Coal Science

The American Conference on Coal Science sponsored by the Pennsylvania State University with the Division of Fuel Chemistry of the American Chemical Society, the Geological Society of America, and the Organic Geochemistry Group of the Geochemical Society, held at Pennsylvania State University, University Park, Pa., June 23–26, 1964

Peter H. Given, *Conference Chairman*

Publication Date: January 1, 1966 | doi: 10.1021/ba-1966-0055.fw001

ADVANCES IN CHEMISTRY SERIES 55

AMERICAN CHEMICAL SOCIETY

WASHINGTON, D.C. 1966

Publication Date: January 1, 1966 | doi: 10.1021/ba-1966-0055.fw001

Library of Congress Catalog Card 66–25071

PRINTED IN THE UNITED STATES OF AMERICA

Advances in Chemistry Series

Robert F. Gould, *Editor*

Advisory Board

Publication Date: January 1, 1966 | doi: 10.1021/ba-1966-0055.fw001

AMERICAN CHEMICAL SOCIETY PUBLICATIONS

In Coal Science; Given, P.;
Advances in Chemistry; American Chemical Society: Washington, DC, 1966.

Publication Date: January 1, 1966 | doi: 10.1021/ba-1966-0055.fw001

FOREWORD

ADVANCES IN CHEMISTRY SERIES was founded in 1949 by the American Chemical Society as an outlet for symposia and collections of data in special areas of topical interest that could not be accommodated in the Society's journals. It provides a medium for symposia that would otherwise be fragmented, their papers distributed among several journals or not published at all. Papers are refereed critically according to ACS editorial standards and receive the careful attention and processing characteristic of ACS publications. Papers published in Advances in Chemistry Series are original contributions not published elsewhere in whole or major part and include reports of research as well as reviews since symposia may embrace both types of presentation.

In Coal Science; Given, P.;
Advances in Chemistry; American Chemical Society: Washington, DC, 1966.

PREFACE

International Conferences on Coal Science have been held in Europe every two years for the last 12 years and have convinced those who have attended them that occasional broad-spectrum conferences on the science of coal serve a very useful purpose. Many organizations in the U. S. from time to time hold symposia concerned with coal, but in recent years they have elected to concentrate on the more applied aspects of coal research, or from their nature they have been obliged to cover only a limited part of the field.

In 1961 a number of coal research workers felt that a conference in the U. S. devoted to fundamental coal studies from many different viewpoints would be useful for those resident in the North American continent. The committee below organized such a conference.

Early in the planning the committee decided to use the organic geochemistry of coal as far as possible as the central theme of the proposed conference. This was for several reasons. In view of the long tradition of research in the U. S. on coal geology and paleobotany and the scale of present activity in these subjects and petrography, it seemed appropriate that the conference should have a strong earth science flavor. Secondly, coal is an exceptionally interesting subject for organic geochemical study, inasmuch as it preserves within its structure a more complete record of its origin and history than any other organic sediment. Finally, it seemed that the subject could provide a central meeting point for all those concerned with basic research on coal; one of the main objectives of the conference was to help build bridges between coal research workers in the geological and physical sciences.

An excellent series of papers was offered, covering a wide range of themes in fundamental coal research. Of the 50 papers presented verbally at the conference, the manuscripts of 47 are included in this volume. Records of the discussions of individual papers and of the general discussions are also incorporated. It is hoped that the book will be of interest not only to those concerned in coal research but also to petroleum geochemistry and to those dealing with general geochemical problems.

The Committee is indebted to the Fuel Chemistry Division of the American Chemical Society, the Organic Geochemistry Group of the Geochemical Society, and the Coal Geology Division of the Geological Society of America for encouragement and for lending their support as co-sponsors. They are grateful to the Pennsylvania State University for extending the hospitality of its campus for the conference. Finally, the Committee wishes to record its sincere appreciation to the Earth Science Division of the National Science Foundation for Grant GP–1679 which enabled a distinguished group of overseas workers,

Publication Date: January 1, 1966 | doi: 10.1021/ba-1966-0055.pr001

In Coal Science; Given, P.;
Advances in Chemistry; American Chemical Society: Washington, DC, 1966.

who contributed notably to the success of the conference, to be specially invited to participate.

PETER H. GIVEN
Pennsylvania State University

IRVING A. BREGER
U.S. Geological Survey

R. A. GLENN
Bituminous Coal Research, Inc.

WILLIAM SPACKMAN
Pennsylvania State University

P. L. WALKER, JR.
Pennsylvania State University

IRVING WENDER
U.S. Bureau of Mines

August 24, 1965

Publication Date: January 1, 1966 | doi: 10.1021/ba-1966-0055.pr001

In Coal Science; Given, P.;
Advances in Chemistry; American Chemical Society: Washington, DC, 1966.

Distribution of Some Organic Substances in Paleozoic Rocks of Central Pennsylvania

FREDERICK M. SWAIN

Department of Geology and Geophysics, University of Minnesota, Minneapolis, Minn.

Publication Date: January 1, 1966 | doi: 10.1021/ba-1966-0055.ch001

Organic substances separated by solvent extraction or by acid treatment from Paleozoic rocks of central Pennsylvania include hydrocarbons, carbohydrates, amino acids, and specifically unidentified compounds of presumed aromatic or heteroaromatic nature. Hydrocarbons and carbohydrates in marine Ordovician and Silurian samples average less than 50 p.p.m.; in marine Devonian samples the average is 50 p.p.m. or more. Amino acid values of Ordovician marine rocks studied are less than 1 p.p.m. in Ordovician and 3–6 p.p.m. in Silurian. Marine Middle Devonian rocks are much richer in amino acids. The data point to a progressive, although possibly not uniform, increase in organic productivity in the seas and nearby lands of this area from Ordovician through Devonian time.

The Paleozoic rocks of central Pennsylvania comprise a thick sequence representing a wide range of lithologic and environmental types. Some of the residual organic substances in the Paleozoic strata were studied to learn whether the organic compounds were related to sedimentary types. If such a relationship were found, the information would be useful for interpreting paleoecological conditions of the Paleozoic of the area.

Because of the small quantities of organic substances that could be separated from the indurated rock samples, their separation and characterization has been difficult. Most of the organic carbon of the rocks is in a form that cannot be extracted with petroleum solvents, mineral acids, or bases. Of the material that can be so extracted, three general types of substances predominate: hydrocarbons, carbohydrate residues, and amino acid residues from protein. These occur in quantities of about 10–150 p.p.m. Other organic matter extracted by petroleum solvents, mineral acids, or bases appears, on the

In Coal Science; Given, P.;
Advances in Chemistry; American Chemical Society: Washington, DC, 1966.

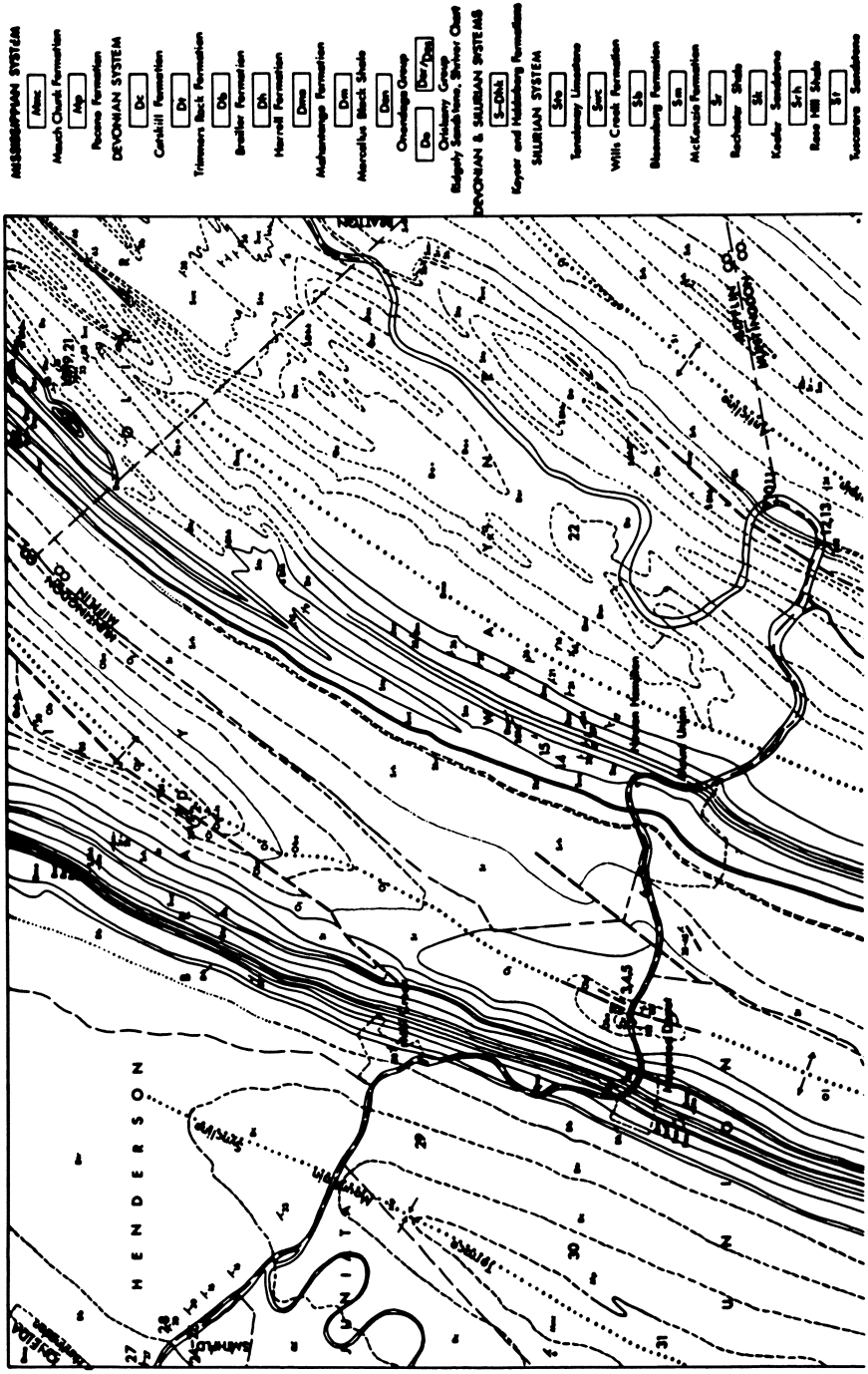

Publication Date: January 1, 1966 | doi: 10.1021/ba-1966-0055.ch001

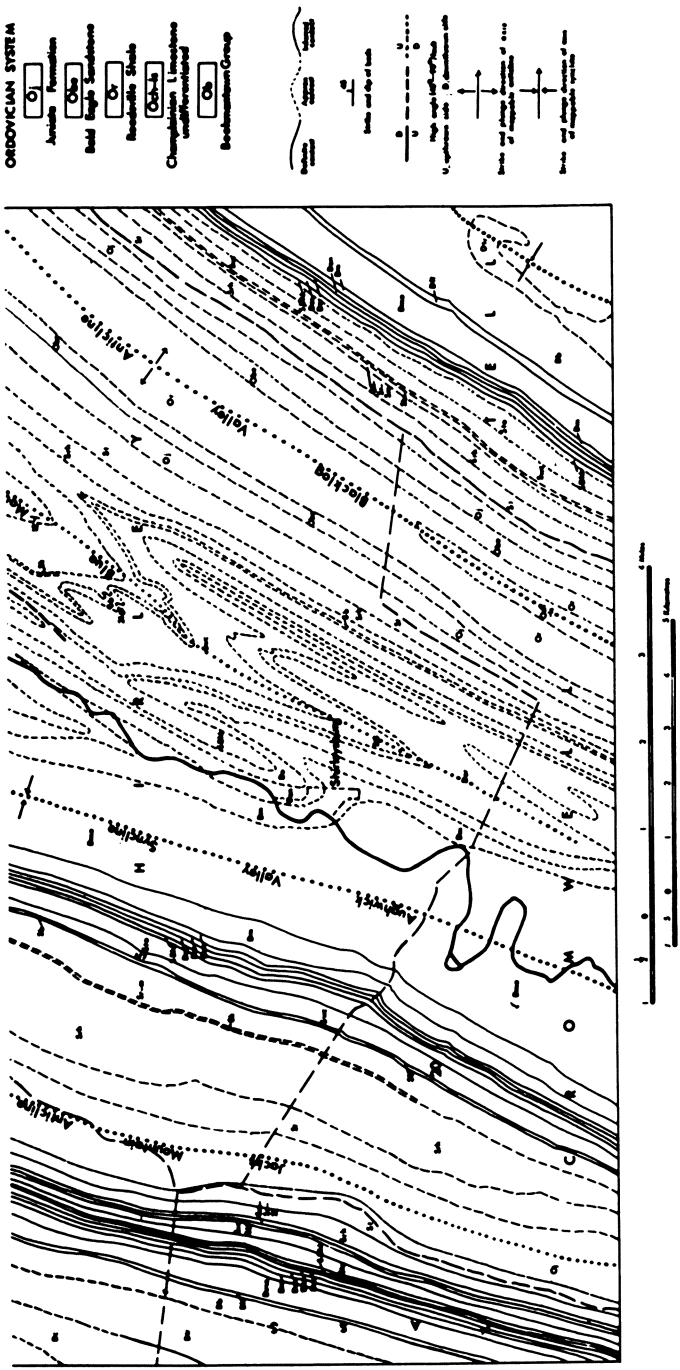

Figure 1. Reconnaissance geologic map by the author of Mt. Union Quadrangle, Huntingdon and Mifflin Counties, Pa. showing location of samples

Publication Date: January 1, 1966 | doi: 10.1021/ba-1966-0055.ch001

basis of preliminary study, to represent mainly aromatic or heteroaromatic compounds and perhaps organic acids that are present only in amounts of 1–10 p.p.m.

Field and Laboratory Procedures

The rock samples on which the study was based were obtained principally in the Mt. Union 15-minute Quadrangle, Huntingdon and Mifflin Counties, Pa. Figure 1 represents a reconnaissance geologic map of the Quadrangle prepared by the writer and shows where most of the samples were obtained. A list of the locations of the samples and of measured sections from which they were obtained is given in the Appendix.

Rock samples were collected from measured sections. Weathered samples were avoided as far as possible, and weathered crusts were later removed in the laboratory. The samples were thoroughly cleaned, treated with chromic acid, crushed, powdered in porcelain ball mills, and stored in glass jars.

Organic carbon analyses were made in duplicate by a combustion train method in the Microanalytical Laboratory, School of Chemistry, University of Minnesota, and Kjeldahl nitrogen analyses were done in triplicate in the Minnesota State Board of Health Laboratory. Averages of the readings are used here (Table III and VI) and are rounded off to the second decimal. Carbonate was removed from the samples by treatment with 0.5*N* hydrochloric acid prior to the carbon analyses.

Bitumen fractions of Middle Devonian rocks (7) were analyzed by extracting 25–50-gram samples in Soxhlet extractors using benzene and methanol 80:20 as solvent; ethyl ether was used in addition for a few samples; the extracts were dried under nitrogen and, after removing sulfur over mercury, were separated on columns of activated alumina using *n*-heptane, benzene, and pyridine plus methanol as successive eluting agents. The fractions were dried under nitrogen and weighed as representatives of saturated hydrocarbons, aromatic hydrocarbons, and asphaltene residual substances in the rock.

Clean and crushed 5-gram samples were treated with concentrated sulfuric acid to degrade carbohydrate materials, and the solutions were tested for total carbohydrates by adding a phenol solution using the procedure of Dubois *et al.* (3). The resulting solutions were measured in a Beckman No. 20 colorimeter, and the total carbohydrates, expressed as glucose equivalent in p.p.m. of rock sample, were calculated by comparing with known samples of D-glucose (Table I, column 5). The colored solutions were scanned in the visible range, and as suggested by Dubois *et al.* (3), the pentose and/or hexose nature of the original substances was estimated from the absorption maxima thus obtained (Table I, column 6).

Individual carbohydrates were separated from some of the rock samples by treatment with 0.5*N* sulfuric acid followed by neutralization, desalting, and paper chromatography as discussed by Palacas *et al.* (6). A much more comprehensive study of the carbohydrates, being made by M. A. Rogers, will be reported later.

Samples of Silurian and Devonian rocks were analyzed for amino acid content by treating with sulfuric acid followed by neutralizing with $BaCO_3$, or by treating with 6*N* hydrochloric acid and ion exchange desalting (9). Paper chromatography was used to separate the amino acids as described earlier (8) (Figure 2). A Spinco amino acid analysis was made of the amino acids from one of the Marcellus black shale samples (Figure 3).

In order to detect furfural degradation products of possible carbohydrates in the rock specimens (4), a 25-gram sample of crushed rock was treated with excess 6*N* hydrochloric acid, and 25 ml. of the resulting solution was collected by boiling into the empty cup of a Soxhlet extractor. Scanning the distillates

Publication Date: January 1, 1966 | doi: 10.1021/ba-1966-0055.ch001

Table I. Bituminous Substances in Ordovician and Silurian Rocks from Mobile Oil Co. No. 1 Long Well, Centre County, Pa.[a]

Geologic Formation	*Beekmantown Dolomite 5138 ft.*	*Beekmantown Dolomite 6972 ft.*	*Antes Shale 14,429 ft.*	*McKenzie Limestone 9010 ft.*
Geologic Age	*Lower Ordovician*	*Lower Ordovician*	*Middle Ordovician*	*Middle Silurian*
Total ether extract	564	640	68	10
Heptane chromat. fraction	12	12	16	2
Benzene chromat. fraction	10	6	30	4
Pyridine + methanol fraction	20	20	10	4
Polar compounds	522	602	386	0
Total benzene + methanol extract, p.p.m.	126	916	442	204
Heptane chromat. fraction	8	4	0	0
Benzene chromat. fraction	10	14	48	12
Pyridine + methanol chromat. fraction	8	8	30	54
Polar compounds	100	894	364	144
Kjeldahl-N	n.d.	0.001	0.09	0.05

[a] Well strata are involved in overthrusting which explains unusual depth figures; values are in p.p.m., corrected for sulfur content.

in the range 200–400 mμ revealed various other substances in addition to furfural (λ max 274 mμ) and 5-hydroxymethylfurfural (λ max 280 mμ). When the distillates were dried under reduced pressure at 50°C. and taken up in ethanol, many showed prominent absorption peaks (Figures 4 and 5). Attempts were made to determine the general chemical nature of these substances as follows. The concentrations of the substances in the present samples were too small for detection by infrared spectrophotometry.

Tests for carboxylic acids were made by paper chromatography using 95% ethanol (100 ml.) and concentrated ammonium hydroxide (1 ml.) as solvent and aqueous bromothymol blue as indicator (*1*). Tests for pyridines were made on their hydrochlorides using butanol:acetic acid:water (4:1:5) as solvent and ammoniacal iron chloride or cysteine-sulfuric acid as indicators. Phenol tests were made using the same solvent and ammoniacal silver nitrate as indicator. Preliminary separations by gas chromatography were attempted using a 15-foot silicone gum column and a hydrogen flame attachment.

Other samples were treated with 10% sodium hydroxide solution, distilled, and subsequently handled in the same way as the acid-treated samples.

The tests showed that a number of substances of aromatic and heteroaromatic nature are present in the samples, but at present they cannot be characterized definitely. The problem of whether or not some of the substances were produced in laboratory treatment of the samples is discussed under Results. Further study of the material is being made.

Publication Date: January 1, 1966 | doi: 10.1021/ba-1966-0055.ch001

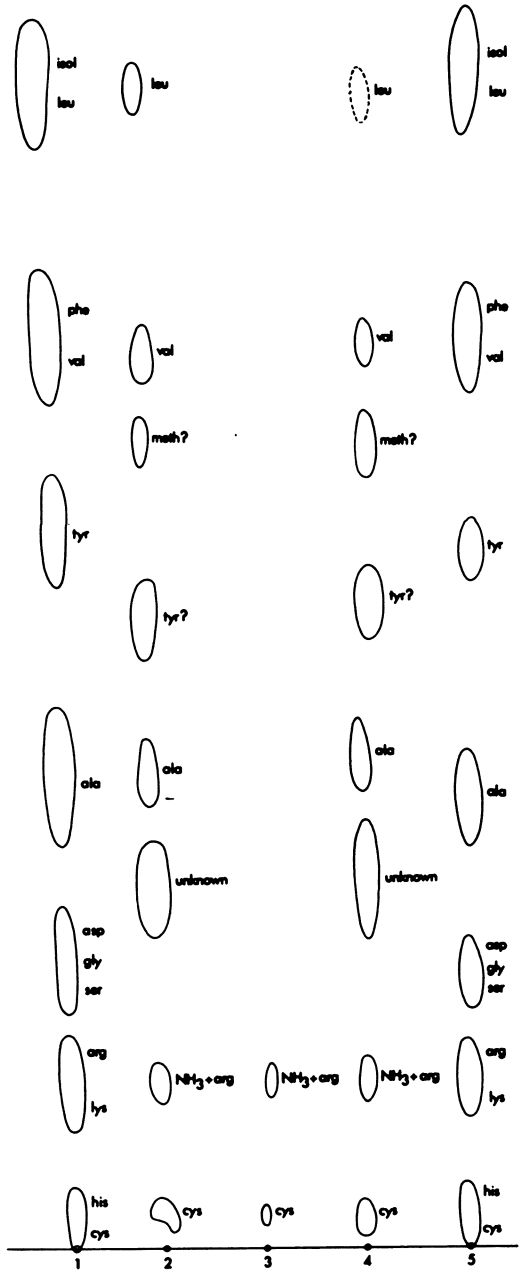

Figure 2. Tracing of paper chromatogram showing amino acids separated from an H_2SO_4 extract of Marcellus shale and Onondaga shale. 1 and 5 are standards; 2 and 4 are Marcellus shale; 3 is Newton Hamilton (Onondaga) shale

Results of Study of Organic Substances

The organic carbon values of the samples examined (Table III) show that the fine-grained, darker colored rocks are typically higher in organic content than the sandstones and lighter colored rocks, but several exceptions occur. Although the Lower and Middle Ordovician samples are relatively high in organic carbon, very little could be extracted, and the carbon is apparently mostly in the pyrobituminous (insoluble) form.

Of the substances studied the most abundant in the Paleozoic rocks of the area are furfurals presumably derived from carbohydrates, higher molecular weight hydrocarbons, and in a few samples, amino acids. Acid and base soluble, low boiling substances having some properties of heterocyclic compounds, phenols, and organic acids exist in smaller amounts.

Bituminous Substances. The distribution of hydrocarbons and other bitumens in some of the Paleozoic rocks of the area is shown in Tables I and II, the latter summarized after Swain (7). The presumed saturated hydrocarbons of the Ordovician, Silurian and Lower Devonian samples are measurably less than in the Middle and Upper Devonian samples. The presumed aromatic hydrocarbons are not as well differentiated. The pyridine-plus-methanol-eluted chromatographic fractions, arbitrarily taken as asphaltic material, also appear, like the aromatic fractions, to be controlled more by local variations than by geologic age.

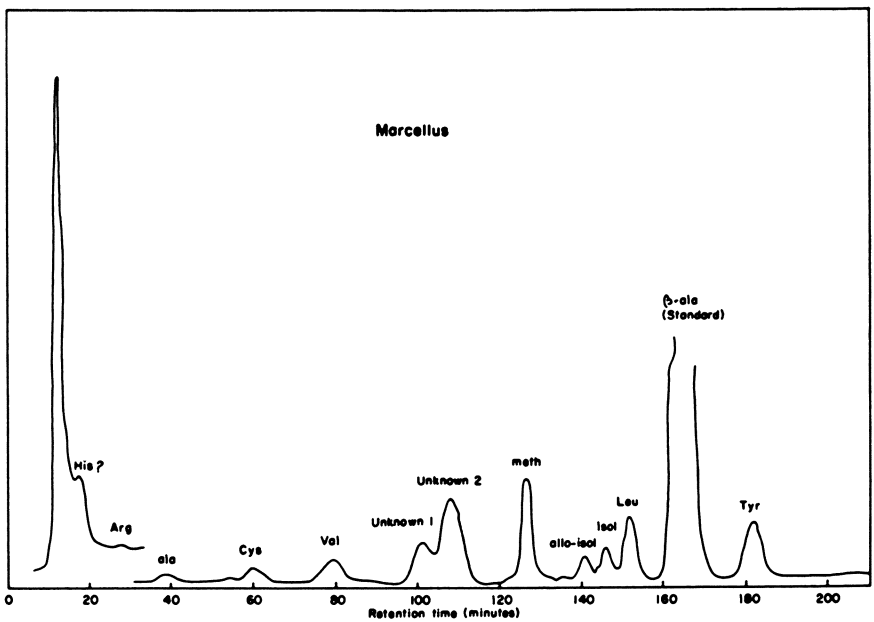

Figure 3. Spinco amino acid chromatogram of H_2SO_4 extract of Marcellus shale run in sodium citrate buffer; column 1 to right eluted 2½ hours at pH 3.25, then 2½ hours at pH 4.25, [Na], 0.2N; column 2 to left eluted with pH 5.28 buffer, [Na], 0.35N

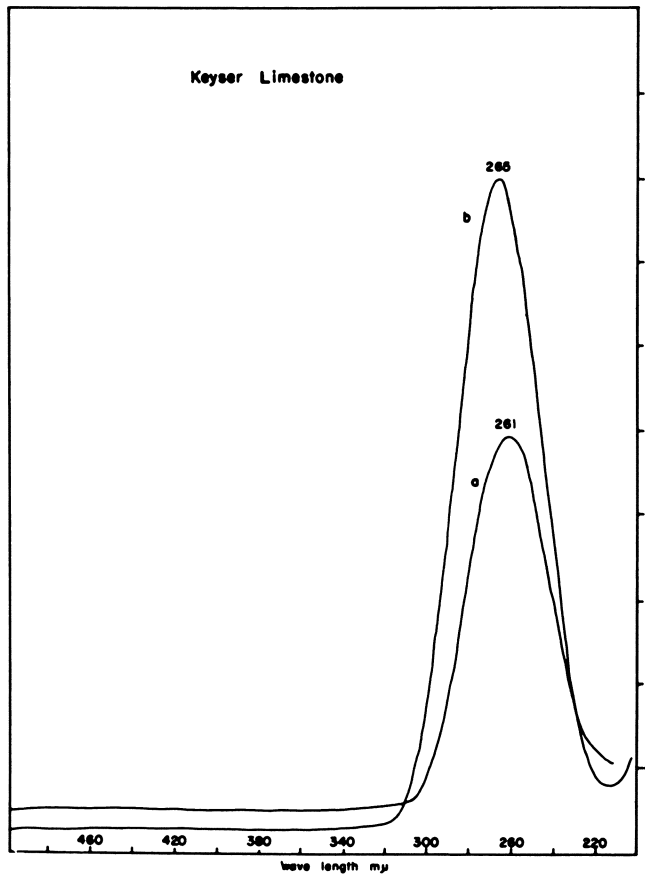

Figure 4. (a) Ultraviolet absorption spectrum of distilled hydrochloric acid extract of upper Keyser limestone, Mt. Union Quadrangle, Pa.; (b) distilled sodium hydroxide extract

Total Carbohydrates. The results of the phenol-sulfuric acid tests for total carbohydrates are listed in Table I. The Lower and Middle Ordovician dolomites and limestones of this area did not yield detectable total carbohydrates, either because they are absent or because of metamorphic degradation. Palacas (*5*) and Palacas, Swain, and Smith (*6*), on the other hand, found traces of glucose and other sugars in Lower and Middle Ordovician rocks of Franklin County, Pa. southeast of the Mt. Union area. It appears that the early and medial Ordovician seas of the Mt. Union area may neither have been receiving much carbohydrate material from the lands nor was much being contributed by organisms to the bottom sediments.

The succeeding Paleozoic deposits all contained more or less carbohydrate residue, ranging from less than 1 p.p.m. to 150 p.p.m. (Table I).

Publication Date: January 1, 1966 | doi: 10.1021/ba-1966-0055.ch001

The total carbohydrates vary according to rock type:

	%C	*Total Carbohydrates, p.p.m.*
Sandstones	0.27	18
Red beds	0.05	23
Shales	0.34	37
Limestones	0.25	55

Absorption spectra of the phenol-sulfuric acid solutions tested for total sugars show that 5-hydroxymethylfurfural from hexoses is more common in the uppermost Silurian and Devonian samples than in the earlier deposits. Furfurals from pentose sugars evidently form the bulk of the residual carbohydrates in these samples, however. There is no definite evidence as to the marine or terrestrial origin of the hexose products in the samples.

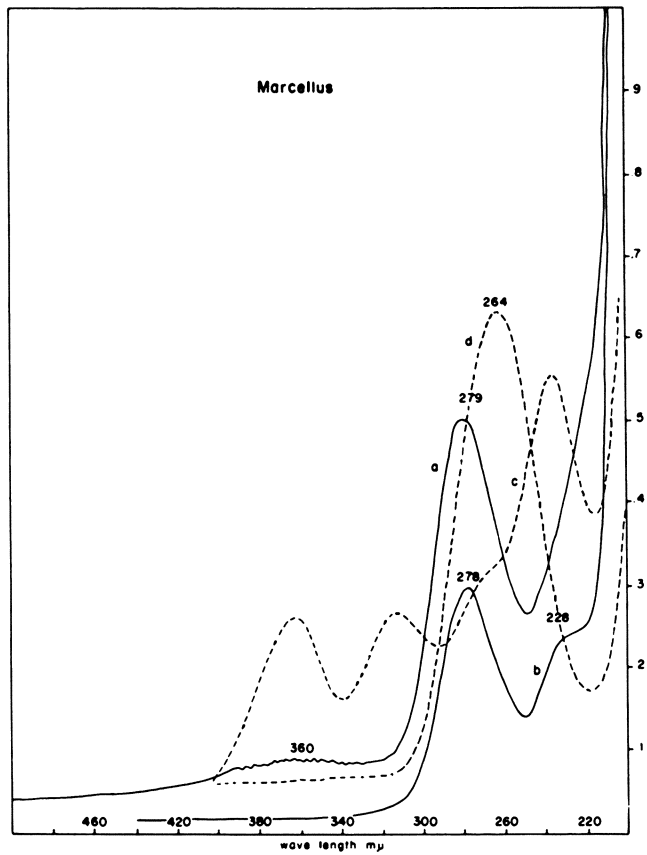

Figure 5. (a) Ultraviolet absorption spectrum of distillate of hydrochloric acid extract of Marcellus Black Shale, Loc. 23, 20-25 ft. above base (b) redistillation of (a); (c) ethanol extract of (a); (d) distillate of sodium hydroxide extract

Table II. Bituminous Substances in Devonian Rocks from Huntingdon County, Pa.[a] (7)

	Ridgeley Sandstone Lower Devonian	*Newton Hamilton Fm., M. Devonian*	*Marcellus Black Shale, M. Devonian*	*Mahantango Fm., M. Devonian*	*Burket Black Shale, U. Devonian*
Number of samples	1	26	8	15	3
Total benzene + methanol extract	191	235	857	324	261
Heptane chromat. fraction	13	41	94	70	46
Benzene chromat. fraction	42	16	11	41	48
Pyridine + methanol chromat. fraction	36	44	71	30	45
Polar compounds	100	134	681	183	122

[a] Values are in p.p.m., corrected for sulfur content.

Table III. Description of Paleozoic Carbon Content and

Description and Interpretation of Origin

P Gr-W, thick-bedded dolomite (offshore marine)

M L Gr, sublithographic, fossiliferous limestone; galena mineralization in fractures (nearshore marine)

M Gr, fissile, silty, calcareous, fossiliferous sh. (nearshore marine)

L Gn-Gr, M-C, argillaceous sandstone (deltaic)

M R Br-Gn, M-C, argillaceous ferruginous sandstone (deltaic)

W, M-F, angular-subrounded, silty silica cemented sandstone (prodeltaic)

P Gr-Br, fissile, calcareous fossiliferous shale, plant fragments (nearshore marine)

P Gr, M-C, conglomeratic calcareous fossiliferous sandstone and sandy limestone (nearshore marine)

M Br-Gr, fissile calcareous fossiliferous shale (nearshore marine)

M Gr, calcarenitic, fossiliferous limestone (nearshore marine)

P R Br, silty, slightly calcareous. ferruginous fissile shale

L G-Gn, platy, finely micaceous calcareous slightly fossiliferous shale (tidal flat)

M Gr, dense to sublithographic, wavy laminated, brecciated limestone (lagoonal)

Individual Carbohydrates. In previous studies (*5*, *6*, *7*) individual sugars from samples of the Marcellus shale from this area were separated by paper chromatography. The following were obtained (Table IV): glucose, galactose, arabinose, xylose, rhamnose, glycerol(?), and several unknown, possibly polysaccharide, compounds. Further study of individual carbohydrates of the Paleozoic rocks of the area is being made by M. A. Rogers.

Amino Acids. Traces of amino acids were found in the Devonian Newton Hamilton and Marcellus Formations in a previous study (*7*). In the present work (Table V) small quantities of amino acids were isolated from the Marcellus shale. In both the earlier work and the present study an amino acid that chromatographed as arginine was found. Other amino acids in the Marcellus black shale are: histidine(?), methionine, alanine, tyrosine, valine, leucine or isoleucine, and two unknowns, possibly including aminobutyric acid of nonprotein origin; in the Newton Hamilton Formation: histidine(?). Ammonia was also present in both the Marcellus and the Newton Hamilton.

Rock Samples, Their Organic Total Carbohydrate Tests[a]

Formation	*Age*	*Org. C %*	*Glucose Eq. p.p.m.*	*Abs. Max. mμ*
Beekmantown	L. Ordovician	0.42	none	—
Chazy-Black River-Trenton	M. Ordovician	0.20	none	—
Reedsville	U. Ordovician	0.30	25.0	±480 (very weak) (f)
Bald Eagle	U. Ordovician	0.14	23.2	n.d.
Juniata	U. Ordovician	0.17	19.8	n.d.
Tuscarora	L. Silurian	0.04	11.2	482, 496 (f + h)
Rose Hill	M. Silurian	0.39	11.4–33	482 (f)
Keefer	M. Silurian	0.89	13.2–37.2	no peak
Rochester	M. Silurian	0.30	24.0–46.2	n.d.
McKenzie	U. Silurian	0.10	18.0–59.0	480–482 (f)
Bloomsburg	U. Silurian	0.03	10.0–32.6	±480 (very weak) (f)
Wills Creek	U. Silurian	0.38	71.6–103.6	482 (f)
Tonoloway	U. Silurian	n.d.	20.0	486 (h)

Table III.

	Description and Interpretation of Origin
	M-D Gr, finely crystalline limestone argillaceous to pure fossiliferous limestone (nearshore marine)
	M Gr, dense to finely crystalline argillaceous, fossiliferous limestone (nearshore marine)
	M Gr, coarsely crystalline argillaceous fossiliferous, calcarenitic limestone (nearshore marine)
	M-D Gr, platy siliceous, calcareous shale and M-T bedded siliceous fossiliferous limestone (nearshore marine)
	W, M-C, subrounded to rounded, partly calcareous, partly porous quartz sandstone (nearshore marine)
	M-L-Gn-Gr, calcareous fossiliferous shale (nearshore marine)
	B, fissile-platy, pyritic shale (offshore marine)
	M, Gr-Gn, silty shale (nearshore marine)
	B, fissile, slightly calcareous fossiliferous shale (offshore marine)
	Gn-Gr, platy silty shale, plant fragments (deltaic)
	Gn-Gr, flaggy, VF-F sandstone and siltstone; plant fragments (deltaic)
	M Gr and M R-Br, silty shale, Gr and W F-C sandstone, marine fossils (nearshore marine-deltaic)
	Pale R-Br, silty micaceous shale and F-C felspathic, hematitic sandstone (alluvial)
	F-M, L Gn-Gr, angular-subrounded, argillaceous micaceous sandstone, rock fragments (alluvial)
	Pale R-Br, silty sandy, micaceous slightly calcareous shale (alluvial)

[a] Abbreviations: P, pale; Gr, gray; W, white; Gn, green; Br, brown; B, black; M, medium; C, coarse; F, fine; R, red; f, furfural; h, 5-

The Silurian Wills Creek, Tonoloway and Keyser Formations were tested for residual amino acids (Table V). The following were found: cystine(?), histidine(?), arginine, glycine(?), aspartic acid(?), glutamic acid(?), threonine, alanine, valine, leucine.

Other Organic Substances. Spectral data on other organic substances detected in samples of the Paleozoic rocks treated with dilute hydrochloric acid and distilled, are given in Table VI. The substances possibly represent aromatic and heteroaromatic compounds such as anthracene, naphthalene, pyridines, and phenols, but a more definite characterization has not been completed. The compounds seem to be present in only a few parts per million.

Publication Date: January 1, 1966 | doi: 10.1021/ba-1966-0055.ch001

Continued

Formation	*Age*	*Org. C*	*Glucose Eq.*	*Abs. Max.*
Keyser	U. Silurian	0.17	11.2–25.2	480–488 (f + h)
Coeymans	L. Devonian	n.d.	150.4	488 (h)
New Scotland	L. Devonian	0.31	21.6–88.4	480–486 (f + h)
Shriver	L. Devonian	0.33	38.8–122.4	480–488 (f + h)
Ridgeley	L. Devonian	0.00	144	484 (f + h)
Newton Hamilton	M. Devonian	0.06–0.29	1–72	n.d.
Marcellus	M. Devonian	0.70–3.61	0.05–86	n.d.
Mahantango	M. Devonian	n. d.	n.d.	n.d.
Burket	U. Devonian	2.33	17.2	480 (very weak) (f)
Harrell	U. Devonian	n.d.	n.d.	n.d.
Brailler	U. Devonian	0.11	14.4	480 (very weak) (f)
Chemung (Trimmers Rock)	U. Devonian	n.d.	100.8	484 (very weak) (f + h)
Catskill	U. Devonian	0.00	21.2	482–492 (f + h)
Pocono	L. Mississippian	n.d.	9.6	n.d.
Mauch Chunk	M.-U. Mississippian	0.00	33.0	482 (f)

hydroxymethylfurfural. Whether λ max suggests furfural or 5-hydroxymethylfurfural is given in parentheses in column 6.

Attempts to separate them by paper chromatography resulted in a few spots that presently cannot be definitely matched with known compounds.

In an attempt to learn to what extent the substances may have been produced in laboratory preparation of the rock samples, specimens of recent marine algae from Oregon and California, freshwater pondweeds from Minnesota, and freshwater lake sediments from several localities were treated with acid and base and distilled in the same manner as the rock samples. The plant distillates yielded large quantities of furfurals only. The absorption spectra of the sediment samples showed several other peaks (mostly small) in addition to furfurals. A few sediment samples had large peaks. If the substances sepa-

Publication Date: January 1, 1966 | doi: 10.1021/ba-1966-0055.ch001

Table IV. Carbohydrate Components of Middle and Upper Devonian Rocks of Central Pennsylvania[c]

Formation	*Galactose*	*Glucose, p.p.m.*	*Mannose*	*Arabinose*	*Xylose*	*Fructose*	*Galacturonic acid*	*Glycerol*
Oranda, M. Ord.,[a] Mechanicsville, Pa.	?	0.36		?				x
Onondaga, M.[a,d] Dev., Newton Hamilton, Pa.								
Marcellus, M.[a] Dev., Huntingdon, Pa.	?	1.3		x	x			x
Mahantango, M.[b] Dev., Newton Hamilton, Pa.		x	x		x			
Harrell, U.[b] Dev., Mill Creek, Pa.		x		x		x	x	
Brailler, U.[b] Dev., Huntingdon, Pa.		x						
Chemung, U.[b] Dev., Huntingdon, Pa.	x	x		x	x			

[a] Paper chromatographic analyses of samples extracted with 0.5*N* sulfuric acid by Palacas, Swain, and Smith (6).

[b] Paper chromatographic analyses of samples extracted with 0.5*N* sulfuric acid by M. A. Rogers.

[c] x indicates substance was present, but quantity not measured.

[d] Carbohydrate reacting material detected but not resolved owing to inorganic salt interference.

Table V. Amino Acids Separated Paleozoic Rock Samples

Formation	*Cys*	*his + arg*	*gly + asp*	*glu + thr*
McKenzie[a] Limestone	0.4	0.8	0.9	0.4
Wills Creek[a] Shale	0.6	4.7	1.0	0.9
Lower Keyser[a] Limestone	0.4	0.4	0.7	0.5
Marcellus Black[b] Shale (1)	tr.	tr (his) tr (arg)	.001 (tyr)	0.001 (unkn. 1) 0.002 (unkn. 2)
Marcellus Black[a] Shale (2)	8.5	32.6	18.1	8.1

[a] Values in p.p.m., obtained by paper chromatography

[b] Values in micromoles per gram, obtained with a Spinco amino acid analyzer

Publication Date: January 1, 1966 | doi: 10.1021/ba-1966-0055.ch001

rated from the rocks were formed primarily in laboratory pretreatment of the samples, similar compounds should have appeared in the recent samples. Thus, although the possibility of contamination or laboratory artifacts cannot be ruled out entirely for the rock samples, the writer believes that the substances, as yet not definitely characterized, obtained by distillation with acid or base, are mainly indigenous.

In general these substances are widely distributed in the acid distillates but appear to increase in number at two stratigraphic levels: (1) in the middle Silurian McKenzie Limestone and (2) in the middle Devonian shales. Furthermore, possible two- and three-ring aromatic or heteroaromatic structures show similar increases. There is also a rough correlation with the Kjeldahl nitrogen content of the samples (Table VI).

The writer believes that there is a direct relationship between these acid distillate compounds and sedimentary environments which favored production and preservation of organic matter.

Relationship of Organic Residues to Sedimentary Environments in Mt. Union Quadrangle

Offshore neritic formations in the Paleozoic rock sequence probably include, on faunal and lithologic grounds, the Lower Ordovician Beekmantown dolomites, Middle Ordovician limestones, and Devonian Marcellus and Burket black shales (Table III). The first two are characterized by 0.1–0.4% organic carbons, very low organic nitrogen, and about 20 p.p.m. hydrocarbons but no carbohydrate residues. The Devonian offshore neritic black shales by contrast

from Sulfuric Acid Extracts of from Mt. Union (Pa.) Area

ala	*val* + *meth*	*leu* + *isol*	Σ	*Remarks*
—	—	0.4	2.9	H_2SO_4 extract neutralized with $BaCO_3$ and developed in BuOH:HAC:H_2O
—	0.2	—	7.4	Same procedure
0.5	0.3	0.2	3.0	Same procedure
tr.	tr (val) .001 (meth)	tr (isol) 0.001 (leu)	—	Run in sodium citrate buffer, pH ranging from 3.25–5.28
.052(t)[c] 16.6 5.2(t)[c]	15.7	0.1(p)[c] 13.5	118.4	HCl extract desalted in ion exchange columns

[c] t = tyrosine; p = phenylalanine.

Publication Date: January 1, 1966 | doi: 10.1021/ba-1966-0055.ch001

Table VI. Spectral Data on Substances Treatment and Distillation

Formation	*Absorption* 220	240	253, 247	252	256	258
Beekmantown Dolomite (Ord.)				x		
Chazy-Black River Trenton Limestone (Ord.)						
Reedsville Shale (Ord.)						
Bald Eagle Sandstone (Ord.)						
Juniata Red Beds (Ord.)						x
Tuscarora Sandstone (Sil.)						
Tuscarora green shale layer in sandstone (Sil.)						
Castanea Red Sandstone (Sil.)						
Rose Hill Shale (Sil.)	x					
Keefer Sandstone (Sil.)				x		
Rochester Shale (Sil.)					x	
McKenzie Limestone (Sil.)	x			x		
Bloomsburg Red Shale (Sil.)						
Wills Creek Shale (Sil.)						
Tonoloway Limestone (Sil.)						
Keyser Limestone (Sil.)						
Coeymans Limestone (Dev.)	x					
New Scotland Limestone (Dev.)						
Shriver Chert (Dev.)						
Ridgeley Sandstone (Dev.)						
Newton Hamilton Shale (Dev.)				x	x	
Marcellus Black Shale (Dev.)				x		
Mahantango Shale (Dev.)				x		
Burket Black Shale (Dev.)						
Harrell Shale (Dev.)						
Brailler Siltstone (Dev.)				x		
Trimmers Rock Sandstone (Dev.)						
Catskill Red Beds (Dev.)						
Pocono Sandstone (Miss.)	x		x			
Mauch Chunk Red Shale (Miss.)			x			

Separated by 6N Hydrochloric Acid from Paleozoic Rock Samples

Maxima, mμ

260	261	264	265	272	314	328-330	340, 276	340	360	364	*Kjeld. N.*
	x		x								0.01
	x		x								0.01
											0.03–0.04
	x										0.01
	x										0.01
	x										0.01
	x										n.d.
	x										n.d.
	x		x								0.02
											0.04
	x										0.02
x	x					x					0.06
	x					x					0.04
x	x					x					0.02
	x		x								0.01
x	x										0.01
x	x										0.02
x	x										n.d.
	x										0.01
											0.01
						x		x		x	0.04–0.05
			x		x		x	x	x	x	
	x										0.04–0.20
		x		x					x	x	0.13
	x										n.d.
											n.d.
x											0.02
	x		x								0.01
											0.01
	x										0.02

have up to 3.6% organic carbon, up to 0.6% nitrogen, about 25 p.p.m. glucose equivalent, and about 100 p.p.m. hydrocarbons.

Closer proximity of the Marcellus and Burket depositional basins to a terrestrial or littoral source of vegetative debris together with anaerobic stagnation of the sea are suggested as accounting for the greater content in Devonian residual organic matter than in the Ordovician deposits.

Many of the formations in the sequence are suggested as being nearshore neritic in origin judging from their faunas and sedimentary structures. The Middle Devonian Newton Hamilton shale and limestone is an example (Table III). Organic carbon varies from less than 0.02% to about 1%; nitrogen averages about 0.02%. Glucose equivalent averages about 25 p.p.m. except in the Middle Silurian where it is about 50 p.p.m. and in the Middle Devonian where it is up to 105 p.p.m. The Devonian rocks have a generally higher hydrocarbon content than the Ordovician and Silurian of this area.

The relative increase in carbohydrates in the Middle Silurian and Middle Devonian is suggested as resulting from a period of increased organic productivity during the deposition of those rocks.

Several of the formations probably represent littoral beach, lagoonal, and tidal flat deposits of various types; these include the Ordovician Bald Eagle sandstone, Silurian Tuscarora and Castanea sandstones, Bloomsburg red siltstones and shales, Wills Creek shale, Devonian Harrell shale, Brailler siltstone, and Trimmers Rock Sandstone (Table III). Organic carbon is less in these than in the neritic deposits, organic nitrogen about the same, and glucose equivalent is greater than in the inner neritic deposits. An increased contribution of debris from shore vegetation is believed to characterize the littoral samples. It is possible that a shore vegetation did not develop in this area until the late Ordovician.

The Ordovician Juniata, Devonian Catskill, and Mississippian Mauch Chunk red beds represent alluvial deposits (Table III). As would be expected because of the oxidizing nature of the environment, organic carbon is much lower than in the other deposits, organic nitrogen is somewhat lower, and glucose equivalent is much lower.

The data and discussion above suggest that differences exist in the organic residues of the Paleozoic Formations of the Mt. Union area as functions of type and amount of source material, rate of deposition, distance from source, and preservative sedimentary conditions. Carbohydrate residues are more abundant in the Silurian and Devonian than in the underlying Ordovician, which may reflect the increase of larger terrestrial and littoral plants in the Silurian and Devonian.

Although there is some evidence for marine sources, the bulk of the organic material in the Paleozoic samples studied probably was from terrestrial or littoral sources rather than from plankton because of the predominance of furfurals, presumably from pentoses, that are common in terrestrial fungi and other low forms of plants, but scarce in modern marine environments. Breger and Brown (*2*) also suggested a terrestrial source for organic matter of the Upper Devonian-Lower Mississippian Chattanooga Black Shale. Although they were not present in the Mt. Union area, it is planned that organic residues

Publication Date: January 1, 1966 | doi: 10.1021/ba-1966-0055.ch001

of sublittoral facies of coal-bearing formations be studied. Under favorable conditions the source material in such facies may be in a less humified state than in the coal beds proper and thus provide knowledge as to some transitory stages in coal formation.

Appendix

The localities from which samples were obtained for this study are listed below.

1. Beekmantown Dolomite, Lower Ordovician, 1 mile northeast of Airydale, Mt. Union Quadrangle.
2. Middle Ordovician limestone, 1.5 miles southwest of Airydale, Mt. Union Quadrangle.
3. Reedsville Shale, Middle Ordovician, Jacks Mountain Gap, 1 mile east of Mapleton, Mt. Union Quadrangle.
4. Bald Eagle Sandstone, Upper Ordovician, Jacks Mountain Gap, 1 mile east of Mapleton, Mt. Union Quadrangle.
5. Juniata Formation, Upper Ordovician, Jacks Mountain Gap, 1 mile east of Mapleton, Mt. Union Quadrangle.
6. Tuscarora Sandstone, Lower Silurian, Jacks Mountain Gap, 1 mile east of Mapleton, Mt. Union Quadrangle.
7. Tuscarora Formation, Jacks Mountain Quarry, 1.5 miles west of Mt. Union, south of Juniata River, Mt. Union Quadrangle.
8. Castanea Sandstone, Lower Silurian, Jacks Mountain, north side of Juniata River, 1 mile west of Mt. Union, Mt. Union Quadrangle.
9. Rosehill Formation, Middle Silurian, north Side of Juniata River, 4 miles east of Mt. Union, Mt. Union Quadrangle.
10. Keefer Sandstone, Middle Silurian, north Side of Juniata River, 4 miles east of Mt. Union, Mt. Union Quadrangle.
11. Rochester Shale, Middle Silurian, north Side of Juniata River, 4 miles east of Mt. Union, Mt. Union Quadrangle.
12. McKenzie Formation, Upper Silurian, south Side of Juniata River, 4 miles southeast of Mt. Union, Mt. Union Quadrangle.
13. Bloomsburg Formation, Upper Silurian, south Side of Juniata River, 4 miles southeast of Mt. Union, Mt. Union Quadrangle.
14. Wills Creek Shale, Upper Silurian, 1 mile northeast of Mt. Union, Mt. Union Quadrangle.
15. Tonoloway Limestone, Upper Silurian, 1 mile northeast of Mt. Union, Mt. Union Quadrangle.
16. Keyser Limestone, Upper Silurian, 9 miles northeast of Mt. Union, Mt. Union Quadrangle.
17. Coeymans Limestone, Lower Devonian, 9 miles northeast of Mt. Union, Mt. Union Quadrangle.
18. New Scotland Limestone, Lower Devonian, 9 miles northeast of Mt. Union, Mount Union Quadrangle.
19. Shriver Formation, Lower Devonian, 9 miles northeast of Mt. Union, Mt. Union Quadrangle.
20. Shriver Formation, 8 miles southwest of Mt. Union, Mt. Union Quadrangle.
21. Ridgeley Sandstone, Lower Devonian, 9 miles northeast of Mt. Union, Mt. Union Quadrangle.
22. Newton Hamilton Formation, Middle Devonian, 2.5 miles northeast of Mt. Union, Mt. Union Quadrangle.
23. Marcellus Formation, Middle Devonian, 2 miles northeast of Mt. Union, Mt. Union Quadrangle.
24. Mahantango Formation, Middle Devonian, south Side of Juniata River, opposite Huntingdon, Huntingdon Quadrangle (not shown on map).

Publication Date: January 1, 1966 | doi: 10.1021/ba-1966-0055.ch001

25. Burket Shale, Upper Devonian, south Side of Juniata River, opposite Huntingdon, Huntingdon Quadrangle (not shown on map).
26. Harrell Shale, Upper Devonian, south Side of Juniata River, opposite Huntingdon, Huntingdon Quadrangle (not shown on map).
27. Brailler Formation, Upper Devonian, north Side of Juniata River, east edge of Huntingdon, Huntingdon Quadrangle (not shown on map).
28. Trimmers Rock Formation, Upper Devonian, east edge of Huntingdon, Mt. Union Quadrangle.
29. Catskill Formation, Upper Devonian, south Side of Juniata River, 1.5 miles west of Mill Creek, Mt. Union Quadrangle.
30. Pocono Sandstone, Lower Mississippian, Sideling Hill, 2 mi. southwest of Mill Creek, Mt. Union Quadrangle.
31. Mauch Chunk Formation, Upper Mississippian, Little Trough Creek Valley, 3 miles southwest of Mill Creek, Mt. Union Quadrangle.
32. Mobile Producing Company No. 1 Long Well, Centre County, Pennsylvania: core samples from Lower Ordovician, Middle Ordovician and Middle Silurian (not shown on map).

Publication Date: January 1, 1966 | doi: 10.1021/ba-1966-0055.ch001

Acknowledgments

The work has been supported by grants from the National Science Foundation and the Graduate School, University of Minnesota. David Dobbins, Larry Nutter, Willard Miller, Gunta Venteris, Mikola Malinowsky, Arturs Studans, Inara Porietis, and M. Alan Rogers assisted in the field and laboratory work. Assistance and advice was also provided by the Pennsylvania Geological Survey. This assistance and support are gratefully acknowledged. Samples from their deep well, the Long No. 1, Centre County, Pa. were kindly supplied by the Mobil Oil Co.

Literature Cited

(1) Block, R. J., Durrum, E. L., Zweig, Gunter, "Paper Chromatography and Paper Electrophoresis," Academic Press, New York, 1955.
(2) Breger, I. A., Brown, Andrew, *Trans. N. Y. Acad. Sci.* **25,** 741 (1963).
(3) Dubois, Michel, Gilles, K. A., Hamilton, J. K., Rebers, P. A., Smith, Fred, *Anal. Chem.* **38,** 350 (1956).
(4) Noller, C. R., "Chemistry of Organic Compounds," W. B. Saunders, Philadelphia, 1951.
(5) Palacas, J. G., Ph.D. Thesis, University of Minnesota, 1959.
(6) Palacas, J. G., Swain, F. M., Smith, F., *Nature* **185,** 234 (1960).
(7) Swain, F. M., *Bull. Am. Assoc. Petrol. Geologists* **42,** 2858 (1958).
(8) Swain, F. M., *Bull. Am. Assoc. Petrol. Geologists* **47,** 777 (1963).
(9) Swain, F. M., Blumentals, A., Millers, R., *Limnol. Oceanog.* **4,** 119 (1959).

Received October 5, 1964.

Discussion

Irving A. Breger: Do the furfural and hyroxymethylfurfural exist as such in the sediments or might they be formed during the extraction process?

Frederick M. Swain: The furfurals are believed to be represented by polymeric carbohydrate compounds in the rocks and to have been produced by distillation of the rock samples with hydrochloric acid (*6*).

Keith A. Kvenvolden: Would you elaborate on your finding of hydrocarbons in acid extracts of Paleozoic rocks?

Dr. Swain: Very little hydrocarbon material was present in the distilled acid extracts, but dried distillates showed small amounts of aromatic hydrocarbons that had distilled over in Soxhlet flasks. Much larger quantities of residual hydrocarbons were extracted with benzene from Devonian rocks of this area in an earlier study (*7*).

Peter H. Given: Are the "unknown amino acids" unknown in the sense that they are not found in the proteins of present living matter?

Dr. Swain: Yes, the amino acids listed as unknown from the Marcellus Formation are not among the common protein amino acids. It is suggested they may be aminobutyric acids, but this has not been verified.

Peter Zubovic: You mentioned a high concentration of vanadium in some of your rocks. Do you know whether this vanadium is associated with the mineral or organic matter?

Dr. Swain: At first we thought it may be associated with the organic matter. However, because of the small amount of organic matter present we are not sure of this. We just don't know how it is associated.

Publication Date: January 1, 1966 | doi: 10.1021/ba-1966-0055.ch001

2

Oxygen Functional Groups in Green River Oil-Shale Kerogen and Trona Acids

J. I. FESTER* and W. E. ROBINSON

Laramie Petroleum Research Center, Bureau of Mines, U.S. Department of the Interior, Laramie, Wyo.

Publication Date: January 1, 1966 | doi: 10.1021/ba-1966-0055.ch002

Carboxyl, ester, amide, hydroxyl, aldehyde, and ketone groups were estimated for oil-shale kerogen and kerogen-derived trona acids from the Green River Formation. Ether groups were estimated by difference. Carboxyl, ester, and ether groups were found to account for the major portion of the oxygen in both the kerogen and trona acid samples. Minor amounts of amide, hydroxyl, aldehyde, and ketone groups were indicated. The reactive oxygen groups, carboxyl and ester, account for about one-half of the total oxygen in kerogen and two-thirds of the total oxygen in trona acids while the unreactive ether group accounts for the other half of the total oxygen in kerogen and one-third of the total oxygen in trona acids.

The production of carbon monoxide, carbon dioxide, and water during low temperature heating of oil shale indicates the presence of oxygen functional groups in kerogen. Evolution of carbon dioxide begins at about 200°C. (*2*) and reaches a maximum at about 260°C. About 30–60% (*5*, *7*) of the total kerogen oxygen appears in the pyrolytic gases from heating kerogen at 350°C. Nearly all of the kerogen oxygen appears in the gases when kerogen is retorted at 500°C. The oxygenated gases may be derived from carboxyl (acids and acid salts), aldehyde, ketone, ester, ether, hydroxyl, and amide groups.

Little quantitative data are available in the literature about the oxygen functional groups in kerogen. A recent report (*3*) describes a modified method for determining the carboxyl groups present in kerogen by utilizing steam distillation in the Fuchs calcium acetate exchange method (*4*).

* Deceased

In Coal Science; Given, P.;
Advances in Chemistry; American Chemical Society: Washington, DC, 1966.

The present report gives the methods used and the data obtained for acid, ester, aldehyde, ketone, amide, hydroxyl, and ether functional groups in kerogen and trona acids. These methods may be applicable also in studying coals and other carbonaceous materials.

Experimental

Sample Preparation. A kerogen concentrate was prepared from Green River oil shale from the Mahogany zone of the Bureau of Mines oil-shale mine near Rifle, Colo. The untreated oil shale contained 35% organic material. The concentration procedure consisted of benzene extraction of the crushed shale (100 mesh) to remove benzene soluble organic material, dilute hydrochloric acid leaching to remove mineral carbonates, and attrition grinding (*8*) in the presence of water and cetane to remove much of the remaining mineral matter. The resulting kerogen concentrate contained 86% organic material and 14% mineral matter consisting of quartz, feldspar, and pyrite.

In all of the functional group tests of kerogen, the inorganic material removed from the oil shale by attrition grinding was used as a mineral blank. Because pyrite was concentrated with the kerogen and was not separated with the mineral, pyrite equivalent to that present in the kerogen concentrate was added to the mineral blank.

The trona acids used in this study are alkali soluble organic acids that have been leached or degraded from the oil shale of the Green River Formation subsequent to deposition by the action of a sodium carbonate-sodium bicarbonate brine, referred to as trona. In certain locations, such as near Rock Springs, Wyo. where the sample was obtained, trona brine containing the organic acids can be pumped from wells drilled into the Green River Formation. In preparing the sample, the brine was acidified with mineral acid which precipitated the organic trona acids out of solution. After water washing, the precipitated trona acids contained 0.8% mineral matter. These trona acids were used as a comparison sample in this study because they contain structures similar to those present in Green River kerogen and are essentially free of mineral matter.

Analytical Methods. The carboxyl group was determined by a modified Fuchs calcium exchange method (*3*). The modified procedure consisted of exchanging the carboxyl groups of the samples with calcium acetate, removing the liberated acetic acid by steam distillation, and determining both the amount of acetic acid liberated and the amount of calcium exchanged. In the procedure, 1 gram of sample was added to a 500-ml. reaction flask to which is added 40 ml. of carbon dioxide-free distilled water and 10 ml. of 1*N* calcium acetate solution. The reaction mixture was steam distilled at an approximate rate of 250 ml. of distillate per hour for 24 hours and titrated with 0.02*N* sodium hydroxide to a cresolphthalein end point. When steam distillation was completed, the sample was filtered and washed with dilute (pH 8-9) sodium hydroxide to remove excess calcium acetate. The sample was dried, and calcium was determined by chemical methods.

The ester function was determined by alkaline hydrolysis followed by precipitating the liberated acids as calcium salts. In the present work, samples of 1–1.5 grams were added to 50 ml. of 0.2*N* aqueous sodium hydroxide and refluxed with continuous stirring under nitrogen for 18–24 hours. After hydrolysis the samples were titrated to a pH of 9 with hydrochloric acid. Then 15 ml. of 1*N* calcium acetate was added, and the sample was stirred rapidly under a stream of nitrogen for 1 hour. The suspension of calcium salt was filtered, washed with dilute base until free of excess calcium acetate as determined by titration with ethylenediaminetetraacetic acid (EDTA), and dried under a stream of nitrogen. Calcium was determined on the dried product.

Publication Date: January 1, 1966 | doi: 10.1021/ba-1966-0055.ch002

Since it was possible that a portion of the amide structure, if present, would react as ester structure in the above hydrolysis, a separate reaction was carried out to estimate the amount of amide present. Since amides are generally more difficult to hydrolyze than esters, the following procedure was used: 2-gram samples were weighed into Kjeldahl flasks, and 200 ml. of 10% sodium hydroxide were added. The mixture was refluxed for 3 hours, and the ammonia was trapped in boric acid solution and determined by titration. The hydrolyzed kerogen concentrate was filtered, washed thoroughly with distilled water, and dried. Because the trona acids are alkali soluble, it was necessary to neutralize the excess base with 5*N* hydrochloric acid; 5 ml. were added in excess. The acids that precipitated out of the solution were filtered, washed thoroughly with water, and dried. The residue from hydrolysis of kerogen and trona acids was suspended in 100 ml. of ether, washed for 1 hour with rapid stirring, filtered, and the resulting residue was dried. The trace of ether soluble material was examined by infrared techniques for primary and secondary amines. The ether-insoluble residues from kerogen concentrate and trona acids then were subjected to Kjeldahl nitrogen determinations to check for decrease in nitrogen owing to loss of ammonia and primary and secondary amines cleaved fr m amide structure.

The hydroxylamine reaction was used to estimate ketone and aldehyde groups. The method used was similar to one described by Kaverzneva and Salova (*6*). A 25-ml. solution of 5% aqueous hydroxylamine hydrochloride (previously adjusted to a pH 7.5–8 with sodium hydroxide) was added to 1.5 grams of sample and allowed to react for 18–24 hours at room temperature. The mixture was filtered, washed with water, and dried. The residue was analyzed for nitrogen, and the amount of aldehyde and ketone structure was calculated from the nitrogen increase.

Attempts were made to reduce any aldehyde and ketone function with sodium borohydride. A 1.5-gram sample was weighed into a 100-ml. reaction flask and suspended in 10 ml. of methanol. A solution of 0.3 gram of sodium borohydride in 25 ml. of 0.1*N* sodium hydroxide was added to the sample over a period of 15 minutes. The mixture was refluxed under nitrogen for 6 hours, filtered, and washed thoroughly with water. The amount of aldehyde and ketone was estimated by the decrease in the 5.8 micron peak in the infrared spectrum of the treated sample as compared with the untreated sample.

Hydroxyl groups were determined by the acetylation method described by Blom *et al.* (*1*). The procedure consisted of treating 1-gram samples with acetic anhydride-pyridine reagent. The acetylated sample was recovered by filtration and thoroughly washed. The amount of hydroxyl function was then determined by hydrolyzing the sample with 0.2*N* sodium hydroxide and measuring the amount of acetic acid liberated when the hydrolyzate was neutralized with sulfuric acid and steam distilled.

The x-ray scattering intensities for kerogen and trona acids were obtained with an XRD-5 diffractometer using zirconium-filtered Mo K alpha radiation. The experimental x-ray intensities were corrected for air scattering, polarization, and absorption and then converted, using data from chemical analysis, to express the scattering per carbon atom.

Calcium was determined by an EDTA method; carbon and hydrogen by the combustion method; total nitrogen by the Kjeldahl method; sulfur by the Eschka method; infrared spectra by the potassium bromide pellet technique.

Results and Discussion

The similarity of kerogen and trona acids is indicated by their elemental compositions shown in Table I. In both materials the carbon to oxygen ratio indicates the presence of considerable quantities of oxygen functional groups.

Publication Date: January 1, 1966 | doi: 10.1021/ba-1966-0055.ch002

Table I. Elemental Composition of Kerogen and Trona Acids

	Weight Percent[1]	
	Kerogen	*Trona Acids*
C	77.7	75.7
H	10.1	9.8
N	2.6	1.9
S	1.1	1.6
O[2]	8.5	11.0
Total	100.0	100.0
	Atomic Ratio	
H/C	1.56	1.56
C/N	34.8	46.4
C/S	190.4	126.2
C/O	12.2	9.2

[1] Mineral free basis
[2] Determined by difference

Figure 1 shows x-ray scattering intensities per carbon atom of the kerogen and trona acid samples. These materials have nearly identical peaks, indicating the presence of similar structures. Similarly, the infrared spectra of kerogen and trona acids (Figure 2) show a structural correlation between the two materials. Particularly significant are the similarities in absorbance in the 3.4 micron region attributed to the C-H aliphatic stretch; the 5.83 micron region attributed to the C=O stretching vibration; the 6.85 micron region attributed

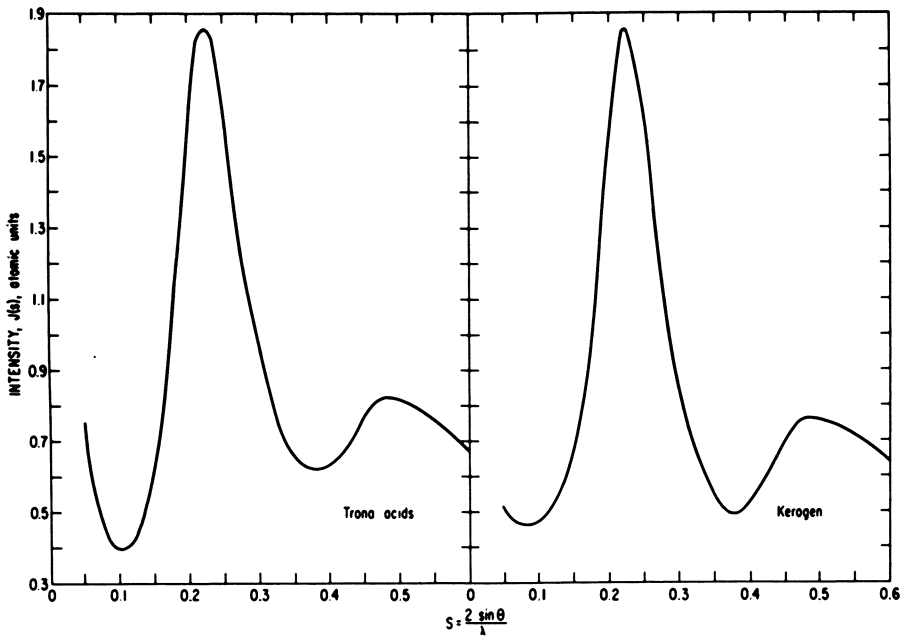

Figure 1. X-ray scattering intensities per carbon atom of trona acids and kerogen from Green River oil shale

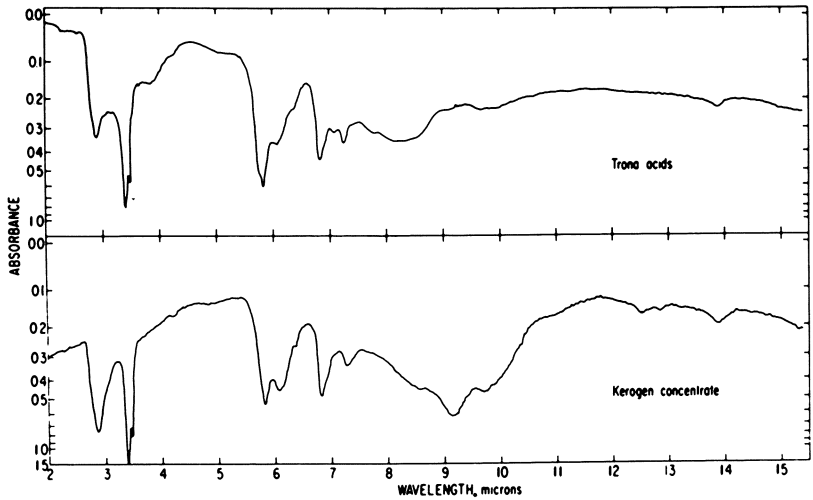

Figure 2. Infrared spectra of trona acids and kerogen concentrate

to aliphatic C-H deformation vibrations; the 7.25 micron region which is associated with the presence of CH_3 groups. The strong absorption of the kerogen sample in the 9-10 micron region is probably caused by the silicate minerals which are still present. Because absorption in the 2.85 micron region is normally observed for all potassium bromide pellets, no significance is attached to the presence of this peak in the spectra.

The results of the calcium exchange method using steam distillation for determining the carboxyl function are shown in Table II. Triplicate determinations were in good agreement and accounted for 15.8% of the kerogen oxygen and 38.9% of the trona acids as carboxyl oxygen. To test the agreement between the amount of acetic acid liberated and the amount of calcium added,

Table II. Carboxyl Content of Kerogen and Trona Acids

	Based on Amount of Acetic Acid Formed		*Based on Amount of Calcium Exchanged*	
	Meq. COOH per gram	*Percent of total oxygen*	*Meq. COOH per gram*	*Percent of total oxygen*
Kerogen[1]	0.41	15.3	0.41	15.3
	0.43	16.2	0.40	15.1
	0.42	15.8	0.40	15.1
Average	0.42	15.8	0.40	15.2
Trona acids	1.34	39.1	1.36	40.0
	1.32	38.2	1.32	38.2
	1.35	39.5	1.34	39.1
Average	1.34	38.9	1.34	39.1

[1] Mineral free basis

Publication Date: January 1, 1966 | doi: 10.1021/ba-1966-0055.ch002

the amount of calcium in the exchanged product was determined. The results of these determinations, calculated on the basis of two carboxyl groups per atom of calcium, also are shown in Table II. These results also agreed closely and accounted for 15.2% of the kerogen oxygen and 39.1% of the trona acid oxygen as carboxyl oxygen.

The results of the ester determinations are shown in Table III. The calcium-exchanged kerogen before hydrolysis contained an equivalent of 8.4 mg. of calcium per gram of sample. After hydrolysis the exchanged kerogen contained 21.5 mg. of calcium per gram of sample. This increase of 13.1 mg. of calcium was equal to the hydrolysis of 0.65 meq. of ester groups per gram of sample and represented 24.7% of the total kerogen oxygen. Similarly, the increase in the calcium exchange owing to hydrolysis of the trona acids was

Table III. Ester Content of Kerogen and Trona Acids Based on Hydrolysis and Calcium Exchange

	Calcium, mg. per gram		*Ester Content*[1]	
	Before hydrolysis	*After hydrolysis*	*Meq. ester per gram*	*Percent of total oxygen*
Kerogen [2]	8.4	22.1	0.68	25.9
	8.4	21.0	0.63	23.5
	8.4	21.5	0.65	24.7
Average	8.4	21.5	0.65	24.7
Trona acids	27.3	41.9	0.73	20.9
	26.4	41.3	0.75	21.8
	26.7	41.6	0.75	21.8
Average	26.8	41.6	0.74	21.5

[1] Calculations based upon two ester groups per calcium atom
[2] Mineral free basis

equal to the hydrolysis of 0.74 meq. of ester groups per gram of sample and represented 21.5% of the total trona acid oxygen. Infrared spectra (Figure 3) of the kerogen concentrate, trona acids, and salts of the treated materials show the relative changes in the 5.5–6.5 micron region with a particular treatment. Spectra A and B are of the starting materials. Spectra C and D show a decrease in absorption in the 5.8 micron region and a corresponding increase in absorption in the 6.3 region caused by calcium exchange and formation of the carboxylate ion. Spectra E and F show additional shifts of absorption to the 6.3 micron region attributed to hydrolysis of ester groups to acid groups and formation of additional carboxylate ion by the exchange with calcium. Spectra E and F show remaining absorption in the 5.8 micron region. Reducing aldehyde and ketone groups with sodium borohydride showed no major decrease in the intensity of the 5.8 micron band. This indicates that groupings other than carbonyl groups may account for some of the absorption in the 5.8 micron region.

The results of the amide determination are shown in Table IV. Hydrolysis of the kerogen produced ammonia equal to 0.052 mg. equivalents of amide

Publication Date: January 1, 1966 | doi: 10.1021/ba-1966-0055.ch002

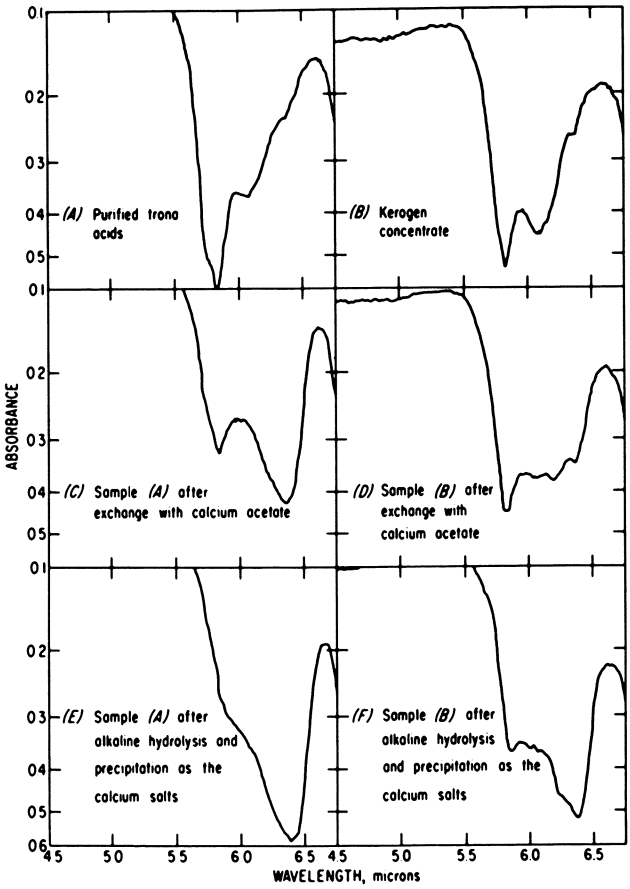

Figure 3. Infrared spectra in the 5.5–6.5 micron region of trona acids and kerogen concentrates and derivatives of these materials

Table IV. Amide Content of Kerogen and Trona Acids

	Meq. amide per gram	*Percent of total oxygen*
Kerogen[1]	0.043	0.5
	0.059	0.7
Average	0.052	0.6
Trona acids	<0.001	<0.1
	<0.001	<0.1
Average	<0.001	<0.1

[1] Mineral free basis

per gram of sample. This amount of amide function is equivalent to 0.6% of the total oxygen. There was no evidence of ammonia evolution from hydrolysis of the trona acids, nor was there any evidence that substituted amides were present in either sample.

Results obtained from the hydroxylamine reaction of carbonyl groups (ketone and aldehyde) are shown in Table V. About 1.2% of the kerogen oxygen and 5.0% of the trona acid oxygen appear to be present as ketone and aldehyde oxygen.

Table V. Aldehyde and Ketone Content of Kerogen and Trona Acids

	Meq. C=O per gram	*Percent of total oxygen*
Kerogen[1]	0.2	1.2
	0.2	1.2
	—	—
Average	0.2	1.2
Trona acids	0.3	4.5
	0.4	5.5
	—	—
Average	0.35	5.0

[1] Mineral free basis

Table VI. Hydroxyl Content of Kerogen and Trona Acids

	Meq. OH per gram	*Percent of total oxygen*
Kerogen[1]	0.2	3.5
	0.3	5.9
	—	—
Average	0.25	4.7
Trona acids	0.1	1.8
	0.1	1.8
	—	—
Average	0.1	1.8

[1] Mineral free basis

Table VII. Distribution of Total Oxygen in Functional Groups, %

	Kerogen	*Trona Acids*
Carboxyl oxygen	15.3	39.1
Ester oxygen	24.7	21.5
Amide oxygen	0.6	0.0
Carbonyl oxygen (aldehyde and ketone)	1.2	5.0
Hydroxyl oxygen	4.7	1.8
Ether oxygen[1]	53.5	32.6
Total	100.0	100.0

[1] By difference

Results of the acetylation test on kerogen and trona acids (Table VI) indicated the presence of 4.7% of the kerogen oxygen and 1.8% of the trona acid oxygen as hydroxyl groups.

A summary of the oxygen functional group determinations are shown in Table VII. Approximately 94% of the kerogen oxygen and 93% of the trona acid oxygen were accounted for as carboxyl, ester, and unreactive oxygen. The remaining oxygen in each sample was indicated to be present as hydroxyl, aldehyde, ketone, and amide groups.

Acknowledgments

The authors wish to thank Sabri Ergun and W. F. Donaldson of the Solid State Physics group at the Bureau of Mines Pittsburgh Coal Research Center for their special assistance in obtaining the x-ray scattering intensities of the samples. We also wish to thank Glenn L. Cook of the Laramie Petroleum Research Center for interpreting the infrared spectra.

Literature Cited

(1) Blom, L., Edelhausen, Van Krevelen, D. W., *Fuel* **36,** 135 (1957).
(2) Bureau of Mines, *U.S. Bur. Mines Rept. Invest.* **4652,** 49 (1949).
(3) Fester, J. I., Robinson, W. E., *Anal. Chem.* **36,** 1392 (1964).
(4) Fuchs, W., *Fuel* **22,** 112 (1943).
(5) Hubbard, Arnold B., Fester, John I., *Chem. Eng. Data* **3,** 147 (1958).
(6) Kaverzneva, E. D., Salova, A. S., *Izv. Akad. Nauk* SSSR, *Otdl. Khim. Nauk* **6,** 782 (1951).
(7) Robinson, W. E., Cummins, J. J., *Chem. Eng. Data* **5,** 74 (1960).
(8) Smith, J. W., Higby, L. Warren, *Anal. Chem.* **32,** 1718 (1960).

RECEIVED October 5, 1964.

Publication Date: January 1, 1966 | doi: 10.1021/ba-1966-0055.ch002

Discussion

Irving Wender: What is the origin of the term trona acids?

John I. Fester: The organic acids that occur in a sodium carbonate-sodium bicarbonate brine are referred to as trona brine in wells drilled in the Green River formation in western Wyoming. Hence the name trona acids.

Dr. Wender: Has the number of double bonds in kerogen or in trona acids been determined?

Dr. Fester: Brower and Graham reported the presence of one double bond in Green River oil-shale kerogen for each 16–22 carbon atoms, (*Ind. Eng. Chem.* **50,** 1059 (1958)).

Kulai A. Kini: I am surprised at the absence of phenolic hydroxyl in kerogen. What method was used to estimate phenolic groups?

Dr. Fester: The acetylation method used would include phenolic hydroxyl. However, the total hydroxyl for kerogen was less than 5% of the total oxygen and less than 2% for trona acids. If present, phenolic hydroxyl would represent only a small part of the total oxygen.

Keith A. Kvenvolden: How do the isoprenoids vary with depth, and what new thoughts do you have concerning the reasons for these variations?

Dr. Fester: The ratio of the C_{20} isoprenoid paraffin to the total isoprenoid paraffins decreased with depth of burial while the ratio of each of the C_{15}, C_{16}, C_{18}, and C_{19} isoprenoids to the total isoprenoid paraffins tended to increase with depth of burial. These variations may be caused by a combination of several factors, one important factor being environmental conditions of the lake at the time of deposition.

Robert B. Anderson: Can you comment on Brook's postulate that alkaline environment leads to oil shale formation?

Dr. Fester: Only to say that most oil shales, including Green River oil shale, were deposited in a slightly alkaline environment.

Publication Date: January 1, 1966 | doi: 10.1021/ba-1966-0055.ch002

3

Similar Compositions of Alkanes from Coal, Petroleum, Natural Gas, and Fischer-Tropsch Product

R. A. FRIEDEL and A. G. SHARKEY, JR.

Bureau of Mines, U.S. Department of the Interior, Pittsburgh Coal Research Center, Pittsburgh, Pa.

Publication Date: January 1, 1966 | doi: 10.1021/ba-1966-0055.ch003

Possible interrelationships of natural substances are important. Similarities of the low molecular weight alkane isomers from crude oil and Fischer-Tropsch synthesis product have been reported. A similar composition for high temperature coal carbonization has been found. The C_4 to C_7 alkane isomers from these sources can be calculated quantitatively with equations developed for Fischer-Tropsch products. A reversal of the concentrations of the monomethyl isomers from C_6 (2 Me > 3 Me) to C_7 (3 Me > 2 Me) occurs in all three products; comparisons at higher carbon numbers indicate some dissimilarities. Naphthene isomers for crude oil and high temperature coal carbonization also have similar compositions. Aliphatic hydrocarbons from low temperature coal processes are considerably different. The C^{13} isotopic composition of pure compounds from the various sources are being compared in order to provide information on their origin.

A similarity between the low molecular weight alkane isomers in crude oil and Fischer-Tropsch catalytic synthesis products has been reported previously (*8*), along with a discussion of the possible significance for the origin of petroleum. It was shown that the composition of the C_4–C_7 alkane isomers in crude oils (*13*) can be calculated quantitatively with equations previously reported for calculating the alkane isomers in Fischer-Tropsch products (*1*, *6*, *21*). The equation for calculating isomer distribution is $\theta_n = kF_n\, a^{n-2}$, where θ_n is the number of moles containing n carbon atoms, k is a constant, and F_n is a function of f, a constant representing the ratio of chain branching, b, over

In Coal Science; Given, P.;
Advances in Chemistry; American Chemical Society: Washington, DC, 1966.

chain lengthening, a. If $b = af$, the lengthening and branching of chains is illustrated as follows:

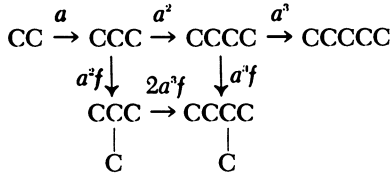

Isomeric Compositions

Crude Oils. Part a of Table I compares branched alkanes observed in Fischer-Tropsch products with those observed in a representative crude oil. Part b predicts Fischer-Tropsch product along with the relative concentrations of isomers in terms of a and f, and part c predicts crude oil compositions. In this last portion of Table I comparisons are given for branched isomers for $f = 0.176$. The comparison of observed and predicted normal C_6 and C_7 is not very similar with $f = 0.176$; however, as noted in the footnote, a change of f value to 0.1 produces a very close comparison for the normal compounds.

One of the interesting points concerning the prediction of crude oil and Fischer-Tropsch compositions is the quantitative success in predicting reversal of methyl isomers. In the C_6's the concentration of 2-methylpentane is found to be greater than that of 3-methylpentane, whereas in the C_7's the situation is reversed as 3-methylhexane becomes greater than 2-methylhexane.

The growth scheme used in this work is a modification of growth scheme B from Anderson *et al.* (*1*): Addition of the carbon atom is permitted on the first two carbon atoms on one end of the growing chain and on substituents on the first three carbon atoms. Results are not very different if branching is allowed on the first three carbon atoms of a chain (*8*). The chain branching factor is f, as usual, except in the formation of quaternary carbons in which case 0.1 f is used because of the low probability of substitution on tertiary carbon atoms.

There are very few data available on alkane isomers above C_7 for comparison of petroleum or any other natural product. Some analyses, however, are available for the C_8 isomers from alkanes from crude oils. Predicted results from the Fischer-Tropsch equation with $f = 0.1$ are given in Table II along with analyses of C_8 alkanes from two crude oils (*2*, *4*). A very definite exception to the predicted values appears in Table I, namely, the predominance of 2-methylheptane over 3-methylheptane. This observation is contrary to the prediction of the equation. According to scheme B (*1*) other C_8 analyses from crudes made available to the author by M. J. O'Neal show the same predominance of the 2-methyl isomers. A total of four C_8 analyses available for comparison represent crudes from western and southwestern United States. As mentioned in (*8*), 11 out of 14 analyses through the C_7's showed the reversal; the three that did not have the predicted reversal also came from the Southwest. It would be of interest to have analyses of C_8's in crudes from other parts of the world in order to study this reversal. For C_9 alkanes only partial analyses are available; they are Ponca City, Okla. crude (*4*) and a commercial mixture

Publication Date: January 1, 1966 | doi: 10.1021/ba-1966-0055.ch003

Table I. Alkane Compositions: Crude Oil and

a. C_6-C_7 branched alkanes observed in crude oil and F.T.

	Crude No. 1	*F.T.*
n-Butane		
2-Methylpropane		
n-Pentane		
2-Methylbutane		
2,2-Dimethylpropane		
n-Hexane	53.9	53.1
2-Methylpentane	38.8	45.0
3-Methylpentane	6.7	1.9
2,3-Dimethylbutane	0.6	—
2,2-Dimethylbutane	—	—
n-Heptane		
2-Methylhexane	35.6	38.4
3-Methylhexane	45.6	56.0
2,3-Dimethylpentane	11.7	4.7
2,4-Dimethylpentane	3.2	0.0
3-Ethylpentane	2.5	—
2,2-Dimethylpentane	0.7	—
3,3-Dimethylpentane	0.5	—
2,2,3-Trimethylbutane	0.2	—
n-Octane		
Methylheptanes		
Dimethylhexanes		

[a] Total branched isomers

[b] For $f = 0.10$, calculated and observed values are: nC_7—56.1 (calc.), 56.4 (obs.); $isoC_7$'s—43.9 (calc.), 43.6 (obs.).

of predominantly straight run material (5). Both of these partial analyses indicate that the reversal recurs and the 3-methyl isomer again predominates. It will be of interest to see what happens in the case of future analyses of C_9 alkanes. Perhaps there is an alternation of predominance of the 2-methyl isomer; perhaps it occurs only for the even carbon numbers (see discussion on tobacco waxes below).

The evidence for an organic origin, or principally organic origin, of petroleum is very strong. Nevertheless, the predictions of the Fischer-Tropsch equation appear to have some significance whether or not an inorganic origin is indicated. The prediction of the equation may indicate the kind of branching that occurs in organic syntheses by living species to form the precursors of

Publication Date: January 1, 1966 | doi: 10.1021/ba-1966-0055.ch003

Fischer-Tropsch Product (F.T.), Mole Percent[c]

b. Predicted and observed isomer distribution in F.T.			*c. Predicted and observed isomer distribution in crude oil, using modified F.T. equations*			
Observed	*Predicted, f = 0.0727*		*Observed, No. 1*		*Predicted, f = 0.176*	
89.4	93.2	a^2	87.4		84.8	
10.6	6.8	a^2f	12.6		15.2	
81.2	82.1	a^3	65.8		65.3	
18.8	17.9	$3a^3f$	33.8		34.5	
			0.4		0.2	
78.8	73.2	a^4	56.6		49.6	
11.2	15.9	$3a^4f$		53.9		52.0
9.5	10.5	$2a^4f$		38.8		40.7
0.4	0.4	$2a^4f^2$		6.7		6.1
				0.6		1.2
			[a]43.4	100.0	[a]50.4	100.0
			100.0		100.0	
66.0	64.6	a^5	56.4		[b]37.7	
13.1	14.0	$3a^5f$		35.6		31.9
19.1	18.7	$4a^5f$		45.6		46.3
1.6	2.0	$6a^5f^2$		11.7		11.9
0.3	0.7	$2a^5f^2$		3.2		3.8
				2.5		4.4
				0.7		0.7
				0.5		0.8
				0.2		0.2
			[a]43.6	100.0	[a]62.3	100.0
			100.0		100.0	
61.0	57.1	a^6				
36.4	37.4	$9a^6f$				
2.6	5.4	$18a^6f^2$				

[c] Data from Friedel and Sharkey (*8*).

petroleum alkanes. A *quantitative* prediction results from the Fischer-Tropsch equation, and it is the only one available at the present time.

Fischer-Tropsch and Crude Oil. Other similarities between crude oil and Fischer-Tropsch products should be mentioned. First, polynuclear condensed aromatics are produced in syntheses involving catalytic hydrogenation of carbon monoxide as shown in the Fischer-Tropsch work of Weitkamp (*3*). The catalysis group in our laboratory attempted catalytic hydrogenations at elevated temperatures and found production of considerable amounts of aromatics as large as pyrene. This evidence is cited to indicate that the aromatics in petroleum could possibly be derived from catalytic syntheses of the Fischer-Tropsch type. Another similarity has been shown by the product obtained from

Publication Date: January 1, 1966 | doi: 10.1021/ba-1966-0055.ch003

Table II. Predicted Composition of Octane Isomers Compared with Values Observed in Two Crude Oils, Mole Percent

C_8 Alkanes	Crude Oils		Predicted, $f = 0.1$
	East Texas (2)	Ponca City (4)	
n-Octane	44.7	51.35	45.5
2-Methylheptane	23.3	19.21	13.7
3-Methylheptane	12.9	11.16*	19.1
4-Methylheptane	5.1	5.58	9.1
2,3-Dimethylhexane	3.5	3.12	2.7
2,4-Dimethylhexane	2.3	2.23	2.8
2,5-Dimethylhexane	2.2	1.56	0.9
3,4-Dimethylhexane	2.0	2.23	2.0
2,3,4-Trimethylpentane	1.1	0.04	0.18
3-Ethylhexane	1.7	*	2.90
2-Methyl-3-ethylpentane	0.9	2.46	0.48
2,2-Dimethylhexane	0.5	0.22	0.18
3,3-Dimethylhexane	0.6	0.67	0.30
2,2,3-Trimethylpentane	—	0.04	0.04
2,2,4-Trimethylpentane	—	0.09	0.03
3-Methyl-3-ethylpentane	—	—	0.03
2,3,3-Trimethylpentane	0.6	0.04	0.05
2,2,3,3-Tetramethylbutane	—	—	0.0001

* 3-Methylheptane + 3-Ethylhexane

catalysts used for many months in the Sasol commercial Fischer-Tropsch plant in South Africa. The spectral characteristics of this product were similar to those obtained for petroleum asphaltenes.

Coal Derivatives. In attempting to extend this investigation to coal products, it was evident that not many isomeric analyses have been carried out. In the case of low temperature tar the predominant species reported have been normal olefins and normal alkanes. Branched alkane isomers are probably very low in concentration. However, limited data for high temperature coal tar (*10*) and for coal hydrogenation products (*7*, *12*) indicate a close comparison of C_7 alkanes with those from crude oil and the values predicted by the Fischer-Tropsch equation (Table III, top). A close comparison is notable also in the bottom part of Table III, which gives data for the C_6 and C_7 naphthenes from high temperature coal carbonization, coal hydrogenation, and a crude oil.

The data recently published by Ouchi and Imuta (*15*) on a chloroform extract of Yubari coal also indicates similarities to petroleum. Branching is greater at the low carbon numbers and drops off at higher carbon numbers as in crudes (*11*) and Fischer-Tropsch product (*17*). The other similarity to crude oil is noted in the odd-even alternation of normal alkanes from C_{19} to C_{25} with the odd carbon number alkanes predominating.

Other data on analyses of coal products have been given by Girling (*9*). A list of alkanes found, but not quantitatively determined, from C_3 through C_7, indicates that the normals and monomethyl isomers predominate. This again is similar to crude oil and Fischer-Tropsch product.

At this stage the comparisons of the analyses are considered interesting but too sparse to draw any conclusions concerning relationships between petroleum and coal.

Publication Date: January 1, 1966 | doi: 10.1021/ba-1966-0055.ch003

Natural Gas. A search has also been made for data on alkane isomers from natural gas. So far the search has been very unsuccessful. Only one isomeric analysis has been found. This was provided by Duane Kniebes of the Institute of Gas Technology and is shown in Table IV. Comparison of natural gas data with those found in crude oil and in predictions of the Fischer-Tropsch equation is not very good, particularly in the C_7's. It is hoped that better data will be forthcoming both from natural gas and from coal. In the search for natural gas data, at least one company contacted has decided that its research department should obtain isomeric data on many natural gases.

Pyrolysis. Many good analytical data are being turned out by tobacco company research laboratories for cigarette smoke and for constituents of tobacco leaves. A recent article on analyses of cigarette smoke by Phillipe *et al.* (*16*) demonstrated that the normal and monomethyl isomers in C_5 and C_6 alkanes were very similar to those obtained from thermal cracking of petroleum. These are data on only a few compounds and no dimethyl isomers were found. It is perhaps not surprising that a slight similarity exists since petroleum compounds in high molecular weight ranges are primarily straight chained, apparently branched only on one end. In fact some researchers have found that the waxes from tobacco have similar structures (*14*). Also, the 2-methyl and 3-methyl isomers predominate alternately.

Thermal cracking of higher components of crude oils can produce low molecular weight alkanes having isomeric compositions similar to the alkanes found in crudes.

Table III. Alkane and Naphthene Compositions: Crude Oil and Coal Derivatives, Mole Percent

Alkanes	*Predicted, F.-T. equation $f = 0.1$*	*Crude No. 1 (13)*	*Coal, high temp. carb. (10)*	*Coal, hydrogenation (7, 12)*
n-Heptane	54.6	56.5	75.6	60
2-Methylhexane	16.4	15.5	14.6	
3-Methylhexane	22.9	19.9	15.2	
2,3-Dimethylpentane	3.4	5.1	9.1	
2,4-Dimethylpentane	1.1	1.4	—	40
3-Ethylpentane	1.2	1.1	3.0	
2,2-Dimethylpentane	0.2	0.2	—	
3,3-Dimethylpentane	0.2	0.2	0.5	
2,2,3-Trimethylbutane	0.03	0.1	—	
Naphthenes				
Cyclohexane		41.4	90.5	28.6
Methylcyclopentane		58.6	9.5	71.4
		100.0	100.0	100.0
Methylcyclohexane		58.5	64.4	35.6
1-1-Dimethylcyclopentane		1.8	2.0	
1-*trans*-2-Dimethylcyclopentane		16.0	14.5	
1-*trans*-3-Dimethylcyclopentane		7.9	13.6	47.8
1-*cis*-2-Dimethylcyclopentane		—	5.5	
1-*cis*-3-Dimethylcyclopentane		7.9	—	
Ethylcyclopentane		7.9	—	16.6

Table IV. Isomeric Analysis of a Natural Gas Condensate*

	Natural Gas	*Crude No. 1*
n-Pentane	65.5	65.8
i-Pentane	35.5	33.8
2,2-Dimethylpropane	—	0.4
n-Hexane	37.5	56.7
2-Methylpentane	45.5	23.3
3-Methylpentane	15.8	16.8
2,3-Dimethylbutane	1.2	2.9
2,2-Dimethylbutane	—	0.3
n-Heptane	12.6	56.5
2-Methylhexane, 2,3-Dimethylpentane	17.8	20.6
3-Methylhexane	12.6	19.9
2,4-Dimethylpentane, 2,2-Dimethylpentane, 2,2,3-Trimethylbutane	23.6	1.7
3-Ethylpentane	19.3	1.1
3,3-Dimethylpentane	14.1	0.2
C_8 Isomers	present	present
Cylohexane	present	present
Benzene	present	present
Toluene	present	present

* Institute of Gas Technology

Carbon-13 Isotope Analyses

It is generally accepted that the lower alkanes in petroleum and in coal products are obtained from cleavage of bonds in higher components. On the other hand, the lower alkanes in crude oil may have originated from synthesis or from chemical reactions of nonhydrocarbons. In coal it is possible that the carbonaceous constituents may have small alkanes adsorbed on them and that these are desorbed at elevated temperatures. In this case scission of bonds would not be involved. It seems important then to attempt to find out whether or not low molecular weight alkanes are really derived from high molecular weight molecules by decomposition processes. One possible way of approaching this problem is to study the content of carbon-13 isotopes in nature. This figure is taken to be 1.1%, and from isotopic work on petroleum it is known that in nature this value varies in small but measurable amounts (*18*). All such measurements have been for the purpose of making total carbon-13 isotopic determinations in a compound with one exception. The work of Stevenson (*19, 20*) and co-workers on small molecules has made it possible to determine the isotopic content of various carbon atoms in these molecules. Calculations involved for other than small molecules appear to be prohibitively complex. The problem has been approached empirically; a standard has been used which is known to be a molecule not derived from any bond scission, namely, *n*-hexane from Fischer-Tropsch synthesis. Fischer-Tropsch products provide the only source of molecules that could not have been formed by decomposition. Any other hexane obtained from nature or from synthesis with smaller molecules may or may not have a history involving bond cleavage.

Publication Date: January 1, 1966 | doi: 10.1021/ba-1966-0055.ch003

Preliminary measurements have been made on Phillip's *n*-hexane, known to be derived from natural gas, and comparisons have been made with the Fischer-Tropsch standard, *n*-hexane. Both products were purified by Dr. B. D. Blaustein of the Pittsburgh Coal Research Center by means of gas chromatography. It is known from the work of Stevenson that breakage of a carbon-12-carbon-12 bond is more probable than breakage of a carbon-12-carbon-13 bond. This means that if the *n*-hexane from natural gas were formed by a bond

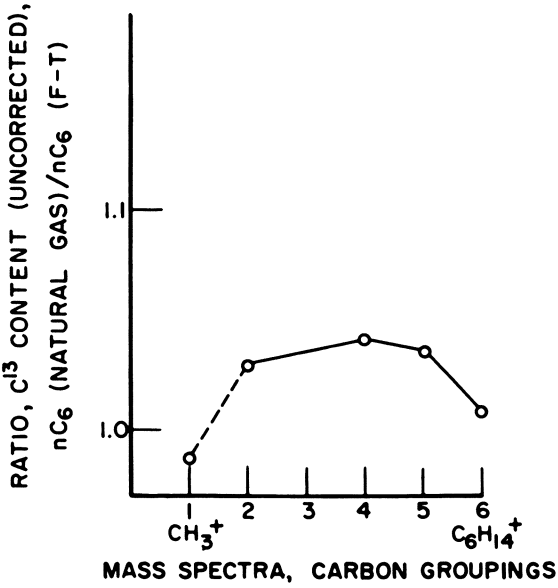

Figure 1. Ratio of carbon-13 contents from mass peaks of n-*hexane, from natural gas and from Fischer-Tropsch synthesis*

scission process, one or both of the end carbon atoms must be low in carbon-13 concentration. Both the standard and the natural gas *n*-hexane examined and the isotopes for CH_3, C_2H_5, etc. up to the molecular ion C_6H_{14} were compared. The results are indicated in Figure 1. As predicted for a decomposition product, the CH_3^+ and $C_6H_{14}^+$ ions, which heavily involve the terminal carbon atoms, show the lowest carbon-13 isotopic content. This result indicates that this *n*-hexane derived from natural gas is indeed a product of bond cleavage. These preliminary results will be expanded.

Literature Cited

(1) Anderson, R. B., Friedel, R. A., Storch, H. H., *J. Chem. Phys.* **19,** 313 (1951).
(2) Bell, M. F., *Anal. Chem.* **22,** 1005 (1950).
(3) Cady, W. E., Launer, P. J., Weitkamp, A. W., *Ind. Eng. Chem.* **45,** 350 (1963).
(4) Desty, D. H., Goldup, A., Swanton, W. T., Proc. 3rd Int'l Symposium on Gas Chromatography, **3,** 83 (1961).

Publication Date: January 1, 1966 | doi: 10.1021/ba-1966-0055.ch003

(5) Dorsey, J. A., Hunt, R. H., O'Neal, M. J., *Anal. Chem.* **35,** 511 (1963).
(6) Friedel, R. A., Anderson, R. B., *J. Am. Chem. Soc.* **72,** 1212 (1950).
(7) Friedel, R. A., Logar, A. F. Jr., Shultz, J. L., *Appl. Spectroscopy* **6,** 24 (1952).
(8) Friedel, R. A., Sharkey, A. G. Jr., *Science* **139,** 1203 (1963).
(9) Girling, G. W., *J. Appl. Chem.* **13,** 77 (1963).
(10) Glick, C. F., Miskalis, A. J., Kessler, T., *Anal. Chem.* **34,** 1692 (1962).
(11) Hood, A., "Mass Spectrometry of Organic Ions," p. 597, ed. F. W. McLafferty, Academic Press, New York, 1963.
(12) Kaplan, E. H., Storch, H. H., Orchin, M., *U.S. Bur. Mines Tech. Paper* **690,** 1946.
(13) Martin, R. C., Winters, J. C., *Anal. Chem.* **31,** 1954 (1959).
(14) Mold, J. D., Stevens, R. K., Means, R. E., Ruth, J. M., *Biochem.* **2,** 605 (1963).
(15) Ouchi, K., Imuta, K., *Fuel* **42,** 445 (1963).
(16) Philippe, R. J., Moore, H., Honeycutt, R. G., Ruth, J. M., *Anal. Chem.* **36,** 859 (1964).
(17) Sharkey, A. G. Jr., Shultz, J. L., Friedel, R. A., *Anal. Chem.* **34,** 826 (1962).
(18) Silverman, S. R., Epstein, S., *Bull. Am. Assoc. Petrol. Geologists* **42,** 998 (1958).
(19) Stevenson, D. P., *J. Chem. Phys.* **19,** 17 (1950).
(20) Stevenson, D. P., Wagner, C. D., Beech, O., Otvos, J. W., *J. Chem. Phys.* **16,** 993 (1948).
(21) Weller, Sol, Friedel, R. A., *J. Chem. Phys.* **18,** 157 (1950).

RECEIVED October 5, 1964.

Discussion

Irving Wender. It is interesting in connection with this paper to note that optical activity in low temperature tar first occurs in fractions boiling at about 122°C. (*4*). While only petroleum fractions boiling over 200°C. are optically active (*1*), a recent paper has revealed that catalytic reforming of petroleum results in the formation of optically active fractions that boil below 200°C. But again, only fractions boiling over 122°C. are optically active (*3*). It would be intriguing to know if the optically active substances in the low boiling fractions from coal and petroleum have similar structures. Examining the lowest boiling optically active fraction would extend the Friedel and Sharkey study by one or two carbon numbers to the C_8 and C_9 hydrocarbons; it is probable that naphthenic structures in these fractions are responsible for the rotation of polarized light.

Robert A. Friedel. It would be interesting to carry out the work suggested by Dr. Wender. Type analyses of C_8 naphthenes from a coal hydrogenation product have been reported (*2*); the types analyzed include ethylcyclohexane, propylcyclopentanes, dimethylcyclohexanes, *gem*-trimethylcyclopentanes, other trimethylcyclopentanes, and methyl-ethylcyclopentanes. Some compounds in these classes could be optically active. Comparable analyses of catalytically reformed petroleum would be of considerable interest in trying to ascertain what optically active components are produced in the reforming.

It is interesting to speculate on possible reasons for the lack of optical activity in the low molecular weight components of crude oils. Dr. Wender and

I have discussed this point. One possible explanation is that these components have abiogenic origins; Fischer-Tropsch products are also optically inactive. Of course the optically active constituents at higher molecular weights could not have come from catalytic synthesis. Another possible explanation is that racemization may have occurred over long periods. But this is not a completely satisfactory answer either. Although low molecular weight components racemize somewhat more rapidly than high molecular weight substances, it is peculiar to observe the tremendous differences found in petroleum—namely, zero activity below b.p. 200°C. and high activity for high boiling fractions.

Robert J. Rosscup. Are the isomers of carbon numbers 6 and 7 near thermodynamic equilibria, or present at compound ratios, i.e.—$\frac{n\ C_7}{\text{2-Me Hexane}}$ near equilibrium, at the temperature of the Fischer-Tropsch reaction? Also will this catalyst system isomerize paraffins?

Dr. Friedel. No. The Fischer-Tropsch synthesis is not an equilibrium process. Thermodynamic equilibrium would predict products with much more extensive branching than is found to occur at Fischer-Tropsch synthesis temperatures.

Concerning isomerization I would like to refer the question to Dr. R. B. Anderson.

Robert B. Anderson. Iron catalysts apparently do not isomerize hydrocarbons; however, there is little experimental evidence besides the products of the Fischer-Tropsch synthesis. In hydrocracking of paraffins on nickel and cobalt catalysts the isomerization does not occur.

Dr. Rosscup. If the formation of hydrocarbons is kinetically rather than thermodynamically controlled, does this suggest that the crude oil was formed at a temperature near that of the Fischer-Tropsch reaction?

Dr. Friedel. Possibly, although only partial formation of crude oil would be possible through synthesis. Constituents such as porphyrins would decompose at synthesis temperatures.

Dr. Anderson. Part of the hydrocarbons in petroleum could have been formed by a Fischer-Tropsch type reaction at say 200°C., at a different place from that in which the petroleum, which contains porphyrins and other thermally labile compounds, is currently found. The broadest interpretation of the similarity between isomers in petroleum and in the Fischer-Tropsch synthesis is that this result suggests that petroleum is produced by radical reactions rather than carbonium ion mechanisms.

Milton Denekas. The implication of the relation of crude oil composition to a Fischer-Tropsch product is that oil has been produced by a synthetic process (building-up) rather than by a degradative process. Can you assume that the products from coal pyrolysis are also produced by a synthetic building-up) process rather than by degradation?

Dr. Friedel. No. Products of the pyrolysis of coal under high temperature carbonization conditions surely must arise from degradation. The quantitative prediction of C_7 alkane isomers from coal may possibly indicate a relationship in compositions of coal and petroleum. The hydrocarbons from each perhaps should be similar since both are supposedly derived from organic plants;

Publication Date: January 1, 1966 | doi: 10.1021/ba-1966-0055.ch003

photosynthesis might have produced similar chain branching in the precursors of both coal and petroleum.

Literature Cited

(1) Fenske, M. R. *et al.*, *Ind Eng. Chem.* **34,** 638 (1942).
(2) Friedel, R. A., Logar, A. F., Shultz, J. L., *Appl. Spectroscopy* **6,** No. 5, **24** (1952).
(3) Sattar-Zade, A. Dzh., Sattar-Zade, I. S., *Azerb. Neft. Khoz.* **42,** 37 (1963); C.A. **60,** 14302a (1964).
(4) Zahn, C., Langer, S. H., Blaustein, B. D., Wender, I., *Nature* **200,** 53 (1963).

Publication Date: January 1, 1966 | doi: 10.1021/ba-1966-0055.ch003

Ratios of Organic Carbon, Nitrogen, and Hydrogen in Recent Sediments

TADASHIRO KOYAMA

Water Research Laboratory, Faculty of Science, Nagoya University, Chikusa-ku, Nagoya, Japan

Publication Date: January 1, 1966 | doi: 10.1021/ba-1966-0055.ch004

The ratios of organic carbon, nitrogen, and hydrogen were determined in a core sample of recent sediments. The vertical distribution of the ratios in the core sample suggests that a relationship between microbiological decomposition rates of organic carbon, nitrogen, and hydrogen in sediments may be of the following order: Org. C < Org. N < Org. H. The decomposition processes of these components were also discussed. The composition of organic matter in sediments gradually changes into a form richer in carbon as a result of microbiological activity.

In nature, organic matter usually decomposes incompletely. Even on land, given proper conditions of aeration, humidity, and chemical composition, organic matter produced by higher plants rarely decomposes completely into its original materials such as carbon dioxide and water.

The decomposition of organic matter in lakes differs from that on land in the following ways:

(1) The chemical composition of the organic matter derived from lake plankton typically is considerably higher in proteins and fats than that derived from terrestrial vegetation.

(2) The availability of oxygen in the bottom water is reduced or is periodically absent.

Laboratory experiments on the decomposition of plankton under aerobic and anaerobic conditions showed that the mineralization of organic matter is practically halted under anaerobic conditions which prevail in the bottom sediments (*1*, *29*).

Experiments dealing with the decomposition of plankton and the regeneration of nutrients in vitro and under laboratory conditions have been performed. Von Brand and Rakestraw (*24*, *25*, *26*, *27*, *28*) reported the process

In Coal Science; Given, P.;
Advances in Chemistry; American Chemical Society: Washington, DC, 1966.

of decomposition and regeneration of nitrogenous organic matter in sea water, and Botan *et al.* (*1*) reported a mechanism for the aerobic decomposition of nitrogenous matter in fresh water under laboratory conditions.

Recently, observations in situ have been reported. Emery and Rittenberg (*2*) and Orr and Emery (*16*) found that the carbon content in California basin sediments decreases with depth while the C/N ratio increases with depth and that more nitrogen than carbon has been regenerated. Tanaka (*23*) noted the occurrence of hydroxylamine as one of the intermediate breakdown products of nitrogenous organic matter in a boundary between anoxic and oxic water layers in lake waters. Oana (*15*) found that denitrified nitrogen is produced in lake water. Kleerekoper (*5*) studied the mineralization of plankton in lake waters, and Saijo (*17*) reported chemical studies on the production and mineralization of plankton in lake waters. Takai *et al.* (*19, 20, 21, 22*) reported the microbial metabolism in paddy soils, and Koyama (*6, 7, 8, 9, 10*) studied the microbiological metabolism in lake sediments and paddy soils. Emery and Hoggan (*3*) studied gases in marine sediments. Motojima (*13*) and Maki (*12*) reported genetic studies on natural gas accumulation and the mineralization of peat.

The object of the present study was to measure the ratios of organic carbon, nitrogen, and hydrogen in the detritus sinking in lake water and in the sediments and to discuss the decomposition processes of these components in order to gain basic knowledge concerning the mechanism of coal formation.

Publication Date: January 1, 1966 | doi: 10.1021/ba-1966-0055.ch004

Method

Sampling. Water and sediments were sampled at the greatest depths of two mountain mesotrophic lakes in Nagano Prefecture, Lakes Kizaki-ko and Nakatsuna-ko. Sampling of the core sediments was made by using a core sampler devised by the author.

Chemical Analysis. Ammonia in the lake waters was analyzed by using pyridine-pyrazolone reagent (*11*); hydroxylamine by using the method of Endres and Kaufmann (*4*); nitrite by using Griess' reagent; nitrate by using copper sulfate, hydrazine sulfate, naphthylamine, and sulfanilic acid reagents (*14*); dissolved oxygen, nitrogen, argon, and methane by using the carbon dioxide method (*18*) modified by the author as well as by using gas-chromatography; total carbon dioxide by using the hydrogen method (*6*). The amount of denitrified nitrogen is calculated on the basis of N_2/Ar ratios of the gases dissolved in lake waters.

The bottom sediments were analyzed for gaseous components, using the author's method (*6*) and gas chromatography; for organic carbon (Org. C), using the wet combustion method modified by the author (*7*) as well as dry combustion method; for organic nitrogen (Org. N), using the Kjeldahl method modified by the author (*7*); for organic hydrogen (Org. H), using the dry combustion method.

The apparatus for determining organic carbon (Org. C) and hydrogen (Org. H) in sediments by the dry combustion method is similar to that of Pregl. It consists of the following three main parts as shown in Figure 1:

(1) A train of washing bottles: (B) containing concentrated H_2SO_4, U-type glass tube (C) charged with glass wool, combustion tube (D), absorption bottles for CO_2 containing NaOH drops (E) and for water containing

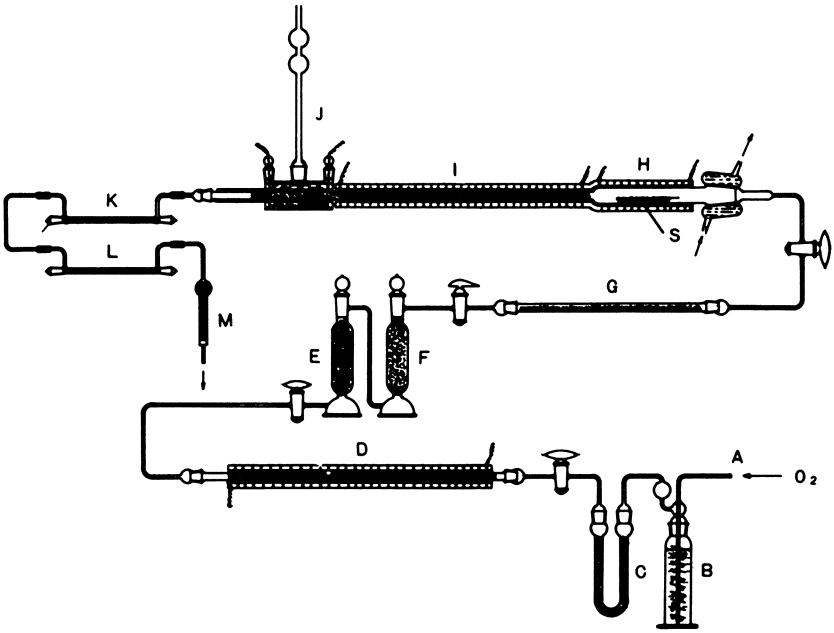

Figure 1. Apparatus for determining C and H in sediments

$CaCl_2$ (F), and absorption tube (G) for water containing P_2O_5. The train is for purifying oxygen.

(2) Main combustion tube of sample (I) similar to Pregl's.

(3) A train of absorption tubes: (K) for water and (L) for CO_2 produced from sample by combustion.

A wet sample of sediment is first dried at 110°C. and then finely ground. A quantity of the ground sample (0.1 gram) is taken in a small weighing bottle (Figure 2 d), and the bottle is put into a vessel of the apparatus for drying sediments (Figure 2 c) and then dried completely under the reduced pressure of 10^{-4} Hg. During this process, to facilitate the dryness, the vessel (c) is warmed to about 60°C. with hot water (e). After the sample has been dried completely, the amount of sample taken is weighed accurately. The sample is mixed well with 0.3 gram of ground $K_2Cr_2O_7$ in a boat (S) (Figure 1) and put into the vessel (c) in order to dry again. After the procedure, the boat is put into a part (H) of the combustion tube (I) (Figure 1), and the carbon and the hydrogen in sediments are determined according to Pregl's procedure. In this case, the measured amount of carbon gives the sum of organic carbon, free carbon, and carbonate carbon and that of hydrogen gives the sum of organic hydrogen and hydrogen of water of crystallization.

The free carbon and the hydrogen of water of crystallization are determined by the following procedure. A small quantity (0.3 gram) of the same sample is weighed in a beaker; 20 ml. of water and 10 ml. of hydrogen peroxide solution (30%) are added. The beaker is warmed in a boiling water bath to facilitate decomposition of organic matter. Every 30 minutes, 10 ml. of hydrogen peroxide solution are added (30 ml. of hydrogen peroxide solution are enough to decompose completely organic matter in sediments). The residue in the beaker is washed thoroughly with water and dried to 110°C. The free

Publication Date: January 1, 1966 | doi: 10.1021/ba-1966-0055.ch004

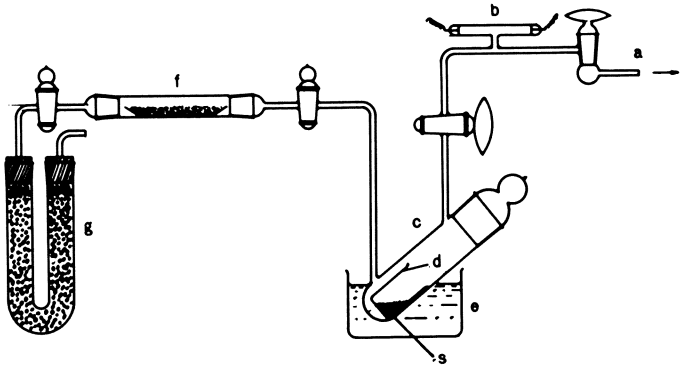

Figure 2. Apparatus for drying sediments

carbon and the hydrogen of water of crystallization in the residue are determined according to the same procedure mentioned above. Carbonate carbon is determined by using the author's method (*6*). Organic carbon (Org. C) and hydrogen (Org. H) in sediments are calculated from the results, assuming that the content of water of crystallization in the sediment is not affected by the treatment with hydrogen peroxide solution. The measured contents of organic carbon, organic hydrogen, and water of crystallization in the same sample did not fluctuate more than 5%.

Results and Discussion

Ratios of Organic Carbon and Nitrogen in Settling Detritus. The ratios of Org. C/Org. N of plankton, sediments collected at 25 meters in water, and surface bottom sediments in Lake Kizaki-ko are 5.7, 9.3, and 15.5, respectively (Table I).

Table I. Average Ratio Organic C/Organic N of Plankton, Detritus Settled at the 25-Meter Level and Surface Bottom Sediments in Lake Kizaki-ko

	Org. C/Org. N
Plankton	5.7[b]
Sediment at 25-meter level	9.3[b]
Surface bottom sediments	15.5

[a] Maximum depth = 28.5 meters
[b] After Saijo (*17*).

Similar relationships apparently occur in Lake Lauzon, Montcalm County, Quebec, Canada, reported by Kleerekoper (*5*) (Table II). Using Kleerekoper's data, Org. C was estimated, assuming that the ratios of Org. C/Loss on ignition of the samples are equal to the average ratio, 0.428, of the sediments from Lakes Kizaki-ko and Nakatsuna-ko in Nagano Prefecture, Japan. The variation in the ratios of Org. C/Org. N of plankton, sediments at 11-meter level, and surface bottom sediments is similar to that in Table I. The facts suggest that the organic nitrogen in plankton is subjected more intensively to

Publication Date: January 1, 1966 | doi: 10.1021/ba-1966-0055.ch004

microbiological decomposition processes than organic carbon in the course of sinking in lake water and also soon after settling on the bottom surface.

In order to clarify the mechanism of microbiological decomposition of organic carbon and nitrogen of detritus in the lake water, the gaseous and nitrogenous components as well as the other chemical characteristics were determined in Lake Kizaki-ko, September 7–8, 1963 and October 28–31, 1963 when stagnation had greatly advanced in the lake.

Table II. Average Chemical Composition of Plankton, Detritus Settled at the 11-Meter Level, and Surface Bottom Sediments, in Lake Lauzon, Montcalm County, Quebec[a, b]

Item	*Plankton average*	*Sediment at 11-Meter*		*Surface bottom sediments*
		July 2 to Aug. 7, 1950	*Sept. 25, 1950 to July 6, 1951*	
	%	%	%	%
Loss on ignition	94.3	52.6	59.7	57.8
Org. N	7.37	1.98	2.68	1.24
Loss on ignition / Org. N	12.8	26.6	22.3	46.6
Org. C[c] / Org. N	5.48	11.4	9.55	19.9

[a] Maximum depth = 27 meters

[b] Data from Kleerekoper (*5*) with addition by this author

[c] Org. C was estimated on the assumption that the ratio C/Loss on ignition of these samples is equal to the average ratio (0.428) of sediments from Lakes Kizaki-ko and Nakatsuna-ko.

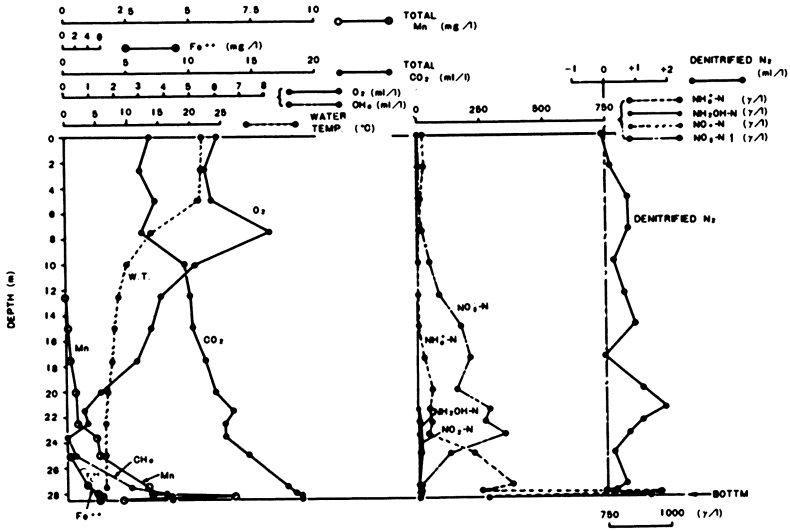

Figure 3. Vertical distribution of various components in Lake Kizaki-ko (Sept. 7–8, 1963)

In Organic Geochemistry; Eglinton, G., Murphy, M.T.J.;
Advances in Chemistry; American Chemical Society: Washington, DC, 1966.

Publication Date: January 1, 1966 | doi: 10.1021/ba-1966-0055.ch004

Figure 3 shows the chemical characteristics in the lake on September 7–8, 1963 and indicates that the dissolved oxygen decreases rapidly with depth and is completely absent in the water layers deeper than 23.5 meters. This results from consumption of oxygen by microorganisms in the hypolimnion by the end of summer stagnation. However, the total carbon dioxide increases remarkably with depth. The total Mn begins to appear in the water layer at 15 meters and increases with depth from 23.5 meters probably as a result of accumulation of Mn^{+2}. In contrast to Mn, Fe^{+2} does not yet appear at 23.5 meters; even dissolved oxygen has already disappeared while Fe^{+2} increases downwards in the water layers deeper than 23.5 meters. Concentration of NH_4^+-N increases with depth and amounts to 970 γ/liter in the water layer lying just over the bottom surface. The ammonium ions will be derived from particulate organic matter raining down into the stagnant bottom water and also from bottom sediments. The latter is probably the main source of the ammonium ions in the lake water. Concentration of NO_3^--N increases with depth to the uppermost layer of anoxic zone to a maximum of 342 γ/liter and then rapidly decreases almost to zero. NO_2^--N and NH_2OH-N first appear in the boundary layer between oxic and anoxic zone which corresponds to 22.5 meters, increase to a maximum at 25.0 meters, and then decrease until they disappear simultaneously. Denitrified nitrogen can be found at almost all depths, however; its highest concentration

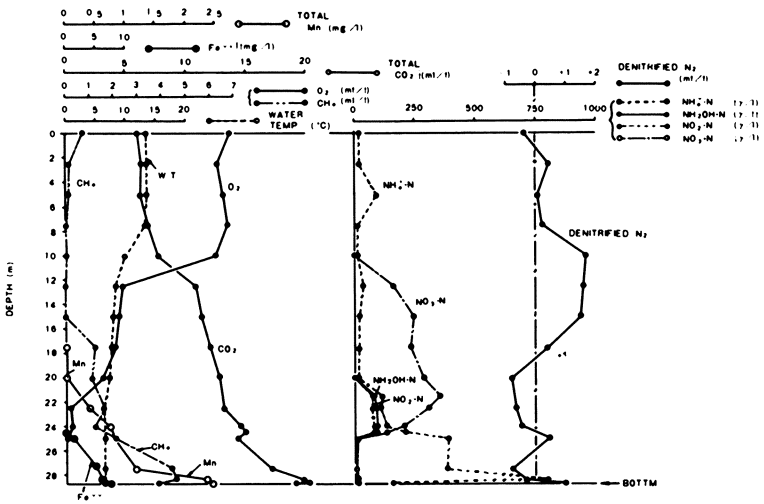

Figure 4. Vertical distribution of various components in Lake Kizaki-ko (Oct. 28–31, 1963)

of 1.86 ml./liter is observed in a water layer at 21.5 meters, in which 0.65 ml./liter of dissolved oxygen is present.

Figure 4 shows the chemical features of the lake on October 28–31, 1963. They differ from those on September 7–8 in the following ways:

(a) A peak of the vertical distribution of NO_3^--N is present in the water layer at 21.5 meters in which dissolved oxygen amounts to 1.47 ml./liter.

(b) NH_2OH-N and NO^{-}_2-N are present in the water layers at depths ranging from 21.5 to 24.5 meters, in which 0.22–1.47 ml./liter of oxygen dissolve, and they amount to about 90 and 80 γ/liter, respectively.

(c) A peak of denitrified nitrogen is found in the oxic zone at depths ranging from 10.0 to 15.0 meters, at which 2.21–6.23 ml./liter of oxygen are present.

(d) Traces of methane are found even in the surface water layers.

(e) Manganese begins to appear in the water layer at 17 meters and increases remarkably with depth from 22.5 meters, in which 0.22 ml./liter of oxygen are present.

All of these irregularities are probably induced by weak circulation of the lake water at mid-autumn.

Table III. Vertical Distribution of Mineralized C and N in Lake Kizaki-ko

September 7–8, 1963

Depth, meters	*Miner. C, mg./liter*	*Miner. N, mg./liter*
0.0	+0.14	—0.12
2.5	—0.30	+0.23
5.0	+0.28	+0.86
7.5	—0.28	+0.91
10.0	+1.61	+0.37
12.5	+1.83	+0.81
15.0	+1.90	+1.30
17.5	+2.43	+0.19
20.0	+2.87	+1.63
21.5	+3.53	+3.09
22.5	+3.27	+1.74
23.5	+3.27	+1.30
25.0	+4.46	+0.64
27.5	+7.29	+1.15
28.0	+8.32	+0.63
28.2	+8.74	+0.99
28.45	+8.75	+1.97

28.5 meters: Bottom

October 28–31, 1963

0.0	—0.29	—0.44
2.5	—0.13	+0.57
5.0	—0.16	+0.19
7.5	+0.19	+0.32
10.0	+0.67	+2.13
12.5	+2.31	+2.17
15.0	+2.55	+2.16
17.5	+2.95	+0.77
20.0	+3.34	—0.68
22.5	+3.55	—0.22
24.0	+4.30	—0.04
24.5	+4.52	—
25.0	+4.08	+0.99
27.5	+5.67	—0.57
28.4	+7.10	+0.46
28.65	+7.34	+1.59

28.7 meters: Bottom

From the vertical distributions of various components, the mineralized carbon (Miner. C) and nitrogen (Miner. N) at various depths were calculated according to the following equations:

$$\text{Miner. C (mg./liter)} = [(\text{Total } CO_2 - \text{Orig. } CO_2 + CH_4] \times 0.536$$
$$= [(\text{Total } CO_2 - 6.53) + CH_4] \times 0.536$$
$$\text{Miner. N (mg./liter)} = \text{Denitrified } N_2 \times 1.25 + (NH_4^+\text{-N} + NH_2OH\text{-N} + NO_2^-\text{-N} + NO_3^-\text{N}) \times 10^{-3}$$

Orig. CO_2: Amount of total carbon dioxide which was not affected by the activity of organisms after the thermal stratification had been established and thus existed originally. In this paper, the amount was assumed to be the average value of the total carbon dioxide in surface water layers which are almost saturated with air.

The calculated values are summarized in Table III. The amounts of total mineralized carbon and nitrogen in a vertical water column of Lake Kizaki-ko, with a sectional area of 100 sq. cm. and with the same depth as the lake's are as follows:

	Miner. C, mg.	*Miner. N, mg.*	$\frac{\textit{Miner. C}}{\textit{Miner. N}}$
Sept. 7–8, 1963	630	254	
Oct. 28–31, 1963	638	194	
Average	634	224	2.83

The fact that the average ratio of Miner. C/Miner. N (2.83) is considerably smaller than the ratio of Org. C/Org. N of plankton (5.7) indicates clearly that the organic nitrogen in plankton is more easily mineralized than the organic carbon by microbiological activities and also that the mineralization processes are active in the lake water. This fact may account for the relationship between the ratios of Org. C/Org. N of plankton, of detritus and of surface bottom sediments, which has been shown previously.

Table IV. Gaseous Components in Core Sample of Sediments from Lake Kizaki-ko[a]

Depth from the bottom surface	O_2	N_2	CH_4	H_2	CO_2
cm.	*ml/l.*	*ml/l.*	*ml/l.*	*ml/l.*	*ml/l.*
	March 1, 1952. Depth: 28.0 meters				
5–20	0	9	79	12	69
20–35	0	0	126	25	48
35–50	0	24	107	8	51
Average	0	11	104	15	56
	Sept. 5, 1952. Depth: 29.5 meters				
0–10	0	2	40	29	100
10–17	0	6	153	15	173
17–25	0	39	95	4	199
25–35	0	2	123	10	130
Average	0	12	103	15	151

[a] The amounts of gases are expressed in relation to one liter of the interstitial water of sediments.

Publication Date: January 1, 1966 | doi: 10.1021/ba-1966-0055.ch004

Table V. Gaseous Components in Core Sample of Sediments from Lake Nakatsuna-ko[a]

Depth from the bottom surface	O_2	N_2	CH_4	H_2	CO_2
cm.	ml/l.	ml/l.	ml/l.	ml/l.	ml/l.
March 3, 1952. Depth: 11.5 meters					
0–15	0	3	44	14	154
15–23	0	0	47	10	191
23–30	0	0	66	13	112
30–40	0	73	12	0	—
Average	0	19	42	9	152
Sept. 6, 1952. Depth: 12.5 meters					
0–10	0	6	58	14	126
10–18	0	—	—	—	183
18–25	0	2	105	3	234
25–35	0	5	80	24	262
Average	0	4	81	14	201

[a] The amounts of gases are expressed in relation to one liter of the interstitial water of sediments.

Ratios of Organic Carbon and Nitrogen in the Bottom Sediments. As is generally known, the mineralization of organic matter is practically halted in anaerobic conditions which will prevail in the bottom sediments. Organic matter in sediments in which microorganisms are active generally will decompose according to the following steps:

Solid state → colloidal state → soluble or gaseous state

In order that the relationship between the microbiological decomposition rates of organic carbon and nitrogen in the bottom sediments be known more fully, the following components were measured:

(1) Gaseous components in the bottom sediments.

(2) Nonvolatile carbonaceous and nitrogenous components dissolved in the interstitial water of the bottom sediments.

(3) Total carbon and nitrogen in peptized aqueous fractions from the bottom sediments. The method for preparing the fractions will be shown later.

(4) Total carbon and nitrogen in the bulk composition of the bottom sediments.

The gaseous components in core sediments from Lakes Kizaki-ko and Nakatsuna-ko are given in Tables IV and V and expressed in ml./liter of the interstitial water of the sediments. Distribution of total carbon (including a small amount of free and carbonate carbon) and total nitrogen (including a small amount of ammonium nitrogen) in the same cores of sediments are given in Table VI and that of nonvolatile as well as gaseous carbon and nitrogen in the interstitial water are also given in Table VI. From the data of Table VI the average amounts of carbonaceous and nitrogenous components in 100 grams of the original sediments were calculated as shown in Table VII. The data show that the ratios of Total C/Total N of ground material and interstitial water of the bottom sediments are 15.8 and 6.6, respectively for Lake Kizaki-ko and 15.7 and 9.0, respectively for Lake Nakatsuna-ko. The results suggest

Publication Date: January 1, 1966 | doi: 10.1021/ba-1966-0055.ch004

Table VI. Distribution of Total Carbon

Location	Depth from the bottom surface	Water content	Total C	Total N
	cm.	%	%	%
Lake Kizaki-ko (Sept. 5, 1952)	0–10	72.0	4.33	0.297
	10–17	70.2	4.66	0.280
	17–25	66.9	5.30	0.341
	25–35	65.5	5.70	0.373
Lake Nakatsuna-ko (Sept. 6, 1952)	0–10	77.7	7.70	0.500
	10–17	73.9	7.88	0.489
	17–25	70.3	8.48	0.538
	25–35	66.3	9.25	0.620

that the organic nitrogen is more easily decomposed than the organic carbon by microbiological activities in the recent sediments.

Some colloidal or higher molecular products exist in the sediments as intermediate breakdown products between the organic matter in solid state and matter in soluble or gaseous state as a consequence of microbiological decomposition. Separating the intermediate breakdown products from the decomposing sediments was accomplished as follows.

After separating interstitial waters from sediments of 60 grams by centrifuging at 3000 r.p.m. for 10 minutes, the residue of 40 grams was mixed well with 30 ml. of oxygen-free water and centrifuged to separate the peptized solution of sediments from the first stage. The same treatment was successively

Table VII. Average Amounts of Total C and Total N in 100 grams of Original Sediments

	Bulk composition	Ground material	Interstitial water		
			Involatile comp.	Gaseous comp.	Total
	mg.	mg.	mg.	mg.	mg.
Lake Kizaki-ko, Sept. 5, 1952					
H_2O	68700				
Total C	1580	1560	7.42	9.35	16.77
Total N	102	99	1.50	1.04	2.54
Total C/Total N	15.4	15.8	4.94	9.0	6.6
Lake Nakatsuna-ko, Sept. 6, 1952					
H_2O	72100				
Total C	2340	2320	5.96	13.2	19.16
Total N	150	148	1.57	0.55	2.12
Total C/Total N	15.6	15.7	3.70	24	9.0

Publication Date: January 1, 1966 | doi: 10.1021/ba-1966-0055.ch004

and Total Nitrogen in Lake Sediments

	Interstitial water				
	Involatile comp.		Gaseous comp.		
Total C / Total N	Total C	Total N	C_{CH_4}	C_{CO_2}	N_{N_2}
	mg./l.	mg./l.	mg./l.	mg./l.	mg./l.
14.6	127	19	22	54	2
16.6	105	20	82	93	8
15.5	82	20	51	107	49
15.3	118	28	66	70	2
15.4	92	14	17	107	11
16.1	90	18	47	133	19
15.0	70	25	63	185	0
15.0	79	30	61	117	0

Table VIII. Distribution of Total Carbon and Total Nitrogen in Lake Sediments

		Total C	Total N	Total C / Total N
Lake Kizaki-ko, March 1, 1952				
Bulk composition, %		5.00	0.323	15.52
Interstitial water, mg./liter		102	20.8	4.90
	No.			
[b] *Peptized aqueous solution of sediments, mg./liter*	1	499	94.2	5.30
	2	753	102.0	7.38
	3	796	98.0	8.12
	4	910	130.2	7.00
	5	1027	144.2	7.12
				Average 6.98
Lake Nakatsuna-ko, June 5, 1952				
Bulk composition, %		8.78	0.579	15.17
Interstitial water, mg./liter		80.5	21.2	3.80
[b] *Peptized aqueous solution of sediments, mg./liter*	1	219	62.0	3.53
	2	407	74.4	5.47
	3	798	112.2	7.12
	4	1010	130.4	7.75
	5	851	113.4	7.50
	6	467	72.1	6.47
				Average 6.31

[a] Core depth = 15–30 cm.

[b] After separation of interstitial waters from sediments of 60 grams by centrifugation under 3000 r.p.m. for 10 minutes, the residue of 40 grams was mixed well with 30 ml. of oxygen-free water and centrifuged to separate the peptized solution of sediments of the first stage. The same treatment was successively repeated on the residue to obtain the peptized solutions of the second, third, and subsequent stages.

repeated on the residue to obtain the peptized solutions of the second, third, and subsequent stages. The colloidal or higher molecular breakdown products probably are concentrated in these peptized aqueous solutions.

Total carbon and nitrogen were analyzed for the core sediments, the interstitial waters, and the peptized aqueous solutions; the results are given in Table VIII. The ratios of Total C/Total N of the bulk composition, interstitial waters of the core sediments, and the average ratios of the peptized aqueous solutions are also summarized in Table VIII.

The relationship between the ratios of Total C/Total N of the bulk composition of the average peptized aqueous solutions and of the interstitial waters suggests that among the various organic components in the sediments, organic nitrogen is more easily decomposed by microorganisms into colloidal or higher molecular breakdown products than is organic carbon. Furthermore, among the organic components in the colloidal breakdown products, organic nitrogen is more intensively subjected to the microbiological activities than organic carbon.

The carbonaceous and nitrogenous components in peat and in the connate waters were determined by Motojima (*13*) and Maki (*12*) and the results are given in Tables IX and X. The relationship between the ratios of Total C/Total N of peat and those of the connate waters suggests that the same micro-

Table IX. Vertical Variation of Carbon and Nitrogen in Peat from Higashiyonesato[a,b]

Depth	*Loss on ignition*	*Inorg. C*	*Org. C*	*Inorg. N*	*Org. N*	*Total C / Total N*
meters	*%*	*mg./g.*	*mg./g.*	*mg./g.*	*mg./g.*	
0	28.9	0.034	96.5	0.023	6.34	15.2
0.4–0.6	78.5	—	344	0.073	14.6	23.4
1.4–1.6	75.7	—	376	0.070	13.5	24.1
2.3–2.6	84.9	—	453	0.044	13.5	33.6
3.2–3.6	93.6	—	447	0.010	13.1	34.1
4.2–4.5	89.2	0.035	387	0.011	11.1	38.7
					Average	28.2

[a] Higashiyonesato is located near Sapporo City, Hokkaido, Japan.
[b] After Motojima (*13*) and Maki (*12*).

Table X. Vertical Variation of Carbon and Nitrogen of Connate Waters in Peat from Higashiyonesato[a,b]

Depth	*Inorg. C*	*Org. C*	*Total C*	*Inorg. N*	*Org. N*	*Total N*	*Total C / Total N*
meters	*mg./l.*	*mg./l.*	*mg./l.*	*mg./l.*	*mg./l.*	*mg./l.*	
0.35	15.0	40.5	65.5	1.11	3.62	4.73	13.9
0.60	24.0	51.3	75.3	1.30	4.44	5.74	13.1
1.00	39.1	52.8	91.9	1.87	4.56	6.43	14.3
2.00	35.4	45.6	81.0	1.56	5.20	6.76	12.0
4.50	69.1	14.2	83.3	3.34	3.42	6.76	12.3
						Average	13.1

[a] Higashiyonesato is located near Sapporo City, Hokkaido, Japan.
[b] After Motojima (*13*) and Maki (*12*).

Publication Date: January 1, 1966 | doi: 10.1021/ba-1966-0055.ch004

Table XI. Vertical Variation of Organic Carbon, Nitrogen, and Hydrogen in a Core Sample of Sediments from Lake Kizaki-ko, Which Was Previously Dried[a]

Depth from the bottom surface	*Total C*[b]	*Free C*	*Org. C*	*Total H*	*Crystal. H_2O-H*	*Org. H*	*Org. N*[c]
cm.	%	%	%	%	%	%	%
0–6	4.34	0.32	4.00	1.06	0.50	0.56	0.292
6–12	4.03	0.31	3.70	1.21	0.55	0.66	0.257
12–19	4.03	0.30	3.71	1.17	0.60	0.57	0.264
21–28	4.07	0.30	3.75	1.01	0.64	0.37	0.300
28–34	5.61	0.22	5.37	1.09	0.56	0.53	0.350
34–40	5.73	0.44	5.27	1.05	0.63	0.42	0.356
40–46	5.80	0.41	5.37	1.08	0.60	0.48	0.435
46–52	5.97	0.40	5.55	1.10	0.62	0.48	0.442
52–59	5.77	0.37	5.38	1.03	0.60	0.43	0.442
59–66	6.83	0.31	6.50	1.05	0.67	0.38	0.428
66–73	6.39	0.21	6.16	0.88	0.63	0.25	0.400
73–80	7.29	0.21	7.07	0.98	0.66	0.32	0.457

[a] September 5, 1952.
[b] Total C = Org. C + Free C + Carbonate C; Carbonate C = 0.02%
[c] Org. N: Including small amount of NH_4^+-N.

biological decomposition processes as those mentioned in lake waters and recent sediments take place even in the peat strata. Perhaps the microbiological decomposition processes which have been taking place for geological time in the peat strata result in the regular increase in the ratios of Total C/Total N from 15.2 to 38.7 with increasing depth (Tables IX and X).

Ratios of Organic Carbon, Nitrogen, and Hydrogen in the Bottom Sediments. In order to clarify the relationship between the microbiological decomposition rates of organic carbon, nitrogen, and hydrogen in recent sediments the carbonaceous, nitrogenous, and hydrogenous components in a core sediment from Lake Kizaki-ko were determined by dry and wet combustion methods. The results are given in Table XI. The total carbon shows the sum of organic, free, and carbonate carbon in the sediments. The carbonate carbon was determined by the method similar to that for determining total carbon dioxide in water. The ratios of Total C/Org. N, Org. C/Org. N, Org. C/Org. H, and Org. N/Org. H, which were calculated from the data in Table XI are given in Table XII. There is no relationship between the ratios of Total C/Org. N as well as Org. C/Org. N and the depth of core sediments because of the young age of the core sample compared with that of peat. The ratios of Org. C/Org. H, however, with a few exceptions, increase regularly from 5.6 to 24.6 with increasing depth. This indicates that organic hydrogen is more intensively subjected to microbiological decomposition than organic carbon in recent sediments.

The vertical variation of the ratios of Org. N/Org. H in the same core sample shows that with a few exceptions the ratios increase regularly with increasing core depth. This means the organic hydrogen is more easily decomposed than organic nitrogen in recent sediments.

Publication Date: January 1, 1966 | doi: 10.1021/ba-1966-0055.ch004

Table XII. Vertical Variation of the Ratios: Total C/Org. N, Org. C/Org. N, Org. C/Org. H, and Org. N/Org. H in a Core Sample of Sediments from Lake Kizaki-ko[a]

Depth from the bottom surface	Total C / Org. N	Org. C / Org. N	Org. C / Org. H	Org. N / Org. H
cm.				
0–6	14.9	13.7	7.1	0.52
6–12	15.7	14.4	5.6	0.39
12–19	15.3	14.0	6.5	0.46
21–28	13.6	12.5	10.1	0.81
28–34	16.0	15.3	10.1	0.66
34–40	16.1	14.8	12.6	0.85
40–46	13.3	12.3	11.2	0.91
46–52	13.5	12.5	11.6	0.92
52–59	13.1	12.1	12.5	1.03
59–66	16.0	15.1	17.1	1.13
66–73	16.0	15.3	24.6	1.60
73–80	16.0	15.4	22.1	1.43

[a] September 5, 1952.

All of the facts found in lake waters and bottom sediments suggest that a relationship between the microbiological decomposition rates of organic carbon, nitrogen, and hydrogen in recent sediments may be of the following order:

$$\text{Organic C} < \text{Organic N} < \text{Organic H}$$

This also suggests that the composition of organic matter in sediments gradually changes into a form richer in carbon as a result of microbiological activity.

Conclusions

The ratios of Org. C/Org. N of plankton, of sediments collected at 25 meters in the water, and of surface bottom sediments in Lake Kizaki-ko are 5.7, 9.3, and 15.5, respectively. Kleerekoper reports that similar relationships apparently occur in Lake Lauzon, Quebec.

The gaseous and nitrogenous components as well as the other chemical characteristics were determined in Lake Kizaki-ko, September 7–8, and October 28–31, 1963 when stagnation was greatly advanced in the lake.

From the vertical distributions of various components, the mineralized carbon (Miner. C) and nitrogen (Miner. N) at various depths were calculated. On the basis of the calculated values, the ratio of Miner. C/Miner. N in a vertical water column of Lake Kizaki-ko was estimated to be 2.83, which is considerably smaller than that of plankton.

The relationships between the ratios of Org. C/Org. N mentioned above indicate that the organic nitrogen in plankton is subjected more intensively to microbiological decomposition processes than organic carbon in the course of their sinking in lake water and also soon after they settled on the bottom surface.

The following components in sediments were measured: (1) gaseous components, (2) nonvolatile carbonaceous and nitrogenous components dis-

Publication Date: January 1, 1966 | doi: 10.1021/ba-1966-0055.ch004

solved in the interstitial water, (3) total carbon and nitrogen in peptized aqueous fractions, and (4) total carbon and nitrogen in the bulk composition.

From the results, the average ratios of Total C/Total N of the bulk composition, of the average peptized aqueous solution and of the interstitial waters of the sediments were estimated to be 15.35, 6.65, and 4.35, respectively.

The facts suggest that among the various organic components in the sediments, organic nitrogen is more easily decomposed by microorganisms into colloidal or higher molecular breakdown products than is organic carbon; furthermore, among the organic components in the colloidal breakdown products, organic nitrogen is more intensively subjected to the microbiological activities than organic carbon.

The carbonaceous, nitrogenous, and hydrogenous components in a core sediment from Lake Kizaki-ko were determined. The ratios of Org. C/Org. H and of Org. N/Org. H in the core sample increase regularly with increasing depth.

All of the facts found in the lake waters and bottom sediments suggest that the microbiological decomposition rates of organic carbon, nitrogen, and hydrogen in recent sediments may be in the following order: Organic C < Organic N < Organic H.

Publication Date: January 1, 1966 | doi: 10.1021/ba-1966-0055.ch004

Literature Cited

(1) Botan, E. A., Miller, J. J., Kleerekoper, H., *Arch. Hydrobiol.* **56,** 334 (1960).
(2) Emery, K. O., Rittenberg, S. C., *Bull. Am. Assoc. Petrol. Geol.* **36,** 735 (1952).
(3) Emery, K. O., Hoggan, D., *Bull. Am. Assoc. Petrol. Geol.* **42,** 2174 (1958).
(4) Endres, G., Kaufmann, L., *Ann.* **530,** 184 (1937).
(5) Kleerekoper, Herman, *J. Fisheries Res. Board Can.* **10,** 283 (1953).
(6) Koyama, T., *J. Earth Sci., Nagoya Univ.* **1,** 107 (1953).
(7) Koyama, T., *J. Earth Sci., Nagoya Univ.* **2,** 5 (1954).
(8) Koyama, T., *J. Earth Sci., Nagoya Univ.* **3,** 65 (1955).
(9) Koyama, T., *J. Earth Sci., Nagoya Univ.* **6,** 1 (1958).
(10) Koyama, T., *J. Geophys. Res.* **68,** 3971 (1963).
(11) Kruse, J. M., Mellon, M. G., *Anal. Chem.* **25,** 1188 (1953).
(12) Maki, S., *Geol. Survey, Japan, Monthly Rep.* **10,** 601 (1959).
(13) Motojima, K., *Geol. Survey, Japan, Rep. No.* **183,** 1 (1959).
(14) Mullin, J. B., Riley, J. P., *Anal. Chim. Acta* **12,** 464 (1955).
(15) Oana, S., *J. Earth Sci., Nagoya Univ.* **5,** 103 (1957).
(16) Orr, W. L., Emery, K. O., *Bull. Geol. Soc. Am.* **67,** 1247 (1956).
(17) Saijo, Y., *J. Chem. Soc. Japan* **77,** 917 (1956).
(18) Sugawara, K., *Bull. Chem. Soc. Japan* **14,** 375 (1939).
(19) Takai, Y., Koyama, T., Kamura, T., *J. Agr. Chem. Soc. Japan* **29,** 967 (1955).
(20) Takai, Y., Koyama, T., *J. Sci. Soil Manure, Japan* **26,** 509 (1956).
(21) Takai, Y., Koyama, T., Kamura, T., *Soil Sci. Plant Nutr.* **9,** 176 (1963).
(22) Takai, Y., Koyama, T., Kamura, T., *Soil Sci. Plant Nutr.* **9,** 207 (1963).
(23) Tanaka M., *Bull. Chem. Soc. Japan* **27,** 200 (1954).
(24) Von Brand, T., Rakestraw, N. W., *Biol. Bull.* **72,** 165 (1937).
(25) Von Brand, T., Rakestraw, N. W., Renn, C. E., *Biol. Bull.* **77,** 285 (1939).
(26) Von Brand, T., Rakestraw, N. W., *Biol. Bull.* **79,** 231 (1940).
(27) Von Brand, T., Rakestraw, N. W., *Biol. Bull.* **81,** 63 (1941).
(28) Von Brand, T., Rakestraw, N. W., Zabor, J. W., *Biol. Bull.* **83,** 273 (1942).
(29) Waksman, S. A., Carey, C. L., Reuszer, H. R., *Biol. Bull.* **65,** 57 (1933).
(30) Yamane I., Sato, K., *Bull. Inst. Agr. Res., Tohoku Univ.* **7,** 239 (1956).
(31) Yamane, I., *Bull. Inst. Agr. Res., Tohoku Univ.* **12,** 261 (1961).
(32) Yamane, I., Sato, K., *Soil Sci. Plant Nutr.* **9,** 28 (1963).
(33) Yamane, I., Sato, K., *Soil Sci. Plant Nutr.* **9,** 32 (1963).

RECEIVED October 5, 1964.

5

Chemistry of Humic Substances in Relation to Coalification

WOLFGANG FLAIG

Institut für Biochemie des Bodens, Braunschweig, Germany

Plant constituents decompose at different rates. Since phenolic substances are more resistant to microbial attack, they are regarded as material essential in forming humic substances. During humification the methoxyl content decreases and nitrogen increases. Lignin decomposition products which are formed undergo different oxidation reaction leading to phenols or quinones and polymerization products. A scheme for the decomposition of lignin and humification according to experimental results with labelled lignin decomposition products is discussed. Under the conditions of coalification the formation of polymerization products derived from quinonoid substances may occur which leads finally to a higher degree of aromatization.

Publication Date: January 1, 1966 | doi: 10.1021/ba-1966-0055.ch005

During humification various plant constituents decompose at different rates. Carbohydrates and proteins serve as an energy source for microorganisms or as materials for forming their body substances while lignin and other phenolic compounds decompose more slowly than the two other main constituents. Therefore, lignin and other phenolic compounds may be regarded as materials essential for forming the dark colored substances in humus.

We have investigated the humification of straw, as an example, under constant conditions of humidity and temperature in a climatic chamber (*4*, *18*) and separated different fractions according to a modified method of Waksman's proximate analysis. The amount of nitrogen present in these processes is the factor limiting the rate of decomposition. Therefore we added nitrogen in form of ammonium nitrate in a quantity of 1% of straw dry weight to a nutrient solution in one experiment while the nutrient solution had no nitrogen in a parallel experiment. Table I shows the calculated data.

Under the condition chosen cellulose decomposes much faster than lignin. Adding nitrogen accelerates the decomposition of holocellulose as well as

In Coal Science; Given, P.;
Advances in Chemistry; American Chemical Society: Washington, DC, 1966.

Table I. Decomposition of Straw, Holocellulose, and Lignin with and without Added Nitrogen

Days	Nitrogen Added	Decrease of Fractions in %		
		Org. Subst.	Holocellulose[b]	Lignin H_2SO_4[b]
0		0	0	0
70	0	10.4	20.2	0.4
	1[a]	49.3	67.5	7.2
120	0	27.7	36.7	9.0
	1	66.4	84.5	24.0
180	0	36.3	44.7	13.3
	1	76.4	92.4	37.7
240	0	48.7	57.4	24.6
	1	80.9	94.7	48.1

[a] 1N = 1% N as NH_4NO_3 per dry weight of straw
[b] Mean value of three analyses

lignin. The lignin fractions have been isolated according to a modified method of Klason with sulfuric acid (23). The values of the elementary analysis are shown in Table II.

Since carbon values decreased and oxygen values increased, oxidative reactions must have occurred during decomposition.

Nitrogen values more than triple on adding ammonium nitrate. The more the straw is rotted, the less nitrogen can be hydrolyzed with hydrochloric acid. A part of the nitrogen in the lignin fractions is fixed as α-amino nitrogen. The quantity decreases from 60% of total nitrogen content in fresh straw to about 20% in rotted straw. A remarkable decrease could be observed for the methoxyl content. This fact can be explained by an enzymatic demethylation process.

The decomposition of lignin is caused by oxidation and demethylation; furthermore, fixation of nitrogen occurs. Nitrogen can be derived from peptides, amino acids, or ammonia. All these compounds can be formed by the decomposition of plant proteins or during the autolysis of the microorganisms.

For further consideration some additional remarks must be made. In coalification not only might lignin alteration itself play an important role, but

Table II. Values of Elementary Analysis of the Lignin Fractions from Experiments with and without Added Nitrogen[a]

Days	Nitrogen	C %	H %	O %	N %	S %	OCH_3 %	ash %
0		62.73	5.64	30.55	0.53	0.55	17.08	6.15
70	0	62.29	5.48	31.20	0.54	0.49	15.53	7.65
	1[b]	61.42	5.25	30.20	1.44	0.69	12.78	9.00
120	0	62.13	5.42	31.41	0.56	0.48	14.99	8.62
	1	60.93	5.41	31.20	1.68	0.78	11.33	10.02
180	0	62.20	5.41	31.30	0.56	0.53	14.37	9.31
	1	60.94	5.38	31.15	1.74	0.79	10.95	11.24
240	0	62.14	5.27	31.03	0.56	0.97	13.46	9.36
	1	59.61	5.13	32.77	1.88	0.61	9.93	11.69

[a] Calculated for ash-free substances
[b] 1N = 1% N as NH_4NO_3 per dry weight of straw

Publication Date: January 1, 1966 | doi: 10.1021/ba-1966-0055.ch005

also possible further reaction of the various primary lignin decomposition products that might occur subsequently during humification. One part of these further decomposition products can be used as an energy source by the lignin-decomposing microorganisms (*6*). Another part reacts alone or with other compounds to form dark colored humic substances (*7*, *8*).

During the rotting of plant materials, different phenolic compounds can be identified (*14*, *16*, *18*, *28*) as shown in Figure 1. These are aromatic compounds with side chains of one or three carbon atoms. They may be derived from the polymeric lignin by cleavage or oxidation reactions whereby the side chain is shortened.

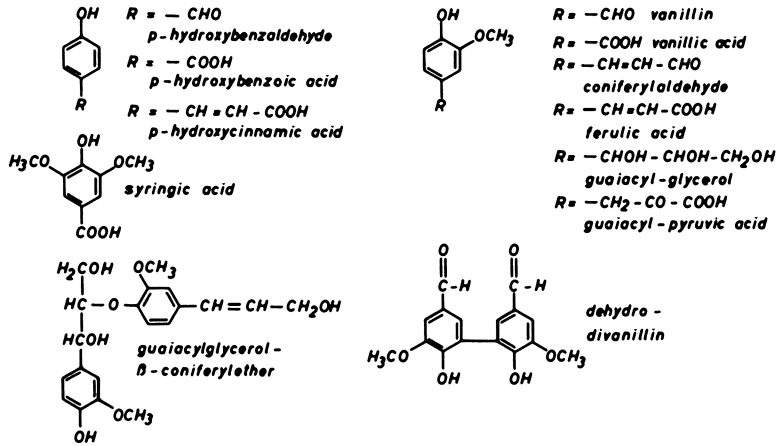

Figure 1. Structure of identified lignin decomposition products

Guaiacylglycerol-β-coniferyl ether is a dimeric decomposition product of coniferous lignin; dehydrodivanillin may be also formed by dimerization of vanillin after formation from lignin. Among the lignin decomposition products are mono-, di- and triphenol derivatives which are derived from the different types of lignin of needle trees, deciduous trees, or graminees.

In our above mentioned experiment the straw lignin had a ratio of vanillic to syringic components of 1.7 : 1. This ratio has been determined by oxidizing the lignin with *m*-nitrobenzenesulfonic acid (*24*). The lignin has been isolated according to the method of Brauns. The question arises: would this ratio be constant during the humification process? Kratzl and Claus (*17*) analyzed the original and rotted straw and determined vanilloylacetyl and syringoylacetyl quantitatively after ethanolysis. They found that the ratio 1.6 : 1 (to be compared with the value 1.7 : 1 that we found with the other method) changed to 2.7 : 1 in the rotted straw after 240 days. This means that during humification the lignin decomposition products of syringyl type are transformed more rapidly than those of guaiacyl type.

However, in the lignin fraction of the rotted straw, the ratio was 0.5 : 1 at the end of the decomposition experiment. Therefore, the syringyl components are split off more slowly from the polymeric lignin than the guaiacyl

Publication Date: January 1, 1966 | doi: 10.1021/ba-1966-0055.ch005

components. Both results agree with other experiments. Thus, syringic acid is more sensitive to oxygen treatment in alkaline solution than vanillic acid. Furthermore the C_2 atoms of the side chain of three carbon atoms are preferred for connecting the monomers of the phenylpropenyl type (*1*, *20*), especially syringyl type. We were able to confirm this result also with labelled compounds.

In Figure 2 the further reactions of the lignin decomposition products, which involve biological oxidation in the soil or in cultures or microorganisms, are summarized. All of the secondary reaction products could be identified.

The essential reactions (*5*) during the further transformations of the decomposition products of lignin are:

(a) cleavage of the side chain (I or II–III)
(b) decarboxylation (III–XIII, VII–IX)
(c) demethylation (III–IV, VI–VII)
(d) demethoxylation (III–V)
(e) hydroxylation (V–IV)
(f) formation of quinones (III–XIII, IV–XI, V–X, VII–XII)
(g) dimerization (VII–VIII or IX, XIII–XIV)
(h) polymerization (II–$(II)_x$ and others such as X, XI, XII)

The dimerization and polymerization of the resulting quinones will be discussed more extensively later in relation to the formation of compounds in which the aromatic structure increases successively during the reactions.

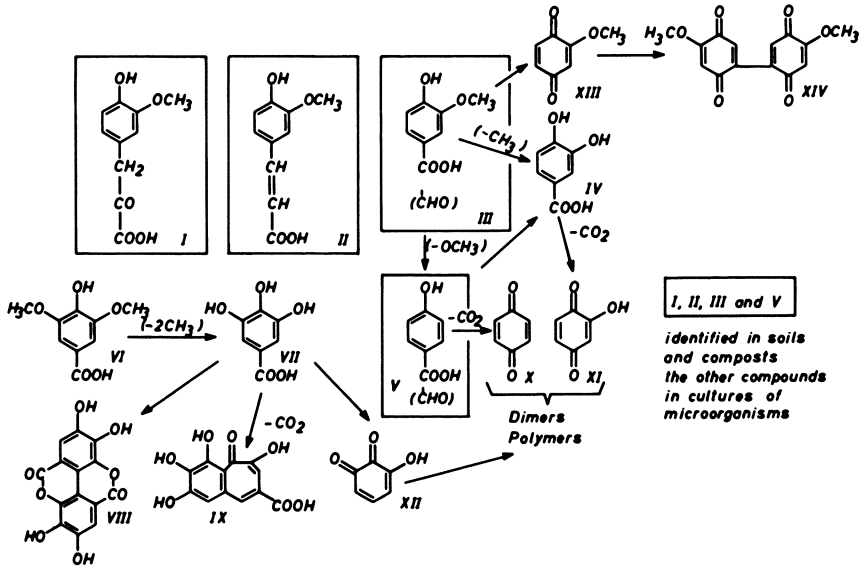

Figure 2. Oxidation of lignin decomposition products

I Guaiacyl-pyruvic acid
II Ferulic acid
III Vanillic acid (vanillin)
IV Protocatechuic acid (-aldehyde)
V *p*-Hydroxybenzoic acid (-aldehyde)
VI Syringic acid
VII Gallic acid
VIII Ellagic acid
IX Purpurogallin
X *p*-Benzoquinone
XI Hydroxy-*p*-benzoquinone
XII 3-Hydroxy-*o*-benzoquinone
XIII Methoxy-*p*-benzoquinone
XIV 3,3'-Dimethoxy-diphenyl-di-quinone-2,5,2',5'

Publication Date: January 1, 1966 | doi: 10.1021/ba-1966-0055.ch005

Polymerizing lignin decomposition products under oxidizing conditions depends on substitution on the phenyl ring, whether there is one OH group alone or whether it is associated with one or two methoxyl groups. Furthermore it is important to know whether the side chain is composed of aldehyde, carboxyl, vinyl alcohol, acrylic acid, or glycerol groups. For three carbon atoms in the side chain the polymer linking can occur through the side chains, through the rings, or through a side chain and a ring in form of a C-C linkage or a C-O-C linkage. In the case of phenyl derivatives with one carbon atom in the side chain the only possibility that exists is linkage between the rings (*11*) (Figure 3).

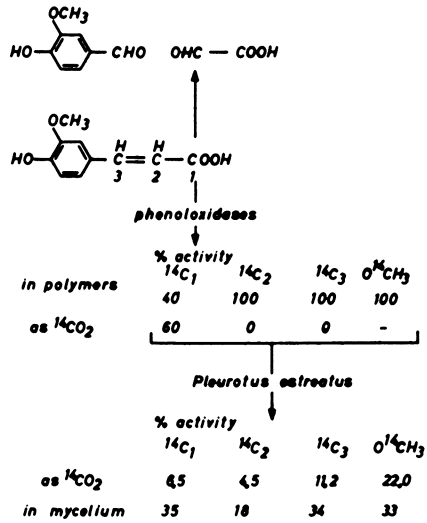

Figure 3. Different decomposition of labelled groups of polymers of ferulic acid

In order to elucidate the mechanism of the further transformations of the primary lignin decomposition products including the cleavage reactions, we synthesized some of the important primary products labelled with C^{14} and introduced these into the cultures of fungi or enzymes. Thus, it could be shown, for example, that the breakdown of the side chain of ferulic acid occurs at the double bond; vanillic acid is found. During polymerization in the presence of phenoloxidases, in the case of carboxyl-labelled ferulic acid, about 60% of the activity is split off as $C^{14}O_2$. The polymers labelled in the 2 and 3 position in the side chain or in the methoxyl group contain the whole applied activity.

If the polymers are shaken in cultures of *Pleurotus ostreatus*, the carbon atom of the methoxyl group is used by the microorganisms to a larger extent than the other carbon atom (Figure 4). It has been mentioned that C_2 atom participates mainly in the linkage of the monomers and therefore is less available for the microorganisms.

Publication Date: January 1, 1966 | doi: 10.1021/ba-1966-0055.ch005

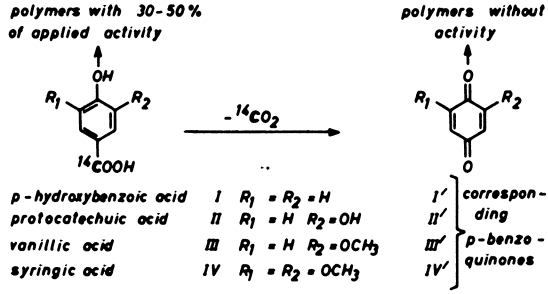

Figure 4. Oxidative degradation of C_6-C_1 compounds

Phenyl derivatives with a carboxyl group, which may be formed also by degradation of C_6-C_3 compounds, split off $C^{14}O_2$ under oxidizing conditions—i.e., during enzymatic oxidation or with weak oxidizing agents. The corresponding *p*-benzoquinones are formed which dimerize or polymerize mostly to colored products. The polymerization of the C_6-C_3 compounds and the C_6-C_1 compounds occurs via radical-like or quinonoid intermediates (*8*). This can be concluded from the results of experiments with appropriately substituted compounds.

Other experiments show that phenolcarboxylic acids labelled in the carboxyl group form radioactive polymers by simultaneously forming $C^{14}O_2$. This means that not all $C^{14}O_2$ is split off, and the polymerization does not occur only through quinones as intermediate steps. Demethylation of the lignin decomposition products is a further important reaction because *o*-benzoquinones can be formed under certain conditions.

We studied the demethylation of lignin decomposition products labelled in the C atom of the methoxyl group. After demethylation the resulting 1,2-diphenols form *p*- or *o*-benzoquinones by further oxidation under mild conditions depending upon the substitution of the side chain, as shown in Figure 5. In the case of demethylation of partially methylated 1,2,3-triphenols, formation

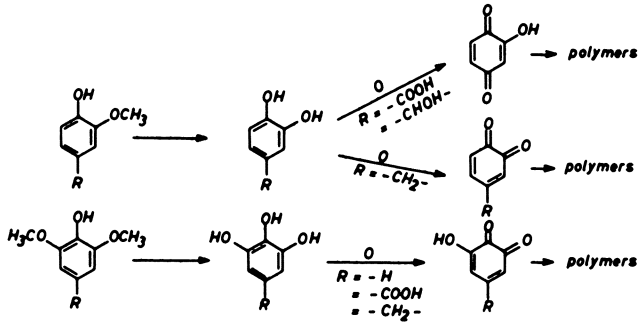

Figure 5. Demethylation of lignin decomposition products

Publication Date: January 1, 1966 | doi: 10.1021/ba-1966-0055.ch005

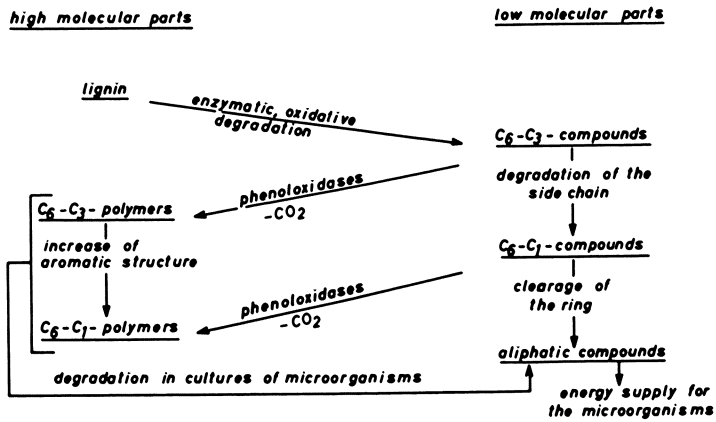

Figure 6. Decomposition of lignin

of 3-hydroxy-*o*-benzoquinones was observed. The different quinones react to form polymers, whereby the hydrogen content decreases.

The various observations and conclusions are summarized in Figure 6 where a complete scheme for lignin decomposition is proposed. It has some interesting implications for the process of humification. As Figure 6 shows, the following steps occur in the decomposition of lignin:

(1) The high molecular lignin is enzymatically degraded to C_6-C_3 compounds or C_6-C_1 compounds; the latter are also formed from the C_6-C_3 compounds by loss of two carbon atoms in the side chain.

Table III. Elementary Analysis of Different Products

Lignins and Coals		*C*	*H*	*O*	*N*	*OCH₃*	*S*	*Humic Acids in % of Org. Subst.*
Björkman-lignin (fresh straw)		60.68	5.79	33.11	0.4	16.74	0	
Lignin (H_2SO_4) (260 days) S-free	before hydrolysis	58.00	5.83	29.93	3.14	7.84	3.9	
		60.3	6.1	31.1	3.3	8.1	0	
	after	58.86	5.61	34.15	1.38	—	0	
Lignitic soft coal[b] (2 samples)		63.2	4.5	32.3	~1	2.5		27.0
Subbituminous coal (10 samples)		73.2	5.3	21.5	~0.8	0.2		8.5
Bituminous coal (5 samples)		84.3	5.3	10.4	0.8	0		nil

Publication Date: January 1, 1966 | doi: 10.1021/ba-1966-0055.ch005

(2) The C_6-C_3 compounds and the C_6-C_1 compounds formed partly repolymerize under oxidizing conditions with loss of carboxyl groups as CO_2 to polymers having a composition different from that of lignin. Another part of the lignin decomposition products is degraded to aliphatic compounds, as finally the polymers are also. The aliphatic compounds formed serve as an energy supply for the microorganisms.

(3) *o*-Diphenols or vicinal triphenols are formed by demethylation of the corresponding methyl ethers. *o*-Benzoquinones as well as *p*-benzoquinones can be derived from these, and this is an additional factor leading to copolymer formation and cross-linking.

(4) The polymers formed contain an increasing proportion of aromatic structure with increasing degradation of the side chain. (This fact is interesting for the problem of coalification.)

(5) In the case of humification, nitrogen compounds react to a different extent in these stages of the reactions when aromatic components are involved. The extent of nitrogen fixation depends on the available α-amino nitrogen compounds and the environmental conditions (9). In the case of natural humification, the biological processes can be considered more or less finished at this stage.

Coalification occurs under conditions which are more anaerobic than those used in the laboratory work and are less favorable for microorganisms. The oxygen tension is lower and decreases with time. More and more oxygen-containing compounds must serve as oxidizing agents. Temperature and pressure increase, and time begins to play an important role.

The results of elementary analyses of lignin isolated from fresh (2, 3) and rotted straw and data for different types of coals and humic acids isolated from these and from chernozem are shown in Table III to illustrate further steps of coalification. The following points should be noted:

(1) The low carbon content of humic acids isolated from rotted straw and chernozem may be caused not only by oxidizing processes but also by the

of Humification, Coalification, and Humic Acids[a]

Isolated "Humic Acids"		*C*	*H*	*O*	*N*	OCH_3
"Humic acids" from straw (260 days, 15.7% of org. subst.)	before hydrolysis	53.74	5.19	37.63	3.44	7.66
	after	57.53	4.58	36.94	0.95	—
Humic acids from chernozem		58.9	3.3	34.2	2.5	0.7
Humic acids from lignitic soft coal (2 samples)		61.2	4.1	34.8	~0.6	—
Humic acids from subbituminous coal (7 samples)		69.2	4.5	26.3	—	—
No humic acids						

[a] % of ash-free substances

[b] Bitumen extracted with alcohol-benzene after treatment with dilute HCl.

Publication Date: January 1, 1966 | doi: 10.1021/ba-1966-0055.ch005

presence of fixed nitrogen compounds. After hydrolysis the carbon content increases because the carbon content of the hydrolyzed amino acids is lower than that of lignin or of altered lignin. The values of the lignin fraction from the material rotted for 260 days show that besides α-amino nitrogen-containing compounds, other carbon-containing compounds are hydrolyzed. H. W. Scharpenseel and R. Krausse (*27*) found that the content of amino acids in coal humic acids accounts for less than one-third of the nitrogen content.

(2) With increasing age of the coals the carbon content increases, and the oxygen and methoxyl content decreases in the material free of bitumen as well as in the isolated humic acids (*29*).

It is possible that the quinones formed as intermediates during early stages of coalification polymerize under mild oxidation conditions in the absence of water, and that the polymers are dehydrated and dehydrogenated under the influence of pressure and higher temperatures. All reactions in which water takes part—e.g., the cleavage of the ring to aliphatic compounds—are no longer possible to such an extent. Furthermore, hydrobenzoquinone, for example, is transformed in the presence of ferric ions into dark colored polymers in nonaqueous solutions or at higher temperatures. *o*-Benzoquinones or 3-hydroxy-*o*-benzoquinones react with themselves in different ways depending upon substitution as shown in Figure 7.

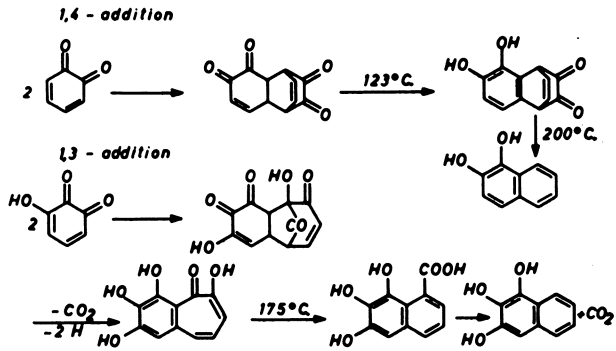

Figure 7. Dimerization of o-benzoquinones and aromatization of the adducts

o-Benzoquinone dimerizes by 1,4-addition by the Diels-Alder reaction (*12, 21*). At higher temperatures a phenolic isomer is formed which is transformed to 1,2-dihydroxynaphthalene at 200°C. (*15*).

Pyrogallol and some derivatives are oxidized to 3-hydroxy-*o*-benzoquinones which dimerize by 1,3-addition. The adducts react to purpurogallin by dehydrogenation and splitting off of CO_2 (*25, 26*). By treating with alkali at 175°C. purpurogallin is transformed into 6,7,8-trihydroxynaphthalene-1-carboxylic acid (*13, 22*). Decarboxylation would be a further step in increasing aromatic character.

The reactions mentioned can only be a few of those that must be identified before the increase of aromatic structure in the course of coalification can be

Publication Date: January 1, 1966 | doi: 10.1021/ba-1966-0055.ch005

fully explained. At the moment we are studying further dimerization reactions of different susbtituted *o*-benzoquinones and the aromatization of the addition products (*19*).

Literature Cited

(1) Adler, E., *Z. Papier* **15,** 604 (1961).
(2) Bjorkman, A., *Nature* **174,** 1057 (1954).
(3) Bjorkman, A., *Svensk Papperstid.* **59,** 477 (1956).
(4) Flaig, W., *Freiberger Forschungsh.* **A254,** 39 (1962).
(5) Flaig, W., FAO-IAEA Technical Meeting on the Use of Isotopes in Soil Organic Matter Studies, Braunschweig, 1963.
(6) Flaig, W., Haider, K., *Arch. Mikrobiol.* **40,** 212 (1961).
(7) Flaig, W., Salfeld, J. C., *Trans. Intern. Congr. Soil Sci., 7th Madison, Wisc.,* **1960,** 648 (1961).
(8) Flaig, W., Salfeld, J. C., Haider, K., *Landwirtsch. Forsch.* **16,** 85 (1963).
(9) Haider, K., Frederick, L. R., Flaig, W., *Plant Soil* **22,** 49 (1965).
(10) Haider, K., Lim, S. U. Flaig, W., *Landwirtsch. Forsch.* **15,** 1 (1962).
(11) Haider, K., Lim, S. U., Flaig, W., *Holzforsch.* **18,** 81 (1964).
(12) Harley-Mason, J., Laird, A. H., *J. Chem. Soc.* **1958,** 1718.
(13) Haworth, R. D., Moore, B. P., Pauson, P. L., *J. Chem. Soc.* **1949,** 3271.
(14) Henderson, M. E. K., *Nature* **175,** 634 (1955)
(15) Horner, L., Dürckheimer, W., *Chem. Ber.* **91,** 2532 (1958).
(16) Ishikawa, H., Schubert, W. J., Nord, F. F., *Arch. Biochem. Biophys.* **100,** 131 (1963).
(17) Kratzl, K., Claus, P., *Monatsh.* **93,** 219 (1962).
(18) Maeder, H., Dissertation, University of Giessen, 1960.
(19) Müller, H. H., *Dipl.-Arbeit* Braunschweig, 1964.
(20) Müller, E., Mayer, R., Spanagel, H., Scheffler, K., *Ann.* **645,** 53 (1961).
(21) Patchett, A., Witkop, B., *J. Org. Chem.* **22,** 1477 (1957).
(22) Perkin, A. G., *J. Chem. Soc.* **101,** 803 (1912).
(23) Ritter, G. J., Seborg, R. M., Mitchell, R. L., *Ind. Eng. Chem. Anal. Ed.* **4,** 202 (1932).
(24) Ruhemann, H., Dissertation, Braunschweig, 1964.
(25) Salfeld, J. C., *Angew Chem.* **69,** 723 (1957).
(26) Salfeld, J. C., Baume, E., *Chem. Ber.* **97,** 307 (1964).
(27) Scharpenseel, H. W., Krausse, R., *Z. Pflanzenernähr., Düng., Bodenk.* **92,** 11 (1962).
(28) Seifert, K., *Holzforsch.* **16,** 102 (1962).
(29) Stach, H., *Das Braunkohlenarchiv Heft* **40,** 1 (1933).

RECEIVED April 19, 1965.

Discussion

Irving Wender. All lignin is optically inactive, but oils derived from coal by low temperature carbonization or by hydrogenation are optically active. It may be possible to follow lignin coalification through the microbiological (enzymatic) stage by following the increase in optical activity on microbiological or enzymatic attack on lignin.

Wolfgang Flaig. We have not done such experiments. I thank you for this proposal for further work.

James M. Schopf. This is a most significant paper. What was the nature of the microorganisms or assemblages of microorganisms used in your experiments?

Dr. Flaig. We worked mostly with different white rot fungi, *Polystictus versicolor* and others.

Peter H. Given. One of the important questions we have to solve in coalification is how polycyclic aromatic substances come to be formed. Was the benzotropolone positively identified? This is an interesting way in which polycyclic compounds are formed from monocyclic. Is it your idea that quinone adducts are formed in the biochemical decay and that these adducts are transformed into polycyclic aromatics by the action of heat after burial?

Dr. Flaig. Purpurogallin and its 8-carboxylic acid have been identified, and the reaction mechanism elucidated (*1*, *4*, *5*, *6*). We were able to identify for the first time the suggested quinone dimers (*2*). After elucidating the mechanism of the formation of purpurogallin through 3-hydroxy-*o*-benzoquinone as an intermediate, we studied other substituted *o*-benzoquinones and their transformation by various treatments. Further work is in progress (*3*).

B. K. Mazumdar. Low rank coals like lignites and natural humic acid derived from such coals are known to contain alicyclic structures in their constitution. How does the author envisage the formation of such structures in the transformation of lignin to humic acid-like substances?

Dr. Flaig. We could show that, by oxidative polymerization of lignin decomposition products with side chains containing one or more carbon atoms, polymer-like humic substances are formed. The polymerization can be carried out with mild oxidizing agents or in the presence of phenoloxydases.

In the case of ferulic acid, dimers are known; one of these has a difuran structure and another a benzofuran structure.

George Kapo. In your experiments on the degradation of lignin you found that adding amino acids catalyzed the decomposition. What are the reactions and mechanisms involved with these added nitrogen compounds?

Dr. Flaig. The mechanism of the reaction between amino acids and oxidized lignin decomposition products can be described by the scheme of Trautner, which involves oxidative deamination.

Irving A. Breger. What proportion of lignin decomposes?

Dr. Flaig. That depends upon the conditions of rotting. For instance, the proportion of lignin which rots under field conditions is lower than that which rots during experiments in climatic chambers.

Dr. Breger. Are the polymeric products soluble?

Dr. Flaig. The polymeric products of lignin decomposition formed in the presence of phenol oxidases are not water soluble.

Literature Cited

(1) Flaig, W., FAO-IAEA Technical Meeting on the Use of Isotopes in Soil Organic Matter Studies, Braunschweig, 1963.
(2) Flaig, W., Salfeld, J. C., Haider, K., *Landwirtsch. Forsch.* **16,** 85 (1963).
(3) Müller, H. H., Dip.-Arbeit, Braunschweig, 1964.
(4) Salfeld, J. C., *Angew. Chem.* **69,** 723 (1957).
(5) Salfeld, J. C., Baume, E., *Chem. Ber.* **97,** 307 (1964).
(6) Steinmetz, A., Dissertation Tech. Univ. Braunschweig, 1956.

Publication Date: January 1, 1966 | doi: 10.1021/ba-1966-0055.ch005

Petrographic Continuity of Pennsylvania Coals

EDWIN F. KOPPE

The Pennsylvania Geological Survey, Harrisburg, Pa.

Publication Date: January 1, 1966 | doi: 10.1021/ba-1966-0055.ch006

Microscopic studies of medium and low volatile bituminous coals in central Pennsylvania were directed toward relating petrographic composition with the geological and geographical distribution of specific coal beds. When coupled with conventional mapping techniques, petrographic analyses of the coal by layers permit solution of some correlation problems. Some beds exhibit uniform lateral petrographic continuity throughout the quadrangle. Others have good lateral continuity of the bed in one direction but not in another. In the "poor" direction, usually across geological structure, one example illustrates that the only laterally continuous zone within the seam forms the basal few inches at one site and, less than eight miles away, becomes the topmost layer. At the two sites the total thickness of the coal is essentially the same.

The data presented here are a result of a research program on the petrographic composition of Pennsylvania coals begun in 1957 by the Pennsylvania Geological Survey. Much of the data are taken from recent studies of medium and low volatile bituminous coals in the Houtzdale 15 minute quadrangle, Clearfield County, Pennsylvania. The quadrangle studies are directed toward relating petrographic composition with the geological and geographical distribution of coal beds as well as determining composition for use in industrial applications.

Local and regional variation in petrographic character of specific coal beds have been investigated actively for more than forty years. Roos (*9*) initiated comprehensive studies demonstrating that the character and quality of a coal seam change from place to place and that detailed sections were necessary for insight into the composition of coal. This important type of study has been continued and extended by several workers (*3*, *4*, *5*, *8*, *10*). In the Australian coals, Taylor and Warne noted that changes in microlithotype

In Coal Science; Given, P.;
Advances in Chemistry; American Chemical Society: Washington, DC, 1966.

composition were not usually marked over distances of one to five miles, but that trends sometimes appear in a seam over wide areas.

To some extent, petrographic changes can be related to the geological history of the associated strata. The writer (*6, 7*) earlier demonstrated that coal layers may be missing from the bed resulting in changed overall petrographic analyses. The presence or absence of basal units was ascribed to local topographic relief which was present immediately prior to coal deposition.

Methods

Routine quantitative petrographic procedures were employed throughout the current study with only minor necessary modifications. Channel samples were collected in the field from each megascopically recognizable coal layer in the bed exposed in strip mines, road cuts, and underground mines. In the laboratory, the samples were crushed to —30 mesh (—590 microns), pelletized

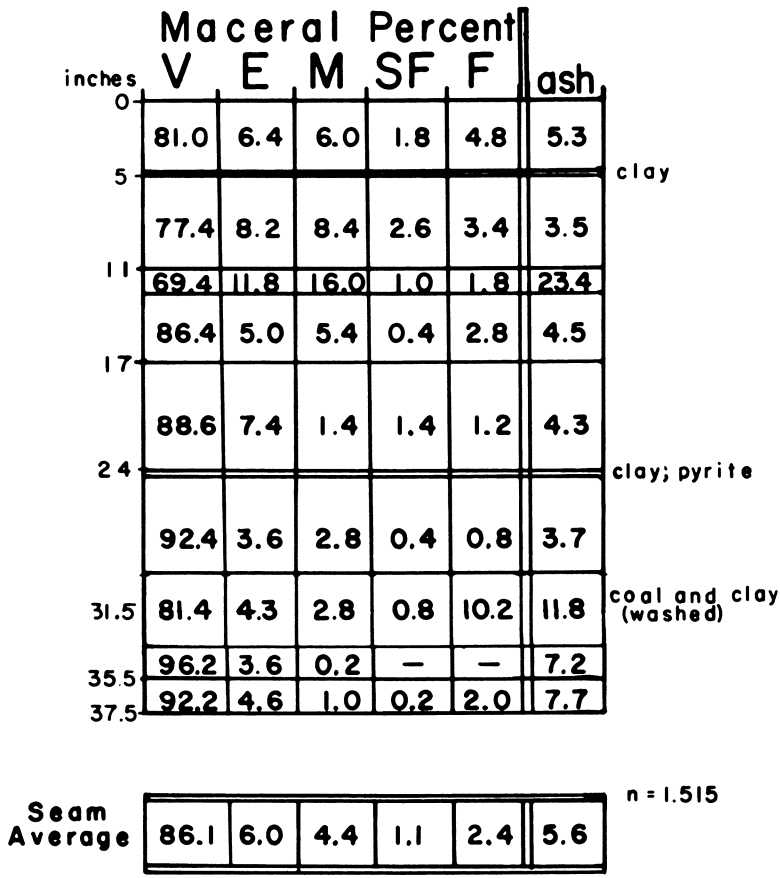

Figure 1. Petrography of Lower Kittanning coal at West Kittanning, Pennsylvania. Symbols: V—vitrinite, E—exinite, M—micrinite, SF—semifusinite, F—fusinite

Publication Date: January 1, 1966 | doi: 10.1021/ba-1966-0055.ch006

Table I. Maceral Composition of Upper Freeport Coal

Bed		Site 1	2	3	4	5
Upper (F)	Vitrinite	78.1	77.0	[d]	73.7	79.0[b]
	Exinite	2.8	2.7		5.2	3.4
	Micrinite	8.5	6.8		12.1	6.8
	Fusinite[a]	9.6	13.8		9.0	10.8
Lower	Vitrinite	89.8	90.7	89.6	89.6	92.4[c]
	Exinite	2.5	1.3	1.2	3.1	2.0
	Micrinite	3.7	2.3	2.1	2.0	2.3
	Fusinite[a]	4.1	5.8	7.1	5.3	3.3

[a] Includes semifusinite
[b] Probable correlative of upper bed in the Houtzdale quadrangle
[c] Average of eight columns
[d] Absent

in Lucite, then ground and polished with a Buehler Automet for examination. All samples were examined under oil with plane and polarized reflected light at a magnification of 310×.

Similar reflectances of some of the macerals (especially exinite and vitrinite) in standard oil of $n = 1.515$ caused difficulties of positive identification. To circumvent this problem, an index oil adjusted to $n = 1.60$ was compounded from 1-bromonaphthalene and cedarwood oil. The mixture provided sufficient differences in reflectivity between macerals for meaningful quantification.

Each layer sample was characterized on the basis of organic entities identified at 500 points using the Chayes method (*1*, *2*). Total bed or seam composition was then calculated by multiplying maceral percentages obtained by the thickness of the layer (in inches), adding the totals, and dividing the sum by the total thickness of the bed. The method of data handling is illustrated in Figure 1. The total seam average was determined from nine layer samples (500 points each) which contribute disproportionate amounts to the seam average. In this example, therefore, 4500 points were necessary to determine the composition of the whole bed.

Results

Table I summarizes the petrography of the Upper Freeport coal examined at five sites shown in Figure 2. Earlier detailed study in the region of the type section (*7*) established a persistence of beds over a distance of 23 miles (sites 1, 2, and 3 in Table I and Figure 2). Irregularities of the basal portion of the coal were not sufficient to obscure the analytical results of the main bed. The petrographic characteristics of mined coal was significantly altered when an overlying bed (F coal) was included as "Upper Freeport" coal. The coal at these three sites are high volatile A bituminous in rank.

Near Coral (site 4, Figure 2 and Table I) there is a repetition of the so-called "Thick Freeport" coal which includes the F coal. There are no significant quantitative petrographic changes between the coal at this site and the sites 22 miles or more to the west. The coal rank at this location is medium volatile bituminous. Reflectivity is greatly increased however. Although no analyses were made, a third patch of "Thick Freeport" coal occurs immediately southwest of the Houtzdale quadrangle (site 5 in Figure 2), suggesting that

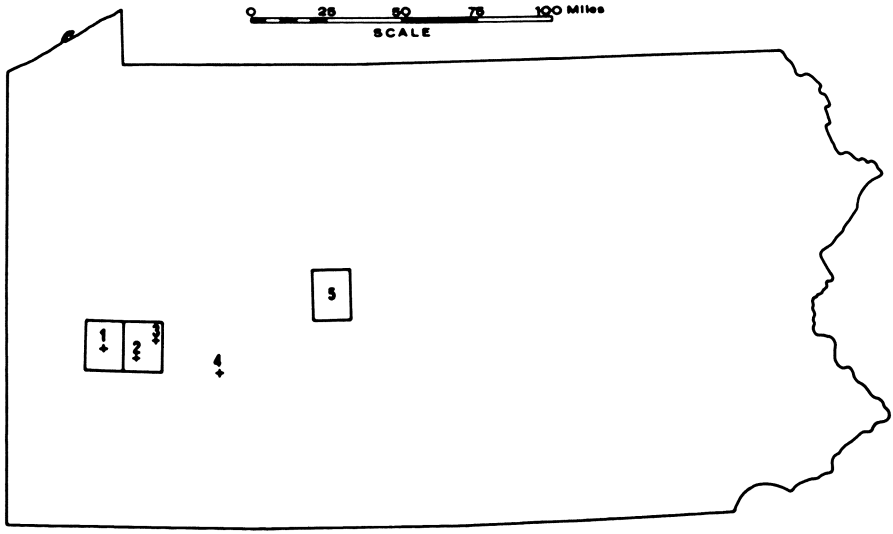

Figure 2. Sample locations—Upper Freeport coal; 1—Harmar Mine, 2—Springdale Mine, 3—Armstrong Mine, 4—Coral strip mine, 5—Houtzdale quadrangle area

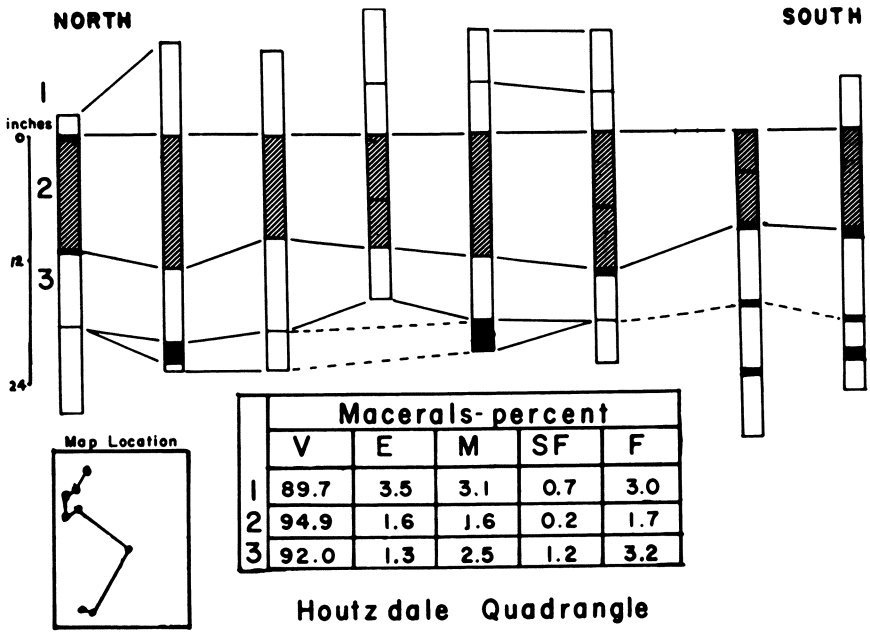

	Macerals-percent				
	V	E	M	SF	F
1	89.7	3.5	3.1	0.7	3.0
2	94.9	1.6	1.6	0.2	1.7
3	92.0	1.3	2.5	1.2	3.2

Houtzdale Quadrangle

Figure 3. Correlation of Upper Freeport coal beds in Houtzdale quadrangle by layers having similar petrographic analyses

Publication Date: January 1, 1966 | doi: 10.1021/ba-1966-0055.ch006

the coal, 20 feet over the Upper Freeport coal of the region, is the same bed analyzed as the upper bed of the "Thick Freeport" complex. Petrographic results shown in Table I support this contention. Average analyses of eight columns of medium and low volatile coal are given for the quadrangle rather than a single column. The data are in agreement between all sites over a distance of 80 miles virtually unaffected by changes in rank.

Within the Houtzdale quadrangle, an area of approximately 226 square miles, examining the layers within the coal beds leads the writer to suggest that most of the Upper Freeport coal here was deposited at the same time. The petrographic characteristics of three layers, correlated in Figure 3, are recorded in Table II. Differences in composition between layers are slight but generally sufficiently diagnostic to distinguish one layer from another. Many of the coals were at least partially weathered. Since weathered coal is difficult to quantify precisely, this might account for the spread of data within individual layers.

Figure 4 illustrates the coals of the Lower Kittanning formation in the Houtzdale quadrangle. In much of western Pennsylvania only one coal is mined as the Lower Kittanning coal (Figure 1). Here, however, there are five beds which may be mineable, at least locally. Most of the beds differ from

Table II. Petrographic Composition of Selected Layers of Upper Freeport Coal

Layer No.	*Column*	*Vitrinite*	*Exinite*	*Micrinite*	*Semifusinite*	*Fusinite*
1	23	88.4	2.2	3.8	0.6	5.0
	28	89.6	2.8	3.4	0.8	3.4
	8[b]	92.8	1.2	2.8	—	3.2
	89	89.2	4.6	2.4	0.4	3.4
	27	88.4	2.9	3.1	0.6	5.0
	61	89.0	5.3	3.1	1.4	1.2
	83[a]					
	84	91.4	1.8	5.0	1.0	0.8
	Average	89.7	3.5	3.1	0.7	3.0
2	23	91.0	2.4	2.2	1.0	3.4
	28	96.4	1.6	0.8	—	1.2
	8[b]	98.4	0.4	1.2	—	—
	89	95.5	1.4	1.3	0.4	1.4
	27	94.8	1.2	2.0	—	2.0
	61	95.0	2.4	1.4	—	1.2
	83	95.6	1.9	1.4	—	1.1
	84	92.8	1.6	2.2	0.4	3.0
	Average	94.9	1.6	1.6	0.2	1.7
3	23	94.0	1.4	1.6	—	3.0
	28	93.6	2.0	1.6	0.8	2.0
	8[b]	91.4	0.6	2.0	2.0	4.0
	89	90.4	0.4	3.2	2.0	4.0
	27	92.0	1.0	3.8	0.2	3.0
	61	92.0	1.8	3.0	0.2	3.0
	83	94.2	2.0	1.4	—	2.4
	84	89.0	1.2	3.2	2.6	4.0
	Average	92.0	1.3	2.5	1.0	3.2

[a] Absent
[b] Badly weathered

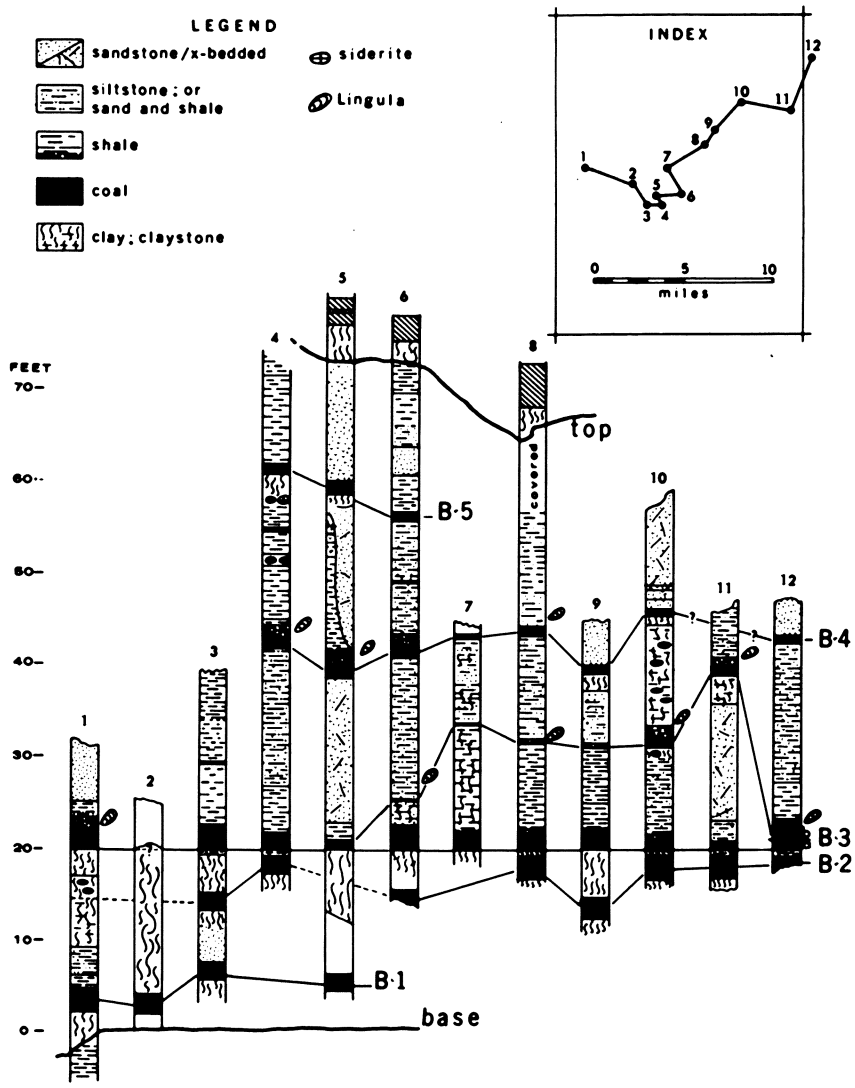

Figure 4. Complex of coal beds in the Lower Kittanning formation of the Houtzdale quadrangle

one another petrographically as shown in Table III. Some of the differences are subtle. For example, beds 1 and 2 were separated primarily as a function of their exinite-micrinite ratios.

When unit B-3b is missing, beds 3 and 4 cannot be recognized solely by quantitative petrography. Here, supplementary geological information is required to effect sensible correlations. Although total bed data yield results which indicate petrographic continuity, layer-by-layer studies indicate that

Publication Date: January 1, 1966 | doi: 10.1021/ba-1966-0055.ch006

Table III. Petrographic Composition of Beds in the Lower Kittanning Coal Complex, %

Bed	Sample No.	Vitrinite	Exinite	Micrinite	Semi-fusinite	Fusinite	Ash	Thickness, inches
B–5	15	84.2	3.1	3.1	2.0	7.6	12.3	20
	69	90.2	1.3	2.8	2.3	3.4	12.5	14
	74	87.0	2.4	3.1	1.0	6.5	17.5	9
	Average	87.1	2.3	3.0	1.8	5.8	14.1	
B–4	11	92.7	2.7	3.5	0.4	0.7	9.5	12.5
	14	90.5	3.6	3.9	0.9	1.1	11.4	11
	48	93.9	4.6	1.1	—	0.4	3.5	9
	49	95.4	2.0	1.5	0.1	1.0	6.9	11
	68	92.8	4.0	1.4	0.3	1.5	3.1	11.5
	73	94.2	4.0	1.5	0.1	0.2	5.4	12.5
	Average	92.2	3.5	2.2	0.3	0.8	6.6	
B–3b	4	88.0	5.8	5.0	0.2	1.0	16.5	9
	13	88.8	4.2	5.5	0.5	1.0	6.0	17
	18	83.0	5.4	7.0	0.6	4.0	6.6	14
	40*	87.9	5.1	3.0	1.6	2.4	8.6	22
	81	81.6	8.6	4.6	—	5.2	8.4	4
	75	84.2	8.8	4.8	0.6	1.6	13.8	6
	82	87.9	4.0	3.7	0.7	3.7	4.6	14
	95-C-lb	88.5	3.9	3.8	1.4	2.4	5.2	13
	Average	86.2	5.7	4.7	0.7	2.7	8.0	
B–3a	2	92.0	3.0	2.6	0.6	1.8	3.5	12
	3a	92.0	4.4	2.0	—	1.6	4.4	9
	17a	92.6	4.2	2.5	—	0.7	10.0	6
	33	93.0	2.4	2.5	—	2.1	8.8	16
	34	94.4	1.9	2.3	0.7	0.7	5.8	20
	35a	91.5	2.8	3.0	1.3	1.4	6.6	21.5
	40*	91.2	3.6	3.2	0.4	1.6	8.2	6
	45	91.3	3.3	2.6	0.3	2.5	3.8	20
	47	92.5	3.5	2.0	0.9	1.1	5.9	17.5
	57	91.9	3.3	2.6	0.9	1.3	6.5	21.5
	60	91.1	3.2	2.3	0.8	2.6	6.6	23.5
	67	93.1	3.2	2.3	0.3	1.1	4.5	22
	72	91.0	3.7	2.1	1.2	2.0	5.6	23
	75*	92.0	2.4	2.2	1.2	2.2	6.3	26.5
	81*	91.7	3.0	2.0	0.1	3.2	7.4	14
	91	94.0	2.2	2.5	0.3	1.0	7.5	22
	95-C-1a	92.8	2.7	1.9	0.8	1.8	9.2	12.5
	Average	92.2	3.1	2.4	0.6	1.7	6.5	
B–2	3b	86.5	4.3	4.7	0.9	3.6	9.1	30.5
	17b	83.9	4.5	4.9	1.4	5.3	12.0	27.5
	35b	80.5	4.7	6.1	1.7	7.0	16.0	22.5
	46	87.6	3.7	3.7	1.6	3.4	12.8	26
	56	85.3	3.7	4.9	1.2	4.9	11.5	17.5
	Average	84.7	4.2	4.9	1.4	4.8	12.3	

Table III. Continued

Bed	Sample No.	Vitrinite	Exinite	Micrinite	Semi-fusinite	Fusinite	Ash	Thickness, inches
B–1	32	87.4	1.9	4.9	0.9	4.9	8.6	21
	51	83.8	2.9	5.4	1.9	6.0	12.1	25
	55	87.8	2.5	3.7	2.2	3.8	6.1	21
	80	87.2	2.4	4.2	1.4	4.8	10.0	48.5
	Average	86.5	2.4	4.6	1.6	4.9	9.2	

• Partial

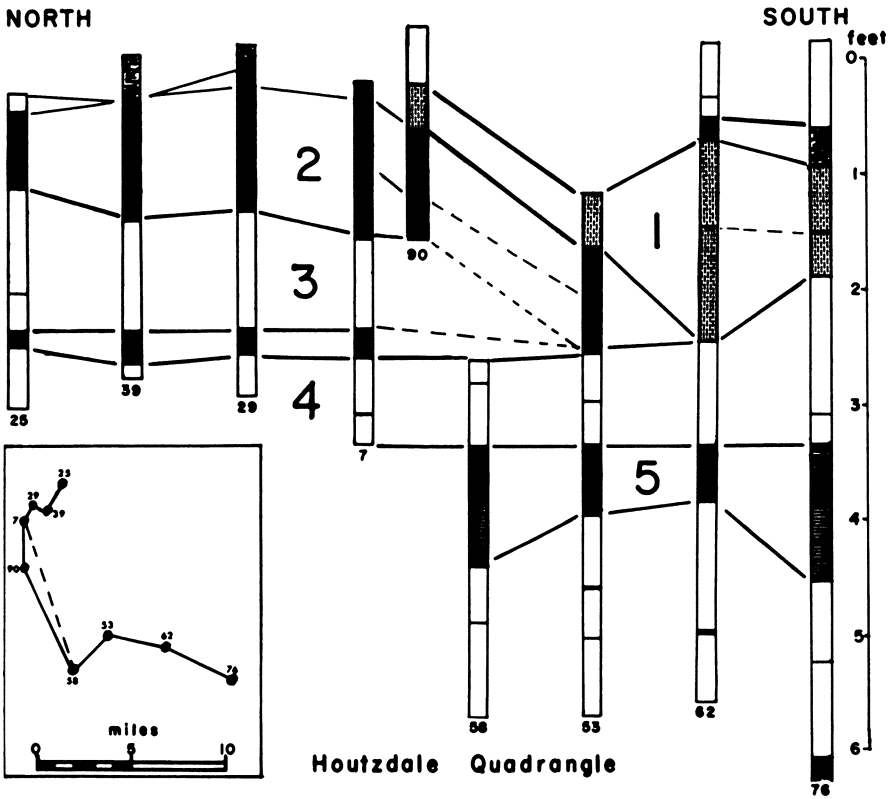

Figure 5. Correlation of layers in the Lower Freeport coal of the Houtzdale quadrangle

relationships within the beds are very complicated. The writer has had only limited success correlating specific layers of the Lower Kittanning coals for more than a few miles in one direction or another. Layer continuity does, nevertheless, seem to be better along the trend of the present geological structures than across the structures. This phenomenon is better discussed in connection with the Lower Freeport coal.

Three major northeast-southwest trending structural features are present in the quadrangle. These are: (1) the Clearfield syncline to the northwest, (2) the Laurel Hill anticline with a few coals remaining on the structure, and (3) the Houtzdale syncline in the southeast. Figure 5 illustrates correlations made in the Lower Freeport coal from the Clearfield syncline across the anticline and into the Houtzdale syncline. Relatively uniform layer-by-layer petrographic continuity was found between columns 25, 39, 29, and 7 (Table IV and Figure 5) in the Clearfield syncline area. Troublesome dissimilarities were found when the above results were compared with results from coals collected to the southeast in the Houtzdale syncline area.

Layers 2 and 3 contribute the bulk of coal in most of the Clearfield syncline. Generally speaking, layer 4 at the base of the coal is not particularly well developed. Eight miles to the southeast, layer 4 is the uppermost layer preserved in the vicinity of column 58. Although closer, column 90 was collected on the flank of the anticline. This column contains none of the layers

Publication Date: January 1, 1966 | doi: 10.1021/ba-1966-0055.ch006

Table IV. Petrographic Composition of Selected Layers of Lower Freeport Coal

Layer	*Column*	*Vitrinite*	*Exinite*	*Micrinite*	*Semifusinite*	*Fusinite*
1	90	77.4	2.2	1.2	1.6	17.6
	53	75.8	2.6	8.8	4.6	8.2
	62	77.6	2.0	11.2	—	9.2
	76	76.0	2.8	10.2	4.3	6.0
	Average	76.7	2.4	8.0	2.6	10.3
2	25	88.8	2.0	4.1	1.3	3.8
	39	87.4	3.3	4.5	1.5	3.3
	29	88.0	2.0	6.6	1.0	2.4
	7	86.7	0.8	6.0	1.2	5.3
	90	84.6	3.6	4.9	1.5	5.4
	53	82.5	2.6	4.5	4.4	6.0
	Average	86.3	2.4	5.1	1.8	4.4
3	25	91.3	1.5	2.9	0.2	4.1
	39	90.6	2.4	3.6	2.2	1.2
	29	90.4	2.0	3.2	0.2	4.2
	7	87.4	1.2	4.4	0.6	6.4
	Average	89.9	1.8	3.5	0.8	4.0
4	25	92.0	1.2	4.2	0.8	1.8
	39	85.6	2.4	5.4	1.6	5.0
	29	87.8	1.8	5.0	1.0	4.4
	7	89.7	1.2	4.7	1.5	2.9
	58	93.0	1.2	3.7	0.7	1.4
	53	90.2	1.6	4.3	0.8	3.1
	62	92.8	—	4.0	1.0	2.2
	76	89.7	1.1	2.9	1.2	5.1
	Average	90.0	1.3	4.3	1.2	3.2
5	58	92.9	0.9	2.1	0.2	3.9
	53	93.2	3.2	1.2	1.0	1.4
	62	95.8	1.2	0.6	0.4	2.0
	76	92.8	2.2	1.4	0.8	2.8
	Average	93.7	1.9	1.3	0.6	2.5

found in the sample to the southeast and only the upper layers found elsewhere in the Clearfield syncline. The normal underclay sequence was present beneath the coal. Although sought, no evidence was found that layers 3 or 4 were deposited at this site. Layer 1 was encountered in most Lower Freeport coal of the Houtzdale syncline but only at the top of column 90 in the northwestern part of the quadrangle. The unit is characterized by a high inert maceral concentration (total of micrinite, semifusinite, and fusinite). The writer suspects that layers 1, 2, and 3 were deposited in the vicinity of column 58 and that they were subsequently removed by erosion. It is possible that the coal represented by column 58 was deposited in another swamp basin; however, two of the three missing upper layers were recognized in column 53 collected nearby in the same synclinal basin. Examining the layers correlated in Figure 5 and the average maceral composition of the layers listed in Table IV largely explains why Lower Freeport coal mined in the northwest part of the study area should not be expected to have the same properties as coal mined in the southeast.

Publication Date: January 1, 1966 | doi: 10.1021/ba-1966-0055.ch006

Conclusion

The quantitative maceral analyses presented above are used to demonstrate petrographic continuity of coals from place to place. The examples used were selected to emphasize different aspects of regional and local situations. Problems encountered in the Houtzdale quadrangle illustrate that some measure of continuity can be established locally in spite of rapid changes in thickness and character of the coal beds involved.

Petrographic continuity of layers may reflect widespread simultaneous deposition of a given maceral composition. If this is true, it is probable that physical and chemical aspects of the peat swamp are more significant factors than local floristic similarities in establishing the organic composition of the layer.

It is neither intended nor implied that the above technique can supplant normal geological data for identifying the major coal horizons. Indeed, much work remains to be done to learn why some Pennsylvania coals yield uniform analyses over great distances and why others, though widespread, can be related only locally through detailed examination of the layers within them.

Literature Cited

(1) Chayes, F., *Am. Mineralogist* **34**, 1 (1949).
(2) Chayes, F., "Petrographic Modal Analysis," Wiley and Sons, New York, 1956.
(3) Hacquébard, P. A., *Mededel. Geol. Sticht. Nederlands*, Ser. C, **3**, Pt. 2, No. 1, 1 (1943).
(4) Hacquébard, P. A., *Geol. Surv. Canada, Bull.* **19**, 1951.
(5) Hacquébard, P. A., *Conf. Origin Const. Coal, 2nd*, **1952**, Nova Scotia, 293.
(6) Koppe, E. F., *Trans. A.I.M.E.* **217**, 185 (1960).
(7) Koppe, E. F., *Pa. Geol. Survey*, 4th Ser., **M–48** (1963).
(8) Marshall, C. E., Draycott, A., *Univ. Sydney Dept. Geol. Geophys. Memoir* **1** (1954).
(9) Roos, G., *Compte Rend. Congr. Avanc. Études Stratigraph. Carbonifèr. 2^e*, **1935**, Heerlen, 1057.
(10) Taylor, G. H., Warne, J., *Proc. Intern. Congr. Coal Petrology, 1st*, **1960**, 75.

RECEIVED April 19, 1965. Published with permission of the State Geologist.

Discussion

Peter A. Hacquebard: It is interesting to note that material evaluations rather than microscopic analyses of the natural bands (microlithotypes) are used in this study. In so doing, the natural stratigraphic sequence within the coal bed is not considered. For geological studies the latter is of great importance, permitting correlation of coal seams and studies of facies changes.

Edwin F. Koppe: There is no doubt that studying the microlithotypes would be extremely helpful. Producing such data is, however, very time consuming. This study of more than 90 profiles was conducted by myself with the help of one assistant in the course of one and a half years, and pressing needs for the data determined the methods employed.

Gilbert H. Cady: Were the measurements of maceral distributions made from columns or from broken coal samples?

Mr. Koppe: From broken coal samples.

Duncan G. Murchison: Could Mr. Koppe tell us how many points were counted in the maceral analyses quoted? In the absence of any deviations on the figures, it would seem that to allow a significant difference between 2.6 and 4.2%, for example, the number counted would have to be very high.

Mr. Koppe: 500 points were counted from pellets of —30 mesh coal for each layer. Thus, the maceral analyses for total coal beds are variable. In some profiles, as few as 1500 points were used; in others 4000 or more. On the total bed basis, I think the difference quoted is significant.

Marie-Therese Mackowsky: Have you ever looked at polished rocks cut parallel to the bedding plane? In this case you could see the effect of transport better than in rocks cut perpendicular to the bedding plane.

Mr. Koppe: This was not done, but it would be helpful to do so. The coal examined is highly fractured in the bed. Often samples were scooped up with a thin paint spatula. Studying oriented block material was impractical for the area in the time available.

Publication Date: January 1, 1966 | doi: 10.1021/ba-1966-0055.ch006

7

Electron Paramagnetic Resonance Studies of Humic Acid and Related Model Compounds

CORNELIUS STEELINK

Department of Chemistry, University of Arizona, Tucson, Ariz.

Humic acids from soils and lignites have been examined by EPR spectrometry. All samples showed a stable free organic radical content of about 10^{18} spins per gram. When these samples were converted to their sodium salts, a marked increase in radical content occurred. This was interpreted to indicate that a quinhydrone moiety exists in the humic acid macromolecule. Synthetic humic acid, prepared by oxidizing catechol in the presence of amino acids, also showed similar EPR spectra, as did selected quinhydrone model compounds. The radical moiety appeared to be stable to severe oxidation and hydrolytic conditions. Reduction in basic media caused an initial decrease in radical species; continued reduction generated new radical species. A proposed model for humic acid based on a hydroxyquinone structure is proposed.

Publication Date: January 1, 1966 | doi: 10.1021/ba-1966-0055.ch007

Since the time of Berzelius, chemists have proposed structures for the amorphous, black substance known as "humic acid." In the past 150 years, much experimental work has appeared on the nature of humic acid, most of it based on classical chemical and microbiological studies. Very little information about the molecular structure of humic acid has resulted from these studies however. Some of the problems plaguing investigators in this field have been (a) variation in the source of humic acid, (b) variation in the definition of humic fractions of soil and coal, (c) lack of crystallinity of the samples, (d) uncertainty of molecular weight measurements, (e) variation in extraction techniques, and (f) variation in elemental composition. The little unambiguous information that exists today is based on extensive degradation of the humic acid polymer and represents only a small fraction of the total molecule.

In recent years investigators have turned to physical methods of analysis in an attempt to elucidate the structure of the undegraded humic acid. These methods have included coagulation studies (*16*), potentiometry (*5*, *21*), pola-

In Coal Science; Given, P.;
Advances in Chemistry; American Chemical Society: Washington, DC, 1966.

rography (*15*), infrared and ultraviolet spectrophotometry (*6, 7, 9, 10, 16, 24*), chelation studies (*14*), NMR spectrometry (*2*), molecular weight measurements (*20*), electron microscopy (*8*), differential thermal analysis (*19*), and other methods. Some of the recent studies are listed in Table I.

Table I. Physical Chemical Methods of Analyzing Humic Acid

Method	*Reference*
Coagulation Threshold	Kononova
Potentiometry	Pommer van Dijk
Polarographic Reduction	Kinney
Infrared Absorption Spectrophotometry	Elofsen Farmer Scharpenseel
Ultraviolet Absorption Spectrophotometry	Kononova Flaig (9)
Molecular Weight	Piret
Differential Thermal Analysis	Mitchell
Chelation Studies	Khanna
NMR Studies	Barton (2)
Electron Microscopy	Flaig (8)

In 1960 Rex (*22*) first reported the use of electron paramagnetic resonance spectrometry as a method for demonstrating the presence of stable organic free radicals in humic acid. We felt that this technique might provide useful information about the structure of humic acid which was not readily available by other physical methods, particularly if relations between EPR spectra and chemically modified humic acids could be demonstrated. Our preliminary studies (*26*) confirmed this presumption.

Experimental

Spectra. All EPR measurements were made with a Varian 100 kc. modulation spectrometer. Spin concentrations were estimated by comparison with solid diphenylpicrylhydrazyl. Numbers of radicals were assumed to be proportional to signal height times width squared. Temperature dependence plots were obtained by controlling the temperature of the resonance cavity with cooled or heated nitrogen. Signal intensities of the temperature plot were estimated by comparing with the intensity of the sample at 25°C.

All infrared absorption spectra were taken with a Beckman IR-4 spectrophotometer on potassium bromide pellets.

Samples. Samples were obtained from the sources listed in Table II.

Extraction. Humic acids were extracted from their sources with 1*N* sodium hydroxide. The solution was acidified with sulfuric acid, and the resulting precipitate was dried under vacuum at room temperature. Fulvic acid was obtained by evaporating to dryness the neutral filtrate from the humic acid mixture.

Sodium Salts. The sodium salts of all samples were prepared by dissolving a given weight of humic acid in 1*N* aqueous sodium hydroxide. Adding a tenfold excess of absolute ethanol to the basic solution precipitated the salt which was filtered, washed with ethanol, and dried at room temperature in

Publication Date: January 1, 1966 | doi: 10.1021/ba-1966-0055.ch007

Table II. Humic Acid Samples and Their Sources

Sample	*Source*
English podzol	Cheshire Forest, B_2 horizon, Cheshire, England
Swiss muck	Extracted from chestnut soil, by Fluka Co., Buchs S. G., Switzerland
Wisconsin podzol	Department of Soils, University of Wisconsin, Madison, Wis.
NALCO Leonardite	Nalco Co., Chicago, Ill.
North Dakota Leonardite	U.S. Bureau of Mines, Grand Forks, N. D.
New Mexico lignite	Surface mine near Farmington, N. M.

vacuo. Preparing these salts in an atmosphere of nitrogen did not change their spin concentrations appreciably from salts prepared under aerobic conditions. The sodium salts of the model hydroxyquinones were prepared in the same manner as above.

"Artificial Catechol Humic Acid." This was prepared by K. B. Roy, Department of Macromolecules, Indian Association for the Cultivation of Science, Calcutta, India, by the air oxidation of catechol in the presence of various amino acids.

Reducing Humic Acid. To an aqueous alkaline solution of humic acid under nitrogen were added stepwise weighed portions of sodium amalgam, according to the procedure of Farmer (7). After each sodium amalgam portion had reacted, an aliquot of this solution was removed and immediately poured into an excess of ethanol. The resulting precipitate was dried under vacuum. The concentrations reported in Figure 7 are those of the sodium salts.

Results and Discussion

Solid samples of soil humic acid gave a single line spectrum (Figure 1) at "*g*" values very close to 2.00. The intensity of the signal corresponded

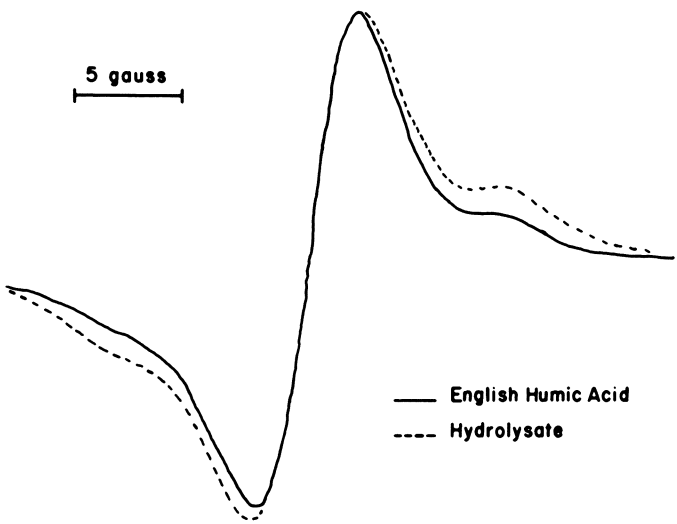

Figure 1. Spectra of English humic acid and hydrolysate

Publication Date: January 1, 1966 | doi: 10.1021/ba-1966-0055.ch007

roughly to 10^{18} spins per gram. Numerous fractionation experiments, including vigorous acid hydrolysis, showed no decrease in spin content. Thus, the radical species was apparently not a contaminant. A survey of various soils by EPR spectrometry indicated the presence of a stable organic free radical in approximately the concentration represented by the humic acid fraction; this indicated that the radical species was not an artifact of the extraction procedure. A temperature dependence study is shown in Figure 2. This suggested that two types of radical species exist in the macromolecule (*26*).

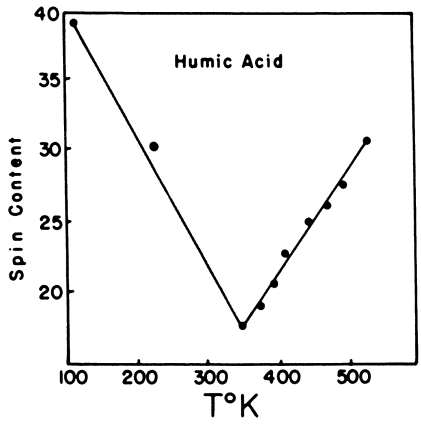

Figure 2. Spin content vs. *temperature for humic acid*

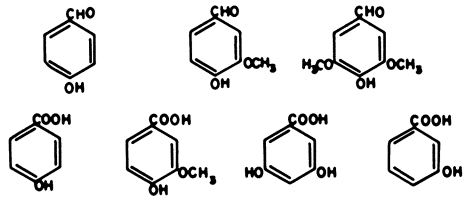

Figure 3. CuO oxidation products for soil humic acid; Farmer (7) and Steelink (13)

Our preliminary proposals, based on the above results, suggested that a stable semiquinone radical species existed in the humic acid molecule along with a noninteracting quinhydrone species. Therefore, we began to assess a number of possible model compounds for humic acid. These models should represent structures which are consistent with the chemical evidence in this field. Degradative work in our laboratory (*13*) and in many other laboratories had shown the presence of the molecular fragments in humic acid as shown in Figures 3 and 4. Flaig (*11*), on the basis of extensive studies with model phenolic systems, had already proposed a partial structure for humic acid (Figure 5). Flaig's model, as well as the chemical evidence, implies the

Publication Date: January 1, 1966 | doi: 10.1021/ba-1966-0055.ch007

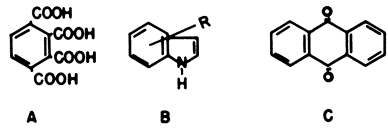

Figure 4. Degradation products of humic acid; A—Schnitzer (25), B—Flaig (11), C—Kumada (17)

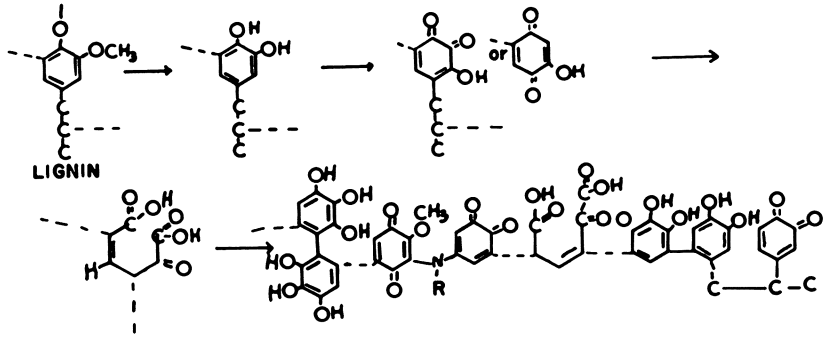

Figure 5. Possible formation of humic acid from lignin; Flaig (11)

existence of catechol and hydroquinone moieties as well as their quinoid and hydroxylated derivatives. Our attention was directed to simple compounds which could contain such structural features.

One of the most striking properties of humic acid is its change in free radical content upon conversion to the solid sodium salt. This change is reversible: upon reacidification of the salt, the spin content returns to its original level (*28*). In general, the line widths increased about 50% on conversion to the salt. Table III illustrates this effect for many different humic acids. These results seem entirely consistent with the known properties of the salts of quinhydrone as shown in Figure 6 (*28*).

Table III. Free Radical Content of Humic Acids and Salts

Humic Acid	*Acid Spins/gram**	*Sodium Salt Spins/gram**	*Increase Factor*
English podzol	0.2	10	50
Swiss muck	0.6	24	40
Wisconsin podzol	0.7	18	26
Wisconsin podzol, fulvic fraction	0.4	0.7	2
NALCO Leonardite humic acid	0.4	6.6	16
North Dakota Leonardite humic acid	0.4	30	75
New Mexico lignite humic acid	2.8	37	12
Artificial catechol-amine humic acid	2.3	54	23

* Spin content $\times 10^{18}$

Publication Date: January 1, 1966 | doi: 10.1021/ba-1966-0055.ch007

Stabilization of a radical anion of humic acid may be caused by an adsorption effect. Bijl (*3*) observed that solid barium hydroxide octahydrate turned blue when placed in a solution of quinhydrone; the blue solid was highly paramagnetic. Under the conditions we used for preparing these salts, insoluble sodium humate (with a large surface area) could have stabilized the anion radical by adsorption from the basic solution. Weiss and McNeil (*18*) observed a similar phenomenon with base soluble xanthenes, and proposed that biradicals may be formed in such a system. His compounds, however, do not appear to have the structural requirements to satisfy such a stabilized system. The recent report by Weber (*29*) on the spin content increase associated with the basification of a naphthoquinone-naphthohydroquinone system seems to parallel our observations quite closely.

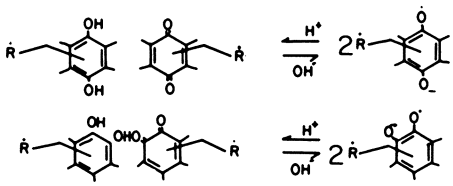

Figure 6. Proposed quinhydrone models for humic acid; R=semiquinone radical

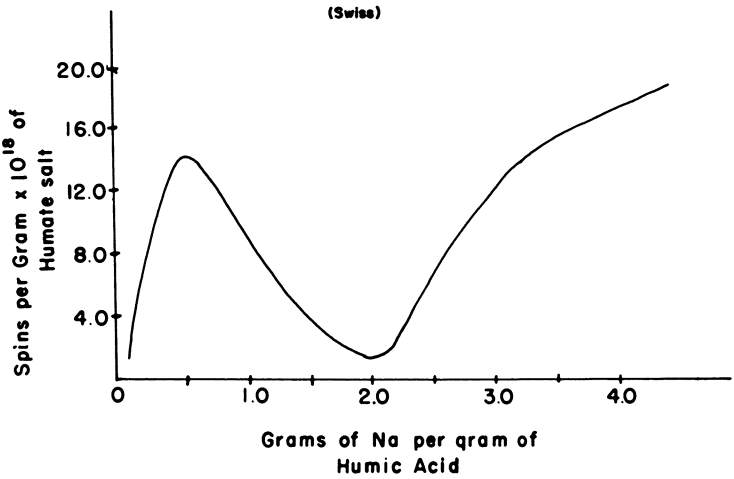

Figure 7. Stepwise reduction of humic acid

Stepwise chemical reduction of humic acid caused a variation in spin content as shown in Figure 7. The initial rise in radical content is attributed to anion radical formation caused by sodium; the following decrease in spin content with further addition of sodium is probably caused by the reduction of these anion radicals. The subsequent increase in radical content could be caused by the one-step reduction of the remaining quinone moieties.

Publication Date: January 1, 1966 | doi: 10.1021/ba-1966-0055.ch007

Controlled electrolytic reduction of humic acid and hydroxyquinones in dimethylformamide in our laboratory (*27*) have shown small initial decreases in spin content followed by an increase up to the first half-wave potential. Since this was carried out in the absence of base, it would correspond to the portion of the curve in Figure 7 after the first maximum. The probable series of competing reactions is illustrated in Figure 8. Austen and co-workers (*1*) have observed similar behavior in coal extracts that were electrolytically reduced.

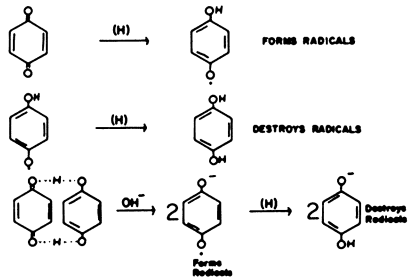

Figure 8. Reduction of model compounds

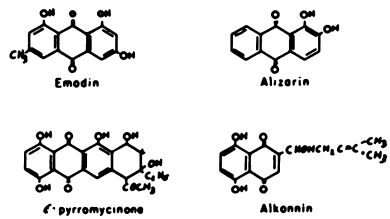

Figure 9. Some naturally occurring hydroxyquinones

All of the above effects can be rationalized on the basis of intermolecular charge transfer systems—i.e., by systems composed of quinone groups of one polymeric chain lying close to hydroquinone groups of an adjacent chain. It occurred to us that perhaps intramolecular quinhydrones might also behave in this manner. Certainly, a number of hydroxyquinones occur naturally, in plants and microorganisms and could be incorporated into the humic acid molecule at some stage of its formation. Some examples of these compounds are shown in Figure 9.

An EPR spectral survey of a selected number of hydroxyquinones showed that they all formed stable radical salts which could be reversibly converted to the acid form of low or negligible spin content. Significantly, many of these hydroxyquinones were stable free radicals in the acid form although the radical content was quite low (Table IV).

Publication Date: January 1, 1966 | doi: 10.1021/ba-1966-0055.ch007

Table IV. Free Radical Content of Some Hydroxyquinones and Their Salts

Sample	Acid Spins/gram*	Salt Spins/gram*	Increase Factor
Emodin	0.03	21	700
Alizarin	0.02	450	22500
ε-Pyrromycinone	0.00	8.6	
Alkannin	0.28	9.3	33
(Quinizarin-2-sulfonic acid)	0.74	140	196

* Spin content × 10^{18}

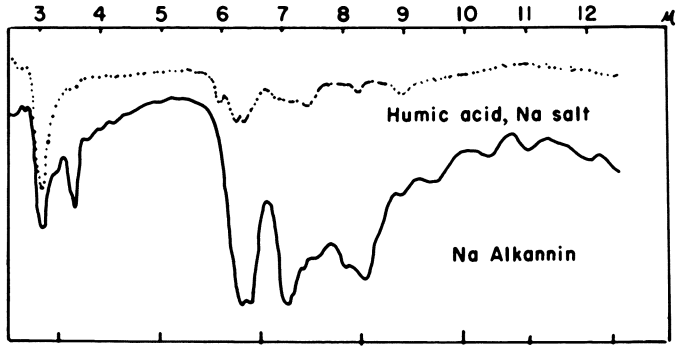

Figure 10. Infrared spectra of sodium salts

In these compounds, free radical centers could arise from intramolecular charge transfer complexes, yielding a biradical such as shown in Figure 11. Alternately, in the solid state, monoradicals could be formed by intermolecular charge transfer between two molecules (Figure 11). The experimental evidence for the presence of biradicals in these systems is very inconclusive (a small signal in the $g = 4.0$ region) and at any rate, represents only a minute fraction of the signal at $g = 2.00$. Therefore, the major contribution to the unpaired spin content probably arises from monoradicals created by intermolecular charge transfer. This phenomenon has been extensively studied by Russell and associates (*23*) in other systems. They have shown that when oxidized and reduced functional groups are present in the same system, radical anions can be created and stabilized by strong base.

The infrared absorption spectra of hydroxyquinone salts indicated strong bands in the 6.0–6.4 μ region as do many of the humic acid salts (Figure 10). Bands in the region 6.35–6.40 μ have been assigned to phenoxy radicals (*4*). Those in the 6.3 μ region correspond to complex hydroxyquinones (*4*) or carboxylate ion (*6*). Unambiguous assignment of functional groups from such IR spectra is not possible; however, the similarity of the spectra of humic acids and the models would indicate closely related structural features.

On the basis of the results cited above, we propose that the species in humic acids responsible for its paramagnetism is a charge transfer complex as described in Figure 11. The presence of an easily ionizable phenolic proton

Publication Date: January 1, 1966 | doi: 10.1021/ba-1966-0055.ch007

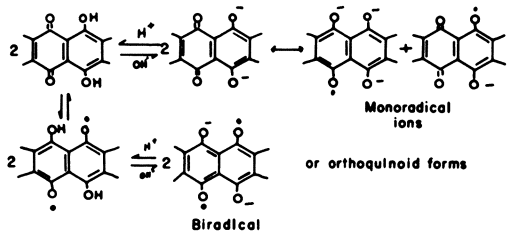

Figure 11. Proposed radical formation in hydroxyquinones

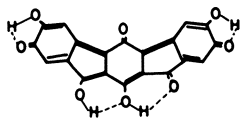

Figure 12. Anthraxylic acid; after Gillet (12)

in the molecule adjacent to a quinoid moiety stabilizes the radical anion upon basification. A rough estimate places the number of spin centers at one per molecule in the salt or a minimum of one charge transfer system per molecule. While one cannot develop a complete formula from these data, it is interesting to note that both Flaig's (*11*) complex formulation and Gillet's (*12*) simple formula (Figure 12) would possess the structural features compatible with this paramagnetic behavior.

Literature Cited

(1) Austen, D. E. G., Given, P. H., Ingram, D. J. E., Peover, M. E., *Fuel* **38,** 309 (1959).
(2) Barton, D. H. R., Schnitzer, M., *Nature* **198,** 217 (1963).
(3) Bijl, D., Kainer, H., Rose-Innes, A. C., *Nature* **174,** 830 (1954).
(4) Chandross, E. A., Kreilick, R., *J. Am. Chem. Soc.* **86,** 118 (1964).
(5) Dijk, H. van, *Sci. Proc. Roy. Dublin Soc.*, Ser. **A1,** No. 4, 163 (1960).
(6) Elofsen, R. M., *Can. J. Chem.* **35,** 926 (1957).
(7) Farmer, V. C., Morrison, R. I., *Sci. Proc. Roy. Dublin Soc.*, Ser. **A1,** No. 4, 85 (1960).
(8) Flaig, W., Beutelspacher, H., *Z. Pflanzenernähr. Dung. Bodenk.* **52,** 1 (1952).
(9) Flaig, W., Scheffer, F., Klamroth, B., *Z. Pflanzenernähr. Dung. Bodenk.* **71,** 33 (1955).
(10) Flaig, W., Schobinger, U., Deuel, H., *Chem. Ber.* **92,** 1973 (1959).
(11) Flaig, W., *Suomen Kemistilehti* **33A,** 229 (1960).
(12) Gillet, A., *Brennstoff-Chem.* **37,** 395 (1956).
(13) Greene, G., Steelink, C., *J. Org. Chem.* **27,** 170 (1962).
(14) Khanna, S. S., Stevenson, F. J., *Soil Sci.* **93,** 298 (1962).
(15) Kinney, C. R., Love, D. L., *Anal. Chem.* **29,** 1641 (1957).
(16) Kononova, M. M., "Soil Organic Matter," Pergamon Press, New York, 1961.
(17) Kumada, K., Suzuki, A., Aizawa, K., *Nature* **191,** 415 (1961).
(18) McNeil, R., Weiss, D. E., *Australian J. Chem.* **12,** 643 (1959).
(19) Mitchell, B. D., *Sci. Proc. Roy. Dublin Soc.*, Ser. **A1,** No. 4, 105 (1960).
(20) Piret, E. L., White, R. G., Walther, H. C. Jr., Madden, A. J. Jr., *Sci. Proc. Roy. Dublin Soc.*, Ser. **A1,** No. 4, 69 (1960).

Publication Date: January 1, 1966 | doi: 10.1021/ba-1966-0055.ch007

(21) Pommer, A. M., Breger, I. A., *Geochim. Cosmochim. Acta* **20,** 30 (1960).
(22) Rex, R. W., *Nature* **188,** 1185 (1960).
(23) Russell, G. A., Strom, E. T., *J. Am. Chem. Soc.* **86,** 744 (1964).
(24) Sharpenseel, H. W., Albersmeyer, W., *Z. Pflanzenernähr. Dung. Bodenk.* **88,** 203 (1960).
(25) Schnitzer, M., Wright, J. R., *Soil Sci. Soc., Amer. Proc.* **24,** 273 (1960).
(26) Steelink, C., Tollin, G., *Biochim. Biophys. Acta* **59,** 25 (1962).
(27) Steelink, C., Haines, D., unpublished work.
(28) Tollin, G., Reid, T., Steelink, C., *Biochim. Biophys. Acta* **66,** 444 (1963).
(29) Weber, M. M., Hollocher, T. C., Rosso, G., *J. Biol. Chem.* **240,** 1776 (1965).

RECEIVED October 5, 1964.

Discussion

Peter Given. I do not think the radicals in bituminous coals can be oxygen radicals similar to these you describe in soil and peat humic acids since acetylation does not change the signal. Acetylation can be shown by IR spectra to be virtually complete.

Cornelius Steelink. It is possible that other systems may give rise to the radical species. However, one of our models for humic acids is a biradical

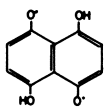

whose radical character would not be changed on acetylation. Our humic acids change very little in spin content on methylation. It would be interesting to form sodium salts from your coals to see if the spin content increased. This would be fairly convincing evidence for oxygen radicals.

Kulai A. Kini. Is there any experimental evidence showing whether the ESR behavior is subject to an oxygen effect? Can one be reasonably sure that the humic acids did not undergo chemical change (possibly altering the free radical concentration) during drying and/or oxygen removal?

Dr. Steelink. The oxygen effect can be ruled out by the following evidence:

(1) Samples made under air and under nitrogen showed little difference in spin concentration.
(2) Samples show high spin concentration when placed in aqueous base.
(3) The magnitude of the spin concentration would rule out trace oxygen effects.
(4) EPR analysis of unextracted soil shows definitely that an organic radical is present in approximately the same concentration as in the isolated humic acid. Thus extraction procedures do not create the radical.

Wolfgang Flaig. You formulated the hydroxyquinone radical as an oxygen radical. Do you observe ether linkages after polymerization?

Dr. Steelink. Although the proposed radical species were written with the unpaired electrons on oxygen (as above and in the ionic state: these electrons are extensively delocalized, and a number of canonical forms can be written with the unpaired electrons on carbon. The electron on oxygen is favored only because of its resemblance to well established phenoxy radicals such as galvinoxyl.

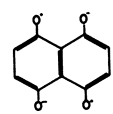

Dr. Flaig. To what extent do your suggestions about radical formation agree with the investigations of M. Eigen *et al.* (*Chem. Ber.* **34,** 3309 (1961))?

Dr. Steelink. Our proposals for radical ions in humates are entirely consistent with the proposals for the formation of hydroxy semiquinone radical ions of Eigen.

Robert A. Friedel. What is your interpretation of the fine structure indicated by your EPR spectrum.

Dr. Steelink. The possible presence of a second radical species or perhaps a chelated form of the first species. We have had a little more luck with alkaline solution spectra of humic acid where three or four lines are evident.

George Kapo. What do you think is the relation between humic acids produced by the oxidation of bituminous coals and the humic acids you worked with?

Dr. Steelink. We have not worked with humic acids from bituminous coals. In general, the carbonyl and phenolic content of an oxidized coal would be the most important structural properties in contributing to EPR phenomena such as we have described.

Loren Hill. Did you observe any change in line width and/or *g*-value on chemical treatment?

Dr. Steelink. The line is narrower under acid conditions. No large variation in *g*-value was observed.

Publication Date: January 1, 1966 | doi: 10.1021/ba-1966-0055.ch007

Analysis and Paragenetic History of Anthraxolite in Ordovician Slate, Eastern Pennsylvania

GEORGE R. STEVENS

Department of Geology, Lafayette College, Easton, Pa.

Publication Date: January 1, 1966 | doi: 10.1021/ba-1966-0055.ch008

Anthraxolite in the Martinsburg slate of eastern Pennsylvania was deformed in Taconic time with the enclosing rock and was probably upgraded to its high present rank at low temperatures early in its history. X-ray diffraction and thermal studies indicate that it has a fair degree of graphitic ordering which improves with thermal annealing and devolatization. It responds to heating more like bituminous substances than like anthracite, indicating that the few volatiles present are low temperature residual types. A clastic origin of the nodules is not supported by the geologic evidence. It is more likely that a viscous, humic parent substance seeped into cavities in the sediments soon after their deposition in the still, deep geosynclinal environment. The existence of anthraxolite and similar substances in rocks of all types and ages throughout the world suggests a continuous, common process.

Slate workers in eastern Pennsylvania quarries have long encountered hard, siliceous "knots" on some cleavage slabs of the slate. Such knots destroy the uniform cleavage, and render the host slate unsuitable for commercial use. During 1963, slate splitters at one of the quarries began to encounter unusual knots containing what appeared to be coal in addition to the usual quartzose matrix (Figure 1). These were called to my attention, and several specimens were provided.

The rarity of the coal-like material in the slate is indicated by the fact that only about 50 nodules have been found during a two-year period. These were all taken from the same portion of one quarry, and all have similar characteristics.

In Coal Science; Given, P.;
Advances in Chemistry; American Chemical Society: Washington, DC, 1966.

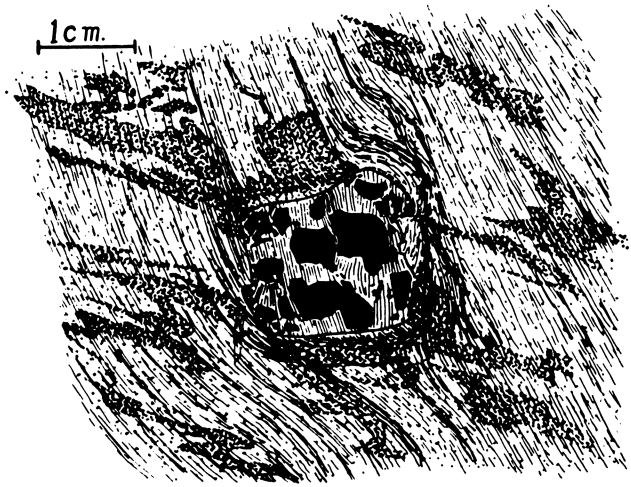

Figure 1. Anthraxolite-bearing nodule in slate, seen on cleavage surface. "Exploded" anthraxolite fragments are engulfed in matrix of quartz and calcite intergrown in comb structure which parallels the tectonic a-lineation of the slate. Darker bands are distorted carbonaceous primary laminae. (Compare with Figure 3.)

The coal-like material has been analyzed and identified as "anthraxolite," a term introduced by Chapman in 1871 (*6*) for anomalous anthracite-like carbon found in veinlets and cavities in Ordovician slates of Ontario and Quebec. The name has since been applied by others to similar veinlets and masses of anthracite-like material found in anomalous host rocks.

Location and Geologic Setting

The anthraxolite-bearing nodules have been found only in the Stoddard Slate Quarry at Pen Argyl, in Northampton County, Pa. (Figure 2). The Pennsylvania "slate belt" consists of the eastern end of the outcrop band of the Ordovician Martinsburg formation, and most of the quarries are situated in this district between the Delaware and the Lehigh Rivers, close to the northern margin of the belt. Blue Mountain (Kittatiny of New Jersey), comprised of Silurian sandstones and conglomerates, marks the northern boundary of the Martinsburg formation. A broad valley underlain by Cambrian and Ordovician limestones and dolomites extends along the south margin. The whole district comprises the southeastern margin of the Valley and Ridge Province of the Appalachian Mountains.

Regional deformation has been extremely complex and intense. Strata have been tightly folded about ENE-trending axes, with nappe-like recumbent folds and thrusts developed in places. Cleavage, especially well developed in the more argillaceous strata, dips to the south at low angles, approximately parallel to axial planes of folds. Cleavage is most perfect in the slate, a consequence of the fine grain size of the original sediment and conditions of defor-

Publication Date: January 1, 1966 | doi: 10.1021/ba-1966-0055.ch008

mation. The slaty character of the Martinsburg formation decreases westward from the vicinity of Allentown as the rock there has been less affected by the metamorphism and deformation which upgraded the parent shale into slate. The slate belt continues northeastward through New Jersey into New York and Vermont but with irregularities in the patterns of metamorphism. Commercial slate occurs only in a few areas within the entire slate belt.

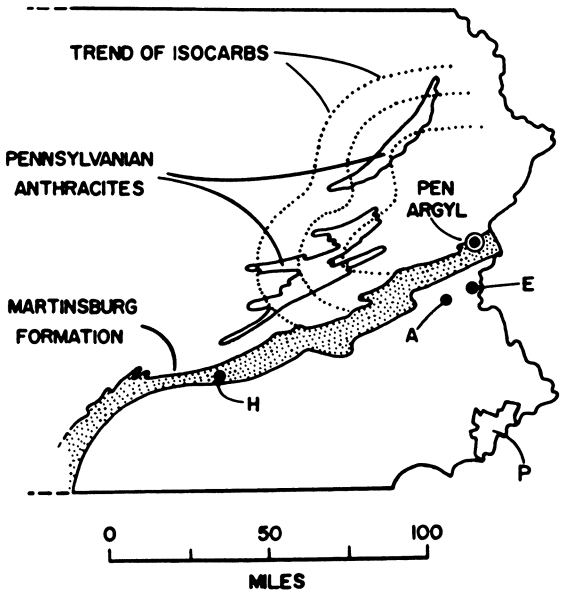

Figure 2. Outline map of eastern Pennsylvania showing extent of Martinsburg formation (stippled), anthracite coal fields, and general trend of isocarbs. Principal cities shown are: H, Harrisburg; A, Allentown; E, Easton; and P, Philadelphia. Anthraxolite locality at Pen Argyl, slate belt

Previous Work

Many authors have studied anthraxolite and related substances since Vanuxem's first account in 1842 (*39*). It has been reported as cavity fillings, veins, and dikes and as laminations in rocks of all geologic ages and types on all continents (e.g., *1*, *15*, *20*, *31*, *32*, *37*, *38*). Except for obvious cases of contact metamorphism near igneous intrusions, earlier workers have generally recognized a fluid origin and low temperature history for these substances.

Dunn and Fisher (*13*) provided a detailed study of New York anthraxolites in 1954, which led, on chemical grounds, to the conclusion that anthraxolite was genetically related more to coal than to oil. Dietrich (*12*) attempted to clarify the relation of anthraxolite to coal and oil using several different analytical approaches, but his results were not conclusive. In 1963, King (*23*) reviewed the general problem of origin of anthraxolite and concluded that it

Publication Date: January 1, 1966 | doi: 10.1021/ba-1966-0055.ch008

was highly aromatic early in its history, fractionated and migrated under aqueous conditions, and was derived from some primary sedimentary organic matter.

The present study is an attempt both to characterize the Martinsburg anthraxolite and to determine its origin and geologic history. Such findings bear directly on the complex question of the metamorphic and structural history of the Martinsburg slate, the metamorphism of coals and carbonaceous sediments in general, and suggest the possible use of anthraxolite and related substances as geologic thermometers for enclosing rocks which have undergone metamorphism.

Character of the Slate

The nodules are found in gray-black commercial slate having fine grain size, uniform color and texture, and well developed slaty cleavage. Such slate occurs in thick strata marked only by thin black bands ("ribbons") of somewhat coarser texture, and by rare, disseminated "knots," siliceous nodules of foreign material. The slate is a mixture of quartz, illite, chlorite, calcite, and muscovite, with minor amounts of pyrite, carbonaceous matter, and heavy mineral grains. The dark color is attributed to finely disseminated carbon and pyrite. An analysis of the slate is given in Table I.

Table I. Analysis of Pen Argyl Slate *(2)*

SiO_2	57.50
Al_2O_3	20.84
Fe_2O_3, FeO	3.51
MgO	3.02
CaO	3.92
Na_2O	1.25
K_2O	3.36
CO_2	3.30
C	0.57
FeS_2	1.39
Ignition loss	0.15
	98.80

The slate contains 0.5% organic carbon, consisting of opaque black "amorphous" carbon and both saturated and aromatic hydrocarbons. The relatively high ratio of saturated to aromatic hydrocarbons (Table II) is a consequence of metamorphic fractionation. Original saturated compounds were evidently more stable than the aromatics and were thus destroyed at a slower rate during metamorphism.

Table II. Organic Analysis of Martinsburg Slate, Stoddard Quarry, Pen Argyl, Pa.[a]

Organic Carbon	0.5 wt.%
Total Benzene Extract	70.7 p.p.m.
Saturated Hydrocarbons	43.6 p.p.m.
Aromatic Hydrocarbons	8.4 p.p.m.
Nonhydrocarbons	18.7 p.p.m.
Sat./Arom. Ratio	5.1

[a] Analysis by Marathon Oil Co.

Publication Date: January 1, 1966 | doi: 10.1021/ba-1966-0055.ch008

There may be a genetic relationship between the organic substances of the slate and the anthraxolite nodules, but clarification of this rests on future studies.

The Nodules

Anthraxolite. The anthraxolite occurs as acorn-size nodules engulfed in a quartz-calcite matrix as "knots" on the cleavage slabs of the slate. Specific gravity (by toluene displacement) ranges from 1.543 to 1.577, placing it well within the anthracite range. The masses tend to have original elongation parallel to bedding but are also flattened into the cleavage, a condition typical of particles in deformed rocks. The anthraxolite has undergone cataclasis into an "exploded" pattern. Cracks and intervening spaces have been filled with a mixture of quartz and calcite in columnar array (Figure 3).

Broken surfaces have a brilliant, glassy luster and are jet-black in color with a perfect conchoidal fracture. Remnants of the precataclasis bounding surface of each nodule retain a dull luster owing to a closely pitted, etched surface. Maximum size of the composite nodule ranges up to 5 cm. but can be as little as 0.5 cm.

Microscopic examination reveals no structures or texture, except for rare stellate groupings of acicular microlites (4 × 18μ) on some fracture surfaces of the shards. These prismatic crystals, which may be organic, radiate from aggregates of particles too small for resolution. They are partially imbedded in the anthraxolite and are not fissure fillings.

Examination of flame-etched surfaces revealed only scattered torus-shaped ring and moat structures, 100–200μ in diameter. These features probably result from differential resistance of anthraxolite and rare impurities to oxidation.

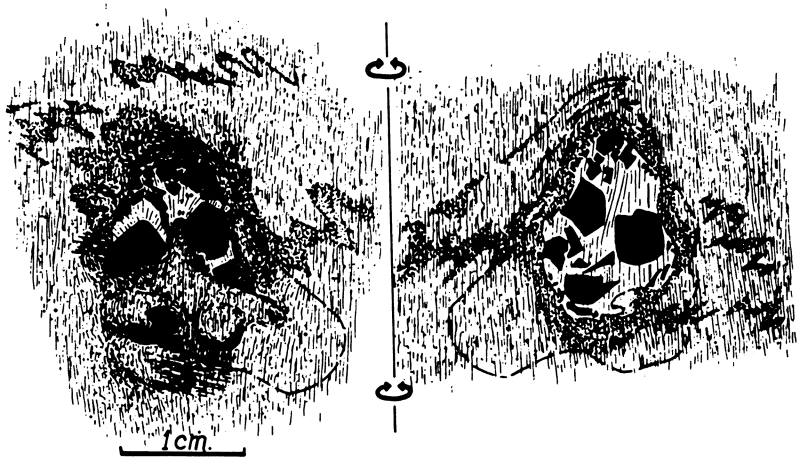

Figure 3. Front and rear views of anthraxolite nodule in cleavage slab 1 cm. thick. Broken line is internal configuration of nodule. Distortion of primary laminae is related to presence of nodule

Pyrite was found in only two specimens, forming roseate "flowers" flattened onto the surface of a microfissure. Thin films of quartz or calcite are the usual material filling such incipient fractures.

The Matrix. Between 50 and 60% of the composite nodule consists of a matrix of quartz intergrown with calcite in "comb" or columnar structure. Prisms of these minerals are oriented into general parallelism with the tectonic *a*-lineation normal to fold axes. This orientation also characterizes all other elongate mineral grains and aggregates in the slate proper, a consequence of the mechanics of cleavage development. Quartz is more abundant than calcite, and prisms of each are uniformly distributed through the bundle of rods which comprise the matrix. Dark calcite predominates, however, in the shell adjacent to the slate, where the prismatic habit is replaced by the more usual rhombohedral habit. Such crystals are also twinned. Two generations may be represented in this bimodal distribution of twinned rhomboidal and untwinned prismatic calcite. Microcrystalline pyrite occurs as irregular patches in the shell calcite adjacent to the slate walls in many of the nodules. It is rare or absent within the matrix proper.

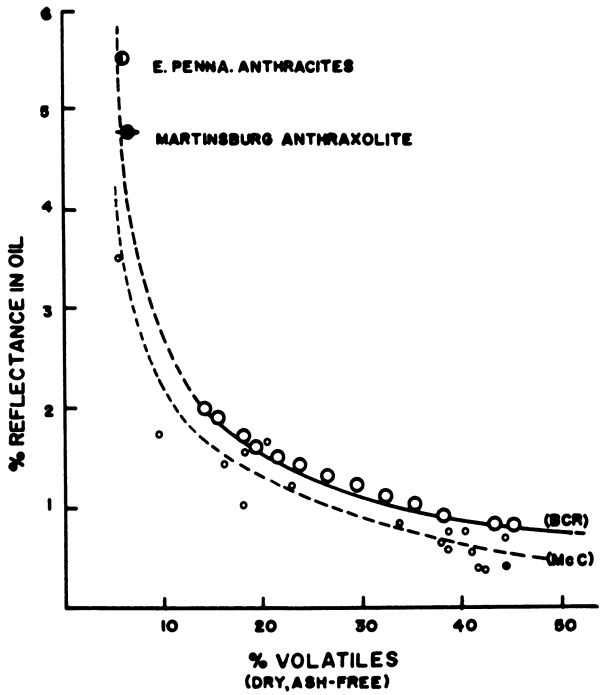

Figure 4. Relation between volatile content and reflectance of coals. Solid curve (BCR) by Bituminous Coal Research, Inc., Pittsburgh. Broken curve (McC) based on data published by McCartney (28). *Reflectance of Martinsburg anthraxolite indicates approximately 7% volatile matter*

Analysis

Optical, infrared, x-ray, thermal, and chemical studies were carried out to characterize the anthraxolite and to determine its geochemical evolution. Some differences in the same properties were noted for different nodules; hence, several nodules were pulverized together in order to have "average" anthraxolite for analyses. Sufficient material for determining compositional extremes and variation was not available. Present understanding suggests that neither properties nor composition vary widely.

Optical Tests. Curves showing the relation between percent reflectance in oil and volatile content for various coals are given in Figure 4. The measure of 4.75% for the Martinsburg anthraxolite was made against known glass and silicon carbide standards. The anthraxolite gave very uniform results, and no anisotropy was recorded. The empirical relation between reflectance and volatile content places the anthraxolite in the anthracite range, with about 93% fixed carbon indicated. This is in good agreement with the elemental analysis of the anthraxolite listed in Table III.

Infrared Absorption. Attempts to determine the nature of carbon-hydrogen bonding by means of a Beckman IR–5 infrared spectrophotometer were not successful, probably because of the near opacity of the anthraxolite and excessive scatter caused by inadequate grinding. Highly graphitized carbons are commonly opaque to infrared radiation because the absorption edge of electronic excitation occurs in the infrared range.

Chemical Analysis. Preliminary attempts to extract hydrocarbon components from the anthraxolite by means of toluene were unsuccessful, even though several percent of nitrogen, oxygen, and hydrogen are known to be present. Table III lists the elemental analysis of anthraxolite blended from five different nodules. Results were reproducible, and the deviation from 100% is thus thought to represent some systematic error.

Table III. Analysis of Martinsburg Anthraxolite[a]

	As Analyzed %	*Adjusted, Ash free* %
Carbon	91.18	94.66
Hydrogen	1.55	1.61
Nitrogen (Kjeldahl)	0.64	0.67
Oxygen (direct)	2.90	3.02
Sulfur	0.03	0.04
Ash (as oxide)	1.00	
	97.30	100.00

[a] Analysis by Gulf Oil Co.

X-Ray Diffraction. Powder samples of a single nodule and of several nodules combined gave patterns very similar to those of anthracite (Figure 5). The anthraxolite pattern is broader in the principal peak region, with a pronounced secondary band near 22.5° 2θ which is absent from the anthracite pattern. This suggests a wider variation in particle or crystallite sizes present in the anthraxolite.

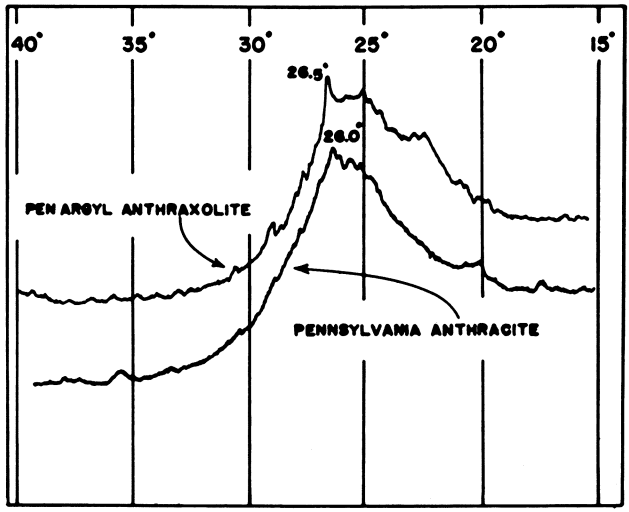

Figure 5. X-ray diffractograms of principal band region for Martinsburg anthraxolite and Pennsylvanian anthracite coal. Main peak at 26.5° 2θ is probably caused by graphitic structure, not quartz. Principal difference between patterns is subordinate anthraxolite band at 22.5° 2θ, not present in anthracite record. Copper Kα radiation. (Compare with Figure 9.)

Crystallite Dimensions. A possible relation between the interlayer spacing of turbostratic graphitic layers and the length of such incipient crystals in the *c*-axis direction (L_c) was proposed by Blayden, Riley, and Taylor (*4*) for carbonized coals. (Their results are generally considered now to be too high.) Interlayer spacings derived from principal peaks of the anthraxolite diffractogram indicate that partially ordered packets of carbon atoms having *c*-axis lengths of 7, 8, 13, 17, and 46 A. are common in the distribution (Figure 6). The 3.35 A. peak, representing packets of 46 A. length is that of pure graphite.

Figure 7 shows several curves which have been proposed to relate carbon content of coals to the *a*-axis crystallite size (*4, 5, 11, 19, 24*). Curves I and II are based on criteria now superseded and are considered to be obsolete. From these data, layer diameters between 8 and 9 A. are suggested for the anthraxolite (94% C). Since these values are close to the *c*-axis lengths (which as reported above may be too large), it is felt that typical crystallites of the anthraxolite may be nearly equidimensional cylinders.

As in many other anthracitic substances, diffuse bands also appear near 43° and 80° 2θ. These represent two-dimensional (*hk*) reflections only since the turbostratic disorder of graphitic layers which characterizes "amorphous" carbons does not permit (*hkl*) three-dimensional atomic planes other than (001). Hirsch (*19*) proposed that the position of the (11) band was a function of carbon content of the sample, related to the crystallite layer diameter (L_a). With increasing rank, the (11) reflection shifts towards smaller 2θ values, representing greater bond lengths and larger crystallite size. Using values

Publication Date: January 1, 1966 | doi: 10.1021/ba-1966-0055.ch008

established by Hirsch as guides, the main (11) peak of the Martinsburg anthraxolite (79° 2θ) indicates a mean layer diameter of about 14 A. and about 94% carbon, most of which is probably in the ordered form. This is a somewhat larger size than given above based on other methods. Minor peaks within the (11) band indicate groups of platelets having diameters (L_c) of 7, 8, 11, 12, 16, 26, and 36 A. in addition to the more abundant 20 A. size class.

Effect of Heat Treatment. Thermal techniques were used to determine retentivity of volatile components and the response of the anthraxolite carbon to thermal reordering. Powdered anthraxolite samples were held 80 minutes at 600°C. and 60 minutes at 1200°C. in nonoxidizing environments and analyzed by x-ray diffraction. Comparison of before and after diffractograms revealed a shift towards greater d-spacing (smaller 2θ values) in the 2-A. peak vicinity (Figure 8), and a surprising intensification of the diffuse (102) graphite band position. This suggestion of ordering is supported by exothermic reactions in the vicinity of 600°C. determined by differential thermal analysis. An anticipated corresponding shift in the position of the (11) band was not recorded.

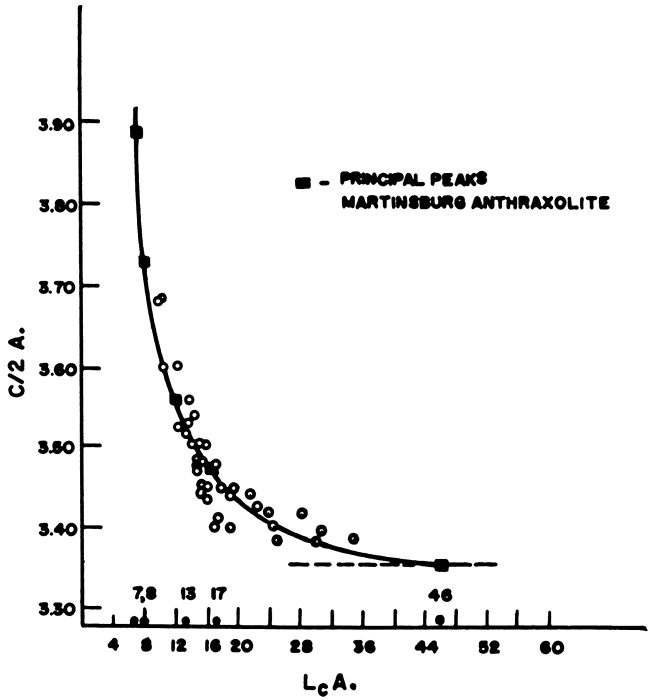

Figure 6. Relation between interlayer spacing (c/2) and size of carbon crystallites in c-axis direction (L_c), in Angstrom units. Black squares represent positions of minor peaks within the principal anthraxolite (002) band region, which correspond to the values of L_c indicated. Curve after Blayden, Riley, and Taylor, (4)

Publication Date: January 1, 1966 | doi: 10.1021/ba-1966-0055.ch008

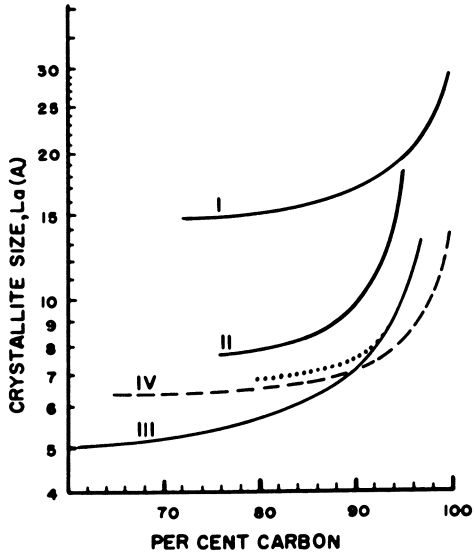

Figure 7. Relations between carbon content and crystallite layer diameter (L_a) in Angstroms. Curve I after Blayden, Riley, and Taylor (4); curve II after Hirsch (19); III after Cartz and Hirsch (5). Curve IV is a synthesis of data from Diamond (11) and MacFarlane (24). Dotted portion of curve III represents vitrains only. Assuming 94% fixed carbon for the Martinsburg anthraxolite, value of L_a should be between 8 and 9 A.

The asymmetry of peak shape is preserved in anthraxolite heated to 1200°C. showing that turbostratic disorder persists in spite of a general enhancement of ordering. The band is also sharper and narrower. This may be interpreted to mean either that fewer class intervals are represented in the crystallite size distribution or that increased ordering of aromatic lamellae has reached the point where graphite (*hkl*) planes are more common. Diffraction peaks of both (100) and (101) fall with the 2-A. band.

The shape and main peak position of the (002) band change markedly in the samples heated to 1200°C. though heating to 600°C. only has little effect. Figure 9 contrasts these features for unheated and heated anthraxolite samples. Heating suppresses the separate 22.5° band, other minor peaks, and the main 25.5° band. The center of gravity of the distribution does not change, remaining centered at about 24.5° 2θ. These changes reflect ordering of carbon crystallites towards a closer, more nearly graphitic spacing. Fewer class intervals in the total size distributions for L_c corresponds to a similar reduction for size classes of L_a, based on the changes noted in the 2-A. band.

Expulsion of volatiles during 600°C. heating amounted to 2.9 weight percent, approximately half of the volatile content, and virtually all volatiles were expelled from anthraxolite heated to 1200°C. It would appear that re-

Publication Date: January 1, 1966 | doi: 10.1021/ba-1966-0055.ch008

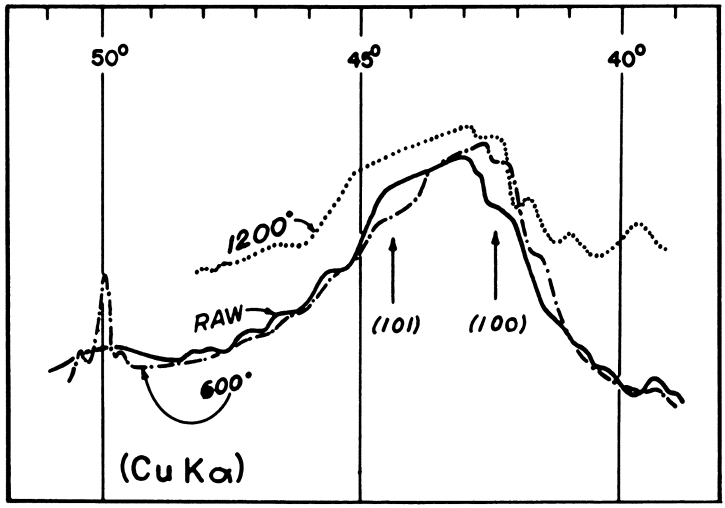

Figure 8. Partial x-ray diffractogram of Martinsburg anthraxolite. Change in shape and position of the 2–A. peak after heat treatments to 600° and 1200°C. Positions of (101) and (100) of graphite are indicated. Copper Kα radiation

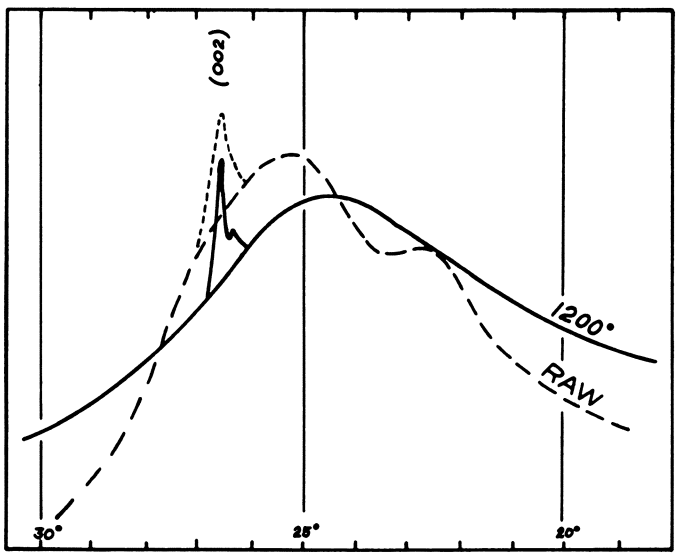

Figure 9. Change in shape (generalized) of the principal x-ray diffraction band of Martinsburg anthraxolite after heating to 1200°C. for 1 hour. Subordinate peak at 22.5° 2θ is eliminated by heating. Curve becomes more symmetric but center of gravity of the band does not change from 24.5°. Copper radiation. (Compare with figure 5.)

Publication Date: January 1, 1966 | doi: 10.1021/ba-1966-0055.ch008

lease of these volatiles was accompanied by some form of aromatic condensation towards graphitic ring structure, probably with lateral layer growth as edge hydrocarbons were expelled. This is suggested by the data in Figure 7, which show a rapid increase in crystallite diameter (L_a) with increasing carbon content.

Differential Thermal Analysis. Several nodules were pulverized, blended, and stored for 6 months. Samples of this material were then heated in a DuPont 900 differential thermal analyzer to 1200°C. in partial vacuum, nitrogen, and low oxygen atmospheres. Thermal behavior was compared with that of a freshly powdered, single nodule specimen heated in a nitrogen atmosphere. Records were made during both programmed heating (15°C. per minute) and free cooling. Approximately 45 mg. of the powdered anthraxolite were packed into a thin-walled platinum cup 3 mm. in diameter and 4 mm. deep. This cup was then sealed over the thermocouple in such a way that it was forced into the sample, which was then tamped by means of a piston. Calcined alumina beads provided the reference material, packed into an identical cup 0.5 cm. away from the first. A 1.5-cm. diameter quartz tube enclosed both cups and thermocouples and provided a closed system for atmosphere control. This assembly fitted inside a Kanthal wound cylindrical furnace. All tests were programmed at the same heating rate and scale factors.

Oxidizing Atmosphere Thermograms. Thermogram traces for two specimens allowed to oxidize during heating are shown in Figure 10. The solid trace shows both exothermic and endothermic peaks representing oxidation,

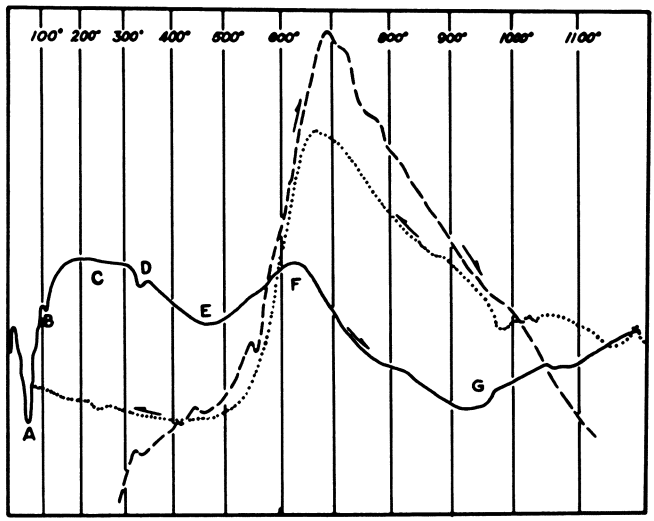

Figure 10. Records of differential thermal analyses of Martinsburg anthraxolite under limited oxidizing conditions. Solid and dotted traces are heating and cooling records of same samples heated in partial vacuum. Broken trace is thermogram of sample heated in nitrogen-enriched air

Publication Date: January 1, 1966 | doi: 10.1021/ba-1966-0055.ch008

volatile loss, and probable graphitic ordering. The sample was heated at low pressure (50 mm. Hg) to 700°C. Above 700°C. the vacuum was held below 1 mm. Hg. The deep endothermic peak at point A is caused by dehydration below 100°C. Expulsion and possible burning of combustible volatiles (CO?) is shown by the broad exotherm at C. Clegg (8) reported both peaks, and attributed oxidation to occluded air. Inflections at B and D appeared on other records also (Figure 11), but their cause is not known.

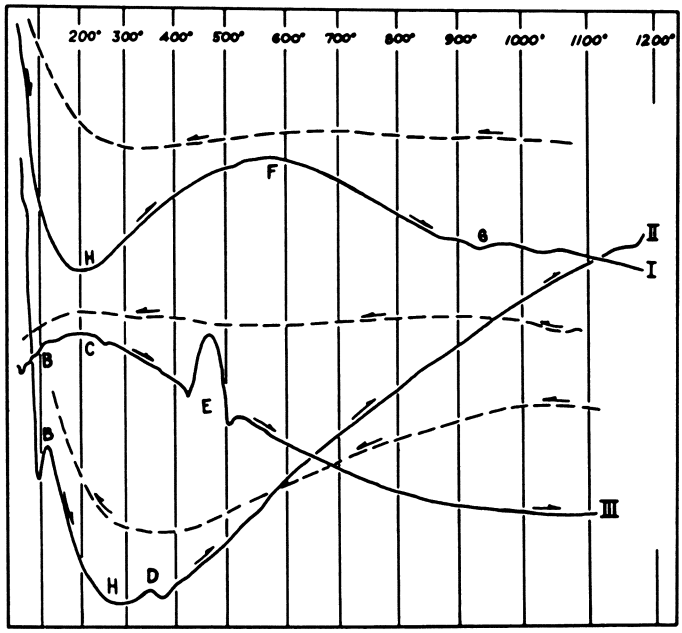

Figure 11. Records of differential thermal analysis of Martinsburg anthraxolite in nitrogen atmosphere. Trace I. single nodule freshly pulverized. Trace II, aged, blended sample. Trace III is the second heating of sample of II. Broken traces are cooling curves

Loss of volatiles occurs chiefly at about 500°C. (endotherm at point E), a process begun at about 300°C. The shallowness of the endotherm is caused by low volatile content and relative ease of gas expulsion.

If vesiculation or decrepitation took place in the carbon at this stage, the increased surface area would enhance subsequent oxidation. Such vesiculation is described by Clegg (9) for carbonized bituminous coals.

Exothermic reactions culminate at about 640°C. (point F), reflecting both accelerated oxidation and crystallite ordering. The down slope of the exothermic peak after 640°C. suggests that combustible volatiles have been depleted, and reactive surface area has been reduced. The trace then tends to reflect the general endothermic character of carbonized coals. Smothers and Chiang (34) have demonstrated that this exotherm (F) is caused mainly by

Publication Date: January 1, 1966 | doi: 10.1021/ba-1966-0055.ch008

oxidation. The peak was also suppressed from thermograms of anthraxolite run in a pure nitrogen atmosphere (Figure 11).

The high temperature endotherm at G appeared on other anthraxolite traces and is reported in coals by Smothers and Chiang (*35*) and by Glass (*16*) who attributed it to evolution of hydrogen concurrent with the beginning of graphitization (which is exothermic).

Both the high temperature endotherm between 900°C. and 1000°C., and the main oxidation exotherm are repeated during cooling (Figure 10). The slight shift of each to higher temperatures may be explained by polymerization of the preheated sample (*35*). Below 600°C. behavior remained endothermic, reinforcing the argument that the exotherm at C is caused by oxidation of low temperature volatiles by occluded air. Approximately one-half of the sample was lost by oxidation during the run.

The general configuration of the thermogram, with three main endotherms and two intervening oxidation exotherms, is similar to that reported by Glass for Michigan peat and lignite (*17*) and for Arkansas lignite, as reported by Smothers and Chiang (*34*). It is unlike the curves Glass recorded for anthracite and related substances, which have only two endotherms (at 120°C. and 620°C.) and a single exotherm at 400°C. (*18*). Glass's data were taken under experimental and atmospheric conditions comparable to my own. He derived a progressive series of thermogram styles based upon volatile content of the coal. The thermal style of the Martinsburg anthraxolite (Figure 10) is typical of that proposed by Glass for highest volatile coals and protocoals. This may mean that its volatiles are more closely related to those found in peat and lignite than to those in high carbon, metamorphosed coals. It suggests that the anthraxolite achieved its high carbon content by a process of low temperature devolatization rather than by high temperature distillation which would have destroyed susceptible hydrocarbons.

A second blended sample was heated under similar conditions, but in a nitrogen stream into which room air was bled at a moderate rate. The resultant thermogram (Figure 10, dashed curve) shows a main oxidation exotherm at 700°C. which masks any other trends. This exotherm centers at a higher temperature than for the preceding run (solid line). Inflections in the curve suggest the existence of the D, E, and G peaks seen on the preceding thermogram.

Inert Atmosphere Thermograms. Elimination of oxygen from the sample atmosphere radically alters the style of the thermograms. Suppression of the 600°C. oxidation exotherm has already been described. The low temperature exotherm centering about 200°C. (Figure 10) is also eliminated when the sample is heated in pure nitrogen. Trace I in Figure 11 is that of a single anthraxolite nodule pulverized just prior to heating. It is characterized by a major endotherm centered at 200°C. (point H), which indicates loss of volatile components early at low temperatures, continuous with dehydration (if any). This agrees with the suggestion above that the volatiles are mainly loosely bound, low temperature types such as those in peat and lignite rather than tightly bound hydrocarbon components such as are associated with true anthracites.

Publication Date: January 1, 1966 | doi: 10.1021/ba-1966-0055.ch008

The broad exotherm centered near 600°C. (point F) is in the same position as the main oxidation exotherm though no oxygen was present. The peak must therefore represent crystallite organization into more nearly graphitic configuration, masked above 600°C. by an endothermic discharge of gasses, culminated by expulsion of hydrogen at 940°C. (endotherm G).

The cooling curve for this sample is shown just above Trace I. There is practically no exothermic rise, indicating that the ordering process responsible for the exotherm during initial heating was essentially completed by 1200°C.

Traces II and III (Figure 11) represent the same sample of blended, aged anthraxolite. Trace II records the initial heating, and Trace III records the second heating 24 hours after cooling. Dehydration at 100°C. is indicated by the sharp endotherm near B on Trace II. The chief response of the sample to heating is endothermic, centering at 300°C. The general exothermic rise above 400°C. stems from the balance between endothermic release of volatiles (which apparently diminishes) and exothermic graphitization (which accelerates). The cooling curve (lowest dashed trace) conforms to the heating curve, but has lower amplitude because less crystallite growth is possible during cooling.

When heated a second time (Trace III), the sample shows a small dehydration endotherm at 50°C. owing to release of absorbed water vapor. Oxygen absorbed during storage permitted exothermic oxidation of the coked anthraxolite, chiefly at 200°C. (peak C). No indigenous volatiles remained in the sample after the first heating. The nearly flat second cooling curve (Figure 11) attests to the inert behavior of the twice-baked anthraxolite. The generally endothermic character of the second heating curve indicates that little or no graphitization took place, except at highest temperatures where the endothermic slope of the trace is nullified. The exothermic peak at 475°C. (point E) coincides with the "main volatiles endotherm" registered during vacuum heating of a previous sample (Figure 10, solid trace). Since no volatiles remained in the sample during this second heating, the peak is probably caused by experimental factors.

Salient Points of the Analyses. The high reflectance and specific gravity of the anthraxolite places it in the high carbon class with anthracite, but its extreme isotropy puts it into a different genetic class. Microscopic crystals imbedded in the anthraxolite survived metamorphic upgrading but are destroyed by the high temperatures and oxidation of flame etching. Ash, comprising only 1% of the material, is uniformly distributed throughout. About 6% of the remainder consists of volatile substances, half of which are expelled on heating to 600°C. creating perlitic decrepitation cracks. Practically all volatile substances are driven off before 1200°C.

The low ratio of hydrogen to oxygen in the anthraxolite (0.534) is similar to that of Pennsylvania anthracites though the latter have, on the average, nearly twice as much of these components.

The similarity between x-ray diffractograms of Pennsylvania anthracite and the anthraxolite suggests a common metamorphic history rather than a common origin. The dimensions of the carbon crystallites in the anthraxolite have been approximated on the basis of published relationships between crystallite dimensions, carbon contents, and interlayer spacing. These data indicate

Publication Date: January 1, 1966 | doi: 10.1021/ba-1966-0055.ch008

crystallites whose layer diameters average about 9 A. and whose stack heights average about 13 A., values in accord with low temperature thermal history.

Heat treatment of the anthraxolite led to sharpening of the diffuse diffractogram bands, probably accompanied by an increase of internal ordering, reduction in the number of crystallite size classes, and growth of individual crystallites by lateral accretion.

The primary thermal response of the anthraxolite during controlled heating in inert atmosphere is endothermic devolatization at rather low temperatures, between 200° and 300°C. At higher temperatures carbon atoms increase their organization towards graphitic structure, and hydrogen is expelled. The anthraxolite responds to heating in a way comparable to very high volatile bituminous coals, peat, and lignite and not like anthracite. This suggests that it has retained low temperature type volatiles during its development.

Publication Date: January 1, 1966 | doi: 10.1021/ba-1966-0055.ch008

Origin and Metamorphic History of the Anthraxolite

Possible Clastic Origin. The obvious participation of the anthraxolite nodules in the deformation and metamorphism of the enclosing Martinsburg slate raises the possibility of clastic origin. The fact that the carbon has been subjected to some metamorphism implies that it was formerly of lower rank than now. Hence any hypothesis of clastic origin requires a pre-Martinsburg source area for "bituminous" particles and a means of transport to the site of deposition consistent with known patterns for the Martinsburg formation. In addition, there should be supporting evidence of association with other clastic particles eroded from the same highland and carried in by the same agent and path. The post-depositional history must account for rank increase, volume reduction, and cataclasis and must agree with the mechanisms of metamorphism for the Martinsburg slate.

The slates and graywacke sandstones of the Martinsburg formation in eastern Pennsylvania constitute a metamorphosed sedimentary sequence, deposited by turbidity currents in deep water where pelagic clays were also accumulating very slowly. McBride (*27*) carefully measured paleocurrent directions throughout the present outcrop belt of the Martinsburg. He concluded that the portion in eastern Pennsylvania and in New Jersey received its sediment load from a nearby highland located southeast of the present slate belt and that sediments were carried into the deep basin by northwest and southwest moving turbidity currents.

The petrography and mineral content of the coarser sediments indicate that they were derived from a low grade metamorphic terrain undergoing rapid erosion. Rock units presently exposed southeast of the slate belt include such lithologies as quartzite, granite, amphibolite, and gneiss, in addition to the pre-Martinsburg lower Paleozoic sequence of carbonate sediments. None of these probable source rocks is known to contain carbonaceous substances in quantity, and it appears unlikely that they could have been the source of the Martinsburg nodules.

Anthraxolite and similar substances have been described from lower Paleozoic dolomites by others (*13*, *15*, *20*, *39*), in vugs, veins, and fossil

cavities. Evidence of plastic flow indicates that the original carbonaceous substance migrated into openings in these sediments some time after their consolidation into rock. If this also took place in rocks prior to Martinsburg time and if such protoanthraxolite were locally very abundant, then the older rocks (possibly including the very earliest Martinsburg sediments) could indeed have been eroded to supply clastic nodules of anthraxolite. Precambrian carbons such as Schungite are unknown in the Precambrian rocks of Pennsylvania and New Jersey though graphite occurs locally.

Carbonaceous nodules and smears reported in the Martinsburg of central Pennsylvania by McCreath (*29*) are associated with graptolite-bearing zones. This has been verified by Pierce in 1964 (personal correspondence) who identified ground-up graptolite fragments in the mylonite of a shear zone near McConnelsburg. This substance is highly bituminous and rich in volatiles and in no way resembles anthraxolite. Its age (syntectonic) is younger than the Martinsburg itself; hence it cannot have provided clastic fragments during Martinsburg deposition. On the other hand, had concentrations of graptolites and similar substances built up locally during deposition, they could well have been modified in situ by subsequent metamorphism to anthraxolite.

The probable absence of any pre-Martinsburg carbon concentrations precludes a clastic origin for the nodules. In any case, they are found in the uniform gray slate (originally mud), which was precipitated in the deep, still basin very slowly and are not associated with the clastic debris of the turbidite sequences. Turbulent conditions would have been needed for transport of such pebbles into the environment.

Epigenetic Origin of Anthraxolite—Evidence of Related Occurrences. Viscous behavior of protoanthraxolite is well attested to in the literature. Such forms as veins, botryoidal masses, cavity and vug fillings, and "frozen plastic buttons" are reputed at many anthraxolite localities (e.g., *15*, *40*). Chapman (*7*) and Hunt (*21*) each reported anthraxolite fillings in Orthoceratite shells, corals, and brachiopods. The host rocks included most of the Paleozoic sedimentary sequence through the Devonian. In all of the cases cited, the anthraxolite had very high carbon content, and was intimately associated with contemporaneous calcite and drusy quartz cavity linings.

Material similar to anthraxolite, but of lower rank, was found in amygdaloidal cavities in the Triassic basalts of New Jersey and Connecticut by Russell (*32*). Both Chapman and Hunt (*7*, *21*) listed Canadian localities where anthraxolite migrated into igneous host rocks, and Arschinow described examples from the Crimea, Siberia, Scandinavia, India, and Argentina (*1*) where quartz and calcite are also associated with the carbon.

All of the authors cited above, and several others, have described vein-anthraxolite and have pointed to epigenetic origin for it. The veins are commonly associated with quartz and calcite but in a few cases with such minerals as barite, fluorite, pyrite, copper, or even gold. The vein of albertite injected into sediments of Carboniferous age in New Brunswick is genetically comparable to the great Sudbury vein, but it is highly bituminous, and of low rank, like the West Virginia Grahamite. Such bituminous dikes may represent the protoanthraxolite not yet affected by metamorphic or diagenetic rank

Publication Date: January 1, 1966 | doi: 10.1021/ba-1966-0055.ch008

increase. In any case, the mobility and fluid nature of the anthraxolite parent substance is evident, both for veins and for small cavity fillings.

Earlier workers recognized the fluid behavior of protoanthraxolite and generally attributed subsequent rank increases to metamorphism. In those cases where the enclosing rock showed no evidence of metamorphism, rank increase had to be explained by some other, less severe diagenetic process. Hunt, for instance, explained the rank increase by a slow process of dehydration, evaporation of volatile hydrocarbons, oxidation, and volume reduction of an originally liquid bitumen in the absence of heat (*21*). He proposed that the bitumen was derived from lower forms of marine "molluscous animals" or marine vegetation in the subaqueous environment in a process similar to coalification, but which retained hydrogen. Modern studies have generally followed Hunt's ideas and elaborated on them, except in cases of obvious igneous metamorphism of earlier carbonaceous matter. The similarity of composition between metamorphic and nonmetamorphic anthraxolites shows that slow diagenesis can be as effective as relatively rapid thermal metamorphism in achieving rank increase.

Hunt, Stewart, and Dickey (*22*) in their study of the Green River shale (Eocene) found no evidence of metamorphism, and correlated the paragenesis of hydrocarbon types with salinity and H_2S content of the aqueous environment of deposition. They found natural hydrocarbons such as gilsonite, albertite, wurtzilite, and ozocerite in veins and cavities in the carbonate sediments much as anthraxolite has been described in Paleozoic rocks elsewhere. The formation of albertite, a high carbon substance characterized by condensed aromatic rings, was correlated with a dolomite-precipitating aqueous environment having relatively low salinity and H_2S content. Subsequent depth of burial to 1 mile would have achieved a geothermal temperature increase to about 70°C. at the most whereas confining pressures could not have exceeded about 400 bars. Such conditions are well below metamorphic levels. Following similar lines of evidence and reasoning for the Paleozoic carbonates of New York, Dunn and Fisher (*14*) concluded that the New York anthraxolite was formed at depths of less than a mile at a temperature near 50°C. They proposed simple dehydrogenation as the chemical path.

The possibility of low temperature generation of protoanthraxolite has been confirmed experimentally by Berl (*3*) and Schuhmacher *et al.* (*33*), who produced asphaltic and coaly substances from pure carbohydrates by heating in a weakly alkaline solution at temperatures between 230° and 340°C. Such changes evidently take place spontaneously over long time periods even in the absence of such heat.

Response of Natural Coals to Metamorphism. The Martinsburg slate and its anthraxolite have clearly been subjected to low grade metamorphism. Presuming a low temperature origin such as suggested in the preceding section, at least part of the anthraxolite rank increase must be caused by this metamorphism. In order to evaluate this contribution to rank increase, it is useful to examine known cases of metamorphism of natural coals. MacFarlane (*25*) studied the thermal effects of intruded olivine basalt sills on Yampa coals (Colorado). He carried out parallel laboratory studies in which unaltered

Publication Date: January 1, 1966 | doi: 10.1021/ba-1966-0055.ch008

samples of these coals were heated to high temperatures at standard pressures, and he recorded progressive changes in properties. The relations thus derived (Figure 12) suggest thermal limits for the protoanthraxolite of the Martinsburg, which underwent low grade regional metamorphism. If it had been of high rank comparable to anthracite prior to its metamorphism with the rock, it might have achieved the present specific gravity (1.577) after heating to only 300°C. On the other hand, if it were bituminous originally, it could have been heated to as much as 600°C. before reaching its present rank and density. From similar experimental studies of coal xenoliths taken from a peridotite dike in Fayette County, Pa., Sosman (*36*) concluded that the coal (which became coked) never exceeded a temperature of about 500°C. in the dike.

Publication Date: January 1, 1966 | doi: 10.1021/ba-1966-0055.ch008

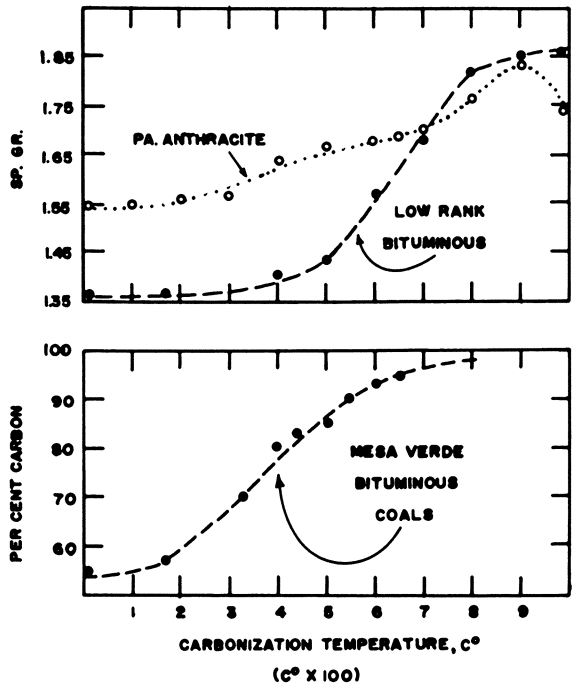

Figure 12. Relations of specific gravity and carbon content of coals to carbonization temperature. After MacFarlane (24). Dashed lines give parameters of Martinsburg anthraxolite

Such findings suggest a thermal history for the anthraxolite of temperatures up to 600°C., but these approaches neglect both the duration of heat treatment and the effect of high confining pressures, factors which could lower the maximum temperature needed to raise the rank to a given level.

Origin and History of Martinsburg Anthraxolite. The morphology of the Martinsburg anthraxolite nodules shows a history of dilation, followed by cataclasis. Quartz and calcite evidently crystallized during the dilation of the

protoanthraxolite to occupy shrinkage space as it was being created. Measurement of 15 nodules shows that the anthraxolite now occupies about 60% of the entire nodule, indicating a shrinkage of 40%. This figure agrees closely with the amount of shrinkage undergone by bituminous coals during carbonization (*25*). The existence of a dark, carbonaceous aureole in the slate adjacent to the nodules (Figures 1 and 3) also suggests a process of distillation since hydrocarbons lost from the anthraxolite during dilation may have become fixed in the adjacent clays.

In the case of the nodules found in lower Paleozoic rocks in New York, shrinkage is believed to have been minor (*13*). The quartz and calcite there crystallized before, during, and after seepage of the proto-anthraxolite into pre-existing cavities in the limestone. In the Martinsburg, however, the quartz and calcite evidently crystallized during dilation and fragmentation of the anthraxolite. Prisms of these minerals fill the gaps between the "exploded" anthraxolite fragments, attesting to their late introduction (Figures 1, 3). Parallelism of these prisms to the tectonic *a*-lineation of the slate proves that the crystallization of the quartz and calcite was controlled by the metamorphism and deformation which produced the slate.

The mineralogy of the slate and the nodule matrix offer further evidence that high temperatures have not been involved. Calcite and quartz will react to form Wollastonite ($CaSiO_3$) at temperatures above 350°C. at atmospheric pressure in the absence of water. At such pressures as exist at geosynclinal depths, the temperature of the reaction would normally increase to about 700°C. Ramberg (*30*) has shown that in "open" systems from which the CO_2 produced by the reaction is lost, the lithostatic pressure of the rocks would exceed the partial pressure of CO_2, and the reaction would proceed at temperatures *below* 350°C. even for very high confining pressures. Yoder (*42*) has shown that the presence of water in such an open system can also drastically reduce the temperature of reaction. It is likely that both CO_2 and H_2O (as CO_3^{-2} and OH^-?) were able to migrate through the Martinsburg sediments with relative ease, owing to the very high porosity and to a high degree of preferred orientation of mineral grains. Maxwell (*26*) proposed that the excellent slaty cleavage of the Martinsburg resulted from the existence of abundant pore water which enhanced grain translations and rotations. The presence of water is also proved by the abundance of hydrous minerals now in the slate.

The absence of such minerals as biotite, which could have formed at temperatures as low as 300°C., supports the assumption of a lower maximum temperature for the rock mass. Fresh chlorite, the low temperature analogue of biotite, is abundant in the slate and is unstable only at higher temperatures. In view of these things, it is proposed that the slate and the anthraxolite were heated together at great depth, to a maximum temperature between 300° and 600°C., but probably much closer to the lower value.

The Martinsburg of eastern Pennsylvania is on the southwest margin of the Taconic and Acadian Orogenic belts. It is believed to have been metamorphosed and deformed at least twice before the more general Appalachian Orogeny (Permian). Its metamorphism and slaty cleavage can be correlated with the Taconic orogeny (late Ordovician) since the cleavage and early folds

Publication Date: January 1, 1966 | doi: 10.1021/ba-1966-0055.ch008

have been deformed by the later tectonism (*26*). Moreover, the post-Taconic rocks are not metamorphosed as is the Martinsburg. The forces which produced the slaty cleavage and metamorphism also caused the fragmentation of the already brittle anthraxolite; thus, the anthraxolite must have attained its present rank and character soon after the deposition of the Martinsburg sediments, in Taconic time. This suggests that an influx of "protoanthraxolite" into rocks has been a continuous process throughout Paleozoic time since anthraxolite has also been reported in many of the younger strata.

The high rank of the anthraxolite, its content of ash, nitrogen, and sulfur, and its low hydrogen-oxygen ratio fit it almost exactly into the pattern of chemical contours and isocarbs established by Deasy and Griess (*10*) for the nearby Pennsylvanian anthracite coals (*see* Figure 2). These anthracites attained their present condition in Permian or Triassic time, during the waning stages of the Appalachian Orogeny. The pattern of metamorphism of the coals, however, transects the regional trend of folds. The Martinsburg sediments, situated several thousand feet lower in the sequence, should also have been influenced by these same forces, at least in part. It is a curious coincidence that the westward diminution of Taconic metamorphism in the Martinsburg conforms to the pattern of later metamorphism for the Pennsylvanian coals. This suggests that late Appalachian Orogeny may have had a more important role in the metamorphism of the Martinsburg sediments than is generally recognized.

Source of the Protoanthraxolite. The field evidence for most anthraxolite occurrences strongly points to some sort of fluid carbonaceous substance which became concentrated in the openings of more or less permeable rock. In his review of the origin of anthraxolite, King (*23*) proposed that primary organic sediments yielded a mobile fraction under low-to-moderate conditions of heat and pressure and that this fraction migrated through rock pores in an aqueous medium. Dunn and Fischer (*14*) concluded that the New York anthraxolites had their origin in coaly, not asphaltic parent material, and they suggested that a process similar to fusinization raised the substance to its high rank without much heat or pressure. Most earlier workers, however, have proposed a bitumin lineage, related to oil, possibly derived from marine sapropels.

The Martinsburg anthraxolite appears to have been emplaced in the bottom muds quite early, possibly as sapropel derived elsewhere from simple marine plants. Emplacement could have been simultaneous with the deposition of the muds, but the absence of stratification suggests that the substance infiltrated into cavities in a way similar to that for the younger New York anthraxolites.

A sapropelic origin is consonant with the geologic environment but is not necessarily supported by the chemistry of the anthraxolite (Table III) which reflects a low hydrogen-oxygen ratio. Relatively abundant oxygen is typical of substances of humic origin whereas relatively high hydrogen content is found in sapropelic or bituminous substances. Figure 13, based on data tabulated by White (*41*), relates the hydrogen-oxygen ratio to the carbon content of natural organic substances. Three main lineages appear from the distribution: algal boghead (sapropelic), cannel, and humic. These lineages are determined by

Publication Date: January 1, 1966 | doi: 10.1021/ba-1966-0055.ch008

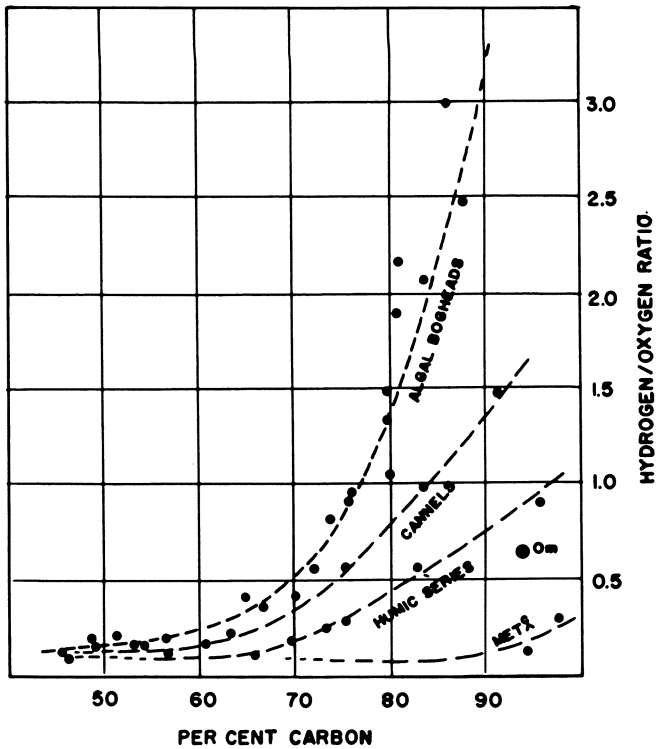

Figure 13. Relation between carbon content and ratio of hydrogen and oxygen for natural carbonaceous substances. Derived from analyses compiled by White (41). Distribution of values suggests three main genetic families. Values for Martinsburg anthraxolite (0_m) and similar substances are positioned near high carbon end of humic series curve

the change of the hydrogen-oxygen ratio with carbon content, and each shows a progressive relative increase in hydrogen and elimination of oxygen as rank increases. This effect is greatest for substances of algal or sapropelic origin, such as bogheads, sapropels, copal, and tasmanite. Coaly substances, derived from woody carbohydrates, have a greater tendency to retain oxygen and to lose hydrogen as rank increases. The cannel lineage, which includes the cannel coals and West Virginia semibituminous coal, is intermediate between the boghead and humic suites. The low hydrogen-oxygen ratio (0.53) of the Martinsburg anthraxolite would seem to place it in the humic series. Other anthraxolites have ratios which range between 0.25 and 1.5. Schungite, which may be derived from Precambrian sapropelic sediments falls exactly on the humic series curve. The Cornbrash asphaltite associated with Cretaceous anthracite coals of the Preussiche-Oldendorf, and almost certainly of humic origin (37) also falls on the curve for the humic series. The Martinsburg anthraxolite is similar in composition to each of these substances. Carbonaceous

Publication Date: January 1, 1966 | doi: 10.1021/ba-1966-0055.ch008

materials having the highest carbon content and lowest hydrogen-oxygen ratios, such as the Sudbury anthraxolite and Rhode Island meta-anthracite, may belong to a separate "metamorphic" suite which reflects accelerated hydrogen loss because of high metamorphic temperatures.

In an attempt to determine whether there might be any relationship between the carbon of the anthraxolite and that of the calcite associated with it, the ratios of stable carbon isotopes were determined for each (Table IV). The results are given as δC^{13} in per mil relative to National Bureau of Standards sample NBS-22 and also relative to the Urey-Chicago Standard (PDB).

Table IV. Carbon Isotope Ratios for Martinsburg Anthraxolite and Calcite[a]

	δC^{13} *vs. NBS-22* (‰)	δC^{13} *vs. PDB* (‰)
Anthraxolite	+ 2.6	—27.2
Associated Calcite	+29.2	— 0.6

$$\delta C^{13} = \frac{\left(\frac{C^{13}}{C^{12}}\right)_{\text{sample}} - \left(\frac{C^{13}}{C^{12}}\right)_{\text{standard}}}{\left(\frac{C^{13}}{C^{12}}\right)_{\text{standard}}} \times 1000$$

[a] Analysis by Marathon Oil Co.

A negative value of δC^{13} indicates that the sample contains less C^{13} than the reference standard; a positive value indicates that it contains more. The greater abundance of C^{13} in the carbonate of the matrix than in the anthraxolite indicates that no genetic relation exists between the two even though it has been proposed that organic carbon in sediments can react (reversibly) with water eventually to produce carbonate ion. If such a process operated, it must have been highly selective, favoring oxidation of C^{13}. The matrix calcite δC^{13} value is within range for inorganic carbonates such as limestone and dolomite. The anthraxolite has isotopic composition typical of biogenic carbonaceous substances such as fossil wood, plants, and coal. Similar measures for the organic carbon of the slate are not yet available.

Summary and Conclusions

Anthraxolite has been found in rocks which range in age from Precambrian through Triassic. It occurs in the Martinsburg slate as fragmented nodules enclosed in prismatic quartz and calcite. Analyses indicate great homogeniety and low volatile and ash content, similar to other anthraxolites. Comparison of x-ray diffraction patterns with published data suggest that the carbon crystallites are roughly equidimensional—about 14 A. wide. Heat treatment tends to expel remaining volatiles, to anneal the disordered carbon atoms into nearly graphitic order, and to increase the average size of the crystallites. Differential thermal analyses show that volatile expulsion begins at temperatures as low as 200°C., followed by exothermic ordering and growth of crystallites to high temperatures. The thermal behavior of the anthraxolite is unlike that of anthracite but is very similar to thermal behavior of high volatile coals and protocoals.

Publication Date: January 1, 1966 | doi: 10.1021/ba-1966-0055.ch008

The implied retention of low temperature-sensitive hydrocarbons in the anthraxolite suggests that it reached its present rank by a low temperature devolatization process rather than by thermal distillation.

It is not likely that the anthraxolite had a clastic origin since no suitable source rocks are known and the environment of deposition was unfavorable. There is much evidence that anthraxolite was originally a semifluid substance which migrated into veins and cavities. Its rank increase has come about in the absence of much heat and pressure by a slow diagenetic process similar to that which has produced aromatic hydrocarbons in Green River shale (Eocene). Experimental evidence supports this view. The hydrogen-oxygen ratio of the anthraxolite suggests that it had a humic rather than sapropelic parent susbtance. A humic origin has also been proposed by others for anthraxolites in Canada and New York. The carbon in the contemporaneous calcite envelope of the nodule is shown to be unrelated to the carbon of the anthraxolite.

Studies of contact metamorphism of natural coals suggest by comparison that the Martinsburg protoanthraxolite was not heated above 600°C. if originally of low rank, nor above 300°C. if originally of high rank. It participated in the regional metamorphism of the enclosing slate which has a low temperature mineral assemblage. Had the slate been subjected to temperatures above about 300°C. at geosynclinal depths, its assemblage would have included minerals not now present, such as biotite.

The metamorphism of the slate and anthraxolite occurred in Taconic time not long after deposition of the Martinsburg. The dilation of the protoanthraxolite culminated with brittle cataclasis at the time the slaty cleavage was forming in the rock. Even though the chemistry of the anthraxolite fits into the pattern of late Appalachian isocarbs of the anthracite coalfields located nearby, there is no direct evidence that Appalachian metamorphism affected the anthraxolite. Assignment of Taconic age to the Martinsburg anthraxolites means that protoanthraxolite has formed and migrated repeatedly throughout geologic time, for anthraxolite occurs in many of the younger strata.

Publication Date: January 1, 1966 | doi: 10.1021/ba-1966-0055.ch008

Acknowledgments

Frank Ceraul and Frank Moretti of the Stoddard Slate Co., Pen Argyl, originally called my attention to the anthraxolite nodules. They have collected all of the specimens during two years of cleaving slate blocks for roofing slates. Louis G. Benedict, of Bituminous Coal Research, Inc., Pittsburgh, performed reflectance measurements on the nodules and provided data from which the curve in Figure 4 was plotted. Elemental analysis of the nodule carbon was arranged by Grover Shrayer of Gulf Research and Development Co., Pittsburgh, and the isotope analysis of the nodule carbon and the organic analysis of the enclosing slate was provided by Donald R. Baker, of the Marathon Oil Co. Research Center at Littleton, Colo. Edwin F. Koppe of the Pennsylvania Geological Survey, Harrisburg, performed independent optical, etching, and gravity measurements whose results paralleled my own. Each of these workers stimulated ideas during the course of several discussions.

Literature Cited

(1) Arschinow, W., Petrographical Institute Lithogaea, *Moscow, Publ.* **G 50** (1914).
(2) Behre, C. H., Penn. Geol. Survey, Ser. 4, *Bull.* **9M,** 97 (1927).
(3) Berl, E., *Science* **80,** 227 (1934).
(4) Blayden, H. E., Riley, H. L., Taylor, A., *J. Am. Chem. Soc.* **62,** 181 (1940).
(5) Cartz, L., Hirsch, P., *Phil. Trans. Roy. Soc. London,* Ser. A, **252,** 569 (1960).
(6) Chapman, E. J., "Minerals and Geology of Central Canada," 2nd ed., p. 145–6, Toronto, 1871.
(7) *Ibid.,* pp. 144–6.
(8) Clegg, K., *Illinois State Geol. Surv., Rept. Invest.* **190,** 12 (1955).
(9) *Ibid.,* p. 14.
(10) Deasy, G., Griess, P., *Proc. Penn. Acad. Sci.* **36,** 237 (1962).
(11) Diamond, R., *Phil. Trans. Roy. Soc. London,* Ser. A, **252,** 204 (1960).
(12) Dietrich, R., *Econ. Geol.* **51,** 649 (1956).
(13) Dunn, J., Fisher, D., *Am. J. Sci.* **252,** 489 (1954).
(14) *Ibid.,* p. 499.
(15) Ellis, W. H., *Chem. News* **76,** 186 (1897).
(16) Glass, H. D., *Econ. Geol.* **49,** 295 (1954).
(17) *Ibid.,* p. 305.
(18) *Ibid.,* p. 297.
(19) Hirsch, P. B., *Proc. Roy. Soc. London,* Ser. A, **226,** 147 (1954).
(20) Hunt, T. S., "Geology of Canada," Chap. 17, Geological Survey of Canada, Ottawa, 1863.
(21) *Ibid.,* p. 524–7.
(22) Hunt, J., Stewart, P., Dickey, P., *Am. Assoc. Petrol. Geol. Bull.* **38,** 1671 (1954).
(23) King, L. H., *Can., Dept. Mines Tech. Surv., Mines Branch, Res. Rept.* **R-116,** (1963).
(24) MacFarlane, G., *Econ. Geol.* **24,** 1 (1929).
(25) *Ibid.,* p. 10.
(26) Maxwell, J., "Petrologic Studies," Buddington Volume, The Geological Society of America, Baltimore, 1962.
(27) McBride, E., *J. Sed. Petrol.* **32,** 69, 85–8 (1962).
(28) McCartney, J., *Econ. Geol.* **47,** 207 (1952).
(29) McCreath, A. S., *Penn. Geol. Surv., 2nd Rept. Analyses* No. 25, **MM,** 102 (1879).
(30) Ramberg, H., "The Origin of Metamorphic and Metasomatic Rocks," p. 49, University of Chicago Press, Chicago, 1952.
(31) Rankama, K., *Geol. Soc. Amer. Bull.* **59,** 389 (1948).
(32) Russell, I. C., *Am. J. Sci.* **16,** 112 (1878).
(33) Schuhmacher, J., Huntjens, F., Van Krevelen, D., *Fuel* **39,** 223 (1960).
(34) Smothers, W., Chiang, Y., *Econ. Geol.* **47,** p. 384 (1952).
(35) *Ibid.,* pp. 394–5.
(36) Sosman, R., *Am. J. Sci.* **35-A,** 353 (1938).
(37) Teichmüller, M., Teichmüller, R., *Z. Deutsch. Geol. Ges.* **100,** 498–517 (1950).
(38) Tyler, S., Barghoorn, E., Barrett, L., *Geol. Soc. Am. Bull.* **68,** 1293 (1957).
(39) Vanuxem, L., "Geology of New York," Pt. III, p. 33, 34, Albany, 1842.
(40) *Ibid.,* p. 29, 33.
(41) White, D., *Trans. Am. Inst. Min., Met. Eng.* **71,** 274 (1925).
(42) Yoder, H. S., *Geol. Soc. Am. Spec. Paper* **62,** 505 (1955).

RECEIVED January 3, 1966.

Discussion

Peter H. Given: In your view, how did metamorphism of the carbonaceous material occur? Was it incorporated in the mineral while in a low rank state and then raised in rank in situ with the slate? Was the rock exposed to a high temperature through deep burial or the presence of igneous bodies?

George R. Stevens: The geologic history of the anthroxolite and the parent slate is complex but generally understood. My feeling is that the upgrading of the carbon probably began by devolatilization prior to metamorphism but was climaxed during the metamorphism of the slate. Volume reduction accompanied this. Fragmentation and emplacement of the gangue minerals were probably effects of a second event. I do not feel that great heat was involved.

E. S. Barghoorn: I question the use of the term "anthraxolite" in describing the material you have studied since this is of Ordovician age. The term was first used for pre-Cambrian carbonaceous substances.

Dr. Stevens: The usage can be defended on basis of composition and perhaps also on basis of mode of occurrence. The type "anthraxolite" at Sudbury is clearly much older. If the age of the substance must be part of its definition, then it would be better to call the nodules simply "carbonaceous matter." Otherwise, "anthraxolite" could be appropriate. Others have so used the term. In any case, the term is more suitable than "anthracite."

Publication Date: January 1, 1966 | doi: 10.1021/ba-1966-0055.ch008

Significance and Use of Optical Phenomena in Uraniferous Caustobioliths

JACQUES JEDWAB

Université Libre de Bruxelles, Bruxelles 18, Belgium

Publication Date: January 1, 1966 | doi: 10.1021/ba-1966-0055.ch009

Optical anomalies are very widespread in uraniferous carbonaceous materials from different geological ages like bituminous and anthracitic coals, coalified logs, bituminous shales, and asphaltic sandstones. These optical anomalies, expressed by high reflectivity and anisotropic halos, are very stable, once acquired, in the course of history of the sediment. At this time it is not yet known if the intensity of optical anomalies is cumulative and proportional to the radioactive doses received. Nevertheless, one may evaluate through this kind of "natural nuclear plates" the time of introduction of uranium, the epigenetic vers. syngenetic type of its origin, and the plastic and fault-like movements of the organic materials.

Among the numerous methods used to study uraniferous organic materials, the microscopic and autoradiographic approaches and interpretation seem rather neglected. This methodological gap is even more striking when one considers that good instrumental commodities are available. Whatever the reasons, geologists and ore microscopists have greatly ignored these fields, the scientific interest of which we shall show here.

Numerous investigators have already noticed and described natural and artificial effects related to irradiation in caustobioliths and other carbonaceous materials: Stach (*24*, *25*), M. and R. Teichmüller (*26*, *27*), Hoehne, (*11*), Friedel and Breger (*8*), Ergun, Donaldson and Breger (*7*), Breger (*2*) and Duchesne, Depireux, and Van der Kaa (*5*) in coals; Davidson and Bowie (*4*), Ramdohr (*20*, *21*, *22*) Liebenberg (*17*), Uytebogaardt (*28*) in "Thucholites and Related Materials;" Zoubov (*30*), Pierce, Mytton, and Barnett (*18*) and Pierce and Rosholt (*19*) in asphalt and bitumen. An early paper by Grip and Ödman (*6*) displayed halo effects but did not explicitly refer to the irradiation as an active agent.

In Coal Science; Given, P.;
Advances in Chemistry; American Chemical Society: Washington, DC, 1966.

Observations from these workers coupled with ours shows that the different organic materials, regardless of their origin and nature, react quite similarly to irradiation.

The effects involved, from an optical point of view, are an increase of reflectivity, and both opacity and anisotropy. These effects, and others—e.g., insolubility or microhardness—appear to be related to an increase in chemical and physical stability. If one considers that these effects are stable towards further geological agents, we now realize that we have in hand a "geological photographic plate." This optimistic approach should not hide the fact that data and information obtained are rather complex and that our understanding of the basic phenomena is still inadequate. We shall thus confine ourselves to describing and interpreting a few typical examples.

Publication Date: January 1, 1966 | doi: 10.1021/ba-1966-0055.ch009

Techniques

The observations are performed with a Leitz Ortholux polarizing microscope equipped with the "Opak" illuminator, lamps for reflected and transmitted light, immersion objectives, and verniers. Characteristics of the polished thin sections and of the nuclear emulsion plates are observed in transmitted light with the same immersion optics after removing the Berek prism.

Polished sections and polished thin sections are prepared according to the usual techniques of coal petrography. They are mounted permanently on quadrangular pieces of transparent Lucite for location purposes. We have described elsewhere a graphical method of micro-surveying which allows an observer to locate any specific autoradiograph on nuclear emulsion plate of a given point in an opaque section (*13*).

Nuclear emulsion plates are Ilford K 5-100 micron. They are processed as recommended by Bowie (*1*).

Irradiation Phenomena

Under Reflected Light. Radioactive minerals (zircon, uraninite, coffinite) enclosed in organic material are surrounded by a clear halo of more than 20 microns width (Figure 1). This halo corresponds to a zone of increased anisotropy, reflectivity, and hardness as first observed by Stach (*24*).

The outline of the halos is determined by those of the radioactive inclusions; therefore they may be circular, banded, or irregular and asymmetrical. Between the mineral inclusion and the clear halo one often finds a dark rim of 2–4 microns width, whose significance is not yet clear (Figure 1b, Figure 2g, Figure 3f).

The reflectivity within the halo is not constant; one observes a maximum close to the radioactive source with a decrease outwards. The tracing of reflectivity curves with a photocell, recorder, and moving stage has shown that the decrease curves are smooth but sometimes stepwise (Figure 1a, b). The width of the halos is difficult to estimate by a subjective method, and our instrumental measurements are still too few to allow definite interpretation. However, the width generally varies between 20 and 50 microns. Preliminary observations suggest that the intensity of the halos is proportional to the quantity of uranium (Figure 4c).

In Coal Science; Given, P.;
Advances in Chemistry; American Chemical Society: Washington, DC, 1966.

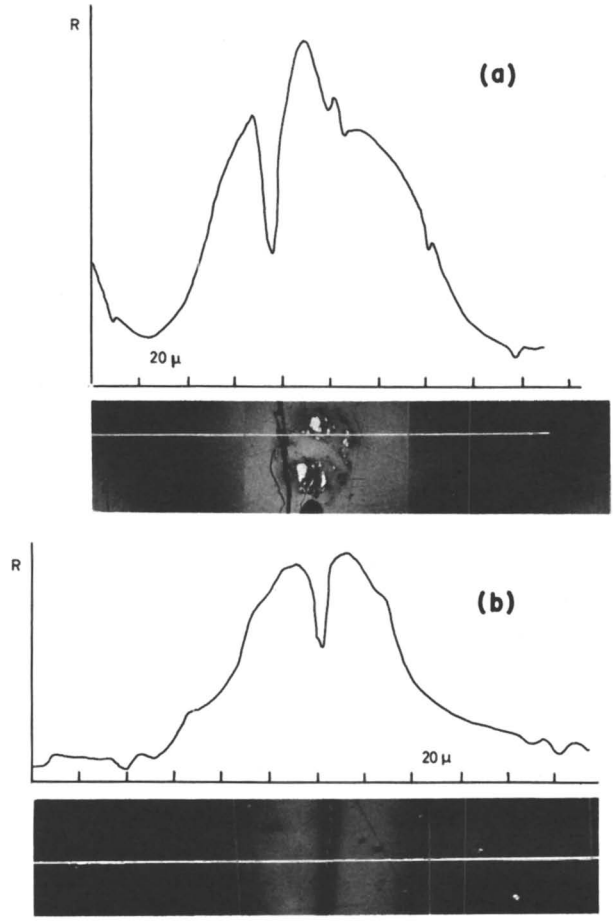

Figure 1. Reflectivity curves of halos around uranium inclusions: (a) in Temple Mountain asphalt, (b) in St. Hippolyte Coal. Ordinate axis (R) gives reflectivity in arbitrary linear units. Recordings were made along the white line drawn on the photographs. Notice the step-wise shape of the curves and their asymmetry

When observing asphalts and low rank coals, introducing a nicol prism increases the contrast between irradiated zones and background. Rotating the stage usually shows a slight pleochroic effect. Anthracitic coals must be observed with two nicol prisms since their high reflectivity masks secondary effects. Rotating the samples between crossed nicols shows cross- or lemniscate-like figures as well as strongly contrasted bands (Figure 5a, b).

Under Transmitted Light. The former reflecting halos correspond to opaque zones of the same outline which become progressively transparent towards the rim. The color is of the same shades as coal or asphalt.

One also observes crosses in polarized light which are deformed when the stage is rotated. This has been attributed to photoelastic effects of stress applied to a point.

Several Uranium-Caustobioliths Associations

Apart from these general characteristics, each association presents its own peculiarities determined by the origin of the carbonaceous material, the original structures, its mechanical history, and the time of introduction of the radioactive elements. These peculiarities are most important from a geological and geochemical point of view. The few cases described hereafter were chosen according to their diversity and exemplary value.

Asphaltized Log from Temple Mountain, Utah. This type of material has been widely described (e.g., *14*). The studied samples come from the North Adit mine (Chinle formation) (Figure 2).

The uraniferous minerals (uraninite and coffinite) form minute isolated inclusions, or are aligned according to the cellular structure of the wood (Figure 2a-g). In the same sample one finds compressed relics of woody structures (Figure 2a), together with cellular cavities filled with uranium (Figure 2d, g). This suggests that uranium was introduced during or before the compression.

The material shows clearly the difference of optical transparency of irradiated zones. It seems that the effect is limited to the range of the α-particles, which would tend to prove that the radioactivity is unable by itself to induce the entire induration of the asphalt. This does not exclude the effect of the released heat.

The nuclear emulsion plates show that the bulk of the activity corresponds to discrete inclusions. The asphalt by itself shows very low activity (Figure 2e, h).

Asphaltic Sandstone from Lodeve-Mas Alary, Herault, France. This rock of Permian age contains, together with uraninite, secondary uranium minerals, sulfides, molybdates, etc. (*12, 15*) (Figure 3).

The asphalt is distributed as little pellets or stringers. In the same samples one finds pellets of high reflectivity and nearby, others of dull appearance (Figure 3a). The last are elastic whereas the former are brittle towards the microhardness test.

Figure 2. Asphaltized log from Temple Mountain, Utah (1 nicol) →

(a) Compressed cellular structure, without uranium (× 180).
(b) The same as a with a few uranium inclusions surrounded by halos (× 180).
(c) The same as a with heavy uranium filling. In the center: structureless asphalt (× 90).
(d) and (g) Cellular structures, showing the shape of halo (d) (× 180) and black narrow bands (g) (× 562).
(e) and (h) Uranium inclusions (× 112) and corresponding autoradiograph (6 hours exposure) (× 112).
(f) Contiguous inclusions of uranium; vanadium and nickel minerals "pushed in the matrix. Obliterated woody structure at left (× 180).

Publication Date: January 1, 1966 | doi: 10.1021/ba-1966-0055.ch009

The most interesting features are the traces of mechanical movements which gave rise to manifold or stretched halos. These movements occurred when the material was plastic and still sensitive to irradiation (Figure 2e, g). One may observe halos separated from the uranium minerals which remain only as fine threads; other elongated halos have one end showing a sharply defined limit, and the other fading out smoothly.

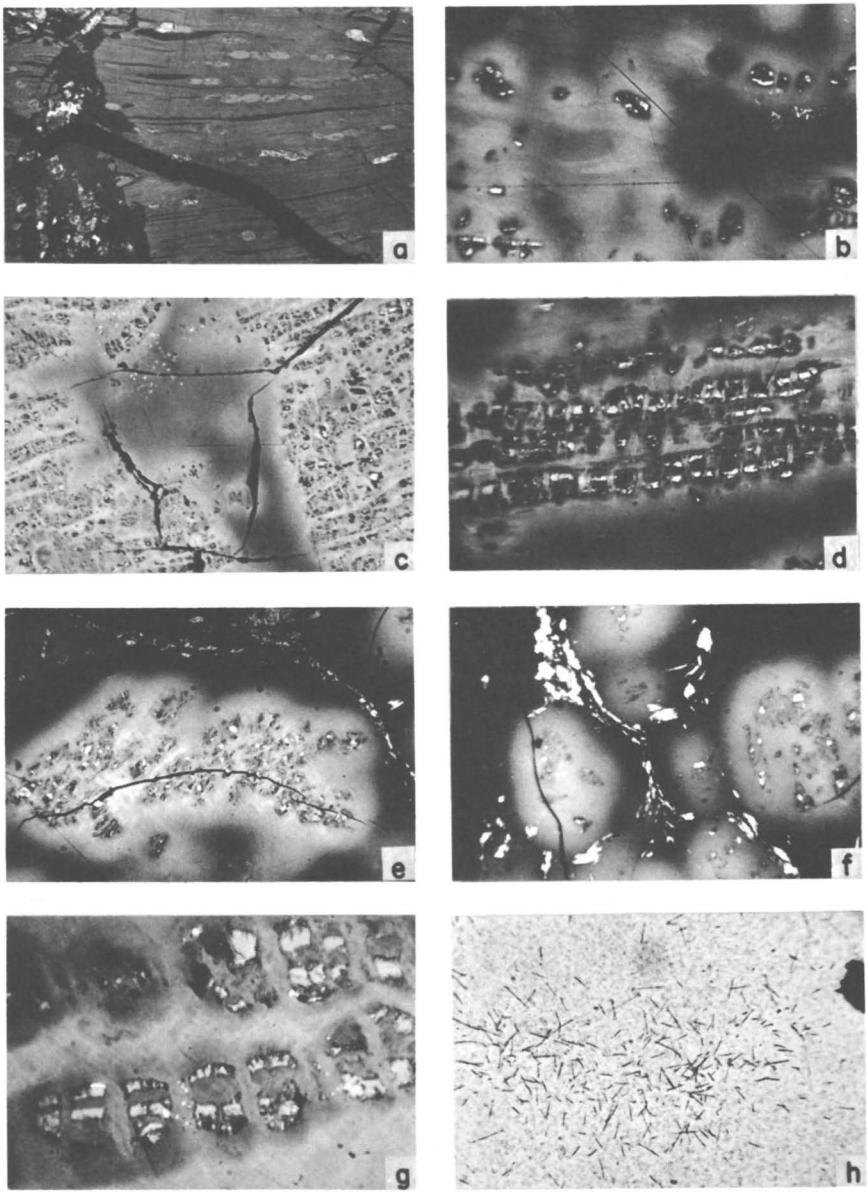

Publication Date: January 1, 1966 | doi: 10.1021/ba-1966-0055.ch009

Coal from St. Hippolyte, Vosges, France. This coal of Stephanian age contains an epigenetic mineralization of uranium (Figure 4) (9). Microscopic uraninite fills cracks of different size especially visible in massive vitrinite (Figure 1b, Figure 3d). Symmetrical halos run along the cracks following their finest details. One observes sometimes thin dark zones between filled crack and bright halos, of unknown origin. These banded halos are similar to oxidation bands found in highly altered coals. However, in the St. Hippolyte coal,

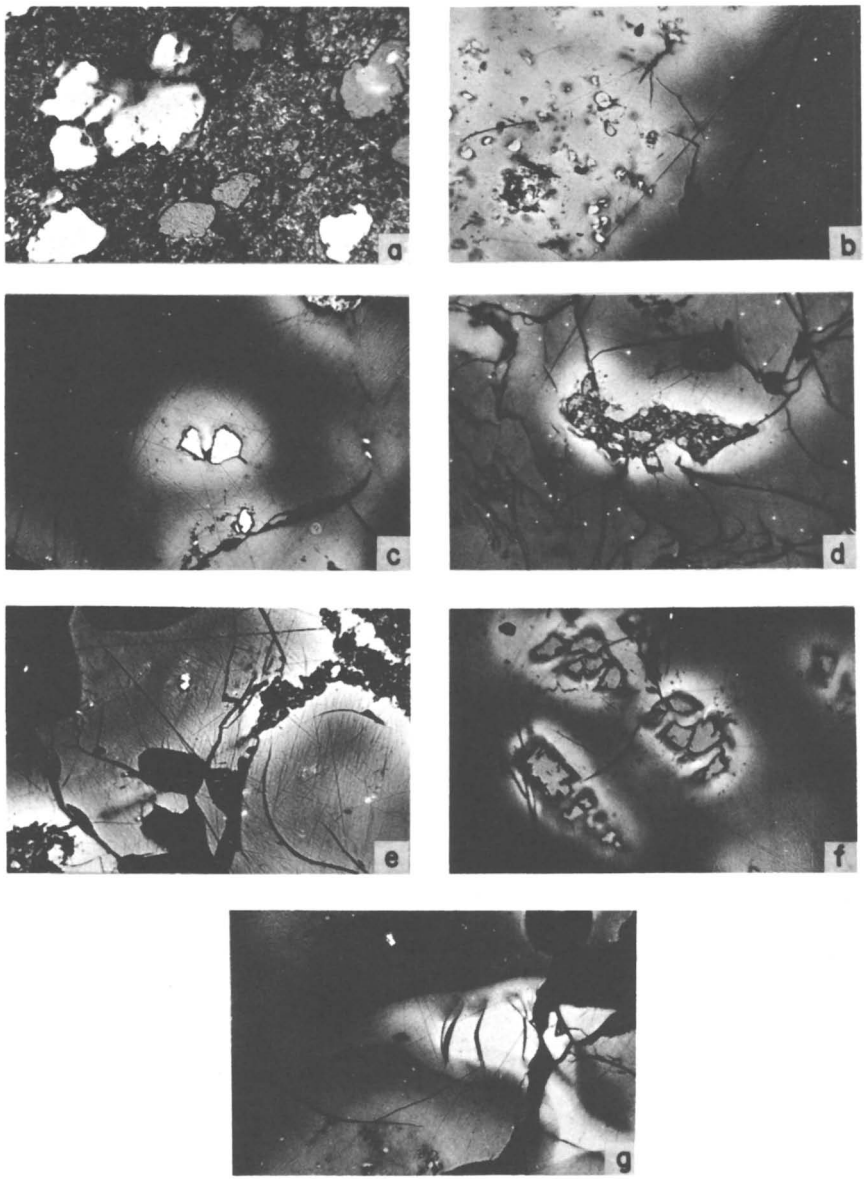

Publication Date: January 1, 1966 | doi: 10.1021/ba-1966-0055.ch009

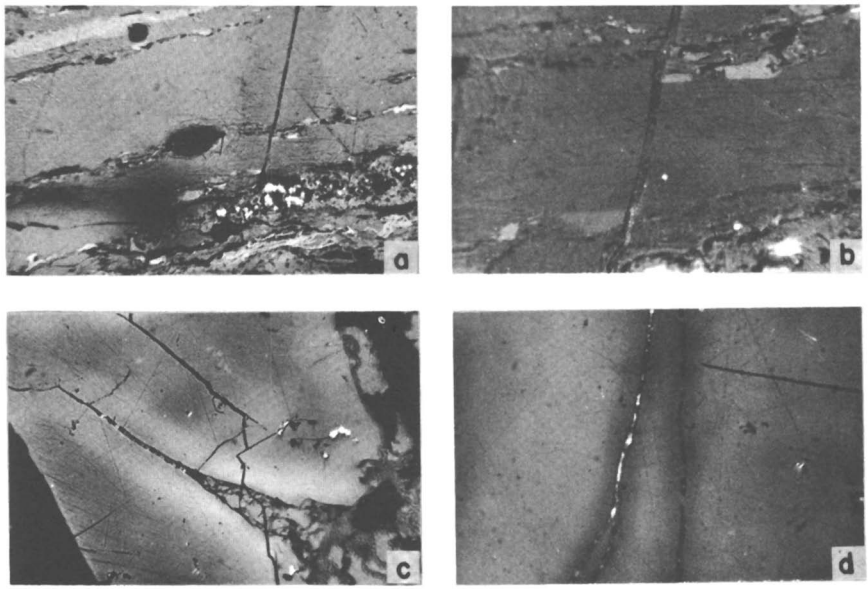

Figure 4. Coal from St. Hippolyte, Vosges, France (1 nicol)
(a) Banded coal with transversal crack in vitrinite. Symmetrical dark grey halo (× 180).
(b) Enlarged part of (a) showing that the crack is actually filled (× 562).
(c) Uranium concentration in massive vitrinite showing the decrease of halo intensity with the narrowing of active zone (× 180).
(d) Two fine veins of uranium. Notice the different reflectivities of left and right sides (× 562).

fractures devoid of uranium filling or filled only with sulfides, are also devoid of halos.

Samples of banded coals show in the vitrinite portion transversal bands of high relief (owing to polishing) with a fine median crack filled with uranium minerals (Figure 4a, b).

Distribution of the radioactivity corresponds to the filled cracks. The main coal shows very low radioactivity.

← *Figure 3. Asphaltic sandstone from Lodève-Mas Alary, Hérault, France (1 nicol, × 200)*
(a) Two types of asphaltic pellets in sandstone: highly reflecting (left) and dull (center and upper right).
(b) Irradiated asphalt containing uraninite (left) and normal asphalt (right) with minute sulphide inclusions.
(c) Uranite inclusion with simple halo.
(d) Irregular inclusion, with complicated fracture system.
(e) Complex uranium concentrations (lower left and upper right) joined by a stretched stringer.
(f) Broken inclusions of uranium mineral with well marked dark bands.
(g) Double halos (center); highly reflecting zone (right) with diffuse end (left).

Publication Date: January 1, 1966 | doi: 10.1021/ba-1966-0055.ch009

Coal from Dorenaz, Valais, Switzerland. This anthracitic coal of Carboniferous age shows interesting peculiarities (Figure 5). In contrast to the former case, the α-activity is arranged along lines parallel to the bedding, either as stars or as bands (Figure 5d, e). In the polished sections one observes elliptical halos without specific mineral inclusions or bands of very fine black particles. The anisotropy effects are very marked as different kinds of crosses or vivid bands (Figure 5a, b).

Tectonic movements affected the coal, and in many instances the halos are cut and displaced; coal brought in front of former halos remains entirely

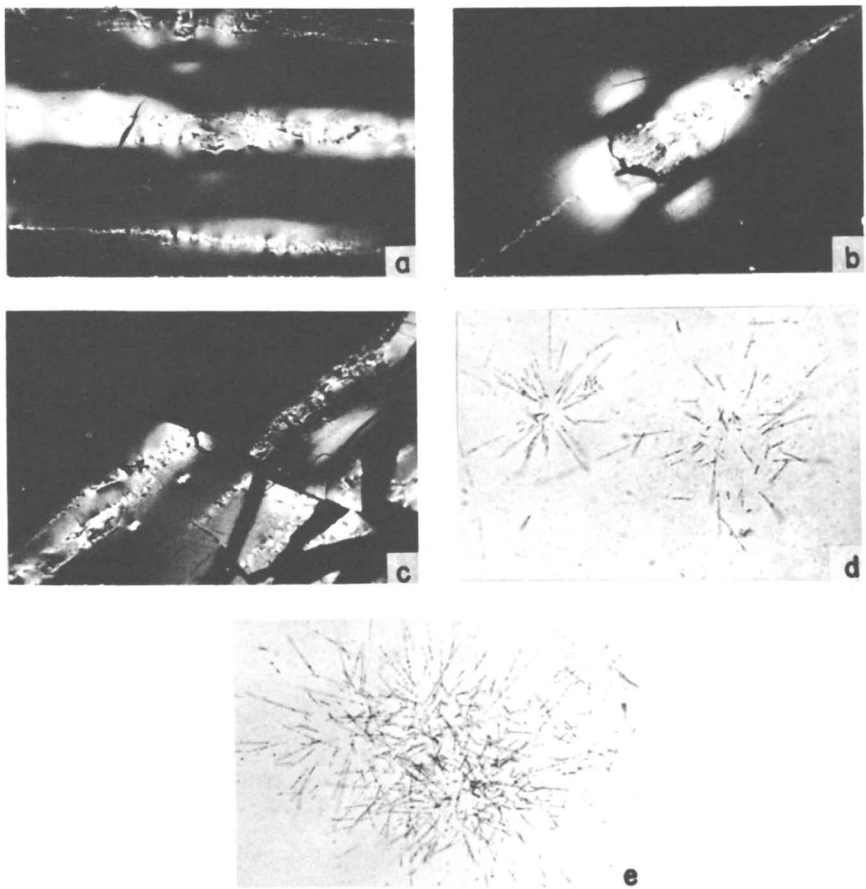

Figure 5. Coal from Dorénaz, Valais, Switzerland (a-c: 2 nicols, × 180)
(a) Two anisotropic bands (center and bottom) and lemniscate-like pattern (upper border).
(b) Big inclusion with anisotropic figure. Notice black traversing crack, a very common feature, also visible in (a), middle left.
(c) Anisotropic bands cut by microscopic fault. Coal in front of active band (left bottom) remains unaffected (center) (× 148).
(d) and (e) Star and cluster-like α-track patterns (× 148).

Publication Date: January 1, 1966 | doi: 10.1021/ba-1966-0055.ch009

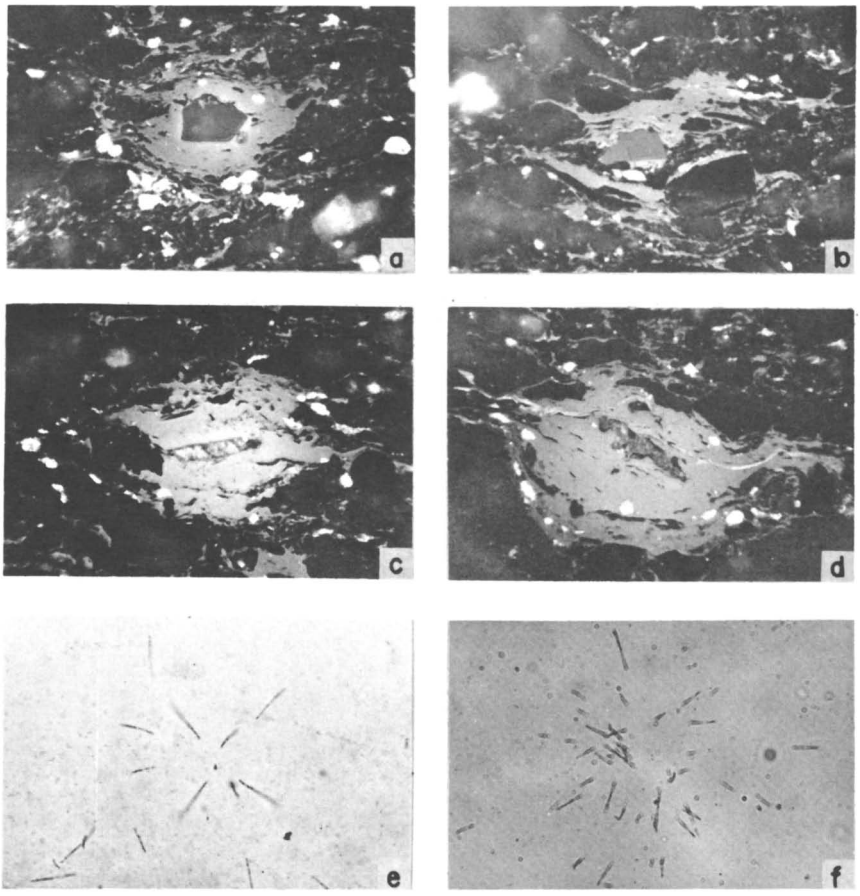

Figure 6. Copper shale from Mansfeld, Germany (1 nicol, × 180)
(a) and (b) Inclusions of zircons (dark grey) in well-shaped organic amygdule (a) or diffuse stringers (b).
(c) and (d) Complex undefined inclusions in organic amygdules. Notice lack of screening effect behind mineral inclusions (in black).
(e) and (f) Autoradiographs of weakly and strongly active inclusions (25 days exposure).

unaffected (Figure 5c). Therefore one may say that the carbonaceous matter exhibited its maximum sensitivity to radiation before the final coalification and/or tectonization. The introduction time of the uranium relative to the tectonics is also given by such observations. One may further infer that introduction of uranium subsequent to the final coalification would have no effect on the optical properties. (More details concerning the radioactivity of this coal will be published in a joint article in *Bull. Soc. Suisse Min. Pétrogr.*, 1965.)

Copper Shale from Mansfeld, Germany. The famous "Kupferschiefer" which has acquired a renewed importance in recent metallogenic theories (*3*, *6*, *29*), is known to be locally uraniferous (*16*, *23*) (Figure 6). Schüller has

Publication Date: January 1, 1966 | doi: 10.1021/ba-1966-0055.ch009

published photographs of "thucholite" in which one sees anisotropic halos surrounding uraninite. The existence of a uranium-organic compound is inferred from contact-print autoradiographs at I/I scale. According to Kohl, the uranium is mainly concentrated in a fine layer of the ore-bed called "Erdpechhiecke," containing numerous droplets of bitumen. Our samples came from an unspecified layer.

The α-activity is bound to two types of compounds (apart from the mentioned uraninite):

(1) To layers of fairly continuous organic remains, in which the activity is randomly distributed and relatively low. There are no optical effects visible in these carbonaceous matters.

(2) To discrete inclusions, sometimes easily recognizable as zircons, (Figure 6a, b) or complex inclusions made up of strongly colored particles (Figure 6c, d). These inclusions have variable radioactivities. (Figure 6e, f).

When these inclusions are associated with organic matter (which acts as binding material of the carbonate grains and amounts to 5–15% of the rock), they produce clear halos (Figure 6a–d).

The spatial relations of the organic material to the zircons seem to be nonfortuitous; one often finds the mineral inclusion in the middle of an amygdule. Apparently, the zircons fixed the very mobile and radiation-sensitive organic matter at an early stage. Such an early induration has also been inferred by Stach (25) in coal.

Publication Date: January 1, 1966 | doi: 10.1021/ba-1966-0055.ch009

Concluding Remarks and Future Problems

The observations described here are not intended to solve any pending problem of ore genesis or organic geochemistry. They are illustrations of the many roads opened to us by the natural introduction during geological times of a kind of photographic plate, and like photographic plates, the irradiation phenomena may be useful for numerous purposes, most of them as yet difficult to foresee.

The parallel with photographic plates may be extended further: we may immediately make use of the displayed images even if we do not fully understand the mechanism of "image formation," as was also the case in the beginnings of photography.

So far as possible now, we may draw a few conclusions:

Irradiation phenomena are very widespread in carbonaceous materials and are found in every case where they might be expected to occur. As the irradiated zones generally contrast well with the poorly reflecting matrix and have a much larger diameter than the radiating particles, the presence of radioactive materials may be easily inferred by trained eyes. (Some confusion with oxidation bands is nevertheless possible).

The same instrument may be used for the microscopy of the sections and of the nuclear emulsion plates. In fact, the microscope builds a bridge between past and present distribution of radioactivity.

The intrinsic properties of carbonaceous materials (ubiquity, variety of genetical types, fair resistance to geological agents, plasticity or brittleness, adsorption of uranium, metamorphic evolution) added to their sensitivity to

radiation may give us complex information regarding the history of radioactive elements and organic matters during their common or separate destiny.

If the available evidence allows us to say that there are relationships between received radiation and the width and reflectivity of halos, quantitative answers should be given to a few important questions if we wish to make further progress:

Are the quantitative characteristics of the halos homogeneous in the same sample (width, maximum reflectivity, shape of profile)?

What are the relationships between these characteristics and the chemical and physical properties of the carbonaceous matter?

What are the agents responsible for the halo formation, and what is the importance of the previous oxidation stage of the material?

Perhaps the answers to these questions will lead us to a geological chronology of the very important uranium-carbon deposits.

Acknowledgment

We would like to acknowledge the National Science Foundation travel grant which allowed us to attend the American Conference on Coal Science. Our gratitude goes to B. and P. Mamet-Bratley who helped in the translation of this paper. We are also indebted to the following for supplying samples used in this work: I. A. Breger, U.S. Geological Survey; M. Louis, I.F.P., Rueil Malmaison, A. Grimbert, C.E.A., Fontenay-aux-Roses; T. Hügi, Bern University; Dipl. Ing. G. Rehwald, Erzlabor-Braunfels, Germany; M. Teichmüller, Geologisches Landesamt Nordrhein, Westfalen, Krefeld who prepared the polished thin sections.

Literature Cited

(1) Bowie, S. H. U., in "Nuclear Geology," Faul, H., p. 47, John Wiley and Sons, New York, 1954.
(2) Breger, I. A., *Intern. Conf. Coal Sci., 4th, Le Touquet, 1961*, D6.
(3) Davidson, C. F., *Mining Mag. London* **110,** 244 (1964).
(4) Davidson, C. F., Bowie, S. H. U., *Bull. Geol. Survey Gt. Brit.* No. **3,** 1 (1950).
(5) Duchesne, J., Depireux, J., Van Der Kaa, J. M., *Geochim. Cosmochim.* Acta **23,** 209 (1961).
(6) Dunham, K. C., *Econ. Geol.* **59,** 1 (1964).
(7) Ergun, S., Donaldson, W. F., Breger, I. A., *Fuel* **39,** 71 (1960).
(8) Friedel, R. A., Breger, I. A., *Science* **130,** 1762 (1959).
(9) Grimbert, A., Carlier, A., *Bull. Serv. Carte Géol. Alsace-Lorraine* **9,** Pt. 2, I (1957).
(10) Grip, E., Ödman, O. H., *Sveriges Geol. Undersökn., Arsbok*, **38,** No. **6** (1944)
(11) Hoehne, K., *Chem. Erde* **19,** 38 (1957).
(12) Jedwab, J., *Bull. Soc. Belge Geol. Paleontol., Hydrol.* **71,** 487 (1962).
(13) Jedwab, J., *Ibid.* **72,** 401 (1963).
(14) Kelley, D. R., Kerr, P. F., *Bull. Geol. Soc. Am.* **69,** 701 (1958).
(15) Kervella, F., *Bull. Inform. Sci. Tech. Comm. Energy At.* **16–19** (1958).
(16) Kohl, E., *Z. Prakt. Geol.* **49,** 99 (1941).
(17) Liebenberg, W. R., *Trans. Proc. Geol. Soc. S. Africa* **58,** 101 (1955).
(18) Pierce, A. P., Mytton, J. W., Barnett, P. R., *Proc. UN Intern. Conf. Peaceful Uses Atomic Energy, 2nd, Geneva, 1958*, **2,** 192.
(19) Pierce, A. P., Rosholt, J. N., *U.S. Geol. Survey, Profess. Paper* No. **424–D,** 320 (1961).
(20) Ramdohr, P., *Abhandl. Deut. Akad. Wiss. Berlin, Kl. Math. Allgem. Naturw.* **5,** (1955).
(21) Ramdohr, P., *Abhandl. Deut. Akad. Wiss. Berlin, Kl. Chem., Geol., Biol.* **2,** (1957).

(22) Ramdohr, P., *Geol. Rundschau* **49,** 253 (1960).
(23) Schüller, A., *Abhandl. Deut. Akad. Wiss. Berlin, Kl. Math. Allgem. Naturw.* **6** (1959).
(24) Stach, E., *Glückauf* **86,** 41 (1950).
(25) Stach, E., *Brennstoff-Chem.* **39,** 329 (1958).
(26) Teichmüller, R., *Congr. Strat. Geol. Carbon 3,' Heerlen,* 615 (1952).
(27) Teichmüller, M., Teichmüller, R., *Geol. Mijnbouw* **20,** 41 (1958).
(28) Uytenbogaardt, W., *Intern. Geol. Congr., Rept. 21st Session, Copenhagen,* **1960,** Pt. 15, 114.
(29) Wedepohl, K. H., *Geochim. Cosmochim. Acta* **28,** 305 (1964).
(30) Zoubov, A. J., *Geol. Rudn. Mestorozhd.* **6** (1960).

RECEIVED October 5, 1964.

Discussion

Marlies Teichmüller. Stach and Dépireux recently performed irradiation experiments using α-rays of polonium 210, acting on the surfaces of polished sections from high and medium volatile bituminous coals. They found an increase in reflectance not only from vitrinite but also from exinite (megaspores and algae), as is shown in Figures A and B. The changes in medium volatile coals are less than in high volatile coals. The rise in reflectivity is explained by the authors as an increase of rank (increase of C-content, decrease of volatile matter) though the irradiated coals have not been studied chemically. Stach, E., Dépireux, J., *Brennstoff-Chem.* **46,** 13 (1965).)

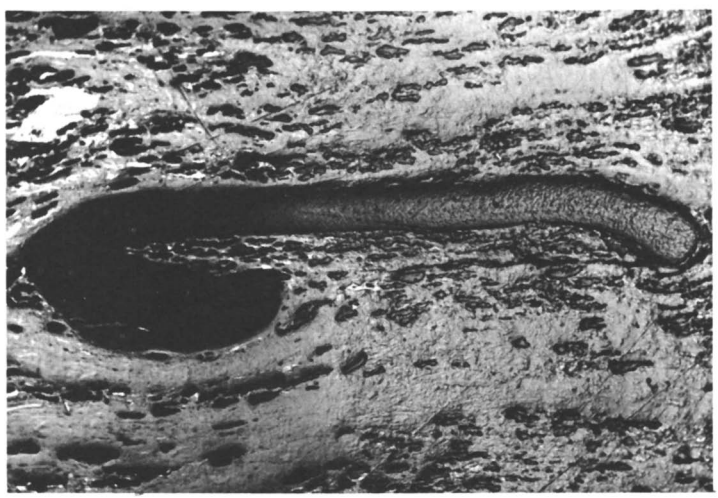

Figure A. Megaspore from a high volatile bituminous coal (37% V.M.), on the left changed by α-irradiation; polished section, oil immersion, × 100 (from Brennstoff-Chemie *46, 13 (1965))*

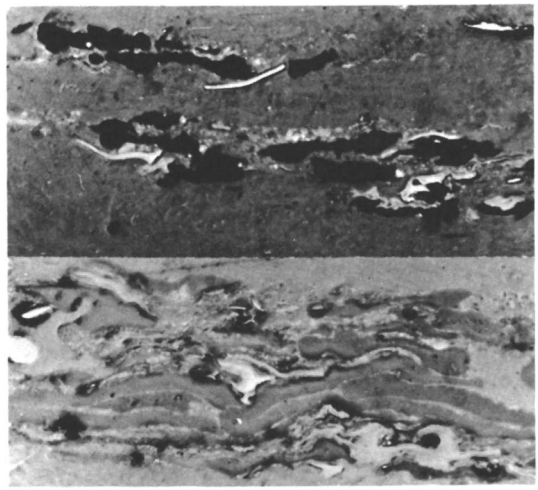

Figure B. Clarite with microspores in a high volatile bituminous coal (37% V. M.). Above: untreated, below: after α-irradiation. The reflectance of vitrinite and exinite increased to the degree of reflectance of a medium volatile coal (with 26% V. M.). Polished section, oil immersion, × 500 (from Brennstoff-Chemie *46, 13 (1965))*

H. S. Gluskoter. What other minerals have been identified in addition to the pitchblende in these sediments?

Jacques Jedwab. We have not identified the minerals ourselves. However, extensive lists of minerals showing uranium organic matter associations have been published as follows:

Temple Mountain: Kelley and Kerr (*14*)
Lodève-Mas Alary: Kervella (*15*). *See also* A. Lenoble and A. Gangloff, *Proc. U.N. Intern. Conf. Peaceful Uses Atomic Energy*, 2nd, Geneva 569, 1958.
St. Hippolyte: Grimbert and Carlier (*9*).
Dorénaz: Sublet (*Eclogae Geol. Helv.* **55,** 23 (1962)
Mansfeld: Wedepohl (*29*). *See also* K. E. Eisenhuth and E. Kautzsch, "Handbuch für den Kupferschieferbergbau," Leipzig, 1954.

Dr. Gluskoter. What is the evidence for a syngenetic origin for the uranium minerals in the Swiss anthracite? Why could this not be secondary deposition along planes of weakness (bedding)?

Dr. Jedwab. The syngenetic origin of uranium in the Dorénaz coal is inferred from the following arguments:

(1) Isolated concentrations of uranium are found in massive vitrinite without any visible connection with a plane of stratification or a fracture.

(2) One does not observe decreasing concentrations of uranium as one follows along a stratification plane produced by fracture.

(3) Certain uranium inclusions consist of block grains of about 1μ diameter intimately and uniformly mixed with the coal. They lie in layers or bands concordant with the stratification without fractures or planes being present. Inclusion of uranium during sedimentation or while the sediment still had a

Publication Date: January 1, 1966 | doi: 10.1021/ba-1966-0055.ch009

high water content explains this type of concentration better than an epigenetic origin.

In fact we are in one of those situations (which many other workers have commented on), where the "syngenetic-epigenetic" nomenclature is very imperfect. In the particular case of coal and uranium, it would strictly be necessary to term "epigenetic" any uranium that did not originate within the living plant species.

Publication Date: January 1, 1966 | doi: 10.1021/ba-1966-0055.ch009

Geological Causes of Coalification

MARLIES TEICHMÜLLER and ROLF TEICHMÜLLER

Geologisches Landesamt Nordrhein-Westfalen, Krefeld, Germany

The effect of pressure, temperature, and time on the diagenesis and metamorphism of coals is tested by geological observations and by experiments. Geological arguments are taken mainly from rank sections and rank maps, based on vitrite analyses. Temperature has most influence on the chemical reactions during the coalification process. Not only the maximum temperature reached but also the duration of exposure is important. The same rank may be reached either by a rapidly acting high temperature or by a long acting lower temperature. Pressure retards the chemical reactions during coalification, but it changes the physical structure of coal. Tectonic pressure can cause occasional and restricted increase of rank.

Publication Date: January 1, 1966 | doi: 10.1021/ba-1966-0055.ch010

In all coal basins the geologist observes a more or less regular alteration of the coals with increasing depth. Low rank coals most noticeably lose moisture; in higher rank coals the volatile matter decreases markedly with increasing depth; in the case of anthracites a loss of hydrogen is most characteristic. Other coal properties also change—e.g., the carbon content, the calorific value, and the optical reflectivity of the vitrinites. All these phenomena have been described by geologists under the general term "coalification."

To study coalification quantitatively and determine its degree ("rank"), it is necessary to work always with one and the same petrological constituent since the changes occur differently in the different macerals. Vitrinite is best suited to comparative rank investigations since it is the most abundant component, is relatively easy to isolate, and changes in the most consistent manner Regarding the type and extent of rank change with depth, investigations of vitrites out of deep borings are most informative.

Over the past 10 years approximately 12 deep borings have been put down in the North of the Ruhr district in order to establish the extent of

In Coal Science; Given, P.;
Advances in Chemistry; American Chemical Society: Washington, DC, 1966.

the reserves of coal. Since the pattern of coal utilization largely depends on rank, the range of coalification featured by these boreholes, which have a depth of up to 1200–1700 meters, was studied in detail. For example, in the Nordlicht-Ost 1 borehole (Figure 1) coal rank has been determined by measuring various properties (volatile matter, moisture, carbon content, calorific value). The unfaulted, fully cored profile, featuring a productive Carboniferous of 1250-meter thickness overall, covers, of course, only a limited range of coal rank. To form a picture of the way in which rank increases with depth from the high volatile bituminous coals to the anthracites, it is necessary to link the rank profiles of individual boreholes in a meaningful order. Patteisky and M. Teichmüller have done this (*17*), and Figure 2 shows the results in

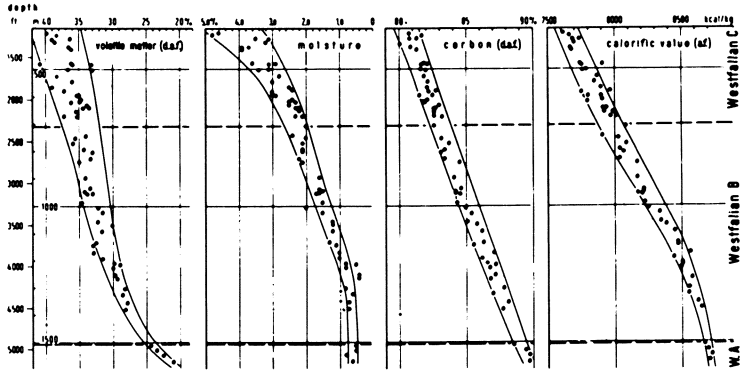

Figure 1. The increase of rank of coal with depth in the Nordlicht Ost 1 well (on the basis of vitrite analyses)

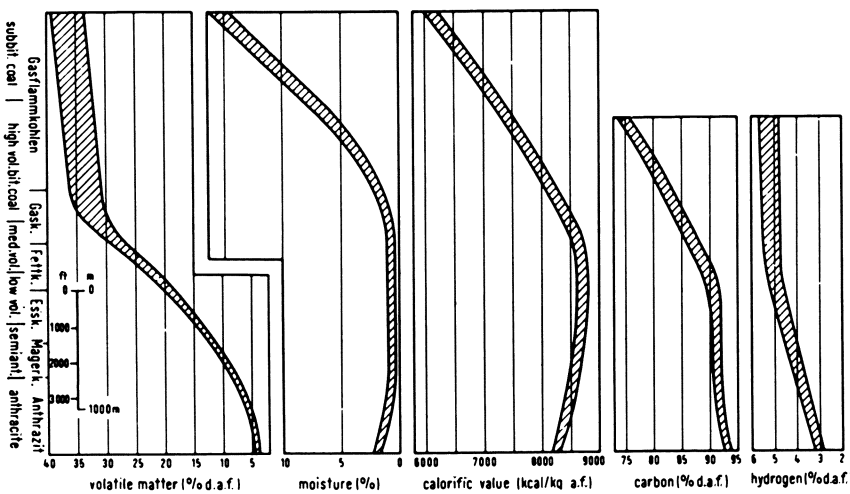

Figure 2. The increase of rank of coal (vitrite) with depth, based on data from deep borings with flat lying beds (scheme according to Patteisky and M. Teichmüller (17))

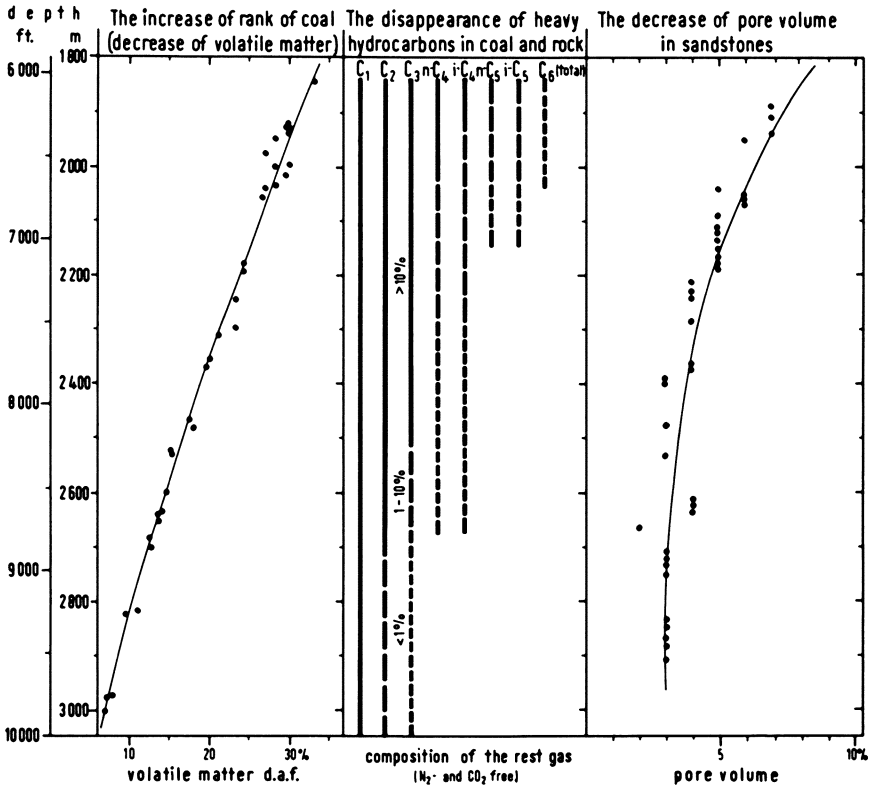

Figure 3. Changes of coals (vitrites) and rocks with increasing depth in the Münsterland 1 well (according to M. Teichmüller (26) Gedenk (5) and Tunn (31))

simplified form. At first volatile matter decreases very little with depth, and the values for the low rank bituminous coals show marked scatter expressed by the broadness of the coalification band. On proceeding downward, however, a considerable decrease is noted in the range of the medium volatile bituminous coals to the semianthracites. With increasing depth the contents of moisture, carbon, and hydrogen, as well as the calorific value likewise show changes of varying degree, which are characteristic for each property as well as for the different ranges of rank. This shows that the evidential value of the different measures of rank vary with the individual rank range. Therefore we used different measures of rank in our studies depending on the rank range being considered.

These rank investigations included not only individual boreholes and shafts but also larger geological cross-sections and whole coal districts, as for instance the Ruhr Basin (*18*), the Saar Basin (*2*), and the Basin of Wealden coals in Lower Saxony (*28*). From such areas rank maps were drawn representing the regional rank changes of one and the same seam.

Publication Date: January 1, 1966 | doi: 10.1021/ba-1966-0055.ch010

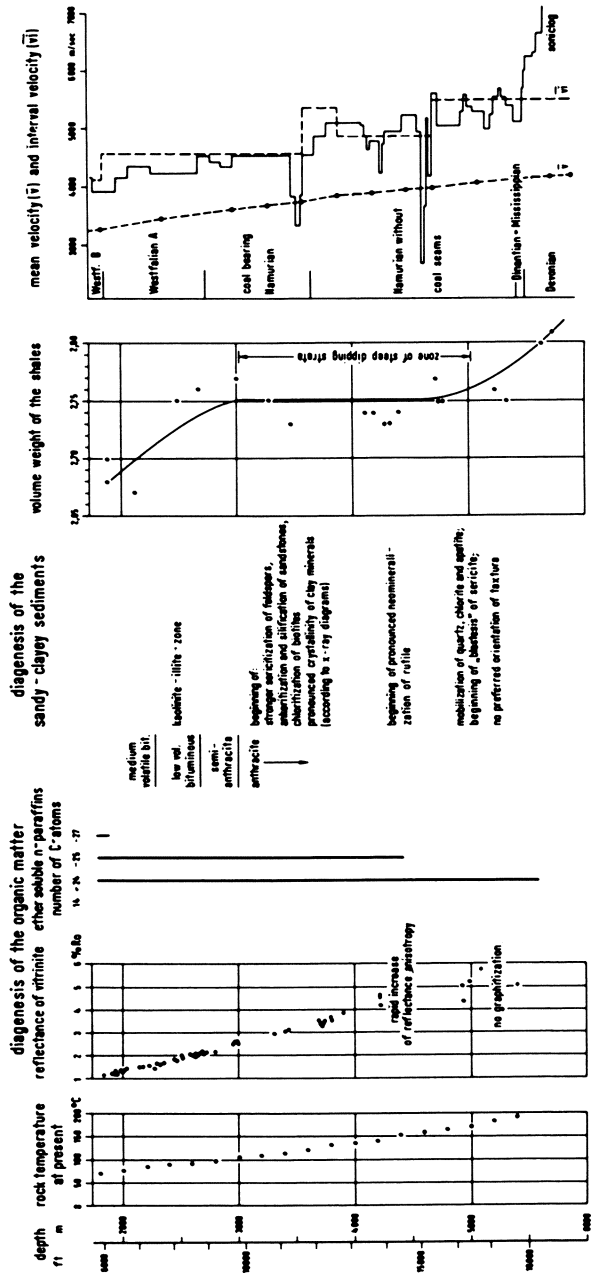

Figure 4. Metamorphism of organic matter and diagenesis of rocks in the Münsterland 1 well (according to Hedemann (7), Lensch (14), Welte (32), Scherp (19), Stadler (21), Strasser and Wolters (24), and Lichtenberg (15))

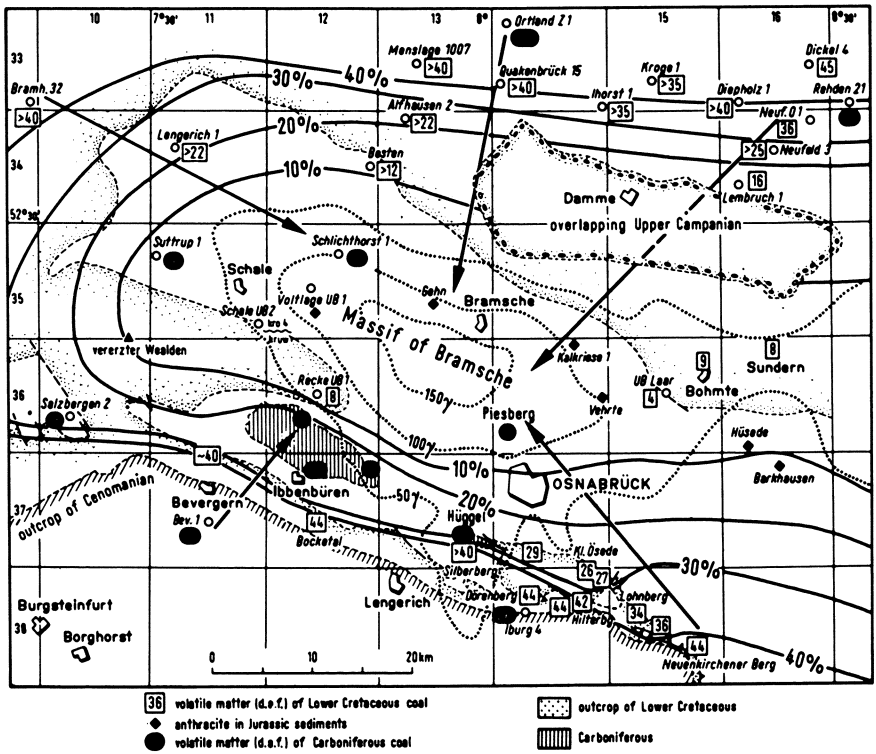

Figure 5. The increase of rank of coal (on the basis of vitrite analyses) towards the magnetic anomaly near Bramsche. kru_w = Wealden (Lower Cretaceous); kro_1 = Cenomanian; kro_4 = Upper Campanian (Upper Cretaceous). The numbers at the margin of the map indicate the numbers of the single topographic maps 1:25 000

On the basis of these investigations it seemed useful to discuss again the causes of coalification, which already have often been discussed by geologists as well as by chemists.

Influence of Temperature

In the Münsterland 1 borehole, the deepest in all Europe, put down in 1961-62 approximately 40 kilometers north of the Ruhr, it was possible to study the rank changes at one point in one continuous profile from a depth of 1800 meters down to 5000 meters. Figure 3 shows the decrease in volatile matter compared with other changes, namely, the disappearance of hydrocarbons from the interstitial gases and the decreasing porosity of the sandstones.

Figure 4 (left) shows the increase in rank of organic matter through the Münsterland 1 borehole in terms of vitrinite reflectance and occurrence of nonvolatile hydrocarbons. Figure 4 (right) shows the degree of diagenesis manifest in the associated sandstones and clayey rocks as well as the changes

Publication Date: January 1, 1966 | doi: 10.1021/ba-1966-0055.ch010

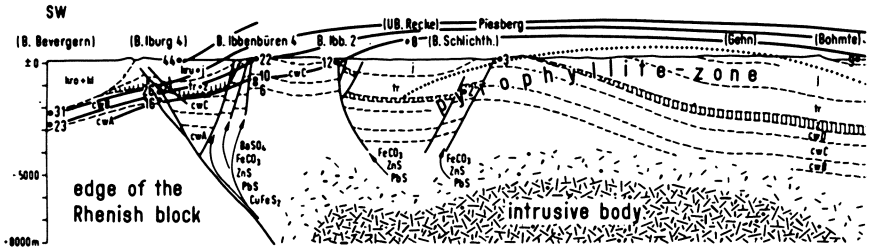

Figure 6. The doming of the isovols in the roof of the Bramsche Massif. B = borehole; cro$_4$ = Upper Campanian (Upper Cretaceous); cro = Upper Cretaceous; cro$_1$ = Cenomanian (Upper Cretaceous); k = Albian (uppermost Lower

in seismic velocity. The unchanged clay minerals, that is the kaolinite-illite zone, extends down to the depths of 3000 meters. Although at 3000 meters the entire process of bituminous coal carbonification (up to the semianthracites) is complete in all stages, this depth only marks the beginning of the various phenomena of mineralogical changes. However, as the anthracites were reached in the Münsterland 1 well, a certain correlation between coal rank and mineral paragenesis in the associated rock became evident.

As a precaution against generalization we next turn to borings some 25 miles farther north. The dotted area in Figure 12 represents the so called Bramsche Massif. This region features a considerable positive magnetic and gravimetric anomaly. Furthermore, the massif is characterized by a mineralization of Cretaceous age and by occasional occurrence of magmatic dykes in Lower Cretaceous sediments. Figure 5 shows a map with the outcrop line of the Lower Cretaceous, with lines of identical magnetic vertical intensity (dotted lines) and with the isovols of the Wealden coals (solid lines). Particularly intensive coalification of the Lower Cretaceous coals, as well as of the Carboniferous coals and of the organic matter in the Jurassic black shales (27), is restricted to the area of high vertical magnetic intensity. It is this area which also represents the culmination of the gently uplifted sediments. Figure 6, a section taken through the Bramsche Massif, shows that the highest rank anthracites (with less than 3% volatile matter) occur together with pyrophyllite. The isovols (solid lines) show a distinct doming. There is no doubt that a large intrusive body lying at great depth must have penetrated the sediments during the Middle Cretaceous and caused considerable heating in its roof. As far as the summit of the massif is concerned the changes displayed by the associated rocks (Westphalian D to Upper Jurassic) are likewise as marked as in the much older strata of the Münsterland 1 borehole at a depth of 5000 meters. This picture, however, changes on the edge of the Bramsche Massif where anthracitization occurred in many coals but where the associated rocks remained unaffected by any diagenetic change of note. At Bohmte, for instance, the anthracites occur together with kaolinite-bearing shales. This example aptly illustrates that coal reacts much more rapidly upon heating than the associated rocks and that temperature evidently plays a major part in the coalification process, for neither folding pressure nor over-

In Coal Science; Given, P.;
Advances in Chemistry; American Chemical Society: Washington, DC, 1966.

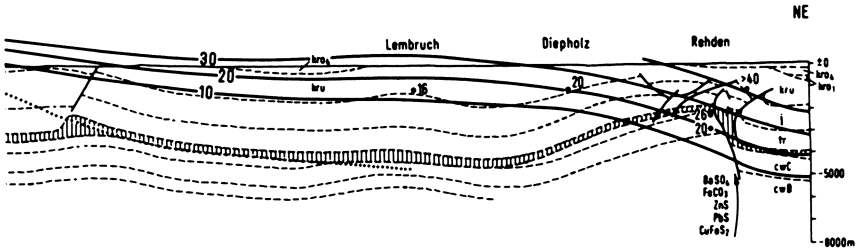

Cretaceous); kru = Lower Cretaceous; j = Jurassic; tr = Triassic; z = Zechstein (Upper Permian); cwc = Westfalian C (Carboniferous); cwb = Westfalian B; cwa = Westfalian A (after Stadler, M. Teichmüller and R. Teichmüller (22))

burden pressure in the Bramsche region can be regarded as being considerable. Spackman and Moses (*20*) explain the occurrence of pyrophyllite in two seams of the southern anthracite coal field of Pennsylvania as a result of intense compressional forces in this area. According to our observations in the Bramsche Massif where tectonic forces were very weak, and on the basis of all experimental work done on the formation of pyrophyllite, we tend to believe that pyrophyllite indicates relatively high temperatures rather than high tectonic forces. A temperature of 300–400°C. is assumed for the transformation of kaolinite into pyrophyllite in the Bramsche Massif area (*22*). This temperature led to an anthracitization (3% volatile matter) of coals within a span of about 5 million years (*22*).

It is well known that the rank of coal increases with depth. This is valid not only at one and the same point where in a vertical section the older seams are more highly coalified than the younger ones (cf. Figures 1, 3, 4), but also over larger areas. The map in Figure 12 shows that in Northwest Germany the rank of coal at the boundary between Westfalian C and Westfalian D is highest where this horizon has subsided to the greatest depth. An exception occurs only in the Bramsche Massif where special thermal conditions prevailed as noted before.

Since the overburden pressure cannot have caused the increase of rank with increasing depth (as will be shown later), only increasing rock temperature can be the reason for the vertical rank variations.

Another proof of the importance of temperature is the fact that there is often a strict relationship between the run of isovols and the run of isotherms in deep profiles, both being influenced no doubt by the varying thermal conductivity of the different rocks. The strong influence of temperature on the rank of coal is obvious in the case of contact-metamorphic coals, whose rank increases distinctly when approaching the intrusive body. Apart from these geological observations, all experiments on artificial coalification have shown that temperature is the decisive factor in the coalification process. Thermodynamic and reaction kinetic considerations (*9*) also support this opinion.

Influence of Pressure

Some earlier authors maintain that folding pressure markedly accelerated metamorphism of the coals. White (*33*) and Stadnichenko (*23*) explain the

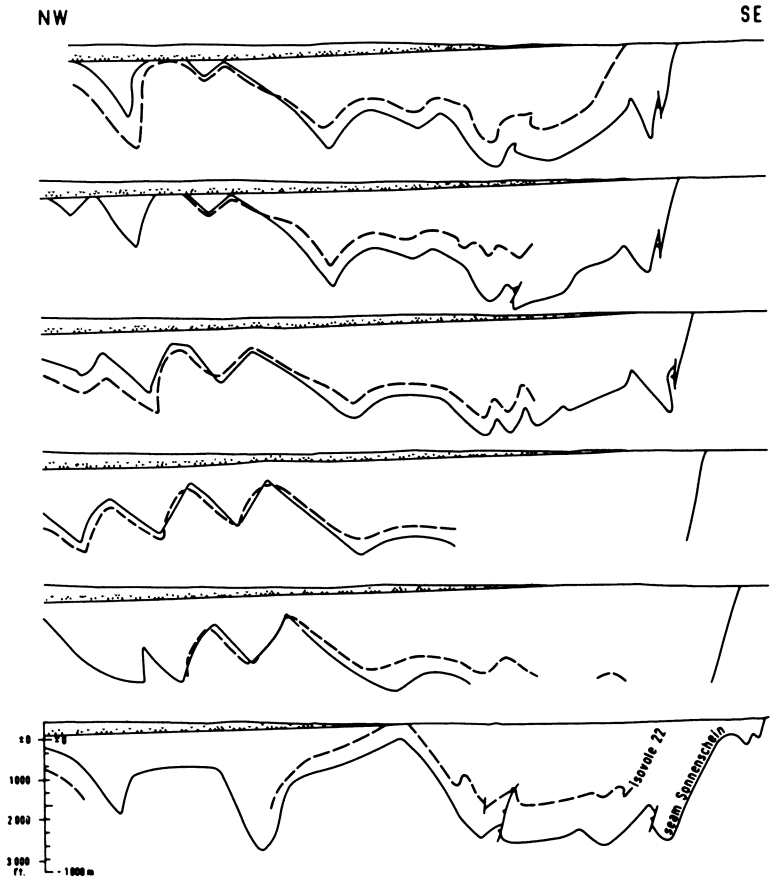

Figure 7. Folds and isovols (22% volatile matter) run parallel in cross-sections through the Bochum Syncline (Ruhr Basin) (after M. Teichmüller (25))

increase of rank of coals from the west to the east in the Appalachian region by an increasing tectonic stress. According to Stadnichenko (23), "the thrust pressure theory furnishes the only satisfactory explanation of the changes in carbonization of the bed [Lower Kittanning] in passing from the Allegheny River to the Allegheny Escarpment in western Pennsylvania." On the other hand, Heck (6) has shown that in the Appalachian area of West Virginia the folded areas generally were the areas of the deepest subsidence prior to folding. Moreover, according to Stadnichenko (23), the rank of the Lower Kittanning seam *decreases* again at the outermost eastern margin of the coal basin being studied, that is in an area where, in her view, the tectonic pressure was at a maximum. Thus, the rank of the Lower Kittanning bed has been found to be surprisingly low in the Horseshoe Mine (35% volatile matter). Perhaps the conditions are similar to those on the southernmost margin of the Ruhr Basin.

Publication Date: January 1, 1966 | doi: 10.1021/ba-1966-0055.ch010

On the southern margin of the Ruhr Basin, where folding is most intensive, coal rank is at a minimum. This is shown clearly by a coalification map of seam Sonnenschein (*18*). The reason is that here, on the edge of the basin of deposition of the Upper Carboniferous, the seam-bearing strata have not undergone the same degree of subsidence prior to folding as those farther north.

From cross-sections through the folded Ruhr Carboniferous near Bochum in Figure 7, in which the locations of the Sonnenschein seam and the 22% volatile matter isovol (obtained by numerous vitrite analyses) have been plotted, it can be seen that the isovol has been folded (so to speak) in the same way as the seams. In other words, the coalification must be older than the folding of the seams. Consequently, it cannot be an effect of the folding. These geological observations suggest that folding pressure is not responsible for the chemical changes undergone by Ruhr coals during their coalification. Since, in any event, folding pressure must have been greater than overburden pressure (otherwise folding would not have been possible), the increase in rank with depth (observed in every borehole) cannot be attributed to the increasing overburden but to the rise of rock temperature.

The latest experiments undertaken by Huck and Patteisky (*8*, *10*) have proved that, far from promoting the chemical process of coalification, static pressure, in fact, even retards it. The chemical changes undergone by a high volatile bituminous coal of 33% volatile matter at an experimental temperature of 350°C. increased with *decreasing* pressure. Under vacuum conditions these changes were great enough to cause the exinite to disappear and the volatile matter to decrease from 33 to 18%. By contrast, at a pressure of 8000 atm. the exinite and the volatile matter remained unchanged. The effect of these changes is illustrated in Figure 8.

On applying "dynamic" pressure accompanied by shearing phenomena, as produced by grinding coal in a rocking ball mill, no reaction took place at room temperature as Jüntgen and Karweil (*11*) found. At temperatures of 200°–300°C., gases such as CO, CO_2, H_2, CH_4, and higher homologues began to be released.

In nature, in coal bearing sediments of the foredeeps we may expect similar shearing phenomena only at great faults—for instance at thrust planes of the Ruhr Carboniferous. There, pent up stresses may occasionally have caused rapid tectonic movements, as has been observed in the course of certain earthquakes. Figure 9 shows the local increase of rank in the immediate vicinity of an overthrust plane, as observed near Bochum in the Ruhr Basin. Very close to the thrust plane the volatile matter of the Sonnenschein seam registers 16.7 and 13.9%, a little farther away 23.2 and 23.8%, respectively. These latter values represent the normal rank of the Sonnenschein seam in this area. However, such great increases of rank at overthrusts are very rare as far as we know from western Europe. In general, tectonic movements take place so slowly in the foredeeps that neither shearing nor friction heat exercise any observable influence over coal metamorphism. The friction heat generally leaks away without effect. (Conditions may be different in orogens

Publication Date: January 1, 1966 | doi: 10.1021/ba-1966-0055.ch010

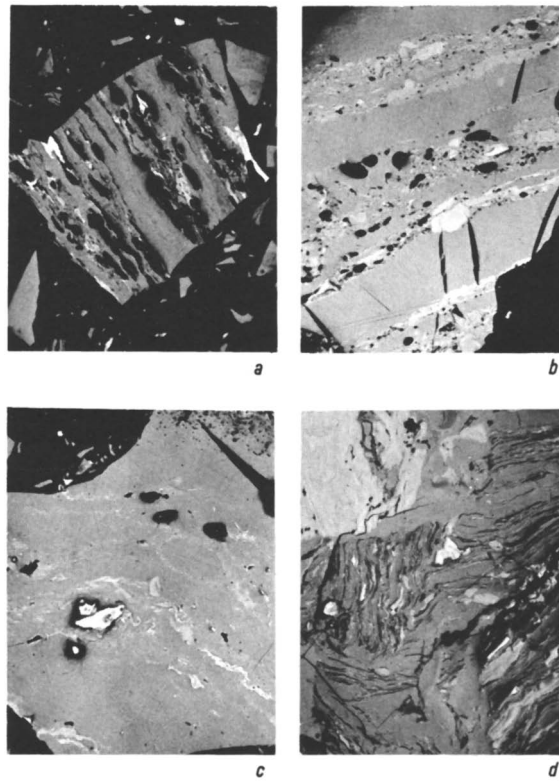

Figure 8. The alterations of macerals during artificial coalification at a temperature of 350°C. in relation to the pressure applied. Microphotographs of polished coal sections, oil immersion, × 100

(a) untreated coal (33% volatile matter) with dark exinite and weakly reflecting vitrinite

(b) coal after treatment in vacuum; the exinite has disappeared, and reflectance of vitrinite has increased greatly; pores and cracks developed by degasification

(c) coal after treatment under normal pressure; the exinite has become much lighter and is hardly visible; the reflectance of vitrinite has increased moderately

(d) coal after treatment under a pressure of 8000 atm.; the color and reflectance of exinite and vitrinite did not change; the coal particles have become briquetted (after Huck and Patteisky (8, 10); photographs by M. Th. Mackowsky and E. Wolff)

Publication Date: January 1, 1966 | doi: 10.1021/ba-1966-0055.ch010

which are impregnated with magma intrusions. In such areas graphitization obviously is promoted by shearing stress.)

The examples show that pressure usually does not promote *chemical* coalification—but undoubtedly it changes the coal physically. As is well known, clays are very sensitive to the action of overburden pressure, under which they lose moisture and porosity. Peats and brown coals have much the same characteristics as clays. This can be readily demonstrated experimentally by compressing brown coals at room temperature. The process does not involve any chemical changes but only a compression and consolidation, attended by an appreciable shrinkage in volume and emission of moisture. Figure 10 shows the action of a pressure of 270 kg./sq. cm. corresponding to an overburden of 1300 meters, upon a xylite from a soft brown coal. The

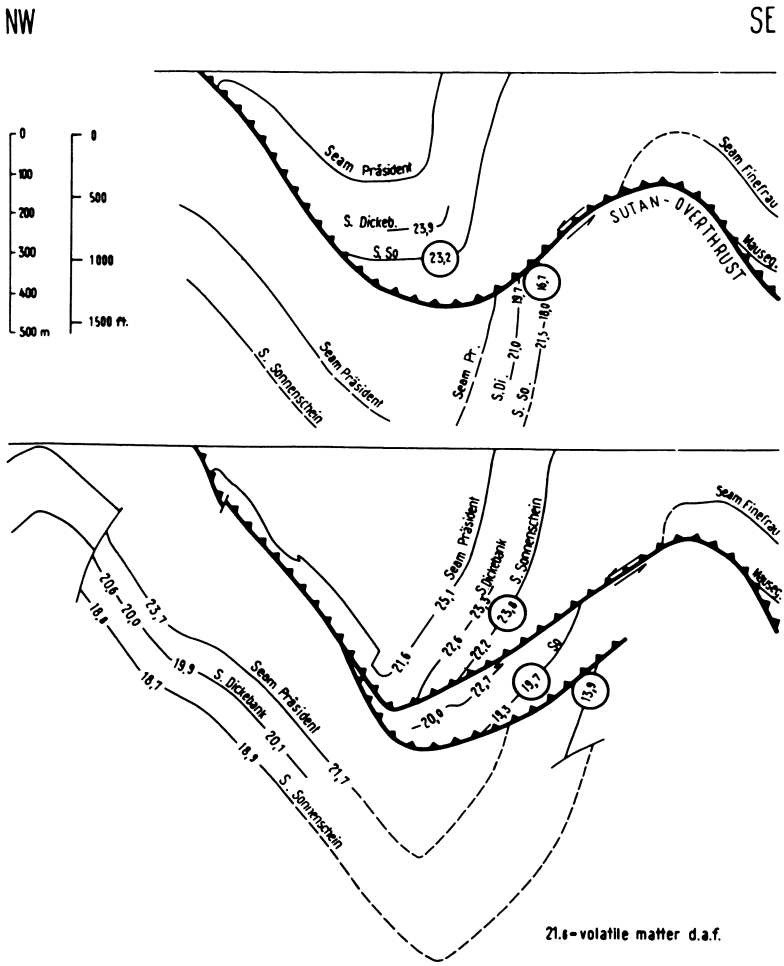

Figure 9. The increase of rank of coal in the immediate vicinity of the Sutan overthrust near Bochum (after M. Teichmüller (25))

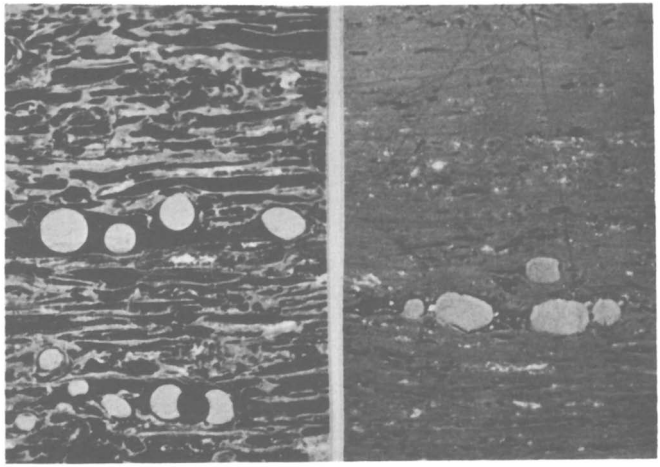

Figure 10. The effect of compression on a xylite (wood) from a soft brown coal (with 60% moisture); (left) as mined; (right) compressed at a pressure of ca. 270 kg./sq. cm. Polished sections under oil immersion, × 250

Publication Date: January 1, 1966 | doi: 10.1021/ba-1966-0055.ch010

decrease in porosity is obvious: the original cell cavities appear compressed, resulting in the formation of vitrite. Figure 11 demonstrates the compression under pressure of a humic tissue and of loosely aggregated detritus into vitrite and clarite. Macroscopically, the brown coals turned visibly darker as a result of compression, and here and there became lustrous.

This clearly indicates that pressure plays an important part in the diagenesis of coals, especially of the low rank coals—but in a purely *physical* sense. Intensely folded coals often contain relatively little moisture (cf. for example Dunningham (*3*), Edwards (*4*), Berkowitz and Schein (*1*). Moreover, we have found that coals encountered in deep wells contain less moisture than coals of similar chemical analyses which have been sampled from mine workings. This may be the effect of the release of pressure on coals exposed in mines, permitting some adsorption of water.

To sum up, according to our observations in different coal-bearing foredeeps the effect of pressure on rank increase is purely physical. The *chemical* reactions are caused by temperature increase, and according to the experimental observations, pressure actually retards them.

Influence of Time

Time generally is considered to have relatively small influence on the coalification process. To prove this it is usual to offer the example of the Mississippian lignites from the Moscow Basin which, despite their great geological age, still lack bituminous characteristics. These coals, however, were never buried to any great depth.

The proof of the influence of time on the rank of coal can be found in the following comparison: Kuyl and Patijn (*13*) have described subbituminous

coals of Eocene age from boreholes in Venezuela lying at depths of 3670–4000 meters with a rock temperature of about 125°C. Because the deep subsidence in this region occurred during Miocene and Pliocene time, the coals were subjected to a temperature of 125°C. for only 10–20 million years at the most. In the Münsterland 1 well, however, Carboniferous *anthracites* were met at almost the same depth and at the same rock temperature, but they had suffered this same temperature for a much longer period—i.e., for at least 70 million years. Hence this appears to demonstrate that—other factors being equal—length of time of coalification influences the rank of coal directly.

Let us take another example. At the U.S. Gulf Coast, the Pleistocene and the Upper Tertiary (Pliocene and Miocene) reach a thickness of more than 6000 meters. Nevertheless, the coalification has only reached the stage of high volatile bituminous at this depth. This observation resulted from our studies of samples from a deep borehole located in Terrebonne Parish, La. By reflectance measurements on humic inclusions in claystones of the uppermost Middle Miocene encountered at a depth of 5440 meters, we obtained a mean value (under oil) of 0.95% reflectance, which is equivalent to the reflectance of vitrinites (out of deep boreholes) with 35–40% volatile matter (daf). On the other hand, we found low volatile bituminous coals (14–16% volatile matter, daf) at a depth of 5100 meters in a borehole in the Lower

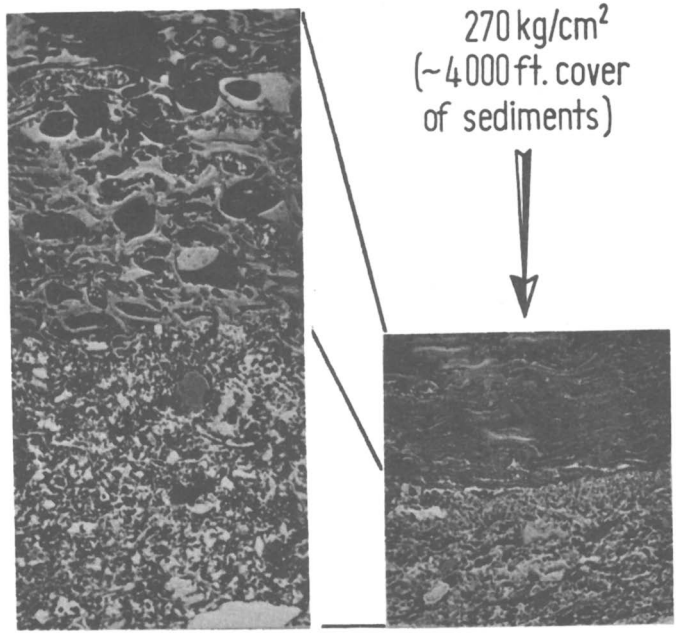

Figure 11. The effect of compression on a humic tissue and on humic degradation matter in a soft brown coal (with 60% moisture); (left) as mined; (right) after pressing. Polished sections under oil immersion, × 250

Elbe Trough in northwestern Germany (Figure 12). In both cases the temperatures are nearly the same. In the Louisiana borehole the temperature amounts to about 141°C. at a depth of 5440 meters, while in the borehole in the Lower Elbe Trough it reaches *ca.* 147°C. at a depth of 5100 meters. It seems conclusive that the Carboniferous coals of Northwest Germany lie in a sinking area which has subsided more and more since Permian time (—i.e., for 270 million years), whereas at the Gulf Coast for the same amount of subsidence a time of only 16 ± 3 million years was available for coalification of the coaly inclusions in the Miocene claystones (*see* Figure 13). Obviously this was not sufficient time for the organic matter to reach the same high degree of coalification as in Northwest Germany.

If such a formation with an incomplete coalification is folded, the run of the isovols will of course be different from that found in the Ruhr Basin as shown in Figure 7. This situation occurs in the Saar-Lorraine Basin. There the planes of equal rank of coal—on the basis of moisture content and calorific

Publication Date: January 1, 1966 | doi: 10.1021/ba-1966-0055.ch010

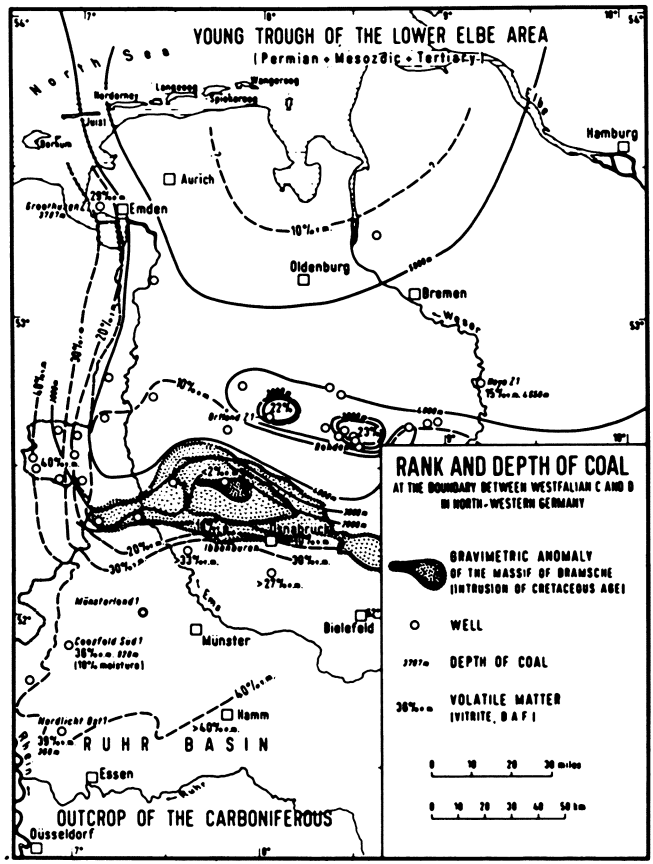

Figure 12. Rank and depth of coal in northwestern Germany

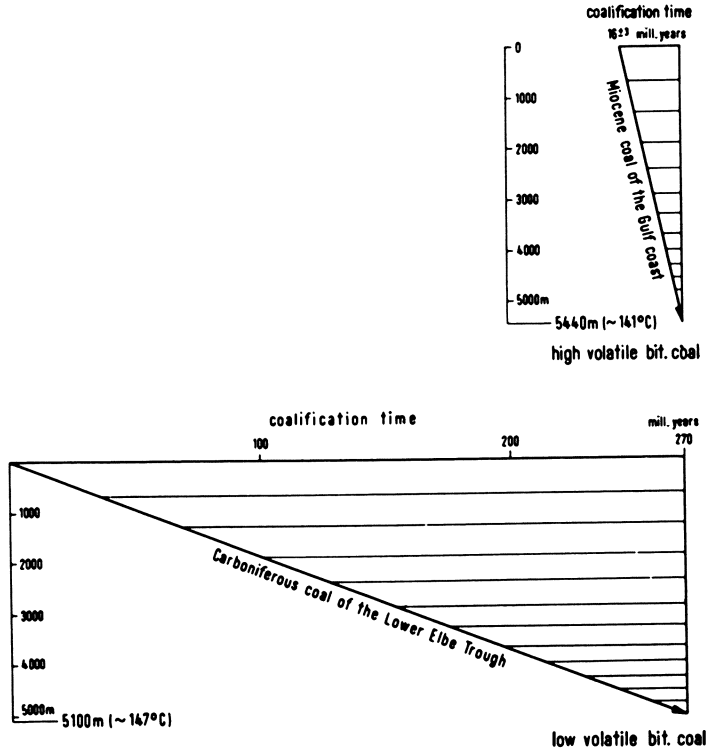

Figure 13. The difference in length of coalification time for coals of the same degree of subsidence; Carboniferous coals of the Lower Elbe Trough and Miocene coals of the U.S. Gulf Coast

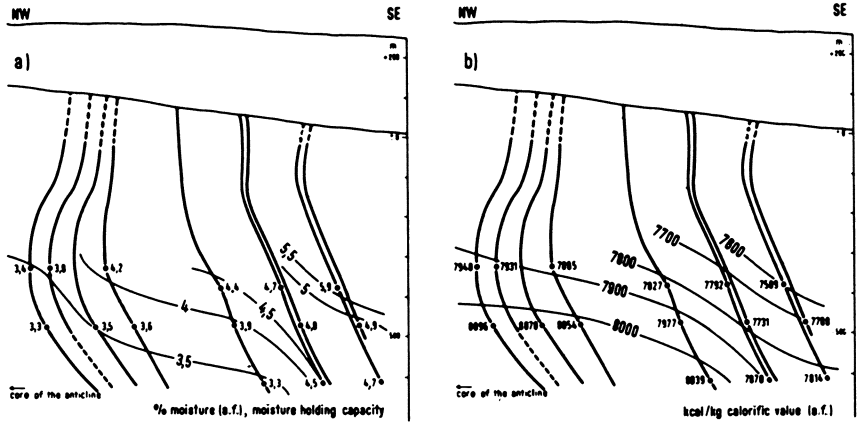

Figure 14. On the steep flank of an anticline in the Saar-Lorraine coal basin the isoplanes for the moisture capacity and the calorific value of vitrites cut the bedding planes

value—do not run parallel to the bedding planes but cut the seams at a considerable angle (Figure 14). In the Saar and in Lorraine the influence of the present depth of the seams is much more pronounced than in the Ruhr Basin (cf. (2)).

A similar picture is shown by the subbituminous coals in the northern foreland of the Alps where the lines of equal moisture content also cut the bedding planes (Figure 15). It is true that in the Hausham Syncline the moisture content of the vitrites decreases with increasing age of the seams, but on the other hand there also is a distinct relation between the moisture content and the present depth of the seams. It is striking that the lines of equal moisture content stand oblique. This may result from the uplifting of the Alps which is still proceeding.

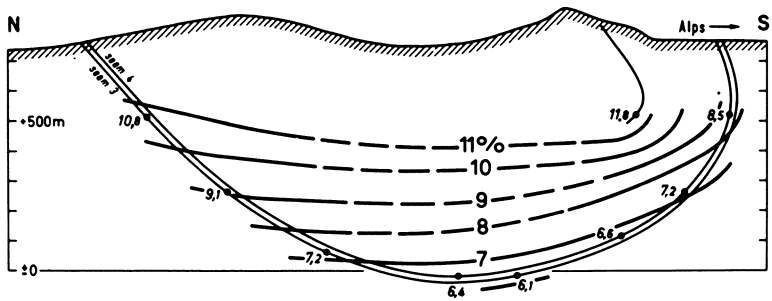

Figure 15. The course of the lines of equal moisture content in Oligocene vitrites of subbituminous stage in the Hausham Syncline, Upper Bavaria

The relation between age of coalification and age of folding may vary widely. The coalification may be preorogenic, synorogenic, or postorogenic. As the case may be, the isovols run conformable or unconformable in regard to the seams (cf. Figure 16). In the Ruhr Basin the coalification is mainly preorogenic (case a in Figure 16, cf. Figure 7). Case b in Figure 16 occurs if the coalification is synorogenic or if a preorogenic coalification is overlaid by a synorogenic or postorogenic one (for instance in Upper Bavaria and in the Saar-Lorraine Basin). A coalification which is exclusively postorogenic probably is not realized in nature.

In general each folding is combined with an uplift. Therefore as a result of folding, the coal commonly comes into cooler horizons, and the coalification will be braked or even stopped. This is true particularly of the top of the anticlines. If later the folded area subsides once more, the coalification may proceed again. In the case that this subsidence is very deep or of very long duration, the postorogenic coalification may be stronger than the preorogenic one.

As a rule the oldest sediments in a coal basin are buried deepest. The folding does not begin before the subsidence of the basin reaches a certain magnitude. Hence the seams of the oldest formations are coalified relatively strongly already before the folding. The situation is different with the

Publication Date: January 1, 1966 | doi: 10.1021/ba-1966-0055.ch010

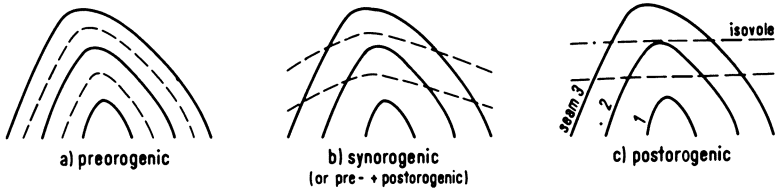

Figure 16. The run of isovols depends on the relationship in time of the coalification process and folding (schematic)

younger strata of the same coal basin. Often the folding begins during their sedimentation. In this case, the coalification of the younger formations of a coal basin is often more synorogenic than preorogenic. Also the geothermal gradient before folding plays a certain role with the age of coalification. If the gradient is steep, the beds are heated more strongly and the coalification proceeds more rapidly. When then the folding starts, the coalification has developed already to a high level. A steep preorogenic geothermal gradient thus gives a considerable chance for a preponderantly preorogenic coalification. Obviously this was the case in the Ruhr District.

In the northern part of the Ruhr Basin M. and R. Teichmüller (*29*) and Mackowsky and Kötter (*16*) have found pebbles of low volatile bituminous coals in the measures of the Lower Westfalian C, which themselves are characterized by seams of high volatile bituminous coal (40% volatile matter; cf. Figure 17). These pebbles can have their parent outcrop only in layers of Namurian C or Lowest Westfalian A age and that at the southern margin of the foredeep, where folding and uplifting took place very early. This suggests a period of coalification extending at most from the Namurian C to the beginning of the Westfalian C, which by our reckoning is a period of approximately 12 million years. This space of time, which is brief from the geological point of view, therefore suffices for a coal to attain the low volatile bituminous stage. The question is—at what temperature? We know only the former depth of burial of these coals. Paleogeographic observations suggest a maximum depth of burial of 2300 meters for the coals found on the southern margin of the Ruhr coalfield (*30*). Assuming a temperature gradient of 1°C./25 meters, this would correspond to a maximum temperature of no more than approximately 110°C. which is surprisingly low and—according to Karweil (cf. Figure 18)—seems pretty unlikely for the formation of low volatile bituminous coals. Indeed, coals of a much lower rank (high volatile bituminous coals, having 5% moisture) are found in the foredeep of the Alps, which have been buried for a longer time (20 million years) at a greater depth (2500 meters). This comparison indicates a strong heating during Carboniferous time in the foredeep of the Variscan Mountains. This assumption is supported by the occurrence of magmatic intrusions and hydrothermal mineralizations in the Variscan foredeep which are not known in the Alpine Tertiary foredeep. All this seems to suggest that a relatively steep geothermal gradient prevailed during the Carboniferous. The same idea has been published already by Kuyl and Patijn (*13*).

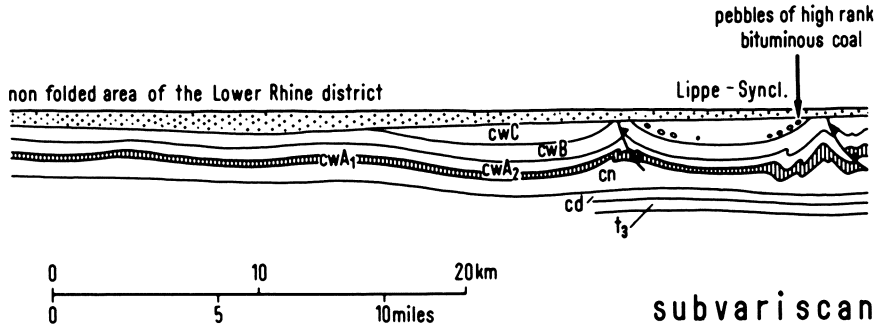

Figure 17. Cross-section through the foredeep of the Variscan orogen in northwestern Germany showing the provenance of high rank coal pebbles found in the low rank Westfalian C of the Lippe Syncline. cw = Westfalian;

Karweil (*12*) tried to illustrate graphically the correlation between coal rank, rock temperature, and duration of heating on the basis of reaction kinetics. In Figure 18 the ordinate records the temperature, and the abscissa indicates coal rank (in terms of volatile matter and a conversion factor = Z).

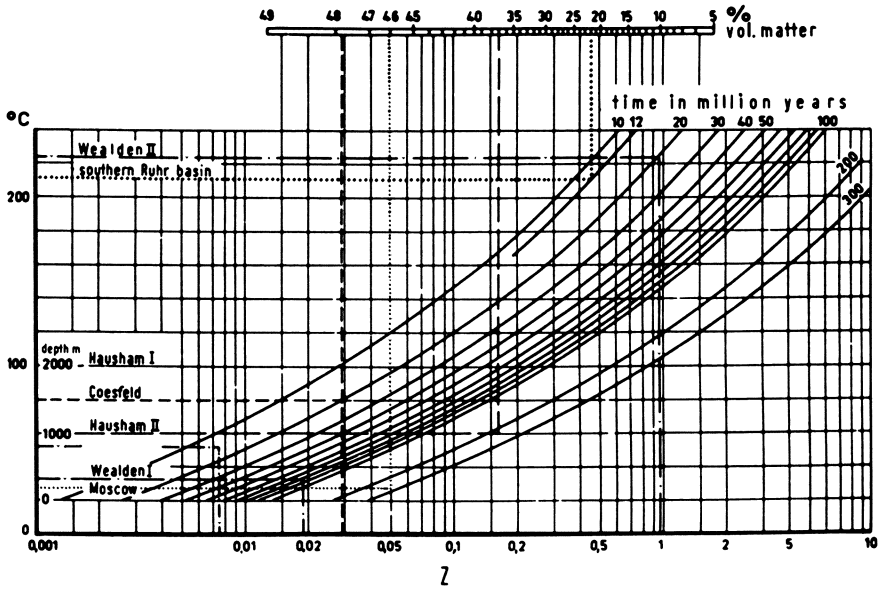

Figure 18. Relations between rank of coal (volatile matter), temperature, and time of coalification (after Karweil (12)) (Z is a conversion factor relating volatile matter to coal rank)

Publication Date: January 1, 1966 | doi: 10.1021/ba-1966-0055.ch010

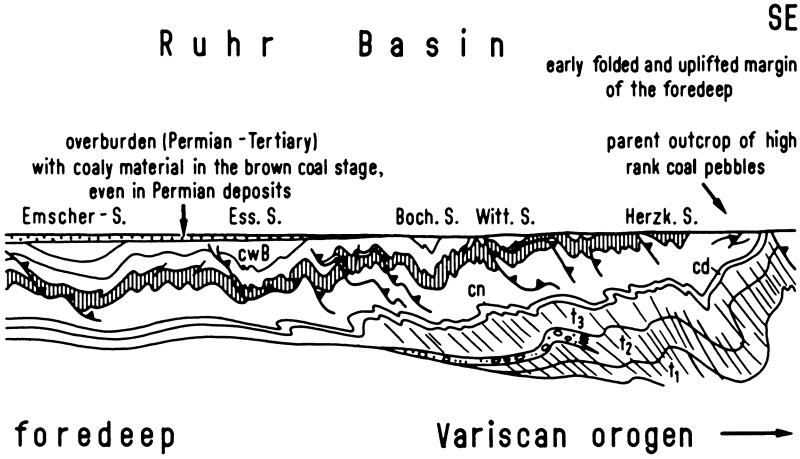

cn =Namurian; cd = Dinantian (Mississippian); t_3, t_2, t_1 = Upper, Middle, Lower Devonian

The series of curves reflects different coalification times. According to this presentation long term mild heating of the coal should result in the same coal rank as short term strong heating. Geological observational data when entered in this diagram are mostly in satisfactory agreement, yielding a temperature gradient of 1°C./25 meters. Only the coals of the southern Ruhr Basin are not consistent with this gradient. The formation of these coals (with 22% volatile matter) taking place over a span of about 12 million years —as we saw above—would imply heating to a temperature of about 210°C. according to Karweil's diagram. For a depth of burial of 2300 meters this would correspond to a geothermal gradient of 1°C./12 meters, consistent with a relatively rapid increase in the temperature of the strata during the Carboniferous.

It is interesting to note in this context that outside of the subalpine basin, plant remains of the German Tertiary attain the bituminous stage only in a region which is characterized by a particularly steep geothermal gradient. A case in point is the rift valley of the Upper Rhine near Worms, where a gradient of 1°C./12 meters is measured today. Here, at a depth of 2100–2300 meters, stems have been found in Oligocene sandstones with coalified matter having a reflectance equivalent to that of high volatile A bituminous coals. In passing it may be mentioned that major bituminous coal deposits of the Tertiary exist notably in Japan, a country known for recent vulcanism.

Conclusions

Geological investigations have shown that undoubtedly temperature has most influence on geochemical coalification. This is proved by such evidence as contact metamorphism of coals, increase of rank with increasing temperature of the earth's crust with depth, increase of rank of the same seam as magma chambers (batholiths) are approached, and relations between the thermal

Publication Date: January 1, 1966 | doi: 10.1021/ba-1966-0055.ch010

conductivity of rocks, rock temperature, and degree of coalification. The decisive influence of temperature has likewise been proved by all experiments in artificial coalification. Above all it is the maximum temperature to which the coal had been subjected over an extensive period of time which has greatest effect in increasing coal rank. In general this temperature had been attained in the major foredeeps shortly before the onset of folding (preorogenic) and rarely exceeded 200°C. However, the metamorphism of coal may also be synorogenic and postorogenic, especially in relatively young layers of a basin (for instance Upper Bavaria, Saar-Lorraine Basin) and in the shelf areas of foredeeps where the seams suffered new subsidence after the orogenic period (for instance in the Münsterland).

The effect of time upon coalification depends on the temperature to which the coal has been exposed during burial. If this temperature is low, the time factor is hardly important. With higher temperatures, however, the length of heating has a marked effect. The same rank may be reached either by a shortly acting high temperature (Ruhr Basin) or by a long acting lower temperature (Northwest Germany). The "normal" temperatures in subsiding areas (120–190°C. according to 3000–5000 meters depth and 1°C./30 meters geothermal gradient) need a certain time to produce the corresponding maximum rank. If the seams were uplifted too early, the maximum rank (corresponding to the maximum subsidence before uplifting) could not be reached (anticlines of the Saar-Lorraine Basin).

Pressure of the overburden does not cause chemical reactions which lead to a higher rank. Experiments have shown that static pressure even retards coalification processes. By contrast, pressure affects the physical properties, notably the porosity and moisture content in low rank coals. Further, the optical anisotropy of vitrinites (which is a tension anisotropy) is caused by pressure. Shearing movements have influenced the chemical coalification only occasionally and locally in the foredeeps that we have studied (for instance in the immediate vicinity of overthrusts). In such cases the tectonic movements probably were so quick that the friction heat and the shearing could operate. Shearing in no way can account for the gradual increase in coal rank with depth.

That the Carboniferous should generally be the age of bituminous and anthracite coals, and the Tertiary that of brown coals, lignites and subbituminous coals must be accepted as being unrelated to differing pressure conditions. Indeed, these rank variations (which exist even if rate and duration of subsidence of the seams and geothermal conditions were equal) may be attributed to the fact that the Carboniferous coals had better chances for a long post-orogenic coalification than the more recent coals of the Tertiary. It is debatable whether the foredeeps of the Carboniferous generally were subjected to more intensive heating than those of the Tertiary. Observations in Northwest and Central Europe appears to suggest that they were.

Acknowledgments

We express our gratitude to the National Science Foundation for enabling us to attend the American Coal Science Conference and to F. Hamilton

(National Coal Board, London) for his assistance in translating the German text.

Literature Cited

(1) Berkowitz, N., Schein, H. G., *Fuel* **31,** 19 (1952).
(2) Damberger, H., Kneuper, G., Teichmüller, M., Teichmüller, R., *Glückauf* **100,** 209 (1964).
(3) Dunningham, A. C., *Proc. Conf. Ultra-Fine Structure of Coals and Cokes, British Coal Utilisation Research Assoc.* **1944,** 57.
(4) Edwards, A. B., *Proc. Australasian Inst. Mining Met.* **150-51,** 101 (1948).
(5) Gedenk, R., *Fortschr. Geol. Rheinland Westfalen* **11,** 205 (1963).
(6) Heck, E. T., *Bull. Am. Assoc. Petrol. Geologists* **27,** 1194 (1943).
(7) Hedemann, H. A., *Fortschr. Geol. Rheinland Westfalen* **11,** 403 (1963).
(8) Huck, G., Paper presented at the Colloquium "Chemie und Physik der Steinkohle," Essen, July 10, 1964 (ref. in *Erdöl Kohle* **17,** 755 (1964)).
(9) Huck, G., Karweil, J., *Brennstoff-Chem.* **36,** 1 (1955).
(10) Huck, G., Patteisky, K., *Fortschr. Geol. Rheinland Westfalen* **12,** 551 (1964).
(11) Jüntgen, H., Karweil, J., *Freiberger Forschungsh.* **A229,** 27 (1962).
(12) Karweil, J., Z. *Deutsch. Geol. Ges.* **107,** 132 (1956).
(13) Kuyl, O. S., Patijn, R. J. H., *Compt. Rend. 4th Intern. Congr. Strat. Géol. Carbonifère* **2,** 357 (1961).
(14) Lensch, G., *Fortschr. Geol. Rheinland Westfalen* **11,** 197 (1963).
(15) Lichtenberg, K., *Fortschr. Geol. Rheinland Westfalen* **11,** 387 (1963).
(16) Mackowsky, M. Th., Kötter, K., *Fortschr. Geol. Rheinland Westfalen* **3,** 1055 (1962).
(17) Patteisky, K., Teichmüller, M., *Brennstoff-Chem.* **41,** 79, 97, 133 (1960).
(18) Patteisky, K., Teichmüller, M., Teichmüller, R., Leistikow, O., *Fortschr. Geol. Rheinland Westfalen* **3,** 687 (1962).
(19) Scherp, A., *Fortschr. Geol. Rheinland Westfalen* **11,** 251 (1963).
(20) Spackman, W., Moses, R. G., *Proc. 1960 Anthracite Conf., Penna. State Univ. Minerals Inds. Expt. Sta. Bull No.* **75,** 1 (1961).
(21) Stadler, G., *Fortschr. Geol. Rheinland Westfalen* **11,** 283 (1963).
(22) Stadler, G., Teichmüller, M., Teichmüller, R., in press.
(23) Stadnichenko, T., *Econ. Geol.* **29,** 511 (1934).
(24) Strasser, B., Wolters, R., *Fortschr. Geol. Rheinland Westfalen* **11,** 419 (1963).
(25) Teichmüller, M., *Compt. Rend. 4th Intern. Congr. Strat. Géol. Carbonifère,* **3,** 699 (1962).
(26) Teichmüller, M., *Fortschr. Geol. Rheinland Westfalen* **11,** 129 (1963).
(27) Teichmüller, M., Khalifeh, Y., Roucache, J., Louis, M., *Rev. Inst. Franc. Pétrole,* **15,** 1567 (1960).
(28) Teichmüller, M., Teichmüller, R., Z. *Deutsch. Geol. Ges.* **100,** 498 (1950).
(29) Teichmüller, M., Teichmüller, R., *Geol. Jahrb.* **65,** 497 (1950).
(30) Teichmüller, R., *Fortschr. Geol. Rheinland Westfalen* **3,** 725 (1962).
(31) Tunn, W., *Fortschr. Geol. Rheinland Westfalen* **11,** 239 (1963).
(32) Welte, D. H., *Fortschr. Geol. Rheinland Westfalen* **12,** 559 (1964).
(33) White, D., *Trans. Am. Inst. Mining Met. Eng.* **71,** 269 (1925).

RECEIVED April 19, 1965.

Discussion

Peter H. Given: I find it difficult to believe that pressure had as little chemical significance as the authors state. I accept their evidence that pressure is not a prime cause of metamorphism, and I am sure that ordinary devolatilization is suppressed at high pressures. However, it seems to me that the

existence of high pressures during active metamorphism must guide or determine the kind of effect that temperature will have—i.e., I think that the metamorphic reactions undergone by coals as a result of long exposure to elevated temperatures took one possible course rather than another because the system was under high pressure.

It has been found (K. E. Walee, *Quart. Rev. (London)* **16**, 267 (1962)) that within a certain temperature range a number of organic compounds will form high polymers if the pressure is very high (but not at atmospheric pressure). If the temperature is too low, the rate of reaction is too slow to yield any useful amount of polymer; if it is too high, the rate of cracking or decomposition exceeds the rate of polymerization, and again no polymer is obtained. Perhaps this is a relevant example of how pressure can determine the kind of change temperature will bring about. Also, it illustrates the fact that condensation or polymerization reactions can be favored by very high pressures because of the increase in density that these reactions produce.

I imagine that during metamorphism of coals, groups such as CH_3 and OH are split off as in a pyrolysis; this would be a result of heating only. The remaining structures, containing free radicals, could then condense and polymerize because they are under high pressure, instead of decomposing further as they would at higher temperatures and lower pressures.

The orientation of large aromatic lamellae parallel to the bedding plane in meta-anthracites (*see* Discussion, p. 282) must be a result of the large unidirectional pressures. It does not seem improbable that the type of aromatic character and perhaps the aromaticity itself are a result of high pressure (though of course pressure could not have this effect unless the temperature had been high enough); certainly the transition from a disordered to a fairly well ordered structure would proceed with a considerably larger decrease in free energy if the pressure were high.

Marlies and Rolf Teichmüller: We quite agree with Dr. Given that high pressures suppress the devolatization of coal, and that consequently at a given temperature the coalification product must be different at different pressures. The question is whether polymerization or condensation reactions may be favored by high pressures as far as the *coal* is concerned. Pressures may favor polymerization only if double bonds are present, which is very probably not the case with coal. The coking process shows that condensation takes place at high temperatures also *without* high pressures.

It is also our opinion that the orientation of the aromatic clusters parallel to the bedding plane is the effect of overburden pressure (cf. M. and R. Teichmüller, *Geol. Rundsch.* **42**, 266 (1954); M. Teichmüller, (*25*)). In this paper only the optical anisotropy (which is a result of this orientation) was mentioned as an effect of the unidirectional pressure during coalification. Folding pressure occasionally may change the orientation of the molecules and lead to an orientation which is oblique to the bedding plane. The result is a nonparallel extinction of the vitrinite under crossed nicols which is oriented to the direction of the folding pressure (e.g., in strongly folded subbituminous coals of Upper Bavaria). As mentioned in this paper graphitization in nature is promoted by shearing stress (in addition to very high temperatures). The

Publication Date: January 1, 1966 | doi: 10.1021/ba-1966-0055.ch010

reason may be that the ideal orientation of the lamellae of a graphite crystal is facilitated by unidirectional pressure (*see also* Jüntgen, H., Karweil, J., *Brennstoff-Chem.* **12,** 356 (1964).

However, we think that the orientation of molecules in a coal is a purely physical effect. For that reason we like to distinguish between chemical processes and physical changes during coalification (cf. *Geol. Rundsch.* **42,** 266 (1954)). We believe that the chemical reactions are promoted only by high temperatures (and long times) but retarded by high pressures. On the other hand, high pressures certainly may change the physical structure of the coal.

George Kapo: At the bottom of the bore holes there was a slight increase in the moisture content of the coal. In other words, with an increase in depth there is a minimum in moisture content. Is this minimum caused by a minimum in the cross-linked structure of the coal here?

Dr. M. Teichmüller: The minimum moisture content in coals with about 20% volatile matter and the reincrease of moisture in lower volatile bituminous coals and in anthracites, as is shown by the rank profiles, is well known. It obviously depends on the change of microporosity which has its minimum also in vitrites with *ca.* 20% volatile matter. As far as I know it is believed that this minimum depends on the chemical structure of medium volatile coals: the oxygen-rich, long bridges and chains of high volatile bituminous coals have been split off already to a considerable degree. Therefore, the space between the aromatic clusters is reduced. An explanation for the increase in microporosity and moisture in low volatile and anthracite coals is hard to give (stronger condensation of the aromatic clusters, more pronounced arrangement into the bedding plane, more production of water during the coalification of anthracites?).

Publication Date: January 1, 1966 | doi: 10.1021/ba-1966-0055.ch010

11

Coal Metamorphism and Igneous Associations in Antarctica

J. M. SCHOPF

U. S. Geological Survey, The Ohio State University, Columbus, Ohio

W. E. LONG

The Ohio State University Institute of Polar Studies, Columbus, Ohio

Publication Date: January 1, 1966 | doi: 10.1021/ba-1966-0055.ch011

Coal has been discovered in many areas along the Transantarctic Mountains by geologic parties since the International Geophysical Year (IGY) of 1957–1958. More than 100 analyses included in this report show that most of the Antarctic coal is high rank and noncaking. Its rank apparently exceeds that from any other comparable Gondwana area. Much Antarctic coal has been altered by heat from igneous intrusions. Analyses show moisture and oxygen tending to be high and variable and hydrogen declining toward the source of heat. Differences in original coal, geologic environment, confining pressure, rate of heating, and total thermal energy are reflected by Antarctic coal deposits igneothermally affected. Natural coke occurs, but coal igneothermally altered commonly appears lithologically similar to anthracite of geothermic and load-metamorphic origin.

This paper is a progress report on the analytic qualities of Antarctic coal. The first report of coal in Antarctica came from the Shackleton Expedition of 1907–09 during the first attempt to reach the South Pole. Seven coal beds were observed at Buckley Nunatak near the head of the Beardmore Glacier, and a small piece was brought back. David and Priestley (*12*) reported a dry, mineral free fixed carbon value of 83.7% for the sample, suggesting that the coal is high rank (low volatile) bituminous (*1*).

On the second Scott Expedition (1910–1913) coal float was found near Gondola Ridge in the Granite Harbor area. The coal first described as "lignite" outcropped in an inaccessible position at Mount Suess. Debenham (*13*), reporting on various aspects of Antarctic geology, indicated that

In Coal Science; Given, P.;
Advances in Chemistry; American Chemical Society: Washington, DC, 1966.

the coal at Mount Suess was high rank and similar to that of the Beardmore region. In the Mawson Expedition to Adelie Land, Madigan (*25*) reported coal from Horn Bluff on the coast bordering the South Indian Basin, but he had to abandon his samples on the journey back to the base station. Later, during the First Byrd Expedition, Gould (*19*) reported the presence of coal in the Queen Maud Mountains but did not collect a sample. On the Second Byrd Expedition Blackburn (*2*) collected an extensive suite of specimens, including coal, from the Mount Weaver area, but only an incomplete report was published and another reference was made to lignite. (Analyses presented in this report show, however, that the coal at Mount Weaver is high rank and comparable with that at other localities along the Transantarctic Mountain chain.) Prior to Deep Freeze program of the U.S. Navy, the IGY expeditions, and more recent geologic explorations this was the extent of information about coal in the Antarctic.

Publication Date: January 1, 1966 | doi: 10.1021/ba-1966-0055.ch011

Recent Coal Discoveries

A number of coal discoveries occurred rapidly during and since the IGY Antarctic operations. The central Horlick Mountain Range was visited for the first time by William E. Long during the Byrd Oversnow Traverse. He collected coal samples and published (*22*) a preliminary description of the coal measures section in that area. The Transantarctic Expedition led by Sir Vivian Fuchs (*17*) collected coal float specimens in the Theron Mountains east of the Weddell Sea. New Zealand parties (*20*) concerned with the exploration of a tractor route leading from the Antarctic plateau to sea level at Ross Island, found coal in several localities including Allan Nunatak and Mount Brooke (formerly called Tent Peak) in Victoria Land farther inland than Mount Suess. P. W. Crohn (*11*) found coal on the other side of the continent in work carried on by Australian IGY parties based on Mawson Station near the Amery Ice Shelf in the Prince Charles Mountains. In this area igneous intrusions in the coal measures apparently are lacking. To judge by the partial analysis given, the coal could have as much as 84.20% carbon and 62.30% fixed carbon on a dry, mineral-free basis. This coal would be relatively low in rank and might correspond to high volatile bituminous coal in the ASTM system of classification.

Work continued in 1960–1963 in the Ohio Range (formerly called the Central Range of the Horlick Mountains) to procure coal for accurate analysis. Samples of outcrop coal and one excellent sample of coal from an adit opened in one bed were collected. Coal samples were taken in 1959 by John J. Mulligan (*31*) at Mount Gran in the vicinity of Frank Debenham and McKenzie Taylor's old Mount Suess locality. The following season Mulligan (*32*) sampled coal farther inland in the Willett Range. Brown and Taylor (*6*) published an analytic report on coal from the Theron Mountains in 1961.

The last two field seasons (1962–63 and 1963–64) in the Antarctic yielded systematic collections of coal by Velon H. Minshew and by William E. Long of the Institute of Polar Studies, The Ohio State University, in the Mount Howe, Mount Weaver, Watson Escarpment, and Thorvald Nilsen areas of the Queen Maud Mountains. During the 1962–63 field season Dwight

L. Schmidt, A. B. Ford, and Robert D. Brown of the U.S. Geological Survey collected a float specimen of natural coke at Aztec Nunatak in the Pensacola Mountains to complete the list of coal localities now known along the Transantarctic Mountains.

One of the most spectacular discoveries of the 1963–64 field season was made by the Minnesota party under direction of Campbell Craddock (*9*) in the Sentinel Range of the Ellsworth Mountains. They submitted a sample of high rank coal accompanied by characteristic elements of the *Glossopteris* flora at a locality about 600 or 700 miles north of the nearest similar occurrences in the Transantarctic Mountains, intermediate in position between them and the Falkland Islands, where a similar flora (but no coal) has been reported from the work of early Swedish Expeditions.

Large areas underlain by coal probably are present all along the mountainous margin of the Antarctic plateau which stretches clear across Antarctica. Only the Amery deposit and that of the Sentinel Mountains occur outside this Transantarctic Mountain area.

Coal Measures Terrain

The extent of Antarctic coal fields is unknown, but some generalizations can be made about the Antarctic coal measures. The coal measures in general are of Permian age, based on plant fossil evidence (*10*, *35*, *37*). The deposits along the Transantarctic Mountains resemble the coal measures of South Africa, parts of South America and Australia in that beds commonly are flat lying; however, the coal appears higher rank, probably as a result of the Antarctic coal measures being more heavily intruded by diabase sills. However, intrusive rocks are not known to be associated with the coal in the Sentinel Mountains. A coke specimen has been collected in the Pensacola Mountains, but field relations have not yet been reported. A similar upper Paleozoic sedimentary section is now recognized in most of the region, with a glacial interval (tillite or related deposits) represented below it, followed by a zone of siltstone and dark shale, and a substantial upper section of coal-measures sandstone, with interspersed shaly beds and coal deposits.

The Antarctic coal beds are apparently less persistent, and locally may be thicker, than many of the beds in Paleozoic coal fields of North America. It is hazardous to generalize about petrographic composition from hand specimens that are available from many of the coal beds, but one obtains the impression that dull, moderately dull, and midlustrous attrital layers are more prevalent than in Paleozoic coal of the Northern Hemisphere. Vitrain bands tend to be relatively sparse and thin; fusain chips and partings generally are present and may be abundant. Many coal specimens are relatively impure, apparently owing to well-dispersed detrital mineral matter.

Such features have often been considered as evidence of allochthonous origin of coal. However, all coal beds contain *some* detrital plant fragments which, according to the peat concept of coal origin, must have been transported to some degree. A greater proportion of attrital coal (derived from vegetable detritus) might suggest a greater *degree* of allochthony, but the distinction surely is not absolute.

Publication Date: January 1, 1966 | doi: 10.1021/ba-1966-0055.ch011

The Antarctic coal measures generally lack marine deposits and underclay. Coal beds commonly grade downward into carbonaceous shale. However, some plant roots can be observed in such shale, apparently in their place of growth penetrating the bedding. Some of the plant material contributing to the coal very probably is essentially in place. The limited lateral extent of particular coal beds suggests a broad piedmont alluvial landscape occupied by somewhat discontinuous fresh water morasses or swamps. All fossil wood, observed as fusain in coal and as petrified logs, shows growth rings—proof of a seasonal climate—with concomitant fluctuation of water level in the swamps. Under these conditions alluviation would favor deposition of shale rather than formation of underclay, and account for detrital bands of impurity within the coal. Similar coal and sedimentary sequences are known in Australia, India, and South Africa.

Publication Date: January 1, 1966 | doi: 10.1021/ba-1966-0055.ch011

Sampling

Problems of access affect any effort to obtain information about Antarctic coal. Coal commonly crops out in inaccessible steep slopes swept clean by the wind and, even where accessible, the climate and the occurrence of permafrost are not favorable for sampling coal beds according to accepted standards. Coal samples obtained in the Antarctic generally are not standard. Even though modern standards of analysis have been used in treating the samples (*14*), no amount of laboratory technique can compensate for inadequacy in sampling. Nearly all of the available analytic data are based on analyses of the available coal specimens which were exposed on surfaces of outcrops. This is the type of "sample" that can be obtained practically under commonly existing conditions of climate and transport.

The weathering effects of the extremely cold and dry Antarctic climate on coal are difficult to evaluate. However, it may be that the changes owing to atmospheric exposure are considerably less than ordinarily would be expected. The possibility of penetration by oxygen-bearing surface water or roots of modern vegetation is nonexistent. Previously Schopf (*37*) had suggested that the high oxygen, variable moisture, and low sulfur content of Antarctic coal might be caused by peculiarities of weathering. However, analyses accompanying this report (*see* Table X) show that the properties of surface samples and adit samples taken up to 12 feet below the surface do not differ greatly. It may be that none of the changes from Antarctic exposure goes much deeper than the surface film of coal that can be warmed by direct sunlight.

In addition, all the coal is now high rank and not as susceptible to alteration by atmospheric exposure as lower rank coal. Apparently the Antarctic atmosphere is less important in altering the analytic properties of the coal than it would be in almost any other situation. For this reason, analyzing crop coal and float coal may be valuable for a rank determination. These results, however, are not to be relied on for evaluating grade or estimating purity, within a particular deposit.

Intrusive Rocks

Igneothermal metamorphism, a result of widespread Jurassic and infrequent Quaternary igneous intrusion, is the most important single factor affecting an evaluation of Antarctic coal. Diabase sills and dikes have been reported or may be inferred for every coal area along the Transantarctic Mountains. The age of diabase (dolerite) intrusions in the Beacon Sandstone of Victoria Land has been rated by the potassium-argon method at 147–163 m.y. (million years) (mid-Jurassic) by McDougall (*27*); slightly older diabase intrusions are reported farther north along the coast (*39*). In virtually every instance, evaluating the coal seems to depend on the relation to intrusive rocks and distance from the intrusive bodies even when obvious effects are lacking. If one is to reconstruct the metamorphic history of the coal, the effects of load and geothermal metamorphism must be disentangled from the superimposed effects of igneothermal metamorphism.

Coal Analyses

Results of a large series of Antarctic coal analyses are given in Tables I–XIV. General sample locations are indicated by table headings; more detailed locations are indicated in the coal localities reference list (Appendix). Only those analyses showing 20% or less ash have been included here. In addition, analyses of coal from South Africa (Table XV), Brazil (Table XVI), Australia (Table XVII), and New Zealand (Table XVIII) have been presented as nearly as possible on a comparable basis for comparative reference. However, precise standards of analysis differ from country to country and from laboratory to laboratory. All coals, except those from New Zealand, probably are comparable in age and geologic setting. Additional proximate analyses of foreign coals are given by Morgan and Barkley (*29*). In general terms, it appears that the average apparent rank of Antarctic coal is higher than that of comparable coal deposits of Australia, India, South Africa, or eastern South America.

Nearly all the Antarctic coal analyses are based upon determinations of the U.S. Bureau of Mines Coal Analysis Section under the supervision of Forrest E. Walker. Sources of other analytic data and sources of collections upon which they are based are cited in the locality listing of respective analyses tabulated. Ultimate values as well as results of proximate determination are given whenever available.

Analytic values on the air-dry basis vary widely. In column 2 (Table II) for example, moisture values range from 19.5–1.2%, with the higher moisture sample actually containing less ash than that having lower moisture. Oxygen values also have a surprising range. Discounting the fact that oxygen has been determined by difference according to standard analytic practice, the range of values is extraordinary. Less variation occurs in the ash-free values, but since mineral matter never occurs in the form of ash, ash-free determinations are less reliable than values corrected to approximate a mineral matter-free condition. The Parr formulation (*33*, *34*) is the most widely accepted basis for approaching mineral-free values for fixed carbon, volatile matter,

Publication Date: January 1, 1966 | doi: 10.1021/ba-1966-0055.ch011

and calorific units. The dry, mineral-free analytic values are probably the best available basis for comparing analyses of high rank Antarctic coal.

Schapiro and Gray (*36*) have shown that microscopic voids commonly occur in Antarctic coals altered by igneous heating. These voids occur without necessarily affecting the megascopic appearance of the coal. Possibly coked coals such as this, which may be called cryptovesicular, include moisture in excess of that which is driven off by standard drying procedure. It is conceivable that unusual moisture relations would be reflected by the unusual samples.

Most of the analyses of Antarctic coal were based on blocks of transportable size taken from surface outcrops. In earlier work, sections of purer coal were cut from the blocks and submitted for analysis. In later work, selected blocks were crushed, and a float fraction of purer coal was submitted to provide analytic data from each deposit. These samples, while not useful for determining coal grade, may be adequate for indicating rank. Practically all of the Antarctic coal, with the exception of that at Amery (which may represent high volatile bituminous coal), corresponds to medium volatile bituminous or higher rank. The high apparent rank Antarctic coal may be classified according to conventional ASTM standards of rank based on proximate analysis, but it seems clear that these results serve only as a first approximation.

Figure 1 shows results of nearly all of the best coal analyses available; none of the analyses plotted here represents coal with more than 20% ash. This chart shows dry, mineral-free values for fixed carbon plotted against dry, mineral-free heating value (B.t.u.). The highest rank coals, represented by points at the top of the plot, are based on samples of coal adjacent to igneous bodies. Below this, we see the major grouping of coals (outlined) which appears to range through semianthracite down to medium volatile bituminous rank according to ASTM standards of classification. The suggestion of an inclined axis is apparent only for the whole group of analyses plotted together. The shape of the grouping suggests that some more general trend of geologic correlation may exist, but the nature of the control for such a correlation is not evident. Values from any single locality commonly seem to cluster roughly in a random pattern. One sample, obtained by flotation and barely sufficient for analysis, showed unexplained high volatile bituminous characteristics (point 24/188). According to comparison with American coals within the ranks indicated, the lower range of coal samples represented here should be agglomerating. However, as far as we are aware, not one of them shows any agglomerating or caking tendency.

A detailed geologic interpretation of the influence of igneous intrusion cannot be based wholly on values of the proximate analysis. On Mount Schopf in an area adjacent to Terrace Ridge in the Ohio Range, the stratigraphic sequence and relation to igneous intrusion is perfectly clear, but there is no graduated sequence of fixed carbon or B.t.u. that corresponds to the relative distance from the overlying diabase sill. Different low ash layer samples taken from the same adit vary widely in heating value. The distance of adit samples from intrusive rock is about 1100 feet. Lack of consistency

Publication Date: January 1, 1966 | doi: 10.1021/ba-1966-0055.ch011

of mineral-free fixed carbon values in relation to known distance from an intrusive sill is shown in Figure 2. The values from ultimate analyses, on the other hand, may have a greater significance for coal which has been affected by igneous heating.

Three explanations have been suggested for the variable, commonly high, oxygen content of Antarctic coal. Brown and Taylor (*6*) suggested (and then apparently abandoned the idea) that high oxygen might have been inherited from an original high oxygen, low rank condition prior to igneous

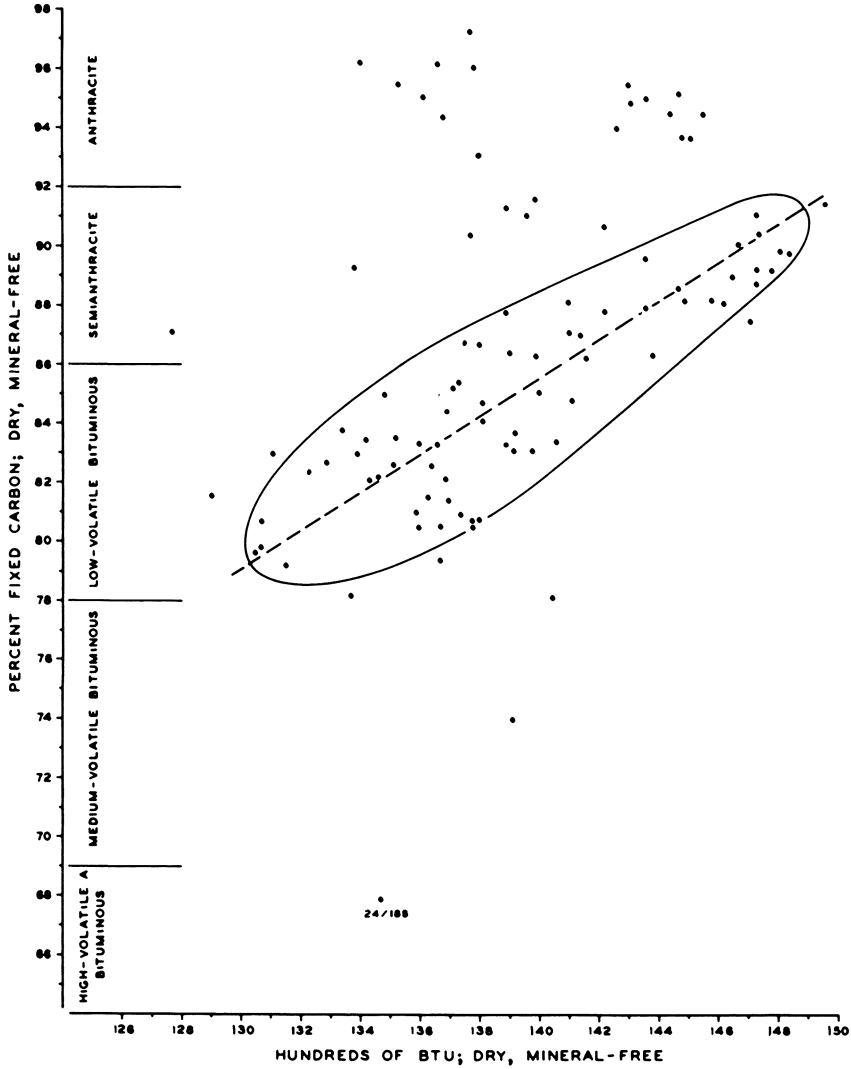

Figure 1. Relation of fixed carbon and heating value (dry, mineral-free basis) for Antarctic coal samples with less than 20% as-received ash

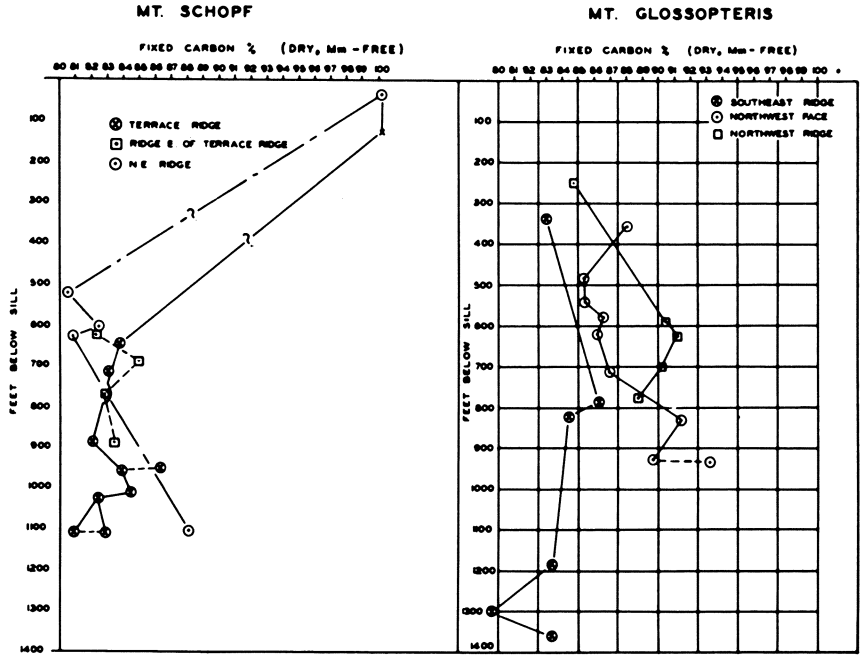

Figure 2. Comparison of fixed carbon (dry, mineral free) with relative stratigraphic position on Mt. Schopf and Mt. Glossopteris. Results of proximate analyses of three measured sections (Long (23)) are plotted in each group

heating. Geologic reasoning also suggests that the Antarctic coals probably had attained about high volatile A bituminous rank by the end of the Triassic. Coal of much lower rank is uncommon in other Gondwana areas. Lower rank original coal with high inherent moisture should show correlated, differential effects of obvious shrinkage in relation to sources of heat. However, the visible cleat, although irregular, is relatively uniform regardless of distance from a sill or dike. The original sedimentary section evidently was thick and adequate to have induced bituminous rank by loading because intrusive rocks rarely show vesiculation as they would if they had been intruded at moderate or shallow depth. The presence of small coke vesicles also indicates that the coal at the time of intrusion possessed coking properties. No vesicles would appear if the coal had been initially below the coking range in rank development. High oxygen probably was not characteristic of the coal before it was affected by intrusion.

If free oxygen had been available, it would have combined with heated coal, but a reasonable source for free oxygen is lacking. It is unlikely that gaseous oxygen could have been dissociated from water or from minerals, even as an accompaniment of igneous intrusion, according to Peter Given (*18*). However, Given also suggests that under certain conditions coal could be oxygenated directly by water without involving elemental gaseous dissociation. Hot water and steam generally are associated with igneous intrusions.

Publication Date: January 1, 1966 | doi: 10.1021/ba-1966-0055.ch011

Exposure to heated water or water vapor also might be somewhat erratic like the oxygen as determined by analysis of this coal. This suggestion, consequently, seems most attractive as a tentative explanation for oxygen anomalies. Possibly some of the unusual moisture determinations may be explained as an accompaniment of this process.

Hydrogen determinations may have special significance in interpreting coal altered by igneous intrusion. Above a temperature of 500°C. hydrogen varies directly with temperature and independently from the original character of the coal (*24*). In addition, the hydrogen content is essentially stable relative to oxidation; it is sensitive to devolatilization and metamorphic changes induced by heat. Possibly, hydrogen values will help to establish the thermal history of "higher temperature" Antarctic coal deposits.

Direct use of hydrogen values, obtained from the usual ultimate analysis, is not appropriate for this purpose. Unless a mineral-free correction is introduced, such values include the hydrogen in water of hydration derived from mineral impurities. Some clay minerals may contain more than 10% water rather tightly bound. We do not know the nature of clay minerals in Antarctic coals, and moisture relations may have been altered by igneous heating. Nevertheless, the standard Parr correction has been applied although discrepancies from this source may be fairly significant. The mineral-free correction, based on the Parr formula, has been carried out as originally devised by Orin Rees and Gilbert Thiessen of the Illinois State Geological Survey. The method was recommended by Gilbert H. Cady (*8*). A carbonate correction has been omitted because no carbonate determinations are available. None of the coal samples analyzed, however, seemed to include an appreciable content of carbonate minerals. All these calculations are based on dry (moisture-free) values. The formula for calculation is as follows:

$$\text{Hydrogen (dry, mineral free)} = \text{H} - \frac{0.16/9\ (\text{Ash} - 1.245\ 2)}{100 - \text{Mineral Matter}}$$

Mineral matter may be evaluated by calculating according to the following equation:

$$\text{Mineral Matter (dry)} = \text{Ash} + 0.625\ \text{S} + 0.16\ (\text{Ash} - 1.245\ \text{S}).$$

Other authors (*15*, *38*) have advocated a somewhat different formulation to achieve about the same result.

Dry, mineral-free hydrogen content of coal may be useful in reconstructing the relative movements of beds in faulted areas. Such a procedure would be based on establishing or assuming a relatively uniform source of heat. Faults are present in two of the coal areas in Antarctica in which the extent of throw (vertical component of dip slip) cannot be accurately determined by correlation. One area involves comparing Terrace Ridge coals (where the relation to the intrusive rock is known) with the Mount Glossopteris coals where the intrusion may have been removed by erosion. These two locations are about five miles apart. The other involves comparing analyses from a fault block area on Mount Weaver, from which the diabase has been eroded, with a section extending to the summit of the mountain where a remnant of

Publication Date: January 1, 1966 | doi: 10.1021/ba-1966-0055.ch011

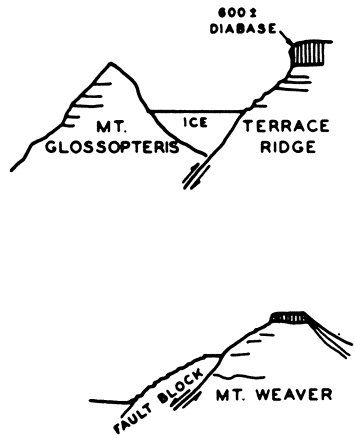

Figure 3. Relations of coal measures strata to diabase sills in the Ohio Range and at Mt. Weaver in the Queen Maud Mountains, Antarctica

the diabase cap is present. Diagrams of these relationships (not drawn to scale) are shown in Figure 3.

Unfortunately, coal analyses suitable for correlating sections in these faulted areas are not very numerous, and results now available are not sufficient to define a curve for hydrogen content that is of practical assistance. However, the data are generally consistent with the postulates suggested by field study. To this extent they help to confirm field interpretation of fault relationships diagrammed in Figure 3. The available dry, mineral-free hydrogen content for samples from each of the four sections is given below tabulated in stratigraphic sequence.

Data from Mount Weaver and from Terrace Ridge, where relations to overlying diabase are evident, show about 3% hydrogen in lower coals. The hydrogen values of all but the uppermost sample from Mount Weaver are slightly higher than those from the lower sequence of coals on Terrace Ridge. About 600 feet of diabase is present above the Terrace Ridge section (23) whereas the remnant of diabase at the summit of Mount Weaver is considerably thinner, estimated at possibly 200 feet (28). The heat reservoir at Terrace Ridge probably was greater than on Mount Weaver. A systematic decline in hydrogen, extending 600–800 feet below the diabase, with hydrogen content depending inversely on distance from the source of heat, seems apparent in both sections. Below the 600–800 foot level, values for mineral-free hydrogen seem fairly uniform.

A minimum of 0.15 and 0.16 hydrogen has been recorded for normal-appearing, banded anthracitic coal specimens taken at Sunny Ridge and at Mount Howe, in the Queen Maud Range, at a location where the coal is close to both an overlying sill and a thick diabase dike. These data suggest that hydrogen is minimal near a sill and that the hydrogen deficiency is detectable

Publication Date: January 1, 1966 | doi: 10.1021/ba-1966-0055.ch011

Ohio Range

Terrace Ridge			*Mt. Glossopteris*		
CGL no.	*H*	*Distance below thick diabase sill (ft.)*	*CGL no.*	*H*	*Distance below summit (ft.)*
134	2.25	630	162	1.62	340
83	1.97	648	150	2.86	625
105	1.98	662	159	2.51	820
108	2.36		51	2.92	<900
114	2.46		126	2.96	1126
		1091			
115	2.30	(Adit)			
117	2.26				
132	3.08	1105			

for a considerable distance from the specific heat source. The coal hydrogen thermometer method may be useful in solving problems in structural geology particularly in areas in which the contrast in hydrogen content is greater and less geologic information can be inferred directly than in the two areas just mentioned.

Igneothermal Alteration of Coal

Regional metamorphism of coal is related to both pressure and temperature attained within the upper part of the earth's crust during the period since deposition of coal-forming material. These effects depend on tectonic and geothermal history of the coal basin and generally are relatively gradual and gradational. Igneous alteration, on the other hand, usually implies conspicuous alteration of the coal adjacent to intrusive rocks. Such local effects noted in commercial coal fields have been studied and described by Marshall (*26*) and others.

Alteration of Antarctic coal seems different from the usual effects attributed to igneous intrusion because the megascopic appearance is not changed much even though there is microscopic evidence of coking (*6*, *36*). The presence of extensive sheets of igneous intrusive rocks in Antarctic coal fields suggests that igneous effects should be more than usually conspicuous there, but it is difficult to distinguish this kind of metamorphic alteration, here indicated as igneothermal, from tectonically induced, pressure-temperature metamorphism for which the geothermal gradient is most important. There seems to be no reason to suppose the geothermal gradient in Antarctica has differed greatly from that of Australia, India, South Africa, or eastern South

Publication Date: January 1, 1966 | doi: 10.1021/ba-1966-0055.ch011

Queen Maud Range

Mt. Weaver			*Fault Block*		
CGL no.	*H*	*Distance below diabase sill at summit (ft.)*	*CGL no.*	*H*	*Distance below Fault Block ledge (ft.)*
246	1.90	225	209	2.22	125
233	3.20	755	203	2.63	365
228	3.21	920	200	2.90	465
223	3.20	1070	198	2.99	507
219	3.10	1240			
216	3.06	1280			
213	3.11	1293			

America, but the higher average apparent rank of coal suggests that its igneothermal history has been somewhat different.

Coal which has been subjected to igneothermal alteration lacks coking or other properties that enhance its present commercial uses. Coal is an economic product limited by availability and utilization, and the lack of any commercial incentive may have served to limit information about natural occurrences of coal that has been affected by igneous activity. Should we ever discover that this type of thermally altered coal possesses some unusual advantage for an important type of chemical processing, our deficit in knowledge could be corrected rapidly. This, in turn, might result in an increased interest in Antarctic reserves of altered coal since they probably exceed the reserves occurring elsewhere. The effects of igneothermal alteration on coal results in a different product than that encountered in destructive distillation of coal during commercial carbonization.

Natural coke is produced at a maximum bulk density from material depositionally aggregated within a coal bed. Except in the immediate proximity of an igneous intrusion, heating rates caused by intrusion probably are so slow that they are beyond range of close comparison with any conditions in commercial coke plants. It is not surprising that the density and small size of coke vesicles in natural coke contrast so greatly with any material produced artificially. Under great overburden pressure, to say nothing of the additional pressure induced by magmatic intrusion, the surprising thing is that as many examples of natural vesicular coke occur as have been noted. Vesiculation and fissuring of natural coke have developed in spite of high pressure confinement in spaces that largely resulted from decomposition and cracking of materials pre-existing in the bed. Virtually the only causal feature

common to both natural and commercial coke is a high enough thermal history to have produced destructive distillation.

It is generally conceded that the products of igneous alteration or pyrolysis of coal strongly reflect and depend on the original state of maturation (rank) that existed prior to heating. There is much less agreement on the importance of compositional variables that reflect the original plant aggregates (type), but in experimental work differences have been noted. The Antarctic coals seem to offer an exceptional opportunity to study the role of coal type in the carbonization of coal. These coals contain a variety of naturally oriented coalified plant materials which have been subjected to bulk densities and heating rates that would be virtually impossible to duplicate experimentally. Carbonized under what we can regard as extreme conditions, much of the Antarctic coal shows so little alteration in appearance megascopically that it may be regarded as a naturally banded natural coke. More specific chemical and physical differences must serve to distinguish this type of natural coke from anthracite of geothermal and tectonic origin.

No general solution to this problem is available at present, and further consideration is beyond the scope of this report. It is evident that the Antarctic coal measures present an unusually favorable opportunity to observe relationships of intrusive rocks and coal if practical general problems of adverse climate and transportation can be solved. Coal chemical and physical criteria might be developed for recognition of a scale of alteration relative to heat source, thus furnishing the geologist with a geothermometer. It is hoped that the analytic data which have been presented will serve to focus additional attention on fundamental problems of coal related to igneothermal alteration.

Publication Date: January 1, 1966 | doi: 10.1021/ba-1966-0055.ch011

Acknowledgments

The authors are particularly indebted to Peter Given, Pennsylvania State University and to Ralph J. Gray, U.S. Steel Applied Research Laboratory, Monroeville, Pa. for most helpful criticism of an earlier version of this manuscript. Phoebe E. Reigle, U.S. Geological Survey, has calculated the mineral-free analytic values and aided in arranging the tables.

Analyses 115–117 by the Dominion Laboratory of the New Zealand Department of Scientific and Industrial Research, covering coal from the Queen Elizabeth and Dominion Ranges, were provided through the kindness of C. A. Fleming of the New Zealand Geological Survey, Lower Hutt.

All analyses of Antarctic coal samples submitted from the U.S. Geological Survey have been analyzed at the U.S. Bureau of Mines, Coal Analysis Section under supervision of Forrest E. Walker. Preparation of samples for analyses as well as field sampling and shipment was supported, in part, by NSF grant G-17216 administered by the Institute of Polar Studies through the Research Foundation, The Ohio State University.

This report has been prepared, in part, with support of NSF grant GA-177 to the U.S. Geological Survey.

Literature Cited

(1) ASTM Standards on Coal and Coke, p. 85-90, ASTM, September 1957.
(2) Blackburn, Q. A., *Geograph. Rev.* **28,** 598 (1937).
(3) Brown, H. R., *Australia, C.S.I.R.O., T.C.* **39** (1960).
(4) Brown, H. R., *Australia, C.S.I.R.O., T.C.* **46** (1962).
(5) Brown, H. R., *Australia, C.S.I.R.O., Misc. Rept.* **245** (1964).
(6) Brown, H. R., Taylor, G. H., *Fuel* **40,** 211 (1961).
(7) Brown, H. R., Waters, P. L., *Trans. World Power Conf., 6th, Melbourne, 1962,* Paper 189.
(8) Cady, Gilbert H., written communication, Nov. 22, 1954.
(9) Craddock, Campbell, Bastien, T. W., Rutford, R. H., Anderson, J. J., *Science* **148,** 634 (1965).
(10) Cridland, A. A., *Am. J. Botany* **50,** 186 (1963).
(11) Crohn, P. W., *Australian Natl. Antarctic Research Expedition Report., Ser. A.* **3,** 249 (1959).
(12) David, T. W. E., Priestley, R. E., *British Antarctic Expedition 1907-9, Sci. Inv., Geol., Report* (1914).
(13) Debenham, Frank, *British Antarctic ("Terra Nova") Expedition, 1910, Natural History Report, Geol.* **1,** 103 (1921).
(14) Fieldner, A. C., Selvig, W. A., *U.S. Bur. Mines, Bull.* **492** (1951).
(15) Francis, Wilfrid, "Coal: Its Formation and Composition," Edward Arnold, Ltd., London, 1954.
(16) Fraser, Thomas, Abreu, Alvaro de Paiva, *Min. Agricultura, Dept. Nac. Prod. Min., Lab. Prod. Min., Bull. No.* **13,** (1943).
(17) Fuchs, Sir Vivian, Hillary, Sir Edmund, "The Crossing of Antarctica," Cassell & Co., Ltd., London, 1958.
(18) Given, Peter, written communication to J. M. Schopf, March 8, 1965.
(19) Gould, L. M., "Cold: the Record of an Antarctic Sled Journey," Brewer, Warren, and Putnam, New York, 1931.
(20) Gunn, B. M., Warren, Guyon, *New Zealand, D.S.I.R., Geol. Surv. Bull. N.S.* **71,** (1962).
(21) Hall, P. E., *J. Chem., Met., Min., Soc. S. Africa* **30,** 195 (1930).
(22) Long, W. E., *Science,* **136,** 319 (1962).
(23) Long, W. E., Ph.D. Dissertation, The Ohio State University, 1964.
(24) Lowry, H. H., Landau, H. G., Naugle, L. L., *Trans. Am. Inst. Min. Met. Eng.* **149,** 297 (1942).
(25) Madigan, C. T., in "The Home of the Blizzard," Douglas Mawson, Vol. 1, p. 334, Lippincott, Philadelphia, 1914.
(26) Marshall, C. E., *Univ. Sydney, Geol. Dept., N.S., Pub. No.* **115** (1952).
(27) McDougall, Ian, *J. Geophys. Res.* **68,** 1535 (1963).
(28) Minshew, V. H., Personal communication to J. M. Schopf, 1964.
(29) Morgan, R. E., Barkley, J. F., *U.S. Bur. Mines, Bull.* **512** (1952).
(30) Morrison, G. K., *J. Chem., Met., Min., Soc. S. Africa* **40,** (1939).
(31) Mulligan, J. J., *et al., U.S. Bur. Mines, Rept. Invest.* **6218** (1963).
(32) Mulligan, J. J., *et al., U.S. Bur. Mines, Rept. Invest.* **6331** (1963).
(33) Parr, S. W., *Univ. Illinois Bull., Eng. Expt. Sta Bull.* **180** (1928).
(34) Parr, S. W., "The Analysis of Fuel, Gas, Water, and Lubricants," McGraw-Hill Book Co., Inc., New York, 1932.
(35) Plumstead, E. P., *Trans-Antarctic Expedition Sci. Rept. No.* **9** (1962).
(36) Schapiro, Norman, Gray, R. J., ADVAN. CHEM. SER. **55,** 196 (1966).
(37) Schopf, James M., *Ohio State Univ., Inst. Polar Studies, Rept. No.* **2** (1962).
(38) Seyler, C. A., *Proc. South Wales Inst. Eng.* **47** (1933).
(39) Starik. I. Ye., Krylov, A. Ya., Ravich, M. G., Silin, Yu. I., *Ann. N.Y. Acad. Sci.* **91,** 576 (1961)
(40) Suggate, R. P., *New Zealand, D.S.I.R., Bull.* **134** (1959).

RECEIVED April 19, 1965. Publication authorized by the Director, U.S. Geological Survey. Contribution No. 70, Institute of Polar Studies, The Ohio State University, Columbus, Ohio.

Appendix

Coal Localities Reference List

1:	CGL 101	Mt. Gran (77°S., 161°E.), adjacent to the Mackay Glacier, 4505 ft. elevation, specimen 1.75 in. thick, 2 ft. below a 50-ft. diabase sill. #2 Coll. Dec. 1960, P. E. Calkin, OSU.
2:	CGL 102	As above, but specimen 2 in. thick, approximately 465 ft. below 200–300 ft. thick diabase sill. #90 Coll. Dec. 1960, P. E. Calkin, OSU.
3:	CGL 103	As above, but specimen 1 in. thick from 2-ft. bed, approximately 448 ft. below 200–300 ft. diabase sill. #12B Coll. Dec. 1960, P. E. Calkin, OSU.
4:	CGL 104	As above, but specimen 1 in. thick from 1-ft. bed, approximately 434 ft. below 200–300 ft. diabase sill. #14 Coll. Dec. 1960, P. E. Calkin, OSU.
5:	12–24–4	Mt. Gran (77°S., 161°E.). Samples collected Dec. 1959, J. Mulligan, U.S. Bureau of Mines. *See* Mulligan *et al. (31).*
6:	12–23–2	*Idem*
7:	12–13–2	*Idem*
8:	12–23–1	*Idem*
9:	12–23–1 E	*Idem*
10:	12–23–1 F	*Idem*
11:	12–23–1 I	*Idem*
12:	1–9–5	*Idem*
13:	12–23–3	*Idem*
14:	1–10–1	*Idem*
15:	12–26–1	*Idem*
16:	B (MS–11)	Allan Nunatak (76°42'S., 159°45'E.). Sample collected 1957–58, G. Warren, N. Z. Geological Survey. *See* Gunn and Warren (*20*).
17:	CGL 255	Allan Nunatak, Mawson Glacier area, Victoria Land, North side midway between NE and NW ridges. AN 12 Coll. Jan. 1964, W. E. Long, OSU.
18:	CGL 256	As above, but specimen from 19-ft. coal bed, near narrow central part of NE ridge. AN 6 Coll. Jan. 1964, W. E. Long, OSU.
19:	CGL 257	As above, but specimen from upper part of 19-ft. coal bed. AN 7 Coll. Jan. 1964, W. E. Long, OSU.
20:	CGL 258	As above, but specimen from lower part of 19-ft. coal bed. AN 7 Coll. Jan. 1964, W. E. Long, OSU.
21:	CGL 259	As above, composite of specimens from 19-ft. coal bed. AN 5, 6, 7 Colls. Jan. 1964, W. E. Long, OSU.
22:	12–21–1	Mt. Robison (77°11'S., 160°20'E.). Samples collected Dec. 1960, J. Mulligan, U.S. Bureau of Mines. *See* Mulligan *et al.* (*32*).
23:	12–21–2	*Idem*
24:	12–21–4	*Idem*

Publication Date: January 1, 1966 | doi: 10.1021/ba-1966-0055.ch011

25:	12–21–5	*Idem*
26:	12–21–7	*Idem*
27:	12–21–11	*Idem*
28:	CGL 251	Queen Maud Range, Thorvald Nilson Mts. (86°7′S., 150°8′W.), Antarctica, Upper Amundsen Glacier area, about 955 ft. above basement contact. Section 7, QM 147 Coll. Jan. 1964, W. E. Long, OSU.
29:	CGL 252	As above, but about 731 ft. above basement contact. Section 13, QM 187 Coll. Jan. 1964, W. E. Long, OSU.
30:	CGL 253	As above, but about 705 ft. above basement contact. Section 13, QM 189 Coll. Jan. 1964, W. E. Long, OSU.
31:	CGL 254	As above, but about 694 ft. above basement contact. Section 13, QM 190 Coll. Jan. 1964, W. E. Long, OSU.
32:	CGL 209	Queen Maud Range, Mt. Weaver (87°S., 152°30′W.). West slope, 125 ft. below "Fault block ledge." MA–130, Coll. 1962–63, V. H. Minshew, OSU.
33:	CGL 203	As above, but 365 ft. below "Fault block ledge." MA–105 Coll. 1962–63, V. H. Minshew, OSU.
34:	CGL 200	As above, but 465 ft. below "Fault block ledge." MA–95 Coll. 1962–63, V. H. Minshew, OSU.
35:	CGL 198	As above, but 507 ft. below "Fault block ledge." MA–93 Coll. 1962–63, V. H. Minshew, OSU.
36:	CGL 197	As above, but 527 ft. below "Fault block ledge." MA–91 Coll. 1962–63, V. H. Minshew, OSU.
37:	CGL 180	Queen Maud Range, Mt. Weaver (87°S., 152°30′W.). QB 80 Coll. 1934 on Second Byrd Expedition by Q. A. Blackburn.
38:	CGL 181	As above, QB 90 Coll. 1934, 2nd Byrd Expedition, Blackburn.
39:	CGL 190	As above, QB 143 Coll. 1934, 2nd Byrd Expedition, Blackburn.
40:	CGL 193	As above, QB 66 Coll. 1934, 2nd Byrd Expedition, Blackburn.
41:	CGL 248	Queen Maud Range, about 5 miles SW of Mt. Weaver summit (87°S., 132°30′W.), about 393 ft. below crest of "Sunny Ridge." MA–216 Coll. 1962–63, V. H. Minshew, OSU.
42:	CGL 249	Queen Maud Range, about 30 miles S of Mt. Weaver, 95 ft. below summit of Mt. Howe, West ridge (87°30′S., 152°30′W.). MA–435 Coll. 1962–63, V. H. Minshew, OSU.
43:	CGL 246	Queen Maud Range, Mt. Weaver (87°S., 152°30′W.), about 225 ft. below summit, central (NE) face. MA–278 Coll. 1962–63, V. H. Minshew, OSU.
44:	CGL 243	As above, but 385 ft. below summit. MA–271 Coll. 1962–63, V. H. Minshew, OSU.
45:	CGL 240	As above, but 490 ft. below summit. MA–266 Coll. 1962–63, V. H. Minshew, OSU.
46:	CGL 237	As above, but 585 ft. below summit. MA–261 Coll. 1962–63, V. H. Minshew, OSU.
47:	CGL 235	As above, but 680 ft. below summit. MA–255 Coll. 1962–63, V. H. Minshew, OSU.

48: CGL 233 As above, but 755 ft. below summit. MA–251, Coll. 1962–63, V. H. Minshew, OSU.

49: CGL 231 As above, but 865 ft. below summit. MA–245 Coll. 1962–63, V. H. Minshew, OSU.

50: CGL 229 As above, but 895 ft. below summit. MA–242 Coll. 1962–63, V. H. Minshew, OSU.

51: CGL 228 As above, but 900 ft. below summit. MA–240 Coll. 1962–63, V. H. Minshew, OSU.

52: CGL 226 As above, but 1010 ft. below summit. MA–237 Coll. 1962–63, V. H. Minshew, OSU.

53: CGL 225 As above, but 1030 ft. below summit. MA–235 Coll. 1962–63, V. H. Minshew, OSU.

54: CGL 224 As above, but 1055 ft. below summit. MA–231 Coll. 1962–63, V. H. Minshew, OSU.

55: CGL 223 As above, but 1070 ft. below summit. MA–229 Coll. 1962–63, V. H. Minshew, OSU.

56: CGL 222 As above, but 1115 ft below summit. MA–228 Coll. 1962–63, V. H. Minshew, OSU.

57: CGL 219 As above, but 1240 ft. below summit. MA–194 Coll. 1962–63, V. H. Minshew, OSU.

58: CGL 216 As above, but 1280 ft. below summit. MA–189 Coll. 1962–63, V. H. Minshew, OSU.

59: CGL 215 As above, but 1286 ft. below summit. MA–187, Coll. 1962–63, V. H. Minshew, OSU.

60: CGL 213 As above, but 1293 ft. below summit. MA–185 Coll. 1962–63, V. H. Minshew, OSU.

61: CGL 212 As above, but 1297 ft. below summit. MA–183 coll. 1962–63, V. H. Minshew, OSU.

62: CGL 131F Ohio Range (84°50'S., 114°W.), Mt. Schopf, ridge E of Terrace Ridge, 625 ft. below diabase sill. 1.75 sp. gr. Float (18/128). H3–87 Coll. 1961–62, W. E. Long, OSU.

63: CGL 130F As above, but 690 ft. below diabase sill. 1.59 sp. gr. Float (22/164). H3–85 Coll. 1961–62, W. E. Long, OSU.

64: CGL 129F As above, but 767 ft. below diabase sill. 1.59 sp. gr. Float (31/122). H3–83 Coll. 1961–62, W. E. Long, OSU.

65: CGL 128F As above, but 883 ft. below diabase sill. 1.59 sp. gr. Float (10/94). H3–81 Coll. 1961–62, W. E. Long, OSU.

66: CGL 136F Ohio Range, Mt. Schopf, NE ridge, 525 ft. below diabase sill. 1.75 sp. gr. Float (70/210). H3–191 Coll. 1961–62, W. E. Long, OSU.

67: CGL 135F As above, but 605 ft. below diabase sill. 1.59 sp. gr. Float (48/223). H3–189 Coll. 1961–62, W. E. Long, OSU.

68: CGL 134F As above, but 630 ft. below diabase sill. 1.59 sp. gr. Float (108/244). H3–188 Coll. 1961–62, W. E. Long, OSU.

69: CGL 133F As above, but 735 ft. below diabase sill. 1.59 sp. gr. Float (24/188). H3–186 Coll. 1961–62, W. E. Long, OSU.

70: CGL 132F As above, but 1105 ft. below diabase sill. 1.59 sp. gr. Float (128/177). H3–182 Coll. 1961–62, W. E. Long, OSU.

71: CGL 83 Ohio Range (84°50'S., 114°W.), Mt. Schopf, Terrace Ridge, 648 ft. below diabase sill. 2-in. specimen at base of 12-ft. coal bed. H2–25 Coll. Dec. 1960, W. E. Long, OSU.

Publication Date: January 1, 1966 | doi: 10.1021/ba-1966-0055.ch011

72: CGL 105F As above, but 662 ft. below diabase sill; coalified stump. 1.70 sp. gr. Float. H2–4P Coll. Jan. 1961, W. E. Long and G. A. Doumani, OSU.

73: CGL 164F As above, but 710 ft. below diabase sill. 1.59 sp. gr. Float (13/163). H3–366 Coll. 1961–62, W. E. Long, OSU.

74: CGL 108 As above, but 1091 ft. below diabase sill at "Dirty Diamond" Adit; 17.5-in. coal, 124.5 in. below top of 11-ft. 10-inch bed. H3–Adit Coll. 1961–62, W. E. Long, OSU.

75: CGL 114 As above, but 9.75-in. coal, 32.8 in. below top of 11-ft. 10-in. bed. H3–Adit Coll. 1961–62, W. E. Long, OSU.

76: CGL 115 As above, but 11.5-in. coal, 20.8 in. below top of 11-ft. 10-in. bed. H3–Adit Coll. 1961–62, W. E. Long, OSU.

77: CGL 117 As above, but 8-in. coal at top of 11-ft. 10-in. bed, about 3 ft. below ground surface. H3–Adit Coll. 1961–62, W. E. Long, OSU.

78: CGL 92 As above, but 1117 ft. below diabase sill. 1-in. specimen from 8-ft. bed. H2–60 Coll. Dec. 1960, W. E. Long, OSU.

79: CGL 145F Ohio Range (84°50'S., 114°W.), Mt. Glossopteris, NW face, 546 ft. below summit. 1.59 sp. gr. Float (22/124). H3–227 Coll. 1961–62, W. E. Long, OSU.

80: CGL 144F As above, but 685 ft. below summit. 1.59 sp. gr. Float (52/292). H3–221 Coll. 1961–62, W. E. Long, OSU.

81: CGL 143F As above, but 740 ft. below summit. 1.59 sp. gr. Float (20/148). H3–220 Coll. 1961–62, W. E. Long, OSU.

82: CGL 142F As above, but 775 ft. below summit. 1.59 sp. gr. Float (28/138). H3–217 Coll. 1961–62, W. E. Long, OSU.

83: CGL 141F As above, but 817 ft. below summit. 1.59 sp. gr. Float (42/125). H3–216 Coll. 1961–62, W. E. Long, OSU.

84: CGL 140F As above, but 905 ft. below summit. 1.59 sp. gr. Float (30/116). H3–211 Coll. 1961–62, W. E. Long, OSU.

85: CGL 139F As above, but 1010 ft. below summit. 1.59 sp. gr. Float (11/121). H3–209 Coll. 1961–62, W. E. Long, OSU.

86: CGL 126F As above, just below "Museum Ledge," 1126 ft. below summit. 1.59 sp. gr. Float (40/260). H3–12/26 Coll. 1961–62, J. M. Schopf, U.S.G.S.

87: CGL 138F As above, 1129 ft. below summit. 1.59 sp. gr. Float (30/260). H3–201 Coll. 1961–62, W. E. Long, OSU.

88: CGL 51 Ohio Range, Mt. Glossopteris, about 1.5 miles NW of summit. H–16 Coll. 1959, W. E. Long, OSU.

89: CGL 153F Ohio Range (84°50'S., 114°W.), Mt. Glossopteris, North ridge, 255 ft. below summit. 1.59 sp. gr. Float (20/196). H3–229 Coll. 1961–62, W. E. Long, OSU.

90: CGL 162F As above, but SE ridge, 340 ft. below summit. 1.75 sp. gr. Float (60/170). H3–418 Coll. 1961–62, W. E. Long, OSU.

91: CGL 160F As above, 790 ft. below summit. 1.59 sp. gr. Float (87/185). H3–405 Coll. 1961–62, W. E. Long, OSU.

92: CGL 159F As above, 820 ft. below summit. 1.59 sp. gr. Float (136/176). H3–402 Coll. 1961–62, W. E. Long, OSU.

93: CGL 158F As above, 1185 ft. below summit. 1.59 sp. gr. Float (66/160) H3–177 Coll. 1961–62, W. E. Long, OSU.

Publication Date: January 1, 1966 | doi: 10.1021/ba-1966-0055.ch011

94: CGL 157F As above, 1300 ft. below summit. 1.59 sp. gr. Float (71/137). H3–174 Coll. 1961–62, W. E. Long, OSU.

95: CGL 156F As above, 1360 ft. below summit. 1.59 sp. gr. Float (76/136). H3–169 Coll. 1961–62, W. E. Long, OSU.

96: CGL 151F As above, but West ridge, 595 ft. below summit. 1.59 sp. gr. Float (36/212). H3–10–JR Coll. 1961–62, John Ricker, OSU.

97: CGL 150F As above, 625 ft. below summit. 1.59 sp. gr. Float (132/160). H3–9–JR Coll. 1961–62, John Ricker, OSU.

98: CGL 148F As above, 700 ft. below summit. 1.59 sp. gr. Float (44/80). H3–6–JR Coll. 1961–62, John Ricker, OSU.

99: CGL 147F As above, 775 ft. below summit. 1.59 sp. gr. Float (12/117). H3–5–JR Coll. 1961–62, John Ricker, OSU.

100: CGL 125F Ohio Range (84°50'S., 114°W.), Canyon Peak, about 2240 ft. above basement contact. 1.59 sp. gr. Float (34/140). H3–38 Coll. 1961–62, W. E. Long, OSU.

101: CGL 123F As above, 2160 ft. above basement contact. 1.59 sp. gr. Float (42/184). H3–34 Coll. 1961–62, W. E. Long, OSU.

102: CGL 122F As above, 2090 ft. above basement contact. 1.59 sp. gr. Float (64/110). H3–29 Coll. 1961–62, W. E. Long, OSU.

103: CGL 120F As above, 2005 ft. above basement contact. 1.59 sp. gr. Float (36/116). H3–24 Coll. 1961–62, W. E. Long, OSU.

104: CGL 119F As above, 1975 ft. above basement contact. 1.59 sp. gr. Float (44/96). H3–22 Coll. 1961–62, W. E. Long, OSU.

105: "A" Theron Mts. (79°11'S., 29°W.), Mt. Faraway. Samples collected 1957 by P. J. Stephenson, Commonwealth Trans-Antarctic Expedition. *See* Brown and Taylor (*6*).

106: "B" *Idem*

107: "C" *Idem*

108: "E" *Idem*

109: "F" *Idem*

110: "G" *Idem*

111: CGL 260F Ellsworth Mountains, Sentinel Range, Polarstar Peak (77°50'S., 85°W.), upper part exposed Polarstar Formation, 64–R Coll. 1964, R. H. Rutford, Univ. Minn.

112: CGL 265 As above, but on East ridge of Polarstar Peak (77°32'S., 86°2'W.), 6-in. bed about 680 ft. above the middle of Polarstar Formation. 64–TB–4 Coll. 1964, T. W. Bastien, Univ. Minn.

113: CGL 266 As above, but about 760 ft. above the middle of Polarstar Formation. 64–TB–68–5 Coll. 1964, T. W. Bastien, Univ. Minn.

114: CGL 267F Pensacola Mountains, Patuxent Range, central nunatak of Aztec group (about 86°S., 70°W.). 1.85 sp. gr. Float (50/148). P–4–GS–106 Coll. 1963, A. B. Ford, U.S.G.S.

115: CS–10,471 Queen Elizabeth Range, N of Law Glacier (84°S., 159°30'E.) at 7450 ft. elevation just east of plateau (50 ft. above Coll. MS–78). AJ 271/7 (MS 79) Coll. Dec. 28, 1961, G. W. Grindley, N. Z.

116: CS–10,465 Dominion Range, Nunatak E (85°25'S., 165°E.), 10-ft. coal bed outcrop on E side. AJ 271/1 (MS–104) Coll. Nov. 20, 1961, V. R. McGregor, N. Z.

Publication Date: January 1, 1966 | doi: 10.1021/ba-1966-0055.ch011

117:	CS–10,467	Dominion Range, between Mill and Keltie Glaciers (85°5′S., 171°30′E.), 10-ft. coal bed, 60 ft. above diabase sill. AJ 271/3 (1.12.2) Coll. Dec. 1, 1961, V. R. McGregor, N. Z.
118:	#1	*See* Hall (*21*).
119:	#4	*Idem*
120:	#10	*Idem*
121:	#15	*Idem*
122:	A	*See* Morrison (*30*).
123:	B	*Idem*
124:	C	*Idem*
125:	#20	*See* Hall (*21*).
126:	D	*See* Morrison (*30*).
127:	#221	*See* Fraser and Abreu (*16*).
128:	#521	*Idem*
129:	#6033	*Idem*
130:	#1321	*Idem*
131:	#1521	*Idem*
132:	#1722	*Idem*
133:	#1821	*Idem*
134:	Greta c.	*See* Brown and Waters (*7*).
135:	Muswellbrook No. 1 c.	*Idem*
136:	17858	*See* Brown (*5*).
137:	17862	*Idem*
138:	17864	*Idem*
139:	17852	*Idem*
140:	Blair Athol L 17 Top 13 ft.	*See* Brown (*3*).
141:	Blair Athol L 17 mid 11 ft.	*Idem*
142:	Blair Athol L 17 85-ft. core	*Idem*
143:	Dawson	*See* Brown and Waters (*7*).
144:	Fiery (top)	*See* Brown (*4*).
145:	Bluff c.	*Idem*
146:	Rob Roy	*Idem*
147:	37	*See* Suggate (*40*).
148:	40	*Idem*
149:	63	*Idem*
150:	68	*Idem*
151:	75	*Idem*
152:	78	*Idem*
153:	89	*Idem*

Publication Date: January 1, 1966 | doi: 10.1021/ba-1966-0055.ch011

Table I. Antarctic Coal Analyses

Central Victoria Land: Mt. Gran (Calkin)

		Proximate Analysis, %				*Ultimate Analysis, %*					
Lab. No.	*Condition*[•]	*Moisture*	*Volatile Matter*	*Fixed Carbon*	*Ash*	*C*	*H*	*N*	*S*	*O*	*B.t.u.*
– 1 –	AR	12.9	10.1	57.7	19.3	60.3	1.7	0.7	0.0	18.0	8,460
CGL–101	DRY		11.5	66.4	22.1	69.2	0.4	0.8	0.0	7.5	9,710
Calkin–2	DAF		14.8	85.2		88.9	0.5	1.0	0.1	9.5	12,470
	DMF		12.9	87.1			0.49				12,770
– 2 –	AR	7.9	5.3	82.7	4.1	82.6	2.3	1.0	0.5	9.5	12,740
CGL–102	DRY		5.7	89.9	4.4	89.7	1.5	1.1	0.5	2.8	13,830
Calkin–9C	DAF		6.0	94.0		93.9	1.6	1.2	0.5	2.8	14,470
	DMF		5.5	94.5			1.51				14,550
– 3 –	AR	9.0	5.3	77.1	8.6	76.8	2.4	1.1	0.3	10.8	11,790
CGL–103	DRY		5.9	84.6	9.5	84.4	1.5	1.2	0.3	3.1	12,960
Calkin–12B	DAF		6.5	93.5		93.2	1.7	1.3	0.3	3.5	14,310
(= 13)	DMF		5.5	94.5			1.51				14,440
– 4 –	AR	8.3	5.9	78.7	7.1	79.8	2.2	1.0	0.2	9.7	12,160
CGL–104	DRY		6.5	85.7	7.8	87.0	1.4	1.1	0.2	2.5	13,270
Calkin–14	DAF		7.0	93.0		94.3	1.5	1.2	0.3	2.7	14,380
(= 15)	DMF		6.3	93.7			1.39				14,480

[•] AD = air dried; AR = as received; DRY = moisture free; DAF = dry, ash free (moisture free and ash free); DMF = dry, mineral free (moisture free and mineral free)

Table II. Antarctic Coal Analyses

Central Victoria Land: Mt. Gran (Mulligan)

		Proximate Analysis, %				*Ultimate Analysis, %*					
Lab. No.	*Condition*[•]	*Moisture*	*Volatile Matter*	*Fixed Carbon*	*Ash*	*C*	*H*	*N*	*S*	*O*	*B.t.u.*
– 5 –	AR	7.8	10.9	66.8	14.5	68.9	2.5	0.9	1.1	12.1	10,600
12–24–4	DRY		11.8	72.5	15.7	74.7	1.8	0.9	1.2	5.7	11,490
	DAF		14.0	86.0		88.5	2.1	1.1	1.4	6.9	13,620
	DMF		12.2	87.8			1.90				13,890
– 6 –	AR	14.1	4.5	71.6	9.8	72.6	2.6	0.6	0.2	14.2	10,890
12–23–2	DRY		5.3	83.3	11.4	84.5	1.2	0.7	0.3	1.9	12,680
	DAF		6.0	94.0		95.4	1.4	0.8	0.3	2.1	14,320
	DMF		4.8	95.2			1.39				14,470
– 7 –	AR	8.8	4.5	78.0	8.7	77.0	2.3	0.5	0.3	11.2	11,690
12–13–2	DRY		5.0	85.4	9.6	84.5	1.5	0.5	0.4	3.5	12,830
	DAF		5.5	94.5		93.4	1.6	0.6	0.4	4.0	14,180
	DMF		4.5	95.5			1.51				14,300
– 8 –	AR	14.9	5.4	66.6	13.1	67.1	2.7	0.4	0.3	16.4	10,110
12–23–1	DRY		6.3	78.3	15.4	78.9	1.2	0.5	0.3	3.7	11,880
	DAF		7.5	92.5		93.3	1.4	0.5	0.3	4.5	14,050
	DMF		6.0	94.0			1.14				14,260
– 9 –	AR	19.5	4.3	67.8	8.4	67.6	3.3	0.4	0.2	20.1	10,250
12–23–1–E	DRY		5.3	84.2	10.5	84.0	1.4	0.5	0.3	3.3	12,730
	DAF		5.9	94.1		93.9	1.5	0.6	0.3	3.7	14,220
	DMF		5.0	95.0			1.39				14,360
– 10 –	AR	16.4	4.5	72.0	7.1	71.8	3.0	0.4	0.2	17.5	10,860
12–23–1–F	DRY		5.3	86.3	8.4	85.8	1.4	0.5	0.3	3.6	12,980
	DAF		5.8	94.2		93.7	1.6	0.5	0.3	3.9	14,180
	DMF		5.1	94.9			1.40				14,310

Publication Date: January 1, 1966 | doi: 10.1021/ba-1966-0055.ch011

Table II. Continued

Lab. No.	Condition*	Proximate Analysis, % Moisture	Volatile Matter	Fixed Carbon	Ash	Ultimate Analysis, % C	H	N	S	O	B.t.u.
– 11 –	AR	14.7	7.3	64.2	13.8	65.4	2.7	0.4	0.3	17.4	9,770
12–23–1–I	DRY		8.6	75.3	16.1	76.7	1.3	0.4	0.3	5.2	11,450
	DAF		10.3	89.7		91.4	1.5	0.5	0.4	6.2	13,650
	DMF		8.7	91.3			1.26				13,890
– 12 –	AR	1.2	4.7	84.4	9.7	85.5	0.5	0.0	0.1	4.2	11,950
1–9–5	DRY		4.7	85.5	9.8	86.5	0.4	0.0	0.1	3.2	12,090
	DAF		5.3	94.7		95.9	0.4	0.0	0.1	3.6	13,410
	DMF		4.4	95.6			0.26				13,530
– 13 –	AR	1.5	4.4	76.1	18.0	76.7	0.6	0.0	0.0	4.7	10,590
12–23–3	DRY		4.5	77.2	18.3	77.8	0.4	0.0	0.0	3.5	10,750
	DAF		5.5	94.5		95.2	0.5	0.0	0.0	4.3	13,150
	DMF		3.7	96.3			0.10				13,400
– 14 –	AR	6.2	6.2	75.0	12.6	74.5	2.4	0.8	0.4	9.3	11,620
1–10–1	DRY		6.6	80.0	13.4	79.4	1.9	0.9	0.4	4.0	12,390
	DAF		7.6	92.4		91.8	2.1	1.0	0.5	4.6	14,310
	DMF		6.3	93.7			1.98				14,510
– 15 –	AR	4.2	5.6	83.1	7.1	83.8	1.1	0.2	0.2	7.6	12,050
12–26–1	DRY		5.8	86.8	7.4	87.5	0.7	0.2	0.2	4.0	12,570
	DAF		6.3	93.7		94.5	0.7	0.3	0.2	4.3	13,580
	DMF		5.6	94.4			0.63				13,680

Table III. Antarctic Coal Analyses

Central Victoria Land: Allan Nunatak

Lab. No.	Condition*	Proximate Analysis, % Moisture	Volatile Matter	Fixed Carbon	Ash	Ultimate Analysis, % C	H	N	S	O	B.t.u.
– 16 –	AR	1.91	12.32	72.85	12.92				4.77		11,600
B	DRY		12.56	74.27	13.17				4.86		11,830
(MS–11)	DAF		14.47	85.53					5.60		13,620
	DMF		11.5	88.5							13,940
– 17 –	AR	3.5	13.9	72.3	10.3	74.7	3.1	1.6	0.8	9.5	12,130
CGL–255	DRY		14.4	74.9	10.7	77.4	2.8	1.7	0.8	6.6	12,570
Long–AN 12	DAF		16.1	83.9		86.7	3.1	1.9	0.9	7.4	14,070
	DMF		15.0	85.0			3.01				14,230
– 18 –	AR	4.1	15.2	70.9	9.8	73.8	3.1	1.7	0.6	11.0	11,900
CGL–256	DRY		15.8	74.0	10.2	77.0	2.8	1.8	0.6	7.6	12,400
Long–AN 6	DAF		17.6	82.4		85.7	3.1	2.0	0.7	8.5	13,810
	DMF		16.7	83.3			2.99				13,970
– 19 –	AR	3.2	13.6	65.9	17.3	68.3	2.9	1.5	0.5	9.5	11,010
CGL–257	DRY		14.0	68.1	17.9	70.6	2.6	1.6	0.5	6.8	11,380
Long–AN 7	DAF		17.0	83.0		86.0	3.1	1.9	0.6	8.4	13,860
	DMF		15.4	84.6			2.90				14,110
– 20 –	AR	3.5	12.0	74.5	10.0	76.3	3.3	1.7	0.7	8.0	12,500
CGL–258	DRY		12.4	77.2	10.4	79.0	3.0	1.8	0.7	5.1	12,950
Long–AN 5	DAF		13.9	86.1		88.1	3.3	2.0	0.8	5.8	14,450
	DMF		12.8	87.2			3.23				14,610

Table III. Continued

Lab. No.	Condition*	Proximate Analysis, % Moisture	Volatile Matter	Fixed Carbon	Ash	Ultimate Analysis, % C	H	N	S	O	B.t.u.
– 21 –	AR	3.9	13.7	70.4	12.0	72.7	3.1	1.6	0.6	10.0	11,810
CGL–259	DRY		14.2	73.4	12.4	75.7	2.8	1.7	0.6	6.8	12,290
Long–AN	DAF		16.3	83.7		86.4	3.2	1.9	0.7	7.8	14,030
5, 6, 7 composite	DMF		15.1	84.9			3.04				14,220

Table IV. Antarctic Coal Analyses

Central Victoria Land: Mt. Robison

Lab. No.	Condition*	Proximate Analysis, % Moisture	Volatile Matter	Fixed Carbon	Ash	Ultimate Analysis, % C	H	N	S	O	B.t.u.
– 22 –	AR	8.1	8.7	72.4	10.8	73.4	2.1	0.8	0.3	12.6	11,040
12–21–1	DRY		9.5	78.8	11.7	79.9	1.3	0.8	0.3	6.0	12,010
	DAF		10.8	89.2		90.6	1.5	0.9	0.4	6.6	13,610
	DMF		9.6	90.4			1.27				13,770
– 23 –	AR	6.8	8.6	76.0	8.6	77.5	2.3	0.8	0.4	10.4	11,920
12–21–2	DRY		9.2	81.6	9.2	83.1	1.6	0.9	0.4	4.8	12,790
	DAF		10.1	89.9		91.6	1.8	1.0	0.5	5.1	14,090
	DMF		9.3	90.7			1.62				14,220
– 24 –	AR	7.7	21.4	57.5	13.4	71.2	2.1	0.8	0.3	12.2	10,820
12–21–4	DRY		23.2	62.3	14.5	77.1	1.4	0.8	0.3	5.9	11,720
	DAF		27.1	72.9		90.1	1.6	0.9	0.4	7.0	13,710
	DMF		26.0	74.0			1.38				13,910
– 25 –	AR	3.7	11.0	73.2	12.1	75.6	2.6	1.2	0.6	7.9	12,040
12–21–5	DRY		11.5	75.9	12.6	78.5	2.2	1.2	0.6	4.9	12,510
	DAF		13.1	86.9		89.8	2.5	1.4	0.7	5.6	14,310
	DMF		11.8	88.2			2.34				14,490
– 26 –	AR	3.6	12.2	66.5	17.7	69.1	2.6	1.2	0.6	8.8	11,100
12–21–7	DRY		12.7	69.0	18.3	71.7	2.3	1.3	0.6	5.8	11,520
	DAF		15.5	84.5		87.8	2.8	1.5	0.8	7.1	14,100
	DMF		13.7	86.3			2.53				14,390
– 27 –	AR	5.6	11.3	72.9	10.2	74.8	2.5	1.2	0.9	10.4	11,830
12–21–11	DRY		11.9	77.3	10.8	79.3	2.0	1.2	0.9	5.8	12,520
	DAF		13.4	86.6		88.9	2.3	1.4	1.0	6.4	14,040
	DMF		12.2	87.8			2.10				14,220

Table V. Antarctic Coal Analyses

Queen Maud Mountains Region: Thorvald Nilsen Mts.

Lab. No.	Condition*	Proximate Analysis, % Moisture	Volatile Matter	Fixed Carbon	Ash	Ultimate Analysis, % C	H	N	S	O	B.t.u.
– 28 –	AR	4.6	18.2	66.4	10.8	69.4	3.0	1.9	0.7	14.2	11,100
CGL–251	DRY		19.1	69.6	11.3	72.7	2.7	2.0	0.7	10.6	11,640
Long–	DAF		21.6	78.4		82.0	3.0	2.2	0.8	12.0	13,110
QM–147	DMF		20.5	79.5			2.90				13,270

Publication Date: January 1, 1966 | doi: 10.1021/ba-1966-0055.ch011

Table V. Continued

Lab. No.	Condition*	Proximate Analysis, % Moisture	Volatile Matter	Fixed Carbon	Ash	Ultimate Analysis, % C	H	N	S	O	B.t.u.
– 29 –	AR	3.4	13.4	76.7	6.5	77.6	2.7	2.0	0.6	10.6	12,330
CGL–252	DRY		13.9	79.4	6.7	80.3	2.4	2.0	0.6	8.0	12,770
Long–	DAF		14.8	85.2		86.1	2.6	2.2	0.7	8.4	13,680
QM–187	DMF		14.2	85.8			2.49				13,780
– 30 –	AR	3.3	15.6	71.2	9.9	73.8	2.9	1.6	0.5	11.3	11,810
CGL–253	DRY		16.2	73.5	10.3	76.3	2.6	1.7	0.5	8.6	12,220
Long–	DAF		18.0	82.0		85.0	2.9	1.9	0.5	9.7	13,620
QM–189	DMF		17.0	83.0			2.76				13,750
– 31 –	AR	4.3	18.8	68.4	8.5	72.0	3.0	1.7	0.6	14.2	11,440
CGL–254	DRY		19.6	71.5	8.9	75.2	2.6	1.8	0.6	10.9	11,950
Long–	DAF		21.5	78.5		82.6	2.9	2.0	0.7	11.8	13,120
QM–190	DMF		20.7	79.3			2.75				13,240

Table VI. Antarctic Coal Analyses

Queen Maud Mountains Region: Mt. Weaver

Lab. No.	Condition*	Proximate Analysis, % Moisture	Volatile Matter	Fixed Carbon	Ash	Ultimate Analysis, % C	H	N	S	O	B.t.u.
– 32 –	AR	3.2	12.4	73.0	11.4	73.6	2.4	1.7	0.8	10.1	11,600
CGL–209	DRY		12.8	75.5	11.7	76.1	2.1	1.8	0.8	7.5	11,980
Minshew–	DAF		14.5	85.5		86.2	2.3	2.0	1.0	8.5	13,570
MA–130	DMF		13.3	86.7			2.22				13,750
– 33 –	AR	2.6	13.5	68.2	15.7	69.4	2.6	1.7	0.7	9.9	11,240
CGL–203	DRY		13.9	70.0	16.1	71.2	2.4	1.8	0.7	7.8	11,530
Minshew–	DAF		16.5	83.5		84.9	2.9	2.1	0.9	9.2	13,750
MA–105	DMF		14.9	85.1			2.63				14,000
– 34 –	AR	2.7	12.9	73.5	10.9	74.4	2.9	1.9	0.6	9.3	12,090
CGL–200	DRY		13.3	75.5	11.2	76.5	2.7	2.0	0.6	7.0	12,430
Minshew–	DAF		15.0	85.0		86.2	3.0	2.2	0.7	7.9	14,000
MA–95	DMF		13.8	86.2			2.90				14,160
– 35 –	AR	2.6	20.1	68.0	9.3	75.6	3.0	1.9	0.7	9.5	12,250
CGL–198	DRY		20.7	69.7	9.6	77.7	2.8	1.9	0.7	7.3	12,590
Minshew–	DAF		22.8	77.2		85.9	3.1	2.1	0.8	8.1	13,920
MA–93	DMF		21.9	78.1			2.99				14,040
– 36 –	AR	2.6	15.2	73.3	8.9				0.7		12,200
CGL–197	DRY		15.6	75.2	9.2				0.7		12,520
Minshew–	DAF		17.2	82.8					0.7		13,790
MA–91	DMF		16.3	83.7							13,920

Table VII. Antarctic Coal Analyses

Queen Maud Mountains Region: Mt. Weaver (Blackburn)

Lab. No.	Condition*	Proximate Analysis, % Moisture	Volatile Matter	Fixed Carbon	Ash	Ultimate Analysis, % C	H	N	S	O	B.t.u.
– 37 –	AR	3.1	15.4	65.8	15.7				0.7		10,890
CGL–180	DRY		15.9	67.9	16.2				0.7		11,230
Blackburn–	DAF		18.9	81.1					0.8		13,400
QB–80	DMF		17.4	82.6							13,640

Publication Date: January 1, 1966 | doi: 10.1021/ba-1966-0055.ch011

Table VII. Continued

Lab. No.	Condition*	Proximate Analysis, % Moisture	Volatile Matter	Fixed Carbon	Ash	Ultimate Analysis, % C	H	N	S	O	B.t.u.
– 38 –	AR	2.1	11.2	69.5	17.2				0.6		11,370
CGL–181	DRY		11.5	70.9	17.6				0.6		11,610
Blackburn–	DAF		13.9	86.1					0.8		14,090
QB–90	DMF		12.1	87.9							14,360
– 39 –	AR	2.8	16.8	73.5	6.9				0.6		12,270
CGL–190	DRY		17.3	75.6	7.1				0.6		12,620
Blackburn–	DAF		18.7	81.3					0.7		13,590
QB–143	DMF		17.9	82.1							13,690
– 40 –	AR	2.3	10.0	74.9	12.8				0.7		12,020
CGL–193	DRY		10.2	76.7	13.1				0.7		12,300
Blackburn–	DAF		11.8	88.2					0.8		14,150
QB–66	DMF		10.4	89.6							14,350
– 41 –	AR	0.9	3.5	80.2	15.4	79.7	0.5	0.1	0.1	4.2	11,350
CGL–248	DRY		3.6	80.9	15.5	80.5	0.4	0.1	0.1	3.4	11,450
Minshew–	DAF		4.2	95.8		95.2	0.5	0.1	0.1	4.1	13,550
MA–216	DMF		2.7	97.3			0.15				13,770
– 42 –	AR	1.7	4.4	78.8	15.1	77.5	0.6	0.1	0.1	6.6	11,150
CGL–249	DRY		4.5	80.2	15.3	78.8	0.4	0.1	0.1	5.3	11,340
Minshew–	DAF		5.3	94.7		93.0	0.5	0.2	0.1	6.2	13,390
MA–435	DMF		3.8	96.2			0.16				13,600

Table VIII. Antarctic Coal Analyses

Queen Maud Mountains Region: Mt. Weaver (Minshew)

Lab. No.	Condition*	Proximate Analysis, % Moisture	Volatile Matter	Fixed Carbon	Ash	Ultimate Analysis, % C	H	N	S	O	B.t.u.
– 43 –	AR	2.9	11.9	66.5	18.7	67.4	2.1	1.5	0.6	9.7	10,600
CGL–246	DRY		12.2	68.5	19.3	69.4	1.8	1.6	0.6	7.3	10,910
Minshew–	DAF		15.1	84.9		85.9	2.2	1.9	0.8	9.2	13,520
MA–278	DMF		13.3	86.7			1.90				13,800
– 44 –	AR	3.1	13.8	63.6	19.5				0.6		10,460
CGL–243	DRY		14.3	65.6	20.1				0.6		10,790
Minshew–	DAF		17.9	82.1					0.7		13,510
MA–271	DMF		15.9	84.1							13,810
– 45 –	AR	2.7	13.6	66.2	17.5				0.6		10,810
CGL–240	DRY		14.0	68.0	18.0				0.6		11,110
Minshew–	DAF		17.1	82.9					0.8		13,550
MA–266	DMF		15.3	84.7							13,810
– 46 –	AR	2.8	14.4	76.1	6.7				0.6		12,680
CGL–237	DRY		14.8	78.3	6.9				0.6		13,040
Minshew–	DAF		15.9	84.1					0.6		14,010
MA–261	DMF		15.2	84.8							14,110
– 47 –	AR	2.6	14.7	65.0	17.7				0.6		10,860
CGL–235	DRY		15.1	66.7	18.2				0.6		11,150
Minshew–	DAF		18.4	81.6					0.8		13,630
MA–255	DMF		16.7	83.3							13,890

Publication Date: January 1, 1966 | doi: 10.1021/ba-1966-0055.ch011

Table VIII. Continued

Lab. No.	Condition*	Proximate Analysis, % Moisture	Volatile Matter	Fixed Carbon	Ash	Ultimate Analysis, % C	H	N	S	O	B.t.u.
– 48 –	AR	2.3	15.5	73.1	9.1	75.6	3.2	2.0	0.6	9.5	12,340
CGL–233	DRY		15.9	74.8	9.3	77.3	3.0	2.1	0.6	7.7	12,630
Minshew–	DAF		17.5	82.5		85.3	3.3	2.3	0.7	8.4	13,930
MA–251	DMF		16.6	83.4			3.20				14,060
– 49 –	AR	2.5	15.9	74.2	7.4				0.5		12,450
CGL–231	DRY		16.3	76.1	7.6				0.5		12,770
Minshew–	DAF		17.6	82.4					0.6		13,820
MA–245	DMF		16.9	83.1							13,920
– 50 –	AR	3.0	18.6	74.5	3.9				0.6		12,670
CGL–229	DRY		19.2	76.8	4.0				0.7		13,060
Minshew–	DAF		20.0	80.0					0.7		13,610
MA–242	DMF		19.5	80.5							13,670
– 51 –	AR	2.8	17.7	70.2	9.3	73.3	3.2	2.0	0.6	11.6	11,990
CGL–228	DRY		18.2	72.2	9.6	75.4	3.0	2.0	0.6	9.4	12,330
Minshew–	DAF		20.2	79.8		83.4	3.3	2.2	0.7	10.4	13,640
MA–240	DMF		19.3	80.7			3.21				13,770
– 52 –	AR	2.6	17.4	72.9	7.1				0.6		12,280
CGL–226	DRY		17.9	74.9	7.2				0.6		12,610
Minshew–	DAF		19.3	80.7					0.7		13,600
MA–237	DMF		18.6	81.4							13,700
– 53 –	AR	2.8	17.0	64.1	16.1				0.6		10,980
CGL–225	DRY		17.5	65.9	16.6				0.6		11,290
Minshew–	DAF		20.9	79.1					0.7		13,530
MA–235	DMF		19.5	80.5							13,780
– 54 –	AR	2.9	18.4	72.8	5.9				0.7		12,320
CGL–224	DRY		18.9	75.0	6.1				0.7		12,680
Minshew–	DAF		20.1	79.9					0.7		13,500
MA–231	DMF		19.5	80.5							13,600
– 55 –	AR	2.5	15.2	68.3	14.0	70.4	3.0	1.7	0.6	10.3	11,500
CGL–223	DRY		15.5	70.1	14.4	72.2	2.9	1.8	0.6	8.2	11,790
Minshew–	DAF		18.1	81.9		84.3	3.3	2.1	0.8	9.5	13,770
MA–229	DMF		16.9	83.1			3.20				13,980
– 56 –	AR	2.2	14.1	63.7	20.0				0.7		10,750
CGL–222	DRY		14.4	65.2	20.4				0.7		11,000
Minshew–	DAF		18.1	81.9					0.8		13,820
MA–228	DMF		16.1	83.9							14,130
– 57 –	AR	2.9	17.5	70.0	9.6	73.5	3.1	1.5	0.5	11.8	11,900
CGL–219	DRY		18.0	72.1	9.9	75.8	2.9	1.6	0.5	9.3	12,260
Minshew–	DAF		19.9	80.1		84.1	3.2	1.8	0.6	10.3	13,600
MA–194	DMF		19.1	80.9			3.10				13,740
– 58 –	AR	2.8	17.8	71.4	8.0	75.3	3.2	1.4	0.5	11.6	12,210
CGL–216	DRY		18.3	73.5	8.2	77.5	2.9	1.4	0.5	9.5	12,560
Minshew–	DAF		20.0	80.0		84.4	3.2	1.5	0.5	10.4	13,680
MA–189	DMF		19.2	80.8			3.06				13,800
– 59 –	AR	3.4	19.8	67.6	9.2				0.7		11,570
CGL–215	DRY		20.5	70.0	9.5				0.8		11,980
Minshew–	DAF		22.6	77.4					0.8		13,240
MA–187	DMF		21.8	78.2							13,370

Table VIII. Continued

Lab. No.	Condition*	Proximate Analysis, % Moisture	Volatile Matter	Fixed Carbon	Ash	Ultimate Analysis, % C	H	N	S	O	B.t.u.
– 60 –	AR	2.9	17.4	69.9	9.8	72.5	3.1	1.7	0.7	12.2	11,740
CGL–213	DRY		17.9	72.0	10.1	74.7	2.9	1.7	0.7	9.9	12,090
Minshew–	DAF		19.9	80.1		83.1	3.2	1.9	0.7	11.1	13,450
MA–185	DMF		19.0	81.0			3.11				13,590
– 61 –	AR	3.2	16.6	67.7	12.5				0.6		11,340
CGL–212	DRY		17.1	70.0	12.9				0.6		11,710
Minshew–	DAF		19.7	80.3					0.7		13,450
MA–183	DMF		18.5	81.5							13,630

Table IX. Antarctic Coal Analyses

Horlick Mountains Region: Ohio Range, Terrace Ridge

Lab. No.	Condition*	Proximate Analysis, % Moisture	Volatile Matter	Fixed Carbon	Ash	Ultimate Analysis, % C	H	N	S	O	B.t.u.
– 62 –	AR	7.2	14.9	61.9	16.0				0.4		10,130
CGL–131	DRY		16.0	66.7	17.3				0.4		10,910
Long–	DAF		19.4	80.6					0.5		13,180
H3–87	DMF		17.9	82.1							13,430
– 63 –	AR	6.4	14.1	78.3	1.2				0.5		12,430
CGL–130	DRY		15.0	83.8	1.2				0.5		13,280
Long–	DAF		15.2	84.8					0.5		13,440
H3–85	DMF		15.0	85.0							13,480
– 64 –	AR	6.9	15.8	73.1	4.2				0.6		11,760
CGL–129	DRY		16.9	78.6	4.5				0.6		12,630
Long–	DAF		17.7	82.3					0.7		13,230
H3–83	DMF		17.3	82.7							13,290
– 65 –	AR	6.9	15.0	72.1	6.0				0.6		11,700
CGL–128	DRY		16.1	77.5	6.4				0.7		12,560
Long–	DAF		17.2	82.8					0.7		13,420
H3–81	DMF		16.5	83.5							13,520
– 66 –	AR	6.8	14.9	58.6	19.7				0.3		9,270
CGL–136	DRY		16.0	62.9	21.1				0.4		9,940
Long–	DAF		20.3	79.7					0.5		12,610
H3–191	DMF		18.4	81.6							12,900
– 67 –	AR	7.2	16.0	72.1	4.7				0.5		11,590
CGL–135	DRY		17.3	77.6	5.1				0.5		12,490
Long–	DAF		18.2	81.8					0.6		13,160
H3–189	DMF		17.6	82.4							13,230
– 68 –	AR	7.7	17.5	71.0	3.8	74.4	2.9	1.4	0.5	17.0	11,520
CGL–134	DRY		19.0	76.9	4.1	80.6	2.2	1.5	0.6	11.0	12,490
Long–	DAF		19.8	80.2		84.1	2.3	1.6	0.6	11.4	13,020
H3–188	DMF		19.3	80.7			2.25				13,070
– 69 –	AR	6.5	28.6	59.0	5.9				0.7		11,720
CGL–133	DRY		30.6	63.1	6.3				0.7		12,530
Long–	DAF		32.7	67.3					0.8		13,370
H3–186	DMF		32.1	67.9							13,470

Publication Date: January 1, 1966 | doi: 10.1021/ba-1966-0055.ch011

Table IX. Continued

Lab. No.	Condition*	Proximate Analysis, % Moisture	Volatile Matter	Fixed Carbon	Ash	Ultimate Analysis, % C	H	N	S	O	B.t.u.
– 70 –	AR	4.1	11.2	76.2	8.5	77.5	3.2	1.5	0.7	8.6	12,660
CGL–132	DRY		11.6	79.6	8.8	80.8	2.9	1.6	0.7	5.2	13,200
Long–	DAF		12.8	87.2		88.6	3.1	1.8	0.8	5.7	14,480
H3–182	DMF		11.9	88.1			3.08				14,620

Table X. Antarctic Coal Analyses

Horlick Mountains Region: Ohio Range, Terrace Ridge

Lab. No.	Condition*	Proximate Analysis, % Moisture	Volatile Matter	Fixed Carbon	Ash	Ultimate Analysis, % C	H	N	S	O	B.t.u.
– 71 –	AR	8.0	14.3	67.5	10.2	70.5	2.6	1.4	0.4	14.9	10,860
CGL–83	DRY		15.5	73.4	11.1	76.6	1.9	1.5	0.4	8.5	11,810
Long–	DAF		17.5	82.5		86.2	2.1	1.7	0.5	9.5	13,290
H2–25	DMF		16.5	83.5			1.97				13,420
– 72 –	AR	7.6	11.9	68.2	12.3	70.5	2.6	1.8	0.4	12.4	10,990
CGL–105	DRY		12.8	73.8	13.4	76.3	1.9	2.0	0.4	6.0	11,890
Long–	DAF		14.8	85.2		88.1	2.2	2.3	0.5	6.9	13,730
H2–4P	DMF		13.6	86.4			1.98				13,900
– 73 –	AR	7.3	15.3	71.7	5.7				0.5		11,580
CGL–164	DRY		16.5	77.4	6.1				0.6		12,490
Long–	DAF		17.6	82.4					0.6		13,310
H3–366	DMF		17.0	83.0							13,390
– 74 –	AR	7.4	17.4	61.6	13.6	65.4	2.8	1.7	0.5	16.0	10,230
CGL–108	DRY		18.8	66.6	14.6	70.6	2.2	1.8	0.6	10.2	11,040
Long–	DAF		22.0	78.0		82.8	2.6	2.1	0.7	11.8	12,930
H3–Adit	DMF		20.8	79.2			2.36				13,140
– 75 –	AR	7.5	17.3	63.1	12.1	65.9	3.0	1.4	0.6	17.0	10,350
CGL–114	DRY		18.8	68.1	13.1	71.3	2.3	1.5	0.6	11.2	11,190
Long–	DAF		21.6	78.4		82.1	2.6	1.7	0.7	12.9	12,880
H3–Adit	DMF		20.3	79.7			2.46				13,050
– 76 –	AR	7.9	17.6	65.9	8.6	69.5	2.9	1.3	0.5	17.2	10,810
CGL–115	DRY		19.1	71.6	9.3	75.4	2.2	1.4	0.6	11.1	11,740
Long–	DAF		21.0	79.0		83.1	2.4	1.6	0.6	12.3	12,940
H3–Adit	DMF		20.2	79.8			2.30				13,070
– 77 –	AR	6.5	15.0	62.6	15.9	65.3	2.7	1.1	0.5	14.5	10,260
CGL–117	DRY		16.0	67.1	16.9	69.9	2.1	1.2	0.5	9.4	10,970
Long–	DAF		19.3	80.7		84.1	2.5	1.5	0.6	11.3	13,210
H3–Adit	DMF		17.8	82.2			2.26				13,460
– 78 –	AR	6.1	14.5	61.1	18.3	63.9	2.5	1.4	0.5	13.4	10,000
CGL–92	DRY		15.4	65.1	19.5	68.1	2.0	1.5	0.5	8.4	10,660
Long–	DAF		19.1	80.9		84.6	2.4	1.9	0.6	10.5	13,240
H2–60	DMF		17.4	82.6			2.16				13,500

Table XI. Antarctic Coal Analyses

Horlick Mountains Region: Ohio Range, Mt. Glossopteris (NW)

		Proximate Analysis, %				*Ultimate Analysis, %*					
Lab. No.	*Condition*[a]	*Moisture*	*Volatile Matter*	*Fixed Carbon*	*Ash*	*C*	*H*	*N*	*S*	*O*	*B.t.u.*
– 79 –	AR	4.6	11.3	79.3	4.8				0.5		12,710
CGL–145	DRY		11.8	83.2	5.0				0.5		13,320
Long–	DAF		12.4	87.6					0.5		14,020
H3–227	DMF		11.9	88.1							14,100
– 80 –	AR	5.9	13.3	72.8	8.0				0.6		11,720
CGL–144	DRY		14.2	77.3	8.5				0.6		12,450
Long–	DAF		15.5	84.5					0.7		13,600
H3–221	DMF		14.6	85.4							13,730
– 81 –	AR	5.5	13.5	72.8	8.2				0.6		11,730
CGL–143	DRY		14.2	77.1	8.7				0.6		12,400
Long–	DAF		15.6	84.4					0.7		13,580
H3–220	DMF		14.8	85.2							13,710
– 82 –	AR	5.0	12.1	76.7	6.2				0.7		12,430
CGL–142	DRY		12.8	80.7	6.5				0.7		13,090
Long–	DAF		13.7	86.3					0.8		14,000
H3–217	DMF		12.9	87.1							14,100
– 83 –	AR	5.2	12.7	74.6	7.5				0.7		12,110
CGL–141	DRY		13.4	78.7	7.9				0.8		12,780
Long–	DAF		14.6	85.4					0.8		13,880
H3–216	DMF		13.7	86.3							13,990
– 84 –	AR	4.8	12.1	74.7	8.4				0.7		12,160
CGL–140	DRY		12.7	78.5	8.8				0.7		12,770
Long–	DAF		13.9	86.1					0.8		14,000
H3–211	DMF		13.0	87.0							14,140
– 85 –	AR	3.2	8.2	68.7	19.9				0.5		11,250
CGL–139	DRY		8.4	71.1	20.5				0.5		11,620
Long–	DAF		10.6	89.4					0.6		14,620
H3–209	DMF		8.5	91.5							14,960
– 86 –	AR	3.3	9.7	73.4	13.6	73.9	3.0	1.4	0.7	7.4	12,150
CGL–126	DRY		10.0	75.9	14.1	76.4	2.7	1.4	0.8	4.6	12,570
Long–	DAF		11.6	88.4		89.0	3.2	1.6	0.9	5.3	14,630
H3–12–26JS	DMF		10.2	89.8			2.96				14,840
– 87 –	AR	3.2	9.6	71.8	15.4				0.7		11,850
CGL–138	DRY		9.9	74.2	15.9				0.8		12,240
Long–	DAF		11.8	88.2					0.9		14,550
H3–201	DMF		10.1	89.9							14,810
– 88 –	AR	3.2	10.4	74.6	11.8	75.4	3.0	1.3	0.7	7.8	12,290
CGL–51	DRY		10.7	77.1	12.2	77.9	2.7	1.3	0.7	5.2	12,690
Long–	DAF		12.2	87.8		88.7	3.1	1.5	0.8	5.9	14,460
H–16	DMF		11.0	89.0			2.92				14,650

Table XII. Antarctic Coal Analyses

Horlick Mountains Region: Ohio Range, Mt. Glossopteris (N,SE&W)

		Proximate Analysis, %				*Ultimate Analysis, %*					
Lab. No.	*Condition*[a]	*Moisture*	*Volatile Matter*	*Fixed Carbon*	*Ash*	*C*	*H*	*N*	*S*	*O*	*B.t.u.*
– 89 –	AR	8.0	14.9	75.3	1.8				0.4		12,000
CGL–153	DRY		16.1	81.9	2.0				0.5		13,040

Publication Date: January 1, 1966 | doi: 10.1021/ba-1966-0055.ch011

Table XII. Continued

Lab. No.	Condition*	Proximate Analysis, % Moisture	Volatile Matter	Fixed Carbon	Ash	Ultimate Analysis, % C	H	N	S	O	B.t.u.
Long–	DAF		16.5	83.5					0.5		13,300
H3–229	DMF		16.2	83.8							13,330
– 90 –	AR	7.9	14.7	67.2	10.2	70.2	2.4	1.0	0.3	15.9	10,620
CGL–162	DRY		15.9	73.1	11.0	76.1	1.6	1.1	0.3	9.9	11,520
Long–	DAF		17.9	82.1		85.6	1.8	1.2	0.4	11.0	12,950
H3–418	DMF		17.0	83.0			1.62				13,110
– 91 –	AR	5.4	12.7	73.7	8.2				0.6		11,980
CGL–160	DRY		13.4	78.0	8.6				0.6		12,660
Long–	DAF		14.7	85.3					0.7		13,850
H3–405	DMF		13.8	86.2							13,990
– 92 –	AR	5.6	14.3	72.7	7.4	74.6	2.9	1.5	0.6	13.0	11,810
CGL–159	DRY		15.1	77.1	7.8	79.0	2.4	1.6	0.7	8.5	12,510
Long–	DAF		16.4	83.6		85.6	2.6	1.7	0.7	9.4	13,570
H3–402	DMF		15.6	84.4			2.51				13,690
– 93 –	AR	5.6	15.0	69.9	9.5				0.6		11,430
CGL–158	DRY		15.9	74.1	10.0				0.6		12,100
Long–	DAF		17.6	82.4					0.7		13,450
H3–177	DMF		16.7	83.3							13,600
– 94 –	AR	5.5	18.2	66.4	9.9				0.6		11,440
CGL–157	DRY		19.2	70.4	10.4				0.6		12,100
Long–	DAF		21.5	78.5					0.7		13,500
H3–174	DMF		20.6	79.4							13,670
– 95 –	AR	6.0	14.7	67.7	11.6				0.6		11,110
CGL–156	DRY		15.6	72.1	12.3				0.6		11,810
Long–	DAF		17.8	82.2					0.7		13,470
H3–169	DMF		16.7	83.3							13,660
– 96 –	AR	3.7	9.2	79.5	7.6				0.6		12,970
CGL–151	DRY		9.5	82.6	7.9				0.6		13,470
Long–	DAF		10.3	89.7					0.7		14,620
H3–10–JR	DMF		9.5	90.5							14,740
– 97 –	AR	3.9	8.6	78.9	8.6	78.7	3.0	1.5	0.6	7.6	12,770
CGL–150	DRY		8.9	82.1	9.0	81.9	2.7	1.6	0.6	4.2	13,280
Long–	DAF		9.8	90.2		90.0	2.9	1.7	0.7	4.7	14,590
H3–9–JR	DMF		8.9	91.1			2.86				14,730
– 98 –	AR	3.8	9.5	76.7	10.0				0.7		12,510
CGL–148	DRY		9.8	79.8	10.4				0.7		13,010
Long–	DAF		11.0	89.0					0.8		14,520
H3–6–JR	DMF		9.9	90.1							14,670
– 99 –	AR	4.4	10.7	75.2	9.7				0.7		12,300
CGL–147	DRY		11.1	78.8	10.1				0.7		12,860
Long–	DAF		12.4	87.6					0.8		14,300
H3–5–JR	DMF		11.4	88.6							14,470

Publication Date: January 1, 1966 | doi: 10.1021/ba-1966-0055.ch011

Table XIII. Antarctic Coal Analyses

Horlick Mountains Region: Ohio Range, Canyon Peak

		Proximate Analysis, %				*Ultimate Analysis, %*					
Lab. No.	*Condition*[•]	*Moisture*	*Volatile Matter*	*Fixed Carbon*	*Ash*	*C*	*H*	*N*	*S*	*O*	*B.t.u.*
– 100 –	AR	3.6	10.2	73.3	12.9				0.7		12,170
CGL–125	DRY		10.6	76.1	13.3				0.7		12,630
Long–	DAF		12.2	87.8					0.8		14,570
H3–38	DMF		10.8	89.2							14,780
– 101 –	AR	3.9	10.1	72.7	13.3				0.7		12,020
CGL–123	DRY		10.5	75.7	13.8				0.7		12,510
Long–	DAF		12.2	87.8					0.8		14,520
H3–34	DMF		10.8	89.2							14,730
– 102 –	AR	3.5	10.4	70.8	15.3				0.6		11,760
CGL–122	DRY		10.7	73.5	15.8				0.6		12,180
Long–	DAF		12.7	87.3					0.7		14,470
H3–29	DMF		11.2	88.8							14,730
– 103 –	AR	4.1	10.8	70.3	14.8				0.6		11,630
CGL–120	DRY		11.2	73.4	15.4				0.6		12,130
Long–	DAF		13.3	86.7					0.8		14,330
H3–24	DMF		11.8	88.2							14,580
– 104 –	AR	4.1	11.7	74.8	9.4				0.7		12,590
CGL–119	DRY		12.2	78.0	9.8				0.7		13,130
Long–	DAF		13.5	86.5					0.8		14,550
H3–22	DMF		12.5	87.5							14,710

Table XIV. Antarctic Coal Analyses

Theron Mts., and Others

		Proximate Analysis, %				*Ultimate Analysis, %*					
Lab. No.	*Condition*[•]	*Moisture*	*Volatile Matter*	*Fixed Carbon*	*Ash*	*C*	*H*	*N*	*S*	*O*	*B.t.u.*
– 105 –	AD	7.8	9.3	64.7	18.2	64.7	1.3	1.4	0.3	6.3	9,700
Brown &	DRY		10.1	70.2	19.7	69.8	1.4	1.6	0.3	7.2	10,520
Taylor–	DAF		12.6	87.4		87.4	1.7	1.9	0.4	8.6	13,120
"A"	DMF		10.7	89.3			1.37				13,380
– 106 –	AD	7.3	7.8	75.3	9.6	74.6	1.5	1.4	0.4	5.2	11,510
Brown &	DRY		8.4	81.2	10.4	80.4	1.6	1.5	0.5	5.6	12,420
Taylor–	DAF		9.4	90.6		89.8	1.8	1.7	0.5	6.2	13,840
"B"	DMF		8.4	91.6			1.63				13,990
– 107 –	AD	8.0	6.6	69.4	16.0	68.9	1.3	1.1	0.4	4.3	10,300
Brown &	DRY		7.2	75.4	17.4	74.6	1.4	1.2	0.5	4.9	11,200
Taylor–	DAF		8.6	91.4		90.6	1.7	1.4	0.6	5.7	13,540
"C"	DMF		6.9	93.1			1.38				13,800
– 108 –	AD	3.1	5.2	76.3	15.4	77.2	0.6	0.4	0.1	3.2	10,920
Brown &	DRY		5.4	78.7	15.9	79.6	0.7	0.4	0.1	3.3	11,270
Taylor–	DAF		6.4	93.6		94.8	0.8	0.5	0.1	3.8	13,400
"E"	DMF		4.9	95.1			0.51				13,610
– 109 –	AD	2.4	4.3	79.8	13.5	79.8	0.7	0.3	0.1	3.2	11,440
Brown &	DRY		4.4	81.8	13.8	81.7	0.7	0.4	0.1	3.3	11,720
Taylor–	DAF		5.1	94.9		94.9	0.8	0.4	0.1	3.8	13,600
"F"	DMF		3.8	96.2			0.54				13,780
– 110 –	AD	7.4	8.2	71.5	12.9	71.3	1.6	1.3	0.4	5.1	10,970
Brown &	DRY		8.9	77.2	13.9	77.0	1.8	1.5	0.4	5.4	11,850
Taylor–	DAF		10.3	89.7		89.6	2.0	1.7	0.5	6.2	13,770
"G"	DMF		8.9	91.1			1.87				13,960

Table XIV. Continued

Lab. No.	Condition*	Proximate Analysis, % Moisture	Volatile Matter	Fixed Carbon	Ash	Ultimate Analysis, % C	H	N	S	O	B.t.u.
– 111 –	AR	5.9	14.2	69.5	10.4	73.9	2.3	0.9	0.3	12.2	11,240
CGL–260	DRY		15.1	73.9	11.0	78.5	1.8	0.9	0.3	7.5	11,950
Rutford–	DAF		17.0	83.0		88.2	2.0	1.1	0.3	8.4	13,430
64–R	DMF		16.0	84.0			1.85				13,570
– 112 –	AR	4.3	12.0	66.5	17.2	69.4	1.9	0.8	0.2	10.5	10,480
CGL–265	DRY		12.6	69.4	18.0	72.5	1.4	0.8	0.2	7.1	10,950
Bastien–	DAF		15.3	84.7		88.4	1.8	1.0	0.3	8.5	13,340
64–TB–68–4	DMF		13.7	86.3			1.37				13,590
– 113 –	AR	4.1	12.0	69.2	14.7	71.9	1.9	0.8	0.2	10.5	10,830
CGL–266	DRY		12.5	72.1	15.4	75.0	1.4	0.9	0.2	7.1	11,300
Bastien–	DAF		14.8	85.2		88.6	1.7	1.0	0.3	8.4	13,340
64–TB–68–5	DMF		13.4	86.6			1.38				13,540
– 114 –	AR	1.0	5.9	87.2	5.9	88.2	1.3	1.1	0.3	3.2	13,060
CGL–267	DRY		6.0	88.0	6.0	89.0	1.2	1.1	0.3	2.4	13,190
Ford–	DAF		6.4	93.6		94.7	1.3	1.2	0.3	2.5	14,030
P–4–GS–106	DMF		5.7	94.3			1.18				14,110
– 115 –	AD	3.9	12.8	68.0	15.3				0.5		11,340
Grindley–	DRY		13.3	70.8	15.9				0.5		11,800
CS–10,471	DAF		16.0	84.0					0.6		14,030
	DMF		14.3	85.7							14,270
– 116 –	AD	6.5	16.2	61.1	16.2				0.5		10,390
McGregor–	DRY		17.3	65.4	17.3				0.5		11,110
CS–10,465	DAF		21.0	79.0					0.6		13,440
	DMF		19.4	80.6							13,690
– 117 –	AD	1.5	3.3	76.6	18.6				0.1		11,670
McGregor–	DRY		3.4	77.7	18.9				0.1		11,850
CS–10,467	DAF		4.0	96.0					0.1		14,610
	DMF		2.3	97.7							14,890

Table XV. South African Coal Analyses

Transvaal: Witbank, Breyten, and Ermelo Districts (Samples 118–125)
Natal: Klipriver District (Sample 126)

Lab. No.	Condition*	Proximate Analysis, % Moisture	Volatile Matter	Fixed Carbon	Ash	Ultimate Analysis, % C	H	N	S	O	B.t.u.
– 118 –	AR	2.71	24.37	62.6	10.32	72.39	4.25	1.76	0.52	10.76	12,350
Witbank	DRY		25.03	64.37	10.60	74.35	4.07	1.81	0.53	8.64	12,690
Hall #1	DAF		28.0	72.0		83.35	4.50	2.00	0.59	9.56	14,190
(1930)	DMF		27.18	72.82			4.45				14,350
– 119 –	AR	2.20	25.07	61.22	11.51	72.85	4.31	1.64	0.63	9.06	12,590
Witbank	DRY		25.62	62.60	11.76	74.46	4.16	1.68	0.64	7.30	12,870
Hall #4	DAF		29.04	70.96		84.60	4.65	1.88	0.71	8.16	14,590
(1930)	DMF		28.11	71.89			4.61				14,770
– 120 –	AR	1.61	34.21	54.43	9.75	72.82	4.97	1.72	1.24	9.50	12,990
Witbank	DRY		34.76	55.33	9.91	73.99	4.87	1.75	1.26	8.22	13,200
Hall #10	DAF		38.59	61.41		82.3	5.35	1.92	1.39	9.04	14,650
(1930)	DMF		37.78	62.22			5.37				14,830

Table XV. Continued

Lab. No.	Condition*	Proximate Analysis, % Moisture	Volatile Matter	Fixed Carbon	Ash	Ultimate Analysis, % C	H	N	S	O	B.t.u.
– 121 –	AR	1.96	27.70	60.42	9.92	72.49	4.31	1.86	1.23	10.19	12,480
Witbank	DRY		28.24	61.65	10.11	73.91	4.18	1.9	1.25	8.65	12,730
Hall #15	DAF		31.42	68.58		82.40	4.60	2.09	1.38	9.53	14,160
(1930)	DMF		30.48	69.52			4.59				14,330
– 122 –	AR	1.7	37.6	52.1	8.6	74.7	5.4		1.0		
Witbank	DRY		38.3	53.0	8.7	76.0	5.3				
Morrison–A	DAF		41.9	58.1		82.6	5.8				
(1939)	DMF		41.3	58.7			5.77				
– 123 –	AR	1.8	34.0	55.3	8.9	74.9	5.1		1.0		
Witbank	DRY		34.6	56.3	9.1	76.2	4.95				
Morrison–B	DAF		38.1	61.9		83.1	5.4				
(1939)	DMF		37.4	62.6			5.40				
– 124 –	AR	2.9	31.0	54.3	11.8	69.9	4.8		1.0		
Breyten	DRY		31.9	55.9	12.2	71.9	4.64				
Morrison–C	DAF		36.3	63.7		80.7	5.2				
(1939)	DMF		35.4	64.6			5.19				
– 125 –	AR	3.19	30.60	53.83	12.38	66.08	4.68	1.79	1.09	13.98	11,470
Ermelo	DRY		31.58	55.65	12.77	68.19	4.48	1.85	1.12	11.59	11,850
Hall #20	DAF		36.19	63.81		78.53	5.05	2.09	1.26	13.07	13,580
(1930)	DMF		35.22	64.78			5.05				13,780
– 126 –	AR	1.6	28.2	57.1	13.1	73.2	4.5		1.0		
Klipriver	DRY		28.7	58.0	13.3	74.4	4.41				
Morrison–D	DAF		33.1	66.9		84.4	5.0				
(1939)	DMF		32.0	68.0			4.99				

Table XVI. South American Coal Analyses

Brazil: Rio Grande Do Sul (Samples 127–129)
Brazil: Santa Catarina (Samples 130–133)

Lab. No.	Condition*	Proximate Analysis, % Moisture	Volatile Matter	Fixed Carbon	Ash	Ultimate Analysis, % C	H	N	S	O	B.t.u.
– 127 –	AR	21.1	26.4	41.7	10.8				1.38		9,390
Fraser &	DRY		33.4	53.0	13.6				1.75		11,900
Abreu #221	DAF		38.7	61.3					2.03		13,770
(1943)	DMF		37.6	62.4							14,020
– 128 –	AR	20.9	34.8	39.1	5.2				0.94		10,230
Fraser &	DRY		44.0	49.4	6.6				1.19		12,930
Abreu #521	DAF		47.1	52.9					1.27		13,840
(1943)	DMF		46.6	53.4							13,960
– 129 –	AR	14.7	29.7	35.8	19.8				0.72		8,810
Fraser &	DRY		34.9	41.8	23.3				0.84		10,330
Abreu #6033	DAF		45.5	54.5					1.10		13,470
(1943)	DMF		43.8	56.2							13,810
– 130 –	AR	0.9	31.6	57.7	9.8				2.21		13,630
Fraser &	DRY		31.9	58.2	9.9				2.23		13,750
Abreu #1321	DAF		35.4	64.6					2.48		15,260
(1943)	DMF		34.3	65.7							15,490

Publication Date: January 1, 1966 | doi: 10.1021/ba-1966-0055.ch011

Table XVI. Continued

Lab. No.	Condition*	Proximate Analysis, % Moisture	Volatile Matter	Fixed Carbon	Ash	Ultimate Analysis, % C	H	N	S	O	B.t.u.
– 131 –	AR	1.2	30.6	58.2	10.0				1.54		13,310
Fraser &	DRY		30.9	59.0	10.1				1.56		13,470
Abreu #1521	DAF		34.4	65.6					1.74		14,980
(1943)	DMF		33.5	66.5							15,180
– 132 –	AR	1.0	29.3	56.5	13.2				2.92		13,480
Fraser &	DRY		29.6	57.1	13.3				2.95		13,620
Abreu #1722	DAF		34.1	65.9					3.40		15,710
(1943)	DMF		32.6	67.4							16,040
– 133 –	AR	1.2	31.6	58.0	9.2				2.17		13,350
Fraser &	DRY		32.0	58.7	9.3				2.20		13,510
Abreu #1821	DAF		35.3	64.7					2.43		14,900
(1943)	DMF		34.2	65.8							15,100

Table XVII. Australian Coal Analyses

New South Wales: Northern coalfield, Lower coal measures (Samples 134–139)
Queensland: Triassic coal measures (Samples 140–146)

Lab. No.	Condition*	Proximate Analysis, % Moisture	Volatile Matter	Fixed Carbon	Ash	Ultimate Analysis, % C	H	N	S	O	B.t.u.
– 134 –	AD	2.2	42.6	48.2	7.0	75.2	5.9		1.62		13,770
Greta c bed	DRY		43.6	49.2	7.2	76.9	5.8		1.7		14,080
Brown and	DAF		47.0	53.0		82.4	6.2		1.8		15,170
Waters 1962	DMF		46.3	53.7			6.28				15,320
– 135 –	AD	2.6	37.4	54.0	6.0	76.5	5.5		0.84		13,660
Muswellbrook	DRY		38.4	55.4	6.2	78.5	5.4		0.9		14,020
No. 1 c bed	DAF		40.9	59.1		83.4	5.7		1.0		14,950
Brown and Waters 1962	DMF		40.4	59.6			5.74				15,050
– 136 –	AD	2.1	28.9	56.0	13.0	73.0	4.6	1.6	1.0	4.7	13,160
Brown–	DRY		29.5	57.2	13.3	74.3	4.8	1.6	1.1	4.9	13,440
17858	DAF		34.1	65.9		86.0	5.4	1.8	1.2	5.6	15,500
(1964)	DMF		32.9	67.1			5.46				15,740
– 137 –	AD	2.4	24.9	56.2	16.5	70.3	4.1	1.5	0.7	4.5	12,530
Brown–	DRY		25.5	57.6	16.9	71.6	4.4	1.6	0.7	4.8	12,840
17862	DAF		30.7	69.3		86.6	5.1	1.9	0.8	5.6	15,450
(1964)	DMF		29.3	70.7			5.14				15,740
– 138 –	AD	2.1	30.1	61.5	6.3	79.6	4.9	1.7	0.8	4.6	14,280
Brown–	DRY		30.7	62.9	6.4	81.3	5.0	1.8	0.8	4.7	14,590
17864	DAF		32.9	67.1		86.9	5.3	1.9	0.9	5.0	15,590
(1964)	DMF		32.3	67.7			5.32				15,710
– 139 –	AD	3.0	21.8	65.8	9.4	77.2	4.2	1.7	1.1	3.4	13,650
Brown–	DRY		22.5	67.8	9.7	79.5	4.4	1.7	1.2	3.5	14,070
17852	DAF		24.9	75.1		88.2	4.8	1.9	1.3	3.8	15,580
(1964)	DMF		23.9	76.1			4.82				15,770
– 140 –	AD	7.2	29.0	58.3	5.5	71.6	4.1	1.6	0.2	9.8	12,240
Blair Athol	DRY		31.3	62.8	5.9	77.0	4.4	1.8	0.2	10.7	13,190
L17 top 13′	DAF		33.2	66.8		81.9	4.7	1.9	0.2	11.3	14,010
Brown (1960)	DMF		32.8	67.2			4.62				14,100

Table XVII. Continued

Lab. No.	Condition*	Proximate Analysis, % Moisture	Volatile Matter	Fixed Carbon	Ash	Ultimate Analysis, % C	H	N	S	O	B.t.u.
– 141 –	AD	5.2	27.0	61.0	6.8	72.4	4.0	1.7	0.2	9.7	12,340
Blair Athol	DRY		28.5	64.3	7.2	76.2	4.3	1.8	0.2	10.3	13,020
L17 mid 11′	DAF		30.7	69.3		82.3	4.6	1.9	0.2	11.0	14,030
Brown (1960)	DMF		30.2	69.8			4.56				14,120
– 142 –	AR	5.2	27.8	59.8	7.2	72.1	4.1	1.6	0.1	9.7	12,310
Blair Athol	DRY		29.3	63.1	7.6	76.0	4.4	1.8	0.1	10.1	12,990
L17 85′ core	DAF		31.7	68.3		82.4	4.7	1.9	0.1	10.9	14,050
Brown (1960)	DMF		31.3	68.7			4.68				14,150
– 143 –	AD	1.0	12.0	80.0	7.0	84.5	4.2		0.48		14,380
Dawson bed	DRY		12.1	80.8	7.1	85.3	4.1		0.48		14,530
Brown-Waters	DAF		13.0	87.0		91.4	4.4		0.52		15,640
(1962)	DMF		12.3	87.7			4.35				15,750
– 144 –	AD	1.5	31.6	52.8	14.1	72.6	4.8	1.4	0.4	5.2	12,890
Fiery (top)	DRY		32.1	53.6	14.3	73.5	5.0	1.5	0.3	5.4	13,090
77″ excl. imp.	DAF		37.4	62.6		86.0	5.7	1.7	0.4	6.2	15,270
Brown (1962)	DMF		36.5	63.5			5.71				15,490
– 145 –	AD	2.6	28.6	49.8	19.0	63.9	4.2	1.0	0.1	9.2	11,140
Bluff c bed	DRY		29.4	51.1	19.5	65.0	4.5	1.1	0.2	9.7	11,440
177″ excl. imp.	DAF		36.4	63.6		81.5	5.4	1.3	0.2	11.6	14,210
Brown (1962)	DMF		35.2	64.8			5.38				14,500
– 146 –	AD	1.8	32.0	49.0	17.2	67.6	4.5	1.4	0.2	7.3	12,020
Rob Roy bed	DRY		32.6	49.9	17.5	68.5	4.7	1.4	0.3	7.6	12,240
65″ excl. imp.	DAF		39.5	60.5		83.6	5.5	1.7	0.3	8.9	14,850
Brown (1962)	DMF		38.4	61.6			5.52				15,110

Table XVIII. New Zealand Coal Analyses

South Island: Cretaceous or younger

Lab. No.	Condition*	Proximate Analysis, % Moisture	Volatile Matter	Fixed Carbon	Ash	Ultimate Analysis, % C	H	N	S	O	B.t.u.
– 147 –	AD	1.1	36.0	57.1	5.8	77.5	5.4	0.9	3.3	7.1	13,960
Buller Dist.	DRY		36.4	57.7	5.9	78.4	5.3	0.9	3.3	6.2	14,120
Suggate–37	DAF		38.7	61.3		83.3	5.6	1.0	3.5	6.6	14,994
(1959)	DMF		37.7	62.3			5.74				15,190
– 148 –	AD	2.2	34.7	60.4	2.7	80.3	5.5	1.2	2.3	8.0	14,500
Buller Dist.	DRY		35.5	61.7	2.8	82.1	5.4	1.2	2.3	6.2	14,830
Suggate–40	DAF		36.5	63.5		84.5	5.5	1.2	2.4	6.4	15,247
(1959)	DMF		35.9	64.1			5.64				15,370
– 149 –	AD	1.8	8.9	86.9	2.4	88.7	3.9	0.8	0.5	3.7	15,020
Fox River	DRY		9.1	88.5	2.4	90.3	3.8	0.8	0.5	2.2	15,300
Suggate–63	DAF		9.3	90.7		92.5	3.9	0.8	0.5	2.3	15,678
(1959)	DMF		8.9	91.1			3.88				15,730
– 150 –	AD	1.4	36.8	57.5	4.3	81.0	5.8	1.3	0.4	7.2	14,530
Greymouth	DRY		37.3	58.3	4.4	82.1	5.7	1.3	0.4	6.1	14,740
Suggate–68	DAF		39.0	61.0		85.9	5.9	1.4	0.4	6.4	15,408
(1959)	DMF		38.7	61.3			5.94				15,480

Table XVIII. Continued

Lab. No.	Condition*	Proximate Analysis, % Moisture	Volatile Matter	Fixed Carbon	Ash	Ultimate Analysis, % C	H	N	S	O	B.t.u.
– 151 –	AD	0.9	35.2	59.2	4.7	80.8	5.6	1.9	0.4	6.6	14,660
Greymouth	DRY		35.5	59.8	4.7	81.6	5.5	1.9	0.4	5.9	14,790
Suggate–75	DAF		37.3	62.7		85.6	5.8	2.0	0.4	6.2	15,529
(1959)	DMF		37.0	63.0			5.75				15,610
– 152 –	AD	1.1	17.6	76.3	5.0	85.3	4.6	1.0	0.4	3.7	14,810
Greymouth	DRY		17.8	77.1	5.1	86.2	4.5	1.0	0.4	2.8	14,970
Suggate–78	DAF		18.7	81.3		90.9	4.7	1.1	0.4	2.9	15,772
(1959)	DMF		18.3	81.7			4.70				15,860
– 153 –	AD	0.5	41.8	51.2	6.5	78.7	5.5	0.7	2.2	6.4	14,130
Greymouth	DRY		42.0	51.5	6.5	79.1	5.5	0.7	2.2	6.0	14,200
Suggate–89	DAF		45.0	55.0		84.6	5.9	0.7	2.4	6.4	15,193
(1959)	DMF		44.3	55.7			5.94				15,360

Discussion

Peter Given, C. R. Binder, and J. Imbalzano. Through the courtesy of Dr. Schopf we have been able to examine the infrared spectra of three of his samples of Antarctic coals, #72 = CGL 105, #29 = CGL 252 and #18 = CGL 256 (*see* Tables III, V, and X).

The spectra were run on potassium bromide discs of the specimens at about 0.35% w/w concentration using a Perkin-Elmer Model 21 spectrometer. Microscopic examination of the discs showed that in spite of long grinding, the coal particle size was relatively large ($\leq 10\mu$, except for CGL 105, which contained many particles in the range 10–50μ). Consequently, a fair amount of scatter was observed in the spectra.

Few bands were visible in the spectra. The main features were a medium intensity band or shoulder at 1690–1710 cm.$^{-1}$, a strong band at 1560–1575 cm.$^{-1}$, and a medium band at around 1375 cm.$^{-1}$. There were also weak bands at 750 and 800 cm.$^{-1}$, which could represent aromatic C–H stretching vibrations, but were quite possibly caused by mineral matter.

The band at 1560–1575 cm.$^{-1}$ is presumably an aromatic skeletal vibration, usually found at 1600 cm.$^{-1}$ in bituminous coals. The band at 1690–1710 cm.$^{-1}$ is interesting, and must represent a carbonyl vibration. It might be caused by quinones or aromatic ketones and if so, would indicate that oxidation had occurred during the thermal alteration; the frequency is rather high for this assignment, however. A more probable assignment is to aromatic esters or possibly phenolic lactones. This interpretation would be consistent with the view that the coals were of lignitous or subbituminous rank before the igneous intrusion occurred.

The absorption of methyl groups occurs at 1375 cm.,$^{-1}$ but this seems an improbable assignment here. Perhaps the band represents a coupling

Publication Date: January 1, 1966 | doi: 10.1021/ba-1966-0055.ch011

between carbonyl and aromatic skeletal vibrations similar to that reported by Hadzi and Sheppard (3) for polycyclic quinones, though at a somewhat higher frequency.

The level of absorption was high for all samples. In the case of CGL 105 this was undoubtedly caused mainly by scattering. With the other samples, the result may indicate that the aromatic systems are so extensive that some electronic absorption is occurring in the infrared.

We have also made some electron spin resonance measurements on one sample, CGL 256, before and after laboratory carbonization (*1*). The results were as follows:

	Unheated	*Carbonized at* 450°C.	550°C.
Free spin concentration, gram^{-1} × 10^{18}	26.8	150.3	103.6
line width, gauss	3.0	3.3	3.3

The line widths are unusually narrow, comparable with those shown by fusinites (*1*) and somewhat narrower than is usually found for carbonized vitrinites. This indicates that a great deal of exchange and delocalization narrowing is taking place, which in turn implies that extensive oriented polycyclic aromatic nuclei have been formed, as would be expected of coals heated under a large unidirectional pressure for a considerable length of time. The moderate free spin concentration of the unheated sample and the sharp rise on carbonization at 450°C. suggest that the maximum temperature experienced *in situ* was not more than about 350°C. or a little higher. The behavior is quite distinct from that of normal coals of the same carbon content (daf) or of anthracites of the same (presumed) degree of aromaticity.

James M. Schopf. As mentioned in the paper, on general geologic grounds I doubt that the coals represented by CGL 105 (No. 72, stump, Terrace Ridge, 662 ft. below diabase), 252 (No. 29, Amundsen section 13, 731 ft. above base) and 256 (No. 18, Allan Nunatak) could have been as low as subbituminous rank prior to the episode of intrusion. At the same time, I appreciate the interest shown by Dr. Given and his colleagues in obtaining infrared spectra of these samples. I only wish that more extensive studies were possible that would clear up a possible conflict of evidence between the detailed physical examination and the reasoning based on geology.

Dr. Given. I am struck by the high oxygen and low hydrogen contents that seem to be characteristic of all the samples studied by Schopf and Long. The result of both laboratory carbonization and thermal alteration by igneous intrusions is normally to decrease considerably both oxygen and hydrogen contents of coals. I submit that we are therefore forced to conclude either that oxygen was added in the course of thermal alteration or that the coals, before the intrusion occurred, contained considerably more oxygen than would correspond with bituminous rank.

It is difficult to believe that oxygen per se was available during metamorphism. However, it is known that at 500°–600°C. steam can react with carbons to give a surface oxide and hydrogen; water would be available from clay minerals and bed moisture in the Antarctic strata, and this reaction could well have occurred at the high pressures prevailing in the seams. On the other hand,

Publication Date: January 1, 1966 | doi: 10.1021/ba-1966-0055.ch011

it is difficult to account for the low hydrogen contents with this view. Sulfate or nitrate ions could possibly act as oxidizing agents and both add oxygen and remove hydrogen, but it is difficult to imagine these ions as being present in significant amounts within the coal seams.

I believe that the most effective way of representing graphically the chemical results of metamorphism of coals is the H/C *vs.* O/C diagram introduced by Van Krevelen (5). A rough sketch of this diagram is shown in Figure A, with the normal coal band drawn in. If a coal of composition represented by any point in the band, A, is carbonized in the laboratory at progressively higher temperatures, the compositions of the products lie approximately

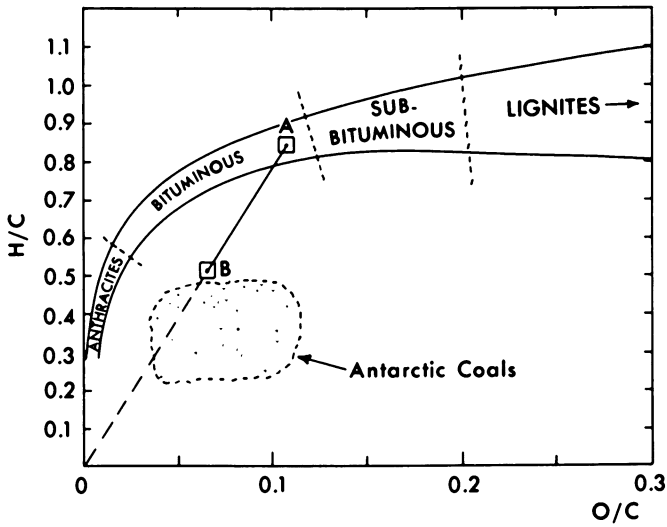

Figure A. Atomic ratios, H/C and O/C, for normal coals and thermally altered coals

on a straight line, ABO, directed towards the origin. Available data indicate that thermal alteration caused by igneous intrusion may have a similar effect on composition (*see* Van Krevelen (5), p. 270, and Francis (2)). Therefore, if one found a thermally altered coal of composition represented by point B, one would draw in the straight line OB and extrapolate it to meet the normal coal band near A; one would then deduce that the coal, before being affected by the intrusion, had a composition somewhere near that represented by point A. The procedure is, of course, very approximate. Since the Antarctic sills are very thick and coals well over 1000 feet from sills have been highly altered, the coals must have been exposed to a *range* of relatively high temperatures, and for a long period (100 years or so?); these factors further complicate the interpretation of the Antarctic data in the manner outlined above.

I have plotted some of the analytical data (daf) of Schopf and Long on the H/C–O/C diagram; the results for a number of samples, including those collected at known depths (taken from the tables of the paper by Schopf and

Publication Date: January 1, 1966 | doi: 10.1021/ba-1966-0055.ch011

Long), are shown in Figure A. Construction lines like OAB suggest that the coals were around subbituminous rank before intrusion; in the complete sequence of seams in the coal measures there might have been a range of rank from high rank lignitous to subbituminous, or subbituminous to very low rank bituminous.

Schopf and Long state that the age of the diabase intrusion in the Beacon Sandstone of Victoria Land is 147–163 m.y. (mid-Jurassic), and slightly older intrusions are reported farther north along the coast. The coals are Permian, presumably late Permian in view of the extensive glaciation early in this era. The intrusion therefore occurred 30–90 m.y. after the coals were laid down, depending on the exact date of the intrusion and the absolute age one wishes to assign to the late Permian of Antarctica. Now it is argued by M. and R. Teichmüller (*4*) that the main factors determining normal metamorphism of coals are the maximum depth of burial, the length of time spent at or near that depth, and the local geothermal gradient. Where the rate of subsidence and the geothermal gradient (°C./100 m.) are high, metamorphism from peat to bituminous rank, in their view, take only 10–20 m.y. Where these factors and the maximum depth of burial are low, the same transition may take 100 m.y. It is, therefore, at least possible that the Antarctic coals had reached only lignitous or subbituminous rank at the time of the intrusions, though this would imply a rather low geothermal gradient.

The few infrared spectra that have been determined do not conclusively show whether the high oxygen contents are caused by oxidation or by a low rank state before alateration; they slightly favor the latter view.

I find it interesting that in the strata studied by Schopf and Long, the sills lay *above* the coal seams. This means that the temperature gradient owing to the sill was of opposite sign to the geothermal gradient, and therefore in sequences of samples like those in the table on pp. 166-7, it is the coals that were initially of lowest rank that were more intensely subjected to thermal alteration. This situation may account for the observed variations in H/C–O/C relations with depth below the sill (which are complex); however, since the samples were not taken from vertical boreholes, some lateral variations in the strata no doubt also affect the relations.

Dr. Schopf. I believe that the first alternative suggested by Dr. Given is more likely to be correct—i.e., that oxygen was added to the coals during the episode of igneous intrusion. I do not have any explanation to account for the missing hydrogen which would be liberated by the hot water or steam reaction other than the observation that the coal beds obviously were not hermetically sealed. Hydrogen could have passed off as a gas.

The only argument against the postulate of very slow incoalation by combined effects of geothermal heat plus pressure that I know of, is that presented by comparison with Gondwana coals outside Antarctica where igneothermal effects are not as evident. One would suppose geothermal gradient and loading would have been about the same, or at any rate, would follow a trend related to depth of burial in all these related areas. Thus far no such trend has been recognized, other than the lower rank suggested by the coal at Amery in the Antarctic. In general, the Permian coal measures of India and the Southern

Publication Date: January 1, 1966 | doi: 10.1021/ba-1966-0055.ch011

Hemisphere are in the upper range of high volatile bituminous rank. Subbituminous and lignitic coals of Permian age are very rare. I am aware of no geological reasons why the coals of Antarctica generally should have been originally of lower rank than those located elsewhere within this related paleogeographic province. It would seem an odd coincidence for all such coals to have been suddenly elevated to a considerably higher rank through igneous activity in the Mesozoic, even though intrusives are exceedingly common. No doubt additional observations and study will throw light upon this problem.

Dr. Given. I think Dr. Schopf misunderstands the situation I was envisaging. Presumably *all* Gondwana coals at some point in time had reached only the lignitous or subbituminous rank. My suggestion is that at this point in time the Antarctic coals were subjected to igneous metamorphism while coals in other parts of Gondwanaland continued to increase in rank slowly up to high volatile bituminous by normal metamorphism in the geothermal gradient. I am not suggesting that of necessity Antarctic coals were originally any different from other Gondwana coals, only that they had a different metamorphic history from the lignite or subbituminous stage onward.

Literature Cited

(1) Austen, D. E. G., Ingram, D. J. E., Given, P. H., Binder, C. R., Hill, L. W., ADVAN. CHEM. SER. **55**, 344 (1966).
(2) Francis, Wilfred, "Coal: Its Formation and Composition," pp. 403, 409-10, 585-89, St. Martins Press, Inc., New York, 1961.
(3) Hadzi, D., Sheppard, N., *J. Am. Chem. Soc.* **73**, 5460 (1951).
(4) Teichmüller, M., Teichmüller, R., ADVAN. CHEM. SER. **55**, 133 (1966).
(5) Van Krevelen, D. W., "Coal," p. 113-20, American Elsevier Pub. Co., New York, 1961.

Publication Date: January 1, 1966 | doi: 10.1021/ba-1966-0055.ch011

12

Physical Variations in Highly Metamorphosed Antarctic Coals

N. SCHAPIRO and R. J. GRAY

Applied Research Center, U.S. Steel Corp., Monroeville, Pa.

Publication Date: January 1, 1966 | doi: 10.1021/ba-1966-0055.ch012

The presence of coal in Antarctica has been known since early 1900. The recent discovery of numerous coal beds, one over 13 feet thick, has stimulated interest in these coals. A set of 36 samples, for which chemical analyses were available, were examined microscopically; optical reflectance, Knoop indention hardness, and electrical resistivity were determined. These coals range in rank from semianthracite to natural coke and are generally high in ash, fixed carbon, and oxygen. The coals have been altered by igneous intrusives; the closer the coal to the source of heat, the higher the rank reflectance and hardness and the lower the electrical resistivity. Changes in physical properties with degree of coal alteration may be useful in estimating the temperature of alteration and rank of coal prior to alteration and in geologic correlation problems.

In the early 1900's petrified trees, imprints of fossil leaves, and thin coal seams were discovered in Antarctica. This discovery was important since it was evidence of forests that once grew in what is now virtually an ice-covered continent. However, between 1957 and 1961 the discovery of numerous coal beds (*2, 5, 7*), some of which are over 13 feet thick, stimulated the interest in Antarctic coals. Coal is the only economically important mineral resource that has been discovered to date in Antarctica. Most of the coal now known to be present occurs in a block-faulted mountainous area that extends almost completely across the continent. Since this exceptional area of rock exposed in an otherwise ice-covered continent contains coal, the exposure of coal-bearing strata may be only an indication of a vast new and previously unsuspected coal field. The amount of coal present is very important, but the rank and grade of

In Coal Science; Given, P.;
Advances in Chemistry; American Chemical Society: Washington, DC, 1966.

the coal will largely determine its potential use and, therefore, the extent to which the coal in Antarctica is exploited. The stratigraphic sequence in which the coals occur is or has been overlain by diabase sills that were formed by molten material. The degree of thermal alteration of the coal depends on the distance of the coal from the heat source as well as the amount of heat available. In addition to generally describing the microscopic characteristics of Antarctic coal, the present investigation was conducted to determine changes that occur in the chemical composition, reflectance, microhardness, and electrical resistivity of the coals caused by thermal alteration.

The Antarctic coal samples are reportedly of Permian age and were collected in 1957 as part of the Antarctic exploration program of the Ohio State University Institute of Polar Studies. The bulk of the samples are from two localities shown in Figure 1: (1) the Terrace Ridge in the Ohio Range of the Horlick Mountains, and (2) Mount Gran in the Granite Harbour area of South Victoria Land. In each instance the coals were sampled from each of the accessible coal seams in the stratigraphic sequence exposed. Thus, these sam-

Publication Date: January 1, 1966 | doi: 10.1021/ba-1966-0055.ch012

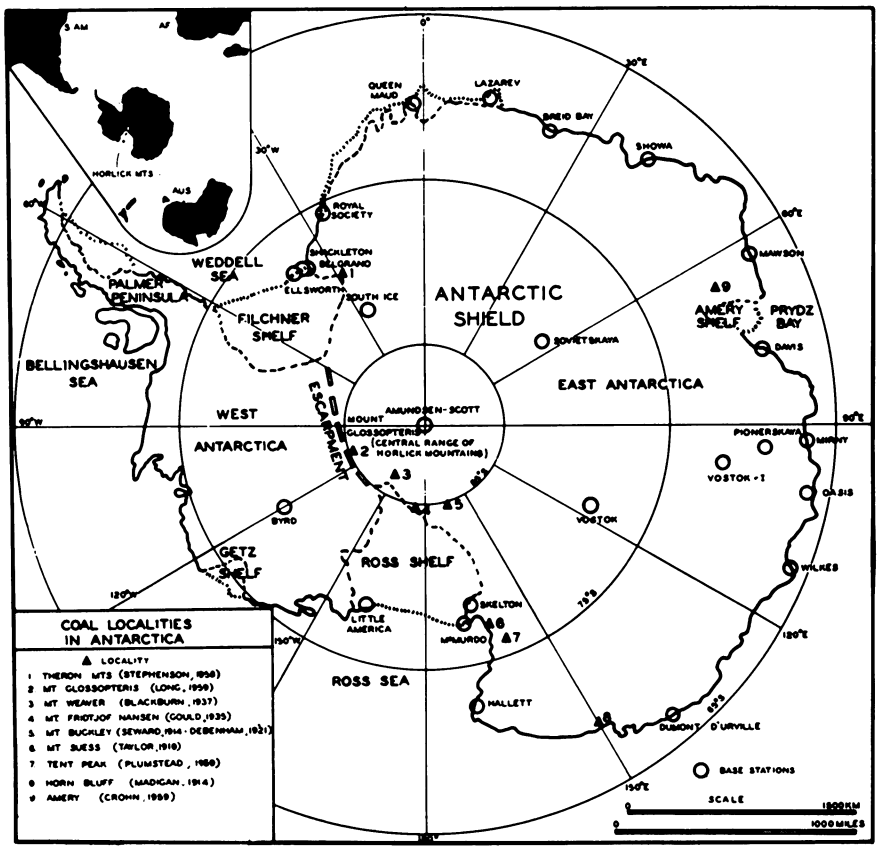

Figure 1. Map of Antarctica showing the general area of coal sample localities

ples represent an oriented sequence ranging from youngest to oldest coal through a thickness of about 1000 feet. For comparison purposes, samples from the Schultheiss escarpment in the Horlick Mountains and also samples from Plunkett Point near the Beardmore Glacier were included in this study. All of these coals occur in association with diabase sills formed by molten material that invaded the coal-bearing sediments in the area. A fairly complete discussion of the geologic sequence that accompanies the coal-bearing strata, together with a more complete description of the physiography of the exploration area is given by Doumani and Long (*2*).

Materials and Experimental Work

The 36 Antarctic coal samples were analyzed chemically (proximate and ultimate analyses) at the U. S. Bureau of Mines in Pittsburgh. The results of these analyses accompanied the samples when received from J. M. Schopf. The samples were collected by W. E. Long in the Ohio Range on NSF grant

Table 1. Chemical, Optical, and Physical

Sample Number	*Description*	*Seam Thickness, feet*	*Distance Below Sill, feet*
77[b]	Coaly Shale	3	52
78[b]	Coal		132
80[b]	Coaly Shale or Impure Coal	2	500
81[b]	Shale, Black Coaly	3	530
82[b]	Coal	4	648
83[b]	Coal	8	652
85[b]	Coaly Shale	3	850
86[b]	Shale, Black, Rough, Blocky	2	878
87[b]	Coal	2	889
88[b]	Coal	3	959
89[b]	Coal	8	962
91[b]	Coal, Blocky and Platy	2	1023
92[b]	Coal	8	1117
94[c]	Coal—Diabase Relation		
95[c]	Coal	3	1167
98[b]	Coal, Impure		1021
100[b]	Coal		962
	Dirty Diamond Adit (Fresh Coal)[a]		1000
12–21–1[d]	No. 1 Coal	2.3	
12–21–2[d]	No. 2 Coal	0.5	
12–21–4[d]	No. 3 Coal	2.8	
12–21–5[d]	No. 4 Coal	2.0	
12–21–7[d]	No. 5 Coal	8.0	
12–21–9[d]	No. 6 Coal	2.5	
12–21–10[d]	No. 7 Coal	1.5	
12–21–11[d]	No. 9 Coal	7.5	
12–23–1[c]	No. 1 Coal, Mt. Grans Seam	4.1	
12–23–2[c]	No. 3 Coal	2.0	
12–23–3[c]	Specimen of No. 1 Coal in Contact with Igneous Rock		
12–24–4[c]	No. 5 Coal	0.7	
1–10–1[c]	Coal Float		

G–17216, and in Victoria Land by John Mulligan, also on an NSF grant to the Bureau of Mines. Each sample was crushed by hand with a mortar and pestle to approximately 0.625 by 0.25 inch. A split of each crushed sample was embedded in epoxy resin, polished, examined microscopically, photographed, and then its reflectance was determined. Knoop indention hardnesses were also determined by using a 20-gram load on the diamond indenter. The indenter was kept in contact with the sample for 15 seconds. Additional splits of each sample were crushed to minus 60 mesh, dried at 100°C. for 24 hours, and their electrical resistivity was determined at 20,000 p.s.i. The sample locations, chemistry, petrography, reflectance, electrical resistivity, and hardness of the 36 Antarctic coal samples studied are included in Table I.

Results and Discussion

Chemistry. The moisture- and ash-free fixed carbon figures for this coal are relatively high (Table I). Most of the samples exceeded 80% fixed carbon, and all the samples exceeded 80% ultimate carbon. About one-third of the

Properties of Antarctic Anthracite

Chemical Analysis (moisture-free)*								
Proximate			*Ultimate*					
VM	*FC*	*A*	*H*	*C*	*N*	*O*	*S*	*Moisture*
1.3	12.2	86.5	0.3	13.0	0.5		0.1	0.6
3.3	32.4	64.3	0.4	33.3	0.7	1.1	0.2	1.7
4.7	16.3	79.0	0.4	18.2	0.7	1.6	0.1	2.9
5.5	19.1	75.4						
13.7	54.9	31.4	1.3	58.2	1.4	7.4	0.3	7.0
15.5	73.4	11.1	1.9	76.6	1.5	8.5	0.4	8.0
		72.3						
		80.1						
13.5	46.3	40.2	1.4	49.3	1.4	7.2	0.5	5.7
11.9	52.5	35.6	1.7	54.2	1.4	6.6	0.5	4.9
14.4	63.6	22.0	2.0	65.6	1.6	8.3	0.5	5.8
13.7	44.7	41.6	1.6	48.7	1.3	6.5	0.3	5.3
15.4	65.1	19.5	2.0	68.1	1.5	8.4	0.5	6.1
6.7	29.1	64.2	1.3	30.9	1.1	2.2	0.3	2.3
6.5	45.6	47.9	1.7	46.4	1.2	2.4	0.4	2.7
11.9	52.6	35.5						5.4
14.0	61.9	24.1	1.8	64.0	1.7	7.9	0.5	5.5
9.5	78.8	11.7	1.3	79.9	0.8	6.0	0.3	6.1
9.2	81.6	9.2	1.6	83.1	0.9	4.8	0.4	6.8
23.2	62.3	14.5	1.4	77.1	0.8	5.9	0.3	7.7
11.5	75.9	12.6	2.2	78.5	1.2	4.9	0.6	3.7
12.7	69.0	18.3	2.3	71.7	1.3	5.8	0.6	3.6
12.8	64.2	23.0	2.1	66.9	1.2	6.0	0.8	3.8
7.9	34.1	58.0	1.2	35.6	0.6	4.1	0.5	2.8
11.9	77.3	10.8	2.0	79.3	1.2	5.8	0.9	5.6
6.3	78.3	15.4	1.2	78.9	0.5	3.7	0.3	14.9
5.3	83.3	11.4	1.2	84.5	0.7	1.9	0.3	14.1
4.5	77.2	18.3	0.4	77.8	0.0	3.5	0.0	1.5
11.8	72.5	15.7	1.8	74.7	0.9	5.7	1.2	7.8
6.6	80.0	13.4	1.9	79.4	0.9	4.0	0.4	6.2

Table I.

Sample Number	Description	Chemical Analysis[a] Proximate VM	FC
77[b]	Coaly Shale	9.6	90.4
78[b]	Coal	9.2	90.8
80[b]	Coaly Shale or Impure Coal	22.4	77.6
81[b]	Shale, Black Coaly	22.4	77.6
82[b]	Coal	20.0	80.0
83[b]	Coal	17.5	82.5
85[b]	Coaly Shale		
86[b]	Shale, Black, Rough, Blocky		
87[b]	Coal	22.6	77.4
88[b]	Coal	18.4	81.6
89[b]	Coal	18.5	81.5
91[b]	Coal, Blocky and Platy	23.4	76.6
92[b]	Coal	19.1	80.9
94[c]	Coal—Diabase Relation	18.7	81.3
95[c]	Coal	12.5	87.5
98[b]	Coal, Impure	18.4	81.6
100[b]	Coal	18.4	81.6
	Dirty Diamond Adit (Fresh Coal)[b]		
12–21–1[d]	No. 1 Coal	10.8	89.2
12–21–2[d]	No. 2 Coal	10.1	89.9
12–21–4[d]	No. 3 Coal	27.1	72.9
12–21–5[d]	No. 4 Coal	13.1	86.9
12–21–7[d]	No. 5 Coal	15.5	84.5
12–21–9[d]	No. 6 Coal	16.7	83.3
12–21–10[d]	No. 7 Coal	18.8	81.2
12–21–11[d]	No. 9 Coal	13.4	86.6
12–23–1[e]	No. 1 Coal, Mt. Gran Seam	7.5	92.5
12–23–2[e]	No. 3 Coal	6.0	94.0
12–23–3[e]	Specimen of No. 1 Coal in Contact with Igneous Rock	5.5	94.5
12–24–4[e]	No. 5 Coal	14.0	86.0
1–10–1[e]	Coal Float	7.6	92.4
	Plunkett Pt. Graphite		

[a] Abbreviations: VM = Volatile Matter; FC = Fixed Carbon; A = Ash; H = Hydrogen; C = Carbon; N = Nitrogen; S = Sulfur.
[b] Terrace Ridge, Mt. Schopf, Ohio Range of Horlick Mts.

samples exceeded 90% ultimate carbon. The hydrogen values ranged from 0.5–3.3%. Although these carbon values are high and the hydrogen values are low, the carbon values are not nearly as high as the reflectance data indicate.

Nearly all the coals examined are relatively high in ash. Only two of the samples from the Terrace Ridge area contain less than 20% ash, on a moisture-free basis. Most of the remaining samples from this area range from impure coal to coaly shale. Most of the mineral matter is finely divided (dehydrated) clay, silica, and pyrrhotite. This is an important point since the proximate and ultimate analyses for material that deviates so widely from what is normally considered coal cannot be considered particularly reliable for comparison pur-

Publication Date: January 1, 1966 | doi: 10.1021/ba-1966-0055.ch012

Continued

(moisture- and ash-free) Ultimate					*Average Reflectance, % (in oil)*	*Micro-Hardness kg./sq. cm.*	*Electrical Resistivity, ohm-cm. (20,000 p.s.i.g.)*
H	*C*	*N*	*O*	*S*			
2.2	93.5	3.6		0.7	11.5	179.8	2.45
1.1	93.3	1.9	3.1	0.6	10.4	188.6	2.67×10^{-1}
1.9	86.7	3.3	7.6	0.5	6.2	77.8	2.70×10^{4}
					7.0	85.8	3.09×10^{4}
1.9	84.9	2.0	10.8	0.4	6.0	69.7	7.73×10^{4}
2.1	86.2	1.7	7.5	0.5	6.8	56.7	2.29×10^{5}
					5.5	40.5	6.62×10^{6}
					4.2	39.1	6.67×10^{7}
2.3	82.4	2.3	12.1	0.9	4.8	42.9	4.55×10^{8}
2.7	84.1	2.2	10.3	0.7	5.4	39.5	2.40×10^{8}
2.5	84.1	2.0	10.7	0.7	4.7	40.4	1.22×10^{8}
2.7	83.4	2.2	11.1	0.6	2.8	33.4	6.02×10^{8}
2.4	84.6	1.9	10.5	0.6	3.1	34.8	1.32×10^{8}
3.6	86.3	3.1	6.2	0.8	2.6	23.8	2.88×10^{8}
3.3	89.1	2.4	4.5	0.7	2.9	35.7	1.85×10^{8}
					3.5	37.8	2.41×10^{8}
2.3	84.3	2.2	10.6	0.6	5.0	42.7	1.28×10^{8}
					3.1	34.3	1.98×10^{9}
1.5	90.6	0.9	6.6	0.4	5.9	116.6	3.98×10
1.8	91.6	1.0	5.1	0.5	5.9	124.7	2.69×10^{2}
1.6	90.1	0.9	7.0	0.4	5.4	91.0	3.34×10
2.5	89.8	1.4	5.6	0.7	4.2	65.0	1.08×10^{5}
2.8	87.8	1.5	7.1	0.8	3.5	49.3	5.06×10^{6}
					6.0	96.6	3.24
2.7	86.8	1.5	8.0	1.0	3.8	60.0	1.34×10^{7}
2.8	84.8	1.5	9.7	1.2	3.8	55.7	8.74×10^{6}
2.3	88.9	1.4	6.4	1.0	4.5	53.2	3.62×10^{5}
1.4	93.3	0.5	4.5	0.3	6.0	69.5	1.20×10
1.4	95.4	0.8	2.1	0.3	5.4	74.0	1.12×10
0.5	95.2	0.0	4.3	0.0	5.5	35.1	3.80×10^{-2}
2.1	88.5	1.1	6.9	1.4	5.1	52.6	2.56×10^{4}
2.1	91.8	1.0	4.6	0.5	5.5	59.8	1.84×10^{3}
					5.9	55.2	3.93
					5.0	34.5	1.84×10
					6.0	27.0	4.00×10^{-2}

[c] Four miles northwest of Mt. Schopf, Ohio Range of Horlick Mts.
[d] Second mountain south of Mackay Glacier.
[e] Mt. Gran, Central Victoria Land.

poses with coal. All except two samples from the Granite Harbour area contain less than 20% ash; however, only one sample contained less than 10% ash. In general, all the coal samples were low in sulfur. Most of the samples contained 0.5% or less sulfur. The oxygen content of these coals, with few exceptions, was unusually high. The reason for considering the dry, ash-free oxygen values exceptionally high is based on comparing the oxygen values to carbon content. All the samples except one exceeded 4.3% oxygen, on an ash- and moisture-free basis. Approximately one-third of all the samples analyzed exceeded 10% oxygen. Brown and Taylor (*1*) indicate that the oxygen occurs in nonacidic functional groups in the Antarctic coal. They also

Publication Date: January 1, 1966 | doi: 10.1021/ba-1966-0055.ch012

demineralized (acid-washed) coal and found that the coal analyzed the same on the ultimate basis, indicating the high oxygen content of the actual coal substance. Chars prepared from brown or subbituminous coals are known to contain a high proportion of nonacidic oxygen. It has been suggested that the unusually high oxygen content may be caused by the weathering conditions in Antarctica (*6*). However, in a recent study of coals that had been altered to natural coke in the Somerset area in Colorado, similar high oxygen contents were reported (*4*).

Coal Petrography. Of the 36 samples examined microscopically, approximately one-half contained gas vacuoles produced by thermal distillation of the coal. Thus, these coals that might otherwise have been referred to the rank of anthracite can be regarded as natural coke. All the samples, including those with gas vesicles, appeared to be fairly dense, with no macroscopic indication of a coke-structure development. The samples with the most advanced vacuole development appeared to be almost metallic in luster. All the coal entities normally encountered—vitrinoids, micrinoids, semifusinoids, and fusinoids—were present, whereas the exinoids and resinoids, which are difficult to identify with certainty in semianthracite or anthracite, were not positively identified in

Publication Date: January 1, 1966 | doi: 10.1021/ba-1966-0055.ch012

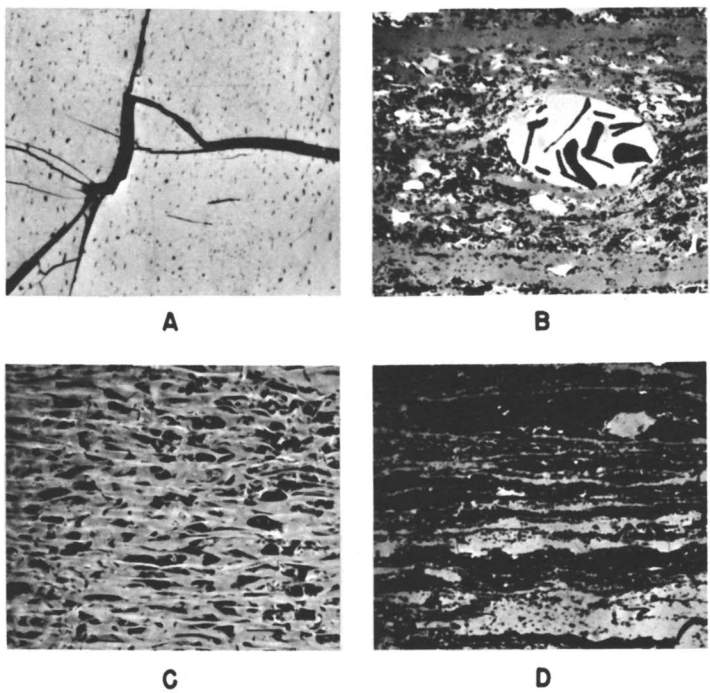

Figure 2. Photomicrographs showing some of the common entities found in Antarctic coals; reflected light, × 150
A—Vitrinoid with cracks. B—Bright inerts in a mixture of vitrinoids (gray) and clays (black). C—Semifusinoids preserving cellular structure. D—Clay minerals (black) containing thin vitrinoid bands (gray)

Figure 3. Examples of the Microstructural variations that accompany the transition from natural coke to coal. The photomicrographs are arranged in sequence of increasing distance below the intrusive (sill) that was the source of heat; reflected light × 255

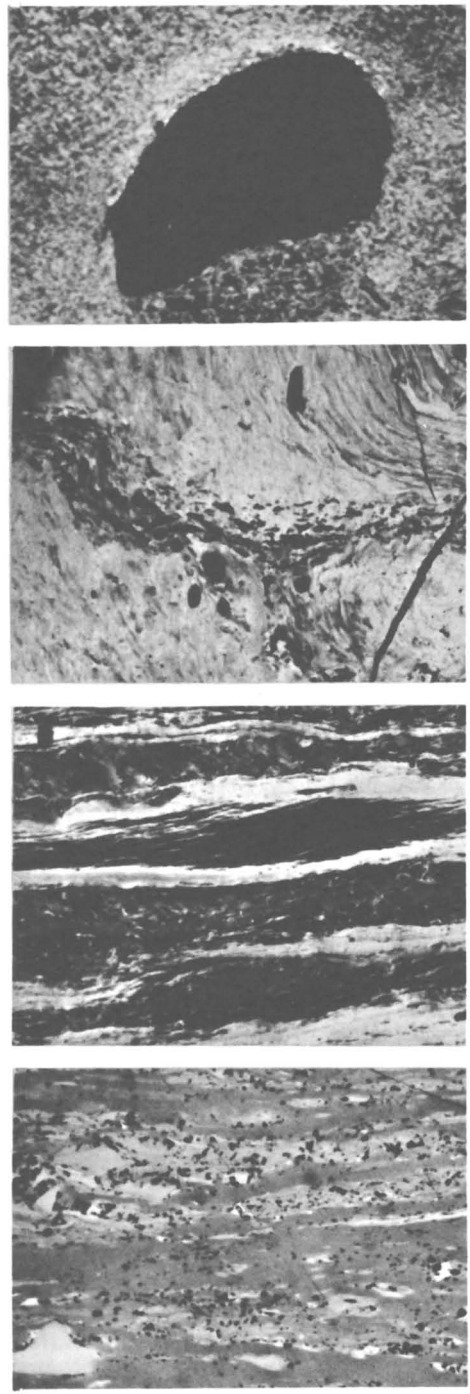

Large vacuole (black) surrounded by coke wall (gray). This natural coke appears 132 feet below a 600-F diabase sill

Small vacuoles (black) surrounded by material transitional between coke and anthracite. This coal occurs 648 feet below the sill

Transitional material between anthracite and coke. The variations in the appearance of the banding are caused by variations in composition and anisotropy. No vacuoles developed. Banding was retained in this unit, which occurs 652 feet below the sill

Semianthracite or anthracite containing recognizable coal entities that do not appear to be altered in this unit, which occurs 1117 feet below the sill

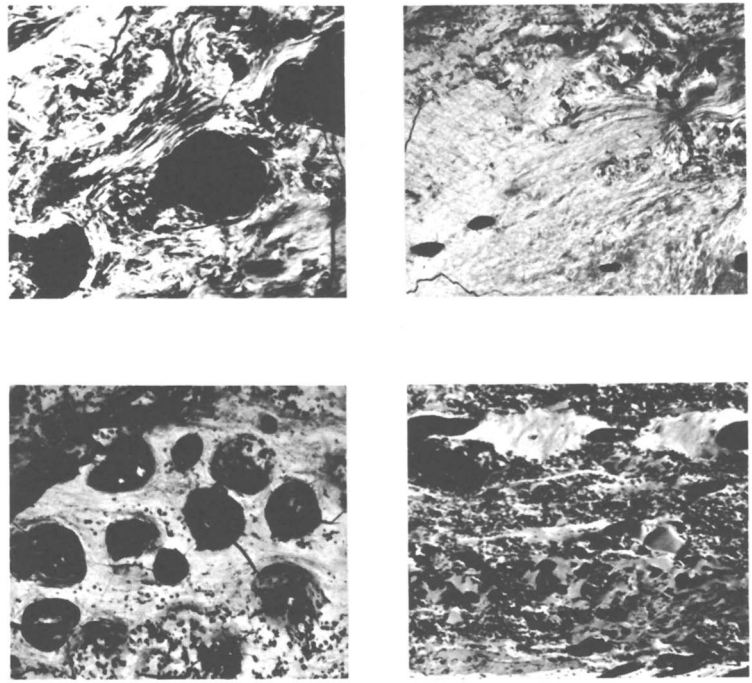

Figure 4. The appearance of natural coke that occurs in the Antarctic coal measures; reflected light × 150

these coals. Representative macerals and maceral associations are illustrated in Figure 2. The natural coke-to-semianthracite sequence is illustrated in Figure 3. All the photomicrographs are of coals from the Terrace Ridge area and are arranged in the order of increasing distance below the sill. The photomicrographs in Figure 4 illustrate the nature of the anisotropic domains developed in the coke. The size and intensity of anisotropy suggests that the cokes are similar to those produced in by-product ovens from marginal high- to medium-volatile rank coals. However, exceptionally high hydrogen coals are known to produce cokes with similar anisotropy, even though they are from high volatile coals. Additional petrographic features are presented in Figure 5, showing pyrolytic graphite, compression-crack patterns in organic inert particles, and two typical areas of a highly mineralized coal. To a petrographer familiar with North American coals the most striking difference in the Antarctic coals, apart from rank, is the abundance of semifusinoids, which is not uncommon for Permian coal deposits in such Southern Hemisphere countries as South Africa and Australia. The coal from each of these areas, including Antarctica, is dominated by a fossil flora known as the *Glossopteris* flora, which is considered characteristic of a postulation of an ancient land mass in the southern hemisphere, known as Gondwanaland. Some of the semifusinoid forms observed are illustrated in Figure 6. The presence of an abundant semifusinoid, fusinoid, or micrinoid content for a coal is usually considered indicative of a poorer coking coal since these macerals either will not fuse or will undergo transient

Publication Date: January 1, 1966 | doi: 10.1021/ba-1966-0055.ch012

fusion during carbonization. This last observation is superfluous because all the entities in the Antarctic coals included in this study are noncoking, being too high in rank to soften during carbonization. However, it is important to consider entity composition because if lower rank coals are found in Antarctica, they are likely to contain an abundance of the poorer fusing macerals.

Reflectance. The optical properties (reflectance) are not in accord with the chemical properties for these coal samples, and the maximum reflectance of the coals indicates that they are higher in rank than would be concluded from the chemical data alone. These discrepancies are not surprising since these coals are thermally metamorphosed and may not follow the normal coalification curve (*8*). For the subject samples, it was decided that chemical data did not suitably indicate rank or the degree of thermal metamorphism, particularly in those instances where the samples contained so much ash that they were not suitable for routine chemical tests. The maximum reflectance in oil of these coals ranges from 2.6% to 11.5% (Table I). The lower reflectance is similar to that encountered in some semianthracites and anthracites, whereas the upper reflectance is more nearly that of graphite or long term, high tem-

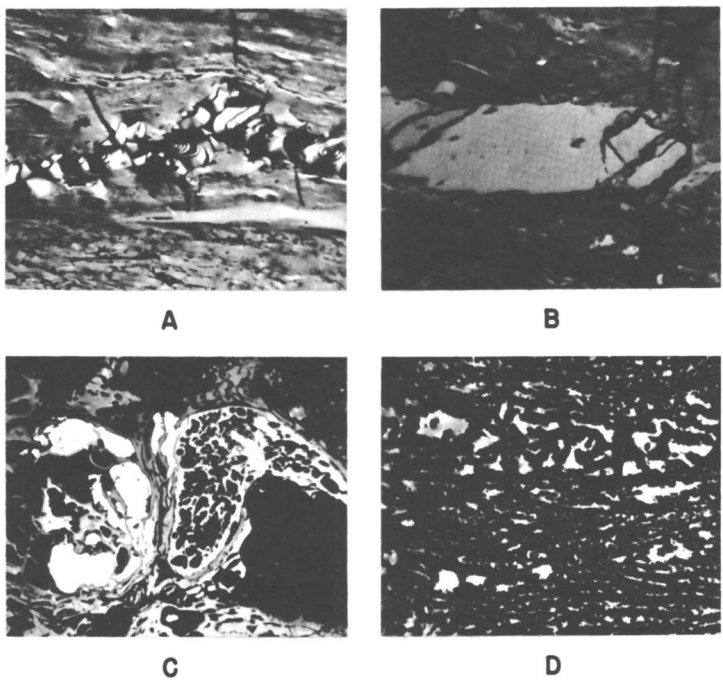

Figure 5. Some of the unusual material or structural features in Antarctic coals; reflected light, × 150

A—Pyrolytic carbon showing ribbon-like structure in vitrinoid bands. B—Faint gray lines define compression cracks in a bright micrinoid particle. C—Pyrrhotite (white) formed by the thermal decomposition of pyrite impregnating semifusinoids (gray). D—Bright coke particles in a baked-bone coal layer

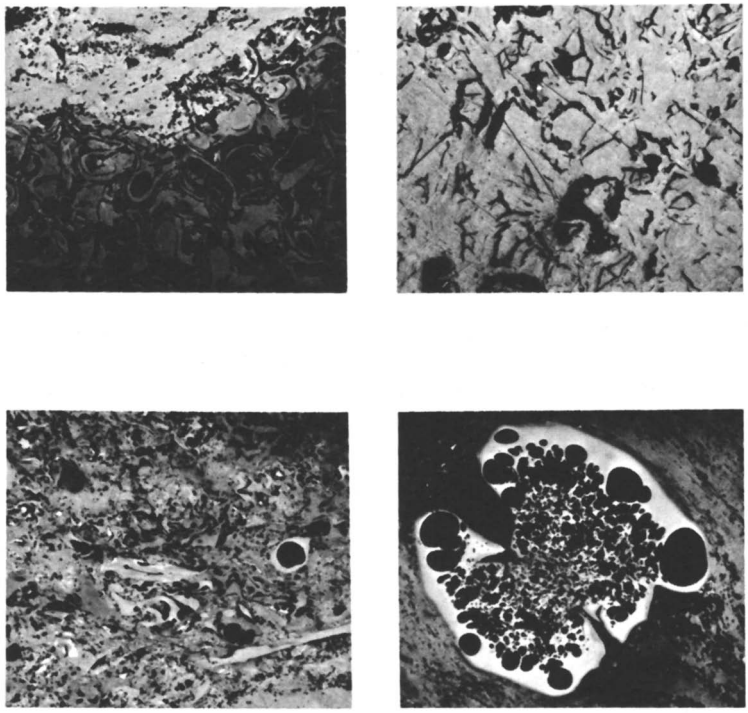

Figure 6. Variations in semifusinoids in Antarctic coals. These semifusinoids are a nonfusing entity present in abundance in these coals; reflected light, × 150

perature coke. In this study the reflectance measurements were used to differentiate the degree of coal alteration. For instance, when the reflectance is plotted against the distance of the coal or coke below the igneous sill in the Terrace Ridge area (Figure 7), the reflectance decreases from 11.5% at a distance of 52 feet below the sill to 2.8% at a distance of 1167 feet below the sill. Thus, the reflectance changes regularly with the distance of the coal below the sill. When the normal rank indicators, namely volatile matter or ultimate carbon, are plotted against distance below the sill, there is no general trend (Figure 8) even when the chemical analyses that are expected to be most erratic (over 50% ash) are eliminated. However, the hydrogen, which is normally considered the best indicator of temperature changes in the coal, does tend to increase as the distance below the sill increases (Figure 9). The hydrogen values in the demonstrations are calculated to a dry, ash-free basis. However, analysis of low ash coal concentrates from which the mineral matter has been removed would be desirable.

Electrical Resistivity. There is a close relationship between the reflectance and electrical resistivity of coal. As the reflectance increases, the resistivity decreases and higher reflecting, higher temperature cokes are less resistant than the lower reflecting, lower temperature cokes. The resistivity of the Antarc-

Publication Date: January 1, 1966 | doi: 10.1021/ba-1966-0055.ch012

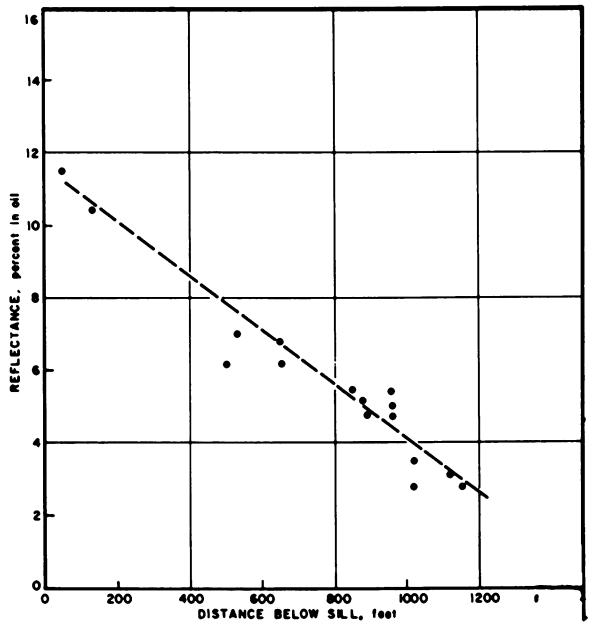

Figure 7. Relation between distance of coal below sill and reflectance

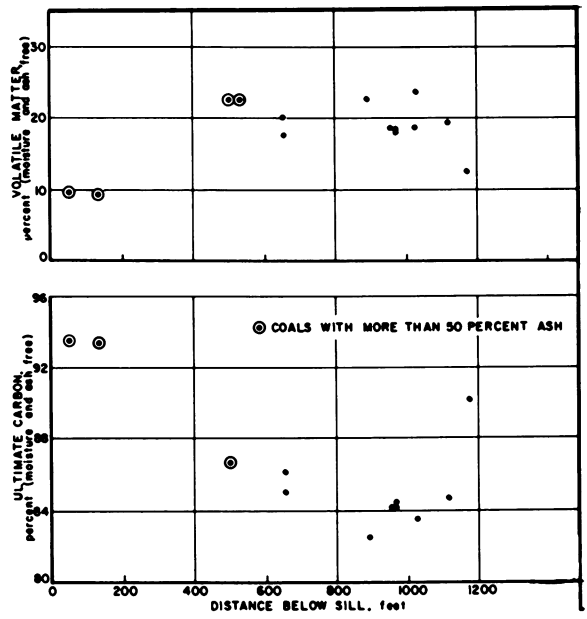

Figure 8. Relation of distance of coal below sill to ultimate carbon and volatile matter

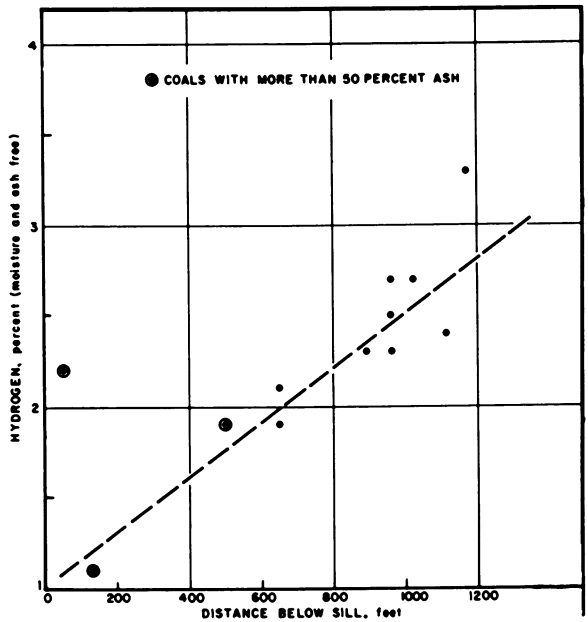

Figure 9. Relation between distance of coal below sill and hydrogen content

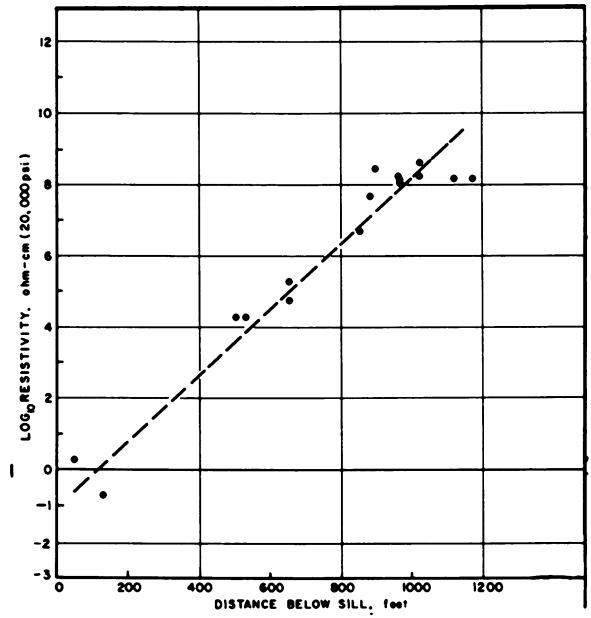

Figure 10. Relation between distance of coal below sill and electrical resistivity

Publication Date: January 1, 1966 | doi: 10.1021/ba-1966-0055.ch012

tic coals ranges from 1.40×10^{-2} ohm-cm. for one of the most thermally altered samples to 6.35×10^{8} ohm-cm. for one of the least altered samples (Table I). In the resistivity determinations, the entire sample was used, therefore, the effect of the kind and amount of mineral matter enters into the results. However, the resistivity changes are much more sensitive to coal rank differences than to changes in ash (mineral) content. The resistivity increases as the distance below the sill increases (Figure 10).

Hardness. The Antarctic coals have Knoop hardnesses that range from 27 kg./sq. mm. to 188.6 kg./sq. cm. (Table I). Other natural cokes are generally the hardest, and the semianthracites are generally the softest. Hardness increases as the distance from the sill decreases for the coals from the Terrace Ridge area (Figure 11). However, when all the samples are considered, the hardness does not necessarily correlate in a completely regular manner with another single set of test data.

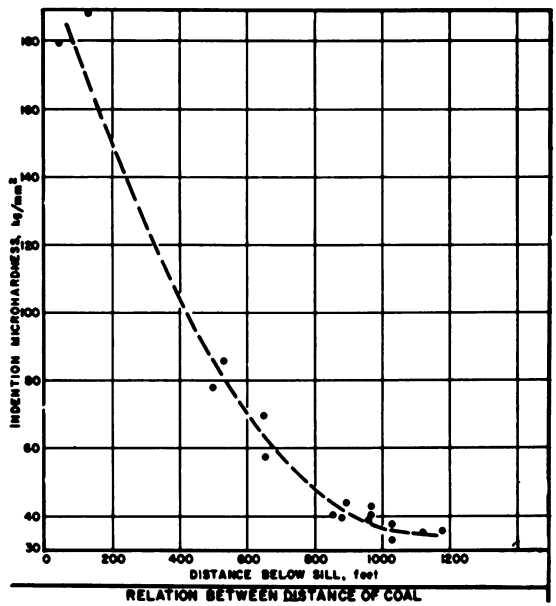

Figure 11. Relation between distance of coal below sill and indention microhardness

The Knoop hardness of coal in the rank range of semianthracite to anthracite increases regularly with rank. However, the hardness of carbonized coal increases with temperature up to about 1200°C. and then decreases at higher temperatures (3). It is possible that coal brought to similar stages of chemical rank may have different hardnesses, these depending upon the agency or method responsible for the rank change. Honda and Sanada (3) indicate that the Knoop hardness numbers of coals carbonized at 1200°C. are in the range of 200–300 kg./sq. cm., whereas those carbonized at 2000°C. are between 100 and 200 kg./sq. cm. Several of the Antarctic coals have Knoop hardness num-

bers between 100 and 200 kg./sq. cm., but this has been interpreted to mean that these coals reached temperatures between 700° and 1000°C. Cokes from coals with lower volatile matter have higher hardness numbers than cokes similarly prepared but from higher volatile coal. Therefore, it is necessary to know the rank of the coal from which the coke was produced before hardness data can be used to postulate accurate temperatures.

Summary

A set of 36 Antarctic coal samples were analyzed chemically, examined microscopically and photographed, and their optical reflectance and electrical resistivity were determined. The coals were associated with intrusives, and in degree of metamorphism they range from semianthracite through anthracite to natural coke. The coals are generally high in ash, fixed carbon, and oxygen and low in hydrogen and sulfur. The oxygen values are unusually high compared to equivalent rank commercial anthracites used in the United States. All of the coals or cokes are too high in rank to be considered for coke production. The entity composition of the coals is similar to that of Pennsylvania anthracites, but the Antarctic coals contain an abundance of semifusinoids. These semifusinoids undergo only transient fusion even in lower rank, higher volatile coals. In general, the reflectance and Knoop indention hardness of the coals increase and the electrical resistivity decreases as the rank of the coal increases. The coals are altered by contact with an igneous sill; the closer the coal to the sill, the greater the alteration, the higher the reflectance and hardness, and the lower the electrical resistivity. Therefore, these physical properties are useful in postulating temperature equivalents and should also be useful in planned exploration if the degree of metamorphism of the coal is to be related to the extensive sill complex in the area.

Literature Cited

(1) Brown, H. R., Taylor, G. H., *Fuel* **40,** 211 (1961).
(2) Doumani, G. A., Long, W. E., *Sci. Am.* **207,** 168 (1962).
(3) Honda, H., Sanada, Y., *Fuel* **36,** 403 (1957).
(4) Johnson, V. H., Gray, R. J., Schapiro, N., "Abstracts of Papers," 145th Meeting, ACS, September 1963, p. 3K.
(5) Mulligan, J. J. *et al.*, *U.S. Bur. Mines Rept. Invest. No.* **6218** (1900).
(6) Schopf, J. M., personal communication.
(7) Schopf, J. M., *U.S. Geological Survey Rept. No.* **2,** (1962).
(8) Van Krevelen, D. W., Schuyer, J., "Coal Science," D. Van Nostrand Co., Inc., New York, 1957.

RECEIVED January 25, 1965.

General Discussion

George Kapo: A recent development (*3*) in the solubilization in water of organic compounds normally insoluble in water such as vitamin A acetate, alizarin, actinomycin C and F, etc., may be useful in humic acid chemistry. The technique of solubilization consists of dissolving the water insoluble compound in a water miscible solvent, adding an aqueous solution of the sodium salt of hippuric or cyclohexylsalicylic acid, and evaporating the solvent. This results in an aqueous solution of the material; removing water by thin film evaporation or freeze drying leaves a water soluble powder. Assuming the effect of the additive can be accounted for, this technique could provide a means of direct titration in aqueous solutions of the functional groups in humic acids. Here the water miscible solvent could be an acetone-water mixture.

Peter H. Given: While listening to the papers of Dr. Flaig and Dr. Spackman (page 695), it occurred to me that perhaps they are discussing essentially the same process from different viewpoints. Dr. Flaig has elucidated much of the chemistry of the microbiological decay of lignin in straw. Dr. Spackman, by petrological methods, has observed the effects of the differential decay of different types of cell wall in fossilized woody tissue. Is Dr. Flaig in fact studying the chemistry of what Dr. Spackman sees under the microscope? On the other hand, if the decay observed by Dr. Spackman is not caused by microorganisms, by what kind of process is it caused? It seems clear that some kind of mechanical breakdown of major plant tissue occurred before this became thoroughly incorporated into the growing sediment. No doubt further biochemical attack took place during this latter stage and before burial.

A colleague (Dr. C. Clagett, Department of Biochemistry, Pennsylvania State University) has recently drawn my attention to some organisms known as the slime molds. These are large multi-nucleate but noncellular saprophytic organisms which can live on particles of organic matter, including decayed and macerated plant tissue, and also on bacteria, using some of the latter's protein for their own metabolism. Although nonphotosynthetic and able to grow in the dark, they develop a pigment when growing in light, and light appears to be necessary for them to produce spores and reproduce by a sexual mode. It occurred to me that these organisms may have played a part, with others, in bringing about the decay of woody tissue in coalification. One interesting point is that they do not bring about the complete breakdown of cellulose and lignin as fungi and bacteria may do if provided with enough oxygen and nutrients.

A third point that may merit some discussion is the origin of nitrogen in coals. Coals commonly contain 1–2% nitrogen, and this represents an appreciably higher N/C ratio than found in woody tissue. Mason (*2*) has suggested that the extra nitrogen is derived from the proteins in the bacteria that brought about the original decay; bacteria have a relatively high total nitrogen content.

Aureal Cross: I really cannot believe that the type of cell-wall alteration seen by Dr. Spackman in the Brandon lignite resulted from microbial attack.

Publication Date: January 1, 1966 | doi: 10.1021/ba-1966-0055.ch012

Such attack can always be detected afterwards by a mottled or pitted appearance of the cell walls. Also, I do not think that Myxomycetes, the slime molds, were important primary agents in the biochemical stages of coal formation because their preferred habitat is, for example, rotting tree stumps rather than a peaty mass.

Norbert Berkowitz: Surely it is possible that the primary alteration of the cell walls is caused by hydrolysis and oxidation by water vapor and air, or they may undergo these reactions inorganically after actual immersion in water. It is of course possible that breakdown products resulting from these reactions were used or altered by microorganisms.

Cornelius Steelink: Perhaps plant cellulosic material, after hydrolysis, could be used by soil microorganisms to produce phenolic substances, which could then be incorporated into humic acids. I think it is significant that nonlignin-derived phenols occur in podzol humic acids.

Dr. Given: Of course, the sort of decay studied by Dr. Flaig, if it affected a major part of the lignin and if the cellulose and hemicelluloses were similarly largely broken down, would cause all cellular organization and even individual cell structure to be destroyed. However, I am not sure how far these two conditions are likely to be met in practice. My original thought was that Dr. Flaig's type of biochemical breakdown had occurred to a small extent or in a small proportion of the cell wall material in the Brandon lignite not sufficient to destroy the cellular organization, but perhaps this is not a very reasonable concept. However, the discussion suggests a further thought—that in a pillar section of a bituminous coal seam the fraction of material retaining fairly massive portions of organized cellular structure is small. Surely, therefore, extensive maceration of cellular tissue must have occurred; this could well have been caused by microbial agencies, and in any case there is not enough dimensionally intact fossilized cell structure left to show the mottling referred to by Cross and others. In other words, where extensive microbiological breakdown to relatively simple molecules has occurred followed by alteration and repolymerization as described by Dr. Flaig, no physical traces of the activities of the organisms can be discerned afterwards from the nature of things.

William Spackman: Only about 20% of the cells of woody tissue contain protoplasm and hence proteinaceous material. It is true therefore that woody tissue is a poor source of nitrogen.

Irving A. Breger: There is little doubt that nitrogen was introduced at a very early stage of coal formation.

R. Stephan: One way in which nitrogen could be fixed in the coal-forming materials is by a reaction between quinones (formed by breakdown of lignin) and amino acids (from plant protoplasm or microorganisms). An alternative possibility is the interaction between reducing sugars (from cellulosic material) and amino acids. These sugars can be either glucose or its oligomers, all derived by chemical and/or bacterial degradation from cellulose. Condensation of amino acids and sugars occurs both in weakly acidic and alkaline media (pH range 5.5–8.5). The resulting complex, once formed, is fairly unstable and rapidly decomposes to dark brown polymers. These polymers contain nitrogen, very likely in the form of ring structures because the α-amino nitrogen as

Publication Date: January 1, 1966 | doi: 10.1021/ba-1966-0055.ch012

found in the starting materials (proteins, peptides or amino acids) can no longer be detected.

Dr. Spackman's point that only about 20% of the cells of woody tissue contain protoplasm and therefore amino acids, does not preclude the above hypothesis. In fact, this amount of nitrogenous material would be more than ample to account for the small percentage of nitrogen found in coal.

Dr. Given: As I understand it, there is not enough protein in woody tissue to account for the 1–2% nitrogen commonly found in coals unless one supposes that a great deal of preferential loss of C and H occurred, with enrichment of N, and this supposition seems most improbable. However, amino acids from enzymes and bacterial cells most probably would be released into the coal-forming mass, and Dr. Stephan's suggestions on how these acids could be built into stable structures retaining the nitrogen are most interesting. Of course, this view of the source of some of the nitrogen in coals implies that a significant amount of carbon and hydrogen in coals originated in microorganisms rather than the plant material; the C/N weight ratio in amino acids is in the range from 2:1 to 8:1 or so.

Marlies Teichmüller: During coalification gelling takes place in the early stage of a Hartbraunkohle (lignite). From a petrographic viewpoint it is the most striking change in the whole rank range (starting from peat and ending with anthracites). The coal at this point of the rank range changes from a brown, dull, earthy and soft substance to a black (almost glass-like) substance of lustrous, tough, and hard appearance. The bedding becomes much more pronounced. Under the microscope one observes that cavities of cell tissues and pores in the detrital matter disappear and that the humic substances have been in a somewhat fluid or at least a plastic state. I would like to draw the attention of organic and physical chemists to this very interesting phenomenon. Perhaps it can be clarified by colloid chemical studies. At least it seems to me that this process is mainly a colloidal, and perhaps purely physical one since the chemical alterations at the boundary between soft and hard brown coals are small (at least as measured by C, H, O, and volatile matter content). Stach (*4*) obtained the same effect by an artificially peptizing humic substances in centimeter pieces of brown coal by means of alkali treatment. After drying the gelled coal pieces at room temperature, he found hard, lustrous, black pieces of "Glanzbraunkohle" (subbituminous coal). The carbon content had not changed.

Dr. Berkowitz: I must question the validity of Dr. Teichmüller's rather definite conclusions about the relative roles of time, temperature, and pressure in the coalification process. From an examination of Ruhr coals, Dr. Teichmüller said that only temperature plays a significant role. I suggest that conclusions drawn from data for coals in other areas (e.g., Alberta and Pennsylvania) would lead to the conclusion that pressure rather than temperature was the determining variable; therefore, I doubt whether Dr. Teichmüller's quite unqualified statements could have general validity. Indeed, from first principles one would deduce a rather complex and variable situation. Thermodynamically, one could perhaps rule out time as an important parameter since, unless one accepted the concept of a "tunnelling factor," time alone will not

Publication Date: January 1, 1966 | doi: 10.1021/ba-1966-0055.ch012

allow a reaction to proceed when such reaction is thermodynamically impossible. If it is thermodynamically possible, temperature would play a much more important role. On the other hand, pressure effects could (depending on the kind of pressure) both accelerate and retard reaction. For example, if pressure operates to retain gaseous reaction products (e.g., methane) in the coal, it will cause retardation; if it operates to produce greater permeability of the strata (and thereby to allow release of gaseous reaction products), pressure would accelerate the reaction. I question the wisdom of needlessly attempting to force nature into a sort of intellectual straightjacket which would obscure rather than elucidate reality.

Dr. Teichmüller: I am sorry that the geological observations are not consistent with Dr. Berkowitz's ideas concerning the influence of pressure on coalification. A greater permeability of the sediments cannot be caused by the overburden pressure since permeability decreases with increasing depth. As to the folding pressure, it commonly leads also to compression. It is true that tectonic pressure may also lead locally to fracturing and mylonitization if shearing occurs. Crushing of the coal and the associated sediments may therefore be observed occasionally at planes of movement, as overthrusts or faults, but according to our observations in different coal fields of Europe, this does not lead to an increase in coal rank. An exception to this rule has been described in our paper from the Sutan overthrust near Bochum where we assume the local increase in rank to be an effect of friction heat caused by exceptionally rapid movement. The geological observation that even in a folded formation coal rank increases with depth (measured from *one* point of the earth's surface) cannot be explained as an effect of folding pressure because this has a more or less horizontal direction.

In the U. S. the influence of the theory of D. White and his students (e.g., Stadnichenko) is very strong. White assumed that the tectonic pressure is the main cause of the coalification process. The same theory has been favored in Europe for a long time, but since systematic studies have been made of the vertical and regional alterations of rank in different coal fields of Europe and since also the chemists—on the basis of experiments and reaction kinetic considerations—concluded that temperature is the decisive factor for rank increase and that pressure even retards the chemical reactions during coalification, this theory has been abandoned more and more. It is true that the most intensely folded areas often bear the highest rank coals, but these areas commonly had subsided to the greatest depth prior to folding. It is a geological rule that the very deep sinking areas (foredeeps, geosynclines) will be folded later most intensely.

Dr. Breger: It seems significant that coal like materials with coking ability have never been produced in artificial coalification experiments using heat as well as pressure.

Dr. Teichmüller: Coking properties seem to depend largely on the physical microstructure of coals (porosity), as Berkowitz and Schein have shown (*1*). The swelling is possible only when the gases are kept from escaping by a too-narrow pore structure. I imagine that for getting such a pore structure, pressure must be applied while heating the coal. This is the case in nature

Publication Date: January 1, 1966 | doi: 10.1021/ba-1966-0055.ch012

where normally coalified coals, during subsidence, are exposed to elevated temperatures as well as to (overburden) pressure. Perhaps the experiments on artificial coalification did not pay attention to the "right" relations (i.e., as in natural conditions) between the temperatures and pressures applied. Moreover, no experiment can imitate the long geological time which was available for the coalification processes in nature. Therefore, in experiments higher temperatures must be used than normally were available during natural coalification. This also may lead to different reactions and different coalification products.

Elso Barghoorn: It is worth noting that in coal balls the organic matter, despite exposure to metamorphosing conditions, is still in the peat stage because it has been protected against pressure by its position in petrified concretions.

Dr. Teichmüller: The excellent structural preservation of plant remains in coal balls (which is the same as in recent peats) of course is caused by the very early petrification in the peat stage. It can be seen easily in thin sections that only the structure of the plant remains is preserved whereas the organic substance has been replaced almost totally by the petrifying mineral (calcite, dolomite). Its former location may be recognized only by a darker, brownish color of the mineral (which may be caused by submicroscopic inclusions of humic matter adsorbed by the formerly colloidal inorganic matter). At least in coal balls from the German Carboniferous the amount of microscopically visible organic matter (mostly fusinite, but sometimes also exinite and vitrinite) is very small. It can be seen and identified best in polished sections. According to my observations on polished sections the organic matter of coal balls has the same rank as the coal in which the concretions occur; at least the reflectance of the vitrinite is the same.

James M. Schopf: Dr. Teichmüller probably has underestimated the significance of the small amount of organic matter in peat-like state of preservation that is present in coal balls. It is, in fact, impossible for excellent structure to be preserved without the presence of the substance. Excellent structural preservation, so common in calcareous coal balls, is not compatible with any theory of replacement. This conclusion is supported most decisively by using the peel technique for preparing microscopical sections of the petrified plant tissues. By this method, the supporting and protecting mineral is removed by etching. The organic substance of the tissues remains intact on the etched surface and is removed as a sheet of microscopic thickness for study by applying a dissolved plastic strong enough (when dry) to be removed in a coherent sheet. The peel technique has virtually replaced thin section methods for paleobotanical studies of petrified plant tissues in recent years. This technique is significant for detailed interpretation of the organic structures preserved by "intracrustation" within the rock. The peel can only remove solid substances. Any vestiges of actual mineral replacement would show only as surface replicas on the peel, and these are generally unsatisfactory for botanical examination. General success of the peel technique for use in European as well as American coal ball studies shows that a substantial part of the original plant substance is still there. From my own observations, I feel that comparing the coal ball tissues with those in peat or in peaty litter is fully justified. It seems evident

Publication Date: January 1, 1966 | doi: 10.1021/ba-1966-0055.ch012

that the tissues were protected from alteration by the mineral medium with which they were permeated.

The coal ball plant fragments can, in fact, be regarded as an excellent sample of the vegetable material present in coal measures peat before any overburden was emplaced. The petrifying medium may be regarded principally as a replacement of the water which saturated tissues and filled the interstices. In such uncompressed peat the water content generally is in the neighborhood of 90%, and this corresponds to about the present proportion of mineral in coal balls to organic residue.

None of the lignocellulosic plant tissues in coal balls has been altered to vitrinite in any of the various European and American coal balls I have examined. It would be very interesting to know the source of Dr. Teichmüller's coal ball vitrinite reflectances. I believe they must refer to streaks of unmineralized peat which can be found associated between centers of coal ball mineralization which had been compressed and coalified rather than actually petrified. None of the plant material within coal balls I have examined can be taken as having any bearing on metamorphism or on the rank of the coal.

Jack Simon: In Illinois the systematic increase in rank from the northwest to southeast can hardly be explained by the increase of subsidence; this, to be sure, does exist in the same general direction, but the increase in depth does not seem to be great enough for this gradual loss of moisture and for the gradual increase in calorific value across the Illinois basin from northwest to southeast.

Dr. Teichmüller: Besides the deeper subsidence perhaps additional heat, caused by intrusive bodies at depth, might be the cause for the higher rank of coals in southeastern Illinois. The igneous activity seems to be greatest in that area according to geological-mineralogical observations. I was informed at least that igneous dikes occur in that area.

Dr. Schopf: A study has been completed recently by L. P. Tan, formerly of the Geological Survey of Taiwan, on the metamorphism of Taiwan Miocene coals. The results of this study will be published soon by the Taiwan Geological Survey. They are very similar to those previously developed for New Zealand Cretaceous coals by Suggate (*5*) except that the Taiwan "coal band" is in effect slightly displaced above the New Zealand coal band, according to the customary plotting. Differences in age of the coal—i.e., the period of incoalation, may explain why New Zealand coal attains about 40% volatile matter at about 3000 ft. maximum overburden depth whereas in Taiwan, the same volatile content is not attained until maximum overburden exceeded 7000 ft. Recent mapping and coal analyses in Taiwan and a favorable geologic setting have provided good control.

It is, of course, very difficult to separate the effects of geothermal gradient from overburden pressure. In a given region the two are intercorrelated.

Dr. Teichmüller: Very often it is impossible to separate the influence of overburden pressure and the influence of rock temperature on rank of coal in a subsidized formation.

Nevertheless sometimes it can be done. In the Saar Basin, where thick sandstone layers occur between claystones, in the coal-bearing Carboniferous

Publication Date: January 1, 1966 | doi: 10.1021/ba-1966-0055.ch012

it can be shown that the degree of rank increase with depth has been influenced by the different thermal conductivity of the rocks. Because of the higher thermal conductivity of sandstones, the increase is slower in the sandy series than in the clayey series.

The question of whether rank increase with depth is caused by overburden pressure or by rock temperature could be clarified best by studying the relations between the course of "isobaths"—i.e., rock isotherms and isorank lines in young sediments. If the overburden pressure is decisive there must be a strict relation between depth and rank of coal whereas if temperature is the main factor there should be a relationship between rock temperature and rank. The rock temperature is determined not only by the depth of subsidence but also by the depth of the basement (which has a high thermal conductivity) and the different thermal conductivities of the overlying rocks. From Russian investigations we know that the depth of the basement (which may vary laterally) greatly influences the course of the isotherms in the overlying rocks. An ideal area for the proposed investigations would be the southern U.S. where measurements of rock temperature as well as basement depth have been made in numerous oil wells. Coal rank could be studied by means of reflectance measurements of vitrinites from coal seams and humic inclusions in claystones out of deep wells.

Publication Date: January 1, 1966 | doi: 10.1021/ba-1966-0055.ch012

Literature Cited

(1) Berkowitz, N., Schein, H. G., *Fuel* **31,** 19 (1952).
(2) Mason, Brian, "Principles of Geochemistry," 2nd ed., p. 226, Wiley and Sons, New York, 1958.
(3) Rothbaum, H. T., *J. Appl. Chem.* **14,** 382 (1964).
(4) Stach, H., *Brennstoff-Chem.* **14,** 201 (1933).
(5) Suggate, R. P., *New Zealand Dep. Sci. Ind. Res. Bull.* **134** (1959).

Physicochemical Properties of Certain Minor Elements as Controlling Factors in their Distribution in Coal

PETER ZUBOVIC

U. S. Geological Survey, Washington, D. C.

Publication Date: January 1, 1966 | doi: 10.1021/ba-1966-0055.ch013

Analyses of sink-float separates of coal show the following order for the organic affinity of the following elements: Ge>Be>(Ga, Ti, B, V) Ni>(Co, Y)>Mo>Cu>Sn>La>Zn. Studies in chelate chemistry show that generally the chelate stabilities of the bivalent metals is Be>Cu>Ni>Co>Zn>Fe. Except for the copper this is the same order for the organic affinity of these metals in coal. Copper could be in a reduced state in the coal depositional environment or precipitated as a sulfide. The trivalent metals—gallium, yttrium, and lanthanum—have the same order for their organic affinity and chelate stability. Most of the metals show a good relation between their organic affinity, ionic potential, and chelate stability.

In a study of the geochemistry of metallic elements in coal or other carbonaceous geological materials, several problems are encountered. Although much data on the minor element content of such materials exists, data on the distribution of elements among the organic matter, syngenetically formed minerals, and detrital minerals are very scarce. Furthermore, except for several general postulations first proposed by Goldschmidt (*6*) the genesis of most minor elements in carbonaceous rocks is almost completely unknown. This paper attempts to correlate the available data on distribution of minor elements in organic and inorganic matter of coal with some of the known chemical properties of these elements and to determine patterns of their accumulation and distribution in organic and inorganic phases of coal. This paper is primarily concerned with the minor elements—beryllium, boron, titanium, vanadium, chromium, nickel, cobalt, copper, zinc, gallium, germanium, molybdenum, tin, yttrium, and lanthanum—and to a lesser extent with the major elements—iron, aluminum, and silicon.

In Coal Science; Given, P.;
Advances in Chemistry; American Chemical Society: Washington, DC, 1966.

Goldschmidt (*6*) proposed three general methods for the accumulation of elements found in organic matter of coal:

(1) Accumulation by plants during growth.
(2) Accumulation by complex formation during decay of plant matter.
(3) Accumulation after burial.

These postulations generally have been accepted by most investigators. The author feels that in large coal deposits the first two are the dominant methods of accumulation and that the last process takes place only on a very limited scale, such as in isolated fragments of carbonized wood and in the tops of some coal beds, and therefore, that the accumulation of these elements is essentially a syngenetic process. Chemical data on the relation of minor elements and the accompanying organic matter are relatively sparse. Breger and others (*3*) suggested that uranium as well as nickel, cobalt, beryllium, molybdenum, titanium, vanadium, chromium, and tin present in a demineralized lignite are held essentially as metal organic complexes. They detected germanium in the mineral fraction but not in the original or the mineral-free part of the lignite, whereas Manskaya and others (*11*) reported that about 80% of the germanium present in a peat was bound to organic matter which is soluble in dilute alkali solutions and that 30% of this was bound to strongly polymerized humic acids.

Table I. Average Organic Affinity of Some Metals Determined by Float-Sink Methods

Element	*Percent organic affinity (18)*	*Percent organic association (9)*
Germanium	87	100
Beryllium	82	75–100
Gallium	79	75–100
Titanium	78	75–100
Boron	77	75–100
Vanadium	76	100
Nickel	59	0–75
Chromium	55	0–100
Cobalt	53	25–50
Yttrium	53	N.D.*
Molybdenum	40	50–75
Copper	34	25–50
Tin	27	0
Lanthanum	3	N.D.*
Zinc	0	50

* N.D.—not determined.

Physical separations of coal by flotation (*9*, *17*, *18*) have produced data showing the organic affinity of a number of minor elements. Horton and Aubrey (*9*) studied the distribution of minor elements in five different density fractions of each of three vitrain samples. By comparing the distribution of the elements with that of the organic and inorganic matter, they calculated the percent association of the elements with the organic matter. Their data are summarized in Table I. Zubovic and others (*17*, *18*) reported on the separation of 13 samples of Eastern Interior Region coals into sink-and-float fractions. The average organic affinity for the elements as derived from the 13 samples

Publication Date: January 1, 1966 | doi: 10.1021/ba-1966-0055.ch013

is also shown in Table I. There is general agreement between the two sets of data in Table I for those elements forming small highly charged ions. Data for cobalt, tin, and zinc show less agreement. These data are plotted in Figure 1 and compared with the ionic potentials of the metals.

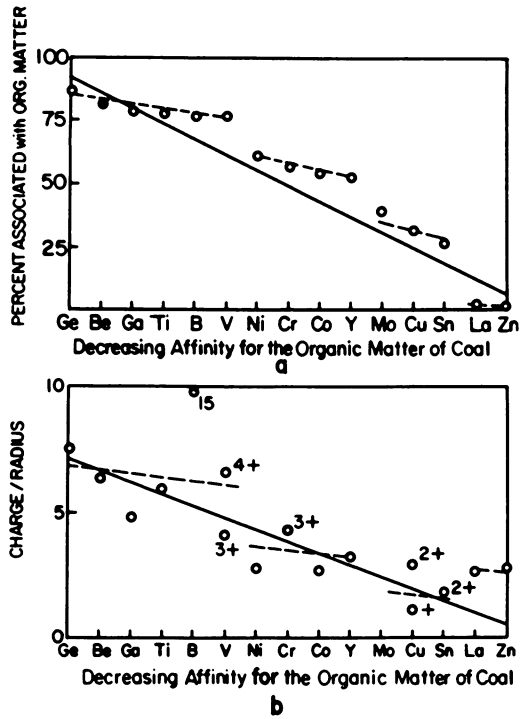

Figure 1. Relation of organic affinity and ionic potential of the elements

When the data for vanadium, nickel, cobalt, copper, and iron in petroleum of the Western Interior Region (*15*) shown below are divided by the average crustal abundance of these elements, the relation, V>Ni>Co>Cu>Fe is derived.

	I *P.p.m. in crude-oil*	*II* *Average crustal abundance in p.p.m.*	*Ratio I/II*
Vanadium	110	100–150	1.0–0.73
Nickel	55	80	0.69
Iron	6	50,000	0.0001
Copper	2	70	0.03
Cobalt	1	23	0.04

This can be considered to be the relation in which these metals have been preferably complexed by the progenitors of petroleum. Except for iron, which

Publication Date: January 1, 1966 | doi: 10.1021/ba-1966-0055.ch013

was not determined in these coals, the relation, V>Ni>Co>Cu, is similar to that derived from coal shown in Table I and Figure 1. From these three sets of data this author believes that the affinity of the elements for naturally occurring organic matter generally follows the sequence shown in Figure 1a. It should be pointed out that for any individual element, considerable variability has been found among the samples, and the data presented in Table I and Figure 1 are the averages for 13 samples.

Relation of Metal-Organic Affinity to Complex Formation

A proof of the validity of the organic affinity series could best be made by studying the complexes, if present, of these metals in coal and other carbonaceous geological materials. However, except for the porphyrin chelates of some of the transition metals, no complexes have been extracted from such materials. Consequently, the only other approach is to assume that this is a stability series for these metals in naturally occurring organic matter and to compare this stability sequence with the stability sequences determined in laboratory studies made on their organic complexes. It must be further assumed that the elements organically associated in geologically old carbonaceous materials are present in the most stable complex possible to survive through geologic time.

The most stable metal-organic complexes are those wherein ring structures are formed; these complexes are called chelates. The most stable chelates form five- and six-membered rings with the metals (*13*). One property of the metals conducive to the formation of stable chelates is the ionic potential (charge/radius) of the metals. Figure 1b shows the organic affinity series plotted against the ionic potentials of the metals. There is general agreement in that the metals with high ionic potentials have high organic affinities in coal, and those with lower ionic potentials have lower organic affinities.

A further indication that the metals associated with the organic matter of coal may be chelated is the correlation between their organic affinity and the stability constants of their chelates as determined in laboratories. Basolo and Pearson (*1*) suggest that for some of the tervalent ions of this report the general order for the stability of their chelates is Ga>Y>La. The same order for these three elements is shown in Figure 1. Furthermore, data from Mellor and Maley (*14*), Irving and Rossotti (*10*), and summaries of these data by Basolo and Pearson (*1*) suggest that the stability of chelates of bivalent ions is Be>Cu>Ni>Co>Zn>Fe. Except for copper, this is the same order of these metals in their organic affinity for coals as shown in Figure 1 and in the subsequent discussion on petroleum. From these observations it appears to this author that that portion of gallium, yttrium, lanthanum, beryllium, nickel, cobalt, and zinc that is bonded to organic matter in coal is held as chelated complexes.

The lack of adequate experimental data on chelates of germanium, boron, titanium, and vanadium prevents a similar comparison for these elements; however, their high ionic potentials do indicate that they should form stable chelates. Vanadium does occur naturally in the very stable vanadium porphyrin complex. For similar reasons, molybdenum and tin are not discussed further.

Publication Date: January 1, 1966 | doi: 10.1021/ba-1966-0055.ch013

In coal, copper shows an organic affinity different from the Mellor and Maley (*14*) series, and zinc appears to be completely associated with the inorganic matter. Copper in the physicochemical environment of coal deposition can be reduced to the univalent state (*5*). Univalent copper cannot be expected to behave like the bivalent metals. The ionic potential of univalent copper fits reasonably well into the organic affinity series (Figure 1a).

In the presence of hydrogen sulfide produced by anaerobic bacterial activity, particularly sulfate reducers, conditions are created whereby sulfides of copper and zinc could be formed. The partition of these metals between the sulfide phase and the organic phase depends on the relation between the stability constants of the complexes and the solubility product of the sulfides of these metals. Elements with small solubility products of their sulfides and low stability constants of their chelates would be expected to go into the sulfide phase when hydrogen sulfide is present. Copper is typical of such elements. Chalcocite has a solubility product of about 10^{-50} and covellite about 10^{-44}, whereas the most stable chelates of copper have stability constants of about 10^{-20}. Consequently, copper could be expected to be accumulated as the sulfide. Zinc sulfide has a much larger solubility product; however, the stability of its chelates is lower. From the fact that zinc appears to be completely associated with the inorganic fraction of coal, it can be assumed that the relation between the solubility product of any of its sulfides and its chelates favors formation of the sulfide. Iron could be expected to follow a similar pattern.

The data in Table I suggest that copper may be associated to some extent with organic matter. This could occur if hydrogen sulfide were not available, owing either to cessation of sulfate-reducing bacterial activity or the paucity of sulfate which could be reduced. It is also possible that a stronger chelating agent is available or that the relation of the concentrations of the chelating agent to hydrogen sulfide favors formation of the chelate.

This approach can also be used for the elements that form insoluble hydroxides in a slightly acid meduim, such as beryllium, aluminum, gallium, and chromium or for any other insoluble inorganic phase which could be formed

All the elements studied show a degree of inorganic association. Unquestionably, a certain, in most cases small, percentage of the elements is incorporated in the detrital mineral matter. Some of these elements generally are found in very resistant minerals: for example, boron in tourmaline, yttrium and lanthanum in rare earth minerals such as xenotime and monazite, and beryllium in beryl. Other elements, such as copper and zinc mentioned previously and perhaps vanadium, gallium, molybdenum, and tin (among the elements studied here), could be syngenetically formed as sulfides under certain conditions. In addition to these elements, iron, as the sulfides pyrite and marcasite, makes up a large portion of the mineral matter of many coals.

Relation of the Metals to Donor Elements

The donor element is an important factor in chelate stability. Generally, certain metals form more stable complexes when bonded to a preferred donor

Publication Date: January 1, 1966 | doi: 10.1021/ba-1966-0055.ch013

atom. Martel and Calvin (*13*) presented a series of preferences of metals for donor elements. For the metals discussed in this report, these are:

O > N	Ga, Ge, Ti, Sn, V(IV), V(V), Co
O = N	Ge, Cr, Fe
N > O	Cu(I), Cu(II), V(III), Ni

Where the valency of a metal is not indicated, the normal valency of the metal is assumed. Beryllium probably is placed in the O=N group because of the stability of its phthalocyanine chelate. Most often Be forms very stable bonds with oxygen as the donor element. Vanadium, nickel, and copper from the N > O group and iron from the O=N group are the elements most frequently found in petroleum, chelated with porphyrin ligands. The porphyrin chelate contains four nitrogens as donor elements.

Publication Date: January 1, 1966 | doi: 10.1021/ba-1966-0055.ch013

Possible Complexing Agents in Decaying Plant Materials

In the presence of decaying plant material a large variety of organic ligand molecules are made available to the metals released from decomposing soil and rock. It is believed that in such a heterogeneous environment the preceding preferences by the metals for certain donor atoms are followed.

This author believes that some of the most stable complex-forming ligands present in decomposing plant remains which would produce stable chelates are chlorophyll, amino acids, and lignin derivatives. The first two could be the chelating agents for trivalent vanadium, nickel, copper, and to some extent iron—i.e., the elements which prefer nitrogen as the donor element. Beryllium, germanium, gallium, titanium, cobalt, aluminum, and silicon would be bonded to the oxygens of lignin derivatives. Other complex formers may be present; however the above are known to have bonding positions whereby stable complexes are formed.

The magnesium of chlorophyll could be replaced by vanadium and the other elements found in metal-porphyrins. Amino acid chelates of the transition metals are quite soluble and could be responsible for long distance transport of some of these elements. Furthermore, this author believes that the preservation

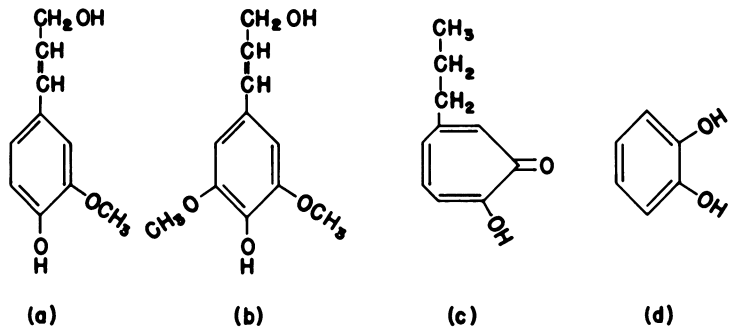

Figure 2. Structures of (a) coniferal alcohol, (b) sinapyl alcohol, (c) β-isopropyltropolone, and (d) catechol.

of amino acids could, in coal, peat, lignite, and other carbonaceous materials, be the result of the formation of stable metal-amino acid chelates. Protected amino acids preserved in fossil bones and shells do not necessarily fall into this category.

The most persistent and stable amino acids appear to be glycine, aspartic acid, and glutamic acid, which were reported in Paleozoic anthracite from Great Britain by Heijhenskjöld and Möllerberg (*8*). Among the most stable amino acid chelates are those formed with copper; however, the stability constants for the α-amino acids of copper do not differ to the point where they indicate that the above mentioned three acids would be preferentially preserved.

In the chelates of glycine, aspartic acid, and glutamic acid all the carbon and nitrogen atoms form part of the ring structure. This probably is the reason why these three acids appear to outlast all others in high rank coal. It should be pointed out that in the presence of hydrogen sulfide, copper is precipitated as the sulfide from copper-amino acid chelates. Thus, copper and perhaps other elements could be transported as amino acid chelates until sufficient hydrogen sulfide was encountered to cause precipitation.

Lignin is considered to be the principal contributor to humic materials which form coal. Lignin is made up of a large number of monomers such as a and b shown in Figure 2. The 4-hydroxy-3-methoxyphenyl group is called the guaiacyl group. There are a large number of such groups in a lignin molecule. Upon its degradation to humic-like substances, the methoxy content of the lignin is greatly reduced. It is possible that during this degradation process a considerable amount of chelation with metals through the guaiacyl oxygens could take place. Very stable chelates are formed with substances such as catechol (d) and the tropolones (c), which have bonding positions

Table II. Stability Constants for Some Metal Complexes of the Tropolones[a,b]

	Be	*Co*	*Cu*	*Ni*
Tropolone	15.4	12.9	16.6[c]	13.8
β-Methyltropolone	17.1	14.1	—	15.0
β-Isopropyltropolone	16.6	14.2	—	15.0
3,4-Benzotropolone	17.1	—	—	15.0
Catechol	—	—	30.7	—

[a] Data shown are log B_2 which is log K_1 K_2.
[b] Data taken from Bjerrum (*2*).
[c] Estimated. (log K_2 = 7.9)

similar to those of the guaiacyl groups. The data for the tropolones (Table II) show that attached structures on the benzene ring further increase the stability of such chelates. As a result, chelation with large humic-like products of lignin should have an unusual stability. Furthermore, since a number of such sites could be available on any one of these partially degraded lignin polymers, these could, through metal linkages, form the very large highly insoluble humic substances found in coal, such as the humins or ulmins. This author does not imply that the insolubility is solely caused by the formation of complexes; loss of polar groups from the degrading lignin plays a dominant role in this phenomenon.

Publication Date: January 1, 1966 | doi: 10.1021/ba-1966-0055.ch013

Manskaya (*12*) suggests that lignin initially degraded to phenylpropane monomers and later condensed structures accumulate in lignite, and that germanium, vanadium, and uranium become fixed with them. This author does not feel that complete degradation of lignin to its monomers has to take place, but rather that large fragments of the degrading lignin can be chelated and subsequently further alteration can take place through loss of easily detached groups to form the humic-like substances.

Another indication that the metals could be bonded to large rather than to small structures is the generally low inherent ash of vitrains and of isolated pieces of coalified wood. Very clean vitrains generally contain about 1% ash. If the metals such as copper were complexed by monomers such as hydroxylconiferyl alcohol, then the copper content of the resulting complex would be about 16% or 20% copper oxide as the ash. However, if metal with similar atomic weight (average about 60) were bonded to degraded lignin molecules (molecular weight about 6000–8000), whereby polymers were formed through the metals, the resulting ash would be about 1%.

The fact that germanium and vanadium frequently are reported in large amounts in isolated fragments of coalified wood (*4*, *7*, *16*) suggests that these two elements form the most stable complexes with degraded woody materials. This author believes that vanadium and germanium replace other metals in existing complexes. Germanium was shown to have the highest organic affinity of the metals in Figure 1, whereas vanadium ranked below some of the other, smaller, highly charged ions such as beryllium, boron, gallium, and titanium. Furthermore, trivalent vanadium forms stronger bonds with nitrogen as the donor element than with oxygen. Tetravalent vanadium, however, forms more stable chelates with oxygen as the donor element. In order to be chelated with the oxygens of lignins, vanadium may be tetravalent. Since the accumulation of large amounts of germanium in these coalified woody materials seems to be a replacement reaction, its emplacement must have occurred after burial and initial degradation of the woody material. The oxidation-reduction potential could have been higher than in the initial phases of degradation, particularly if bacterial activity ceased when the replacement by vanadium occurred.

The other alternative is that trivalent vanadium is replacing elements chelated to the nitrogens of the humic matter. If such is the case, then it would appear that the germanium forms the most stable chelates of those elements bonded to oxygen and trivalent vanadium to those bonded, completely or partially, to nitrogen. When the availability of these two elements were sufficient they would be the two elements complexing a large part of the organic matter that exists as metal chelates in the isolated fragments of coalified wood.

Replacement reactions with pre-existing chelates is suggested largely because this author feels that additional chelation cannot take place after compaction and solidification of the organic mass. Reorientation of large organic ligands into positions to provide strain-free chelates would be difficult in a solid. If some additional enrichment took place, the metals would be held as simple complexes, not as chelates.

In large deposits of coal, the availability of the best complex-forming metals is quite low. Consequently other metals assume a dominant role in

Publication Date: January 1, 1966 | doi: 10.1021/ba-1966-0055.ch013

complex formation. Among the minor elements listed in Table I and Figure 1, titanium is found in largest amounts. This may result from the fact that its crustal abundance is the highest of these metals. The other abundant elements in the earth's crust, silicon and especially aluminum, probably account for the largest share of the metal-organic complexes in such coals. Solubility of the minerals in which these metals occur is also a controlling factor in their availability. The position of iron in this scheme is uncertain. Under most conditions, if hydrogen sulfide is being produced by bacterial activity, most or all of the iron would be expected to form sulfides. As the availability of the metallic elements increases in relation to the amount of organic matter able to form stable complexes, replacement reactions cause retention of those metals which form the more stable complexes. Such conditions generally are found in small isolated lenticular bodies of coal, in thin-bedded coals, and also in strata representing the initial and last phases of coal-bed deposition. This is probably why tops and bottoms of coal beds and thin beds frequently are rich in germanium. The end product of increasing metal and decreasing organic availability is found in the germanium, vanadium, and at times in uranium-rich, isolated coalified fragments of trees.

Publication Date: January 1, 1966 | doi: 10.1021/ba-1966-0055.ch013

Summary

Analyses of float-sink separates of coal reveal a systematic variation of the minor elements with the organic matter which can be arranged into an organic affinity series. This series appears to be related to the chelating properties of the metals. Deviations in this series may be explained by the chemical nature of the depositional environment.

It is believed that most of the transition metals are complexed to nitrogen donors, such as are found in amino acids or derivatives of chlorophyll, and that the metals with high ionic potentials, such as beryllium, boron, germanium, titanium, gallium, and major elements such as aluminum and silicon, may be bonded to oxygen donors of degraded lignin.

Complexing of amino acids by some metals of the transition series may be the reason why some amino acids are preserved in coal through geologic time. Furthermore, the complexing of the humic substance derived from lignin by metals may play a role in forming the highly insoluble fractions of coal. The amount of any given element that is complexed depends upon its availability with respect to the amount of available organic matter and to its position in a complex stability series of the competing elements.

Literature Cited

(1) Basolo, F., Pearson, R. G., "Mechanisms of Inorganic Reactions," p. 16, John Wiley and Sons, Inc., New York, 1958.
(2) Bjerrum, J., Schwarzenbach, G., and Sillen, L. G., "Stability Constants of Metal-Ion Complexes Part I. Organic Ligands," Chemical Society, London, 1957.
(3) Breger, I. A., Deu, M., Rubenstein, S., *Econ. Geol.* **50**, 2 (1955).
(4) Breger, I. A., Schopf, J. M., *Geochim Cosmochim. Acta* **7**, 290 (1955).
(5) Garrels, R. M., "Mineral Equilibria at Low Temperatures and Pressures," pp. 173-200, Harper, New York, 1960.
(6) Goldschmidt, V. M., *Ind. Eng. Chem.* **27**, 1101 (1935).

(7) Hallam, A., Payne, K. W., *Nature* **171,** 1008 (1958).
(8) Heijkenskjold, F., Mollerberg, H., *Nature* **181,** 335 (1958).
(9) Horton, L., Aubrey, K. V., *J. Soc. Chem. Ind.* **69,** Suppl. 1, 541 (1950).
(10) Irving, H., Rossotti, H., *Acta Chem. Scand.* **10,** no. 1, 72-93.
(11) Manskaya, S. M., Drozdova, T. V., Kravtsova, R. P., Tobelko, K. I., *Geokhimiya* **1964,** 455.
(12) Manskaya, S. M., Kodina, L. A., *Geokhimiya* **1963,** 389.
(13) Martell, A. E., Calvin, M., "Chemistry of Metal Chelate Compounds," p. 169, Prentice-Hall, Inc., New York, 1952.
(14) Mellor, D. P., Maley, L. E., *Nature* **161,** 436 (1948).
(15) Moore, J. W., Dunning, H. N., *U. S. Bur. Mines Rept. Invest.* **5370,** 13 (1957).
(16) Stadnichenko, T. M., Murata, R. J., Zubovic, P., Hufschmidt, E. L., *U. S. Geol. Surv. Circ.* **272,** 15 (1953).
(17) Zubovic, P, Sheffey, N. B., and Stadnichenko, T. M., *U. S. Geol. Surv. Profess. Papers No.* **400-B,** B84-B87 (1960).
(18) Zubovic, P., Sheffey, N. B., Stadnichenko, T. M., *U. S. Geol. Surv. Profess. Papers No.* **424-D,** D345-D348 (1961).

RECEIVED January 25, 1965. Publication authorized by the Director, U.S. Geological Survey.

Discussion

M.-Th. Mackowsky. Have you found any characteristic associations of macerals with any particular elements?

Peter Zubovic. We have very little such data. We have separated some macroscopic vitrain and fusain bands from blocks of coal and analyzed these. Generally germanium, beryllium, boron, and gallium are more concentrated in the vitrain samples. Fusain samples generally contain less of most of the elements than is found in the whole block of coal.

Jacques Jedwab. We have studied in our laboratory the ratios Ca/Mg/Be. We have observed a positive correlation between Ca/Mg and Be, indicating a relationship between the enrichment of beryllium in the coal seams (particularly in the roof and walls) and the circulation of ground water.

G. R. Hill. Comparing the ratio of ionic charge to ionic radius is good for metals which form simple ions. For elements like boron, which exist always as complex anions, the ratio may not be meaningful. This may explain the anomalous position of boron in Figure 1. Do we have any information about the nature of the complexes formed by borates in plants?

Mr. Zubovic. I do not have any data on the nature of complexes formed by boron in plants. I do believe that the boron we find associated with organic matter in coal is the result of its accumulation by plants. Bjerrum does not list any boron complexes in his compilation of stability constants of metal-ion complexes. Martel and Calvin suggest that boron complexes resemble esters. I do not believe that the high organic affinity and high ionic potential shown by boron in Figure 1 is any indication that it forms stable chelates. Rather its high organic affinity just shows that it is accumulated by plants and is retained in the organic fraction during coalification.

H. J. Gluskoter. What are the differences, if any, in analytical results between samples ashed at lower and higher temperatures?

Mr. Zubovic. We ashed several samples at higher temperatures—i.e., about 750°C. All of our coals were normally ashed at a maximum of 450°C. Comparing those samples ashed at 750°C. with the same sample ashed at 450°C. showed no loss of any of the elements. However, I must point out that both ashings were done at a slow rate of temperature increase. I suspect that if a sample were placed in a furnace preheated to 750°C. a loss of some of the elements may take place.

Bhupendra Mazumdar. The author's results show that a sample of weathered coal was found to contain appreciably more of metal complexes than the unweathered coal. I would be glad to know if Mr. Zubovic can explain this phenomenon. Has he studied any correlation between extra metal retention and additional acidic groups (in particular COOH groups) usually found in weathered coals?

Mr. Zubovic. We have not made any additional studies of these weathered samples. I do not know if there is any correlation of the elements with a larger number of acidic groups in this coal. I do believe that the additional amounts of elements found in the weathered coals are not held there as chelates but rather as simple complexes such as are formed in ion exchange reactions.

Publication Date: January 1, 1966 | doi: 10.1021/ba-1966-0055.ch013

14

Minor Element Distribution in Coal Samples of the Interior Coal Province

PETER ZUBOVIC

U. S. Geological Survey, Washington, D. C.

Publication Date: January 1, 1966 | doi: 10.1021/ba-1966-0055.ch014

Distribution patterns of 13 minor elements in 54 coal samples indicate that beryllium, boron, germanium, and gallium—the metals forming small, highly charged ions (high ionic potential)—are concentrated near the source areas of a coal basin. The other elements show various distribution patterns which suggest differences in their transport characteristics. Yttrium and lanthanum concentrations demonstrate a fractionation whereby the Y/La ratio is highest in those coals nearest the source areas of the elements. Vanadium and, to a lesser extent, chromium are preferentially enriched in Kentucky bed 9 and its correlative Illinois bed 5. The high concentration of minor elements in weathered samples, relative to unweathered samples, suggests that weathering processes may significantly increase the minor element content in coal.

The distribution of beryllium, boron, titanium, vanadium, chromium, cobalt, nickel, copper, zinc, gallium, germanium, tin, molybdenum, yttrium, and lanthanum in the principal coal-producing beds of the Interior Province has been studied by the U. S. Geological Survey. Data, methods of sampling, and analyses are discussed by Zubovic and others (*11*, *12*). This chapter discusses the occurrence of 13 of these elements with respect to geological and geochemical environments of coal deposition and chemical properties of the elements. Zinc and tin are not included in this study because they were detected in only a few samples.

Distribution of the Elements

Figure 1 shows the area covered in this report. The solid line shows the extent of the Pennsylvanian strata that contain coal beds; the dots represent locations from which samples were taken. The arrows indicate the directions

In Coal Science; Given, P.;
Advances in Chemistry; American Chemical Society: Washington, DC, 1966.

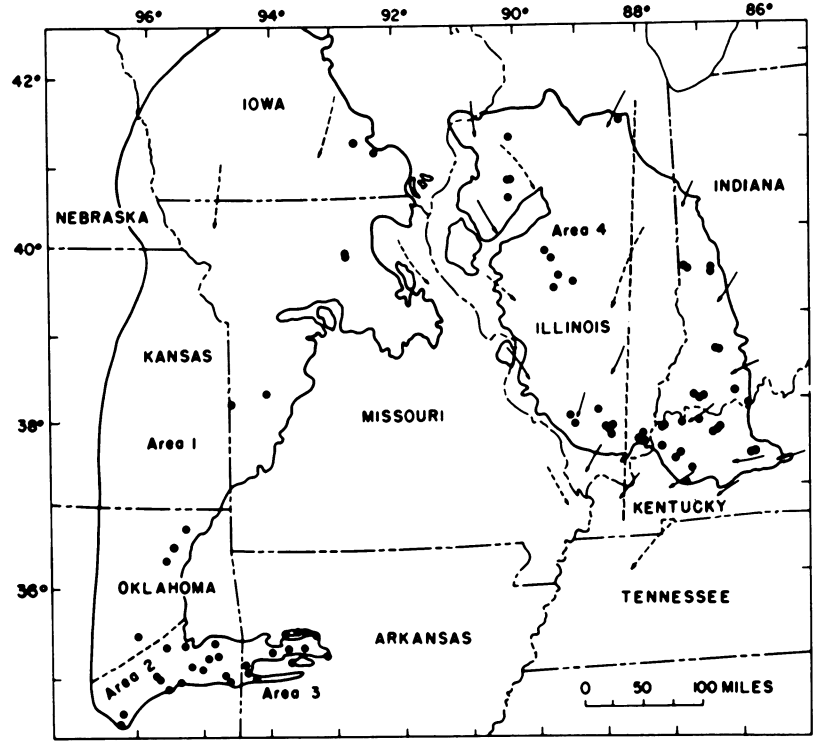

Figure 1. Distribution of the samples in the Interior Province. Solid line indicates extent of Pennsylvania sediments containing coal beds; arrows indicate sedimentary transport directions of basal Pennsylvanian sandstones taken from Potter and Siever (6)

of sedimentary transport of the basal Pennsylvanian sediments as reported by Potter and Siever (*6*). Other reports by Potter (*4*, *5*) show that these same general trends have prevailed throughout Pennsylvanian time in the Eastern Interior Region.

The samples of the Eastern Interior Region considered here are those shown in Figure 1 west of the dashed north-south line in Illinois. All these samples are from Illinois beds 5 and 6. This selection was made to obtain a series of samples located at increasing distances from the source area of the sediments. Because the sedimentary source for the Indiana and Kentucky coal areas are less certainly known (*6*), the samples from those areas are not considered here. Except for beryllium and vanadium, the minor element content of samples from those areas is comparable to samples from western Illinois. The beryllium content of all these coals was reported by Stadnichenko and others (*8*). The unusually high vanadium content of some of the southern coals of the Eastern Interior Region is discussed below.

Distribution of the elements in coal beds of four areas is shown in Figures 2–8. Reading from left to right, the first column shows the minor element

Publication Date: January 1, 1966 | doi: 10.1021/ba-1966-0055.ch014

content of the samples from Iowa, Missouri, and northern and central Oklahoma; samples are arranged in a north to south direction. The second column, reading from left to right, shows the elemental distribution of the samples from west to east in the Oklahoma portion of the Arkansas-Oklahoma Basin; the third column shows the same arrangement of samples from the Arkansas portion of the basin; the last column shows the samples from Illinois arranged from south to north. The areas are numbered 1–4, and these numbers will be used in reference to these areas.

Vanadium and chromium distributions (Figure 2) decrease toward low values in areas 2 and 3. The highest medians are found in area 4. The data show that vanadium is much more dispersed than chromium. Vanadium distribution also increases from north to south in Illinois.

Cobalt and nickel (Figure 3) are distributed similarly. The highest medians are for the samples from areas 1 and 3 and the lowest for areas 2 and 4. The cobalt values show a very large spread. Copper (Figure 4) is distributed similarly to, but more uniformly than, cobalt or nickel. Molybdenum (Figure 4) is erratically distributed.

Publication Date: January 1, 1966 | doi: 10.1021/ba-1966-0055.ch014

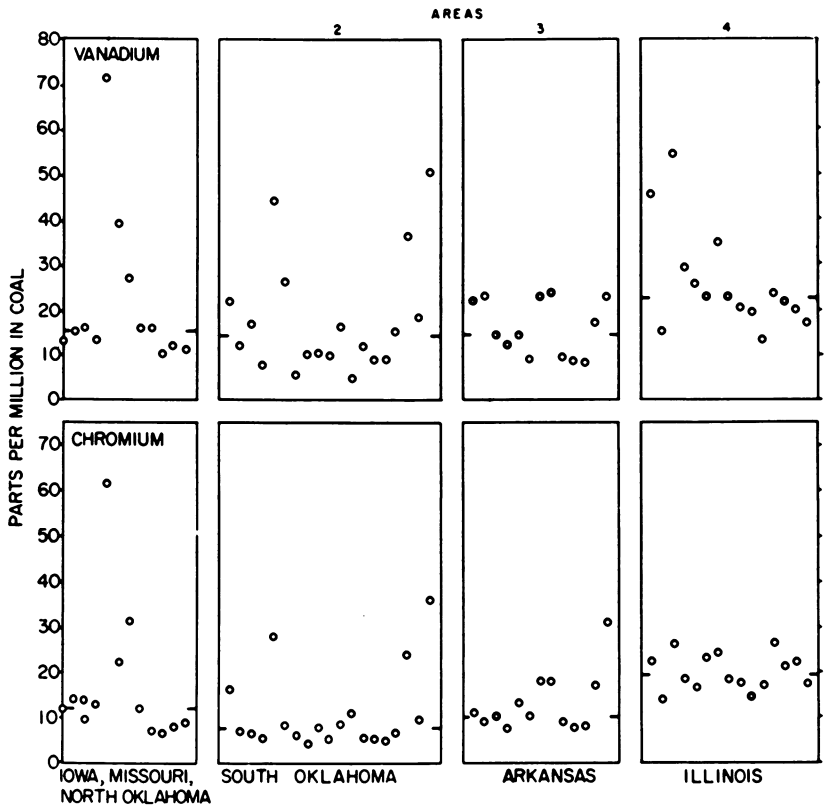

Figure 2. Distribution of vanadium and chromium. Tick marks indicate medians for the elements in the samples

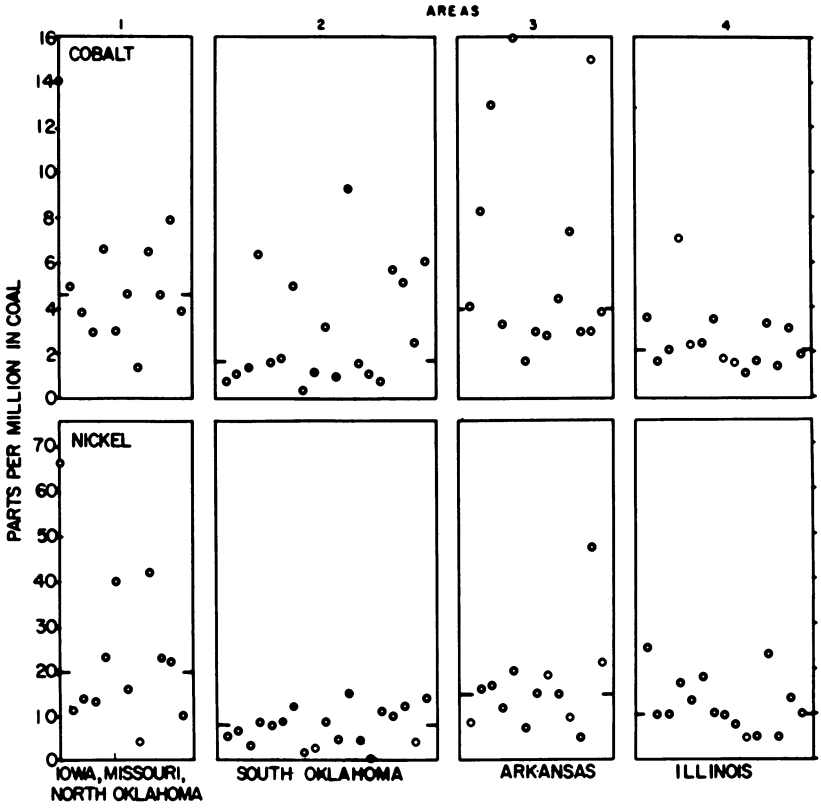

Figure 3. Distribution of cobalt and nickel. Tick marks indicate medians for the elements in the samples

Yttrium values of the samples (Figure 5) decrease significantly in a southerly direction in area 1, but are uniformly distributed in areas 2 and 4 and show an extensive spread in area 3. Lanthanum increases in a southerly direction in area 4, is uniformly distributed in areas 1 and 2, and shows considerable spread in area 3.

Titanium (Figure 6) is found in largest amounts in the area 4 coals and increases in a southerly direction in this area. The lowest concentrations are found in area 2. The Y/La ratios show southerly decreases (increasing distance from source areas) in areas 1 and 4 and uniform low values in areas 2 and 3. This distribution of the Y/La ratios suggests fractionation of these two elements as the distance from source areas increase.

The data for the next four elements suggest a near-source enrichment which would be expected from their chelating properties. Concentrations of beryllium and boron (Figure 7) and germanium and gallium (Figure 8) decrease in a southerly direction (increasing distance from source area) in areas 1 and 4. The germanium values are considerably spread in area 1. The content of beryllium, boron, and germanium in coal are uniformly low in areas 2 and 3.

Publication Date: January 1, 1966 | doi: 10.1021/ba-1966-0055.ch014

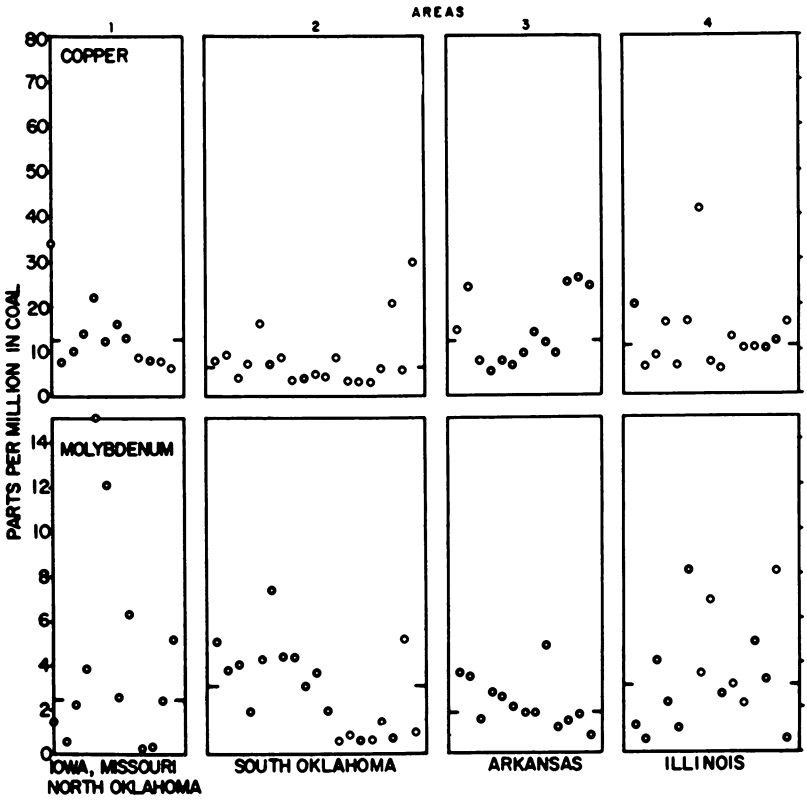

Figure 4. Distribution of copper and molybdenum. Tick marks indicate medians for the elements in the samples

Gallium, although low in these areas, shows more spread than the other three elements.

The data from these last four elements suggest that the nontransition elements, which form small highly charged ions, should be preferentially concentrated in carbonaceous rocks deposited in the near-source areas and depleted as the distance from source increases. The transition elements and those forming larger ions with lower ionic potentials appear to be transported farther from the source before being incorporated into the sediments; this suggests that beryllium, boron, gallium, and germanium form more stable and insoluble complexes than do the transition elements. The insoluble complexes would be more rapidly precipitated than the soluble complexes.

As suggested in the preceding chapter (9), the bonding of elements such as beryllium, boron, germanium, silicon, and aluminum with oxygens from the phenylpropane structures of lignin could be instrumental in further polymerizing these units into large, highly insoluble coal fractions. The transition elements, on the other hand, could be complexed with the nonpolymerizable,

Publication Date: January 1, 1966 | doi: 10.1021/ba-1966-0055.ch014

more water soluble amino acids and could be transported over greater distances within the coal swamp.

It is suggested here that the greater insolubility of the humic fraction of coal may be the result, in part, of polymerization by complexing with metals, particularly aluminum and silicon. These elements are suggested because of their presumed greater availability. The minor elements also play a part, however, only in relation to their availability compared with major elements such as aluminum and silicon.

To this author, the diverse distribution patterns of these elements appear to confirm the paleogeological setting of the sedimentary conditions in the Interior Coal Province in Pennsylvanian time. Schuchert (7) showed that the drainage of the eastern parts of the inland sea in Pennsylvanian time was to the west between the Ozark uplift and the upland south of the present Ouachita Mountains. McDaniel (3) stated that the sedimentary transport direction of the Hartshorne Sandstone was from east-northeast to west-southwest. Most of

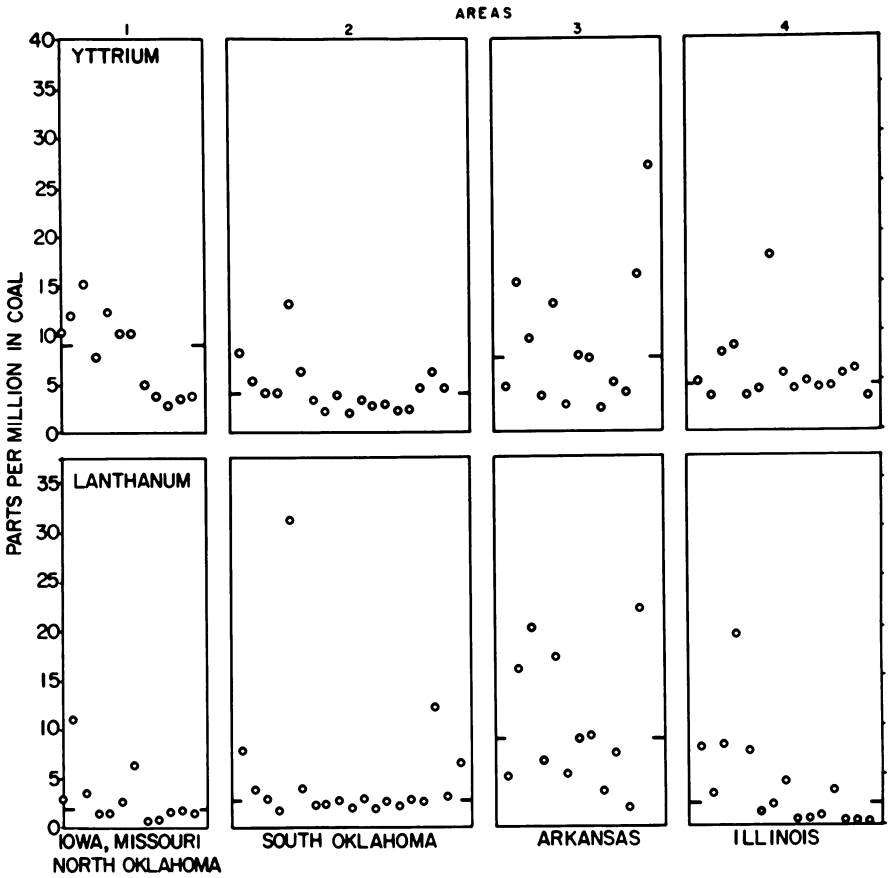

Figure 5. Distribution of yttrium and lanthanum. Tick marks indicate medians for the elements in the samples

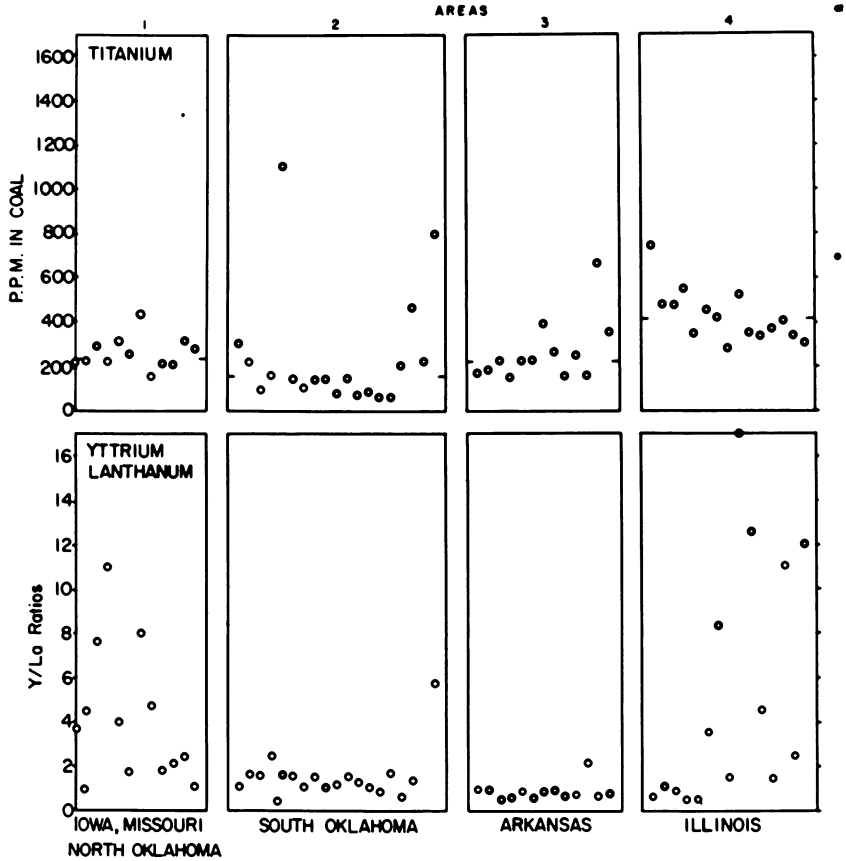

Figure 6. Distribution of titanium and the yttrium/lanthanum ratios. Tick marks indicate medians for the elements in the samples

this sandstone unit lies between the two main coal beds, the lower and upper Hartshorne coals, which were sampled in the Oklahoma-Arkansas Basin. This implies that the sampled portions of the Oklahoma-Arkansas basin were probably a long distance from their sedimentary source area. Uplifted eroding areas existed south of the basin; however, it appears that during deposition of the coals the drainage from these areas was deflected by that from the eastern inland sea. If this did occur, little or no soluble material from the southern source area reached the northern shelf areas where the sampled coals were deposited. The extremely low and uniform values for beryllium, boron, germanium, and gallium found in these coals particularly suggest such an environment. Drainage from the eastern inland sea was rapidly depleted in these elements in the near-source areas. This is not to imply that coal beds were continuously and syngenetically deposited over the entire province. While humic materials were accumulating rapidly in the Oklahoma-Arkansas Basin, the waters entering this basin must have passed through other areas which

Publication Date: January 1, 1966 | doi: 10.1021/ba-1966-0055.ch014

contained sufficient organic matter to deplete the solutions of beryllium, boron, gallium, and germanium. Such organic matter could be the thin organic zones found in numerous areas throughout the Interior Province or in organic-rich nonmarine shales.

Weathered Samples

During the coal studies it was noted that the minor element content of four coal samples from Arkansas was persistently higher than that of other Oklahoma-Arkansas Basin coal samples. These four samples, collected in road cuts, were very badly weathered. Data for these samples are listed in Table I along with the averages of the other 32 samples from the same basin. It is obvious that most of the elements were considerably enriched, particularly beryllium, yttrium, and lanthanum. Although the nature of this enrichment was not investigated, it seems reasonable that coal weathering (oxidation) could produce numerous sites for bonding the metals with the organic matter.

Publication Date: January 1, 1966 | doi: 10.1021/ba-1966-0055.ch014

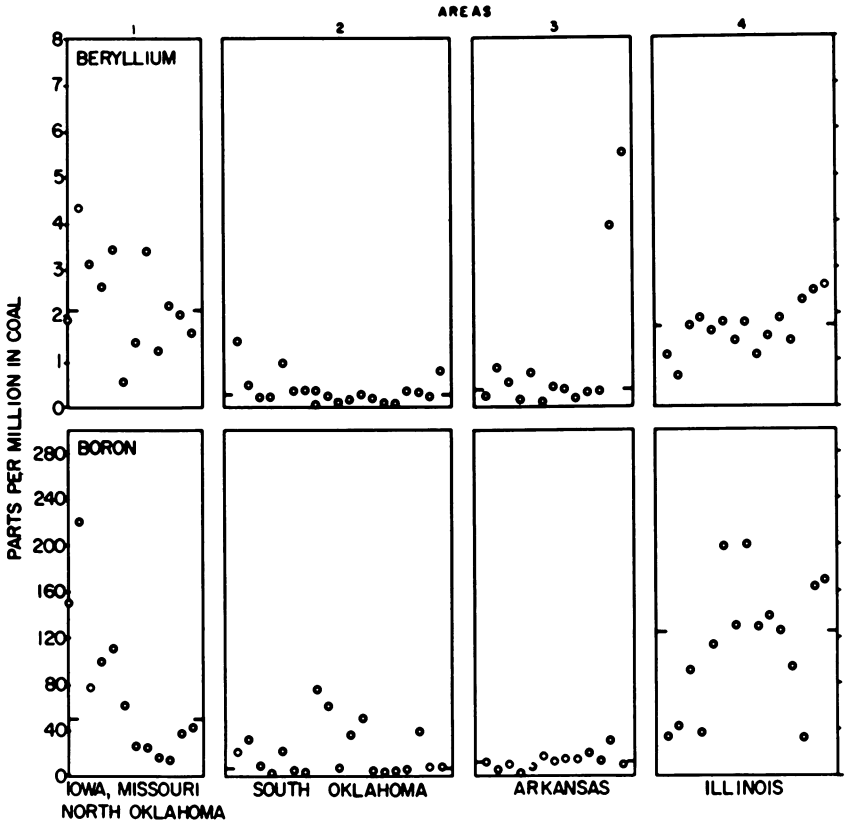

Figure 7. Distribution of beryllium and boron. Tick marks indicate medians for the elements in the samples

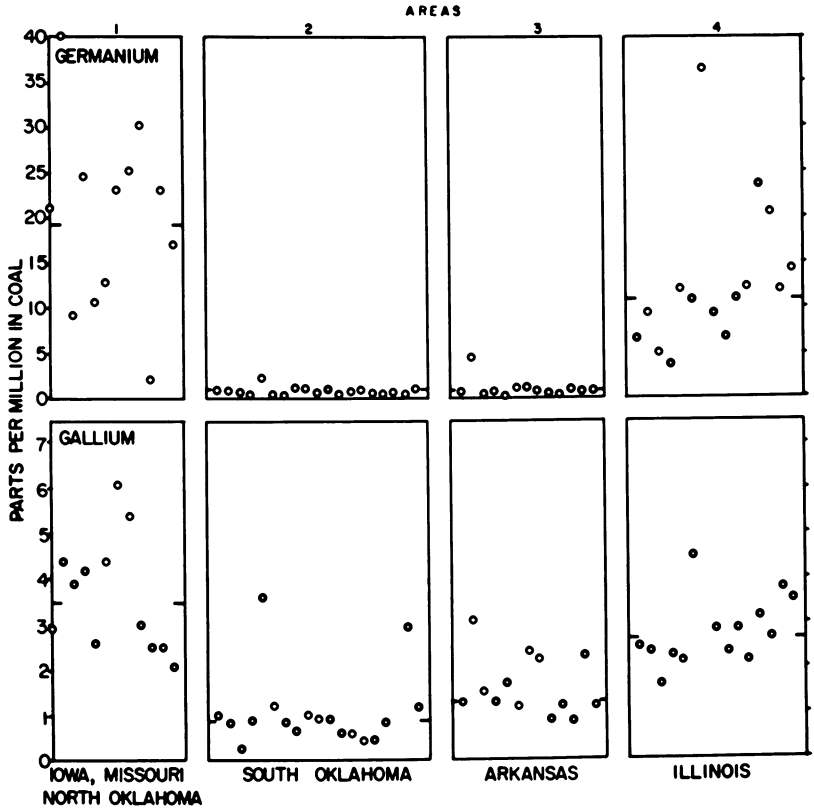

Figure 8. Distribution of germanium and gallium. Tick marks indicate medians for the elements in the samples

Table I. Comparison of Weathered and Unweathered Samples[a]

Element	*Weathered Samples (4)*	*Unweathered Samples (32)*	*Ratio, Weathered/ Unweathered*
Beryllium	13	0.64	20.3
Boron	47	18	2.6
Titanium	1700	250	6.8
Vanadium	70	17	4.1
Chromium	64	12	5.3
Cobalt	15	4.4	3.4
Nickel	95	11	8.6
Copper	72	11	6.5
Gallium	9.1	1.4	6.5
Germanium	1.6	1.0	1.6
Molybdenum	3.4	2.6	1.3
Yttrium	110	7.2	15.3
Lanthanum	93	7.2	13.0

[a] Data are in p.p.m. in coal

Publication Date: January 1, 1966 | doi: 10.1021/ba-1966-0055.ch014

However, the author believes that the metals in the weathered samples are held in ion exchange positions or as simple salts of the organic matter rather than by chelation, and that the accumulation of these abnormally large amounts of most of the elements was synchronous with the weathing process. Data from these samples suggest that basing minor element distribution in carbonaceous rocks on data from weathering samples could lead to erroneous interpretation.

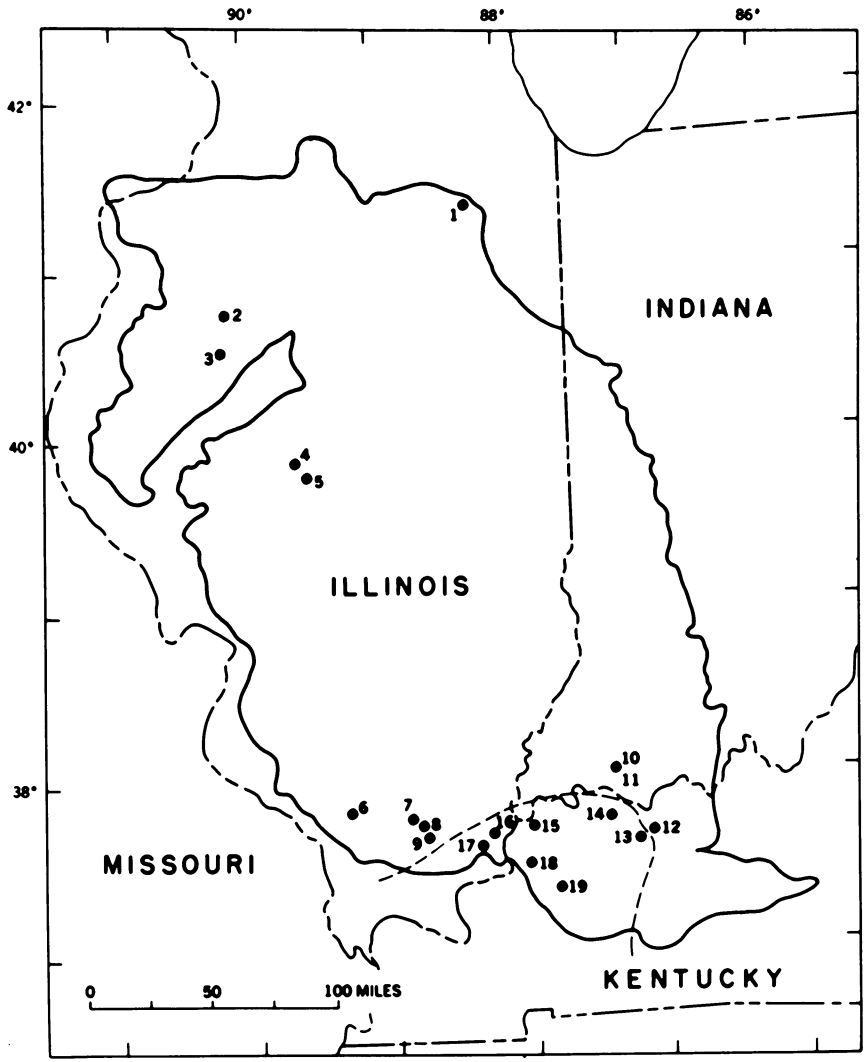

Figure 9. Distribution of samples of bed No. 5 of Illinois and correlatives of bed No. V of Indiana and bed No. 9 of western Kentucky. Dashed line delineates samples with large amounts of vanadium

Publication Date: January 1, 1966 | doi: 10.1021/ba-1966-0055.ch014

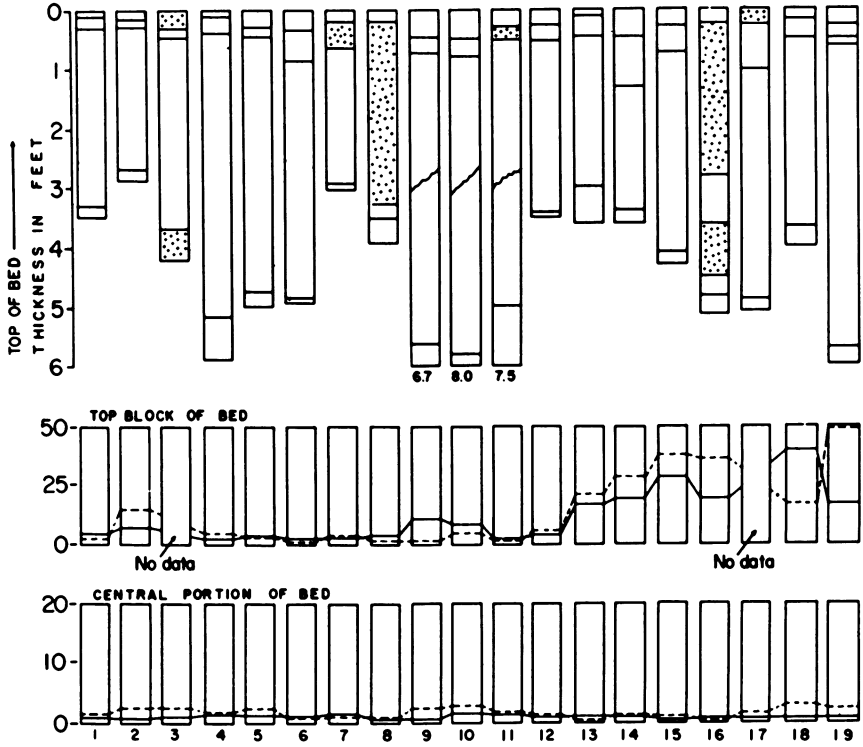

Figure 10. Vanadium/chromium and vanadium/nickel ratios of the top and central portions of the bed. Numbers 1–9 indicate samples taken from localities shown in Figure 9. Solid line are vanadium/chromium ratios, dashed line vanadium/nickel ratios. Stipled areas of columnar samples were not analyzed

Table II. Vanadium, Chromium, and of Illinois and Its Correlatives in

Columnar Samples	*1*	*2*	*3*	*4*	*5*	*6*	*7*	*8*	*9*
Block 1	44	170	nd[c]	96	22	28	21	79	44
Block 2	4.8	88	10	24	88	14	nd	nd	22
Central part	14	14	13	12	16	13	14	11	16
Last block	68	34	nd	36	68	58	100	31	130
Block 1	23	60	nd	92	14	32	21	74	11
Block 2	5.3	50	10	18	53	13	nd	nd	33
Central part	16	19	19	10	15	14	14	34	21
Last block	31	27	nd	16	42	31	38	24	29
Block 1	21	12	nd	18	8.6	27	6.1	84	22
Block 2	5.3	5.0	5.0	5.8	16	2.3	nd	nd	6.5
Central part	8.9	6.6	5.6	3.3	7.7	21	14	23	7
Last block	38	8.5	nd	14	45	70	40	51	85

[a] Data in p.p.m. in coal
[b] Block 3
[c] nd = not determined

Publication Date: January 1, 1966 | doi: 10.1021/ba-1966-0055.ch014

Vanadium-Rich Coals in the Eastern Interior Region

An unusual concentration of vanadium was found in the upper part of bed 9 of western Kentucky and in two samples of its correlative bed 5 of Illinois (*10*). The distribution of the columnar samples from this bed is shown in Figure 9. The dashed line delineates areas where samples contain high vanadium values.

Figure 10 graphically shows data for the columnar samples of coal bed 5 of Illinois and its correlative in Indiana and Kentucky. The thicknesses of the beds at the localities sampled and of the top (block 1), the adjacent blocks, and the bottom blocks are also shown. The sizes of the blocks of the central portions of the columns are not shown. Data for vanadium, chromium, and nickel from these sections of the bed are shown in Table II. Samples 1–12 contain normal amounts of vanadium; samples 13–19 contain large amounts of vanadium in the top part.

Some parts of several columnar samples were not analyzed including the top blocks of samples 3 and 17. In sample 19, block 1 and block 2 contain 2080 p.p.m. vanadium; hence, block 3 is used for comparison with block 1 instead of block 2.

It is apparent from the graphs that vanadium is enriched relative to chromium and nickel in the top part of columnar samples 13–19. Enrichment in some of the other columns also is present in the top part relative to the central portion of bed, but not to the same extent. Chromium is also higher in these samples while nickel is not. No significant enrichment was found for the other elements studied.

Figure 11 shows the ratios of vanadium, chromium, and nickel in the top (block 1) compared with the central parts of the columns. Vanadium enrichment again is apparent. The median for the vanadium content of samples 13–19 (M_2) compared with that of samples 1–12 (M_1) illustrates the differences in enrichment of the three elements.

Nickel Contents of Coal Samples from Bed 5 Indiana and Western Kentucky[a]

10	*11*	*12*	*13*	*14*	*15*	*16*	*17*	*18*	*19*
33	48	28	950	580	1050	1600	nd	570	2080
32	nd	31	110	13	22	nd	140	21	8.4[b]
38	14	16	11	20	15	6.7	12	9	13
13	130	220	21	73	50	15	37	27	26
11	15	18	150	78	92	213	nd	36	310
32	nd	21	25	9.1	15	nd	9.9	21	10[b]
28	9.2	20	8.8	17	19	8.5	14	11	21
13	41	260	42	37	11	17	38	55	130
7.6	9.5	4.6	47	21	28	45	nd	36	42
9.6	nd	9.4	8.9	3.6	3.7	nd	2.4	5.1	6.3
14	8.7	13	36	18	12	9.5	6.6	3.0	6.1
6.7	24	73	32	55	38	17	70	17	32

Publication Date: January 1, 1966 | doi: 10.1021/ba-1966-0055.ch014

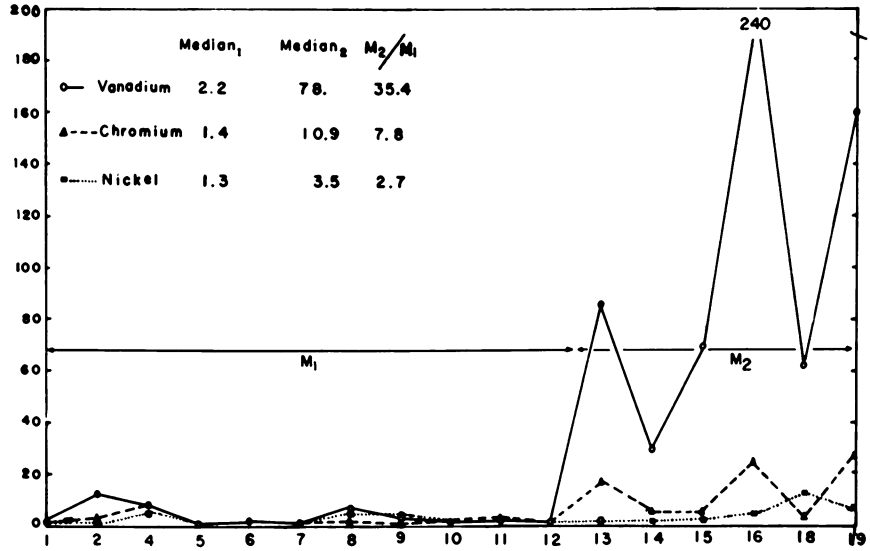

Figure 11. Comparison of the preferential enrichment of vanadium over chromium and nickel. Samples 1–12 are not enriched; samples 13–19 are enriched. Figures show ratios of the elemental content of the top block compared to that of the central portions of the beds.

The vanadium enrichment in the top part of the bed in the area shown cannot be explained with certainty. One of the geological factors to be considered is the apparently thicker shale sequence that overlies the coal bed in Kentucky. Generally in Illinois (*2*), the thickness of the overlying shale ranges from 1 to 5 feet. All this shale is black marine shale. In Kentucky the shale sequence ranges to 50 feet (*1*); however, only a small part of it is black shale. It is not known whether this thick shale sequence in Kentucky correlates with the outline of the enriched vanadium zone shown in Figure 9. If it does, the thicker shale sequence in Kentucky may indicate an initial local downwarp before the sea transgressed over the rest of the region. If such were the case, the more soluble portions of the coal-forming swamp lying north and east of the enriched zone might have been washed into the enriched zone and incorporated into the upper part of the coal bed. If the preceding were true, then other elements having similar transport characteristics and solubilities as shown in the distribution patterns, such as chromium, cobalt, nickel, copper, and titanium, should show a comparable enrichment. This, however, did not occur. Thus this process by itself could not account for the singular enrichment of vanadium.

Analyses of five specific gravity fractions of block 1 of columnar sample 15 and of block 2 of sample 18 gave the data shown in Figure 12. Only those elements pertinent to this problem are shown. The cumulative curves for vanadium, copper, and gallium show a large degree of inorganic association in the top or enriched block and a completely organic association in the unenriched block 2. Nickel shows a dominant organic association in both blocks.

Publication Date: January 1, 1966 | doi: 10.1021/ba-1966-0055.ch014

Chromium shows a small increase in organic association in the unenriched block. The enriched block 1 of column 15 contained abundant pyrite, and many pyritized fossils were found immediately overlying the coal. This suggests a large degree of anaerobic sulfate-reducing bacterial activity. As suggested in the preceding chapter (9), vanadium, gallium, and copper could initially have been accumulated as sulfides in this enriched block and in all the enriched top parts of this bed. Nickel and cobalt could not form sulfides in aqueous acid environments and were transported through the enriched area. Gallium was not enriched similar to vanadium because of its near-source depletion. Copper is not enriched because of its different transport characteristics compared with those of vanadium. Vanadium shows a significant southerly increase in Illinois and may have reached a normal enrichment peak in

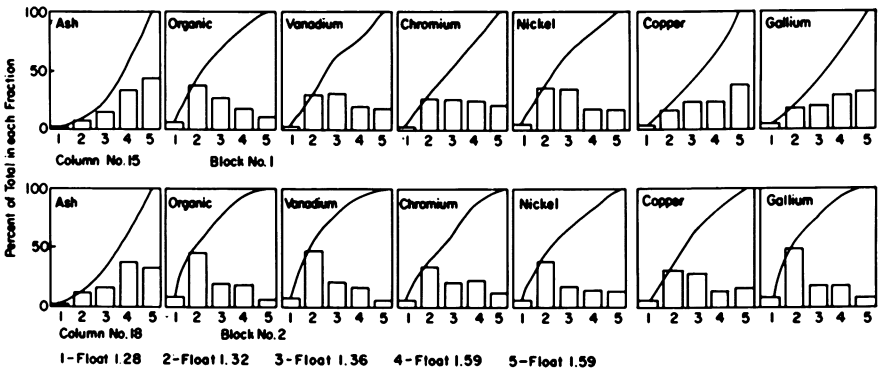

Figure 12. Comparison of the elements in various specific gravity fraction of the top part of bed 9.

the enriched area. Copper, on the other hand, shows a relatively uniform distribution throughout Illinois and into the Oklahoma-Arkansas Basin. Thus, a combination of sulfide precipitation and washing-in of the vanadium-rich humic materials of the adjacent areas into the vanadium-rich zone shown in Figure 9 could account for the high vanadium values found in these coals.

Another form of emplacement which may be considered is that the vanadium was originally present as complexes in the oil of the overlying black shales, and upon compaction of the shale these vanadium-rich components were squeezed into the underlying, more porous coaly substances. However, vanadium should then show a dominant organic association in the sink-float data. Furthermore, elements which are frequently found associated with vanadium in petroleum, such as nickel, copper, and cobalt, should also be enriched; however, they are not. Moreover, oil-bearing black shales of comparable thickness are present throughout Illinois, but there is no comparable vanadium enrichment of the underlying coals. The above-mentioned observations do not support the possibility that the vanadium in the vanadium-enriched coals was derived from the overlying black shales.

Publication Date: January 1, 1966 | doi: 10.1021/ba-1966-0055.ch014

Summary

Three principal findings are reported here.

(1) Metals forming smaller more highly charged ions, which generally form more stable bonds, are concentrated in near-source areas of a coal basin and are depleted elsewhere.

(2) The weathering of coal samples can produce anomalous minor-element concentrations.

(3) Vanadium is preferentially enriched in Kentucky bed 9 and its correlative Illinois bed 5 in a small part of the southern part of the basin.

Other discussions in this paper are largely speculative because of lack of data on the behavior of these elements in biogeochemical systems. Complications result from the fact that the exact geological setting of the depositional basins and the extent of tectonic influence, as suggested for the enriched vanadium samples, are unknown. For example, how close were the samples high in beryllium, germanium, boron, and gallium to the northern edge of the original depositional basin? Also, what would be the maximum concentration of these elements in such an area? At the other end of the basin do the elements with greater transport characteristics concentrate at different distances? If so, what are the chemical mechanisms for their differential accumulations? The yttrium and lanthanum fractionation may be caused by the stability of their chelates; generally yttrium forms more stable chelates than does lanthanum; or the fractionation may be caused by differences in the resistance to weathering and abrasion of the minerals in which these elements are found. Of prime importance is the need for experimental work on biogeochemical systems involving the first transition series and nearby metals.

Literature Cited

(1) Kehn, Thomas M., personal communication.
(2) Lamar, J. E., Armon, W. J., Simon, J. A., *Illinois State Geol. Survey Circ.* **208,** 13 (1956).
(3) McDaniel, G., "Tulsa Geological Society and Fort Smith Geological Society Guidebook," p. 68, 1961.
(4) Potter, P. E., *Illinois State Geol. Survey Circ.* **339** (1962).
(5) Potter, P. E., *Illinois State Geol. Survey Rept. of Invest.* **217** (1963).
(6) Potter, P. E., Siever, R., *J. Geology* **64,** 242 (1956).
(7) Schuchert, C., "Atlas of Paleogeographic Maps of North America," Fig. 51, John Wiley and Sons, Inc., New York, 1955.
(8) Stadnichenko, T. M., Zubovic, P., Sheffey, N. B., *U. S. Geol. Survey Bull.* **1084 K.** (1961).
(9) Zubovic, P., ADVAN. CHEM. SER. No. **55,** 221 (1966).
(10) Zubovic, P., Stadnichenko, T. M., Sheffey, N. B., *U. S. Geol. Survey Profess. Papers* **400 B,** B84 (1960).
(11) Zubovic, P., Stadnichenko, T. M., Sheffey, N. B., *U. S. Geol. Survey Bull.* **1117-B** (in press).
(12) Zubovic, P., Sheffey, N. B., Stadnichenko, T. M., *U. S. Geol. Survey Bull.* **1117-C** (in press).

RECEIVED January 25, 1965.

Discussion

Edwin F. Koppe. With reference to the vanadium-rich area of coal No. 9 in the Kentucky area, would you care to comment on the character of the roof sediments?

Peter Zubovic. The coal is overlain by a black shale sequence which, in places, contains abundant pyritized marine fossils. Above the black shale there generally is a gray shale sequence. The thickness of the two units varies from place to place. The total thickness ranges from about 3–50 feet. I do not know the mineralogy of the shale. I suspect that there is a relation between the total thickness of the shale and the vanadium content of the coal. Parts of this area are being mapped at present, and in the near future we expect to have the data necessary to show if this suggested relation is valid.

Donald R. Baker. It seems to me that your results on the distribution of boron and gallium have important implications for the work of others who have concluded that these elements are depositional environmental indications. I wonder if the *enrichment* of these elements in nonmarine rocks of Pennsylvanian age in the eastern U.S. may simply reflect their *proximity* to the source area and not have any real bearing on the depositional environment. And conversely, the lower content of these elements reported for *marine* shales may be caused by deposition of these facies in areas far removed from the source areas. What is your opinion?

Mr. Zubovic. I feel that the relations shown by boron and gallium in their distribution in coal would be operative in these studies you mention. Depositional environment is important in that organic matter is needed in the near-source nonmarine rocks in order to entrap these elements as well as germanium and beryllium. The other elements, such as vanadium and chromium, should be found more uniformly distributed.

Glenn C. Soth. Was manganese distribution studied? I have encountered an Oklahoma coal (medium volatile) with manganese high enough to interfere with the usual Eschka sulfur determination.

Mr. Zubovic. We have not studied manganese in any of the coals.

Publication Date: January 1, 1966 | doi: 10.1021/ba-1966-0055.ch014

In Coal Science; Gould, P.; Advances in Chemistry; American Chemical Society: Washington, DC, 1966.

15

A Microscopic Study of the Optical Anisotropy of Some Cokes Near Their Resolidification Temperatures

SIMONE PREGERMAIN and JACQUES DEDUIT*

Centre d'Etudes et Recherches des Charbonnages de France
Verneuil-en-Halatte, Oise, France

Publication Date: January 1, 1966 | doi: 10.1021/ba-1966-0055.ch015

A comparative study has been made by optical and electron microscopy of the anisotropic texture of several cokes from caking coals and pitches carbonized near their resolidification temperature. A simple technique made it possible to examine, by both methods, the same area of each sample and to identify the corresponding zones of the two very similar images. The anisotropy observed in polarized light appears in electron microscopy as differences in contrast resulting not from inequalities in electron absorption, but, as revealed by microdiffraction and dark field examinations, from diffraction phenomena depending on the general orientation of the carbon layers within each anisotropic area.

Cokes prepared from caking coals and pitches with a low oxygen content have an anisotropic texture. The anisotropy, often observed under a polarizing microscope either by transmitted (*14*, *15*) or reflected light (*1*), appears at a temperature slightly below that marking the end of the plastic zone (*9*); then the texture solidifies, and the appearance visible through the microscope undergoes little further change while carbonization takes place.

The microscopic image shows a juxtaposition of differently orientated areas whose sizes, varying between a few microns and several tens of microns, are associated particularly with the elementary composition of the initial carbonaceous material (*4*, *18*, *19*). The formation of a texture of this type, often called "a mosaic structure," can be compared (*20*) to the crystallization of a supersaturated solution; areas, each characterized by a definite orientation, develop from nuclei up to the total "consumption" of the isotropic material surrounding them.

* Paper presented by A. Ladam

In Coal Science; Given, P.;
Advances in Chemistry; American Chemical Society: Washington, DC, 1966.

The texture observed on the scale of the micron is the result of an underlying structure which appeared to be all the more worthy of study since the transformations up to the end of the zone of plasticity largely determine the physicochemical properties of the cokes. Thus the important problem of the texture of cokes and industrial carbons is stated.

We shall first examine the microscopic techniques which allowed us to study these transformations and to show the striking analogy between the images obtained by optical microscopy in polarized light and by electron microscopy with ultrathin sections, despite the difference of the absorption mechanisms of light and electrons. Once this analogy was established, we sought to use electron microscopy and electron microdiffraction to learn more about the texture and structure of the anisotropic areas.

Publication Date: January 1, 1966 | doi: 10.1021/ba-1966-0055.ch015

Experimental Techniques

Raw Materials and Their Carbonization. The original materials are vitrain-enriched fractions of three different rank caking coals (Table I) and two pitches of different types (Table II), from which certain mixtures have been prepared.

Table I. Analysis of Original Coals

Name of Coal and International Class	*Proximate Analysis*		*Ultimate Analysis (daf)*[a]					*Resolidification Temperature °C.*
	Ash (dry basis) %	*Volatile Matter % (daf)*[a]	*C %*	*H %*	*O %*	*N %*	*S %*	
Camphausen (634)	2.2	34.9	86.3	5.4	5.6	1.1	0.5	475
Dourges (435)	2.0	25.0	89.1	5.1	4.1	1.5	0.6	500
Drocourt (434)	3.0	21.0	90.6	4.5	3.3	1.5	0.6	495

[a] daf: on a dry and ash free basis

Table II

	Proximate Analysis		*Ultimate Analysis (daf)*			*Softening Temperature KS*[a] *°C.*	*Resolidification Temperature °C.*
	Fixed Carbon %	*Ash %*	*C %*	*H %*	*O %*		
H.T. Pitch	43	0.4	92.9	4.6	1.1	88	533
L.T. Pitch	20	0.7	81.6	6.8	9.6	98	455

[a] KS: Kraemer-Sarnow method of determination

The first pitch—a low temperature (l.t.) pitch—with a high content of oxygen and paraffinic components, is produced by carbonizing, in a fluidized bed at 480°C., a high volatile bituminous coal (international class 711), giving a nongraphitizing coke at a high temperature. The second pitch—a high temperature (h.t.) pitch—is intended for electrodes, with a high carbon content and low oxygen content, of essentially aromatic composition, producing a

graphitizing coke. Mixtures of the two pitches in various proportions provide carbons of intermediate properties (*8*).

The coals and pitches or their mixtures were carbonized up to temperatures around the resolidification temperature, the test being stopped as the temperature reaches its maximum value; the rate of heating adopted was 3°C. $min.^{-1}$ for coals and 0.5°C. $min.^{-1}$ for pitches only in order to avoid, in the latter case, an excessive foaming in the product.

Microscopic Techniques. The samples were embedded in an epoxy resin (Epon 812) and the blocks obtained were cut by a Porter-Blum microtome equipped with a diamond knife. The thin sections were examined under an electron microscope while the corresponding surface of the block was observed directly in white light by means of a metallographic polarizing microscope. The cut surfaces have a fairly small area—of the order of 0.01 sq. mm.—so that observation with an optical microscope poses a problem which could be resolved as follows. The sample, attached by means of a rod to the cup of a metal spherical joint, whose ball is fixed and rests on the microscope stage, is positioned so that the center of rotation of the mobile part of the joint coincides approximately with the center of the area to be observed. The whole is then adjusted so that the optical axis of the microscope passes as close as possible to that center. Hence, it is possible to change the orientation of the area with considerable angular deflection, without its leaving the field of view.

Publication Date: January 1, 1966 | doi: 10.1021/ba-1966-0055.ch015

Results

Under the optical microscope the texture of products derived from the three coals studied show an anisotropy of the type which already has been described for similar materials (*1*, *4*, *9*). The texture of the l.t. pitch coke is entirely isotropic, whereas the h.t. pitch coke is characterized by a pronounced anisotropy in bands. The anisotropy of the carbonization products of mixtures of l.t. and h.t. pitches varies linearly as a function of the composition of the mixture (*8*).

The analogy between the optical and electronic images of the same area is brought out clearly by comparing Figures 1a and 2b relative to the 500°C. semicoke of the mixture of 75% l.t. pitch and 25% h.t. pitch. The optical photographs were taken in polarized light without an analyzer (Figure 1a) and between crossed nicols (Figure 1b); the electronic ones were obtained in bright (Figure 2a) and dark fields (Figure 2b). Correlation between the optical and electronic images is facilitated by the heterogeneity of the field examined, and the dimensions of the areas in the central zone are very suitable for the two techniques of observation. There is a particularly clear analogy between Figures 1a and 2b; the optical image between crossed nicols (Figure 2a) is more difficult to compare with the other images; the tangled black zones and lines which appear in it, owing to the extinction of vibrations at right angles to the direction of the analyzer, are not directly superimposed on the geometry of the areas as designed on the other three photographs.

The next figures represent some of the most typical aspects observed by electron microscopy. The grainy texture of the Dourges semicoke (Figure 3) and the fibrous texture of the Drocourt semicoke (Figure 4) are already known by examination under the optical microscope. Figures 5 and 6 show the importance of observing in dark field, particularly for studying a product with a fine granular structure (Camphausen); Figures 7a and b show a piece of

fusain adhering to a very fine granular area, the surrounding substance being formed of more extensive areas. The transition between zones of different textures appears in Figures 6a and b: the sizes of the finest "grains" go down to a few hundred A, while the largest reach several tenths of a micron; resolution of these areas is therefore beyond the scope of optical microscopy.

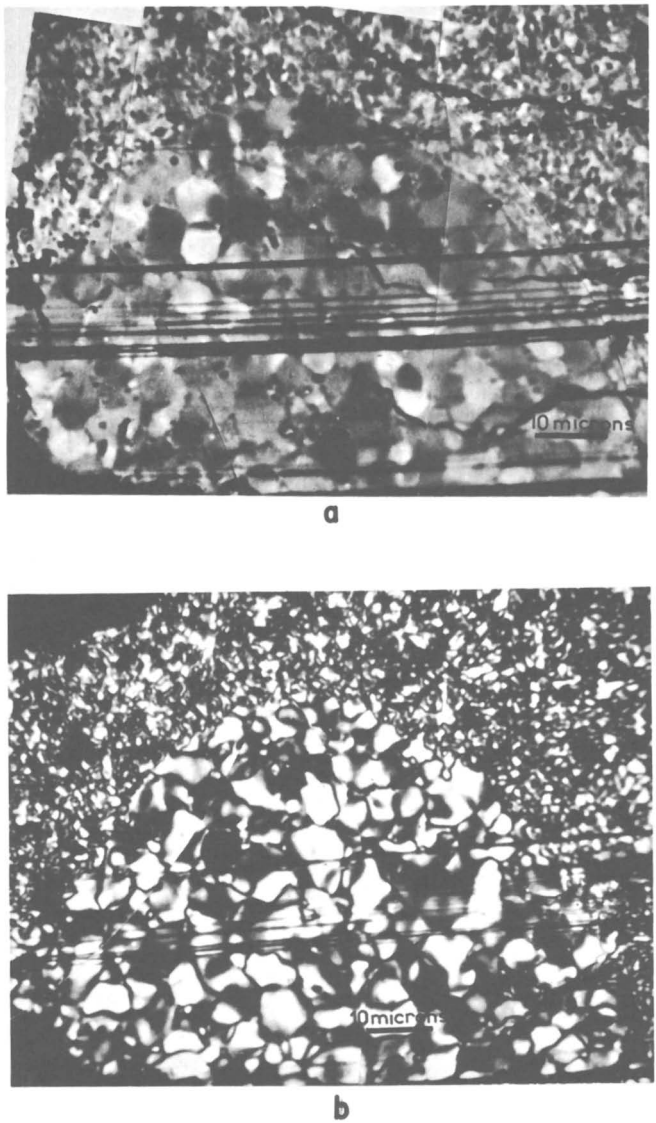

Figure 1. Pitch coke 500°C., 75% l.t., optical microscopy by reflection on block from microtome; × 900 photomontage; (a) polarized light without analyzer; (b) optical photos taken between crossed nicols

Publication Date: January 1, 1966 | doi: 10.1021/ba-1966-0055.ch015

Discussion

Optical Microscopy. The reflectance of an anisotropic surface in normal incidence depends on the degree of polarization of the light and the crystalline orientation of the surface in relation to the light vibrations. In polarized light and in the case of an opaque birefractive crystal, whose absorption coefficients

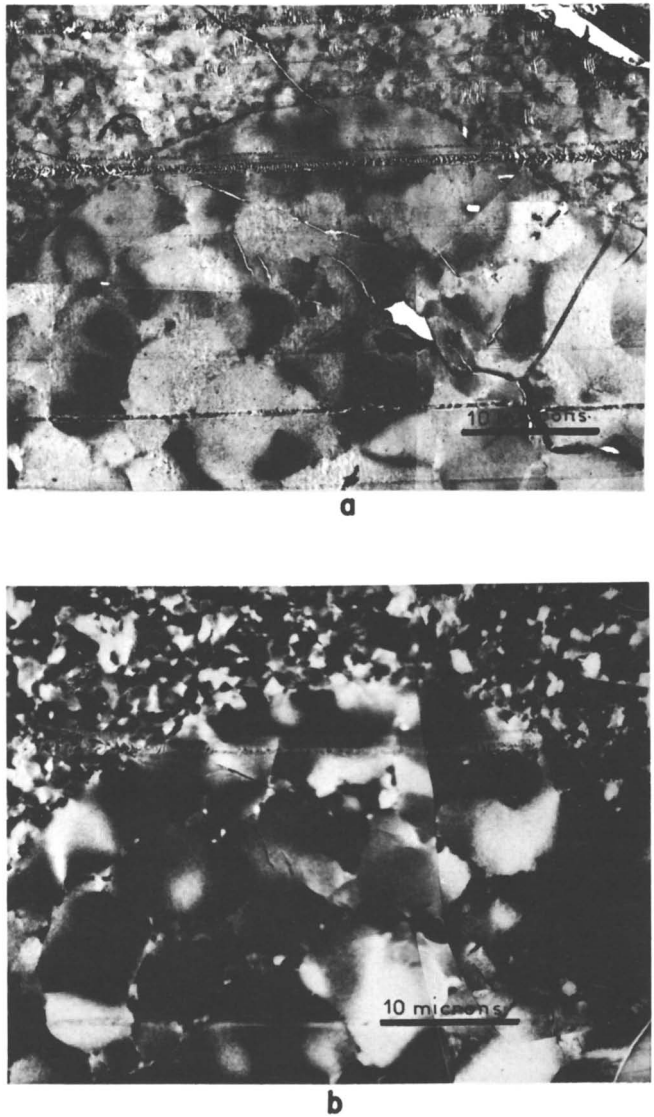

Figure 2. Pitch coke 500°C., 75% l.t., electron microscopy on a section from the block observed by optical microscopy; × 1800 photomontage; (a) in bright field; (b) in dark field

Figure 3. Dourges coke 525°C., section observed in bright field; anisotropy of grainy type; × 1800

Figure 4. Drocourt coke 500°C., section observed in bright field; anisotropy of fibrous type; × 2718

k_1 and k_2 are small compared with the refractive indices n_1 and n_2, there are two privileged orthogonal directions of vibration. If the polarization plane of the incident light forms an angle, α, with one of these two directions, the reflectance, R, will then follow the equation:

$$R = \frac{(n_1 - n)^2 + k_1^2}{(n_1 + n)^2 + k_1^2} \cos^2 \alpha + \frac{(n_2 - n)^2 + k_2^2}{(n_2 + n)^2 + k_2^2} \sin^2 \alpha$$

Publication Date: January 1, 1966 | doi: 10.1021/ba-1966-0055.ch015

n being the index of the medium surrounding the crystal (air or immersion liquid as the case may be).

If the stage is rotated through one complete turn, the reflectance at each point will pass through two maxima and two minima, the extreme values corresponding to $\cos \alpha = 0$ and $\sin \alpha = 0$, respectively.

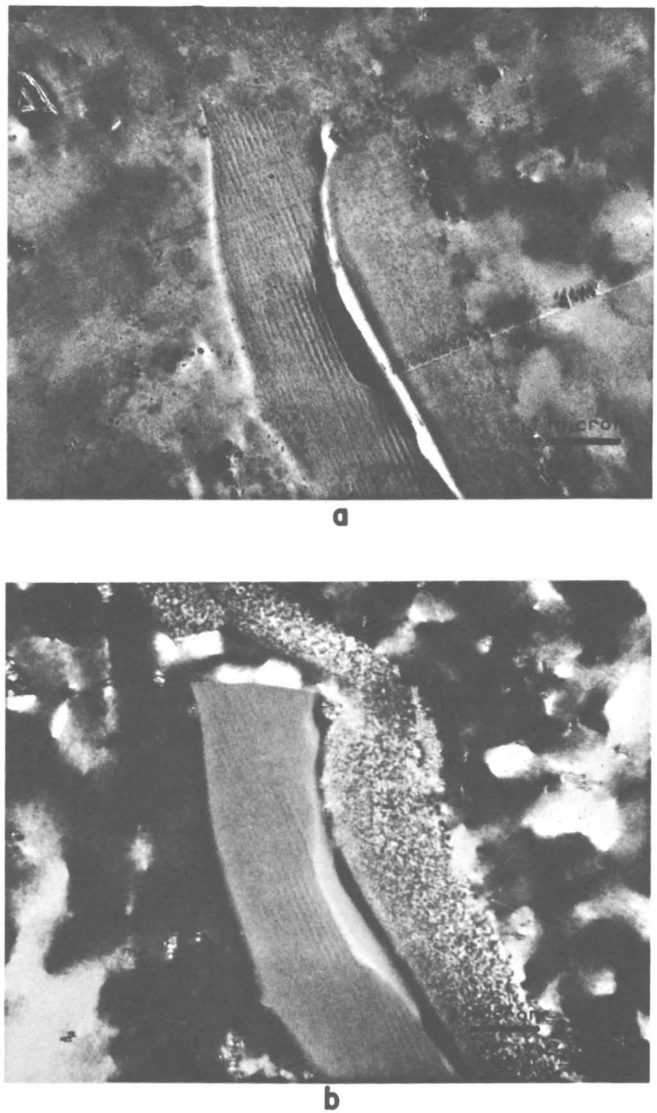

Figure 5. Camphausen coke 500°C.; (a) section observed in bright field; (b) section observed in dark field; anisotropy of granular type; fragment of fusain to which a very fine granular zone is attached; × 8520

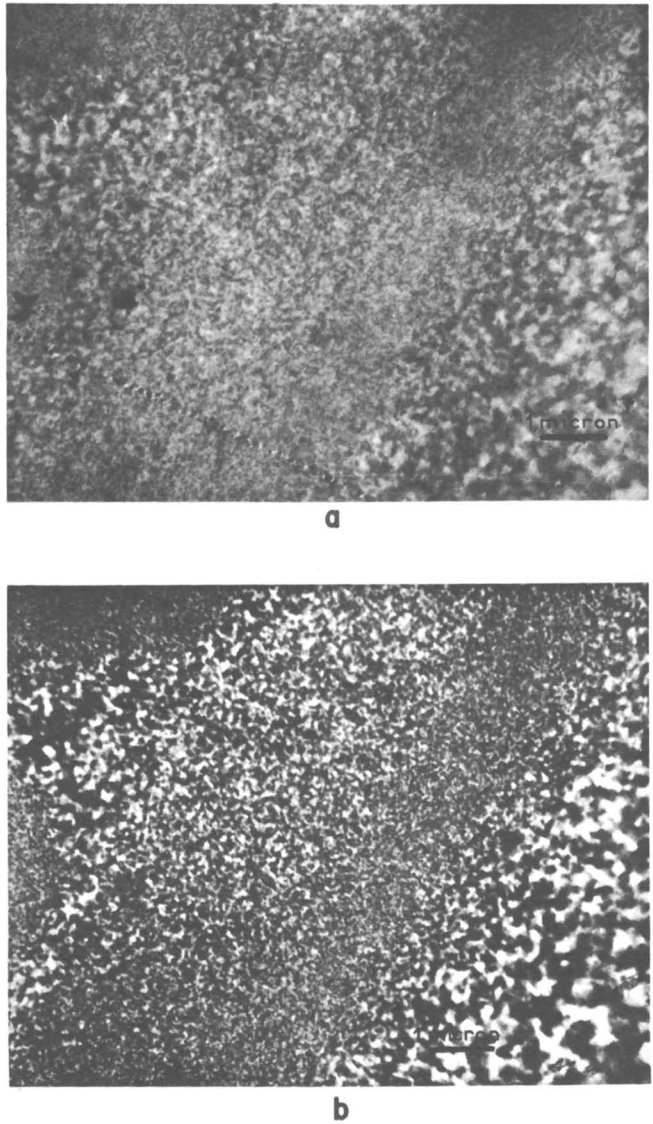

Figure 6. Camphausen coke 525°C.; (a) section observed in bright field; (b) in dark field; transitions between more or less fine granular zones; × 8520

In the case of objectives with a large numerical aperture, account must be taken also of the oblique reflection, and the reflectance will then also depend on the angles of incidence (*7*, *10*).

The samples of coals and pitches carbonized up to about 500°C. possess relatively unorganized structures. The carbon atoms are arranged in layers and form large, aromatic-type molecules, approximately plane and including

Publication Date: January 1, 1966 | doi: 10.1021/ba-1966-0055.ch015

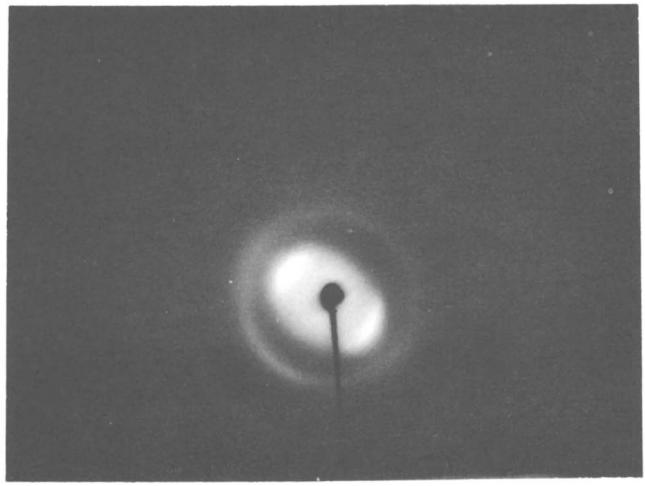

Figure 7. Microdiffraction on pitch coke 500°C., 50% l.t.

particularly oxygen and hydrogen. These layers, stacked roughly parallel to one another, correspond to a probable molecular structure which is still very far from that of graphite but which is nevertheless anisotropic; the reflectance varies as a function of the general orientation of the layers in relation to the direction of the light vibrations. Careful examination of Figure 1a (polarized light without analyzer) shows, too, that despite their fairly marked individualization, the reflectance is not uniform within the areas.

This is confirmed by observation between crossed nicols which shows a reticulation of more or less fine black fringes, some of which coincide approximately with the contours of the areas which appear (for example, on Figure 1a). The rotation of the stage of the microscope sets up a rolling extinction within the various areas. The theory of reflection of polarized light on an isotropic surface hardly applies to interpreting quantitatively the phenomena observed on materials whose structure is so little known. However, the observation of the black fringes gives information as to the orientation of the stacks of carbon layers in relation to the direction of incidence of vibration. It thus appears that the orientation within an area, although it may show considerable local variations, can be represented on the whole by an average direction which is fairly variable from one area to another.

Electron Microscopy. To explain the contrast observed on electron micrographs, the first idea which suggested itself was of thickness differences according to the areas. Lacking accurate methods of measuring the thickness of the sections made it difficult to check this hypothesis. Comparison with photographs of several carbon blacks with particle sizes varying between 200 and 1000A., however, showed that differences in thickness would have to reach an order of magnitude approaching the thickness of the section itself (300A. approximately) to account for the observed contrast. The absence of any noticeable relief on the shadowed preparations and the appearance of the

Publication Date: January 1, 1966 | doi: 10.1021/ba-1966-0055.ch015

images obtained in dark field by microdiffraction confirmed that the origin of the contrast could not be sought in thickness differences. The microdiffraction diagrams, obtained by selecting areas 1 micron in diameter, show either simply two circular rings, more or less diffuse, corresponding to interferences of 10 (2.11A.) and 11 (1.23A.), or, in addition to the two rings deformed into an ellipse, two much more intense arcs owing to the reflection 002 (Figure 7). The movement of the preparation in its plane without rotation, while observing the diagram, turns these two arcs progressively so that in some cases they disappear.

The reflections 10, 11, and 002 are characteristic of the carbonized products with a turbostratic structure—i.e., where the layers stacked roughly parallel are mutually disoriented; in this case diagrams proper to bidimensional structures are obtained, both by electron diffraction (*3*, *11*) and x-ray diffraction (*21*). The reciprocal lattice of a structure of this type in fact consists of a series of 001 points, arranged regularly along the C-axis, and straight lines *hk* parallel to this axis and situated on cylindrical surfaces. The low value of the associated wavelength makes it possible, in electron diffraction, to assume the Ewald sphere to be a plane which cuts the concentric cylinders 10 and 11 along two circles when the electron beam is parallel to the C-axis. Otherwise, the intersection consists of two ellipses.

The diagrams thus show, on the scale of the anisotropic areas, a fiber texture similar to that described by Kuroda (*2*, *13*) for petroleum cokes and Kakinoki (*12*) for thin films of carbon. The presence of the arcs 002, when the electron beam is not perpendicular to the C-axis, is caused by the fact that the texture axis shows some dispersion. This, however, does not prevent each area from having an average direction of the axis 002 different from that of the adjacent ones.

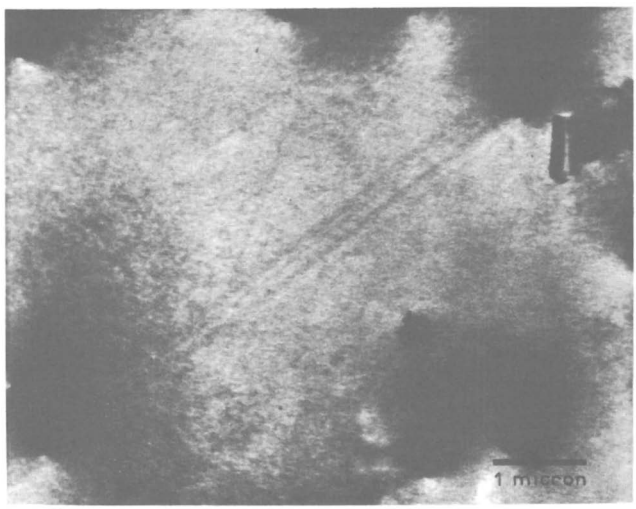

Figure 8. Micrograph of area from which Figure 7 was obtained; dark field; × 12,000

Publication Date: January 1, 1966 | doi: 10.1021/ba-1966-0055.ch015

The contrast observed on the micrographs results essentially from the variations in intensity of the electron beam diffracted by the 002 interferences as a function of the direction of the C-axis, both in bright field where the diffracted rays are stopped by the contrast diaphragm and in dark field where the image is formed by these rays alone. This result has been demonstrated theoretically, at least, in the case of elastic diffusion. It is found that the energy scattered in a given direction by a pregraphitic structure depends on the orientation of the lattice in relation to the incident beam (*17*).

Figure 8 represents a micrograph in dark field, with a relatively high magnification, of isolated areas obtained by selecting part of the 002 arc of the diffraction diagram by means of the objective diaphragm of 50 microns. The image is luminous enough to allow for correct focusing, but the resolving power of the microscope is very poor so that more interesting results are obtained at a low magnification, which allows, moreover, the build up of large areas of the sample by several successive photographs; the position of the contrast diaphragm was in this case determined empirically in order to obtain the maximum contrast over the whole field.

Comparing Figures 2a and b shows that the image in dark field gives many more details; it is possible, in particular, to distinguish the grain boundaries in the zone where the areas have much larger sizes. The variation in the illumination inside a given grain again confirms that the direction of the C-axis is not strictly constant.

Publication Date: January 1, 1966 | doi: 10.1021/ba-1966-0055.ch015

Conclusions

Observing the same area of a sample by optical and electron microscopy has almost always depended, to our knowledge, on the technique of replicas (*5*). The technique of thin sections, already applied to coals (*6*, *16*) and here extended to their carbonization products, nevertheless has great advantages. Apart from its greater resolving power, it makes it possible to study the diffraction diagram of a well-defined zone of the section whose image is known. The device for examining, under the optical microscope, the surface of the block from which the section has been cut is easy to handle and has proved quite satisfactory.

The results obtained and discussed above leave no doubt as to the origin of the optical anisotropy and electronic contrast owing to differences in the orientation of the stacks of carbon layers in relation to the incident beam. The existence of this fibrous structure is confirmed by the diffraction diagrams which showed, at the carbonization temperatures examined, a distribution of intensity similar to that found on cokes carbonized up to much higher temperatures and with better known structures.

It should, however, be emphasized that the transformations occurring up to the end of the plastic range lead to a structure which is already sufficiently organized not to be greatly affected by further carbonization. The graphitizability, which affects a number of physicochemical properties of the cokes (*8*), can therefore be judged at this stage which shows the basic interest of the most detailed knowledge possible of the structure of carbonaceous products at

a moment when their fundamental characteristics seem to be unaffected by any further influence.

Our objective was to attract attention to this essential point by indicating techniques which seem most suitable for improving this knowledge. We hope their intensive application to wider ranges of products, in particular to mixtures of pitches whose properties can be modified progressively by a judicious choice of their composition, will facilitate the theoretical interpretation of results which is still overshadowed by the descriptive aspect.

Literature Cited

(1) Abramski, C., Mackowsky, M. T., "Handbuch der Mikroskopie in der Technik," Vol. II, Pt. 1, p. 311, H. Freund, ed., Umschau Verlag, Frankfurt am Main, 1952.
(2) Akamatu, H., Kuroda H., *Proc. Conf. Carbon, 4th, Buffalo, 1959*, 355 (1960).
(3) Alexanian, C., *Compt. Rend.* **246,** 957 (1958).
(4) Alpern, B., *Brennstoff-Chem.* **37,** 194 (1956).
(5) Bradley, D. E., "Techniques for Electron Microscopy," p. 138, D. Kay, ed., Davis, Philadelphia, 1961.
(6) Brown, H. R., Taylor, G. H., *Nature* **193,** 1146 (1962).
(7) Capdecomme, L., Orcel, J., *Rev. Optique* **20,** 47 (1941).
(8) Chiche, P., Deduit, J., Durif, S., Pregermain, S., *J. Chim. Phys.* **62,** 382 (1965).
(9) Echterhoff, H., Mackowsky, M. T., *Glückauf* **96,** 618 (1960).
(10) Ehrenberg, H., "Handbuch der Mikroskopie in der Technik," Vol. I, Pt. 2, p. 89, H. Freund, ed., Umschau Verlag, Frankfurt am Main, 1960.
(11) Ergun, S., McCartney, J. T., *Science* **134,** 1620 (1961).
(12) Kakinoki, J., *Proc. Conf. Carbon, 5th, Univ. Park, Penna., 1961*, **2,** 499 (1963).
(13) Kuroda, K., *Bull. Chem. Soc. Japan* **32,** 728 (1959).
(14) Luther, H., Abel, O., Monostory, F., *Brennstoff-Chem.* **44,** 246 (1963).
(15) Marshall, C. E., *Fuel* **24,** 120 (1945).
(16) Pregermain, S., Guillemot, C., *Proc. Intern. Conf. Electron Microscopy, 4th*, 384 (1960).
(17) Renard, M., to be published.
(18) Schmidt, W. J., "Handbuch der Mikroskopie in der Technik," Vol. I, Pt. 1, p. 206, H. Freund, ed., Umschau Verlag, Frankfurt am Main, 1957.
(19) Stach, E., "Handbuch der Mikroskopie in der Technik," Vol. II, Pt. 1, p. 1, H. Freund, ed., Umschau Verlag, Frankfurt am Main, 1952.
(20) Taylor, G. H., *Fuel* **40,** 465 (1961).
(21) Warren, B. E., *Phys. Rev.* **59,** 693 (1941).

RECEIVED October 5, 1964. Partly financed by the High Authority of the European Coal and Steel Community.

Discussion*

Geoffrey H. Taylor. Can the authors interpret the granular structure to which they referred? Our work has shown that it is possible to observe domain structure in statistically isotropic coals using microdiffraction.

Simone Pregermain and Jacques Deduit. We think that it is possible, by microdiffraction, to find organized areas in a statistically isotropic coal. We do not know, however, any statistically isotropic cokes which are graphitizable. It may be asked whether the organization as shown in a statistically isotropic coal is pregraphitic.

* These comments were written after the Conference by the authors.

James Bayer. Would the authors define what they mean by ordered arrangement of micelles or degree of anistropy in semicokes, as related to rank and fluidity?

Drs. Pregermain and Deduit. It was not the object of our work to study the degree of anisotropy of semicokes as related to the rank and fluidity of coal. The change of anisotropy and the size of the orientated areas as a function of the rank were studied in CERCHAR by B. Alpern (*4*).

M.-Th. Mackowsky. Have you recognized a relation between rank and the size of the anisotropic domains? We believe that we have found an increase in the size of the anisotropic domains with rank and the degree of plasticity. In cokes from anisotropic coals we have two types of anisotropy, one related to the coal and the other formed in the plastic zone.

Drs. Pregermain and Deduit. Yes. The size of the areas as related to the rank of coal was studied by B. Alpern (*4*).

Publication Date: January 1, 1966 | doi: 10.1021/ba-1966-0055.ch015

Ultrafine Structures in Coal Components as Revealed by Electron Microscopy

J. T. McCARTNEY, H. J. O'DONNELL, and S. ERGUN

Bureau of Mines, U.S. Department of the Interior, Pittsburgh Coal Research Center, Pittsburgh, Pa.

Publication Date: January 1, 1966 | doi: 10.1021/ba-1966-0055.ch016

Electron microscopic studies have been made of several petrologic components of coals of different rank. The ultrathin specimens utilized, from 500 to 2000 A. thick, have been cut on a microtome with diamond knives. Structures in various size ranges have been observed. Some that have been resolved or partly resolved with optical microscopes have been more clearly and definitely characterized using the electron microscope. Ultrafine structures not resolvable optically have been revealed in electron micrographs. There appear to be two general ranges of these ultrafine structures in a number of components, one of the order of hundreds of angstroms, the other less than 100 angstroms. Particles having the general form of spheroids, curved cylinders, and round and polygonal platelets have been observed.

Perhaps the earliest attempt to study ultrafine structures in coal with an electron microscope was reported by Preston and Cuckow (*13*). However, they did little more than present a method for preparing thin-film replicas of coal cleavage surfaces and show electron micrographs of such replicas at low magnification. McCartney (*7*) presented electron micrographs of microspores and cell structures in vitrinite. These were taken of replicas of polished and etched coal surfaces. Waisman, Krivitzkii, and Krigman (*17*) showed micrographs of natural cleavage replicas (coal component unspecified). They observed pores as small as 200 A. in diameter and channels connecting the pores. Alpern and Pregermain (*1*) observed several kinds of fine granular structure in replicas of polished surfaces. The grains in a vitrinite were of the order of 200–300 A. in diameter, while those in the "ciment" surrounding spores (probably granular micrinite) were about 1000 A. A still different granularity, of unspecified size,

In Coal Science; Given, P.;
Advances in Chemistry; American Chemical Society: Washington, DC, 1966.

was observed in massive micrinite. Interpreting these granular structures was not attempted. Mackowsky and Nemetschek (*6*) subjected vitrite particles to intense bombardment by the electron beam and observed that the residues were porous aggregates of 100–300 A. particles. Electron diffraction patterns indicated that graphitization had occurred.

In 1959 Pregermain and Guillemot (*11*) first described a technique for cutting ultrathin sections of coals (500–2000 A.) using a microtome with a diamond knife. These proved to be good specimens for electron microscopy. Structures were observed in vitrinites consisting of grains ranging in average size from 250 A. in a lignite to 100 A. in a semianthracite. Such granular details were not seen in graphite fragments. A relation was supposed between these granular structures and the porous texture indicated by adsorption methods; however, no quantitative relation was traced. Pregermain (*12*) later reported studies of ultrathin sections of semicoke carbonized at 500°C. She observed in these sections granular structures similar to those in the raw coal and containing pores from 20 to 50 A. in diameter. These sizes were compared favorably with those obtained by Bond (*2*) in adsorption measurements. McCartney, Walline, and Ergun (*8*, *9*) prepared ultrathin sections by the method of Pregermain and presented electron micrographs of apparent cell structures and striations in vitrinites. It was cautioned that these might be preparation artifacts. Brown and Taylor (*3*) discussed this latter work and stated that the structures shown were definitely artifacts. They also pointed out the general improvement in resolution of familiar structures by electron microscopy.

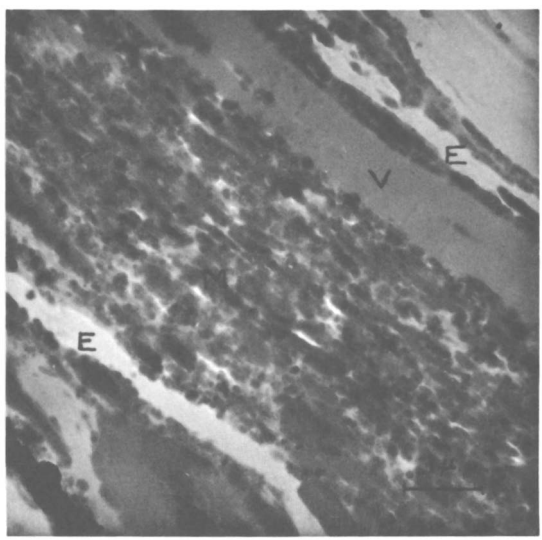

Figure 1. Electron micrograph of an ultrathin section of a dull attrital layer (durain) in a high volatile A bituminous (hvab) coal. V—vitrinite, E—exinite, M—granular micrinite. × 10,500

Publication Date: January 1, 1966 | doi: 10.1021/ba-1966-0055.ch016

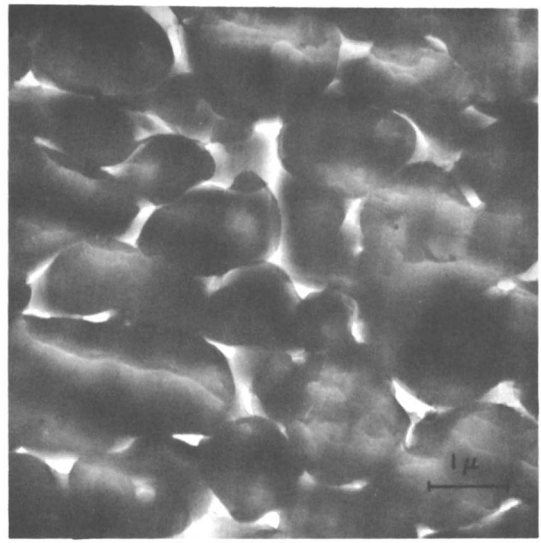

Figure 2. Electron micrograph of an ultrathin section of a megaspore from a Michigan spore coal. × 10,500

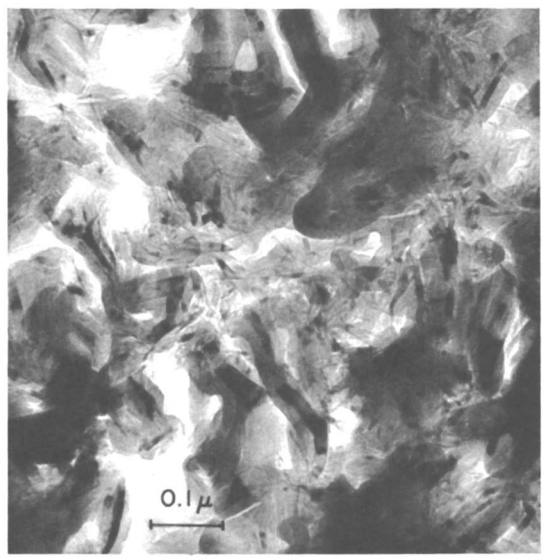

Figure 3. Electron micrograph of an ultrathin section of an apparent vitrain band in a meta-anthracite from Leoben, Austria. × 87,500

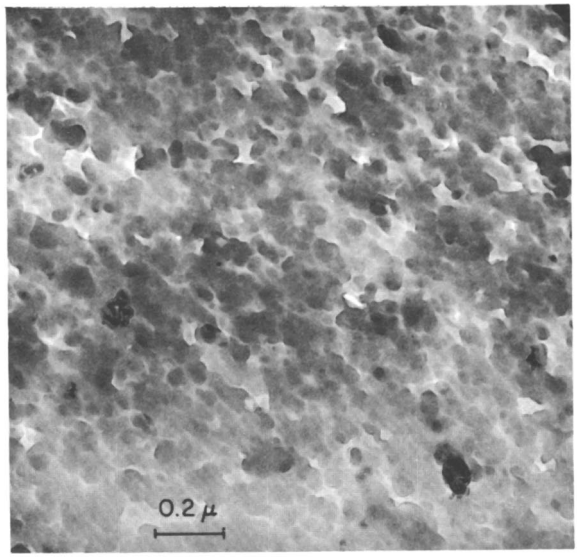

Figure 4. Electron micrograph of an ultrathin section of a resin inclusion in vitrain in a Wyoming subbituminous coal. × 42,000

Since the work reported by McCartney *et al.* (9), ultrathin sections of other, more heterogeneous components and mixtures of components of coals of different rank have been prepared and observed. Procedures for minimizing artifacts have been learned and followed, and experience in observation has led to avoiding obvious faults. These sections were often not as large and continuous as those of homogeneous vitrinites, but adequate areas were available for electron microscopy. Observations of these various components revealed ultrafine structures of different size and form. Some of the structures can be correlated with those deduced from other direct or indirect study techniques; others are unfamiliar and novel, and suggested interpretations are tentative.

Results and Discussion

The physical or petrographic components of coal are defined or described in various ways. In one system, which depends on microscopic observation, the principal components are called exinite, vitrinite, micrinite, and fusinite. Transparency of these in a thin section decreases in that order, whereas reflectance from polished surface increases in the same order. Vitrinite, the major component of most coals, occurs in bands or strands and is usually uniform in appearance, though sometimes shows cell structure; exinite consists of the remains of plant spores, pollen, and cuticles with characteristic shape; micrinite occurs in very fine granular form or massive structureless, irregular form; fusinite shows characteristic fibrous, cellular structure. Semifusinite is transitional between vitrinite and fusinite. On a macroscopic scale, vitrain and

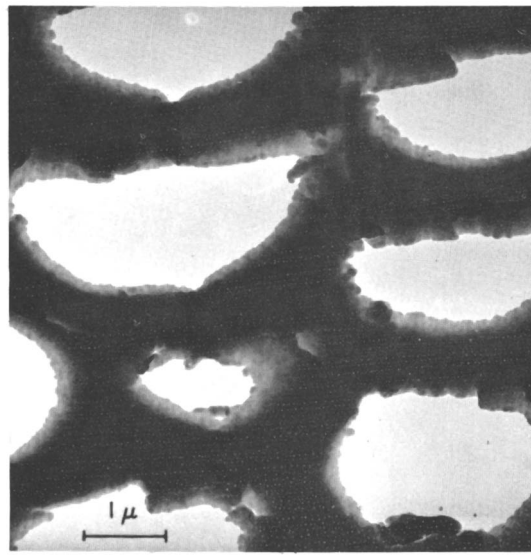

Figure 5. Electron micrograph of an ultrathin section of semifusinite (bogenstructure) in hvab coal. × 10,500

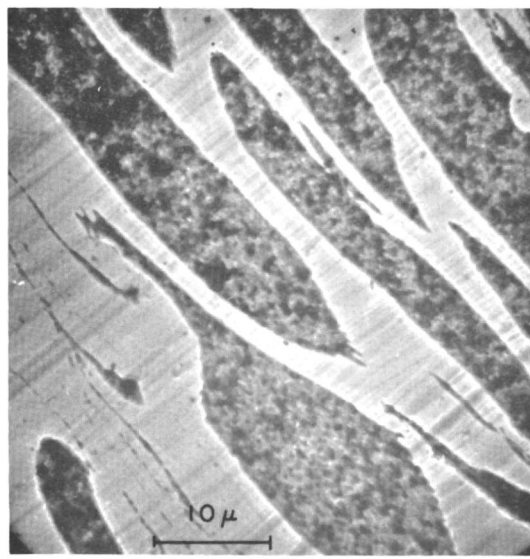

Figure 6. Electron micrograph of a replica of granular micrinite in vitrain in hvab coal. × 1,400

fusain are less homogeneous counterparts of vitrinite and fusinite. Resinous inclusions of ovoid or rodlike form occur in association with the main components.

The general appearance in the electron microscope of an ultrathin section of a heterogeneous area of dull coal (high volatile A bituminous) is illustrated in Figure 1. Components readily identifiable as vitrinite, exinite, and granular micrinite are indicated. Distinguishing the other variously shaded areas is not so positive, but identification can usually be established from shape, density, and association.

Figure 2 shows a vertical section of a megaspore from a Michigan spore coal. This was cut perpendicular to the large, flat surfaces of the platelike spore. The ovoid bodies are about 1 micron in diameter and are apparently composed of folded doughy masses.

Figure 3 shows a typical electron micrograph of an ultrathin section cut from a relatively homogeneous band in meta-anthracite from Leoben, Austria (*14*). This band is probably the product of metamorphosis from a vitrain band in the bituminous stage. Although the section appeared to be continuous, the micrograph reveals a jumble of thin platelets interspersed with many holes. Many of the platelets are nearly parallel to the plane of the micrograph, and their oval or polygonal outlines can be traced. Some have a roughly hexagonal shape. Both x-ray and electron diffraction patterns of this material have shown most of the characteristic sharp lines of graphite (*4*, *10*). Estimations of crystallite size from measurements of line broadening in the x-ray patterns have yielded a value of the order of 800 A. for this coal. Measuring the diameters of about a dozen clearly defined platelets in electron micrographs resulted

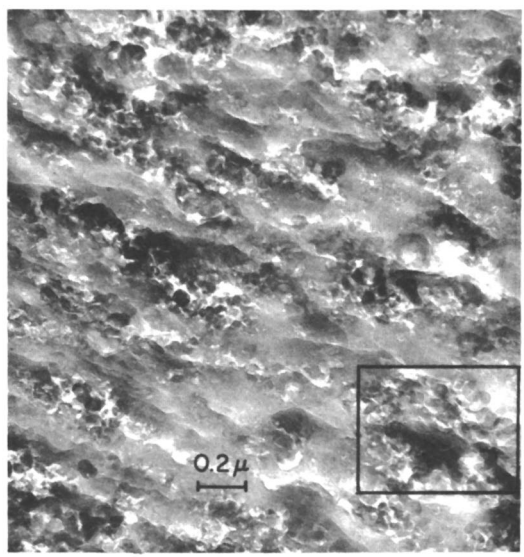

Figure 7. Electron micrograph of an ultrathin section of granular micrinite in vitrain in hvab coal. × 30,800

Publication Date: January 1, 1966 | doi: 10.1021/ba-1966-0055.ch016

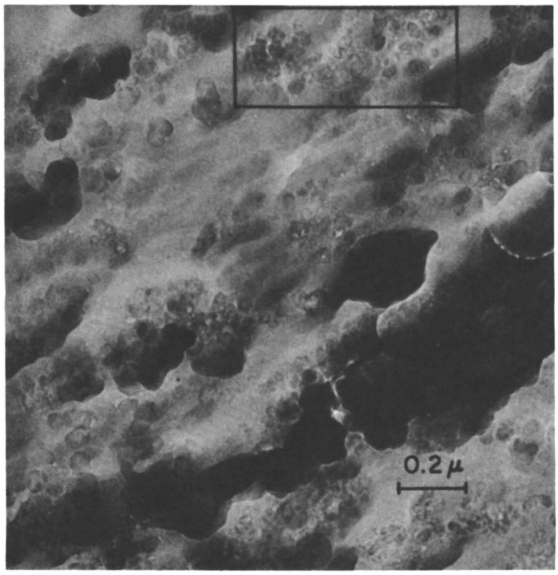

Figure 8. Electron micrograph of an ultrathin section of granular micrinite in vitrain in hvab coal. × 42,000

in an average diameter of the order of 800 A. A reasonable "order-of-magnitude" agreement is indicated. A logical interpretation is that the platelets are crystallites of graphite that have formed and grown from aromatic layer clusters during metamorphosis of this meta-anthracite.

An ultrathin section of a resin inclusion in vitrain from a subbituminous coal is shown in Figure 4. This variety of resin appeared to have a very fine granular structure in the light microscope. The micrograph shows that this consists of nearly spherical particles ranging from 300 to 700 A. in diameter.

Figure 5 is a micrograph of a section of semifusinite. Examining the thinner areas surrounding the cell spaces reveals density maxima or "particles" ranging in size from 300 to 800 A.

A very interesting component in coal from the standpoint of electron microscopy has been granular micrinite. In the early studies by the Bureau of Mines (1948), striking micrographs were obtained of replicas of this material concentrated in cell spaces of vitrain. These structures were brought out by etching in chrome-sulfuric acid. Figure 6 shows such a replica. Of special interest in this micrograph are the fine white lines running between the filled cells. These represent the middle lamella or dividing membranes between the cell walls. Much of the granular material was evidently torn out in stripping and adhered to the replica, accounting for the strong contrast. Despite the attractiveness of these micrographs, little was attempted in the way of quantitative measurements of particle size because of the doubtful resolution and other uncertainties of a replica method.

Publication Date: January 1, 1966 | doi: 10.1021/ba-1966-0055.ch016

Ultrathin sections of granular micrinite yielded apparently better images of the particles. Figure 7 shows a section of such material in a vitrain cell. The particles occur in a rather structureless matrix material. Close inspection reveals that they are platelets rather than spheroids and that portions of the boundaries are angular, suggesting a crystallite structure (*see* outlined area). It is possible that graphitic crystallite growth has progressed to some extent in this micrinite component of a high volatile bituminous coal. These possible crystallites, ranging in diameter from 300 to 1000 A., are smaller and less angular than those of the meta-anthracite discussed previously. Thiessen (*15*) had postulated from light microscope studies that the granules ranged in size from 0.5 to 1 micron. Probably he observed unresolved aggregates of the smaller particles. Figure 8 illustrates, in addition to particles like those in Figure 7, commonly occurring particles of different appearance but of about the same size (outlined area). These seem to have denser rims which are sometimes broken, giving the appearance of coiled, elongated particles. Interpretation of this structure is not attempted.

Figure 9, a fuzzy micrograph at very high magnification, is presented to show an apparent porous structure in fusain. The pores, the small light spots interspersed in the dark matrix, are less than 100 A. in diameter. A previous study has indicated that fusain is the most porous of coal components (*5*). Of course these ultrafine pores are much smaller than those associated with the ordinary cells of fusain.

Finally, highly speculative evidence of an extremely fine structure is presented in Figures 10, 11, and 12. The first shows exinitic material that appears to have a granular structure consisting of coiled particles (dark in the

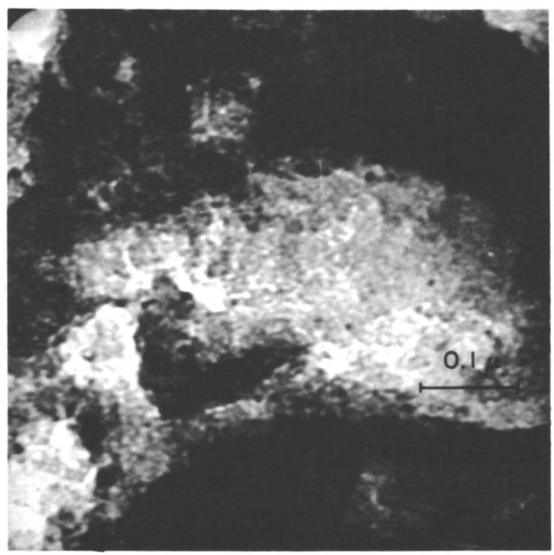

Figure 9. Infrared spectra of samples of resinite from section of fusain in hvab coal. × 122,500

Publication Date: January 1, 1966 | doi: 10.1021/ba-1966-0055.ch016

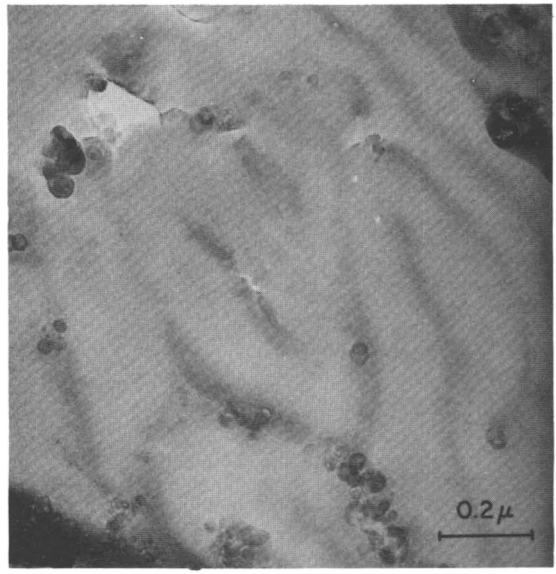

Figure 10. Electron micrograph of an ultrathin section of exinite in hvab coal. × 42,000

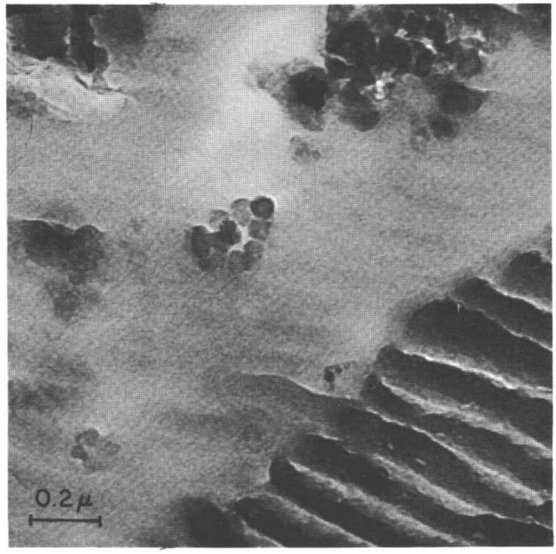

Figure 11. Electron micrograph of an ultrathin section of fusain in hvab coal. × 58,800

micrograph) about 50 A. in diameter. Figure 11 shows a very similar granularity in a fusain sample. The dark ribbed structure is a cutting artifact, but in thinner areas the coiled elongated "particles" also can be seen. Figure 12

Publication Date: January 1, 1966 | doi: 10.1021/ba-1966-0055.ch016

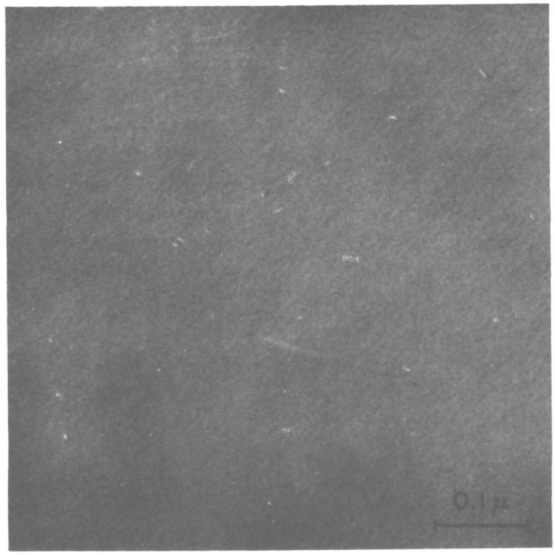

Figure 12. Electron micrograph of an ultrathin section of vitrinite in hvab coal. × 116,900

shows a highly magnified area of apparently homogeneous vitrinite from a high volatile bituminous coal. In this also an ultrafine granularity is observable, possibly not having the form of the two previous examples but comparable in size. The significance of these ultrafine structures is difficult to assess. They may well be artifacts because they occur similarly in different components and because they are sometimes not observable in other specimens of the same components, although this latter circumstance may be caused by unfavorable conditions of preparation or observation. Further high resolution studies are desirable.

As discussed earlier concerning the work of Pregermain, a pertinent question involves the relation of the sizes of structures observed in coals by electron microscopy and the pore structures deduced indirectly from adsorption studies. Van Krevelen (*16*), after analyzing many investigations of internal surface of coals (including that of Bond (*2*)), suggests that the micropore system, which is dominant in determining the internal surface area, consists of 20–40 A. pores with probable 5–8 A. restrictions in the interconnecting channels. In the present study some deductions concerning porosity can be related to the sizes of the apparent particles. For this purpose an assumption of close packing would require that the interstices be about an order of magnitude smaller in size than the granules. Thus, for the 300–1000 A. granules or platelets observed, pores of the order of 30–100 A. could be supposed, while granules of 50 A. diameter could be interspersed with pores of about 5 A. Various combinations of components with these two ranges of pores could be consistent with some of the observed adsorption results.

The micrographs presented here illustrate the potentialities of electron microscopy of ultrathin sections in revealing extremely fine details of crystallite,

Publication Date: January 1, 1966 | doi: 10.1021/ba-1966-0055.ch016

granule, or pore structure in various coal components. Such studies will aid in developing a more complete understanding of the nature of the structural units in coal.

Literature Cited

(1) Alpern, B., Pregermain, S., Bull. Microscop. Appl. **6**, 16 (1956).
(2) Bond, R. L., Spencer, D. H. T., "Industrial Carbon and Graphite," p. 231, Society of Chemical Industry, London, 1958.
(3) Brown, H. R., Taylor, G. H., *Nature* **193**, 1146 (1962).
(4) Ergun, S., McCartney, J. T., *Science* **134**, 1620 (1961).
(5) Ergun, S., McCartney, J. T., Mentser, M., *Econ. Geol.* **54**, 1068 (1959).
(6) Mackowsky, M. Th., Nemetschek, Th., *Naturwiss.* **43**, 442 (1956).
(7) McCartney, J. T., *Econ. Geol.* **44**, 617 (1949).
(8) McCartney, J. T., Walline, R. E., Ergun, S., *U. S. Bur. Mines Rept. Invest.* **5885** (1961).
(9) McCartney, J. T., Ergun, S., Walline, R. E., *Nature* **191**, 1361 (1961).
(10) Mentser, M., O'Donnell, H. J., Ergun, S., *Fuel* **41**, 153 (1962).
(11) Pregermain, S., Guillemot, C., *Fourth Intern. Kongr. Elektronenmikroskopie*, Vol. 1, p. 384, Springer-Verlag, Berlin, 1960.
(12) Pregermain, S., *European Regional Conf. Electron Microscopy*, Vol. 1, p. 516, Nederlandse Vereniging voor Electronenmicroscopie, Delft, 1961.
(13) Preston, G. D., Cuckow, F. W., "Ultra-fine Structure of Coals and Cokes," p. 334, British Coal Utilization Research Association, 1944.
(14) Simon, J. A., private communication.
(15) Thiessen, R., Sprunk, G. C., *Fuel* **15**, 304 (1936).
(16) Van Krevelen, D. W., "Coal," p. 137, Elsevier Publishing Co., Amsterdam, 1961.
(17) Waisman, B. A., Krivitzkii, M. D., Krigman, F. E., *Dokl. Akad. Nauk SSSR* **97**, 1031 (1954).

RECEIVED January 25, 1965.

Discussion

Marlies Teichmüller. In what direction have the samples of meta-anthracite been cut—vertical or parallel to the bedding plane? As the aromatic clusters are oriented parallel to the bedding plane you should get quite a different picture depending on the direction of cutting, supposing that you really can see the clusters under the electron microscope.

James McCartney and Sabri Ergun. The ultrathin sections of meta-anthracite were cut in an undetermined direction with reference to the bedding plane. The micrograph apparently shows crystallites oriented at various angles to the film plane. It could be surmised that the stresses imposed during cutting caused a scrambling of the crystallites into different orientations. If cutting had been done parallel to the bedding, probably this scrambling would have been minimized. Selected orientation of the particle during cutting would have been desirable, but was not done, partly because of the difficulty of maintaining orientation during embedding.

Subsequent to this Conference, sections were cut parallel and perpendicular to the bedding, and these were studied by electron microscopy and electron diffraction. Orientation of the crystallites can indeed be verified by both methods. A report of these studies appears in *Nature*, **205**, 962 (1965).

George Kapo. What percentage of the carbon in meta-anthracite coal do you think is in the platelets (800–1000 A.) you observed?

Mr. McCartney. From a study of electron micrographs, we estimate that a very large proportion of the apparent vitrain band in this meta-anthracite consists of graphite crystallites or platelets. The intensity and sharpness of graphite peaks in diffraction patterns supports this view.

Dr. Kapo. In low rank coals, platelets of the order of 1000 A. probably do not exist while pores of 1000 A. do. It would seem then, that your tentative analogy between platelet and structural unit size does not hold here. Do you have any comments on this?

Mr. McCartney. The comparison of size ranges of structure seen in electron micrographs with those suggested for pore systems in coals could be based on the assumption of close-packed systems in which the sizes of the interstices are smaller by an order of magnitude than the diameter of the granules. If pores of 1000 A. or greater exist in low rank coal, this would signify the presence of cell structural entities of 1 μ or greater.

Wolfgang Flaig. Could it be that the particles with a diameter of 50 A. are humic acids or humine? We found that the particle size of humic acids is between 50 and 100 A.

Mr. McCartney. It would be possible for the 50-A. granular structure of the vitrinite specimen of Figure 12 to have been derived from the colloidal structure of humic acids. However, the similar structures of Figures 10 and 11 in exinite and fusain could hardly be ascribed to such an origin.

Kulai Kini. You mentioned the findings of Van Krevelen that in vitrinites there are pores of diameter 20–30 A. Did you find evidence of these in your electron microscopic work?

Mr. McCartney. Figures 10–12 show evidence of structures of the order of 50 A. in several coal components. If valid, they could account for a system of pores having diameters of a few angstroms.

John Harrison. Can you distinguish between collinite and telinite?

Mr. McCartney. No direct comparison of collinite and telinite in the electron microscope was made.

In general, details of cell structure in vitrinite are distinguished only with great difficulty in ultrathin sections in the electron microscope, probably because of insufficient contrast between cell parts. If cell spaces are filled with another component the cellular structure becomes evident.

N. H. Skau. Did the rounded structures and domains of size 300 A. and the curved filaments of size 50–70 A. pre-exist in the coal or were they created by beginning cokefaction?

Mr. McCartney. Presumably Dr. Skau refers to possible effects of heat absorbed from the electron beam. No changes were observed in larger structures during observations in the electron microscope. For example, the shapes and outlines of spores remained the same, and no evidence of fusion was observed.

Dr. Skau. Did the electron microscope reveal anything about finely subdivided mineral matter in the otherwise nearly mineral-free coal components?

Publication Date: January 1, 1966 | doi: 10.1021/ba-1966-0055.ch016

Mr. McCartney. No serious attention was paid to possible mineral matter in these observations. Very black small spots were seen casually in many of the sections, particularly of heterogeneous components. Our general impression is that no evidence was seen of extremely fine mineral matter in homogeneous vitrinite.

Marie Mackowsky. Have you ever recognized an influence of the electronic beam on the structure of coal? Nemetschek and I observed that the energy of the electronic beam can graphitize the coal, especially if one uses high magnification.

Mr. McCartney. We have not observed any appreciable effect of the electron beam on ultrathin sections of coal or structures therein. As stated in the reply to Dr. Skau, spores and other well-defined entities show no evidence of fusion.

Publication Date: January 1, 1966 | doi: 10.1021/ba-1966-0055.ch016

17

The Electron Microscopy of Vitrinites

G. H. TAYLOR

Division of Coal Research, Commonwealth Scientific and Industrial Research Organization, Chatswood, N.S.W., Australia

Publication Date: January 1, 1966 | doi: 10.1021/ba-1966-0055.ch017

Examination of ultrathin sections of coal in the electron microscope has revealed that one type of vitrinite (vitrinite A) is homogeneous, while the remaining vitrinite (vitrinite B) is a two-component material, the components having similar properties to vitrinite A and exinite, respectively. The material similar to exinite occurs in sheets no more than 1000 A. thick and is responsible for the lower reflectance and higher volatile matter yield of vitrinite B. Exinite, micrinite, and semifusinite have been identified in ultrathin sections. By using a technique of impregnation with a lead salt the ultrafine pore structure of vitrinite has been made visible.

The theoretical lower limit of resolution of the light microscope is about 0.2 micron—i.e., 2000 A. This figure can be reduced in favorable circumstances by using phase-contrast or interference microscopy. Ultraviolet microscopy of coal was attempted at the Division of Coal Research, but without success owing to the opacity of coal to ultraviolet radiation. Vigorous attempts are being made to develop x-ray microscopy, and its limit of resolution is already an order better than that of the light microscope.

The electron microscope has a practical limit of resolution of 10 A. or less for favorable specimens and a theoretical resolution of less than half this. One of the practical limiting factors is the difficulty of getting the specimen into a form suitable for electron microscopy. The specimen must be thin for two reasons: first, electrons will not penetrate thicknesses much in excess of a few hundred angstrom units; second, high resolution is not feasible in a specimen which is very thick compared with the dimensions of the structures being resolved. Preparing suitable specimens has sometimes proved difficult, coal being a comparatively hard and brittle material to section, using what are primarily biological techniques.

In Coal Science; Given, P.;
Advances in Chemistry; American Chemical Society: Washington, DC, 1966.

The ability to resolve fine structure is desirable not only for extending the light microscopy of coal (which has proved a very fruitful field of study) but also for confirming and supplementing data from physical or chemical observations.

Results

Low-Magnification Electron Microscopy of Vitrinite. In this context, the words "low magnification" are intended to mean magnifications of 10,000 or less on photographic negatives. Most of the data described below have come from examining ultrathin sections of coal, cut with a Si-ro-flex ultramicrotome using a diamond knife. (The Si-ro-flex ultramicrotome has been developed by the Fairey Aviation Co. of Australasia Pty., Ltd., from a design by the Division of Chemical Physics, CSIRO, Australia.)

The contrast observed in electron microscopy depends largely on differences in atomic composition of the specimen. In this respect the coal macerals do not differ greatly from one another, and so very high contrast between them would not be expected and is not in fact obtained. Despite attempts to overcome this difficulty low contrast remains a serious limiting factor in observing structure. It is possible that staining techniques, as used in electron microscopy of biological specimens, may prove useful.

Figures 1, 2, and 3 are from ultrathin sections of high volatile bituminous coals. It is possible to distinguish microspores, micrinite fragments, and the

Figure 1. Vitrinite containing thin sheet-like structures of material similar to exinite in many of its properties. × *6750*

Publication Date: January 1, 1966 | doi: 10.1021/ba-1966-0055.ch017

Figure 2. Several spores in a ground mass of vitrinite. The vitrinite contains contorted sheets and shreds of exinite-like material. × 3375

vitrinite ground mass. Micrinite and other macerals of the inertinite group behave as harder material than vitrinite and exinite during section cutting. Since cutting conditions usually cannot be adjusted to suit both harder and softer macerals, artifacts sometimes occur. Thus, the striations in the micrinite (Figure 3) are artifacts.

Apart from the exinite and micrinite, all the other coal material in this section is vitrinite and would be counted as such in a maceral analysis. These macerals were identified not only from their form, which is often characteristic, but by direct comparison of the light-microscope picture of the facet from which the ultrathin section was cut (*1*). By using this technique, each maceral occurrence of sufficient size could be positively identified.

The relative degree of denseness (i.e., opacity to electrons) of the macerals is: exinite least dense, vitrinite intermediate, and inertinite most dense of the coal maceral groups. That is, the light/dark relations are similar to those observed in the usual thin sections examined in the light microscope.

Even at magnifications of 10,000 maceral boundaries are sharply defined, and there is no suggestion of transitions between most maceral occurrences.

Much of the vitrinite in Figures 1, 2, and 3 contains fine structure which is beyond the resolution of the light microscope. (Figures 1, 2, 3, 5, and 6 relate to Greta seam coal, Figure 4 to Homeville, and Figure 7 to Young Wallsend. All coals are of bituminous rank and Permian age and are from the Northern Coalfield of New South Wales.) The lines in much of the vitrinite

Publication Date: January 1, 1966 | doi: 10.1021/ba-1966-0055.ch017

in the micrographs represent sheets rather than fibers, as could be seen from serial sections. These sheets form sinuous, contorted, anastomosing patterns, usually with several sheets together folded into similar structures. The sheets are at most 0.1 μ thick, and many are much less than this. They are frequently about 0.1 μ apart. Their electron denseness is the same or almost the same as that of exinite, and it would be reasonable to assume the same to be true of their composition. Sometimes these structures can be followed to closure in the plane of the section and give the appearance of collapsed cell walls. However, some such closures occur within 2 μ and frequently in less than 10 μ. Although in general the structures will not exhibit their greatest extent in random sections, they nevertheless seem small for plant cells. These structures are not artifacts, as can be demonstrated by rotating the specimen in the ultramicrotome and cutting further ribbons of ultrathin sections with different specimen orientations. The perfection of development of these sheets varies from one vitrinite layer to the next. In some layers the sheets form half or more than half of the vitrinite; in others they are scarcely discernible. Although the sheets of exinite-like material appear to vary somewhat in their properties, the material with which they are associated—the "basic" vitrinite—appears to be homogeneous and uniform at a magnification of 10,000.

Figure 4 shows the light-microscopic appearance of coal in which much of the vitrinite is laminated. The laminae in Figure 4 actually represent aggregates of much finer sheets.

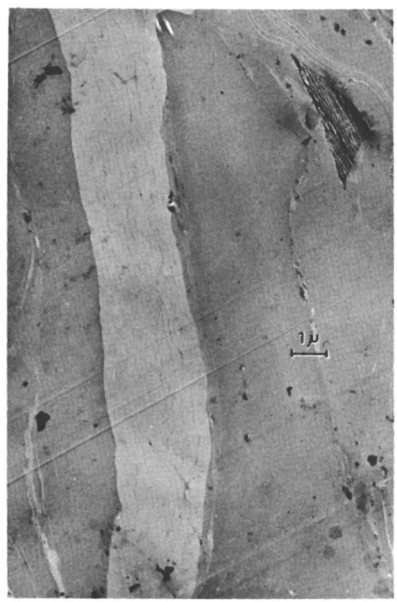

Figure 3. A band of exinite showing fine structure. The associated vitrinite is almost entirely homogeneous. × 4725

Publication Date: January 1, 1966 | doi: 10.1021/ba-1966-0055.ch017

Figure 4. Light micrograph of a polished surface of a high volatile bituminous coal. The fine banding is caused by groups of sheets which cannot be resolved individually with the light microscope. × 185

Thus some vitrinite appears to be a two-component material with the proportions of components varying over a wide range. By relating the field of the electron microscope to the corresponding field of the light microscope, it has been found that the reflectance of the vitrinite varies in relation to the number of exinite-like sheets which are present. The higher the proportion of these sheets, the lower the reflectance. This again is consistent with the sheets being like exinite in their properties.

The vitrinite without any sheets appears to correspond to what Brown, Cook, and Taylor (*2*) have called vitrinite A; that with sheets appears to correspond to vitrinite B. The existence of this kind of laminar structure helps to explain the observation that vitrinite B has a higher volatile matter yield than vitrinite A although some of the coking properties of the two vitrinite types seem fairly similar. Many of the coking properties in fact appear to be primarily related to the "matrix" vitrinite.

In some polished surfaces of vitrinite, as seen in the light microscope, irregular areas of lower reflectance occur. Some of these might reasonably be called resinite, but some are only a little lower in reflectance than the undoubted vitrinite. Sometimes these areas are regularly distributed throughout vitrinite, and sometimes they occur irregularly in heterogeneous coal. Unlike the laminate structures described above, such areas appear uniform and homogeneous within themselves in the electron microscope. They are either similar

Publication Date: January 1, 1966 | doi: 10.1021/ba-1966-0055.ch017

to exinite or intermediate between vitrinite and exinite in their electron denseness.

Exinite, Micrinite, and Semifusinite. Although this paper is primarily concerned with vitrinite, a few comments about the other maceral groups may be relevant. As shown above, microspores, cuticles, and fragments of exinite have sharp boundaries and are readily distinguishable in ultrathin section. The spores especially appear to be very clean and free of mineral particles, although they are frequently surrounded by fine spherical grains—usually between 100 A. and 1000 A. across—often in aggregates. These grains are evidently not crystalline as they gave no well-defined electron diffraction pattern. Electron probe examination results were inconclusive. Comparison with some micrographs obtained by McCartney, O'Donnell, and Ergun (3) suggests that these grains may be a form of fine micrinite. Occasional fragments of exinite show an internal structure. The body in Figure 3 may represent a sporangium, perhaps in an early stage of development.

Fragments of the more usual type of micrinite are often quite angular, with sharply defined boundaries (Figure 3). Micrinite fragments vary in electron denseness, some being a little darker and others a lot darker than the associated vitrinite. The darker fragments are harder and more prone to show striations formed during cutting. There is thus a close analogy between opacity

Figure 5. Contact between semifusinite (showing cellular structure) and vitrinite. This junction appeared to be transitional in the light microscope but at this magnification appears sharp. × *4390*

Publication Date: January 1, 1966 | doi: 10.1021/ba-1966-0055.ch017

of micrinites to electrons and reflectance of micrinite in the light microscope. The fragments have compaction structure around them just as occurs on a larger scale.

Semifusinites behave like micrinites of similar reflectance. Examining several specimens by electron microscopy, where light microscopy had shown apparently gradual transitions from vitrinite to semifusinite, suggested that the transition was at least partly step-wise in nature (Figure 5). In some semifusinite, the actual cell walls could be observed within the generally cellular structure (Figure 5).

Effect of Rank. Most of the above observations were made on high volatile Australian coals of bituminous rank. These coals, whether of Permian, Triassic, or Jurassic age, tended to give fairly similar pictures.

With increasing rank, the differences between macerals become progressively smaller in electron as in light microscopy. Exinite in particular becomes difficult to distinguish in medium volatile coals, and could not be positively identified in the electron micrographs of low volatile bituminous coals so far examined. Similarly, the laminate structure of vitrinite described above could not be observed in low volatile bituminous coals.

In an attempt to make any such structures visible in coals of low volatile bituminous rank, replicas were prepared of both polished and natural fracture surfaces (Figure 6). Indications of such structures were obtained with medium volatile but not with low volatile bituminous coals. Replicas of naturally frac-

Figure 6. Replica of a high volatile coal (polished surface) showing sheet-like structures in vitrinite. × *4050*

Publication Date: January 1, 1966 | doi: 10.1021/ba-1966-0055.ch017

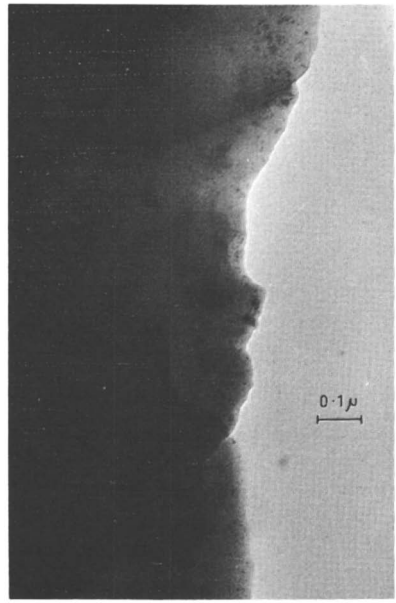

Figure 7. Thin edge of vitrinite which had been impregnated with lead acetate. The dark spots are believed to represent infilled pores. × *57,400*

tured surfaces proved difficult to use owing to the presence of numerous surface irregularities.

High-Magnification Structure. For the structures discussed above, increased magnification gives an enlarged picture but, in general, no new information. At the highest magnifications, the thin sections appear nebulous and without any discernible ultrafine structure.

It was considered likely that any fine structure present might not be obvious owing to lack of contrast. In an attempt to reveal any structures present, samples of vitrinite were evacuated at 10^{-6} mm. Hg for several days and then impregnated with a saturated aqueous solution of lead acetate. The solution was allowed to dry over a period of several days and then some of the vitrinite was freed from the encrusting lead acetate, crushed finely, and dispersed on a carbon-collodion filmed grid.

Using this technique, evidence of structure was found repeatedly in thin edges of vitrinite (Figure 7). The structure was usually that of electron-dense areas, 10 A.–100 A. across. These areas were not visible in similarly prepared dispersions of the same vitrinite which had not been impregnated with lead acetate, and it is suggested that they are pores within the vitrinite which have been filled, partly or wholly, with lead acetate. The pores appear to be roughly equidimensional, although somewhat irregular, and have various sizes even in the same vitrinite grain.

Publication Date: January 1, 1966 | doi: 10.1021/ba-1966-0055.ch017

It is not yet known how efficient this impregnation process is, and much more work will be necessary to obtain quantitative data. Nevertheless, preliminary results suggest that, with further work, direct comparisons with pore distributions as recorded by the BET method, for example, may be possible.

Acknowledgments

The support of H. R. Brown, Chief of the Division of Coal Research, C.S.I.R.O., is gratefully acknowledged. J. F. Corcoran prepared many of the samples used for electron microscopy.

Literature Cited

(1) Brown, H. R., Taylor, G. H., *Nature* **193,** 1146 (1962).
(2) Brown, H. R., Cook, A. C., Taylor, G. H., *Fuel* **43,** 111 (1964).
(3) McCartney, J. T., O'Donnell, H. J., Ergun, S., ADVAN. CHEM. SER. **55,** 261 (1966).

RECEIVED January 25, 1965.

Discussion

G. R. Stevens. It would be interesting to have the author's comments on the 100-A. ultrafine banding shown in some of the electron micrographs. Such bands may not be biogenic. Similar or analogous structures are to be seen in natural glasses such as obsidian, which have undergone gravity flattening and flowage. There is an obvious difference in scale, but electron microscopy of obsidians might well reveal analogous patterns, the result of deformation, that might help to clarify our understanding of such patterns in coals which have suffered flattening and laminar movements parallel to the bedding plane. Could these ultrafine bands in coals be mechanical in origin rather than biogenic?

Geoffrey H. Taylor. I am skeptical about this, because some of these forms seem to be closed, as collapsed vesicles.

Dr. Stevens. I suggest further that such apparently closed forms could also be generated during micro-flowage as laminae refold over themselves. This effect is well known in strongly sheared rocks.

Dr. Taylor. At the moment such an effect seems to me to be unlikely, but I am grateful for the suggestion.

Gilbert H. Cady. How do your findings correlate with the usual classification of vitrinite into collinite and telinite?

Dr. Taylor. Much of our vitrinite A would be telinite, and much of our vitrinite B would be collinite. However, we have found great difficulty in using the concepts of collinite and telinite because whether or not one sees cell structure to some extent depends upon the techniques used.

Robert A. Friedel. Can you take an electron micrograph of an organic sample at high magnification—e.g., 50,000 ×—and then obtain exactly the same picture on taking a second shot of the same spot? It is my impression that the newest equipment with careful techniques can do this, but that with

equipment designed more than two years ago diffuseness of the second picture would occur owing to condensation on the sample of impurities from the vacuum system liberated during the initial exposure.

Dr. Taylor. Yes, we can do this when suitable precautions have been taken. In fact, we have for some years past made use of a resolution test in which two successive pictures are taken of the same field. The contamination problem has been largely overcome in recent years, as you suggest.

John A. L. Campbell. Did you test for calcium in analyzing the unknown particle with the electron probe?

Dr. Taylor. Yes. We tested for all elements of atomic number greater than 12 which are common in coal.

Marlies Teichmüller. We have observed dark spots in vitrinites (especially in anthracites) under the electron microscope *without* impregnating the coal. The technique was to grind the coal in a rocking ball mill, and treat the very fine particles obtained by this process as "thin sections," (cf. R. Meldau and M. Teichmüller, *Öl Kohle* **37**, 751 (1961)).

Dr. Taylor. Naturally, we also looked at coals (but not anthracites) which were not impregnated. However, the only fine particles observed were minerals, as could be confirmed by electron diffraction.

Peter Hacquebard. Were you able to observe any difference in the texture of vitrinite present in distinct vitrite bands and the vitrinite that occurs as ground mass in clarite and durite bands? Your excellent photomicrographs seem to portray only the vitrinite that lies between the spores and similar material.

Dr. Taylor. The vitrinite in vitrite layers was mostly either featureless or showed traces of cell wall structures similar to those in ordinary thin sections. Some vitrinite of this type is to be seen in the photographs shown (*see* Figure 3).

Publication Date: January 1, 1966 | doi: 10.1021/ba-1966-0055.ch017

18

Petrographic Investigation of Two Gondwana Seams from Madhya Pradesh, India

S. K. BABU and RUSSELL R. DUTCHER

Department of Geology and Geophysics,
The Pennsylvania State University, University Park, Pa.

Publication Date: January 1, 1966 | doi: 10.1021/ba-1966-0055.ch018

The basic petrographic composition of two seams of Gondwana age, collected from Chirmiri Colliery, Central India, has been determined. The petrographic work was undertaken to delimit petrography, to allow comparison with coals from the United States, Africa, and Australia, and to apply the information gained to future studies of other Indian coals. The two seams from India of Gondwana age vary considerably in their petrography, chemistry, and physical properties from many of the coals of the United States. Further, the two seams are characterized by macerals of varying types and by a high "inert" content, both of which point to the heterogeneity of organic debris forming the macerals and to changes in environment during the formation of the coal swamp consistent with the "Drift" theory of origin for Gondwana coals.

The two seams, namely Seam No. 2 and Seam No. 4, of Gondwana age collected from Chirmiri Colliery, Central India, were studied to ascertain their basic petrographic composition, chemical variation, and other physical properties in order that the information gained from these studies might be applied to future studies of Indian coals. There is no significant petrographic data available for these specific coals. The study of these two seams was sponsored by the Fulbright-Smith Fund grants for a period of nine months. The studies were carried out at the Organic Sediments Laboratory, Department of Geology and Geophysics, The Pennsylvania State University.

General Geology

The two seams are located along Long. 82° 24′ and Lat. 23° 13′ at the town of Chirmiri in Central India. It lies east of the Hasdo River in Korea

In Coal Science; Given, P.;
Advances in Chemistry; American Chemical Society: Washington, DC, 1966.

State and covers 48 square miles of hilly country. Fermor (*6*) has recognized two colliery; he treated the field in two sections. That to the east of the road, southward from Kurasia to Dabchola, he named the Kurasia area while that to the west he termed the Chirmiri area. The coal bearing beds are known as "Barakars," of lower Permian age of the Gondwana formations. These Barakars are completely isolated and almost entirely surrounded by Talchairs (Upper Carboniferous) on which they lie almost horizontally. To the north of these coal fields near Chitajohr there is a belt of dolerite and basalt which overlies both Talchairs and Barakars. This igneous rock is of Deccan trap age, and there seems to be little doubt that in this region it is all of intrusive character.

As regards the Chirmiri areas from where the two seams have been collected, Fermor (*6*) considered the most important exposure as that at the waterfall known as Karar Khoh in the Korea nala, where 36 feet of coal in seven beds occur in 48 feet of strata. The coal seams are underlain and overlain by coarse to medium grained sandstones and black carbonaceous shales. Seam 2 is at the top of the section while Seam 4 is below. The two seams are separated by 40 feet. Seam 2 is 4 feet thick, while Seam 4 is actually 12 feet thick, but in the mines the mined portion is only 6 feet thick. Pillar columns were collected from these two seams for the present investigation; they form the subject matter of this paper.

Publication Date: January 1, 1966 | doi: 10.1021/ba-1966-0055.ch018

Techniques and Importance of Study

The studies carried out consist of the megascopic description of the master columns study of thin sections for maceral assessment, determination of maceral composition on polished blocks in reflected light, determination of mean maximum reflectance values on polished pellets, proximate analyses of selected petrographic zones, hot stage studies on vitrinoids to determine the thermal behavior at various temperatures, electron microprobe and spectrochemical studies of selected zones to determine the nature of ash forming elements, analyses of certain zones petrographically important to determine the variation of total carbon, and hydrogen and microhardness determinations on certain macerals.

Employing various research techniques, we undertook the petrographic work on these two seams to delimit their petrography, to compare with coals from the United States, Africa, and Australia, and to apply the information gained to future studies of other Indian coals. We also wished to explore the possibilities of better industrial exploitation from the petrographic information. Finally, we hoped that the results would contribute to the basic knowledge of Gondwana coals and the problems associated with the origins of these deposits.

Chemistry of the Seams

All the samples were air-dried before analyses. Chemical analyses were conducted according to standard techniques; in the case of total carbon and hydrogen, the samples were sent to England for analysis. The average values for the chemical analyses for both the seams are presented in Tables I and II.

In Coal Science; Given, P.;
Advances in Chemistry; American Chemical Society: Washington, DC, 1966.

Table I. Average Values Obtained from Duplicate Microchemical Analysis

Zone No.	Fixed Carbon	Volatiles	Ash Content	Moisture	Sulfur	Hydrogen	Total Carbon
Seam No. 4	%	%	%	%	%	%	%
1.	53.43	31.52	12.68	2.37	0.24	4.19	70.92
2.	50.84	29.60	17.60	1.96	0.48	3.83	63.34
3.	47.88	41.40	8.60	2.12	0.36	5.15	73.92
4.	51.73	26.80	18.96	2.51	0.40	3.57	62.33
5.	53.46	28.80	15.60	2.14	0.28	3.89	69.77
6.	51.50	24.80	17.60	6.02	0.24	3.50	64.58
7.	56.83	31.04	10.00	2.13	0.04	3.95	71.77
8.	54.98	24.80	14.00	6.22	0.08	3.49	68.86
9.	59.03	29.20	9.20	2.57	0.20	4.04	73.05
10.	60.73	28.00	8.80	2.47	0.20	3.92	72.04
11.	49.99	26.00	14.00	10.01	0.20	3.96	68.46
12.	54.20	32.40	11.00	2.40	0.20	4.08	74.18
13.	54.30	28.20	15.40	2.10	0.20	3.46	66.22
14.	55.42	30.40	11.80	2.38	0.28	3.91	69.83
15.	52.69	29.80	15.40	2.11	0.26	3.76	66.80
16.	57.32	33.20	7.40	2.08	0.26	4.05	73.75
17.	54.61	26.80	17.32	1.27	0.44	3.49	64.60
18.	53.24	30.00	14.48	2.28	0.24	3.79	66.53
19.	52.95	28.92	15.68	2.45	0.20	3.60	66.52
20.	51.00	29.60	17.40	2.00	0.28	3.78	62.71
21.	45.58	35.20	17.64	1.58	0.48	3.72	62.09
22.	49.34	35.20	13.32	2.14	0.60	4.04	69.17
23.	51.65	37.40	9.24	1.70	0.60	4.45	71.54
24.	58.73	26.80	12.76	1.71	2.68	4.15	67.04
25.	54.18	30.56	13.60	1.66	0.48	3.99	67.97
Seam No. 2	%	%	%	%	%	%	%
1.	48.88	36.96	11.48	2.68	0.63	4.29	66.10
2.	47.92	37.96	10.32	3.80	0.52	4.48	67.38
3.	48.30	36.76	10.60	4.34	0.75	4.33	67.35
4.	51.53	34.88	10.52	3.07	0.52	4.04	67.80
5.	44.87	36.36	11.88	6.89	1.70	4.09	63.83
6.	46.78	37.00	10.84	5.38	0.58	4.36	66.98
7.	38.49	35.16	16.88	9.47	0.72	3.97	62.27
8.	44.50	39.32	12.40	3.78	0.75	4.40	65.26
9.	45.81	40.16	10.00	4.03	0.64	4.63	66.94
10.	47.12	37.40	11.40	4.08	0.48	4.36	66.94
11.	45.77	39.96	10.00	4.27	0.52	4.31	67.44
12.	48.08	36.08	12.44	3.40	0.44	4.25	66.49
13.	48.98	37.00	11.84	2.18	0.46	4.28	66.96
14.	47.05	41.08	9.80	2.07	0.62	4.13	65.28
15.	47.97	41.04	8.04	2.95	0.51	4.21	66.56

Total Carbon. The total carbon in Seam 4 varied between 62.09 and 74.18%, while in Seam 2 it varied between 62.27 and 67.80%. The total carbon presented in Table I is not on an ash-free basis, but on a moisture-free basis. The total carbon does not vary widely in either of the seams. However, it appears to vary more in Seam 4 than in Seam 2.

Volatile. The volatile percentages range from 24.80 to 41.40% in Seam 4, and from 34.88 to 41.08% in Seam 2. According to the volatile percentage proposed by Moore (*12*), these coals fall under the category of medium to high volatile coals, Seam 2 being distinctly in the high volatile range. These two coals are poorly coking as evidenced from the character of the residue left after volatile determinations.

Publication Date: January 1, 1966 | doi: 10.1021/ba-1966-0055.ch018

Ash Content. The ash percentages vary from 8.6 to 18.9% in Seam 4 and from 8.04 to 16.88% in Seam 2, the average ash content being 13.21% for the two seams. The ash content is relatively more in Seam 4 than in Seam 2. The ash colors vary from ash-gray and bluish-gray to brown and chocolate brown.

Sulfur. These coals are generally low in sulfur and seldom exceed more than 1.5%. The sulfur percentage varies from 0.04 to 2.68% in Seam 4 and from 0.44 to 1.70% in Seam 2. The high percentage values—namely, 2.68 and 1.70%—are confined to one zone of each seam where megascopically recognizable pyrite grains are present.

Table II. Average Values Obtained from Duplicate Microchemical Analysis on daf Basis

Zone No.	*Carbon*	*Volatiles*	*Sulfur*	*Total Carbon*	*Hydrogen*
Seam No. 4	%	%	%	%	%
1.	62.89	37.11	0.28	83.48	4.63
2.	63.20	36.80	0.60	78.74	4.49
3.	53.63	46.37	0.40	82.79	5.51
4.	65.90	34.10	0.51	79.37	4.19
5.	64.99	35.01	0.34	84.82	4.42
6.	67.43	32.57	0.31	84.55	3.68
7.	64.68	35.32	0.05	81.68	4.22
8.	68.92	31.08	0.10	86.31	3.52
9.	66.91	33.09	0.23	82.79	4.26
10.	68.44	31.56	0.22	81.19	4.11
11.	65.78	34.22	0.26	90.09	3.75
12.	62.59	37.41	0.23	85.66	4.41
13.	65.82	34.18	0.24	80.27	3.91
14.	64.58	35.42	0.33	81.37	4.25
15.	63.88	36.12	0.31	80.98	4.28
16.	63.32	36.68	0.29	81.47	4.22
17.	67.08	32.92	0.54	79.35	4.11
18.	63.96	36.04	0.29	79.92	4.25
19.	64.67	35.33	0.24	81.25	4.07
20.	63.28	36.72	0.35	77.80	4.42
21.	56.42	43.58	0.59	76.86	4.39
22.	58.36	41.64	0.71	81.82	4.49
23.	58.01	41.99	0.67	80.33	4.78
24.	68.66	31.34	3.13	78.38	4.63
25.	63.94	36.06	0.57	80.21	4.50
Seam No. 2					
1.	56.94	43.06	0.73	77.00	4.76
2.	55.80	44.20	0.60	78.46	4.73
3.	56.78	43.22	0.88	79.18	4.53
4.	59.63	40.37	0.60	78.46	4.40
5.	55.24	44.76	2.09	78.58	4.10
6.	55.84	44.16	0.69	79.95	4.49
7.	53.26	46.74	0.95	82.31	3.86
8.	53.09	46.91	0.89	77.86	4.75
9.	53.29	46.71	0.74	77.86	4.86
10.	55.75	44.25	0.56	79.20	4.63
11.	53.39	46.61	0.61	78.66	4.48
12.	57.13	42.87	0.52	79.00	4.60
13.	56.97	43.03	0.53	77.88	4.70
14.	53.39	46.61	0.70	74.07	4.42
15.	53.89	46.11	0.57	74.78	4.36

Publication Date: January 1, 1966 | doi: 10.1021/ba-1966-0055.ch018

Hydrogen Content. The hydrogen content presented in Tables I and II is corrected for moisture. It varies between 3.46 and 5.15% in Seam 4 and between 3.97 and 4.63% in Seam 2. There is no marked variation in the hydrogen content of either of the seams.

Moisture. The moisture determinations are not very reliable since the coals were sampled and then shipped to the laboratories at The Pennsylvania State University for this study. Several months elapsed between the time of sampling and analysis. However, the moisture determinations do provide some basis to demarcate the zones which are highly absorbent. The moisture content ranges from 1.58 to 10.01% in Seam 4 and from 2.07 to 9.47% in Seam 2.

Fixed Carbon. The fixed carbon (calculated as 100 — (ash + volatile + moisture) after A.S.T.M.) varies from 45.58 to 60.73% in Seam 4 and from 38.49 to 51.53% in Seam 2.

There seems to be a steady increase in the fixed carbon content in the bottom portion of Seam 4 followed by a gradual decrease towards the top portion, while it is fairly uniform throughout in Seam 2. The ash and volatiles bear an antipathetic relationship in Seam 4 while they are pretty closely similar to each other in Seam 2. The sulfur is low throughout in Seam 4 with a tendency to increase at the top; it is uniform throughout except in the bottom portion of Seam 2. The histograms in Figure 1 show the average chemical composition of Seams 4 and 2, respectively; Figure 2 portrays the variation of ash, volatile matter, moisture, sulfur, and fixed carbon in Seams 4 and 2.

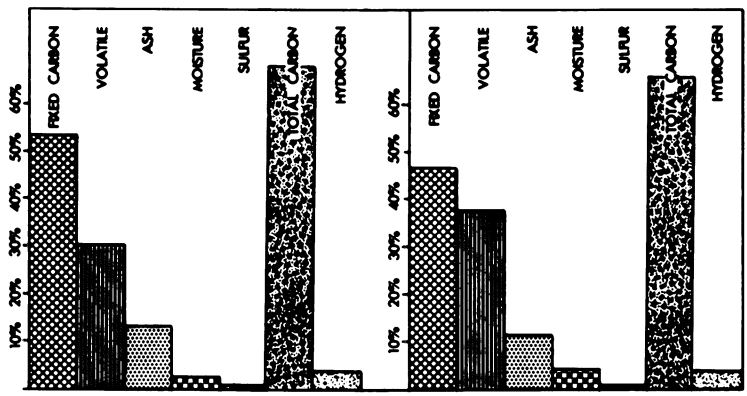

Figure 1. Histogram showing the average chemical composition of Seam 4 (left) and Seam 2 (right)

Electron Probe Studies

Electron microprobe studies were conducted on certain petrographically delimited zones to obtain information about the distribution of ash-forming elements. Scanning the pellet surfaces for aluminum, iron, and silicon in a majority of cases gave a positive reaction confirming the presence of clay minerals and detrital silicon and iron minerals. However, in a few cases the electron probe gave patterns indicating that some of the mineral matter, though

Publication Date: January 1, 1966 | doi: 10.1021/ba-1966-0055.ch018

not in bulk, is calcium and magnesium bearing. When the specimens were scanned for sulfur, the concentration of this element coincided with the positions for iron thereby confirming the presence of pyrite where otherwise it is not detectable.

Spectrochemical Study of Ash

The ash obtained from proximate analyses was run through an emission spectrograph to ascertain the nature of elements constituting the ash. This study was instituted since the ash residues were of varying colors. The spectrochemical analyses of the ashes from both the seams are presented below.

	Sample, %	
Element	*No. 4*	*No. 2*
Si	12.62	26.98
Al	8.47	10.58
Ca	0.56	1.50
Mg	0.33	0.60
Fe	2.59	6.78
Ti	0.66	1.02
Mn	0.035	0.11

The above analyses point to clay mineral and iron-bearing minerals as well as detrital quartz grains as constituting the bulk of ash-forming material. However, the presence of 0.66–1.02% titanium is somewhat unusual in coal ash, but recently, occurrence of titanium in high proportions has been reported from the coal of the interior province by Zubovic *et al.* (*20*). The titanium present may be caused by acicular inclusions of rutile in detrital quartz, or it may be present as an organic complex in the original plant material. The variation in color of the ash can be attributed to the presence of iron, titanium, and manganese principally.

Previous Petrographic Work

Apparently nothing has been published regarding the petrography of these two seams in the literature. However, their proximate analyses have been given by Fermor. (*6*). Field descriptions of these seams were given by Huges (*10*) and subsequently by Fermor (*6*). Fox (*7*) has mentioned these seams in his memoir of Lower Gondwana coal fields.

Petrography

Megascopic Description. In addition to the macroscopic log prepared from the freshly broken surfaces of the reference pillars of Seams 2 and 4, polished blocks covering the thickness of each of the coal seams were examined under a stereobinocular microscope to delimit the lithotypes. Seam 4 is rich in clarain intimately associated with vitrain, with sporadic occurrences of durain. Fusain bands occur localized in certain portions of the seam. Seam 4 can be classed as semidull coal, Seam 2 as semibright coal. The microbanding seen in these coals is not as continuous and regular as the banding seen in American coals. In particular, vitrain bands occur as discrete lenticles and irregular bands of varying thickness. On the basis of megascopic descriptions, 25 zones

Publication Date: January 1, 1966 | doi: 10.1021/ba-1966-0055.ch018

in Seam 4 and 15 in Seam 2 were demarcated for further detailed petrographic and chemical studies. The vitrain has a tendency to occur sometimes massively with a highly cracked appearance. Figure 3 presents the megascopic descriptions of the column samples of Seam 2 and 4, respectively.

Microscopic Description of the Seams. The zones delimited by observing the polished columns were studied further, both in transmitted and reflected light. A set of 40 thin sections from Seam 4 and 35 sections from Seam 2 were

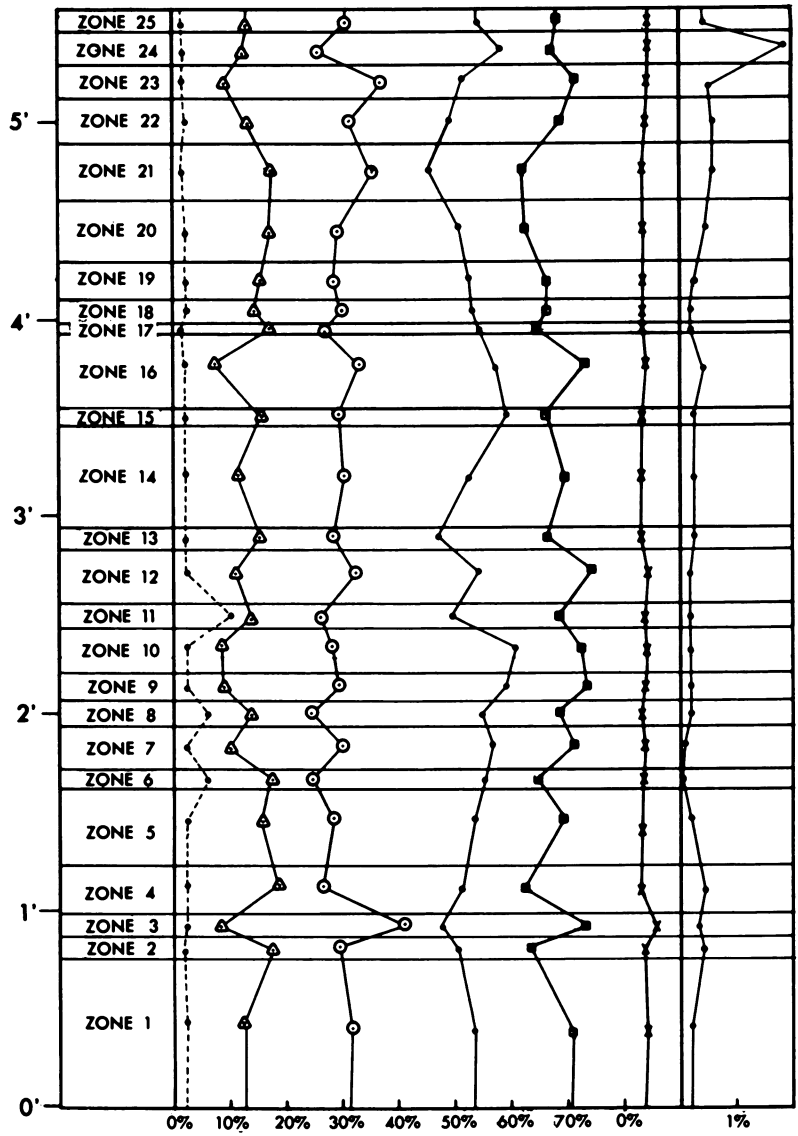

Figure 2. Variation of ash, volatile matter, moisture, sulfur, and fixed carbon

Publication Date: January 1, 1966 | doi: 10.1021/ba-1966-0055.ch018

prepared for studies in transmitted light. A total of 40 polished blocks corresponding to the 40 zones from both the seams were prepared for studies in reflected light. The results of these investigations are presented in Figures 4 and 4a, respectively. In these diagrams, the frequencies of the macerals are plotted instead of percentages after Evans, Hayman, and Majeed (5). The average petrographic composition of both seams is presented by the histograms in Figure 5. The maceral data for each zone is presented in Table III.

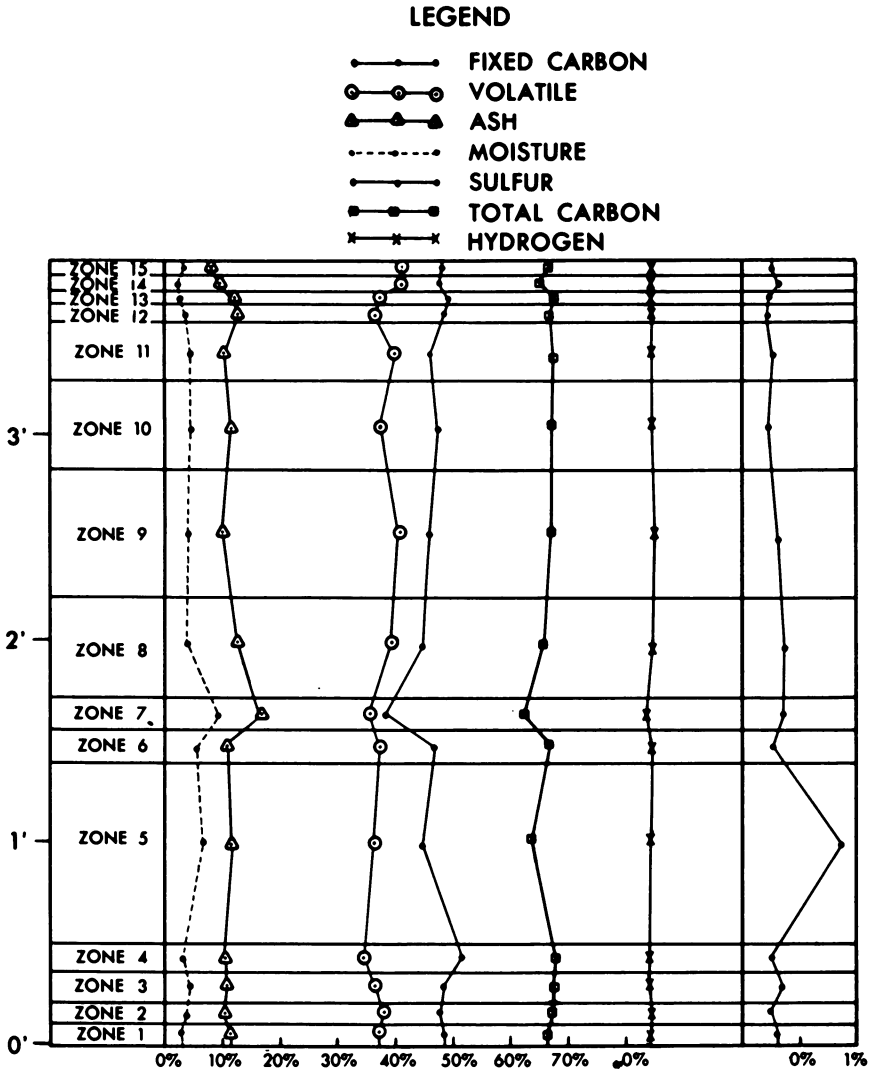

in Seam 4 and Seam 2

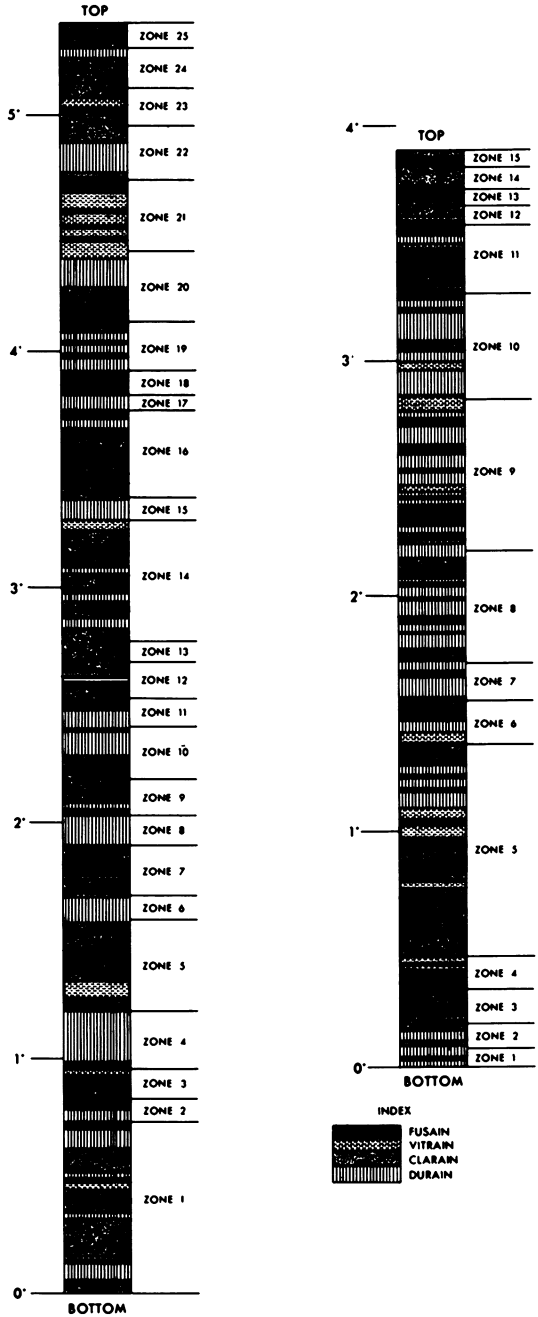

Figure 3. Megascopic descriptions of the column samples of Seam 4 (left) and Seam 2 (right)

Transmitted Light Studies. The maceral counts were conducted on a Leitz Panphot microscope at 500× using a point count technique. Five traverses were made on each section, 20 fields were measured in each traverse, and nine points were counted for each field. The thin section studies are summarized in the following sections. The terms used are those suggested by Spackman (*18*). Representative transmitted light photographs of the major macerals of the two seams are presented as Figure 6.

VITRINOIDS. Before describing the macerals in thin sections, it should be pointed out that the sections were prepared maintaining the uniform thickness throughout and the same standard conditions. As such, vitrinoids were distinguished on the basis of color as yellow, red, reddish-brown, and vitrinoids of any color with structure. The cell cavities of vitrinoids with structure are frequently filled by granular mineral matter, namely clay minerals. Sometimes fine grained micrinite is also observed in association with the mineral matter in the cell cavities of vitrinoids with structure.

Semifusinite is also included in the vitrinoid group of macerals. It is distinguished from fusinite by a degree of translucence in thin section and lower reflectivity in polished specimens. Semifusinites may be subgrouped according to appearance, which however was not attempted. The semifusinites very often occur as a transition stage between vitrinoids and fusinoids.

FUSINOIDS. Fusinite occurs in three forms, namely:

(1) Fusinite with small cells which show a sharp contact with the adjoining maceral and the cells are more or less granular in appearance.

(2) Fusinite with large cells which are not sharply defined from the adjoining macerals and the cells are irregular in appearance.

(3) Fusinite masses which may be mistaken for massive micrinite, but for its size. It is generally free from cell structure and occurs as lenticular masses.

Sclerotia are very rare in Seam 4 but are fairly common in Seam 2. They occur as lenticular or elliptical bodies with "cell" structure. These apparently represent the remains of fungal bodies, their form and size being irregular.

MICRINOIDS. Two types of micrinoids were distinguished—namely, (1) fine grained micrinoid and (2) massive micrinoid. The fine grained micrinoid material is generally associated with spores often filling up the spore cavity or sometimes filling the cell cavities of vitrinoids with structure.

It is possible to distinguish massive micrinoid from "massive" fusinoid. The massive micrinoid exhibits varying brightness and reflectance in reflected light. The differences in brightness of massive micrinoid in one and the same layer are not the same, which may suggest differences in sedimentary conditions. Generally the presence of cell structure is diagnostic for the fusinoids.

EXINOIDS. This group includes the macerals sporinite, cutinite, and resinite. On the basis of size, two types of spore material were recognized—namely, megaspores and "small spores." These are mostly confined to the durainic portions of the seams. The microspores are thin walled and are very small while the megaspores are relatively thick walled. In general, all the spores observed were pale yellow in color. The degree of preservation of the spores is better in the clarain portion than in the durain portion of the seam.

Publication Date: January 1, 1966 | doi: 10.1021/ba-1966-0055.ch018

Seam 4 is particularly characterized by the ribbon-like wavy bands of cutinite confined to the top portion of the seam. These cuticular bodies occur as long, thin, wisp-like bands open at both ends.

Figure 4. Petrographic

Publication Date: January 1, 1966 | doi: 10.1021/ba-1966-0055.ch018

In Coal Science; Given, P.;
Advances in Chemistry; American Chemical Society: Washington, DC, 1966.

Resinite was scarce in the above seams. It occurs as globular bodies in vitrinoids and occasionally as rodlets. Most of the time it was red in color, although in a few cases yellow color was not uncommon. Similar resinoid

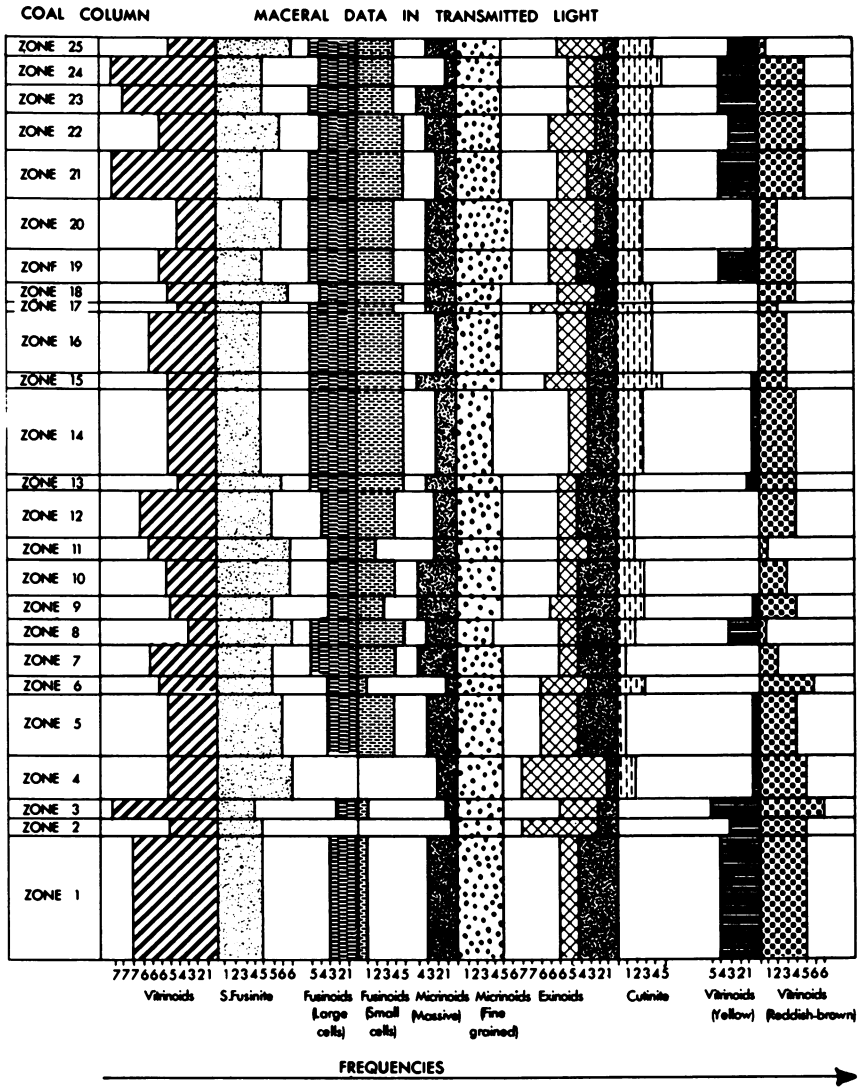

composition of Seam 4

Publication Date: January 1, 1966 | doi: 10.1021/ba-1966-0055.ch018

bodies, globular in appearance but interpreted as sclerotia, have been reported by Pareek (*13*) from Talchair coal.

MICROLITHOTYPES. On the basis of the percentage and proportion of the macerals, several microlithotypes can be distinguished in the above two seams. The first of these is vitrite consisting almost exclusively of the vitrinoid maceral with other macerals constituting less than 5%. It is generally and mostly monomaceralic in character. Megascopically it occurs as bright coal and occurs as bands of 1 cm. thickness. Sometimes clay minerals may occur as disseminations. It is noteworthy that invariably it is the red-colored vitrite that is generally associated with structure, while the yellow one is free (*4*).

The vitrite content varies considerably in the seams of Chirmiri and always constitutes less than 19%. In this respect, it closely resembles South

Publication Date: January 1, 1966 | doi: 10.1021/ba-1966-0055.ch018

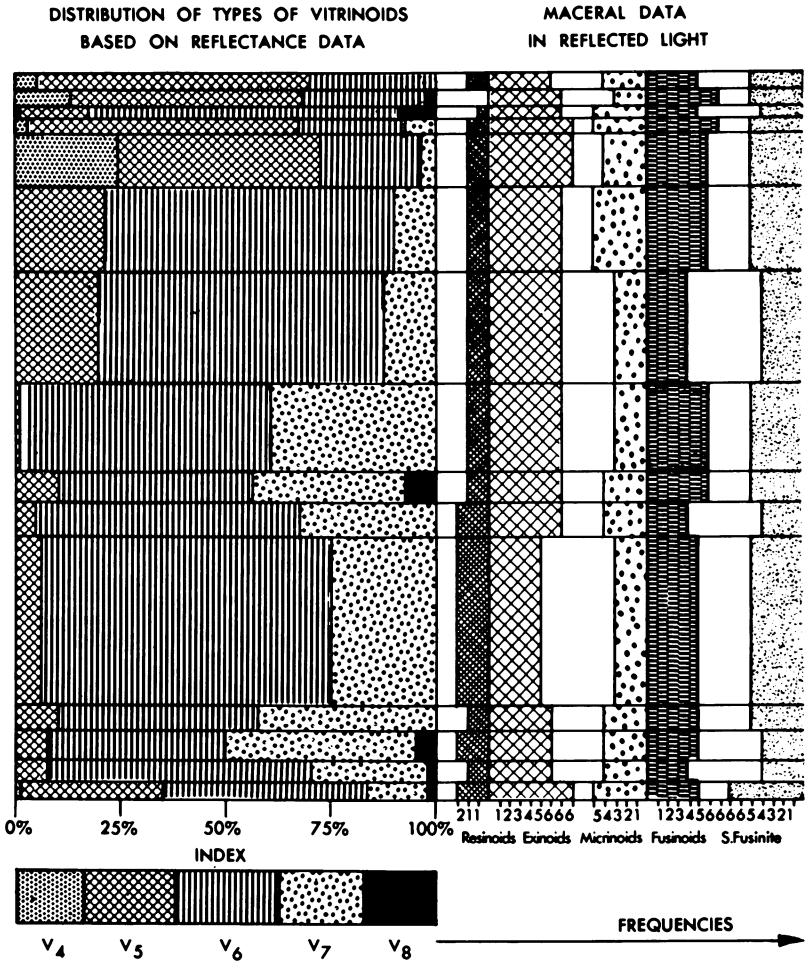

Figure 4a. Petrographic

African coals described by Snyman (*17*) and Australian coals described by Taylor (*19*) and differs from the European and American coals which contain as much as 50% vitrite described by Abramski *et al.* (*1*).

The chief microlithotypes noticed in the coals of Chirmiri are duroclarite and clarodurite. Duroclarite is dominant in zones 1–7 of Seam 4, while the microlithotype clarodurite is dominant in zones 8–25. Seam 2 is characterized by the microlithotype vitrinertinite V. This lithotype is predominant in the top and middle portion of the seam, while in the bottom portion duroclarite is predominant.

Interspersed between the above dominant lithotypes, fusite is common. A gradual transition from clarodurite to fusite is common in most cases.

Publication Date: January 1, 1966 | doi: 10.1021/ba-1966-0055.ch018

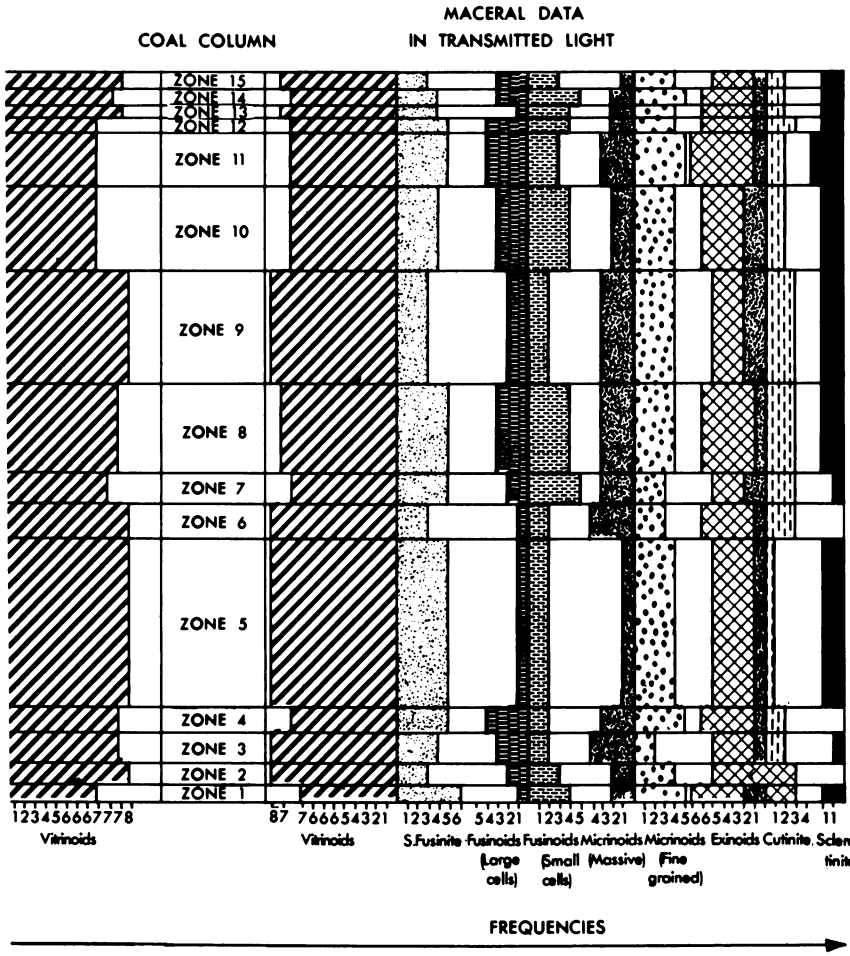

composition of Seam 2

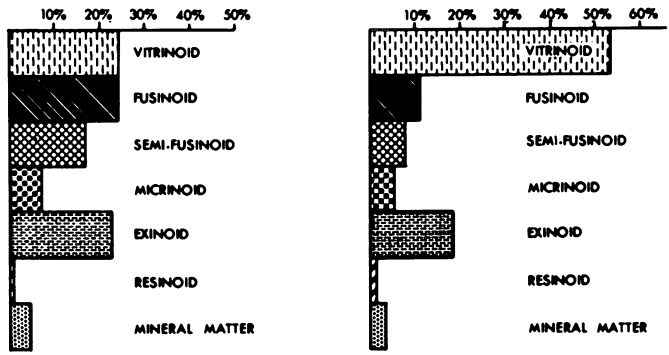

Figure 5. Average petrographic composition of Seam 4 (left) and Seam 2 (right)

On this basis of petrographic data from both transmitted and reflected light techniques, the seams can be classified into three units in the case of Seam 4 and four units in the case of Seam 2. These are:

Seam 4	I	Zones	17–25
	II	Zones	7–16
	III	Zones	1–6

Seam 2	I	Zones	11–15
	II	Zones	8–10
	III	Zones	4–7
	IV	Zones	1–3

This classification of the seams is justified and is well reflected in the proximate analyses and distribution of the vitrinoid types distinguished on the basis of reflectance values. The variation of the different macerals in each zone is shown in Figures 4 and 4a.

Thermal Studies

To ascertain the thermal characteristics of the reactives of the seams such as the temperature of initial melting, temperature of maximum fluidity, and the temperature of solidification, certain portions of vitrinoid bands were carefully selected and removed by microdissection, to avoid contamination, and stored in glass vials. A few pieces of the selected vitrinoids were placed in a Leitz hotstage where an inert atmosphere was maintained by circulating nitrogen. The temperature was raised gradually at a rate of 2°C. per minute. The effect of increasing temperature upon the vitrinoids was continuously observed using the Panphot microscope. No major change occurred in the vitrinoids even when they were held for one hour at temperatures as high as 650°C. The only change observed was that most specimens took on a light gray cast. In this respect they closely resemble the Gondwana coals described from Africa by Snyman (*18*) and by Hall (9). By contrast, many of the high volatile bituminous coals from North America become fluid even at temperatures of 450°C., attain maximum fluidity in the 550°C. range, and begin to solidify at 600°C.

Giesler plastometer tests were conducted on the vitrinoids of Seams 2 and 4, respectively. They did not show any fluidity characteristics at all, and the

Publication Date: January 1, 1966 | doi: 10.1021/ba-1966-0055.ch018

residue in the plastometer was a charred, noncoherent, granular material. This nonfluid nature can be attributed to an overabundance of "inerts" and a lack of the reactive vitrinoids such as types V_0 and V_{10}. Though Seam 2 is abundant in vitrinoids, they are all of the types below 0.9% reflectance.

Reflectance Studies

Polished pellets were prepared from all the zones of both the seams for reflectance measurements. These reflectance measurements were carried out on equipment standard in coal petrographic laboratories in North America. Two pellets were examined for each zone, and three traverses for each pellet and 20 readings for each traverse were recorded. The determinations were conducted maintaining the same standard conditions throughout the investiga-

Table III. Maceral Composition of Seam No. 4 and Seam No. 2

Zone No.	*Vitrinoids*	*Fusinoids*	*Micrinoids*	*Exinoids*	*Resinoids*	*Mineral Matter*	*Total*
Seam No. 4							
1.	43.9	16.6	14.8	18.8	0.3	5.6	100.0
2.	24.6	0.5	12.7	46.4	2.9	12.9	100.0
3.	62.0	6.2	10.4	16.5	1.1	3.8	100.0
4.	35.4	—	11.7	39.4	4.4	9.1	100.0
5.	30.4	13.1	13.7	31.6	5.6	5.6	100.0
6.	35.6	6.7	8.0	35.4	7.4	6.9	100.0
7.	37.4	28.0	11.5	19.6	1.7	1.8	100.0
8.	29.4	42.2	8.6	12.4	3.1	4.3	100.0
9.	24.9	26.4	15.2	27.6	3.1	2.8	100.0
10.	36.2	20.2	15.7	24.1	1.5	2.3	100.0
11.	40.3	23.9	8.3	22.5	1.8	3.2	100.0
12.	36.5	22.9	11.9	23.1	2.4	3.2	100.0
13.	25.4	39.7	8.8	21.4	1.2	3.5	100.0
14.	24.9	44.4	6.5	18.2	2.5	3.5	100.0
15.	23.3	24.2	14.9	31.8	2.6	3.2	100.0
16.	34.8	31.9	8.4	20.3	2.7	1.9	100.0
17.	15.6	9.8	25.4	40.2	3.5	5.5	100.0
18.	37.3	27.8	12.1	18.8	1.2	2.8	100.0
19.	27.8	20.1	17.3	28.3	3.3	3.2	100.0
20.	23.9	20.2	21.2	27.4	1.7	5.6	100.0
21.	45.5	16.3	10.6	21.1	4.2	2.3	100.0
22.	32.8	20.5	13.5	25.9	2.5	4.8	100.0
23.	38.8	27.0	11.6	16.4	4.3	1.9	100.0
24.	48.9	14.2	12.1	19.0	3.2	2.6	100.0
25.	31.1	27.4	14.1	20.2	2.6	4.6	100.0
Seam No. 2							
1.	47.51	10.19	12.32	22.84	1.96	5.18	100.0
2.	65.37	4.46	6.43	15.53	5.53	2.68	100.0
3.	66.92	9.04	6.26	13.31	1.17	3.30	100.0
4.	55.91	7.67	13.39	17.50	1.96	3.57	100.0
5.	70.69	6.88	4.49	12.74	1.54	3.66	100.0
6.	64.03	5.53	7.58	18.04	1.34	3.48	100.0
7.	53.55	17.12	5.34	18.02	2.76	3.21	100.0
8.	55.19	14.74	7.41	16.90	2.28	3.48	100.0
9.	65.16	6.49	5.69	17.08	2.50	3.08	100.0
10.	53.76	13.50	8.04	19.09	2.54	3.07	100.0
11.	46.72	16.69	10.18	21.33	2.32	2.76	100.0
12.	52.91	16.70	8.03	16.84	2.49	3.03	100.0
13.	57.97	9.47	5.58	19.66	3.21	4.11	100.0
14.	46.35	21.78	9.00	18.93	1.08	2.86	100.0
15.	61.23	12.69	5.18	12.15	3.93	4.82	100.0

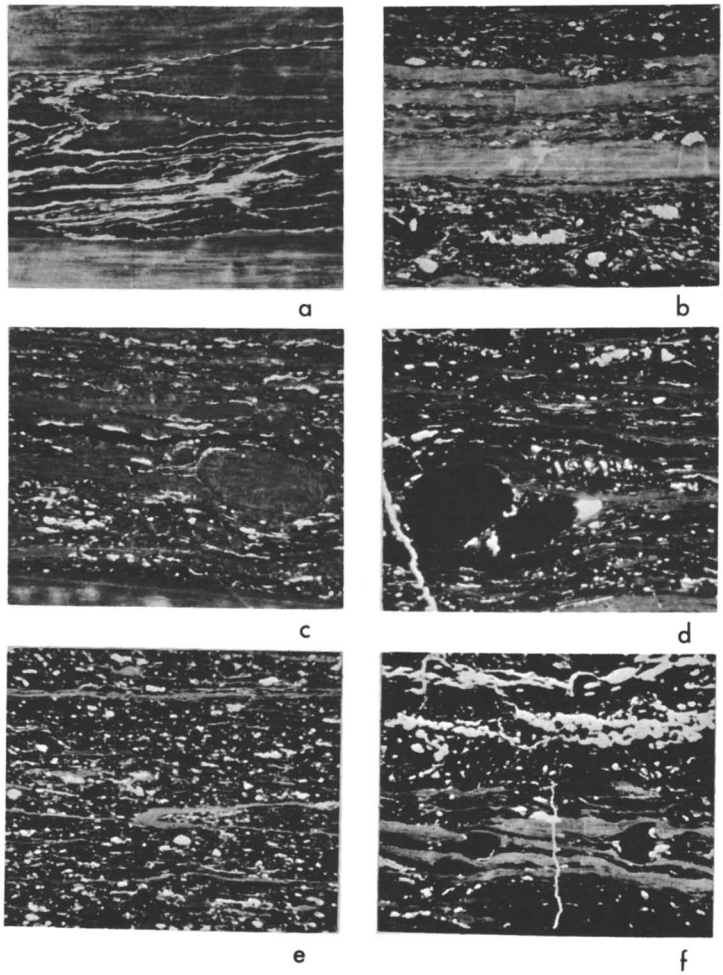

Figure 6. Representative maceral assemblages encountered in Seams No. 2 and 4, Madhya Pradesh, India

Photograph a—Red vitrinoid material with abundant yellow cuticular remains, some microspore remains also present. Both of the latter items are recorded as exinoids.

Photograph b—Bands of yellow vitrinoid across center of picture, abundant micrinoid and fusinoid material present throughout remainder of photograph.

Photograph c—Large, red resin body appears at right center of picture, with a band of micrinoid material extending across photograph above the red resinoid. Abundant microspores (exinoid) and finely divided micrinite (micrinoid) together with vitrinoids comprise the remainder of this section.

Photograph d—Two bodies of massive micrinoid material are shown at the left center of the picture. Abundant fusinoids, micrinoids and stringers of red vitrinoids comprise the remainder of the field of view.

Photographs e and f—Both photographs show typical occurrences of "inert" macerals with well developed large and small cells in the fusinoids. Stringers of vitrinoid material make up the bulk of the remainder of each photograph, with some spore material (exinoids) distributed in Photograph e.

Publication Date: January 1, 1966 | doi: 10.1021/ba-1966-0055.ch018

tions. The standard used had a reflectance value of 1.01%. The photomultiplier reading was checked for every 20 readings to determine current drift; whenever the drift was more than one dial reading, the readings were discarded.

Figure 7 represents the variation of the reflectance values in each zone of both the Seams 2 and 4. The distribution of the various types of vitrinoids encountered in various zones are represented in Figures 4 and 4a, respectively. Principally, the types of vitrinoids encountered are V_4, V_5, V_6, V_7, and V_8 with an abundance of V_6 type of vitrinoid. Next in abundance to V_6 are V_5 and V_7 followed by V_4 and V_8. From Figures 4 and 4a, it is noticed that V_8 is more abundant in Seam 4 than in Seam 2. Seam 4 is 40 feet below Seam 2, and as such, a general slight metamorphic grade may be expected.

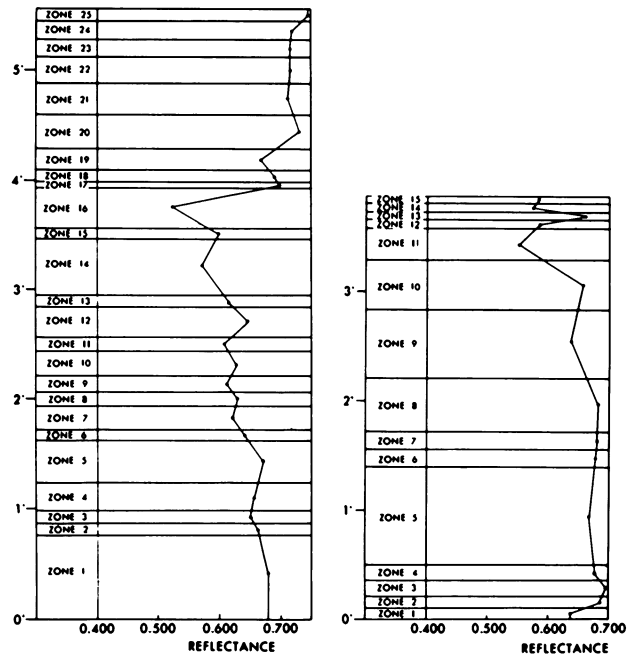

Figure 7. Variation of mean maximum reflectance in various zones of Seam 4 (left) and Seam 2 (right)

The histograms in Figure 8 show the distribution of vitrinoids in both the seams. Both the histograms generally show the same type of distribution with a peak of V_6, V_4, and V_8 on either side of the tail. The mean maximum reflectance values for each zone are presented in Table IV.

One of the authors had an opportunity to read the reflectance values of some of the coals of Permian age from Africa, Australia, and South America. These samples were randomly selected to ascertain the nature and types of vitrinoids present. This was possible through the courtesy of the Anthracological Laboratories of Bituminous Coal Research, Inc. The types of vitrinoids encountered varied from V_4 to V_9, with an abundance of V_6. In this respect

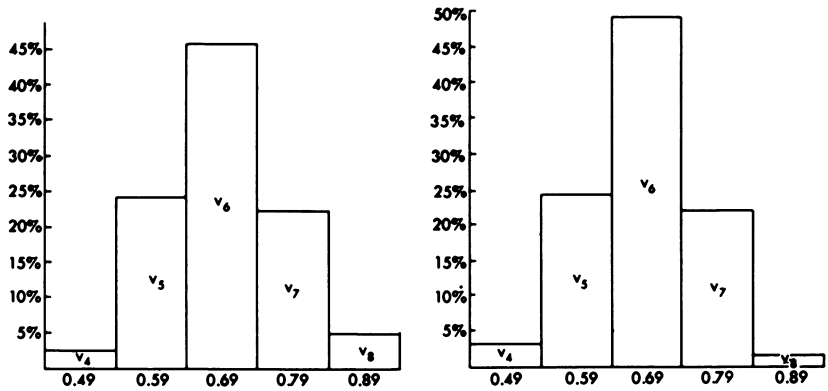

Figure 8. Histograms showing the distribution of vitrinoids based on reflectance. Seam 4 (left), Seam 2 (right)

there is a close similarity with the coals from Chirmiri of Gondwana age, while the vitrinoids encountered in the Carboniferous coals of North America are principally of V_8, V_9, V_{10} onwards excepting the coals from Illinois. This helps to explain why most of the American coking coals are of fluid type, and the coals of Gondwana age are of a nonfluid type.

Microhardness Studies

In order to ascertain the variation in hardness of the coal, microhardness investigations were conducted on vitrain bands using a Leitz microhardness tester. Polished blocks corresponding to the petrographically selected zones were used for the investigation. A set of 10 readings were taken on 10 spots randomly selected along the vitrain band. Table V represents the average hardness of 10 readings expressed in kg./sq mm. The hardness values range from 17.26 to 21.93 kg./sq. mm. in Seam 2 and from 16.50 to 22.78 kg./sq. mm. in Seam 4. There is no marked difference in the hardness value between the seams. The variations of hardness in different zones of both the seams are shown in Figure 9. Three distinct groups of zones in Seam 4 and four zones in case of Seam 2 could be recognized. They are:

Seam 4	Zone	18–25	Seam 2	Zone	12–15
	Zone	6–17		Zone	7–11
	Zone	1–5		Zone	3–6
				Zone	1–2

These zones are very close to the subdivisions established by petrographic studies except for some minor differences. The vitrains of these coals have lower hardness values than those of the high volatile bituminous coals of North America.

Palynological Investigations. All the zones petrographically delimited were macerated for the study of spore and pollen assemblages. They were macerated using Schulze's solution and then treated with 7% potassium hydroxide. The spores and pollen were mounted in glycerol jelly The spore and

Publication Date: January 1, 1966 | doi: 10.1021/ba-1966-0055.ch018

Table IV. Reflectance Values for Both Seams

Zone No.	Mean Maximum Reflectance	
	Seam No. 4	Seam No. 2
1.	0.680	0.639
2.	0.663	0.687
3.	0.652	0.696
4.	0.655	0.677
5.	0.673	0.668
6.	0.643	0.678
7.	0.623	0.680
8.	0.629	0.683
9.	0.611	0.638
10.	0.627	0.655
11.	0.608	0.555
12.	0.646	0.585
13.	0.614	0.660
14.	0.573	0.573
15.	0.598	0.581
16.	0.520	
17.	0.698	
18.	0.690	
19.	0.667	
20.	0.732	
21.	0.711	
22.	0.715	
23.	0.715	
24.	0.717	
25.	0.746	

pollen content of these coals is very close to that reported for the Gondwana coals of Africa and Australia by Snyman (*18*) and Balme and Hennelly (*2*). The detailed palynology of these seams is presently being investigated and will be presented at a future date.

Comparison of the Chirmiri Coals of Gondwana Age with Paleozoic Coals from Other Areas

The two coals from Chirmiri area are very similar in their petrography with the coals of Gondwana age described by Taylor (*19*) from Australia, by Snyman (*18*) and Plumstead (*14*) from Africa, by Marshall (*11*) from lower Gondwana coal fields, by Ganju (*8*) and Banerjee (*3*) from India, and by Schopf (*16*) from Antarctica. On the other hand, they vary considerably from the other Paleozoic coals of North America and Europe. The petrography of the two seams is very close to the petrography of the Australian and African coals except for slightly higher percentages of exinoids. Many of the coals of Gondwana age are of nonfluid types, generally characterized by vitrinoid types V_4, V_5, V_6, V_7, V_8 (of low reflectance), with a predominance of V_6. These Gondwana coals are characterized by a wide variation in their petrographic composition (*18*). Further, they are all characterized by a high percentage of ash.

Conversely, the paleozoic coals of North America and Europe are richer in vitrinoids and exinoids, falling under the category of clarite or durite poor in inertinoids. The abundance of granular micrinite (in North American coals)

Publication Date: January 1, 1966 | doi: 10.1021/ba-1966-0055.ch018

and the rare occurrence of massive micrinite characteristic of Gondwana coals, establishes an important difference between them. Besides, North American coals are generally lower in their ash content.

Economic Geology

In addition to contributing towards the basic petrographic knowledge of the coal seams, this detailed work, employing various techniques, was undertaken on these two seams to explore the possibilities for greater industrial exploitation. The primary use of this coal presently is for steam generation, mainly in railway locomotives.

The results of studies initiated indicate that these two coal seams may well possess a greater utilization potential than heretofore suspected. The petrographic studies have proved that these coals are noncoking as they do not have the required types of vitrinoids to induce fluidity during the coking process. Further, the ratio of optimum inerts to reactives, calculated after Schapiro, Gray, and Eusner (*15*), has shown that Seam 4 contains three times more inerts over optimum inerts, while Seam 2, although containing the required amount of inerts, does not have the types of vitrinoids necessary to induce fluidity during the coking process. Experimental tests conducted on these two seams indicate that some of the inerts could be eliminated by sizing and fractionating finer meshes. Petrographically it seems possible that a product with suitable coking characteristics may be produced by proportionally blending selected size fractions of these coal seams with a good coking coal, and thereby a portion of the good coking coal can be conserved. Secondly, it is good for

Publication Date: January 1, 1966 | doi: 10.1021/ba-1966-0055.ch018

Table V. Microhardness Determinations on Vitrain Bands for Seams No. 4 and 2

Seam No. 4		*Seam No. 2*	
Zones	*H.V. in kg./sq. mm.*	*Zones*	*H.V. in kg./sq. mm.*
1.	17.64	1.	21.93
2.	18.79	2.	20.94
3.	18.73	3.	17.26
4.	17.36	4.	17.89
5.	19.67	5.	18.95
6.	20.13	6.	18.66
7.	17.42	7.	20.27
8.	22.78	8.	19.06
9.	17.86	9.	21.04
10.	17.71	10.	18.55
11.	21.01	11.	21.09
12.	19.05	12.	18.55
13.	20.10	13.	18.25
14.	17.98	14.	18.85
15.	17.42	15.	19.38
16.	19.54		
17.	16.50		
18.	21.22		
19.	19.26		
20.	21.07		
21.	17.36		
22.	21.06		
23.	19.68		
24.	19.15		
25.	17.19		

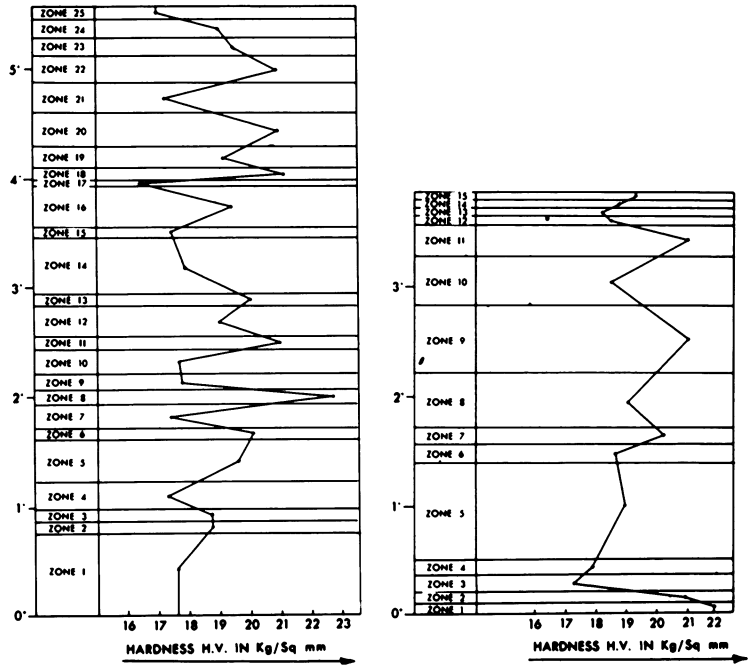

Figure 9. Variation of hardness in vitrinoids in each zone of Seam 4 (left) and Seam 2 (right)

steam generation, and it is possible to set a steam generation power plant at the mine site to supply power to a whole group of collieries and for other electrical energy demands as they develop in the area.

Conclusions

The two seams are characterized by macerals of varying types: for example, yellow, red, or reddish-brown vitrinoids with or without structure, fusinite with large and small cells, micrinite of massive and fine-grained variety, which points to the heterogeneity of the organic debris forming the macerals and to changes in environments during the formation of the coal swamps, consistent with the "Drift" theory of origin for Gondwana coals. Further, the amount of detrital mineral matter is high, which would indicate a movement of water bringing in sediments, probably periodic over-flooding of the area while the deposit was being formed.

The variation in petrographic composition is very pronounced in these two seams of Gondwana age as compared with the carboniferous coals of the United States. The two seams from Chirmiri are characterized by a wide variation in the percentages of vitrinoids and inertinoids, and they are high in exinoids and in ash content. The transition stages of massive micrinite are very pronounced, and the granular micrinite is scarce. Further, the gradual transition from vitrinoid to semifusinoid is very frequent.

These petrographic properties perhaps could be explained by differences in climate and vegetation as compared with the coals of the United States of autochthonous origin. The differences can possibly be explained better by envisaging different conditions of origin for these coals of Gondwana age from India, namely a drift origin.

Acknowledgments

The authors express their thanks to the Chirmiri Colliery staff for granting permission to sample their seams and to Diwan and Bala Krishna for help in sampling. The first author thanks the Fulbright authorities for providing a grant to carry out the above investigations. Finally, the authors thank the many people who have helped in one way or the other in the above investigations, particularly William Spackman, Director of Coal Research at The Pennsylvania State University.

Literature Cited

(1) Abramski, C., *et al.*, "Atlas Für Angewandte Steinkohlenpetrographie," Gluckauf, Essen, 1951.
(2) Balme, B. E., Hennelly, J. P. F., *Australian J. Botany* **3,** 89 (1955).
(3) Banerjee, A. K., *Records Geol. Surv. India* **66,** 333 (1932).
(4) Dutcher, R. R., Ph.D. thesis, The Pennsylvania State University, 1960.
(5) Evans, P., Hayman, R., Majeed, R. J., *Quart. J. Geol. Mining Met. Soc. India* **6,** 40 (1934).
(6) Fermor, L. L., *Mem. Geol. Surv. India* **41,** 150 (1914).
(7) Fox, C. S., *Mem. Geol. Surv. India* **59,** 207 (1934).
(8) Ganju, P. N., *Mem. Geol. Surv. India* **83,** 1 (1955).
(9) Hall, P. E., *Fuel* **9,** 373 (1930).
(10) Huges, T. W.H., *Mem. Geol. Surv. India* **21,** 59 (1885).
(11) Marshall, C. E., *Econ. Geol.* **54,** 20 (1959).
(12) Moore, E. S., "Coal," p. 69, John Wiley and Sons, New York, 1940.
(13) Pareek, H. S., *J. Palaeontol. Soc. India* **3,** 214 (1958).
(14) Plumstead, E. P., "Coal in Southern Africa," p. 24, Witwatersrand Univ. Press, Johannesburg, 1957.
(15) Schapiro, N., Gray, R. J., Eusner, G. R., *Trans. A.I.M.E.* **21,** 89 (1961).
(16) Schopf, J. M., *Ohio State Univ. Inst. Polar Studies, Rept.* **2,** 40 (1962).
(17) Snyman, C. P., *Pub. Univ. Pretoria* **15,** 5 (1961).
(18) Spackman, W., *Trans. N. Y. Acad. Sci.* **20,** 411 (1958).
(19) Taylor, G., Warne, S. St. J., *Proc. Intern. Comm. Coal Petrology, No. 3* (1958).
(20) Zubovic, P., Stadnichenko, T., Sheffey, N. B., *U.S. Geol. Surv. Bull.* **1117-B** (1964).

Received April 21, 1965. Contribution No. 64-18, Mineral Industries Experiment Station.

Properties of Coal Macerals

Infrared Spectra of Resinites and Their Carbonized and Oxidized Products

DUNCAN G. MURCHISON

Department of Geology, University of Newcastle, England

Publication Date: January 1, 1966 | doi: 10.1021/ba-1966-0055.ch019

Infrared spectra of resinites varying in rank were recorded between 4000 and 667 cm.$^{-1}$ and fell into two contrasting groups linked only by a transitional spectrum of thermally metamorphosed resinite. Resinites from bituminous coals display strong absorption from nonaromatic C-H groups, a weak carbonyl absorption and weak aromatic bands that indicate a similar type of substitution to sporinites of equivalent rank. Carbonization causes increase in structureless absorption, probably owing to growth of aromatic lamellae and reduction of aliphatic groups which are also lost during oxidation when the carbonyl band strengthens. Intense absorption from aliphatic or alicyclic groups, a strong carbonyl band, and an absence of the 1600 cm.$^{-1}$ absorption typify lower rank resinites. Of extremely low aromaticity, they fail to give an aromatic char when carbonized and show little spectral change on oxidation.

Until Bent and Brown (*2*) in 1961 published a series of infrared spectra of the group macerals vitrinite, exinite, and inertinite, that were separated from coals of different rank by Fenton and his colleagues (*7*), only the spectral characters of vitrinite had been intensively studied. Monnot and Laddam (*15*) earlier had published infrared spectra of vitrinite and associated exinite in one coal, and Dormans, Huntjens, and Van Krevelen (*5*) had likewise discussed the spectra of vitrinite, exinite, and micrinite from a single coal. The picture that emerged from Bent and Brown's investigation was that spectra of vitrinite and exinite show many similar features: these contrast with spectral characters of the inertinite group which display strong structureless absorption that is probably of electronic origin. The main difference between the vitrinites and

In Coal Science; Given, P.;
Advances in Chemistry; American Chemical Society: Washington, DC, 1966.

exinites lay in their degree of aromaticity. Exinite was found to be substantially lower than vitrinite of the same coal, but the aromaticity increased and became more similar to that of vitrinite with increasing coalification. Besides higher nonaromatic C-H absorption, the exinites of lower rank also showed a weak absorption band at 1700 $cm.^{-1}$ that was attributed to a C=O group; this band does not occur in the spectrum of fresh vitrinite.

The term exinite refers to a group of four macerals of which three—sporinite, resinite, and cutinite—occur ubiquitously in autochthonous coals. The fourth maceral, alginite, is encountered less frequently since it is almost exclusively a constituent found in allochthonous coals. In any single normal coal the bulk of the sporinite, resinite, and cutinite will display broadly similar properties under the microscope, but sporinite usually far exceeds resinite and cutinite in amount. Because of this the "float and sink" method used by Fenton and others to concentrate the group macerals yields fractions that are rich in sporinite. Bent and Brown's spectra thus referred essentially to sporinites in a range of bituminous coals with vitrinites of carbon content extending from 79.6 to 88.6% (dmmf).

Successfully applying the method used by Fenton to prepare his concentrates depends upon two factors. First, there must be adequate density differences between the macerals in the sample, and second, there must be an initially high concentration of the required maceral. In attempting to separate either resinite or cutinite from sporinite of the same coal, neither of these conditions can be fulfilled, at least when the coal is of bituminous rank or higher. If, however, samples on a semimicroscale are acceptable, it is possible to prepare concentrates of resinites of satisfactory purity from bituminous coals by simple mechanical means. The method has been described by Murchison and Jones (*17*) and mainly involves picking with fine probes on differently prepared surfaces of coal under a stereoscopic microscope. Resinites from lignites pose less of a problem because their occurrence in fairly substantial lumps is quite common; these and fossil resins such as kauri gum and amber usually can be prepared to a purity of almost 100% with ease.

Definition and Microscopic Characters of Resinite

The appearance of resinite under the microscope is well known to coal petrologists. Unfortunately, the term when used as presently defined in the International Handbook of Coal Petrography (*10*), can refer to constituents in a single coal which, although they might all have originally been resins, are now variably polymerized and exhibit marked differences in optical properties which presumably reflect chemical differences. If physical and chemical constitution, instead of origin and morphology, are used as a basis for classification, the bulk of these constituents would be grouped under exinite, but many of the remainder would be classed under vitrinite and the rest with inertinite. It was the lack of a meaningful, quantitative definition to describe the constituent isolated from various bituminous coals that led the present author and a colleague to refer in a recent article (*11*) to "resinite (sensu stricto)." Although no more than a temporary solution to the problem, this was an

Publication Date: January 1, 1966 | doi: 10.1021/ba-1966-0055.ch019

attempt to exclude from consideration those resinites which, on grounds of microscopical characters that reflected their physical and chemical constitution, could not be properly grouped under the term exinite. Typical resinite isolated for infrared and other studies is shown in Figure 1. Such resinite, although similar in properties to the sporinite of the same coal, is not necessarily homogeneous in appearance but may display areas with reflectivities that lie between that of the bulk of the resinite and vitrinite of the same coal. This is a very characteristic feature of globules and other masses of resinite; further comment will be made on this point later in the text. The concentrates of the bituminous coal resinites employed for this study contained differing amounts of material whose reflectivity exceeded that of the main mass of the exinite in the coals, but this was always less than 10% by volume.

Publication Date: January 1, 1966 | doi: 10.1021/ba-1966-0055.ch019

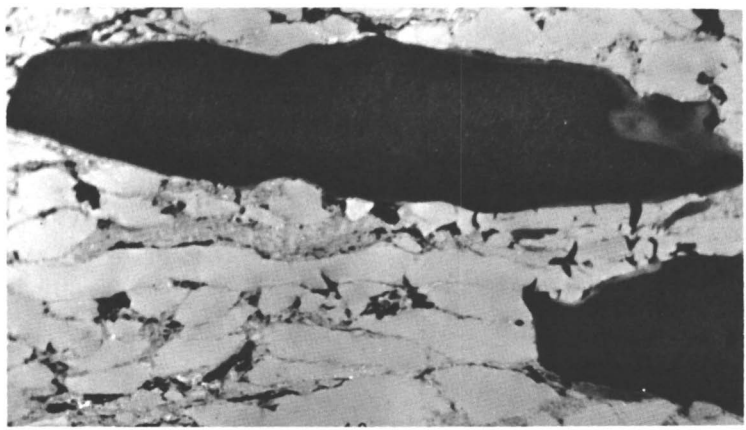

Figure 1. Dark gray, low reflecting resinite globules in bituminous coal, typical of the material isolated for chemical study; relief-polished surface, oil immersion, incident light; × 350

The resinites isolated from lignites, the other fossil resins, and the gums that were studied did not present any classification difficulties. There would be no hesitation in placing all those samples referred to here in the exinite group. The gums have differing origins. Three of the gums were taken from a bottled departmental collection (samples 2, 3, and 4, Table I); unfortunately no information exists about the environment in which these gums were found, but there is little doubt from their appearance that they were either hardened lumps which lay on the surface or were below ground for a very short period of time. The kauri gum was taken from a young peat, and the amber came from the East Prussian Tertiary deposits. With the exception of the amber, these samples can be regarded as very young fossil resins barely influenced by any biochemical processes operating at the start of peat formation. They have been included here primarily because their spectra may show many, if not all, the spectral characters of the precursors of resinites in coals and because they also form the earliest stage in the resinite coalification series.

Elementary Composition of the Samples

Complete analytical details of most of the samples referred to here were given in an earlier article (*18*). The results are summarized in Table I and are presented on a dry ash-free basis fully corrected for contamination by other macerals.

Table I

			Analysis[a]				
		Equivalent				*Atomic ratios*	
Sample	*Locality*	*vitrinite*	*C*	*H*	*O*	*H/C*	*O/C*
1. Kauri Gum	New Zealand	—	76.8	10.1	13.2	1.57	0.129
2. White Angola	West Africa	—	78.9	10.5	9.6	1.59	0.091
3. Gum Dammar	Batavia	—	81.4	11.0	6.6	1.61	0.061
4. Gum Mastic	Isle of Chios	—	74.5	9.7	14.8	1.55	0.149
5. Amber	Baltic	—	74.1	9.4	15.8	1.51	0.160
6. Resinite (L)[c]	Mücheln, near Merseburg	—	81.9	10.3	6.1	1.50	0.056
7. Resinite (L)	Schleenhain, E. of Leipzig	—	—	—	—	—	—
8. Resinite (L)	Edderitz, N. of Halle	—	—	—	—	—	—
9. Resinite (L)	Goitsche (Bitterfeld)	—	79.7	10.0	8.5	1.50	0.080
10. Duxite (L)	Ervenice (Seestadtl)	—	82.2	10.0	5.3	1.45	0.048
11. Resinite (B)[b]	Yard Seam, Northumberland	83.0	81.1	9.2	7.0	1.35	0.065
12. Resinite (B)	Grey Seam, Northumberland	82.7	81.2	8.9	7.8	1.28	0.071
13. Resinite (B)	Plessey Seam, Northumberland	84.5	82.6	7.4	7.9	1.04	0.070
14. Resinite (B)	Winter Seam, Yorkshire	84.1	83.3	8.2	7.6	1.16	0.068
15. Resinite (B)	Top Busty Seam, Northumberland	84.5	84.1	8.2	6.5	1.16	0.058
16. Resinite (B)	Three Quarter Seam, Northumberland	85.1	84.3	7.4	6.2	1.04	0.055

[a] Percent by weight; dry, ash free
[b] (B)—Bituminous Coals
[c] (L)—Lignites

Experimental

The spectra were obtained using varying concentrations of finely ground samples dispersed in translucent pressed plates of potassium bromide. This technique was chosen primarily because of its convenience and because potassium bromide does not produce any specific absorptions in the region studied—4000 to 667 cm^{-1} (2.5–15 microns). The principal objection to this technique is the development of an OH band centered close to 3450 $cm.^{-1}$ which is caused by moisture absorption, either by the sample or by potassium bromide during preparation. This and other regions in which OH absorptions occur is more satisfactorily studied by grinding the sample in a mull of Nujol, hexachlorobutadiene, or other suitable liquid after drying under vacuum at 100°C. In the case of the resinites, however, certain ones of low rank showed a tendency to dissociate under weak vacuum even at room temperature; kauri gum, for

Publication Date: January 1, 1966 | doi: 10.1021/ba-1966-0055.ch019

example, liberated substantial quantities of α-pinene under these conditions. This behavior of resinites was a further incentive at the time of this investigation to use the potassium bromide technique and avoid rigorous drying of the samples.

The resinites were first ground, only several minutes grinding being necessary to reduce the maceral to very fine particle size. No improvement in the spectra was achieved if the resinites were subjected to preliminary grinding for several hours in an agate ball mill before blending with potassium bromide. Blending the finely ground resinite and dried potassium bromide was carried out by hand using an agate pestle and mortar, the mixing taking between 3 and 4 minutes. The most satisfactory spectra of resinites from bituminous coals were obtained using proportions by weight of 1:150 sample to potassium bromide. Lower rank resinites gave better spectra with weight proportions of between 1:125 and 1:100 sample to potassium bromide. Because of the small amounts of resinite from bituminous coals available for all investigations, only sufficient resinite to prepare a single potassium bromide disc was abstracted at any one time. This saved grinding the whole concentrate to fine particle size which would not have been economical in terms of material; the procedure did not appear to introduce any significant sampling error.

Spectra were obtained with a Grubb Parsons double beam GS2 spectrometer with a fore-prism unit of interchangeable calcium fluoride (5000–2000 $cm.^{-1}$: 2–5 microns) and potassium bromide (2000–667 cm.: 5–15 microns) prisms, a reflection grating for final dispersion and automatic slit programming. The instrument charts gave a plot of percentage absorption against wavelength in microns. For convenience and ease of comparison, the spectra have been "stacked" in the figures of this paper.

Publication Date: January 1, 1966 | doi: 10.1021/ba-1966-0055.ch019

Results

Spectra of Untreated Resinites. Bituminous Coals. The resinite spectra have been arranged in three groups (Figures 2–4). Those from bituminous coals are shown in Figure 2. Because resinite and sporinite from any coal of this general level of rank are more similar in their properties to one another than to any other maceral of the coal, their infrared spectra would not be expected to show striking differences. All the main absorption bands occurring in the spectra of lower rank sporinites are found in the resinite spectra. The relative intensities of these absorptions are similar for both macerals at the same level of rank. It should be noted, however, that the resinites from bituminous coal discussed here come from a more restricted rank range (vitrinite carbon contents: 82.7–85.1%) than the sporinites examined by Bent and Brown (vitrinite carbon contents: 79.6–88.6%). Resinite with the microscopical characters referred to earlier in this paper has not been found by the writer in coals with vitrinites of carbon content higher than about 86.5%. If it does occur in higher rank coals, then it is unlikely that the maceral can be separated by the mechanical method described earlier.

The most striking feature of the resinite spectra is the strong absorption arising from nonaromatic hydrogen groupings. Aromatic hydrogen is responsible only for weak or very weak absorptions that occur mainly at 750 $cm.^{-1}$, 812 $cm.^{-1}$, and between 855 and 870 $cm.^{-1}$. These bands appear to bear a similar relationship to one another as do those occurring in lower rank vitrinites (3) and sporinites (2) which suggests the same form of aromatic substitution. While most of the sporinites examined by Bent and Brown displayed

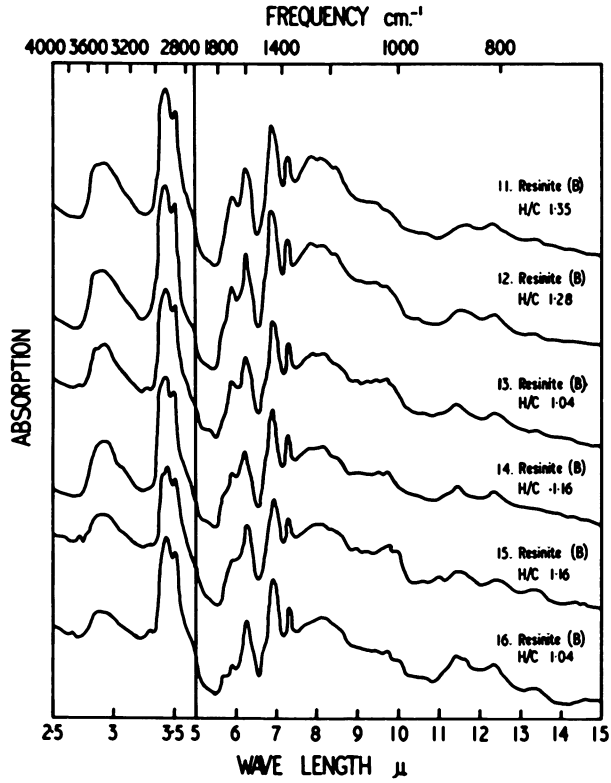

Figure 2. Infrared spectra of resinites from bituminous coals

an aromatic C-H stretching absorption close to 3030 cm.$^{-1}$ that increased in intensity with rising coalification, only the spectra of samples 13, 15, and 16 show a weak band near to this wave number. Samples 13 and 16, which have the lowest atomic ratios, H/C, show the strongest development of this absorption, which is most probably caused by aromatic C-H stretching vibrations although it is centered nearer to 3050 cm.$^{-1}$ than to 3030 cm.$^{-1}$.

As in sporinites the very intense and broad band with peaks at 2860 and 2912 cm.$^{-1}$ testifies to the presence of large numbers of CH_2 groups in resinites. Both macerals show a strong C-H deformation vibration at 1450 cm.$^{-1}$, but this is accompanied in the resinites by an absorption of weak to medium intensity at 1370 cm.$^{-1}$ that is absent or very weak in the sporinite spectra.

Little comment can be made about the hydrogen-bonded OH groups that absorb close to 3300 cm.$^{-1}$. It is unlikely, however, within the rank range of resinites covered here that much variation in the intensity of this absorption would be recorded. The broad region of absorption between 1100 and 1300 cm.$^{-1}$ common to vitrinite and sporinite spectra is also found in the resinite spectra. The peak at 1270 cm.$^{-1}$ almost certainly corresponds to the 1250 cm.$^{-1}$ band assigned by other workers to hydrogen-bonded phenolic structures. Fol-

Publication Date: January 1, 1966 | doi: 10.1021/ba-1966-0055.ch019

lowing the pattern of other maceral spectra, the level of absorption in this region lessens with advancing coalification.

The now familiar and much discussed absorption at 1600 cm.$^{-1}$ that may be caused by several groupings (C=C, oxygen-containing groups and hydrogen-bonded carbonyl groups), also occurs in the resinite spectra. As in the sporinite spectra the band is accompanied by an absorption near to 1700 cm.$^{-1}$ that must be assigned to carbonyl groups. The intensity of this absorption decreases with increasing coalification. The relative intensities of the 1600 cm.$^{-1}$ and the 1450 cm.$^{-1}$ bands of resinite and vitrinite from the same coal show considerable differences. In the vitrinites either the two bands peak at similar absorption levels or the 1600 cm.$^{-1}$ band is the stronger; in the resinites the 1600 cm.$^{-1}$ band is invariably much less intense than the 1450 cm.$^{-1}$ absorption. Perhaps the influence of groupings contributing to the 1600 cm.$^{-1}$ band is greater in the case of the vitrinites. On the other hand, it seems more likely that the absolute intensity of the 1600 cm.$^{-1}$ band for both macerals is similar and that the stronger 1450 cm.$^{-1}$ absorption in the resinites reflects larger amounts of aliphatic (or alicyclic) material in this maceral.

Because of the method used to separate the resinites from the coals, absorption bands caused by mineral matter may occur. Clay minerals or mixtures of clay minerals form the most frequent contaminant, and their presence has had to be accepted as an unavoidable hazard, although contamination can usually be kept to a minimum. There seems to be no economical way however of removing finely dispersed and intermixed syngenetic mineral matter from mechanically separated concentrates that are small in size. Fortunately, most of the clay mineral absorptions lie away from the main maceral absorptions, although a number do interfere with interpretation at frequencies above 900 cm.$^{-1}$. Carbonates also produce absorptions that affect this region, but in addition they cause an intense and broad band centered at 1430 cm.$^{-1}$. Clay mineral absorptions are present in spectra 13–16. Taking sample 15 which shows the most severe contamination as an example, the weak absorptions centered close to 3700, 1100, 1030, 1005, and 915 cm.$^{-1}$ almost certainly belong to kaolinite or a mixture containing large amounts of kaolinite. Other absorptions from this mineral will be obscured in the region 690–800 cm.$^{-1}$ by C-H out-of-plane vibrations caused by the resinite. The absorption appearing near to 870 cm.$^{-1}$ in this and other samples may in part be owing to the presence of carbonates. On the basis of the strength of this absorption, however, the amounts present are probably small, but there will be some enhancement of the resinite 1450 cm.$^{-1}$ band by the carbonates which possess a strong absorption close to 1430 cm.$^{-1}$

Lignites and Lower Rank Deposits. Of several infrared studies of vitrinites or coals with high vitrinite contents, only one (*12*) extended over the complete coalification series from cellulose and lignin to anthracite. The spectra of this investigation demonstrated gradual changes in frequencies and the relative intensities of absorption bands with rising rank. Accepting the view of normal coalification that is widely held at the present time where each constituent undergoes a continuous but not necessarily uniform alteration, it might be expected that resinites would display similar spectral changes if

Publication Date: January 1, 1966 | doi: 10.1021/ba-1966-0055.ch019

examined over a wide enough range. The difficulty of obtaining resinites higher in rank than those isolated has already been explained. Lower rank resinites were, however, obtained quite easily from a number of sources; their spectra are shown in Figures 3 and 4.

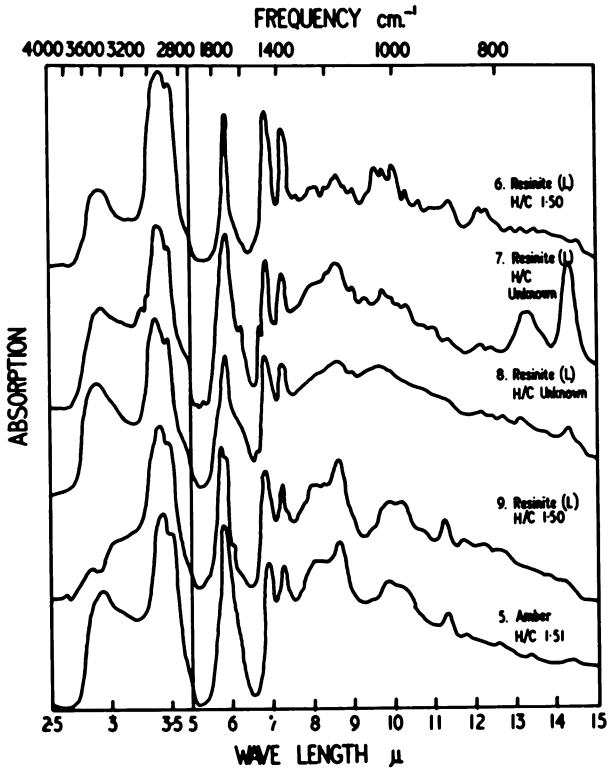

Figure 3. Infrared spectra of amber and resinites from lignites

Both groups of spectra show greater complexity than the spectra of resinites from bituminous coals, particularly in the region below 1250 cm.$^{-1}$ in which numerous but generally weak absorption bands occur. A complete and realistic interpretation within this region would be virtually impossible without considerable chemical study, and it was not the intention of the present investigation to cope with this problem. It was hoped to establish how the absorption pattern of lower rank resinites compared with that of the maceral in bituminous coals and in particular to see what spectral characters were possessed by possible precursors of bituminous coal resinites.

Most of the variation between the spectra of Figures 3 and 4 occurs below 1250 cm.$^{-1}$. Above this frequency all the spectra are strongly similar in pattern, and some of these similarities extend to the spectra of Figure 2. Common to all the spectra is the intense absorption from nonaromatic C-H groups with

Publication Date: January 1, 1966 | doi: 10.1021/ba-1966-0055.ch019

the bands caused by C-H stretching vibrations around 2900 cm.$^{-1}$ showing close similarity. In the lower rank resinites, however, there is some variability in the relative intensities of the absorptions resulting from deformation vibrations at 1450 cm.$^{-1}$ and 1370 cm.$^{-1}$. Generally, the lower the rank, the more intense is the absorption at 1370 cm.$^{-1}$ and the more similar it becomes in strength to the 1450 cm.$^{-1}$ band. In the spectra of resinites from bituminous coals, it is usually of weak to medium intensity, but it is a medium to strong band in the spectra of all the lower rank resinites. This argues for substantial numbers of CH_3 groups in the initial resinite structure; these are reduced with increasing coalification.

Friedel and Queiser (9) in a discussion of the anthraxylon (vitrinite) spectrum, have stated that aliphatic chains would produce a band at 1464 cm.$^{-1}$ whereas CH_2 groups in rings would absorb at 1450 cm.$^{-1}$. Almost all the

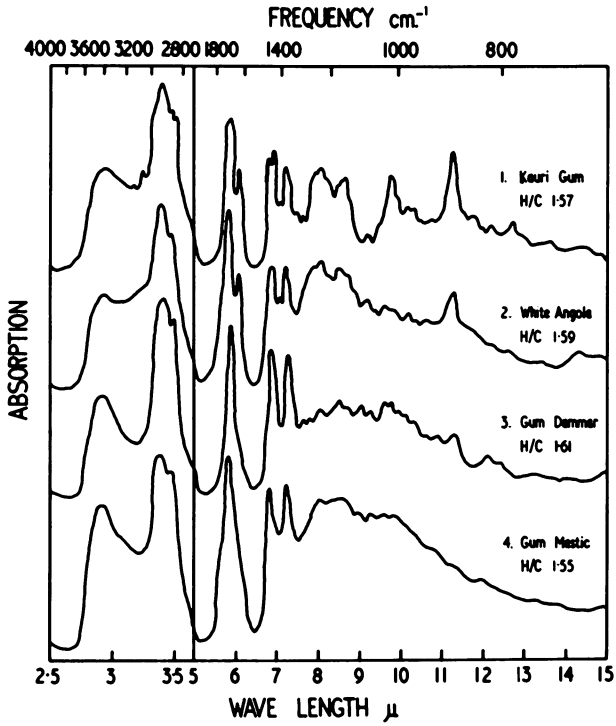

Figure 4. Infrared spectra of fossil gums

resinite spectra show an intense band with a peak at 1450 cm.$^{-1}$, although in several cases the original trace shows either a faint shoulder on the main band or a very weakly developed second peak occurring at about 1465 cm.$^{-1}$. It would be unwise, however, on the basis of this evidence alone to make specific assignments to rings and chains. Bellamy (*1*) gives 1465 ± 20 cm.$^{-1}$ as the frequency for either rings or chains and points out that various

Publication Date: January 1, 1966 | doi: 10.1021/ba-1966-0055.ch019

factors including physical state may affect the position of the band. Furthermore, the C-CH_3 vibration also lies at 1450 ± 20 cm.$^{-1}$. While the precise nature of the groups contributing to the 1450 cm.$^{-1}$ band cannot be decided, there is certainly evidence for the presence of olefinic groups in the lowest rank resinites, for example, kauri gum and white angola. Absorptions occur in these spectra near to 885, 1640, and 3070 cm.$^{-1}$; these could be attributed to a grouping of the type $CR_1R_2{=}CH_2$. Amber also shows a weaker development of these same bands, but they are apparently absent in the higher rank materials.

While intense absorption from nonaromatic C-H groups is common to all the spectra, pronounced differences are found between resinites of bituminous coals and those of lower rank in the spectral region extending from 1500 to 1800 cm.$^{-1}$. The band owing to carbonyl absorption in low rank resinites is extremely strong and contrasts with the weak absorption at almost the same frequency in resinites of higher rank coals. Bent and Brown (*2*) have suggested that this absorption may have arisen in their sporinite spectra as a result of oxidation during separation of the sporinites from the bituminous coals. Also, the writer was unable to collect the resinites from lignites and lower rank deposits himself. These were obtained from many different sources in which the resinites no doubt existed under varying storage conditions. It is possible that these samples became oxidized to varying degrees between the time they were collected and received in the laboratory for study. The intense carbonyl band at 1700 cm.$^{-1}$ would then have to be attributed to this oxidation.

Dealing first with the possibility of oxidation of the sporinite during preparation, the time required to prepare such a sporinite sample by grinding and flotation methods can be as long as 24 hours during which oxidation could feasibly occur. Murchison (*16*), has, however, pointed out that a resinite sample sufficient for infrared study can be isolated from bituminous coal and prepared in a potassium bromide disc in a much shorter period of time, perhaps as little as 20 minutes. A weak carbonyl absorption, similar to that in the sporinite spectrum, still occurs. Even when the resinite is ground for as long as 30 minutes in a stream of oxygen before blending with potassium bromide, the intensity of this absorption is unaffected. It is difficult to believe that if a sample were reactive enough to take up oxygen when initially isolated from the coal, it would fail to take up more oxygen when subjected to prolonged grinding in an oxygen stream. If the lower rank resinites have oxidized during storage, then the strength of the carbonyl absorption suggests that the oxidation has been severe. However, there seems to have been no reduction in absorption owing to nonaromatic C-H groups which would surely have been expected with such severe oxidation. The writer, therefore, prefers to regard the carbonyl band in resinite (and in sporinite), as resulting from a group inherent in the structure, at least from the time the resinite was deposited, if not even earlier in its history. There would be ample opportunity for both resins and spores to oxidize partially under atmospheric influences before their incorporation in the coal-forming peat rather than later when their reactivity had been reduced by diagenetic and metamorphic processes that raised their rank.

Publication Date: January 1, 1966 | doi: 10.1021/ba-1966-0055.ch019

The precise nature of the carbonyl groups giving rise to the absorption near to 1700 cm.$^{-1}$ is uncertain. The range of wave number involved is very small. With one exception which shows peaking at 1689 cm.$^{-1}$, the bituminous coal resinites display this absorption at 1695 cm.$^{-1}$ The resinites from lignitous coals show the absorption between 1703 and 1709 cm.$^{-1}$ and the lowest rank resinites examined have the band between 1694 and 1702 cm.$^{-1}$; amber has its peak at 1730 cm.$^{-1}$, but there may be a weak shoulder around 1709 cm.$^{-1}$ in this substance. In the region covered by these absorptions, carboxylic acids and aldehydes absorb, particularly the aryl aldehydes. The range is generally too low for ketonic carbonyl absorptions, although Bellamy (*1*) quotes both saturated open chain ketones and six- and seven-membered ring ketones absorbing as low as 1705 cm.$^{-1}$ One of the more interesting substances in relation to resinites and their carbonyl absorptions near to 1700 cm.$^{-1}$ is the diterpene abietic acid which is an important component of rosin that occurs in various species of pine. The spectrum of the acid shows an intense absorption centered round 1698 cm.$^{-1}$ as does the triterpene oleanolic acid. In several of the spectra of the lower rank resinites a weak absorption also occurs between 1720 and 1730 cm.$^{-1}$ as a shoulder on the main carbonyl band. Since a similar band develops in the spectrum of abietic acid when it undergoes air oxidation, this suggests that some of the lower rank resinites may be partially oxidized.

The absence of an intense absorption band at 1600 cm.$^{-1}$ in low rank resinite is probably the most striking difference between these substances and the resinites of higher rank; a strong absorption at this frequency is characteristic of the spectra of all coal macerals so far reported. The 1600 cm.$^{-1}$ band is strong even in the spectrum of lignin, and it also occurs in the spectra of fresh wood, peat, and brown coal. In these materials it is accompanied by a band close to 1510 cm.$^{-1}$, and the association of these two absorptions is highly characteristic of an aromatic ring. The 1510 cm.$^{-1}$ band does not appear however in the condensed polynuclear structures that occur in most constituents of coals of bituminous and higher rank. Within the exinite group, even the spectrum of modern spore cases displays the 1600 cm.$^{-1}$ and 1510 cm.$^{-1}$ bands, and the spores themselves show peaks at 1637 and 1510 cm.$^{-1}$ in a broad complex absorption suggesting that these also possess an aromatic structure. The low rank resinites however give little indication of aromatic rings in their spectra and they appear to be the coal constituents of lowest aromaticity encountered so far. Sample 7 is an exception. Absorptions at 1600 and 1490 cm.$^{-1}$ indicate the presence of an aromatic ring. Furthermore, a strong absorption at 700 cm.$^{-1}$ and a band of medium intensity at about 753 cm.$^{-1}$ in the same spectrum is strong evidence for a monosubstituted aromatic.

It is interesting that in macerals of bituminous rank or higher, the 1600 cm.$^{-1}$ band represents groupings that are evidently extremely stable because this absorption persists as long as structure can be detected in the trace, even up to high rank coals. At lower levels of rank it seems that the general absorption pattern illustrated in Figures 3 and 4 remains virtually unmodified over much of the earlier part of the coalification series. Resinite with similar spectral characters to those shown in Figure 3 has recently been isolated in this department in substantial quantities from Egyptian coal whose rank lies near

Publication Date: January 1, 1966 | doi: 10.1021/ba-1966-0055.ch019

to the boundary of the subbituminous and bituminous ranges. Thus, if all the resinites referred to in this article belong to a natural series whose members show a variation in properties with increasing coalification, then at least certain of the changes in constitution involved must take place rapidly within a relatively narrow rank range. This would be consistent with other evidence referred to below.

It is possible, but seems less likely, that the contrasts between the resinites of Figure 2 and those of Figures 3 and 4 might be explained by different precursors. The resinites of bituminous rank referred to here were isolated from coals of Carboniferous age. Those of lower rank came from deposits in the Cainozoic and almost certainly originated in plants that were more highly evolved and organized than any of those found in the late Palaeozoic. There could thus be a fundamental difference in the overall composition and structure of the resins originating in the plants of the two eras. This again seems unlikely if resins have been produced by plants for essentially the same purposes throughout geological time. It seems more realistic at present to attribute the differences between the two groups of resinites to geological rather than to botanical causes.

Publication Date: January 1, 1966 | doi: 10.1021/ba-1966-0055.ch019

Relationship between Resinites in Bituminous Coals and in Coals of Lower Rank

Schopf (*19*), in discussing variable coalification and the processes involved in coal formation, has commented on the very small changes that occur in macerals of the exinite group during the diagenetic and early metamorphic history of coals. He states that only when the coalification processes have been sufficient to raise the rank of the coals to the medium volatile bituminous level do the exinite macerals display pronounced changes in composition. Schopf suggests that once the compositional changes begin, they then take place rapidly and continue at this rate until the exinite macerals are similar in composition to vitrinite of the higher rank coals.

These views are partly in accord with those expressed by Murchison and Jones (*17*, *18*) on the basis of changes observed in the elementary compositions of resinites of different rank. However, the appearance and properties of the resinites in bituminous coals and those of lower rank were sufficiently different to suggest that a major change in resinite composition and structure occurred below or at the boundary between the lignite and high volatile bituminous coals. This is supported by the contrasting appearance of the infrared spectra in Figures 2 and 3. Within the range of bituminous coals studied, the rate of change of properties is quite gradual, but whether this later increases strongly to account for the relatively rapid disappearance of resinite from coals with vitrinite of carbon contents greater than approximately 86% is a matter for further study. In the present article there is more concern with what happens to resinite in coals lower than bituminous rank.

In developing the typical spectrum of a bituminous coal resinite from that of a lower rank resinite, the following major changes would have to take place. The intensity of the carbonyl absorption close to 1700 $cm.^{-1}$ would have to be

much reduced. At the same time a 1600 cm.$^{-1}$ band would have to be established and intensify rapidly. Removal of the considerable number of weak absorptions at frequencies lower than approximately 1250 cm.$^{-1}$ would be accompanied by the growth of bands associated with aromatic C-H out-of-plane vibrations between 900 and 700 cm.$^{-1}$. While absorption from non-aromatic C-H groups would remain strong, there would be some reduction in its intensity, particularly in the band caused by methyl groups at 1370 cm.$^{-1}$. Spectra with an absorption pattern intermediate in character between those of Figures 2 and 3 would be expected for resinites in coals of a restricted rank range, but no such resinites have yet been found in coals of the normal coalification series. Unfortunately, the writer has only had the opportunity to examine a limited number of resinitic coals of lignitous rank. However, the spectrum of a thermally metamorphosed resinite (Duxite) from brown coal does show the intermediate characters expected, but is closer in type to bituminous than to lignitous coal resinite. The formation of the black, lustrous Duxite that occurs in veins and "lakes" was described by Kuhlwein (*14*). Resinite in the brown coals was affected to varying degrees depending upon its proximity to a complex and massive igneous intrusion of Tertiary age that underlies the Bohemian coalfield. Kuhlwein suggested that the conditions under which the Duxite formed were for much of the time similar to those in the process of "bertinization." In this process coals are treated at temperatures well below those that are used for low temperature carbonization; carbon dioxide and water are removed, oxygen split off, and the primary bitumen liquefied.

In the spectrum of Duxite (Figure 5) the carbonyl absorption is still strong, but it is only slightly more intense than the now well established 1600 cm.$^{-1}$ band. There is evidence of aromatic C-H out-of-plane vibrations developing to give peaks close to 870 and 810 cm.$^{-1}$, characteristic frequencies for these bands in the spectra of resinites from bituminous coals. An absorption of medium intensity occurs at 717 cm.$^{-1}$ and this again may be an intermediate feature. The band might possibly arise from a long chain of the type $-(CH_2)_n-$, where n is 4 or more, but it is more likely to be caused by a C-H out-of-plane

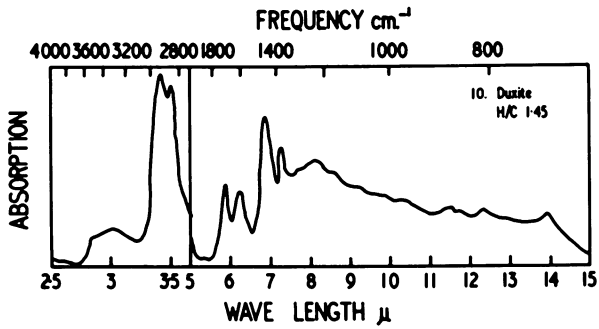

Figure 5. Infrared spectrum of Duxite, a resinite from thermally metamorphosed lignite

Publication Date: January 1, 1966 | doi: 10.1021/ba-1966-0055.ch019

vibration on the ring. Similarly, the weak but distinct band on the original trace at 1510 cm.$^{-1}$ that is normally associated with aromatic compounds but not with bituminous coal spectra published so far, belongs much more to the spectra of lower rank resinites. It seems, therefore, that the Duxite spectrum is that of a maceral in which aliphatic structures dominate, but one in which aromatic clusters are just beginning to develop.

The fact that Duxite was formed through a natural pyrolysis and yielded an intermediate form of spectrum was an encouragement to examine the spectra of resinites carbonized in the laboratory. It was possible that the lower rank resinites would alter on heating to give spectra similar to those of resinites in bituminous coals. Also, the experiments allowed a comparison between the spectra of carbonized resinites and vitrinites in bituminous coals, the latter having been studied by Brown (*4*) some years ago.

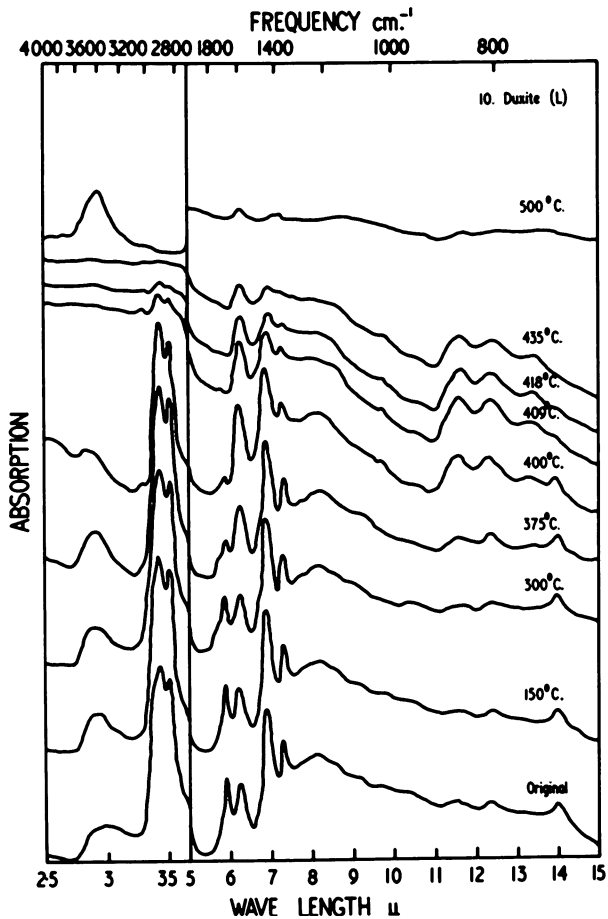

Figure 6. Infrared spectra of samples of Duxite carbonized to different temperatures

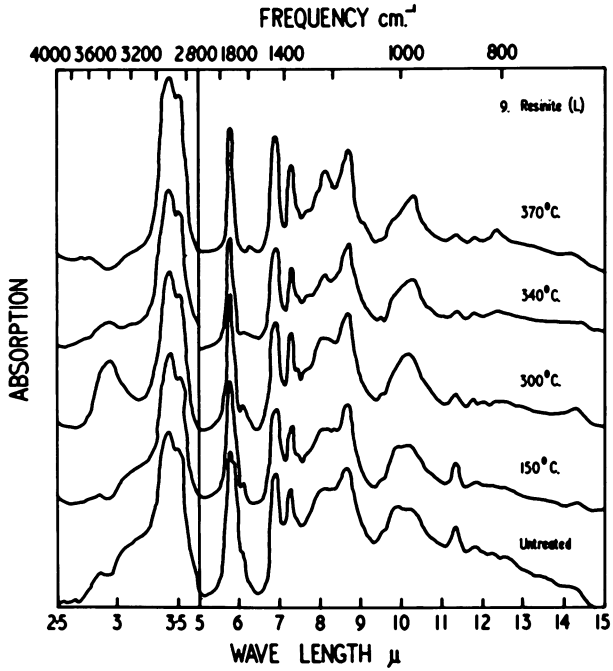

Figure 7. Infrared spectra of samples of resinite from lignite carbonized to different temperatures

Spectra of Carbonized Resinites

Several of the resinite samples were carbonized in nitrogen at various temperatures up to 800°C. using a heating rate of 1.75°C. for one hour. The alterations in the infrared absorption curves of Duxite and resinite from bituminous coals have already been reported (*18*) and shown to be similar to one another and comparable to the changes produced in the spectrum of carbonized low rank vitrinite.

In the Duxite spectrum between 150° and 400°C. the carbonyl absorption at 1700 cm.$^{-1}$ is gradually reduced, and this is accompanied by some increase in intensity of the 1600 cm.$^{-1}$ band (Figure 6). The main changes to the spectrum take place above 400°C. when the resinite has become highly fluid and is decomposing heavily with rapid evolution of volatiles, particularly in the range 400°–435°C. Nonaromatic C-H groups are quickly eliminated together with the absorption at 717 cm.$^{-1}$. A third absorption associated with C-H out-of-plane vibrations develops close to 750 cm.$^{-1}$, the others being centered near to 870 and 810 cm.$^{-1}$. These absorptions intensify above 400°C. as condensation of the aromatic clusters proceeds, but there is apparently no shift of frequency which Brown observed in the spectra of carbonized vitrinites at higher temperatures. The frequencies of the absorptions caused by aromatic C-H out-of-plane vibrations in the spectra of resinites of bituminous coals and

Publication Date: January 1, 1966 | doi: 10.1021/ba-1966-0055.ch019

their carbonized products correspond with those quoted by Brown for semi-anthracitic and anthracitic vitrinites, but not with those of lower rank vitrinites. The relative intensities of the absorptions in this region do, however, differ for the two macerals and the type of substitution of carbonized resinites and high rank vitrinites may thus also differ to some extent. At temperatures higher than 500°C. aromatic hydrogen is lost from the resinites, background absorption increases, and the structureless nature of the spectra suggests that growth of extensive aromatic lamellae has occurred.

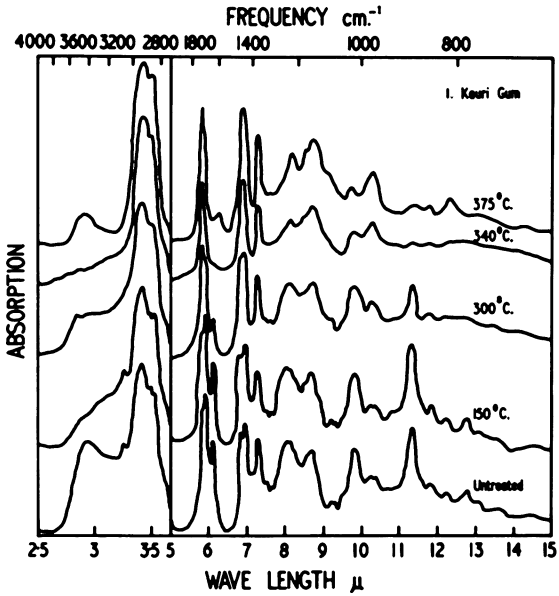

Figure 8. Infrared spectra of samples of kauri gum carbonized to different temperatures

The changes induced in the spectra of Duxite and resinites from bituminous coals were not observed in the spectra of lower rank resinites on heating. Modifications of the spectra of kauri gum and of resinite from a lignite were slight (Figures 7 and 8). There was some simplification of the spectra below about 1250 cm.$^{-1}$ over the temperature range covered. For example, there is the gradual elimination of the strong absorption close to 886 cm.$^{-1}$ and those associated with it at 1642 cm.$^{-1}$ and 3070 cm.$^{-1}$, all of which are caused by an olefinic group of some type. The intensity of the C=O band at 1700 cm.$^{-1}$ is apparently reduced to some extent, but the expected reduction of absorptions caused by nonaromatic C-H groups does not occur. Aromatic C-H systems are apparently not established, and there is no development of an absorption band at 1600 cm.$^{-1}$.

The difference in response of the low and higher rank resinites to carbonization over relatively short periods of time must lie in their initial structures. Those resinites containing condensed ring structures before carbonization

Publication Date: January 1, 1966 | doi: 10.1021/ba-1966-0055.ch019

evidently undergo increase in aromaticity on heating without difficulty. The resinites that are largely aliphatic in character distill gently away when heated rather than polymerizing. Even at relatively low temperatures such resinites yield only a very thin film of material in the silica boat after pyrolysis. However, as Figures 7 and 8 show, in the attempt to carbonize low rank resinites, the spectra at the highest temperatures employed display two new but weak absorptions, one close to 1600 cm.$^{-1}$, the other at 812 cm.$^{-1}$. The 1600 cm.$^{-1}$ band develops as the 1642 cm.$^{-1}$ absorption is eliminated and seems likely to represent the beginnings of the much more intense band at this frequency that has come to be associated with higher rank macerals. The other new absorption developed at 812 cm.$^{-1}$ lies at one of the characteristic frequencies for aromatic C-H out-of-plane vibrations in coal macerals. Attempts to observe further development of a "coal-like" spectrum failed because insufficient material to make potassium bromide discs was left in the boats after carbonization at temperatures higher than 370°C. However, even the limited development achieved was encouraging in view of recent results published by Friedel (*8*). In experiments to pyrolize cotton and pine sawdust at 200°C. in air, Friedel observed little change to the materials over a short period of time. Heating at the same temperature for a period of 10 months produced chars that bore no resemblance to the starting materials. A new and intense absorption arose at 1610 cm.$^{-1}$, indicating the importance of time in these reactions. Similar long term experiments on low rank resinites might induce comparable changes and the same results might also be achieved by carbonizing the resinites for short periods under elevated pressures.

Spectra of Oxidized Resinites

The resinites of different rank were subjected to treatment with molecular oxygen to determine if the low rank material again showed little response. It was also hoped that the experiment might help to explain certain features displayed by the resinites from bituminous coals under the microscope.

Three resinites were ground to pass BS 30 mesh and be retained on BS 170 mesh screen. Individual samples of each resinite were then oxidized for periods of 3, 24, and 48 hours at temperatures well below the softening points of the resinites. Resinite from bituminous coal and the Duxite were oxidized at 140°C. and the resinite from lignite at 120°C. Each oxidized sample was divided into two parts. One was further ground for infrared examination, and the other was retained at the original particle size for microscopic study.

The spectra of the oxidized resinites are shown in Figures 9–11. Again it is the spectra of the higher rank resinites that show greatest modification. There is little apparent change in the spectra of samples 10 and 14 with oxidation during the first 3 hours except for a slight increase in the 1700 cm.$^{-1}$ band. With continued oxidation this absorption intensifies and becomes the strongest in the spectra. Van Krevelen (*13*), quoting the results of various investigations of the numbers of carboxyl groups in coal, states that while carboxyl oxygen occurs in brown coals and lignites, it is virtually absent in coals with carbon contents higher than 80%. However, he also refers to an experiment in which an "oxycoal" was prepared from a vitrain of 87% carbon by oxidation for 48

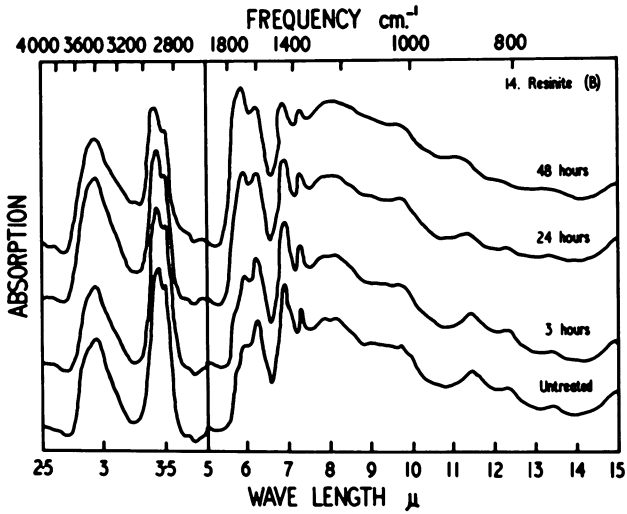

Figure 9. Infrared spectra of samples of resinite from a bituminous coal oxidized at 140°C. for different periods of time

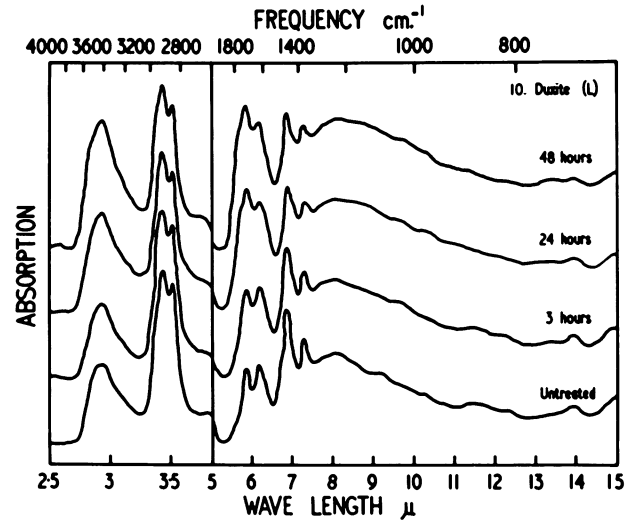

Figure 10. Infrared spectra of samples of Duxite oxidized at 140°C. for different periods of time

hours at 275°C. In this sample oxygen in carboxyl groups was dominant. Presumably if resinite from bituminous coal oxidizes in a manner similar to vitrain, then carboxyl groups substantially contribute to the intensified absorption at 1700 cm.$^{-1}$.

Publication Date: January 1, 1966 | doi: 10.1021/ba-1966-0055.ch019

Growth of the 1700 cm.$^{-1}$ band is accompanied by reduction in the intensity of all absorptions associated with nonaromatic C-H groups. Currently held views are that aliphatic structures are destroyed during the oxidation of coal, and the changes in absorption pattern support this.

Because of the changes in intensity affecting absorptions on either side of the 1600 cm.$^{-1}$ band, it is difficult to decide whether or not its intensity is modified during oxidation. If it is, then the change is slight, indicating that the group or groups producing the band are relatively stable under oxidizing conditions. There does however appear to be a loss of aromatic hydrogen from both resinites as oxidation proceeds because the C-H out-of-plane absorptions are gradually diminished and in the case of Duxite, are virtually removed from the spectrum after 48 hours of oxidation.

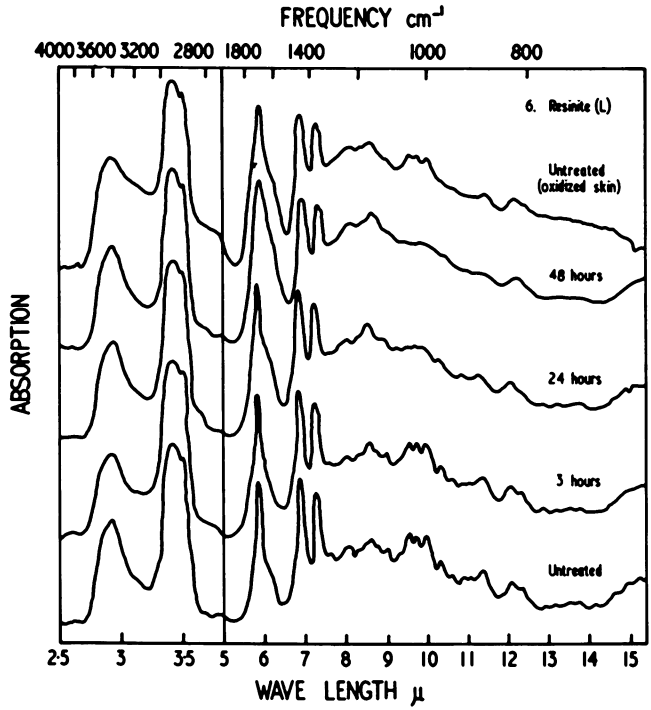

Figure 11. Infrared spectra of samples of resinite from lignitous coal oxidized at 120°C. for different periods of time

In the spectrum of resinite from lignite there is also some loss of nonaromatic C-H groups that is shown particularly in the region below approximately 1250 cm.$^{-1}$. The absorption at 1700 cm.$^{-1}$ becomes less sharp and widens on the low frequency side as oxidation proceeds. A distinct kink in the trace does develop at 1600 cm.$^{-1}$, and it will be interesting to establish if broadening of the absorption band continues with prolonged oxidation and whether or not a separate band may eventually arise at the lower frequency. For com-

parison the spectrum of the thin, dark brown skin that coats lumps of this resinite is also shown. The skin is presumably an oxidized layer; its absorption pattern is similar to that of the fresh resinite after it has been oxidized for 48 hours.

Samples of the resinites at each stage of oxidation were examined with the microscope by incident light under oil immersion. Corresponding to the general darkening in color observed with increasing length of oxidation, the reflectivity of the resinite particles gradually rises. After oxidation for 3 hours there are certain features on the resinite particles that have some bearing on the structure of resinites as they appear on polished surfaces of fresh coals under the microscope. At this stage of oxidation all the particles of Duxite and resinite from bituminous coal displayed distinct rims (Figures 12 and 13). These rims possessed a lower reflectivity than the main mass of the particles, but their reflectivity was probably higher than that of the fresh resinite although no quantitative measurements were made.

Publication Date: January 1, 1966 | doi: 10.1021/ba-1966-0055.ch019

Figure 12. Particle of Duxite displaying an oxidized rim after oxidation for 3 hours at 140°C.; relief-polished surface, oil immersion, incident light; × 378

The occurrence of rims of lower reflectivity than the main mass of the particles after a short period of oxidation was unexpected and will require further investigation. Van Krevelen (*13*) illustrates vitrinite particles with oxidation rims that show a higher reflectivity than the remainder of the particles but does not mention the occurrence of particles with lower reflecting margins. Illustrations of vitrinite particles oxidized by nitric acid however, in a recent paper by Edwards, Jones, and Newcombe (*6*), suggest that acid oxidation at

Figure 13. Particles of resinite from bituminous coal displaying oxidized rims after oxidation for 3 hours at 140°C.; relief-polished surface, oil immersion, incident light; × 395

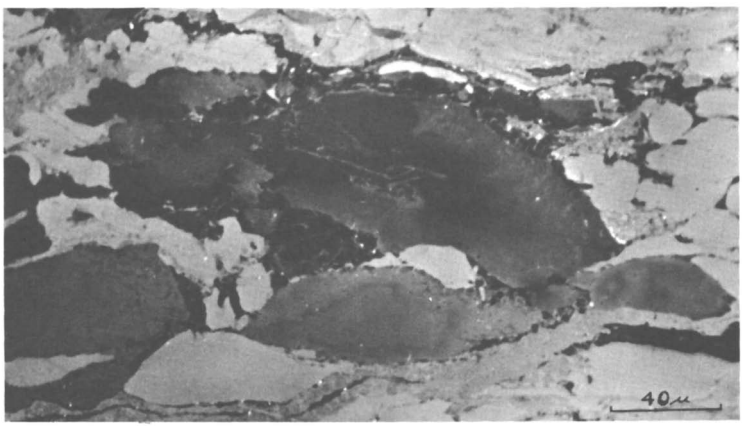

Figure 14. Resinite masses in fresh bituminous coal showing variable reflectivity, possibly owing to oxidation effects at time of deposition or earlier in their history; relief-polished surfaces, oil immersion, incident light; × 350

least can produce rims that are higher or lower reflecting than the main mass of the particles, even on a single particle. Jones and Murchison (*11*), discussing the occurrence of resinite in bituminous coals, have published figures of resinite bodies showing altered marginal areas of which there may be several

Publication Date: January 1, 1966 | doi: 10.1021/ba-1966-0055.ch019

differing in reflectivity. As a result of Stach's conclusions in his petrographical study on the biochemical coalification of exinite (*20*), Jones and Murchison referred these areas of higher reflectivity to oxidized zones formed at the time of deposition of the resin in the coal-forming peat. Typical examples of this type of material are shown in Figure 14. These same authors noted a number of instances in which the margins of the resinite bodies were seemingly unaffected, but the main mass of the resinite altered. Occurrences of this type were attributed to cracks that penetrated the globule after it hardened at the time of deposition and allowed easy access of oxygen to the center of the body.

Summary and Conclusions

Publication Date: January 1, 1966 | doi: 10.1021/ba-1966-0055.ch019

The results described in this article form only part of an interim report on the maceral resinite. Infrared studies suggest that there are two contrasting groups of resinites that are probably linked by intermediate types. The resinites of lignites and lower rank deposits are dominantly aliphatic or alicyclic in structure. They yield an infrared absorption pattern that is in many respects uncharacteristic of coal macerals already examined, but one that is apparently stable through to high rank lignites. They show little reactivity during short term pyrolysis or during oxidation.

Aliphatic structures are still of major importance in the second group of resinites, those of the bituminous coals, but aromatic structures are present in significant amounts. The spectra of these resinites display the type of absorption pattern that has come to be associated with other coal macerals, particularly the sporinites and to a large extent the vitrinites. This pattern is established in the resinites of the high volatile bituminous coals. Furthermore, resinites of this group are reactive during carbonization and oxidation processes in which their behavior parallels that of similarly affected vitrinites of equivalent rank.

The only link found so far between the infrared absorption patterns of the two resinite groups is the spectrum of a thermally metamorphosed resinite from lignite which shows intermediate characters. However, if coalification is a process which causes continuous compositional changes to all coal constituents, then infrared spectra with patterns intermediate to those of the lignitic resinites and the resinites from bituminous coals should be found ultimately. These resinites will come from coals in a very restricted range of the normal coalification series lying near to or including the transition from lignitic to bituminous coals.

If the observations above are correct, then they suggest that the rate of coalification of resinite is by no means regular. Stability of the structure possessed by the resinite at the time of deposition is apparently maintained during its early metamorphic history. When affected by the temperature/pressure conditions possibly required to produce coals of high lignitic rank, the structure must then break down quite rapidly to give the new structure responsible for the absorption pattern of resinites in bituminous coals. Further changes at this general level of rank are apparently more gradual, at least until coals of approximately 86% carbon are formed. Infrared spectra are not available for

resinites from coals above this rank, and microscopical studies show that resinite has virtually disappeared from such coals. This suggests that the rate of compositional changes may have again increased owing to the temperature/pressure conditions in operation at this stage of the coalification process. The rapid changes in absorption pattern that are associated with pronounced reactivity of the resinites from bituminous coals over a narrow temperature range during carbonization support the view that the properties of resinite are modified rapidly somewhere in the range of the medium volatile bituminous coals.

A proper understanding of the nature and behavior of resinite at all levels of rank will require considerable further effort. Petrographic examination of coals will no doubt yield additional data, but a more profitable line of attack would seem to lie in studying fresh and laboratory treated samples by a proper combination of microscopical and chemical analytical techniques.

Publication Date: January 1, 1966 | doi: 10.1021/ba-1966-0055.ch019

Acknowledgments

The writer would like to thank W. F. K. Wynne-Jones for allowing him to use the facilities of the spectroscopy laboratory in the School of Chemistry of the University of Newcastle during the time of this research. He would also like to thank F. J. McQuillin of the Department of Chemistry, University of Newcastle, for considerable assistance and originally suggesting the infrared examination of the resinites, R. A. Friedel of the U.S. Bureau of Mines, Pittsburgh for much helpful discussion, and I. A. Breger, U.S. Geological Survey, Washington for reading the manuscript and making critical comments upon it. He is grateful to J. Booker, I. Prendergast, and A. Scott for assistance in preparing the manuscript and figures. Acknowledgment is also made to the National Coal Board for a grant during the initial stages of this research, but the views expressed are those of the author and not necessarily those of the Board.

Literature Cited

(1) Bellamy, L. J., "The Infra-Red Spectra of Complex Molecules," 2nd Ed., Methuen, London, 1958.
(2) Bent, R., Brown, J. K., *Fuel* **40,** 47 (1961).
(3) Brown, J. K., *J. Chem. Soc.* **1955,** 744.
(4) Brown, J. K., *J. Chem. Soc.* **1955,** 752.
(5) Dormans, H. N. M., Huntjens, F. J., van Krevelen, D. W., *Fuel* **36,** 321 (1957).
(6) Edwards, A. H., Jones, J. M., Newcombe, W., *Fuel* **43,** 55 (1964).
(7) Fenton, G. W., Smith, A. H. V., *Conf. on Sci. Use Coal, Sheffield* **1958,** C-20.
(8) Friedel, R. A., *Appl. Optics* **2,** 1109 (1963).
(9) Friedel, R. A., Queiser, J. A., *Anal. Chem.* **28,** 22 (1956).
(10) International Committee for Coal Petrology, "International Handbook of Coal Petrography," 2nd Ed., Centre National de la Recherche Scientifique, Paris, 1963.
(11) Jones, J. M., Murchison, D. G., *Econ. Geol.* **58,** 263 (1963).
(12) Kinney, C. R., Doucette, E. I., *Nature* **182,** 785 (1958).
(13) Krevelen, D. W. van, "Coal," p. 167, 238–247, Elsevier, Amsterdam, 1961.
(14) Kuhlwein, F. L., *Fuel* **30,** 25, (1951).
(15) Monnot, C. A., Ladam, A., C. R., *Acad. Sci., Paris* **241,** 1939 (1955).
(16) Murchison, D. G., *Nature* **198,** 254 (1963).
(17) Murchison, D. G., Jones, J. M., *Fuel* **42,** 141 (1963).

(18) Murchison, D. G., Jones, J. M., "Advances in Organic Geochemistry," p. 49, Pergamon Press, London, 1964.
(19) Schopf, J. M., *Econ. Geol.* **43,** 207 (1948).
(20) Stach, E., *Brennstoff-Chem.* **43,** 71 (1962).

RECEIVED January 25, 1965.

Discussion

Robert A. Friedel: The spectra having no 1600 cm.$^{-1}$ band and those having progressively stronger 1600 cm.$^{-1}$ bands constitute an interesting series. Quantitative comparisons between the 1600 cm.$^{-1}$ band and the long wavelength aromatic bands in such series should give interesting information on the question of the assignments of these bands. Have you made any quantitative measurements?

Duncan G. Murchison: No quantitative comparisons have so far been made between absorption bands in different parts of the spectra. It would be useful indeed if the particular comparison suggested by Dr. Friedel would help to elucidate the nature of the 1600 cm.$^{-1}$ (6.25 micron) band which at present is still rather unsatisfactorily assigned to two or possibly more groupings.

Marlies Teichmüller. In regard to the resinite that you describe as behaving like vitrinite, it may be of interest to you that Soos (Budapest) described vitrinite-like "resinous" bodies from Tertiary coals of Hungary which really are phlobaphenes—i.e., excretions of plant cells which have phenolic groups. They have been described as "resinite" by the coal petrologists though they have the same or even a higher reflectance than the humified cell wall. They are frequently in the wood of the conifers *Taxodiaceae*, as Soos found by studies of xylites from brown coals compared with studies of wood of the living plants.

Dr. Murchison: I am not familiar with this work of Soos, and I am grateful to Dr. Teichmüller for drawing my attention to it. In general, I think it is easier to decide upon the origin of a particular coal constituent, the lower is the rank of the coal. I feel that it might, therefore, be difficult to distinguish coalified phlobaphenes from resinites, as they are now defined in the International Glossary, in coals of bituminous rank, although this may well be possible in brown coals. Also, phlobaphenes are decomposition products, anhydrides of tannins. In the cell contents of some Gymnosperms the amount of resin is inversely proportional to the tannin content, and it is thought that the tannin may be an intermediate stage in resin production. If this is true, then I think that besides the difficulty of distinguishing tannins, phlobaphenes, and resins from one another in coals that have undergone some degree of coalification, these constituents would probably display spectral similarities.

Bhupendra K. Mazumdar: Have you any views on the nature of the carbonyl groups—quinonoid or nonaromatic ketonic?

Dr. Murchison: I am afraid that I can offer no help on this point now. We have not investigated the nature of the carbonyl groups of the resinites.

Wolfgang Flaig: Measurements of exchange capacity compared with the decrease or increase of the intensity of C=O band in the infrared spectra might be useful, as in the case of rotted lignin.

Irving A. Breger: Is it possible that your 6.2 μ absorption is merely water?

Dr. Murchison: It seems most unlikely that the 6.25 μ absorption in the spectra of resinites from bituminous coal is caused by water. If it were, then I would also expect this absorption to appear in the spectra of lower rank resinites many of which display a substantial OH absorption in the region around 3 μ like those from bituminous coals.

Leo Duffy: Does oxidation result in broadening of the C=O band? If so, what is the possibility of quinone formation during oxidation?

Dr. Murchison: Oxidation of the resinite from lignitous coal does seem to cause broadening of the C=O absorption and makes the appearance of this band very similar to that in the spectrum of the oxidized layer from a weathered sample. It is too early to say whether or not this a general feature that affects all oxidized resinite. The possibility of quinone formation during oxidation has not been studied.

Publication Date: January 1, 1966 | doi: 10.1021/ba-1966-0055.ch019

20

A Comparative Study of Exinite, Vitrinite, and Micrinite

H. TSCHAMLER* and E. DE RUITER

Union Carbide European Research Associates, S.A., Brussels 18, Belgium

Publication Date: January 1, 1966 | doi: 10.1021/ba-1966-0055.ch020

An exinite, vitrinite, and micrinite of the same rank were investigated. From elementary analysis alone it follows that their structures must be different. Combining the results from IR and PSR measurements, the hydrogen distribution, the aliphatic group distribution, and possible intervals for the aromaticity are derived. Exinite possesses the biggest aliphatic position with the highest relative amount of CH_2 groups, and micrinite possesses the smallest aliphatic position with the lowest relative amount of CH_2 groups. From x-ray measurements and hydrogen distribution, limits for the aromatic cluster size are derived; exinite has the smallest clusters, micrinite the largest. Finally, the presence of nonaromatic rings is demonstrated, of which at least a part should be hydroaromatic or alicyclic.

For several years the structural features of a vitrinite (83.9%C) have been intensively studied. The two macerals, exinite and micrinite, which accompany the above mentioned vitrinite in the dull coal were also examined.

Separating the three macerals from the dull coal was difficult. The petrographical purity of the exinite is 86% and that of the micrinite 94%. For both macerals, vitrinite is the main "impurity." Since the vitrinite has a petrographical purity of 99%, it is not difficult to calculate the values for the pure exinite and pure micrinite from the experimental data on the highly enriched maceral fractions. All values reported in the tables are corrected ones. Table I summarizes the results of elementary analysis (maf) and the percentage of volatile matter.

The reported values fully agree with those found by other investigators (*2*, *8*) on exinites, vitrinites, and micrinites of the same rank. The atomic H/C

* Present address: Kupkagasse 6, Vienna VIII, Austria.

In Coal Science; Given, P.;
Advances in Chemistry; American Chemical Society: Washington, DC, 1966.

Table I. Analytical Data (maf) for an Exinite, Vitrinite, and Micrinite

Sample	Volatile Matter	Elementary Analysis (maf)					
		%C	%H	%O	%N	$\%S_{(Diff)}$	H/C
Exinite	66.7	84.1	7.0	6.3	1.3	1.3	0.991
Vitrinite	35.2	83.9	5.5	8.0	1.4	1.2	0.780
Micrinite	22.9	85.7	3.9	8.0	1.2	1.2	0.542

ratio (last column in Table I) remarkably decreases from exinite over vitrinite to micrinite, mainly owing to the large decrease in hydrogen content. From a structural point of view this fact can be explained by (1) a considerable difference in the number of aliphatic groups whereby the mean aromatic cluster size remains the same for all three samples, (2) a considerable difference in the mean aromatic cluster size, the number of aliphatic groups being constant, or (3) a combination of these two extreme cases. Finally, from the volatile matter (%V) and the carbon content (%C) the aromaticity f_a ($= \frac{C_{ar}}{C}$) can be estimated (*10*):

$$f_a = \frac{1200(100 - \%V)}{1240(\%C)} \quad (1)$$

It is, however, known that the f_a values from Equation 1 must be regarded as being too low because not only the aliphatic part but also small aromatic systems are split off during determination of the volatile matter (*11*). Furthermore, these f_a values make sense only as long as the %V is not too high. This method is, therefore, limited to the vitrinite ($f_a = 0.75$) and micrinite ($f_a = 0.87$).

An interesting comparison can be made on the basis of the hydrogen distribution of the three macerals. The aromatic hydrogen content ($\%H_{ar}$) has been calculated from the total area of the infrared absorption between 11 and 14 μ (aromatic HCC rocking vibrations) (*6*). The aliphatic hydrogen content ($\%H_{al}$) has been derived from the absorption of the aliphatic H-C stretching vibration between 3.3 and 3.6 μ (*7*). The values found for the three macerals under investigation are reported in Table II, columns 3 and 4.

Table II. Hydrogen Distribution of an Exinite, Vitrinite, and Micrinite

Sample	%H	$\%H_{al}$	$\%H_{ar}$	$\%H_{OH(Diff.)}$	H_{al}/H	H_{ar}/H
Exinite	7.0	5.4	1.4	0.2	0.77	0.20
Vitrinite	5.5	3.3	1.9	0.3	0.60	0.35
Micrinite	3.9	1.7	2.0	0.2	0.44	0.51

The values of $\%H_{OH}$ in column 5 are the difference between %H and ($\%H_{ar} + \%H_{al}$), and agree fairly well with those which follow from the experimentally determined $\%O_{OH}$ (*1*, *2*). Furthermore, it can be seen from the results in Table II that H_{ar}/H increases considerably, and consequently H_{al}/H decreases strongly in the sequence exinite, vitrinite, and micrinite.

Publication Date: January 1, 1966 | doi: 10.1021/ba-1966-0055.ch020

Using H/C, H_{a1}/H, and H_{a1}/C_{a1} (mean composition of the aliphatic groups) the true aromaticity can be calculated:

$$f_a = 1 - \frac{C_{a1}}{C} = 1 - \frac{(H_{a1}/H) \cdot (H/C)}{(H_{a1}/C_{a1})} \quad (2)$$

Since the structural parameter H_{a1}/C_{a1} cannot be determined experimentally, only particular f_a values can be derived; for example, the theoretically highest f_a value follows from the assumption that $H_{a1}/C_{a1} = 3$, which means that the entire aliphatic portion consists of CH_3 groups. A more realistic value of f_a follows if in Equation 2 $H_{a1}/C_{a1} = 2$ (the aliphatic portion consists either only of CH_2 groups or of the same number CH_3 and CH groups with or without CH_2 groups) is used. These two theoretical but meaningful f_a values are 0.92 and 0.88 for the micrinite, 0.84 and 0.77 for the vitrinite, and 0.75 and 0.62 for the exinite.

The upper limit for f_a follows from the hydrogen distribution and aliphatic group distribution derived from proton spin resonance measurements at the temperature of liquid nitrogen (3). Table III shows all structural parameters obtained directly from the second moment ΔH^2 (in gauss^2) together with H_{a1}/H.

Table III. Aliphatic Hydrogen Distribution Derived from PSR Measurements and H_{a1}/H for an Exinite, Vitrinite, and Micrinite

Sample	ΔH^2(gauss^2)	$a = \frac{H_{CH_2}}{H}$	$b = \frac{H_{CH_3} + H_{CH}}{H}$	b/a	$\frac{H_{CH_2}}{H_{a1}}$	$\frac{H_{CH_3} + H_{CH}}{H_{a1}}$
Exinite	18.5	0.53 ± 0.03	0.24 ± 0.03	0.46	0.69	0.31
Vitrinite	14.2	0.28	0.32	1.14	0.47	0.53
Micrinite	12.1	0.16	0.28	1.75	0.36	0.64

The experimentally found decrease in the second moment from the exinite over the vitrinite to the micrinite establishes that H_{CH_2}/H is highest in the exinite and lowest in micrinite. It follows then from H_{CH_2}/H_{a1} $\left(= \frac{H_{CH_2}}{H} \Big/ \frac{H_{a1}}{H}\right)$ that in the exinite about two-thirds, in the vitrinite about one-half, and in the micrinite about one-third of the aliphatic hydrogen atoms are present in CH_2 groups.

The structural parameter in column 5 of Table III

$$b/a = \frac{H_{CH_3} + H_{CH}}{H_{CH_2}} \quad (3)$$

is very important because all possible aliphatic group distributions can be calculated from it. The upper limit for H_{a1}/C_{a1}, and thus for the aromaticity, is reached if in Equation 3 $H_{CH} = 0$, and therefore $b/a = H_{CH_3}/H_{CH_2}$. The content of CH groups can now be increased stepwise (accompanied by the corresponding decrease of CH_3 groups) until only CH and CH_2 groups are present. This aliphatic group distribution determines the lower limit of H_{a1}/C_{a1}

Publication Date: January 1, 1966 | doi: 10.1021/ba-1966-0055.ch020

and of f_a. For the three macerals, all possible aliphatic group distributions together with the corresponding H_{al}/C_{al} and f_a values are presented in Table IV.

Table IV. Aliphatic Group Distribution per 100 C_{total} of an Exinite, Vitrinite, and Micrinite

Sample	CH_3	CH	CH_2	H_{al}/C_{al}	f_a
Exinite	8	0	26	2.23	0.66
	7	3	26	2.11	0.64
	6	6	26	2.00	0.62
	5	9	26	1.90	0.60
	4	12	26	1.81	0.58
	3	15	26	1.73	0.56
	2	18	26	1.65	0.54
	1	21	26	1.58	0.52
	0	24	26	1.52	0.50
Vitrinite	8	1	11	2.35	0.80
	7	4	11	2.14	0.78
	6	7	11	1.96	0.76
	5	10	11	1.81	0.74
	4	13	11	1.68	0.72
	3	16	11	1.57	0.70
	2	19	11	1.47	0.68
	1	22	11	1.38	0.66
	0	25	11	1.31	0.64
Micrinite	5	0	4.3	2.54	0.90
	4	3	4.3	2.09	0.88
	3	6	4.3	1.77	0.86
	2	9	4.3	1.54	0.84
	1	12	4.3	1.36	0.82
	0	15	4.3	1.22	0.80

Some important conclusions follow from the results:

(1) From the possible ranges for f_a (exinite 0.50–0.66, vitrinite 0.64–0.81, micrinite 0.81–0.91) it follows definitely that the exinite possesses the smallest and the micrinite the highest aromaticity because there is no overlapping of the f_a intervals of the three macerals.

(2) The number of CH_2 groups per 100 C_{total} of the exinite is more than the double of that of the vitrinite and six times higher than that of the micrinite. Thus, it is very probable that to a first approximation H_{al}/C_{al} of the exinite equals 2, a value which corresponds to $f_a = 0.62$. The most probable f_a value for the vitrinite has been found to be 0.77 (*4*), a value which also requires H_{al}/C_{al} near 2. For the micrinite an f_a value $\sim$ 0.89 seems reasonable.

(3) If the f_a values under (2) are the true ones, exinite has one CH_3 group per four CH_2 groups, vitrinite has one CH_3 group per two CH_2 groups, and micrinite has one CH_3 per one CH_2 group.

A further structural parameter which can now be calculated from H/C, H_{ar}/H, and f_a is the aromatic substitution index S_{ar}:

$$S_{ar} = \frac{C_{ar(subst)} + C_{ar(cond)}}{C_{ar}} = 1 - \frac{H_{ar}}{C_{ar}} = 1 - \left(\frac{H_{ar}}{H} \cdot \frac{H}{C} \cdot \frac{1}{f_a} \right) \qquad (4)$$

Table V shows the $\overline{S}_{ar}$ values of the three macerals depending, within a reasonable range, on f_a and H_{ar}/H. The $\overline{S}_{ar}$ values are always of the same order of magnitude. Since (as will be shown in the next paragraph) $\overline{C}_{ar}$ of the mean

Publication Date: January 1, 1966 | doi: 10.1021/ba-1966-0055.ch020

aromatic cluster increases from the exinite over the vitrinite to the micrinite, the term $C_{ar(cond)}/C_{ar}$ in Equation 4 also increases, and, therefore, to have the same $\bar{S}_{ar}$ value for all three samples, the term $C_{ar(subst)}/C_{ar}$ must decrease. This is, of course, the case if $\bar{C}_{ar(subst)}$ decreases, or remains constant and at the same time $\bar{C}_{ar}$ increases, but also if $\bar{C}_{ar(subst)}$ increases, its increase however being smaller than that of $\bar{C}_{ar}$.

Table V. Values of the Aromatic Substitution Index $\bar{S}_{ar}$, depending on aromaticity f_a and H_{ar}/H for an Exinite, Vitrinite, and Micrinite

Sample	*H/C*	H_{ar}/H	f_a	$\bar{S}_{ar}$
			0.64	0.69
Exinite	0.991	0.20	0.62	0.68
			0.60	0.67
		0.18		0.71
		0.20	0.62	0.68
		0.22		0.65
			0.79	0.66
Vitrinite	0.780	0.35	0.77	0.65
			0.75	0.64
		0.32		0.68
		0.35	0.77	0.65
		0.38		0.62
			0.90$_5$	0.70
Micrinite	0.542	0.51	0.89	0.69
			0.87$_5$	0.68
		0.46		0.72
		0.51	0.89	0.69
		0.56		0.66

The $\bar{C}_{ar}$ values for the three macerals can be obtained by x-ray structural analysis (5). From the mean lamellae diameter $\bar{N}$ values can be calculated which principally measure the mean number of atoms in a hexagonal network and in the same plane. Therefore, $\bar{N}$ can represent either only the C_{ar} atoms of the cluster or the C_{ar} atoms and also atoms like C_{al}, O, N, and S which are directly linked to the aromatic cluster. In the first case, $\bar{N}=\bar{C}_{ar(max)}$ and in the second case $\bar{N}=\bar{C}_{ar(min)} + \bar{X}$, $\bar{X}$ being the number of substitution places ($\bar{C}_{ar(subst)}$) except direct bonds.

With the help of the aromatic substitution index $\bar{C}_{ar(max)}$ and $\bar{C}_{ar(min)}$ as well as the corresponding $\bar{R}_{ar(max)}$ and $\bar{R}_{ar(min)}$ can be calculated. The results of Table VI show clearly that the mean size of the aromatic cluster $\bar{R}_{ar}$ is smallest for the exinite and biggest for the micrinite. Based on the experience of a few model substances the most probable $\bar{R}_{ar}$ value should lie approximately in the middle between the reported extreme values.

A further comparative study will now be made on the number of nonaromatic rings per structural unit ($\bar{R}_{nar}$). If it can be assumed that H/C and

Publication Date: January 1, 1966 | doi: 10.1021/ba-1966-0055.ch020

Table VI. Maximum and Minimum Size of the Aromatic Clusters for an Exinite and Micrinite

Sample	$\overline{S}_{ar}$	$\overline{N}$	$\overline{C}_{ar(max)}$	$\overline{R}_{ar(max)}$	$\overline{C}_{ar(min)}$	$\overline{R}_{ar(min)}$	$\overline{C}_{ar(subst.)}$
			15.7	3.46			5.8
Exinite	0.68	15.7					
					10.8	2.20	5.0
			18.0	4.08			5.5
Vitrinite	0.65	18.0					
					13.0	2.75	4.9
			22.3	5.18			7.0
Micrinite	0.69	22.3					
					16.2	3.60	6.0

f_a of a polymer are also valid for its monomer (= structural unit), the following relation is also valid (9):

$$\frac{2(R - 1/m)}{C} = 2 - f_a - \frac{H}{C} \tag{5}$$

where R is the total number of rings ($R = R_{ar} + R_{al} + R_{hetero}$) and m the number of monomers per molecule. In Equation 5, C can be replaced by C_{ar}/f_a. Furthermore, if $m >> 1$, the term $1/m$ can be neglected, so that

$$R = \frac{C_{ar}(2 - H/C)}{2 f_a} - \frac{C_{ar}}{2} \tag{5a}$$

On the other hand, an f_a value can be derived from Equation 5 which corresponds to the limiting case, that $R_{nar} = 0$, or in other words $R = R_{ar}$:

$$f_{a(R=Rar)} = \frac{C_{ar}(2 - H/C)}{2(R_{ar} - 1/m) + C_{ar}} \tag{5b}$$

Each true f_a value which is smaller than $f_{a(R=Rar)}$ requires the presence of nonaromatic rings. For the three macerals under investigation there is no doubt that $1/m = 0$ can be used.

The values in Table VII show that 12 nonaromatic rings should be present for nine mean structural units in the case of exinite, 10 in the case of vitrinite, and 16 in the case of micrinite. Since all $f_{a(R=Rnar)}$ values are higher than the highest ones obtained from the aliphatic group distribution (see Table IV), all samples must contain nonaromatic rings even if the most probable f_a values

Table VII. Mean Number of Nonaromatic Rings, $\overline{R}_{nar}$ per Structural Unit and $f_{a(R=Rar)}$ of an Exinite, Vitrinite, and Micrinite

Sample	$\overline{C}_{ar}$	R_{ar}	f_a	R	$\overline{R}_{nar}$	$f_{a(R=Rar)}$
Exinite	13.25 ± 2.45	2.83 ± 0.63	0.62	4.05 ± 0.75	1.32 ± 0.12	0.71 ± 0.01
Vitrinite	15.50 ± 2.50	3.42 ± 0.66	0.77	4.53 ± 0.73	1.11 ± 0.07	0.85 ± 0.01
Micrinite	19.25 ± 3.05	4.39 ± 0.79	0.89	6.14 ± 0.97	1.75 ± 0.18	1.00 ± 0.01

Publication Date: January 1, 1966 | doi: 10.1021/ba-1966-0055.ch020

(column 4 in Table VII) are not the true values. If the true f_a values are somewhat higher, the R_{nar} values will be somewhat lower than those reported in Table VII, column 6, and vice-versa.

The nonaromatic rings can be either only alicyclic (hydroaromatic) or only heterocyclic, but it is also possible that both types are present simultaneously. The heterocyclic rings may contain N, S, and/or "nonreactive" oxygen. If it is assumed that *all* N, S, and nonreactive oxygen is present in heterocyclic form, these heteroatoms can build at most 0.8 heterocyclic rings per mean structural unit. The minimum number of alicyclic rings is then given by $\overline{R}_{al(min)} = \overline{R}_{nar} - 0.8$, whereas the maximum number of alicyclic rings is reached if $R_{hetero} = 0$, and therefore $\overline{R}_{al(max)} = \overline{R}_{nar}$. If tetra-substituted aliphatic carbon atoms are excluded, only CH_2 and CH groups can form alicyclic rings. The mean number of CH_2 and CH groups per structural unit can be calculated from the aliphatic group distribution and $\overline{C}_{al}$, which follows from $\overline{C}_{ar}$ and f_a. If it is assumed to a first approximation that mainly five- and six-membered rings with at least two and at most four alicyclic carbon atoms are present, $C_{alicyclic(min)}$ equals 2 $R_{al(min)}$ and $C_{alicyclic(max)}$ equals 4 $R_{al(max)}$ but it is evident that $C_{alicyclic}$ can never exceed the sum of all CH_2 and CH groups.

Table VIII shows that in the case of the exinite and the vitrinite $\overline{C}_{al(min)}$ is determined by 2 $\overline{R}_{al(min)}$ whereas $\overline{C}_{al(min)}$ of the micrinite is given by the smallest value for $\overline{C}_{(CH_2 + CH)}$; $\overline{C}_{al(max)}$ equals 4 $\overline{R}_{al(max)}$ only for the exinite; for the vitrinite and the micrinite it follows from the highest value for $\overline{C}_{(CH_2 + CH)}$.

Table VIII. Maximum and Minimum Number of Alicyclic Rings and Alicyclic Carbon Atoms in an Exinite, Vitrinite, and Micrinite

Sample	f_a	$\overline{C}_{al}$	$\overline{C}_{(CH + CH)}$	$\overline{R}_{al(min)}$	$\overline{R}_{al(max)}$	$\overline{C}_{alicycl(min)}$	$\overline{C}_{alicycl(max)}$
Exinite	0.62	8.13 ± 1.50	6.85 ± 1.26	0.40	1.44	0.80	5.76
Vitrinite	0.77	4.63 ± 0.75	3.32 ± 0.54	0.24	1.18	0.48	3.86
Micrinite	0.89	2.39 ± 0.37	1.54 ± 0.24	0.77	1.93	1.30	1.78

Table IX. Maximum and Minimum Portion of Alicyclic Carbon Atoms of C_{al} and C_{tot} for an Exinite, Vitrinite, and Micrinite

Sample	$(C_{alicycl}/C_{al})_{min}$	$(C_{alicycl}/C_{al})_{max}$	$(C_{alicycl}/C)_{min}$	$(C_{alicycl}/C)_{max}$
Exinite	0.12	0.60	0.05	0.23
Vitrinite	0.12	0.72	0.03	0.17
Micrinite	0.64	0.64	0.07	0.07

From the values of columns 3, 7, and 8 in Table VIII together with C_{tot} per structural unit, the results summarized in Table IX can be obtained. The range of $C_{alicycl}/C$ (columns 4 and 5, Table IX) is particularly important because $C_{alicycl}/C$ follows also directly from dehydrogenation reactions.

The results of column 3 in Table IX show that in all three macerals more than half of the aliphatic carbon atoms may be present in alicyclic or/and hydroaromatic rings. The micrinite has no range but only one value because even 2 $R_{al(min)}$ is bigger than the smallest value for $(CH_2 + CH)$. There is no doubt that in the case of the micrinite even small errors in the values of the

Publication Date: January 1, 1966 | doi: 10.1021/ba-1966-0055.ch020

structural parameters would allow only a small difference between $(C_{alicycl}/C_{al})_{min}$ and $(C_{alicycl}/C_{al})_{max}$.

Finally, the alicyclic fraction of H_{al} should be discussed. This structural parameter can be calculated from:

$$\frac{H_{alicycl}}{H_{al}} = \frac{H_{alicycl}}{C_{alicycl}} \cdot \frac{C_{alicycl}}{C} \cdot \frac{C}{H} \cdot \frac{H}{H_{al}} \tag{6}$$

if $\frac{H_{alicycl}}{C_{alicycl}}$ is known. This ratio corresponds to:

$$\frac{H_{alicycl}}{C_{alicycl}} = \frac{(H_{CH_2})_{alicycl} + (H_{CH})_{alicycl}}{C_{alicycl}} = \frac{2(CH_2)_{alicycl} + (C_{CH})_{alicycl}}{C_{alicycl}} \tag{7}$$

and with $(C_{CH})_{alicycl} = C_{alicycl} - (C_{CH_2})_{alicyl}$ one obtains from Equation 7:

$$\frac{H_{alicycl}}{C_{alicycl}} = \frac{(C_{CH_2})_{alicycl} + C_{alicycl}}{C_{alicycl}} = 1 + \frac{(C_{CH_2})_{alicycl}}{C_{alicycl}} \tag{7a}$$

On the other hand, from Equation 7 and with $(C_{CH_2})_{alicycl} = C_{alicycl} - (C_{CH})_{alicycl}$, one obtains:

$$\frac{H_{alicycl}}{C_{alicycl}} = \frac{2C_{alicycl} - (C_{CH})_{alicycl}}{C_{alicycl}} = 2 - \frac{(C_{CH})_{alicycl}}{C_{alicycl}} \tag{7b}$$

In general, the following can be said about $\frac{H_{alicycl}}{C_{alicycl}}$:

(1) If $C_{alicycl(max)} \leqslant C_{CH_2}$ $H_{alicycl}/C_{alicycl}$ can be 2. If $C_{alicycl(max)} > C_{CH_2}$ then $(C_{CH_2})/C_{alicycl} < 1$ and thus $H_{alicycl}/C_{alicycl} < 2$ (Equation 7a).

(2) If $C_{alicycl(min)} \leqslant C_{CH}$, $H_{alicycl}/C_{alicycl}$ can be $= 1$. If $C_{alicycl(min)} > CH$, then $(C_{CH})_{alicycl}/C_{alicycl}$ is < 1 and therefore $H_{alicycl}/C_{alicycl}$ is > 1 (compare Equation 7b).

Table X shows, in columns 2 and 5, the numbers of CH and CH_2 groups per structural unit which can be calculated from the results of Table IV. The values in columns 3 and 4 originate from Table VIII. The data from columns 2 and 5 lead to the values in columns 6 and 7, which give finally the $H_{alicycl}/C_{alicycl}$ values in columns 8 and 9 of Table X. As expected the micrinite possesses only one value for $H_{alicycl}/C_{alicycl}$ (see Table IX). In the case of the exinite, as long as the true number of alicyclic carbon atoms per 10 structural units is not greater than 10–11, all $C_{alicycl}$ atoms can be once substituted, and therefore $H_{alicycl}/C_{alicycl}$ can be 1. As soon as the true value of $C_{alicycl}$ exceeds the value 11, CH_2 groups have to be used to complete $C_{alicycl}$ and therefore $H_{alicycl}/C_{alicycl}$ increases (this value lies in the extreme case of 57–58 $C_{alicycl}$ atoms per 10 structural units at 1.74). Since the maximum possible number of alicyclic carbon atoms is smaller for exinite than the number of CH_2 groups present, all alicyclic C atoms can be unsubstituted, and therefore $H_{alicycl}/C_{alicycl}$ can reach the value 2. The situation is somewhat different for the vitrinite. As long as the true number of alicyclic carbon atoms is not greater than 9–10 per 10 structural units, all $C_{alicycl}$ atoms can be once substituted, and therefore the value 1 for $H_{alicycl}/C_{alicycl}$ is possible. If only up to 25–26 alicyclic C atoms are present, all of them can be unsubstituted, and the value

Publication Date: January 1, 1966 | doi: 10.1021/ba-1966-0055.ch020

Table X. Maximum and Minimum Portion of Alicyclic

Sample	$\bar{C}_{CH}$	$\bar{C}_{alicycl}$ min	$\bar{C}_{alicycl}$ max	$\bar{C}_{CH_2}$	$C_{CH}/C_{alicycl(min)}$
Exinite	1.05	0.80	5.76	6.59	> 1
Vitrinite	0.93	0.48	3.86	2.57	> 1
Micrinite	0.53	1.30	1.78	1.05	0.41

2 for $H_{alicycl}/C_{alicycl}$ is possible. If more than 9–10, or, respectively, more than 25–26 alicyclic C atoms are present, in the former case $H_{alicycl}/C_{alicycl} > 1$ and in the latter case < 2. This leads to the result that in the limiting case of 38–39 alicyclic C atoms, only the value $H_{alicycl}/C_{alicycl} = 1.67$ is valid.

With the help of these results and with Equation 6 the possible range of $H_{alicycl}/C_{alicycl}$ can be calculated. The data are reported in the last two columns of Table X. It can be concluded that in all three macerals, up to about half of the aliphatic hydrogen can be alicyclic and/or hydroaromatic.

Publication Date: January 1, 1966 | doi: 10.1021/ba-1966-0055.ch020

Summary

From *elementary analysis alone* it follows that the structural features of an exinite, vitrinite, and micrinite of the same rank (%C in the vitrinite = 83.9) must be different (strong decrease of %H in the sequence exinite, vitrinite, micrinite). The hydrogen distribution (H_{ar}/H, H_{al}/H, H_{OH}/H, is derived from infrared measurements and elementary analysis: H_{ar}/H increases, and hence H_{al}/H decreases from exinite over vitrinite to micrinite. From the measurement of the second moment at liquid nitrogen temperature (PSR) H_{CH_2}/H is calculated. From this parameter and H_{al}/H, $(H_{CH_3} + H_{CH})/H$ is obtained. It is now possible to establish sets of aliphatic group distributions, the limits being $H_{CH} = 0$ and $H_{CH_3} = 0$. From the possible aliphatic group distributions, possible intervals for the aromaticity ($C_{ar}/C = f_a$) have been obtained. There is no overlap between the f_a intervals of the three macerals: exinite possesses the lowest aromaticity and micrinite the highest. Most probable f_a values and the corresponding aliphatic group distributions (expressed in aliphatic groups per 100 C_{total} atoms) are: exinite: $f_a = 0.62$; 6 CH_3, 6 CH, and 26 CH_2 groups; vitrinite: $f_a = 0.77$; 6–7 CH_3 · 6–5 CH, and 11 CH_2 groups; micrinite: $f_a = 0.89$; 4 CH_3, 3 CH, and 4 CH_2 groups. The amount of CH_3 groups is certainly not negligible; its contribution to the aliphatic portion increases in the sequence exinite → vitrinite → micrinite. Exinite possesses the highest CH_2 content, and this may be related to the presence of aliphatic chains.

From x-ray measurements, $\bar{N}$, the mean number of atoms in a planar hexagonal arrangement can be calculated. $\bar{N}$ includes all aromatic C atoms (C_{ar}) and—to an unknown extent—all atoms except hydrogen directly attached to the aromatic systems. Knowing the number of substitution places (X) from hydrogen distribution, limits for $\bar{C}_{ar}$ (C_{ar} per mean unit) as well as $\bar{R}_{ar}$ (cond. arom. rings per mean unit) can be established, the upper limit being $C_{ar} = \bar{N}$ and the lower limit being $\bar{C}_{ar} = \bar{N} - X$. Results are: exinite: $\bar{R}_{ar} = 3.5$–2.2,

Hydrogen of H_{al} for an Exinite, Vitrinite, and Micrinite

$C_{CH_2}/C_{alicycl(max)}$	$\frac{H_{alicycl}}{C_{alicycl}}$	$\frac{H_{alicycl}}{C_{alicycl}}$	$\frac{H_{alicycl}}{H_{al}}$	
			min	*max*
>1	1	1	0.07	0.60
0.67	1	1.67	0.06	0.61
0.59	1.59	1.59	0.47	0.47

vitrinite: $\bar{R}_{ar} = 4.1$–2.75, micrinite: $\bar{R}_{ar} = 5.2$–3.6. The aromatic cluster size thus increases definitely from exinite over vitrinite to micrinite.

From aromaticity and elementary analysis the total number of rings per mean unit ($\bar{R}$) can be derived. The number of nonaromatic rings is then given by $\bar{R}_{nar} = \bar{R} - \bar{R}_{ar}$ and includes alicyclic and heterocyclic rings. If all hetero atoms were to form a ring, there could be a maximum of ~ 0.8 such rings per unit in all three macerals. Limits for the number of alicyclic rings per unit ($\bar{R}_{al}$) are obtained as follows: $\bar{R}_{al(max)} = \bar{R}_{(max)} - \bar{R}_{ar(min)}$ and $\bar{R}_{al(min)} = \bar{R}_{(min)} - \bar{R}_{ar(max)} - 0.8$. If it is taken into account that only CH_2 and CH groups can form alicyclic rings and that these rings contain not more than four and not less than two C atoms, limits for $\bar{C}_{alicycl}$ (alicyclic C atoms per unit) can be calculated. Results are: exinite: $\bar{R}_{al} = 0.40$–1.44, $\bar{C}_{alicycl} = 0.80$–5.76; vitrinite: $\bar{R}_{al} = 0.24$–1.18, $\bar{C}_{alicycl} = 0.48$–3.86; micrinite: $\bar{R}_{al} = 0.77$–1.93; $\bar{C}_{alicycl} = 1.30$–1.78. Taking into account the improbability of the extreme limits, all samples should contain alicyclic structures in not negligible amounts.

Acknowledgment

The maceral separation has been carried out at the Technische Hochschule, Aachen, and the authors want to express their thanks to C. Kröger.

Literature Cited

(1) Brown, F. B., Davis, H., private communication.
(2) Given, P. H., Peover, M. E., Wyss, W. F., *Fuel* **39,** 323 (1960).
(3) Oth, J. F. M., Tschamler, H., *Fuel* **42,** 467 (1963).
(4) de Ruiter, E., Tschamler, H., *Brennstoff-Chem.* **45,** 15 (1964).
(5) Ruland, W., Sandor, V., *Fuel* **44,** 39 (1965).
(6) Tschamler, H., de Ruiter, E., *Brennstoff-Chem.* **44,** 280 (1963).
(7) Tschamler, H., de Ruiter, E., *Brennstoff-Chem.* **43,** 16 (1962).
(8) Van Krevelen, D. W., "Coal," p. 323, American Elsevier Publishing Co., New York, 1961.
(9) *Ibid.*, p. 435.
(10) Van Krevelen, D. W., Chermin, H. A. G., *Fuel* **33,** 338 (1954).
(11) Van Krevelen, D. W., Schuyer, J., "Coal Science," p. 193, American Elsevier Publishing Co., New York, 1957.

RECEIVED October 5, 1964.

Discussion

H. L. Retcofsky: How did you derive the extinction coefficients which you used for determining H_{al} from the infrared spectra of macerals?

Hubert Tschamler: They were derived either from mean values observed for model compounds of known structure or from the properties of solvent extracts of coals. In the latter case an accurate value for $\%H_{al}$ can be derived by measuring proton spin resonance in solution and this, combined with the optical densities observed in the infrared spectra, gives the specific extinction coefficients. (*See* J. F. M. Oth, E. de Ruiter and H. Tschamler, *Brennstoff-Chem.* **42**, 378 (1961); also Ref. 7).

Bhupendra Mazumdar: Our dehydrogenation studies indicate that a coal of around 84% carbon content has an alicyclicity of about 0.23. Do you feel that your values of aromaticity are compatible with published alicyclicities?

Dr. Tschamler: I have recently compiled a table comparing the various published values of $C_{alicycl}/C$ for coals, together with a figure recently obtained by R. Fuks. It is as follows.

Author	*Method*	*%C in Coal*	$C_{alicycl}/C$
M. E. Peover (1960)	*p*-Benzoquinone	80.0	0.35
		84.0	0.27
		88.0	0.20
B. K. Mazumdar (1962)	Sulfur; > 200°C.	82.5	0.25 (0.18)
		85.0	0.22 (0.16)
		87.5	0.17 (0.13)
		90.0	0.11 (0.09)
I. Wender (1963)	$Pd/CaCO_3$; 350°C.	80.0	0.20
		85.0	0.14
		90.0	0.01
P. H. Dicker (1963)	Sulfur; < 200°C.	81.0	0.16 ± 0.02
		85.5	0.11 ± 0.02
R. Fuks (ERA) (1964)	Phenanthrenequinone 150°C.	84.0	0.13 ± 0.02

The figures of B. K. Mazumdar *et al.* shown in parentheses are the revised values computed by these authors after it had been pointed out that at temperatures above 200°C. the sulfur dehydrogenation method they used is capable of removing hydrogen from aromatic nuclei as well as alicyclic rings. The revised figure for a coal of 85% C was 0.16, not 0.23.

Various methods and assumptions give for a vitrinite of 84% C content, values of aromaticity, f_a, ranging from 0.64 to 0.81 (3). A number of arguments suggest that H_{al}/C_{al} should be at least 1.65, which raises the minimum value for f_a to 0.71. For various reasons (4) we believe 0.77 is the most probable value, which would mean that C_{al}/C is 0.23. Certainly not all aliphatic carbon is alicyclic, so that $C_{alicycl}/C$ must be smaller than C_{al}/C. Hence we feel that the data of Peover in the above table are unrealistic, but all the other values (including the revised figures of Mazumdar *et al.* but not

Publication Date: January 1, 1966 | doi: 10.1021/ba-1966-0055.ch020

the original data) are in reasonable agreement and fit into the overall concept of the distribution of carbon and hydrogen.

Our own results (R. Fuks, 1964) by chemical dehydrogenation indicate that $C_{alicycl}/C$ is 0.13 for a vitrinite of 84% C. If $f_a = 0.77$, then on the average 57% of the aliphatic carbon atoms are alicyclic, which seems reasonable since we found that the range of $C_{alicycl}/C_{al}$ is 0.45–0.72 if $R_{hetero} = 0$, and 0.26–0.72 if $R_{hetero} = 0.5$. Details have been published (*4*).

Dr. Mazumdar: The revised values of alicyclicity referred to by Dr. Tschamler are to be treated as minimum estimates since we had possibly overcorrected for the suspected side reaction during sulfur dehydrogenation. more recent work on reduced coals ("Abstracts of Papers," 142nd Meeting, ACS, September 1962, p. 3K) suggests that in fact side reactions quite possibly do not occur with the Vesterburg technique, and therefore we believe that the alicyclicity of the coal studied by Dr. Tschamler may well be as high as 23%. Hence, I feel that the aromaticity deduced by Dr. Tschamler from physical data may be somewhat on the high side.

Peter H. Given: Whereas Tschamler and Fuks, and Peover studied more or less pure vitrinites, Mazumdar apparently worked with whole coals. Moreover, Indian coals, being from Gondwanaland strata, are most probably of very different petrographic composition compared with European and North American coals (rich in exinites and inert macerals; *See* p. 284). Quite apart from the question whether sulfur dehydrogenation really is free of side reactions, there may well be a spread of data at any level or rank because of petrographic differences.

I object to the use of the term "alicyclicity" in this connection. The methods used by Peover, Wender, and Fuks are selective for that group of alicyclic substances capable of yielding aromatic structures on dehydrogenation—i.e., for *hydroaromatic* rings. If the sulfur method really dehydrogenates *any* alicyclic structures (e.g. cyclooctane or camphene), then it would yield olefins rather than aromatics and could probably also convert saturated chains to olefins. On the other hand, if it attacks only hydroaromatic structures, then "alicyclicity" is an incorrect and misleading expression, and "hydroaromaticity" should be used.

Publication Date: January 1, 1966 | doi: 10.1021/ba-1966-0055.ch020

21

Electron Spin Resonance Study of Pure Macerals

D. E. G. AUSTEN[1] and D. J. E. INGRAM[2]
Department of Electronics, University of Southampton, England

P. H. GIVEN, C. R. BINDER, and L. W. HILL
Department of Fuel Technology, Pennsylvania State University, University Park, Pa.

Publication Date: January 1, 1966 | doi: 10.1021/ba-1966-0055.ch021

The concentration of unpaired spins in a series of pure macerals from British and North American bituminous coals has been determined. The concentration in vitrinites increases consistently with rank and rises sharply above about 90% carbon content. Values for spore-rich exinites lie somewhat below those found for the associated vitrinites. The corresponding fusinites have unpaired spin concentrations much higher (2–5 times) than those of the other macerals, and the half-peak width of the signal is much narrower. On pyrolysis in nitrogen at temperatures up to 550°C. the signals given by the vitrinites and exinites increase in height and sharpness, whereas those given by the fusinites undergo little change in either characteristic. The results suggest that the origin of the fusinites studied involved exposure of woody tissue to moderately high temperatures.

Electron spin resonance studies of whole coals and vitrinites, before and after laboratory carbonization, were published some years ago (*2, 14, 15, 17*). Some measurements on exinites and micrinites from German coal seams have also been described (*14*). An extensive series of vitrinites, exinites, and fusinites were studied by two of the authors (D. E. G. Austen and D. J. E. Ingram) in 1959, but the results have been reported previously only in a doctoral thesis (*1*). This study formed the starting point for the other three authors, who have continued the investigation to ascertain how much electron spin resonance studies can

[1] Present address: Esso Research Ltd., Abingdon, Berkshire, England.
[2] Present address: Department of Physics, University of North Staffordshire, Keele, Staffordshire, England.

In Coal Science; Given, P.;
Advances in Chemistry; American Chemical Society: Washington, DC, 1966.

elucidate the origins of coal macerals; this aspect of the data has not been considered previously. The same set of samples (from British coal seams) has been used in both series of experiments, but in the later work it was supplemented by specimens from North American seams.

The basis of electron spin resonance can be explained briefly as follows. In normal covalently bonded molecules all the electrons occur in pairs. Each pair is described by the same orbital—i.e., the two electrons are of equal energy. However, the spins of the electrons are opposed; hence the net magnetic moment of a pair is zero. Molecular species are known in which there is one unpaired electron in the molecule, and these are commonly known as "free radicals." Such free radicals are paramagnetic, and under the influence of a magnetic field the energy level corresponding to an unpaired electron can be split in two. One can then observe transitions between the two levels; the energy gap between them can be altered by an externally applied magnetic field, and measurements are normally made with applied magnetic fields of some 3000 gauss and microwave radiation of 3-cm. wavelength (about 10^{10} c.p.s.). This is the phenomenon known as electron spin resonance or electron paramagnetic resonance.

Normally, species containing unpaired electrons are unstable, rapidly decomposing or dimerizing to give a new species in which the two odd electrons are paired in one new orbital. Free radicals can be relatively stable if the unpaired electrons are delocalized over an extensive conjugated system of double bonds, for example in certain aromatic molecules. Most forms of carbon, including coal macerals and the asphaltic bitumens of petroleum, are highly aromatic; moreover, since they are solid, the molecular movement necessary for dimerization is effectively prevented. Such "trapped" radicals in carbons are known to be very stable, though in some cases the signal is weakened and broadened by absorbed oxygen which is paramagnetic.

Experimentally, the sample to be studied is placed in an intense, homogeneous, magnetic field and irradiated with microwave radiation of accurately known frequency, generated by a klystron and conducted through wave guide channelling. The magnetic field intensity is varied through a narrow range, and the absorption is measured with suitably balanced electronic circuits. The concentration of free spins can be calculated from the absorption signal as one passes through the critical field intensity, and some information about the character of the free spins can be deduced from the shape of the signal, particularly its width.

Experimental

Samples Studied. FROM BRITISH SEAMS. The suite of samples was collected and separated by the Coal Survey of the National Coal Board under the direction of Dr. G. W. Fenton, and the authors are indebted to Dr. Fenton for the gift of the samples. The suite consisted of the vitrinites, spore-rich exinites, fusinites and, in one case, the micrinite from five British coal seams of Carboniferous age together with the vitrinites from two coals of higher rank from which it was impracticable to separate the other macerals. The exinites were separated by float-and-sink methods from selected black durain bands, as also

Publication Date: January 1, 1966 | doi: 10.1021/ba-1966-0055.ch021

was the micrinite. The fusinites were similarly separated from relatively thick lenses of fusain occurring as partings in the seams.

A brief description of the separation methods and of some properties (volatile matter, coking properties, density) of the macerals was given by Fenton and Smith (*7*). Elementary analyses and an extensive organic study have been reported previously by various authors (*9*, *10*), and the infrared spectra have been reported by Brown and Bent (*4*). General information on the stratigraphy and fossil distribution of the seams is contained in Trueman's book (*19*). Some properties of the macerals are collected in Table I together with some values of the reflectance under oil immersion (determined by Mr. R. C. Neavel, Department of Geology and Geophysics, Pennsylvania State University). Since, as will be shown later, the greatest interest attaches to the results obtained for the fusinites, the reflectance distribution (50–75 points, also determined by Mr. Neavel) of these macerals is given in Figure 1 as a further aid to identifying the samples used.

North American Samples. These materials have so far been less well characterized than the British samples, and the fusinites were less petrographically pure. They had, however, been more recently collected. Available information is included in Table II.

Table I. Properties of Macerals from British Seams

Coal Colliery, Seam	Vitrinite		Exinite	Fusinite	Micrinite
	% C, daf	Reflectance in oil, %	% C, daf		
1. Cannock Wood, Shallow	79.6	—	81.0	90.3	n.s.
2. Teversal, Dunsil	81.5	—	n.s.	87.7	n.s.
3. Markham Main, Barnsley	82.3	0.674	81.6	91.6	n.s.
4. Dinnington Main, Barnsley	85.1	—	84.3	n.s.	n.s.
5. Aldwarke Main, Silkstone	86.9	1.109	87.1	92.1	86.9
6. Chislet, No. 5	88.6	—	89.1	92.2	n.s.
7. Roddymoor, Ballarat	88.8	1.304	n.s.	n.s.	n.s.
8. Coegnant, Gellideg	91.4	—	n.s.	n.s.	n.s.
9. Blaenhirwaun, Pumpquart	93.8	—	n.s.	n.s.	n.s.

n.s. = no sample available.
Petrographic purities: mostly 90–98%.
Ash content: 0.3–1.0% for vitrinites and exinites, 2–4% for fusinites and micrinite.
For reflectance of fusinites *see* Figure 1.

Pyrolysis Procedure and Sample Preparation. Pyrolyzed samples were prepared by heating 0.1–0.2 gram maceral in a boat under a stream of oxygen-free nitrogen at 10°/min. to the desired temperature, and maintaining the sample at that temperature for 1 hour.

In the original measurements by the Southampton workers, measurements were made on dried samples in air and sealed under vacuum. Oxygen effects

Publication Date: January 1, 1966 | doi: 10.1021/ba-1966-0055.ch021

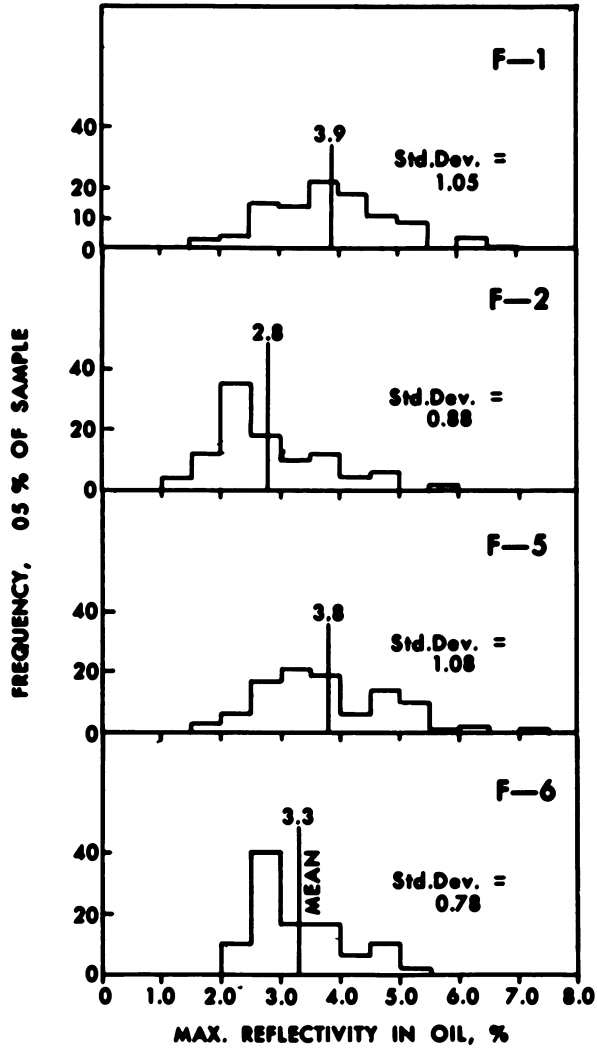

Figure 1. Reflectance distribution in British fusinites

were found for the higher rank vitrinites and all the fusinites, and therefore only the in vacuo measurements are reported here. In the Penn State work, all samples were evacuated at 100°C. and about 10^{-5} torr for 15–24 hours and then sealed while still evacuated. About 0.1-gram sample was used for each measurement.

Instrumentation. Two electron spin resonance spectrometers have been used in the course of the work. The Southampton instrument was built in the laboratory, using a Varian magnet, and operated at 3 cm. wavelength. It employed an H_{014} rectangular cavity and obtained high sensitivity by magnetic field modulation at 100 kc.p.s. with a crystal detector; phase sensitive detection

Table II. Macerals from American Seams

Coal Location, seam	Vitrinite % C (estimated)	Vitrinite R_o, %	Fusinite R_o, mean, %
Ellsworth, Pa., Pittsburgh Seam	84.0	0.90	4.2 (approx.)
Buckhannon, W. Va., Redstone Seam	84.5	0.95	4.7[a]

[a] Range of reflectance values, 1.5–6.5%; sample contained roughly 5% vitrinite as impurity.

was also used as and when necessary to determine or check results. Free radical concentrations were obtained by comparing the integrated signal strengths with those from standard samples.

The Penn State measurements were made in a spectrometer constructed by Dr. H. Atwater in the Department of Electrical Engineering, which operated at a frequency of 9.11×10^9 c.p.s., and employed a Varian Type V 4612A magnet. Phase sensitive detection was used, in conjunction with a bolometer detector. The cylindrical cavity operated in the H_{011} mode.

In order to obtain absolute measurements of spin concentrations, a series of standards was made up, which consisted of known weights of diphenylpicrylhydrazyl (DDPH) diluted with potassium chloride (the mixtures were blended in a vibrating ball mill). A suitable standard was run immediately after each unknown at identical settings of instrument gain so that recorder traces of standard and unknown could be directly compared.

Results

Preliminary Tests of Significance of Instrumental Data. The electron spin resonance band given by a solid material normally consists of a symmetrical curve with a single maximum. The shape and width of the band is determined by the nature of the operative relaxation processes; the excess energy associated with the upper energy level can be dissipated to other parts of the system in various ways, and the relative importance of these determines the form of the signal (*12*). It is also possible that unresolved hyperfine structure from the hydrogen atoms can contribute to the observed line width. Double resonance measurements on such carbons have indicated a coupling between the unpaired electrons and the protons. In ideal cases, the shape is that of either the Lorentzian or Gaussian distribution curves. In these cases an experimental curve can be fully characterized by two parameters, and integration of the curve to give the total signal strength can be performed analytically; this is true also when the experimental recorder trace is the first differential of the absorption curve, as it is when phase sensitive detection is employed.

The absorption curves given by coal macerals approached the horizontal (magnetic field strength) axis more slowly than a Gaussian distribution curve. Shape analysis (*16*) showed that over much of the curve, the form closely approximated a Lorentzian distribution curve, but both positive and negative deviations were found in the wings of the curves (that is, in various examples, the curves approached the axis either somewhat more or somewhat less rapidly

than a true Lorentzian curve). In these circumstances, it is necessary to perform a double integration on the experimental first-differential curve in order to obtain a number proportional to spin concentration. Such integration was therefore performed, by graphical methods, on all curves obtained in the work reported here including the DDPH standards, and absolute spin concentrations were obtained as ratios of unknown to standard.

The line widths recorded are the distances, in gauss, between the two maxima of the differential curve and thus represented the width of the absorption curve at the level of maximum slope. For a curve of Lorentzian shape, this width is equal to $0.577/T_2$, where T_2 is the spin-spin or "transverse" relaxation time (*12*). Since the curves were not strictly Lorentzian (though they were so to well below the region of maximum slope) and in any case were not of identical shape, the recorded line widths do not have this exact theoretical significance, and small differences in width between two samples could be caused by shape differences rather than variations in relaxation phenomena. Nevertheless, since the conclusions drawn later from the observed line widths depend on major differences in level rather than subtle differences in numerical value, they should be perfectly valid.

Tests for the "skin effect" were made on a few of the samples by making measurements on macerals diluted to various extents with potassium chloride (*16*). The number of spins per gram of coal was found to be independent of dilution, and so there is no evidence of a skin-effect. It was established that saturation of the energy transitions was not occurring by varying the microwave power by a calibrated attenuator; the spin concentration found did not depend on power in the range covered (5–30 milliwatts).

Results on Unheated Samples. The results obtained in Southampton for the set of British samples are shown in Figures 2 and 3. In Figure 2 the spin concentration of each maceral is plotted against the carbon content (daf) of the associated vitrinite, and the points for each set of macerals from one coal are joined by a vertical line. It can be seen that the vitrinite series forms a well-defined narrow band which curves upwards sharply at about 90% carbon, and the data resemble closely those presented earlier by Austen and Ingram for whole coals. The values of exinites form a wider, approximately horizontal band lying a little below the vitrinite band, while the fusinite data appear to vary at random but lie consistently well above the vitrinite band and are appreciably higher than vitrinites of the same carbon content (90–92%) would be.

Figure 3 shows that the line widths of the vitrinite signals are 4.5–7.0 gauss, decreasing with increasing rank; these values are typical for low temperature carbons (it should be noted that values previously reported by Ingram and Austen (*2*) are widths at half-peak height and are therefore 1.73 times greater than the figures given here (*12*). The fusinites give unusually narrow signals (2–3 gauss), and in strength and width the signals are very reminiscent of those previously reported for pyrolyzed coals and carbons.

Measurements on the same set of samples have been repeated in the Penn State laboratories. In spite of the fact that the samples had been stored for 5 years (in sealed ampoules under nitrogen) and in spite of the difference in

Publication Date: January 1, 1966 | doi: 10.1021/ba-1966-0055.ch021

instrumentation, the general pattern displayed by the data was found to be the same, and the actual numerical data were repeated within about ±20%. The line widths were reproduced more closely than this indicating that little, if any, addition of oxygen had occurred in the intervening time.

Results for Pyrolyzed Samples. The complete set of data obtained is collected in Table III and some typical trends are shown in Figures 4 and 5. For consistency, the figures shown for unpyrolyzed samples are all data obtained by the Penn State group. At 550°C. the vitrinites suffered about 25%

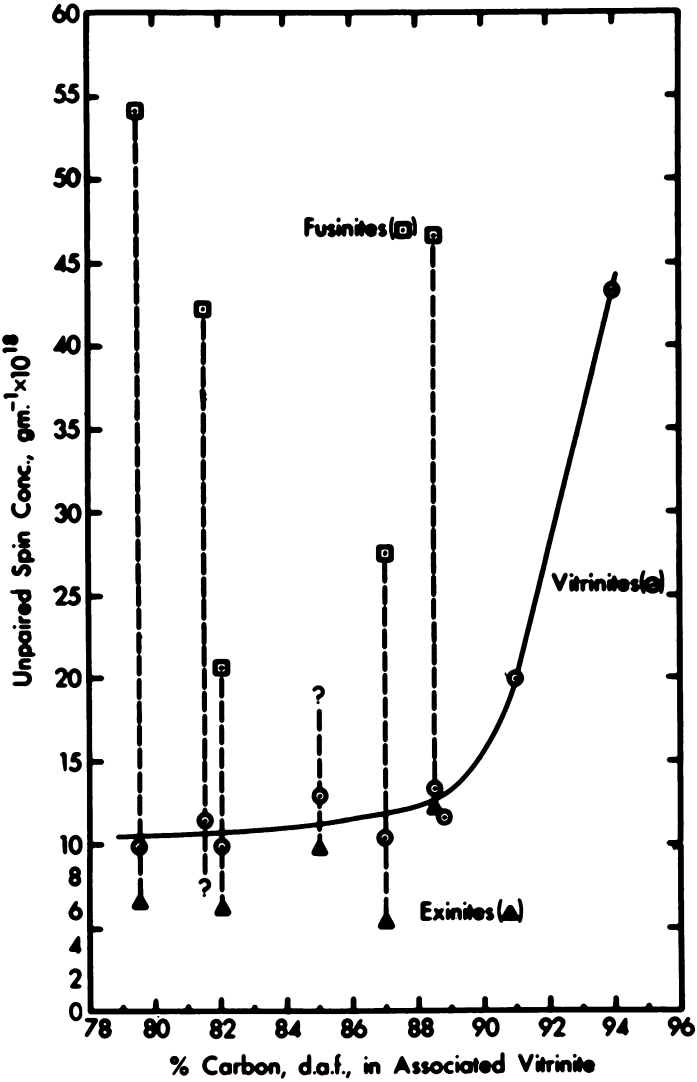

Figure 2. Unpaired spin concentration in pure macerals

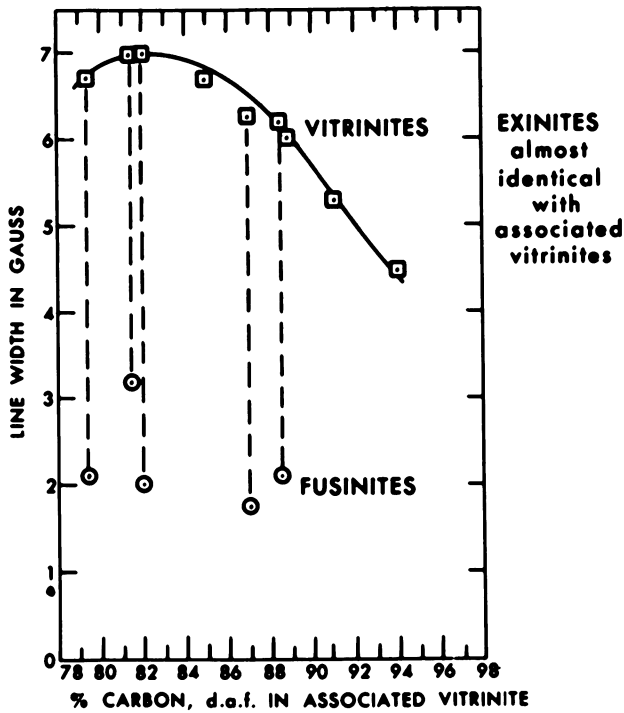

Figure 3. Line width in pure macerals

loss in weight, the exinites 40–50%, and the fusinites and micrinite 2–10%.

The changes in spin concentration and line width recorded for vitrinites and exinites are typical of what has been observed previously with whole coals and many types of low temperature carbons (*2*, *12*, *14*, *15*, *17*). On the other hand, the signals given by fusinites either did not change in strength or width within the limits of experimental error, or there was a small increase in strength with virtually no change in width. The single micrinite sample available behaved similarly to the fusinites and to the micrinites previously studied by Kröger (*14*); its signal strength increased a little on pyrolysis. In all cases the *g* values (2.0027–2.0037) were very close to the free spin value (2.0023), indicating that as a result of delocalization of electrons in aromatic systems, there is little coupling between the spin and orbital motions of the electrons.

Discussion

Vitrinites and Exinites. We have seen that the changes in ESR behavior of exinites and vitrinites are very much like those of low temperature carbons, and so they call for no particular discussion. Interpreting the changes shown by vitrain has been discussed by Van Krevelen and Smidt (*13*, *17*) and by Austen and Ingram (*2*, *12*). It may, however, be added here that the nearly Lorentzian shape of the signals obtained indicates that exchange narrowing

Publication Date: January 1, 1966 | doi: 10.1021/ba-1966-0055.ch021

Table III. Unpaired Spin Concentrations and Line Widths of Macerals before and after Laboratory Pyrolysis

Sample	Unheated		350° C.		450° C.		550° C.	
	[a]Line Width	[b]Conc.	Line Width	Conc.	Line Width	Conc.	Line Width	Conc.
1. Cannock Wood								
exinite	7.0	3.2	8.0	12.2	4.6	45.7	2.5	123.4
fusinite	1.6	44.3	1.9	51.7	1.8	43.3	1.5	58.5
2. Teversal								
vitrinite	6.7	5.53	5.4	10.2	5.0	34.9	3.7	39.5
fusinite	1.5	56.1	3.3	49.5	3.4	61.6	3.2	52.9
3. Markham Main								
vitrinite	8.0	6.36	8.7	18.8	6.3	31.7	2.7	65.9
fusinite	1.4	31.1	3.0	28.6	2.1	32.4	2.1	42.0
4. Dinnington Main								
vitrinite	7.9	9.88	7.5	12.1	8.0	32.1	2.8	90.3
5. Aldwarke Main								
vitrinite	8.1	12.0	7.9	10.9	7.2	19.0	4.7	28.5
fusinite	2.0	43.5	2.7	42.0	2.5	49.0	3.6	53.9
micrinite	1.9	53.1	2.3	35.1	2.3	33.2	3.4	45.6
6. Chislet								
vitrinite	7.9	9.87	8.0	12.1	7.1	27.4	4.9	81.7
exinite	5.5	7.32	5.9	12.1	5.9	97.9	3.1	145.4
fusinite	1.7	73.4	2.3	77.0	3.0	78.2	2.8	89.3
7. Ellsworth								
vitrain	7.2	1.73	8.4	3.54	3.8	86.2	5.3	18.5
fusain	4.8	30.70	5.9	19.90	3.2	18.9	3.6	21.3
8. Redstone								
vitrain	6.4	4.96	5.3	8.92	6.7	10.8	3.7	120.0[d]
fusain	2.2	40.80	3.1	54.00	3.2	45.2	2.3	39.9[c]

[a] All line widths in gauss.

[b] All concentrations in spins/gram $\times 10^{18}$.

[c] Pyrolyzed at 650°C., line width 3.0 gauss 38.3 $\times 10^{18}$ spins/gram and at 750°C., line width 5.7 gauss, 27.2 $\times 10^{18}$ spins/gram.

[d] Pyrolyzed at 650°C., line width 2.8 gauss, 113.9 $\times 10^{18}$ spins/gram and at 750°C., line width 2.5 gauss, 2.72 $\times 10^{18}$ spins/gram.

and/or delocalization narrowing (Ref. *12*, pp. 127–8) occur and increase when the samples are pyrolyzed.

The chief question of geochemical interest is how the radicals came to be in the macerals in the first place and why the change with rank is as found. Although it has been known for some years that whole coals contain appreciable concentrations of free radicals, this question appears not to have been discussed previously in any general way. Three possible answers suggest themselves.

(1) Stable radicals were formed during diagenesis of the organic sediment, and they have persisted ever since. The detailed mechanism of enzymatic reactions is not well understood, but it is known that stable free radicals can be produced. Steelink (*18*) has found that humic acids from soils, peats, and lignites have moderately high concentrations of free radicals, and since the

Publication Date: January 1, 1966 | doi: 10.1021/ba-1966-0055.ch021

signal increases in strength on treatment with alkali, he believes the radicals are mainly of a semiquinone character and exist in quinhydrone structures.

It seems therefore that stable radicals *are* formed during diagenesis (possibly by aerial oxidation as well as enzymatic action), but it may be questioned whether it is these radicals that survive metamorphism and are observed in bituminous coals. One of the main chemical consequences of metamorphism is that much of the combined oxygen in peats is eliminated, and one would expect that if the majority of the free radical centers in peats were localized on oxygen atoms, they would mostly be eliminated during metamorphism.

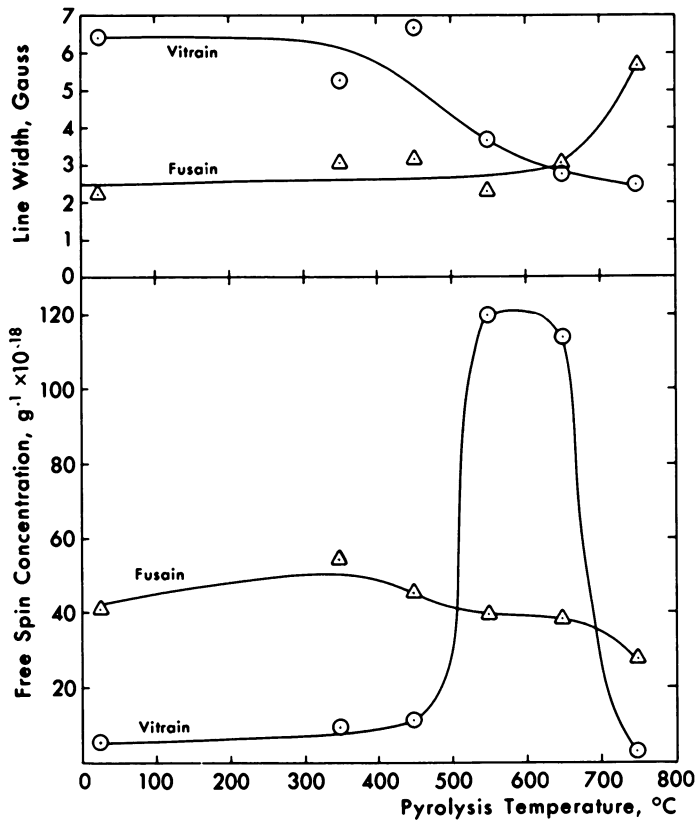

Figure 4. Free spin concentration and line width; Redstone vitrain and fusain

Moreover, the radicals in bituminous vitrinites do not have the characteristics of oxygen radicals. For one thing, it was concluded from the g value (2.007) of the signal given by the semiquinone radical produced from anthraquinone that the unpaired electron was largely localized on the oxygen, in contrast to aromatic hydrocarbon radicals where the electron is largely delocalized (3). The g values found in the present work were appreciably smaller, indicating

Publication Date: January 1, 1966 | doi: 10.1021/ba-1966-0055.ch021

delocalization of the electrons; the line widths and nearly Lorentzian shape suggest a similar conclusion. Furthermore, phenoxy radicals might be expected to bring about homolytic splitting of acetic anhydride during acetylation and hence lose their radical character, whereas it was found that acetylation does not change the radical concentration appreciably.

It is, of course, possible that oxygen radicals present in peats are indeed largely eliminated during metamorphism but leave an aromatic structure behind over the carbon atoms of which the odd electron is delocalized. This remains a reasonable possibility.

(2) Radicals are formed in pyrolytic reactions during metamorphism. The differences in elementary composition and functional group concentration between peats, lignites, and bituminous coals can be accounted for by postulating a progressive elimination of such simple substances as methane, water, and carbon dioxide during metamorphism. Moreover, these substances do occur abundantly in coal measures, and it seems quite likely that they result from decomposition of methyl and methoxyl, hydroxyl and carboxyl groups, respectively. Such decomposition would certainly take place by homolytic splitting, and a proportion of the radicals thus left behind in the solid structure may well be stabilized (a) because they are trapped inside a structure in which little mobility is possible, and (b) by delocalization of the unpaired electrons over the aromatic system.

From this view, the number of radical centers *formed* in a coal by splitting off side groups would increase with rank. Simple calculation shows that only a small fraction (on the order of 0.1–1%) of these centers survive in modern bituminous coals. The level of rank at which the spin concentration in vitrinites begins to increase rapidly is more or less the level at which, according to the x-ray studies of Hirsch *et al.* (*11*), the size of the aromatic nuclei begins to grow rapidly. Presumably, then, the high unpaired spin concentration in high rank vitrinites is caused not only by an increased number of radicals produced during metamorphism, but also by survival of a greater fraction as a result of more effective stabilization in the large aromatic lamellae.

(3) The radicals are produced during metamorphism by radiation from radioactive materials in the mineral matter. None of the common radioactive elements (U, Th, K^{40}) has much of its radiation energy in neutron emission, and so we need consider only α-particles and electrons. Typical concentrations of potassium in the mineral matter of coal are known, and from the K^{40}/K^{39} abundance ratio, one can easily estimate probable levels of K^{40} concentration. Little is known of the concentrations of U and Th, except that they are lower in shaley materials than in any other kind of rock, but one can assume an approximate level of one part in 10^7 parts of mineral matter.

The range of α-particles in organic solids is around 40 microns, and of electrons 1–2 mm.; the greater proportion of the available energy is in α-radiation. When an α-particle of 4 m.e.v. energy passes through organic matter, it removes electrons and occasionally protons in its path and loses a small proportion of its energy at each collision. Calculation shows that in 300 million years the number of unpaired electrons that would have been produced per gram of bituminous coal is of the order of 10^{20}–10^{21}, which is similar to the number

Publication Date: January 1, 1966 | doi: 10.1021/ba-1966-0055.ch021

that could have been produced by metamorphic scission of methyl groups, etc. The two mechanisms of radical production could perhaps be combined by suggesting that radiation effects supply at least part of the activation energy for scission.

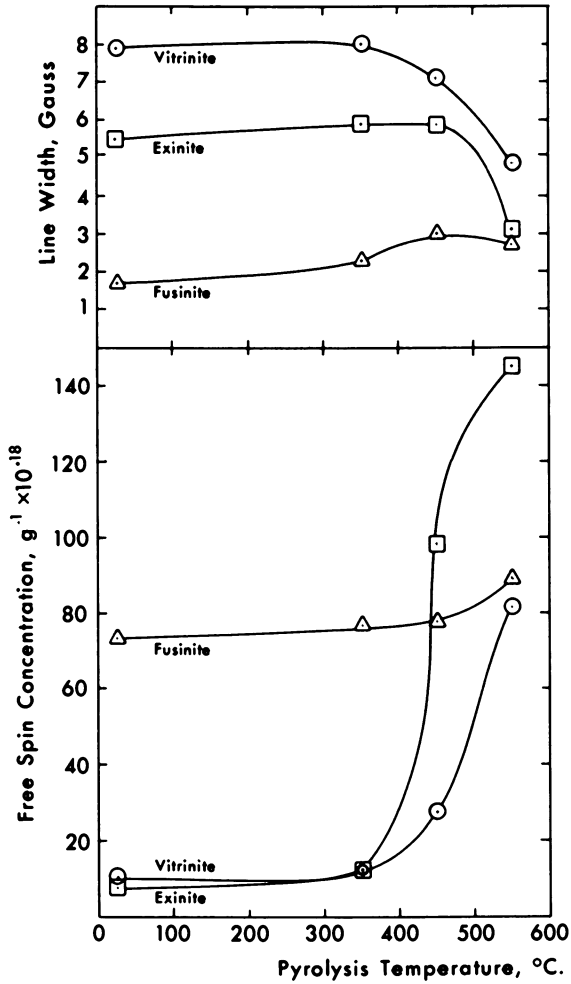

Figure 5. Free spin concentration and line width for macerals from Chislet, No. 5, coal

Breger and Friedel (*8*) showed that irradiation of two high rank coals (89.5 and 90.3% carbon) with neutrons does indeed increase the spin concentration, but low rank coals were not affected in this way. Breger, Ergun, and Donaldson (*6*) showed that in coalified logs containing exceptionally high concentrations of epigenetic uranium, the organic material was extensively altered but along a path different from that of normal metamorphism (the

Publication Date: January 1, 1966 | doi: 10.1021/ba-1966-0055.ch021

effect of radiation having been to cause cross-linking of alicyclic structures rather than aromatization).

Duchesne, Dépireux, and van der Kaa (*5*) found that the radiation yield when lignites were irradiated with γ-radiation from Co^{60} and high energy α-particles (16 m.e.v.) was in the range 0.2–6 × 10^{-3} radicals produced per 100 e.v. absorbed. On this basis, calculation from U + Th contents measured by α-scintillation showed that the radicals in the particular lignites they studied (which had rather high contents of U + Th: 10^{-6}–10^{-3} g/g of whole coal) could have been produced largely by radiation effects. They stated that in bituminous coals the U + Th contents are much lower (5 × 10^{-9} g/g) and concluded that only a small proportion of the radicals could have been produced by radiation. As general propositions these conclusions appear contradictory since bituminous coals have presumably passed through a lignitous stage (unless one assumed that lignites acquire much epigenetic uranium and lose it again during metamorphism to higher rank).

All three possible explanations of the presence of relatively high concentrations of unpaired spins in vitrinites and exinites from bituminous coals seem reasonably plausible. It is likely that all three mechanisms made some contribution, but one cannot at present assess their relative importance.

Fusinites and Micrinite. The fusinites studied in the present investigation were characterized by higher spin concentrations than the macerals associated with them, and the line widths were much narrower. These characteristics did not change much on pyrolysis up to at least 550°C., again in contradistinction to the other macerals.

It is immediately obvious that there is some ambiguity in the results of previous ESR studies of whole coals since the behavior of a series of samples both before and after pyrolysis will depend on their relative petrographic make-up and particularly on their fusinite contents. However, since most of the samples that have been studied were vitrainous, the results can be taken without too much ambiguity as referring to vitrinites.

It is interesting to compare the figures reported here for fusinites with those found for coals by Smidt and van Krevelen. (*13*, *17*). These authors studied a range of "hand-picked vitrains of high purity, which could almost be considered as vitrinites," covering a range of carbon content 71.7–96.5%; their measurements were made during carbonization at temperatures up to about 600°C. They found no change in spin concentration on pyrolysis of the lignite of 71.7% carbon and of the high rank anthracites (95.1 and 96.5% carbon), but the width of the signal given by the materials changed considerably on heating (in fact, it *increased* markedly). The high rank coals are undoubtedly highly graphitic, and the ESR signal observed may be caused largely by conduction electrons rather than free radicals; at any rate, a different kind of phenomenon is probably being observed.

At the level of carbon content of the fusinites studied (90–92%) Smidt and Van Krevelen found little change of signal width below about 450°C., but the spin concentration increased by a factor of 3–4 between about 420° and 550°C. Experience with carbons prepared in the laboratory shows that if certain ESR characteristics are developed by exposure to a certain heat treatment

Publication Date: January 1, 1966 | doi: 10.1021/ba-1966-0055.ch021

temperature, then subsequent reheating to the same temperature does not alter the characteristics (of course, this is not true if very short periods of time are involved in the initial heat treatment). It would be of great assistance in understanding geothermal effects if one could reverse this statement—i.e., if one could assert that the minimum temperature at which changes in ESR behavior are observed represents the maximum temperature to which the carbonaceous material had been exposed in its previous history. In what circumstances can this form of the statement be true?

In general, free radical centers that are produced in a carbonaceous solid by pyrolysis result from the scission of bonds during the release of volatile matter and are stabilized by aromatization of the structure. Activation energies for scission processes are normally of such a magnitude that temperatures of several hundred degrees (Centigrade) must be reached before they proceed at a rate that can be observed in the laboratory. Therefore, if free radical centers can be produced in a carbonaceous solid at low temperatures, for example by irradiation with α-particles or electrons or by slow pyrolysis taking place in geological time, then heating to at least 300°–400°C. may be necessary in the laboratory before any perceptible change occurs in the ESR behavior. This is, in fact, the situation with vitrinites: in the studies of van Krevelen and Smidt almost no change in signal strength or width was found for coals of any rank below about 400°C., and in the present work changes were sometimes observed after pyrolysis at 350°C., but they were small. In normal metamorphic processes coals have at no time been exposed to temperatures above about 200°C.

We see, therefore, that the minimum temperature at which changes in ESR characteristics are observed may be considerably higher than the maximum temperature to which the sample has been heated previously. But this minimum temperature is not likely to be higher than about 400°C. since any carbonaceous solid containing atoms other than carbon will start to decompose at least by this temperature. Hence, if it is found that the signal strength *and* width shown by such a solid does not begin to change until some higher temperature, $T°$, is reached, it is very probable that the solid has been heated previously at least approximately to $T°$.

Now, since fusinites have higher carbon contents and aromaticities than the other associated macerals, their structures could stabilize a higher proportion of free radical centers produced during metamorphism (by whatever means), and the signal would be subject to considerable exchange and delocalization narrowing. The unpaired spin concentration in the high rank coals of 90–93% carbon studied by Van Krevelen and Smidt (i.e., of the same range of carbon contents as the fusinites we have studied) increased by a factor of 3–4 on pyrolysis at 450°–550°C., while the concentration in the fusinites hardly changed at all in this range.

Thus we are led to the conclusions that fusinites achieved both their high carbon contents and their unpaired spin concentration before incorporation into the sediment and most probably by exposure to elevated temperatures. A commonly held view of the origin of some fusinites is that pyrolysis occurred as a result of forest fires, perhaps ignited by lightning or meteorites. An alternative

Publication Date: January 1, 1966 | doi: 10.1021/ba-1966-0055.ch021

suggestion is that during the activity of thermophilic bacteria in decaying vegetable matter, spontaneous combustion starts from hot spots and carbonizes some of the material. Obviously, if a portion of the original woody material were subjected to pyrolysis before incorporation into the sediment, a highly carbonaceous material would result, which would undoubtedly contain a high concentration of stable free radicals whose spin concentration and line width would not change much on laboratory pyrolysis until relatively high temperatures were reached. But an alternative view must be considered.

In principle, highly carbonaceous material could be produced by either chemical or biological oxidation. However, such oxidation would have to be highly selective in burning off combined hydrogen so that the remaining carbon skeletal structures could polymerize to an aromatic charcoal-like substance. It is difficult to envisage such a highly selective reaction as occurring naturally; so far as the authors are aware, no enzymatic process of this kind is known. Moreover, it is difficult to imagine the reaction as proceeding uniformly through pieces of woody tissue, or that the ESR signal would not change on heating at 550°C. However, since not very much is known about microbial decay processes in subtropical swamp environments, one cannot exclude this possibility. Perhaps some kind of fungal attack selectively oxidizes woody tissue, making it somewhat more carbonaceous and leaving it in such a state that a small degree of geological metamorphism converts it into a highly aromatic fusinite that does not change much on further exposure to metamorphosing conditions.

The range of fusinites studied here is relatively small, being restricted to samples from thick fusain lenses in bituminous coals of Carboniferous age taken from two coal basins in the northern hemisphere. The present data, therefore, do not justify any general statement about the origin of fusinites. It can be stated, however, that the properties noted for the fusinites studied are consistent with the view that they were subjected to some kind of pyrolysis to perhaps 400–600°C. before incorporation in the organic sediment.

The behavior of the single micrinite studied was similar to that of fusinites. It would be premature to try to draw any general conclusion from this fact.

Acknowledgements

One of the authors (D. E. G. Austen) is indebted to the British Coal Utilisation Research Association for a grant supporting his research (1957–1959). The Penn State authors gratefully acknowledge support from the Earth Science Division of the National Science Foundation; they are also indebted to Dr. H. Atwater, Department of Electrical Engineering, for assistance in using the electron spin resonance spectrometer, to Dr. L. Singer for discussions on interpreting data, and to Mr. R. C. Neavel for his reflectance measurements and assistance in collecting and preparing samples for study.

Literature Cited

(1) Austen, D. E. G., Ph.D. Thesis, University of Southampton, 1958.
(2) Austen, D. E. G., Ingram, D. J. E., *Conf. on Sci. Use Coal, Sheffield* **1958**, A–39.
(3) Austen, D. E. G., Ingram, D. J. E., Given, P. H., Peover, M. E., *Fuel* **38**, 309 (1959).

(4) Bent, R., Brown, J. K., *Fuel* **40,** 47 (1961).
(5) Duchesne, J., Dépireux, J., van der Kaa, J. M., *Geochim. Cosmochim. Acta* **23,** 209 (1961).
(6) Ergun, S., Donaldson, W. F., Breger, I. A., *Fuel* **39,** 71 (1960).
(7) Fenton, G. W., Smith, A. K. V., *Gas World (Coking Section)* **149,** 81 (1959).
(8) Friedel, R. A., Breger, I. A., *Science* **130,** 1762 (1959).
(9) Given, P. H., Peover, M. E., Wyss, W. F., *Fuel* **39,** 323 (1960).
(10) Given, P. H., Peover, M. E., Wyss, W. F., paper presented to 4th International Conference on Coal Science, Le Touquet, France, 1961.
(11) Hirsch, P. B., *Phil. Trans. Roy. Soc. London,* **252A,** 68 (1960).
(12) Ingram, D. J. E., "Free Radicals as Studied by Electron Spin Resonance," Butterworth, London, 1958.
(13) Krevelen, D. W., van, "Coal," pp. 394–399, Elsevier, Amsterdam, 1961.
(14) Kröger, C., *Brennstoff-Chem.* **39,** Sonderausgabe, 62–7 (1958).
(15) de Ruiter, E., Tschamler, H., *Brennstoff-Chem.* **42,** 290 (1960).
(16) Singer, L. S., "Proceedings of Fifth Carbon Conference," Vol. 2, p. 37, Pergamon Press, Oxford, 1963.
(17) Smidt, J., van Krevelen, D. W., *Fuel* **38,** 355 (1959).
(18) Steelink, C., ADVAN. CHEM. SER. No. **55,** 80 (1965).
(19) Trueman, A., Ed., "The Coalfields of Great Britain," Arnold, London, 1954.

RECEIVED April 19, 1965.

Discussion

Geoffrey H. Taylor. Tertiary bituminous coals examined in C.S.I.R.O. (Sydney) contain fusinite but little micrinite, sometimes virtually none. This would seem to preclude a genetic connection between fusinite and micrinite origin.

Peter H. Given. This is interesting information, and I agree with the conclusion, at least for the coals referred to.

Edwin Koppe. In the Tertiary lignites of the western United States, many of the coals I have studied, unlike those referred to by G. H. Taylor, have rather high micrinite concentrations as well as fusinite in "normal" concentrations. I agree with Dr. Hacquebard that the fusinite is formed very early while peat is accumulating. Microscopic studies show that fusinites have high internal strength and retain their form throughout compaction of the coal. With regard to semifusinite, the physical properties are intermediate between the high strength of fusinite and the lack of original strength of the vitrinitic components. Semifusinites show a characteristic wavy extinction with polarized light, which is of diagnostic value and is probably a strain phenomenon.

Duncan G. Murchison. If he does not already know, Dr. Given might like to know that work by Terres *et al.* in Germany on the specific heats of fusinites showed that they formed at temperatures similar to those quoted from the ESR study. Furthermore, the work on specific heats also indicated that semifusinites formed under less severe charring conditions.

As far as the measurements on micrinite are concerned, might not the term "micrinite" as used here in fact refer to several inert macerals, namely, semifusinite, sclerotinite, and micrinite? This would seem likely in view of the "float and sink" methods used to concentrate the vitrinite.

Dr. Given. I appreciate Dr. Murchison's drawing my attention to the work of Terres, which is certainly interesting. From discussions I have heard between my petrographic colleagues, it certainly does seem more difficult to characterize micrinites than some other macerals, and therefore I agree that materials of different nature and origin may be confused, particularly in a float-and-sink separation. I wonder whether the difficulty of recognition and characterization lies behind the contrasting observations of Taylor and Koppe?

H. Tschamler. Dr. E. de Ruiter and I have also made electron spin resonance measurements on macerals (E. de Ruiter and H. Tschamler, *Brennstoff-Chem.* **42**, 290 (1961)). We found quite similar results for micrinites to the single value reported by Given *et al.*

Bhupendra K. Mazumdar. It is difficult for us to accept the view that temperatures of the order of 600°C. or so must have been involved in forming fusinites. One would have to imagine the raging of forest fires during primordial times in all areas of coal formation and right in peat bogs.

On the other hand, we have in the course of our dehydrogenation studies observed points of similarity between fusain and dehydrogenated vitrain—e.g., the percent hydrogen in both is of a similar order (3.5 ± 0.5), both are noncaking and yield no tar, and the difference in V.M. content between vitrain and the corresponding fusain is nearly equal to the yield of tar from the vitrain. Moreover the V.M. content of dehydrogenated vitrain and fusain are of a similar order. On the basis of such considerations we are led to believe that oxidative dehydrogenation caused by microorganisms and aided by aerial attack must have transformed the exposed portions of vegetable debris to what may be envisaged as the primordial fusain substance. The difference in physical and chemical properties this brought about at the peat-bog stage, between one portion of vegetable debris and the other, persists through the geochemical stage until normal dehydrogenation (which appears to set in at or immediately after the 85% carbon content level of rank) wipes it out at about 92–92% carbon; at this point the macerals should have similar analysis and behavior. This is in fact observed to be so.

Further, the fusain samples we examined contained methyl groups (in amounts comparable to those in higher rank coals). The presence of such group in fusains would itself rule out the forest fire theory or any other concept which envisages exposure to high temperatures (600°C.) in forming fusains.

Dr. Given. Dr. Mazumdar finds it difficult to imagine forest fires sweeping through peat bogs. In the first place I would point out that the fire has to sweep through the forest, not the bog. Secondly, modern research on combustion processes in forest fires makes it clear that, once ignited, a fire could perfectly well sweep through a semi-tropical forest in conditions of high humidity, and the humidity would actually contribute to the fierceness of the fire (the steam condenses at high altitudes and thus increases the "chimney draft" at the vortex of the fire). The difficulty is to visualize a suitable ignition process; lightning, the falling of meteorites, the ignition of marsh gas (spontaneously or by lightning), and the activities of thermophilic bacteria are possibilities.

Publication Date: January 1, 1966 | doi: 10.1021/ba-1966-0055.ch021

It is worth bearing in mind that nowhere in the world at present are large amounts of peat accumulating like they did in Carboniferous times (subsequently leading to the formation of substantial coal measures); geomorphic and climatic conditions do not seem to be suitable. It is therefore difficult for us to visualize conditions in the forests that gave rise to the major coal measures when world climate and morphology were quite different.

I do not find convincing Dr. Mazumdar's arguments in favor of dehydrogenation and the properties he lists are not very sensitive criteria for detecting structure similarities. Moreover, I find it difficult to believe in a severe microbiological oxidation which (a) preserves cellular structure, (b) burns off hydrogen but not carbon, and does not add oxygen, and (c) operates in the same matrix and on the same substrate as other, much less severe processes. However, I will admit a possibility that the initial aerobic attack leaves some portions of woody tissue as particularly suitable oxygen sources for anaerobic bacteria, condensation and aromatization occurring as secondary consequences of oxygen abstraction, but this is not primarily a dehydrogenation process.

I agree that methyl groups are very unlikely to survive pyrolysis at 600°C. although, depending on time of exposure, some might survive 400–450°C. However, the data referred to were presumably obtained by the Kuhn-Roth procedure. Many chemists doubt whether this procedure, developed for elucidating certain features in the structure of terpenoid hydrocarbons, can properly be applied to carbonaceous solids of much more complex structure. At the same time it must be admitted that available separation methods yield materials having a wide range of reflectance values, which have presumably been exposed (in our view) to different temperatures. If there are indeed methyl groups in pure fusinites, they may be present in those portions that were exposed to relatively low temperatures.

Norbert Berkowitz. I find it difficult to accept ESR data on fusain as proof of thermal history. Below 400°C. ESR signals of coals show, quite generally, little change with carbonization temperature; and signal widths of the order of 3 gauss or so have been recorded with a fair number of coal-like materials (e.g. synthetic "humic acids" prepared by oxidative polymerization of phenols). I conclude therefore that the constancy of the ESR signal height at $T < 400$°C. and the narrowness of the signal do not, in themselves, constitute proof of a forest fire origin of fusain specimens examined by the authors—although viewed in conjunction with other evidence (e.g., Nandi's data on specific heats), they might *suggest* it. Perhaps it is a matter of semantics, perhaps the authors' conclusion ought to be rather less definite.

Dr. Given. I feel that the significant findings for fusinites are not only that the line width is narrow and relatively invariant, but that the large maximum in signal strength, found with all other carbonaceous solids carbonized at 500–600°C., is absent when fusinites are carbonized at these temperatures. We do not claim that the results establish a forest fire origin for fusinites, only that they make it probable that fusinites were exposed to temperatures of 450–600°C. before burial.

Publication Date: January 1, 1966 | doi: 10.1021/ba-1966-0055.ch021

Cornelius Steelink. We have found line widths of less than 4.0 gauss for humic acids and model compounds.

Dr. Koppe. Does anyone have any spin concentration data on charcoal?

Dr. Given. Yes. The results depend on the temperature at which the wood has been charred, but if this is around 500–600°C., similar results are found to those we report for fusinites.

James M. Schopf. I was interested in Dr. Given's conclusion of similarity of micrinite and fusinite. The petrologic associations of micrinite are even more difficult to associate with its origin as a result of forest conflagration. From its geologic occurrences it seems to me very unlikely that all fusain occurrences can be explained by forest fires. For this reason it is most appropriate to examine alternative methods by which fusain and micrinite could originate.

Dr. Given. I did not "conclude" that fusinites and micrinites have similar origins. I submit that the results reported support the view that fusinites had been exposed to moderately high temperatures before burial and consolidation with the accumulating sediment. How this exposure occurred is a matter of guesswork, but one obvious possibility is in forest fires. With regard to micrinites, I said that if the observation on one sample is substantiated by studies of other samples, then one would have to consider an origin that also involved exposure to heat.

Peter Hacquebard. As regards the origin of fusain, quantitative studies carried out on coals from the Dutch and Nova Scotia coal fields have shown that there is no relationship between rank and amount of fusain. Anthracitic and low volatile coals do not contain more fusain than high volatile bituminous coals. This observation is considered as evidence for the primary origin of fusain during the peat stage; it does not support the hypothesis of metamorphic origin of fusain brought about during the coalification process.

Douglas S. Montgomery. Dr. Hacquebard stated that in his experience there was no more fusinite in anthracite than in low rank coals, and fusinite therefore did not, in his opinion, result from the coalification process. Could the same statement be made concerning the semifusinite?

Dr. Hacquebard. Yes, I think it could.

Publication Date: January 1, 1966 | doi: 10.1021/ba-1966-0055.ch021

Anthracite Lithology and Electrokinetic Behavior

S. C. SUN and JOHN A. L. CAMPBELL

Department of Mineral Preparation, The Pennsylvania State University, University Park, Pa.

Publication Date: January 1, 1966 | doi: 10.1021/ba-1966-0055.ch022

In an effort to establish the mechanism of coal flotation and thus establish the basis for an anthracite lithotype separation, some physical and chemical parameters for anthracite lithotype differentiation were determined. The electrokinetic properties were determined by streaming potential methods. Results indicated a difference in the characteristics of the lithotypes. Other physical and chemical analyses of the lithotypes were made to establish parameters for further differentiation. Electron-microprobe x-ray, x-ray diffraction, x-ray fluorescent, infrared, and density analyses were made. Chemical analyses included proximate, ultimate, and sulfur measurements. The classification system used was a modification of the Stopes system for classifying lithotypes for humic coals.

This research was undertaken to determine some physical and chemical parameters for anthracite lithotype differentiation. The program was the first step in an effort to establish the mechanism of anthracite flotation and thus establish the basis for an anthracite lithotype separation. Presented results will show that anthracite lithotypes are different, and that in order to interpret research results from anthracite coals correctly, a petrographic knowledge of the coal is necessary.

Most coal petrographers agree that the higher rank coals, including the normal anthracites, exhibit the same components, constituents, and types as the lower rank coals but with original differences of physical properties and chemical composition greatly reduced (*4*). However, other than the work of Turner (*9*, *10*) and a few other scientists (*5*, *6*, *11*, *12*) little actual work has been performed in anthracite petrology. In fact, not only are the physical and chemical properties of anthracite not well known, but the presence of anthracite lithotypes is not even recognized by many research groups.

In Coal Science; Given, P.;
Advances in Chemistry; American Chemical Society: Washington, DC, 1966.

Lithotype Classification

Coal seams display two different modes of variation: rank and type. The rank of the material under consideration is anthracite. Regarding type, coal is composed of different bands of materials, distinctly contrasted in regard to physical and chemical composition. These bands are termed lithotypes in this paper, after the word coined by Seyler (2) in 1954.

A megascopic examination of 11 anthracites revealed three megascopically distinct homogeneous lithotypes (Figure 1). The classic description of bituminous coal lithotypes by Stopes was found to be quite adequate for recognizing these three lithotypes in anthracite, vitrain, durain, and fusain. The Stopes system, however, recognizes a fourth type, clarain or bright coal. Vitrain is the brilliant constituent, and clarain is bright, being composed of alternating bands of vitrain and durain. The term durain is used for dull coal, and fusain for fossil charcoal.

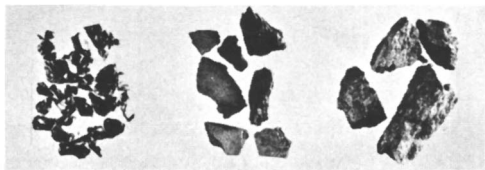

Figure 1. A megascopic illustration of lithotypes

Table I. Designation and Source of Anthracite Samples

Sample Designation	*Sample*
SP–BRA	Bottom Red Ash• 110 Tunnel 23 East
SP–C	Carbondale Co. Top and Bottom Clark
SP–H	Hillman• 95 Tunnel 1 West
SP–T	Holmes Seam #10 Trevorton, Pa.
SP–J	Jeddo—Highland Coal Co.
SP–B	Mills Kidney• Bliss
SP–CH	Mills Kidney• Corgan Hollenback
SP–CN	Mills Kidney• Corgan Newport
SP–R	Russian Anthracite Donetz
SP–Wa	Wanamie #19• Bottom Red Ash 14 Plane 1 West
SP–W	Welsh Anthracite

• Glen Alden Corporation

Table II. Designation and Source of Lithotype Samples

Sample		
Designation	*Type*	*Source*
SP–BRA–V	Vitrain	Bottom Red Ash 110 Tunnel 23 East
SP–BRA–D	Durain	Bottom Red Ash 110 Tunnel 23 East
SP–C–V	Vitrain	Carbondale Co. Top and Bottom Clark
SP–C–D	Durain	Carbondale Co. Top and Bottom Clark
SP–H–V	Vitrain	Hillman 95 Tunnel 1 West
SP–H–D	Durain	Hillman 95 Tunnel 1 West
SP–T–V	Vitrain	Holmes Seam #10 Trevorton
SP–J–V	Vitrain	Jeddo—Highland Coal Co.
SP–B–V	Vitrain	Mills Kidney Bliss
SP–B–D	Durain	Mills Kidney Bliss
SP–B–F	Fusain	Mills Kidney Bliss
SP–CH–V	Vitrain	Mills Kidney Corgan Hollenback
SP–CN–V	Vitrain	Mills Kidney Corgan Newport
SP–CN–D	Durain	Mills Kidney Corgan Newport
SP–R–V	Vitrain	Russian Anthracite Donetz
SP–Wa–V	Vitrain	Wanamie #19 Bottom Red Ash 14 Plane 1 West
SP–Wa–D	Durain	Wanamie #19 Bottom Red Ash 14 Plane 1 West
SP–Wa–F	Fusain	Wanamie #19 Bottom Red Ash 14 Plane 1 West
SP–W–V	Vitrain	Welsh Anthracite
SP–W–D	Durain	Welsh Anthracite
SP–W–F	Fusain	Welsh Anthracite

The lithotype clarain, admittedly present, was not used in this study. Clarain is by definition a heterogeneous material composed of vitrain and durain bands, of less than an arbitrarily chosen thickness, generally 3–5 mm. For the purpose of this study, it was felt that this material could be described adequately if the vitrain and durain constituents were described.

The following standard visual parameters were used to identify the lithotypes.

Vitrain. Occurs in uniform bands up to ½ inch in thickness. The bands are a brilliant black, having the luster of broken glass, and complete homogeneity. Breakage into cube-like pieces and pieces with conchoidal fractures are common.

Publication Date: January 1, 1966 | doi: 10.1021/ba-1966-0055.ch022

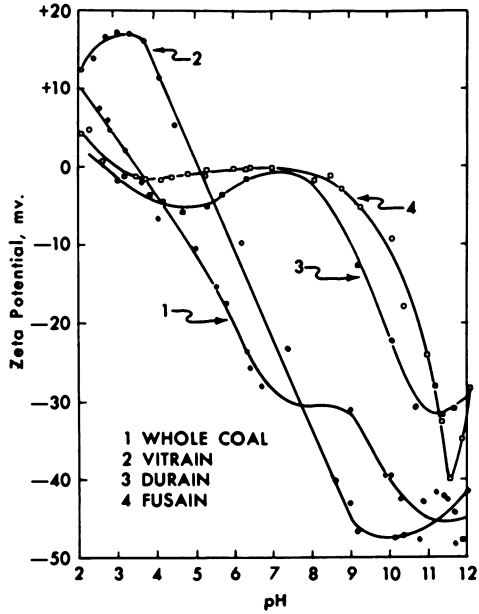

Figure 2. Variation of bliss anthracite zeta potential with pH

Durain. Appears dull black or dull gray and gives a black streak on a porcelain plate. Surfaces appear homogeneous and slate like. A roughness or granular appearance may be noticed upon close inspection of a surface. Some faces may have a slightly higher reflectance and have a slightly silky appearance. Irregularly shaped pieces are obtained upon breakage.

Fusain. Has the exact appearance of charred wood. Surfaces are dull in appearance, very irregular and rough, and upon closer inspection appear to be fibrous in nature. Surfaces may also appear velvety if held at a correct angle to the light. Pieces break very easily into irregularly shaped particles.

Electrokinetic Properties

All of the anthracites used in this investigation were from Pennsylvania except two, a Russian anthracite and a Welsh anthracite. Tables I and II indicate the various designations and sources of the anthracite and lithotype samples.

The electrokinetic properties were determined by streaming potential methods (*1*). Results indicated that the surface characteristics of the lithotypes are different. Hydronium and hydroxyl ions appeared to be potential-determining ions for coal. Results of a typical streaming potential investigation are shown in Figure 2. Potential-determining ions may be loosely defined as those ions which participate in the the electrolytic reaction that establishes equilibrium at the solid-liquid interface. When the potential-determining ions

Publication Date: January 1, 1966 | doi: 10.1021/ba-1966-0055.ch022

in solution are in a certain concentration, an electrical double layer does not exist, and the surface of the solid in solution is uncharged. This condition is described as the zero-point-of-charge (ZPC).

At the ZPC maximum hydrophobic characteristics of the coal are exhibited. One can establish better froth flotation, flocculation, and/or filtration conditions if this point is known.

Points for five anthracites and 10 lithotypes are listed in Table III. The ZPC for vitrains occurred between a pH of 4.0 and 6.5. For durains and fusains the points occurred between a pH of 2.0 and 4.5, while in the whole anthracites the ZPC occurred between a pH of 2.5 and 4.5.

Other physical and chemical analyses of the lithotypes were made to establish parameters for further differentiation.

Table III. Isoelectric Points of Anthracites and Lithotypes Investigated

Sample		*Isoelectric Point*
Designation	*Type*	*pH*
SP–W	Coal	3.5
SP–W–V	Vitrain	6.5
SP–W–D	Durain	2.0
SP–W–F	Fusain	7.0
SP–R–V	Vitrain	4.0
SP–T–V	Vitrain	4.3
SP–B	Coal	3.5
SP–B–V	Vitrain	5.2
SP–B–D	Durain	2.6
SP–B–F	Fusain	3.0
SP–Wa–D	Durain	4.5
SP–Wa	Coal	2.7
SP–J	Coal	3.9
SP–C	Coal	4.3

Table IV. Distribution of Lithotypes in Anthracite Coal Samples

Sample	*Vitrain, %*	*Durain, %*	*Fusain, %*
SP–J	87	9	4
SP–R	76	11	13
SP–H	72	25	3
SP–W	71	20	9
SP–CH	69	25	6
SP–CN	63	29	8
SP–B	59	9	32
SP–Wa	42	54	4
SP–C	35	64	1
SP–BRA	31	15	54

Physical Properties

Using polished pellets 1 inch in diameter, a microscopic particle classification analysis for lithotypes, developed for this research by the authors (*1*), was made of the various coals. Only vitrain, durain, and fusain were counted. Results are presented in Table IV. Standard visual parameters were used for particle identification. An analysis of this type, although not necessarily conclusive, is important for a relative comparison. Results of a check between

operators were within 4%. The anthracites were generally found to contain 60–80% vitrain, 10–30% durain, and 1–10% fusain. Mean reflectance readings of the vitrinites in the whole coal (Table V) ranged from 4.5 to 6.1.

The apparent specific gravity of the various lithotypes was measured. Results (Table VI) indicate that the order of increasing density for the lithotypes is vitrain, durain, and fusain. For Pennsylvania anthracites, the specific gravity for vitrain was found to vary between 1.36 and 1.53; for durain between 1.43 and 1.73; for fusain between 1.93 and 2.30.

X-ray diffractometric analysis of the vitrains resulted in wide, diffuse bands or continuous background patterns. This indicated that the vitrains have an amorphous character and/or that any crystalline material present (small crystallites) is of nonregular arrangement. However, Turner (*9*, *10*), who found anthracite composed of three constituents—anthraxylon, attritus, and fusain—stated that "the anthraxylon particle is similar to graphite carbon and gives a diffraction pattern resembling cellulose thus showing a definite arrangement of colloidal micelles. The attritus contains almost all the mineral matter of anthracite." It should be stated that Turner used the more accurate x-ray powder camera techniques.

Publication Date: January 1, 1966 | doi: 10.1021/ba-1966-0055.ch022

Table V. Mean Reflectance (R_0) of Vitrinites from Selected Anthracites

Sample	*R_o Percent*
SP–C	4.46
SP–B	4.48
SP–BRA	5.50
SP–J	6.08

Table VI. Specific Gravity of Investigated Lithotypes

Sample	*Vitrain*	*Durain*	*Fusain*
SP–W	1.33	1.59	1.78
SP–C	1.36	1.43	•
SP–CN	1.38	1.69	•
SP–CH	1.39	•	•
SP–H	1.39	1.57	•
SP–Wa	1.40	1.66	2.30
SP–T	1.41	•	•
SP–B	1.42	1.73	1.98
SP–BRA	1.44	1.60	•
SP–R	1.52	•	•
SP–J	1.53	•	•

• Lithotypes not obtainable

Chemical Properties

Proximate and ultimate analyses results (Tables VII and VIII, respectively) show that fixed and total carbon content of the lithotypes decrease in the order vitrain, durain, and fusain. The reverse of this trend is found for percent ash content, vitrain having the least and the durains and fusains having the most. Durain was found to have the highest percentage of volatile matter; vitrains have the highest percentage of sulfur.

Table VII. Proximate and Sulfur Analysis

Sample		Fixed Carbon	Ash	Sulfur	Vol. Mat.	Moisture
Designation	Type	% (dry)	% (dry)	% (dry)	% (dry)	% (as recd.)
SP-J	Whole Coal	92.2	2.8	0.44	4.6	1.1
SP-R-V	Vitrain	91.6	2.0	0.96	5.4	1.3
SP-W-V	Vitrain	89.6	1.1	1.38	7.9	0.88
SP-T-V	Vitrain	89.2	0.2	0.76	9.8	1.2
SP-B-V	Vitrain	88.9	3.2	0.68	7.2	2.4
SP-W	Whole Coal	85.1	3.7	0.72	10.5	1.3
SP-C	Whole Coal	84.5	8.0	0.62	6.9	2.0
SP-Wa	Whole Coal	83.8	8.4	1.46	6.3	2.6
SP-B	Whole Coal	83.1	9.7	0.77	6.4	2.0
SP-Wa-D	Durain	70.0	22.8	0.46	6.7	0.90
SP-W-F	Fusain	58.1	20.8	0.23	20.9	0.42
SP-W-D	Durain	54.3	36.2	0.45	9.0	0.90
SP-B-D	Durain	50.9	40.8	0.42	7.9	1.1
SP-B-F	Fusain	43.5	52.4	0.11	4.0	0.64

Table VIII. Ultimate Analysis of Anthracites and Lithotypes

Sample				Oxygen and
Designation	Type	Carbon,%	Hydrogen,%	Nitrogen,%
SP-R-V	Vitrain	89.56	2.44	5.0
SP-T-V	Vitrain	89.37	3.74	5.9
SP-W-V	Vitrain	89.12	3.93	4.5
SP-B-V	Vitrain	87.41	2.46	6.3
SP-W	Whole Coal	86.16	3.87	5.6
SP-J	Whole Coal	85.73	2.29	8.7
SP-C	Whole Coal	83.60	2.85	4.9
SP-B	Whole Coal	80.93	2.68	5.9
SP-Wa	Whole Coal	80.88	2.30	7.0
SP-Wa-D	Durain	69.00	2.25	5.5
SP-W-F	Fusain	62.41	2.20	14.4
SP-W-D	Durain	54.63	2.75	6.0
SP-B-D	Durain	50.38	1.73	6.7
SP-B-F	Fusain	43.88	1.32	2.3

Using procedures similar to Kinney (3) the infrared spectra were investigated. Results illustrated in Figure 3 indicate that the adsorption bands present in lower rank coals have disappeared, not only for the whole coal as reported by Kinney, but also for the various lithotypes.

Emission spectroscopy analyses of the anthracites (Table IX) show that 90% of the ash of Pennsylvania anthracites is composed of silicon, aluminum, and iron-bearing minerals.

An iron content in some of the lithotype ashes was indicated by their brownish-red to dark earth brown colors. An x-ray fluorescence analysis (Table X) of the ash substantiated the presupposed presence of iron. Iron was generally found in all of the lithotypes. Detectable amounts of calcium were found in all the vitrains.

An electronmicroprobe x-ray analyzer was used to determine how and what type of mineral matter is distributed on the surface of the various lithotypes. Results indicated that the mineral matter located at the surface is vastly different among the various lithotypes. The mineral matter appearing on the flat, homogeneous vitrain surface (Figure 4) was found to be distributed

Publication Date: January 1, 1966 | doi: 10.1021/ba-1966-0055.ch022

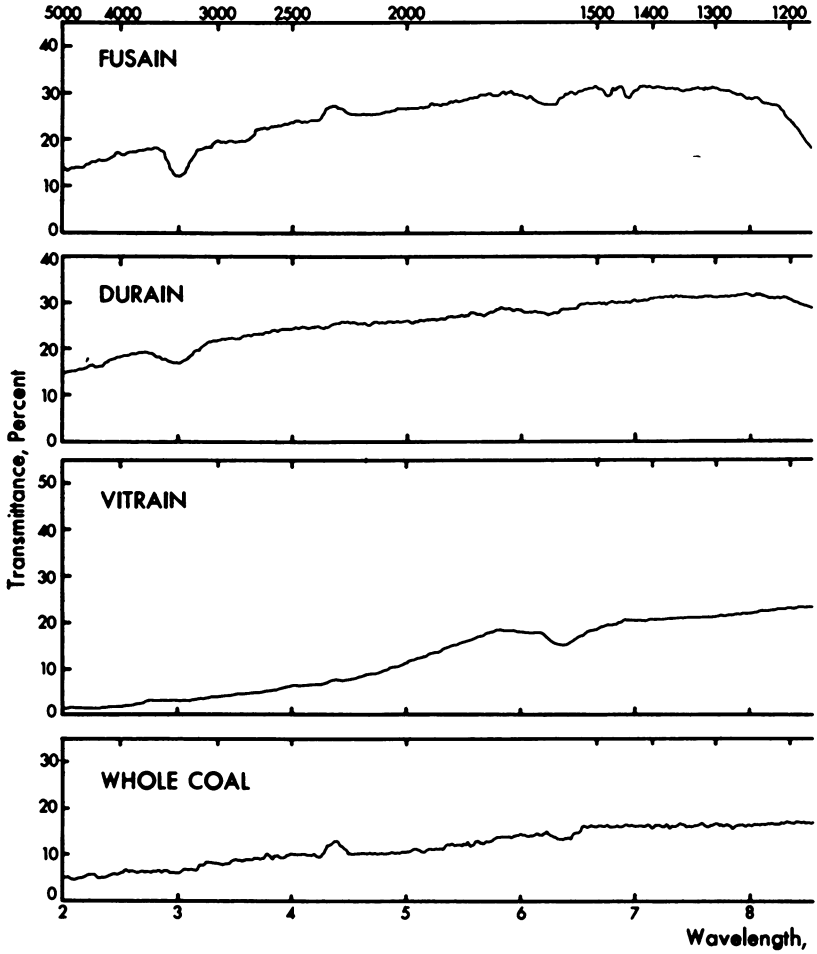

Figure 3. Infrared spectra of Mills

Table IX. Analysis of Selected Anthracites by Emission Spectroscopy

Sample Whole Coal	*Si Wt. %*	*Al Wt. %*	*Fe Wt. %*	*Ca Wt. %*	*Mg Wt. %*	*Ti Wt. %*	*V Wt. %*	*Mn Wt. %*
SP–B	2.50	1.65	0.32	0.04	0.05	0.09	0.004	0.0020
SP–BRA	2.47	2.05	0.20	0.01	0.03	0.04	0.002	0.0080
SP–Wa	2.09	1.65	0.50	0.03	0.15	0.09	0.003	0.0020
SP–CN	1.92	1.24	0.62	0.09	0.08	0.06	0.031	0.0500
SP–C	1.90	1.74	0.15	0.03	0.03	0.11	0.040	0.0005
SP–H	1.42	0.98	0.62	0.05	0.02	0.10	0.001	0.0008
SP–CH	1.14	0.84	0.38	0.01	0.02	0.04	0.002	0.0004
SP–W	0.58	0.67	0.31	0.14	0.07	0.02	0.002	0.0020
SP–R	0.45	0.39	0.72	0.08	0.07	0.01	0.003	0.0050

Publication Date: January 1, 1966 | doi: 10.1021/ba-1966-0055.ch022

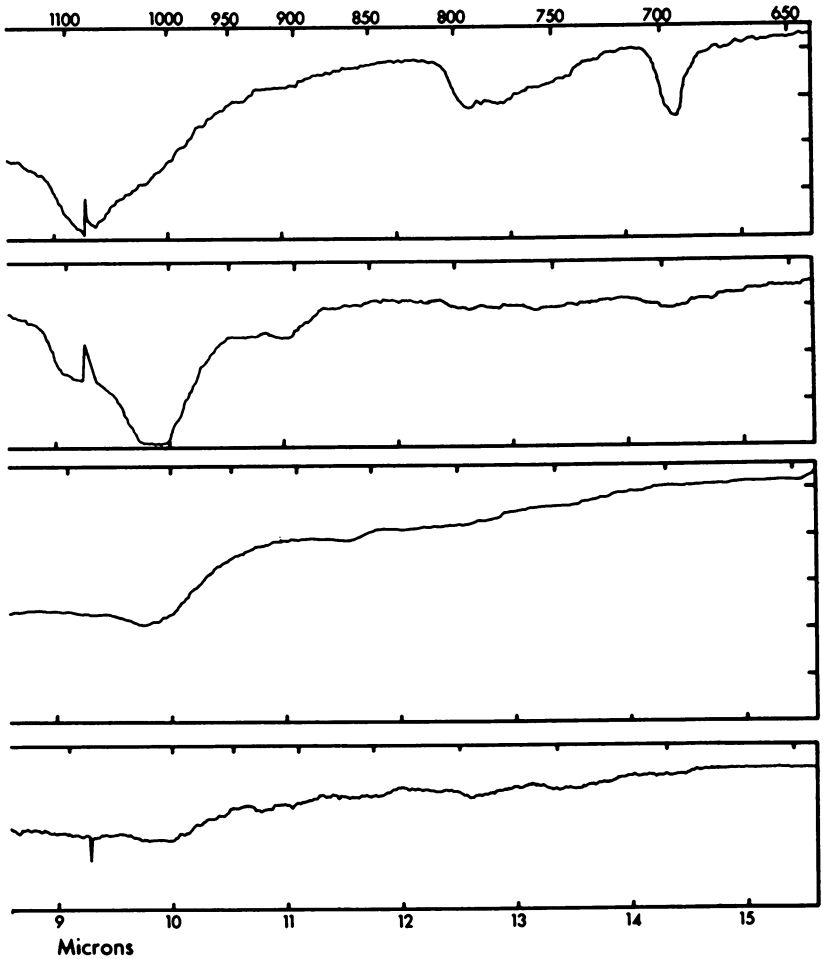

Kidney Bliss anthracite and lithotypes

Table X. X-ray Fluorescence Analysis of Lithotypes*

Sample				
Designation	*Type*	*Iron*	*Calcium*	*Magnesium*
SP–W–V	Vitrain	Medium	High	High
SP–W–D	Durain	Medium	Low	Absent
SP–W–F	Fusain	High	Low	High
SP–B–V	Vitrain	Medium	High	Absent
SP–B–D	Durain	Medium	Absent	Absent
SP–B–F	Fusain	Medium	Absent	Absent
SP–R–V	Vitrain	High	High	Medium
SP–Wa–D	Durain	Medium	Absent	Absent

* Qualitative analysis, relative amounts indicated

Publication Date: January 1, 1966 | doi: 10.1021/ba-1966-0055.ch022

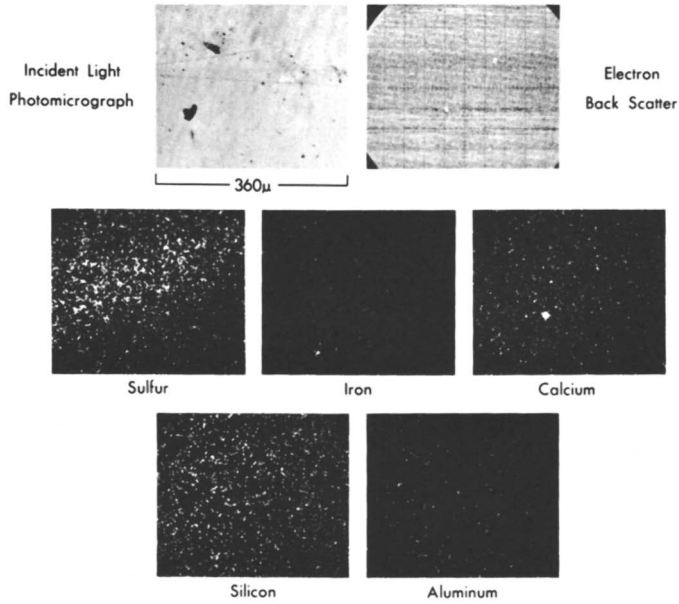

Figure 4. Mills Kidney Bliss vitrain electronmicroprobe analysis

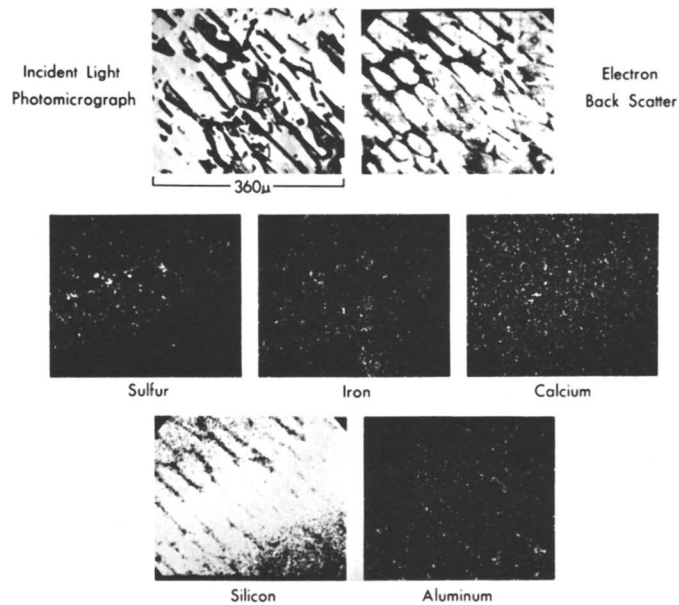

Figure 5. Mills Kidney Bliss fusain electronmicroprobe analysis

Publication Date: January 1, 1966 | doi: 10.1021/ba-1966-0055.ch022

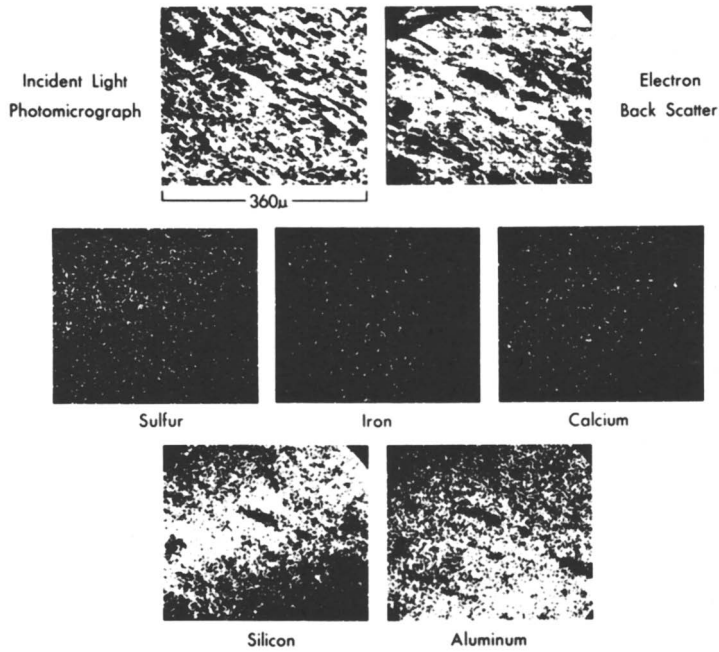

Figure 6. Mills Kidney Bliss durain electronmicroprobe analysis

fairly uniformly. However, some pockets of calcium were found in the one or two pits appearing on the surface of the vitrain particles. Fusain was found to consist of what appears to be high carbon cellular structure filled with quartz (Figure 5). The durain surface (Figure 6) is seen to be impregnated with a matted aluminum and silicon substance which is most likely a kaolinite type of material.

Conclusions

From the foregoing it is evident that the lithotypes of anthracite are different. Differences in adsorption characteristics, surface structure, physical properties, and chemical composition conclusively demonstrate that the anthracite lithotypes are unalike and are distinct entities. It is also evident that to interpret research results of anthracite coals correctly, a petrographic knowledge of the coal is necessary. Anthracite cannot be regarded as a homogeneous substance.

Acknowledgment

The authors wish to acknowledge and thank the Coal Research Board of the Commonwealth of Pennsylvania which made this research project possible.

Literature Cited

(1) Campbell, J. A. L., Sun, S. C., *Penn. State Univ., Mineral Ind. Exp. Sta., Spec. Res. Rept. No.* **SR-44** (1964).
(2) "International Handbook of Coal Petrology," 1st Ed., p. 25, Centre National de la Recherche Scientifique, Paris, 1957.
(3) Kinney, C. R., Doucette, E. I., *Nature* **182,** 785 (1958).
(4) Marshall, C. E., "Coal Petrology," A. M. Bateman, ed., Part II, The Economic Geology Publishing Co., Lancaster, 1955.
(5) Middleton, B. D., Inouye, K., Spackman, W., *Penn. State Univ., Mineral Ind. Exp. Sta., Spec. Res. Rept. No.* **SR-27** (1961).
(6) Prasad, D., personal communication, 1963.
(7) Stopes, M. C., *Proc. Roy. Soc. London, Ser. B,* **90,** 470 (1919).
(8) Stopes, M. C., *Fuel* **14,** 4 (1935).
(9) Turner, H. G., *Trans. AIME* **71,** 127 (1925).
(10) Turner, H. G., Anderson, H. V., *Ind. Eng. Chem.* **23,** 811 (1931).
(11) Wagner, H. C., *U.S. Geol. Survey, Bull.* **995-A** (1953).
(12) Walsh, M. Jr., Dutcher, R. R., *Penn. State Univ., Mineral Ind. Exp. Sta., Spec. Res. Rept. No.* **SR-11** (1959).

RECEIVED January 25, 1965.

Discussion

J. W. Ramsey: How extensive are the anthracite samples in which lithotypes can be distinguished and separated?

John A. L. Campbell: A set of 11 anthracites was investigated. Table IV lists the distribution of lithotypes in these anthracite samples. The anthracites were found generally to contain 60–80% vitrain, 10–30% durain and 1–10% fusain.

It is felt that any anthracite seam will readily yield such lithotypes. Because fusain is relatively soft and friable and is likely to be ground to fines during handling, it may appear only as coatings or fine bands in other coal types. The durain in many cases looks like slate. Not realizing these two factors one could, without close inspection, be easily misled into believing that the major lithotype, vitrain, is the only lithotype present in a particular seam.

Bernard D. Blaustein: If different macerals have different electrokinetic characteristics and this turns out to be generally true for different types of coal, could one not separate macerals by electrophoresis? In a recent paper in *Analytical Chemistry,* mixtures of solids (presumably fine mesh) are separated electrophoretically. If this has not been tried as a means of separating macerals, I would like to suggest that someone attempt it.

Mr. Campbell: Anthracite lithotypes were investigated for their electrokinetic characteristics to establish a basis for separation, utilizing froth flotation methods. The electrokinetic characteristics of macerals were not investigated. However, results from the lithotype work does imply that macerals have different electrokinetic characteristics. I believe electrophoretic methods could be used effectively to separate macerals for laboratory purposes.

Coal has been investigated by electrophoretic and streaming potential methods; however, to my knowledge successfully separating macerals by electrophoresis has not been accomplished.

Peter H. Given: I think Dr. Blaustein's suggestion is extremely interesting and worth following up. It might be possible to separate the macerals of bituminous coals in this way, provided they were finely enough ground to remain in suspension and to migrate in the electric field. But if very finely ground, could the macerals be identified again after separation?

Marie-Therese Mackowsky: Yes, in favorable cases and provided careful study of the coal is made before separation.

Irving A. Breger: Was anything known about elements or minerals present in samples on which zeta potentials were studied?

Mr. Campbell: Elements present in the lithotypes were determined by ultimate analysis, emission spectroscopy, and x-ray fluorescence analysis. The presence of certain minerals was inferred from the determined elements. A direct mineralogical analysis was not undertaken.

Publication Date: January 1, 1966 | doi: 10.1021/ba-1966-0055.ch022

Diffusion of Argon from Coals of Different Rank

S. P. NANDI and P. L. WALKER, JR.

Fuel Science Department, The Pennsylvania State University, University Park, Pa.

Publication Date: January 1, 1966 | doi: 10.1021/ba-1966-0055.ch023

Unsteady state release of argon has been measured from 200x325 mesh samples of 12 coals of volatile matter ranging from 2 to 45% over the temperature range 25°–100°C. The micropore diffusion parameter ($D^{1/2}/r_o$) has been evaluated. Argon diffusion is found to be activated for all coals except meta-anthracite, which is shown to have lost its microporosity. Activation energies increase monotonically from 3.2 kcal./mole for the anthracite (4.5% VM), to 6.5 kcal./mole for the medium volatile bituminous coal (27.0% VM), and then decrease with further increases in volatile matter to 4.3 kcal./mole for the high volatile bituminous coal (45.4% VM). The magnitude of the activation energies indicates that the size of the micropores in the coals closely approaches the size of the argon atom.

In a recent communication (*6*) the role of diffusion in establishing equilibrium in the adsorption of nitrogen and carbon dioxide on coals has been clearly indicated. The different internal surface area values obtained from nitrogen adsorption at 77°K. and carbon dioxide adsorption at 195°K. are caused primarily by the different diffusion velocities of the two gases in the micropore structure of coal under the conditions of measurement.

Unsteady state diffusion data obtained by various workers (*4, 6, 9, 10, 12*) have shown that diffusion of simple gases like methane, nitrogen, oxygen, and argon in coal is activated. That is, diffusion is proportional to $\exp(-E/RT)$ instead of $T^{1.5}$ as in bulk diffusion, or $T^{0.5}$ as in Knudsen diffusion. Diffusion of gases through a porous solid can only become activated if the diameter of the pores (through which diffusion occurs) is comparable with the diameter of the diffusing gas. When the diameter of the gas molecules becomes greater than that of the pores, the activation energy of diffusion increases sharply.

In Coal Science; Given, P.;
Advances in Chemistry; American Chemical Society: Washington, DC, 1966.

Therefore, data on the activation energy for the diffusion of a noble gas from coals of different rank permit an estimate of, at least, the trend of micropore size in coal with rank.

The only published work on the diffusion of gas in coals of different rank appears to be that of Bolt and Innes (*2*) who studied the diffusion of carbon dioxide from eleven samples of coal at 38°C. They found the diffusion coefficient to range from 3.5 to 9.2 x 10^{-8} sq. cm./sec., with no apparent correlation with coal rank. Diffusion data on coals of different rank at temperatures higher than 38°C. have only been reported by the present authors (*6*). It has been shown (*7*) that the diffusion of inert or noble gases from coal above room temperatures can be rigorously analyzed by using simple diffusion theory, and that true diffusion parameters of the micropore systems can be obtained. In this paper our measurements on the unsteady state release of argon from coals of various rank, over a temperature range, are reported.

Publication Date: January 1, 1966 | doi: 10.1021/ba-1966-0055.ch023

Experimental

Coals Used. Twelve coals of 200 × 325 Tyler mesh particle size were used in this study. Analyses of the coals are given in Table I.

Table I. Analyses of Coals

		Composition, as Received, Wt %					*Volatile Matter*
Coal	*State*	*H_2O*	*Ash*	*C*	*H*	*S*	*% daf*
Meta-anthracite	R. I.	0.7	43.5	55.1	0.2	...	2.1
St. Nicholas	Pa.	1.6	9.1	84.2	2.4	0.5	4.5
Dorrance	Pa.	0.7	9.9	82.9	2.5	0.7	5.8
Treverton	Pa.	0.5	9.7	...	...	1.1	9.0
Upper-Kittanning	Pa.	0.5	9.5	80.4	4.2	1.4	18.0
Kelley	Pa.	0.7	4.7	82.9	5.7	...	27.2
Pratt	Ala.	0.8	7.9	78.8	4.8	1.6	29.2
Upper-Freeport	Pa.	0.4	7.9	79.8	5.0	1.6	33.0
Pittsburgh	Pa.	1.1	5.6	77.5	5.3	1.5	37.4
Pittsburgh	Pa.	1.4	6.6	76.2	5.4	2.2	39.5
Pittsburgh 8	Ohio	1.5	16.4	65.5	4.9	4.5	42.4
Illinois No. 6	Ill.	1.9	7.6	66.1	5.5	2.8	45.4

Unsteady State Diffusion. The apparatus, experimental procedures, and the computational procedures used to calculate the diffusion parameter $D^{1/2}/r_o$ (where D is the diffusion coefficient and r_o is the diffusion path length) have been described in detail previously (*6, 8*). A differential experimental system was used to avoid errors caused by small temperature fluctuations. In principle, the procedure consisted of charging the sample under consideration with argon to an absolute pressure of 1204 ± 12 torr (an equilibrium time of about 24 hours was allowed) and then measuring the unsteady state release of the gas after suddenly reducing the pressure outside the particles back to atmospheric.

Prior to being charged with argon, the coal samples were degassed for 24 hours at temperatures ranging from 450°C. for the anthracites to 130°C. for the lowest rank Illinois coal. The temperatures of degassing were in every case higher than the temperatures of diffusion measurements. The temperature range over which diffusion was investigated was 25°–100°C.

For computing the diffusion parameter, $D^{1/2}/r_o$, Fick's diffusion equation was assumed to be applicable to the system, with D independent of concentration of the diffusing species. Solving Fick's law for a spherical particle, where the external gas pressure is constant gives:

$$\frac{V_t - V_o}{V_\infty - V_o} = 1 - \frac{6}{\pi^2} \sum_{n=1}^{\infty} \frac{1}{n^2} \exp\left(\frac{-Dn^2\pi^2 t}{r_o^2} \right)$$

where V_o, V_t and V_∞ are volumes at time $t = 0$, $t = t$, and $t = \infty$. The above equation was used in conjunction with experimental V_t *vs.* $t^{1/2}$ curves to calculate $D^{1/2}/r_o$ by a procedure described by Nelson and Walker (8).

Results and Discussion

The experimental diffusion parameters, $D^{1/2}/r_o$, at 30°C. are presented in Table II for all the coals. Clearly, no correlation exists between diffusion parameter and rank. If r_o is taken as the average particle radius for the 200 × 325 mesh samples, an upper limit to the values of diffusion coefficient, D, is obtained. The diffusion coefficient ranges from 1.92×10^{-9} sq. cm./sec. for Kelley coal to 1.41×10^{-8} sk. cm./sec. for the Dorrance anthracite. Our previous studies on the change of $D^{1/2}/r_o$ with particle size suggested that r_o is not necessarily the particle radius (7) but is a smaller distance related to the average length of the micropores in the particles. That is, the calculated

Table II. Diffusion of Argon from Coals of Different Rank

Coal	$D^{1/2}/r_o$ *at 30°C.* $sec.^{-1/2}$	$D_o^{1/2}/r_o$ $sec.^{-1/2}$	*Activation Energy kcal./mole*
St. Nicholas	0.0182	0.262	3.2
Dorrance	0.0424	0.785	3.6
Treverton	0.0181	0.603	4.2
Upper-Kittanning	0.0261	2.53	5.5
Kelley	0.0157	3.47	6.5
Pratt	0.0229	3.33	6.0
Upper-Freeport	0.0197	1.92	5.5
Pittsburgh	0.0172	0.676	4.3
Pittsburgh	0.0169	2.49	6.0
Pittsburgh 8	0.0193	1.13	4.9
Illinois No. 6	0.0279	1.00	4.3

Publication Date: January 1, 1966 | doi: 10.1021/ba-1966-0055.ch023

diffusion coefficients varied with particle size when r_o was taken as the average particle size in a sieve size fraction.

The temperature dependence of the diffusion parameter for all coals could be described by Arrhenius plots. Figure 1 shows typical plots for two of the bituminous coals. Table II summarizes the activation energy and pre-exponential data for all coals, where $D^{1/2}/r_o = D_o^{1/2}/r_o \exp(-E/2RT)$. Since r_o should be independent of diffusion temperature, the activation energy

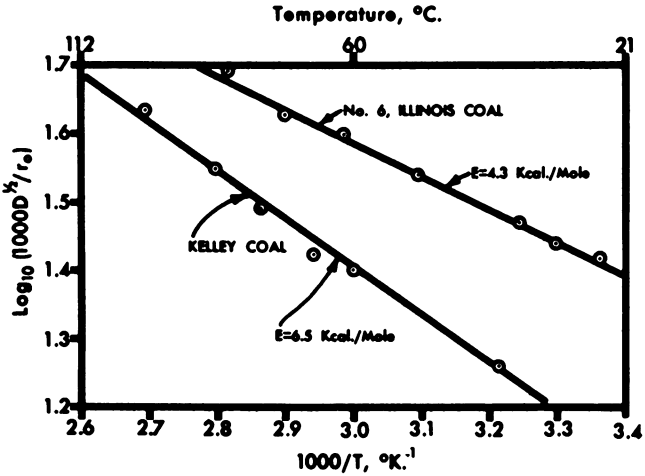

Figure 1. Activation energy plot for the diffusion of argon from two coals (200 × 325)

values can be taken as representing the temperature dependency of the diffusion coefficient. In Figure 2 the activation energy values for argon diffusion are plotted against volatile matter content of the coals. A volcano-shaped curve is obtained with its peak at a volatile matter content of *ca.* 27% (carbon content on daf basis of *ca.* 87%). The correlation towards the high volatile coals shows some spread which is not understood at this time. Two curves are drawn on the high volatile matter side of the curve primarily to emphasize the spread of values.

Curves of helium density (*11*), heat of wetting (*1*), and butane adsorption (*3*) *vs.* coal rank show minima at *ca.* 85–90% carbon content. These results are consistent with the correlation between activation energy for diffusion and coal rank found in this paper. A maximum in activation energy between 85 and 90% carbon indicates that the average size of the micropores in coal goes through a minimum at this point. This would result in the internal microporosity in coals of 85–90% carbon content being most inaccessible to displacement and adsorbing fluids.

The meta-anthracite sample behaved in a completely different way compared with the rest of the coals. It had a negligible capacity for argon; consequently, diffusion measurements could not be made. Helium, even at 250°C., could not enter into its micropores. Helium was shown to be able to pene-

Publication Date: January 1, 1966 | doi: 10.1021/ba-1966-0055.ch023

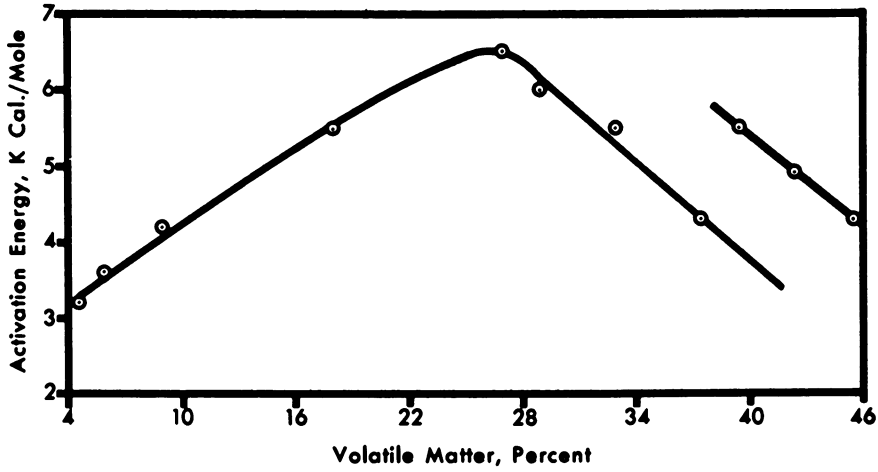

Figure 2. Activation energy for the diffusion of argon from coals (200 × 325) of different rank

trate the pores of a 1700°C. heat-treated St. Nicholas anthracite at 200°C. (7) even though heat treatment at this temperature removed most of its microporosity. From this, it appears that the meta-anthracite has a very small microporosity.

This result is to be expected from the x-ray structure of meta-anthracites. Ergun *et al.* (5) showed that a significant degree of graphitization in anthracite by the natural process of metamorphism is attained when the graphite-like layers reach a size of 25–30A. In the same paper it was shown that the L_c and L_a values for a meta-anthracite were 200 and 2500A., respectively, compared with values of 20 and 30A for the L_c and L_a dimension of a typical anthracite. The x-ray diffraction pattern of the meta-anthracite was strikingly similar to the pattern given for Ceylon graphite. From these evidences, meta-anthracite should be considered to be a highly graphitic substance and consequently nonporous.

Conclusions

The results of argon diffusion from coals have shown that the minimum size of the micropore system in coals is a function of the rank. The activation energy values show that the critical dimension of the pores go through a minimum in the range of good coking coals. Because the diffusion of argon is activated, it is concluded that the minimum dimension of the micropores is comparable to the size of the argon atom.

The critical dimension of the micropores in anthracite is large compared with that in coking bituminous coal, but when the meta-anthracite region is reached the microporosity disappears.

The minimum dimension of the micropores increases in the low rank coals, but the correlation between rank and activation energy is poor in this

Publication Date: January 1, 1966 | doi: 10.1021/ba-1966-0055.ch023

region. Bituminous coals are more complex than anthracites. They contain varying proportions of the petrological components, with these components undoubtedly having different micropore properties. Therefore, with bituminous coals, petrologically homogeneous components should be studied.

Acknowledgments

We wish to acknowledge the financial support of the Coal Research Board of the Commonwealth of Pennsylvania for making this research possible.

Literature Cited

(1) Berkowitz, N., *Can. J. Technol.* **33,** 169 (1955).
(2) Bolt, B. A., Innes, J. A., *Fuel* **38,** 333 (1959).
(3) Gregg, S. J., Pope, M. I., *Fuel* **38,** 501 (1959).
(4) Joy, A. S., *Conf. Sci. Use Coal, Sheffield, 1958,* **A–67** (1958).
(5) Mentser, M., Donnell, H. J., Ergun, S., *Fuel* **41,** 153 (1962).
(6) Nandi, S. P., Walker, P. L. Jr., *Fuel* **43,** 385 (1964).
(7) Nandi, S. P., Ph.D. Thesis, Pennsylvania State University, 1964.
(8) Nelson, E. T., Walker, P. L., Jr., *J. Appl. Chem.* **11,** 358 (1961).
(9) Pruss, W., 2nd Intern. Conf. Coal Sci., *Brennstoff-Chemie* **S35** (1958).
(10) Sevenster, P. G., *Fuel* **38,** 403 (1959).
(11) Van Krevelen, D. W., Schuyer, J., "Coal Science," p. 153, Elsevier Publishing Co., Amsterdam, 1957.
(12) Zwietering, P., Overeem, J. F., Van Krevelen, D. W., *Fuel* **35,** 66 (1956).

RECEIVED January 25, 1965.

Discussion

George Kapo. What is the cause of the minimum in pore diameter you observed as one increases the percent carbon in the coal?

S. P. Nandi. Many parameters (e.g., helium density, heat of wetting, butane adsorption, etc.) for correlating coal rank pass through a minimum at *ca.* 85–90% carbon content. In the present paper another parameter—the average size of the micropores—has been shown to follow the same pattern.

One plausible explanation of the above phenomenon can be given as follows. During the biochemical change from wood to peat, with the production of a hydrosol, there is a pronounced swelling, and the greater proportion of the water is contained in the bigger capillaries. The loss of moisture during the production of the hydrogel of lignite is accompanied by shrinkage of the larger pores without much diminution in the number or size of the smaller pores. The change from lignite to bituminous coal is a continuation of the process of conversion of peat to lignite, with a continued loss of water and a reduction in the number of pores of all sizes, but especially of the larger pores, until a carbon content of about 89% is reached. With further increase in rank the liberation of methane (as a result of carbon to carbon bond formation) again increases the porosity of coal (W. Francis, "Coal," pp. 667–716, Edward Arnold Ltd., London, 1961).

Bhupendra K. Mazumdar. Dr. Nandi mentioned that prior to diffusion studies, degassing the anthracite sample was carried out at 450°C. or so, and he commented that such high temperatures could be used satisfactorily. However, we wonder if this temperature of treatment is safe since, in our experience, at this temperature pyrolysis may set in to a certain extent.

Dr. Nandi. Outgassing at 450°C. is thought to have produced a negligible change in the ultrafine structure of St. Nicholas and Dorrance anthracites (S. P. Nandi, V. Ramadass and P. L. Walker, Jr., *Carbon* **2**, 199 (1964)). The carbon dioxide surface areas of raw and 700°C. heat-treated St. Nicholas anthracite are 220 and 215 sq. meters/gram, respectively, and those for the raw and 500°C. heat-treated Dorrance are 215 and 235 sq. meters/gram, respectively. In case of the higher volatile matter Treverton anthracite, this outgassing temperature apparently produced a significant change.

Publication Date: January 1, 1966 | doi: 10.1021/ba-1966-0055.ch023

24

Equilibrium Sorption Studies of Methane on Pittsburgh Seam and Pocahontas No. 3 Seam Coal

R. B. ANDERSON, J. BAYER, and L. J. E. HOFER

Pittsburgh Coal Research Center, Bureau of Mines, U.S. Department of the Interior, Pittsburgh, Pa.

Publication Date: January 1, 1966 | doi: 10.1021/ba-1966-0055.ch024

As a part of the Bureau of Mines studies on the storage and release of methane from coal, the equilibrium sorption of methane on Pocahontas No. 3 (lvb) coal from the Bishop mine of western Virginia and on Pittsburgh seam (hvab) coal from the Pursglove mine of northern West Virginia has been investigated. The results show that on the two coals methane is adsorbed at atmospheric pressure and 30°C. according to the Freundlich isotherm with exponents of 0.81 (lvb) and 0.88 (hvab) and with amounts at equilibrium of 2.89 cc (STP)/gram (lvb) and 1.97 cc. (STP)/gram (hvab). The two coals differ markedly in pore volume (difference between the mercury and helium specific volumes) with 0.136 cc./gram (lvb) and 0.020 cc./gram (hvab).

The release of methane during coal mining is a major safety problem. Modern mining machinery, which increases the rate of mining, has also increased the rate of evolution of methane. The Bureau of Mines is conducting studies on this problem, both in actual mining situations and in the laboratory. Studies on free flow of methane from holes drilled in the face and with displacement of methane by infusion of water into bore holes have been reported for West Virginia mines, the Pittsburgh seam coal at the Humphrey No. 7 mine at Osage (*7*), and the Pocahontas No. 4 seam at the Olga mine (*8*). Laboratory studies have been made on similar Pittsburgh and Pocahontas coals to provide basic information on the release of methane from coal. The present paper reports equilibrium adsorption measurements.

Several investigations have been reported on the adsorption of methane on coal (*4,5,9,10,12,14,15*). Methane adsorption at room temperature is usually highest for anthracite, passes through a minimum for bituminous coals

In Coal Science; Given, P.;
Advances in Chemistry; American Chemical Society: Washington, DC, 1966.

(of 86% carbon maf) (*9,10*), and then increases again for lower rank coals. Methane isotherms at room temperature and up to 1 atm. are either linear or have a slight curvature characterized by the Freundlich equation with an exponent slightly less than unity. Differential heats of adsorption for methane on coal of 4.2 and 4.9 kcal./mole have been reported (*5,10,15*). The rate of adsorption of methane is apparently controlled by an activated diffusion process, and the rate increases with increasing temperatures (*14*). Equilibrium can usually be obtained at temperatures above —78°C.; however, at —183°C. to —196°C. smaller amounts of methane are adsorbed than at —78°C. (*10*). These results are similar to those obtained at the Bureau of Mines for the adsorption of nitrogen on coal (*1*). At room temperature and 1 atm. the volume of methane adsorbed was 2–6 times the volume of nitrogen (*4,15*).

The adsorption of methane on coal has been determined at room temperature and pressures up to 1000 atm. (*9,12*). The amount of methane as a function of rank follows essentially the same pattern described above; however, the volumes adsorbed at 1000 atm. were 21–70 cc. (STP)/gram (*9,12*) compared with 1–8 cc. (STP)/gram at 1 atm.

This paper presents isotherms for the adsorption of methane, nitrogen, carbon dioxide, and water vapor on a Pocahontas No. 3 (lvb) and a Pittsburgh (hvab) coal. Rate data for the adsorption of methane on these coals will be described in a subsequent paper.

Experimental

Channel samples of Pocahontas No. 3 seam (lvb), Bishop mine, Tazewell County, Va., and Pittsburgh seam (hvab), Pursglove No. 15 mine, Monongalia County, W. Va. coals were collected under nitrogen at the mine face and sent to Bruceton in a closed container filled with nitrogen.

The samples were quartered as quickly as possible in air and then crushed and sieved in a dry box containing a nitrogen atmosphere. This procedure was followed to minimize oxidation of the coal during the sizing operations. Fractions of 6–8 mesh and 80–100 mesh were used.

Chemical analyses of the two coals are shown in Table I. The Bishop coal has a higher carbon content but lower volatiles and oxygen content than the Pursglove coal.

Helium and mercury densities were determined on the 6–8 mesh fraction. The larger mesh size was used to avoid the possibility that mercury would not penetrate the space between particles in the mercury density measurements. The coal was placed in a calibrated density tube, evacuated at room temperature for one hour, and then heated at 100°C. in vacuo for 2 hours. The weight of the coal after this treatment was used to compute the densities. Helium densities were determined at 30°C. by the method of Rossman and Smith (*11*). Mercury densities were determined by admitting mercury at an absolute pressure of 1140 torr to the coal sample after evacuation, following the helium density measurement.

Sorption studies were performed on the 80–100 mesh fraction. The coal was placed in a glass tube and evacuated in the manner used for the density measurements except that, because of the finer mesh size of the sample, it was evacuated more cautiously to avoid the loss of coal. The weight of the coal after this treatment was used to compute the amount adsorbed per gram.

Publication Date: January 1, 1966 | doi: 10.1021/ba-1966-0055.ch024

Table I. Chemical Analyses of Coals

	Pittsburgh, wt. %		*Pocahontas, wt. %*	
	mf[a]	*maf*[b]	*mf*	*maf*
Ash	6.6		6.2	
Volatile matter	36.3	38.9	22.3	23.8
Hydrogen	5.2	5.6	4.6	4.9
Carbon	79.2	84.8	84.5	90.1
Nitrogen	1.7	1.8	1.2	1.3
Oxygen	6.0	6.4	2.9	3.1
Sulfur	1.3	1.4	0.6	0.6

[a] Moisture-free basis.
[b] Moisture-ash-free basis.

Nitrogen, methane, and carbon dioxide isotherms were determined by the conventional volumetric method (3). Nitrogen isotherms were obtained at three different temperatures in the following order: —195°, —78°, 0°, —78°, and —195°C. without intervening evacuation in the sequence of experiments. Methane isotherms were determined at the following temperatures and in the following order: —195°, —78°, 0°, 30°, 50°, 0°, —78°, and —195°C. Here, too, no evacuations were performed between isotherm measurements. Methane isotherms at —195°C. are of lower accuracy than other isotherms because they are determined at pressures less than 10 torr, the vapor pressure of methane at —195°C. In determining methane isotherms at —195°C., the gas buret was used like a McLeod gauge—i.e., the stopcock to the sample was closed, and the mercury in the gas buret was raised to the next or higher reference position so that the pressure was increased by a factor of 10 or 20

Table II. Pore Volumes and Surface Areas

Coal	Pittsburgh	Pocahontas
Density, grams/cc.:		
By helium	1.313	1.435
By mercury	1.278	1.201
Pore volume, cc./gram	0.020	0.136
Volume adsorbed at saturation, calculated as normal liquid, cc./gram		
N_2	0.002 (0.008[a])	0.006 (0.014[a])
CH_4	0.0007	0.0005 (0.022[a])
CO_2	0.062	0.071
H_2O	0.025	0.013
Surface area, sq. meters/gram		
N_2	0.62 (7.9[a])	0.78 (17.9[a])
CH_4	0.75	0.25 (61[a])
CO_2	114[b]	140[b]
H_2O	36.6	11.6

[a] Values obtained from isotherms at —195°C. after adsorption sequence at higher temperatures.
[b] Recent work indicates that surface areas from CO_2-isotherms on coal should be determined by the Langmuir rather than the BET equations. Surface areas calculated using the Langmuir equation were 174 and 200 sq. meters/gram for the Pittsburgh and Pocahontas coals, respectively.

Publication Date: January 1, 1966 | doi: 10.1021/ba-1966-0055.ch024

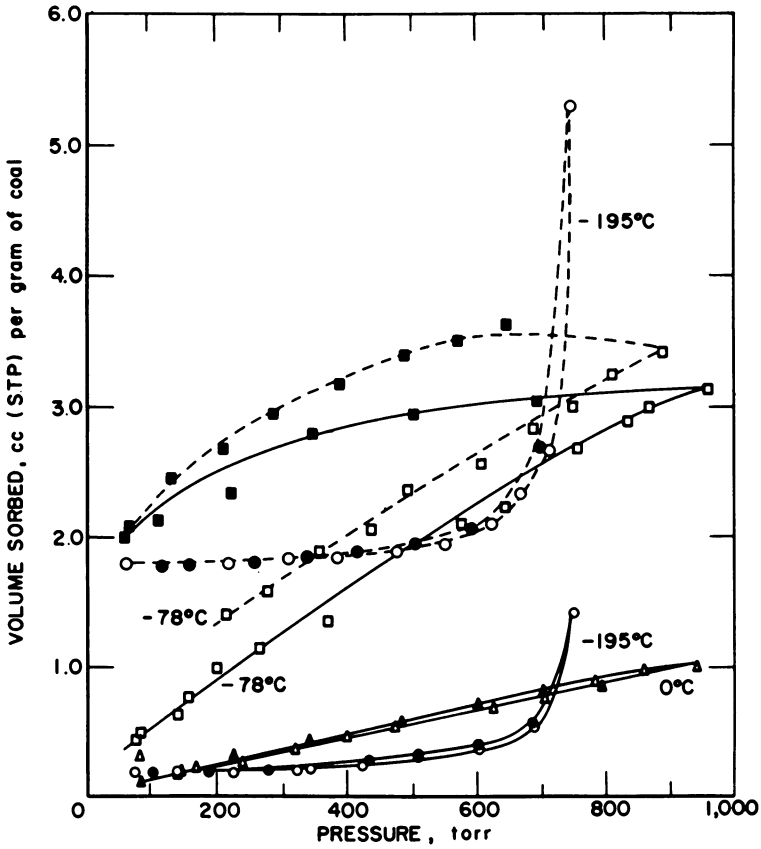

Figure 1. Nitrogen sorption on Pittsburgh coal; desorption points are solids; solid curves indicate isotherms of ascending temperature sequence and broken curves, descending temperature sequence

to permit pressure determination with moderate accuracy on a conventional mercury manometer. Carbon dioxide isotherms were determined at —78°C.

Water isotherms were determined in the following way: Samples of 80–100 mesh coal were evacuated at 100°C. for 2 hours in a glass tube and were then transferred to weighing bottles. The dried samples were exposed in a vacuum desiccator to water vapor from a series of saturated salt solutions with relative pressures ranging from 0.11 to 0.96 (*6*). The desiccator was kept in an air thermostat maintained at 35 ± 0.5°. It was evacuated to a pressure of less than 5 mm. and then closed for equilibration. Seven days were allowed for equilibration at each sorption point. In previous work (*1*) this time was found to be sufficient for attaining equilibrium.

Results

The density measurements given in Table II indicate that the Pittsburgh seam coal has a low pore volume compared with that of the Pocahontas coal.

Publication Date: January 1, 1966 | doi: 10.1021/ba-1966-0055.ch024

For both coals the time necessary to make the nitrogen adsorption isotherm at —195° and 0°C. was short, and the experimental points were taken at about hourly intervals. The isotherms at 0°C. represent equilibrium. Nitrogen adsorption at —195°C. is rapid in the macropores but too slow to detect in the micropores. The isotherm at —195°C., therefore, represents only the adsorption in macropores. At —78°C. nitrogen adsorption is also rapid in the macropores and is slow but detectable in the micropores. Therefore, at —78°C., 8–24 hours were allowed to elapse before each reading. Equilibrium was not attained at —78°C. as shown by the irregular isotherms and the large

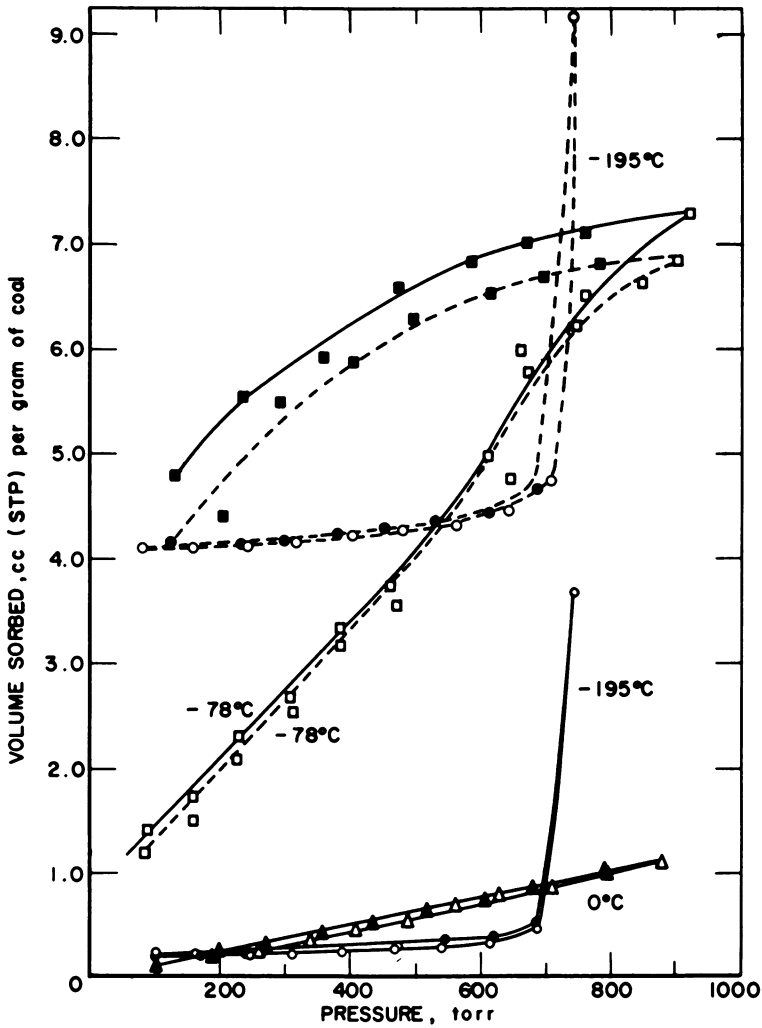

Figure 2. Nitrogen sorption on Pocahontas coal; desorption points are solids; solid curves indicate isotherms of ascending temperature sequence and broken curves, descending temperature sequence

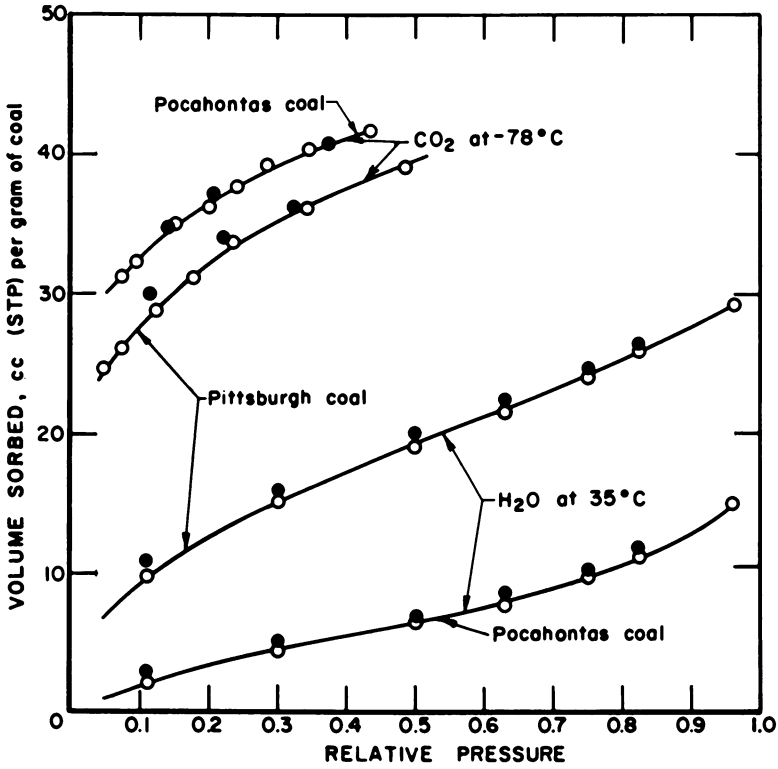

Figure 3. Adsorption of water vapor and carbon dioxide on coal; desorption points are solid

hysteresis loops. Figures 1 and 2 show the initial isotherms at —195° and —78°C. (ascending temperatures) as solid curves. The final isotherms at —78° and —195°C. (descending temperatures) are shown as dashed curves. The nitrogen isotherms for Pittsburgh and Pocahontas coals are qualitatively similar in that the sorption at —78° is greater than the initial adsorption at —195° and than the adsorption at 0°C.

Water isotherms determined at 35°C. are shown in Figure 3. The amount of water sorbed by the Pittsburgh coal is about twice the amount taken up by Pocahontas coal. These isotherms represent equilibrium measurements. Hysteresis loops that do not close at relative pressures less than 0.3 are characteristic of water adsorption on coal.

Carbon dioxide isotherms at —78°C. are also shown in Figure 3. The adsorption of CO_2 was relatively slow; however, adsorption and desorption points taken at 24-hour intervals seem to represent equilibrium conditions. The pressure scale for CO_2 isotherms is given as observed pressure divided by an extrapolated liquid vapor pressure at —78°C. (A plot of the logarithm of vapor pressure of liquid CO_2 as a function of reciprocal absolute temperature is linear, and this straight line was the basis of extrapolation. At —78°C. the

Publication Date: January 1, 1966 | doi: 10.1021/ba-1966-0055.ch024

vapor pressure of liquid CO_2 is 1.86 times the vapor pressure of the solid.) This convention is consistent with the general observation that the adsorbate is usually more nearly like liquid than solid. The isotherm for Pocahontas coal showed no hysteresis, but for Pittsburgh coal desorption points were higher than adsorption points.

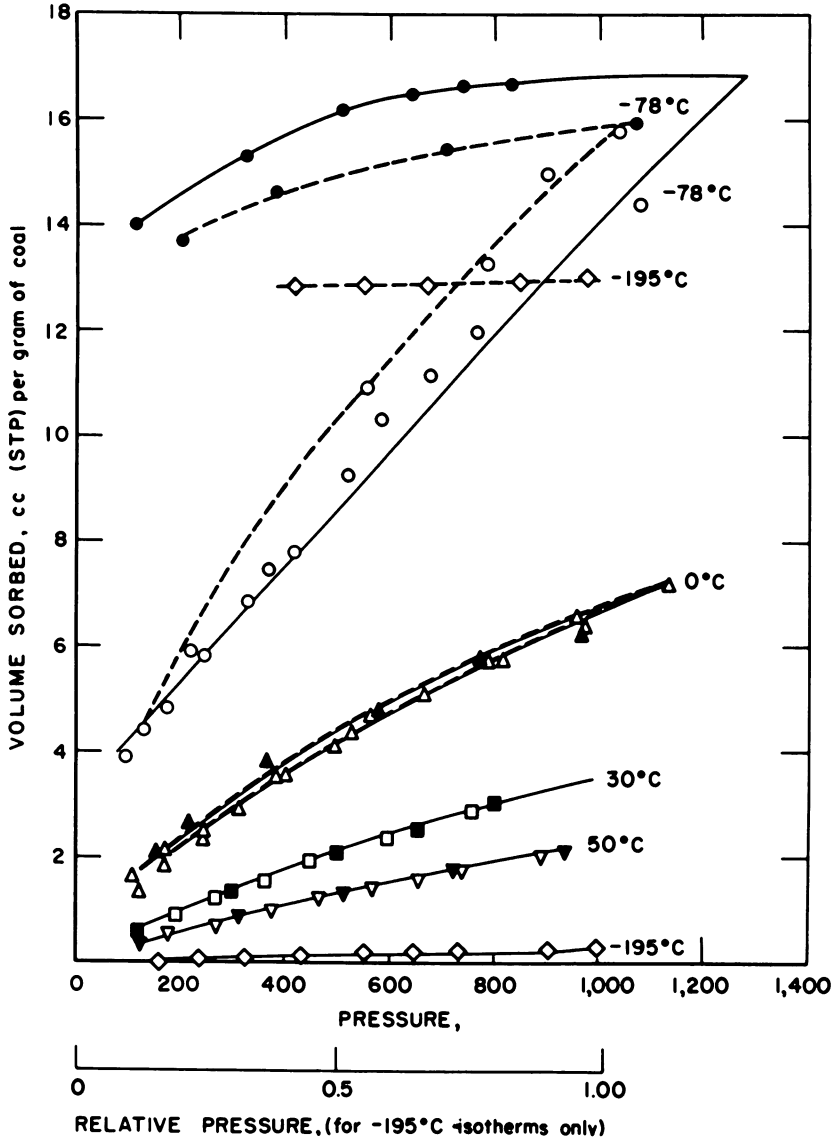

Figure 4. Methane isotherms on Pocahontas coal; solid symbols represent desorption; solid curves indicate isotherms of ascending temperature sequence and broken curves, descending temperature sequence

Publication Date: January 1, 1966 | doi: 10.1021/ba-1966-0055.ch024

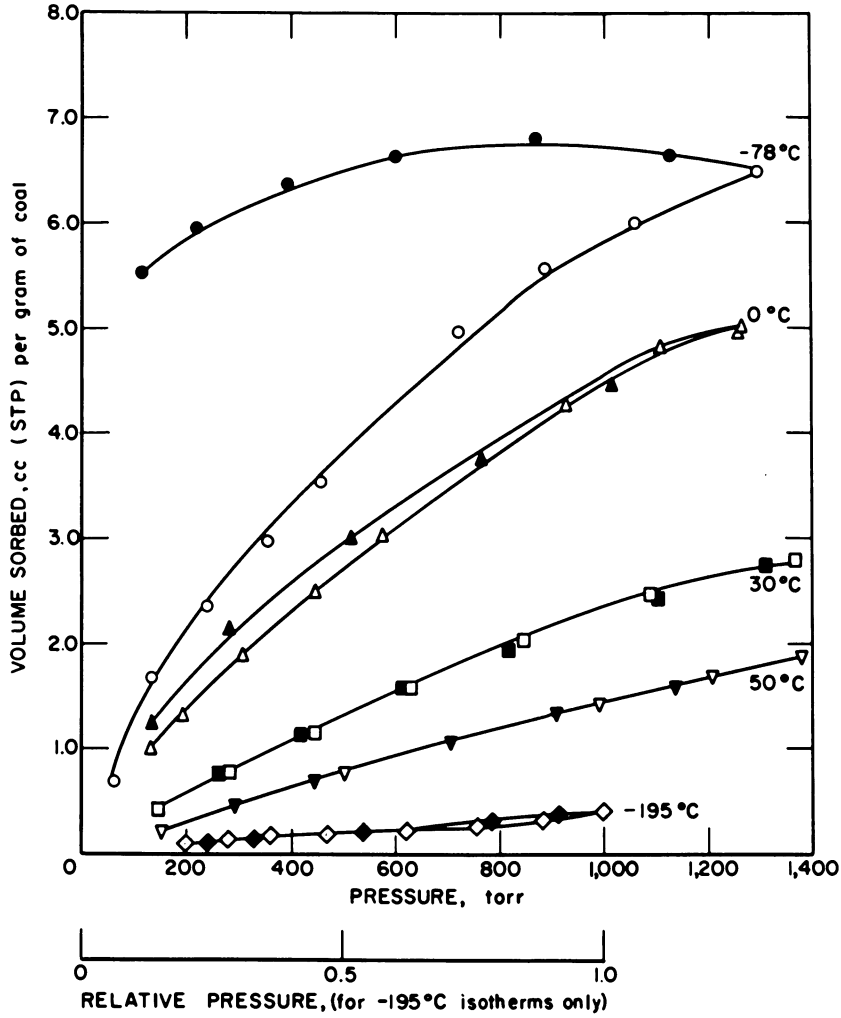

Figure 5. Methane isotherms on Pittsburgh coal determined in increasing temperature sequence; desorption points are solid

In Figure 4 for Pocahontas coal the methane isotherms at —195°, —78°, 0°, 30°, and 50°C., determined in the sequence indicated, are shown as solid curves, and the isotherms at 0°, —78° and —195°C. after the initial sequence are shown as dashed curves. For the Pittsburgh coal, only the isotherms in a rising series of temperatures were determined (Figure 5). Figures 4 and 5 show a plot of methane isotherms at —195°C. on a relative pressure basis (pressure of methane/vapor pressure) because the vapor pressure is only about 10 torr. Isotherms determined at —195°C. represent metastable equilibrium and those at 30°, 50°, and possibly 0°C. equilibrium. Adsorption was

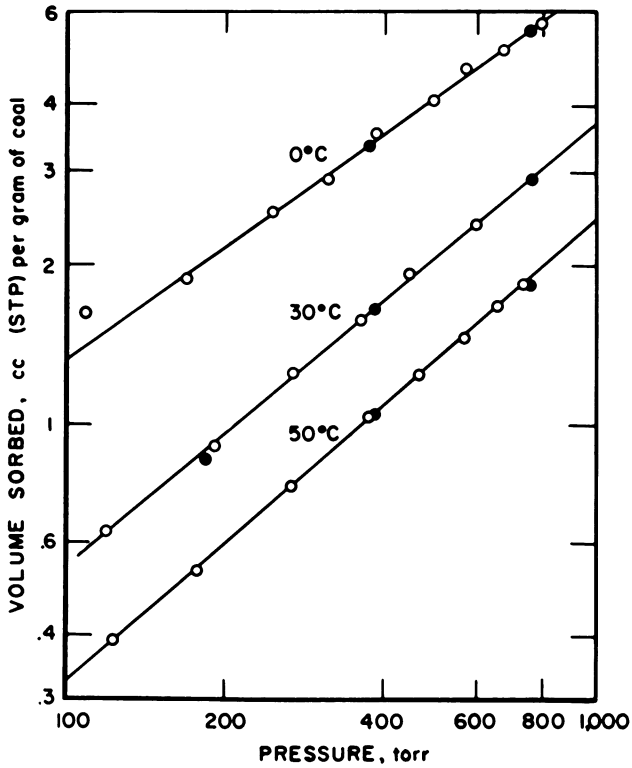

Figure 6. Plots of Freundlich equation for methane on Pocahontas coal; solid circles were obtained using manostatic sorption apparatus

slow at —78°C., and the irregular adsorption points and the large hysteresis loops indicate that equilibrium was not obtained. However, at —78°C. a greater amount of methane was adsorbed than at all other temperatures except for the final isotherm at —195°C. In the temperature range 0°–50°C. the amount adsorbed decreased regularly with increasing temperature.

Surface areas estimated from the isotherms in Figures 1–5 are given in Table II.

Logarithmic plots of the Freundlich equation, $Q = kp^n$, where Q is the amount of methane adsorbed at a pressure p, and k and n are constants, for methane adsorption at 0°, 30° and 50°C. in Figures 6 and 7 indicate that the equation is valid up to at least 1000 torr. Equilibrium sorption points obtained on different samples in a manostatic adsorption apparatus are shown as solid points in Figures 6 and 7. The exponent n varied from 0.72 at 0° to 0.87 at 50°C. for the Pocahontas coal and from 0.78 at 0° to 0.94 at 50°C. for Pittsburgh coal (Table III).

Differential heats of adsorption for methane calculated with the Clapeyron equation from isotherms at 0°, 30° and 50°C. are given in Table III. The

Publication Date: January 1, 1966 | doi: 10.1021/ba-1966-0055.ch024

heats of adsorption were in the range 4.7–7.8 kcal./mole and decreased with increasing amounts adsorbed.

The Langmuir equation

$$Q = cV_s p/(1 + cp)$$

in the form

$$1/Q = 1/cV_s p + 1/V_s,$$

where Q is the amount of methane adsorbed at pressure p, V_s is the limiting amount of methane adsorbed at high pressures, and c is a constant, represent the adsorption data in the pressure range 200–1000 torr as shown in Figure 8. Constants for the Langmuir equation are given in Table III.

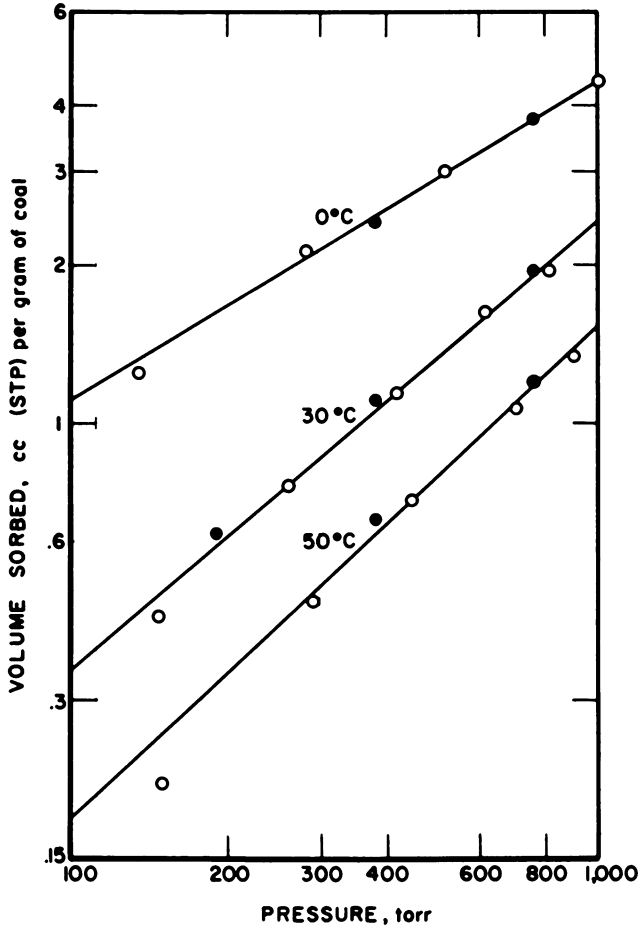

Figure 7. Plots of Freundlich equation for methane on Pittsburgh coal; solid circles were obtained using manostatic sorption apparatus

Discussion

Coal is a unique adsorbent. At —195°C. most coals act as 4-A. molecular sieves, and molecules such as nitrogen, methane, and argon are not adsorbed in large amounts. These molecules do not enter the pore structure with openings of molecular sizes at an appreciable rate. At —78°C. nitrogen, methane, and argon adsorb slowly but in amounts significantly larger than at —195°C. As temperature is increased above —78°C., the rate continues to increase, but the amount adsorbed at equilibrium decreases. Carbon dioxide adsorbs slowly in large amounts at —78°C., and has been proposed as a method of measuring surface area of coal (*2*).

From 0° to 35°C. most coals behave as a 5-A. molecular sieve adsorbing large amounts of *n*-butane but little isobutane. The idea that pore openings may become larger as temperature increases seems consistent with the moderately large coefficient of thermal expansion of coal. Methanol and water vapor adsorb relatively rapidly and in large amounts at about room temperature; however, their adsorption is apparently complicated by chemical interactions of these molecules with polar groups within the coal and extensive swelling of the coal. The shape of isotherms for methanol and water and hysteresis phenomena are not characteristic of physical adsorption on molecular sieves and charcoals. Adsorption studies of CO_2 on carbon blacks at —78°C. in this and other laboratories (*13*) suggest that the adsorption of CO_2 may also be affected by the oxygen content of the carbon black.

Surface areas reported in Table II show some of the difficulties in estimating a significant surface area for coal. Areas from the initial nitrogen and methane isotherms at —195°C. probably represent only the external area of

Table III. Constants of Freundlich and Langmuir Isotherms and Heats of Adsorption for Methane

	Pittsburgh Coal, T °C.			*Pocahontas Coal, T °C.*		
	0	*30*	*50*	*0*	*30*	*50*
Constant *n* of Freundlich equation	.78	.88	.94	.72	.81	.87
Langmuir equation						
V_m, cc.(STP)/gram	8.7	9.2	8.8	12.9	10.6	10.0
c (torr)$^{-1} \times 10^3$	1.035	0.348	0.198	1.013	0.524	0.308
Heat of adsorption, kcal./mole		5.9			4.3	
Differential heat of adsorption from Clapeyron equation, kcal./mole, for following amounts adsorbed, cc.(STP)/gram	*Temperature Ranges, °C.* 0–30	30–50		*Temperature Ranges, °C.* 0–30	30–50	
1.0	7.80	5.60		6.18	5.24	
1.5	6.82	5.18		5.69	5.14	
2.0	6.07	—		5.38	4.91	
2.5				5.11	4.86	
3.0				4.92	4.74	

Publication Date: January 1, 1966 | doi: 10.1021/ba-1966-0055.ch024

the particles plus the area of the pores with openings larger than 4-A. The volumes of nitrogen or methane adsorbed at a relative pressure of one, calculated as normal liquid, are very much less than the pore volume computed from

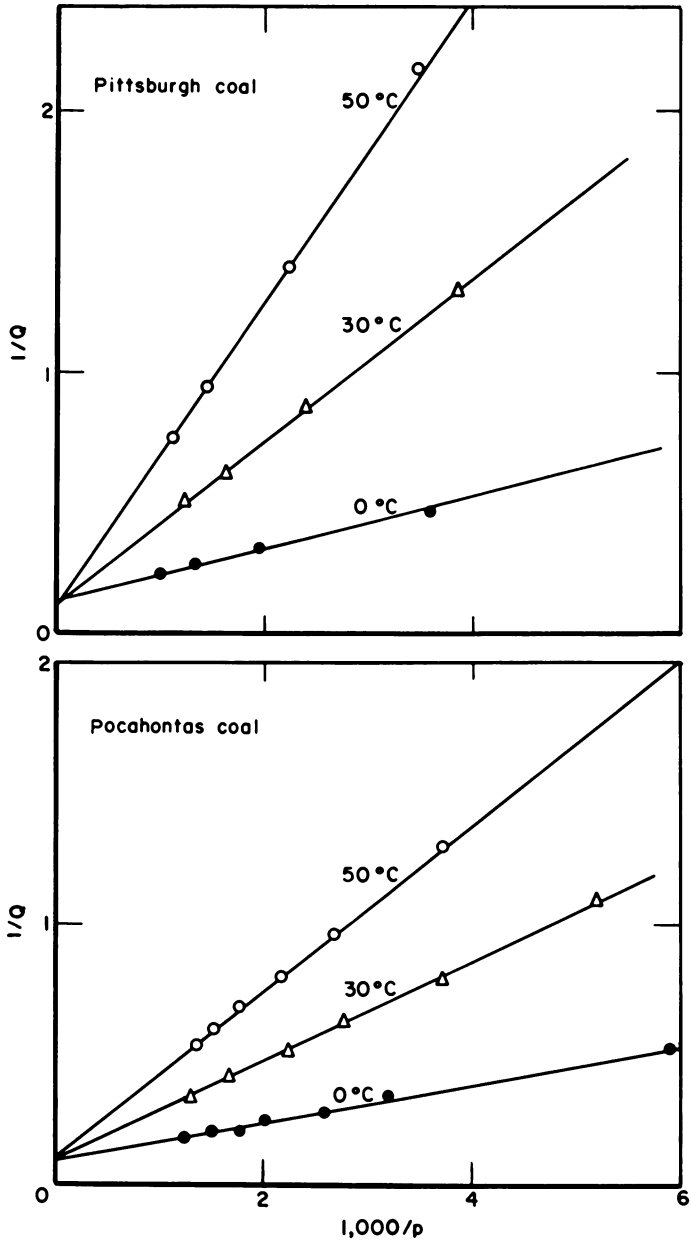

Figure 8. Langmuir plots for adsorption of methane on coal

mercury and helium densities. At —78°C. and higher temperatures, nitrogen or methane enter pores with openings of molecular dimensions, and subsequent isotherms at —195°C. are displaced upward by about this amount.

Surface areas from CO_2 isotherms at —78°C. were 114 and 140 sq. meters/gram for Pittsburgh and Pocahontas coals which are of the same magnitude as areas from methanol adsorption, 113 and 110 sq. meters/gram, obtained previously (*1*) on other samples of Pittsburgh and Pocahontas coals. For the Pittsburgh coal the volume of liquid CO_2 adsorbed at saturation pressure exceeded the pore volume but not for the Pocahontas coal. Surface areas from water adsorption were lower than those from CO_2 adsorption, 36.6 and 11.6 sq. meters/gram for Pittsburgh and Pocahontas coals. The volume of water as liquid adsorbed at saturation exceeded the pore volume for Pittsburgh but not for Pocahontas coal.

Publication Date: January 1, 1966 | doi: 10.1021/ba-1966-0055.ch024

Methane adsorption at 0°C. and 1000 torr was about 4 and 6 cc. (STP)/gram for Pittsburgh and Pocahontas coals compared with about 1 cc. (STP)/gram for nitrogen. At 0°C. nitrogen isotherms are essentially linear, but methane isotherms have a small curvature. Methane isotherms at 0°, 30°, and 50°C. are represented accurately by the Freundlich equation and in the pressure range 200–1000 torr by the Langmuir equation. Because the isotherms have only slight curvature, it may be expected that the two dissimilar adsorption equations will fit the same data. The values of the Freundlich exponent, n (Table III), increase toward 1 with increasing temperatures, consistent with the general observation that the exponent tends to approach 1 as temperature increases and the amount adsorbed decreases. The values of n for nitrogen at 0°C. are nearly unity, consistent with the smaller amount of nitrogen adsorbed on coal.

The Langmuir isotherm may be expected to be more reliable at high than at low pressure because complicating factors not included in the derivation, such as variation of the heat of adsorption with the amount adsorbed, become less important. The Langmuir equation permits extrapolating to the limiting amount adsorbed at high pressure, V_s. The values of V_s were about 9 cc. (STP)/gram for Pittsburgh and 11 for Pocahontas coals. The validity of the V_s values as estimates of the limiting amount of methane adsorbed at high pressure may be questioned since these values are less than half of those determined on European coals of similar rank (*9*, *12*).

Differential heats of adsorption of methane at 0° and 50°C. (Table III) varied from 4.7 to 7.8 kcal./mole. These values are of the magnitude of a normal (Trouton's rule) liquid boiling at room temperature, 6.3 kcal./mole; therefore, the adsorption may be regarded as a physical process. For both coals the heats of adsorption decrease exponentially with amount adsorbed and decrease with increasing temperature. The heat of adsorption for Pittsburgh coal is slightly larger than for Pocahontas coal. Heat of adsorption estimated from the temperature dependence of the constant c of the Langmuir were of the same magnitude as heats from the Clausius-Clapeyron equation for large amounts adsorbed.

The following summary is made on the two coals:

(1) The Pocahontas coal has a larger pore volume than Pittsburgh coal.

(2) The surface area estimated from CO_2 isotherms was larger for Pocahontas (140 sq. meters/gram) than for Pittsburgh coal (114 sq. meters/gram). Since these results vary in the opposite order to the oxygen content of the coals, possible complications of enhanced adsorption or inhibition of CO_2 by the oxygen of the coal do not invalidate the conclusion that Pocahontas coal has a larger surface area than Pittsburgh coal.

(3) In the temperature range 0°–50°C., Pocahontas coal adsorbs more methane than Pittsburgh coal consistent with 1 and 2.

Literature Cited

(1) Anderson, R. B., Hall, W. K., Lecky, J. A., Stein, K. C., *J. Phys. Chem.* **60,** 1548 (1956).
(2) Anderson, R. B., Hofer, L. J. E., Bayer, J., *Fuel* **41,** 393 (1962).
(3) Emmett, P. H., "Advances in Colloid Science," Vol. I, pp. 1–36, E. O. Kraemer, Ed., Interscience Publishers, New York, N. Y., 1942.
(4) Ettinger, I. L., *Izvest. Akad. Nauk SSSR, Otd. Tekhn. Nauk* **1949,** 1719.
(5) Joy, A. S., *Conf. Sci. Use Coal, Sheffield,* **1958, A–67.**
(6) Mellon, E. F., Korn, A. H., Hoover, S. R., *J. Am. Chem. Soc.* **69,** 827 (1947).
(7) Merritts, W. M., Poundstone, W. N., Light, B. A., *Bur. Mines Rept. Invest.* **5977,** 1962.
(8) Merritts, W. M., Waine, C. R., Mokwa, L. P., Ackerman, M. J., *Bur. Mines Rept. Invest.* **6326,** 1963.
(9) Moffat, D. H., Weale, K. E., *Fuel* **34,** 449 (1955).
(10) Nandi, S. P., Kini, K. A., Lahiri, A., *J. Sci. Ind. Research* **18B,** 511 (1959).
(11) Rossman, R. P., Smith, W. R., *Ind. Eng. Chem.* **35,** 972 (1943).
(12) Sommen, van der, J., Zwietering, P., Eillebrecht, B. J. M., Van Krevelen, D. W., *Fuel* **34,** 444 (1955).
(13) Spencer, W. B., Amberg, C. H., Beebe, R. A., *J. Phys. Chem.* **62,** 719 (1958).
(14) Zwietering, P., Overeem, J., Van Krevelen, D. W., *Fuel* **35,** 66 (1956).
(15) Zwietering, P., Van Krevelen, D. W., *Fuel* **33,** 331 (1954).

RECEIVED October 5, 1964.

Publication Date: January 1, 1966 | doi: 10.1021/ba-1966-0055.ch024

Discussion

Philip L. Walker, Jr. Your adsorption results show carbon dioxide to be adsorbed to a greater extent than water on bituminous coals. Since these molecules are close to the same size, do you interpret this to mean that water is only adsorbing on the hydrophilic part of the surface whereas carbon dioxide is adsorbing on all of the available surface?

Robert B. Anderson. Dr. Walker's statement is a good general summary of the data on these and other coals. The hydrophilic character of coal may be expected to increase with oxygen content. For example, on anthracite the adsorption of water at low relative pressures is small compared with the adsorption of CO_2. On lignite the adsorption of both water and CO_2 is large.

25

Kinetics of the Sorption of Methanol on Coal

MAURICE M. MITCHELL, JR.* and PAUL FUGASSI

Coal Research Laboratory, Carnegie Institute of Technology, Pittsburgh, Pa.

Kinetic and equilibrium studies of the sorption of methanol on various coals and on partially acetylated samples of these coals have been used to elucidate a mechanism for this process. The data are interpreted in terms of partial acetylation blocking surface sites and perhaps interfering with intermolecular hydrogen bonding. It is proposed that the rate-determining step is a set of parallel, competing, second-order reactions involving transfer of methanol from the surface to the interior of the coal. All types of surface sites appear to participate, and the pressure-independent rate constant is considered to be the sum of the rate constants for each type of surface site. The dependence of the experimental rate constant on methanol pressure is a characteristic of the coal rank.

Publication Date: January 1, 1966 | doi: 10.1021/ba-1966-0055.ch025

The use of methanol sorption as a possible tool for studying coal and its structure has been the subject of numerous investigations and discussions. Dryden gives a summary of much of this work (*4*). Most of these studies have been concerned with justifying the wide differences in the amount of sorption on coals obtained with other sorbates of different polarities and the resulting large discrepancies in surface areas calculated from these data. Interpreting heats of wetting data from the standpoint of functional groups contained within the coal structure, in particular hydroxyl, has been a part of these studies. Values of hydroxyl contents of coals calculated from these data generally have been lower than those obtained from other methods of determination. It is argued that, because of the necessary assumptions about energies of interaction and the small, experimentally obtained differences in heats of wetting between those of methanol and of nonpolar sorbates, methanol sorption as measured calorimetrically is not a reliable tool for assessing the oxygen-containing groups

* Present address: The Atlantic Refining Company, Research and Development Department, 500 South Ridgeway Ave., Glenolden, Pa. 19036

In Coal Science; Given, P.;
Advances in Chemistry; American Chemical Society: Washington, DC, 1966.

in coal. However, it is generally accepted that methanol, because of its polar hydroxyl group, wets the coal through hydrogen bonding, and that the groups in the coal which are most involved in this sorption are hydroxyl and carbonyl (e.g. quinone). The methanol molecule easily fits within a cube 4 A. to a side, and it should penetrate the cracks and pores within the coal. These have been estimated to be about 40 A. wide and interconnected by constrictions of 5–8 A. width.

In recent years the Coal Research Laboratory has been investigating the kinetics and isotherm behavior of methanol sorption on coal (*6*, *7*, *10*) along with the sorption of other vapors on coal (*6*) and of polar vapors on swelling gels (*9*, *10*). Methanol sorption was shown to be reversible on coal, and its sorption behavior supports the model of coal as a gel or mixture of gels in its physical structure. All indications (*1*, *6*, *7*) are that its interaction is with specific and a fixed number of sites for a particular coal sample. Although the sorption of methanol is reversible, coal exhibits sorption behavior which is interpreted in terms of an irreversible swelling of the coal gel upon initial exposure to methanol vapor. As a result of these studies, an isotherm and experimental rate equation for the sorption and desorption were derived that fit the observed data. The isotherm derived for methanol sorption on coal was:

$$W_e = \frac{AKK_1P^\circ c}{[1 + (K_1P^\circ - 1)c]\,(1 - c) + KK_1P^\circ c} \qquad (1)$$

where A is the total sites per unit weight within the coal susceptible to methanol sorption, K is the equilibrium constant for the transfer reaction of methanol from the surface to the interior of the coal, K_1 is the equilibrium constant for adsorption of methanol from the vapor onto a vacant surface site, P° is the vapor pressure of methanol at the temperature of the experiment, and c is the relative pressure of the methanol vapor and is equal to P/P°. P is the experimental methanol pressure at which W_e, the equilibrium amount of sorption per unit weight of coal, is measured. The experimental rate equation derived for the sorption of methanol on coal was:

$$\frac{dW}{dt} = k_s\,(W_e - W)^2 - k_d W^2 \qquad (2)$$

In this equation dW/dt is the rate of sorption, k_s is the experimental rate constant for sorption, W_e is the equilibrium sorption, W is the amount of sorption at time $t = t$, and k_d is the experimental rate constant for desorption. Thus, the sorption rate was found to be proportional to the square of the concentration of unoccupied sites, and the desorption rate was proportional to the square of the concentration of occupied sites. These rate equations are not general solutions to Fick's law of diffusion. The experimental rate constants for sorption were found to be non-linearly dependent on methanol pressure and seemed to correlate with the amount of surface sorbed methanol in different ways for coals of various rank.

This paper deals with a series of studies on coals of ranks indicated by their carbon contents of between 65 and 81%. It was believed that a detailed study of methanol sorption on these coals, including an investigation of the

role surface sites play in their kinetic and isotherm behavior, would contribute to an understanding of coal structure. It was expected that by blocking some of the surface sites irreversibly, changes in the magnitudes of rate constants and isotherm parameters might be achieved. A clarified mechanism would be obtained by interpreting these changes. Acetylation with acetic anhydride vapor was chosen as the means to block sites because its large molecular size and relatively high vapor pressure would permit control of the reaction to include only surface sites, and the by-product of acetylation (acetic acid) is volatile, its sorption on coal being reversible (*8*). The data of Mazumdar *et al.* (*11*) on the heats of wetting of coals and acetylated coals by methanol indicate that at total acetylation the heat of wetting is essentially zero. Thus, the acetate group introduced into the coal does not significantly sorb methanol, and partial acetylation should result in blocking certain sites on the surface of coal.

Publication Date: January 1, 1966 | doi: 10.1021/ba-1966-0055.ch025

Experimental

Apparatus. The sorption of methanol on coal was measured in the apparatus shown schematically in Figure 1. It consisted of three McBain-Bakr type balances, the springs for which were formed from 0.005-inch Ni-Span-C alloy wire annealed at 600°C. The diameters of these springs were about 1.5 cm.,

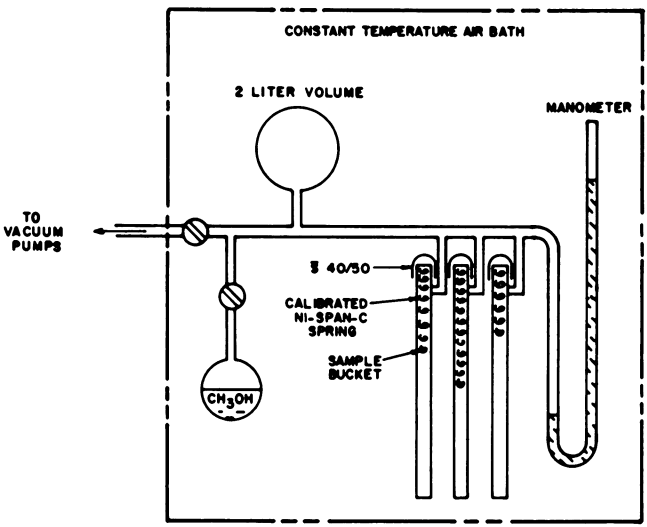

Figure 1. Schematic diagram of sorption apparatus

and their spring constants were 1.923, 1.563, and 1.539 mg./mm. The balances were contained in tubes 40 mm. in diameter and 60 cm. long. The caps were sealed with a beeswax-rosin vacuum wax. The coal samples were carried in glass buckets weighing about 120 mg. which were hung on the ends of the springs. The coal samples weighed about 200 mg. and the spring elongations were determined by means of a cathetometer reading to 0.1 mm. The springs were calibrated for loads up to 1.5 gram, and to that point their response was

linear. Over the temperature region of these studies the temperature coefficients of the spring constants were negligible. The volume of the system was such that the methanol pressure during a kinetic run varied less than 1 mm. The constant-temperature air bath which housed the entire apparatus was controlled to ±0.02°C. during the significant portion of the kinetic runs and to about ±0.05°C. over the relatively long periods of time necessary to obtain equilibrium sorptions. The apparatus was connected on the outside of the air bath to a vacuum line consisting of a three-stage mercury diffusion pump backed by the usual mechanical vacuum pump. In addition, means were provided to admit air dried over anhydrous calcium sulfate when releasing vacuum.

The coals were acetylated in the apparatus shown in Figure 2. The reaction chamber was 40 mm. in diameter and about 15 cm. long. This apparatus was connected to the same vacuum line as the sorption system. A steel rack, shaped to fit within the reaction chamber and provided with a taut nichrome wire to hold the sample buckets, is shown in Figure 3.

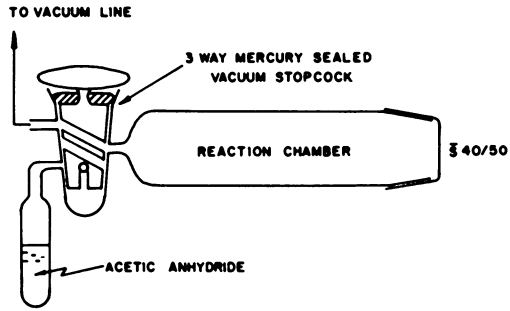

Figure 2. Schematic diagram of acetylation apparatus

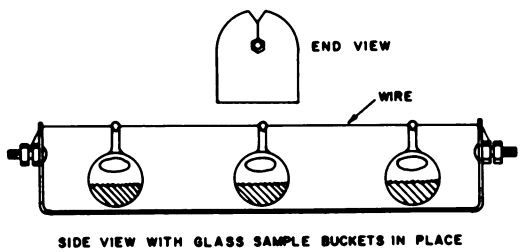

Figure 3. Sample rack for acetylation apparatus

Materials. The five American coals used in this work and their ultimate analyses are listed in Table I. Table II shows data on maximum obtainable vapor phase acetylations and oxygen contents for these coals.

The coals were crushed to —20 mesh but were not further size segregated to avoid selective separation of the petrographic constituents of the coal. Analytical reagent grade methanol was obtained from Fisher Scientific Co. and used without further purification. It was stored over anhydrous calcium sulfate and degassed by intermittent evacuation of the storage flask. Reagent

Table I. Ultimate Analysis of the Coal Samples[a]

	C	*H*	*N*	*O*	S	*Ash*
Upper Freeport	78.7	4.8	0.9	4.6	1.7	9.3
Illinois No. 6 (Clinton)	65.2	4.9	1.2	10.4	4.0	14.3
Lower Kittanning	77.9	4.7	0.9	4.1	2.3	10.1
Upper Kittanning	80.6	3.8	1.1	3.7	1.3	9.5
Wyoming Elkol	74.3	5.3	1.2	15.2	0.6	3.4

[a] Moisture-free basis

Table II. Oxygen Contents and Maximum Obtainable Vapor Phase Acetylations by Acetic Anhydride[a]

	Milliatom weight oxygen per gram of coal	*Maximum Obtainable Vapor Phase Acetylation, millimole acetyl per gram coal*
Upper Freeport	2.88	0.71
Illinois No. 6 (Clinton)	6.50	3.33
Lower Kittanning	2.56	0.83
Upper Kittanning	2.31	0.76
Wyoming Elkol	9.50	4.17

[a] Moisture-free basis

Publication Date: January 1, 1966 | doi: 10.1021/ba-1966-0055.ch025

grade Baker and Adamson acetic anhydride was used as the acetylating agent. It was degassed, and the more volatile acetic acid, if any were present, was removed by expansion several times from the acetic anhydride reservoir into the evacuated, empty reaction chamber.

Procedure. Three glass buckets were dried in a desiccator over calcium sulfate for two to three days and then weighed. About 200 mg. of raw coal were then added to each bucket. The buckets were reweighed, and the coal was returned to the desiccator for drying. After one day in the desiccator, the buckets were placed on the metal rack and sealed within the acetylation apparatus. The apparatus was evacuated for one to two days including at least 12 hours with the diffusion pump running. The samples were then removed and reweighed. The difference in weight between the dry, empty bucket and the dry, full bucket was taken as the sample weight.

The buckets were returned to the acetylation apparatus, sealed, and re-evacuated, usually overnight. Three to four more hours evacuation with the diffusion pump was followed by admission of the acetic anhydride vapor. The amount of acetylation was controlled by varying the temperature of the liquid acetic anhydride and the time of contact of the vapor with the coal. The acetylation apparatus was then evacuated for three days including 12–15 hours with the diffusion pump. This amount of evacuation was sufficient to remove all traces of acetic acid and acetic anhydride. After evacuation dry air was admitted, the cap removed, and the samples were withdrawn and reweighed. The difference in weight before and after acetylation was taken as the amount of acetylation.

Each sample bucket was then attached to a spring and sealed within a tube of the sorption apparatus. The sorption system was immediately evacuated, the air bath temperature raised to 45°C., and a set of spring elongations measured by means of the cathetometer. For those samples that were not to be acetylated, the procedure was to vacuum-dry the coal directly on the spring balances. The dry sample weight was determined by subtracting the loss of weight during this evacuation from the sample weight determined on desiccator-dried material.

Methanol vapor was then admitted to the system at a relative pressure of 0.85 to 0.90. The vapor was kept in contact with the coal for three days, after which the system was evacuated until the spring elongation returned to the original value for zero pressure (four to six days). This "aging" at a high relative pressure was necessary to assure reproducible behavior in subsequent kinetic experiments (*6*, *7*). After returning to the original spring elongations, the coal samples were ready for kinetic studies.

Each kinetic run was started by simultaneously admitting methanol to the system and starting a timer. From 10 to 40 seconds were required to reach the desired methanol pressure, the higher pressures of course taking the longest times. The surge of methanol vapor caused a slight oscillation of the springs that was not damped sufficiently for accurate readings until an additional 60–80 seconds had elapsed. Readings of each of the spring elongations were then taken at about every 90 seconds for 20 minutes, every 120 seconds for another 20 minutes, and every 300 seconds for yet a third 20-minute interval. Time was read to the nearest second and spring elongations to 0.1 mm. Equilibrium readings were taken at 24 hours and confirmed at 36 hours. After the equilibrium spring elongations were read, the system was evacuated until return to the initial spring elongations was achieved.

Concurrent with taking the equilibrium spring elongations, the standard pressure of methanol at equilibrium was obtained and was considered to be the pressure of the kinetic run.

Experimental runs were made at relative pressures between 0.1 and 0.85 at temperatures of 45° and 35°C. The vapor pressures of methanol were obtained by plotting the data of Stull (*13*) and reading the 35°C. and 45°C. values (201 and 320 mm., respectively).

At least five runs were made at each of the two temperatures. The 45°C. set of runs was made first, and the order of occurrence was low pressure to higher pressure runs. Upon completion of the 35°C. set, the system was again evacuated until the spring elongations returned to their initial values. The sample buckets were removed and reweighed. This final weighing was a secondary check against weight changes caused by possible splattering of the coal during its many manipulations and by possible solvolysis of the acetylated coal by methanol.

The fundamental data obtained by this procedure were weights of dry coals, amounts of acetylation, spring elongations *vs.* time, equilibrium spring elongations, and pressures of methanol. These data in conjunction with the spring constants and vapor pressures of methanol allowed for calculating the kinetics and isotherms of the sorption of methanol.

Computations. Before a sample had been placed in the experimental apparatus or acetylated, its weight of dry coal was known. Since this value did not change during an experimental series, all calculations were made on a dry, unacetylated coal basis.

A program was written for an IBM 650 digital computer to obtain the experimental rate constant, k_r from a given set of kinetic data. This program was written according to a modification of the interpretive system devised by V. M. Wolontis (*14*). The program was constructed to produce a least-squares fit of the data to the linear equation,

$$(f/1\text{-}f) = k_r W_r t \qquad (3)$$

where f is equal to the fraction of reaction, and k_r is the experimental rate constant. This is the integrated form of Equation 2 with only the sorption reaction included. This program had a testing procedure built into it to detect

Publication Date: January 1, 1966 | doi: 10.1021/ba-1966-0055.ch025

and reject deviations from the simplified rate equation. These deviations could be caused by either the reverse desorption reaction or first-order diffusion reaction's becoming significant. Since these deviations occurred only after 75% reaction, sufficient experimental data that fit the simplified equation were always obtained.

For evaluating the isotherm equation, Equation 1 is rearranged to

$$c/W_s = \alpha + \beta c - \gamma c^2 \qquad (4)$$

where $\alpha = 1/AKK_1P^\circ$, $\beta = (KK_1P^\circ + K_1P^\circ - 2)/AKK_1P^\circ$, and $\gamma = (K_1P^\circ - 1)/AKK_1P^\circ$. Simultaneous solution of three equations like Equation 4 would lead to values of α, β, and γ. The isotherm parameters are then obtainable through the relations:

$$A = 1/(\alpha + \beta - \gamma),\ K = (\alpha + \beta - \gamma)/(\alpha + \gamma),\ \text{and}\ K_1 = \left(\frac{\gamma}{\alpha} + 1\right)/P^\circ.$$

To obtain the three equations for simultaneous solution, nine sorption values, W_s, were read from the isotherm plots of the equilibrium sorptions for each coal at relative pressures of 0.09, 0.18, 0.27, 0.36, 0.45, 0.54, 0.63, 0.72, and 0.81. Another computer program was written that took the nine values of W_s and the corresponding values of c and summed them into three sets of combined c/W_s's. The program went on to solve the three resulting equations and then evaluated A, K, and K_1. The program also calculated theoretical values for the isotherm data, and both the theoretical and experimental values of W_s at the nine relative pressures were tabulated for comparison. This tabulation constituted a means of determining if experimental conditions caused equilibrium sorption behavior not predicted by the isotherm equation and allowed proper selection of data summation order. Any order of summing the nine values into three equations was possible in this program. The order finally used in all isotherm calculations was consecutive. That is, the first equation was the sum of c/W_s for c values of 0.09, 0.18, and 0.27; the second was for c values of 0.36, 0.45, and 0.54; the third equation was the sum of c/W_s for the highest three relative pressures.

According to the rate equation evolved below the experimental rate constant, k_r, is equal to the product of the rate constant for the slowest step in the mechanism, k_4, times a function of the concentration of methanol on the surface. A third computer program was devised that calculated from the experimental values of c, K_1, and P° the surface functions:

$$\Theta_1,\ \Theta_2,\ \Theta_3,\ \sum_{n=1}^{\infty} \Theta_n,\ \sum_{n=2}^{\infty} \Theta_n,\ \sum_{n=1}^{\infty} n\Theta_n,\ \text{and}\ \sum_{n=2}^{\infty} n\Theta_n.$$

Input to this third program also included the k_r values corresponding to the coal sample and temperature for which K_1 had been determined. Each k_r was divided by each of the surface functions corresponding to the same relative pressure. The final operation of the program was to average the k_4's obtained and to tabulate all results (surface functions, trial k_4's and trial average k_4's) and input data. Inspecting the trial individual and average k_4's to find the set

Publication Date: January 1, 1966 | doi: 10.1021/ba-1966-0055.ch025

with minimum deviation from its average permitted selection of the surface function characteristic of the coal under study.

Experimental Results

The five coals were acetylated to different extents to produce eight samples of partially acetylated coals. These coal samples and their degrees of acetylation appear in Table III.

Table III. Partially Acetylated Coal Samples[a]

Coal	*Vapor Phase Acetylation, % of Maximum Obtainable (Table II)*	*Total Oxygen Acetylated, %*
Upper Freeport	19.0	4.7
Illinois No. 6 (Clinton)	6.5	3.3
	18.4	9.4
Lower Kittanning	6.9	2.2
	17.9	5.8
Upper Kittanning	27.1	8.9
Wyoming Elkol	5.6	2.5
	18.3	8.0

[a] Moisture-free basis

Because of the uncertainty involved in determining ash contents of coals, caused by the high ignition temperatures employed, it was thought best to include the ash with the coal. Separate experiments showed that sorption of methanol on an ash obtained from Pittsburgh seam coal was negligibly small. Furthermore, the sorption of methanol on known, finely divided mineral constituents of coals such as $CaSO_4$ and FeS_2 was also found to be negligible. Consequently, all equilibrium sorptions, rate constants, and isotherm parameters are on a moisture-free basis only. No error in interpreting results is expected except when comparing different coals of different ash contents. The basis of coal composition will be indicated for all comparisons made. It is to be noted, however, that the percent acetylation and percent of total oxygen acetylated are independent of ash contents.

Kinetic Results. Without exception the sorption of methanol on the eight acetylated and five unaltered samples of coal was found to obey a second-order rate expression over better than 75% reaction. Deviations from the second-order equation in the latter stages of reaction were most pronounced at the lower relative pressures. The experimental rate constants varied with pressure, and two classes of such behavior were observed. For high oxygen ($0 > 6$ mmoles/gram), low rank coals, the experimental rate constants decreased with increasing methanol pressure. Sometimes a maximum value at low pressures was detected. With low oxygen ($0 < 5$ mmoles/gram), high rank coals, a steady increase of experimental rate constants was observed with increasing pressure.

It was determined that only two surface functions were necessary to correlate all of the rate data. The experimental rate constants of the high oxygen coals (Illinois and Wyoming) correlated with θ_1, the fraction of surface sites

Publication Date: January 1, 1966 | doi: 10.1021/ba-1966-0055.ch025

holding only one molecule of methanol. For the low oxygen coals, $\sum_{n=1}^{\infty} \Theta_n$, the sum of all fractions of sites occupied, correlated with the experimental rate constants. From these facts it is concluded that for high oxygen coals the rate behavior is controlled by surface sites holding just one molecule, but for low oxygen coals all occupied sites feed to the interior of the coal one molecule of methanol at a time and with about equal probability.

The function $\sum_{n=1}^{\infty} n\Theta_n$, which is an average concentration of sorbed methanol per mole of sites, did not fit the data, indicating that the methanol on the surface does not act like a continuous film in supplying molecules for the interior reaction. Likewise, the surface functions $\sum_{n=2}^{\infty} \Theta_n$ and $\sum_{n=2}^{\infty} n\Theta_n$ did not correlate with the rate data, thus ruling out any very strong attractions between the first sorbed molecule and a surface site. The various possible surface functions investigated are illustrated in Figures 4 and 5.

The controlling surface functions did not change for a given coal over the range of acetylation (27%) studied. Table IV lists the pressure-independent rate constants computed from experimental data and corresponding surface functions.

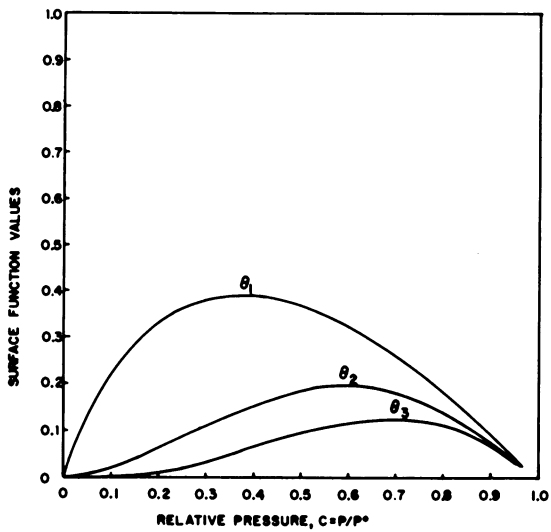

Figure 4. Typical surface functions—fractions of sites covered

Publication Date: January 1, 1966 | doi: 10.1021/ba-1966-0055.ch025

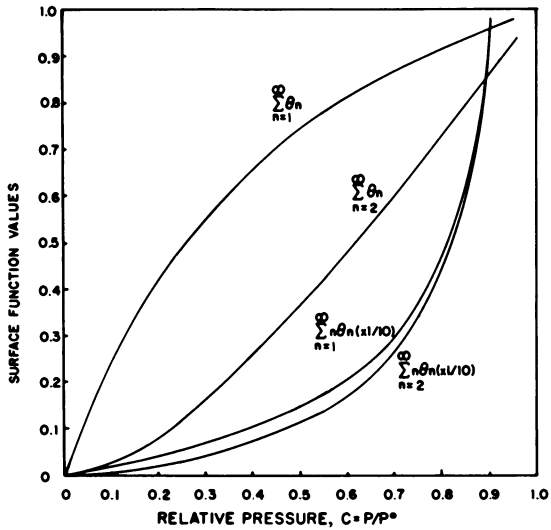

Figure 5. Typical surface functions—sums of sites and surface concentrations

Table IV. Rate Constants and Controlling Surface Function

Coal	*Amount of Acetylation*[a]	$k_4 \times 10^{-4}$ *at 35°C.*[b]	$k_4 \times 10^{-4}$ *at 45°C.*[b]	*Controlling Surface Function*[c]
Upper Freeport	none	4.1	4.9	B
	19.0	2.5	4.8	B
Illinois No. 6 (Clinton)	none	18.5	26.1	A
	6.5	12.9	19.6	A
	18.4	15.2	18.9	A
Lower Kittanning	none	7.5	14.3	B
	6.9	8.3	12.7	B
	17.9	7.3	8.8	B
Upper Kittanning	none	10.9	15.0	B
	27.1	5.8	8.6	B
Wyoming Elkol	none	12.6	15.4	A
	5.6	7.3	11.9	A
	18.3	9.3	11.1	A

[a] Amount of acetylation—percent of maximum vapor phase acetylation obtainable.
[b] k_4 in grams dry coal per mole methanol per hour.
[c] $A = \theta_1$, $B = \sum_{n=1}^{\infty} \theta_n$

Inspecting Table IV reveals that partial acetylation, though not changing the mechanism or controlling surface functions, does affect the value of the pressure-independent rate constant. Considering a probable overall accuracy of only ±5% caused mainly by coal sample inhomogenity, it is concluded that partial acetylation generally decreases the rate. Its effect is not too severe between about 6% and 18% of maximum obtainable acetylation. On the basis of the one high rank coal studied at 27% acetylation, it is inferred that high amounts of acetylation will greatly reduce the rate constants. The observed decrease in rate constants with increasing amounts of acetylation is

Publication Date: January 1, 1966 | doi: 10.1021/ba-1966-0055.ch025

interpreted to mean that the rate is proportional to the concentration of surface sites and that acetylation has the effect of reducing this concentration. The implication, of course, is that where k_4 is a rate constant that is a function of temperature alone and hence may be called a "true rate constant," it is in fact only so for a particular coal.

Equilibrium Results. Table V shows all of the isotherm parameters computed for the sorption of methanol on the acetylated and unaltered coals. These values are on a moisture-free basis.

Table V. Compilation of Isotherm Parameters

Coal	*Amount of Acetylation*[a]	A^{25}[b]	A^{45}	K^{25}	K^{45}	K_1^{25}[c]	K_1^{45}
Upper Freeport	none	2.30	2.20	1.47	2.16	14.7	7.50
	19.0	1.32	1.39	2.76	1.23	13.7	10.9
Illinois No. 6 (Clinton)	none	6.03	4.93	0.730	0.837	23.3	15.7
	6.5	6.19	6.08	0.667	0.569	34.3	17.4
	18.4	5.87	5.62	0.634	0.669	39.4	21.0
Lower Kittanning	none	1.64	1.61	1.43	1.94	22.2	7.88
	6.9	1.59	1.54	3.51	3.63	7.51	3.43
	17.9	1.63	1.57	2.36	2.65	11.2	6.60
Upper Kittanning	none	1.57	1.62	3.24	2.86	9.34	6.15
	27.1	1.70	1.71	2.46	1.93	16.1	10.5
Wyoming Elkol	none	7.16	6.49	0.745	0.798	23.5	17.5
	5.6	7.53	6.61	0.650	0.732	43.2	14.9
	18.3	7.51	7.12	0.643	0.645	41.9	26.4

[a] Amount of acetylation—percent of maximum vapor phase acetylation obtainable.
[b] Superscripts on parameters denote temperature at which determined; A is in units of mmoles/gram of coal.
[c] K_1 is in units of atmospheres^{-1}.

From inspecting Table V the following observations are made. The total sites per gram of coal, A, do not vary significantly with temperature for high rank coals, but low rank coals show a definite decrease in A with increased temperature. Acetylation of high rank coals except Upper Freeport causes essentially no change in A. With Upper Freeport coal, a large decrease in A is incurred upon 19% acetylation possibly by blocking of pores by the acetyl groups. Low rank coals exhibit a slight increase in A upon acetylation to 6% of maximum followed by a slight decrease at 18% acetylation. Also, with increased acetylation the temperature dependence of A is almost eliminated.

From the above observations it is concluded that partial acetylation has the primary effect of opening pores and/or decreasing intermolecular hydrogen bonding of hydroxyl groups between adjacent molecules, thus causing a slight increase in A for high oxygen, low rank coals. For low oxygen, high rank coals there is probably very little intermolecular bonding and, hence, little effect from either acetylation or temperature changes.

The surface reaction equilibrium constants, K_1, always decrease with increasing temperature indicating the expected exothermic nature of surface sorption. Acetylation increases K_1 for low rank coals which can be interpreted to mean that energetic sites are freed, through acetylation of adjacent sites, from intermolecular hydrogen bonding. For high rank coals K_1 goes through a minimum upon increased acetylation. This is interpreted to mean that if,

Publication Date: January 1, 1966 | doi: 10.1021/ba-1966-0055.ch025

as postulated above, in high rank coals little intermolecular bonding occurs, then small amounts of acetylation attack the most energetic hydroxyl groups first, thus decreasing K_1. Further acetylation exposes hydroxyl groups not considered on the surface of unacetylated coals to attack through opening of pores.

The equilibrium constant for the reaction between methanol on surface sites and internal sites, K, is the most complex in its temperature and acetylation dependence. In some coals temperature dependences shift about from exothermic to endothermic reactions, and no overall pattern for high rank and low rank coals seems to exist.

Mechanism and Rate Equation

Because of the results obtained for the kinetics of sorption of methanol on both acetylated and unacetylated coals, the mechanism for sorption of methanol on coal must explain the following experimental observations: sorption follows a second-order rate equation; the experimental rate constants vary with pressure, and two different behaviors are noted; the rate constants decrease upon partial acetylation; at equilibrium one molecule of methanol is sorbed on one site. In addition, the mechanism must also account for the observations that the reverse desorption experimental rates are independent of the original pressure of sorption, and increased acetylation substantially decreases the rate of desorption. The following mechanism is postulated:

$$G + S \rightleftharpoons G \cdot S \tag{1}$$

$$G + G \cdot S \rightleftharpoons G_2 \cdot S \tag{2}$$

$$G + G_{n-1} \cdot S \rightleftharpoons G_n \cdot S \tag{3}$$

$$G \cdot S + 2D \rightarrow 2(D \cdot 1/2G) + S \tag{4a}$$

$$G_2 \cdot S + 2D \rightarrow 2(D \cdot 1/2G) + G \cdot S \tag{4b}$$

$$G_n \cdot S + 2D \rightarrow 2(D \cdot 1/2G) + G_{n-1} \cdot S \tag{4c}$$

$$G_{n-1} \cdot S + 2(D \cdot 1/2G) \rightarrow G_n \cdot S + 2D \tag{5}$$

$$G_n \cdot S + 2(D \cdot 1/2G) \rightleftharpoons 2D \cdot G + G_{n-1} \cdot S \tag{6}$$

Reactions 1, 2, and 3 represent surface sorption of methanol, G, on surface sites, S. These reactions are in rapidly established equilibrium. Reactions of type 4a, 4b, and 4c are the slow, rate-determining steps of the sorption of methanol on internal sites, D. The generalized Reaction 5 is the reverse of reactions of type 4 and accounts for the reversibility of the methanol sorption. Reaction 6 is a rapidly established equilibrium whose inclusion in the postulated mechanism is necessary because of the isotherm prediction of one molecule of methanol per site at equilibrium.

Interpreting this mechanism requires the further postulation that for low rank coals, k_{4a} is much larger than any other k_{4i}'s. Therefore, the measured k_4 approximates k_{4a}, and Θ_1 correlates with the behavior of experimental rate constants with pressure. For high rank coals, $k_{4a} \sim k_{4b} \sim k_{4c}$, and the measured k_4 equals the sum of all k_{4i}'s (5). Therefore, for high rank coals $\sum_{n=1}^{\infty} \Theta_n$ is the

Publication Date: January 1, 1966 | doi: 10.1021/ba-1966-0055.ch025

controlling surface function. The decrease in the measured k_4 because of a decrease in surface sites through mild acetylation is consistent with the postulated mechanism. This mechanism requires that a methanol molecule be held on two internal sites as the product of the rate-determining step. Dissociation of methanol into ions is not likely because of the high energies required. No irreversible sorption is detected, and it is difficult to imagine free radicals forming from methanol in the coal without their reacting with the coal. Hence, it is assumed that methanol is held intact on two adjacent sites. This mechanism is consistent with the experimentally observed second-order kinetics because the third reactant, methanol on surface sites, is of constant concentration for a given coal sample at a given and constant methanol pressure. Finally, the mechanism explains the desorption or reverse reaction if it is assumed that all surface sites participate in receiving methanol from the interior. The rate of desorption is independent of sorption pressure but depends on total available surface sites and hence on the amount of acetylation.

The rate equation is derived as follows:

In general:

$$dW/dt = \sum_{n=1}^{\infty} k_s (G_n \cdot S)(D)^2 - \sum_{n=1}^{\infty} k_d (G_{n-1} \cdot S)(D \cdot 1/2G)^2$$

where

W = sorption in moles CH_3OH/gram coal,
t = time
k_s = true rate constant for sorption
k_d = true rate constant for desorption

Let S_o equal the concentration of surface sites per gram of coal.

$$\text{Then } dW/dt = \sum_{n=1}^{\infty} k_s S_o \Theta_n (D)^2 - \sum_{n=0}^{\infty} k_d S_o \Theta_n (D \cdot 1/2G)^2$$

But $\sum_{n=0}^{\infty} \Theta_n$ is defined as unity and from Reaction 6 of the mechanism,

$$K_6 = (D \cdot G)^2 (G_{n-1} \cdot S)/(D \cdot 1/2G)^2 (G_n \cdot S) =$$

$$(D \cdot G)^2 S_o \sum_{n=1}^{\infty} \Theta_n \Big/ (D \cdot 1/2G)^2 S_o \sum_{n=1}^{\infty} \Theta_n$$

$$\text{Therefore, } \frac{dW}{dt} = \sum_{n=1}^{\infty} k_s S_o \Theta_n (D)^2 - k_d S_o (D \cdot G)^2 / K_6$$

Now, $(D) \sim W_\infty - W$ and $(D \cdot G) \sim W$

Publication Date: January 1, 1966 | doi: 10.1021/ba-1966-0055.ch025

So, $dW/dt = \sum_{n=1}^{\infty} k_a S_n \Theta_n (W_\infty - W)^2 - (k_d S_n / K_6) W^2$

For low rank coals, $\sum_{n=1}^{\infty} k_a S_n \Theta_n \sim k_a S_n \Theta_1$

For high rank coals, $\sum_{n=1}^{\infty} k_a S_n \Theta_n \sim k_a S_n \sum_{n=1}^{\infty} \Theta_n = \frac{k_a S_n \Theta_1}{1-c}$

since $\sum_{n=1}^{\infty} \Theta_n$ can be shown to equal $\Theta_1/(1-c)$.

But, in either case $\sum_{n=1}^{\infty} k_a S_n \Theta_n = k_r$, the experimental rate constant;

$k_a S_n = k_4$ the pressure-independent rate constant; and $k_5 = k_d S_n / K_6$ for the desorption rate constant.

Simplifying the constants, $\frac{dW}{dt} = k_r (W_\infty - W)^2 - k_5 W^2$. Dividing by W_∞ and recognizing that the fraction of reaction, $f = W/W_\infty$,

$$\begin{aligned} df/dt &= k_r (W_\infty - 2W + fW) - k_5 W f \\ &= k_r W_\infty (1-f)^2 - k_5 W_\infty f^2 \\ &= k_r W_\infty [(1-f)^2 - B f^2] \end{aligned} \quad (5)$$

where $B = k_5/k_r$.

Rearranging and integrating Equation 5 between the limits o–f and o–t leads to:

$$\frac{1}{2\sqrt{B}} \cdot \ln \frac{1 - f(1-\sqrt{B})}{1 - f(1+\sqrt{B})} = k_r W_\infty t \quad (6)$$

Expanding all terms for low rank coals (Θ_1 controlling);

$$\text{Equation } 6 = k_a S_n \Theta_1 W_\infty t = k_4 \Theta_1 W_\infty t$$

and

$$B = k_d / k_a K_6 \Theta_1$$

Similarly, for high rank coals ($\sum_{n=1}^{\infty} \Theta_n = \Theta_1/(1-c)$ controlling);

$$\text{Equation } 6 = k_a S_n \Theta_1 W_\infty t/(1-c) = k_4 \Theta_1 W_\infty t/(1-c)$$

and

$$B = k_d (1-c)/k_a K_6 \Theta_1.$$

B is independent of S_n but is a function of K_6. This equilibrium constant must be quite large to account for the observed isotherm behavior, but its evaluation is not readily obtained. Because of the large magnitude of K_6, B must be small and can be neglected at relative pressures above 0.1 for at least 75% of the

Publication Date: January 1, 1966 | doi: 10.1021/ba-1966-0055.ch025

reaction. When B is neglected, $df/dt = k_s W_s (1 - f)^s$ and $\int_o^f df/(1-f)^s = \int_o^t k_s W_s dt$. Thus:

$$f/(1-f) = k_s W_s t = k_4 \Theta_1 W_s t \quad (7)$$

for low rank coals, and:

$$f/(1-f) = k_4 \Theta_1 W_s t/1 - c) \quad (8)$$

for high rank coals.

Discussion

It was the simplified integrated Equations 7 and 8 that were found sufficient for handling the experimental data. However, the fact that B is independent of S_s explains the qualitative observation that for slower sorptions —e.g., on acetylated coals—deviations from the simplified equations occurred at lower fractions of reaction than for faster reactions. This observation is consistent with the conclusion that acetylation merely reduces the concentration of all surface sites, and the acetate group itself is rather inert to methanol sorption.

From the above derivation it appears that all that is necessary to obtain the true rate constant for sorption, k_s, is to evaluate S_s, the concentration of all surface sites. Unfortunately, there is no convenient method for doing this. It is known (*1*, *3*, *4*) that methanol on coal yields unusually high sorptions because of internal penetration by the methanol molecules. But this sorption is on specific sites, and any nonspecific sorptions, even though strictly on the surface, can not yield sufficient data, in themselves, to produce a good value for S_s. Moreover, any attempt to correlate k_4 with either oxygen content or total sites is fruitless. This indicates that either S_s is not proportional to A or oxygen content, or the simplifying assumption used in the derivation that $k_4 = k_s S_s$ is being pushed too far, and that k_4 is really an average over all types of possible sites (hydroxyl, quinone, etc.). The latter possibility seems the more plausible.

Figure 6 is a plot of the calculated total sites, A, as a function of total oxygen contents for the coals on a dry, ash-free basis. Pseudo-oxygen contents for the partially acetylated coals were calculated by subtracting the amount of acetylation from the total oxygen contents. This plot has a slope of 0.75 which indicates that three of every four oxygen-containing groups, as an average over all ranks of coal, are susceptible to methanol sorption. This conclusion agrees with that of Dryden (*3*) that 70–90% of the oxygen in bituminous coals occurs as hydroxyl and quinone groups. Other data by Blom *et al.* (*2*) also generally fit this plot. The fact that any other type of manipulating the oxygen contents of acetylated coals yields greater deviations from the linear plot of Figure 6 indicates that the acetate group is indeed relatively inert to methanol sorption.

The rate and equilibrium constants are known at two temperatures and the calculations of associated energies should be possible. However, because of the limited accuracy associated with studies on coal, detailed values seem

Publication Date: January 1, 1966 | doi: 10.1021/ba-1966-0055.ch025

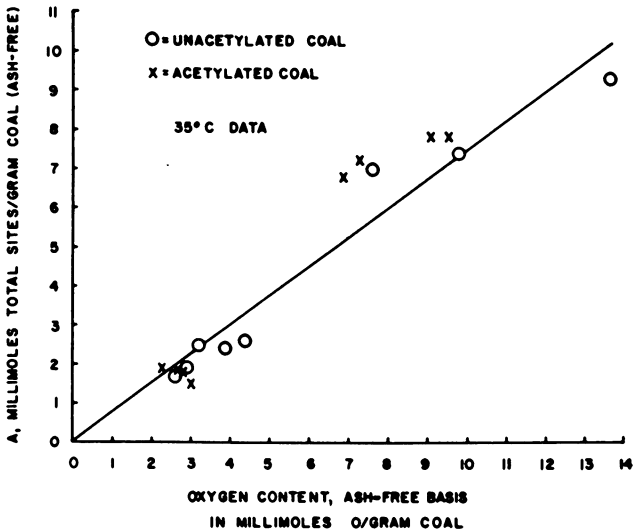

Figure 6. Total sorption sites as a function of oxygen content of coals

pointless. Hence, for the external reaction, the free energies associated with K_1 have a range of —0.8 to —2.3 kcal./mole with enthalpies of about —8 to —10 kcal./mole and entropies of —20 to —30 cal./deg.-mole. For the internal reaction, K is not well defined at all, but the enthalpies range from about —2 to +5 kcal./mole. These energies for the sorption of methanol on coal are small compared to normal chemical reactions but are comparable to those values normally associated with hydrogen bond formation. Incidentally, the heat of condensation of methanol, which involves formation of hydrogen bonds, is about —11 kcal./mole.

Table VI lists the activation energies calculated for the sorption reaction. Since the ratio of k_4's is involved in their calculation, the energies are independent of ash contents or concentrations of total surface sites of the coals.

Table VI. Activation Energies for Sorption

Coal	*Vapor Phase Acetylation, % of Maximum Obtainable*	E_a *kcal./mole*
Upper Freeport	none	2.7
	19.0	13.1
Illinois No. 6 (Clinton)	none	6.7
	6.5	8.2
	18.4	4.2
Lower Kittanning	none	12.8
	6.9	8.3
	17.9	3.6
Upper Kittanning	none	6.3
	27.1	7.7
Wyoming Elkol	none	3.9
	5.6	9.6
	18.3	3.6

Publication Date: January 1, 1966 | doi: 10.1021/ba-1966-0055.ch025

Table VI shows that the changes of activation energy with acetylation closely parallel the changes in A (Table V). The maximum in E_a observed for low rank coals is consistent with the hypothesis that mild acetylation of these coals first unbinds energetic sites, then upon further acetylation the remaining available sites possess lower average bonding energies. The steady decrease in the high rank coal, Lower Kittanning, is consistent with the belief that in these coals little intermolecular hydrogen bonding occurs, and acetylation steadily reduces the average available energy.

Acknowledgments

The authors would like to acknowledge the support of this work by the Coal Research Board, Commonwealth of Pennsylvania. This paper was taken partly from the thesis by M. M. Mitchell, Jr., submitted in partial fulfillment of the requirements for the degree of Doctor of Philosophy at Carnegie Institute of Technology. The experimental data on unaltered coals was obtained by G. J. Ostapchenko (*12*).

Literature Cited

(1) Anderson, R. B., Hall, W. K., Lecky, J. A., Stein, K. C., *J. Phys. Chem.* **60,** 1548 (1956).
(2) Blom, L., Edelhausen, L., Van Krevelen, D. W., *Fuel* **36,** 135 (1957).
(3) Dryden, I. G. C., *BCURA Monthly Bulletin* **24,** 289 (1960).
(4) Dryden, I. G. C., "Chemistry of Coal Utilization," Suppl. Vol., Chap. 6, H. H. Lowry, Ed., John Wiley and Sons, Inc., New York, 1963.
(5) Frost, A. A., Pearson, R. G., "Kinetics and Mechanism," 2nd Ed., p. 164, John Wiley and Sons, Inc., New York, 1961.
(6) Fugassi, P., Hudson, R., Ostapchenko, G., *Fuel* **37,** 25 (1958).
(7) Fugassi, P., Ostapchenko, G., Trammell, R., *Fuel* **37,** 36 (1958).
(8) Fugassi, P., Trammell, R., and Masciantonio, P., "Abstracts of Papers," 134th Meeting, ACS, September 1958, p. 3K.
(9) Fugassi, P., Ostapchenko, G., *Fuel* **38,** 259 (1959).
(10) Fugassi, P., Ostapchenko, G., *Fuel* **38,** 271 (1959).
(11) Mazumdar, B. K., Bhangale, P. H., Lahiri, A., *Fuel* **36,** 254 (1957).
(12) Ostapchenko, G. J., Ph.D. Thesis, Carnegie Institute of Technology, 1958.
(13) Stull, D. R., *Ind. Eng. Chem.* **39,** 517 (1947).
(14) Wolontis, V. M., *Technical News Letter,* No. **11,** IBM Applied Science Division (1956).

RECEIVED January 25, 1965.

Discussion

Robert Anderson: Your adsorption equation is similar to the BET equation except for an added term in the denominator. Can this additional term be related to the fact that coal swells during the adsorption of methanol?

Maurice M. Mitchell: This term accounts for the swelling property of the gel. For a derivation of the isotherm equation *see* ref. 9.

Kulai A. Kini: It was mentioned that the rate of sorption of methanol is altered by partial acetylation. Have any surface area measurements been done on the coal samples before and after acetylation? In absence of these it

is too risky to ascribe the change in rate of sorption to blocking of surface sites.

Dr. Mitchell: No, surface area measurements were not compared in this way. However, in view of the extremely mild acetylation conditions used (brief exposure to acetic anhydride *vapor*), it is difficult to believe that any material change in physical structure resulted.

Bhupendra K. Mazumdar: My colleagues and I found a few years ago that blocking of hydroxyl groups in coals by acetylation leads to a marked decrease in moisture sorption capacity and heat of wetting in methanol—a decrease that was proportional to the amount of hydroxyl blocked. We also found a linear relation between water sorption at 60% R.H. and total oxygen functional group content. We concluded that polar groups have an important effect on water sorption by hydrogen bonding or other mechanisms.

Publication Date: January 1, 1966 | doi: 10.1021/ba-1966-0055.ch025

26

Sorption of Polar Vapors by Crystalline Polynuclear Compounds with Polar Functionalities

PHILIP MASCIANTONIO, WILLIAM H. WILMOT, and PAUL FUGASSI

Coal Research Laboratory, Carnegie Institute of Technology, Pittsburgh, Pa.

Publication Date: January 1, 1966 | doi: 10.1021/ba-1966-0055.ch026

Experimental evidence indicates that small, polar gaseous molecules, such as water and methanol, can permeate and be sorbed reversibly by solid crystalline lattices at temperatures far removed from the melting point of the lattice provided that the molecular units composing the lattice are large, unsymmetrical, rigid, and contain polar groups of the type of carbonyl, acetate, and methoxy. Polar groups on adjacent carbon atoms, which may interact intramolecularly, are relatively inactive in the sorption process. These results make it probable that local order in coals involving molecular structures of this type will not decrease the sorption of polar gaseous molecules by the coals.

The sorption of polar vapors by coal has been the concern of this laboratory, and in connection with our work a question has arisen concerning the permeation of gas molecules into ordered regions of the coal gel. In general, polar, gaseous molecules might be expected to permeate a gel if (1) the gel contains polar groups, (2) the gas molecule is sufficiently small, and (3) the gel does not possess high order or crystallinity. It has been established that the sorption of a polar molecule, like water, by cellulose takes place mainly in nonordered regions and that the water molecule does not permeate the ordered regions (3). The permeation of an ordered lattice by a gas molecule would be expected to occur if the lattice were thermally disorganized as happens near the melting point of the lattice. Although coal seems to possess little order from x-ray measurements (*1*), there must be present, in higher rank coals, condensed structures which to some extent form more ordered regions. To investigate these phenomena, studies have been made of the sorption of small polar molecules by crystalline solid dyes possessing highly condensed aromatic structures and a number of polar groups. All the compounds used have high melting points, far above the temperatures at which the sorption measurements have been made.

In Coal Science; Given, P.;
Advances in Chemistry; American Chemical Society: Washington, DC, 1966.

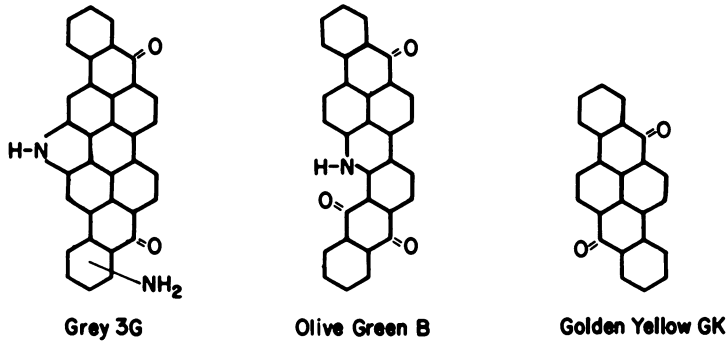

Figure 1. Aromatic adsorbents

Experimental

The solids used were Grey 3G, Olive Green B, Golden Yellow GK, 1-aminoanthraquinone, and various derivatives of violanthrene prepared from Violanthrone and Oxybenzon. The dyes were commercial products and were kindly donated by the Koppers Co. Figure 1 shows the structural formulas of the first three dyes. Figure 2 illustrates the structural formulas of the various derivatives of violanthrene that were used. These derivatives were prepared by conventional methods from purified Violanthrone and Oxybenzon using dimethyl sulfate for the methoxy derivatives and anhydride for acetate derivatives (*4*). The dyes were purified by dissolution in various solvents followed by reprecipitation. In some cases they had to be reduced chemically to be appreciably soluble in alkaline aqueous solutions and were afterwards recovered by air oxidation. The reprecipitated material was washed repeatedly with water and with methanol. These treatments gave materials whose ash content was low and of the order of a few tenths of a percent. Under the low powered microscope all of the solids appeared to be crystalline. Through the kindness of William Robinson of the Metallurgy Department, Carnegie Institute

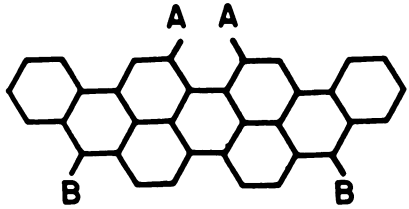

Figure 2. Violanthrene derivatives

Derivative	*Group A*	*Group B*
Violanthrone	H	O
Oxybenzon	OH	O
Diether	H	OCH_3
Tretraether	OCH_3	OCH_3
Diacetate	H	$OCOCH_3$
Tetra-acetate	$OCOCH_3$	$OCOCH_3$
Tetraquinone	O	O

of Technology, x-ray powder spectra were taken of the violanthrene derivatives. Only those derivatives were used which gave sharp line spectra. Such spectra show that the compounds were crystalline and that the individual crystals were not of colloidal dimensions. The surface area of the samples is thus normal and not exceptionally large. Distilled water was the source of water vapor, and absolute methanol (ACS standard), stored over Drierite was the source of methanol vapor. These liquids were thoroughly out-gassed by chilling and repeated exposure to a high vacuum (10^{-5} mm.).

Sorptions were measured by direct weighing using Jolley balances. For the water work, tungsten springs were used having a sensitivity of about 4 mg. per mm. extension. For the methanol work Ni-Span-C springs with a sensitivity of about 1.6 mg. per mm. extension were employed. Spring elongations were measured to 0.1 mm. using an Eberbach cathetometer. The sorption apparatus was mounted in an air thermostat held to ±0.2°C. The general procedure employed has been described (2). In the sorption experiments samples were exposed to a given pressure of vapor for periods of 24–48 hours. Rate measurements with methanol proved that such periods were quite adequate for attaining equilibrium. In all cases the sorptions were reversible by pumping. The weight of sample desorption was always very close to the initial weight, indicating that no chemical reaction involving a weight change had taken place.

Results and Discussion

At a given temperature the experimental values obtained are the weight of gas sorbed per given weight of solid, W, expressed as moles of gas per mole of solid and the corresponding relative pressure, C, which is the pressure of vapor divided by the vapor pressure of the liquified vapor at the selected temperature. The data have been fitted to the empirical equation:

$$X = a + bC$$

where X is the mole fraction of sorbed gas or $W/(1 + W)$, C is the relative pressure, and a, b are empirical constants. This equation is valid from $C = 0.2$ to $C = 0.9$. Measurements at lower values of C have low precision with the Jolley springs now in use, and at values of C greater than 0.9 it is possible for the vapor to condense upon the spring or upon the glass bucket used to hold the sample. Using an empty bucket it has been shown that condensation at $C = 0.9$ or lower does not take place with methanol and with water. While the

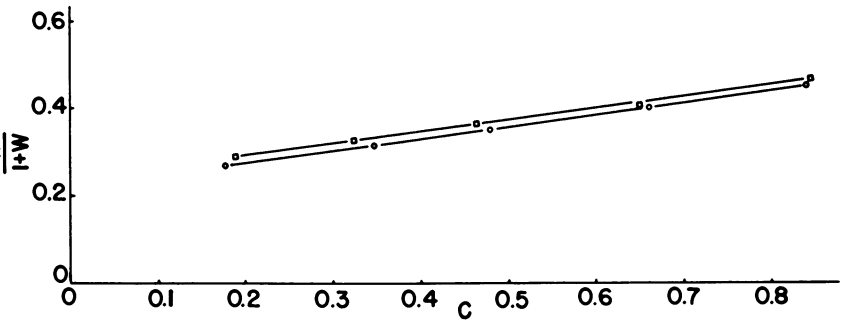

Figure 3. Violanthrone-methanol system; ○—45°C., □—35°C.

value of X extrapolated to $C = 1$ is significant, the extrapolation of X to $C = 0$ is meaningless since theoretically W must approach 0 as C approaches 0, and X must likewise approach 0. A typical plot of the data appears in Figure 3.

The sorption data for methanol vapor and water vapor are given in Tables I and II, respectively. Column 7 of each table shows the calculated ratio of sorbed gas molecules to molecules of solid at a relative pressure, C = 1. These extrapolated values are deemed significant because they correlate with the chemical composition of the solid. Experimentally, the adsorption of water or methanol vapor is very low on hydrocarbons having polycyclic aromatic structures. For all substances listed, the ratio of sorbed gas to solid (molecular basis) is around 1 or higher except for Golden Yellow G.K. (0.25) and 1-aminoanthraquinone (0.04). Golden Yellow G.K. has a structure composed of

Publication Date: January 1, 1966 | doi: 10.1021/ba-1966-0055.ch026

Table I. Sorption of Methanol on Violanthrene Derivatives

Compound	*T°C.*	*a*	*b*	*X(C=1)*	*Polar Groups per Molecule Solid*	*Molecule CH_3OH / Molecule Solid*	*Type Polar Group*
Violanthrone	35	0.239	0.279	0.518	2	~ 1.0	C=O
	45	0.219	0.271	0.490			
Diacetate	35	0.183	0.216	0.399	2	~ 0.66	$COOCH_3$
(3, 8)	45	0.174	0.216	0.390			
Tetra-acetate	35	0.488	0.185	0.673	4	~ 2.0	$COOCH_3$
(3, 8, 12, 13)	45	0.488	0.185	0.673			
Dimethoxy	35	0.211	0.276	0.487	2	~ 1.0	$COCH_3$
(3, 8)	45	0.190	0.273	0.467			
Tetramethoxy	35	0.191	0.307	0.498	4	~ 1.0	$COCH_3$
(3, 8, 12, 13)	45	0.164	0.278	0.444			
Tetraquinone	35	0.260	0.248	0.508	4	~ 1.0	C=O
(3, 8, 12, 13)	45	0.238	0.250	0.488			
Oxybenzon	35	0.280	0.233	0.513	4	~ 1.0	C=O
	45	0.264	0.244	0.518			C—OH

Table II. Sorption of Water on Various Dyes

Compound	*T°C.*	*c*	*b*	*X(C=1)*	*Polar Groups per Molecule Solid*	*Molecule H_2O / Molecules Solid*	*Type Polar Group*
Violanthrone	45	0.330	0.345	0.675	2	~ 2.0	C=O
	55	0.365	0.288	0.673			
Oxybenzon	45	0.280	0.385	0.665	4	~ 2.0	C=O
	55	—	—	—			C—OH
Olive Green B	45	0.079	0.482	0.561	4	~ 1.0	C=O
	55	0.220	0.255	0.475			N—H
Grey 3G	45	0.369	0.371	0.740	4	~ 2.6	C=O
	55	0.375	0.345	0.720			N—H
Golden Yellow GK	45	0	0.2	0.2	2	~ 0.25	C=O
	55	0.025	0.180	0.205			
1-aminoanthraquinone	45	0.011	0.034	0.045	3	~ 0.036	C=O
	55	0.013	0.032	0.045			N—H

six condensed rings, and 1-aminoanthraquinone has a structure of three condensed rings; all the other compounds have structures involving eight or more rings. It appears that in order for gas molecules to permeate the crystal lattice,

the molecules making up the solid lattice must have considerable bulk, sufficient dissymmetry and rigidity so that a close-packed lattice cannot be formed.

For Violanthrone the ratio is two for water vapor and one for methanol vapor. Two possible reasons for this behavior are: (1) the water molecule is smaller than the methanol molecule and might penetrate regions that the methanol cannot, or (2) water molecules might form a more stable bond with the polar groups than methanol. In this connection a discussion of the driving force leading to sorption is in order. For the types of molecules under discussion, the constituents of the crystal lattice are held in place by Van der Waals forces and by a more specific interaction between polar groups located on adjacent molecules, such as hydrogen bonding. The lattice structure for an unsymmetrical molecule must represent a compromise between these two types of forces. On adding a polar gas to the system, competitive reactions result so that a given polar group can either bond intermolecularly with a polar group on a neighboring molecule or can bond with the gas molecule. If water forms a stronger hydrogen bond with a given polar group than methanol does, then intermolecular bonds between polar groups on adjacent molecules might be broken by water vapor and not by methanol vapor. The second explanation is favored because methanol and water do not differ much in size. There is, however, a known "sieve effect" since experimentally, isopropyl alcohol is sorbed by violanthrene derivatives to only about 20–50% of the methanol sorption, both on a mole basis. Unfortunately the desorption of isopropyl alcohol, by evacuation for periods up to 5 days, is so slow that the process is irreversible from a practical standpoint.

Considering methanol sorption on violanthrene derivatives it appears that such sorption can result if the polar groups at the widely separated 3, 8 positions are acetate, carbonyl, or methoxy. In general, small polar groups at the adjacent 12, 13 positions seem to contribute little to the sorption. On the other hand, the larger acetate group at the 12, 13 positions raises the extent of sorption considerably. Perhaps adjacent polar groups can interact with each other to form an intramolecular bond which cannot be broken by the methanol molecule. The effect of the acetate group might be caused by its larger size or a weak interaction with a similar acetate group. Such intramolecular interaction might well explain why water vapor sorption is lower than expected for Oxybenzon, Olive Green B, Grey 3G, and Golden Yellow GK since in all these compounds two polar groups on the same molecule are adjacent to each other.

Over the valid range of the empirical isotherm equation, the heat of the sorption process is given by:

$$\Delta H = \frac{RT^2}{b}\left[\frac{1}{C}\frac{da}{dT} + \frac{db}{dT}\right]$$

In this equation ΔH is the heat of the process, R is the gas constant, T is the absolute temperature, and the remaining symbols a, b, C are those appearing in the empirical isotherm. The equation arises from the empirical isotherm and the following thermodynamic relationships: $\Delta F = H - T\Delta S$, $\Delta F = RT \ln C$, and $\frac{\partial \Delta F}{\partial T} = -\Delta S$ where ΔF, ΔH, and ΔS are the changes in free energy, heat content, and entropy, respectively. For the methanol experiments da/dT is

Publication Date: January 1, 1966 | doi: 10.1021/ba-1966-0055.ch026

always negative and greater than db/dT which is sometimes positive and sometimes negative. With one exception the value of ΔH varies from about —5000 cal./mole (exothermic) to about +1000 cal./mole as C goes from 0.2 to 0.9. The one exception is the tetra-acetate of violanthrene for which ΔH is 0. The heat effect for water vapor sorption on Violanthrone differs considerably from that for methanol. For water the value of ΔH is about 4000 cal./mole at $C = 0.2$, goes through 0 at $C = 0.6$, and is negative thereafter. In fact, for all the compounds studied, the value of ΔH for water sorption is positive at low values of C, later shifting to negative at higher values of C. Since sorption of the gas molecule by the solid involves forming a bond between gas and solid, breakage and formation of intermolecular and in some cases intramolecular bonds between solid molecules, and expansion (swelling) of the lattice, it is difficult to attribute changes in the overall experimental ΔH to any one process. The sorption of polar gases by solid dyes must be accompanied by swelling of the solid and perhaps modification of the lattice. However, no quantitative experiments along these lines have been made.

If ordered structures involving aromatic polycyclic skeletons of the type studied here were present in coal, it would indicate that such structures would be permeated by methanol, and that surface area measurements based on methanol sorption would give values greater than the true surface area as that area is normally defined.

Acknowledgment

The authors wish to thank the Coal Research Board, Commonwealth of Pennsylvania, for their support of this work, and J. T. Wang for assistance in the calculations. The contents of this paper are abstracted from the dissertations submitted by P. Masciantonio and W. H. Wilmot to the Graduate School, Carnegie Institute of Technology, for the Ph.D. degree.

Literature Cited

(1) Ergun, S., Tiensun, V. H., *Fuel* **38**, 64 (1959).
(2) Fugassi, P., Ostapchenko, G., *Fuel* **38**, 259 (1959).
(3) Hermans, P. H., "Colloid Science," Vol. II, H. R. Kruyt, Ed., p. 540, Elsevier Publishing Co., New York, 1949.
(4) Stallman, Otto, U. S. Patents 2,183,627 and 2,183,628 (Dec. 19, 1939).

RECEIVED January 25, 1965.

Discussion

Martin D. Neuworth: The author did not make any distinction between sulfur in completely aromatic rings and sulfur in hydroaromatic or nonaromatic ring structures. Since the stability of sulfur in completely aromatic structure is higher than in other configurations, the dyes might be separated on this basis independently of available hydrogen or volatile matter.

Philip X. Masciantonio: All of the model compounds have aromatic structural units; however, no data are available on the relative aromaticity of these model compounds. Dr. Neuworth's suggestion may be helpful in getting a better correlation of the data if aromaticity could be evaluated quantitatively for these compounds.

Peter H. Given: J. R. Jones and I have studied the pyrolysis of some aromatic sulfur compounds, including dibenzothiophene and thioxanthone (dibenzothiopyrone). Much of the sulfur is lost from the thioxanthone as volatile products, whereas much of the sulfur in dibenzothiophene is retained in the char. The difference in behavior no doubt arises from some difference in aromatic stability between the two sulfur heterocycles; hence, aromaticity or aromatic character may well be a general factor determining how much sulfur is retained in the char on pyrolysis.

Dr. Masciantonio: Of the 10 model compounds studied, four contain structures similar to the types described by Dr. Given. The sulfur retention observed for these compounds does not show any obvious trend; however, insufficient data are available. It is interesting that the same model compound Ciba Orange R exhibits sulfur retention values in the range 3–100% in the blending experiments. These data indicate that sulfur retention can be controlled by appropriately modifying the elemental environment during pyrolysis. Therefore parameters such as molecular size, structure, and aromaticity may not be of major importance during high temperature pyrolysis.

Publication Date: January 1, 1966 | doi: 10.1021/ba-1966-0055.ch026

Kinetics and Mechanism of Solution of High Volatile Coal

GEORGE R. HILL, HASSAN HARIRI, R. I. REED, and LARRY L. ANDERSON

Department of Fuels Engineering, University of Utah, Salt Lake City, Utah

Publication Date: January 1, 1966 | doi: 10.1021/ba-1966-0055.ch027

A kinetic study of the dissolution of a Utah high volatile bituminous coal in tetralin has been conducted. Equipment for obtaining rate data during the early stages of the reaction has been developed. The data are interpreted in terms of a pseudo second-order rate constant, average heats of activation, and apparent entropies of activation, the numerical values of these functions depending on the degree of extraction. The rate of solution in tetralin of this coal is not an equilibrium phenomenon but is a kinetically controlled reaction in which the average activation energy increases as the reaction proceeds.

While solvent extraction is used to convert coal to valuable liquid and gaseous products, it also may be used to study coal structure and composition. Thermal dissolution of coal (solvent extraction with a reaction temperature above the boiling point of the solvent) with various solvents has been studied extensively for a number of years (*5*, *9*, *10*, *12*, *13*). In fact, a voluminous literature has been presented and reviewed which deals directly with the extraction of coal and extraction conditions. This paper describes experimental result of kinetic studies together with a new approach to the theory and mechanism of solvent extraction.

Experimental Procedure

The coal used for this study was taken from a working face of Utah Spring Canyon Coal Mine. The analysis as given by Commercial Testing and Engineering Co. for the sample (calculated on a dry basis) is shown below.

The coal was ground in the laboratory and sized to pass 200 mesh. Ash determinations on the ground coal sample were made, and an average value of 5.2% was used to correct for the ash content of the extracted coals.

In Coal Science; Given, P.;
Advances in Chemistry; American Chemical Society: Washington, DC, 1966.

Ultimate Analysis		*Proximate Analysis*	
Carbon	72.88	Water	—
Hydrogen	5.58	Ash	8.37
Nitrogen	1.51	Volatile Matter	45.71
Oxygen	10.82	Fixed Carbon	45.92
Sulfur	0.65		
Chlorine	0.19		

Heating value—13,237 B.t.u./lb.

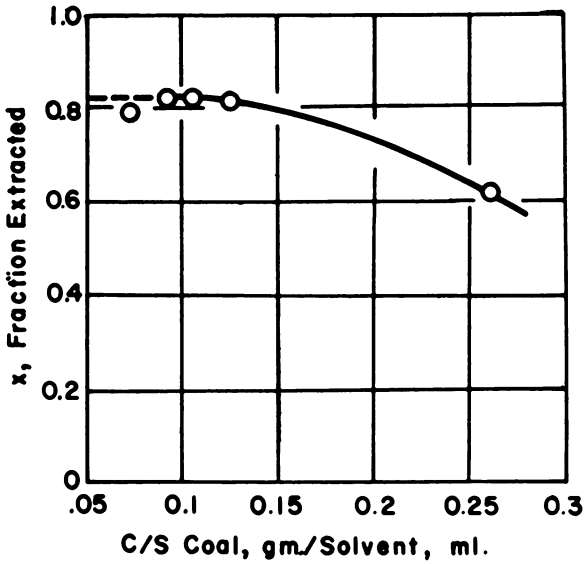

Figure 1. Determination of coal/solvent ratio for optimum extraction

To find the optimum ratio of coal/solvent (C/S), a series of solubility experiments were performed at constant temperature and time but with different C/S. It was found that at ratios smaller than 1:8 the quantity of coal dissolved did not increase (Figure 1). All kinetic studies were made at ratios of 1:10 to ensure that excess solvent was always present.

For each run, coal samples of approximately 50 grams were dried at 100°C. for 4 hours and weighed after cooling in a desiccator for ½ hour. In the early experiments, coal and solvent were mixed in the autoclave, and runs were performed. It was found that the time necessary for the autoclave and mixture to be heated from room temperature to reaction temperature was 1½–2 hours. When extraction fraction *vs.* time was plotted, it showed that at higher temperatures more than 80% of the total possible extraction of coal dissolved before the system reached the reaction temperature. Consequently, the data obtained in the first 2 hours were incorrect.

To overcome this problem a coal injector was designed and constructed. The coal injector was a stainless steel cylinder, 8 inches long, 3 inches outside diameter, and 1.5 inches inside diameter. One side of the cylinder was open, and the other was provided with a 0.25-inch stainless steel female fitting (Figures 2 and 3). A piston, provided with an "O" ring gasket, was used for the open side of the cylinder and could move back and forth by a mechanical

Publication Date: January 1, 1966 | doi: 10.1021/ba-1966-0055.ch027

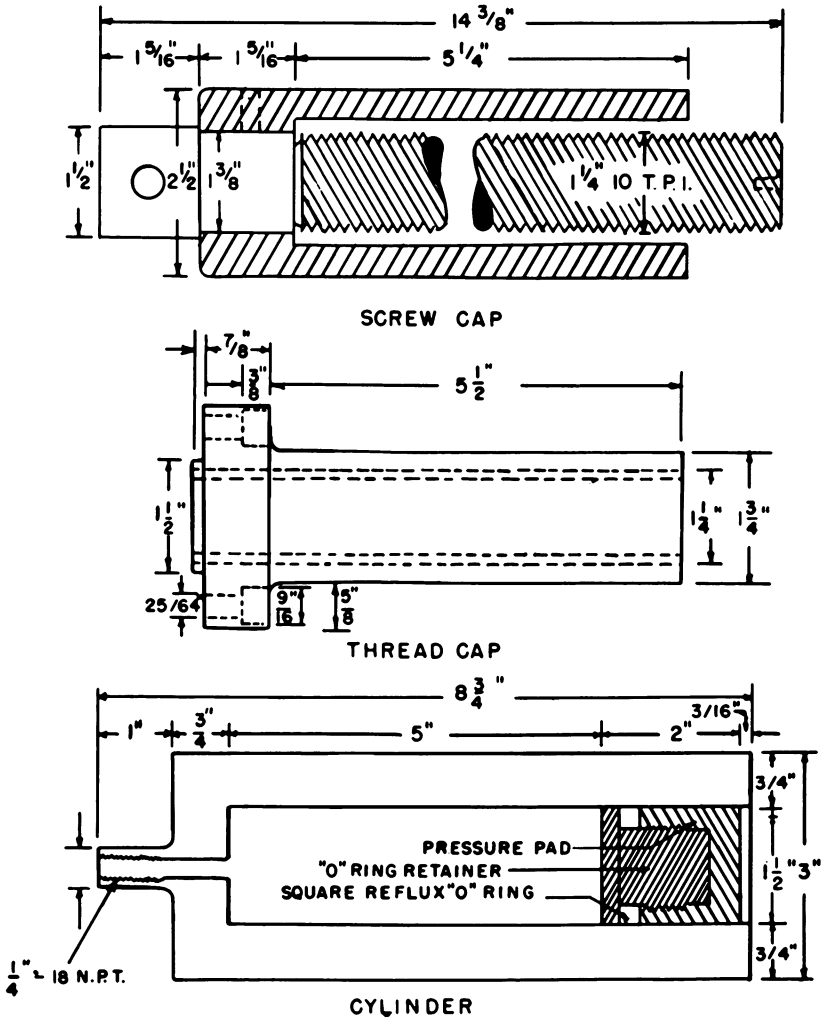

Figure 2. Major parts of coal injector with their measurements

screw system. The outside body of the coal injector's cylinder was graduated and calibrated in cubic centimeters injected per linear inch drive of the cylinder.

To use the coal injector, equal amounts of coal and tetralin (approximately 50 grams of coal which was prepared by the above mentioned procedure and 50 cc. of tetralin) were used in each run and mixed in the coal injector. While preparing coal paste in the coal injector, 450 cc. of tetralin were being heated in the autoclave to reaction temperature. When the autoclave containing tetralin reached the reaction temperature, the coal paste was injected into the autoclave through a fitting on the autoclave. The temperature was carefully observed during this operation, and it was found that after 1 or 2 minutes the system returned to the reaction temperature (Figure 4).

In Coal Science; Given, P.;
Advances in Chemistry; American Chemical Society: Washington, DC, 1966.

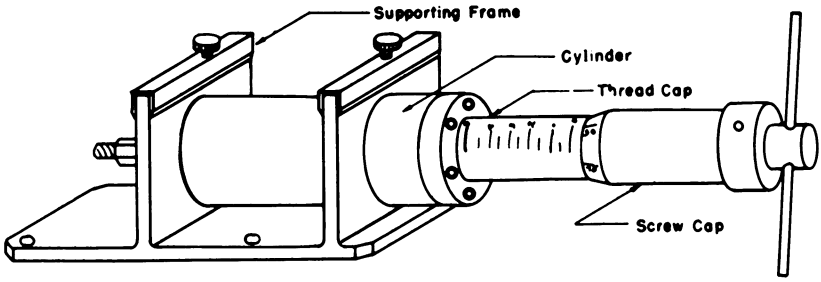

Figure 3. Coal injector used for solvent extraction

The autoclave used for this study was a 1-liter capacity Magne Drive autoclave made by Autoclave Engineers. It is provided with a liquid sample line, a gas sample line, quenching tubes, Magne Drive stirrer, pressure gauge, heating jacket, and two extra connections for special uses. One of these connections was used for injecting the coal paste into the autoclave. The autoclave design pressure of 5000 p.s.i.g. proved adequate for all runs.

Each run was continued for about 25–30 hours, and about 25 liquid samples were taken during this time. The volume of each sample was between 15 and 30 cc. Samples taken in each run were treated similarly. They were transferred into Soxhlet thimbles which had already been dried for ½ hour. The thimbles were placed in the Soxhlet extraction unit using benzene as the solvent. The extraction was continued until the liquid circulating in the unit became clear and colorless (indicating pure benzene).

The thimbles were then removed from Soxhlet extraction tubes and placed in the oven at 100°C. for ½ hour and weighed. The difference between the weight of the thimbles before and after Soxhlet extraction was the weight of residues.

For each run, the ratio of coal in grams to the mixture (coal plus tetralin) in cubic centimeters used in the experiment was carefully measured; to obtain the initial amount of coal in each sample taken, that ratio was multiplied by

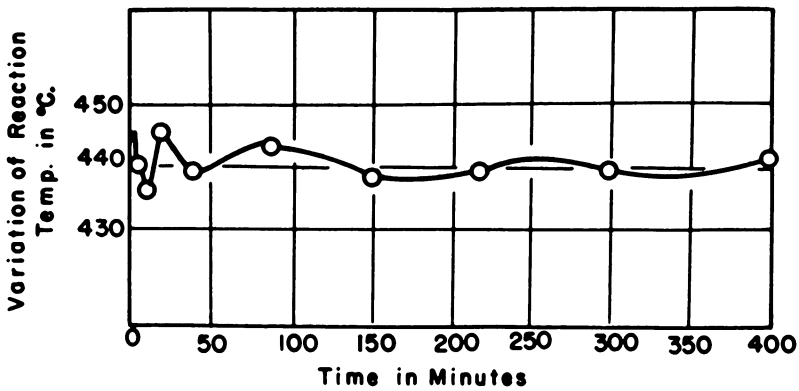

Figure 4. Variation of temperature during process of solvent extraction at 440°C.

the volume of the sample. This procedure is valid if the following assumptions are accepted:

(1) The mixture in the autoclave is homogeneous. This was insured by keeping the Magne Drive stirrer always at a steady 1500 r.p.m. It was experimentally proved that even distribution of coal and tetralin in the autoclave is a fair assumption because the fraction extracted from the last portion of mixture, which remained in the autoclave and was taken after the system cooled to room temperature and the autoclave was opened, was found to be very close to the yield obtained from the last sample taken from the system through the sample lines at reaction temperature.

(2) The volume of the coal before and after extraction does not change very much. This also was found to be a fair assumption because in all the runs the initial and final volumes were accurately measured and gave C/S ratios of approximately 1/10. Generally, the total volume after extraction was about 20 cc. less than the initial volume of the mixture. Since some of the coal converts to gas and some adheres to the wall of the autoclave, it is concluded that the density of the mixture at the start and end of the run did not change significantly. However, even the ratio of coal (grams)/total volume (cc.), (C/V), for this small change was corrected.

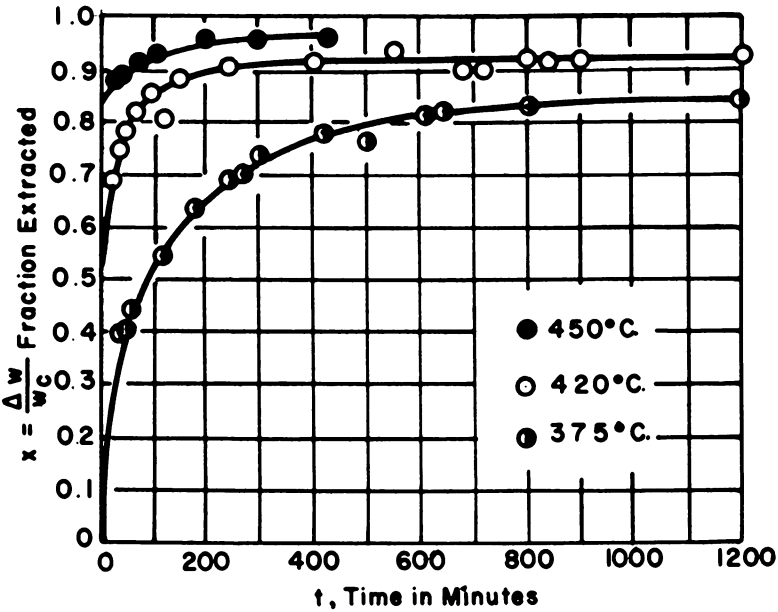

Figure 5. Time-yield curve for thermal dissolution of bituminous coal in tetralin

Theory and Mechanism

The conventional mechanism and mathematical treatment for solvent extraction kinetics was proposed by Oele *et al.* in 1951 (*11*) and has since been accepted and used by others. Oele assumed that the coal will enter the liquid solvent in accordance with a zero-order rate law up to a certain time;

then not only is the zero-order reaction maintained, but now a reverse reaction occurs, which was assumed to be unimolecular.

While interpreting our experimental data (Figures 5, 6, 7) by this and other mathematical expressions, we concluded that there are other mechanisms which represent the data better than Oele's model. The tetralin solutions were found not to be saturated with dissolved coal in the experiments performed by us.

When $\ln\left(1 - \frac{x}{x_{eq}}\right)$ was plotted *vs.* t, a straight line was obtained by the method of least squares; it did not pass the second boundary condition of Oele's equation—i.e., at time zero, x was not zero. Charlot (*1*) used this model, and his graph of $\ln\left(1 - \frac{x}{x_{eq}}\right)$ *vs.* time does not satisfy the second boundary condition of Oele (*11*).

The dissolution of coal by solvent action raises several problems as to the probable mode of action of the solvent and the possible kinetic consequences of such reaction.

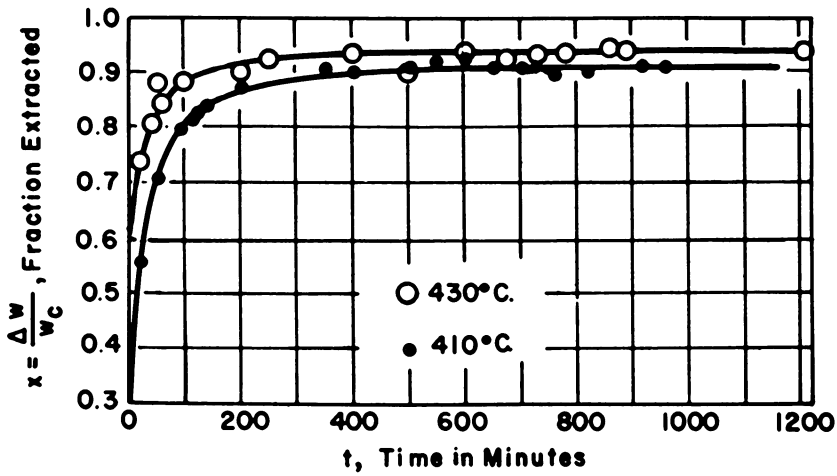

Figure 6. Time-yield curve for thermal dissolution of bituminous coal in tetralin

A coal particle can be considered as made up of a main structure permeated by both macro and micro pores and other materials which are lodged in the coal and are accessible to the action of the solvent, tetralin. This conventional picture of coal has received some experimental support (*3*, *8*). Moreover, good evidence exists that the pores present range in size from an ultrafine structure having gaps a few Angstroms wide (the result of the random packing of relatively large channels) up to 100 A. wide (*14*). Still larger capillaries and fissures are present. Dissolution of such coal can occur

Publication Date: January 1, 1966 | doi: 10.1021/ba-1966-0055.ch027

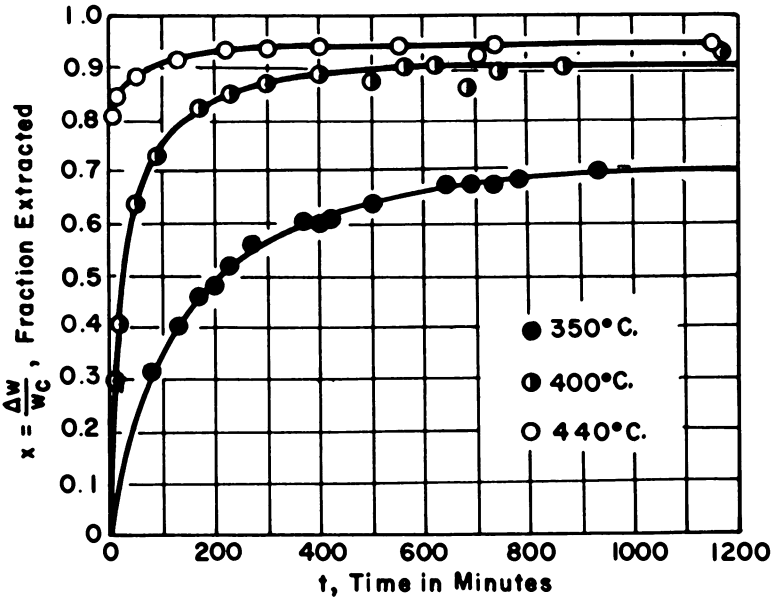

Figure 7. Time-yield curves for thermal dissolution of coal in tetralin

in several ways, and some of them have distinct kinetic consequences. These include:

	Kinetic Consequence	*Rate Constant*
(1) Dissolving out of included materials	1st and/or 2nd	k_e
(2) Dissolution of the coal structure in the presence of a large volume of solvent	1st	k_f
(3) Diffusion out of the micropores	2nd	k_e
(4) Hydrogen transfer reactions	2nd	k_e
(5) Solvent imbibition	1st or 2nd	k_f, k_e

Dissolving out the organic materials which are not part of the main coal structure depends upon the size of the micropore. It may become the rate-controlling step and represent the diffusion of the solution of the organic material in the solvent tetralin, from out of the pore, which implies that the process of solution will be first order with respect both to the coal and solvent. If, however, the material dissolves in a large port or fissure, then the diffusion process may be so rapid that the reaction will be first order with respect to the coal only.

The hydrogen transfer reaction will be a second-order process since the transfer reaction from the tetralin to the coal will not be an abundant process at the temperatures used here.

Solvent imbibition would result in swelling of the coal particles with its consequent effect upon the porous structure. This consideration does not seem important in the present experiments since little swelling of the coal has been reported (*4*). It is known that solvents which swell the matrix can release

Publication Date: January 1, 1966 | doi: 10.1021/ba-1966-0055.ch027

the material (a colloidal matrix of bonded or interlocked units) which forms the residue of the low temperature extraction. At higher temperatures the nature of the solvent is much less critical, although peptization can sometimes occur.

Since more than one of these dissolution processes might occur in the coal extraction experiments, it is necessary to allow for concurrent chemical reactions when constructing a rate equation. Since reactions are either first or second order, a kinetic expression having concurrent reactions of first and second order must be derived.

$$+\frac{dx}{dt} = k_f(a - x) + k_s(a - x)(b - x)$$

Here, a represents the initial concentration of coal, b that of tetralin; k_f is the first-order reaction rate constant, and k_s is the second-order constant. The other symbols have their usual significance.

Rearranging:

$$\frac{+\,dx}{k_f(a - x) + k(a - x)(b - x)} = +\,dt$$

The quadratic denominator has the roots:

$$x = \frac{k_f + k_s b}{k_s} \text{ and } a.$$

Integrating by parts after substitution and between the limits $x = 0$, $t = 0$; $x = x$, and $t = t$, one obtains:

$$\ln\left(\frac{k_f + k_s b - k_s x}{k_f + k_s b}\right)\left(\frac{a}{a - x}\right) = (k_f - k_s a + k_s b)$$

When t $\sim$ 0, x $\sim$ 0, and therefore in the initial stages of reaction the expression simplifies to:

$$\ln\frac{a}{a - x} \sim t(k_f - k_s a + k_s b)$$

When the reaction is near completion, $x \sim a$. Then $\log\frac{a}{a - x}$ changes rapidly with small variations in x, and one may consider the bimolecular contribution as overshadowed by the first-order reaction. This follows since b, the concentration of the solvent, which is in excess, is much greater than a, the concentration of coal.

$$\text{(E)} \quad \ln\left(\frac{k_f + k_s b - k_s x}{k_f + k_s b}\right)\left(\frac{a}{a - x}\right) \sim \frac{k_s x}{k_f + k_s b} + \ln\frac{a}{a - x}$$

The complete rate equation (E) reduces to the following approximation on substituting, simplifying, and returning to Briggsian logarithms:

$$2.303 \log\frac{a}{a - x} = \frac{k_s x}{k_s b + k_f} + t(k_f - k_s a + k_s b)$$

Publication Date: January 1, 1966 | doi: 10.1021/ba-1966-0055.ch027

If $k_s b \sim k_f$, the equation simplifies to:

$$2.303 \log \frac{a}{a - x} = \frac{x}{2b} + t(k_s b - k_s a + k_f)$$

From this research, $k_f = 2.26 \times 10^{-4}$ sec.$^{-1}$ From an Arrhenius plot of the data $k_f = 10^{13.4} e^{-60.5/RT}$. For the extraction of the interspersed materials in the coal, k_s is $9.10^5 e^{-29/RT}$.

A detailed analysis of the data in terms of the simplified equation (E) demonstrates that the constant k_f for the "chemical" dissolution is an average value and that the process involves a series of reactions with increasing activation energies.

Considering the fundamental structure of coal as proposed by Hill and Lyon (7), the high volatile coals consisted of large alkylated, polynuclear, oxygenated, aromatic, and heterocyclic nuclei. These are held together by oxygen and sulfur atoms cross-bonded to carbon-carbon bridges and three-dimensional tetrahedral bonds which form the basic porous structure of the coal matrix. With this structure in mind it is believed that at the beginning of reaction the materials which enter the liquid phase are those which were trapped in the coal pores and which may be weakly bonded to the main coal structure. These require the lowest activation energy to separate from the matrix of the coal. The remainder of the coal dissolves with the breaking of chemical bonds, consequently requiring a greater activation energy, and as the extraction continues the activation energy of extraction increases. This is illustrated by the following:

$$\text{Coal} \xrightarrow{k_1} R_1 + L_1 + G_1 \quad (1)$$

$$R_1 \xrightarrow{k_2} R_2 + L_2 + G_2 \quad (2)$$

$$R_2 \xrightarrow{k_3} R_3 + L_3 + G_3 \quad (3)$$

$$R_n \xrightarrow{k_n} R_{n+1} + L_{n+1} + G_{n+1} \quad (4)$$

$$\text{where } k_1 > k_2 > k_3 > \ldots > k_n$$

In the first step, all the coal bulk which is readily available in the mixture of coal and solvent goes to R_1 which is solid, L_1 which is liquid, and G_1 which is gas. The rate constant for this unimolecular reaction is k_1. When Reaction 1 is well advanced, Reaction 2 becomes the main route with the extraction of R_1 (rate constant k_2) and so on. According to Dryden (2), extraction occurs by the removal of units of colloidal size directly from the coal, and he proposes a model for extraction as follows:

> A matrix of larger and more strongly linked micelles, which can be partly and progressively dispersed in a suitable solvent by increasing the temperature, is intimately associated with a proportion of

Publication Date: January 1, 1966 | doi: 10.1021/ba-1966-0055.ch027

smaller, less strongly bonded micelles that are normally trapped within this matrix unless it is first swollen by the solvent. The difference between these two classes of micelles was supposed to be one of degree rather than kind. Possibly they formed a continuous series, the dividing line being determined by the temperature. The micelles, assumed to be rigid and comparatively indestructible, would be extracted as individuals by diffusion through the swollen pores of the matrix.

Dryden's model may describe the extraction at low temperatures, but at temperatures above 350°C. the assumption of indestructible micelles is not tenable. Apart from the idea of an indestructible micelle, Dryden's model is similar to the one described above. Moreover, in this study, no distinction is made between the colloidal part of the coal and the lighter hydrocarbons. Of course it was observed that the liquified coal extracted at 350°C. had a higher average molecular weight than the one at 450°C. Distilling these samples showed that extracts taken at lower reaction temperatures have higher boiling points. In the above proposed scheme it is assumed that at any instant one of these steps predominates and all the reactions are forward reactions only. If there are any reverse reactions, they must have very slow rates and can be neglected. To support the above assumptions—i.e., that the reverse reaction is negligible and that there is no equilibrium between forward and backward reaction—the following experiment was performed.

A sample of 50 grams of coal and 500 cc. of tetralin was placed in the autoclave, and the temperature was raised to 443°C. After 3 hours at this temperature, a liquid sample was taken. The temperature was then lowered to 350°C., maintained for about 6½ hours, and another sample taken. This process was repeated twice with the following results (Table I):

Table I. Experimental Results Testing Reverse Order Mechanism in Solvent Extraction of Coal[a]

Sample No.	W_i	W_f	W	W_e	$x = \frac{\Delta W}{W_e}$	t	T, °C.
1	3.6457	0.4450	3.2007	3.4561	0.93	180	443
2	2.7296	0.2895	2.4401	2.5877	0.94	500	350
3	4.5217	0.5340	3.9877	4.2866	0.93	850	267
4	4.3855	0.5418	3.8437	4.1574	0.926	1450	246

[a] All samples heated initially to 433°C. and kept at that temperature for 180 minutes.

Table I shows that the fraction extracted is constant within experimental error. Hence, one may conclude that there is very little, if any, reverse reaction involved. A similar procedure was employed in other experiments, and the same result was obtained.

The model developed here assumes that only unimolecular reactions are involved, but that the "first-order reaction velocity constant" varies with the fraction extracted. To derive a suitable mathematical relationship between the first-order reaction velocity constant, k, and the fraction extracted, x, one proceeds as follows:

$$\frac{dx}{dt} = k(1 - x)$$

Publication Date: January 1, 1966 | doi: 10.1021/ba-1966-0055.ch027

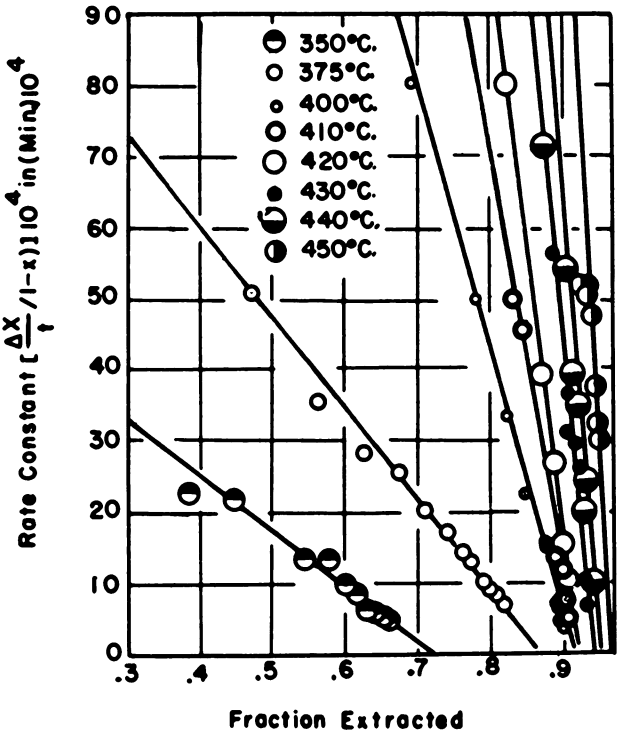

Figure 8. Fraction extracted vs. the rate constant

$$\frac{dx/dt}{1 - x} = k$$

At each temperature, the method of finite differences was used and $\frac{x}{t}$ evaluated for a series of x. The plot of $(\Delta x/\Delta t)/1 - x = k$ *vs.* x closely approximated a straight line (Figure 8). It is therefore considered that the rate constant, k, changes linearly with x, the fraction extracted.

$$k = C_1 - C_2 x$$

$$k = C_1(1 - \frac{C_2}{C_1} x)$$

If $C_1 = k_\circ$ and $C_2/C_1 = a$

then, $k = k_\circ(1 - ax)$

The parameters $k_\circ$ and a were found experimentally (Table II); a is found to be the reciprocal of the maximum possible extraction, (x_∞), at a given temperature, (t); $k_\circ$ was the intercept.

Publication Date: January 1, 1966 | doi: 10.1021/ba-1966-0055.ch027

The above equation then becomes:

$$\frac{dx}{dt} = k_o(1 - ax)(1 - x)$$

where k_o is a pseudo second-order rate constant.

$$\frac{dx}{(1 - ax)(1 - x)} = k_o dt + C \quad \text{and}$$

$$\ln\left(\frac{1 - x}{1 - ax}\right) = (k_o t + C)(a - 1)$$

Table II. Comparison of k_o and a in $k = k_o(1 - ax)$ in Integrated Form

$T°C.$	k_o	a	$\frac{1}{x_{max}}$
350	0.0059	1.390	1.387
375	0.0120	1.142	1.188
400	0.0372	1.111	1.111
410	0.0542	1.092	1.099
420	0.0760	1.088	1.088
430	0.110	1.067	1.066
440	0.142	1.064	1.061
450	0.2210	1.057	1.042

Using the boundary conditions: $t = 0$, $x = 0$, and $t = \infty$, $ax = 1.0$; substituting the first boundary condition $C = 0$, the final equation becomes

$$\ln\left(\frac{1 - x}{1 - ax}\right) = k_o t(a - 1)$$

For all temperatures from 350° to 450°C. k_o was calculated from the above equation for a series of x and t and then averaged. The k_o average was fairly close to the intercept of k *vs.* x.

From the original x and t, the curve which best represented the experimental data was plotted, and the data used for calculating the k_o's were taken from that curve. The maximum rate constant is represented by k_o.

An Arrhenius energy of activation, E, and Eyring enthalpy of activation, $\Delta H^{\ddagger}$, were obtained by plotting $\ln k_o$ and $\ln (k_o/T)$ *vs.* $1/T$. The values were 32.0 kcal./mole for the Arrhenius activation energy and 31.0 kcal./mole for the Eyring activation enthalpy (Table III and Figures 9 and 10).

Table III. Final Results of Solvent

T, °K.	$1/T$	(k_o/T)	k_o
623	16.050×10^{-4}	8.988×10^{-6}	0.0059
648	15.428×10^{-4}	17.1162×10^{-6}	0.0120
673	14.859×10^{-4}	51.0407×10^{-6}	0.0372
683	14.640×10^{-4}	79.6709×10^{-6}	0.0542
693	14.430×10^{-4}	107.5035×10^{-6}	0.0760
703	14.225×10^{-4}	153.8437×10^{-6}	0.1100
713	14.025×10^{-4}	162.9705×10^{-6}	0.1420
723	13.831×10^{-4}	275.375×10^{-6}	0.2210

[a] $E_o = 31.8$ kcal. for Arrhenius plot; $\Delta H_o^{\ddagger} = 30.8$ kcal. for Eyring plot

Publication Date: January 1, 1966 | doi: 10.1021/ba-1966-0055.ch027

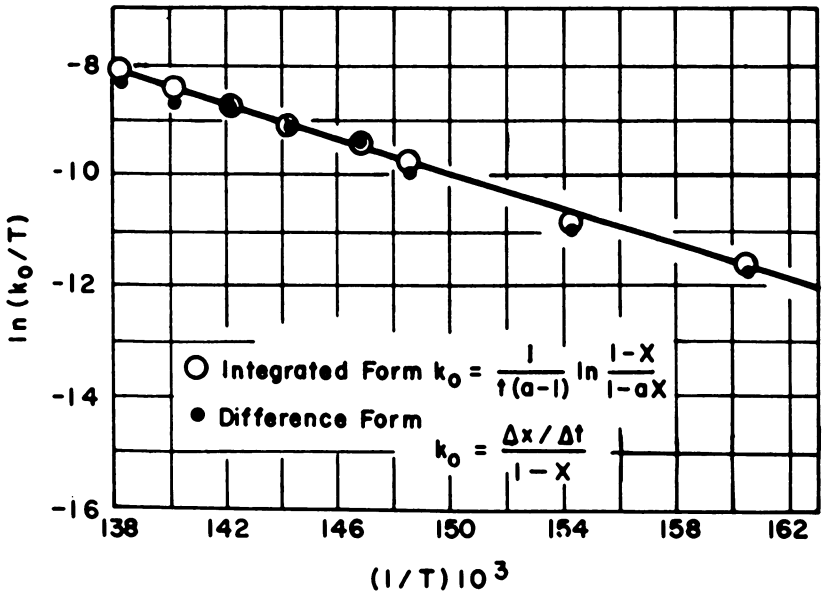

Figure 9. Plot of k_o/T for calculating the enthalpy of activation

The reaction rate constant at the beginning of the experiment—i.e., at $x = 0$—is k_o; it should not be mistaken for a zero-order rate constant.

To investigate the quantitative variation of enthalpy of activation and entropy of activation with x, a series of rate constants with different temperatures for each value of x were taken, and by using the theory of absolute reaction rates (*6*):

$$k' = \kappa \frac{k_B T}{h} e^{-\Delta H^{\ddagger}/RT} e^{\Delta S^{\ddagger}/R}$$

where k_B is the Boltzmann constant and h is the Planck constant.

Values for the average $\Delta H^{\ddagger}$ and the apparent $\Delta S^{\ddagger}$ were obtained for four different values of x and are given in Table IV. At the beginning of the reaction the apparent entropy of activation was negative, but as the reaction continued, it increased to zero and then became positive. An explanation for this

Extraction of Coal with Tetralin[a]

(k_o/T)	$\ln(k_o)$	$\ln(k_o/T)$
9.4695×10^{-6}	—5.2728	—11.5674
18.5040×10^{-6}	—4.4232	—10.8923
57.2855×10^{-6}	—3.2941	—9.8037
78.0×10^{-6}	—2.9150	—9.4416
109.8680×10^{-6}	—2.5770	—9.1155
156.4750×10^{-6}	—2.2072	—8.7633
199.155×10^{-6}	—1.9519	—8.5200
305.6651×10^{-6}	—1.5559	—8.1400

Publication Date: January 1, 1966 | doi: 10.1021/ba-1966-0055.ch027

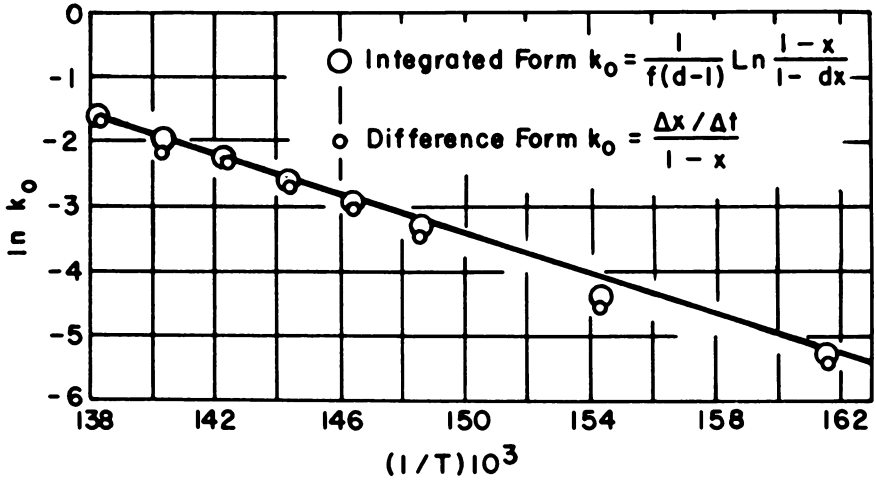

Figure 10. Arrhenius plot for calculating the activation energy

behavior based on an increase in number of sites available for reaction is being checked and will be published.

Solvent extraction of coal can be explained by a series of independent first-order reactions, the residue of one reaction being the reactant for another reaction. It can be formalized as follows:

$$\text{Coal} \rightleftharpoons X_0^{\ddagger} \xrightarrow{k_0'} R_1 + L_1 + G_1$$

$$R_1 \rightleftharpoons X_1^{\ddagger} \xrightarrow{k_1'} R_2 + L_2 + G_2$$

$$R_2 \rightleftharpoons X_2^{\ddagger} \xrightarrow{k_2'} R_3 + L_3 + G_3$$

$$R_n \rightleftharpoons X_n^{\ddagger} \xrightarrow{k_n} R_{n+1} + L_{n+1} + G_{n+1}$$

Where $X^{\ddagger}$'s are activated complexes for the reactions.

These reactions should not be confused with consecutive reactions since in this case R_1, R_2, and R_n are the remaining unreacted coal rather than a new product.

Table IV. Variation of Enthalpy and

	T, °K.	$1/T$(°K.)$^{-1}$	$x = 0$
k_1/T_1	623	1.605×10^{-3}	0.0947×10^{-4}
k_2/T_2	648	1.542×10^{-3}	0.1850×10^{-4}
k_3/T_3	673	1.486×10^{-3}	0.5527×10^{-4}
k_4/T_4	683	1.464×10^{-3}	0.7935×10^{-4}
k_5/T_5	693	1.443×10^{-3}	1.0907×10^{-4}
k_6/T_6	703	1.422×10^{-3}	1.5647×10^{-4}
k_7/T_7	713	1.4025×10^{-3}	1.9915×10^{-4}
k_8/T_8	723	1.383×10^{-3}	3.0570×10^{-4}
$\Delta H^{\ddagger}$ (kcal./mole)			37.2
$\Delta S^{\ddagger}$ (cal./mole °K.) apparent			—19.5

Publication Date: January 1, 1966 | doi: 10.1021/ba-1966-0055.ch027

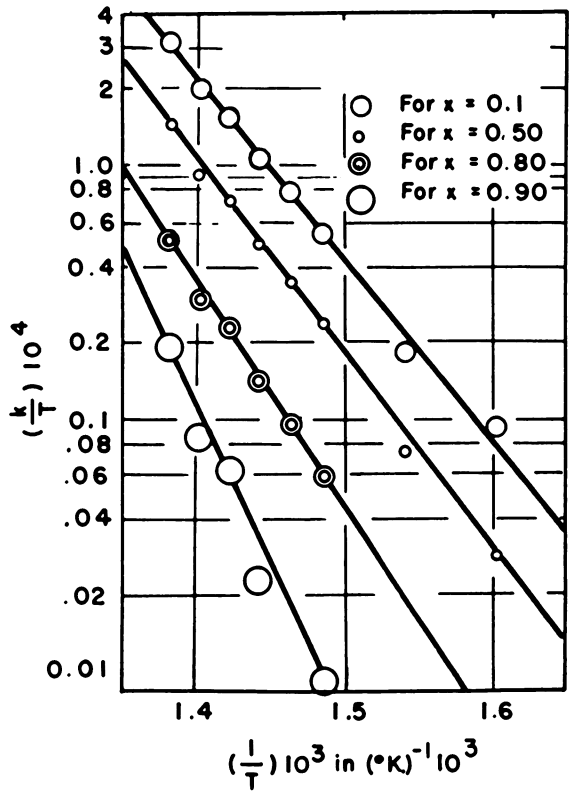

Figure 11. Plot of k/T vs. 1/T for evaluating activation enthalpies

The value of —19.5 e.u. for the apparent entropy of activation obtained at the beginning of the extraction includes a term for the limited number of sites where dissolution could occur (Table IV and Figure 11). It is considered probable that the dissolution of material from the pores (process R_f) occurring simultaneously can account for part of the large negative value. Charlot (*1*)

Entropy of Activation with Fraction Extracted

$x = 0.5$	$x = 0.8$	$x = 0.9$
0.0290×10^{-4}		
0.07514×10^{-4}	0.0091×10^{-4}	
0.2459×10^{-4}	0.0618×10^{-4}	
0.3579×10^{-4}	0.0966×10^{-4}	0.0095×10^{-6}
0.5003×10^{-4}	0.1426×10^{-4}	0.0234×10^{-6}
0.7312×10^{-4}	0.2310×10^{-4}	0.0640×10^{-6}
0.9327×10^{-4}	0.2973×10^{-4}	0.08555×10^{-6}
1.4661×10^{-4}	0.51170×10^{-4}	0.1936×10^{-6}
40.0	51.8	85.5
—16.8	—2.1	41.0

Publication Date: January 1, 1966 | doi: 10.1021/ba-1966-0055.ch027

found that a two-stage mechanism fits the lower temperature range of dissolution well.

To determine whether the low temperature "physical" dissolution could be separated from the processes with higher activation energies, the following experiments were conducted.

Coal and tetralin with a ratio of about 1 gram of coal to 10 cc. solvent were mixed in the autoclave, and the temperature was raised to 250°C. This was the temperature at which transition of a diffusion process to a surface reaction process takes place as postulated by Charlot (*1*). The contents of the autoclave were divided into three parts and placed in three thimbles, which were already treated and weighed according to the procedure previously described (Figures 12 and 13).

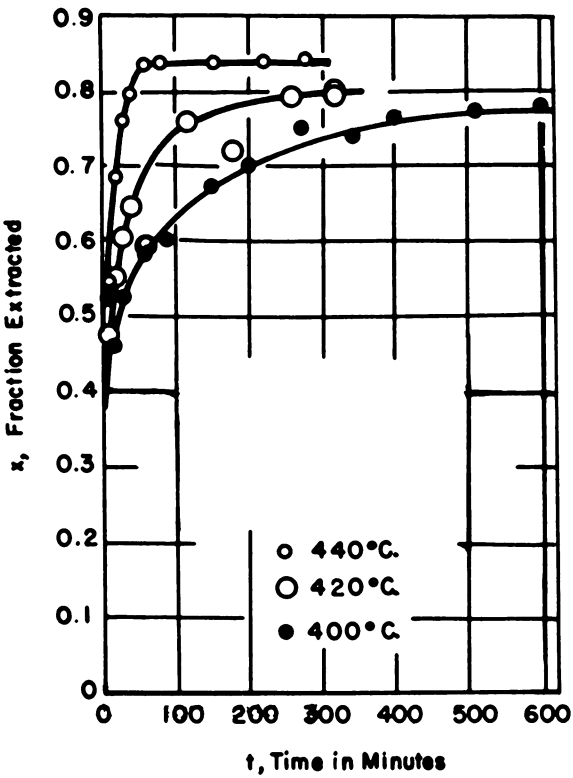

Figure 12. Variation of fraction extraction with time for the second stage of two-stage solvent extraction of coal; first stage at 250°C. for 8 hours not shown

The thimbles were treated in the Soxhlet extraction apparatus using benzene. The residue left in the thimbles was dried and carefully weighed. A total of 12% coal was extracted in this manner. These three coal samples were extracted with fresh tetralin at reaction temperatures of 400°, 420°, and 440°C.

The experimental procedure was the same as previously described—i.e. part of the tetralin was heated in the autoclave to the selected reaction tem-

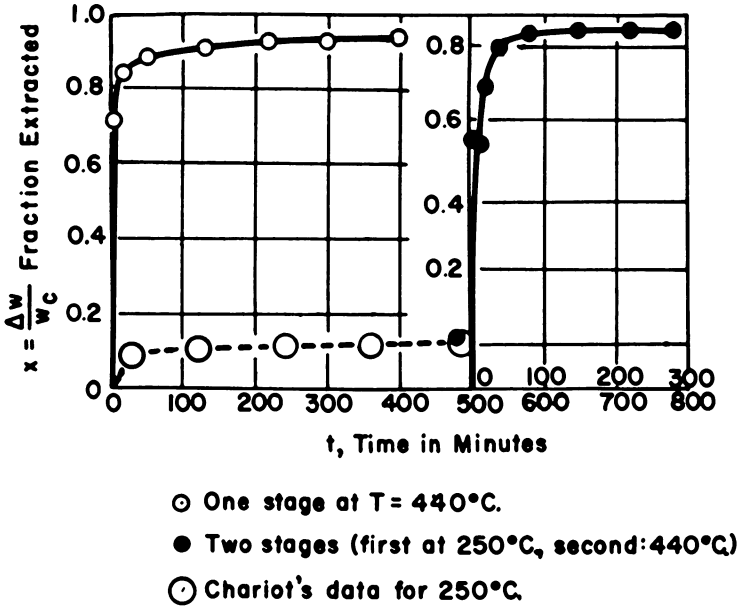

Figure 13. Comparison of one-stage and two-stage extraction of coal

Table V. Final Results for Second Stage of Two-Stage Solvent Extraction of Coal[a]

T, °C.	X_m	$1/X_m$	$\left(a = \frac{1}{X_m}\right)$	k' for $x = 0$	k' for $x = 0.7$	$1/T$
440	0.84	1.19	1.1914	0.1914	0.0362	0.0014025
420	0.80	1.25	1.276	0.0506	0.0060	0.0014430
400	0.79	1.265	1.266	0.0140	0.0014	0.0014859
	$\Delta H^{\ddagger}$ in kcal.			60.0	75.0	
	$\Delta S^{\ddagger}$ (for $\kappa = 1.0$)			+6.2 e.u.	+25.5 e.u.	

[a] First stage—250°C. for 8 hours; 12% was extracted and is not shown here.

perature and the coal paste which was prepared by mixing the coal sample with the remaining solvent in the coal injector was then injected into the reactor. A series of samples was taken to determine the amount of residue left.

The data obtained were treated exactly as those obtained in former experiments, and a series of average enthalpies of activation and apparent entropies of activation was obtained for different x's (Table V, Figures 14 and 15).

It was found that removing only 12% of coal during the first stage of extraction increased the initial apparent entropy of activation from a negative to a positive value. It further shows that this value increases as x increases. This is expected if the surface area available for reaction increases during the course of the reaction.

Publication Date: January 1, 1966 | doi: 10.1021/ba-1966-0055.ch027

The experimental results confirm the idea that at the initial stage of the experiment, the reaction is under diffusion control. This process has a very low activation energy, and when combined with thermal disintegration of the coal at higher temperatures, it lowers the average free energy of activation for the reaction.

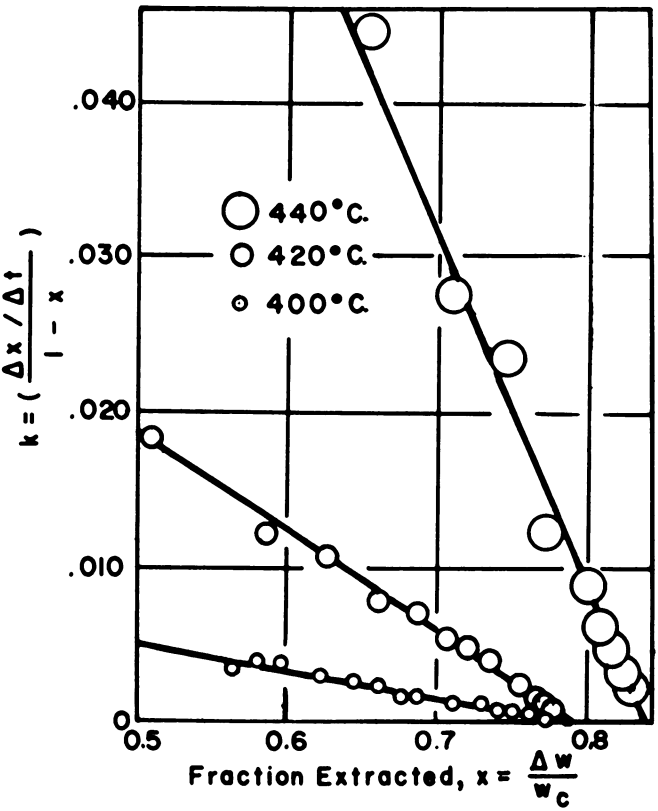

Figure 14. Variation of rate constant with x for the second stage of two-stage extraction of coal; first stage at 250°C. for 8 hours not shown

Conclusion

Coal is a complicated material, and more than one simple chemical process takes place during solvent extraction. The activation energy necessary for dissolving coal increases with the extent of the process up to a point; at a certain temperature insufficient energy is available for more extraction. When the activation energy necessary for extraction becomes more than maximum energy supplied, additional coal will not dissolve. The rate constants, average heats of activation, and apparent activation entropies predict the dissolution

Publication Date: January 1, 1966 | doi: 10.1021/ba-1966-0055.ch027

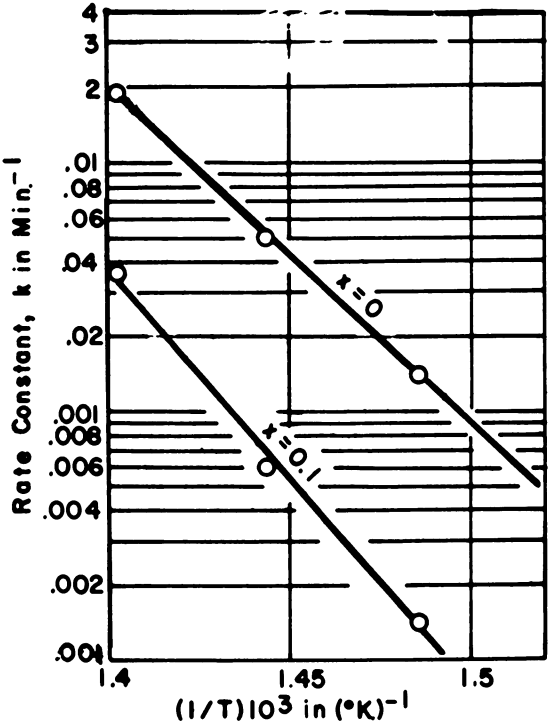

Figure 15. Arrhenius plot for the second stage of a two-stage extraction of coal for two values of x; first stage at 250° not shown

rate of this coal in tetralin. The heat of activation increases, and the apparent entropy of activation becomes increasingly negative during the course of the reaction.

Acknowledgment

Appreciation is expressed to Yacob Shifai, Norbert Kertamus, and Larry Charlot for their contribution to this paper. The research reported here is supported by the Office of Coal Research, Department of the Interior under Contract No. 14-01-0001-271 and by the University of Utah Research Fund.

Literature Cited

(1) Charlot, L. A., Master's thesis, University of Utah, 1963.
(2) Dryden, I. G. C., "Chemistry of Coal Utilization," H. H. Lowry, Ed., p. 248, Wiley and Sons, New York, 1963.
(3) Dryden, I. G. C., *Fuel* **37**, 444 (1958).
(4) D'yakova, M. K., Davtyan, N. A., *Bull. Acad. Sci. URSS, Classe Sci. Tech.*, **1945**, 203; *J. Appl. Chem.* **21**, 113 (1948).

(5) D'yakova, M. K., "Production of Synthetic Liquid Fuels and Chemical Products by Thermal Dissolution of Solid Fuels," p. 86, Academy of Science of the U.S.S.R., 1957.
(6) Glasstone, S., Laidler, K. J., Eyring, H., "The Theory of Rate Processes," McGraw-Hill Book Co., 1941.
(7) Hill, G. R., Lyon, L. B., *Ind. Eng. Chem.* **54,** 36 (1962).
(8) Huck, Kartweil, *Brennstoff-Chem.* **34,** 97, 129 (1953).
(9) Kiebler, M. W., "The Chemistry of Coal Utilization," H. H. Lowry, Ed., Vol. I, p. 724, Wiley and Sons, New York, 1945
(10) Lowry, H. H., Rose, H. J., *Bur. Mines Inform. Circ.* **7420** (1947).
(11) Oele, A. P., Waterman, H. I., Goedkoop, M. L., Van Krevelen, D. W., *Fuel* **30,** 169 (1951).
(12) Pilipetz, M. G., Kuhn, E., Friedman, S., Storch, H. H., *U.S. Bur. Mines, Rept. Invest.* **4546** (1949).
(13) Storch, H. H., *Chem. Rev.* **29,** 483 (1941).
(14) Van Krevelen, D. W., "Coal," p. 178, American Elsevier Publishing Co., New York, 1961.

RECEIVED October 5, 1964.

Publication Date: January 1, 1966 | doi: 10.1021/ba-1966-0055.ch027

Discussion

George Kapo: In your opinion what is the extent of the available internal area for solution?

George R. Hill: In the low temperature "physical" solution process the surface area would probably be that determined by BET adsorption measurements. In the high temperature process, apparently the coal structure is opened up, and the surface would be the total surface of all the "molecular" units. This occurs, as the dissolution proceeds, by a combination of chemical bond breaking and solvent action with hydrogen transfer to the free radicals produced.

Dr. Kapo: How does diffusion influence the kinetics of solution?

Dr. Hill: In the low temperature solution process the activation energy value suggests that a physical process—probably diffusion—is rate controlling. The large (and increasing) value of the heat of activation for the major portion of the dissolution reaction requires that the rate is a chemically controlled process—very likely the breaking of chemical bonds.

Kulai A. Kini: You said that there was no swelling when coal was extracted with aromatic solvents. What method was used to measure swelling?

Dr. Hill: No direct measurements other than usual observation were made on the swelling of the coal. The bulk volume remained unchanged.

Norbert Berkowitz: I think the kinetic treatment of the experimental data is of questionable validity. The extraction process is evidently accompanied by considerable changes in the geometry of the coal particles (e.g., swelling and dispersion); there is the unresolved question of whether the extract forms a solution or dispersion; finally, there is an obvious but somewhat indefinite effect of coal decomposition. The latter point alone would make determining a temperature effect (and hence, calculating an "activation energy") very difficult practically, if not impossible.

Dr. Hill: The point is well made that the solution of coal in solvents is a complicated process involving separation of macerals, breaking of relatively weak hydrogen bonds, and, increasingly at high temperatures, the rupture of covalent chemical bonds. The "activation energy" calculated from a plot of log of rate *vs.* $1/T$ obviously must be an average value for all the processes which are occurring.

The slope of the line obtained from this plot is, however, independent of the final state of the coal in solution and is meaningful in terms of the "minimum" average chemical bond strength of those bonds broken in the dissolution reaction. Observing a low activation energy at low temperatures requires the conclusion that a primarily physical separation process is occurring below 280°C., but that above that temperature the breaking of chemical bonds of increasing strength becomes rate controlling. The data also require a conclusion that the degree of solution (and pyrolytic decomposition) is determined by a rate process and is not an equilibrium phenomenon. The very high (80 kcal.) average heat of activation obtained at high temperatures suggests that many carbon-carbon bonds are being severed in the high temperature range.

It is agreed that a physical interpretation of the entropy of activation is most tenuous; nevertheless, it is a useful beginning for understanding what is occurring. The absolute value of $\Delta S^{\ddagger}$ has no meaning unless the initial state is well defined and constant. However, the change in $\Delta S^{\ddagger}$ as the reaction proceeds is significant and requires an explanation like the one proposed. If a better method of utilizing the data can be suggested, we should be pleased to apply it.

Leslie Reggel: Could you say more about the structure of the coal "molecule" you showed us? Is enough hydroaromatic hydrogen included?

Dr. Hill: The coal "molecule" (reproduced from *Ind. Eng. Chem.* **54,** 36 (1962)) does in fact include hydroaromatic hydrogens. All of the R° N alicyclic rings (some six or seven in the diagram) have hydroaromatic hydrogens as does the alicyclic ring in the lower left hand corner of the model. In this "average structural unit" some 14.7% of the hydrogen is aromatic, 77% of the hydrogen is alicyclic and aliphatic, and 8.3% of the hydrogen is in functional groups. The percentage of hydroaromatic hydrogen corresponds to that reported by Given (*Fuel* **39,** 147 (1960)).

28

Phenanthrene Extraction of Bituminous Coal

LASZLO A. HEREDY[1] and PAUL FUGASSI

Coal Research Laboratory, Carnegie Institute of Technology, Pittsburgh, Pa.

Three bituminous coal samples were extracted at 350°C. with phenanthrene, labeled in one series with tritium, in another with C^{14}. The extract yield was 80–90%. Results: converting coal to soluble products breaks C-H bonds; 10–15% of the hydrogen content of the coal exchanged with that of the phenanthrene during extraction; 3–8% chemically linked phenanthrene was found in the extracts; less than 1% hydrogen exchange took place between pure model compounds (anthracene, *p*-benzylphenol) and tritiated phenanthrene under similar experimental conditions. Thus, chemical reactions take place during phenanthrene extraction of bituminous coals. The role of phenanthrene in this process is probably an interaction with the free radicals which are formed in the thermal decomposition of coal.

Publication Date: January 1, 1966 | doi: 10.1021/ba-1966-0055.ch028

Most solvents which have been used for coal extraction can be divided into two groups. Extraction with the first group of solvents is based on purely physical effects and gives low extract yields. Most monocyclic aromatic compounds belong to this group. On the other hand, the extract yield is high when coal is treated with hydroaromatic solvents at higher temperatures. In that process chemical interactions take place, and hydrogen is transferred from the solvent to the coal substance. The higher yields with hydroaromatic solvents result from the hydrogenative cleavage of carbon-carbon and carbon-oxygen linkages in the coal polymer and the formation of lower molecular weight, more soluble materials. The results of Orchin and co-workers (*1*, *2*) on the extraction of coal with phenanthrene and other polynuclear aromatic compounds do not fit into this classification. They reported that at a temperature of about 350°C. phenanthrene and other related angular condensed aro-

[1] Present address: Atomics International, Research and Advanced Development Division, Canoga Park, Calif.

In Coal Science; Given, P.;
Advances in Chemistry; American Chemical Society: Washington, DC, 1966.

matic hydrocarbons gave extract yields as high as 90–95% without effecting any hydrogenation. It was shown by material balance that the total weight and the overall elemental composition of the coal extract did not change compared with the original coal. Also, the phenanthrene could be recovered quantitatively in high purity from the extraction products. These findings suggested very strongly that the phenanthrene did not react irreversibly with the coal. The authors (3) concluded that "although the mechanism of the dispersing action of phenanthrene remains unknown, it seems probable that phenanthrene has a selective solvent action on those constituents of the coal that act as binding agents for the micellar portion of the coal. Removal of the binding material leads to complete disintegration of the colloidal structure of the coal and peptization of the micelles in the solvent."

The effect of temperature on the phenanthrene extraction was also studied by Orchin and his co-workers. The extract yield at 280°C. was only 10%, and it increased very sharply as the temperature was raised: 40% at 300°, 85% at 320°, and 95% at 340°C. In our opinion, this strong temperature dependence suggests that the dissolving effect of phenanthrene may not be a purely physical interaction with the coal, but chemical reactions might take place during the extraction. Since it was shown by the authors that the phenanthrene could be recovered completely in high purity and there was no change in the overall elemental composition of the coal substance during extraction, there appeared to be only one conceivable chemical change involving phenanthrene which might have taken place: the exchange of hydrogen between phenanthrene and the coal, which could not be observed in the original work without using isotope tracer techniques. We carried out a brief experimental study of this problem, using tritiated and C^{14} labeled phenanthrene in the extraction.

Publication Date: January 1, 1966 | doi: 10.1021/ba-1966-0055.ch028

Experimental

The composition of the three coal samples studied is shown in Table I. All were high volatile (HVA-type) bituminous coals. The composition of the Bruceton coal was very similar to that of the coal which was used in earlier

Table I. Elemental Analysis of Coals[a]

	Ireland Mine Coal	*Ireland Mine Vitrain Conc.*	*Bruceton Mine Coal*
C	82.2	82.5	83.4
H	5.8	5.7	5.7
N	1.3	1.3	1.4
O	8.9	8.7	8.3
Organic S	1.7	1.7	1.2[b]
Mineral Matter	7.9	5.4	3.3

[a] Composition in wt. %, dmmf basis
[b] Total S

studies by Orchin *et al.* (*1*, *2*). The coal samples were ground to —100 mesh, dried in vacuum at 100°C., and stored under nitrogen until required.

The tritiated phenanthrene was prepared by the method of Yavorsky and Gorin (*4*). Approximately 10 grams of phenanthrene (highest purity) were

dissolved in 400 ml. cyclohexane and stirred for 6 hours at 60°C. with tritiated phosphoric acid-boron trifluoride complex. The organic layer was separated and washed with distilled water. The cyclohexane was distilled off, and the residue was mixed with 100 grams phenanthrene. This diluted reagent had a specific radioactivity of 26.0 microcuries per gram.

Phenanthrene labeled with C^{14} was purchased from Tracerlab, Waltham, Mass. A diluted reagent (specific radioactivity: 1.1 microcuries per gram) was prepared by dissolving the labeled material in excess high purity phenanthrene.

Extraction. Separate extraction experiments with the two labeled phenanthrenes were carried out using a technique similar to that used by Orchin *et al.* (*1*, *2*). Phenanthrene was refluxed in a flask, and the sample of the powdered coal (about 6 grams), wrapped in a piece of glass filter cloth, was placed on a support directly under the reflux condenser so that it was in contact with the ascending vapor and the refluxing condensate of the solvent. A 15:1 solvent to coal weight ratio was used in every experiment. After extracting for 6 hours the wrapped filter cloth was transferred into a Soxhlet extractor and extracted with benzene for 24 hours. The weight of the dried residue gave the amount of the phenanthrene insoluble material. The phenanthrene solution containing the coal extract was poured into 1 liter of benzene. The black precipitate which was formed was filtered, extracted with benzene for 24 hours, dried, and weighed (phenanthrene soluble fraction). The benzene solution was distilled at atmospheric pressure to remove the benzene and then vacuum-fractionated in a spinning band column to recover the phenanthrene. The residue was dissolved in 10 ml. benzene and poured into 200 ml. of *n*-hexane. A brown precipitate was formed. It was filtered, washed with *n*-hexane, and dried (benzene soluble fraction). The hexane solution, containing a small fraction of the coal extract and some phenanthrene, was not further separated. The recovered phenanthrene was tested for purity after each run by gas chromatography and NMR spectroscopy. It was shown to be of high purity.

Table II. Phenanthrene Extraction of Bituminous Coals

	Extract Yield[a]				
Fraction	*Ireland Mine Vitrain Conc.*		*Ireland Mine Coal*	*Bruceton Mine Coal*	
Benzene Soluble	9.9	7.5	11.1	6.9	7.0
Phenanthrene Soluble	65.0	70.7	66.8	72.8	72.5
Phenanthrene Insoluble	5.8	7.3		14.6	14.7
Hexane Soluble + Losses	19.3	14.5	22.1	5.7	5.8

[a] Corrected for phenanthrene content, dmmf basis, wt. %

Model Compounds. The experiments with model compounds were carried out as follows. A mixture of 1 gram *p*-benzylphenol and 1 gram tritiated phenanthrene was heated in a sealed tube at 350°C. for 6 hours. The product was dissolved in benzene and extracted with aqueous sodium hydroxide solution. The extract was washed with benzene, acidified, and extracted with benzene. The aqueous solution was distilled, and the condensate was analyzed for tritium. The benzene solution was evaporated, and the residue (*p*-benzylphenol) was assayed for tritium. The degree of tritium exchange of the phenolic hydrogens was calculated by analyzing the water condensate, that of the rest of the hydrogens by analyzing the residue. A similar experiment was carried out with a mixture of 1 gram anthracene and 1 gram tritiated phenanthrene, which was refluxed for a period of 6 hours at 350°C. The product was treated with warm alcohol, and the anthracene was recovered in high purity from the solution by crystallization.

Publication Date: January 1, 1966 | doi: 10.1021/ba-1966-0055.ch028

Assay. The products were assayed for tritium content by a liquid scintillation as follows. The sample (about 0.25 gram) was burned in a stream of dried oxygen and helium. The water content of the gas leaving the oven was collected in traps kept at dry-ice temperature, weighed, and recovered by rinsing the traps with distilled water. The diluted tritiated water was weighed again, and a 0.5 ml. sample was used for tritium count in a Model 314 Ex Tri-Carb liquid scintillation spectrometer. The scintillation liquid was a solution of 2,5-diphenyloxazole (POP) and 2,2'-*p*-phenylene-bis(5-phenyloxazole) (POPOP) in a mixture of ethyl alcohol and toluene. The specific radioactivity of the sample and the corresponding tritium content were calculated from the scintillation count rate by comparing it with that of a standard containing a known amount of tritiated water. The degree of apparent tritium exchange was calculated using the following formula:

$$\text{Apparent Tritium Exchange} = \frac{(\text{Tritium count/Hydrogen content}) \text{ of coal extract}}{(\text{Tritium count/Hydrogen content}) \text{ of phenanthrene}}$$

The products were analyzed for chemically combined phenanthrene content by radio assay, based on the beta radiation emitted by the C^{14} atoms of the labeled phenanthrene. The radiation count rate of the labeled phenanthrene, measured under standard conditions, was used as a reference. The combined phenanthrene content of subsequent samples was calculated from a direct proportionality between the observed count rate of the samples and their labeled phenanthrene content. The beta radiation of the samples was counted with a thin-window (1.4 mg./sq. cm.) Geiger-Müller tube and a scaler (Nuclear-Chicago Corp., Model No. 186.).

The infrared spectra of the coal and the various extracts were recorded on a Baird, Model GY–1 (Ireland Mine vitrain concentrate) and on a Perkin Elmer Model 337 spectrophotometer (Bruceton coal). The samples were prepared by the potassium bromide pellet technique. The high resolution proton NMR spectrum of the benzene soluble extract from Ireland Mine vitrain concentrate was recorded on a Varian A-60 spectrometer in 10% deuterated chloroform ($CDCl_3$) solution, using tetramethylsilane internal standard.

Table III. Elemental Analysis of Products from Phenanthrene Extraction of Bruceton Coal[a]

Fraction	*C*	*H*	*N*	*O*	S	*Mineral Matter*
Coal	83.4	5.7	1.4	8.3	1.2	3.3
Benzene Soluble	81.9	6.2	0.9	10.0	[b]	0.06
Phenanthrene Soluble	82.4	5.0	1.5	10.3	0.9	0.17
Phenanthrene Insoluble	82.0	4.9	1.1	8.7	3.3	17.70

[a] Wt. %, dmmf basis
[b] Insufficient sample for analysis

Discussion

The extract yields are shown in Table II. More than 90% of the organic coal substance was dissolved in the extraction of Ireland Mine vitrain concentrate and about 85% in the case of Bruceton coal. The yield of the phenanthrene soluble fraction was not determined in the extraction of Ireland Mine coal. In that run the products were worked up with a different procedure, and the phenanthrene soluble and phenanthrene insoluble fractions were not separated.

Publication Date: January 1, 1966 | doi: 10.1021/ba-1966-0055.ch028

The elemental analyses of the products from the extraction of Bruceton coal are shown in Table III. The mineral matter was separated from the extract quite efficiently as shown by the ash content of the extracts and the insoluble residue. The elemental composition of all fractions was quite similar to that of the original coal. Only the hydrogen content varied to some extent, increasing with increased solubility. The elemental analysis of the products from the extraction of Ireland Mine coal was incomplete.

Tritium Exchange. The results of the radioactivity assays are summarized in Table IV which also shows the calculation of the extent of tritium exchange and the amount of chemically combined phenanthrene in the various extracts. Significant tritium exchange took place during the extraction of both coals. The Ireland Mine coal was nearly twice as reactive as the Bruceton Coal. Although on a weight percent basis the amount of chemically linked phenanthrene was also significant, clearly hydrogen exchange was the predominant reaction. It

Table IV. Summary of Radioactivities—Calculation of Tritium Exchange

Fraction	*Yield*[a] *%*	*Apparent Tritium Exchange*[b] *%*	*Correction for Phenanthrene Content*[c] *%*	*Tritium Exchange*[d] *%*	$\frac{1 \times 4^e}{100}$	$\frac{1 \times 3^f}{100}$
Ireland						
C_6H_6 Sol.	14.3	27.2	20.5	6.7	1.0	2.9
$C_{14}H_{10}$ Sol. + $C_{14}H_{10}$ Insol.	85.7	21.4	4.3	17.1	14.8	3.7
Sum of Fractions					15.8	6.6
Bruceton						
C_6H_6 Sol.	7.4	30.3	15.2	15.1	1.1	1.1
$C_{14}H_{10}$ Sol.	76.9	12.7	2.6	10.1	7.8	2.0
$C_{14}H_{10}$ Insol.	15.7	4.7	1.7	3.0	0.5	0.3
Sum of Fractions					9.4	3.4

[a] Yield is given on a loss-free basis. It refers to the sum of benzene soluble, phenanthrene soluble, and phenanthrene insoluble fractions.
[b] Apparent tritium exchange as calculated from the tritium assay.
[c] Correction as calculated from the C^{14} assay.
[d] The extent of tritium exchange, given by *b* and *c*.
[e] Calculation of tritium exchange in sum of fractions.
[f] Calculation of chemically linked phenanthrene content in sum of fractions.

would be very difficult to determine which structures participated preferentially in the hydrogen exchange reaction. Since only hydrogen atoms in phenolic hydroxyl groups could be examined in this respect, the following procedure was carried out.

A mixture of 1 gram benzene insoluble residue from the extraction of Ireland Mine coal and 10 ml. 10% aqueous sodium hydroxide solution was sealed in a glass vial and heated at 100°C. for 4 days in a thermostat. After cooling to room temperature the vial was opened, the aqueous solution decanted, distilled over, and analyzed for tritium content. The solid residue was filtered, washed thoroughly with distilled water, dried, and analyzed for tritium.

The two analyses agreed well and showed that the tritium content of the residue decreased from 21.4 to 15.8%. The difference (5.6%) corresponds approximately to that fraction of the hydrogen content of coal which is present

Publication Date: January 1, 1966 | doi: 10.1021/ba-1966-0055.ch028

in phenolic hydroxyl groups. This test, although not completely conclusive, suggests strongly that all phenolic hydrogens participated in the tritium exchange.

Hydrogen Exchange. Experiments were carried out with model compounds to study the interaction of tritiated phenanthrene with phenolic and other aromatic compounds in order to obtain information about the nature of hydrogen exchange. The experiments were performed under similar conditions

Table V. Tritium Exchange in Model Experiments

Substrate	*Phenanthrene to Substrate Ratio*	*Extent of Tritium Exchange, %*
p-Benzylphenol	1:1	0.15 (OH hydrogens) 0.6 (aromatic and CH_2 hydrogens)
Anthracene	1:1	1.3
Anthracene in the presence of Ireland Mine coal	1:1:1	4.2
Ireland Mine coal pretreated with phenanthrene	15:1	15.6[a]

[a] Sum of tritium content from tritium exchange and chemically linked tritiated phenanthrene. The corresponding value in Table IV is 15.8 + 6.6 = 22.4%.

(at 340°–350°C. temperature, for 6 hours) as the coal extractions. The results are shown in Table V. Although the ratio of reagents was changed in these experiments (the concentration of tritiated phenanthrene was decreased from 94 to 50%), the results clearly indicated that the rate of hydrogen exchange was much less with the model compounds than with coal. The very low value for the exchange of phenolic hydroxyl hydrogens is particularly interesting since in coal extraction apparently all phenolic hydrogens participated in the exchange reaction. The effect of the presence of coal on the hydrogen exchange was investigated in the third experiment, in which a mixture of 1 gram anthracene, 1 gram tritiated phenanthrene, and 1 gram Ireland Mine coal were heated at 340°C. for 6 hours. The result was a definite increase in the degree of hydrogen exchange between anthracene and phenanthrene.

Comparing the results of the coal extractions and the model experiments shows quite clearly the greater reactivity of coal. Furthermore, Experiment No. 3 in Table V indicates that the highly reactive coal has the effect of promoting hydrogen exchange between anthracene and phenanthrene. These experiments present sufficient evidence to conclude that the extraction of bituminous coal with phenanthrene is not a purely physical process. The net result of these reactions is a hydrogen exchange between the coal substance and the phenanthrene and a simultaneous depolymerization of the coal as evidenced by the high extract yields. The exploratory experiments presented in this paper are not sufficient to clarify the mechanism of the extraction process. If it is assumed that hydrogen exchange causes solubilization, it is possible to propose a course of reaction which agrees with the experimental results. This process, essentially a free-radical chain reaction, is outlined as follows.

Publication Date: January 1, 1966 | doi: 10.1021/ba-1966-0055.ch028

Coal is known to contain free radicals. In a high volatile bituminous coal their concentration is about 2×10^{18} free radicals per gram, which means that there is one unpaired electron for every 2500 carbon atoms in the coal structure. Additional free radicals are formed in the thermal cracking of coal. This reaction starts slowly above 300°C. and proceeds with a measurable rate at the temperature of the phenanthrene extraction. The first step in the proposed free-radical chain reaction would be the abstraction of hydrogen from phenanthrene by a free radical derived from coal. In the second step, the phenanthrene free radical thus formed abstracts a hydrogen atom from the coal, producing a new free radical. Some of the free radicals produced from coal are probably so unstable that they split into a smaller, more stable molecule and a new free radical, which then abstracts hydrogen from another phenanthrene molecule. The formation of the phenanthrene free radical thus completes the "propagation cycle" of the chain reaction. The net result of such a cycle can be illustrated by the following example:

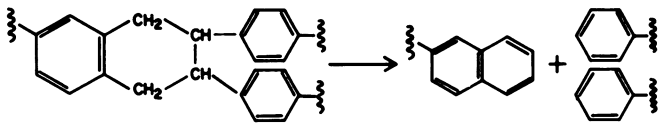

The process shown is thermal cracking and simultaneous hydrogen disproportionation, leading to aromatization of the hydroaromatic structure. A hydroaromatic unit was used in this example because such units are believed to have a predominant role in the coal structure.

If reactions of the above type occur during extraction, one would expect that gradually less hydrogen exchange takes place as the extraction proceeds because the number of reactive groups decreases. This assumption was tested in the last experiment shown in Table V. The coal was heated for 6 hours at 340°C. with nontritiated phenanthrene prior to extraction with tritiated phenanthrene. When this pretreated coal was extracted, the tritium content of the product was only 15.6% as compared with 21.4%, in the nonpretreated product. This decreased tritium content supports the above assumption and agrees with the proposed reaction mechanism.

Spectra. The infrared and NMR spectra of some of the extracts were studied briefly to obtain information about their chemical structure. The infrared spectra of the two coals and the benzene soluble and phenanthrene soluble fractions are shown on Figures 1 and 2. The spectra of the extracts in general are similar to those of the starting coals, and no detailed evaluation will be given. Special attention is called only to one feature of the spectra—namely, that the relative intensity of the aromatic hydrogen absorption band at 3000 to 3050 $cm.^{-1}$ appears to be greater in the phenanthrene soluble extract than in the original coal. Although strong interference by the phenolic hydrogen absorption renders a quantitative evaluation of the spectra impossible, the increased intensity of the aromatic hydrogen absorption band is qualitatively quite well recognizable, particularly in the phenanthrene soluble extract from the Ireland Mine vitrain concentrate. The apparent increase in

Publication Date: January 1, 1966 | doi: 10.1021/ba-1966-0055.ch028

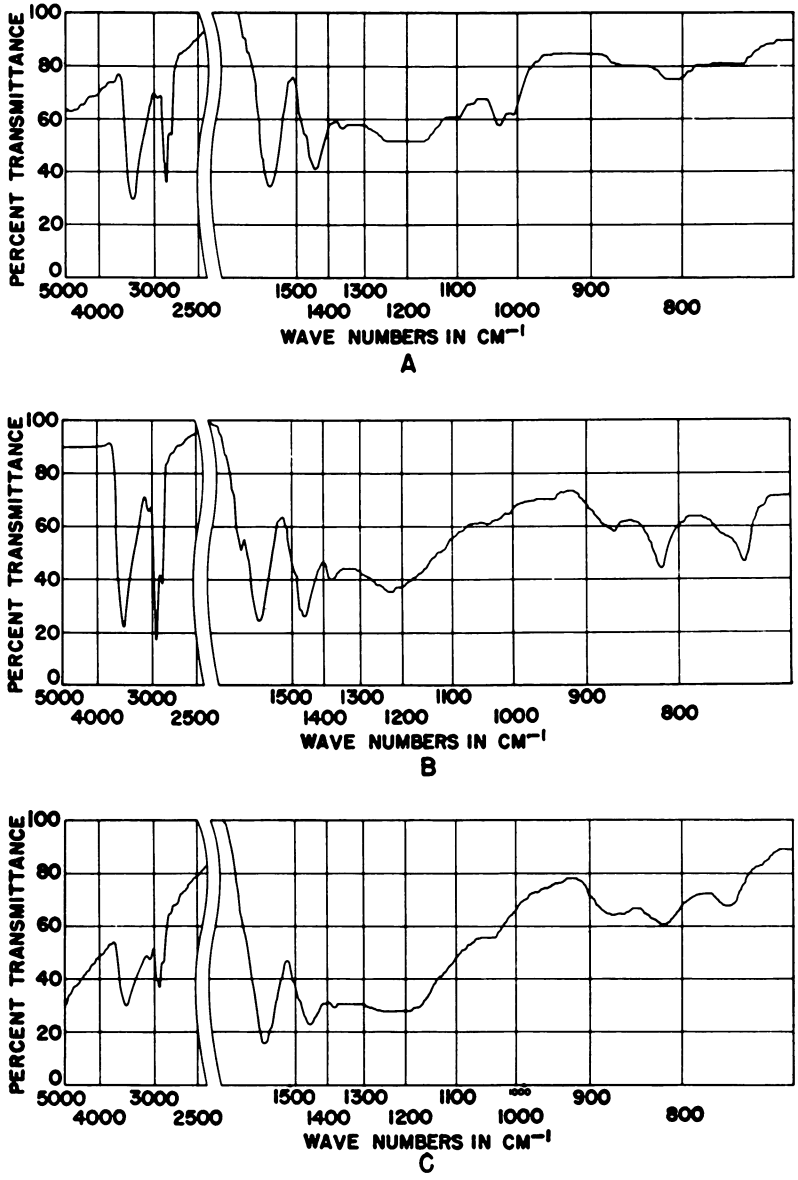

Figure 1. Infrared spectra of: (A) Ireland Mine vitrain concentrate, (B) benzene soluble fraction, (C) phenanthrene soluble fraction

the aromaticity of the products agrees with the reaction scheme suggested above. The results of this qualitative study, however, should be confirmed with more detailed infrared spectroscopic investigations. It was pointed out that there seems to be a noticeable difference in the intensities of the aliphatic

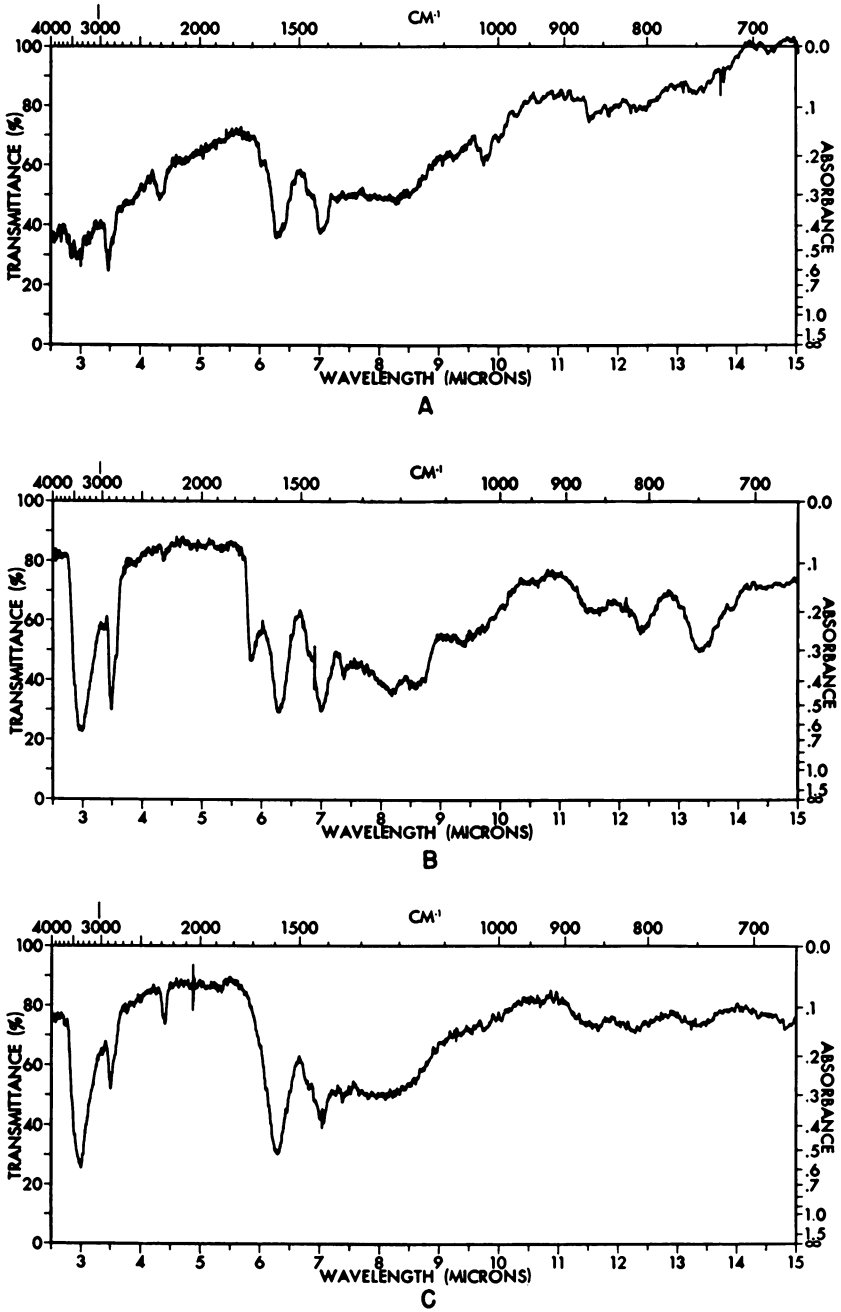

Figure 2. Infrared spectra of: (A) Bruceton coal, (B) benzene soluble fraction, (C) phenanthrene soluble fraction

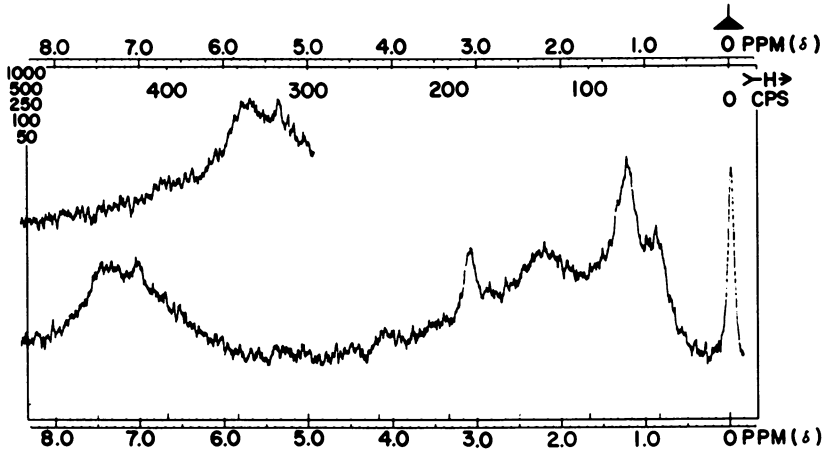

Figure 3. NMR spectrum of benzene soluble fraction of Ireland Mine Vitrain concentrate

Table VI. Hydrogen Type Distribution in Benzene Soluble Fraction, Ireland Mine Vitrain Concentrate

Hydrogen Type	*Absorption Range c.p.s.*	*Distribution %*
Aromatic Hydrogens[a]		
Condensed Aromatic Structures	430–525	16.3
Monocyclic Aromatic Structures + Phenolic OH	360–430	14.7
Aliphatic Hydrogens		
α^2, $\alpha\beta$ and αCH, CH_2, and CH_3 Groups	120–255	29.6
β^-CH and CH_2 Groups	60–120	31.2
β^-CH_3 Groups	35–60	8.2

[a] α hydrogens are on aliphatic carbon atoms directly linked to aromatic rings; α^2 hydrogens are on aliphatic carbon atoms directly linked to two aromatic rings; β hydrogens are on aliphatic carbon atoms which are directly linked to an aromatic ring on one side and in β position with respect to another aromatic ring on the other side; β^- hydrogens are on aliphatic carbon atoms which are not directly linked to an aromatic ring.

C-H infrared band in the phenanthrene soluble fraction relative to the original coal and also a shift in the position of the bands. These observations agree with the postulated mechanism.

The high resolution NMR spectrum of the benzene soluble extract from Ireland Mine vitrain concentrate is shown in Figure 3. The full recording covers the range 0–500 c.p.s. from the absorption peak of tetramethylsilane at 0 c.p.s; the trace above the full recording covers the range of 400–600 c.p.s. The hydrogen type distribution calculated from the spectrum is given in Table VI. The amount of hydrogen in condensed aromatic structures agrees well with the chemically linked phenanthrene content of this fraction. It appears that the "coal-part" of this fraction consists mostly of tetralin-type and cyclo-paraffin structures.

Publication Date: January 1, 1966 | doi: 10.1021/ba-1966-0055.ch028

Summary

(1) Chemical interactions take place between the solvent and bituminous coal during phenanthrene extraction. The net effect of the interaction is hydrogen exchange between phenanthrene and the coal. The formation of chemical bonds between phenanthrene and coal also occurs to a small extent, as a side reaction.

(2) The formation of the coal extract was interpreted as a free-radical chain reaction leading to the depolymerization of coal and aromatization of some of the hydroaromatic structures. It was suggested that phenanthrene possibly plays the role of a chain carrier in this process.

Acknowledgment

The authors wish to thank the Coal Research Board, Commonwealth of Pennsylvania, the American Oil Co. and Consolidation Coal Co. for their support. Special thanks are due to the management of the Research Division of Consolidation Coal Co. for permitting the use of the facilities in their radiological laboratory. The spectra were recorded at Spectra Research Laboratories, Altadena, Calif. by David Lawson, whose kind cooperation is gratefully acknowledged.

This paper was abstracted from the thesis submitted by L. A. Heredy to the Carnegie Institute of Technology, in partial fulfillment of the requirements for a Ph.D. degree in Chemistry.

Literature Cited

(1) Golumbic, C., Anderson, J. E., Orchin, M., Storch, H. H., U.S. *Bur. Mines, Rept. Invest.* **4662** (1950).
(2) Orchin, M., Golumbic, C., Anderson, J. E., Storch, H. H., *U.S. Bur. Mines, Bull.* **505** (1951).
(3) *Ibid*, p. 7.
(4) Yavorsky, P. M., Gorin, E., *J. Am. Chem Soc.* **84**, 1071 (1962).

RECEIVED January 25, 1965.

Discussion

Irving Wender: Did you make any experiments with labeled anthracene? Anthracene is a poorer solvent for coal than phenanthrene, and if hydrogen exchange takes place, this might cast doubt on your conclusions.

Laszlo Heredy: We did make experiments with labeled anthracene, but the results were inconclusive as to whether any tritium exchange took place; at any rate it is very small. It seems that the linear compound is simply less efficient both as solvent and reactant than an angular hydrocarbon like phenanthrene.

Maurice Mitchell, Jr.: The answer to Dr. Wender's question, in my opinion, is that where solubility is an equilibrium phenomenon, Heredy's work shows a mechanism for solubilizing coal. Thus, although the differences in

solubility between anthracene and phenanthrene are not explained, the fact that anthracene may exchange a little hydrogen does not preclude Heredy's mechanistic conclusions for the phenanthrene solubilization of coal.

Milton Denekas: Isn't the solubility of coal in phenanthrene a function of temperature of extraction, and therefore a partial thermal cracking process? Isn't this reaction somewhat different from the action of tetralin on coals since the latter solvent has hydrogen available for hydrogenation?

Dr. Heredy: We agree that cracking probably occurs, and the resulting radicals react with phenanthrene. However, we are not sure how important hydrogen availability is for the dissolution process; although hydrogen exchange does occur with coal, it occurs only to a small extent or not at all in the dissolution of model compounds.

Leo Duffy: Was any hydrogenated phenanthrene found?

Dr. Heredy: No, there was not.

Mr. Duffy: Doesn't this seriously affect your comments regarding the infrared evidence of increased aromatic hydrogen?

Dr. Heredy: The facts are as stated, but I agree that there may be a little difficulty in accounting for them. However, surely hydrogen transfer reactions, perhaps via the solvent, could place hydrogen from aliphatic structures on free radicals centers created by C-C bond scission on aromatic nuclei.

Publication Date: January 1, 1966 | doi: 10.1021/ba-1966-0055.ch028

29

Correlation Between Rank and Reactivity in Liquid Phase Oxidation

GEORGE KAPO

Department of Chemical Engineering, Central University of Venezuela, Caracas, Venezuela

Publication Date: January 1, 1966 | doi: 10.1021/ba-1966-0055.ch029

The rate of surface oxidation of coal between 74 and 90% carbon using molecular oxygen in aqueous sodium hydroxide was measured directly in a flow reactor. The results agree well with the correlation between the rank and the reactivity a coal exhibits in alkaline permanganate oxidations but are in disagreement with phosphoric acid-dichromate and acid permanganate oxidations. This difference between acidic and alkaline oxidations is explained on the basis of solubility considerations. Also, it is concluded that the available internal area in coal for a liquid phase oxidation is no greater than 10^2 sq. cm/gram and, hence, bears no relation to the area which is measured by gas absorbtions and whose value ranges from 10^4 to 10^6 sq. cm./gram.

Liquid phase oxidation of coal has been studied for three reasons: (1) to produce commercially organic acids from coal; (2) to provide a simple chemical reaction for assessing rank; (3) to determine various structural parameters of coal. The last reason includes studies on the reaction products as well as on the magnitude of the reaction rate. This paper will be concerned with the relation between the rank of coal and its rate of liquid phase oxidation. By rank is meant the sum total of the functional groups (phenols, alkyl side chains, etc.) and the structural characteristics (degree of cross-linking, etc.) which affect the reactivity. However, the criterion of rank will simply be per cent carbon (daf).

The reaction rate per gram can be equated to the product of three functions:

$$r = f(\text{rank})\ g(\text{specific surface area})\ h(\text{reaction conditions}) \qquad (1)$$

In a simple heterogeneous reaction the rate per gram is proportional to the sum of the external area, a_e, and the available internal area for reaction, a_i; or

In Coal Science; Given, P.;
Advances in Chemistry; American Chemical Society: Washington, DC, 1966.

$$g(\text{specific surface area}) = (a_e + a_i) \quad (2)$$

Generally we will be interested in comparing the relation between reaction rate and rank under different reaction conditions. If we define the reactivity of a coal under certain reaction conditions as the ratio of its reaction rate to the reaction rate of a standard coal, from Equations 1 and 2 we can write that

$$\text{reactivity} = r' = \frac{r}{r_0} = \frac{(a_e + a_i)\, f(\text{rank})}{(a_e + a_i)_0\, f(\text{rank})_0} \quad (3)$$

By definition the reactivity of the standard coal (subscript 0) is 1.

Data on these systems indicate strongly that $a_e >> a_i$. If density and shape variations among different ranks are small, in experiments where specified screen cut are used Equation 3 then reduces to

$$r' = bf(\text{rank}) \quad (4)$$

where b = a constant = $1/f(\text{rank})_0$

This equation will be referred to as the correlation between rank and reactivity. In this paper the various correlations between rank and reactivity in the literature will be compared with the correlation presented here for liquid phase oxidation of coal with molecular oxygen in alkali.

Coal Sampling and Analyses

Table I presents the proximate and the ultimate analyses of the coals used in the study. Coals A, B, D, and E were obtained from and analyzed by the United States Bureau of Mines. The coal samples were crushed by the Bureau to pass through 60 mesh before analyzing them. The coal which passed through 60 and was retained on 100 mesh was used in this study. Coal C was obtained directly from the mine and was analyzed by the Commercial Testing and Engineering Co., Cleveland, Ohio.

The sample of Coal C consisted of about 50 pounds of coal ranging from 5 to 10 inches in size. To reduce the size of this coal it was first cut into approximately 1-inch pieces before crushing and sieving to give the desired size. The technique used in sieving was to take one cut at a time by using only two screens, crushing the coal sample until it all went through the larger screen, collecting the material on the smaller screen, and discarding any coal which passed through the smaller screen. Table II shows the proximate analyses of the different sizes of coal C. Since the difference between volatile matter of the least and the most volatile petrographic ingredient in coal is about a factor of two (5), it would appear that no serious segregation occurred during sieving.

Apparatus and Procedure

All the available data on the rate of liquid phase oxidation of coal have been taken in batch reactors. Interpreting this data is complicated by the homogeneous oxidation of the intermediate organic acids formed and the con-

Publication Date: January 1, 1966 | doi: 10.1021/ba-1966-0055.ch029

Table I. Proximate and

Coal	Source			Proximate Analysis			
	Mine	County	State	Moisture	Ash	Volatile matter (daf)	Fixed carbon (daf)
A	Coronet Jewel #1, Buckanan, Va.			3.2	2.8	21.9	78.1
B	Crossbrook #2, Wise, Va.			2.4	14.5	37.2	62.8
C	Hazard #9, Perrone, Ky.			1.37	5.17	40.6	59.4
D	Big Bend Mine, Lucas, Iowa			17.8	10.8	46.4	53.6
E	Sandow, Milam, Texas			3.1	15.0	51.0	49.0

Table II. Proximate Analyses of Different Sizes of Coal C

	Moisture	Ash	Volatile Matter (daf)	Fixed Carbon (daf)
Original Coal	1.4	5.2	59.4	40.6
—2 + 3 mesh	2.3	4.5	57.0	43.0
—20 + 28 mesh	1.9	4.8	58.6	41.4
—80 + 100 mesh	1.5	5.1	55.4	44.6

tinual reduction in the concentration of the reactants. To avoid these problems the rather elaborate flow reactor system shown in Figure 1 was constructed. With this apparatus the surface oxidation rate was measured directly at constant oxygen concentration. Induction time for the reaction, homogeneous oxidations, and diffusion effects were also measured.

The apparatus consisted of a flow reactor containing the coal and an oxygen absorber. A fixed bed reactor was used for studies on large coal particles, while a spout reactor was used for studies on small coal particles. Both reactors had a volume of about 400 cc. and were designed so that both wall and end effects were eliminated. Experimental residence time distributions indicated that the fixed bed reactor approximated a plug flow reactor, while the fluidized bed spout reactor had perfect mixing.

The absorber pump constantly recycled the fluid through the oxygen absorber so that the fluid was always essentially saturated with oxygen. A small side stream was removed from the gas absorber recycle by the reactor pump. The side stream could either flow through the reactor or bypass the reactor. The reactor bypass was used when it was desired to study the decomposition in solution of the humic acids. Down stream from the reactor was a filter to remove any coal fines produced, a sight glass to observe the fluid, a flow colorimeter to measure the rate of production of humic acids, and a flow rate indicator.

The oxygen absorber, the reactor, and the connecting tubing were immersed in a constant temperature oil bath whose temperature was controlled within ± 0.2°C. The oxygen uptake by the coal was recorded, and the pressure in the system was controlled with Swarthout electronic transmitters and recorders. Pressure control was within ± 10^{-3} atmospheres, while experiments were made up to 9 atmospheres total pressure.

The apparatus was constructed entirely of stainless steel. The pump packing, valve packing, O-rings and solenoid valve seats were all made of Teflon.

Publication Date: January 1, 1966 | doi: 10.1021/ba-1966-0055.ch029

Ultimate Analyses of Coal

Ultimate Analysis (daf)					*B.t.u. (daf)*
C	*H*	*N*	*O*	*S*	
90.0	5.2	1.5	2.4	0.9	15760
84.8	5.5	1.6	7.1	1.0	15100
82.5	5.5	1.5	8.6	1.9	15160
79.1	5.4	1.5	10.2	3.6	13980
74.1	5.5	1.5	16.7	2.2	12900

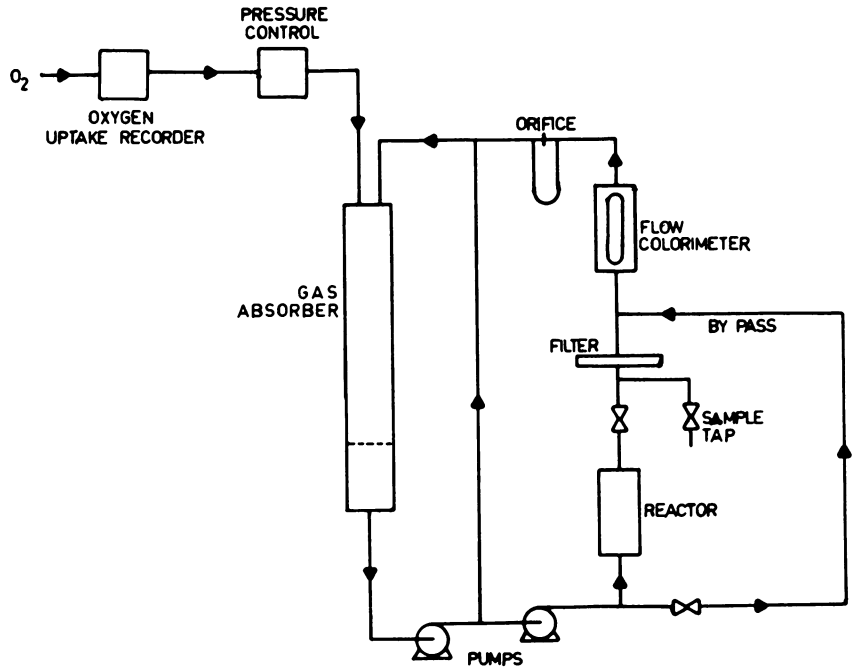

Figure 1. Apparatus

The inside lining of the reactor holding the coal was constructed of polypropylene; during the experiment no apparent decomposition of the polypropylene was observed.

The heterogeneous reaction taking place on the coal surface was separated from the homogeneous decomposition in solution by keeping the concentration of organic acids low by periodic flushing of the system. Utilizing the reactor bypass, it was determined that the oxygen uptake associated with the homogeneous reactions was never more than 5% of the total oxygen uptake by the system. The use of an oxygen absorber in conjunction with the reactor assured that the concentration of oxygen remained constant during the entire experiment. The combination of a large liquid volume, a moderate concentra-

tion of alkali, and frequent flushing of the system assured that the concentration of sodium hydroxide was essentially constant during an experiment.

Discussion

Figure 2 shows the kind of data one can obtain from the apparatus described here. The absorption values from the flow colorimeter are plotted directly *vs.* time; assuming Beer's law, the slope of the locus of this data is the rate of production of humic acids. This rate exhibited a definite induction time. For this experiment, between time zero when the coal was introduced and 10 hours, the rate of production of humic acids increased by a factor of 5. After the induction time of 10 hours the rate of production of humic acids remained constant.

In Figure 2 the rate of oxygen uptake in the experiment is plotted directly against time. As can be seen there is little variation in this rate during the induction period. The gradual increase is caused by increasing homogeneous oxidation of the humic acid whose concentration is increasing.

The rates of oxygen uptake reported in this paper were the rates existing shortly after the induction period ended and after the accumulated organic acids were flushed from the apparatus. A material balance during the induction period indicated that less than 1% of the coal was consumed here. Hence, the rates reported here are related directly to the original coal charged to the reactor with no complications arising from changes of surface area and of petrographic composition.

The following may be taken as conclusive evidence that the reaction was not diffusion controlled:

(1) The Reynolds number in the reactor was varied from 0.0003 to 0.003 with no effect on reaction rate.

(2) The rate of oxygen uptake increased by a factor of 1.7 with a 10°C. increase in temperature.

(3) The calculated rate of mass transfer of oxygen to the coal surface was several orders of magnitude higher than the rate of consumption of oxygen at the coal surface.

Table III presents the reaction rate and the induction time for reaction (as defined in Figure 2) for the five coals studied. These data were taken under the following conditions: 109.5°C., 1 *N* sodium hydroxide, and 8.5 atm. of oxygen partial pressure. The mesh size of the coals was through 60 mesh on 100 mesh. The reaction rates are based on the external area of the coal particles.

Available Area for Reaction

This section should be related to the paper on the surface area of coal presented in the Conference by Dr. Bond (*20*).

In liquid phase oxidations diffusivities are about $1/10^4$ times those existing in the gas phase, and from the pores humic acids and benzenoid acids are removed whose mean diameters are very large compared with the average pore diameter in coal and molecules such as nitrogen and methanol.

Publication Date: January 1, 1966 | doi: 10.1021/ba-1966-0055.ch029

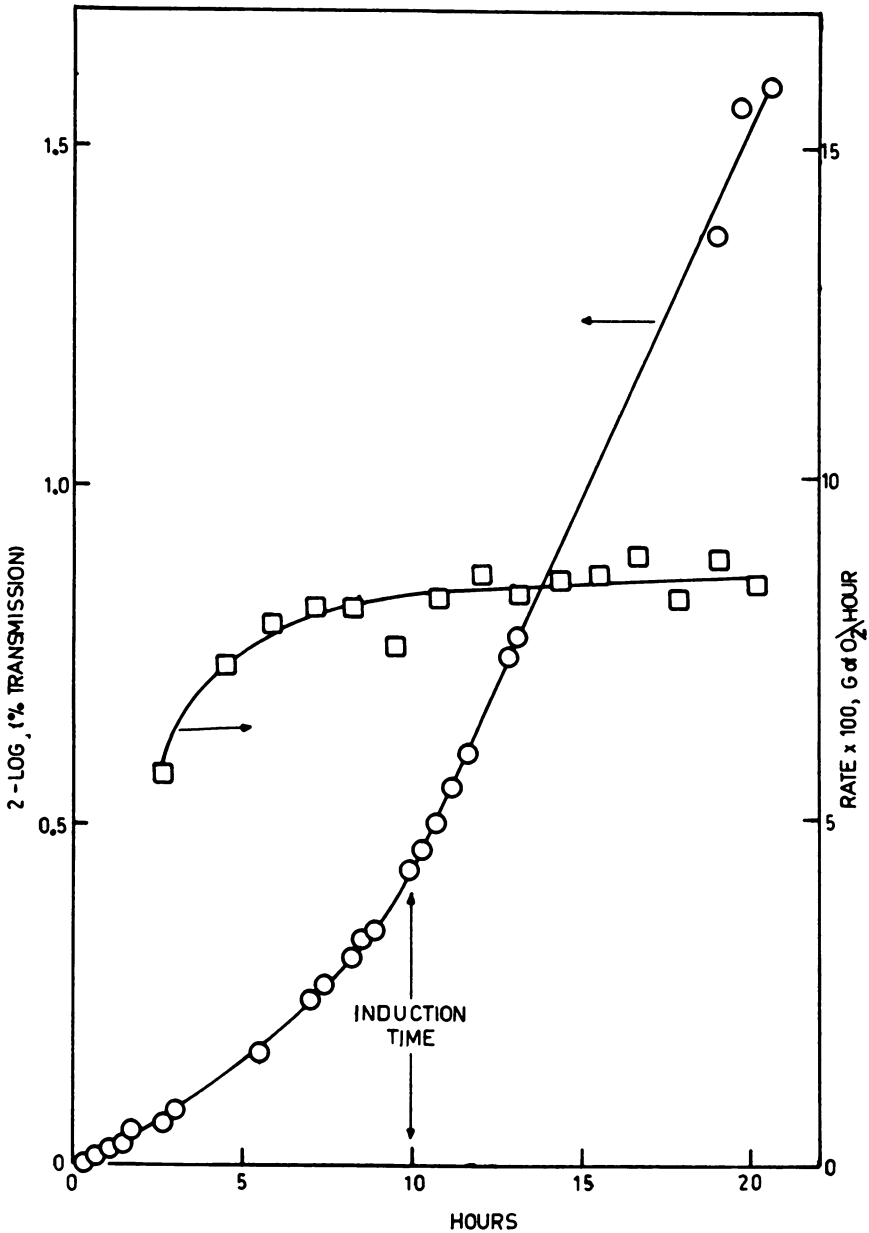

Figure 2. Determination of induction time and reaction rate; concentration of humic acids proportional to 2-log (% transmission); Coal C: —2+3 mesh, 1.16N NaOH; 6.4 atm. O_2 partial pressure, 109.2°C.; □ = rate of oxygen uptake; ○ = concentration of humic acids

Table III. Results

Coal	*% Carbon, (daf)*	*Reaction Rate × 10^6 grams oxygen/hr-sq. cm.*	*Induction Time, hours*
A	90.0	6	44
B	84.8	14	21
C	82.5	33	10
D	79.1	108	4
E	74.1	201	0

Publication Date: January 1, 1966 | doi: 10.1021/ba-1966-0055.ch029

The available area for a liquid phase oxidation, then, should have little relation to the surface area determined by a gas absorptions and heat of wetting experiments.

In 1933, Francis (*4*) measured the rate of the alkaline permanganate oxidation of coal at screen cuts of through 60 on 100 and through 100 on 200 mesh. He found that the rate of reaction was directly proportional to the external area of the different coal samples, thus inferring that there is little internal area available for reaction. In 1936 Gauzelin and Crussard (*8*) reached the same conclusion in similar experiments. Since 1933 a vast and complicated pore structure of coal has been discovered. However, the discovery of this pore structure does not invalidate the experimental results of Francis as some authors (*19*) have suggested.

Other related work in surface area was the phosporic acid-dichromate oxidation of coke by Riley. In an early paper (*2*), on the basis of reaction rates on different particles sizes, Riley suggested that coke smaller than 60 mesh had no available internal area. Later (*1*) Riley reversed himself and suggested that different cokes had different amounts of available internal area. In this paper both vapor absorptions and reactivity measurements were made on different cokes. However, no correlation was found between these two items.

Recently, Honda and Hirose (*13*), on the basis of Riley's experiments on coke, suggested that the available internal area of coal in a phosphoric acid-dichromate oxidation should be proportional to the internal area of the coal as determined by a vapor absorption.

The effect of particle size from 2½ mesh to 90 mesh on the rate of liquid phase oxidation was investigated in the present study. Assuming that the available internal area of the coal is independent of particle size, we can write:

$$r = ka_i + ka_e \tag{5}$$

where:

r = reaction rate, grams of oxygen/hr.-gram
a_i = available internal area for reaction, sq. cm./gram
a_e = external area for reaction, sq. cm./gram
k = reaction rate constant, grams of oxygen/hr.-sq. cm.

A plot of r *vs.* a_e should be a straight line of slope k and with an intercept of ka_i; hence, a_i can be calculated.

Figure 3 shows the results of the experiment. From the slope and the intercept of the line through the three data points the available internal area of this coal is estimated to be 46 sq. cm./gram.

Since the external area of 80 mesh coal is about 400 sq. cm./gram it can be concluded—as Francis did—that for the coals of 80 or higher mesh essentially all of the reaction area for the liquid phase oxidation is on the external surface of the coal with little or no internal area available for reaction.

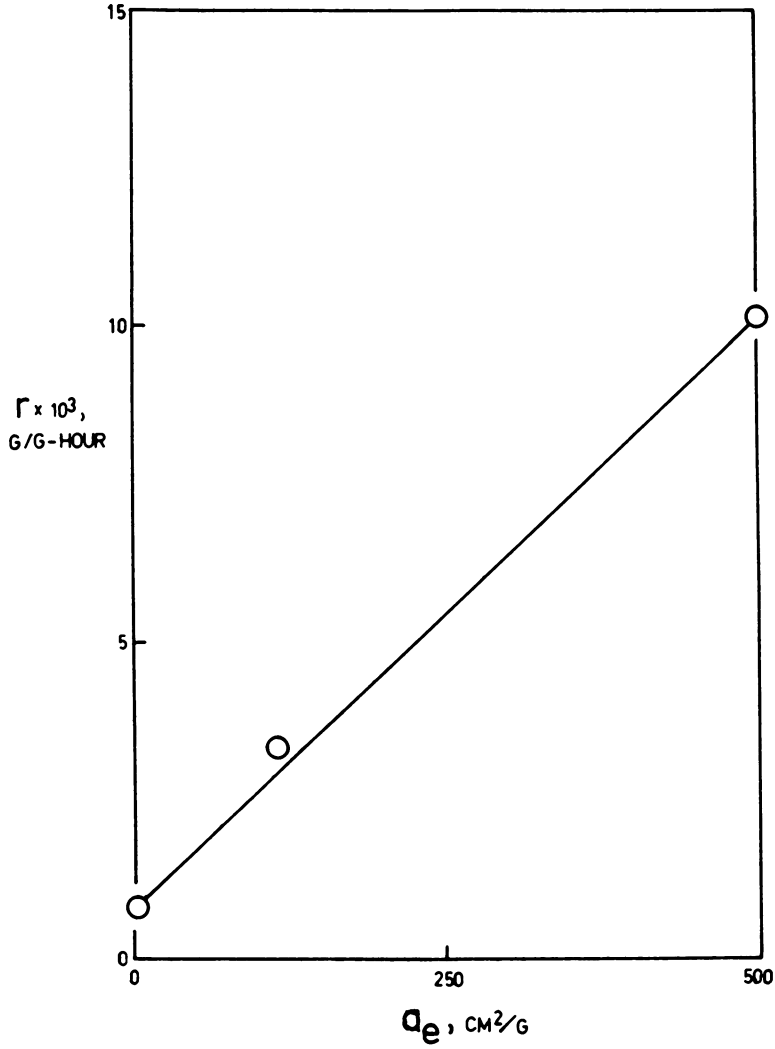

Figure 3. Determination of internal area; Coal C—1N NaOH; 6.4 atm. O_2 partial pressure, 98.3°C.

An alternative explanation of the data presented in Figure 3 is that the majority of the macropore structure is available for reaction, and by breaking up the coal one is simply opening up hitherto sealed pores. However, this does not seem likely since—to explain the results in Figure 3— one would have to assume that from 2½ to 90 mesh the exposed internal area of the coal increases by a factor of 12. Mercury penetration data on Coal C indicates that the macropore area increased only 7% going from 2½ to 90 mesh (*see* Discussions). Also, Malherbe (*16*) found for three bituminous coals that in going from 5 to 270 mesh the BET area only increased by a factor of 2. Furthermore, the helium density of coal is independent of particle size indicating no sealed pores exist at least in respect to the accessibility of helium (*14*).

It would appear then that the results of Smith and Mapstone (*19*), where simply —200 mesh coal instead of a specific screen cut was used, are meaningless. For, presuming that reaction is mostly on the external surface of the coal particle, it is impossible to determine the reactivity of their coals unless one makes the rather stringent assumption that all coals when pulverized to —200 mesh have the same weight average particle size. Fortunately, in all other papers on the rate of a liquid phase oxidation as a function of rank, specified average screen cuts of 80 or larger mesh were used. Hence, reactivities can be calculated directly from the reaction rates reported in the papers, and Equation 4 can be used to compare the results of the different papers.

Publication Date: January 1, 1966 | doi: 10.1021/ba-1966-0055.ch029

Correlation Between Rank and Reactivity

Figure 4 is a semi-log plot of reactivity (r') *vs.* per cent carbon (daf) for the results of this study with molecular oxygen and sodium hydroxide. Coal E (% carbon = 74.1) was chosen as the standard coal; hence, its reactivity is equal to 1 (*see* Equation 4). The solid line is the best straight line through the results of this study. Also in Figure 4 are plotted the results of the alkaline permanganate oxidations of Gauzelin and Crussard (*8*), of Francis (*4*), of Erdman and Ramsay (*3*), and of Olin and Waterman (*17*), the phosphoric acid-dichromate oxidation of Honda and Hirose (*13*), the acid permanganate oxidation of Gauzelin and Crussard (*9*), and the recent reactivity measurements of coal extracts by Van Krevelen and Bakker (*21*). The value of the constant b in Equation 4 in all of the alkaline oxidations and in the coal extracts oxidation was chosen so that there was as close agreement as possible with the solid line. The value of b in the acid-dichromate oxidation was chosen for the best agreement with the solid line when per cent carbon was less than 80. The value of b in the acid permangate oxidation was chosen so that there was as close agreement as possible with the acid-dichromate oxidation. The dashed lines through the two acid oxidations are from the original papers.

Interpreting the Results

There is good agreement between the alkaline oxidations with permanganate and with oxygen. The strong decrease in reactivity with rank here can

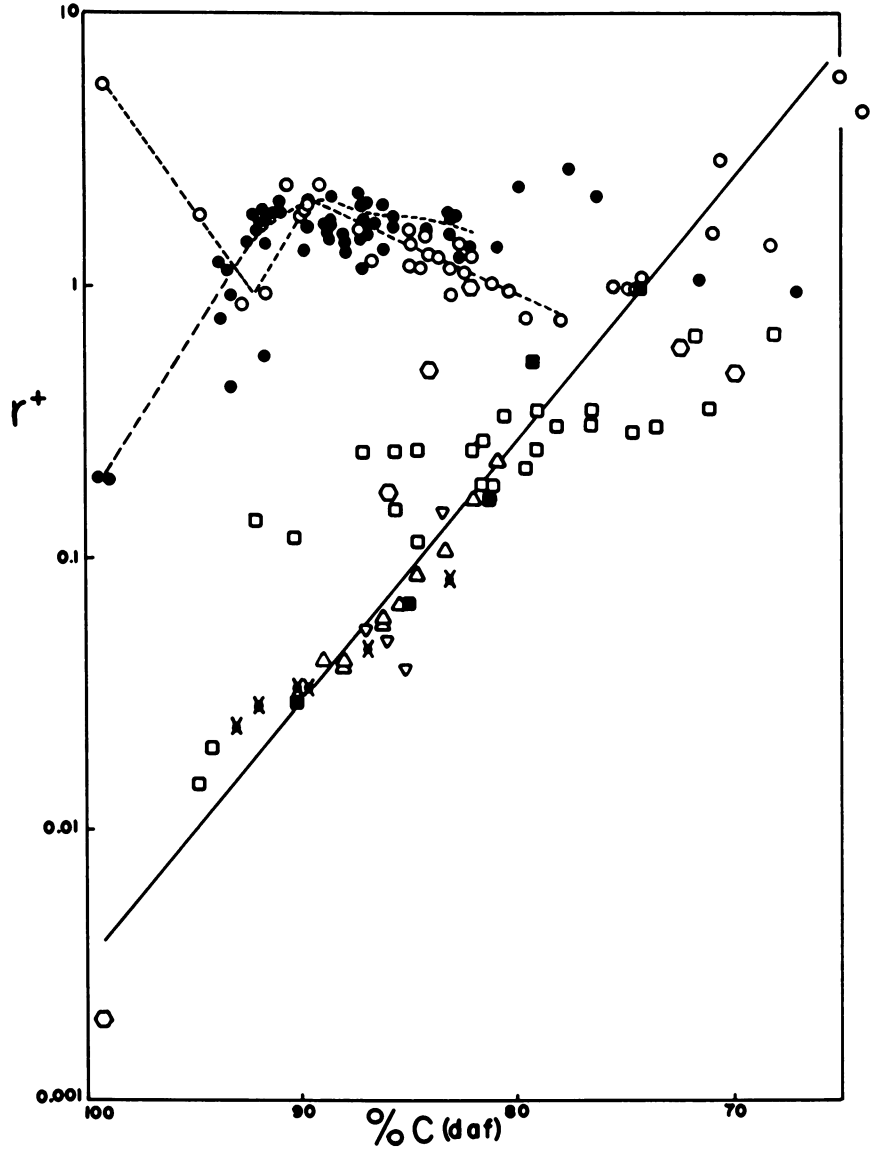

Figure 4. Correlation between rank and reactivity; ■ = this study, NaOH-O_2; △ = Francis, alkaline permanganate; □ = Olin and Waterman, alkaline permanganate; ⬡ = Erdman and Ramsay, alkaline permanganate; ⬟ = Gauzelin and Crussard, alkaline permanganate; ▽ = Van Krevelen and Bakker, quinoline-O_2 (coal extracts); ○ = Honda and Hirose, phosphoric acid-dichromate; ● = Gauzelin and Crussard, acid permanganate.

In Coal Science; Given, P.;
Advances in Chemistry; American Chemical Society: Washington, DC, 1966.

be attributed to at least three factors: (1) the decrease in oxygen content, (2) the decrease in aliphatic carbon content (*7*), and (3) the increase in size of the aromatic nuclei (*23*).

It has been found that oxygen-containing substitutents (particularly phenols) and alkyl substitutents on an aromatic nucleus increase dramatically the susceptibility to oxidation of the original aromatic compound (*18*, *24*, *25*). Oxidation of the aromatic nuclei in coal undoubtedly takes place at periphery sites; hence, an increase in size of aromatic nuclei would be expected to lower the oxidation rate owing to a decrease in the number of oxidation sites per unit area of coal surface.

The results for the two oxidations in acid medium are in good agreement with each other but almost in complete disagreement with the results in alkali. The majority of Honda's data is between 78 and 90% carbon and show a rise in reactivity of a factor of three as rank increases; the results in alkali over the same range show a decrease in reactivity of a factor of 10. Honda suggests that his increase in reactivity is caused by the decrease in cross-linking in coal which is believed to occur here. The decrease of hardness of coal with increase in per cent carbon in this range is attributed, at least in part, to decrease in cross-linking. Also, the fact that only coals between 88 and 91% carbon form very compact cokes is ascribed partly to their relatively low degree of cross-linking and hence, to a high mobility of their structural units upon heating (*6*, *11*, *22*). Finally, it has been suggested that the minimum in internal area in this region (*12*) and the maximum in amount of reduction possible (*10*) is caused by a decrease in the degree of cross-linking with increase in rank.

Admitting that the degree of cross-linking may determine the reactivity of a range of coals in acid oxidations, the immediate question is still why the alkaline oxidations do not give the same results as acidic ones. Solubility considerations can afford an explanation. The initial product of an alkaline oxidation of coal is primarily humic acids (high molecular weight water insoluble acids), while in acidic (except HNO_3) and neutral oxidations the main products are benzenoid acids (low molecular weight water soluble acids) and carbon dioxide (*15*). Hence, in acidic oxidations there is a large degradation of the original coal structure, and the reaction rate here will depend more on how strongly cross-linked the structural units are in coal rather than on the reactivity of individual bonds in the coal. On the other hand, in alkaline oxidations there is relatively little degradation of the coal structure; hence, the reaction rates here will depend more on the susceptibility of individual bonds to oxidation rather than on the cross-linked structure of the coal.

As suggested by Honda the decrease in reactivity in his acidic oxidation with increase in rank below 78 and between 90 and 93% carbon for his coals is caused by increasing cross-link structures here. This can also explain the decrease in reactivity above 90% carbon for the acid permanganate results. The increase in reactivity noted by Honda going from 93% carbon to graphite is caused by ability of the concentrated phosphoric acid to disperse graphite-like structures.

Publication Date: January 1, 1966 | doi: 10.1021/ba-1966-0055.ch029

Literature Cited

(1) Balfour, A., Blayden, H. E., Carter, A. H., Riley, H. L., *J. Soc. Chem. Ind.* **57,** 1 (1938).
(2) Blayden, H. E., Riley, H. L., *J. Soc. Chem. Ind.* **54,** 159 (1935).
(3) Erdman, J. C., and Ramsey, V. G., "Abstracts of Papers," 138th Meeting, ACS, September 1960, p. 8R.
(4) Francis, W., *Fuel* **12,** 128 (1933).
(5) Francis, W., "Coal," 2nd ed., p. 357, Edward Arnold, London, 1961.
(6) *Ibid.*, p. 711.
(7) *Ibid.*, p. 726.
(8) Gauzelin, M., Crussard, M., *Fuel* **17,** 19 (1938).
(9) Gauzelin, M., Crussard, M., *Fuel* **17,** 36 (1938).
(10) Given, P. H., Lupton, V., Peaver, M. E. Residential Conference on Science in the Use of Coal, p. A–38 (April 15–17, 1958).
(11) Hirst, W., "The Ultra-Fine Structure of Coals and Cokes," (B.C.U.R.A.), p. 39–42 Cheney & Sons, Banbury, England, 1944.
(12) *Ibid.*, p. 37.
(13) Honda, H., Hirose, Y., *Fuel* **37,** 323 (1958).
(14) Lowry, H. H., "Chemistry of Coal Utilization," suppl. vol. p. 107, Wiley, New York, 1963.
(15) *Ibid.*, Vol. I, p. 358.
(16) Malherbe, P. le R., *Fuel* **30,** 97 (1951).
(17) Olin, H. L., Waterman, W. W., *Ind. Eng. Chem.* **28,** 1024 (1936).
(18) Randall, R. B., Benger, M., Groocock, C. M., *Proc. Roy. Soc.* (London) **165A,** 432 (1938).
(19) Smith, J. W., Mapstone, G. E., *Fuel* **36,** 191 (1957).
(20) Spencer, D. H. T., Bond, R. L., ADVAN. CHEM. SER. **55,** 724 (1966).
(21) Van Krevelen, D. W., Bakker, C. A. P., *Fuel* **43,** 137 (1964).
(22) Van Krevelen, D. W., "Coal," 2nd ed., p. 340, Elsevier, New York, 1961.
(23) *Ibid.*, p. 358.
(24) Yohe, G. R., Hill, D. R., Dunbar, J. E., Scheidt, F. M., *J. Am. Chem. Soc.* **75,** 2688 (1953).
(25) Yokokawa, C., Watanabe, Y., Kajiyama, S. and Takegami, Y., *Fuel* **41,** 209 (1962).

RECEIVED January 25, 1965.

Discussion

Robert B. Anderson. Some information on mass transfer processes may be obtained from activation energies. If a reaction were moderately rapid and diffusion in the liquid phase were rate controlling, the apparent activation energy should be 1–2 kcal./mole. If reaction occurs in pores and were diffusion plus reaction controlled, the activation energy should be one-half that of the surface process, which should still be a large value. What apparent activation energy was found in your oxidation reactions?

George Kapo. In my studies (*2*) I had the opportunity of measuring the activation energy of the overall surface reaction consuming oxygen as well as

the specific surface reactions producing the various types of products. The results are shown in the following table:

Reaction	*Activation Energy kcal./mol*
Oxygen uptake	13
Humic Acid production	17
Benzenoid plus oxalic acids production	17
Volatile-acids production	8
Carbon dioxide production	13

The overall reaction rate may be affected by diffusion if the mass transfer from the bulk fluid to the coal surface and/or the pore diffusion steps are relatively slow. I have made tentative estimates of both these diffusion effects. The following equation can be written (2) for the rate of oxygen uptake of a porous solid such as coal, assuming the oxygen to be consumed in an irreversible first-order reaction.

$$r_o = \frac{(1 - e)(O_2)}{\frac{1}{kn} + \frac{1}{K}} + \frac{pA_i (O_2)}{\frac{1}{kn} + \frac{L^2}{2RD} + \frac{2L}{KR}}$$

where: r_o = rate of oxygen consumption, moles/hr.-sq. cm. (external area)
e = void volume = void surface of coal, dimensionless fraction
(O_2) = bulk oxygen concentration, moles/cc.
k = chemical reaction rate constant, cc./hr.-site
n = number of reaction sites per unit area, sites/sq. cm.
K = liquid phase mass transfer coefficient for oxygen, cm./hr.
p = number of pores per unit area, pores/sq. cm.
L = average pore length, cm.
R = average pore radius, cm.
A_i = internal area of one pore = $2\pi RL$, sq. cm.
D = diffusivity of oxygen in water, sq. cm./hr.

The first term represents the reaction rate on the external area (no pore diffusion), while the second term represents the reaction rate occurring inside the pores. The terms in the denominators represent chemical and diffusion processes; it is the relative size of these terms which determine whether or not diffusion is affecting the rate of the chemical reaction. The following table gives estimates of the size of these terms as well as the name of the process which they represent.

Term	*Name*	*Value, hr./cm.*
$1/kn$	chemical reaction	6000
$1/K$	mass transfer to external area	0.1
$2L/KR$	mass transfer to pore mouth	100
$L^2/2RD$	pore diffusion	600

These results show that the chemical reaction term is at least an order of magnitude greater than any diffusion terms; hence, we would conclude that the reaction is not diffusion controlled. High temperature liquid phase oxida-

Publication Date: January 1, 1966 | doi: 10.1021/ba-1966-0055.ch029

tions (*1*) exhibit diffusion effects; these effects have been predicted on the basis of the above equation and the activation energy presented in the first table.

Norbert Berkowitz. I suggest that *initial* reaction data cannot justify the author's rather definite conclusions since a diffusion-controlled component of the overall reaction would be relatively slow compared with an initial surface reaction and therefore more or less completely masked by it. Moreover, if the oxidation reaction were carried out in a liquid medium, swelling and dispersion of the solid reactant would accompany it, and in a dry (gaseous) medium, oxidation is known to cause some "eating out" of pores, etc. In both cases, therefore, continuous changes in reactant geometry accompany the reaction, and the critique applying to Hill *et al.* applies to Kapo.

Dr. Kapo. The reaction rates presented in this paper were taken before more than several percent of the original coal charged to the reactor was consumed. It would appear then that there was no complication owing to large changes in reactant geometry because of loss of reactant. If any dispersion of the coal had occurred, the dispersed particles would be washed out of the reactor and thus not affect the measurement of the reaction rate of the solid coal in the reactor. If reaction occurs in the pores, swelling could complicate the problem. Compared with organic solvents of the type used by Dr. Hill, however, the swelling effect of dilute alkali on coal would be small. Diffusion of oxygen to and diffusion of products away from the external surface of the coal did not control the reaction (*see* reply to R. B. Anderson).

The availability of the pores for reaction is a difficult problem in any gas or liquid phase reaction with coal. Liquid phase oxidation of coal in alkali

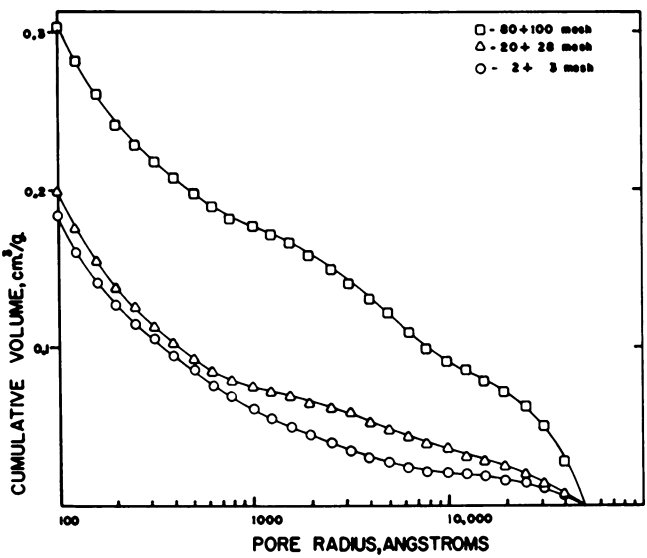

Figure A. Pore size distributions of different screen cuts of coal C

Publication Date: January 1, 1966 | doi: 10.1021/ba-1966-0055.ch029

represents an extreme situation where the main products of the reaction are macromolecular humic acids. It is difficult to imagine how these large humic acid molecules can diffuse out (at any reasonable velocity) of a pore system where the size of many of the pores approach the molecular diameter of the humic acids. We may be fortunate in that the initial humic acids formed will plug the pores shut so that oxygen can no longer diffuse in and reaction in the major part of the pore structure will drop to zero. If this is the case, the kinetic problem is simply one of a shrinking sphere, and the measured reaction rate truly reflects the chemical structure of the coal with no complications arising from the nature of the pore structure.

The only proof of the above contention are the results in Figure 3 of the paper where reaction rate is approximately proportional to external area. Figure A here shows the pore size distribution (from mercury penetration (*3*)) of each particle size, confirming that little additional pore structure was opened up during coal grinding. This would rule out the possibility that the effect measured in Figure 3 was caused by opening up entrances to sealed pores.

For diffusion control of reaction in pores the reaction rate per gram will be inversely proportional to particle size (hence, external area per gram) and will exhibit an activation energy equal to one-half the activation energy of the intrinsic reaction, which still can be a high number (*4*). Hence, another interpretation of the data in Figure 3 and the activation energies reported in the reply to R. B. Anderson is that the overall reaction was controlled by diffusion in the pores. The controlling diffusion would not be that of the oxygen's diffusion in, but of the humic acids' diffusing out. The question could only be settled by determining reaction rates on coals where the pore structure had been destroyed or made inaccessible.

Peter H. Given. It is wrong to speak of humic acids as macromolecular if their molecular weights are a few thousands at most. Such molecules, if fairly compact, might be some tens of angstroms in diameter, but certainly not hundreds of angstroms. The tobacco mosaic virus molecule is about 1200A. long and 50A. diameter and has a molecular weight of, I think, 14 million. This gives an idea of scale of true macromolecules.

Dr. Kapo. I must agree with Dr. Given here, and I retract my original statement about the size of the regenerated humic acid molecule. However, it should be noted that one would expect repulsion between the identically charged carboxylate groups in the molecule, resulting in an expanded structure for the sodium salt of the humic acid solution. This would result in at least one dimension of the molecule being much larger than the average pore diameter in coal. Also, an expanded structure will cause the rate of diffusion of the humic acids even out of the larger pores in coal to be very small.

Literature Cited

(1) Kamiya, Y., *Fuel* **40,** 149 (1961).
(2) Kapo, G., Ph.D. Thesis, Case Institute of Technology, Cleveland, Ohio, 1964.
(3) Nichols, J. R., Chemical Research Department, Atlas Chemical Industries, Wilmington, Del.
(4) Satterfield, C. N., Sherwood, T. K., "The Role of Diffusion in Catalysis," Addison-Wesley, London, 1963.

Publication Date: January 1, 1966 | doi: 10.1021/ba-1966-0055.ch029

Aliphatic Structures in Coal

B. K. MAZUMDAR, S. GANGULY, P. K. SANYAL, and A. LAHIRI

Central Fuel Research Institute, Jealgora, India

Publication Date: January 1, 1966 | doi: 10.1021/ba-1966-0055.ch030

From C-methyl contents determined in coals and reduced coals by the Kuhn-Roth method, it appears that more methyl groups are present, especially in higher rank bituminous coals, (C > 86%), than have hitherto been believed. A truer assessment of methyl groups is sought by interpreting the pyrolysis behavior (at 600°C.) of coal. Studies on a series of coals, dehydrogenated coals, and reduced coals are presented, and probable mechanisms of methane formation during pyrolysis are discussed. Most of the methane formed during low temperature pyrolysis is a maximum measure of the methyl content in coals. The total distribution of carbon in coal is discussed, and it is believed that the aliphatic side chain is constituted mainly of methyl groups.

A decade of work on the distribution of carbon (and also hydrogen) has now led to a fair assessment of the aromatic and hydroaromatic contents of coals although there may still be differences of opinion about the accuracy of these values (*16*). Our information on the aliphatic structures present in coal is, however, less complete.

It had been observed earlier (*17*, *18*, *19*) that in coals of 80-90% carbon content (on dmf basis) the sum of aromatic and hydroaromatic fractions appears always to be almost constant at 92 ± 2% of the total carbon in coal. The balance of 6–10% could thus be aliphatic carbon. The accuracy of such an estimate obviously would depend upon the accuracy of the aromaticity and hydroaromaticity values. The conclusion that the sum of aromatic and hydroaromatic carbon fractions is nearly constant at the region of 92–93% of the total carbon has also emerged from the recent deductions made by A. F. Gaines (*11*) and the authors (*20*) by interpreting infrared and NMR data.

In Coal Science; Given, P.;
Advances in Chemistry; American Chemical Society: Washington, DC, 1966.

Methyl Groups in Coal

Thus far the only aliphatic structures definitely known to exist in coal are the methyl groups, but only 2–4% of carbon in coal (C = 80–90%) appears to be in methyl groups as estimated by the Kuhn-Roth method (*5*, *14*, *15*). However, the method is not quantitative in the case of methyl groups directly linked to aromatic structure. Proton spin resonance studies by Oth and Tschalmer (*26*) on coal extracts indicate that about 33% of hydrogen is in methyl form—i.e., about twice the values obtained by Kuhn-Roth reaction on normal coal samples. Studies made on reduced coals indicate that there may be more methyl groups than have been estimated by Kuhn-Roth method. (A similar conclusion has since been obtained by R. Bent, W. K. Joy, and W. R. Ladner (*1*) from methyl measurements on a reduced coking coal.) Earlier, a number of coals were reduced following the technique of Reggel *et al.* (*28*) for a series of chemical studies (*3*, *12*). C-methyl has since been determined by the Kuhn-Roth method on three of these reduced samples. The values thus obtained are considerably higher (50–70%), especially in the case of the higher rank coal samples (C = 90%), than those obtained on the starting coal samples (Table I).

Table I. Comparative Study of C-Methyl Determinations on Normal and Corresponding Reduced Coals by Kuhn-Roth Method

Samples[a]	*Rank* *%C dmf*	*Extent of Reduction* *Hydrogen added per 100 C atoms*	*%C as C—CH_3*	*% Increase in Estimation of C-Methyl Consequent on Reduction*
Vitrain 6	89.8	—	1.6	—
Reduced	—	21	2.5	56
Vitrain 7	90.4	—	1.5	—
Reduced	—	44	2.6	73
Reduced	—	25	2.2	47
Vitrain 1	83.5	—	3.2	—
Reduced	—	23	3.4	6
Vitrain	83.6	—	3.6	—
Reduced	—	18	4.1	14

[a] Except for the last sample, others were reduced earlier for some other chemical studies (*3*, *12*). The numbers of vitrain samples correspond to those given in earlier papers (*3*, *12*).

Reduction apparently creates fresh hydroaromatic structure (at the expense of the aromatics), and thus the methyl groups attached to the aromatic structures are likely to become amenable to quantitative estimation (by the Kuhn-Roth procedure), provided that the particular aromatic ring is reduced to hydroaromatic. Significantly, the reduced samples of the lower rank coals did not yield much higher values for methyl groups than the original samples. Thus, it would appear that Kuhn-Roth estimation does not completely measure the true C-methyl content in coals, especially in high rank coal samples.

It is, however, likely that not all aromatic rings with attached methyl groups may have been reduced (*6*), in which case the values for C-methyl

Publication Date: January 1, 1966 | doi: 10.1021/ba-1966-0055.ch030

content obtained on reduced coals will not represent the total or the true values for the original coal samples.

A correlation between the hydroaromatic carbon and the C-methyl carbon as determined by Kuhn-Roth method is shown in Figure 1. The relationship is more or less linear. It had been determined earlier (*14*) that the proportion

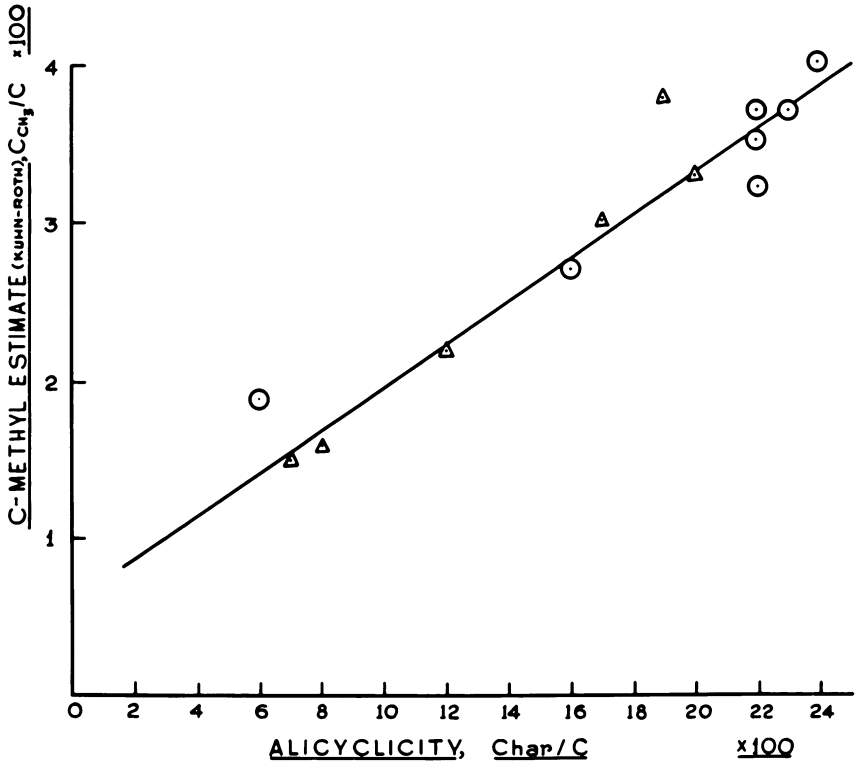

Figure 1. Relation between the C-methyl content (Kuhn-Roth method) and the alicyclic carbon content of coal
⊙ *values from Kaiser et al. (14);*
△ *values determined by the present authors*

of C-methyl carbon (determined by Kuhn-Roth method) remained almost constant at about 4% of the total carbon between 80 and 85% carbon coal, but beyond 85% carbon the value abruptly changes and then decreases progressively to less than half this value at 90–92% carbon rank. It was presumed at the time that the decrease in the C-methyl value was caused by demethylation during coal metamorphism. However, an interpretation of Figure 2 which depicts the variation of C-methyl values by Kuhn-Roth method and the hydroaromaticity of coal against rank when considered with the evidence presented in Figure 1 would indicate that methyl groups are perhaps chiefly present in hydroaromatic structures in low rank coals, and that with progressive aromatization of the hydroaromatic structures the character of

Publication Date: January 1, 1966 | doi: 10.1021/ba-1966-0055.ch030

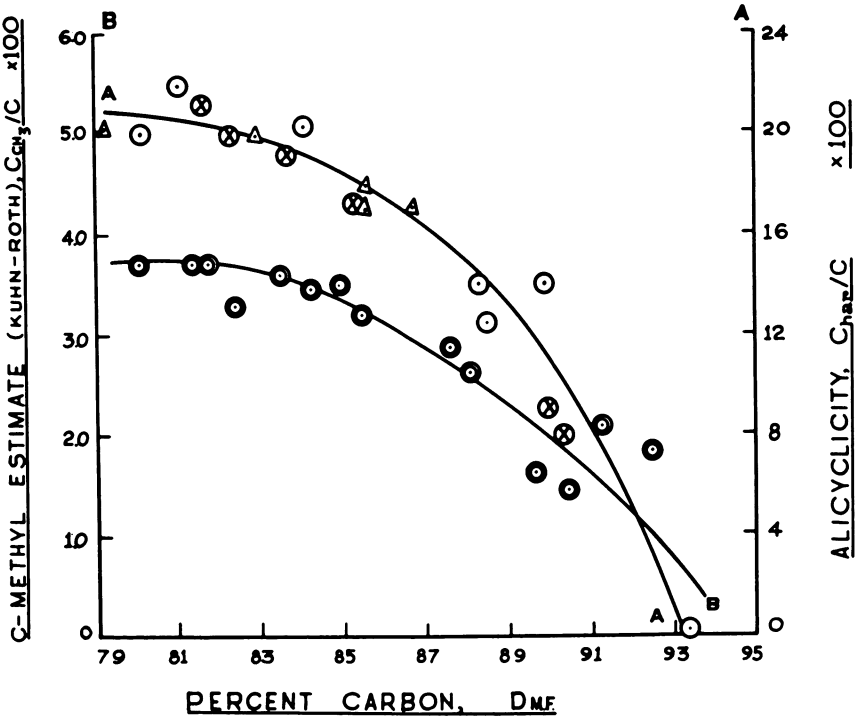

Figure 2. The nature of variation of alicyclic and methyl-carbon (Kuhn-Roth) contents with coal rank
⊙ *Kuhn-Roth estimate;*
⊙ △ ⊗ *Estimate of alicyclicity (7, 8, 13)*

the methyl groups changes progressively, and they become less and less amenable to Kuhn-Roth estimation.

The apparent decrease in values of C-methyl content with increase in rank observed earlier (*14*) would now appear to be caused largely by progressive aromatization of methyl-substituted hydroaromatic structures rather than demethylation. Since the Kuhn-Roth method has limitations, an alternative method for assessing the C-methyl content in coals is desirable.

Pyrolysis of Coal and Methane Formation

In 1947, Kinney (*15*) drew attention to a direct relationship between the amount of acetic acid formed on oxidizing coal with nitric acid and potassium dichromate and the yields of methane obtained by low temperature carbonization. The oxidation method leading to acetic acid is a variation of the standard Kuhn-Roth procedure, and hence what Kinney indicated as the "methane yielding structure" is obviously the methyl groups in coal. However, the relationship he pointed out can only be qualitative since true C-methyl content (as shown in the present work) cannot be obtained by any

Publication Date: January 1, 1966 | doi: 10.1021/ba-1966-0055.ch030

oxidation method, and there can be more than one source of methane formation.

Interpreting the likely sources of methane formation requires a clearer understanding of the mechanism of coal pyrolysis. This appears to be possible now in view of the mechanism (*21*) of coal pyrolysis advanced by the present authors. The major postulates of the mechanism are (1) that all the aromatic carbon of coal be effectively retained in the coke/char during low temperature carbonization (600°C.); and (2) that virtually all the hydroaromatic carbon in coal forms tar. More recently the suggested mechanism was remarkably confirmed by parallel studies on reduced coals (*3*, *12*). It has been shown (*3*) that the additional carbon volatilized in the case of reduced coals during pyrolysis is equal to the aromatic carbon rendered hydroaromatic during reduction. This is claimed as direct proof of the selective and complete volatility of the nonaromatic structure of coal during pyrolysis. Further, it has also been found (*12*) that virtually all the freshly created hydroaromatic carbon forms tar. Thus, in the light of such a mechanism of coal pyrolysis it is possible to interpret the source or sources of gas formation, particularly methane formation.

The link between the methyl groups and methane formation is obvious, but there might be other mechanisms which also lead to methane formation during pyrolysis. Ouchi and Honda (*27*), from studying the pyrolysis of phenolformaldehyde resins, suggest that the following reactions may also occur, leading to the formation of hydrocarbon gases:

$$CH_2 + H_2 \rightarrow CH_4 \quad (1)$$

$$CH_2 + CH_2 \rightarrow C_2H_4 \quad (2)$$

$$C_2H_4 + H_2 \rightarrow C_2H_6 \quad (3)$$

$$CH_3 + CH_3 \rightarrow C_2H_6 \quad (4)$$

$$C_2H_6 + CH_2 \rightarrow C_3H_8 \quad (5)$$

Further, Fitzgerald and Van Krevelen (*10*), on the basis of Dent's findings (*8*) consider another possibility of methane formation—e.g., through autohydrogenation:

$$C + 2H_2 \rightarrow CH_4 \quad (6)$$

The reaction is favored under pressure; however, even under atmospheric pressure significant amounts of methane have been claimed as being formed at 500–600°C (*8*, *10*).

The possibility of the above reactions, their extent, and hence the main source of methane formation (which is the chief hydrocarbon in pyrolysis gases) have been examined in the present work by carrying out pyrolysis studies on coals, dehydrogenated coals, and reduced coals.

Experimental

Nine samples of coal (mostly vitrains), including a lignite and an anthracite, have been studied. The analytical and structural data on the samples

Publication Date: January 1, 1966 | doi: 10.1021/ba-1966-0055.ch030

Table II. Analytical and

Coal No.	% Ash dry basis	Analysis, % dmf basis C	H	N	O
1.	13.4	81.6	5.4	2.4	10.0
2.	11.0	82.4	5.4	2.3	9.4
3.	6.4	83.6	5.5	2.8	7.9
4.	3.2	85.5	5.2	1.9	6.6
5.	5.6	87.9	5.3	1.8	4.5
6.	4.3	89.8	4.8	2.1	2.8
7.	7.4	90.4	4.6	2.3	2.2
8.	6.2	69.7	4.6	1.5	24.0
9.	3.4	93.2	3.1	1.3	2.4

[a] By pyrolysis.

Table III. Pyrolysis of Coals Showing

Coal No.	Rank %C dmf	Gray-King Assay % yield on dmf basis[a] Coke/ Char	Tar	Liquor	Gas (by diff.)	Volume of gas per 100 gm. dmf coal c.c. at NPT
1.	81.6	69.5	12.1	7.0	11.4	13.620
2.	82.4	68.5	14.3	6.4	10.8	12,800
	82.4	69.0	14.0	6.6	10.4	12,900
3.	83.6	70.1	12.9	6.7	10.3	12,740
4.	85.5	75.6	10.8	4.0	9.6	13,790
5.	87.9	77.5	10.0	3.5	9.0	12,000
6.	89.8	85.1	6.7	1.3	6.9	11,950
7.	90.4	87.6	5.5	1.2	5.7	12,780
8.	69.7 (Lignite)	51.5	13.6	10.0	24.9	21,160
9.	93.2 (Anthracite)	98.5	nil	nil	1.5	6.190

[a] The retort is inserted at 300°C., and carbonization is carried out by heating at the rate of 5°C./minute to 600°C. where it is maintained for an hour.

are presented in Table II. The results of Gray-King assay on the samples are given in Table III. The analysis of gas, the yield of methane, the percentage of carbon appearing as methane as well as the total carbon in gas (as methane hydrocarbons, unsaturated hydrocarbons, carbon monoxide, and carbon dioxide) are also presented in Table III. The composition of gas was determined in the usual way by Orsat and Haldane apparatus. The saturated hydrocarbon gases are reported roundly as methane in Table III because this was the most prevalent among them. The pyrolysis gas for only two samples (samples 2 and 6), however, was analyzed by infrared spectroscopy, and a semiquantitative analysis indicates that ethane is present to the extent of about 2–3% in the gases; still higher hydrocarbons appear to be present only in traces.

Publication Date: January 1, 1966 | doi: 10.1021/ba-1966-0055.ch030

Structural Properties of the Coals

Functional Oxygen Groups % dmf basis				Structural Parameters		
				Aromaticity[a]	Hydro-aromaticity[b]	
O_{OH}	O_{CO}	O_{COOH}	Unaccounted	f_a	f_{har}	$f_a + f_{har}$
5.5	1.8	0.9	1.8	0.72	0.21	0.93
5.2	0.9	0.7	2.6	0.73	0.20	0.93
4.4	0.6	0.4	2.5	0.74	0.19	0.93
3.0	0.8	0.1	2.7	0.75	0.17	0.92
1.4	0.5	nil	2.6	0.78	0.14	0.92
0.5	0.2	nil	2.1	0.87	0.08	0.95
—	—	—	—	0.89	0.07	0.96
10.2	2.7	6.1	5.0	0.64	0.22	0.86
nil	—	nil	—	0.99	nil	0.99

[b] Dehydrogenation by sulfur (*17*, *18*).

the Distribution of Carbon in Gases

Gas Analysis, % v/v					Yield of Methane per 100 gm. dmf coal c.c. at NTP	Percent Carbon Appearing as:	
CO_2	CO	Unsaturated	H_2	CH_4[b]		Methane	Total Gases
11.0	16.2	4.0	20.6	48.2	6560	4.3	7.5
11.8	10.5	4.9	18.9	53.9	6900	4.5	7.2
12.3	11.9	3.7	15.7	56.4	7290	4.7	7.4
8.7	12.6	3.9	17.9	56.9	7250	4.6	7.0
6.9	11.2	3.4	25.4	53.1	7330	4.6	6.8
7.8	5.2	2.6	24.6	59.8	7180	4.4	5.6
1.1	7.6	2.0	33.2	56.1	6700	4.0	4.9
4.9	6.2	2.3	37.2	49.4	6310	3.4	4.9
41.9	20.5	3.0	10.7	23.9	5060	4.0	15.0
6.8	4.0	1.1	51.3	36.8	2280	1.3	1.7

[b] This includes small proportions of ethane and traces of other higher hydrocarbons which are lumped together with methane and reported here in terms of methane. For samples 2 and 6 the content of ethane was separately determined in a semiquantitative way by infrared spectroscopy, and these values are 3.2 and 2.5%, respectively. The range of values may be taken to be typical for other samples as well.

In another set of experiments the effect of prior dehydrogenation on the yields of gases (especially that of methane) was studied. As shown earlier, dehydrogenation with either sulfur (*17*, *18*) or iodine (*22*) leads to the complete inhibition of tar formation and "fixation" of the corresponding carbon (alicyclic) in char. It is thus possible to study the contribution, if any, of the hydroaromatic structure towards gas formation by partial or complete "fixation" of the hydroaromatic carbon in char.

Discussion

It was observed earlier (*17*, *18*, *22*) that the yield of methane from pyrolyzing dehydrogenated coals (including the methane evolved during de-

Publication Date: January 1, 1966 | doi: 10.1021/ba-1966-0055.ch030

Table IV. Effect of Partial or Complete Dehydrogenation

Coal No.	*Conditions of Treatment with Sulfur Prior to Pyrolysis*	*Gray-King Assay % yield on dmf basis*		*Volume of Gas per 100 gm. dmf coal, c.c. at NTP*
		Char	*Tar*	
2. Starting vitrain				see Table III
(a)	Heated with sulfur up to 360°C. for partial dehydrogenation (40%) followed by pyrolysis	82.0	nil	11,000[a]
(b)	Partial dehydrogenation (20%) followed by pyrolysis	77.0	5.0	11,200[a]
(c)	Heated with *excess* sulfur for hours ensuring complete dehydrogenation followed by pyrolysis of the dehydrogenated coal	82.9	nil	27,010[b]
7. Starting vitrain				see Table III
(a)	Partial dehydrogenation as in 2(a) followed by pyrolysis	93.0	nil	10,270[a]
3. Starting vitrain				see Table III
(a)	Heated with *excess* sulfur up to 360°C. but dehydrogenation not prolonged	88.5	nil	31,580[b]
4. Starting vitrain				
(a)	Treatment as in 3(a)	89.1	nil	24,990[b]

[a] Gas freed of H_2S

[b] Including H_2S formed during dehydrogenation stage

hydrogenation reaction) is practically the same as obtained by pyrolyzing untreated coals. Similar results appear to have been obtained by Berkovitch and McCulloch (2), at least in one of their experiments on coal-sulfur reactions, though Dicker, Gaines, and Stanley (9) have reported recently that their findings on methane yield are "somewhat different from those of the Indian school." They found that the yield of methane from pyrolyzing two coals of 401 and 902 rank after complete dehydrogenation with sulfur was less by about 33 and 60%, respectively compared to the untreated samples.

It appears that the discrepancy in the results reported above is caused chiefly by the difference in the method of conducting the coal-sulfur reaction. If coal and sulfur are mixed intimately (in 2:1 proportion) and heated in a Gray-King assay retort from room temperature to 360°C. for one hour and maintained at this temperature for another hour (as was done by Mazumdar *et al.* (17, 18) in their initial studies on coal dehydrogenation), followed by

on the Yield of Methane During Subsequent Pyrolysis

Gas Analysis % v/v						Methane Yield per 100 gm. dmf coal c.c. at NTP	Percent decrease in Methane Yield (consequent on pretreatment)
H_2S	CO_2	CO	Unsaturated	H_2	CH_4[d]		
						7,290	—
—	12.9	13.3	nil	11.0	62.8	6,910	5.2
—	12.1	14.1	3.1	7.6	63.1	7,060	3.2
78.6		1.0	nil	nil	20.4	5,510[c]	24.4[c]
						6,310	—
—	2.9	3.5	4.0	27.8	61.8	6,350	nil
						7,250	—
72.0		1.1	1.6	4.4	20.9	6,600	8.9
60.8		2.1	1.9	7.7	27.5	6,870	6.3

[c] This confirms Dicker's experiment (*9*). It is significant that in other cases where there was residual hydrogen in gas the yield of methane did not decrease substantially.
[d] *See* footnote *b* under Table III

the usual rates of heating up to 600°C. as in Gray-King assay, then the yield of methane is about the same as obtained from the untreated coals although invariably slightly lower. On the other hand, if dehydrogenation is prolonged to ensure completion (100%) (as was done by Dicker *et al.* (*9*)) and the completely dehydrogenated coals are carbonized (after removing the free sulfur) up to 600°C., the yield of methane is substantially reduced (Table IV) as observed by Dicker *et al.*

However, the considerable decrease in methane yield in the above case does not indicate the contribution of the hydroaromatic structure towards methane formation. It has been established (*19*, *23*) that complete or even a partial dehydrogenation inhibits tar formation completely (though a minimum dehydrogenation is necessary for this effect) and retains all the hydroaromatic carbon in the char. The decrease in methane yield on pyrolysis of

Publication Date: January 1, 1966 | doi: 10.1021/ba-1966-0055.ch030

Table V. Results of Pyrolysis of Reduced Coals Showing the

Coal No.		Reduced Coal[b] grams, dmf	Ethylene-diamine per 100 gm. starting vitrain, gm.	f_{bar}	Gray-King Assay % yield, dmf basis			
					Coke	Tar	Liquor	Gas
1.	Starting vitrain	—	—	0.18	69.5	12.1	7.0	11.4
	Reduced	111.4	8.5	0.28	59.9	23.4	7.1	9.6
2.	Starting vitrain	—	—	0.17	68.5	14.3	6.4	10.8
	Reduced	107.4	7.5	0.30	54.7	31.0	5.1	9.2
3.	Starting vitrain	—	—	0.18	70.1	12.9	6.7	10.3
	Reduced	118.5	13.3	0.36	51.5	30.2	7.3	11.0
7.	Starting vitrain	—	—	0.07	87.6	5.5	1.2	5.7
	Reduced	101.5	0.3	0.32	65.7	27.7	0.4	6.2

[a] See footnote *b* under Table III

completely dehydrogenated coals may be the result of insufficient hydrogen to form methane with the methyl radicals present. The source of hydrogen at this low temperature pyrolysis stage is mainly the hydroaromatic material and, therefore, complete dehydrogenation will result in evolution of very little hydrogen during the pyrolysis stage (Table IV, *see* expt. No. 2).

In order to verify this hypothesis, a few experiments have also been done with smaller proportions of sulfur so as to cause partial dehydrogenation only to the extent necessary to ensure that 100% of the hydroaromatic carbon is retained in char during subsequent pyrolysis (Table IV). The yield of methane remains practically the same as with the untreated coals (Table IV), indicating that hydroaromatic carbon as such does not contribute to methane formation. At the same time, the hydrogen evolved from such structures is necessary for forming methane.

It has been shown earlier (*3*) that the aromatic carbon rendered hydroaromatic by reduction is quantitatively devolatilized, and virtually all the freshly created hydroaromatic carbon forms tar (*12*) with little extra carbon liberated as a gas. In the present work some of the previously reduced samples as well as one recently prepared have been studied with special emphasis on the volume and composition of the gas. The essential data on the reduced samples and the results of pyrolysis are presented in Table V.

Results of Pyrolysis on Normal, Dehydrogenated, and Reduced Coals

Table III shows that values for the percent yield of methane (including small amounts of ethane reported as methane) in the bituminous range (C = 81–90% on dmf basis) are largely the same and may be put at 7000 ± 500 cc. at NTP, although strictly speaking the yield tends to decrease somewhat between 88 and 90% carbon coal. However, when the yield is expressed as

Publication Date: January 1, 1966 | doi: 10.1021/ba-1966-0055.ch030

Effect of Extra Hydroaromatic Structure on the Yields of Gases

Volume of gas per 100 gm. starting vitrain c.c. at NTP	*Gas Analysis % v/v*					*Methane Yield per 100 gm. starting vitrain c.c. at NTP.*	*Carbon in the form of gases, %*
	CO_2	*CO*	*Unsaturated*	H_2	CH_4[a]		
13,620	11.0	16.2	4.0	20.6	48.2	6560	7.5
16,640	8.5	10.8	5.0	37.7	38.0	6320	7.2
12,800	11.8	10.5	4.9	18.9	53.9	7290	7.4
13,200	9.1	9.7	5.1	18.1	58.0	7660	7.5
12,740	8.7	12.6	3.9	17.9	56.9	7250	7.0
16,820	2.9	4.5	3.7	39.7	49.2	8280	7.0
12,780	4.9	6.2	2.3	37.2	49.4	6310	4.9
18,320	4.6	4.8	3.7	52.4	34.5	6320	5.5

[a] Per 100 grams dmf starting vitrain

the percentage of total carbon in coal, it works out to an almost constant value—e.g., about 4.6% in coals having 81–86.0% carbon (dmf) and about 4% carbon in the case of highest rank bituminous coal. For lignite the percent yield of methane is considerably lower, but when expressed as percentage of carbon it is again of an order similar to that in bituminous coals.

Another significant feature is the total carbon in gas appearing in the form of different gases—i.e., methane (including small proportions of ethane), carbon monoxide, carbon dioxide, etc. Once again, in the bituminous coals having less than 86% carbon almost a constant proportion of carbon (e.g. about 7%) appears in the form of gases, but in the 90% carbon coal it is only about 5%. Thus, 93–95% carbon in the bituminous coals is distributed between their coke/char and tar, and the sum of the aromatic and the alicyclic fractions determined for these coals is also of a similar order (Table II). Further, prior dehydrogenation (complete or partial) followed by pyrolysis leads to a similar proportion of carbon retained in the char (Table VI). Likewise, the proportion of carbon appearing as a gas for the lignite sample is also complementary to that retained in its char consequent upon prior dehydrogenation (Table VI).

All these observations indicate that hydroaromatic structures do not as such contribute significantly to methane formation. Evidently this is also true for the amount of carbon dioxide and carbon monoxide found in low temperature pyrolysis gases.

The above conclusions are supported by the results obtained by pyrolyzing reduced coals (Table V). Although the hydroaromatic content of the coals was doubled or even quadrupled by reduction, the yield of methane (including small proportions of ethane) from carbonizing the reduced samples was about the same as from untreated coals. In one case, however, the yield of

Publication Date: January 1, 1966 | doi: 10.1021/ba-1966-0055.ch030

Table VI. Pyrolysis Behavior (600°C.) of Coal with or without Sulfur Showing the Compatibility of the Carbon in Gas and That Retained in Char with Pretreatment

Coal No.	*Carbon Retained during Pyrolysis in Presence of Sulfur,* %*	*Carbon Delivered in the Form of Gases During Normal Pyrolysis, %*
2. (i)	92.0	7.3
(ii)	93.1	7.3
3. (i)	92.9	7.0
(ii)	91.5	7.0
4. (i)	92.0	6.8
(ii)	93.1	6.8
7. (i)	95.5	4.9
(ii)	96.0	4.9
9. (i)	85.5	15.0

* The first figures in each set obtained in presence of smaller proportions of sulfur (insufficient for complete dehydrogenation but optimum (*19,23*) for complete fixation of hydroaromatic carbon in char), and the second were obtained in presence of excess sulfur. In the presence of iodine (*22*) the same results are also obtainable.

methane was found to be significantly higher (14% in excess over the normal yield). This odd behavior may be caused by the fact that this particular sample had an unusually high ethylenediamine content. In support of this hypothesis it may be observed that the reduced sample of the high rank coal (C = 90%, dmf basis) which had no adsorbed ethylenediamine yielded practically the same amount of methane as the original coal. This is all the more significant since, in this sample, the total hydroaromatic content was nearly five times that of the original sample.)

The fact that the freshly created hydroaromatic structure in reduced coals contributes little to the formation of gases (except for some unsaturates, Table V) is perhaps also evident from the correlation shown earlier between the yield of extra tar and the extra hydroaromatic carbon created by reduction (*12*). These results are recast in Figure 3 to show more effectively the pyrolysis characteristics of reduced coals and hence throw light on the formation of gases.

The sum total yields of coke and tar from the original coals are almost equal to the sum total yields of coke and tar from the correspondingly reduced coals although the yields of tar in the case of some of these reduced samples were as high as six times the original yield of tar from the original coals (Figure 3).

It is evident, therefore, that the aromatic carbon alone yields coke, and hydroaromatic carbon yields tar. Since neither appears to contribute substantially to the formation of gases (during the low temperature pyrolysis), it seems certain that the gases of low temperature pyrolysis owe their origin largely to the aliphatic structure in coal. At least it is now certain that methane formation is quite independent of the aromatic and hydroaromatic structures in coal.

However, the possibility of methane formation by autohydrogenation still has to be considered. A few experiments have been done to ascertain such contribution, if any, towards methane formation during low temperature pyrolysis (600°C.).

Publication Date: January 1, 1966 | doi: 10.1021/ba-1966-0055.ch030

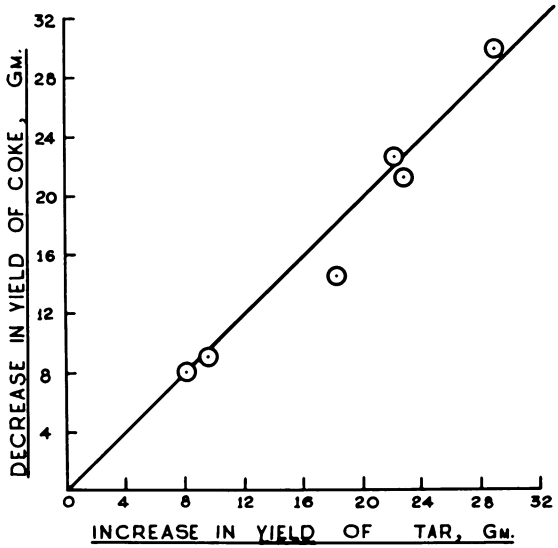

Figure 3. The correspondence of the increase in the yield of tar with the decrease in the yield of coke consequent upon reduction

Experimental

Two samples of coke prepared at 600°C. were crushed to 72 B.S. mesh size and treated with hydrogen from 300–600°C. for an hour, and the treatment was continued for another hour at 600°C. (to simulate Gray-King assay conditions). The stream of hydrogen gas (including other gases formed) was collected. The gas was analyzed, and the results are presented in Table VII.

Results

Results show that though some methane is formed, the quantities are relatively small (about 5% or even less of the total methane obtainable by low temperature pyrolysis of coal) even though a considerable excess of hydrogen was used in the experiments.

The foregoing results and discussions indicate that methane is specifically derived from the methyl groups in coal. If the above hypothesis is agreed to, then the following conclusions emerge:

(1) The methyl content in bituminous coals (carbon 80–90%) ranges from 4.0–4.6% of the total carbon.

(2) The methyl content is virtually constant in coals having 80–86% carbon, and it progressively decreases with increasing coal rank.

These conclusions are however subject to the validity of the tacit assumption made here that the small proportion of ethane (2–3%) which invariably accompanies methane formation owes its origin also to the methyl groups in coal. Dicker *et al.* (9) however are of the opinion that ethane mainly origi-

Publication Date: January 1, 1966 | doi: 10.1021/ba-1966-0055.ch030

Table VII. Reaction of Semicoke (600°C.)

Coke Samples	*Conditions of Treatment with Hydrogen*
Prepared from Coal No. 2	Heated from room temperature to 600°C. for one hour and then maintained at 600°C. for another hour.
Prepared from Coal No. 5	Same as above
Prepared from Coal No. 7	Same as above

[a] The volume of hydrogen reacting with coke is about 10 times that obtainable *in situ* during pyrolysis of coal at and up to 600°C.

Publication Date: January 1, 1966 | doi: 10.1021/ba-1966-0055.ch030

nates from pyrolysis of the hydroaromatic structure. In view of the formation of similar amounts of methane hydrocarbons (at least in terms of carbon appearing in the form of hydrocarbon gases) from the pyrolysis of coals, partially dehydrogenated coals, and reduced coals, the present authors believe that most of the ethane is formed by the combination of methyl radicals originating from the methyl groups in coals. Both views are moot questions at the present state of our knowledge. Fortunately, proportions of ethane in relation to methane are rather small, and as such, the above conclusions with regard to methyl content in coal would not involve any serious error, provided that the basic supposition of the relationship between methyl groups in coal and methane formation during pyrolysis is held to be true.

The presence of a considerable proportion of methylated bodies in low temperature tar and its origin must be explained. The fact that the yield of methane remains largely the same even when tar formation is completely inhibited would indicate that the methyl groups of coal possibly do not participate in forming the methylated bodies in tar. It is not unlikely, therefore, that such methylated bodies in tar are "synthesized" during pyrolytic reaction of the hydroaromatic structure (via methylenes).

It is also almost certain that the methyl groups are completely eliminated during pyrolysis at 600°C. Infrared (*7*) and chemical studies (*24*) on semicoke indicate that semicoke is about 100% aromatic in character and hence contains no methyl carbon.

The distribution of carbon in the form of aromatic, hydroaromatic, and methyl carbon (as assessed in the present work) is presented in Table VIII. The sum of the three forms of carbon accounts for about 97.5–98.0% of the total carbon in lower rank bituminous coal (C < 86% carbon, dmf basis) and about 99.4% of the total carbon in case of the highest rank bituminous coal (C = 90.4%) studied. Small proportions of carboxyl groups are present in lower rank bituminous coal, and if this carbon is taken into account, it may bring the total up to 98% at the maximum.

and Hydrogen under Atmospheric Pressure

"Volume of Hydrogen Passed per 100 gm. daf coke, c.c. at NTP	Gas Analysis, %					Methane Formed by Hydrogenation, c.c. at NTP/100 gm. daf coke
	CO_2	CO	Unsaturated	H_2	CH_4	
32,480	0.6	3.1	0.6	94.1	1.6	520
21,500	1.9	6.0	0.6	90.0	1.5	320
20,400	1.0	1.0	0.5	97.5	nil	nil

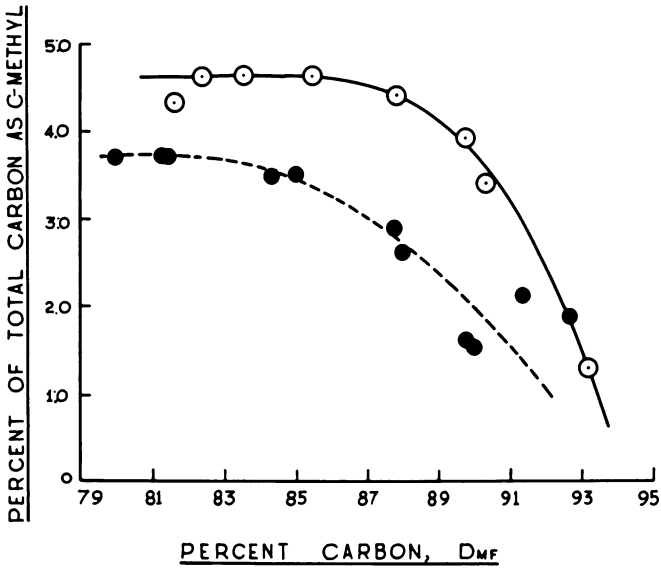

Figure 4. Variation of the true methyl content of coal with rank and its comparison with the Kuhn-Roth estimate
- - - - values by Kuhn-Roth method;
—— values derived from pyrolysis.

The difference of about 2% carbon in case of the lower rank bituminous coal does not appear to be entirely caused by cumulative errors in assessing the different forms of carbon. Remarkably, (Table VI) the amount of carbon retained in char consequent on prior dehydrogenation (and which according to our interpretation represents the sum of aromatic and hydroaromatic car-

Publication Date: January 1, 1966 | doi: 10.1021/ba-1966-0055.ch030

Table VIII. The Self-Consistency of the Maximum Estimate of C-Methyl

Coal No.	*Rank %C, dmf basis*	*$f_a + f_{ha.r.}$,[a] % of total carbon*	*C-Methyl, % of total carbon*	*Carboxylic Carbon, % of total carbon*
2	82.4	93.0	4.6	0.3
3	83.6	93.0	4.6	0.2
4	85.5	93.1	4.6	nil
7	90.4	96.0	3.4	nil
8	69.7	86.0	4.0	3.3

[a] This is derived from the retention of carbon in char consequent upon prior dehydrogenation (Table VI) and is considered to be the maximum estimate of the sum of the aromatic and hydroaromatic carbon. Individual determinations of aromatic and hydroaromatic carbon also lead to a similar assessment (Table II).

[b] These values of carbonyl oxygen are not determined by the present authors but are taken rank-wise from Blom's determination by hydroxylamine method (*4*). These values are considered to be the maximum estimate for carbonyl oxygen and are about double the estimate obtainable by phenylhydrazine method (Table II). The latter method is suspect

bon) and the carbon delivered into the gas during *normal* carbonization in the form of hydrocarbons and oxides of carbon add up almost precisely to 100% of the total carbon in c al.

In accounting for 98% of the total carbon in the form of aromatic, hydroaromatic, and methyl carbon (Table VIII), the carbon which is released into the gas in the form of carbon oxides has not been included. It is significant to recall once again that the formation of carbon monoxide and carbon dioxide *prima facie* appears to be independent of the aromatic and hydroaromatic fractions of coal (Tables III and V). This fact obviously raises a question as to the source of formation of the carbon oxides (particularly carbon monoxide), invariably found in low temperature gases. Gasification reactions involving the reaction of water and carbon during pyrolysis cannot explain the formation of the substantial proportions of carbon monoxide (and carbon dioxide) found in gases because most of the acetylatable hydroxyl groups in coal appear in the form of water during low temperature pyrolysis (*9*). The formation of carbon monoxide (and a good part of carbon dioxide—i.e., over and above that caused by decarboxylation of minor proportions of carboxyl groups) would thus appear to be caused largely by the carbonyl groups in coal. In spite of uncertainties in the true estimate of carbonyl oxygen, if the values obtained by Blom *et al.* (*4*) by oxime formation or titanometric reduction are accepted as truer estimates of carbonyl oxygen contents for the ranks of coal studied, a fair correlation appears to exist between the amount of carbon monoxide and carbon dioxide formed during pyrolysis and the carbonyl oxygen content of coal (Table VIII).

The nature of carbonyl groups in coal is not yet known unambiguously. It may be quinonoid and/or ketonic (*13*) in character. In the latter case, the carbonyl carbon will have to be grouped with the aliphatic carbon, and in

Publication Date: January 1, 1966 | doi: 10.1021/ba-1966-0055.ch030

(Assessed From Pyrolysis) with Other Forms of Carbon in Coal

Sum of Aromatic, Hydroaromatic, C-Methyl, and Carboxylic Carbon, % of total carbon	*Carbonyl Oxygen Content Vis-a-Vis Unaccounted Carbon*		
	Probable O_{CO} content,[b] % dmf coal	*Oxygen Appearing as CO and CO_2 during Pyrolysis[c] % dmf coal*	*Carbonyl Carbon, % of total carbon*
97.9	3.1	2.6	2.8
97.8	3.0	2.3	2.7
97.7	2.9	2.3	2.5
99.4	1.0	1.4	1.2
93.3	7.2	9.7	7.7

owing to various complications. (*4*). In spite of uncertainties still remaining about the most probable estimate of carbonyl oxygen in coal, it is of interest to note that it corresponds largely to the amount of carbon monoxide and carbon dioxide formed during pyrolysis (Table III). Further, the "carbonyl" carbon is also roundly consistent with the unaccounted carbon left over after accounting for all other known forms of carbon. The coincidence is possibly more than fortuitous.

[c] This is corrected for the carbon dioxide which would form during pyrolysis owing to carboxyl group in coal.

case of the former it should be added to the aromatic carbon since it is obviously lost during pyrolysis. If this is true then we may account practically for the total carbon in coal in the various structures (Table VIII), even in the case of the lignite sample containing appreciable proportions of carbonyl and carboxyl groups.

The technique for estimating the total aliphatic carbon (especially methyl carbon) in coal may require further refinements. However, in view of the foregoing discussions on the self-consistency of the estimated methyl content with other forms of carbon in coal, it seems unlikely that there are side chains longer than methyl group in normal coals.

Literature Cited

(1) Bent, R., Joy, W. K., Ladner, W. R., *Fuel* **43,** 5 (1964).
(2) Berkovitch, I., McCulloch, A., *Fuel* **25,** 36, 69 (1946).
(3) Bhattacharyya, A. C., Mazumdar, B. K., Lahiri, A., *Fuel,* **43,** 181 (1964).
(4) Blom, L., Thesis, Delft, 1960.
(5) Brooks, J. D., Durie, R. A., Sternhell, S., *Australian J. Appl. Sci.* **9,** 303 (1958).
(6) Brooks, J. D., Durie, R. A., Silberman, H., *Australian J. Chem.* **17,** 55 (1964).
(7) Brown, J. K., *J. Chem. Soc.* **1955,** 744.
(8) Dent, F. J., *Proc. Intern. Conf. Gasification Mineil Coal, Liege,* 1954.
(9) Dicker, P. H., Gaines, A. F., Stanley, L., *J. Appl. Chem.* **13,** 455 (1963).
(10) Fitzgerald, D., Van Krevelen, D. W., *Fuel,* **38,** 17 (1959).
(11) Gaines, A. F., *Fuel* **41,** 112 (1962).
(12) Ganguly, S., Mazumdar, B. K., *Fuel* **43,** 281 (1964).
(13) Given, P. H., Peover, M. E., *J. Chem. Soc.* **1960,** 394.
(14) Kaiser, F., Rao, H. S., Lahiri, A., *Proc. Symp. Nature Coal, Jealgora,* **1959,** 245.
(15) Kinney, C. R., *J. Am. Chem. Soc.* **69,** 284 (1947).
(16) Mazumdar, B. K., Lahiri, A., "Abstracts of Papers," 142nd Meeting, ACS, September 1962, p. 3K.
(17) Mazumdar, B. K., Choudhury, S. S., Chakrabartty, S. K., Lahiri, A., *J. Sci. Ind. Res.* **17B,** 509 (1958).

Publication Date: January 1, 1966 | doi: 10.1021/ba-1966-0055.ch030

(18) Mazumdar, B. K., Chakrabartty, S. K., Choudhury, S. S., Lahiri, A., *Proc. Symp. Nature Coal, Jealgora,* **1959,** 219.
(19) Mazumdar, B. K., Chakrabartty, S. K., Lahiri, A., *Fuel* **41,** 129 (1962).
(20) Mazumdar, B. K., Lahiri, A., *Fuel* **41,** 487 (1962).
(21) Mazumdar, B. K., Chakrabartty, S. K., Lahiri, A., *Proc. Symp. Nature Coal, Jealgora,* **1959,** 253.
(22) Mazumdar, B. K., Choudhury, S. S., Lahiri, A., *Fuel* **39,** 179 (1960).
(23) Mazumdar, B. K., De, N. G., Lahiri, A., *J. Sci. Ind. Res.* **21A,** 36 (1962).
(24) Mazumdar, B. K., Chakrabartty, S. K., Saha, M., Anand, K. S., Lahiri, A., *Fuel* **38,** 469 (1959).
(25) Mazumdar, B. K., Bhattacharyya, A. C., Ganguly, S., Lahiri, A., *Fuel* **41,** 105 (1962).
(26) Oth, J. F. M., Tschamler, H., *Fuel* **40,** 119 (1961).
(27) Ouchi, K., Honda, H., *Fuel* **38,** 429 (1959).
(28) Reggel, L., Raymond, R., Steiner, W. A., Friedel, R. A., Wender, I., *Fuel* **40,** 339 (1961).

RECEIVED October 5, 1964.

Discussion

Laszlo A. Heredy: There is NMR spectroscopic evidence for the presence of both α- and β-CH_3 groups in coal, based on depolymerization work with phenol-BF_3 reagent. For example, isopropyl groups were shown to be present in a high volatile bituminous coal. Is there a distinct difference in the behavior of these two types of CH_3 groups with respect to the reagent used in wet analytical methyl group determination?

Martin B. Neuworth: The Kuhn-Roth method has a number of limitations. These were discussed by Brandenberger *et al.* (*Anal. Chem.* **33,** 453 (1961)). The normal method for estimating C-methyl groups is based on a determination of total acidity calculated as acetic acid. Brandenberger has shown that other acids can be produced during the oxidation—e.g., benzoic acid, and these acids steam distil with the acetic acid. Therefore, when the classical Kuhn-Roth procedure is applied to a substance like coal, it would lead to methyl group values of questionable significance.

Bhupendra K. Mazumdar: We have not worked on the nature of the methyl groups in coal but have sought to assess the total methyl content by interpreting the sources of methane formation during low temperature (600°C.) pyrolysis.

We are aware that the Kuhn-Roth method is not specific for all types of methyl groups. This is exactly the point that we have made in our paper.

Regarding the question of the presence of isopropyl groups in coal, we do not think this point has been proved beyond doubt because (1) the content found by Heredy *et al.* was hardly 0.4% of coal, and (2) the low rank bituminous coal they studied may well have contained significant proportions of foreign inclusions like plant resins. The isopropyl groups identified by the authors may be structural parts of such resins (abietic) rather than of the real matrix of coal structure.

31

Studies on the Structure of Coals of Different Rank

Hydrogen Distribution of Depolymerization Products

LASZLO A. HERETY, ANDREW E. KOSTYO, and MARTIN B. NEUWORTH

Research Division, Consolidation Coal Co., Library, Pa.

Publication Date: January 1, 1966 | doi: 10.1021/ba-1966-0055.ch031

The distribution of hydrogen types in the soluble fractions from the depolymerization of a series of coals has been determined by NMR analysis. The aromatic hydrogen content varies from 20 to 32% of the total hydrogen, and no simple relationship exists with coal rank. β-Paraffinic plus naphthenic hydrogens, the major type, exceed the α-hydrogens and comprise 38–66% of the nonaromatic hydrogens. The most striking variation in the structure of the six coals is the number of methylene bridges. The degree of depolymerization with phenol-BF_3 can be correlated directly with the number of methylene bridges found in the soluble fractions. A general coal structure in accord with our results consists of large units (MW > 4000) and smaller units (MW, 300–600) connected by methylene bridges.

The distribution of hydrogen types in coals continues to be a subject of considerable interest in coal structure studies. Published data indicate that the fraction of aromatic hydrogens usually increases with increasing rank, but the absolute values depend on the specific analytical method used (7). Hydrogen type analysis of a single coal based on the application of NMR spectroscopy to the soluble fraction from depolymerization with phenol-BF_3 has been reported by us (3). The conversion of coal to soluble fragments in substantial yields under very mild conditions permits a reliable determination of the hydrogen types by NMR analysis, and these results can be extrapolated to the parent coal with considerable confidence.

This procedure has now been extended to a series of coals varying in rank from lignite (70% C) to a low volatile bituminous coal (91% C). In addition to determining the amount of aromatic and aliphatic hydrogens, the aromatic group will be further subdivided into monocyclic and polycyclic types. A more

In Coal Science; Given, P.;
Advances in Chemistry; American Chemical Society: Washington, DC, 1966.

detailed breakdown of the aliphatic hydrogens into methylene, α, β, and β^+ types will be reported.

Experimental

Details of the depolymerization, solvent separations, and product analyses were described previously (*3*, *4*). Molecular weights of the benzene-, methanol-, and phenol-soluble fractions were determined cryoscopically using sulfolane as the solvent (*11*).

All NMR spectra were recorded on a Varian A–60 spectrometer at room temperature by Nuclear Magnetic Resonance Specialties, Inc., New Kensington, Pa. Benzene soluble fractions were recorded in deuterated chloroform solution ($CDCl_3$) while dimethyl sulfoxide-d_6 (DMSO-d_6) was the solvent employed for other fractions. (Deuterated chloroform with enrichment of 99.8% was purchased from Bio-Rad Laboratories and dimethyl sulfoxide-d_6 with enrichment of 99.6% from Merck, Sharp, and Dohme of Canada.) The internal standard used with the $CDCl_3$ solutions was tetramethylsilane and hexamethyldisiloxane (chemical shift 7 c.p.s.) with DMSO-d_6. Prior to preparation for NMR recording, the samples were thoroughly dried in a vacuum at 110°C. The NMR tubes were sealed to minimize the absorption of atmospheric moisture. The chemical shifts given in c.p.s. are referred to tetramethylsilane.

A planimeter was used for area measurement. Corrections were made for hydrogen in $CDCl_3$, DMSO-d_6, and chemically combined radioactive phenol so that the final data represent only the hydrogen associated with the coal. A correction for hydrogen in the solvents could be made from the known weight and the deuterium enrichment. The quantity of combined radioactive phenol in each sample was determined from the radioactivity count, and with these data the appropriate correction was made in the aromatic and hydroxyl proton regions. Total hydroxyl proton content was determined by titration with sodium aminoethoxide in ethylenediamine. The resonance line for the hydroxyl proton in $CDCl_3$ is in the 390–370 c.p.s. region. In DMSO-d_6, however, hydroxyl protons are seen as two peaks from 580–525 c.p.s. and from 250–190 c.p.s. These assignments were verified by recording several spectra of depolymerization products at 120°C. Unlike the protons in hydrocarbons, the position of the OH hydrogen depends strongly on temperature. At 120°C. no absorption is obtained in the 580–525 area, and in the 250–190 c.p.s. region, the absorption is equivalent only to particular aliphatic protons. The hydroxyl proton in phenol dissolved in DMSO-d_6 produces a broad peak from 580–525 c.p.s. In the spectra of coal depolymerization products, the peak in the 580–525 region is equivalent to OH protons in the combined radioactive phenol. Evidently, the second line (250–190 c.p.s.) obtained in the spectra of depolymerization products is the result of hydroxyl protons on coal fragments. Therefore, the calculations for hydroxyl protons in samples recorded in DMSO-d_6 were made in the following manner. The broad peak at lower field was assigned completely to hydroxyl protons. Sufficient area to account for remaining hydroxyl protons was subtracted from the second peak at higher field and any remaining area in this region was assigned to aliphatic protons. The strong peak at 150 c.p.s. is caused by residual protons in the DMSO which have not exchanged with deuterium, and a correction is made for these protons in the analysis.

Discussion

Area assignments used for determining hydrogen types and two typical NMR spectra of coal depolymerization products are shown in Figure 1. These

Publication Date: January 1, 1966 | doi: 10.1021/ba-1966-0055.ch031

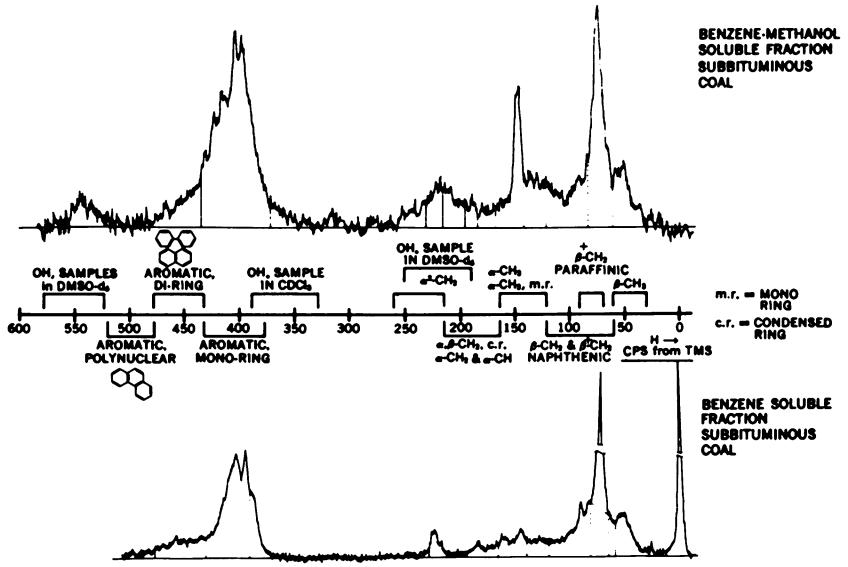

Figure 1. Integration limits and typical NMR spectra

assignments are based on the unpublished work of W. R. Ritchey of Standard Oil of Ohio, on the work of Yen and Erdman (*12*), and also on the spectra of model compounds evaluated by us. Ritchey's assignments are based on careful evaluation of the spectra of approximately 150 model compounds. This number included 80 aromatics, 60 paraffins and cycloparaffins, and about 10 olefins. The data derived from model compounds were used by Ritchey to evaluate the hydrogen distribution of petroleum fractions with a probable error of less than 5%.

In the aromatic region, a division is made between the monocyclic and bicyclic aromatics of the naphthalene and biphenyl type at 433 c.p.s. and between two-ringed compounds and more highly condensed aromatics at 480 c.p.s. The methylene bridge (α^2-CH_2) hydrogens absorb at 260–215 c.p.s. (Methylene protons in cyclic ethers like tetrahydrofuran and dihydropyran absorb in the same region as methylene bridge protons and would be included in estimates of methylene bridge hydrogens.) The region 215–166 c.p.s. is assigned to α,β-CH_2 groups in ethylene bridges, α-CH and α-CH_2 on condensed rings. α-CH_2 protons on monocyclic aromatics and α-CH_3 absorb from 120 to 166 c.p.s. Absorption from 120 to 60 c.p.s. is attributed to β and β^+-CH_2 protons. The intense narrow peak at approximately 73 c.p.s. is the result of a sizable number of protons in similar environment, identified as paraffinic chains β^+ to aromatic rings. A line was drawn at the base of the high peak. The area above the line is equivalent to β^+-CH_2 in chains, and the area below the line from 120 to 60 c.p.s. is equivalent to β-CH_2 and β^+-CH_2 naphthenic hydrogens. The area from 60 to 40 c.p.s. represents those protons in β-CH_3 groups.

Publication Date: January 1, 1966 | doi: 10.1021/ba-1966-0055.ch031

Table I. Hydrogen Distribution

Coal	Code No.	C % dmmf	Aromatic: Di + Cond. Ring	Aromatic: Mono Ring
Lignite	1	70.6	14.3	16.4
Subbituminous B	2	76.7	15.3	7.3
Bituminous HVA	4	82.4	8.4	11.2
Bituminous HVA	5	85.1	12.7	19.2
Bituminous HVA	6	85.8	7.4	16.6
Bituminous LV	7	90.7	18.0	13.0

• To condensed aromatic

Table II. Aliphatic and Aromatic

Coal	Code No.	Benzene Soluble: Aromatic	Benzene Soluble: Aliphatic	Benzene-Methanol Soluble: Aromatic	Benzene-Methanol Soluble: Aliphatic
Lignite	1	6.1	89.1	25.9	66.0
Subbituminous	2	16.0	82.4	24.3	63.5
Bituminous HVA	4	19.0	78.2	—	—
Bituminous HVA	5	22.5	74.3	21.4	63.5
Bituminous HVA	6	26.5	71.0	—	—
Bituminous LV	7	28.8	69.0	—	—

Detailed Breakdown of Hydrogen Types in Soluble Fractions. A detailed breakdown of hydrogen types based on NMR analysis of the total soluble material for each coal is summarized in Table I. Aromatic hydrogens in two-ring aromatics and condensed aromatics are combined in column 3. Condensed aromatic hydrogens are present in relatively small amounts, representing 10–15% of the total aromatic hydrogens. The bulk of the hydrogen in this group is associated with naphthalene and biphenyl structures. The absence of a significant number of hydrogens on three-ring and more highly condensed aromatics in coals of these types is in accord with the published results of many investigators, using other structural tools (*8*). Hydrogens attached to single-ring aromatics vary from 7 to 19% of the total hydrogen and make up from 30 to 70% of the aromatic type. No particular relationship with rank is evident.

Hydrogen in hydroxyl groups tends to decrease with increasing rank. Hydrogen in methylene bridges (column 6) varies over a factor of 5 from 2.4 to 14.0% of the total hydrogens. The implications of this information will be discussed in greater detail.

The next column includes α-CH_2, α-CH, and α,β-CH_3 groups, the latter representing ethylene bridges. This group of hydrogens decreases in general with increasing rank. This is followed by α-CH_3 and some types of α-CH_2 (column 7). These values would represent the maximum amount of α-CH_3 groups. Again, there is no apparent relationship with rank. The hydrogens in column 9 designated β- and β^+-CH_2 are the major type in the coals studied, comprising 20–37% of the total hydrogen. This group would include hydrogens attached to β-carbons in naphthenic rings. The total β-CH_2 and β^+-CH_2 protons in paraffinic chains and naphthenic rings are combined because of the overlap of zones of absorption of the NMR spectra. Chemical dehydrogenation

Publication Date: January 1, 1966 | doi: 10.1021/ba-1966-0055.ch031

of Total Soluble Material, %

	Aliphatic				
Hydroxyl	α -CH_2-	α-CH_2[a] α-CH α,β-CH_2	α-CH_2[b] α-CH_3	β and β^+ CH_2	β CH_3
4.6	14.0	12.6	13.1	20.8	2.9
5.2	4.5	7.2	15.8	37.5	7.2
4.7	5.3	11.1	19.6	29.3	8.5
3.8	2.5	6.2	17.4	29.2	9.0
3.5	2.4	5.6	16.1	36.7	11.5
3.9	3.2	4.7	16.3	32.3	6.2

[b] To monocyclic aromatic

Hydrogen in Soluble Fractions, %

Phenol Soluble		Total	
Aromatic	Aliphatic	Aromatic	Aliphatic
33.7	61.7	30.7	64.7
26.3	66.6	22.6	72.2
19.9	70.5	19.6	75.7
35.6	60.3	31.9	64.3
28.4	67.5	24.0	72.9
32.3	59.2	31.0	65.1

(*10*) of coals provides very strong evidence for the presence of significant amounts of naphthenic rings. The last column contains the β-CH_3 hydrogens and, except for the lignite (coal No. 1) with 2.9% shows little variation with rank.

Aliphatic-Aromatic Distribution of Fractions Separated by Solvent Extraction. The aromatic and aliphatic content of the depolymerization fractions separated according to solvent solubility are shown in Table II. In the lowest molecular weight, benzene-soluble material, the aromatic hydrogens increase with increasing rank. This relationship between aromaticity and rank has been reported by others (*1*, *2*, *9*). Since the benzene-soluble fractions from depolymerization of coal represent only a small part of the coals, the data reported in columns 2 and 3 are probably not representative of the whole coal. In the case of coal No. 1, the value of 89.1% aliphatic hydrogen for the benzene-soluble fraction reflects the concentration of hydrogens in methylene bridges as condensation products with tagged phenol from "aromatic interchange." In general, the aromatic character of the fractions increases with increasing molecular weight (*3*) if one compares benzene-methanol soluble with benzene-soluble and phenol-soluble with benzene-methanol soluble. The values for the benzene-methanol soluble fraction from coals No. 4, 6, and 7 were combined with phenol-soluble values because the intermediate solvent separation with benzene-methanol was omitted. Aromatic hydrogen values for the phenol-soluble fraction and the combined soluble material do not show any apparent relationship with rank.

Aromatic-Aliphatic Hydrogen Distributions in Coals of Different Rank. The aromatic hydrogen content of coals of different rank has been reported by a number of investigators using different analytical techniques (*1*, *5*, *6*, *9*).

Publication Date: January 1, 1966 | doi: 10.1021/ba-1966-0055.ch031

These values are summarized in Figure 2 and compared with our results on the soluble fractions from depolymerization. Van Krevelen (*9*) reported aromatic hydrogen values ranging from 23 to 54% for coals containing 76 to 89% carbon. Aromatic hydrogen content varies directly with rank. Brown (*1*) obtained values of 19–42% for a series of vitrains and showed a similar relationship with rank displaced toward lower aromatic values. Ladner and Stacey (*5*) analyzed two additional coals using the procedure developed by Brown, and the results fit Brown's correlation.

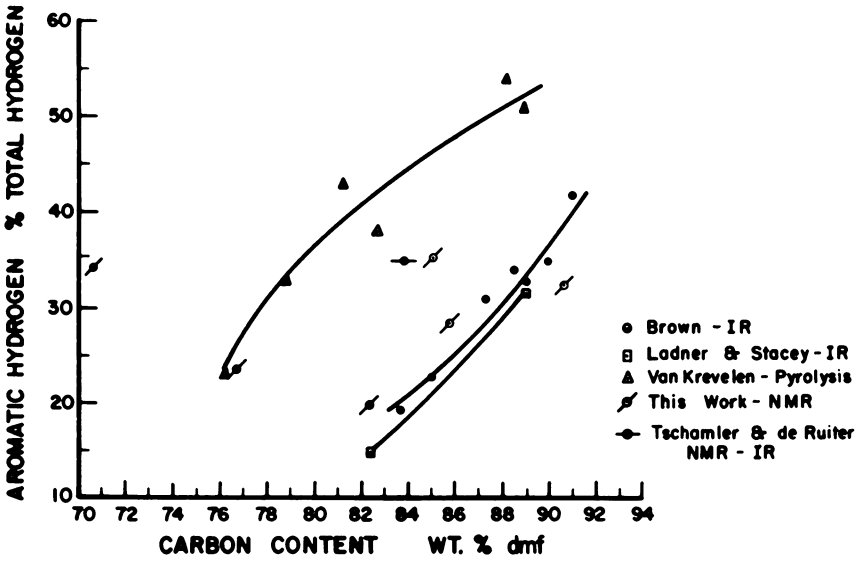

Figure 2. Aromatic hydrogen content vs. *coal rank*

Van Krevelen measured the amount of aromatic hydrogen in a coal by determining the residual hydrogen in a low temperature char and assumed that this residual hydrogen was completely aromatic. This assumption was not substantiated by carbonization of model compounds containing hydroaromatic structures. Hydroaromatic structures are accepted as an important part of the coal unit, and would not necessarily dehydrogenate completely at the temperatures used to prepare the char. High values for the aromatic hydrogen content would result. Brown determined the ratio of aromatic to aliphatic hydrogens by measurement of the infrared absorption at 3.3 and 3.34 μ and application of an arbitrary molar extinction coefficient. The aromatic C-H absorption band is part of the shoulder of the phenolic OH band which makes quantitative measurement difficult in low rank coals. Tschamler and de Ruiter (*6*) refined this method by calculating the ratio of the molar extinction of the solvent extracts from a coal, using NMR analysis to define the aromatic-aliphatic ratio and extrapolating this ratio to the parent coal. While this represents an improvement, the interference from the phenolic OH absorption with measurement of the aromatic C-H absorption is not reduced.

Publication Date: January 1, 1966 | doi: 10.1021/ba-1966-0055.ch031

The values reported from our own work were derived from the NMR analysis of the phenol-soluble extracts from which the benzene-soluble fraction was excluded. The benzene-soluble fractions contain a higher aliphatic hydrogen content than the higher molecular weight fractions. Over the range of coals studied, the aromatic hydrogen values derived from high resolution NMR do not vary directly with rank. A direct comparison cannot be made over the entire range of coals because a lignite was not included in the previous studies cited. Since coals No. 1 and 4 produced the highest yield of soluble material, the analyses of the depolymerization products from these coals should represent most closely the hydrogen distribution of the parent coals. Values for these coals of 33.7 and 19.9% represent an inverse relationship with rank. The value of 19.9% reported for coal No. 4 is somewhat lower than the figure (24%) reported in our earlier paper (3). The higher value was derived from NMR data which we believe are less precise because of the lower purity of the solvent used and the necessity of using high temperatures in the spectrometer.

For coals higher in rank than No. 4, there is a suggestion of increasing aromatic hydrogen content with rank. Coal No. 7 gave a very low yield of soluble material, and one can assume that the aromatic hydrogen value is low because the insoluble fraction shows a much lower H/C ratio than the soluble fraction. There is reasonably good agreement between our data and those of Brown (1) for coals containing 82–91% carbon. It is not surprising that there is no simple relationship between aromatic hydrogen content and rank. Rank, as defined by carbon content alone, does not fully describe the possible variations in chemical and petrographic composition.

Relationship Between Number of Methylene Bridges and Degree of Depolymerization. A relationship between the number of methylene bridges in a coal and the extent of depolymerization was mentioned briefly by us (3) in a recent publication. The data were based on NMR analysis of the benzene-

Table III. Methylene Bridges and Associated Monomeric Units

Coal	Code No.	Not Phenol[a] Soluble Product Wt. % dmmf Coal	Methylene Bridge Hydrogens Wt. % Total H in Coal	Calc. Mol. Wt.[b] of Monomeric Unit per CH_2	Mol. Wt. of Soluble Part of Coal
Lignite	1	73.0 (2.4)[c]	11.6	346	328
Subbituminous B	2	71.1 (6.3)	0.85	4500	311
Bituminous HVA	4	29.1 (18.0)	3.5	1100	689
Bituminous HVA	5	17.1 (11.7)	0.85	4100	632
Bituminous HVA	6	18.5 (6.5)	0.89	4100	570
Bituminous LV	7	8.7 (1.1)	0.57	7600	344

[a] Total soluble material—blank phenol soluble.
[b] Calculated as $R\text{-}CH_2$.
[c] Figures in parenthesis are blank phenol soluble yields.

Publication Date: January 1, 1966 | doi: 10.1021/ba-1966-0055.ch031

soluble fractions, which represent a relatively small part of the coal. Since the amount of methylene bridge hydrogens in the entire soluble fraction from each of six coals was now available, the quantitative contribution of the methylene bridges to depolymerization was re-examined. The yield of depolymerization products and the fraction of total hydrogen in methylene bridges are shown in Table III. Yields of depolymerization products for each coal were measured by subtracting the blank phenol-soluble material from the total phenol-soluble product. There appears to be a direct correlation between the number of methylene bridges in the coal and the amount of net phenol-soluble material recovered. Coal No. 1 with 11.5% methylene bridge hydrogens produced the highest yield of soluble material, 73.0%, and coal No. 7 with 0.5% methylene bridge hydrogens, the lowest yield, 8.7%. In the case of these two coals, the blank phenol-soluble yield was very small and would not contribute to the methylene bridges found in the soluble material. Coal No. 4 with 3.5% methylene bridge hydrogens gave the next highest amount of product, 29.1%. Coals No. 6, 2, and 5 follow in the order of the number of methylene bridges.

The role of methylene bridges in depolymerization can be evaluated further by comparing the calculated value for the size of a monomeric unit per CH_2 group with the experimentally determined average molecular weight of the soluble products. In the case of coal No. 1, the calculated and experimental values are 346 and 328, respectively, indicating that the methylene bridges are probably the sites for the depolymerization, and essentially all the bridges were cleaved. The yield of 73% soluble material confirms this. The residue was shown to be free of vitrain (3), which comprised 80% of the original lignite. If we compare the calculated molecular weight per CH_2 group of 1100 for coal No. 4 with the experimental molecular weight of 689, it is clear that methylene bridges are also responsible for the bulk of the depolymerization in this coal. The calculated molecular weights per CH_2 group for coals No. 2, 5, 6, and 7 are 7–25 times higher than the experimental molecular weights. This can be interpreted to mean that these coals contain large units connected to small units by CH_2 groups. Cleavage of the methylene bridge would yield a small soluble fragment accompanied by a larger insoluble fragment.

Publication Date: January 1, 1966 | doi: 10.1021/ba-1966-0055.ch031

Literature Cited

(1) Brown, J. K., *J. Chem. Soc.* **1955,** 744.
(2) Brown, J. K., Ladner, W. R., Sheppard, N., *Fuel* **39,** 79 (1960).
(3) Herédy, L. A., Kostyo, A. E., Neuworth, M. B., Intern. Conf. Coal Sci., *5th, Cheltenham,* 1963; *Fuel,* in press.
(4) Herédy, L. A., Neuworth, M. B., *Fuel* **41,** 221 (1962).
(5) Ladner, W. R., Stacey, A. E., *Fuel* **43,** 13 (1964).
(6) Tschamler, H., de Ruiter, E., *Brennstoff-Chem.* **43,** 212 (1962).
(7) Van Krevelen, D. W., "Coal," p. 449, Elsevier, New York, 1961.
(8) *Ibid.,* p. 333.
(9) Van Krevelen, D. W., Wolfs, P. M. J., Waterman, H. I., *Brennstoff-Chem.* **40,** 371 (1959).
(10) Wender, I., *et al., Fuel* **43,** 229 (1964).
(11) Wood, J. C., Moschopedis, S. E., Elofson, R. M., *Fuel* **40,** 193 (1961).
(12) Yen, T. F., Erdman, J. G., "Abstracts of Papers," 142nd Meeting, ACS, September 1962, p. 6S.

RECEIVED January 25, 1965.

Discussion

Peter H. Given: What was the petrographic purity of your vitrains? Have you any information about the behavior of other macerals than vitrinite?

Martin B. Neuworth: In some prior work, which will be published, we analyzed the six coals for petrographic composition and found they contained from 73 to 87% vitrain. In the case of coal No. 1, we compared the petrographic composition of the residue with the original lignite. On the basis of these analyses we would conclude that the vitrinite, resinite, and exinite fractions will undergo depolymerization with the rupture of certain aliphatic linkages. The semifusinite, micrinite, and fusinite appear to be inert.

Bhupendra Mazumdar: We consider the presence of isopropyl groups rather unlikely in coal in spite of the evidence put forward by Neuworth *et al.* These authors have worked on a lower rank bituminous coal, and the quantities of isopropyl groups obtained by them were rather small compared to the total methyl group content in such coals (as estimated by Kuhn-Roth method). Further, lower rank coals very often contain appreciable proportions of resins and waxes, and it is not unlikely that the isopropyl chain transfer during depolymerization with phenol-BF_3 reagent could have been caused by resins or similar bodies which may well be present as foreign inclusions in coal. Thus the evidence supporting the presence of isopropyl groups in coal structure is not unambiguous. On the other hand, we have worked mainly with vitrains, and from a study of the compatibility of the maximum estimate of methyl groups (from pyrolysis) with other forms of carbon in coal we are of the opinion that the aliphatic side chain is constituted mainly of methyl groups.

Dr. Given: I think that in his comment Dr. Mazumdar is using the expression "coal structure" to mean vitrinite structure. Surely "coal" is the total assembly of lithotypes and macerals found in any given location. I do not question the finding of Neuworth *et al.* that isopropyl groups were present in their coal samples. I do, however, question the significance of the result. Since the samples used sometimes contained as little as 73% vitrinite, the remainder consisting of other macerals, it is perfectly possible that the isopropyl groups are derived from some member of the exinitic group of macerals. It is already known that the latter macerals are more aliphatic than the associated vitrinite in bituminous coals and may well contain some terpene-derived material, so that the suggestion is reasonable. I suggest that the following calculation might be informative. Assume that all the isopropyl groups derive from a coal component accounting for 15% by weight of the whole coal. Does the calculated concentration of isopropyl groups in this component seem unreasonable if the component has 6.5–7% H (total), aromaticity (f_a) = 0.6 and H_{ar}/H_{al} = 0.15–0.2?

Dr. Neuworth: Our work on "whole" coal samples provided unequivocal evidence of isopropyl groups attached to aromatic nuclei. Obviously it is not possible to associate these isopropyl groups with particular macerals. However these isopropyl groups are not derived from "terpenes or related aliphatic pre-

Publication Date: January 1, 1966 | doi: 10.1021/ba-1966-0055.ch031

cursors." The acid-catalyzed transfer of an intact isopropyl group will occur only if the isopropyl group is attached to an aromatic nucleus. We did not intend to create the impression that isopropyl groups were the major types of aliphatic linkage in coals.

Leo Duffy: How accurate are the aliphatic hydrogen ratios reported?

Dr. Neuworth: Probably of the order of 10%.

Publication Date: January 1, 1966 | doi: 10.1021/ba-1966-0055.ch031

Proton and Carbon-13 NMR of Coal Derivatives and Other Carbonaceous Materials

H. L. RETCOFSKY and R. A. FRIEDEL

Pittsburgh Coal Research Center, Bureau of Mines, U. S. Department of the Interior, Pittsburgh, Pa.

Publication Date: January 1, 1966 | doi: 10.1021/ba-1966-0055.ch032

Complementary use of proton and carbon-13 nuclear magnetic resonance techniques has been applied to studying the mean structural units present in coal derivatives and other carbonaceous materials. The method requires using quantitative data from both proton and C^{13} spectra. Although PMR intensity measurements are known to be quite reliable, the corresponding C^{13} measurements have been explored very little. Intensity-concentration calibration curves for a series of alkyl aromatics and hydroaromatic compounds suggest that quantitative C^{13} data can be used with reasonable assurance of accuracy. The technique has been applied to several coal derivatives and chemically reduced coal derivatives.

The literature contains several papers on applying high-resolution proton nuclear magnetic resonance to studying both hydrogen and carbon distributions in coal and other carbonaceous materials (*1,2,3,4,5,7,8,10,11,13,14,15*). The structural parameters generally derived from the spectral data include the aromaticity, degree of aromatic ring substitution, and average size of the condensed ring system (*2,3,7,14*) although more recent work has been concerned with the aliphatic hydrogen distribution (*10*). In all material published to date, however, assumptions generally were made concerning one or more of these parameters before the others could be calculated. As one example, aliphatic branching indices were necessarily estimated before aromaticity calculations could be made for vacuum distillation products from coal (*8*). We propose to eliminate this and a number of other assumptions by complementing and sometimes replacing the proton NMR data with in-

In Coal Science; Given, P.;
Advances in Chemistry; American Chemical Society: Washington, DC, 1966.

formation gained from another NMR technique—namely, carbon-13 spectra of the materials.

To perform the C^{13} experiments we rely upon NMR signals arising from only naturally occurring carbon-13 in the material. The low natural abundance, $\sim 1.1\%$, along with its other unfavorable characteristics, does not allow the use of conventional NMR techniques such as those used to detect proton signals. Unlike hydrogen NMR signals, C^{13} signals are difficult to detect and possess unsymmetrical line shapes which make absolute intensity measurements impossible. The technique, at present, is limited in sensitivity and requires the use of neat liquids or highly concentrated solutions as samples. Later we will discuss methods for improving sensitivity.

We wish, now, to report what we believe is the first successful attempt to derive quantitative data from C^{13} NMR spectra and in particular to discuss application of the method to simple organic mixtures, to a liquid coal derivative, to two coal derivatives having desirable solubility characteristics, and to a crude oil.

Publication Date: January 1, 1966 | doi: 10.1021/ba-1966-0055.ch032

Experimental

All spectra were obtained on a Varian high-resolution instrument equipped with 60 mc./sec. and 15.085 mc./sec. radio-frequency units for the proton and carbon-13 studies, respectively. Magnetic fields of about 14.1 kg. were employed. Proton spectra were obtained using conventional operating techniques—i.e., observing the absorption mode under slow-passage conditions. The C^{13} spectra, however, were of the rapid-passage dispersion mode type previously described by Lauterbur (*13*). A constant sweep rate and transmitter power level were used when operating at the lower frequency. The double resonance experiments were performed using an NMR Specialties SD-60 spin decoupler.

Proton Spectra

Proton NMR spectra of coal derivatives generally give rise to either broad peaks or complicated multiplets which can be easily divided into band envelopes. For example, the H^1 spectrum of a coal-hydrogenation asphaltene (*4*) consists of three peaks, two of which overlap. A broad peak at lowest field is caused by protons in aromatic and phenolic systems, whereas two higher field peaks are caused by protons bonded to carbons situated α to aromatic rings and those bonded to other nonaromatic carbons, respectively. The ratios of these spectral areas are the same as the ratios of the hydrogens in each of these three hydrogen classes. This accounts for one of the most important characteristics of proton NMR spectra—namely, no calibration data are necessary.

Carbon-13 Spectra

The most valuable information one should be able to obtain from the carbon spectrum of a coal derivative is the ratio of aromatic to nonaromatic carbon atoms. We know of no other direct method by which this value can be obtained. Since the literature pertinent to C^{13} NMR is sparse, we wish to

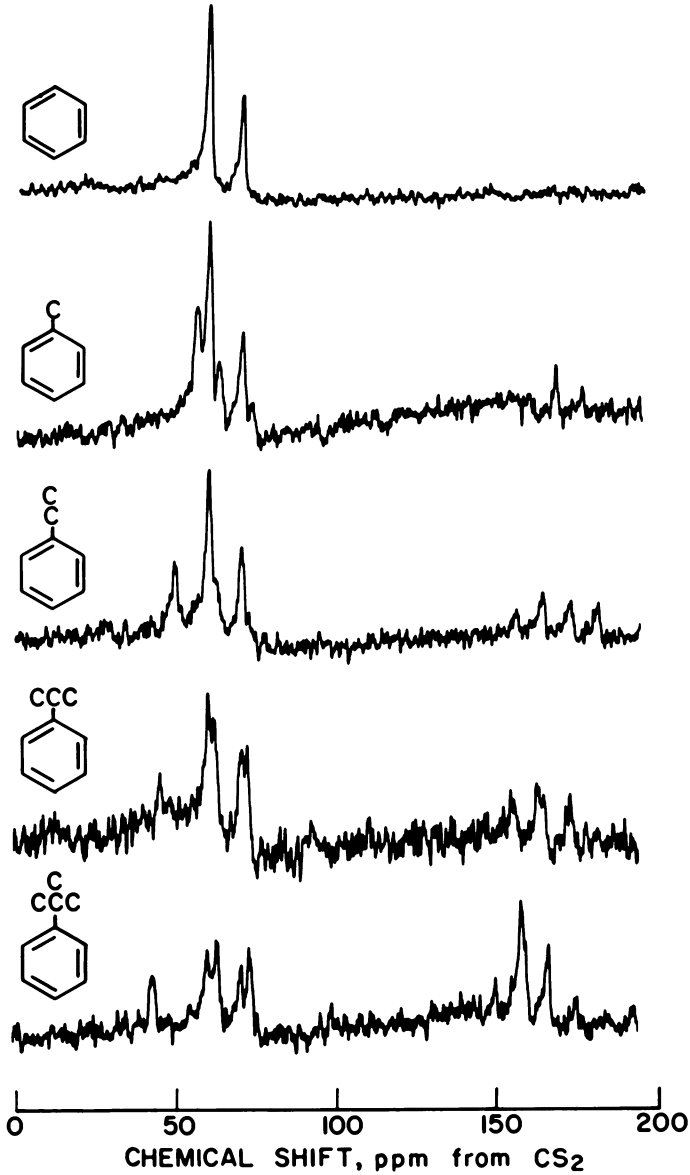

Figure 1. C^{13} spectra of aromatic compounds

discuss the spectra in more detail. Figure 1 presents some illustrative spectra of pure organic compounds. In spectra of alkylbenzenes, as well as in spectra of other materials, the aromatic carbon signals are found at low field, well separated from signals caused by saturated carbon atoms. Olefinic atoms exhibit signals in the same general region as aromatic carbons, triply bonded

carbons have their signals midway between those caused by saturated carbons and those caused by aromatic carbons, while carbonyl signals span a region below aromatic signals extending to very low magnetic fields (*14*). These chemical shifts are referred to carbon disulfide, whose C^{13} signal is taken arbitrarily as 0 p.p.m. In general it can be said that these chemical shifts depend on electron density, electronic excitation energies, and the bond multiplicities of the carbons under study (*15*).

Intensity measurements using rapid-passage dispersion mode spectra have been little explored to date. It became necessary, therefore, to study the quantitative aspects of C^{13} NMR. Our early work was limited to measurements on alkyl aromatic and hydroaromatic compounds. The results of intensity measurements on the C^{13} spectra of 15 compounds are illustrated graphically in Figure 2. Each point is the average of measurements on at least eight spectra, four of which were obtained with sweep increasing and four

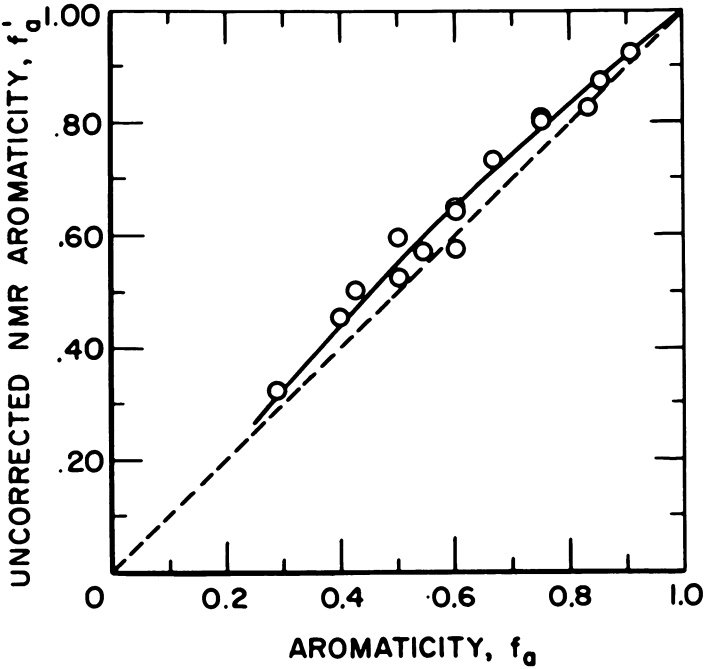

Figure 2. Aromaticity calibration curve for a C^{13} NMR spectrometer

with it decreasing. The liquid samples were run neat, while the solid ones were run as saturated carbon disulfide solutions. Plotted along the abscissa is the quantity which we designate f_a, the fraction of total carbons in the material which are present as aromatic carbons. The ordinate, f_a', refers to the fraction of the total area under the NMR curve assignable to aromatic carbon resonances. These 15 points were fitted to a second degree equation by the

Table I. Test of Least Squares Fit of C^{13} NMR Calibration Data

Compound	*Aromaticity*		
	Known	*C^{13} NMR*	*Dev.*
1-Methylnaphthalene	0.090	0.913	+.004
Toluene	0.857	0.850	—.007
2,3-Dimethylnaphthalene	0.833	0.791	—.042
p-Xylene	0.750	0.768	+.018
o-Xylene	0.750	0.775	+.025
Mesitylene	0.667	0.692	+.025
Tetralin	0.600	0.599	—.001
1,2,3,4-Tetramethylbenzene	0.600	0.610	+.010
tert-Butylbenzene	0.600	0.525	—.075
1-Methyl-4-*tert*-butylbenzene	0.545	0.522	—.023
1,3,5-Triethylbenzene	0.500	0.548	+.048
Hexamethylbenzene	0.500	0.476	—.024
Octahydrophenanthrene	0.429	0.452	+.023
1,3,5-Triisopropylbenzene	0.400	0.411	+.011
2,4,6-Tri-*tert*-amylphenol	0.286	0.295	+.009
			Av. ±0.023

method of least squares; the solid line shown is a plot of the calculated equation. The dotted line would result if the measured areas were directly proportional to the carbon distribution. It should be pointed out that the scatter of these points does not result from errors in reproducibility but is caused by characteristics of the nuclear signals involved.

The differences between the known aromaticity values and those calculated from the least squares equation are given in Table I. The mean value of the deviations, ±2.3% absolute, indicates the accuracy of the method, although in reality it only tests the fit of the calculated equation. The deviations were surprising in that they were smaller than anticipated.

Figure 3 indicates how well this aromaticity calibration curve is reproduced by C^{13} measurements on a series of benzene-cyclohexane blends. Here the dotted line is the calibration curve shown previously (Figure 2), while the solid line passes through the experimental points for the blends. The difference between the two curves is about 2%.

Interpreting the Data

It is appropriate now to re-emphasize just what reasonably quantitative data one can derive from the proton and C^{13} spectra. In this early work we assume that atoms other than carbon and hydrogen are present in only negligible amounts. The atomic hydrogen to carbon ratios can be evaluated from the elemental analyses of the materials and can be used to normalize the hydrogen and carbon NMR measurements so that they add to unity. The proton spectrum gives, after this minor modification, three items of information: h_{ar}, the fraction of total atoms in the material which is present as hydrogen atoms directly bonded to aromatic carbons; $h\alpha$, the fraction bonded to carbons situated α to aromatic rings; and $h\beta$, the fraction bonded to other nonaromatic carbons. The carbon spectrum in conjunction with the aromaticity calibration curve yields c_{ar}, the fraction of total atoms in the material

Publication Date: January 1, 1966 | doi: 10.1021/ba-1966-0055.ch032

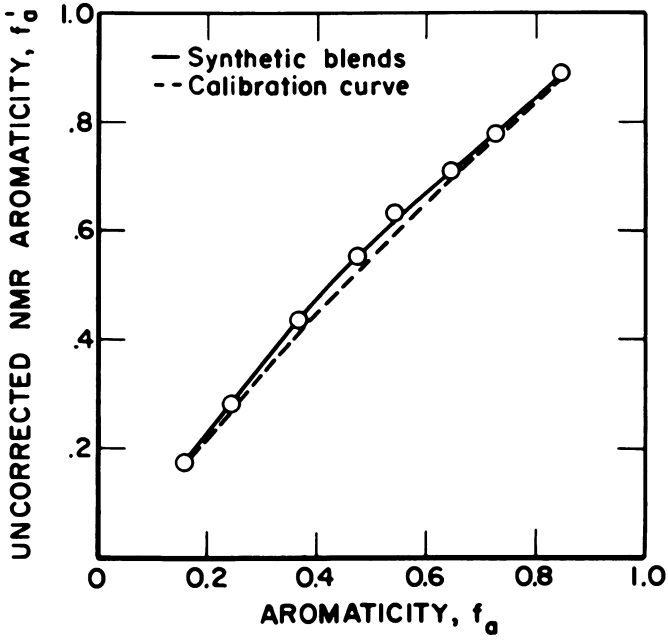

Figure 3. C^{13} NMR intensity data for benzene-cyclohexane blends

present as aromatic carbons, and c_{sat}, the fraction present as nonaromatic carbons. It is unfortunate that signals arising from saturated carbons located α to aromatic rings cannot be separated from signals caused by aliphatic carbons further removed from the rings. It will be shown later that this fact prevents precise calculations of certain structural parameters. Knowing these five quantities one can proceed to develop equations which will yield information as to the structure of an average molecule of the material under study.

Three of the more important structural parameters which can be derived from the H^1 and C^{13} data are the aromaticity, f_a, degree of aromatic ring substitution, σ, and the atomic hydrogen to carbon ratio for the hypothetical unsubstituted aromatic material, $[\frac{H}{C}]_{aru}$. The last parameter indicates the size of the condensed aromatic ring system. The first parameter, f_a, can be calculated utilizing only C^{13} spectral data and the calibration curve (Figure 1). It is important to note that no assumptions about the structure of the material need be made before f_a is calculated.

The other two parameters can be evaluated from complementary use of the C^{13} and proton data. In order to calculate these precisely, one needs to know the number of aliphatic carbons located α to aromatic rings and the number of those further removed. Unfortunately, as pointed out before, there is considerable overlap between these signals; the best one can do is to evaluate the total aliphatic carbon content, c_{sat}. By complementing the C^{13} data

Publication Date: January 1, 1966 | doi: 10.1021/ba-1966-0055.ch032

with proton data, upper and lower limits can be placed on $c\alpha$ and $c\beta$, and thereby on σ and $[\frac{H}{C}]_{aru}$. Since any carbon atom in an aliphatic grouping can bond to 0, 1, 2, or 3 hydrogen atoms, the minimum values for $c\alpha$ and $c\beta$ will be $h\alpha$ and $h\beta$, respectively. This corresponds to a molecule containing no saturate groups other than methyl groups. The maximum $c\alpha$ value occurs when $c\beta$ is minimized and vice-versa; therefore:

$$\frac{h\alpha}{3} \leq c\alpha \leq \left[c_{sat} - \frac{h\beta}{3} \right]$$

and

$$-\frac{h\beta}{3} \leq c\beta \leq \left[c_{sat} - \frac{h\alpha}{3} \right]$$

It can be shown that:

$$\frac{\frac{h\alpha}{3}}{h_{ar} + \frac{h\alpha}{3}} \leq \sigma \leq \frac{c_{sat} - \frac{h\beta}{3}}{h_{ar} + \left[c_{sat} - \frac{h\beta}{3} \right]}$$

and:

$$\frac{h_{ar} + \frac{h\alpha}{3}}{c_{ar}} \leq \left[\frac{H}{C} \right]_{aru} < \frac{h_{ar} + \left[c_{sat} - \frac{h\beta}{3} \right]}{c_{ar}}$$

The ratio $c\beta/c\alpha$ can also be evaluated, giving some information as to the chain length of the aliphatic or naphthenic systems. It is important to remember that one does not obtain a single value for these last three parameters but rather a range of values.

Applications

Synthetic Blend. To test the applicability of the equations, a six-component synthetic blend composed of two alkylbenzenes, two hydroaromatics, and a three- and a four-condensed ring aromatic was prepared, dissolved in CS_2, and spectra recorded. A comparison of spectral data and those known from the composition of the blend is given in Table II.

The first five parameters were obtained directly from intensity measurements on the proton and C^{13} spectra. The largest error is in the C^{13} measurement, although its magnitude is only about 4%. The aromaticity value and the limits placed on sigma and on the H/C ratio for the hypothetical unsubstituted aromatic nucleus are in reasonable agreement with the known values. It should be pointed out that three of the six components of the blend were not used in the original calibration curve.

Publication Date: January 1, 1966 | doi: 10.1021/ba-1966-0055.ch032

Table II. C^{13} and H^1 NMR Studies of a Six-Component Synthetic Blend

Structural Parameter	*Known Value*	*Spectral Value*
c_{ar}	0.35	0.36
c_{sat}	0.14	0.12
h_{ar}	0.22	0.23
$h\alpha$	0.17	0.17
$h\beta$	0.13	0.13
f_a	0.72	0.75
σ	0.25	0.19–0.26
$\left[\frac{H}{C}\right]_{ars}$	0.85	0.78–0.85

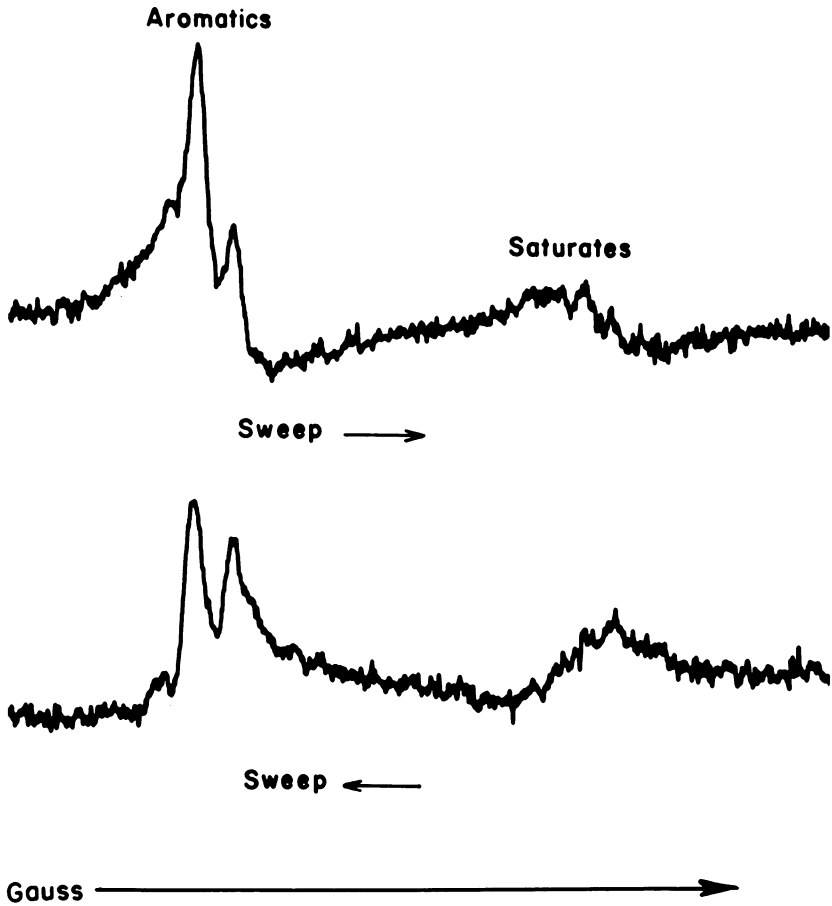

Figure 4. C^{13} NMR spectra of a neutral oil from 700°C. cracking of a 450°C. carbonization product from coal

Coal Derivatives. As our first test of the applicability of the method to a coal derivative we chose a material which is liquid at room temperature and whose structure had been studied extensively by other methods. The C^{13} spectrum of the material, a neutral oil obtained by cracking a coal-carbonization product, is shown in Figure 4. Both increasing and decreasing field sweeps are shown. Values of c_{ar} and c_{al} were obtained from these spectra. The proton spectrum, published elsewhere, gave values of h_{ar}, $h\alpha$, and $h\beta$ (*12*). The spectral data used in conjunction with the elemental analysis of the material indicated an average molecule of the neutral oil to be 70% aromatic and to consist of a naphthalene ring system bearing 2–3 saturate side chains. The side chains contain less than three carbon atoms. This information is consistent with other studies on the material. In particular, agreement with mass spectrometric studies is excellent.

The second application of the method to coal derivatives resulted from a series of studies on reduction products from coal derivatives. The extent of chemical reduction can, of course, be followed by measuring the hydrogen uptake by the material. Proton spectra give some indication as to where the hydrogen is going. Proton spectra of a wax oil (or heavy creosote) from coal and chemically reduced wax oil (Figure 5) illustrate the increase in intensity of the aliphatic hydrogen peaks and the decrease in the aromatic to nonaromatic hydrogen ratio in going from the original material to the reduced

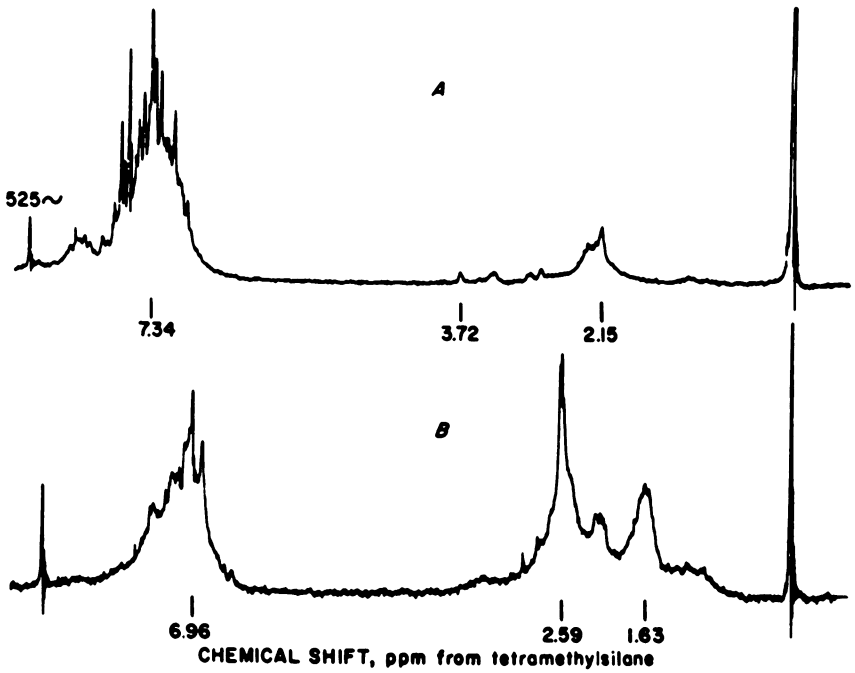

Figure 5. Proton magnetic resonance spectra of a wax oil from coal (a) and its reduction product (b)

material. Figure 6 shows the C^{13} spectra of the same two materials. The original material, the so-called wax oil, is seen to have a spectrum consisting only of aromatic carbon signals. Any other peaks are too weak to be observed. The spectrum of the reduction product indicates the appearance of a band in the aliphatic spectral region. Complementary use of data from the two spectral techniques suggested that the aromaticity of the material had decreased from about 0.95 to 0.75, the degree of ring substitution had increased, and the average size of the condensed ring system had decreased by approximately one ring. This is what one would expect from the results of similar studies on pure compounds.

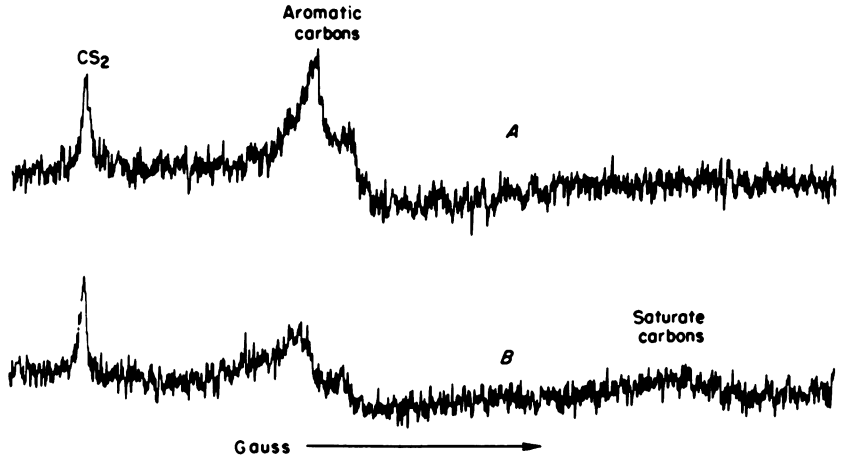

Figure 6. C^{13} NMR spectra of a wax oil from coal (a) and its reduction product (b)

Crude Petroleum. This method, in principle, should be applicable to all carbonaceous materials regardless of origin. Preliminary C^{13} measurements made on a sample of Ponca City crude oil (original petroleum of Project 6, American Petroleum Institute) yielded an aromaticity value of 0.15.

Methods of Signal Enhancement

Two methods of signal enhancement are particularly useful in C^{13} NMR experiments where signal-to-noise is rather poor owing to the low natural abundance of the isotope. Both can be performed using commercially available instrumentation although one of the methods has only recently been applied to NMR work.

The first method uses an averaging technique and can be performed using a computer of average transients (CAT). The CAT is able to sum and, in effect, average a large number of responses. That is, signals arising from nuclei will add to a finite number, whereas noise signals should integrate to

Publication Date: January 1, 1966 | doi: 10.1021/ba-1966-0055.ch032

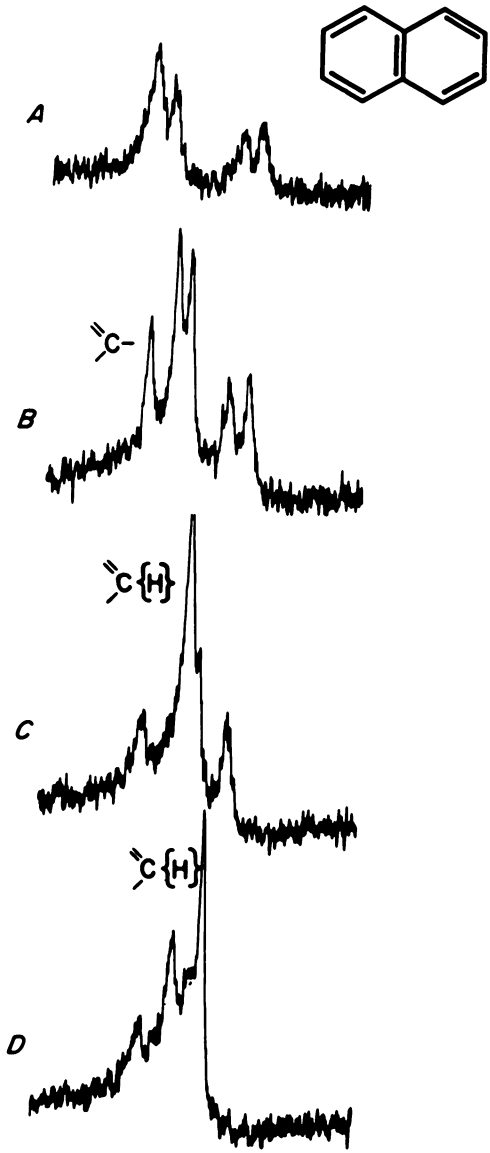

Figure 7. C^{13} NMR spectra of naphthalene

about zero. The signal-to-noise ratio improves by the square root of the number of accumulations. The equipment is rather expensive and requires an accurate sweep reproducibility by the NMR instrument used. We do not have a CAT at the Bureau of Mines at present but are aware of successful operation in other laboratories.

The second method is the so-called double resonance or spin-decoupling technique by which one nucleus is observed at its natural precessional frequency while another is irradiated at its own natural frequency in the same applied magnetic field. This produces a spectrum devoid of fine structure resulting from spin-spin interactions between the two different nuclei and results in not only a signal enhancement, but also a spectrum simplification. An example is shown in Figure 7—the C^{13} NMR spectra of naphthalene. The normal naphthalene spectrum (Figure 7a) should consist of a single line for the bridgehead carbon atoms plus two doublets (spin-spin multiplets) for the two different groups of aromatic atoms bearing hydrogens. The two doublets are easily seen, but the single line is not readily observable. By applying a second RF field close to the decoupling frequency, we see the components of the doublets move closer together (Figure 7b); at the same time a single line is revealed at low field. The last two spectra (Figure 7c and d) show the patterns obtained as each of the two doublets is collapsed. The low-field line remains fixed in position and is thereby assigned to the bridgehead carbon signals.

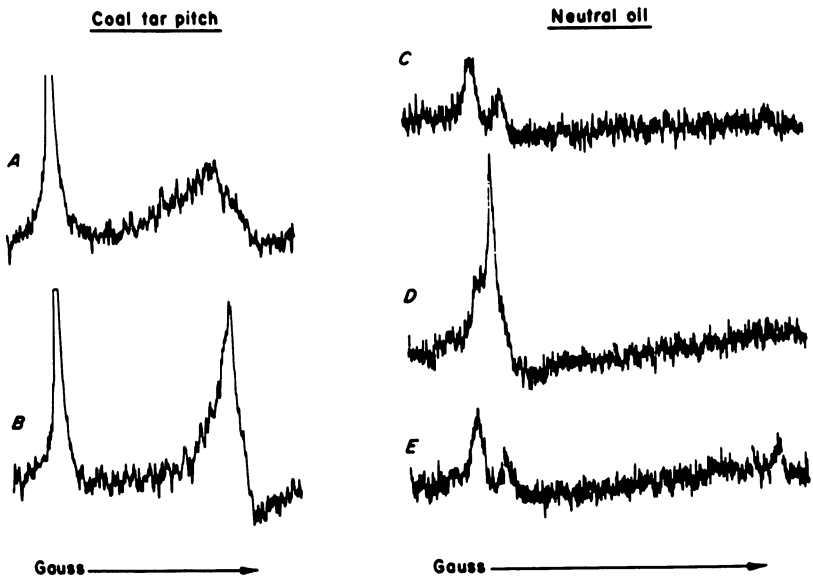

Figure 8. C^{13} NMR spectra of coal derivatives

Figure 8 presents the results of initially applying the spin-decoupling technique to two coal derivatives—a carbon disulfide extract of coal-tar pitch and the neutral oil discussed previously. The normal pitch spectrum exhibits a broad peak resembling a doublet in the aromatic region of the spectrum. No aliphatic carbon signals could be observed. The strong signal at low field is caused by the solvent. The double resonance spectrum at the bottom clearly demonstrates the signal enhancement one can obtain (Figure 8b).

The neutral oil spectrum exhibits both aromatic and aliphatic carbon signals. The aliphatic signals are more easily seen in Figure 4. Double irradiation of the aromatic region produces a strong signal enhancement and reveals low-field signals (Figure 8d) which are assignable to bridgehead carbons and to carbon atoms bearing alkyl or naphthenic substituents. The bottom spectrum shows the signal enhancement of the aliphatic carbon peaks when they are doubly irradiated.

Acknowledgments

The authors are indebted to the Organic Chemistry Project of the Pittsburgh Coal Research Center for supplying samples of the coal derivatives and for carrying out the catalytic hydrogenation of the sample of wax oil, and to Dr. B. Mair of the American Petroleum Institute who supplied a sample of the original petroleum of API Project 6. The samples of API research hydrocarbons used in this study were purified and made available by the American Petroleum Institute Project 58B at the Carnegie Institute of Technology. Most of these were synthesized by the API Research Project 58A at the Ohio State University.

Literature Cited

(1) Brown, J. K., Ladner, W. R., Sheppard, N., *Fuel* **39**, 79 (1960).
(2) Brown, J. K., Ladner, W. R., *Fuel* **39**, 87 (1960).
(3) Dewalt, C. W. Morgan, M. S., *Preprints Papers Symp. Tars, Pitches, Asphalts, Atlantic City, 1962*, ACS, Div. Fuel Chem., p. 33.
(4) Friedel, R. A., *J. Chem. Phys.* **31**, 280 (1959).
(5) Friedel, R. A., *Proc. Conf. Carbon, 4th, Buffalo, 1959*, p. 321, Pergamon Press, New York, 1960.
(6) Friedel, R. A., Retcofsky, H. L., *J. Am. Chem. Soc.* **85**, 1300 (1963).
(7) Friedel, R. A., Retcofsky, H. L., *Proc. Conf. Carbon, 5th, Univ. Park, Penna., 1961*, Vol. 2, p. 149, Macmillan, New York, 1963.
(8) Ladner, W. R., Stacey, A. E., *Fuel* **40**, 295 (1961).
(9) Lauterbur, P. C., "Determination of Organic Structures by Physical Methods," Vol. 2, pp. 472–475, F. C. Nachod and W. D. Phillips, Eds., Academic Press, New York, 1962.
(10) Oth, J. F. M., Tschamler, H., *Fuel* **42**, 467 (1963).
(11) Oth, J. F. M., Tschamler, H., *Brennstoff-Chem.* **43**, 177 (1962).
(12) Pople, J. A., *Mol. Phys.* **7**, 301 (1963–4).
(13) Williams, R. B., *ASTM Special Tech. Publ.* No. **224**, 168 (1958).
(14) Williams, R. B., *Spectrochim. Acta* **14**, 24 (1959).
(15) Winniford, R. S., Bersohn, M., *Preprints Papers Symp. Tars, Pitches, Asphalts, Atlantic City, 1962*, ACS, Div. Fuel Chem., p. 21.
RECEIVED October 5, 1964.

33

Electrochemical Reductions in Ethylenediamine

H. W. STERNBERG, C. L. DELLE DONNE, R. E. MARKBY, and I. WENDER

U. S. Bureau of Mines, Pittsburgh Coal Research Center, Pittsburgh, Pa.

The effect of operating variables on the electrochemical reduction of tetralin used as a model compound for the hydrogenation of coal is described. The effect of adding a proton donor (*tert*-butyl alcohol) on the reduction of an olefin was also investigated.

Publication Date: January 1, 1966 | doi: 10.1021/ba-1966-0055.ch033

Electrochemical reduction of coal in ethylenediamine in the presence of lithium chloride has proved to be a powerful method for hydrogenating coal under extremely mild conditions. As much as 53 hydrogen atoms were added per 100 carbons. The reduced coal was light grayish-tan and was 78% soluble in pyridine and 30% soluble in benzene at room temperature (7). At present, this method of reduction is time consuming mainly because the current efficiency is low, only 10–20%. Further, the carbon cathode became brittle and eroded and had to be replaced repeatedly. This paper describes the effect of cation, anion, and cathode material on current efficiency in reducing tetralin, a model substance for the hydrogenation of coal.

The complete reduction of coal proceeds from aromatic rings through rings containing olefinic double bonds to saturated compounds. While reduction of the benzene ring takes place at a current efficiency of about 80% (*8*), current efficiency for reducing an olefin (1-decene) is only 27% as shown in this paper. The slow step in the coal reduction may very well be reduction of olefinic double bonds. An increase in the rate of olefinic double bond reduction may therefore lead to a considerable increase in current efficiency.

Since proton addition is known (*3*, *4*) to be a rate-determining step in the chemical reduction of aromatic and olefinic double bonds in the alkali-amine system, the effect of adding a proton donor (*tert*-butyl alcohol) on current efficiency in the electrochemical reduction of 1-decene was investigated.

Experimental

Reductions were carried out in the electrolysis vessel shown in Figure 1. One reduction (No. 14) was carried out in a divided cell provided with a

In Coal Science; Given, P.;
Advances in Chemistry; American Chemical Society: Washington, DC, 1966.

coarse, fritted disc of 40 mm. diameter. The following experimental conditions prevailed for the runs listed in Table I except where marked by footnotes:

Temperature: 30°–35°C.

Surface of electrode: 7 sq. cm.

Electrolyte: 100 ml. ethylenediamine, 0.33*M* in electrolyte.

Substrate: 3 ml. (0.022 mole) peroxide-free tetralin, prepared by shaking tetralin with equimolar amounts of solid sodium bisulfate and ferrous sulfate, giving a solution 0.22*M* in tetralin.

Applied voltage: 110–150 volts.

Current: 0.45–0.50 amp.

The current was integrated by a current integrator described by Lingane (5) to give the amount of Faradays passed through the solution, an amount corresponding to 42.4% conversion of the tetralin to hexalin at 100% current efficiency. To isolate the reduction products, the solution was poured onto ice, and the resulting aqueous solution was extracted with pentane; the extract was

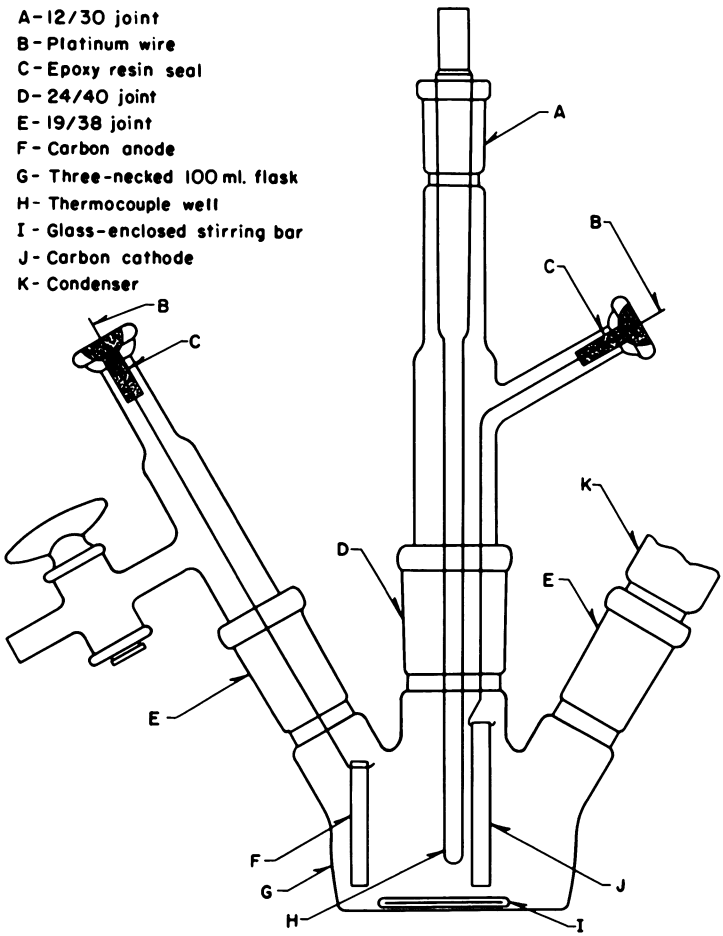

Figure 1. Electrolysis vessel

Publication Date: January 1, 1966 | doi: 10.1021/ba-1966-0055.ch033

treated in turn with dilute acid, bicarbonate, and water, dried over anhydrous calcium sulfate, filtered, and the bulk of the pentane removed by fractional distillation as described previously (*8*). The residue was analyzed mass spectrometrically. The results are summarized in Table I.

Table I. Reduction of Tetralin

No.	Electrolyte	Cathode	Current Efficiency, %	Product Distribution, % Hexalin	Octalin
1	LiCl	Carbon	76.8	85.9	14.1
2	LiCl	Platinum	49.1	82.0	18.0
3	LiCl	Lead	49.5	66.9	33.1
4	LiCl	Copper	37.1	81.9	18.1
5	LiCl	Aluminum	82.0	64.2	35.8
6	LiI	Aluminum	44.3	86.4	13.6
7	RbI	Aluminum	46.6	55.7	44.3
8	$(C_4H_9)_4NI$	Aluminum	14.8	86.3	13.7
9[a]	$(CH_3)_4NCl$	Aluminum	5.8	92.3	7.7
10	$(C_2H_5)_4NCl$	Aluminum	0.4	100.0	0.0
11[b]	$(CH_3)_3SCl$	Aluminum	5.7	77.8	22.2
12	$(C_2H_5)_4NClO_4$	Aluminum	2.9	37.5	62.5
13[c]	LiCl	Aluminum	8.3	63.0	37.0
14[d]	LiCl	Aluminum	27.3	9.3	90.7

[a] Conc., 0.16*M* (sat.); applied potential, 300 volts; current, 0.15 amp.; time, about 3.3 hours.
[b] Conc. 0.22*M* (sat.).
[c] Temp., 80°C.
[d] Divided cell; applied potential, 185 volts; current, 0.3 amp.; time, about 1.7 hours.

Reduction of 1-decene had to be carried out at a lower concentration (0.073*M*) since decene was not completely soluble at the concentrations used in the case of tetralin (0.22*M*). Electrolysis was interrupted after 0.0062 Faradays were passed through the solution, corresponding to 42.2% conversion of 1-decene to decane at 100% current efficiency. In these runs, a carbon cathode was used. Current efficiency for reducing 1-decene was 27.3%. In the presence of an equimolar amount of *tert*-butyl alcohol (0.073*M*), the current efficiency for 1-decene was 38.6%, corresponding to a 41% increase.

Discussion

Effect of Cathode Material. Cathode material has a pronounced effect on current efficiency and product distribution. Highest current efficiency and highest percentage of octalin was obtained with aluminum as may be seen by comparing run 5 with 1, 2, 3, and 4. A high percentage of octalin was also obtained with a lead electrode (run 3), but current efficiency was low.

Effect of Cation. Of all alkali chlorides, only lithium chloride is sufficiently soluble in ethylenediamine to act as an electrolyte. On the other hand, all alkali iodides are soluble in ethylenediamine. Since the anion has a large effect on current efficiency, a common anion such as the iodide ion must be used to compare the effect of the various cations. The results of runs 6 and 7 show that the current efficiency was slightly higher and the percentage of octalin formed much greater when rubidium iodide was used instead of lithium iodide. The metallic cations Li^+ and Rb^+ give markedly better current efficiency than the organic cations (runs 6, 7, 8, and runs 5, 9, 10, 11).

Effect of Anion. Comparing runs 5 and 6 shows that the halide anion has a large effect on both current efficiency and the amount of octalin formed. The

Publication Date: January 1, 1966 | doi: 10.1021/ba-1966-0055.ch033

drop in current efficiency is probably caused by iodide's catalyzing the reaction of amine with lithium to give hydrogen and amide:

$$2Li^{\cdot} \ldots e^{-} + 2RNH_2 \xrightarrow{I^-} 2RNHLi + H_2$$

Experimental evidence in support of this explanation is the fact that lithium added to a solution of lithium iodide in ethylenediamine dissolves without imparting a blue color to the solution—i.e., reacts immediately to give the amide. By contrast, lithium added to a solution of lithium chloride in ethylenediamine dissolves and imparts a deep blue color to the solution. The catalytic effect of iodide anion may be related to the effect of iodide anion on the electron spin resonance (ESR) absorption of solutions of alkali metals in liquid ammonia. Catterall and Symons (*2*) observed a drastic change in the presence of alkali iodides but very little change in the presence of alkali bromides or chlorides. They attributed this change to interaction of the solvated electron with the 6 *p* level of the iodide anion.

Perchlorate anion gives higher current efficiency than chloride anion (runs 10 and 12). The low current efficiency in these runs is caused by the presence of the organic cation.

Effect of Temperature and Cell Divider. Increase in temperature (runs 5 and 13) lowers current efficiency but does not affect product distribution. Using divider (runs 5 and 14) decreases current efficiency but shifts product distribution drastically in favor of octalin over hexalin. Similar results were obtained by Benkeser *et al.* (*1*) in their electrochemical reduction of aromatic compounds in methylamine.

Effect of Proton Donor. The increase in current efficiency on adding a proton donor is consistent with the work reported by Krapcho and Bothner-By (*3*) and Krapcho and Nadel (*4*). These authors showed that the rate of reduction of the benzene ring and of olefins by alkali metals in liquid ammonia and amines is proportional to the concentration of alkali metal, substrate, and proton donor.

The 41% increase in current efficiency on reducing 1-decene achieved by adding an equimolar amount of butyl alcohol may prove significant in connection with the reduction of coal. It has been shown previously (*6*) that current efficiency for coal reduction is about 15%. An increase of 41% in current efficiency would represent a substantial saving in time and current.

Conclusion

Based on results of electrochemical reductions of tetralin in ethylenediamine, current efficiency is highest with aluminum as cathode material and with lithium chloride as electrolyte. A substantial increase in current efficiency was obtained in reducing 1-decene by adding a proton donor.

Literature Cited

(1) Benkeser, R. A., Kaiser, E. M., Lambert, R. F., *J. Am. Chem. Soc.* **86,** 5272 (1964).
(2) Catterall, R., Symons, M. C. R., *J. Chem. Soc.* **1964,** 4342.

Publication Date: January 1, 1966 | doi: 10.1021/ba-1966-0055.ch033

(3) Krapcho, A. P., Bothner-By, A. A., *J. Am. Chem. Soc.* **81,** 3658 (1959).
(4) Krapcho, A. P., Nadel, M. E., *J. Am. Chem. Soc.* **86,** 1096 (1964).
(5) Lingane, J. J., "Electroanalytical Chemistry," p. 346, Interscience Publishers, Inc., New York, 1959.
(6) Markby, R. E., Sternberg, H. W., Wender, I., *Nature* **199,** 997 (1963).
(7) Markby, R. E., Sternberg, H. W., Wender, I., "Abstracts of Papers," 145th Meeting, ACS, Sept. 1963, p. 4K.
(8) Sternberg, H. W., Markby, R. E., Wender, I., *J. Electrochem. Soc.* **110,** 425 (1963).

RECEIVED January 25, 1965.

Discussion

Laszlo A. Heredy: What is the evidence for the conclusion that carbon-carbon linkages are not broken during reduction?

Heinz W. Sternberg: Many organic compounds have been reduced at 90–100°C. with lithium in ethylenediamine (L. Reggel, R. A. Friedel, I. Wender, *J. Org. Chem.* **22,** 891 (1957)). Recovery and analysis of the reaction products showed that carbon-carbon bonds were not broken in this reaction. We therefore do not think that any carbon-carbon bonds are broken during electrolysis which is carried out under even milder conditions (35°C.) than the chemical reduction (90°–100°C.).

George Kapo: Did you say that the reduction between the lithium and the coal was a homogeneous reaction?

Dr. Sternberg: We believe that it is the solvated lithium cation that is being reduced at the cathode to solvated zero charged lithium atom. The solvated lithium then reacts with the coal. This latter reaction may be homogeneous or heterogeneous depending on whether the coal molecule is solvated or not.

George A. Hill: Were any kinetic measurements made at low lithium chloride concentrations to determine the reality of Li^+ transfer of the electron from the electrode to the coal?

Dr. Sternberg: No kinetic measurements were carried out with coal. We did carry out measurements with tetralin using lower lithium chloride concentrations and found a marked decrease in the rate of reduction. However, interpreting the results will have to await perfection of a better technique (now under study) for carrying out these reductions at a controlled potential.

General Discussion

Hubert Tschamler: Four papers deal with soluble products representing a high percentage of the starting coal and which have been obtained by:

(1) Tetralin extraction at 250°C. (Chap. 27).

(2) Phenanthrene extraction at the atmospheric boiling point of the solvent (Chap. 28).

(3) The phenol-boron trifluoride reaction at 100°C. (Chap. 31).

(4) Electrochemical reduction in ethylenediamine (Chap. 33).

At the Fifth International Conference on Coal Science at Cheltenham in 1963, R. Brücker (Bergbau-Forschung GmbH, Essen-Kray) reported on the high solubility of coals, especially vitrinites in tetrahydroquinoline at 300°C. in an autoclave. Based on these preliminary experiments Dr. de Ruiter and I studied this reaction more carefully. As starting material a vitrinite (83.9% C, petrographic purity > 99%) as well as its pyridine-insoluble residue have been

Table A. Analytical Data and Structural Parameters of the Pyridine-Soluble, Benzene-Insoluble Part of a Vitrinite and the Corresponding Pyridine-Insoluble Residue After THQ Treatment Compared with Those of the Starting Materials

	Vitrinite			*Pyridine-Insoluble Residue*	
Parameter	*Original*	*THQ[b]—Treatment*		*Original*	*THQ*
Reaction temp. (°C.)		300	350		320
Pyridine soluble (wt%)	25	~95	~95	0	~90
Pyridine soluble-Benzene insoluble (wt%)	20	85	56	0	69
$\bar{M}$		2400 ± 300	2400 ± 300		2500 ± 300
Volatile matter (%)	35	43	42	34	38
C (maf)	83.9	84.2	84.4	83.3	84.4
H (maf)	5.5	5.6	5.8	5.4	5.6
O (maf)	8.0	6.0	5.2	9.0	6.4
N (maf)	1.4	2.3	3.2	1.4	1.5
$S_{(diff.)}$	1.2	1.9	1.4	0.9	2.1
H/C	0.780	0.792	0.819	0.772	0.791
R_{ar}(UV)	3.40 ± 0.70[a]	4.1	4.1	3.45 ± 0.65[a]	4.1
f_a(UV)	0.77[a]	0.76	0.76	0.77[a]	0.76
$\frac{H_{ar} + H_{ol}}{H}$ (PSR)			0.40		0.41
$\frac{H_{al}}{H}$ (PSR)			0.60		0.59
% H_{al} (IR)	3.3	3.5	3.3	3.2	3.5
$\frac{H_{al}}{H}$	0.60	0.62	0.57	0.59	0.62
% H_{ar} (IR)	1.9	(2.0)	(2.4)	1.95	2.0
$\frac{H_{ar}}{H}$	0.35	0.36	0.41	0.36	0.36

[a] From x-ray analysis
[b] THQ = tetrahydroquinoline

Publication Date: January 1, 1966 | doi: 10.1021/ba-1966-0055.ch033

used. Results are summarized in Table A. The reaction temperature was chosen between 300° and 350°C., and after tetrahydroquinoline (THQ) treatment, between 90 and 95% of the starting materials had gone into solution. During the reaction some H_2O, H_2S, and NH_3 were formed. To separate the soluble material from the excess of THQ and some quinoline formed during the reaction, a benzene extraction was carried out. The benzene-insoluble material was more or less free from impurities and decreased from 85 to 56% with increasing temperature. The mean molecular weight, determined in pyridine (method of Hill Baldes) is of the order of 2500 ± 300. The mean molecular weight of the benzene-insoluble fraction is of the order of 1300 when the reaction temperature is about 375°C. Table A shows that volatile matter and elementary analysis for %C and %H are comparable for all samples whereas there is a definite decrease in the oxygen content and sometimes a definite increase of the nitrogen content (still small amounts of solvent present).

The structural parameters so far obtained (Table A) are practically the same for all samples, and it can be assumed therefore that mainly only weak bonds (C-O-C, C-S-C . . .) have been broken by the reaction. Finally, one may ask the authors of the four papers mentioned above whether they have determined the mean molecular weights of the soluble products they have obtained in a completely different way.

Martin B. Neuworth: The molecular weights of the soluble fractions from our work were determined cryoscopically in sulfolane. Values of the order 300–700 were obtained. Using phenol solubility as a criterion of degradation limits the upper molecular weight to values below 1000.

George R. Hill: Molecular weight determinations are now being made with an osmometer. We assumed that molecular weight decreases with degree of extraction (or increase in temperature).

Bhupendra K. Mazumdar: Several papers relate to solubility or coal dispersion in different solvents and at different temperatures. Was any knowledge concerning the nature of linkage between the "units" of coal structure derived from these studies on the kinetics of solvation?

Dr. Hill: We agree with Dr. Mazumdar that a detailed knowledge of the specific nature of the linkages broken in "solvation" and dissolution processes is needed. The data reported in our paper give "activation energy" averages for many simultaneously occurring processes. At this point one can only say that in the low temperature region (below 280°C.) with this high volatile coal in tetralin, the bonds broken are not stronger than physical adsorption forces or hydrogen bonds. An average heat of activation of 80 kcal. found in the high temperature region plainly points to extensive rupture of normal covalent bonds (i.e., pyrolysis) accompanying and accounting for the increased solubility of the coal. Differential solution tests on once extracted coal may make it possible to evaluate more specific rate-determining steps.

Peter H. Given: I should like to remark on "model structures" for coals. Chemists have often been criticized for offering information about "coal structure" based on experiments with whole coals or with imperfectly characterized materials. Even when one works with what is believed to be reasonably pure materials, there may be questions raised.

Publication Date: January 1, 1966 | doi: 10.1021/ba-1966-0055.ch033

There has been available for some years unarguable evidence that each of the major macerals groups has a distinct set of structural characteristics, and that the major macerals in any one coal do differ materially in chemical structure from each other. We must therefore admit that chemical "structures" alleged to represent whole coals are futile, and that basic chemical research should use single macerals in as pure a state as possible. On the other hand, some believe that pure vitrinite macerals at least can be represented usefully by a model structure.

At the same time, it is perhaps not unreasonable to ask coal petrographers to refrain from undue criticism unless they are prepared to help us select, separate, and characterize suitable materials for chemical research.

Marie-Therese Mackowsky: I would like to make a suggestion. In Germany, France, Belgium, and Holland we have a so-called "central store" for pure macerals. This is the laboratory of Dr. Kröger. Consequently, we have a "maceral bank," and we can ask Prof. Kröger to send us a few grams of vitrinite, exinite, or micrinite. Perhaps you could have the same here, located perhaps at Pennsylvania State University.

Dr. Given: I think this is an excellent suggestion which we must follow up.

Irving Wender: Where can I find coals from which micrinites can be separated without too much difficulty?

James M. Schopf: Micrinites cannot be found readily in the coals of Pennsylvania, but several coals in West Virginia yield them in separable form.

Dr. Hill: Any general model structure for high volatile bituminous coal is at best an average representation containing the proper percentages of each kind of functional atom and group of atoms. The present state of knowledge does not allow us to define precisely a coal "molecule" if indeed there is "one." All coals differ, and each individual coal sample contains a heterogeneous mixture of high molecular weight aggregates, the average constitution of which can be represented by a model.

Publication Date: January 1, 1966 | doi: 10.1021/ba-1966-0055.ch033

Microscopic Investigations of Pore Formation during Coking

MARIE-THERESE MACKOWSKY and EVA-MARIE WOLFF

Bergbau-Forschung G.m.b.H., Essen-Kray, Germany

Publication Date: January 1, 1966 | doi: 10.1021/ba-1966-0055.ch034

Early work has shown that coke strength can be calculated from the results of maceral analyses and reflectance measurements, assuming that the coking conditions are constant. Juranek, Ritter, Mackowsky, and Wolff have contributed information on the influence of particle size, bulk density, and coal rank on coke formation. The results of these latter investigations are summarized, and the effect of varying the rate of heating between 0.5 and 300°C./min. is reported. Coals of different rank behaved differently as the rates of heating were varied. Hence, coke formation should not be described solely in terms of coal composition. Finally, an attempt is made to explain some anomalies in the coking behavior of coals, particularly expansion, in terms of differences in the chemical composition of the coals.

Investigating the relationship between coal rank and maceral composition on the one hand, and coking properties on the other hand, has been one of the main topics of applied coal petrography for more than 30 years. From studies by Amossow and Eremin (*1*, *6*) Berry (*2*), Harrison (*7*), and Schapiro, Gray, and Eusner (*14*, *15*), it was possible to calculate coke strength with considerable accuracy on the basis of known maceral composition and reflectance distributions. Paralleling these studies, Mackowsky and Echterhoff (*5*, *10*, *11*), Ritter and Juranek (*12*, *13*), and recently Brown and Taylor (*3*) have studied the transformation of coal to coke. Some results of these studies on coke formation are discussed.

The first insight into processes occurring in the plastic zone resulted from research by Echterhoff and Mackowsky (*5*). Figure 1 represents an overall picture of the microscopic research findings. A plastograph curve has been

In Coal Science; Given, P.;
Advances in Chemistry; American Chemical Society: Washington, DC, 1966.

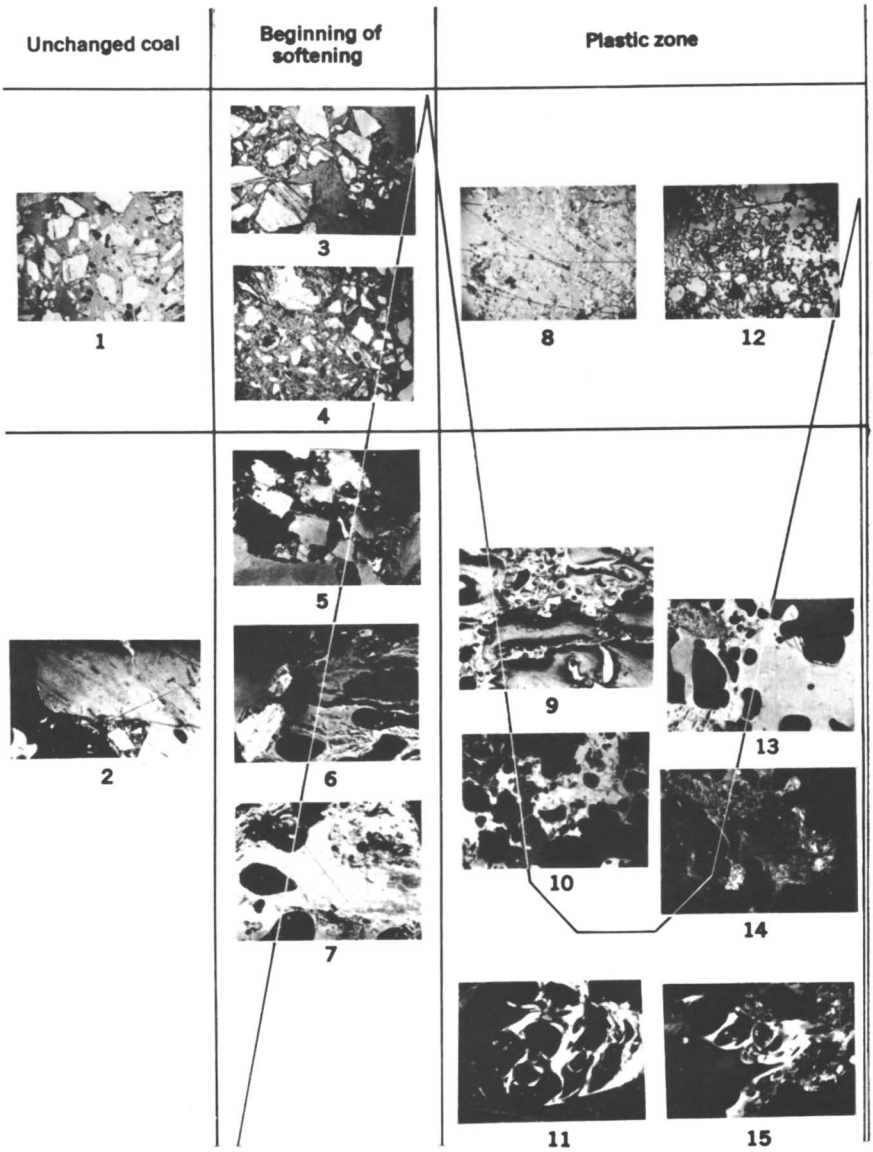

Figure 1. Conversion of coal into coke according to Echterhoff and Mackowsky (5). *Photographs 1, 3, 4, 8, 12, 18, and 21: 9.5 ×. Photographs 2, 5, 6,*

drawn in the same figure to clarify the results presented. The samples used for the investigation were taken from the pilot coking furnace at Bergbau-Forschung. The coking coal carbonized had a volatile content of 29.9% daf, and the bulk density at normal input size distribution was 0.078 kg./cc. Until

Publication Date: January 1, 1966 | doi: 10.1021/ba-1966-0055.ch034

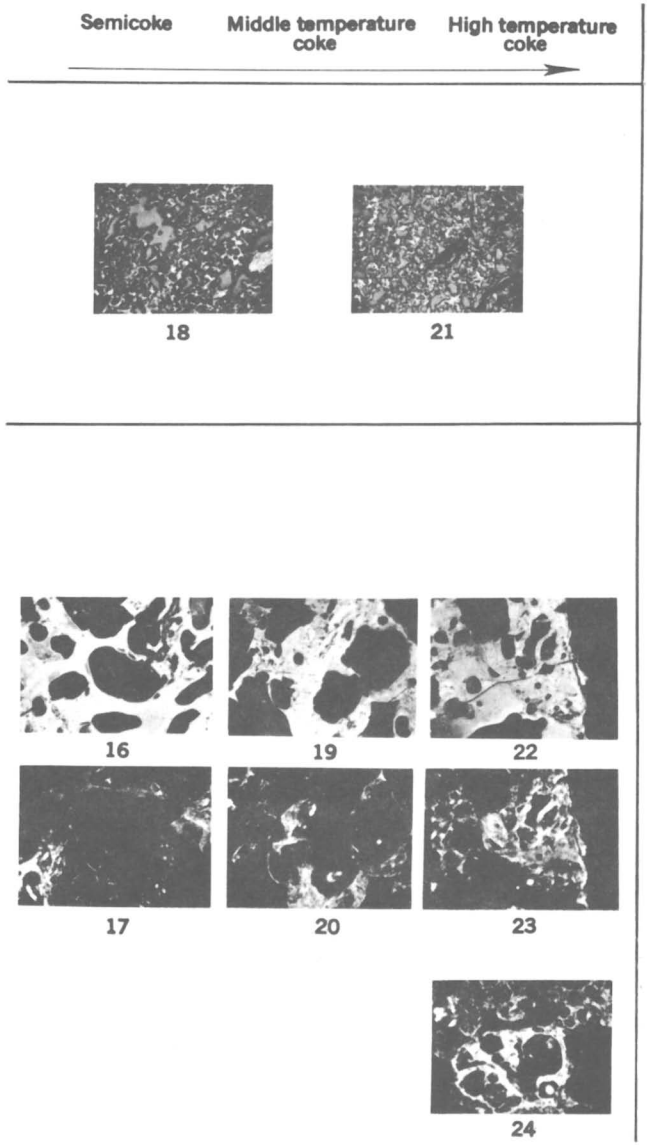

and 7: 190×. Photographs 9, 10, 11, 13, 14, 15, 16, 17, 19, 20, 22, 23, 24: 95×.

softening begins, it is not possible to observe any change under the microscope. Softening begins with a fusion of the grain boundaries, and during this process, so-called cementing pores (Verkittungs-poren) develop. Immediately following the fusion around the grain boundaries, the first devolatilizing pores are

Publication Date: January 1, 1966 | doi: 10.1021/ba-1966-0055.ch034

formed in the vitrinite. The exinite remains unchanged although it is the latter that determines the form of the pore in a particle. As a result of increasing the temperature only a few degrees centigrade, the exinite decomposes rapidly, leading to an apparently homogeneous melting seen only under the microscope. It is only the strongly inert fusinite that can be distinguished by its strong relief (Figure 10). The first stage of the plastic zone is completed when this state is reached. This first stage is characterized by a low viscosity and strong devolatilization. In the second stage of the plastic zone, the substance changes continuously and becomes noticeably more viscous as a result of the beginning of the resolidification. During this period anisotropic regions (often characteristic of a coke) are formed which will maintain their size during further heating. The strength of the anisotropy increases.

Based on the above research Ritter and Juranek (*12*) have developed a small coking furnace for conducting carbonization experiments on a laboratory scale. The samples taken during these experiments allowed us to make an exact microscopic study of the stages of transformation of coal into coke. In the first series of experiments carried out with this apparatus various coal types were carbonized, each of the samples consisting of a mixture of different sieve fractions. We intended to compare the behavior of coal particles of different size ranges during the carbonization process. The average bulk density, and hence the packing density, in the carbonization cylinder was 0.05 kg./cc., which is lower than the usual bulk density in technical or pilot plant carbonization. The rate of heating was 3°C./min. These experiments have substantiated the results of Echterhoff and Mackowsky (*5*). For example, in using a coal of 23% volatile matter daf it was shown how different particle size fractions behaved during the carbonization.

Figure 2 shows the beginning of softening as seen under the microscope. The softening cannot start with fusion of the particle boundaries owing to the low packing density, but it is noticeable by the formation of devolatilization pores in the large particles, accompanied by the simultaneous deformation of

Figure 2. Onset of softening of a coal of 23.0% volatile matter daf at 390°C. Pore formation in the coarse sieve fraction. Magnification 110 ×, oil immersion

Publication Date: January 1, 1966 | doi: 10.1021/ba-1966-0055.ch034

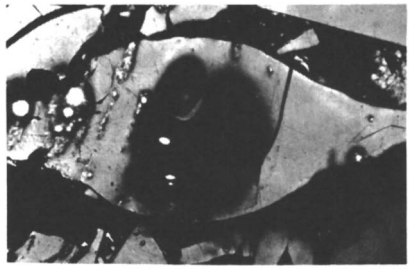

Figure 3. Expansion of particles into the void volumes at 400°C. Coal of 23.0% volatile matter daf. Magnification 110 ×, oil immersion

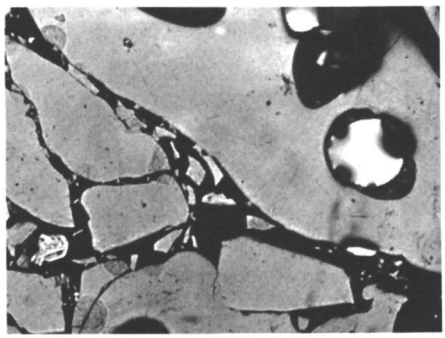

Figure 4. Incipient rounding of the smaller particles as visible evidence of softening. Coal of 23.0% volatile matter daf. 110 ×, oil immersion.

Publication Date: January 1, 1966 | doi: 10.1021/ba-1966-0055.ch034

these particles into the available void volumes. The smaller particle size fractions seem to remain unchanged. Pore formation is introduced by devolatilization during sample heating. If the mass of gas formed in a particle at a given temperature and in unit time is greater than that transported by diffusion, the resulting pressure inside the particle will cause both pore formation and simultaneous deformation of the particle. For particles of decreasing size the pressure drop from the inside toward the outside of the particle decreases until finally there is no pore formation. Thus, small particles will have no pores or at least considerably fewer pores per particle than larger particles.

Figure 3 shows again that formation of the devolatilization pores is connected with the deformation of the particle into the void volume. This is accompanied by a simultaneous increase of the particle volume. At a temperature of 420°C. the smaller particles of this coal sample are spherical (Figure 4), which can be interpreted as a sign of softening around particle boundaries. However, because of the small particle size, devolatilization pores cannot be formed.

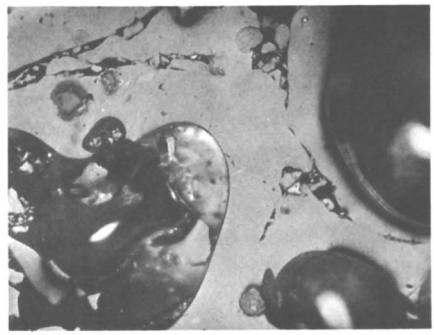

Figure 5. Fusion of particles at 435°C. Coal of 23.0% volatile matter daf. 110 ×, oil immersion.

The fusion of the particles begins in the plastic zone in which the smaller particles fuse to the surface of larger ones (*see* Figure 5). The low bulk density delays melting until this stage. With the void volumes so large, particle fusion is possible only when the phase of the highest fluidity is reached, and it is accompanied by a strong gas formation in the particle in the plastic zone.

The results of this experimental series leads to the conclusion that formation of the devolatilization pores depends on particle size and that pore formation is accompanied by deformation of the particles in the available void volumes. Further, the volume increase of the particles owing to their deformation must also depend on particle size.

In order to elucidate the effect of the particle size during the carbonization process, a so-called granular carbonization experiment was carried out (Figure 6). In this experiment single particle-size fractions of coals of different

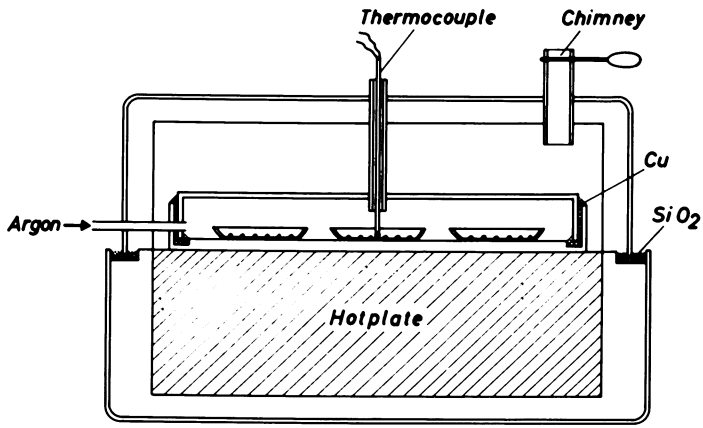

Figure 6. Furnace for "granular coking test"

Publication Date: January 1, 1966 | doi: 10.1021/ba-1966-0055.ch034

ranks were distributed so loosely in flat crucibles that the single particles did not touch each other. The agglomeration of single particles to form a cake was thereby prevented, and bulk density effects were also eliminated. The rate of heating was 2°C./min. To avoid oxidation effects, the experiment was carried out in an argon atmosphere.

Figure 7 shows carbonized coal particles of the sieve fraction 5 to 3 mm. It can be seen that for all types of coals practically all particles display devolatilization pores. This result, obtained by counting, is particularly interesting for the low volatile bituminous coal (No. 6 in Figure 7) because in high temperature cokes produced under normal conditions from another coal of the same rank, the particles of carbonized coal show no pores and will be found as so-called unmelted particles in the coke.

Publication Date: January 1, 1966 | doi: 10.1021/ba-1966-0055.ch034

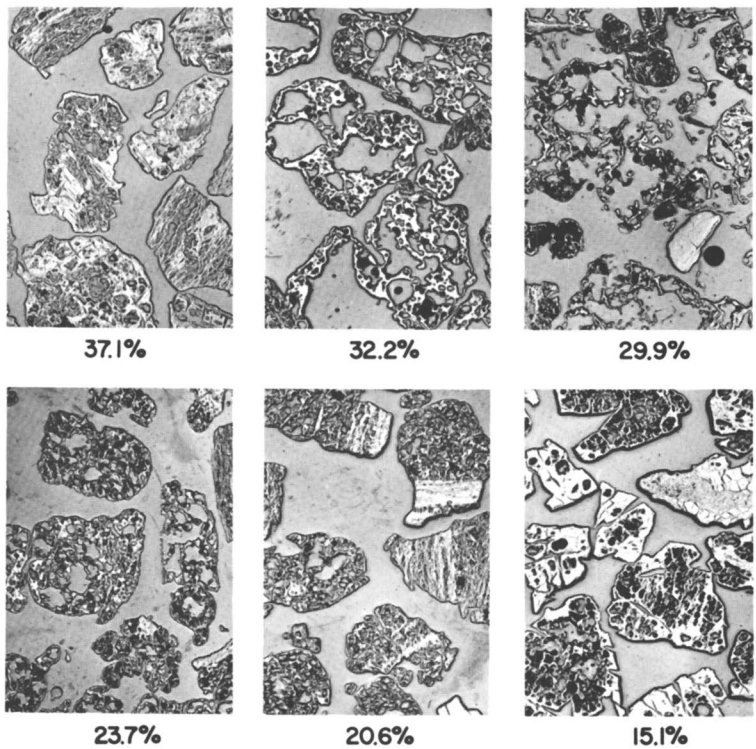

Figure 7. Granular coking of a coalification series % volatile matter daf of raw coal. Screen size: 5–3 mm. Magnification, 2.5 ×

The size, form, number of pores per particle, and porosity are different for coals of different rank. Table I shows quantitative results obtained by counting particles with devolatilization pores.

In general the number of particles showing pores decreases with decreasing particle size, the magnitude of the effect depending on rank. This result is consistent with the qualitative observations of Ritter and Juranek (*12*) from

Table I. Portion of Coked Screen Sizes in Particles with Degassing Pores[a]

	VM daf of Raw Materials					
Sieve size, mm.	*37.1%*	*32.2%*	*29.9%*	*23.7%*	*20.6%*	*15.1%*
5–3 mm.	100	100	100	100	100	94
3–1 mm.	98	100	100	100	100	95
1–0.2 mm.	98	100	100	100	100	78
0.2–0.5 mm.	62	94	95	88	89	23
under 0.2 mm.	23	41	37	30	25	—

[a] Fusite and mineral-free coking material

their carbonization experiments. Coke pore formation depends greatly on particle size for the coal with 15.1% volatile matter daf (*see* No. 6, Figure 7) and fairly strongly for the poorly coking "Gasflamm" coal (37.1% volatile matter daf). The effect is less marked for coals of intermediate rank. The reason for these differences lies in the ability of smaller particles of high volatile coals to release considerable amounts of gas. Within the domain of the easily fusible "Gas" and "Fett" coals (high volatile A bituminous and medium volatile, respectively) it is found that only in the transition range to particle sizes below 0.2 mm., that the proportion of devolatilization pores decrease considerably with decreasing volatile matter content of the original coal. Tables II and III give values of average pore diameter and pore frequency per particle. Both these parameters decrease with decreasing particle size, and the relationship between pore diameter and pore frequency is inversely proportional. The average pore size under the conditions of these carbonization experiments, where expansion possibilities are not limited, is greater than in normal cokes. The different coal types tend to behave similarly as the particle size decreases.

Table II. Mean Pore Diameter, in mm.

	VM daf of Raw Materials					
Sieve size, mm.	*37.1%*	*32.2%*	*29.9%*	*23.7%*	*20.6%*	*15.1%*
5–3 mm.	0.1 mm.	0.3 mm.	0.6 mm.	0.3 mm.	0.1 mm.	0.16 mm.
3–1 mm.	0.09	0.2	0.3	0.2	0.2	0.1
1–0.5 mm.	0.05	0.1	0.1	0.2	0.1	0.2
0.5–0.2 mm.	0.08	0.1	0.1	0.09	0.09	0.15
under 0.2 mm.	0.06	0.05	0.06	0.05	0.06	—

Table III. Pore Frequency per Particle in Particles with Degassing Pores

	VM daf of Raw Materials					
Sieve size, mm.	*37.1%*	*32.2%*	*29.9%*	*23.7%*	*20.6%*	*15.1%*
5–3 mm.	14	7	5	9	10	10
3–1 mm.	7	7	3	3	3	4
1–0.5 mm.	3	3	2	2	3	2
0.5–0.2 mm.	2	2	1	1	1	1
under 0.2 mm.	2	1	1	1	1	—

Publication Date: January 1, 1966 | doi: 10.1021/ba-1966-0055.ch034

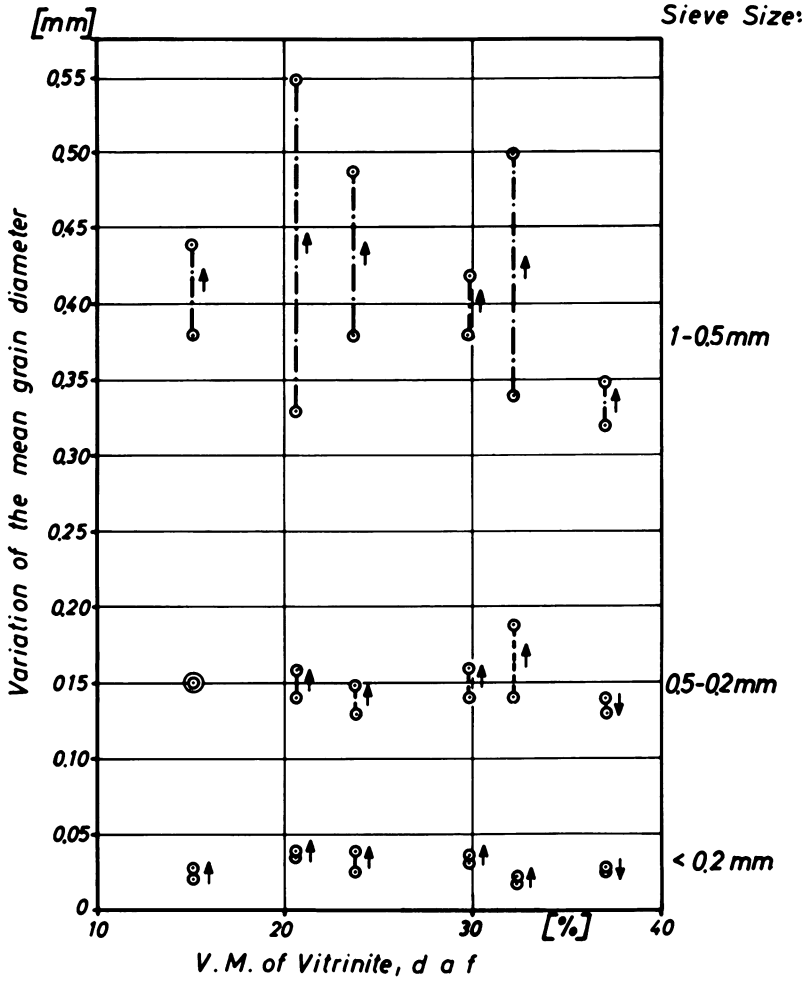

Figure 8. Particle diameter of the granular coking material

These results substantiate the assumption that the internal pressure resulting from the ratio of the gas release per unit time to the rate of diffusion is of determining importance in pore formation. Luther and co-workers (9) succeeded in calculating the internal gas pressure and concluded that it decreases with decreasing particle size. Pore formation causes a plastic deformation of the softened coal particles as shown by the first series of experiments discussed above. From measurements of mean particle size in both the original and carbonized samples, we determined how far deformations produced volume increases. The results are given in Figure 8. It was only the sieve fractions below the 1-mm. level that could be used for the above study because it was only for these fractions that enough particles were available for a statistical evaluation. To understand the values, it is necessary to mention that the

Publication Date: January 1, 1966 | doi: 10.1021/ba-1966-0055.ch034

average particle size determined by a microscopic method is liable to give low results because it is unlikely that the particles are cut in the plane of the largest particle diameter. Despite this, the results are useful because both the original material and the end product were analyzed by the same method. Except for the sample with 32.2% volatile matter daf it can be stated that for the particle size range between 1 and 0.5 mm. the average particle diameter of the carbonized sample increases considerably with increasing rank up to the region of 20% volatile matter and then decreases again. For finer sieve fractions there is no longer a marked increase in mean particle size on carbonization. This difference in behavior of sieve fractions of coal originating from the same seam has the same cause as has the variation in pore formation. The different behavior of a size range, for instance that between 1 and 0.5 mm., for increasing rank can be explained by the fact that the coals of different rank shrink differently on carbonization. In this way the swelling is strongly compensated. As a rough approximation it can be said that coal shrinkage decreases with increasing rank. According to the model of Hirsch (*8*) the fine structure of coal consists of condensed ring systems which are interconnected by numerous long side chains. The number and the length of the side chains is higher for coals of lower rank than for those of higher rank. As a result, the distance between the aromatic nuclei is greater in lower rank coals.

Hence, the specific concentration of the aromatic lamellae increases with rank. Since carbonization results in greater aromatization and greater ordering of the lamellae, shrinkage on carbonization ought to decrease with increasing rank. Strong swelling coupled with insufficient shrinkage causes dangerous swelling pressures to develop. Since shrinkage cannot be directly influenced, the pressure danger in a coal can be decreased only by a decreased degree of swelling. This latter can be obtained by grinding the charge more finely. The opinion held in the past that the decrease in swelling pressure by finer grinding is caused by decreased bulk density cannot be substantiated. Practical experiments have shown that by adding oil to the finely ground coal it is possible to increase the bulk density to almost its initial value (before the fine grinding) without preventing large swelling.

The strong increase in mean particle diameter of the sieve fraction 1.0–0.5 mm. for the coal with 32.2% volatile matter cannot be explained on the basis of the relationships discussed. The unusually high swelling ability in this case is caused by a very high proportion of exinite (21%) in the sample and the correspondingly very small proportion of inertinite (*9*).

Summarizing the results of these experimental studies it can be stated that the pore size and pore concentration are properties which depend on particle size when seam coals of a given rank are compared. Further, swelling and shrinking of good coking coals on carbonization to the semicoke stage make a strong volume increase in the single particles impossible. In the case of the coals that develop dangerous swelling pressures the swelling is not sufficiently compensated by shrinkage.

In a third experimental series the void volume in the coal sample was greatly reduced. For this purpose seam coals were carbonized in a dilatometer so that particle size dependence could be observed. The size ranges investi-

Publication Date: January 1, 1966 | doi: 10.1021/ba-1966-0055.ch034

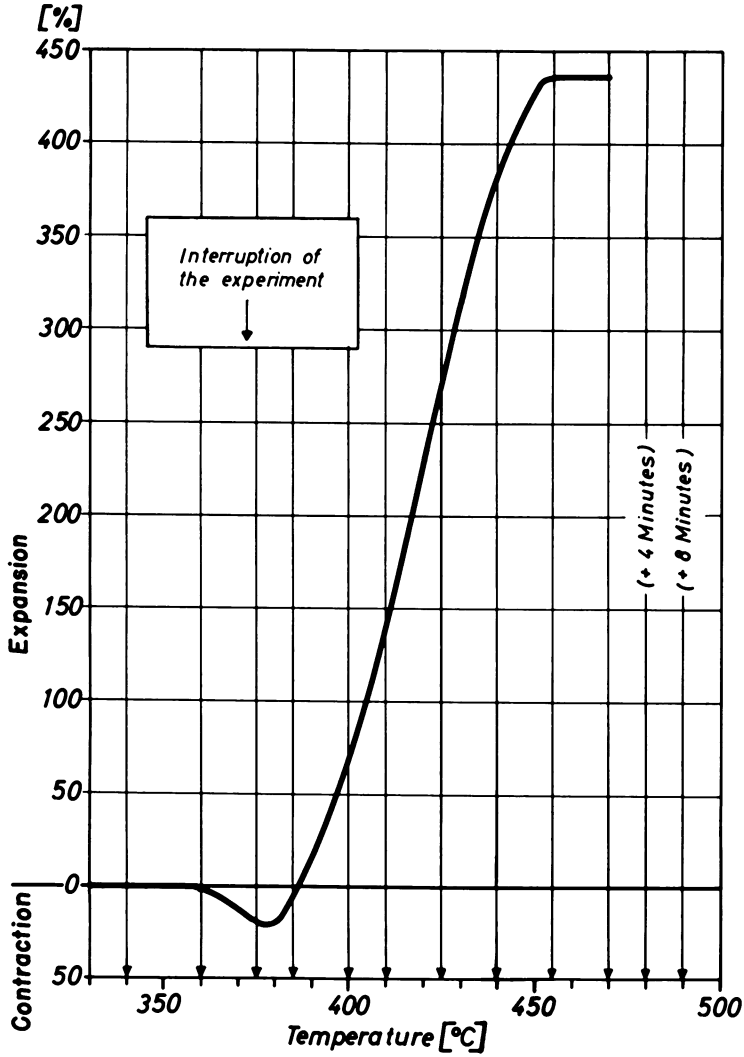

Figure 9. Expansion vs. temperature

gated were below 1 mm., below 0.2 mm., and below 0.06 mm. The dilatometer test was interrupted at characteristic temperatures as shown by Figure 9.

Figure 10 shows results of the microscopic studies of the polished samples of a seam coal and for the particle size below 1 mm. In agreement with previous observations, there is no change in the coal until the beginning of contraction, which can be considered as occurring at the softening temperature for the coal in question. The beginning of softening can be observed in the dilatometer, not by pore formation but by a dense association of the particles owing to fusion. The softening of the single particles begins most probably with the

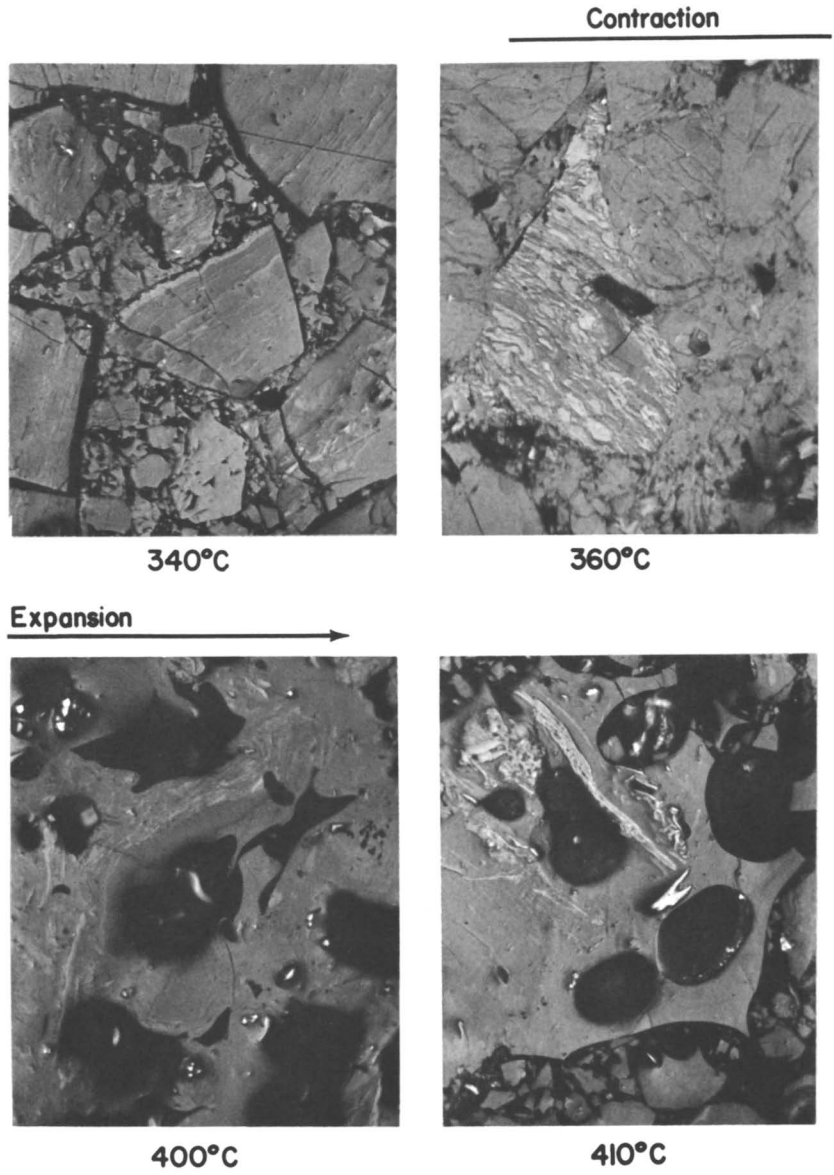

Figure 10. Behavior of a coal of 28.6% volatile

release of decomposition products at the particle boundaries, which causes single particles in the densely packed beds to stick together. This will also enable some particles to slip into the available void volumes of the test sample. Concurrently, a certain swelling and agglutination of the single particles can lead to fusion of the particles into a solid mass. The slipping and fusion of the

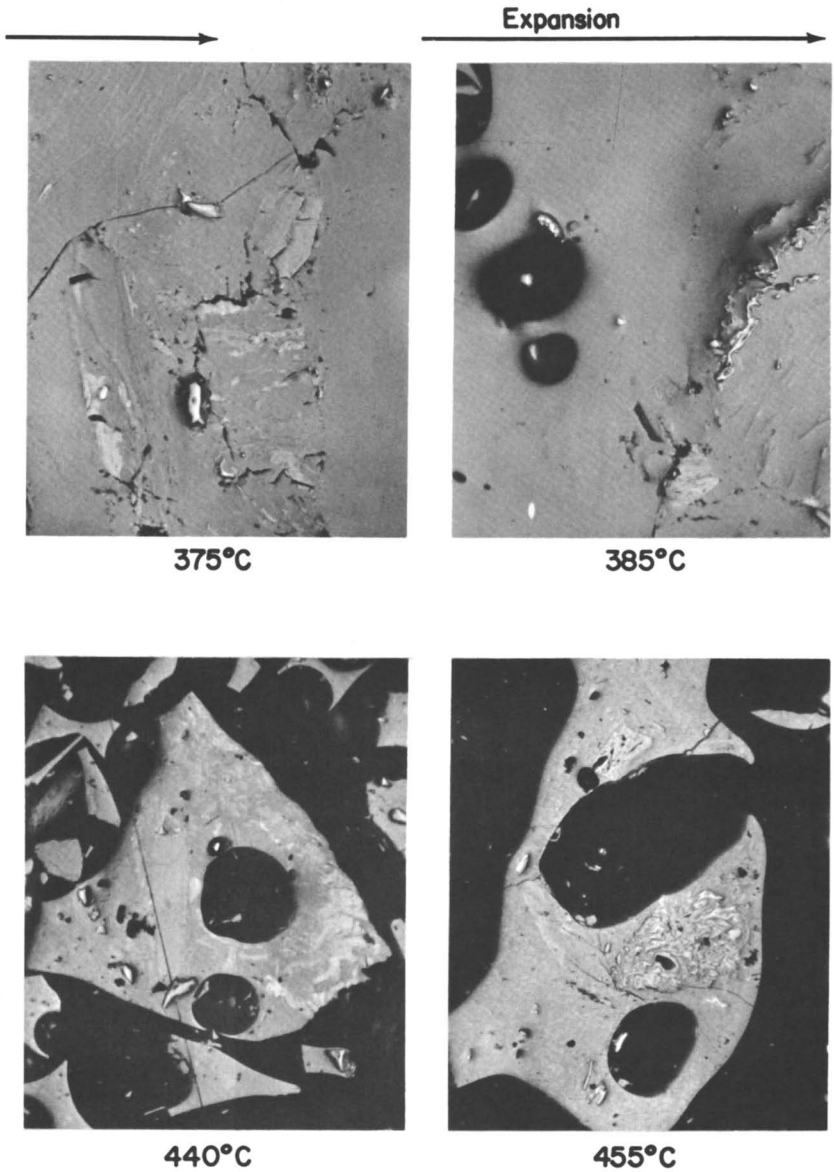

matter daf during heating in the dilatometer

particles will be measured in the dilatometer as a contraction. The contraction is therefore not a collapse of the particles in the physical sense but the result of the beginning of their softening. An anthracite that does not soften shows neither contraction nor expansion in the dilatometer. Figure 11 shows the microphotographs of an anthracite briquet before and after the heating in the

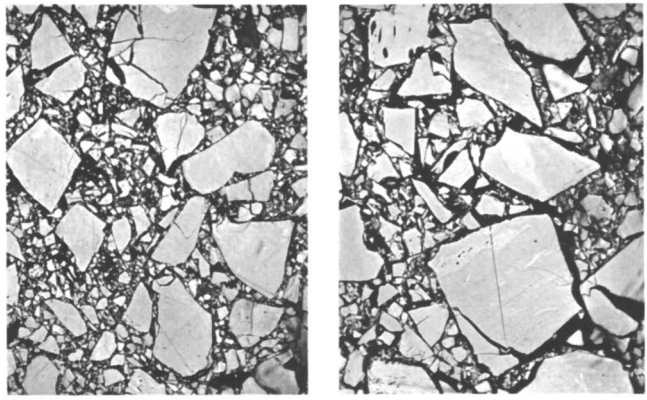

Figure 11. (A) Anthracite; starting material for test carbonization in dilatometer. (B) Anthracite heated in dilatometer to 505°C. Magnification 110 ×, oil immersion

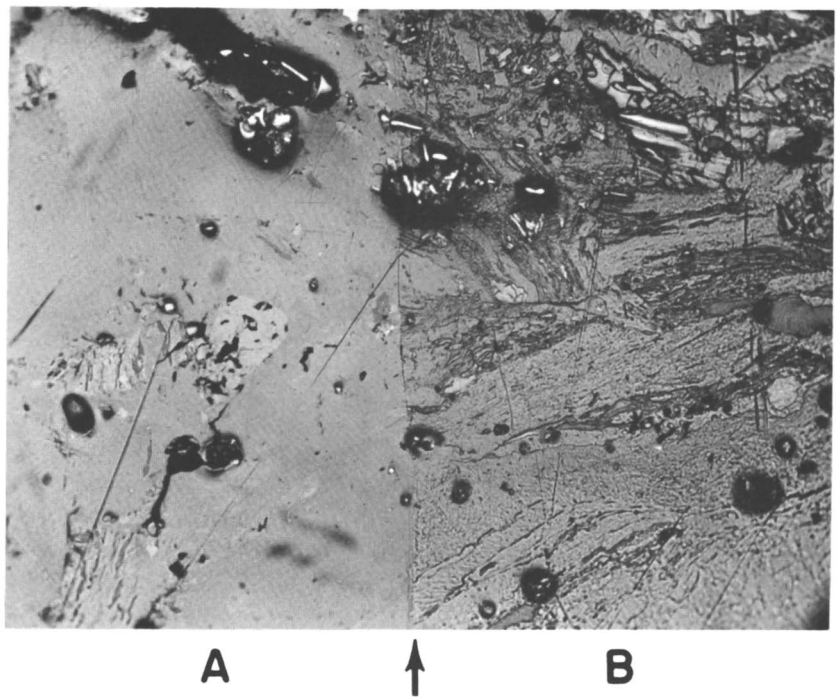

Figure 12. Coal of 28.6% volatile matter daf heated at 375°C. in dilatometer. (A) unetched sample. (B) etched sample. Magnification 220 ×, oil immersion

Publication Date: January 1, 1966 | doi: 10.1021/ba-1966-0055.ch034

dilatometer. No difference can be found between these two samples. In order to explore the processes of contraction, the polished surface of the heated briquet was etched.

Figure 12 shows the etched and unetched part of the sample that was heated at 375°C. As a result of the etching, particle boundaries that could not be identified in the unetched, polished sample became visible. Plastically deformed particles can also be seen. The plastic deformation indicates that softening must have begun without any pore formation. Although the internal gas pressure in the coal is still too low, it is sufficient to cause a small expansion of the particles so that the void volumes in the briquet are filled. As shown by other experiments, pore formation is accompanied by a considerable volume increase of the single particles, which however, is not possible under the conditions in the dilatometer immediately after the beginning of the softening.

A volume increase is possible only when the whole sample briquet has already been deformed (the deformation of the sample being in fact measured as an expansion). When the expansion begins (*see* Figure 10, 385°C.), pore formation in the vitrinite sets in. The size of the pores formed in the dilatometer experiment is on the average smaller than in a loose bulk owing to the fact that deformation of single particles into void volumes is impossible in the dilatometer. Figure 13 compares the dependence of pore formation on bulk density for three coke types.

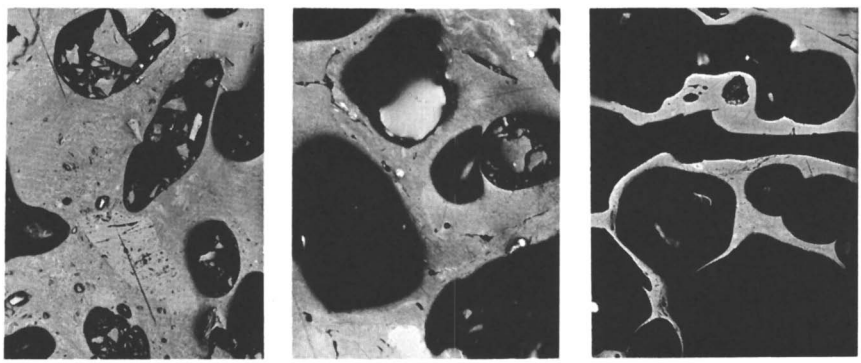

Figure 13. Variation of pore size and count in relation to bulk density. Volatile matter of raw materials: ca. 24% daf. Bulk density: (A) ca. 0.1 kg./cc., dry; (B) ca. 0.05 kg./cc., dry. Particle size: (A) 1 mm., (B) 1–0.5 mm., (C) 1–0.5 mm. Magnification 97 ×, oil immersion

Once the expansion starts in the dilatometer carbonization, complete softening of the coal sets in. The plastic zone will be terminated by resolidification.

Microscopic investigations of samples of other particle sizes (below 0.2 and below 0.06 mm.) of the same coal showed the same changes in the coal in the dilatometer experiments as were found for the coarser particle size. Nevertheless, the effect of particle size does make itself felt in the dilatometer carbonization, as can be observed in the photomicrograph at the temperature

Publication Date: January 1, 1966 | doi: 10.1021/ba-1966-0055.ch034

of the maximum contraction and at beginning of the expansion, respectively. Here pore formation sets in while the pore sizes and number of pores are considerably smaller in the fine particles than in the coarse particles.

The magnitude of expansion also depends on particle size as shown in Figure 14. Expansion decreases with decreasing particle size, varying in extent with coal rank. This effect is to be expected because it is determined not by the gas released per unit time, but only by the magnitude of the internal pressure in the sample briquet, which is lower for a small initial particle size than it is for a coarse sample. This in turn indicates that contrary to what the micrograph shows, the inter-particle bond cannot be without voids absolutely after contraction has occurred since this would mean that the dilatation depends on particle size. Figure 15 shows the relationship between rank and particle-size dependence in the dilatometer carbonizations; the volatile matter is represented on the abscissa.

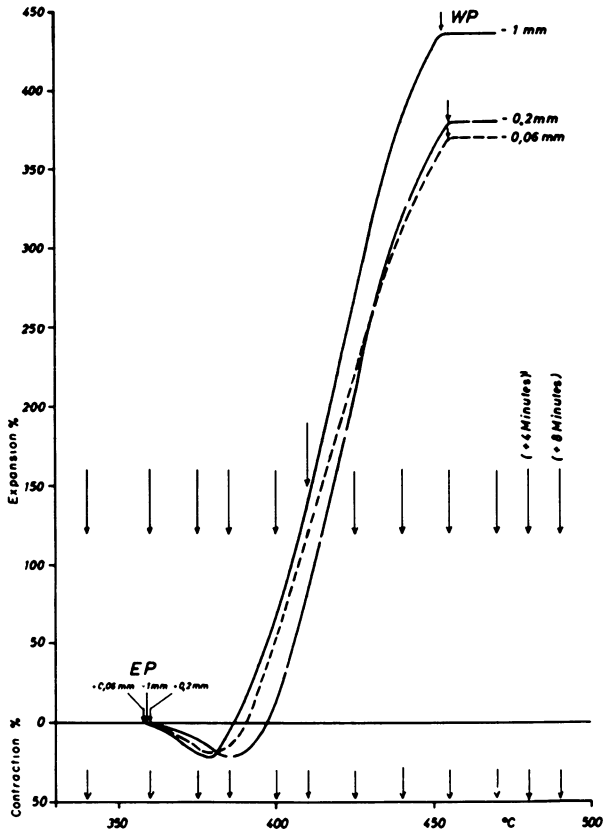

Figure 14. Dependence of expansion on initial particle size, % volatile matter daf of raw coal (a) Beeckerwerth Flöz Katharina, 28.6% VM

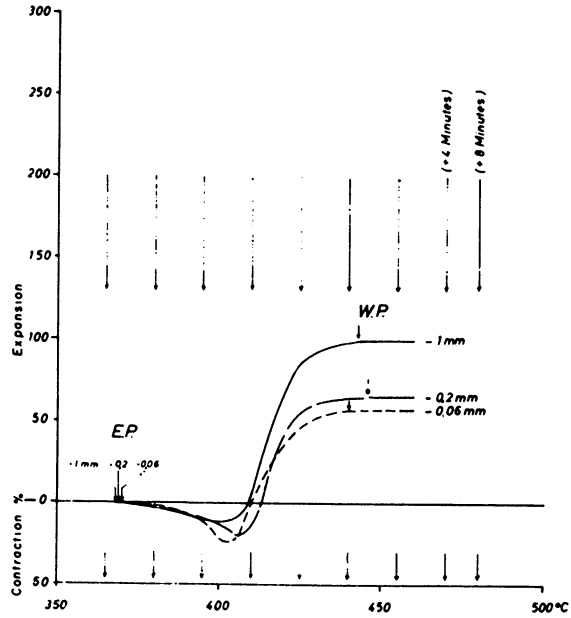

(b) Westende Flöz Zollverein, 29.6% VM

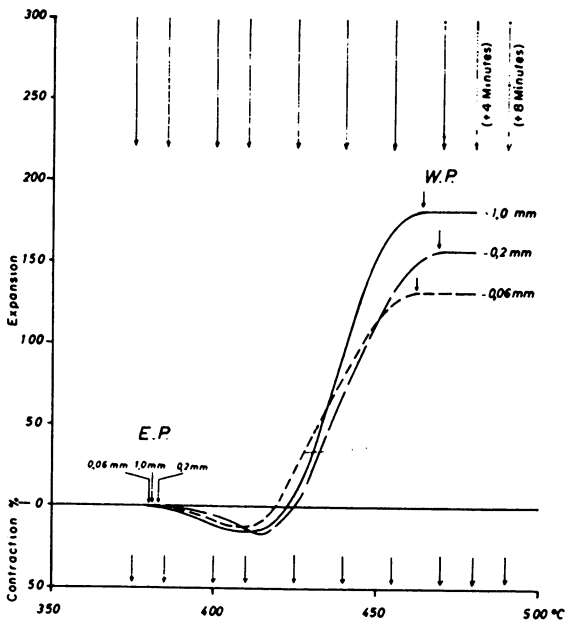

(c) Friedrich Thyssen Flöz Gretchen, 24.3% VM

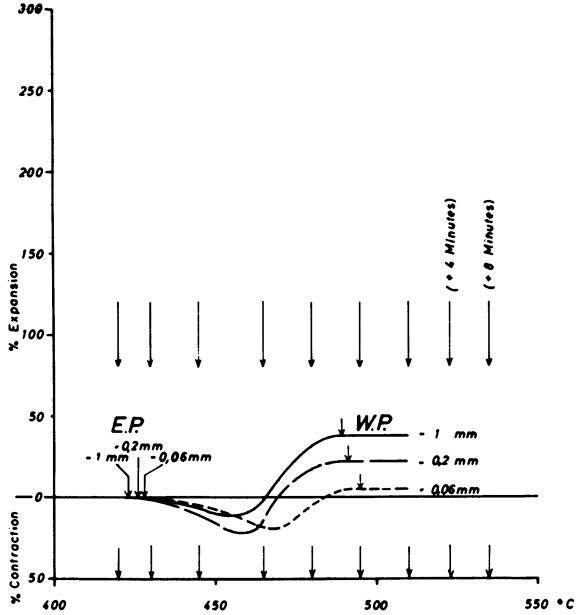

(d) Westende Flöz Prasident, 19.0% VM

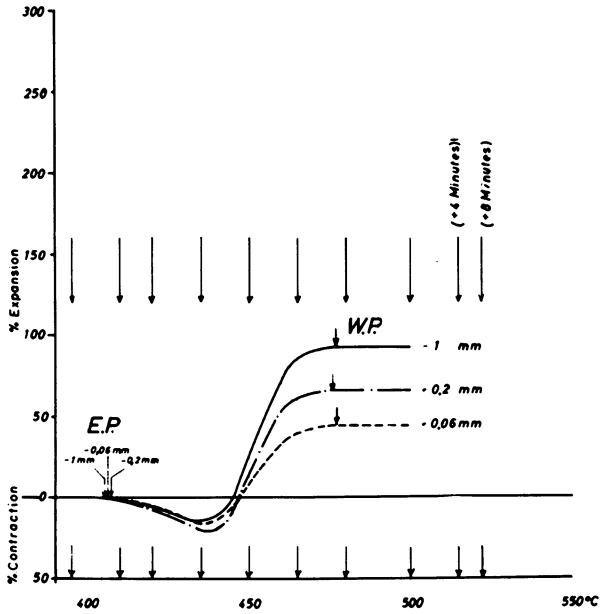

(e) Westende Flöz Sonnenschein, 16.8% VM

The expansion of the particle size range below 0.2 mm., the normal input size for the dilatometer test, is taken as 100%, and the ordinate represents the deviation, in percent, for coarser and finer particle sizes. The particle-size dependence of the expansion can then be distinguished for different stages of coalification. The smallest differences are found among the prime coking coals while the effect of particle size is much stronger for the low and high volatile matter coals. This indicates unambiguously that relationships between expansion and coking ability exist only when the carbonizations take place under strictly identical conditions, which is seldom the case in practice. In connection with the particle-size dependence of the expansion, the results of the granular coking experiments should be recalled. It was found in both experimental series that poorly coking coals strongly depend on particle size for their ability to form coke than do prime coking coals.

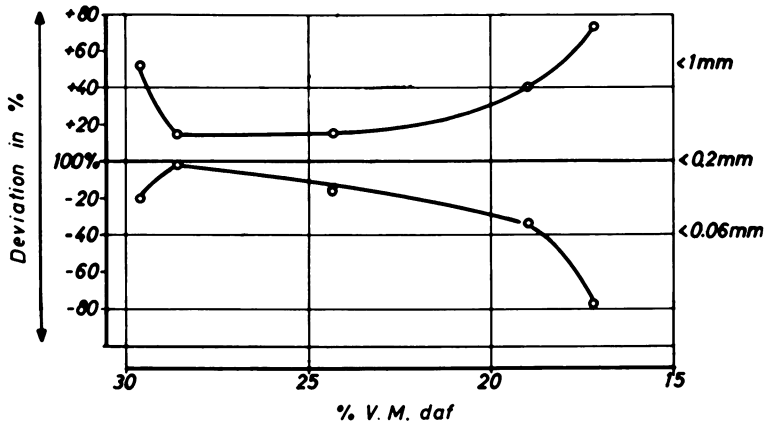

Figure 15. Relationship between rank and particle size dependence in dilatometer carbonizations

By comparing experimental results obtained in carbonizations at high packing density (dilatometer samples) with those carried out on loose bulk samples it can be shown that the processes during carbonization are qualitatively the same despite quantitative differences.

In a last experimental series, which is not yet completed, the effect of the heating rate is investigated. Dulhunty and Harrison (*4*) have carbonized 1953 coals of particle sizes between 0.5 and 0.4 mm. with a low rate of heating (carbonization time longer than 60 hours). They concluded that there was no volume increase in their samples. In a related investigation, a coal with 23.8% volatile matter daf was carbonized by heating to a final temperature of 600°C. at heating rates of 260°C./min., 3°C./min., and 0.5°C./min. Tables IV and V give proportions of the particles showing pores, together with the average particle size of the carbonized samples.

The results available so far substantiate, in general, the statements of Dulhunty and Harrison. Even with a particle size distribution of 1–0.5 mm.

Publication Date: January 1, 1966 | doi: 10.1021/ba-1966-0055.ch034

Table IV. Portion of Coked Screen Sizes in Particles with Degassing Pores, in %

Sieve size, mm.	*Rate of Heating*		
	260°C./min.	*3°C./min.*	*0.5°C./min.*
5–3	100%	100%	100%
3–1	100	100	100
1–0.5	100	98	98
0.5–0.2	100	90	36
under 0.2	69	38	14

Table V. Average Particle Diameter Before and After Coking, in mm.

Sieve size, mm.	*Raw Coal*	*Rate of Heating*		
		260°C./min.	*3°C./min.*	*0.5°C./min.*
5–3	2.34 mm.	6.27 mm.	3.43 mm.	2.64 mm.
3–1	0.97	2.41	1.45	1.04
1–0.5	0.38	0.67	0.49	0.44
0.5–0.2	0.17	0.29	0.15	0.13
under 0.2	0.06	0.06	0.04	0.06

no volume increase was found when the sample was heated at a low heating rate. In the sieve fraction 5 to 3 mm., the volume increase, however, was about 10%. In complementing the statements by Dulhunty and Harrison we can state that there is no net volume increase, swelling, or pore formation when the heating rate is low. The swelling is, however, completely compensated for by the subsequent shrinkage. When the heating rate is very high, the pore formation increases in all sieve fractions as might be expected. In addition, considerable differences in the pore sizes and in the number of pores per particle can be observed, especially in the coarse size fractions. Figure 16 shows these differences.

Based on the fact that the pore formation increases at higher rates of heating, an attempt was made to produce a porous coke by applying high rates of heating to a coal that showed no coking characteristics at normal heating rates. A lean coal with 10.6% volatile matter daf was used, and the

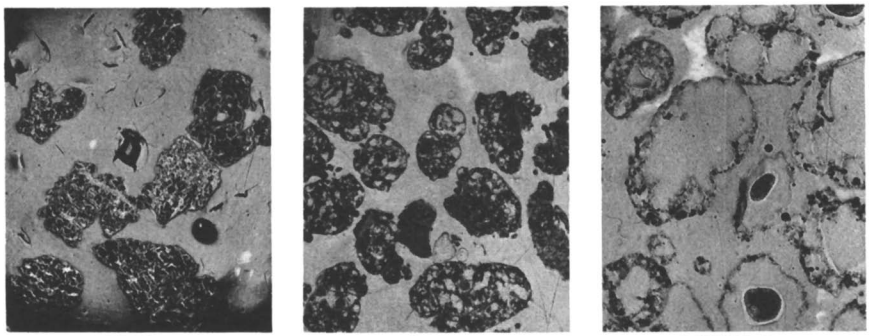

Figure 16. Shape and number of degassing pores in relation to the rate of heating. Volatile matter of the raw coal—23.8% daf; sieve size 5–3 mm. Magnification 1.6 ×

Publication Date: January 1, 1966 | doi: 10.1021/ba-1966-0055.ch034

rate of heating was 300°C./min. The experimental results are presented in Tables VI and VII.

The high rate of heating converted a considerable proportion of this coal to coke. The volume increase found, however, was caused by formation of pores whose size was below the range of the optical microscopic. This latter suggestion is supported by results of determinations of the internal surface

Table VI. Portion of Coked Screen Sizes in Particles with Degassing Pores, in %

	Rate of Heating	
Sieve size, mm.	*300°C./min.*	*3°C./min.*
5–3	42%	10%
3–1	38	4
1–0.5	35	4
0.5–0.2	26	1
under 0.2	12	—

Table VII. Average Particle Diameter Before and After Coking, in mm.

		Rate of Heating	
Sieve size, mm.	*Raw Coal*	*300°C./min.*	*3°C./min.*
5–3	1.53 mm.	2.00 mm.	1.75 mm.
3–1	0.99	1.25	0.75
1–0.5	0.40	0.32	0.33
0.5–0.2	0.18	0.15	0.13
under 0.2	0.03	0.04	0.03

area by gas adsorption. The swelling described as caused by the formation of suboptical microscopic pores does not occur in size fractions below 1 mm. because devolatilization products can be released without the build-up of internal pressure, which is the cause of particle swelling.

Investigations are in progress with high rates of heating and coals of varying rank, such as "Ess" coals (low volatile bituminous), "Gas" and "Gasflamm" coals (high volatile bituminous A, B, C), in order to test how far it is possible to change poorly coking or noncoking coals into coking coals. This is surely of great interest in view of the permanently decreasing amount of good quality coking coals.

Literature Cited

(1) Amosov, J. L., Eremin, I. V., Sukhenko, S. J., Oshorkova, L. S., *Koks Khim.* **12,** 9 (1957).
(2) Berry, W. F., "Abstracts of Papers," 135th Meeting, ACS, April 1959, p. 7J.
(3) Brown, H. R., Taylor, G. H., Cook, A. C., *Fuel* **43,** 43 (1964).
(4) Dulhunty, J. A., Harrison, B. L., *Fuel* **32,** 441 (1953).
(5) Echterhoff, H., Mackowsky, M.-Th., *Glückauf* **96,** 618 (1960).
(6) Eremin, I. V., *Trans. Fossil Fuel Inst.* **8,** 14 (1959).
(7) Harrison, J. A., *Proc. Illinois Mining Inst.* **69,** 17 (1961).
(8) Hirsch, P. B., *Proc. Roy. Soc. (London)* **226,** 143 (1954).
(9) Luther, H., Bussmann, B., Traustel, S., *Brennstoff-Chem.* **43,** 353 (1962); **44,** 65 (1963).
(10) Mackowsky, M.-Th., *Erdöl Kohle* **15,** 441 (1962).
(11) Mackowsky, M.-Th., "Abstracts of Papers," 145th Meeting, ACS, September 1963, p. 2K.

In Coal Science; Gould, R. F.; Advances in Chemistry; American Chemical Society: Washington, DC, 1966.

(12) Ritter, H., Juranek, G., *Brennstoff-Chem.* **41,** 170 (1960).
(13) Ritter, H., Juranek, G., *Brennstoff-Chem.* **42,** 17 (1961).
(14) Schapiro, N., Gray, R. J., *Proc. Illinois Mining Inst.* **68,** 83 (1960).
(15) Schapiro, N., Gray, R. J., Eusner, G. R., *Trans. AIME* **20** (1961).

RECEIVED July 27, 1965.

Discussion

Peter Hacquebard: What kind of petrographic analyses were carried out on the grains? Were these only maceral determinations or also microlithotype analyses?

Marie-Therese Mackowsky: We carried out maceral and microlithotype analyses. Besides these we determined the reflection of the pure vitrinites in oil.

Kulai Kini: Were any strength measurements made on cokes formed at high rates of heating?

Dr. Mackowsky: It was not possible to make any strength determination since the coke particles were so small. It was possible to crush the particles with the fingers without any difficulty.

Publication Date: January 1, 1966 | doi: 10.1021/ba-1966-0055.ch034

Development of Order in the Formation of Coke

J. D. BROOKS and G. H. TAYLOR

Division of Coal Research, Commonwealth Scientific and Industrial Research Organization, Chatswood, N.S.W., Australia

Publication Date: January 1, 1966 | doi: 10.1021/ba-1966-0055.ch035

Previous work had shown that low temperature coke is formed from coals heated to between 450° and 500° C. by a process of nucleation and growth of spherical bodies in the plastic vitrinite. An essentially similar process has now been found to occur with coke-oven and petroleum pitches, with polyvinyl chloride, and with some polynuclear hydrocarbons, all of which yield carbons which graphitize readily at high temperatures. The process is probably general for the initial stages of formation of such carbons from the liquid phase. Some control of the solidification process has been achieved on the laboratory scale, and the physical and chemical structure of the spherulites has been investigated.

It is well known that under the microscope, cokes made from the vitrinite of most coking coals or from petroleum residues exhibit complex patterns of optical anisotropy. The cokes are composed of a mosaic of optically anisotropic units each showing individual extinction behavior; the average size of mosaic units in vitrinite coke varies from less than 1 to about 5 microns and occasionally more. This mosaic pattern may often be observed in vitrinite coke from the solidification temperature (about 470°C.) to well above 1000°C. Once formed, the mosaic pattern does not change throughout this temperature range, except for minor shrinkage, although the degree of anisotropy and the maximum reflectance both increase steadily with temperature. The process of development of the mosaic texture at these comparatively low temperatures just prior to solidification is of great importance because it determines the texture of high temperature cokes and of graphitizing carbons which may be obtained from them. The texture is in turn thought to be related to the strength, mode of breakage, reactivity, and (possibly) conductivity of the coke-like carbons.

In Coal Science; Given, P.;
Advances in Chemistry; American Chemical Society: Washington, DC, 1966.

Recent work in this Division has shown that various substances other than vitrinites, such as pitches from coal tars and petroleum tars, polyvinyl chloride, and polynuclear hydrocarbons, develop similar mosaic structures on heating. In fact this effect occurs with most high carbon materials which pass through a plastic stage during carbonization.

The process of development of a mosaic texture was observed by Taylor (2) first in thermally metamorphosed coals and then in partially carbonized vitrinite. He noted the appearance of spherical bodies in the plastic vitrinite, their growth, and the final development of the mosaic texture which is characteristic of the walls of the vesicular coke structure. From their appearance and behavior in polarized light it was deduced that the spherical bodies probably had a single plane of preferred orientation—i.e., a lamellar structure.

In the present studies this work has been carried further to gain a deeper understanding of the physical and chemical processes involved and to assess the possibilities of exercising control over the solidification process and thus over the texture and properties of the coke.

Publication Date: January 1, 1966 | doi: 10.1021/ba-1966-0055.ch035

Experimental

It was established in the early stages of this investigation that on carbonization, coal-tar and petroleum-tar pitches and some other substances behaved like the vitrinite of a coking coal. For pitch, the sequence of events was exactly the same as for vitrinite, except that the temperature range over which the changes occurred was wider and the absolute temperatures were lower.

The various kinds of pitch used here were carbonized in a porcelain boat within a heated horizontal cylindrical retort. The temperature of the sample, which was measured by means of a thermocouple placed just above the boat, could be maintained constant to within ± 1°C. All carbonization runs were carried out with an atmosphere of oxygen-free nitrogen. The heated material was cooled to room temperature before examination.

The partially carbonized materials were embedded in a cold-setting polyester resin and examined with a Leitz Ortholux microscope using mainly reflected polarized light. Preparing polished surfaces of such a soft material as pitch was difficult, especially since the pitch sometimes contained comparatively hard inclusions, but after the specimen had been chilled with solid carbon dioxide, satisfactorily polished surfaces could be prepared. A JEM-5Y microscope was used for electron microscopy and diffraction, the accelerating voltage being 80 kv. throughout.

Results

Examining a variety of carbonized products showed that cokes from vitrinite, coal-tar and petroleum pitches, polyvinyl chloride, and various polynuclear hydrocarbons all gave a similar mosaic-type structure when carbonized (Figure 1). All these materials passed through a plastic or fluid stage. Solvent-soluble fractions of coke-oven pitch were chosen to exemplify the sequence of changes occurring during carbonization. However, the findings described here probably apply in most respects to all the starting materials mentioned.

The temperatures at which the pitch fractions solidified were between 410° and 435°C. Prior to solidification, spheres had developed within the

Figure 1. Naphthacene carbon-mosaic structure in semi-coke. × 189

pitch, but the structure had not reached completion in a mosaic texture. The optical properties of the pitch surrounding the spheres did not appear to be profoundly changed.

In plane-polarized light the spheres appeared as optically anisotropic bodies of varying size (Figure 2). Until about half the pitch had been converted, little interference between spheres occurred. Most spheres, even when quite large, were accurately circular in outline, but a few had elliptical shapes or protuberances (Figure 3). The elliptical or flattened shapes were presumed to be caused by disproportionate growth of the spheres in directions where the availability of unconverted pitch was greater than in areas where another sphere was competing for material. It was noticeable that the nucleation of spheres was inhibited close to the surface of large

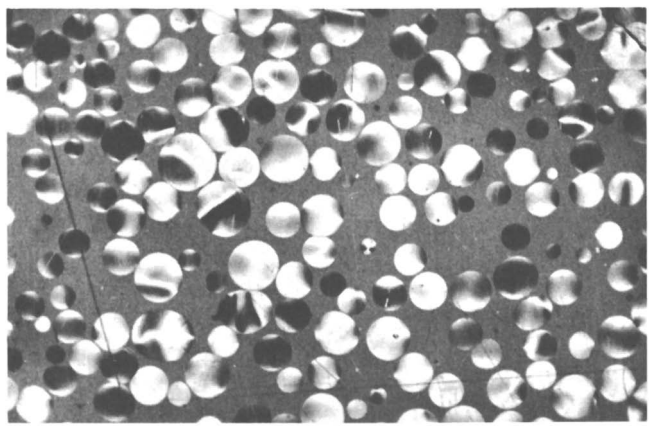

Figure 2. Spheres in toluene-soluble fraction of coke-oven pitch. An intermediate stage of solidification. × 216

Publication Date: January 1, 1966 | doi: 10.1021/ba-1966-0055.ch035

spheres, which were often surrounded by zones from newly forming spheres at the limits of optical microscopy (Figure 4). The protuberances were caused by the capture of small spheres by larger ones. This did not happen often, however, at least in the earlier stages, and small spheres sometimes appeared

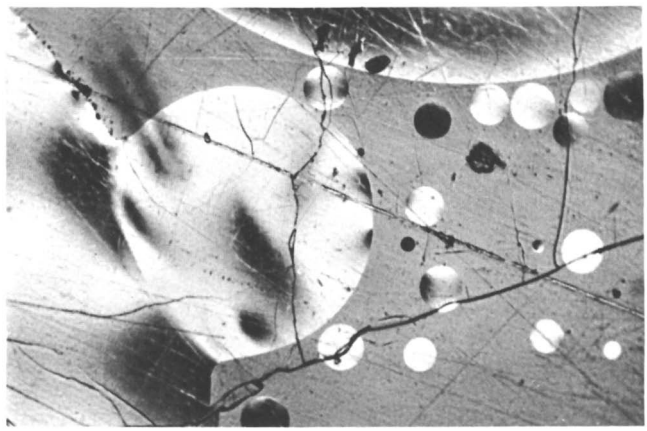

Figure 3. "Capture" of one sphere by another; see also Figure 5. × 238

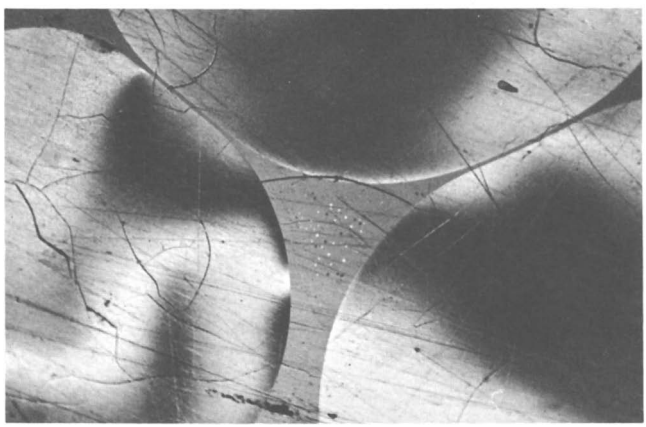

Figure 4. Large spheres closely approaching each other. Small spheres are being nucleated in the interstitial pitch, but there is a zone around the large bodies which is free of these small spheres. × 189

to have been pushed ahead of the rim of a large sphere during its growth. After two or more spheres had contacted, they appeared to remain together, and further enlargement seemed to occur (Figure 5).

Optical extinction was sharpest and most regular in spheres less than 5 microns across. In the largest spheres, extinction patterns were quite com-

Publication Date: January 1, 1966 | doi: 10.1021/ba-1966-0055.ch035

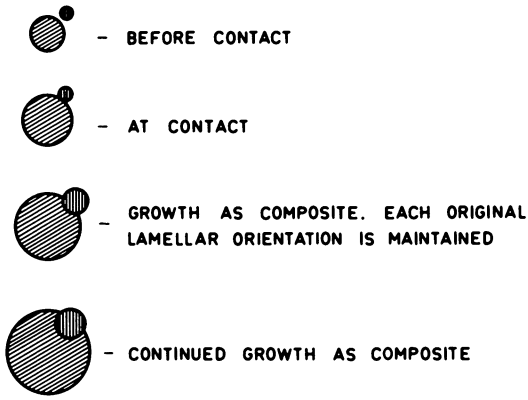

Figure 5. Stages in growth of two spheres making contact.

plex, with the edges exhibiting more undulose and irregular extinction than the centers (Figure 6).

In the original pitches, insoluble, irregular particles were present initially. It was noticeable that at an intermediate stage of solidification the spheres were associated with these insoluble particles, and where insolubles were locally lacking, few or no spheres were present until an advanced stage in the solidification process had been reached. However, such particles were generally excluded from growing spheres, and thus each sphere was surrounded by a ring of particles (Figure 7). On complete solidification, the coke from such pitches contained a network of these insoluble particles (Figure 8) which made it possible to observe the true boundaries of the mosaic units.

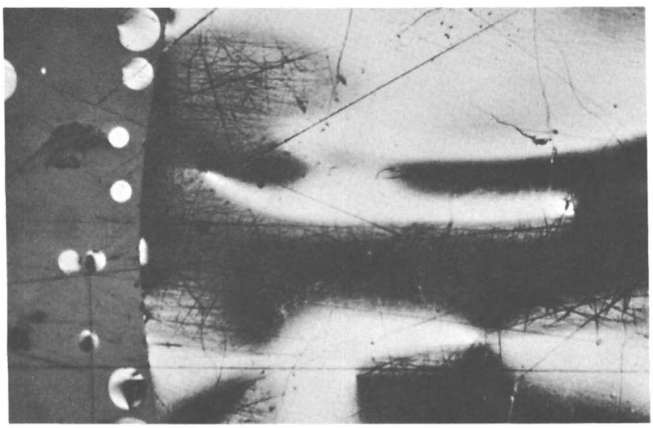

Figure 6. Edge of large sphere showing complex polarization effects. × 124

Publication Date: January 1, 1966 | doi: 10.1021/ba-1966-0055.ch035

Ultrathin sections of partly carbonized pitches were prepared for electron-microscopic examination. The spheres were extremely hard to distinguish from unconverted pitch by microscopy, although their position was revealed if insolubles were present. However, by using electron diffraction and microscopy in conjunction, spheres could be located fairly systematically. The spheres behaved as harder objects than the unconverted pitch during microtomy, and there were frequently cracks or folds around the margins of spheres in ultrathin sections. The spheres were slightly compressed during sectioning but remained approximately spherical. Their margins were sharp and regular so far as could be determined (Figure 9).

Publication Date: January 1, 1966 | doi: 10.1021/ba-1966-0055.ch035

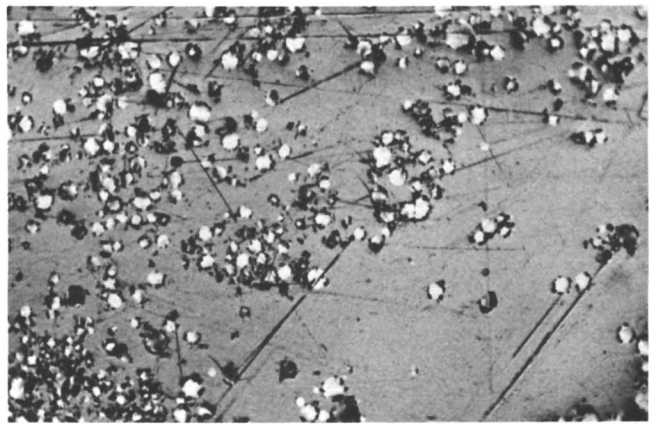

Figure 7. Spheres and insoluble components showing association between them. × 216

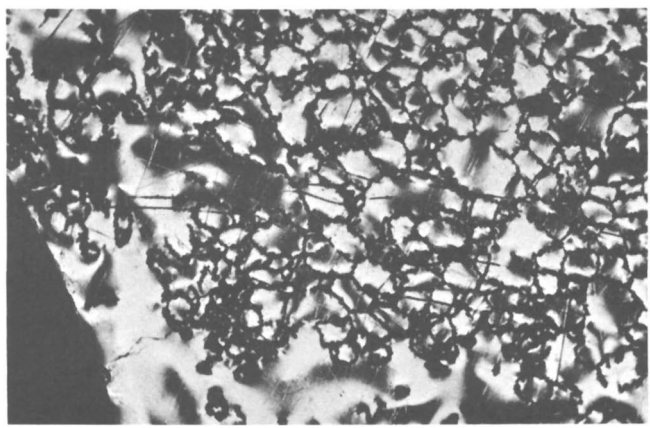

Figure 8. Boundaries of mosaic units in semicoke as revealed by quinoline-insoluble material. × 189

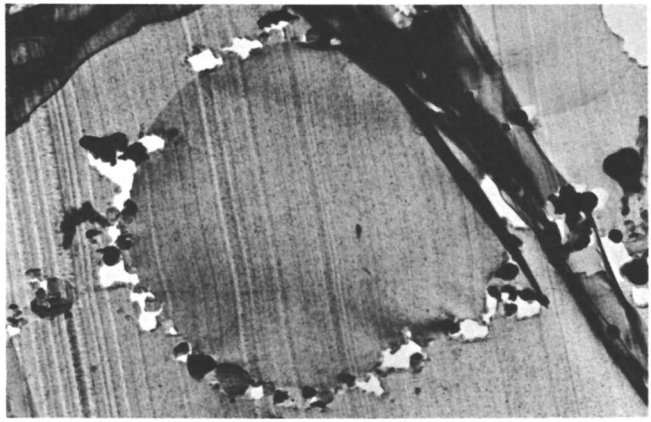

Figure 9. Ultrathin section of sphere. The irregularities around much of the margin are caused by quinoline insoluble particles. Where the edge of the sphere can be seen it is quite sharp. × 5508

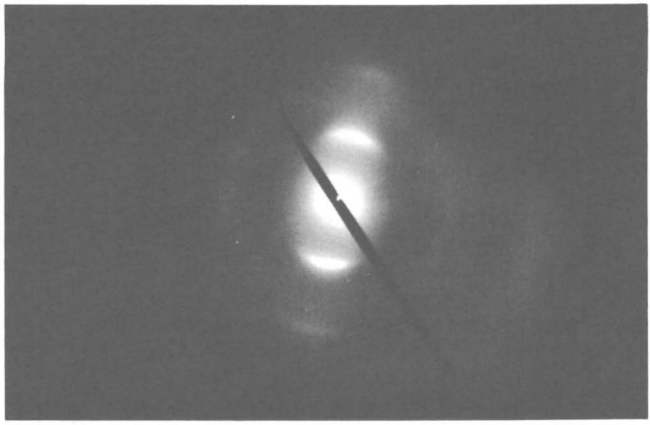

Figure 10. Selected-area diffraction pattern from an ultrathin section of the whole of one sphere

The spheres were observed in the electron microscope at sizes varying from 10 microns down to 0.1 micron, and less. At the lower end of this range the spheres could be located by selected-area diffraction but often could not be resolved because of lack of contrast.

The electron-diffraction pattern yielded by a single body typically contained two arcs, and usually second, and sometimes third orders of these (Figure 10). The pattern was substantially constant over the extent of the sphere. However, as the selected area was reduced symmetrically towards the center of the circular section of the sphere, the pattern became sharper, and the angular extent of the arcs lessened (Figure 11). This was most noticeable where the lamellar direction of the body was perpendicular, or

Publication Date: January 1, 1966 | doi: 10.1021/ba-1966-0055.ch035

nearly so, to the plane of the section. In a similar way, a selected area from near the margin of such a body gave a more diffuse pattern than an area of identical size at the center. Not only was the pattern from the center less diffuse, but the angular extent of the arcs was smaller. The angular extent of arcs at their smallest—i.e., in small central areas of favorably oriented bodies—was about ±12 degrees from a median diameter.

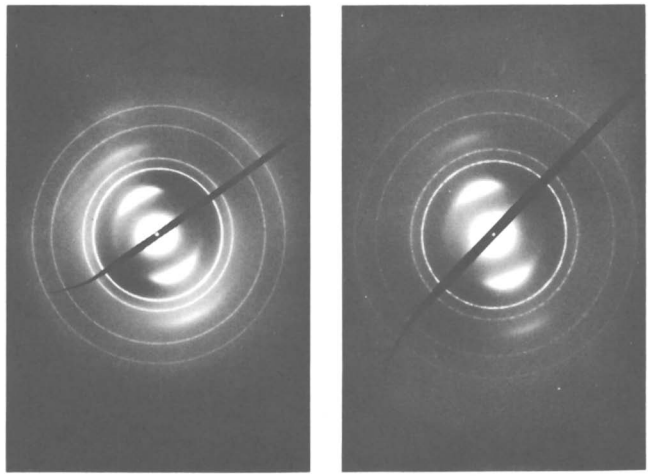

Figure 11. Electron diffraction pattern of the whole of a sphere (a) and of a small central area of the same sphere (b)

An internal aluminum standard was used to calibrate the spacings, which were measured with a photo-microdensitometer. The peak intensity of the main arcs corresponds to an interlamellar spacing of 3.47 A. ± 0.02 A. (compare graphite, 3.35 A., with second and third orders at appropriate spacings). Other peaks present were at 2.07 A. ± 0.02 A. and 1.20 A. ± 0.02 A. These appear to represent (10) and (11) spacings, respectively. Only an extremely diffuse pattern, without evidence of preferred orientation, was obtained from the pitch surrounding the spheres.

Electron-diffraction patterns of spheres were also obtained at their temperature of formation (about 400°C.). The patterns obtained at room temperature and at 400°C. were almost identical, and there was little if any systematic sharpening of the pattern at the higher temperature.

Chemistry of the Solidification Process

The identifiable compounds in coke-oven and petroleum pitches are mainly polynuclear aromatic hydrocarbons. Proton magnetic resonance spectra of solvent-soluble fractions of these materials show that over 90% of the protons are attached to aromatic rings. Under the conditions of carbonization it would

Publication Date: January 1, 1966 | doi: 10.1021/ba-1966-0055.ch035

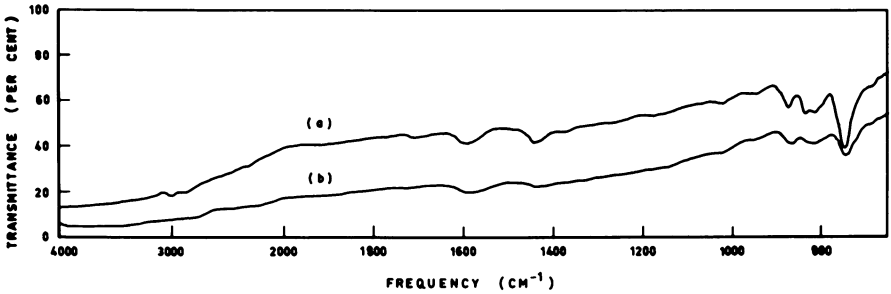

Figure 12. Infrared spectra of fractions of partly carbonized toluene-soluble coke-oven pitch: (a) toluene soluble; (b) toluene insoluble (largely spheres)

be expected that compounds with boiling points up to about 500°C. would be removed by distillation or sublimation. The ultraviolet spectra of benzene- and pyridine-soluble fractions of the partly carbonized coke-oven pitch (i.e., that part of the pitch which remained unconverted) showed envelopes with an absorption edge between 3700 and 4500 A. The average molecular weights of these fractions were 395 and 470, respectively; if composed of single aromatic units, each molecule would contain at least eight to 10 condensed rings. Many compounds of this size would be expected to have pronounced absorption much farther into the ultraviolet visible region, and probably the components in the pitch from which the sphere is formed consist partly of two or more smaller ring systems joined in a nonplanar fashion, presumably by diaryl-type linkages or by a small proportion of CH_2 groups (hydroaromatic structures).

The ultimate analysis of a partly converted pitch containing 27% by volume of spheres corresponded to $C_{100}H_{75}O$ and differed little from that of the solvent-insoluble residue consisting mainly of spherical bodies, of which the analysis corresponded to $C_{100}H_{49}O_{1.4}$. However, the infrared spectrum of the residue showed strong (95%) absorption to 3500 $cm.^{-1}$ (Figure 12), indicating that condensation of compounds in the original pitch had occurred to form larger, extended, conjugated structures having a similar C/H ratio.

The pitch matrix was almost entirely removed by extracting the partly carbonized material with benzene and pyridine (Figure 13). The spheres as a whole were not dissolved although some—especially the larger ones—were badly cracked and in some cases disintegrated into angular fragments during the extraction process (Figure 14). The optical properties of the fragments were similar to those of the material of the original spheres. The crack pattern may have arisen partly from the additional mechanical handling of the spheres but appeared to be, at least in part, a result of slight shrinkage (perhaps owing to the dissolution of a small proportion during the extraction). Since only very rarely could any of these fissures be interpreted as possible solution channels, it is probable that if any material were removed, it came from positions throughout the sphere.

A coke-oven pitch fraction which had been partly carbonized and contained about 30% by volume of spheres was reduced with lithium in ethylene-

Publication Date: January 1, 1966 | doi: 10.1021/ba-1966-0055.ch035

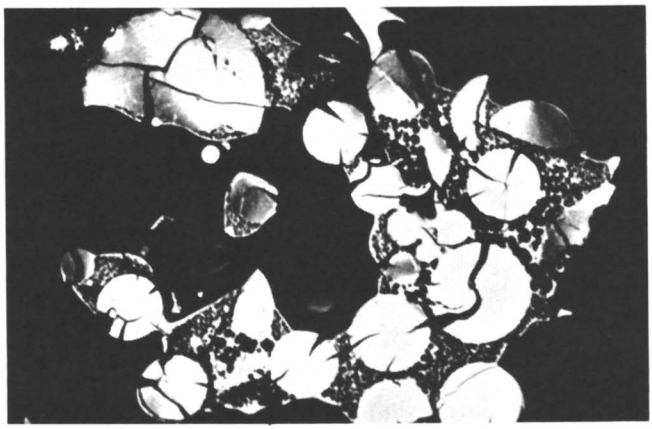

Figure 13. Spheres after extraction. The cracks are perhaps a result of a small amount of shrinkage. × 356

diamine. The hydrogen content increased, the empirical composition changing from $C_{100}H_{53}$ to $C_{100}H_{113}$. The infrared spectrum of the product indicated the virtual absence of aromatic CH groups, and the ultraviolet spectrum showed only end absorption. Measurement of molecular weights in solution in chloroform using a vapor pressure osmometer showed that the unreduced pitch contained: a benzene-soluble fraction (26%), molecular weight 395; a pyridine-soluble fraction (46%), molecular weight 468; and an insoluble fraction (27%), mainly of sperical bodies. After reduction the product was entirely soluble in chloroform, and its molecular weight was found to be 790. The reduction converts polynuclear aromatic structures to polycyclic, partly unsaturated compounds and does not lead to ring opening or molecular weight degradation (*1*). The calculated average molecular weight of the reduction product of the insoluble fraction, and hence the approximate molecular weight of the material of which the spheres are composed, was 1690.

Control of Nucleation and Growth of Spheres

When coke-oven or petroleum-tar pitches were heated to an appropriate temperature (about 420°C.) and quenched, the product contained spheres of various sizes mostly in the range 0–10 microns. The spheres were normally, fairly regularly distributed through the pitch matrix, with small and larger spheres intermixed. When the toluene-soluble extract of the pitch was carbonized to the same temperature, fewer spheres were present in the product, but their diameters were considerably greater. Under these conditions many spheres were more than 10 microns across, and some exceeded 50 microns. This result suggested that nucleation occurred less commonly or less easily in the toluene-soluble pitch fraction and was associated with the presence of 'C1'-insoluble material.

Another factor affecting growth was the time during which the spheres were able to grow. The size, after heating for 5 hours at 412°C., was appre-

Publication Date: January 1, 1966 | doi: 10.1021/ba-1966-0055.ch035

ciably greater (up to 2 mm. in some cases) than when the same pitch was heated for 1 hour at 420°C., its final temperature. Extending the "soaking" time to 5 hours resulted in only a small increase in size over that attained after 1 hour.

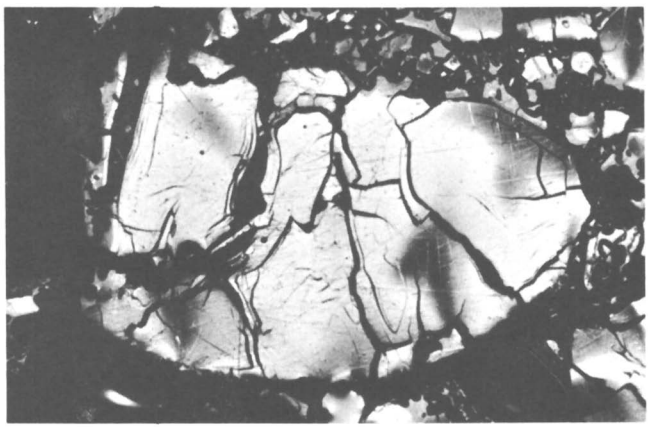

Figure 14. Part of a large sphere after extraction. The sphere is shattered, perhaps partly as a result of mechanical treatment, but the fragments have very similar optical properties to the spheres before extraction. × 216

Publication Date: January 1, 1966 | doi: 10.1021/ba-1966-0055.ch035

Conclusions

Each sphere has a lamellar structure and a single preferred orientation but shows systematic variations in the optical extinction patterns, which indicate some variation from a strictly lamellar arrangement; this is most noticeable at the poles of spheres. As they grow and meet obstructions to their enlargement in particular directions, their extinction behavior becomes increasingly complex, especially when the pitch nears solidification and the complete mosaic structure is formed.

The number of spheres appears to be related to the number of actual or potential nuclei present. The growth of the spheres is related to temperature and time and is limited by the amount of material available, as when two or more spheres are competing for this.

The spheres are composed of condensation products of polynuclear aromatic hydrocarbon, which are planar in configuration.

The condensation products are mainly or wholly insoluble in organic solvents but do not differ markedly in C/H ratio from the high-boiling pitch compounds from which they have separated. The average molecular weight of the pitch shortly before conversion to spheres was about 450 and that of the material of the newly formed spheres was about 1700. Presumably further condensation reactions occur within the ordered structure of the spheres at higher temperatures after complete conversion to low-temperature coke.

Acknowledgments

The authors gratefully acknowledge the support of H. R. Brown, Chief of the Division of Coal Research, C.S.I.R.O. and the assistance of many of their colleagues.

Literature Cited

(1) Brooks, J. D., Duric, R. A., Silberman, H., *Australian J. Chem.* **17,** 55 (1964).
(2) Taylor, G. H., *Fuel.* **40,** 465 (1961).

RECEIVED October 5 1964.

Discussion

Philip L. Walker, Jr. Dr. Taylor has been describing results for the carbonization of a coal tar pitch which was very low in quinoline insolubles (QI). In this case the mosaic unit which he finds in the cokes is quite large. I am wondering if he has looked at pitches of a higher QI content and if the mosaic size in the cokes decreases with increasing QI content in the original pitch?

G. H. Taylor: Yes. We have looked at pitches with varying amounts of quinoline insolubles and find that the mosaic size is limited by these insolubles. Within limits, the higher the QI content, the smaller the mosaic size.

Ralph J. Gray. Dr. Taylor states that the transformation of plastic vitrinite or coal-tar pitch into low temperature coke has some of the characteristics of a crystallization process. The authors place much emphasis on the development of spherical bodies in both vitrinite and pitch. My question concerns the type of pitch, the method of its production, and the method of pitch coke production.

It is my contention that the optical and physical properties and the optical structure produced during the destructive distillation or thermal decomposition of vitrinite is closely related to mode of carbonization and, in the case of pitch, is intimately related to the method of pitch preparation. For instance, a pitch may be produced from a high or low temperature tar, from a primary cooler tar, or from a flushing liquor tar. In addition, it may be air blown, thermally or chemically treated, straight distilled, or cut back, just to mention a few. Under similar carbonization conditions almost any one of these pitches will produce a coke which has certain characteristics that are related to the parent pitch. Even pitches similarly processed from the tar can differ in the content of quinoline- and benzene-insoluble material and β-resin, and can contain more than one distinct liquid phase. None of these points of difference has been discussed by Dr. Taylor or even recognized in the preparation. To interpret the structure of pitch coke divorced from a knowledge of the pitch source and/or carbonization conditions can lead to erroneous conclusions. These are pertinent data omitted by the authors.

To illustrate the possibility of producing distinctly different pitch cokes with different microstructure from two pitches that are nearly identical in physical and chemical characteristics, a series of photomicrographs are included (Figure A). These photomicrographs show the distribution of phases in a cut-back pitch and a pitch produced from straight distillation. The phase separations can be explained without resorting to a theory involving crystallization. In each instance at 450°C. the quinoline-insoluble fraction appears as bright solid particles, and the fraction least soluble in benzene is gray and nearly anisotropic while the fraction most nearly related to anthracene is strongly anisotropic. In my interpretation of a pitch coke, the most important phase differences occur between 450°C. and 550°C. In this range, the low boiling fractions separate and begin to rise as they distill off. The pitch fraction

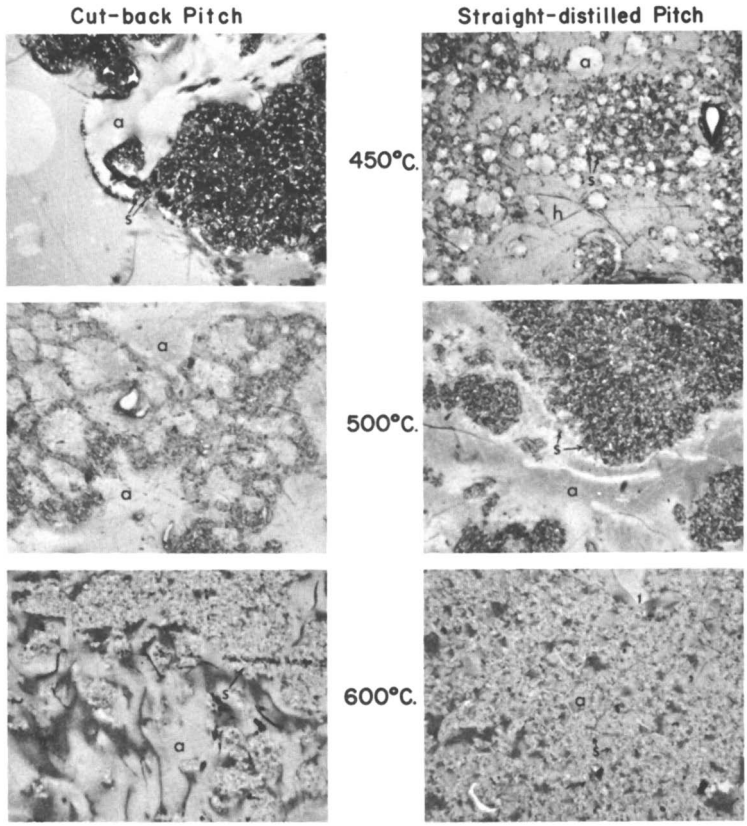

Figure A. The distribution of optically distinct materials in the cut-back and straight-distilled refractory pitches are different. The strongly anisotropic materials (oil phase) (A) contrast with the fine solids (S) in an amorphous resin from the original pitch and with the material which is more isotropic (I). At 450°C. another distinct isotropic phase (H) exists in the straight-distilled pitch, Reflected light × 500

most nearly related to anthracene rises and forms droplets that, in part, rise to the surface of the hot liquid where some are entrapped and some escape and deposit on available surfaces. The sea of higher boiling point materials is more nearly related to the parent coal substance, and it is the viscosity and amount of this phase which determine the extent to which liquid phase separation occurs. This helps explain why a cut-back pitch made from materials widely separated in boiling point separates to produce more distinctly different materials than when the entire spectrum of materials of different boiling points are present. The suspended solids remain in association with the high boiling point liquid phase and, to a large extent, affect its viscosity and are centers of coke formation by nucleation. Thus, the microstructural elements of a pitch coke produced below 550°C. when interpreted as evidence of a crystallization process can better be explained as products of a distillation process that precedes the crystallization process. In considering Dr. Taylor's presentation, one should be aware of this alternative and more realistic explanation for the microstructures in low temperature pitch coke. In addition, these points of difference in interpreting pitch coke microstructure should be at least partially resolved before we try to project our interpretation of pitch-coke structures into our studies of coal-coke structures.

Publication Date: January 1, 1966 | doi: 10.1021/ba-1966-0055.ch035

G. H. Taylor and J. D. Brooks. The pitches studied were produced by straight distillation and were not cut-back pitches. The intention of the present paper is to describe and interpret the series of changes which leads to the formation of semicoke from the vitrinite of a coking coal, many kinds of pitch, or for that matter polyvinyl chloride and many organic chemical compounds. We can take this approach because we find the sequence of events closely similar in each case. The sequence applies to those substances which pass through a plastic stage and form a semicoke with mosaic structure and which graphitize on heating to elevated temperatures. We are aware that pitches vary considerably and that, for example, pitches from air-cycle fluidized-bed carbonization do not behave in this way. We have referred in the paper to some of the effects observed when quinoline-insoluble particles are present.

Dr. Gray, so far as we can understand him, appears to consider the spheres to be comprised of material "most nearly related to anthracene," and further that the spheres rise in the pitch being carbonized. Neither of these suppositions is, in general, true. First, we have calculated the average molecular weight of the sphere material to be about 1700; the spheres represent the largest hydrocarbon molecules present and not the smallest (disregarding the quinoline-insoluble particles present in the pitch prior to carbonization). Second, we have evidence from carbonizing pitch in deep vessels that the spheres sink and aggregate near the bottom of the vessel in the absence of strong convection currents. There is normally, of course, some distillation during the carbonization of pitch, but removing material by distillation is not essential to the sequence of events we have described. We have shown this to be so by carbonizing pitch under reflux conditions where virtually no loss of pitch material occurs. We therefore conclude that in a straight-distilled pitch, for example, the following changes occur in the soluble fraction: condensation reactions cause the formation of larger planar molecules than previ-

ously existed; these larger molecules aggregate into anisotropic spheres having the order described; the spheres grow in size and number at the expense of the pitch in which they occur; eventually all the pitch is converted to such anisotropic material.

Dr. Gray's photographs appear entirely consistent with our interpretation of the carbonization process. His suggestions, however, are incompatible with our observations, quite unrealistic, and provide no alternative explanation of the process of coke formation.

Publication Date: January 1, 1966 | doi: 10.1021/ba-1966-0055.ch035

36

Petrography and Carbonization Characteristics of Some Western Canadian Coals

A. R. CAMERON[1] and J. C. BOTHAM[2]

Department of Mines and Technical Surveys, Ottawa, Ontario, Canada

Publication Date: January 1, 1966 | doi: 10.1021/ba-1966-0055.ch036

Petrographic and carbonization studies were carried out on samples from two seams in the Crowsnest Pass area of British Columbia. Swelling was measured by the free swelling index test and fluidity by the Gieseler test; strength measurements were made on coke from the 500 lb. capacity, movable-wall test oven. Petrography is expressed in both macerals and microlithotypes. Of interest is the somewhat anomalous distribution of the fusinitic constituents in the size fractions of one of the seams examined. Fluidity correlates better with the content of the microlithotype vitrite than with the total vitrinite. Calculated stability factors on six cokes suggest that a textural variety of vitrinite, described as mylonitized or pitted, has a deleterious effect on coke strength.

This paper covers some of the information revealed during a study made by the Department of Mines and Technical Surveys on the petrography and coking properties of two high rank coals from western Canada. The Geological Survey of Canada carried out the sampling and petrographic evaluation while the chemical analyses and the carbonization tests were carried out by the Mines Branch. The coals in question are Lower Cretaceous in age and occur in the Crowsnest Pass area of the Canadian Rockies. They are marginal with respect to coking and are not typical of some of the better coking coals from this area. One of the coals is medium volatile bituminous, and the other is low volatile bituminous, by ASTM rank classification. The medium volatile coal will be treated in considerable detail.

[1] Geological Survey of Canada
[2] Mines Branch

In Coal Science; Given, P.;
Advances in Chemistry; American Chemical Society: Washington, DC, 1966.

Experimental Procedures

Two 1000-lb. samples of the medium volatile coal were collected at a fresh face underground and represent the top and bottom halves of a 12-foot thick seam. Each of these gross samples was screened into eight size fractions, namely, +2 inch, 2 × 1½ inch, 1½ × 1 inch, 1 × ¾ inch, ¾ × ½ inch, ½ × ¼ inch, ¼ × ⅛ inch, and —⅛ inch. Each of these size fractions was weighed, and the results have been plotted in weight percent histograms on Figure 1. Each of the size fractions was crushed to 80% —⅛ inch, and each was sampled for petrographic analysis, chemical analysis, and swelling and fluidity tests. The original gross samples were then reconstituted by blending the fractions back together.

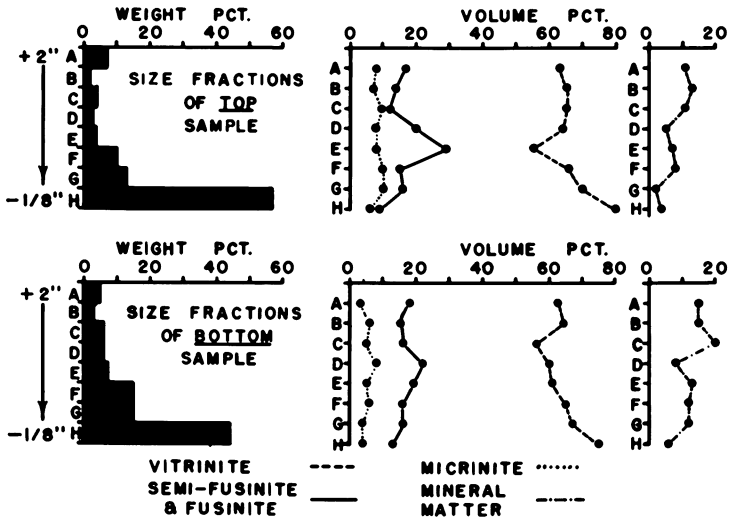

Figure 1. Maceral compositions in size fractions of medium volatile coal

The chemical analysis and the bench-scale and technical-scale testing were carried out either by standard tests or by tests under consideration for standardization by ASTM. Analytical data from these tests for the size fractions of the medium volatile coal are given in Table I.

In addition to the fluidity and swelling tests and the chemical analyses, three charges of the medium volatile coal were coked in the 500-lb. capacity test oven, one representing the top sample, one the bottom sample, and one a 50-50 blend of top and bottom. Also, three charges were coked of the low volatile coal. These represented three commercial size fractions—namely, +1⅝ inch, 1⅝ × ¼ inch, and —¼ inch. Chemical analyses of these six samples, prior to coking, are given in Table II. The technical-scale oven used for this part of the study is the movable-wall type and has been in service for the past three years. The coking chamber is approximately 38 inches deep, 34 inches high, and 12 inches wide. The walls of silicon carbide tile are heated electrically by (silicon carbide) heating elements. With standardized operating conditions the quality of the cokes produced in the test oven duplicates closely that of the commercial cokes made from the same coals under equivalent conditions. Particle size, moisture, and bulk density are given in Table

Publication Date: January 1, 1966 | doi: 10.1021/ba-1966-0055.ch036

Table I. Analyses of Screen Fractions for Top

Identification	*A*	*B*	*C*
Screen Fraction, inch	+2	2 × 1½	1½ × 1
Proximate analysis, %			
Moisture	0.9	0.9	0.9
Ash	24.4	29.2	24.1
Volatile matter	21.2	20.5	21.2
Fixed carbon	53.5	49.4	53.8
Free swelling index	7	5½	6½
Gieseler plasticity[a]			
Start, °C.	443	447	444
Max. fluid temp. °C.	469	477	471
Max. fluidity, ddm	13	8	14
Melting range, °C.	46	49	49
Proximate analysis, %			
Moisture	1.0	0.9	1.2
Ash	22.7	35.3	31.9
Volatile matter	22.8	21.2	20.8
Fixed carbon	53.5	42.6	46.1
Free swelling index	8	6½	7½
Gieseler plasticity[a]			
Start, °C.	445	433	442
Max. fluid temp., °C.	475	472	470
Max. fluidity, ddm	27	16	17
Melting range, °C.	54	57	53

[a] Constant torque plastometer; ddm—dial division per minute.

VI, and the heating rate was programmed according to the recommendations of Eddinger and Mitchell (*1*).

The petrographic analyses of both the size fractions and the samples for carbonizing were carried out microscopically by reflected light on duplicate pellets, prepared in each case from —20 mesh material. For each fraction, macerals and microlithotypes were identified and their proportion recorded. For the samples prepared for coking, only the macerals were recorded. The point count method was used to determine the maceral content, with 300 points being counted per pellet or a total of 600 per sample. The integrating stage was used to assess quantitatively the microlithotypes—60 mm. of coal were traversed per pellet, making a total of 120 mm. per sample.

Petrography of Medium Volatile Coal

Figure 1 shows the variations in maceral distribution of the size fractions making up the top and bottom samples. Also shown in weight percent histograms are the quantities of coal occurring in each size fraction. Examining these diagrams shows that this is a very friable coal, with about 50% of each gross sample occurring in the —⅛ inch fraction. The petrographic plots show that in this seam, fusinite and semifusinite are the major inert macerals and the most variable in terms of proportions present in each fraction. The amount of micrinite is remarkably constant throughout the size fraction series of both samples. Fusinite and semifusinite are found in greatest quantity in the inter-

Publication Date: January 1, 1966 | doi: 10.1021/ba-1966-0055.ch036

and Bottom Samples of Medium Volatile Coal

D 1 × ¾	*E* ¾ × ½	*F* ½ × ¼	*G* ¼ × ⅛	*H* —⅛
Top				
0.8	0.8	1.0	1.1	1.1
18.7	19.8	19.6	13.4	9.2
22.0	21.4	21.7	22.5	23.7
58.5	58.0	57.7	63.0	66.0
7	5½	7½	8	9+
448	450	444	444	441
473	473	472	474	478
9	11	10	35	81
41	43	47	52	58
Bottom				
1.1	1.0	1.2	1.0	1.1
26.1	22.0	21.9	19.8	15.0
21.2	21.5	21.2	22.4	23.0
51.6	55.5	55.7	56.8	60.9
7½	8	8	8	9
444	447	443	440	438
474	478	477	476	473
23	19	17	39	73
54	55	52	56	60

mediate sizes and not in the fines. Vitrinite is least abundant in the intermediate sizes and most abundant in the —⅛ inch fraction, especially in the top sample. This concentration of vitrinite in the —⅛ inch fraction, without an accompanying increase of fusinite, is a favorable feature of this coal. It represents a natural segregation of reactive and inert macerals in a coal that overall has an overabundance of inerts. Exinite was identified in all samples, but in amounts that never exceeded 2%; hence its distribution has not been plotted in Figure 1. Table III presents the detailed maceral data for each size fraction.

Because exinite is a minor constituent in this coal, the microlithotypes defined represent variations in a two-component system of vitrinite and the inert macerals semifusinite, fusinite, and micrinite. Whole particles were considered in the microlithotype analysis—i.e., the maceral composition of a particle was estimated, and on the basis of this estimation the whole particle was assigned to a particular microlithotype. Figure 2 shows the triangular arrangement of the microlithotypes, with the more heavily lined part on the right side being applicable in the present study.

Vitrite and fusite were recognized, as well as carbargilite and shale; the remainder of the material fell into the category of vitrinertite, of which four varieties were noted—namely, vitrinertites 1, 2, 3, and 4. The boundaries of these four varieties of vitrinertite are so drawn that vitrinertite 1 corresponds

Publication Date: January 1, 1966 | doi: 10.1021/ba-1966-0055.ch036

roughly to clarite, vitrinertite 2 to duroclarite, vitrinertite 3 to clarodurite, and vitrinertite 4 to durite.

Figure 3 shows the compositions of the size fractions in terms of the microlithotypes just described. The fractions of the top sample differ from those of

Table II. Analyses of Coals as Prepared for Carbonization in Test Oven

Identification	*Med. Volatile Coal*			*Low Volatile Coal*		
	Top	*Bottom*	*50-50 Blend*	*+1⅝ inch*	*1⅝ × ¼ inch*	*—¼ inch*
Proximate analysis, %						
Moisture	1.1	0.8	0.9	0.6	0.8	0.4
Ash	11.9	18.0	16.0	15.7	15.3	14.3
Volatile matter	25.5	23.1	22.8	18.2	18.7	19.6
Fixed carbon	61.5	58.1	60.3	65.5	65.2	65.7
Ultimate analysis, %						
Carbon	76.85	70.41	—	75.00	74.66	76.05
Hydrogen	4.57	4.29	—	4.06	4.23	4.19
Sulfur	0.54	0.39	0.49	0.23	0.63	0.45
Nitrogen	1.41	0.98	—	0.92	0.89	0.95
Ash	11.92	18.15	—	15.66	15.33	14.27
Oxygen (by diff.)	3.65	5.19	—	3.52	3.49	3.69
Free swelling index	9	8	8½	2½	4	7½
Gieseler plasticity[a]						
Start, °C.	443	445	444	466	467	460
Max. fluid temp., °C.	478	479	477	483	479	486
Max. fluidity, ddm	66	57	61	2	2	6
Range, °C.	61	60	58	26	29	44

[a] Constant torque plastometer; ddm—dial division per minute.

Table III. Maceral Composition of Size Fractions of Medium Volatile Coal

Sample	*Vitrinite*	*Semifusinite*	*Fusinite*	*Micrinite*	*Exinite*	*Min. matter*
Top						
+2 inch	63.4	3.7	13.3	8.3	0.8	10.5
2 × 1½	65.3	4.2	9.5	7.1	0.9	13.0
1½ × 1	65.9	3.0	8.5	10.4	1.2	11.0
1 × ¾	65.0	3.3	16.8	8.1	2.0	4.8
¾ × ½	55.0	5.8	22.7	8.0	1.5	7.0
½ × ¼	65.9	2.1	12.8	9.9	1.8	7.5
¼ × ⅛	70.0	1.8	14.4	9.7	1.9	2.2
—⅛ inch	80.1	1.8	6.7	6.1	1.3	4.0
Average[a]	73.7	2.3	9.8	7.6	1.4	5.2
Bottom						
+2 inch	61.7	4.7	13.3	3.3	1.7	15.3
2 × 1½	63.7	4.6	10.3	6.7	1.0	13.7
1½ × 1	57.0	5.3	11.0	6.0	1.7	19.0
1 × ¾	60.2	8.3	15.0	6.5	1.3	8.7
¾ × ½	61.3	5.0	14.0	5.7	1.0	13.0
½ × ¼	63.6	4.3	10.7	7.4	1.0	13.0
¼ × ⅛	67.1	5.6	9.8	4.0	0.7	12.8
—⅛ inch	76.0	4.7	8.6	4.4	1.7	4.6
Average[a]	68.7	5.0	10.3	5.1	1.4	9.5

[a] Calculated from compositions of fractions.

Publication Date: January 1, 1966 | doi: 10.1021/ba-1966-0055.ch036

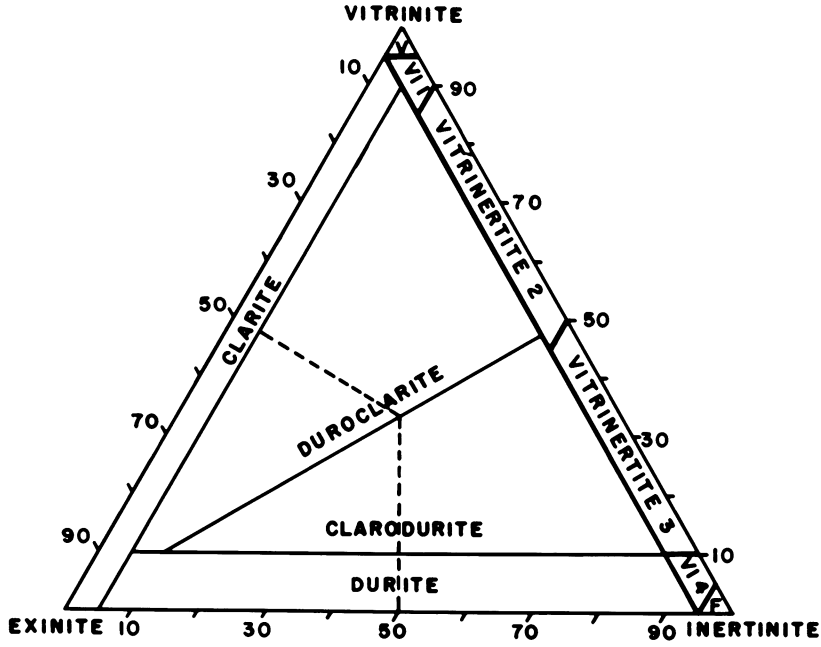

Figure 2. Triangular diagram showing maceral compositions of microlithotypes

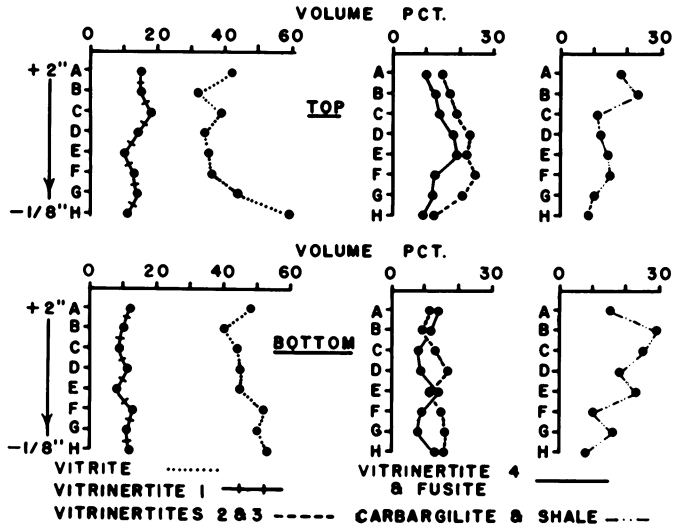

Figure 3. Microlithotypes in size fractions of medium volatile coal

Publication Date: January 1, 1966 | doi: 10.1021/ba-1966-0055.ch036

the bottom sample in certain details. There is more variation in the vitrite content from the coarse fractions to the fine in the top sample as compared with the bottom sample. There is also greater variation in the contents of vitrinertites 2 and 3 and vitrinertite 4 and fusite in the top sample. These last mentioned four microlithotypes concentrate in the intermediate fractions of the top sample while no such concentration is apparent in the bottom sample. Carbargilite and shale decrease in a somewhat erratic fashion from coarse fractions to fine fractions in both samples. Table IV gives the detailed composition of each fraction in terms of microlithotypes.

Relation of Fluidity and Swelling to Petrography

Fluidity data were determined by the Gieseler apparatus on the 16 size fractions of the medium volatile coal. The values obtained were relatively low, ranging from 8 to 81 dial divisions per minute. An attempt was made to correlate these results with petrographic data. Some of the possible relations examined are shown in Figure 4. A plot of the maceral vitrinite against fluidity shows considerable scatter as does a plot of the ash content *vs.* fluidity. The ash content was determined by proximate analysis (*see* Table I) and is included here for comparison.

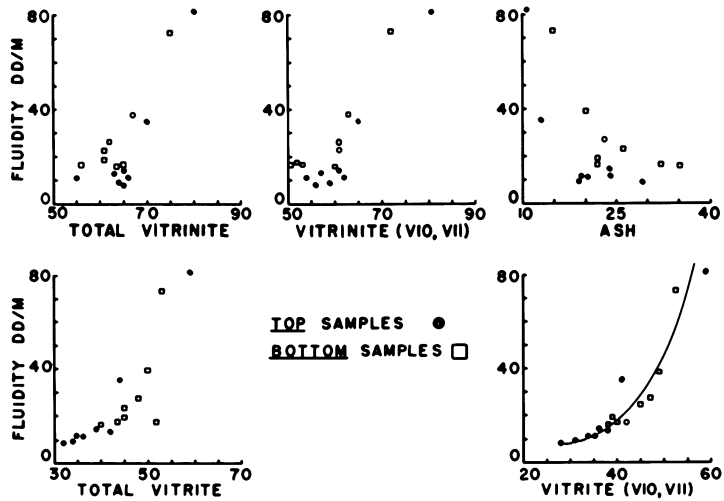

Figure 4. Relation of fluidity (Gieseler) to some petrographic parameters

However, when the content of the microlithotype vitrite was plotted against fluidity, the result was a considerable improvement though several points still fell off the trend line. To examine this relation between vitrite content and fluidity further, we used reflectivity data that had been obtained on the vitrinitic portion of each size fraction. The reflectance types ranged from V10 to V13. (The term reflectance type as used in this paper is equivalent to vitrinoid type as used by Schapiro *et al.* (2)). The vitrite content of

Publication Date: January 1, 1966 | doi: 10.1021/ba-1966-0055.ch036

Table IV. Microlithotype Composition of Size Fractions of Medium Volatile Coal

Sample	*Vitrite*	*VI*$_1$[a]	*VI*$_2$	*VI*$_3$	*VI*$_4$	*Fusite*	*Carb.*	*Shale*
Top								
+2 inch	42.0	14.8	7.8	7.2	0.9	9.1	7.5	10.7
2 × 1½	32.2	15.4	13.6	3.7	2.9	9.6	7.7	14.9
1½ × 1	38.5	18.0	9.7	9.4	1.9	11.7	4.7	6.1
1 × ¾	33.8	13.5	13.1	9.6	4.1	13.8	6.0	6.1
¾ × ½	35.3	9.8	14.4	7.3	4.5	14.6	9.3	4.8
½ × ¼	35.6	12.8	17.7	6.8	0.9	11.6	9.6	5.0
¼ × ⅛	44.3	14.1	15.4	4.8	5.5	6.1	9.7	0.1
—⅛ inch	59.4	11.0	6.9	5.5	2.7	6.5	7.4	0.6
Average[b]	50.8	12.2	9.9	5.9	2.9	7.9	7.9	2.5
Bottom								
+2 inch	47.6	11.5	9.5	3.0	1.9	11.2	2.8	12.5
2 × 1½	40.0	10.4	7.3	2.7	3.5	6.7	9.2	20.2
1½ × 1	44.4	8.9	9.2	4.1	1.7	6.7	8.5	16.5
1 × ¾	45.1	11.0	11.1	5.7	0.5	8.7	6.1	11.8
¾ × ½	45.1	7.5	8.3	3.6	1.7	11.0	13.3	9.5
½ × ¼	52.3	12.8	10.3	5.0	1.8	7.4	5.9	4.5
¼ × ⅛	49.6	10.9	10.5	5.1	4.4	3.4	9.8	6.3
—⅛ inch	52.5	11.8	12.1	3.0	0.7	11.8	5.3	2.8
Average[b]	50.2	11.3	10.9	4.0	1.7	8.6	7.0	6.3

[a] Vitrinertites 1, 2, etc.
[b] Calculated from compositions of fractions.

each fraction was calculated to include only vitrite composed of reflectance types V10 and V11. This calculation is based on an assumption that may be open to criticism, and the result is included here only because it seems to show the best relationship with fluidity of all the petrographic parameters plotted. It was assumed that the reflectance types (V10, V11, etc.) are equally distributed in all the microlithotypes—i.e., that the vitrinite of vitrite contains the same proportions of reflectance types as does the vitrinite of other microlithotypes, vitrinertite 2 for example. Because vitrite is virtually 100% vitrinite, it is possible to use the proportions of the various reflectance types to calculate that part of the vitrite content that is devoid of the higher reflectance types, V12 and V13. The resulting calculation and the relation with fluidity are shown on the fifth graph of Figure 4. It seems to be an improvement over the graph in which total vitrite is plotted against fluidity. Figure 4 shows that a similar calculation for the maceral vitrinite failed to produce much improvement. These four plots of the maceral vitrinite and the microlithotype vitrite suggest that for this coal at least, the most significant relation as far as fluidity is concerned is shown not by the total vitrinite content but rather by that part contained in the larger bands and lenses, which part is expressed by the vitrite content. Furthermore, this relation seems to be improved if only a part of the vitrite content is considered—namely, that part made up in this coal of reflectance types V10 and V11.

The free swelling index (FSI) was determined on each of the size fractions; for the top samples the values ranged from 5½ to 9, whereas the bottom size fractions ranged from 6½ to 9 (*see* Table I). In each case the lowest values occur in the intermediate size fractions—namely, those ranging from 2 × 1½ inch to ¾ × ½ inch. These show a rough relationship with the increase in fusinite and semifusinite and the decrease in vitrinite in these

Publication Date: January 1, 1966 | doi: 10.1021/ba-1966-0055.ch036

fractions. It is interesting that both the fluidity values and the swelling indices in the size fractions of the bottom sample are higher than those of the corresponding size fractions of the top sample in spite of the fact that the ash values (Table I) tend to be higher and the vitrinite values lower in the former.

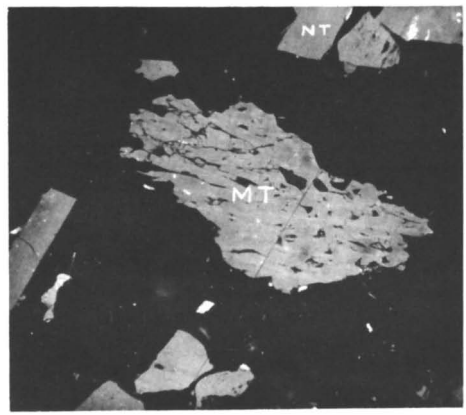

A

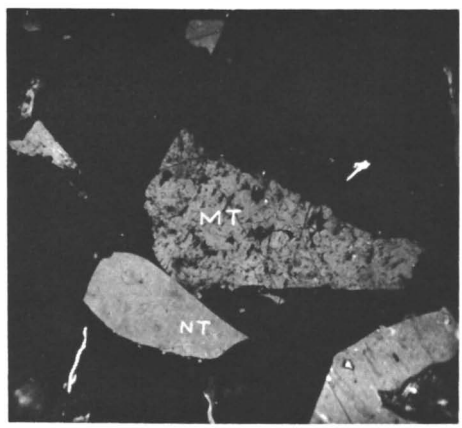

B

Figure 5. Photomicrographs of particles of medium volatile coal showing pitted vitrinite. (A) Particle composed of mylonitized or porous vitrinite (MT) in center. Note similarity of reflectance with particle of normally textured vitrinite (NT) at top center. (B) Pitted vitrinite particle (MT) in center. Smaller particle (NT) immediately below is normally textured vitrinite. Both photomicrographs taken under oil, × *175*

Publication Date: January 1, 1966 | doi: 10.1021/ba-1966-0055.ch036

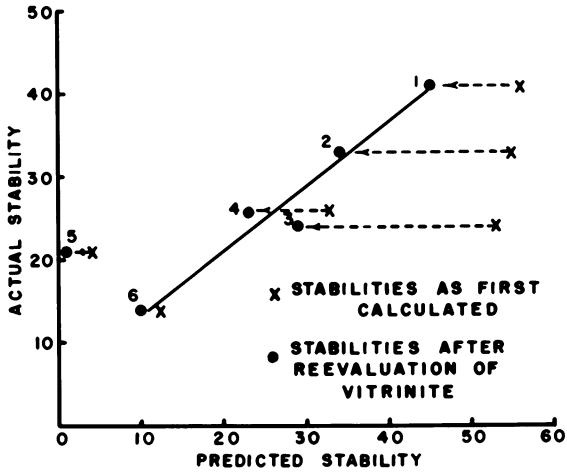

Figure 6. Relation of predicted to actual stabilities for medium volatile and low volatile samples

However, the vitrite values for the bottom size fractions are higher than the corresponding values for the top size fractions (Table IV).

These differences in the petrography of the top and bottom size fractions suggest the value of a microlithotype analysis. The microlithotype analysis provides some idea of the texture of the coals involved. The vitrinite contents of the bottom size fractions are lower than those of the top size fractions, yet the vitrite content is greater in the bottom than in the top. This indicates that a much higher proportion of the vitrinite in the bottom size fractions is concentrated in relatively pure bands and lenses. This textural difference may be of considerable technological significance as indicated by the relation of swelling (and especially fluidity) with vitrite content.

Coke Stability and Petrography

Petrographic analyses, including reflectivity measurements, were made on the six charges coked in the test oven, and stability factor predictions were calculated according to the method described by Schapiro, Gray, and Eusner (2). In four of the six samples involved the predictions were higher than the actual values obtained. The samples were re-examined petrographically, and a portion of the material originally designated as vitrinite was recorded in a separate category. This is vitrinite with a pitted, sometimes granular texture, often heavily impregnated with mineral matter. Figure 5 shows photomicrographs of particles of this material compared with particles of more normally textured vitrinite. Some coal petrographers might place a part of this material in semifusinite, but at least some of it is mylonitized or crushed

Publication Date: January 1, 1966 | doi: 10.1021/ba-1966-0055.ch036

Table V. Petrographic Data

Sample	Vitrinite[a] V10	V11	V12	V13	V14	V15	V16
Medium Volatile							
Top (1)[c]	12.3	44.1	1.5	0.1	—	—	—
Bottom (3)	12.1	30.7	3.1	—	—	—	—
50-50 (2)	12.2	36.6	2.4	0.1	—	—	—
Low Volatile							
+1⅝ inch (5)	—	—	—	10.0	22.7	6.4	0.7
1⅝ × ¼ (6)	—	—	—	6.2	29.3	7.6	1.3
—¼ inch (4)	—	—	—	9.8	34.3	6.7	1.0

[a] V10–V16, reflectance types; V_p Pitted, mylonitized vitrinite.
[b] Mineral matter calculated according to Parr's formula (*2*).

Table VI. Evaluation of Coal Samples in Movable-Wall Test Oven

Identification	Med. Volatile Coal Top	Bottom	50-50 Blend	Low Volatile Coal +1⅝ inch	1⅝ × ¼ inch	—¼ inch
Condition of coal charged						
Moisture,%	1.3	2.6	1.2	0.9	1.2	1.2
Size (⅛ × 0 inch), %	95.0	92.0	93.0	77.2	81.5	80.6
Oven bulk density (dry) lb./cu. ft	51.3	49.4	51.8	55.8	58.5	56.0
			see Table II			
Mean coke size, inches	3.2	3.4	3.2	3.6	3.6	3.4
Drop shatter test for coke 1½-inch sieve, %	81.8	79.8	80.8	72.8	79.0	74.2
Tumbler test for coke (cumulative percent retained on)						
Stability factor, 1-inch sieve	40.7	24.3	32.5	20.2	13.6	26.4
Hardness factor, ¼-inch sieve	63.4	50.3	58.3	66.3	58.6	66.1
Apparent specific gravity	0.94	0.93	0.93	—	—	—
Carbonization pressure Maximum, p.s.i.g.	1.5	1.0	1.1	1.5	1.2	3.8

vitrinite, a constituent to be expected in view of the tectonic history of these coals.

The stability factors were recalculated, and the pitted or mylonitized vitrinite was treated as semifusinite with two-thirds of it being assigned to inerts. Figure 6 shows the relation of the predicted stabilities to the stabilities actually obtained on the coke. Two sets of points are shown, one indicating the position of the stabilities as first calculated and the other the stabilities after re-evaluating the vitrinite. The second calculation is a considerable improvement in the relation of predicted to actual stabilities. The complete data upon which these calculations were made are shown in Table V, while other data pertinent to the evaluation of the samples coked in the movable-wall oven are given in Table VI. The position of the coal represented by point 5 was not improved by recalculation. This coal gave an actual stability of 20.2.

Publication Date: January 1, 1966 | doi: 10.1021/ba-1966-0055.ch036

Used in Stability Calculations

V_r	Semifus.	Fus.	Mic.	Ex.	Min. mat.[b]
11.4	5.1	10.2	7.2	1.4	6.7
18.9	7.5	11.5	5.5	0.9	9.8
15.1	6.4	10.9	6.4	1.1	8.8
5.7	12.3	23.1	10.6	—	8.5
9.0	15.3	14.7	8.2	—	8.4
10.1	7.2	13.6	9.4	—	7.9

[b] (1), (2), etc., sample numbers on Figure 5.

However, its high ash content and its high quantity of inert materials put it in a category of coals where predictions of stability are difficult. A comparison of the FSI values (Table II) for the +1⅝ inch material (point 5 in Figure 5) with the 1⅝ × ¼ inch coal (point 6) suggests that the stability factor of the first-mentioned coal should be lower. This comparison substantiates to some degree the predictions made concerning the +1⅝ inch coal. It is possible that the pitted or mylonitized component, because of its open porous structure, is more susceptible to oxidation than is the more normally textured vitrinite, and this could explain the apparently deleterious effect that this material has on coke quality.

In addition to the relationships discussed, the data presented here suggest one further conclusion of a more general nature—namely, it is well to remember that coal seams have individual characteristics even though possessing many features in common and being subject to many valid generalizations concerning their use. These characteristics are perhaps related to age, or type of parent material, or type of depositional environment, or tectonic history, therefore, the critical petrographic or chemical details governing the utilization properties of one seam may not be as critical with another.

Literature Cited

(1) Eddinger, R. T., Mitchell, J., *Trans. AIME* **15,** 148 (1956).
(2) Schapiro, N., Gray, R. J., Eusner, G. R., *Trans. AIME* **20,** 89 (1961).

Received January 25, 1965.

Discussion

Marie-Therese Mackowsky: Have you ever tried to plot the vitrite and clarite content against fluidity?

Alexander Cameron: Yes, but the correlation with fluidity was not as good as with the vitrite content alone.

John Harrison: The method of mining can effect size distribution. What method of mining was used for this coal? Have you been able to correlate the "pitted" vitrinite with collinite?

Dr. Cameron: The coal was dug by hand from a fresh face underground, and the screen analyses were carried out on this "mine run" coal. No, we have not attempted this correlation.

Publication Date: January 1, 1966 | doi: 10.1021/ba-1966-0055.ch036

Further Applications of Coal Petrography

LOUIS G. BENEDICT and WILLIAM F. BERRY

Bituminous Coal Research, Inc., Monroeville, Pa.

In order to determine the effect of coal rank (as established by reflectance measurement of vitrinite in coal) on the reactions of coal as related to carbonization, gasification, combustion, and other processes, a wide range of bituminous coals were studied. The results show that reflectance measurements can be used effectively: (1) to determine accurately yields of coal carbonization products such as coke, tar, gas, light oil, and liquor from pilot and commercial coke oven; (2) to obtain the heating value and specific gravity properties of gases from these processes; (3) to determine the free swelling index and B.t.u. content of coals; (4) to categorize coals for certain combustion uses; (5) to monitor the oxidation tendencies of coals; (6) to subdivide coals in certain areas of the present coal classification framework.

Publication Date: January 1, 1966 | doi: 10.1021/ba-1966-0055.ch037

During the past several years coal petrography has gained acceptance in certain areas of coal utilization, preparation, and mining as a useful analytical tool. The rapid evolution of this analytical technique can be attributed to the development and subsequent refinement of quantitative methods for measuring the reflectance characteristics of vitrinite in coal (*8*, *14*, *15*, *16*). Mean maximum reflectance has been shown to be directly related to coal rank (*14*, *16*). Moreover, it is known that rank is important in determining certain carbonization and chemical properties.

In this paper, we demonstrate how mean maximum reflectance of vitrinite in oil (hereafter referred to as R_o) can be used in place of conventional chemical-rank parameters (volatile matter and fixed carbon) to estimate the relative yields of carbonization products, specific properties of gas produced by carbonization, and chemical properties of coal such as calorific value and free swelling index (*FSI*). Further, we illustrate that measured R_o can be used to detect coal oxidation, to categorize coals for certain combustion uses, and to help classify coals by rank.

In Coal Science; Given, P.;
Advances in Chemistry; American Chemical Society: Washington, DC, 1966.

Experimental

A wide range of bituminous coals, representing most of the major U. S. coal fields, were microscopically and chemically analyzed in this study. The samples tested, approximately 200 in all, were obtained through various coal producers. However, analytical data were not available for all samples; carbonization, chemical, and by-product gas data for these subject coals were assumed to be the same as those reported previously in published sources (*7, 9, 10, 11, 17, 18*). Only those carbonization data obtained from tests conducted in 18-inch pilot coke ovens at 900°C. are included. The remaining analytical data, approximately one-tenth of the total test results, were obtained from full scale commercial coke oven tests. Because these latter data were not sufficiently represented in the study, they were not considered in computing correlation coefficients (r).

The method used to analyze the R_o of vitrinite in coal is consistent with that reported by others (*8, 14, 15, 16*). Reflectance and chemical properties of the various samples are listed in Appendix I. Carbonization yields and by-product gas properties are shown in Appendix II.

Relation between Reflectance and Volatile Matter, Calorific Value, and FSI

Previous investigations (*14, 15*) have shown that R_o increases as the fixed carbon content increases and decreases as the volatile matter content increases. The relation of R_o to volatile matter for coals included here is similar to that reported by other investigators (*14, 15*); a progressive increase in R_o is accompanied by a corresponding decrease in volatile matter content, as shown in Figure 1.

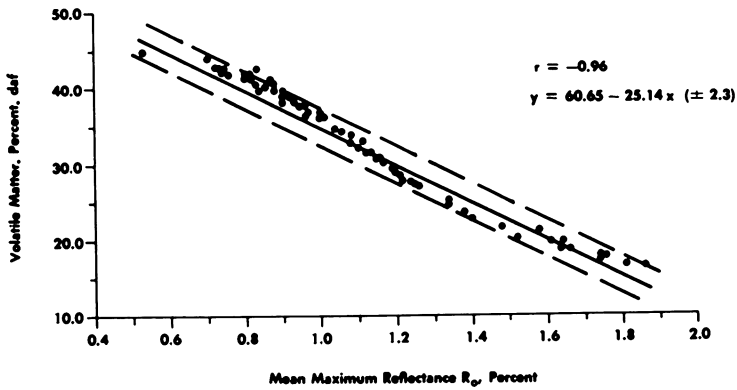

Figure 1. Relationship between reflectance and volatile matter, % daf

Others have related fixed carbon and volatile matter content to calorific value (*4, 5*) and *FSI* (*12*). However, we found that reflectance correlated better with these chemical properties ($r = 0.95$ and 0.87, respectively). Figure 2 shows the relationship between R_o and calorific value for the coals in this study. In general the calorific value increases sharply with increases in R_o in the 0.5–1.1% range, increases slightly in the 1.1–1.7 R_o range, then levels off

Publication Date: January 1, 1966 | doi: 10.1021/ba-1966-0055.ch037

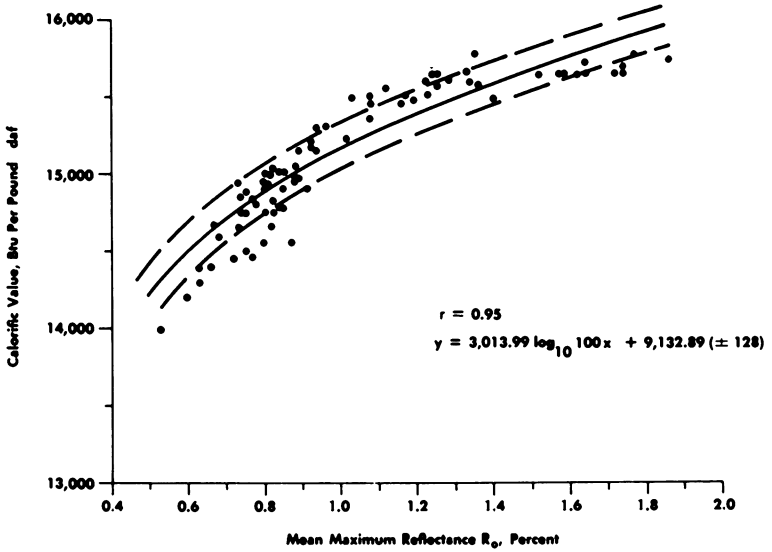

Figure 2. Relationship between reflectance and calorific value

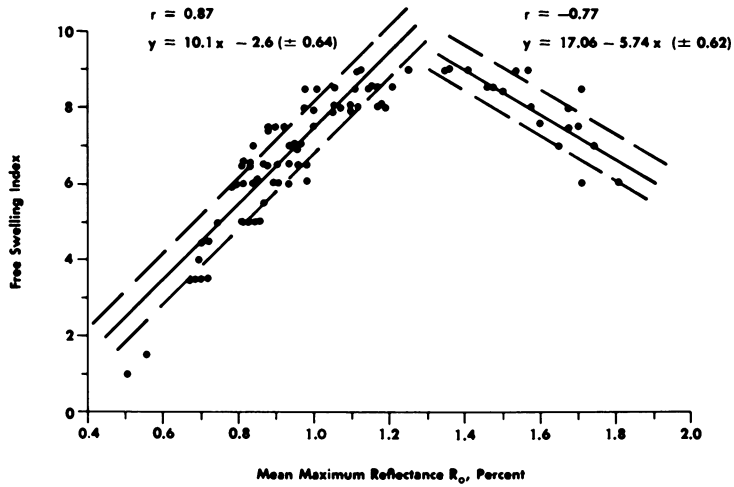

Figure 3. Relationship between reflectance and free swelling index

in calorific value with increased R_o above 1.7%. This work is in general agreement with previous studies in which correlations between calorific value and chemical-rank parameters were presented (*4*, *5*).

The correlation between R_o and *FSI* is shown in Figure 3. It is apparent that *FSI* increases linearly in the 0.5–1.25 R_o range, reaches a maximum in the 1.2–1.4 range, and then decreases rapidly as R_o increases above 1.4. The plotted data are divided into two distinct groups, with the division being made

Publication Date: January 1, 1966 | doi: 10.1021/ba-1966-0055.ch037

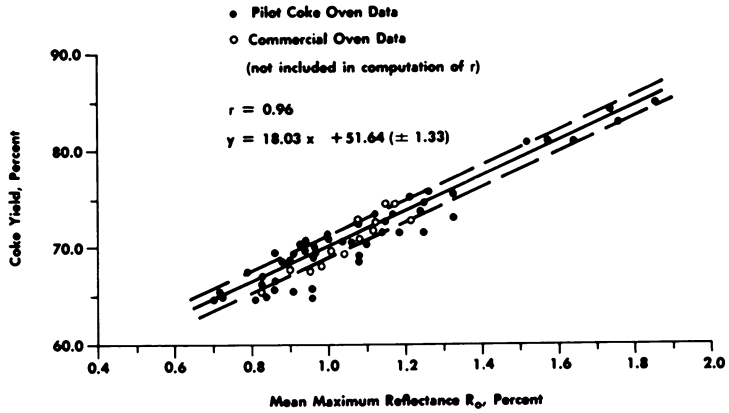

Figure 4. Relationship between reflectance and coke yield

at the 1.25 R_o level. Correlation coefficients for these data ($r = -0.77$ and 0.87) are computed and expressed, respectively, for those points falling above and below the 1.25 R_o threshold (Figure 3).

Yields of Carbonization Products

Yields of carbonization products from coal can be estimated from chemical-rank parameters such as volatile matter and fixed carbon content (*10, 11*). Since R_o is directly related to these chemical-rank parameters (Figure 1), this petrographic-rank parameter should correlate with these same carbonization

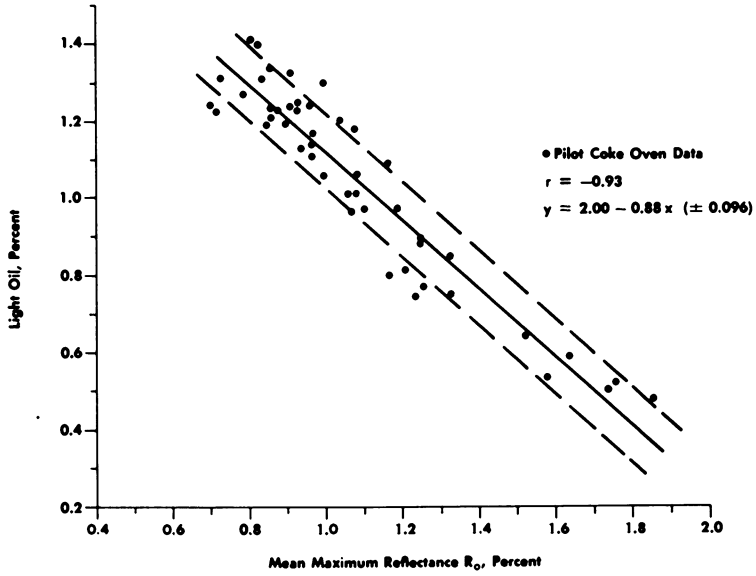

Figure 5. Relationship between reflectance and light oil, %

Publication Date: January 1, 1966 | doi: 10.1021/ba-1966-0055.ch037

properties. Figure 4 demonstrates the relation between R_o and coke yield ($r = 0.96$) as determined in pilot coke ovens. This observed relationship was expected since R_o varies inversely with coal volatility. Figure 4 shows that coke yield increases steadily with increasing reflectance over the entire R_o range, 0.7–1.9.

Figures 5 and 6 show the relation between reflectance and the yield of light oil ($r = -0.93$ and -0.87) expressed successively in weight percent and in gallons per ton of coal. In general, as the average R_o values increase, the yield of light oil decreases rapidly and uniformly through the entire bituminous R_o range.

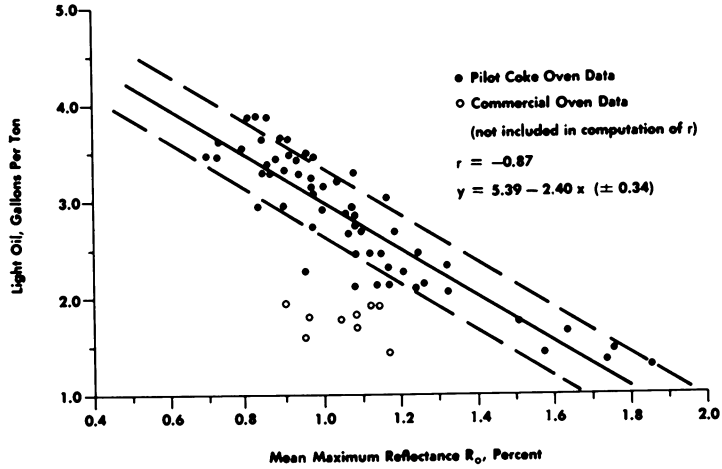

Figure 6. Relationship between reflectance and light oil, gallons per ton

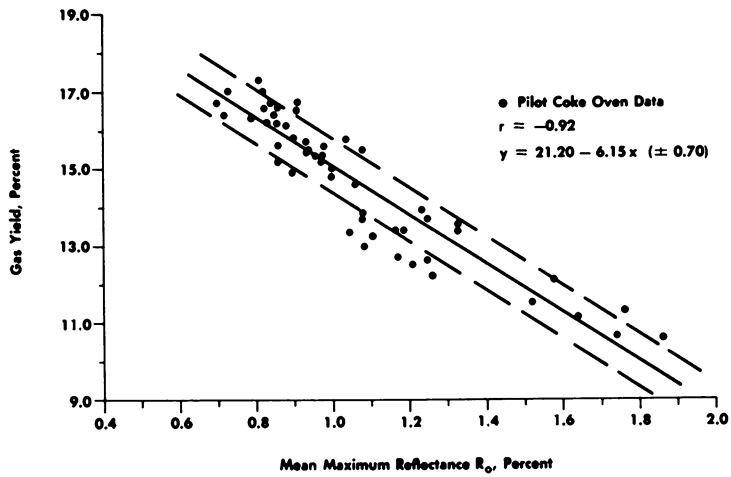

Figure 7. Relationship between reflectance and gas yield, %

Publication Date: January 1, 1966 | doi: 10.1021/ba-1966-0055.ch037

Figure 7 depictes the correlation for R_o of vitrinite and by-product gas yield ($r = -0.92$). As was the case in the correlation of R_o with light oil, the yield of by-product gas exhibits a sharp decrease as coal rank (R_o) increases from 0.7–1.8%.

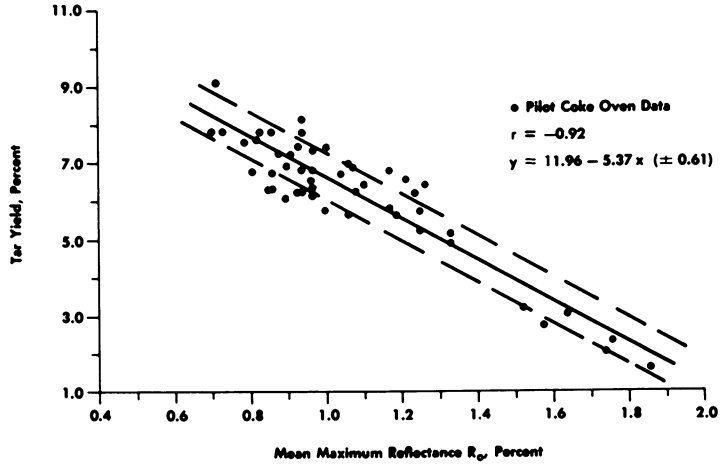

Figure 8. Relationship between reflectance and tar yield, %

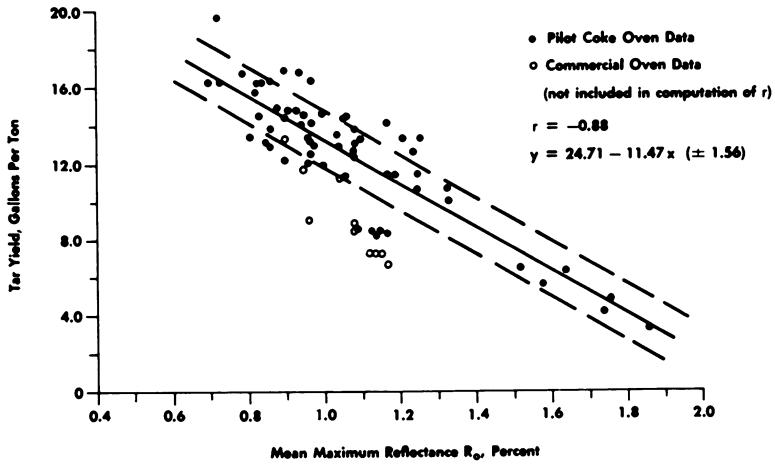

Figure 9. Relationship between reflectance and tar yield, gallons

Figures 8 and 9 show that the total tar product correlated reasonably well with R_o ($r = -0.92$ and -0.88, respectively), and that maximum tar yields are obtained from coals at the high volatile rank level while minimum yields are exhibited by low volatile rank coals. Generally, the tar product of a carbonization process is expressed in combination with the yield of light oil. The relation between the yield of tar plus light oil and R_o was much improved over

Publication Date: January 1, 1966 | doi: 10.1021/ba-1966-0055.ch037

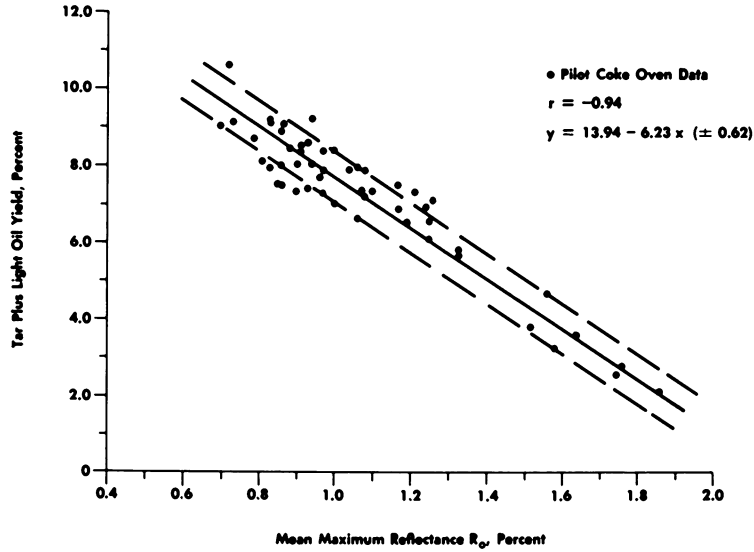

Figure 10. Relationship between reflectance and tar plus light oil, %

the correlations obtained singly for tar or light oil (r = —0.94 and —0.90, respectively). Figure 10 represents the correlation between yield of tar plus light oil (in weight percent of coal) and R_o. Again, these data show that tar plus light oil yields decrease rapidly from the high to low volatile end of the

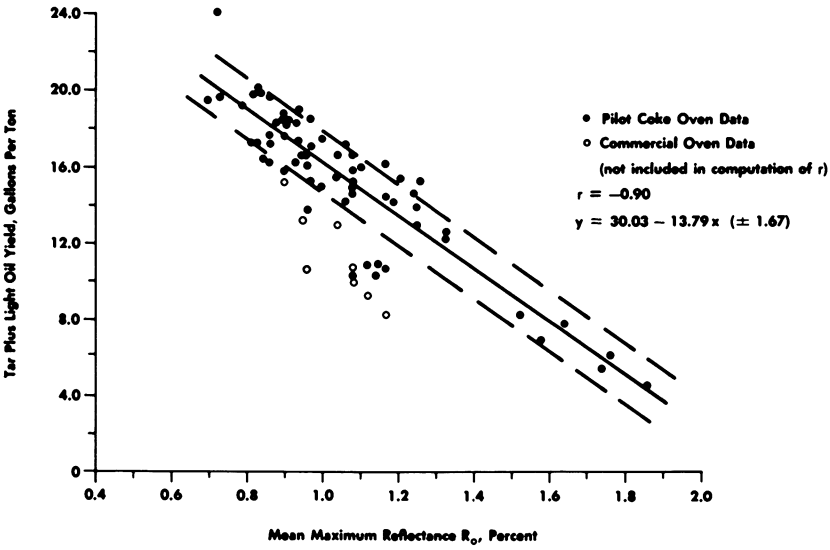

Figure 11. Relationship between reflectance and tar plus light oil, gallons per ton

Publication Date: January 1, 1966 | doi: 10.1021/ba-1966-0055.ch037

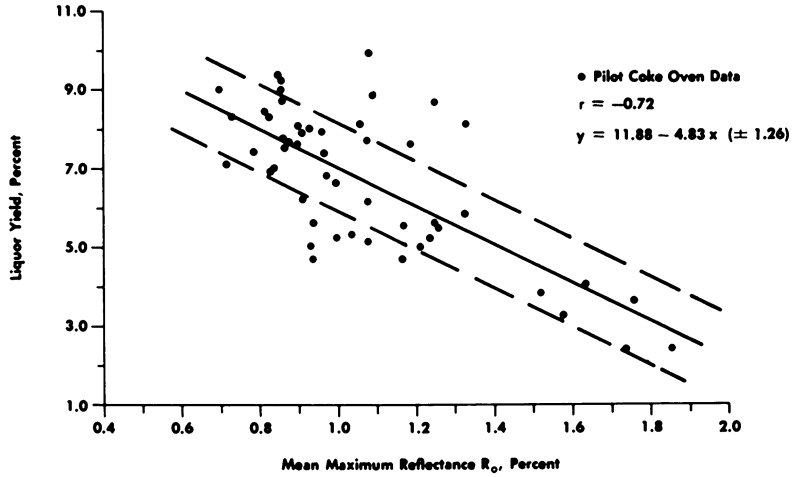

Figure 12. Relationship between reflectance and liquor yield, %

coalification series. Figure 11 shows the relationship between the combined products and R_o expressed in gallons per ton of coal. These data exhibit the same sharp linear decrease in tar plus light oil with corresponding increase in R_o.

Figure 12, the correlation between liquor yield and R_o, shows that the liquor product decreases as the average vitrinite R_o increases. However, the correlation between R_o and liquor is poor ($r = -0.72$). The degree of scatter ($Sy = \pm 1.26$, where Sy = standard estimate of error for y) is probably a function of moisture differences in the subject coals; high percentages of moisture increase liquor yields (*17*).

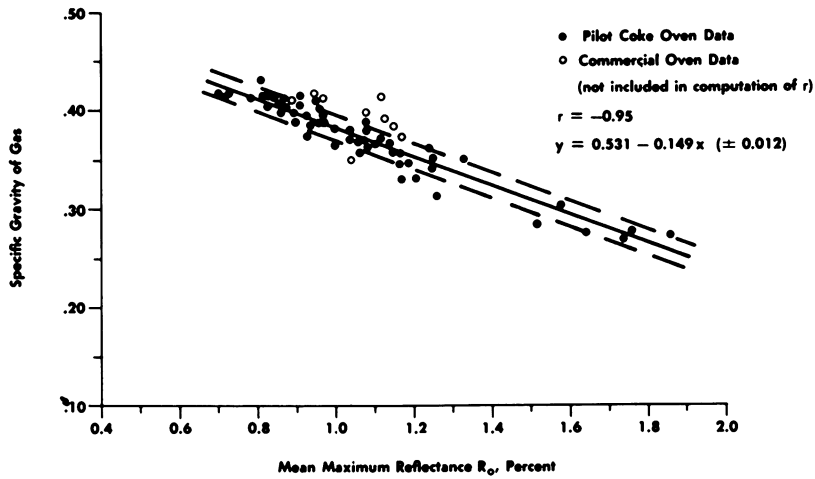

Figure 13. Relationship between reflectance and specific gravity of gas

Publication Date: January 1, 1966 | doi: 10.1021/ba-1966-0055.ch037

Specific Properties of By-product Gas

Since R_o is related to volatile matter content (Figure 1), it would be reasonable to expect a correlation between this rank parameter and specific properties of by-product gas. Our results show that gas specific gravity and gas heating value can, in fact, be estimated fairly accurately from reflectance data.

Figure 13, the correlation between specific gravity of by-product gas and R_o ($r = -0.95$), illustrates that the specific gravity of the gas decreases rather uniformly with rank increase.

A similar correlation was obtained for R_o and the heating value of by-product gas. Figure 14 compares gas heating value (B.t.u. per cubic foot) with R_o ($r = -0.87$) and demonstrates that the heating value of gas decreases gradually as coal rank increases through the 0.7–1.9 R_o range.

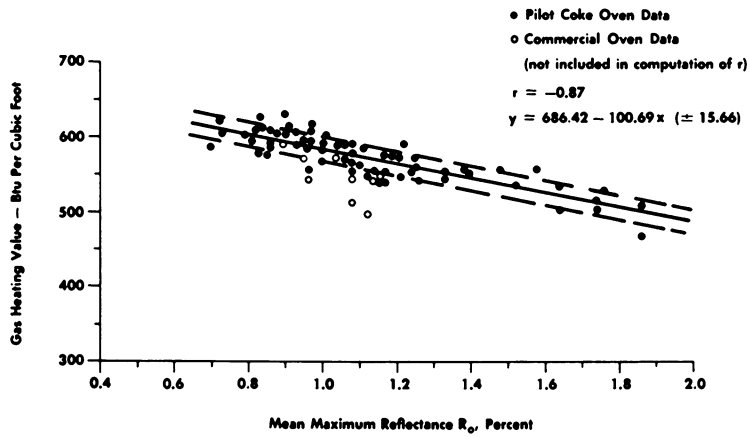

Figure 14. Relationship between reflectance and heating value of gas, B.t.u. per cubic foot

Figure 15 compares the heating value of gas, as expressed in B.t.u. per pound of coal, to the R_o of the samples analyzed. In general, as the R_o of vitrinite in coal increases, the heating values decrease ($r = -0.72$). As indicated by the low coefficient of correlation in Figure 5 ($r = -0.72$), a close relationship between R_o and gas heating value does not exist. Therefore, any reference to these data can only be in very general terms.

Effects of Oxidation on Reflectance

Chemical and physical properties of coal are altered by oxidation (2, 3), and this is especially true of volatile matter content and the average R_o of vitrinite. However, there is no accurate method for detecting and subsequently determining the rate and degree of change in these properties for a given sample at a given point in time. Recent studies at Bituminous Coal Research, Inc. (BCR) revealed that the R_o of coal, along with a volatile matter deter-

Publication Date: January 1, 1966 | doi: 10.1021/ba-1966-0055.ch037

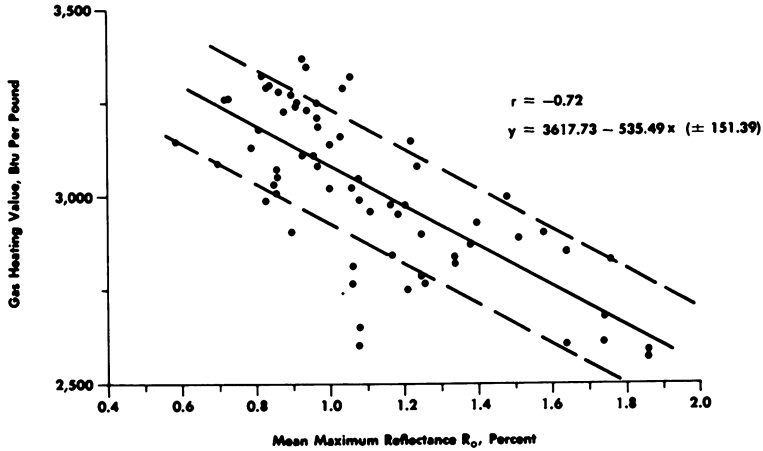

Figure 15. Relationship between reflectance and gas heating value, B.t.u. per pound

mination, could be used to detect oxidation. A correlation between volatile matter content and R_o is shown in Figure 1 ($r = -0.96$, $Sy = \pm 2.3\%$). The analytical data plotted were obtained by analyzing "fresh" or newly mined coal samples. After approximately one year some of these same samples were re-analyzed and again plotted on this graphical framework. In replotting these data, significant deviations from the "base" or original volatile matter-R_o correlation line were observed. Figure 16 illustrates the R_o and volatile matter differences in the re-analyzed coal ($r = -0.88$, $Sy = \pm 3.65\%$). Considerably more scatter is apparent in this plot than in that of the corresponding data in Figure 1. Figure 16 shows that:

(1) Oxidation changes are most pronounced in coals having vitrinite with an average R_o below 0.8%.

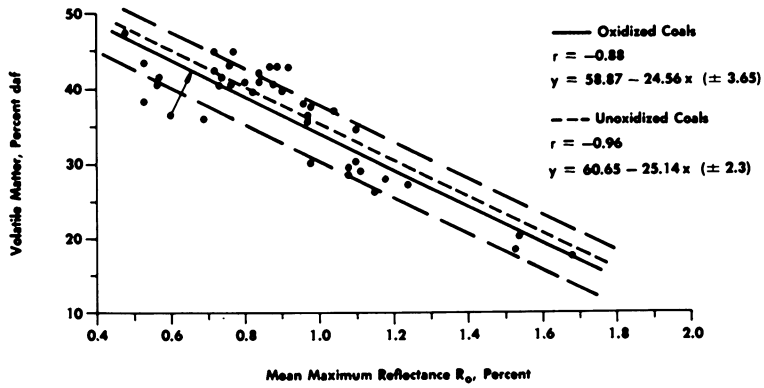

Figure 16. Effects of oxidation on reflectance and volatile matter

Publication Date: January 1, 1966 | doi: 10.1021/ba-1966-0055.ch037

(2) Coals occupying the 0.8–1.4 percent R_o range are least affected by oxidation.

(3) Coals which are characterized by reflectances above 1.4% have intermediate degrees of alteration.

All coals submitted to BCR for petrographic analysis are routinely checked for "oxidation" by comparing "as-received" analytical results with the established "fresh coal" R_o-volatile matter curve shown in Figure 1. Coals falling within reasonable limits of this correlation line (within $Sy = \pm 2.3\%$) are accepted as unoxidized; all others are considered oxidized.

This method for assessing coal oxidation can be used to good advantage when attempting to predict petrographically coke stabilities from highly oxidized coal samples. Using the relationship presented in Figure 16, it is possible to extrapolate back to the rank of the original or fresh coal. As shown in Figure 16, this is accomplished by connecting, at right angles, the as-received analysis value with the established fresh coal volatile matter-R_o curve, the point

Table I. Comparison of Coke Oven Stabilities Predicted from Highly Oxidized Coals on an As-Received and Corrected Basis

Coal Blend No.	*A 500-lb. Oven Stability*	*B As-Received Basis*	*A-B*	*C Corrected for Oxidation*	*A-C*
1	37.8	37.0	0.8	37.0	0.8
2	44.0	41.0	3.0	43.0	1.0
3	50.6	45.3	5.3	49.0	1.6
4	37.5	35.0	2.5	37.0	0.5
5	44.9	39.5	4.4	43.0	1.9
6	50.6	43.2	7.4	49.0	1.6
7	37.6	37.0	0.6	37.0	0.6
8	43.6	41.0	2.6	43.0	0.6
9	49.9	45.0	4.9	49.0	0.9
10	56.0	47.0	9.0	53.0	3.0
11	56.0	48.0	8.0	54.0	2.0
12	57.0	51.0	6.0	56.0	1.0
13	57.0	51.0	6.0	56.0	1.0
14	56.0	43.0	13.0	54.0	2.0

of intersection being the fresh coal rank as determined by the subject parameters. This method of rank inference has been employed at BCR with considerable success. Table I illustrates several cases in which this oxidation correction technique was used to predict coke oven stabilities from highly oxidized coals. The table compares 500-lb. coke oven stabilities with stabilities calculated from petrographic analysis. The stabilities calculated on an as-received basis were found to deviate considerably from the actual oven values, deviations being as high as 13 stability points. However, stabilities predicted from data which were corrected for oxidation compare favorably with the empirical test results—i.e., ±2 stability points.

Combustion Characteristics

Previously it had been thought that combustion characteristics of coals could be determined only from actual tests (*6*). However, testing in a full

Publication Date: January 1, 1966 | doi: 10.1021/ba-1966-0055.ch037

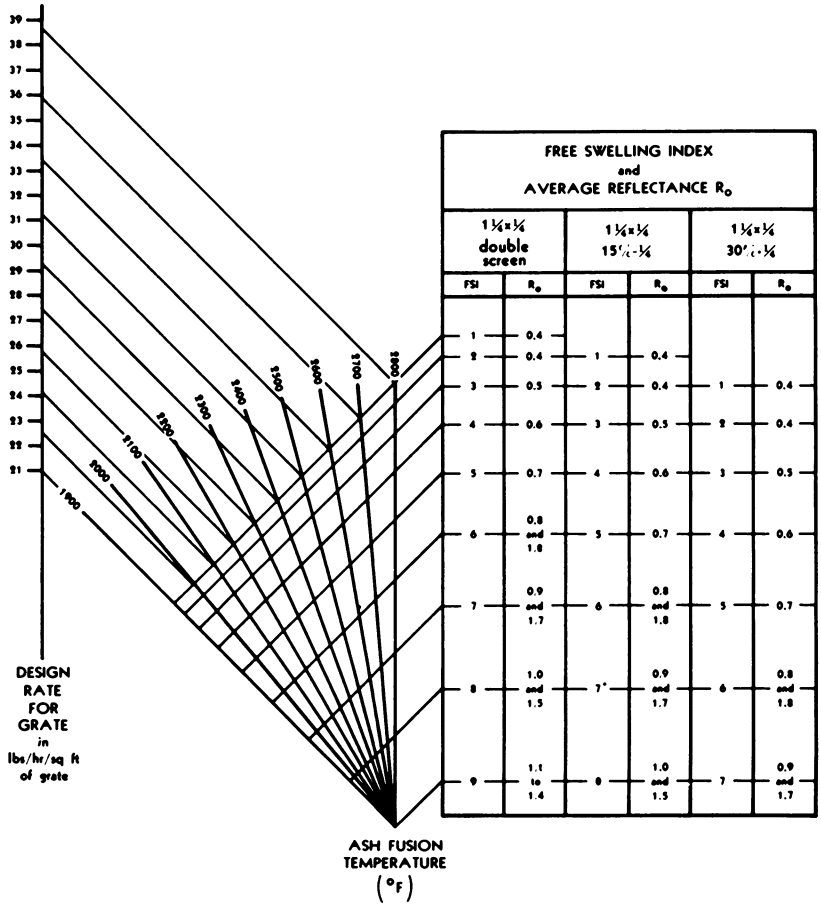

Figure 17. Relationship between reflectance, FSI, screen size, ash fusion, temperature, and combustion performance

scale combustion unit is time consuming and expensive. Many attempts have been made to correlate the domestic stoker characteristics of coal with laboratory test results and with chemical and physical properties. The results of these studies indicated that the combustion behavior of coal could be determined best from full scale tests (*6*).

Work is being conducted presently at BCR to relate petrographic characteristics to coal combustion performance. Preliminary results of the study, although incomplete, show a reasonable correlation between certain petrographic properties and coal combustion behavior.

Advancement in this research area was made possible through the development of the BCR 7-lb. combustion furnace (*13*, *19*). In this furnace, coals can be classified quantitatively in terms of their relative combustion perform-

Publication Date: January 1, 1966 | doi: 10.1021/ba-1966-0055.ch037

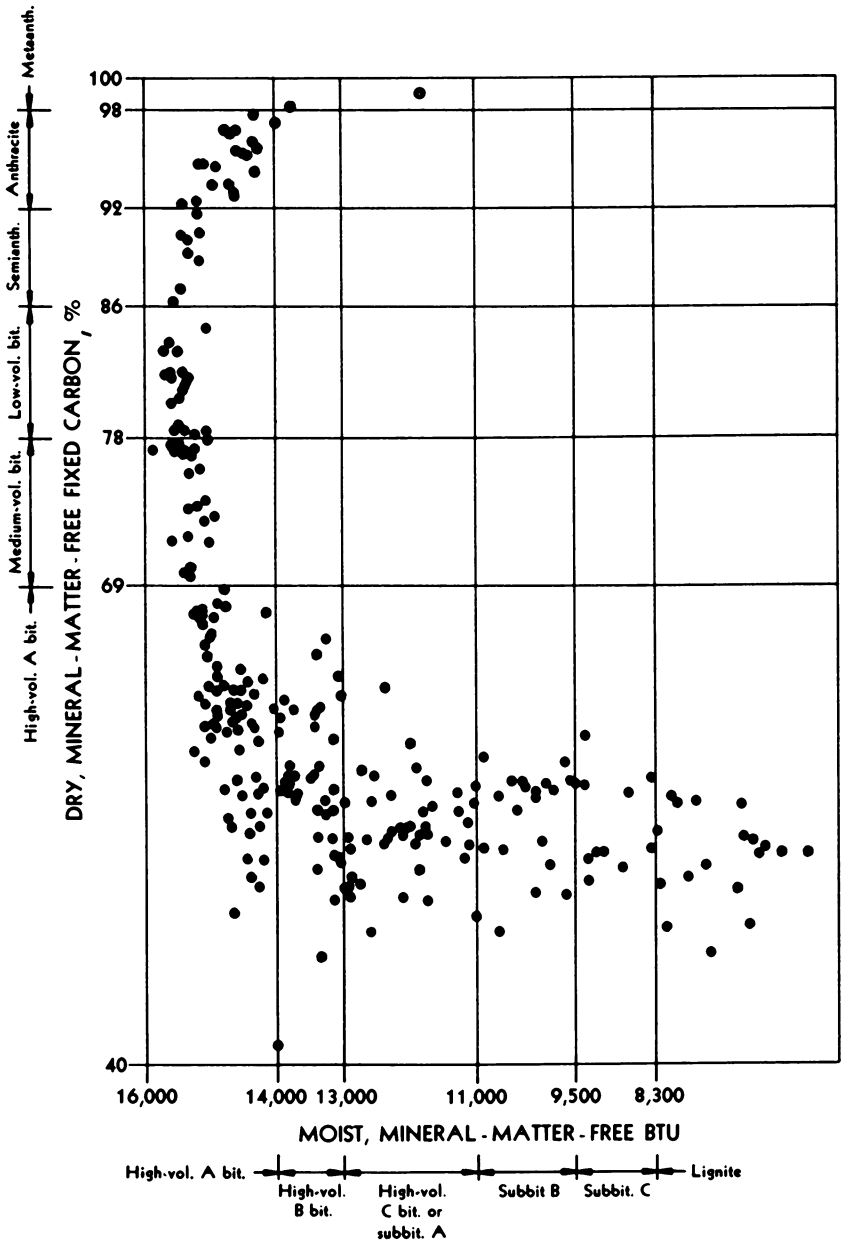

Figure 18. Typical U.S. coals graphed according to standard classification by rank (12)

ance. Prior to development of this test equipment, it was not possible to determine adequately combustion characteristics on such a conveniently small scale.

Several approaches are being taken in an attempt to relate petrographic composition with combustion behavior. Figure 17 shows how R_o along with *FSI* and ash fusion data may be used to predict the burning rate of coals in a specific combustion type (cross-feed stoker). In general, as R_o and *FSI* increase and ash fusion temperatures decrease, coals require more grate surface to insure optimum burn-out and minimum loss of combustibles in the ash.

At present, a petrographic combustion correlation is being worked out which should provide ultimately a general classification of coals for use in several combustion processes. The results of this study will be reported at a later date.

Publication Date: January 1, 1966 | doi: 10.1021/ba-1966-0055.ch037

Classification of Coal by Reflectance

The coal rank classification system commonly used in the U.S. is based on the relationship between calorific value and fixed carbon content (*1*). For the most part, the system serves to classify effectively coals having fixed carbon contents greater than 69%, but it is not possible to classify adequately coals

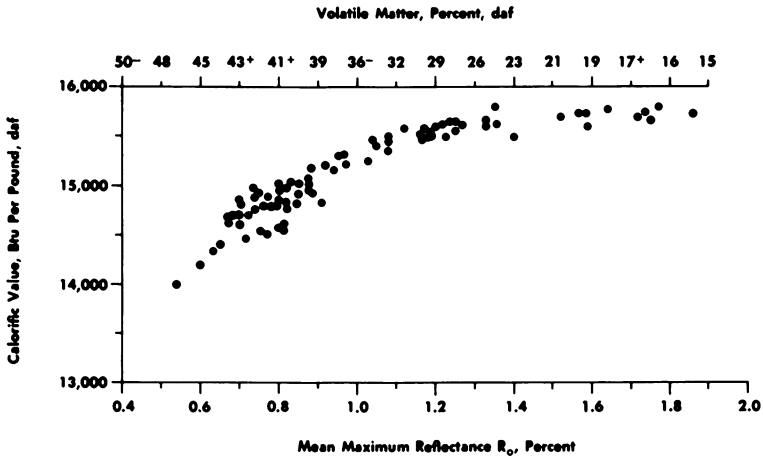

Figure 19. Classification of coals by petrographic and chemical parameters

below this fixed carbon level. Since a correlation exists between chemical-rank parameters and R_o (Figures 1 and 2), there is reason to believe that these problem area coals could be categorized more accurately if petrographic-rank parameters were included in the current coal classification system. Figure 18 illustrates the present method for classifying coals on the basis of chemical composition; Figure 19 illustrates a tentative R_o chemical rank classification. Obviously, insufficient data are presented in Figure 19 to substantiate whether this classification scheme is, in fact, an improvement over that shown in Figure

17. Figure 19 does show, however, that the modified classification improves the correlation in the high volatile rank range—i.e., coals with R_o values in the rank range below 1.1%.

With additional analytical data, the authors feel that a rank classification system of this type could be established on reflectance-chemical properties which would be consistent throughout the entire coalification series.

Summary

This investigation shows that the average reflectance of vitrinite in coal (R_o) can be used to estimate carbonization product yields, by-product gas properties, chemical properties, oxidation effects, and combustion behavior. Moreover, R_o along with calorific value and volatile matter content might be employed to classify accurately and consistently coals of all ranks.

Publication Date: January 1, 1966 | doi: 10.1021/ba-1966-0055.ch037

Literature Cited

(1) American Society for Testing Materials, Philadelphia, Pa., D-388-38.
(2) Bayer, J. L., Denton, G. H., Chang, M. C., "Abstracts of Papers," 145th Meeting, ACS, September 1963, p. 2K.
(3) Benedict, L. G., Berry, W. F., Presented at the Coal Division of the Geological Society of America, Miami, Florida, 1964.
(4) Fieldner, A. C., Selvig, W. A., Frederic, W. H., *U. S. Bur. Mines, Rept. Invest.* **3296R** (1936).
(5) Francis, W, "Coal," p. 317-8, Edward Arnold Publisher, Ltd., London, 1954.
(6) Helfenstine, R. J., *Illinois State Geol. Surv., Rept. Invest.* **151** (1951).
(7) Isenberg, N., Jackman, H. W., "Investigation of Beckley Seam Coal Blended with Wheelwright Coal for Use in the Production of Metallurgical Coke," Inland Steel Co., East Chicago, 1945.
(8) Kotter, K., *Brennstoff-Chem.* **41**, 263 (1960).
(9) Montgomery, C. R., Verno, L. J., *Trans. Mining Soc., AIME*, Preprint **62F82** (1962).
(10) Parry, V. F., *U. S. Bur. Mines, Rept. Invest.* **3482** (1939).
(11) Perch, M., Russell, C. C., Presented at Joint Fuels Conference of Coal Division, AIME and Fuels Division, ASME, November 1948.
(12) Rose, H. J., Presented at the Joint Solid Fuels Meeting of the Coal Division of Fuels Division of AIME and ASME, October 1958.
(13) Saltsman, R. D., *Trans. Mining Soc., AIME*, Preprint **64F35** (1964).
(14) Shapiro, N., Gray, R. J., *Proc. Illinois Mining Inst.* **68**, 83 (1960).
(15) Shapiro, N., Gray, R. J., Eusner, G. R., *Proc. Blast Furnace, Coke Oven, Raw Mater. Comm.* **20** (1961).
(16) Van Krevelen, D. W., Shuyer, J., "Coal Science," p. 164-8, Elsevier Publishing Co., New York, 1957.
(17) Wolfson, D. E., Birge, G. W., Lynch, J. H., *U. S. Bur. Mines, Rept. Invest.* **5628** (1960).
(18) Wolfson, D. E., Reynolds, D. A., *U. S. Bur. Mines, Tech. Paper* **693** (1946).
(19) Zawadzki, E. A., du Breuil, F., *ASME, Tech. Paper* **59FU3**, 1959.

RECEIVED October 5, 1965.

Appendix I. Chemical and Petrographic Data

Coal No.	Petrographic Data	Chemical Data		
	Reflectance, R_o	Volatile Matter, daf	B.t.u., daf	FSI
1	1.08	33.1	15,365	—
2	1.04	34.5	15,470	—
3	1.08	33.1	15,505	—
4	1.08	32.9	15,500	—
5	1.19	29.3	15,527	—
6	1.17	30.0	15,560	—
7	1.25	27.2	15,670	—
8	1.33	25.0	15,625	—
9	1.33	25.0	15,675	—
10	1.25	27.3	15,570	—
11	1.24	27.7	15,660	—
12	1.58	20.8	15,765	—
13	1.76	17.9	15,830	—
14	1.64	19.7	15,800	—
15	1.52	20.2	15,725	—
16	1.86	16.0	15,730	—
17	1.74	17.4	15,770	—
18	0.93	38.1	—	6
19	0.96	37.7	—	6½
20	0.86	40.3	—	5
21	0.88	39.7	—	6½
22	0.90	39.4	—	—
23	0.97	37.2	—	—
24	0.97	37.1	—	7
25	1.00	36.8	—	—
26	0.85	40.2	—	6
27	0.90	38.9	—	6½
28	0.91	38.5	—	6
29	0.94	37.9	—	6½
30	0.94	37.8	—	—
31	0.93	37.2	—	—
32	0.83	40.8	—	6½
33	0.86	39.9	—	—
34	0.97	37.0	—	8
35	0.72	43.6	—	—
36	0.79	42.0	—	6
37	0.86	40.4	—	5
38	0.86	39.7	—	—
39	1.08	33.4	—	—
40	0.97	37.2	—	—
41	1.04	34.5	—	—
42	1.12	31.6	—	—
43	1.14	30.8	—	—
44	1.17	30.3	—	—
45	1.15	30.5	—	—
46	0.95	37.4	—	—
47	0.96	36.9	—	—
48	1.08	32.8	—	—
49	0.90	38.7	—	—
50	0.81	41.6	—	5

Publication Date: January 1, 1966 | doi: 10.1021/ba-1966-0055.ch037

Appendix I. Continued

Coal No.	Petrographic Data Reflectance, R_o	Volatile Matter, daf	Chemical Data B.t.u., daf	FSI
51	0.82	41.6	—	—
52	0.91	38.9	—	—
53	0.84	39.7	—	6
54	1.08	33.0	—	8
55	1.06	33.7	—	8
56	1.10	32.0	—	8
57	1.80	16.3	—	6
58	1.15	30.3	—	8
59	0.73	43.0	—	5
60	0.83	40.6	—	5
61	1.06	33.6	—	8½
62	0.70	43.7	—	4½
63	1.00	36.0	—	7½
64	1.26	27.1	—	9
65	1.17	30.1	—	8
66	1.21	28.6	—	8½
67	1.80	16.3	—	6½
68	1.74	17.6	—	—
69	1.66	18.3	—	—
70	1.64	18.9	—	—
71	1.61	19.6	—	—
72	1.48	21.5	—	—
73	1.40	22.8	—	—
74	1.38	23.5	—	—
75	1.33	24.9	—	—
76	1.21	27.2	—	—
77	1.22	28.0	—	—
78	1.20	29.0	—	—
79	1.14	31.5	—	—
80	1.11	33.0	—	—
81	1.00	34.0	—	—
82	1.01	36.0	—	—
83	0.97	36.7	—	—
84	0.90	38.0	—	—
85	1.34	24.6	—	—
86	1.00	36.2	—	—
87	1.58	19.8	—	8
88	1.46	23.0	—	8½
89	1.47	23.0	—	8½
90	1.54	20.4	—	9
91	0.80	42.0	—	—
92	0.72	44.0	—	—
93	1.41	23.2	—	9
94	0.81	41.0	—	6½
95	0.94	37.3	—	7
96	1.64	18.8	—	—
97	0.56	47.8	—	1½
98	0.97	37.1	—	7
99	1.60	19.2	—	7½
100	1.10	32.0	—	8

Publication Date: January 1, 1966 | doi: 10.1021/ba-1966-0055.ch037

Appendix I. Continued

Coal No.	Petrographic Data	Chemical Data		
	Reflectance, R.	Volatile Matter, daf	B.t.u., daf	FSI
101	1.14	29.4	—	8
102	1.16	30.5	—	8½
103	1.68	18.2	—	8
104	1.68	18.5	—	7½
105	1.73	17.8	—	—
106	1.70	18.0	—	7½
107	1.00	35.4	—	8
108	1.01	35.2	—	8½
109	1.11	32.5	—	8½
110	1.05	34.5	—	8
111	1.74	17.4	—	7
112	1.65	18.5	—	7
113	1.71	17.7	—	6
114	1.12	31.4	—	6
115	1.08	33.0	—	—
116	0.93	38.2	—	—
117	0.88	39.3	—	—
118	0.91	38.5	—	—
119	1.19	29.6	—	8
120	1.18	29.2	—	—
121	1.12	31.8	—	8
122	0.94	38.0	—	—
123	0.95	37.0	—	—
124	0.88	41.2	—	6½
125	0.84	40.1	—	6
126	0.79	41.8	—	—
127	0.82	41.4	—	—
128	0.82	41.8	—	6½
129	0.74	42.5	—	4½
130	0.80	41.6	—	6
131	0.72	42.7	—	3½
132	0.63	46.1	—	—
133	0.94	38.2	—	7½
134	0.90	39.7	—	7½
135	0.88	40.5	—	7½
136	0.83	40.4	—	6½
137	1.03	36.1	—	8½
138	0.80	41.5	—	6
139	0.74	42.0	—	—
140	1.27	27.0	15,630	—
141	1.40	23.3	15,540	—
142	1.59	19.9	15,620	—
143	1.75	18.0	15,680	—
144	0.68	—	14,600	—
145	0.67	—	14,690	—

Publication Date: January 1, 1966 | doi: 10.1021/ba-1966-0055.ch037

Appendix I. Continued

Coal No.	Petrographic Data Reflectance, R.	Chemical Data Volatile Matter, daf	B.t.u., daf	FSI
146	0.73	—	14,690	—
147	0.75	—	14,500	—
148	0.77	—	14,490	—
149	0.74	—	14,750	—
150	0.73	—	14,950	—
160	0.74	—	14,850	—
161	0.75	—	14,900	—
162	0.76	—	14,750	—
163	0.77	—	14,850	—
164	0.78	—	14,800	—
165	0.80	—	15,000	—
166	0.80	—	14,950	—
167	0.80	—	14,900	—
168	0.80	—	14,750	—
169	0.80	—	14,550	—
170	0.81	—	14,650	—
172	0.82	—	14,740	—
173	0.82	—	14,750	—
174	0.82	—	14,830	—
175	0.81	—	14,950	—
176	0.81	—	15,000	—
177	0.85	—	15,000	—
178	0.85	—	14,900	—
179	0.85	—	14,780	—
180	0.88	—	15,050	—
181	0.88	—	14,980	—
182	0.88	—	14,950	—
183	0.89	—	14,950	—
184	0.89	—	15,150	—
185	0.91	—	14,820	—
186	0.92	—	15,200	—
187	0.96	—	15,300	—
188	1.02	—	15,230	—
189	1.03	—	15,500	—
190	1.08	—	15,350	—
191	1.08	—	15,450	—
192	1.08	—	15,500	—
193	1.12	—	15,550	—
194	1.16	—	15,450	—
195	1.17	—	15,450	—
196	1.17	—	15,500	—
197	1.19	—	15,450	—
198	1.22	—	15,600	—
199	1.23	—	15,500	—
200	1.25	—	15,550	—
201	1.24	—	15,650	—
202	1.25	—	15,650	—
203	1.28	—	15,600	—
204	1.35	—	15,800	—
205	1.34	—	15,550	—

Appendix I. Continued

Coal No.	Petrographic Data Reflectance, R_o	Chemical Data Volatile Matter, daf	B.t.u., daf	FSI
206	1.33	—	15,650	—
207	1.30	—	15,550	—
208	1.40	—	15,450	—
209	1.52	—	15,650	—
210	1.57	—	15,650	—
211	1.58	—	15,650	—
212	1.72	—	15,650	—
213	1.59	—	15,600	—
214	1.64	—	15,750	—
215	1.74	—	15,650	—
216	1.74	—	15,700	—
217	1.77	—	15,800	—
218	1.86	—	15,750	—
219	—	—	—	—

Appendix II. Yields of Carbonization

Coal No.	Yield, percent by weight of Coal[a] Coke	Tar	Light Oil	Gas	Liquor
1	71.4	6.2	1.20	13.9	6.1
2	70.7	6.7	1.20	15.8	5.3
3	71.3	6.9	1.06	15.5	5.1
4	71.2	6.2	1.01	13.8	7.7
5	71.4	5.6	0.97	13.4	7.6
6	73.9	5.8	1.11	13.4	4.7
7	74.3	5.7	0.88	13.7	5.6
8	73.2	5.1	0.75	13.6	8.1
9	75.7	4.9	0.85	13.7	5.8
10	71.7	5.2	0.89	12.6	8.7
11	73.8	6.2	0.75	14.2	5.2
12	80.8	2.7	0.51	12.3	3.2
13	82.7	2.3	0.52	11.3	3.6
14	80.6	3.0	0.59	11.1	4.0
15	80.1	3.2	0.64	11.5	3.8
16	84.3	1.6	0.48	10.6	2.4
17	84.0	2.0	0.50	10.6	2.7
18	68.0	6.2	1.25	15.6	8.0
19	68.8	6.5	1.24	15.3	7.9
20	69.5	6.3	1.20	15.2	7.8
21	68.1	7.2	1.23	16.1	7.7
22	69.6	6.0	1.31	14.9	7.6
23	70.0	6.2	1.14	15.2	7.4
24	69.8	7.3	1.17	15.2	6.8
25	71.1	5.7	1.32	14.8	6.6

Appendix I. Continued

Coal No.	Petrographic Data Reflectance, R_o	Chemical Data Volatile Matter, daf	B.t.u., daf	FSI
		Commercial Coke Oven Data[1]		
220	1.08	33.4	—	—
221	1.04	34.5	—	—
222	1.12	31.6	—	—
223	1.14	30.8	—	—
224	1.17	30.3	—	—
225	1.15	30.8	—	—
226	0.95	37.4	—	—
227	0.96	36.9	—	—
228	1.08	32.8	—	—
229	0.90	38.7	—	—

[1] Data not used in computing correlation coefficients (r).

Products and By-Product Gas Data[1]

Yield per ton of Coal[2]		Properties of Gas Heating Value		
Tar, (gal.)	Light Oil in Gas (gal.)	Specific Gravity	B.t.u. per cubic foot	B.t.u. per pound of Coal
12.6	3.30	0.364	592	2990
13.5	3.20	0.379	599	3290
13.8	2.91	0.387	576	3050
12.4	2.75	0.380	554	2640
11.5	2.69	0.349	580	2960
11.5	3.02	0.345	578	2980
11.5	2.44	0.352	563	2900
10.6	2.07	0.352	555	2840
10.0	2.34	0.351	545	2820
10.6	2.47	0.341	573	2790
12.6	2.08	0.362	559	3080
5.5	1.41	0.302	555	3000
4.7	1.45	0.279	527	2830
6.2	1.63	0.275	533	2850
6.5	1.77	0.282	533	2890
3.2	1.29	0.274	506	2590
4.1	1.36	0.267	500	2610
12.9	3.48	0.393	589	3110
13.3	3.47	0.383	587	3110
12.9	3.33	0.405	601	3010
14.9	3.42	0.401	606	3230
12.2	3.64	0.399	585	2900
13.0	3.17	0.389	595	3080
15.3	3.25	0.383	601	3190
11.9	3.16	0.381	587	3020

Publication Date: January 1, 1966 | doi: 10.1021/ba-1966-0055.ch037

Appendix II.

Coal No.	Yield, percent by weight of Coal[a]				
	Coke	Tar	Light Oil	Gas	Liquor
26	66.7	6.3	1.19	16.4	9.4
27	67.7	6.9	1.19	15.8	8.1
28	69.1	7.2	1.24	16.7	6.2
29	70.6	6.8	1.22	15.5	5.6
30	69.7	8.1	1.13	15.4	4.7
31	70.4	7.4	1.23	15.7	5.0
32	66.2	7.8	1.40	16.6	6.9
33	65.8	7.8	1.22	16.3	8.7
34	70.1	6.8	1.11	15.3	6.8
35	65.3	9.4	1.23	16.4	7.1
36	67.6	7.5	1.27	16.3	7.4
37	66.6	6.7	1.34	15.6	9.0
38	66.4	6.7	1.23	16.6	9.2
39	72.4	—	—	—	—
40	69.4	—	—	—	—
41	69.3	—	—	—	—
42	73.4	—	—	—	—
43	71.7	—	—	—	—
44	73.3	—	—	—	—
45	72.7	—	—	—	—
46	67.0	—	—	—	—
47	64.7	—	—	—	—
48	98.2	—	—	—	—
49	68.4	—	—	—	—
50	65.1	6.7	1.41	17.3	7.5
51	63.1	7.7	1.47	17.0	8.4
52	65.4	7.2	1.32	16.6	7.9
53	65.4	7.8	1.31	16.7	7.0
54	68.9	6.3	1.01	12.9	10.0
55	70.2	7.0	0.96	13.3	8.1
56	70.0	6.4	0.97	13.2	8.9
57	—	—	—	—	—
58	—	—	—	—	—
59	64.9	7.8	1.31	17.0	8.3
60	67.0	6.9	1.03	16.2	8.3
61	70.2	5.6	1.02	14.6	8.1
62	64.3	7.8	1.24	16.7	9.0
63	70.8	7.4	1.05	15.0	5.2
64	75.7	6.4	0.77	12.0	5.5
65	73.5	6.8	0.77	12.7	5.6
66	75.0	6.5	0.81	12.5	5.0
67	—	—	—	—	—
68	—	—	—	—	—
69	—	—	—	—	—
70	—	—	—	—	—
71	—	—	—	—	—
72	—	—	—	—	—
73	—	—	—	—	—

Continued

Yield per ton of Coal[a]		Properties of Gas Heating Value		
Tar, (gal.)	*Light Oil in Gas (gal.)*	*Specific Gravity*	*B.t.u. per cubic foot*	*B.t.u. per pound of Coal*
13.1	3.33	0.413	578	3030
14.4	3.30	0.388	602	3270
14.8	3.46	0.406	592	3340
14.0	3.41	0.386	606	3230
15.8	3.29	0.381	606	3350
14.9	3.41	0.375	607	3370
16.2	3.89	0.407	627	3290
16.3	3.39	0.400	607	3280
14.1	3.07	0.382	603	3210
19.7	3.43	0.414	621	3260
15.7	3.54	0.417	601	3130
13.9	3.85	0.399	589	3050
13.8	3.40	0.409	587	3070
12.3	2.46	0.370	574	—
12.6	2.73	0.394	586	—
12.9	2.69	0.372	581	—
8.4	2.46	0.373	548	—
8.2	2.14	0.368	552	—
8.3	2.32	0.358	542	—
8.5	2.45	0.359	544	—
14.6	2.15	0.413	596	—
12.0	1.89	0.405	558	—
8.4	2.05	0.375	565	—
15.9	2.97	0.389	630	—
13.4	3.86	0.432	597	3180
15.8	4.04	0.416	611	3320
14.8	3.64	0.416	614	3250
16.2	3.63	0.413	614	3300
13.0	2.82	0.369	555	2610
14.6	2.67	0.358	573	2810
13.3	2.70	0.356	564	2760
—	—	—	—	—
—	—	—	—	—
16.1	3.63	0.419	606	3260
14.5	2.87	0.416	577	2990
11.4	2.85	0.368	576	3020
16.1	3.46	0.419	583	3090
14.6	2.92	0.365	590	3140
13.2	2.14	0.312	544	2770
14.1	2.15	0.330	557	2840
13.2	2.26	0.330	545	2750
—	—	—	466	2570
—	—	—	515	2680
—	—	—	—	—
—	—	—	500	2610
—	—	—	—	—
—	—	—	555	3000
—	—	—	550	2930

Appendix II.

Coal No.	Yield, percent by weight of Coal[a] Coke	Tar	Light Oil	Gas	Liquor
74	—	—	—	—	—
75	—	—	—	—	—
76	—	—	—	—	—
77	—	—	—	—	—
78	—	—	—	—	—
79	—	—	—	—	—
80	—	—	—	—	—
81	—	—	—	—	—
82	—	—	—	—	—
83	—	—	—	—	—
				Commercial Coke	
220	72.8	—	—	1.08	—
221	69.6	—	—	1.04	—
222	71.5	—	—	1.12	—
223	72.5	—	—	1.14	—
224	74.1	—	—	1.17	—
225	74.4	—	—	1.15	—
226	67.1	—	—	0.95	—
227	65.7	—	—	0.96	—
228	70.8	—	—	1.08	—
229	67.4	—	—	0.90	—

[a] Carbonized at 900°C. in 18-inch pilot coke ovens.

[b] Coke, tar, and light oil are reported on dry basis.

Publication Date: January 1, 1966 | doi: 10.1021/ba-1966-0055.ch037

Discussion

John Harrison: We have noticed that the moisture content of a coal, either before a briquet is made or as a result of adding water during the wet polishing process, can drastically affect the reflectance. This is true of high volatile coals and to a lesser extent the low volatile coals. Other things being equal, coal with the higher moisture content has the lower reflectance. What standards have you set up or what precautions have you taken to prevent this effect from influencing your R_o values?

Louis G. Benedict: We have not observed any significant changes in mean maximum reflectance in a given coal sample with increasing moisture content. We have observed, however, that significant alterations in reflectance result from oxidation. As fresh coal is progressively oxidized, mean maximum reflectance decreases, reaches a minimum, and then increases steadily with con-

Continued

Yield per ton of Coal[a]		Properties of Gas Heating Value		
Tar, (gal.)	*Light Oil in Gas (gal.)*	*Specific Gravity*	*B.t.u. per cubic foot*	*B.t.u. per pound of Coal*
—	—	—	556	2870
—	—	—	—	—
—	—	—	575	2980
—	—	—	592	3200
—	—	—	—	—
—	—	—	—	—
—	—	—	586	2960
—	—	—	592	3320
—	—	—	602	3160
—	—	—	616	3250
Oven data[a]				
8.8	1.80	0.385	544	—
11.1	1.79	0.390	574	—
7.2	1.92	0.414	490	—
7.2	1.90	0.390	542	—
6.7	1.42	0.378	542	—
—	—	—	543	—
11.6	1.60	0.417	571	—
9.0	1.80	0.412	544	—
8.4	1.73	0.397	525	—
13.3	1.97	0.409	584	—

[a] Data not used in computing correlation coefficients (r).

tinued oxidation. This pattern of alteration was observed in coals occupying the reflectance rank range 0.7–1.7%.

Briquets prepared at BCR for petrographic analysis are maintained in a desiccator for an extended period prior to microscopic analysis. Specific high moisture coals have been analyzed for reflectance at regular intervals following their insertion in the desiccating atmosphere; under these conditions of continued desiccation, reflectance remained relatively constant.

Publication Date: January 1, 1966 | doi: 10.1021/ba-1966-0055.ch037

38

Kinetics of Volatile Matter Release from Pennsylvania Anthracites

E. T. NELSON, JEAN WORRALL, and P. L. WALKER, JR.

Fuel Technology Department, The Pennsylvania State University, University Park, Pa.

Publication Date: January 1, 1966 | doi: 10.1021/ba-1966-0055.ch038

Experimental results obtained under both isothermal and non-isothermal conditions are presented on the rates of H_2 and volatile matter release from Pennsylvania anthracites. The effects of particle size and heating rate were investigated, and for two of the anthracites the volatile matter evolved was subjected to chromatographic analysis. For linear heating rates ranging from 2° to 16°C. per min. and for temperatures between 760° and 1000°C. the rate of volatile matter release with respect to temperature has been found to be essentially constant for particle sizes within the range of 200x325 mesh (Tyler) to pieces of approximately 1.2 cm. equivalent radius. Under isothermal conditions rates of H_2 evolution obey a logarithmic time law and exhibit a complex dependency upon particle size.

Despite the fact that the Pennsylvania anthracite fields are located near major steel-producing areas, the role of anthracite as a metallurgical fuel has fallen to that of a minor blending component in producing metallurgical coke. Attempts to use raw anthracite for modern blast furnace and cupola operations have repeatedly shown that it is less satisfactory than coke. Although suitable in all other respects for use in present day metallurgical processes, anthracite is restricted by the following two unfavorable characteristics:

(1) The physical strength of the raw anthracite, as indicated by the ASTM tumbler and drop-shatter tests for coke (*1*, *2*), is inferior to that of metallurgical coke.

(2) Raw anthracite decrepitates when subjected to appreciable temperature gradients.

In Coal Science; Given, P.;
Advances in Chemistry; American Chemical Society: Washington, DC, 1966.

These two characteristics give rise to excessive pressure drop during cupola and blast furnace operations, with the ultimate pressure drop increasing beyond blower capacity. This leads to irregular descent of the furnace charge, pressure fluctuations, and partly frozen stock columns. These difficulties are partly caused by improvements in furnace design during the present century which have led to increased heating rates and hence to increased thermal shock.

Of the two objectionable features of anthracite mentioned above, thermal decrepitation appears to be the more serious. Neither of the two physical strength tests appear to be related to the behavior of the fuel in either blast furnace or cupola operations except with respect to handling and load carrying ability. The problem of handling can be overcome by using appropriate transport equipment. Although it appears possible that the load carrying problem can be overcome by using shorter stock columns, this characteristic is probably more closely related to thermal decrepitation than to physical strength alone. Thus, if methods could be developed to reduce thermal decrepitation, anthracite would be much more widely used as a metallurgical fuel.

With this point in mind, the Fuel Technology Department in 1953 began to investigate the possibility of improving the strength of anthracite by a heat treatment process which would increase its thermal stability. This work has led to the view that the release of volatile matter during the primary thermal decomposition of anthracite is the most important controlling factor with regard to decrepitation and that a relationship should exist between the average particle size and the critical heating rate. As a result of these conclusions, several attempts have been made to heat-treat anthracite in such a way that the rate of release of volatile matter does not lead to an internal pressure exceeding that required to overcome the physical strength of the material. Some success has been achieved in this direction.

The thermal decrepitation of anthracite is undoubtedly caused by a combination of factors such as moisture evolution, crystallite growth, the differential thermal expansion of its petrographic constituents and mineral matter, as well as volatile matter evolution. For anthracite containing a large percentage of moisture, the internal pressure produced by the presence of superheated steam within the micropore structure will obviously influence its thermal stability. However, anthracites of high moisture content would probably be avoided for metallurgical applications; with regard to anthracites of normal moisture content, the moisture would probably be reduced below that percentage which would cause excessive internal pressures by countercurrent contact with hot effluent gases. Crystallite growth was originally suggested as a possible decrepitation mechanism; however, x-ray diffraction studies have yielded no distinct correlation between crystallite dimensions and decrepitation (*5*). Consequently, this explanation has received little attention by recent investigators. With regard to differential thermal expansion, it has been shown by previous investigators (*6*) and also by qualitative tests carried out by the authors that there appears to be no preferential rupture along planes of inhomogeneity within the material. Thus, it is reasonable to assume that the release of volatile matter is a major factor in thermal decrepitation, and a more

Publication Date: January 1, 1966 | doi: 10.1021/ba-1966-0055.ch038

complete understanding of the mechanism involved would assist considerably in developing a process for producing thermally stable anthracite.

In this paper the kinetics of volatile matter release from anthracites have been studied in some detail. Rates of volatile matter release from different particle sizes of anthracite as a function of heating rate and temperature have been measured. The change in composition of the volatile matter with volatilization temperature has been studied.

Experimental Procedure

Measurement of Volatile Matter Release Rates. Volatile matter release rates from anthracite were determined by using the apparatus shown diagrammatically in Figure 1. The power input to the 1-kw., 20-volt Hoskins tube furnace and transformer was controlled by means of a Leeds Northrup duration-adjusting type program controller which permitted linear heating rates up to 20°C. per min. to be selected with varying soak times and temperatures. A maximum temperature of 1000°C. was used since this was the maximum temperature at which the furnace could be operated continuously. The temperature of the furnace was measured by a chromel-alumel thermocouple inside a

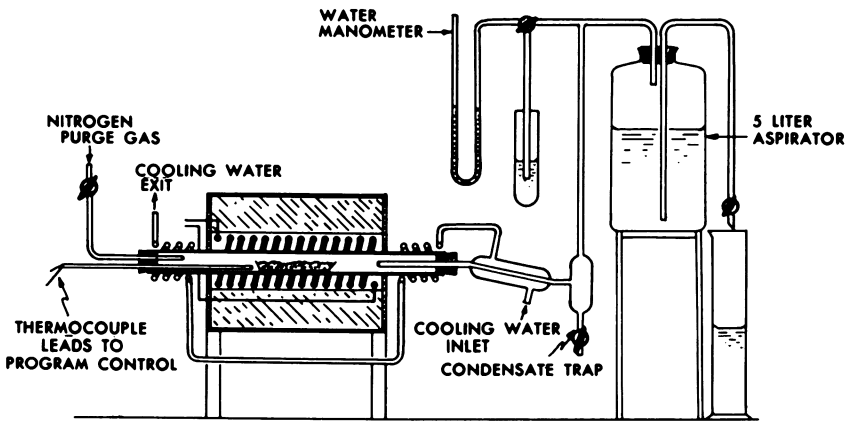

Figure 1. Apparatus for measuring volatile matter release rates

protecting tube and was recorded by the program controller. The controller was capable of maintaining a preset temperature within ±1°C.

Essentially two types of heating runs were made. In one case, the rate of heating up to maximum temperature was held constant (not greater than 20°C. per min.). In the second case, the rate of heating to maximum temperature was more rapid than 20°C. per min. and was not held constant as temperature was increased. In the first case, we were interested in the rate of volatile matter release as a function of heating rate and soak time at maximum temperature. In the second case, we were interested only in the rate of volatile matter release at maximum temperature for more extended soak times. In both cases the following procedure was used for a run. An as-received sample of anthracite of known weight was placed inside the 1-inch internal diameter Coors Sillimanite furnace tube. Nitrogen (of greater than 99.9% purity) was then passed through the apparatus for about 10 minutes to provide an inert atmosphere. With the N_2 turned off and the system open only to the water manometer, the power to the furnace was turned on. The volatiles evolved

Publication Date: January 1, 1966 | doi: 10.1021/ba-1966-0055.ch038

were then passed through a water-cooled condenser and were allowed to displace water from a 5-liter aspirator at constant pressure. The pressure, as indicated by the water manometer, was held at atmospheric pressure by allowing water to flow from the aspirator to the measuring cylinder.

Analysis of Volatile Matter Evolved. An attempt was made to establish the particular volatile component or components responsible for decrepitation by using a Beckman gas chromatography apparatus as described below. It was considered that comparing the analyses obtained at different temperatures with the corresponding rate of volatile matter evolution from the experimental work described previously would perhaps indicate the presence of a thermal decomposition reaction of controlling importance.

The furnace, as shown in section in Figure 1, was coupled to a gas chromatograph apparatus as shown in Figure 2. A supply of carrier gas was provided for the chromatograph apparatus and for purging the system prior to the commencement of each run in order to provide an inert furnace atmosphere. The electrical output from the thermal conductivity detector cell was fed to a Minneapolis-Honeywell 1-mv. range recorder which traced a curve showing the separation of the sample into its components. The instrument was calibrated for each component by plotting peak height against percentage composition. Several gas mixtures of known composition were used for this purpose together with commercial gas cylinder samples of the pure components.

The most satisfactory column for estimating H_2 was found to be a 6-foot length of Linde 13× molecular sieves used in conjunction with argon as a carrier gas. The remaining components found to be present in significant quantities were CO_2, CO, and CH_4. These were estimated by using a 4-foot silica gel column in conjunction with helium as a carrier gas. This column was also found to be satisfactory for ethane; however, this component was not present in sufficient quantity to be detected.

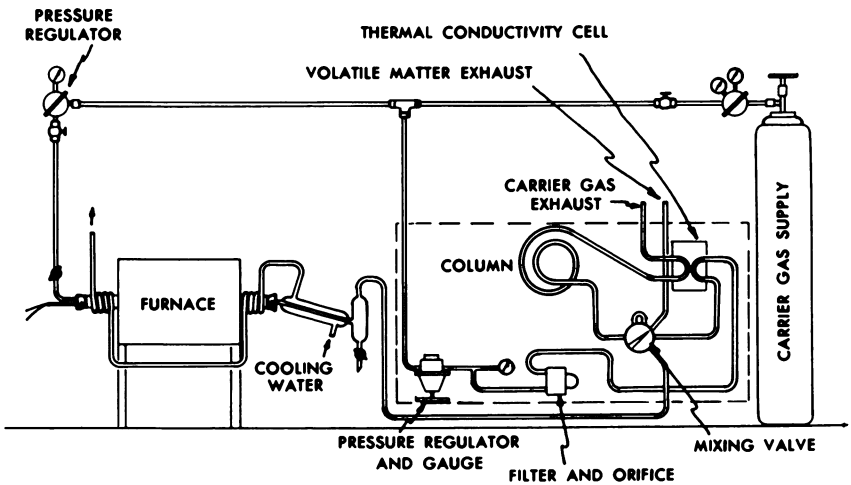

Figure 2. Flow diagram of volatile matter analysis apparatus

Analyses of Anthracites Used. For most of the experimental work an anthracite from the St. Nicholas breaker was used. Its proximate analysis (dry basis) was as follows: C, 84.3%; V.M., 4.5%; ash, 11.2%. Anthracites from other breakers used in this program had the following volatile matter contents

Publication Date: January 1, 1966 | doi: 10.1021/ba-1966-0055.ch038

(dry basis): Jeddo, 2.9%; Dorrance, 4.9%; Loree, 5.4%; Glen Burn, 6.1%; Woodward, 7.5%.

Results

Volatile Matter Release Rates from Anthracites as a Function of Heating Rate and Particle Size. A typical experimental run, expressing the total volume of gas released as a function of temperature for St. Nicholas anthracite, is plotted in Figure 3. At a temperature of about 760°C. there is a sharp increase in the amount of gas released with increasing temperature. Above 760°C. there is an extended region of temperature (760°C. to the maximum

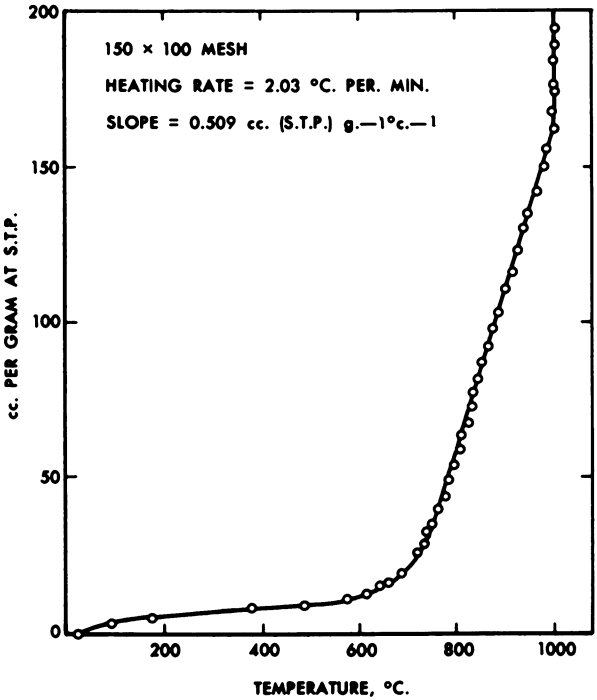

Figure 3. Relationship between the volume of volatile matter evolved and temperature for St. Nicholas anthracite

temperature of 1000°C.) where the amount of gas released per degree rise in temperature is constant. The temperature at which this region commences will be referred to as the critical temperature. Once the maximum temperature of 1000°C. is reached, the volatile matter continues to be evolved if the temperature is held at 1000°C. for some soaking period.

Table I summarizes the volatile matter release rates from St. Nicholas anthracite above the critical temperature. The data show that these rates are essentially independent of heating rate or particle size of the anthracite over the ranges studied. The critical temperature is found to increase, on the aver-

Publication Date: January 1, 1966 | doi: 10.1021/ba-1966-0055.ch038

Table I. Volatile Matter Release Rates in cc. (S.T.P.)/gm./°C. for Varying Particle Size and Heating Rates of St. Nicholas Anthracite Above the Critical Temperature

Particle Size (Tyler Mesh)	*Nominal Heating Rates in °C. per minute*				
	2	*4*	*8*	*12*	*16*
200 × 325	0.541	0.524	0.475	0.500	0.590
100 × 150	0.509	0.489	0.490	0.533	0.600
42 × 65	0.476	0.484	0.535	0.543	0.600
28 × 35	0.506	0.491	0.489	0.520	0.615
12 × 16	0.520	0.514	0.500	0.526	0.593
consolidated pieces (approx. 2.4 cm. in equiv. dia.)	0.611	0.625	0.550	0.585	0.659

age, by *ca.* 70°C. with an increase in heating rate from 2°C. per min. to 16°C. per min. However, at a constant heating rate, the critical temperature is not affected by particle size. From the loss in weight of the anthracite and the total volume of volatile matter released after heating, the average molecular weight of the volatile matter can be calculated. For all the runs on St. Nicholas anthracite the mean average molecular weight was 6.9 ± 0.7. This value did not show a trend with variation in heating rate or particle size.

The rate of volatile matter release for a heating rate of 8°C. per min. was also determined on 150 × 200 mesh fractions of Loree and Woodward anthracites. Three separate runs were made on each sample. For the Loree, the rate of volatile matter release above the critical temperature (740°C.) was 0.611 ± 0.013 cc./gram/°C. For the Woodward the rate of volatile matter release above the critical temperature (770°C.) was 0.666 ± 0.014 cc./gram/°C. The mean average molecular weights of the volatile matter released from the Loree and Woodward were 9.2 ± 0.1 and 7.8 ± 0.3, respectively. As might be expected, the volatile matter release rate increased as the volatile

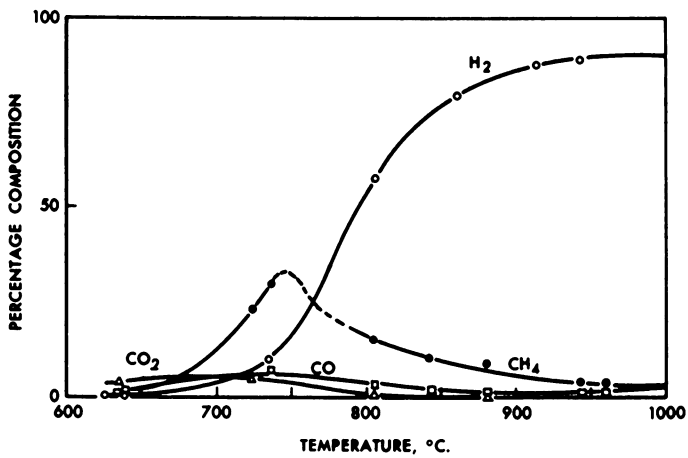

Figure 4. Relationship between volatile matter composition and temperature for a 150 × 200 mesh fraction of St. Nicholas anthracite

matter content of the anthracite increased. Of course, the rate of volatile matter release would also be expected to be a function of the molecular weight of the volatile matter and the distribution of the pore sizes in the anthracite.

Composition of Volatile Matter Evolved from St. Nicholas and Woodward Anthracites as a Function of Temperature and Soak Time. Figure 4 shows the composition of the volatile matter released from a 150 × 200 mesh fraction of St. Nicholas anthracite *vs.* temperature. The difference between 100% and the sum of the percentages of H_2, CH_4, CO, and CO_2 is the percentage of N_2 in the product gas. It is recalled that before commencing a heating run the apparatus was flushed with N_2. Up to 650°C., the rate of release of volatile matter was too low for analysis. The rapid rate of gas evolved above the critical temperature can be attributed primarily to a large increase in the rate of H_2 evolution. Below the critical temperature, more CH_4 is in the product gas than H_2, but the percentage of CH_4 decreases rapidly until at 1000°C. only about 1% is in the product gas. No ethane was detected. Only small percentages of CO and CO_2 were evolved during the heating-up period, but during the constant temperature period at 1000°C. the percentage of CO in the product gas progressively increased to a value of 19% after a soak time of 164 minutes. The last item is shown in Figure 5 where the composition of the gas is plotted against the cumulative time the sample was above 600°C.

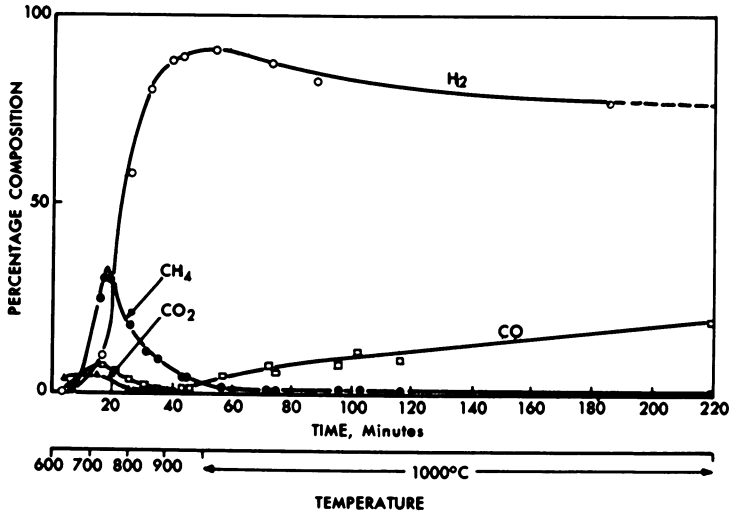

Figure 5. Relationship between volatile matter composition, temperature, and time for a 150 × 200 mesh fraction of St. Nicholas anthracite

Figure 6 shows the composition of the volatile matter released from a 150 × 200 mesh fraction of Woodward anthracite *vs.* temperature. The percentage of N_2 analyzed is also shown. Some significant differences between Figures 6 and 4 are noted. For the Woodward anthracite, much larger percentages of CO and CO_2 are found in the product gas released below 700°C.

Publication Date: January 1, 1966 | doi: 10.1021/ba-1966-0055.ch038

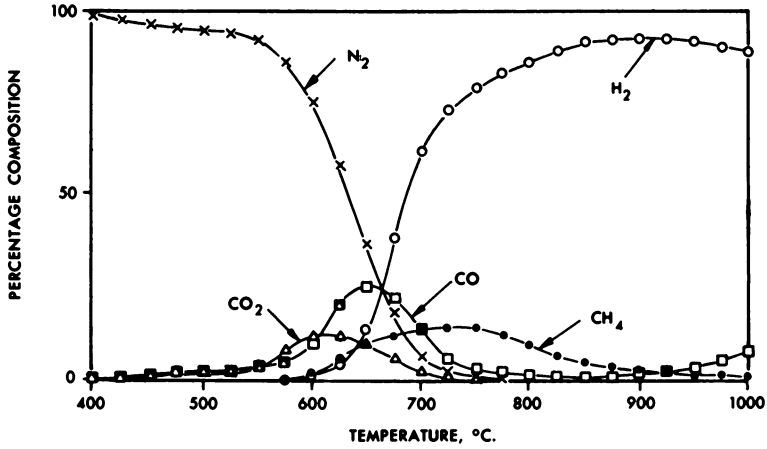

Figure 6. Relationship between volatile matter composition and temperature for a 150 × 200 mesh fraction of Woodward anthracite

than are found for the St. Nicholas anthracite. This increase in the percentage of carbon oxides in the product gas for the Woodward anthracite is accompanied by a decrease in the maximum percentage of CH_4 found in the product gas. For the St. Nicholas anthracite the maximum percentage of CH_4 found in the product gas was 30% (at 737°C.); for the Woodward anthracite the maximum percentage of CH_4 found was 15% (at 735°C.). The relative positions of the H_2 and CH_4 curves for the two anthracites should also be noted. For the St. Nicholas anthracite, the maximum amount of CH_4 in the product gas was found at a position where only *ca.* 15% H_2 was in the product gas. For the Woodward anthracite, the maximum amount of CH_4 in the product gas was found where 75% H_2 was in the product gas. These data indicate some fundamental difference in the desorption kinetics of H_2 and CH_4 from the two anthracites. The formation of CH_4 is presumably caused by the rupture of C-C single bonds, whereas the progressively increasing concentration of H_2 with increasing temperature is probably related to the increasing rupture of the higher energy C-H bonds at the surface and also in the gas phase, for example from methane.

Rate of Release of Hydrogen from St. Nicholas Anthracite at Selected Temperatures as a Function of Soak Time. Initial rates of H_2 release from a 150 × 200 mesh fraction of St. Nicholas anthracite were determined at temperatures between 700° and 755°C. and are shown in Figure 7. Zero time starts when the sample reached the designated maximum temperature. It is seen that after the carrier gas was displaced from the apparatus, the rate of H_2 release at each temperature studied was constant over the interval of times plotted in Figure 7—i.e., the rate of H_2 release did not depend on the amount of H_2 remaining on or in the anthracite. From these initial rates of H_2 release an activation energy of 96 kcal./mole is calculated. When the soak time at a particular temperature below 755°C. was extended sufficiently, the rate of

Publication Date: January 1, 1966 | doi: 10.1021/ba-1966-0055.ch038

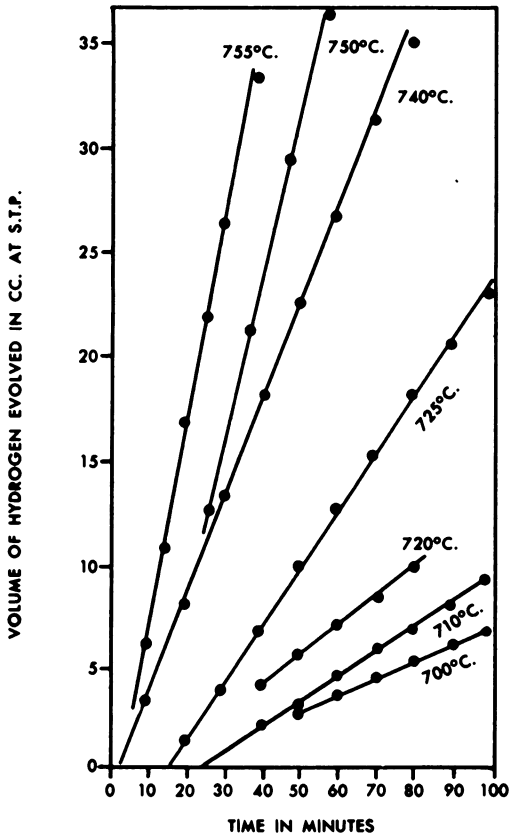

Figure 7. Variation of initial hydrogen release rates with temperature for 5.5 grams of 150 × 200 mesh St. Nicholas anthracite

evolution of H_2 progressively decreased with time. Indeed, at temperatures above 760°C. the initial rate of H_2 release was so rapid that only the region of decreasing evolution rate was apparent. For this region of decreasing evolution rate, a linear plot is obtained if the volume of H_2 evolved is plotted against the log of time. Such plots are shown in Figure 8 for desorption studies in the temperature range 800°–860°C. As discussed by Redmond and Walker (*7*), among others, this type of plot (frequently called an Elovich plot) can be explained theoretically on the basis of a linear increase in activation energy of desorption of H_2 with decrease in surface coverage. If desorption rates at different temperatures are taken at the same value of surface coverage (same volume of H_2 evolved), activation energies at fixed values of coverage can be determined from Arrhenius plots. This was done for the data in Figure 8. The activation energy for H_2 evolution was found to increase linearly with decreasing fractional coverage (θ) from 96 kcal./mole at $\theta \rightarrow 1$ to 137 kcal./mole at $\theta = 0.5$ (or ½ of the total H_2 removed from the anthracite).

Publication Date: January 1, 1966 | doi: 10.1021/ba-1966-0055.ch038

Effect of Particle Size on the Rate of Desorption of Hydrogen from St. Nicholas Anthracite at Constant Temperature. If the rate of evolution of H_2 is controlled by the rate of desorption of H_2 from the surface of anthracite and not by the rate of transport of the H_2 from the pore system, the rate of evolution should be independent of particle size. However, this was not found to be the case. For St. Nicholas anthracite, the initial rate of H_2 release was determined on a 12 × 16 mesh fraction over the temperature range 700°–750°C. and compared with the previous results for initial rate of release on a 150 × 200 mesh fraction. Results are summarized in Table II. The results show clearly that the rate of H_2 evolution at all temperatures studied was more rapid from the larger particle sized sample. The activation energy for H_2 evolution at $\theta \rightarrow 1$ from the 12 × 16 mesh fraction is calculated as 89 kcal./mole, compared with 96 kcal./mole for the 150 × 200 mesh fraction over the same temperature interval.

The initial H_2 release rate at 750°C. was investigated for different particle sizes ranging from a consolidated piece of approximately 2 cm. equivalent

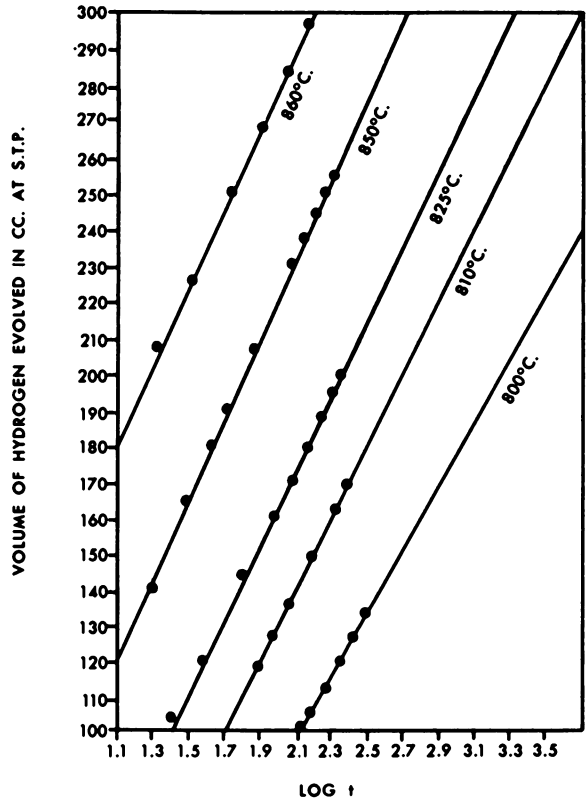

Figure 8. Variation of dq/d log t with increasing temperature for 5.5 grams of 150 × 200 mesh St. Nicholas anthracite

Publication Date: January 1, 1966 | doi: 10.1021/ba-1966-0055.ch038

Table II. Effect of Particle Size on the Rate of Hydrogen Release from 5.5 Grams of St. Nicholas Anthracite

Particle Size (Tyler Mesh)	*Temperature °C.*	*Rate cc./min.*
12 × 16	700	0.17
150 × 200	700	0.08
12 × 16	710	0.27
150 × 200	710	0.13
12 × 16	725	0.41
150 × 200	725	0.30
12 × 16	740	1.00
150 × 200	740	0.50
12 × 16	750	1.50
150 × 200	750	0.85

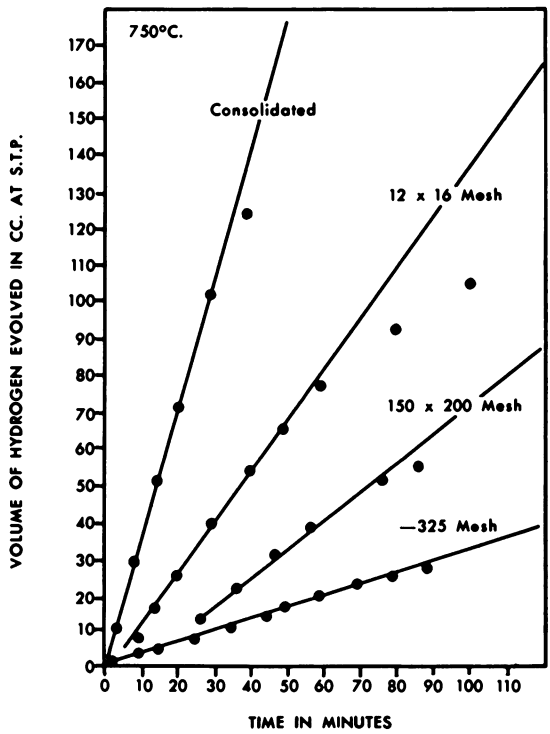

Figure 9. Variation of the initial rate of hydrogen release with particle size for 5.5 grams of St. Nicholas anthracite

diameter to a —325 mesh fraction. The results are shown in Figure 9. The marked decrease in H_2 evolution rate with decrease in particle size is clearly seen.

Effect of Particle Size on the Rate of Volatile Matter Release at Constant Temperature from Different Anthracites. On the basis of the results for St.

Nicholas anthracite, we investigated the effect of particle size on the rate of volatile matter release at constant temperature from other anthracites. In all cases H_2 represented a large fraction of the total volatile matter released. Evolution rates were measured at 800°C. on 5.5-gram samples. As previously discussed, at 800°C. plots of the volume of volatile matter released *vs.* the log of time gave straight lines, with the slope of these lines ($dq/d \log t$) being a measure of the relative rate of volatile matter release. Results are summarized in Table III and Figure 10. The effect of particle size on volatile matter release rate is complex and depends upon the anthracite studied. However, in every case particle size has a pronounced effect on volatile matter release rate at constant temperature.

Table III. Rates of Volatile Matter Release from 5.5-gram Samples of Selected Anthracites at 800°C.

Anthracite	*Particle Size (Tyler Mesh)*	*dq/d log t, cc.*
St. Nicholas	—325	142.0
	150 × 200	160.0
	12 × 16	183.0
Loree	—325	217.0
	150 × 200	191.0
	16 × 20	176.5
Dorrance	—325	153.0
	150 × 200	83.0
	12 × 16	191.5
Glen Burn	—325	158.6
	150 × 200	123.0
	16 × 20	190.0
Jeddo	—325	166.6
	150 × 200	170.0
	16 × 20	131.8

Publication Date: January 1, 1966 | doi: 10.1021/ba-1966-0055.ch038

Discussion

Our primary objective has been to present the experimental results in a convenient, combined form rather than to discuss their significance in great detail. In view of the extreme physical and chemical complexity of anthracite and the limited amount of experimental investigation to which the material has been subjected at present, an elaborate theoretical discussion would be pointless. Indeed, it is improbable that the kinetics of volatile matter release for such a complex material will ever submit to a satisfactory correlation by simple functional relationships. In spite of these difficulties, it is of interest to discuss some of the general trends exhibited by the experimental data and their interpretation by suggesting approximate theoretical and mathematical models for the release mechanism.

A Chemisorption Mechanism for the Release of Hydrogen from Anthracite. In recent years considerable experimental justification has been obtained for the view that in many cases surface interactions during chemisorption can give

rise to a linear dependency of activation energy upon surface coverage. By assuming a velocity equation of the type

$$-\frac{d\Theta}{dt} = Ae^{-(E_0 - \beta\Theta)/RT} \quad (1)$$

where Θ is the fraction of surface coverage, E_0 is the activation energy at $\Theta = 0$, and β is the change in activation energy as Θ goes from 1 to 0, it can be shown that by making appropriate simplifying assumptions a logarithmic time law can result. The assumptions and theoretical considerations involved have been fully discussed by Redmond and Walker (7), and for our purpose it is sufficient to state that a relationship between surface coverage and time under isothermal conditions can be expressed in the form:

$$\Theta = k_1 + k_2 \log t \quad (2)$$

where the constants k_1 and k_2 are related to the constants appearing in Equation 1.

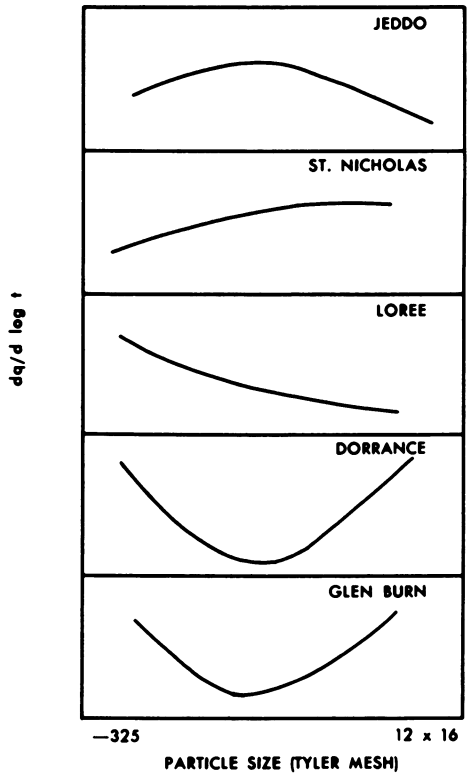

Figure 10. Qualitative variation of dq/d log t with particle size for various anthracites at 800°C.

Publication Date: January 1, 1966 | doi: 10.1021/ba-1966-0055.ch038

In view of the linearity of the curves presented in Figure 8 and the high activation energies obtained by using Equation 1 at constant values of Θ, there seems to be considerable justification for the chemisorption model of volatile matter release. The fact that the initial rates of H_2 release show a zero-order dependency may be attributed to the fact that for raw anthracite the fraction of surface coverage is practically unity. Under these conditions, where almost all of the sites available for H_2 adsorption are filled, Equation 1 leads to the result that the rate of change of coverage with respect to time is initially constant.

On the basis of a chemisorption hypothesis, no dependency upon particle size would be expected; consequently the results presented in Table II and Figure 9, showing that the release rate increases with increasing particle size, are difficult to explain. Although it is conceivable that, owing to the existence of size-dependent temperature gradients within the material there could be a tendency for the rate of release to increase with increasing particle size, it would be preferable to await further experimental evidence before attempting to fit particle size dependency to the proposed model. As Table III and Figure 10 show, anomalous results were also obtained with respect to particle size for other anthracites. However, as with results for St. Nicholas anthracite, it would be preferable to await further experimental evidence before attempting to attach any significance to this complex behavior. In the isothermal work a significant time was required for the furnace to reach its controlled temperature, and this may have resulted in an apparent size dependency. No such dependency was observed for the volatile matter release data at the linear heating rates shown in Table I where the samples were not subjected to discontinuities in thermal treatment.

Although the use of linear heating rates introduces considerable complexity into the mathematics, it is of interest to note that the slope of the curve (above the critical temperature) shown in Figure 3 can be related to desorption theory. By differentiating Equation 1 with respect to time, it follows that

$$-\frac{d^2\Theta}{dt^2} = Ae^{-(E_0 - \beta\Theta)/RT}\left[\frac{\beta}{RT}\frac{d\Theta}{dt} + \frac{E_0 - \beta\Theta}{RT^2}\frac{dT}{dt}\right] \tag{3}$$

When $d^2\Theta/dt^2 = 0$, it follows that

$$-\frac{d\Theta}{dt} = \frac{E_0 - \beta\Theta}{\beta T}\frac{dT}{dt} \tag{4}$$

or, since $1 - \Theta = V_t/V_\infty$, it follows that in terms of volatile matter release

$$\left(\frac{dV_t}{dT}\right)_{H_2} = \frac{V_\infty E_0 - \beta(V_\infty - V_t)}{\beta T} \tag{5}$$

where V_t equals the volume of H_2 released at time (t) and $V\infty$ equals the total amount of H_2 released. Substituting $E_0 = 178$ kcal./mole, $\beta = 82$ kcal./mole, $T = 1073°$K., $V_t = 30$ cc./gram, and $V\infty = 135$ cc./gram leads to the result that $(dV_t/dT)H_2 = 0.16$. Since the volatile matter is approximately 50% H_2

Publication Date: January 1, 1966 | doi: 10.1021/ba-1966-0055.ch038

at 800°C., it follows that dV_t/dT for the total volatile matter should be about 0.32, which at least agrees in order of magnitude with the tabulated values given in Table I. In this calculation, the value of $V\infty = 135$ cc./gram was derived from the original data used to prepare Figures 4 and 5. The value of $V_t = 30$ cc./gram was obtained from Figure 3 assuming that the cumulative volatile matter was 50% H_2 at 800°C. Although the point of inflection in Figure 3 is not well defined, it is clear that such a point must exist, and the apparent linearity of Figure 3 could be caused by the existence of an extensive region in which the second derivative, $d^2\Theta/dt^2$, is almost zero.

A Diffusional Mechanism for the Release of Volatile Matter from Anthracite. The fact that the quantity of H_2 released appeared to be related linearly to the logarithm of time could lead to interpreting the isothermal results in terms of surface chemistry as shown. However, Figure 11 shows that within the limits of experimental error, the solution to the unsteady state diffusion

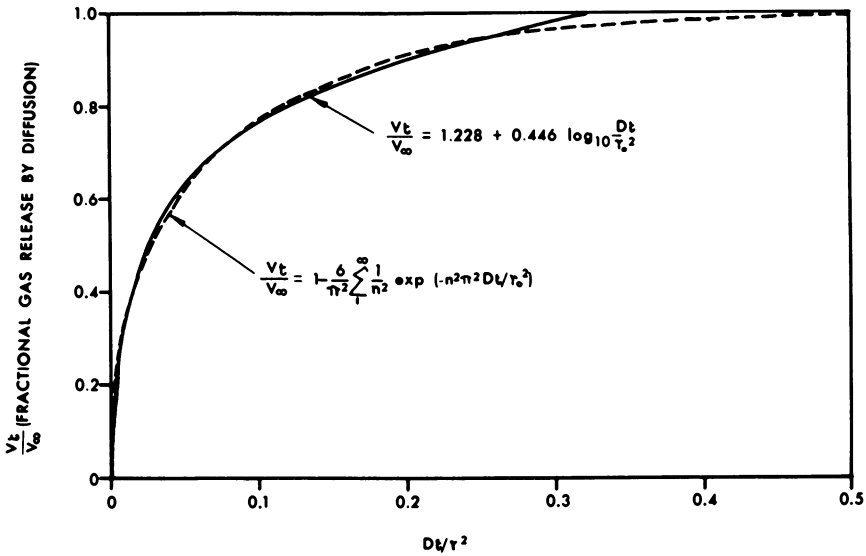

Figure 11. Diffusion theory compared with an approximating logarithmic time law

problem can be represented by a logarithmic time law up to 97% completion of the diffusion process as well as by the conventional equation for diffusion from a spherical particle (*4*). This suggests that the isothermal kinetics of volatile matter release could be interpreted equally well as a pure diffusion process in which the chemical release rate is almost instantaneous compared to the subsequent slow diffusion process through the anthracite. Although, for a homogeneous medium, a diffusion controlled process would not lead to release rates independent of particle size, it is conceivable that the release of volatile matter could be diffusion controlled within relatively nonporous structural units of much smaller dimensions than the external dimensions of the particles them-

Publication Date: January 1, 1966 | doi: 10.1021/ba-1966-0055.ch038

selves. It is analogous to the reasoning used in an attempt to explain the rate of fission product release from uranium oxide (3).

In an attempt to provide further information relative to the validity of the diffusion mechanism, a typical set of results was selected from the isothermal release work, and the volume of volatile matter released was plotted against the square root of time. For a pure diffusion process such a plot should be almost linear initially (4) whereas for a true logarithmic time law, $dV_t/dt^{1/2}$ should tend to infinity for very small values of $t^{1/2}$. Figure 12 shows that by this criterion the rate controlling mechanism appears to be diffusion and not chemisorption. The fact that the curve does not pass through the origin is undoubtedly caused by the fact that it was not possible to heat the sample to

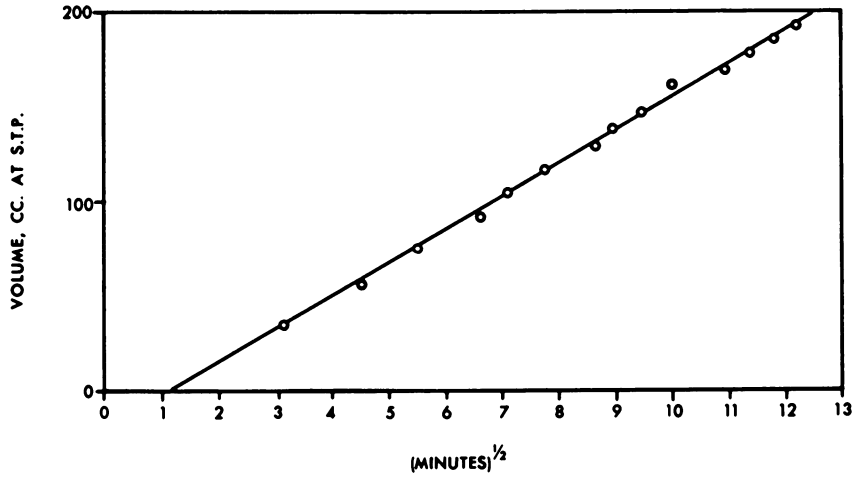

Figure 12. Volatile matter released from 5.57 grams of 150 ×200 mesh St. Nicholas anthracite at 700°C.

the control temperature at $t = 0$. Owing to the sensitivity of the diffusion process to such errors in the initial conditions, no further diffusion interpretations of the isothermal data were attempted.

The high activation energies resulting from the chemisorption hypothesis appear to favor its validity. However, it is possible that such a high activation energy could be caused by an equilibrium between the undecomposed coal molecules and the diffusion species resulting from thermal decomposition. That is, for diffusion in the Z dimension only, a simplified mass balance would lead to a differential equation of the form

$$D \frac{\partial C^*}{\partial Z^2} = \frac{\partial C}{\partial t} \tag{6}$$

where C^* represents the concentration of diffusing species, and C represents the total concentration of "available" volatile matter. If C^* and C were related by an equilibrium constant K such that $C^*/C = K = \exp(-\Delta F/RT)$, then

Publication Date: January 1, 1966 | doi: 10.1021/ba-1966-0055.ch038

the diffusion coefficient would appear to possess an exponential temperature dependency of the type suggested by the following change of variable,

$$De^{-\Delta F/RT}\frac{\partial^2 C}{\partial Z^2} = \frac{\partial C}{\partial t} \quad (7)$$

Although a pure diffusion process can give rise to an apparent logarithmic time law and the initial release of volatile matter is linearly related to $t^{1/2}$, insufficient evidence has been presented to indicate positively that the release is diffusion controlled.

Since the chemisorption and diffusion mechanisms appear to be almost equally acceptable, it is suggested that both of them be regarded as somewhat questionable until they can be investigated by further experimental work.

Acknowledgments

The authors take pleasure in acknowledging the financial support of the Coal Research Board of the Commonwealth of Pennsylvania for making this research possible.

Literature Cited

(1) American Society for Testing Materials, Philadelphia, Pa., D-141-48.
(2) American Society for Testing Materials, Philadelphia, Pa., D-294-50.
(3) Cottrell, W. B., Scott, J. L., Culver, H. N., Yarosh, M. M., *U.S. At. Energy Comm.* **ORNL-2935** (1960).
(4) Crank, J., "The Mathematics of Diffusion," p. 85, The Clarendon Press, Oxford, 1956.
(5) Delvaux, L., M.S. Thesis, The Pennsylvania State University, 1955.
(6) Jackson, E. G., Grace, R. J., *Pennsylvania State Univ. Mineral Ind. Expt. Sta., Anthracite Progress Rept. Nos.* **53** and **54.**
(7) Redmond, J. P., Walker, P. L., Jr., *J. Phys. Chem.* **64,** 1093 (1960).

RECEIVED January 25, 1965.

Publication Date: January 1, 1966 | doi: 10.1021/ba-1966-0055.ch038

Discussion

Marie-Therese Mackowsky: Have you ever determined the mechanical resistance or the strength of the different anthracites? It may be that the independence of the grain size is caused by the fact that a cracking has taken place and in reality you have nearly the same grain size in all the tests.

Philip L. Walker: Hardgrove grindability data for many Pennsylvania anthracites have been determined and reported on in the Proceedings of the 1956 Anthracite Conference held at Pennsylvania State University.

We would agree that grinding should produce some macrocracks in the particles and that these macrocracks can open up previously closed-pore volume. This, in turn, will affect the kinetics of volatile matter release.

Bhupendra Mazumdar: Dr. Walker obtained small amounts of gas by carbonizing anthracite up to 600°C. (about 10 cc./gram) whereas our results

obtained from a South Wales anthracite (C = 93.2%) indicate that about 60 cc./gram of gas is formed at and up to 600°C., owing to pyrolysis. I would like to know about the rank of the anthracite sample to which Dr. Walker's results refer. Further, I would also appreciate his general comments on the degassing of anthracite at 450°C.—is it really safe to do so?

Dr. Walker: We discuss the release of volatile matter from different anthracites in another paper (*Carbon* **2**, 199 (1964)). For a low volatile matter anthracite such at St. Nicholas, weight loss for a heat treatment temperature of 500°C. is 1.7%; for a high volatile matter anthracite such as Treverton (V.M. = 9.0%), weight loss for heat treatment to 500°C. is 4.8%. The difference in weight loss for these two anthracites heated to 500°C. can be accounted for almost entirely by differences in the amount of CO and CO_2 released. Thus, the higher the volatile matter content of the anthracite, the lower the temperature to which the anthracite can be heated and still not significantly change the magnitude of its available micropore volume. That is, release of CO and CO_2 unblocks some previously unavailable micropores.

L. L. Newman: Dr. Mackowsky has already asked you if you related your studies on the kinetics of volatile matter release from Pennsylvania anthracites to the petrographic constituents of the coal. Can you not say in effect that the coals from the various collieries differ from each other quite significantly with respect to their petrographic composition and that identification of a coal by source may identify it petrographically to some extent? How do the results of these studies relate decrepitation actually experienced in industrial operations?

Dr. Walker: We have not related our studies of kinetics of volatile matter release from anthracites to their petrographic consituents. This type of work is planned for the future.

Generally, the decrepitation resistance of anthracites increases with decreasing volatile matter content, but in some cases differences in physical properties of the coals appear to nullify this relation.

George R. Hill: Have you planned to study the kinetics of methane decomposition over anthracite in a long packed column at constant temperature? This should help resolve the unanswered mechanism questions.

Dr. Walker: We have not planned to study the decomposition of methane over anthracite as you suggest. I think it would be more interesting to study the decomposition of methane as it diffuses out of the micropore structure of anthracite. At least two effects are possible: (1) since two moles of hydrogen are produced for each mole of methane decomposing, an increase in the number of moles of gas diffusing from the pores per unit time could result; (2) the carbon produced by methane decomposition could block pores and/or decrease their size, which could result in a decrease in the number of moles of gas diffusing from the pores per unit time.

Norbert Berkowitz: I once again question the admissibility of the kinetic approach. Hydrogen yields at the various temperatures are *not normalized*, and that implies the quite untenable assumption that hydrogen yields at all experimental temperatures would all be the same provided sufficiently long degasification periods were allowed. I doubt whether the authors actually do imply that, but if they don't, they ought to bear in mind that classical kinetics

Publication Date: January 1, 1966 | doi: 10.1021/ba-1966-0055.ch038

cannot be used to describe a reaction whose final product-yields at t_∞ vary with temperature. Most certainly, the initial slopes observed with such a reaction do not allow calculation of an activation energy.

Dr. Walker: Using the Elovich concept (—i.e., a varying activation energy for desorption with surface coverage) is not using classical kinetics. I would agree that this situation is complex because of the possible production of hydrogen from at least two sources: (1) direct desorption of hydrogen from the anthracite surface, and (2) production of hydrogen from the decomposition of methane, which is produced first. Because the situation is complex, stating an activation energy for initial rates of hydrogen release is useful only to give an expression for rate variation with temperature. Certainly this activation energy cannot be used to decide upon a final mechanism for hydrogen release.

Publication Date: January 1, 1966 | doi: 10.1021/ba-1966-0055.ch038

The Dry Oxidation of Subbituminous Coal

E. J. JENSEN, N. MELNYK, J. C. WOOD, and N. BERKOWITZ

Research Council of Alberta, Edmonton, Canada

Publication Date: January 1, 1966 | doi: 10.1021/ba-1966-0055.ch039

Detailed results of a study on the formation of humic acids during dry oxidation of a typical subbituminous coal are reported. The reaction was carried out in a closed circuit system at temperatures between 180°–300°C. and oxygen concentrations in the range 10–90% and was allowed to proceed for approximately 100 hours in most test runs. Particular attention was directed to the development of acidity and alkali solubility in the reactant mass. Data thus obtained are used to outline a general reaction path and to delineate some of the principal chemical changes which appear to occur during the oxidation process. Of special interest is the observation that significant formation rates are confined to a strictly limited temperature range and that even here, alkali solubility and acidity may be consequences of two essentially unrelated reactions.

By a convention which apparently originated from observations by C. Vauquelin (*14*), A. Klaproth (*6*), and R. Jameson (*5*), alkali soluble organic constituents of soil and coal are designated as "humic acids." Collectively, these substances make up an ill-defined series of dark colored, weakly acidic solids which form whenever plant components (such as lignin) are exposed to fungal oxidases, or when coal is allowed to weather or otherwise oxidize. Some evidence now exists that humic acids isolated from these varied sources do indeed contain several common peripheral structures (*2, 11, 16*), but by any more discriminating test, the term possesses little chemical significance or fixed meaning.

Prevailing uncertainties are perhaps most clearly illustrated by the properties of humic acids obtained from a nominally single source—e.g., oxidized coal. Such humic acids will resemble each other in color and typically have equivalent weights around 250. However, depending upon factors which are

In Coal Science; Given, P.;
Advances in Chemistry; American Chemical Society: Washington, DC, 1966.

still not fully understood, their molecular weights can range from less than 600 to more than 10,000. Their acidities can assume values between *ca.* 7 and 12 meq. per gram. Their -OH/-COOH ratios can vary from 0.8 to 2.5. While a rather close structural relationship between them and the parent coal possibly may be taken for granted, the nature of this relationship and the manner in which humic acids form from coal remain equally unknown. All that can be asserted with confidence is that humic acids are, in themselves, reaction intermediates which can be easily further degraded by oxidation.

In these circumstances—and in view of increasing industrial interest in coal-based humic acids as chemical source materials (*4*)—we thought it pertinent to reinvestigate the mechanism of humic acid formation and, as a first step, to direct particular attention to the development of acidity and alkali solubility during progressive uncatalyzed oxidation of a subbituminous coal (Table 1) with dry oxygen. The choice of this particular system is, *prima facie*, arbitrary since conversion of coal into humic acids can, in principle, be accomplished by several methods. (Among those commonly used are reactions

Table I. Composition of Coal

	Proximate Analysis		*Ultimate Analysis*	
	Equilibrium Moisture Basis	*Dry Basis**	*% daf*	
Moisture %	23.0	0.6	Carbon	72.1
Ash %	7.3	9.4	Hydrogen	4.3
Volatile Matter %	28.6	36.9	Sulphur	0.4
Fixed Carbon %	41.1	53.1	Nitrogen	1.4
	100.0	100.0	Oxygen (by diff.)	21.8
				100.0

* As charged to reactor

of static or fluidized coal beds with air or oxygen; "wet" reactions with H_2O_2, $KMnO_4$, or HNO_3, the latter yielding so-called nitro humic acids; reactions with aqueous alkali and air or oxygen under pressure.) It is, however, worth recalling that oxidizing coal with liquid-phase reagents, while usually much faster than dry oxidation, is characteristically less subject to control, and its greater severity will also result in reduced yields of humic acids (and in correspondingly greater proportions of secondary degradation products—notably water soluble acids—in the reactant mixture). These unnecessary complications we wished to avoid.

Experimental Procedures

In order to permit meaningful measurements which could be related to particular reaction conditions, the oxidations were carried out in the apparatus shown in Figures 1 and 2. This gas-tight, closed circuit installation allowed pressure and temperature control, gas monitoring, and periodic withdrawals of small coal samples while reaction proceeded. The total free volume of the apparatus amounted to some 2200 cc.

Publication Date: January 1, 1966 | doi: 10.1021/ba-1966-0055.ch039

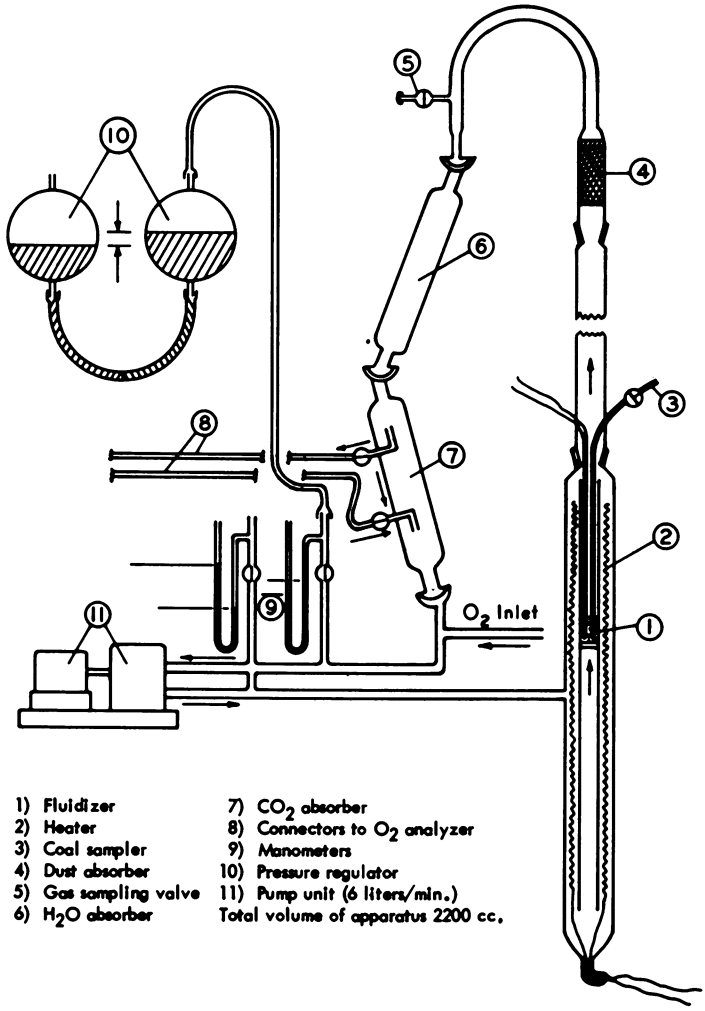

Figure 1. Coal oxidation apparatus (not to scale)

For each run, the fluidized bed reactor was charged with 15.0 grams of freshly ground (–65 + 150 mesh) coal which had been dried in vacuo at 50°C. Operating pressures were always kept to a few millimeters above atmospheric, but temperatures in the different test runs varied between *ca.* 180° and 300°C. (Below 180°C., little or no reaction occurs even when reaction periods are extended to several hundred hours; above 300°C., excessive burn-off, as evidenced by very high H_2O and CO_2 yields, is encountered.)

Oxygen concentrations in the various runs ranged from 10 to 90% and were closely controlled by admitting oxygen at rates which always just balanced the rates of oxygen consumption. The latter were measured by a calibrated cylinder which formed one-half of the constant-head oxygen supply bottle (Figure 2), and instantaneous oxygen concentrations were continuously monitored on a Beckman F3 oxygen analyzer. During the first 30 minutes or so

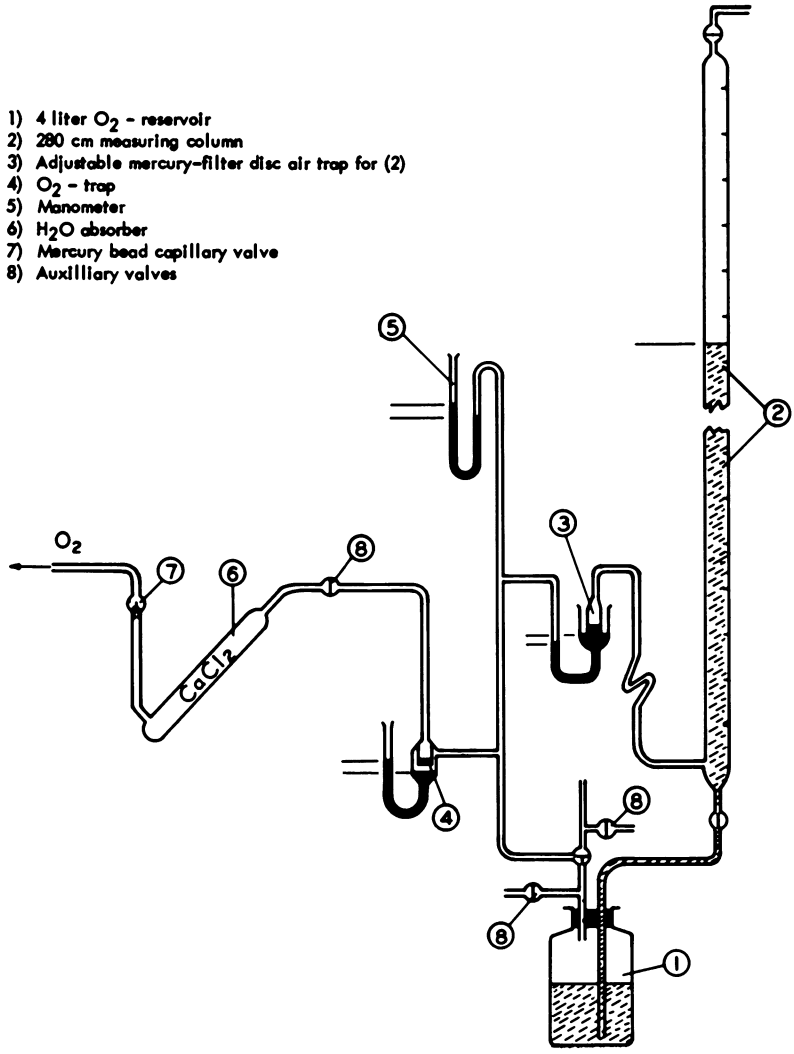

Figure 2. Oxygen supply apparatus (not to scale)

after start-up and attainment of reaction temperature, oxygen consumption rates would occasionally exceed the capacity of the supply valve; when this happened, an auxiliary oxygen source was switched into the line. In no case, however, did oxygen concentrations in the system deviate from the chosen value by more than a few percent.

The principal off-gases (H_2O and CO_2) were routinely collected in tared scrubbers and quantitatively determined by weighing. However, as each run progressed, 1-cc. gas samples were also withdrawn from time to time and analyzed by gas chromatography. Particular attention was paid to oxygen (to check the performance of the Beckman analyzer) and to carbon monoxide. At

Publication Date: January 1, 1966 | doi: 10.1021/ba-1966-0055.ch039

regular intervals 0.1–0.2-gram coal samples were withdrawn for infrared spectroscopy, elemental analysis, and functional group determinations.

Measurements of alkali solubles in these coal samples—conventionally accepted as indices of humic acid concentrations—were initially performed by using Kreulen's method (7). However, even when the most stringent precautions were taken to exclude air, this method yielded markedly time-dependent results (presumably owing to oxidation of the coal by the relatively strong alkali solution), and a more satisfactory colorimetric technique (by J. F. Fryer) was therefore employed. This entailed extracting the coal sample with 0.1*N* aqueous sodium hydroxide for 16–20 hours in an inert atmosphere and subsequent photoelectric scanning of the extract solutions. Actual humic acid concentrations were then obtained from specially constructed reference curves which related optical density (at an appropriate wavelength) to humic acid contents. The inherent error in this determination is estimated at less than 10%.

Total acidities and concentrations of carboxylic acid groups were measured by what are now well-established procedures (*1*, *8*).

Results

The resultant data, exemplified by Figures 3 to 15 and by the material balances summarized in Table II, outline a definite and rather characteristic pattern.

As might have been anticipated, carbon and hydrogen contents of the oxidizing coal decrease progressively as reaction proceeds and tend towards limiting values which depend on the severity and duration of the reaction. (Under the conditions of the present study, these limits lie in the neighborhood of 61% and 1.5%, respectively).

Similarly, total acidity and carboxyl contents (with the difference between these two parameters almost entirely accounted for by the concentration of phenolic-OH) rise rapidly towards asymptotic limits from which, however, they will again decline if reaction conditions are severe—i.e., if reaction temperatures and oxygen concentrations are high. Concentrations of —COOH typically remained below *ca.* 5 meq. per gram, while the total acidity attained values which, depending on conditions, could range from 9 to 12 meq. per gram. (In the parent coal, which contained only traces of alkali soluble matter, —COOH and total acidity amounted to *ca.* 0.6 and 6 meq. per gram, respectively.)

On the other hand, concentrations of humic acids—i.e., of alkali solubles in the reacting coal mass, start in the range 0–5% (consistent with minimal concentration in the parent coal) and show a very pronounced, if somewhat diffuse, general dependence on reaction conditions. For example, at 180°C. and oxygen concentrations below about 20%, conversion to humic acids is negligible, and significant reaction rates at this temperature are only observed when [O]>50%. However, as temperatures rise, reaction rates at all oxygen levels increase until, at 250°C., even relatively low oxygen concentrations will generate large humic acid yields within a few hours. At still higher temperatures, oxygen concentrations in excess of 20% cause very rapid conversion and, thereafter, destruction of humic acids by secondary degradation. Graphs of humic acid concentration *vs.* time will therefore then pass through a more or less clearly discernible maximum.

Publication Date: January 1, 1966 | doi: 10.1021/ba-1966-0055.ch039

Significantly, very rapid conversion of coal into humic acids is always accompanied by a sharp increase in oxygen consumption rates, formation of large quantities of water and carbon dioxide, and a marked decline in the amounts of recoverable coal—i.e., by all the symptoms of extensive combustion. However, similar (if less rapid) carbon losses to burn-off are also observed under much less severe reaction conditions, and such losses will steadily accumulate even when the net rate of humic acid formation has fallen to zero—i.e., when concentrations of humic acids in the oxidizing coal mass have become independent of reaction time. Steady evolution of carbon dioxide and water is therefore a general feature of the reaction. Except at relatively low temperatures and oxygen levels, where conversion to humic acid is slow and where stripping losses can be more or less effectively balanced by adding oxygen to the reacting coal mass, this manifests itself also in increasing weight

Publication Date: January 1, 1966 | doi: 10.1021/ba-1966-0055.ch039

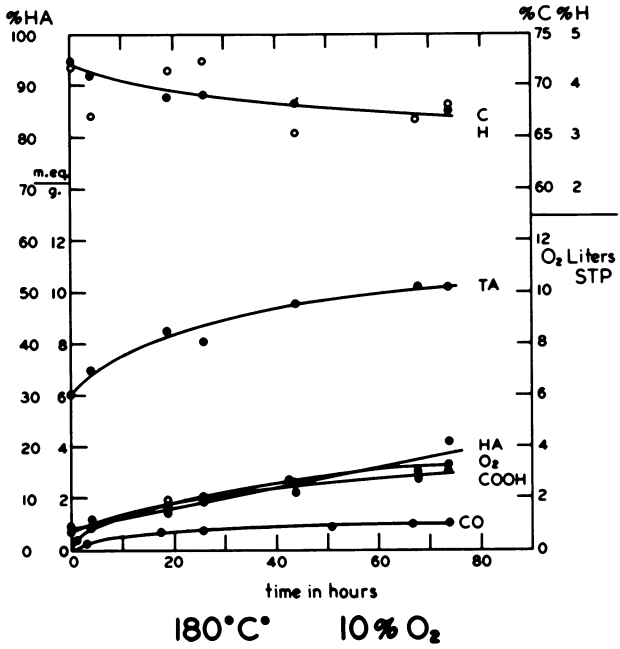

Legend and Explanation for Figures 3–15

Experimental conditions are indicated under each graph.
The following abbreviations and symbols are used:

- ● C = carbon content (%) of solid reactant
- ○ H = hydrogen content (%) of solid reactant
- ◐ TA = total acidity in meq./gram
- ◒ COOH = carboxyl content in meq./gram
- ◒ HA = "humic acid"—i.e., alkali soluble material in w/w % of reactant
- ⊙ O_2 = cumulative oxygen consumption in liters (STP)
- ◑ CO = carbon monoxide content in volume % of reactor gas

The abscissae and ordinates are self-explanatory, but note that the CO ordinate should be read on the 0–100% (HA) scale.

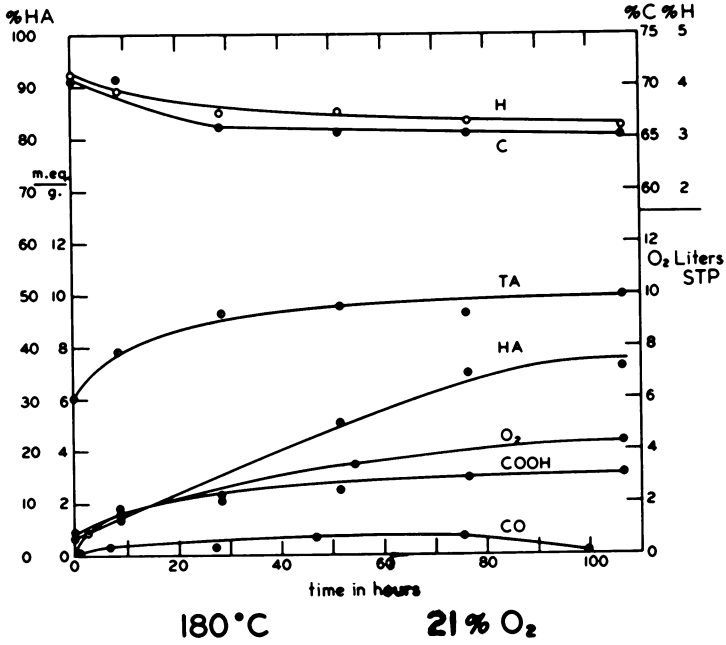

Figure 4

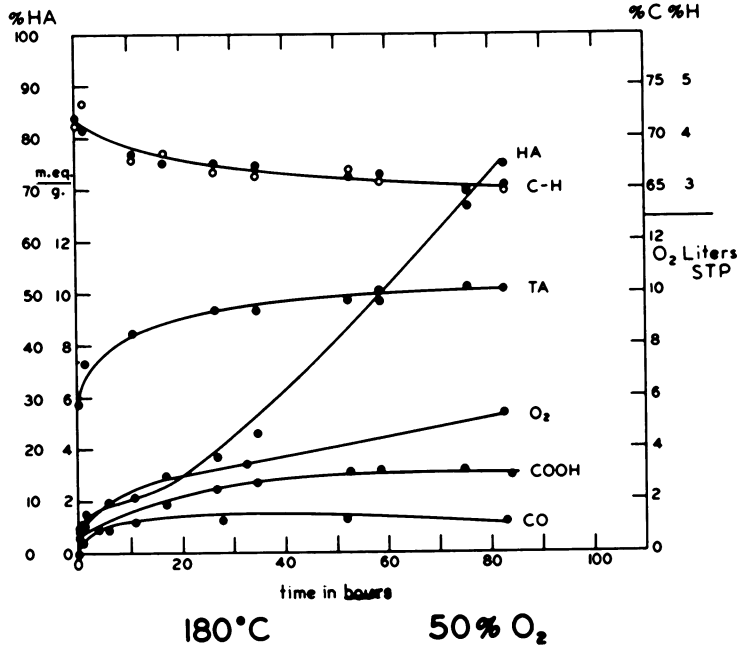

Figure 5

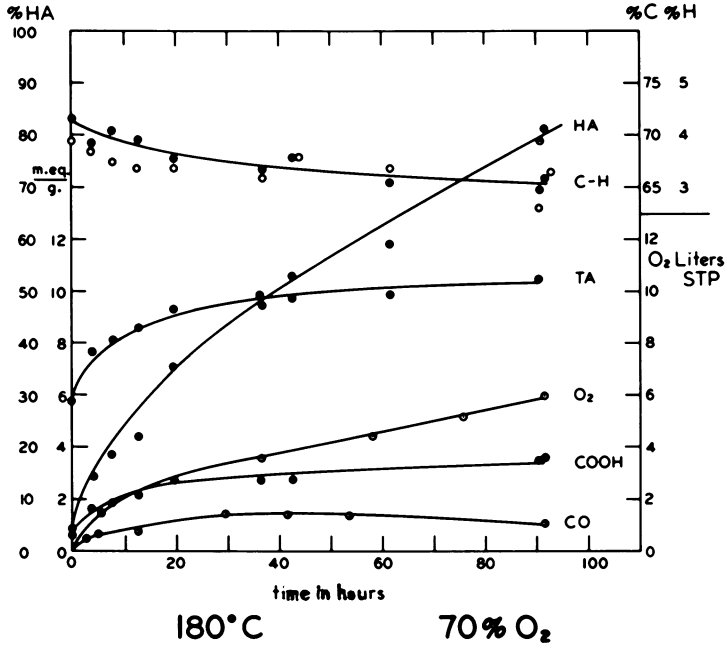

Figure 6

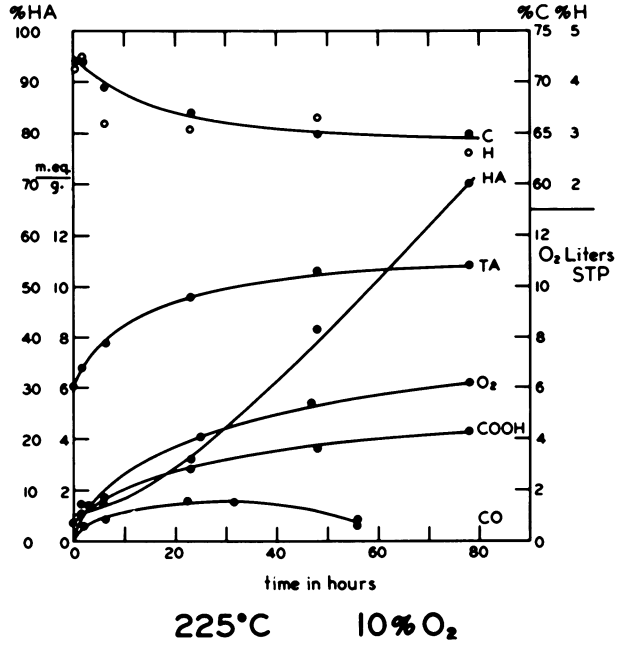

Figure 7

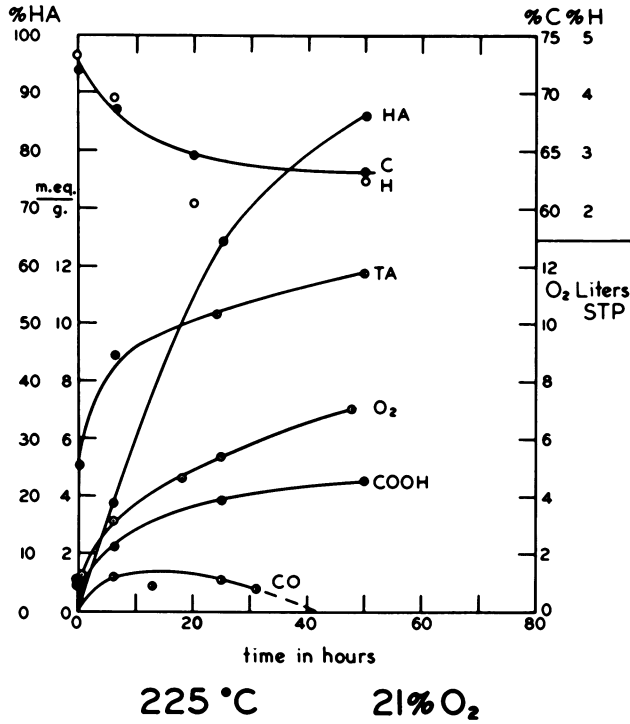

Figure 8

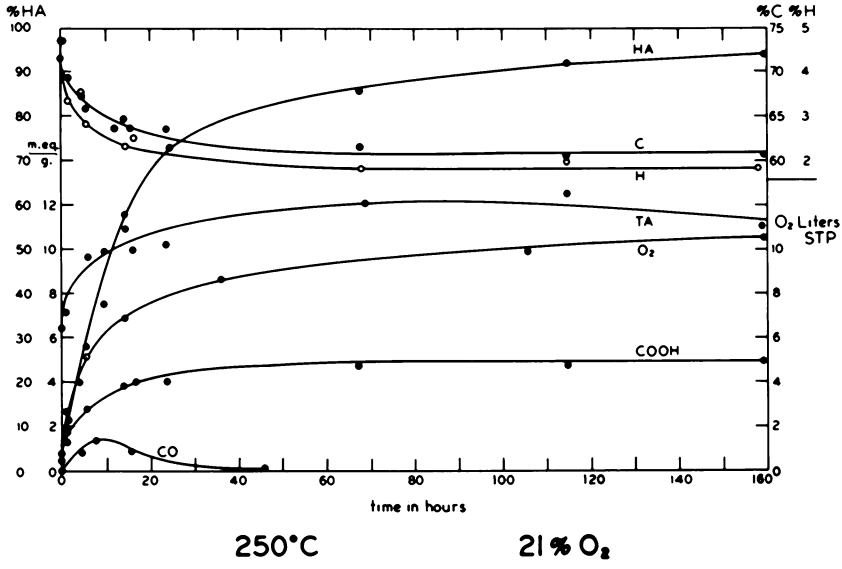

Figure 9

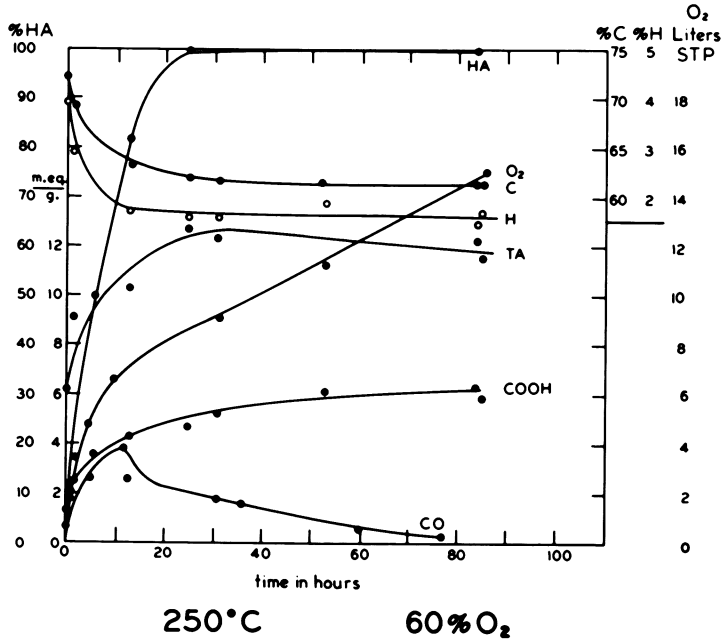

Figure 10

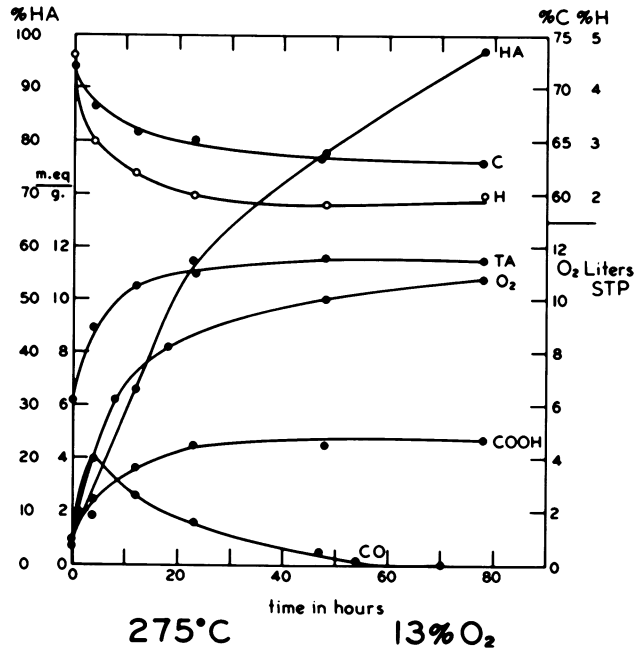

Figure 11

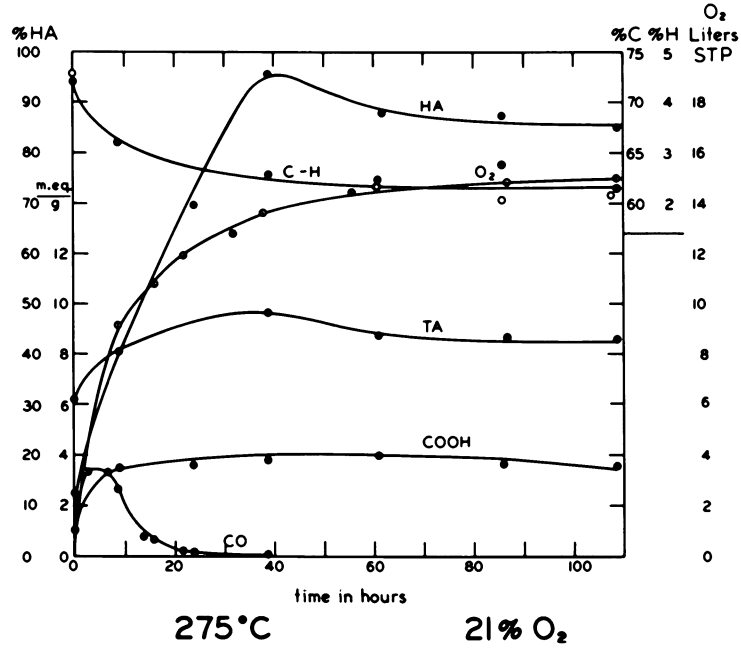

Figure 12

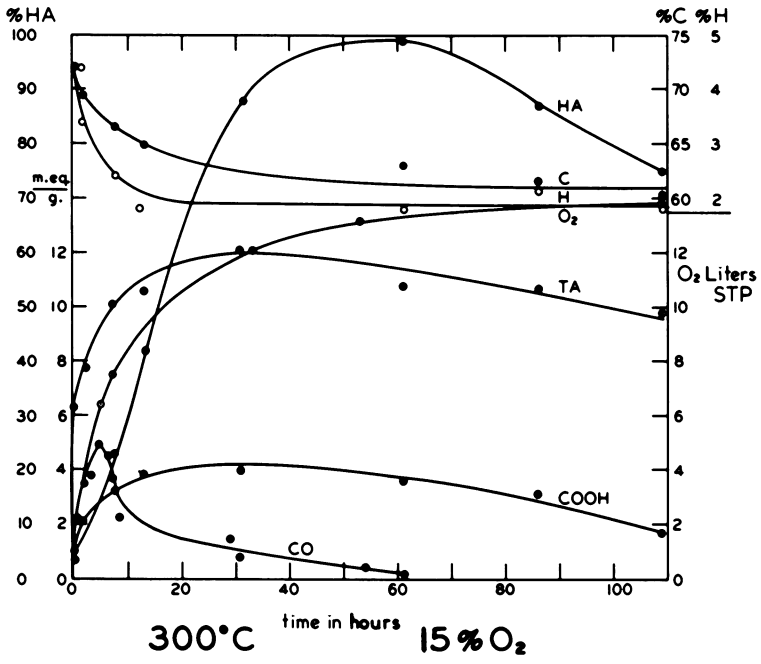

Figure 13

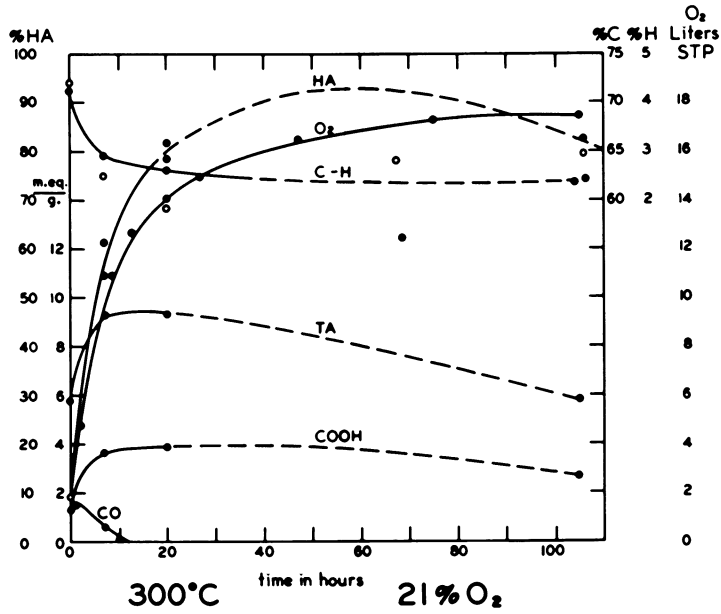

Figure 14

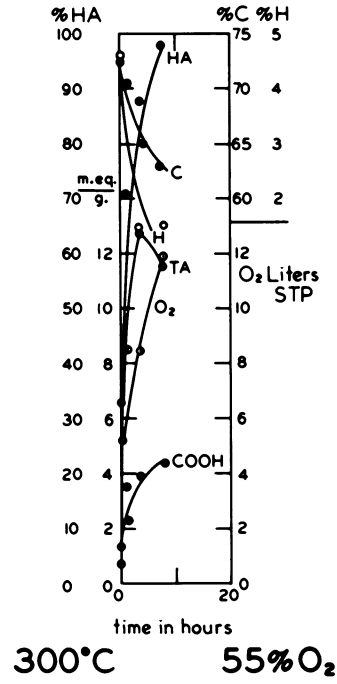

Figure 15

Publication Date: January 1, 1966 | doi: 10.1021/ba-1966-0055.ch039

losses. Figure 16 illustrates this by (estimated) weight loss curves which were calculated from the ash contents of coal samples withdrawn from the apparatus at various stages of reaction.

In sharp contrast to carbon dioxide, carbon monoxide—always a minor reaction product—followed a pattern which was fairly insensitive to reaction conditions: concentrations of carbon monoxide always rose to a peak value in the early stages of oxidation and then rapidly declined to zero.

One experiment not shown graphically is an oxidation reaction which was initiated at 300°C. and 100% oxygen but which led quickly to a violent run-away combustion reaction. This result is of interest only inasmuch as it delineates the upper limiting conditions for controlled oxidation of the coal here under test.

Discussion

Concurrent studies in these laboratories (*15*) indicate that humic acids heated to temperatures around 300°C. (or higher) will, even in the presence of oxygen, tend to lose their acidic functional groups and revert to an essentially coal-like material. In view of this and observations made in the course of the investigations reviewed here, the overall reactions occurring during dry oxidation of coal can be put in the form:

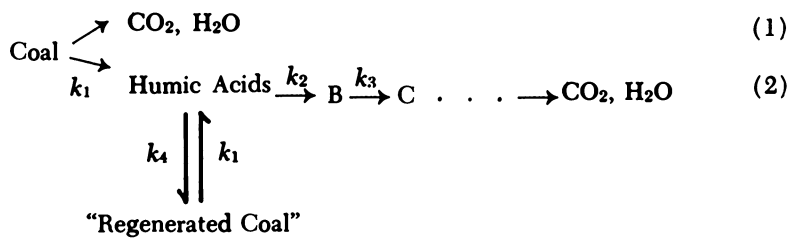

In this scheme, Reaction 1 represents a direct (pre-ignition) combustion reaction which may or may not be accompanied by formation of carbon monoxide; Reaction 2 describes the oxidation reaction (and its sequences) examined in the present study. B and C in Reaction 2 denote degradation products of humic acids (e.g. hymatomelanic, fulvic, and/or so-called water soluble coal acids), and k_1, k_2, etc. represent the corresponding rate constants.

Thus put, details of the individual reactions—which are, in any event, certain to be complex—remain as undetermined and debatable as before. What becomes clear (and consistent with experiment) is that (a): product gases such as carbon dioxide can form via two fundamentally unrelated paths; (b) humic acids can be abstracted by secondary degradation or by stripping reactions such as decarboxylation (i.e. by reactions respectively characterized by k_2, k_3, etc. and by k_4); (c) in a sequential reaction series such as Reaction 2, a zero rate of humic acid formation denotes establishment of a steady state condition rather than formation of a simple equilibrium of the type: coal$\rightleftarrows$ humic acids.

Table II.

Temp., °C.	*180*				*225*	
O_2 %	10	21	50	70	10	21
Coal, grams	15.00	15.10	15.00	15.00	15.00	15.04
O_2, grams	3.88	5.19	6.41	7.09	7.27	8.50
Input	18.88	20.29	21.41	22.09	22.27	23.54
Solids	13.86	14.22	13.91	13.35	12.69	.....
CO_2, grams	2.89	4.21	6.14	6.65	5.36	.....
H_2O, grams	1.82	1.81	1.64	1.18	3.39	3.21
Output	18.57	20.24	21.69	22.18	21.34	.....

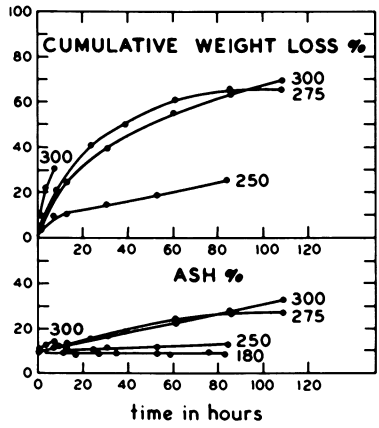

Figure 16. Cumulative weight loss during oxidation at various temperatures (calculated from ash contents of reacting coal). Numbers on each curve denote reaction temperatures

These matters offer a convenient frame of reference for examining two general facets of humic acid formation. The first concerns the influence of reaction conditions on k_1 and the velocities of the various "decay reactions." In each of the test runs forming a part of the present study, excess oxygen may be presumed to have been present, and since oxygen was always admitted to the reactor as fast as it was consumed, the effective oxygen concentration, [O], remained constant throughout each run. Nevertheless, the time to given percent conversion of coal into humic acids—or, more formally, the half-life—appears to depend on [O] as much as on the reaction temperature T, and two quasi-critical temperatures, which limit the practically useful reaction range, seem to exist. Below some temperature T' (in this case $\sim$ 150°C.) no significant conversion at any oxygen level occurs even though slow direct oxi-

Publication Date: January 1, 1966 | doi: 10.1021/ba-1966-0055.ch039

Material Balances

250		275		300		
21	60	13	21	15	21	55
15.02	15.00	15.00	15.00	15.00	15.00	15.03
12.38	13.83	12.77	17.70	16.36	20.56	13.95
27.40	28.83	27.77	32.30	31.36	35.56	28.98
9.40	9.83	9.71	7.34	6.67	4.06	8.90
13.60	12.77	10.85	22.85	18.10	24.05	15.17
3.19	5.13	5.71	3.41	6.47	7.00	6.72
26.19	27.73	26.27	33.60	31.24	35.11	30.79

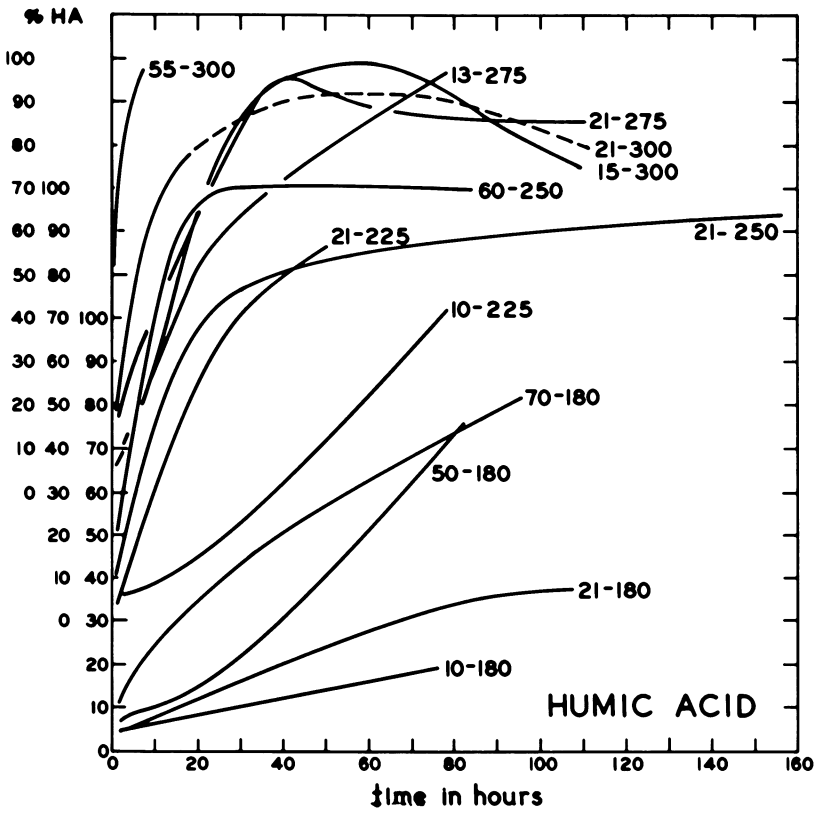

Figure 17. Composite of HA curves shown in Figures 3–15 (note offset ordinates). The first number on each curve denotes oxygen concentration; the second denotes the reaction temperature

dation to carbon monoxide, carbon dioxide, and water takes place. Above some temperature T'' (in this case ~ 300°C.) humic acids represent progressively less stable intermediates—i.e., $k_1 < k_2$, k_3, etc. (as well as $< k_4$), and the system comes, in the limit, to be dominated by combustion—i.e., by Reaction 1 rather than 2. Only when $T' < T < T''$ will the time to given percent conversion vary inversely with T.

Variations in the oxygen level [O] modify this pattern only to the extent that there is a *de facto* interchangeability between [O] and T (Figure 17). Thus, when $T - T'$ is small (e.g., at 180°C.), conversion rates remain low even when [O] assumes very large values. But at higher temperatures, a definite "overlap" becomes evident, with reaction conditions at one temperature and oxygen level effectively equivalent to those at a somewhat higher temperature and correspondingly reduced oxygen concentration. In other words, under near-optimum conditions for converting coal into humic acids, a system defined by T and [O] is roughly equivalent to another defined by $T - \Delta T$ and [O] + Δ[O]. However, as already mentioned, whenever rapid conversion occurs (whether because of high temperatures or high oxygen concentrations), there is also heavy loss of coal material to carbon dioxide and water. For example, even under optimum conditions appropriate for oxidizing

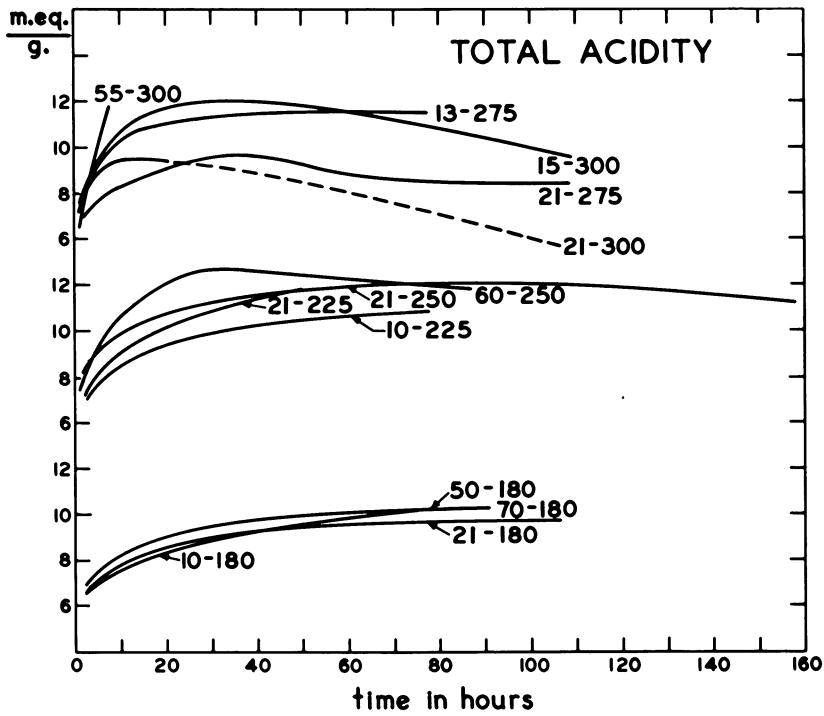

Figure 18. Composite of TA curves shown in Figures 3–15. The first number on each curve denotes oxygen concentration; the second denotes the reaction temperature

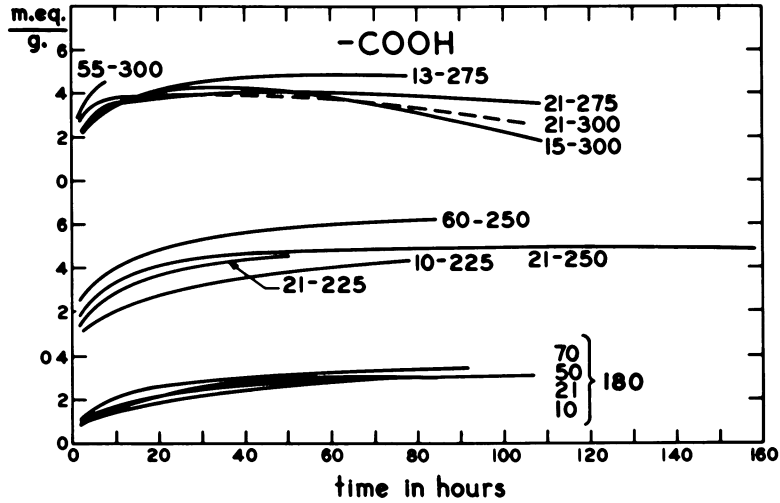

Figure 19. Composite of COOH curves shown in Figures 3–15. The first number on each curve denotes oxygen concentration; the second denotes the reaction temperature

the coal here under test—i.e., at T = 250°–275°C. and [O] $\sim$ 20%, when recoverable humic acids in the residual coal mass reach 80% after about 40 hours oxidation—about one-third of the original charge is lost.

The second point relates to the relationship between total acidity and alkali solubility of the oxidizing coal mass. A striking feature of graphs showing the variation of total acidity and carboxyl concentration with time (Figures 18 and 19) is that they are, even quantitatively, almost independent of reaction temperature and oxygen concentration. Thus, for the cases reviewed here, total acidity starts at about 6 meq. per gram (but negligible solubility in alkali) and then rises to a limit ($\sim$ 12 meq. per gram) which varies only very slightly with T and [O]. Only near the upper end of the useful reaction range—i.e., in the range 275°–300°C.—can a temperature effect (manifested as a poorly defined maximum along the time coordinate) be detected. The same is qualitatively true of the carboxyl concentrations.

If it is also recalled that alkali soluble material (humic acid) builds up much more slowly than acidity (and always markedly dependent on T and [O]), and that the distinctly acidic parent coal is effectively insoluble in alkali, it becomes evident that acidity and alkali solubility are not necessarily covariant, and that accepted definitions of "humic acid" are, chemically speaking entirely arbitrary. Under the conditions of this study the oxidation appears to involve two simultaneous but seemingly unrelated reactions which result in the development of acidity and in molecular (skeletal) breakdown, respectively, and this suggests that alkali solubility is mainly a consequence of degradation which is only coincidentally connected with the formation of acidic functional groups. Figure 20 illustrates this concept qualitatively and leads to the inference that the wide spread in molecular weights of humic acids reported

Publication Date: January 1, 1966 | doi: 10.1021/ba-1966-0055.ch039

in the literature may be quite real—i.e., depending on reaction conditions, an average molecular weight of, say, 600 may be as valid as one of 10,000.

In view of these considerations and the uncertainty surrounding details of the oxidation mechanism, attempts to give kinetic expression to directly measured humic acid concentrations are quite unjustified. In terms of Reaction 2, instantaneous humic acid concentrations will only reflect the momentary balance or imbalance between formative and destructive reactions—i.e., between k_1, on the one hand, and k_2, k_3, etc. on the other. Unless humic acids per se are

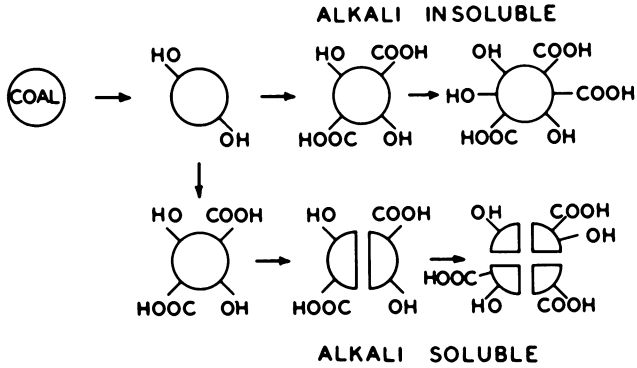

Figure 20. Skeletal breakdown during oxidation

much more sharply and unequivocally distinguished from their degradation products (such as hymatomelanic and fulvic acids), neither gravimetric nor colorimetric methods of determining humic acid concentrations can ever be expected to yield data for kinetic interpretation. In a sequential reaction such as 2, all solid degradation products of humic acid will be retained within the reactant mass and included in gravimetrically determined "humic acid contents." Further, since hymatomelanic acids and, to a lesser extent, fulvic acids are not much less intensely colored than humic acids (*3*), their presence in a product mixture extracted with aqueous alkali will also go largely undetected by colorimetric techniques. However, some useful comments about the mechanism of the coal → humic acid transformation can be made.

Two minor points worthy of note are: (a) formation of carbon dioxide and water at temperatures below *ca.* 300°C. appears, from the evidence of this study, to be caused mainly by Reaction 1—i.e., at such relatively low temperatures, Reaction 2 does not proceed significantly towards its ultimate conclusion; (b) abstraction of humic acids by stripping of functional groups—i.e., by reactions characterized by k_4, is likewise minimal at $T < 300$°C. (The fact that no observable "decay" of humic acids occurs during extended oxidation unless reaction temperatures approach 300°C. is, perhaps, a direct consequence of (a) and (b).)

It can also be reasonably concluded that skeletal breakdown during oxidation (cf. above and Figure 20) occurs primarily in the saturated alicyclic structures within the parent molecule. Thus, humic acids contain not only less

Publication Date: January 1, 1966 | doi: 10.1021/ba-1966-0055.ch039

aliphatic hydrogen than their parent coals, but they will also yield much less tar on pyrolysis. It is, however, possibly significant that not all hydroaromatic structures are eliminated during oxidation and that even some active methylene groups seem capable of surviving it (*10*).

Finally and most important, available evidence is beginning to allow us to delineate the peripheral changes induced by oxidation.

As early as 1940, B. V. Tronov (*13*) advanced (but did not further elaborate upon) a series of postulates which envisaged a reaction sequence beginning with formation of phenols and proceeding via quinones and acid anhydrides to carboxylic acids (Figure 21). One aspect of this series—the formation of phenols—was later qualitatively confirmed by G. R. Yohe *et al.* (*17*) who showed that oxygen uptake by low rank coals and the susceptibility of known phenols to oxidation could both be greatly reduced by methylation. However, more directly relevant in this context is our observation that comparatively large amounts of phenolic structures appear well before appreciable proportions of carboxylic acids can be detected. Concentrations of -COOH became significant only after the reaction had progressed for some time; oxidation after attaining a steady state condition did not alter the -COOH/-OH ratio (or the total acidity) even though evolution of carbon dioxide and water continued.

A second requirement of the Tronov postulates—formation of acid anhydrides—is met by evidence from infrared spectra of oxidized coal samples periodically withdrawn from the reactor. As a matter of experimental record, it should be observed that such anhydrides did not appear until the later stages of reaction, by which time -COOH concentrations were already quite high. However, since initial carboxyl formation probably occurs in aliphatic structures present in the parent coal (*9*), appearance of anhydrides after rather

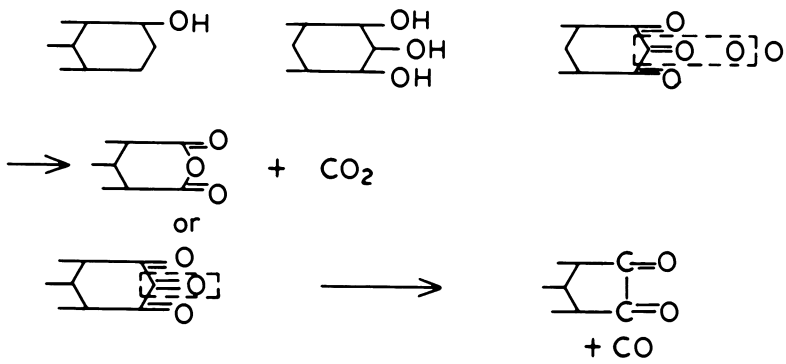

Figure 21. Coal oxidation (Tronov (13))

than before development of carboxylic acids does not necessarily conflict with the Tronov series. (There is, of course, some question of what proportion of anhydrides forms by simple dehydration of carboxylic acids. However, there are strong indications that they do not entirely form by this process: if an anhydride-bearing oxidized coal is hydrolyzed and then reheated in nitrogen

Publication Date: January 1, 1966 | doi: 10.1021/ba-1966-0055.ch039

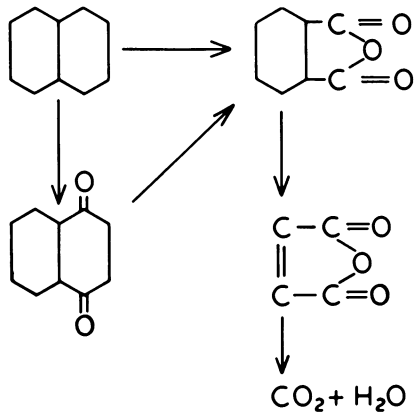

Figure 22. Naphthalene oxidation

to the temperatures which originally produced the anhydride, a material with greatly reduced anhydride and carboxyl concentration is obtained.)

Bearing in mind the generally accepted mechanism for commercially producing phthalic and maleic anhydrides by gas-phase oxidation of naphthalene (Figure 22), Tronov's postulates and the results of the present study could therefore, *prima facie*, be synthesized into a sequence (Figure 23) for which some fairly strong presumptive evidence can be adduced from previous studies in these laboratories (*11*, *16*). For example, while humic acids will react with hot acetic anhydride to produce materials whose infrared spectra show a very strong 1785 $cm.^{-1}$ band, this absorption can be markedly inhibited by methylating and hydrolyzing humic acids prior to reaction with acetic anhydride (*16*). The 1785 $cm.^{-1}$ band therefore was assigned mainly to esters, but it was pointed out that infrared absorption in this region is normally only shown by esters of polyfunctional phenols (such as gallic acid or pyrogallol). In support of this, it was further noted that the C—O stretching absorption of humic acids after reaction with acetic anhydride (1187 $cm.^{-1}$) corresponded very well with equivalent absorptions of triacetoxybenzene (at 1175 $cm.^{-1}$) and triacetoxybenzoic acid (at 1188 $cm.^{-1}$).

In a recent study S. E. Moschopedis (*11*) produced some direct evidence for the presence of quinones and hydroxyquinones in coal and humic acid, and infrared examination of products obtained in the course of the present investigation clearly indicated the existence of five-membered cyclic anhydrides in the reactant mixtures.

No matter how the oxidation process is now formulated (or how it may ultimately come to be described), there can be no doubt that humic acids per se represent relatively unstable solids which are generally as susceptible to oxidation and decomposition as the parent coal and which will also undergo almost continuous changes in functionality. This is perhaps best demonstrated by one experiment in which the coal was oxidized for some 400 hours after

Publication Date: January 1, 1966 | doi: 10.1021/ba-1966-0055.ch039

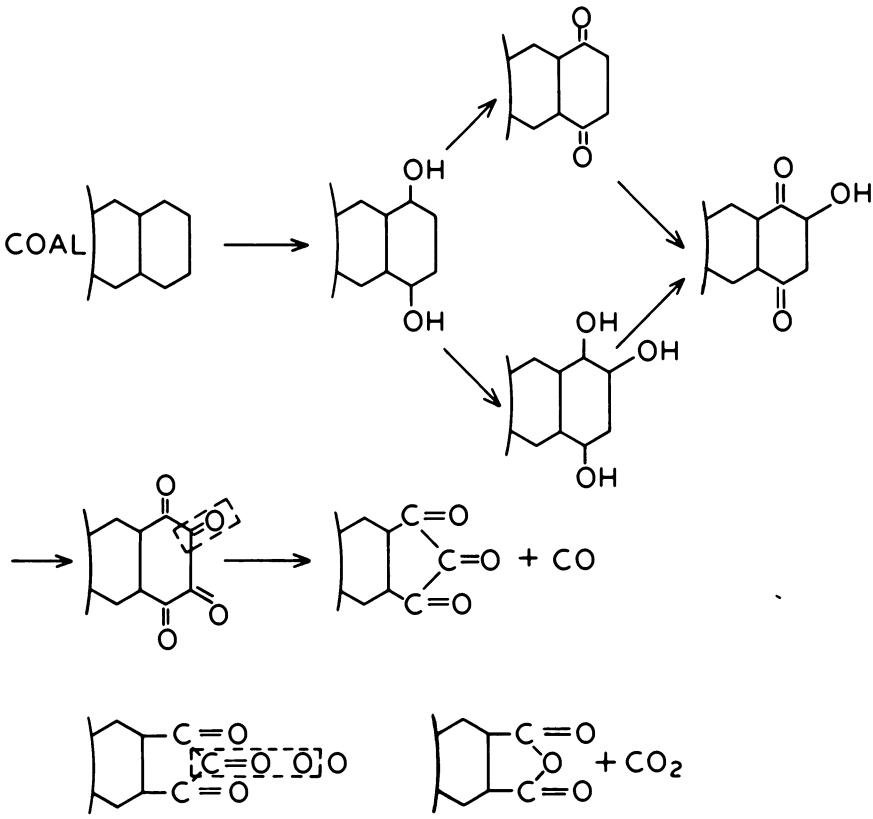

Figure 23. Coal oxidation

a steady state was attained. While oxygen was continuously consumed throughout this period and there was a correspondingly steady evolution of carbon dioxide and water, samples taken from the reactor showed no significant changes except in ash contents (which rose progressively). In the light of this observation and of the data shown in Figures 3–15, we consider that oxidation of coal under the conditions of the present study will always lead to establishment of a steady state (unless $k_2 > k_1$), but that there is never, as some have suggested (*12*), actual termination of oxidation by saturation of oxidation sites.

Acknowledgments

We are greatly indebted to J. F. Fryer for the many analyses and humic acid determinations which were required for this study, and we would also like to than R. A. S. Brown for some helpful discussions and his assistance in compiling the experimental results.

Literature Cited

(1) Brooks, J. D., Sternhell, S., *Australian J. Appl. Sci.* **8** (1957) 206.
(2) Flaig, W., ADVAN. CHEM. SER. No. **55**, 58 (1966).
(3) Francis, W., "Coal," p. 205, Edward Arnold Ltd., London, 1961.
(4) Inukai, Toyoharu, *J. Fuel Soc. Japan* **35**, 301 (1956); *C.A.* **50**, 17383 d (1956). (see also: Council of Scientific & Industrial Research. Central Fuel Research Institute; Report of Director for the Year 1955–56 (p. 34) April 1956, Jealgora, India and *Chem. Eng.* **69**, No. 1, 38 (1962))
(5) Jameson, R., "Outline of the Mineralogy of the Shetland Islands," p. 202, Edinburgh, 1798.
(6) Klaproth, A., *Gehlen's J.* **4**, 329 (1804).
(7) Kreulen, D. J. W., "Elements of Coal Chemistry," p. 61, Nijgh & Van Ditmar, N.V., Rotterdam, 1948.
(8) Lynch, B. M., Brooks, J. D., Durie, R. A., Sternhell, S., *Sci. Proc. Roy. Dublin Soc., Ser. A*, **1**, No. 4, 123 (1960).
(9) Mazumdar, B. K., Anand, K. S., Roy, S. N., Lahiri, A., *Brennstoff-Chem.* **38**, 305 (1957).
(10) Moschopedis, S. E., Wood, J. C., Fryer, J. F., Elofson, R. M., *Fuel* **43**, 289 (1964).
(11) Moschopedis, S. E., *Fuel* **41**, 425 (1962).
(12) Oreshko, V. F., *Izvest. Akad. Nauk S.S.S.R., Otdel. Tekh. Nauk* **1949**, 249 (*C.A.* **44**, 2200i); *Ibid.* **1949**, 748 (*C.A.* **44**, 2201f); *Ibid.* **1949**, 1642 (*C.A.* **44**, 2202e).
(13) Tronov, B. V., *J. Appl. Chem. (U.S.S.R.)* **13**, 1053 (1940); *C.A.* **35**, 1966.
(14) Vauquelin, C., *Ann. Chim.* **21**, 39 (1797).
(15) Wood, J. C., unpublished work.
(16) Wood, J. C., Moschopedis, S. E., and der Hertog, W., *Fuel* **40**, 491 (1961).

RECEIVED October 5, 1964.

Discussion

Bhupendra K. Mazumdar. The authors believe that there is a critical temperature below which humic acid is not formed to any significant extent. This is surprising. Would Dr. Berkowitz indicate roughly what this temperature is?

In our experience at all temperatures oxidation would lead to the formation of humic acids; of course, it is a question of time at lower temperatures.

Norbert Berkowitz. Mazumdar and his colleagues state that they obtained substantial conversions of coal into humic acids at appreciably lower temperatures than the lower limit (*ca.* 150°C.) which we imposed on the "useful reaction range." Coal characteristics may well play an important part in determining the useful reaction range. However, I feel that the Indian data may be partly unreal owing to the analytical procedures used to determine humic acid contents in oxidized coal samples; in particular, Mazumdar *et al.* used extended extraction with rather strong aqueous alkali and therefore, since there is very marked oxidation of the coal *during* such extraction, their observed humic acid yields may reflect not what was produced during the controlled oxidation at > 100°C., but rather what was produced during oxidation at > 100°C., *plus* humic acids formed during extraction.

Gases from Flash and Laser Irradiation of Coal

A. G. SHARKEY, JR., J. L. SHULTZ, and R. A. FRIEDEL

U.S. Department of the Interior, Bureau of Mines, Pittsburgh Coal Research Center, Pittsburgh, Pa.

Publication Date: January 1, 1966 | doi: 10.1021/ba-1966-0055.ch040

Gases from the flash and laser irradiation of Pittsburgh seam (hvab) coal were investigated to determine the action of high temperatures on coal. Temperatures in excess of 1000°C. were reached with both types of irradiation. Craters about 300 microns in diameter were produced in the coal with millisecond pulses from the laser unit rated at 1.7 joules output. Gaseous products from the laser and flash irradiations showed 21% and 8% acetylene, respectively. Diacetylene, vinylacetylene, and other products to molecular weight 130 were indicated in the mass spectrum of the gas from the laser study. The results indicated that the distributions of products obtained from the flash and laser irradiations of coal were different from that produced in high temperature carbonization.

In a previous investigation at the Pittsburgh Coal Research Center of the Bureau of Mines it was shown that the distribution of gaseous products produced by the flash irradiation of coal is different from that obtained by high temperature carbonization (*2*). Rau and Seglin have described a similar investigation which also included a study of the change in gas composition with the rank of the coal (*4*). Bond and co-workers reported on the production of acetylene from coal using a plasma jet (*1*). In all of these studies with the high temperature, rapid irradiation of coal, only a solid residue and gases were produced in detectable quantities.

Laser techniques can be used to produce extreme temperatures for short durations, possibly as high as several thousand degrees centigrade. Honig and Woolston described a combined laser mass spectrographic technique to study laser-induced emission from solids (*3*).

In Coal Science; Given, P.;
Advances in Chemistry; American Chemical Society: Washington, DC, 1966.

Experimental

Figure 1 shows the experimental arrangement used in the present study of the flash and laser irradiation of coal. For the flash irradiations the ruby rod and lens were removed. The sample tube was placed in the position shown for the rod. Energy from a 4000-joule supply was discharged through a xenon lamp for the flash irradiations of about 1 msec. duration. A thin section of coal as shown in Figure 1, a ⅜-inch cube, or in some instances about 150 mg. of through-200 mesh coal, was placed in a sample tube ½-inch in diameter and 6 inches long. The tubes were evacuated and sealed and, for experiments with ground coal, were rotated to deposit as much sample as possible on the inner surface of the tubes in the direct path of the energy. A ruby crystal with an output of about 1.7 joules at 6943A. was used for most of the laser studies.

Publication Date: January 1, 1966 | doi: 10.1021/ba-1966-0055.ch040

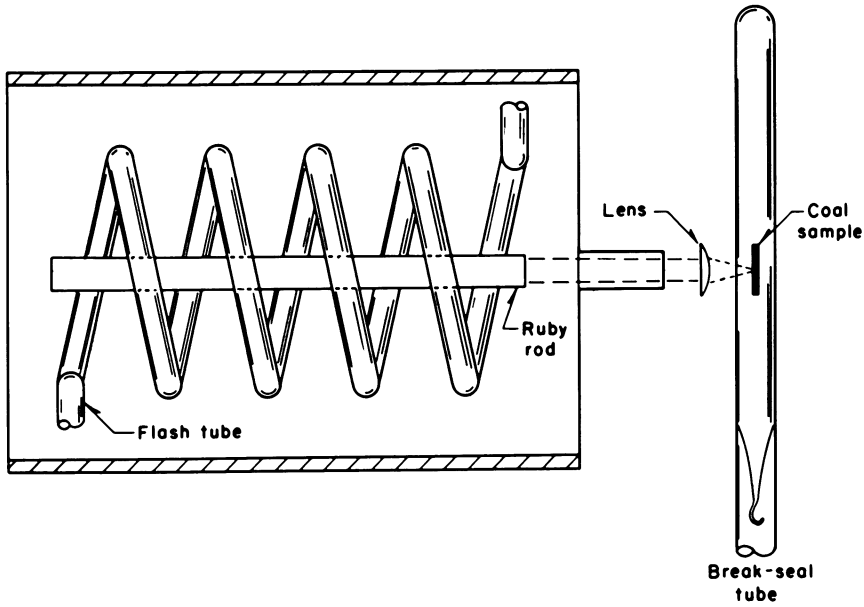

Figure 1. Optical laser head

A unit capable of producing higher energies was used for the 8- and 10-joule experiments. Gases produced by the flash and laser irradiations were analyzed by mass spectrometry after fractionation using the following baths: liquid nitrogen, dry ice, ice water, water at room temperature, and water at 60°C.

Results

Figure 2 shows that craters about 300 microns in diameter were produced using focused energy from the 1.7-joule source. It should be noted that there was evidence of carbonization at the periphery of the craters. Figure 3 shows a replica of the crater produced using laser energy of about 8 joules. From this replica the depth was found to be about one-half the diameter.

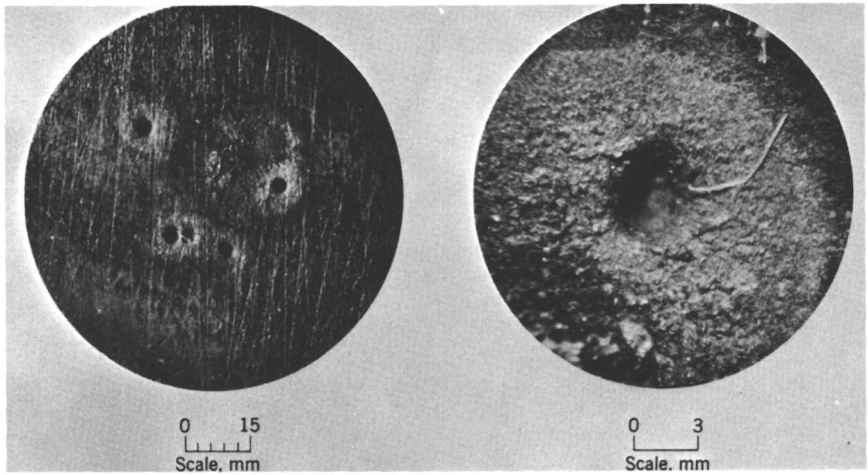

Figure 2. Laser irradiation of Pittsburgh seam (hvab) coal, 84% carbon; section 0.9 mm. thick

An attempt was made to use the volume of the craters to estimate the amount of coal irradiated and to relate this amount of coal to the gaseous product. It was difficult to determine the actual amount of material exposed to the laser beam. Some of the gas was probably produced in the peripheral region of the craters, and also there is evidence that a portion of the sample was simply "blown" from the crater. The yield of gaseous product based on the crater volume is given in Table I.

Total gaseous products obtained by combining data from the five fractions are shown in Table I as well as the analysis of gas from a typical 900°C. car-

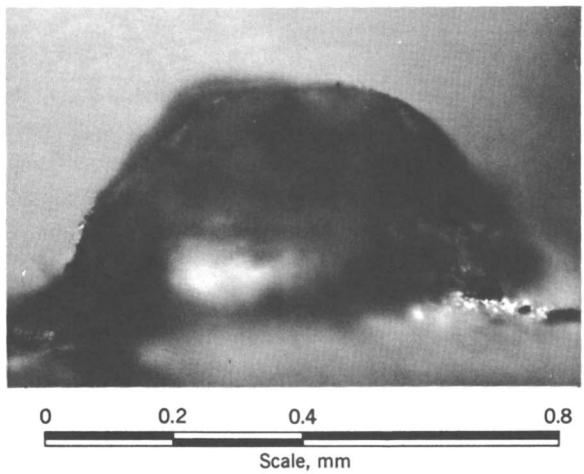

Figure 3. Replica of crater produced by laser irradiation of Pittsburgh seam (hvab) coal

Publication Date: January 1, 1966 | doi: 10.1021/ba-1966-0055.ch040

bonization of coal. The maximum temperature reached by the coal could not be determined but was estimated to be greater than 1000°C. with both types of irradiation. Thermodynamically, acetylene is favored as a product in high temperature pyrolysis of hydrocarbons. A higher percentage of acetylene was obtained with the laser irradiations than with the flash, probably indicative of a higher temperature in these experiments.

Table I. Gaseous Products from Laser and Flash Irradiations and High Temperature Carbonization of Pittsburgh Seam (hvab) Coal

	Mole Percent, H_2O Free Analysis		
Energy Source and/or Treatment	*Ruby Laser (~ 1.7 joule output)*	*Xenon Lamp (~ 4000 joule input)*	*Carbonization at 900°C.*
Components			
H_2	45.4	69.2	55.6
CO	14.4	16.1	7.4
CH_4	4.8	4.1	31.5
C_2H_2	20.9	7.8	0.05 (max.)
C_2H_4	4.9	0.05 (max.)	3.4
C_2H_6	0.6	0.1	1.2
HCN	1.4	1.7	—
CO_2	2.0	0.5	0.4
Σ Hydrocarbons above C_2	5.6	0.4	0.5
Above gases as weight percent of coal	[a] 60.0	[b] 18.0	[c] 15.0

[a] Estimation based on volume of craters in surface following irradiation.
[b] Estimated from weight of coal on inner surface of tube—*see* text.
[c] Carbonization product supplied by J. G. Walters, Bureau of Mines, Pittsburgh Coal Research Center.

Comparing gases from the flash irradiation and the high temperature carbonization of coal confirms previously reported results that flash irradiation produces gas richer in acetylene, carbon monoxide, and hydrogen and poorer in methane and C_2 hydrocarbons other than acetylene (*2*). In addition hydrogen cyanide was observed in the gas from the flash irradiation. Hydrogen cyanide was also found in the previous investigation of the flash irradiation of coal by the Bureau of Mines although it was not reported by Rau and Seglin (*4*). Based on an estimate of 11 mg. of powdered coal being flash irradiated, the gaseous product (exclusive of water) amounted to about 18% of the coal irradiated.

Gas from the laser irradiation showed higher percentages of acetylene, ethylene, and C_3 and higher hydrocarbons than gas from the 900°C. carbonization or from the flash irradiation. Approximately the same percentages of

Publication Date: January 1, 1966 | doi: 10.1021/ba-1966-0055.ch040

methane and carbon monoxide were produced in the flash and laser irradiations. As shown in Table II, components with molecular weights up to 130 were found in the gas from the laser irradiation. Diacetylene and vinylacetylene, recognized as pyrolysis products of acetylene, accounted for 2.4% of the product. The decrease in the percentage of hydrogen, relative to the product

Table II. Hydrocarbons in Gaseous Product from Laser Irradiation of Pittsburgh Seam (hvab) Coal

Molecular Weight	*Compound(s)*	*Mole Percent*
40	Methylacetylene (propyne)	0.6
42	Propylene (propene)	0.7
44	Propane	0.2
50	Diacetylene (butadiyne)	1.9
52	Vinylacetylene (butenyne)	0.5
54	Butadiene; butyne	0.2
56	Butene	0.2
66	Pentenyne	0.1
68	Pentyne; pentadiene	0.1
76	—	0.1 (est.)
78	Hexadiyne	0.1
78, 92	Benzene; toluene	0.2
40–130	Unidentified material[a]	0.7 (est.)
	Total	5.6

[a] Includes trace peaks at masses 116 and 128 corresponding to indene and naphthalene, respectively.

from the flash irradiation, is possibly related to the increase in partially saturated structures such as ethylene and propylene. In the pyrolysis of vinylacetylene at 700°C., Stehling, Frazee, and Anderson observed increases in acetylene, ethylene, ethane, and methane when hydrogen was added (5). Based on the volume of the craters it is estimated that 60% of the coal irradiated produced gaseous product.

As another phase of this investigation single experiments were conducted in which the energy of the irradiation, particle size of the coal, and atmosphere were varied. One experiment was conducted with micronized coal—coal with particle sizes less than 10 microns—coating the inside of the tube. A second experiment, using a cube of coal, was conducted with a unit having an output of up to 10 joules of energy per burst. A third experiment was conducted in a helium atmosphere at 20 mm. pressure rather than in vacuum. Gaseous products were studied using the same experimental technique described previously. Product from the irradiation of the cube of coal with 5 bursts of 1.7 joules energy is considered the standard for this series of tests.

Table III shows that gaseous product from the irradiation of less than 10 micron coal (micronized) showed higher methane and lower acetylene than coal from the cube. Other particle sizes will have to be investigated to determine if particle size is a parameter for maximum acetylene production.

In Coal Science; Gorin, E., et al.;
Advances in Chemistry; American Chemical Society: Washington, DC, 1966.

Publication Date: January 1, 1966 | doi: 10.1021/ba-1966-0055.ch040

Table III. Gaseous Products from Laser Irradiation of Pittsburgh Seam Coal[a]

Sample form	*Cube*	*Micronized*	*Cube*	*Cube*
Joules	*1.7*	*1.7*	*10*	*1.7*
Atmosphere	*Vacuum*	*Vacuum*	*Vacuum*	*Helium*
Number of shots	*5*	*5*	*5*	*5*
Hydrogen	46.5	46.0	42.8	30.7
Carbon monoxide	17.9	22.9	26.0	13.2
Carbon dioxide	12.3	7.6	2.6	23.5
Methane	5.2	7.3	1.1	10.5
Acetylene	16.1	9.4	25.9	6.2
Ethylene	—	0.6	0.6	7.9
Ethane	0.1	1.0	0.03	1.9
Methylacetylene	0.3	—	0.03	—
Diacetylene	0.4	0.5	0.8	0.2
Hydrogen cyanide	1.2	2.4	0.1	0.2
Σ Other hydrocarbons above C_2	—	2.3	—	5.7

[a] Mole percent

Table IV. Hydrocarbons Produced by Laser Irradiation of Pittsburgh Seam Coal in Vacuum[a]

Gaseous hydrocarbons	*Mole percent*
Acetylene	90.9
Methane	3.9
Diacetylene	2.8
Ethylene	2.1
Methylacetylene	0.2
Ethane	0.1

[a] Energy—10 joules

The highest acetylene content observed in our studies was 25.9%. This value was found for the experiment in which 5 bursts of 10 joules energy were used to irradiate a cube of coal (Table III). The distribution of the hydrocarbons obtained in this experiment is given in Table IV, showing that acetylene accounted for approximately 91% of the hydrocarbon product.

Another experiment was conducted under the same conditions as the standard except that 20 mm. of helium was introduced rather than having the sample tube evacuated. The purpose was to determine if the inert helium gas would absorb some of the energy associated with the products and reduce secondary thermal effects. As shown in Table III, relative to the standard, the gaseous product showed higher methane, lower acetylene, and more saturation in the higher hydrocarbons, indicative of lower temperature. It is interesting that even though the distributions of the C_2 products, acetylene, ethylene, and ethane are different for the standard and the experiment with the helium atmosphere, the total C_2 product is approximately the same—namely, 18.6% for the standard and 16.0%.for the irradiation with the helium atmosphere.

Publication Date: January 1, 1966 | doi: 10.1021/ba-1966-0055.ch040

Conclusions

The conclusions that can be drawn from this study of the irradiation of hvab coal under extreme temperatures are:

(1) The products are gaseous and essentially a char with little evidence for the formation of liquids or tarry components.
(2) The percent of vaporization is high, probably in excess of 60%, using focused energy from a 2- to 10-joule source.
(3) The products obtained using high energy for milliseconds are different from products produced by conventional pyrolysis at moderate temperatures for minutes or hours. The gaseous products are richer in unsaturates with acetylene predominating.
(4) The distribution of products appears to be a function of energy of irradiation, atmosphere, and probably particle size of the sample.
(5) While the high energy, short duration irradiation of coal produced a simple mixture of low molecular weight gases, it gave little information concerning the chemical structure of coal.

Acknowledgments

The flash irradiations were performed at the B. F. Goodrich Research Center and the laser irradiations at Westinghouse Research Laboratories.

Literature Cited

(1) Bond, R. L., Galbraith, I. F., Ladner, W. R., McConnell, G. I. T., *Nature* **200,** 1313 (1963).
(2) Hawk, C. O., Schlesinger, M. D., Hiteshue, R. A., Bureau of Mines Rept. Investigation **6264** (1963).
(3) Honig, R. E., Woolston, J. R., *Appl. Phys. Letters* **2,** 138 (1963).
(4) Rau, E., Seglin, L., *Fuel* **43,** 147 (1964).
(5) Stehling, F. C., Frazee, J. D., Anderson, R. C., "Proceedings of the Eighth Symposium on Combustion," Williams and Wilkens Co., Baltimore, 1962.

RECEIVED October 5, 1964.

41

Reaction of Coals under Conditions of High Energy Input and High Temperature

R. L. BOND, W. R. LADNER, and G. I. T. McCONNELL

The British Coal Utilisation Research Association, Leatherhead, Surrey, England

Publication Date: January 1, 1966 | doi: 10.1021/ba-1966-0055.ch041

The reaction of coal in an argon plasma jet produces gas and soot, with an absence of tar. The main gaseous products are hydrogen, acetylene, and carbon monoxide. The reaction depends strongly on the rank and particle size of the coal, the extent of the reaction being greatest for high volatile coals of particle diameter less than 50μ; an anthracite shows negligible reaction. For a coal of 36% volatile matter, fed at 0.3 gram/min. into an argon plasma, acetylene represents over 95% of the hydrocarbons formed, corresponding to a 20% conversion of the carbon in the coal to acetylene. Conversion to acetylene is increased to 40% on adding hydrogen to the plasma; adding nitrogen produces hydrogen cyanide.

Treating coals at very high temperatures yields products that are quite different from those obtained by conventional carbonization processes (*10*). High temperature treatment followed by rapid cooling of the products produces appreciable quantities of unsaturated hydrocarbons, particularly acetylene.

Thermodynamic data on hydrocarbons show that at temperatures above 1300°C. ethylene, acetylene, and carbon are more stable than methane or other saturated hydrocarbons; however, although data of this kind will indicate the species likely to be formed at high temperatures, the amounts of unsaturated hydrocarbons and carbon produced will depend on the rates of the reactions involved and on the temperature cycle used.

The rates of heating and cooling associated with electric arcs are especially favorable for reactions which require rapid heating followed by quenching. For example, an arc process has been particularly successful for producing, on an industrial scale, acetylene from hydrocarbons (*2*). Brief references have been made in some of the early arc work to using coal as the raw material (*6*, *7*, *14*).

In Coal Science; Given, P.;
Advances in Chemistry; American Chemical Society: Washington, DC, 1966.

In recent years there has been renewed interest in treating coal at high temperatures both by rapid processing in the more conventional type of carbonization apparatus (*1*) and by using such devices as flash tubes (*5, 12, 13*), lasers (*13*), arc image furnaces (*9, 11*), and plasma jets (*3*). All these methods produce conditions whereby the coal can be heated rapidly to a temperature well in excess of 1000°C. followed by quenching of the products. The work described here is an investigation into the reactions of coal in a plasma jet and has been reported briefly elsewhere (*3*).

Experimental

Apparatus. PLASMA JET. A section of the plasma arc gun is shown in Figure 1. A direct current arc was struck between the thoriated tungsten rod, which acted as the cathode, and the copper tube anode. Both electrodes were

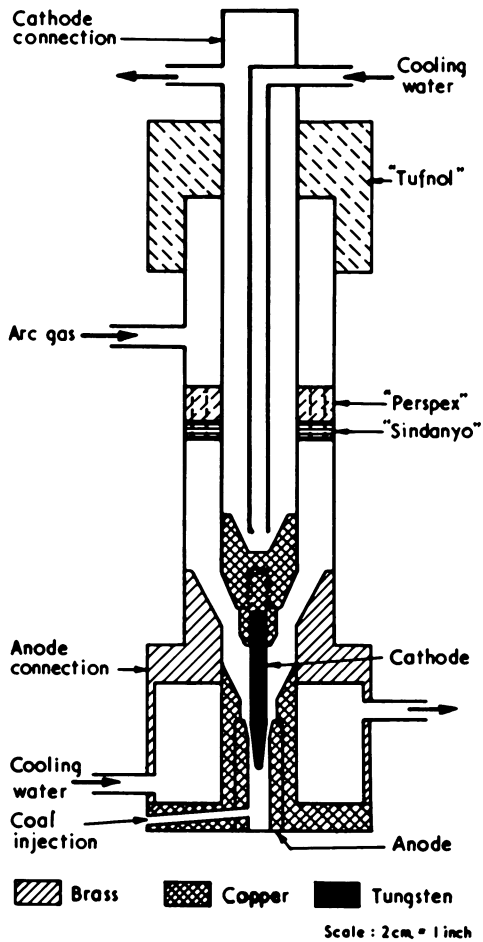

Figure 1. Section of plasma arc gun

Publication Date: January 1, 1966 | doi: 10.1021/ba-1966-0055.ch041

water cooled. The arc gas (argon, hydrogen, or nitrogen) was passed through the electrode space at flow rates varying between 5 and 20 liters/min. On striking the arc by means of a high frequency discharge, a cone of hot gas 2–3 cm. long was produced at the orifice in the anode. Temperatures at the center of this cone were estimated to be between 10,000° and 15,000°C., falling to about 4000°C. at the edge. At gas flow rates of 15 liters/min. or more, the plasma gases mixed rapidly with the surrounding atmosphere, resulting in extremely quick quenching of the hot gases leaving the jet. Reducing the gas flow to about 7.5 liters/min. produced a condition of laminar flow, which gave rise to a much longer zone of hot gas.

Power. Direct current for the arc was supplied from one of two generators—either a rotary welding generator, having an open circuit voltage of 80 volts and giving currents up to 300 amp. or a plasma arc generator with continuously variable power settings at either 185 or 320 volts open circuit and currents up to 350 amp. The current-voltage characteristics of both generators were such that the output terminals could be short circuited without damaging the generator.

The open circuit voltage necessary to maintain a stable plasma varies with the nature of the arc gas; this voltage is lowest for pure argon and highest for pure hydrogen. The operating voltages and currents for the various gases are given in Table I.

Table I. Plasma Operating Voltages and Currents

Gas	*Operating Voltage, volts*	*Operating Current, amp.*	*Input Power, kw.*
Argon	16–20	280–300	4.5–6.0
90% Argon 10% Hydrogen	25–30	275–285	6.9–8.6
90% Argon 10% Nitrogen	25–27	277–282	6.9–7.6
Nitrogen	48–50	260–270	12.5–13.5
90% Nitrogen 10% Hydrogen	45	265	11.9

The energy supplied mainly heats the plasma gas and the cooling water supplied to the electrodes; some of the energy is lost as radiation although this is usually less than about 5%. The proportion of electrical energy lost to the cooling water varies considerably according to the design and operation of the plasma jet (*8*) and can be between 30 and 70%. This has not been measured in the present work.

Method. Coal Injection. The coal was injected into the plasma by suspending it in a stream of argon (or nitrogen with the 100% nitrogen plasma) using the fluidized bed shown in Figure 2. The rate of coal feed was adjusted by varying the proportion of gas passing through the coal bed. This method gave a reasonably even coal feed although the fluidizer tended to feed selectively the fine particles into the plasma and to retain the coarser particles within the bed. The total gas flow through the hole in the anode was held constant at 2 liters/min.

Initially the coal-argon stream was fed with the main gas flow supplying the jet. However, the coal particles then had to pass the cathode (whose tip

Publication Date: January 1, 1966 | doi: 10.1021/ba-1966-0055.ch041

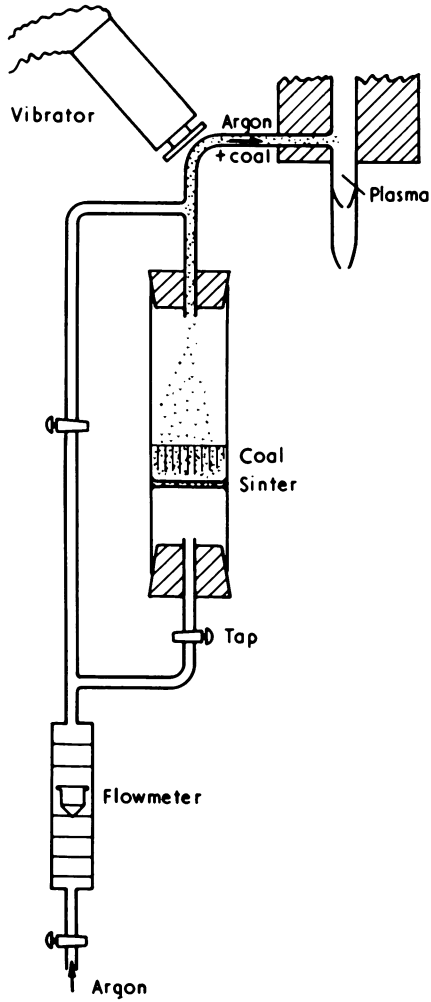

Figure 2. Coal injection

reaches its melting point during operation of the arc) causing severe erosion. The injection method adopted was to feed the coal through a small hole drilled radially in the anode (Figure 1). This prevented the coal particles from coming into contact with the cathode and greatly reduced electrode erosion.

Gas Collection. The plasma jet was enclosed in a metal container fitted to the underside of the jet assembly by means of a large water cooled brass flange. The container, shown in Figure 3, was 2 ft. long, 6 inches in diameter and was fitted with windows for viewing the jet. The gases, after leaving the arc, passed through the water cooled extension tube, cooled rapidly within the metal chamber, and were then led away for sampling and collection. A filter was incorporated between the trap at the bottom of the metal chamber and the collecting vessel to prevent carry-over of the soot, which collected mainly on the inside walls of the cooling chamber and in the trap.

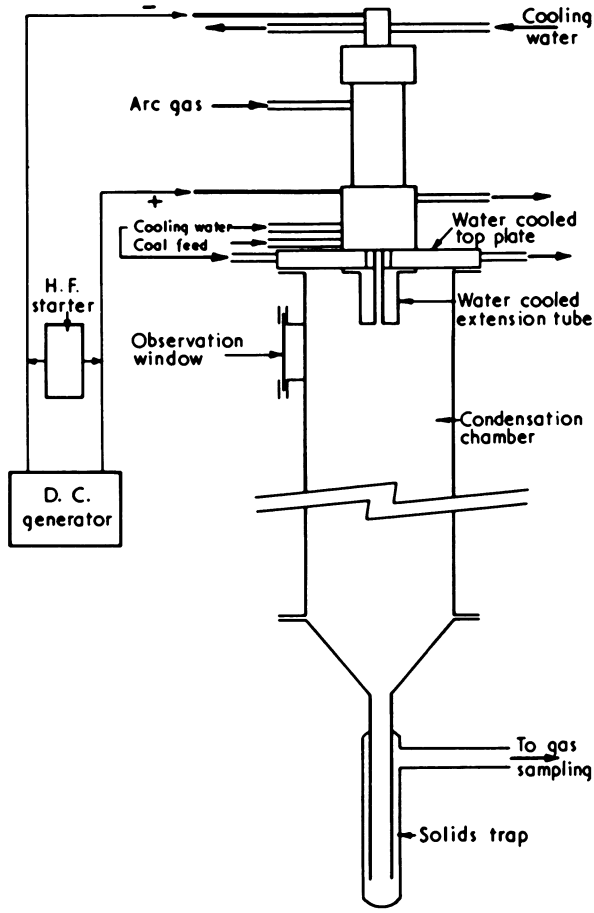

Figure 3. High temperature reaction apparatus

The total gas sample during an experiment, usually between 100 and 200 liters, was collected in a bag made from a roll of Polythene tubing sealed at each end and fitted with an inlet nozzle. The Polythene tube, when lying flat, was 1 ft. wide, and when it was filled with 100 liters of gas at atmospheric pressure, it produced a cylindrical bag about 10 ft. long. Only a very small pressure difference was required between the inside and the outside of the bag for filling and emptying.

"Average" gas samples were also taken from the gas leaving the metal container by sucking gas from the main stream into a gas sampling bottle (200 ml.) at a steady rate throughout an experiment.

Gas Analysis. Most of the analyses were carried out either on the "average" sample taken during an experiment or on a sample extracted from the total gas sample. Some spot samples were also taken to investigate the variation in composition during an experiment. The gas analyses were carried out mainly using either gas chromatographic or infrared methods, but in some cases the

Publication Date: January 1, 1966 | doi: 10.1021/ba-1966-0055.ch041

total quantity of acetylene was determined by a wet chemical method to check the procedure.

Gas Chromatography. The concentrations of the hydrocarbons were determined using a 2-ft., 6-inch alumina-silicone oil column with nitrogen as the carrier gas and a flame ionization detector. Hydrogen, oxygen, nitrogen, and carbon monoxide were determined using a column packed with molecular sieve 13X and argon as carrier gas. The detector was a katharometer. Carbon dioxide was determined using a silica gel column and a katharometer detector.

Infrared. The measurements were carried out with a Unicam SP100 spectrophotometer using a 10-cm. gas cell. The concentration of acetylene was estimated by measuring the optical density of the absorption band at 729 $cm.^{-1}$ and that of hydrogen cyanide from the optical density of the absorption band at 712 $cm.^{-1}$

Chemical. To check against the possibility of errors either in the sampling procedure or in the value taken for the total volume of gas passed through the arc, the total amount of acetylene produced was estimated by a wet chemical method. The total volume of gas collected in the Polythene bag was used for this analysis. Acetylene determination was made using potassium mercuric iodide, dissolved in potassium iodide, in the presence of sodium hydroxide.

$$C_2H_2 + K_2HgI_4 + 2NaOH \rightarrow C_2Hg + 2KI + 2NaI + 2H_2O$$

The precipitation of mercuric acetylide resulted in alkali consumption so that titrating the excess hydroxide gave a direct measure of the amount of acetylide and hence the concentration of acetylene in the gas mixture. The more usual method, precipitating silver acetylide from ammoniacal silver nitrate, was unsatisfactory in this case since the carbon monoxide in the product gases reduced the silver nitrate to silver.

Materials. Analyses. The coal analyses are given in Table II; both black durain and cannel coals are rich in sporinite material while the remainder are highly vitrainous. Two experiments were also carried out with material other than coal; one with Neospectra carbon black and the other with a soot residue formed by the reaction of coal (CRC 802) in the plasma. The analysis (% daf basis) of the Neospectra carbon black was as follows: C, 92.0; H, 0.8; N, 0.05; O by difference, 7.2; volatile matter, 9.2. All the materials were vacuum dried at 110°C. for several hours prior to use.

Size. The following size ranges of Prince of Wales coal (CRC 802) were used. For convenience these have been arranged into three groups (Table III) according to their method of preparation. The coals in the size ranges in groups 1 and 2 were prepared by sieving the dry coal through mesh sieves. Those shown in group 3 are size fractions obtained with a centrifugal classifier.

It must be remembered that the size ranges given are those of the material in the fluidized bed and that, in general, the material reaching the plasma will contain a higher proportion of the smaller particles. Size distributions have been determined for the CRC 802 coal in group 1 both for the material used in the fluidized bed and for that which was fed into the plasma. These are given in Figure 4 which shows a marked difference between the size dis-

Publication Date: January 1, 1966 | doi: 10.1021/ba-1966-0055.ch041

Table II.

NCB[a] Coal Rank Code No.	Colliery	Seam	Air Dried Coal % Moisture	Ash
902	Haunchwood	High Main	12.0	2.2
802	Prince of Wales	Top Haigh Moor	8.8	2.6
301b	Thornley	Bottom Busty	1.0	6.2
203	Britannia	Seven Feet	0.8	8.8
102	Pentreclwdau	Nine Feet	1.3	2.6
Black Durain	Peckfield	Beeston	3.9	1.3
Cannel	Lady Victoria		2.2	4.0

[a] British system of coal classification used by the National Coal Board (*15*).

Table III. Size Ranges of Coal

Group	Size: B.S. Mesh Sieve, Less than	B.S. Mesh Sieve, Greater than	Equivalent in Microns, Less than	Equivalent in Microns, Greater than
1	72	0	210	0
	25	72	590	210
	72	100	210	149
2	100	150	149	105
	150	200	105	74
	200	300	74	53
3			50	40
			40	30
			25	15
			10	0

tribution of the coal in the fluidized bed and that which is fed into the plasma. For this reason, narrower size fractions (groups 2 and 3) were used. Variations in the size of the coal entering the jet were further reduced by feeding only a fraction (<20%) of the coal in the fluidizer. The remainder was discarded after each experiment.

Results

Influence of Feed Rate. Experiments in an argon plasma using coal feed rates usually up to 0.5 gram/min. showed that the products were almost entirely solid or gaseous, there being negligible amounts of the tarry material which is normally associated with the products from the thermal treatment of coal at relatively low temperatures and slow rates of heating. The gases from the coal consisted mainly of acetylene, hydrogen, and carbon monoxide. Acetylene was the most important hydrocarbon produced from the coal and in some cases represented over 95% of the hydrocarbons present. A gas chromatogram of the hydrocarbons present in a typical arc gas produced when the 802 coal was processed in a pure argon plasma is shown in Figure 5, and the corresponding gas analysis is given in Table IV.

Publication Date: January 1, 1966 | doi: 10.1021/ba-1966-0055.ch041

Analyses of Coals

B.S. Swelling No.	Ultimate Analysis dmf, %					Volatile Matter dmf, %
	C	H	N	S	O by diff.	
1	80.6	5.2	1.4	0.9	11.9	41.1
2	83.6	5.3	2.0	0.9	8.2	36.4
8	89.0	5.2	1.5	0.7	3.6	28.1
6	91.7	4.5	1.5	0.7	1.6	16.1
0	93.2	3.5	1.5	0.7	1.1	6.2
—	84.5	6.0	1.2	0.8	7.5	50.7
—	84.6	7.2	1.5	1.0	5.7	55.1

Publication Date: January 1, 1966 | doi: 10.1021/ba-1966-0055.ch041

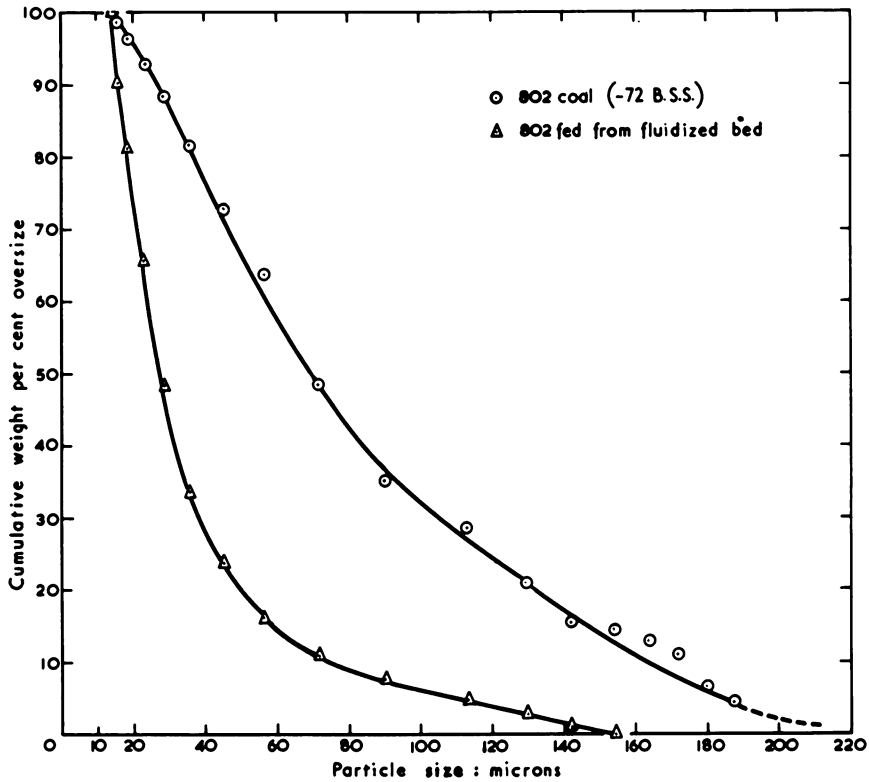

Figure 4. Size distributions of coal in fluidizer and feed from fluidizer

The effect of feed rate upon the conversion of the 802 coal (size group 1, —72 B.S. mesh) to acetylene is shown in Figure 6 both for reactions carried out in an argon plasma and in a 90% argon plus 10% hydrogen plasma. The rectilinear portions of the graph, represented by the unbroken lines, corre-

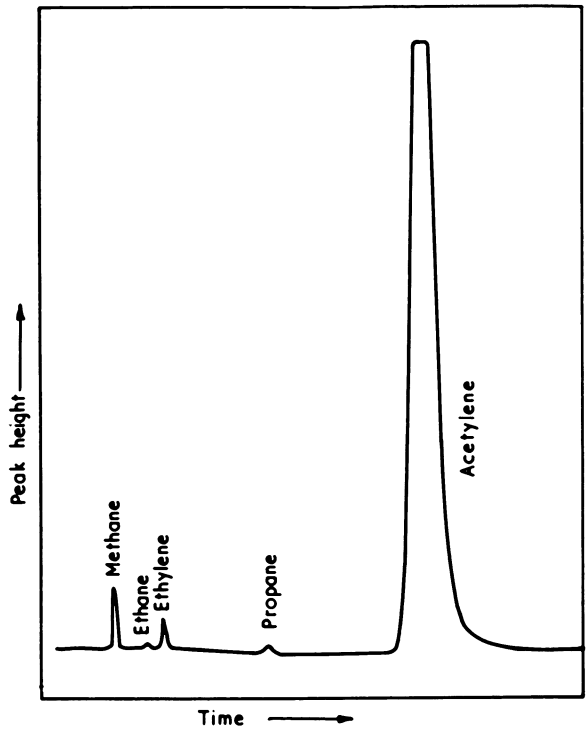

Figure 5. Gas chromatogram of hydrocarbon gases from the plasma jet

Table IV. Analysis of the Arc Gas from 802 Coal in an Argon Plasma

Gas	*Ar*	C_2H_2	CH_4	C_2H_6	C_3H_8	C_2H_4	H_2	*CO*	CO_2	*HCN*
Conc. v/v %	98	0.54	0.014	0.001	0.004	0.005	0.86	0.33	0.005	0.03

spond to a 20% conversion of the carbon in the coal to carbon in acetylene in the pure argon plasma and to 40% conversion to acetylene in the 90% argon plus 10% hydrogen plasma. At coal feed rates exceeding about 0.3 gram/min. the yield of acetylene falls. This could be caused by either inefficient heating of the solid feed material or inadequate quenching of the gaseous products, or both.

Influence of Particle Size. The experiments were carried out with an 802 coal in an argon plasma using size fractions shown in groups 2 and 3 of Table III. The results are given in Figure 7 where the percentage conversion of the carbon to acetylene is plotted as a function of the size fraction in the fluidizer. The extent of the reaction, as expected, strongly depends upon the particle size, particles with diameters greater than about 200μ scarcely reacting. Figure 7 shows that for particles of 50μ or less in diameter a 20% yield of acetylene is reached, which is the yield obtained for the 802 coal ground to pass a 72

Publication Date: January 1, 1966 | doi: 10.1021/ba-1966-0055.ch041

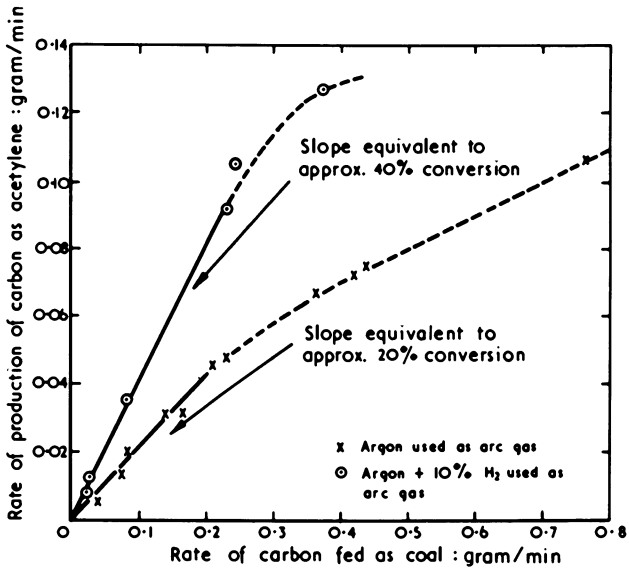

Figure 6. Effect of coal feed rate on conversion to acetylene

B.S. mesh sieve. The explanation for the apparently high yield from the —72 coal used in the initial experiments (3) is that approximately 80% of the material blown out from the fluidizer was less than 50μ in diameter as shown in Figure 4.

Influence of Coal Rank. The effect of the rank of the coal on the reactions in the plasma jet was studied by carrying out experiments in an argon plasma with the range of coals shown in Table II. The size range used for these measurements was 53–74μ. The conversions of the various coals to acetylene, which was taken as a measure of the extent of the reaction, are shown in Figure

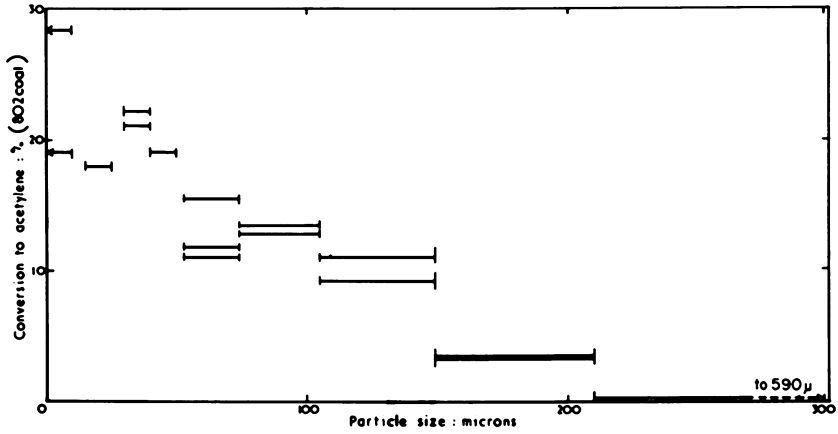

Figure 7. Effect of particle size on acetylene yields

8 where the percentage yields are plotted against the volatile matter as determined by the B.S. test (*4*) (comparatively slow rate of heating to 925°C.). Experiments on two coals, 802 and cannel, showed that the weight loss on heating to about 2800°C. (over 3 hours) is only slightly greater than that measured by the standard volatile matter determination. The 802 coal (standard volatile matter 36.4%) gave a weight loss of 38.3%, and the corresponding value for cannel (standard volatile matter 55.1%) was 54.4% weight loss.

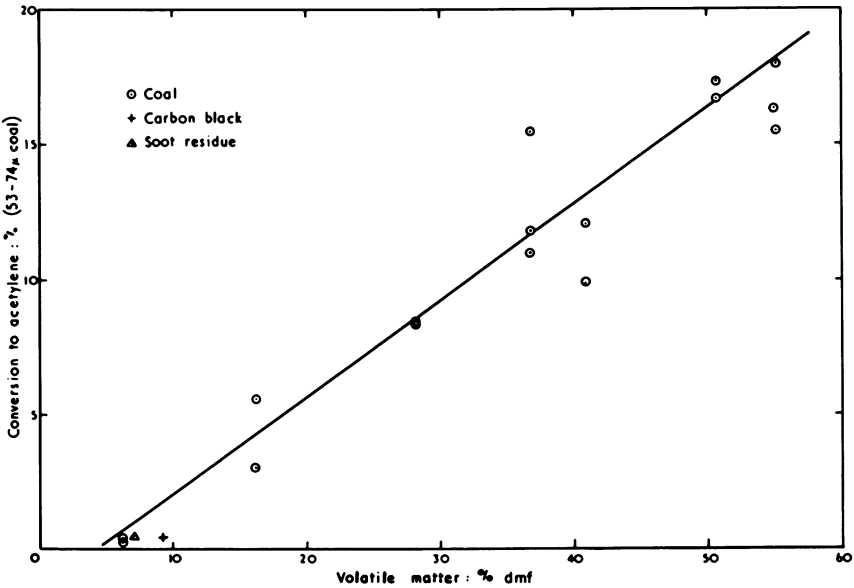

Figure 8. Effect of coal rank on acetylene yield

Under the conditions of rapid heating used, the quantity of volatile matter might well have proved quite different from that obtained with slow rates of heating. Nevertheless, Figure 8 shows that the yield of acetylene under the present conditions is directly proportional to the standard volatile matter of the coal, irrespective of whether the coal consists mainly of vitrinite or sporinite. This suggests that the acetylene is derived mainly from the coal volatiles rather than from complete volatilization of the coal. The small extent of reaction with Neospectra carbon black, and the soot itself when returned for further reaction, show that there is little volatilization of these materials even though they have a very small particle size.

Influence of Residence Time. An approximate calculation of the residence time of the particles in the jet, assuming that they reach the gas velocity instantaneously (which is probably true for the small particles), shows that this time is about 1 msec. Estimating the rate of heating of particles of various sizes shows that particles less than 50μ in diameter will reach a temperature of 1000°C. in approximately 1 msec., assuming a gas temperature of 4700°C. —an average heating rate of 10^6°C. per sec. These estimates indicate that

Publication Date: January 1, 1966 | doi: 10.1021/ba-1966-0055.ch041

particles of 50μ or less in diameter will probably reach a temperature exceeding 1000°C. while they pass through the jet. However, these calculations are only approximate since the temperature distribution in the jet is not known with any certainty.

The effect of the residence time of the particles in the plasma jet was studied in two ways—by varying the gas flow through the jet and by varying the length of the water cooled extension tube (*see* Figure 3).

Experiments with the 802 coal (—72 B.S. mesh) in an argon plasma were undertaken using total gas flow rates through the jet ranging from 5–20 liters/min. at coal feed rates less than 0.3 gram/min., where under the normal experimental conditions (i.e., total gas flow 9.5 liters/min. and the 10-cm. extension tube) a 20% conversion to acetylene was obtained. The conversions to acetylene for various flow rates are given in Table V. Optimum flow conditions appear to be reached at rates between 10 and 15 liters/min.

The length of the extension tube might also be expected to influence the heating time available to the coal particles. However, tubes up to 25 cm. long were tried without any significant change in the acetylene yield (Table V). This somewhat surprising result may be caused by a compensation of the increase in the resulting efficiency of heating by a decrease in the efficiency of the quenching process, with the result that any additional acetylene produced may have decomposed.

Table V. Effect of Flow Rate and Length of Extension Tube on Acetylene Conversions

	Rate of Gas Flow (liters/min.) (10-cm. Extension Tube)				*Length of Extension Tube (cm.) (Flow rate 9.5 liters/min.)*			
Percentage	*5*	*10*	*15*	*20*	*0*	*2.5*	*10*	*25*
Conversion to Acetylene, %	13	22	20	14	21	25	22	20

Influence of Other Atmospheres. HYDROGEN. The results of experiments using a mixture of 90% argon plus 10% hydrogen as the plasma gas have already been given in the section on the influence of feed rate and in Figure 6. An increase in the hydrogen concentration in the plasma from less than 1% (argon plus coal experiments) to 10% produced a two-fold increase in the yield of acetylene. However, at hydrogen concentrations above 10%, the copper anode became severely eroded. Attempts to improve the cooling of this electrode were unsuccessful. The constant erosion of the anode augmented the widely varying arc conditions inherent in the hydrogen plasma jet, with the result that reproducibility was unobtainable at hydrogen concentrations greater than 10%. Nevertheless, the results of the experiments at hydrogen concentrations greater than 10% did not suggest that the yield of acetylene would be substantially greater than the 40% yield obtained with the 90% argon plus 10% hydrogen mixture.

NITROGEN. The gas analysis given in Table IV shows that the nitrogen in the coal was converted to hydrogen cyanide in the plasma jet. The results of experiments on adding nitrogen to the jet are summarized in Table VI. As the concentration of nitrogen in the jet was increased, the conversion of the

Publication Date: January 1, 1966 | doi: 10.1021/ba-1966-0055.ch041

Table VI. Summary of Experiments

NCB Coal Rank Code No.	Size μ	Compositions of Arc Gas % v/v Ar	N_2	H_2	Voltage volts
802	−74 + 53	90	10	—	25
802	−74 + 53	90	10	—	25
802	−74 + 53	90	10	—	26
802	−74 + 53	70	30	—	35
802	−74 + 53	—	100	—	48
102	−74 + 53	90	10	—	27
Cannel	−53	—	100	—	50
Cannel	−53	—	90	10	45

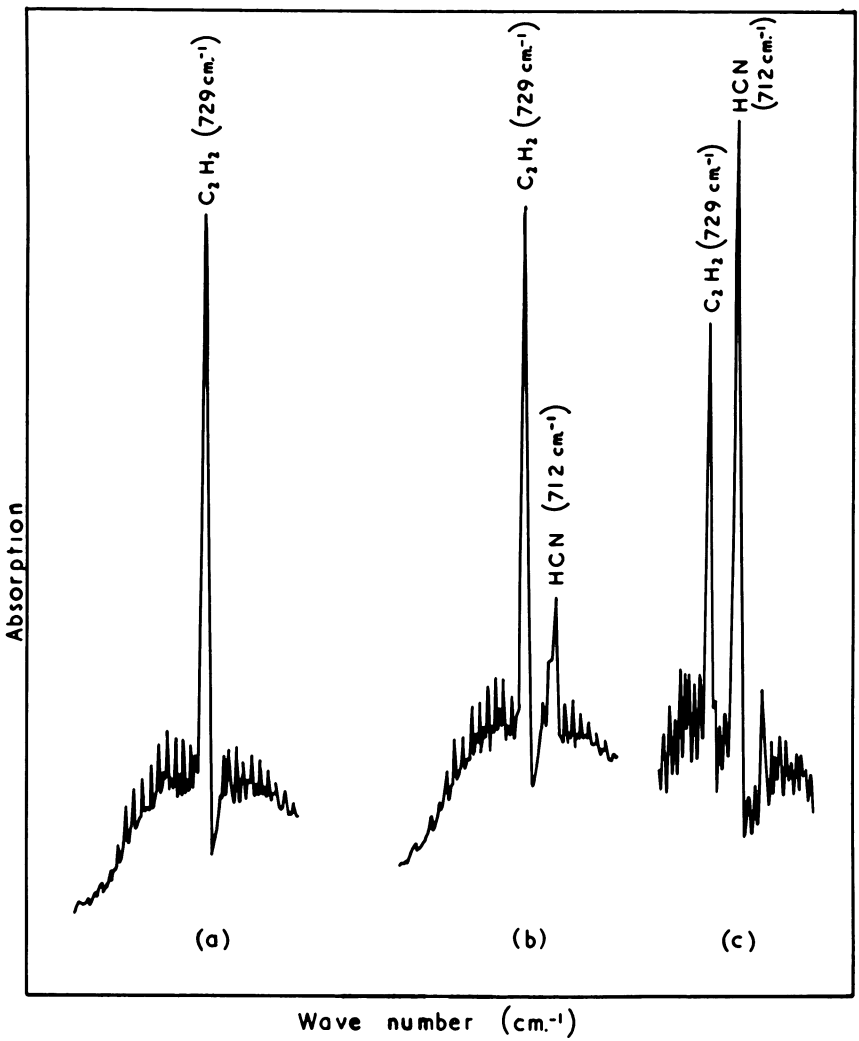

Figure 9. Infrared spectrum of (a) pure acetylene, (b) gases from argon plasma arc, (c) gases from nitrogen plasma arc

Publication Date: January 1, 1966 | doi: 10.1021/ba-1966-0055.ch041

Using Nitrogen Plasmas

Current amp.	Coal Feed gram/min.	Carbon Percentage Conversion w/w C_2H_2	HCN	CH_4
282	0.44	12.9	7.8	0.3
280	0.06	3.4	12.8	0.8
282	0.10	6.6	15.1	0.7
277	0.08	2.5	18.2	0.8
270	0.31	2.7	19.0	0.1
279	0.38	0.4	2.4	0.3
262	0.50	4.6	18.1	0.1
265	0.80	7.4	24.1	0.2

coal to hydrogen cyanide increased while that to acetylene decreased. For the high volatile coal (802) the total conversion of carbon to hydrogen cyanide plus acetylene, in most cases, was approximately equal to the acetylene yield obtained in the pure argon plasma (i.e., approximately 20%). An experiment with the 102 (low volatile) coal in a 90% argon plus 10% nitrogen plasma produced a low yield of hydrogen cyanide, again showing that it is largely the volatile matter from the coal that gives rise to the gaseous components formed in the plasma jet.

In one experiment a 90% nitrogen plasma was used (Table VI). Although using a coal feed rate of 0.8 gram/min., this produced a yield of acetylene plus hydrogen cyanide of 31.5%, which for this feed rate (higher than normally employed) is similar to the acetylene yield achieved in the experiments using the 90% argon plus 10% hydrogen plasma. Again hydrogen cyanide predominated. The changes in the relative amounts of acetylene and hydrogen cyanide are shown by the infrared spectra of gases from the argon and nitrogen plasmas (Figure 9).

The Soot Produced. The soot, which collected mainly on the inside of the metal container, was very finely divided; optical and electron microscope studies indicated that most of the soot particles were submicron in size. The conversion of the coal particles of diameters originally up to 100μ into this finely divided soot may well have resulted from a shattering of the coal particles since it is likely that a violent evolution of gas occurred under the extremely rapid heating. The analyses of the soots from three experiments with the 802

Table VII. Analyses of Some of the Soots from 802 Coal Together with the Analyses of Carbonized Coals of Similar Carbon Content

Sample		Proximate Analyses (Air dry basis %) Moisture	Volatile Matter	Ash	Ultimate Analyses (dmf, %) C	H	O
Soot		1.0	—	4.6	89.7	2.5	5.7
Soot		0.8	7.4	6.6	94.3	1.0	2.8
Soot		2.1	6.8	6.8	95.0	1.2	2.2
Carbonized Coal[a]	600°C.	2.7	6.9	2.0	91.6	2.4	4.0
	700°C.	6.7	5.9	1.9	93.3	0.5	3.6
	900°C.	3.6	1.5	1.7	96.4	0.5	1.5

[a] Thorne, High Hazel, C 83.6%; N.C.B. Rank Code 702.

Publication Date: January 1, 1966 | doi: 10.1021/ba-1966-0055.ch041

coal in an argon plasma are given in Table VII together with the analyses for a coal of similar carbon content carbonized at 600°, 700°, and 900°C. The chemical analyses of the soots show considerable variation but it can be seen that they exhibit certain similarities to those of carbonized coal. However, the H/C ratios of the soots are appreciably higher than those of the carbonized coal. The soots still yield a fairly high proportion of volatile matter in the B.S. test. This became even more apparent for the soots from the coals of very high volatile matter (>50%) where the residual volatiles of the soots from these coals often exceeded 20%.

Conclusions

The plasma jet provides a tool for rapidly heating coal and quenching the products. Its main disadvantages are that it is difficult to ascertain the temperatures and residence times to which the particles are subjected.

The extent of the reactions of coal in the plasma jet depend upon the combination of a physical effect (the influence of the particle size on the rate of heating) and a chemical effect (the subsequent rapid release of volatile material leading, it is thought, to shattering of the particles). As a consequence of these two effects, high volatile coals of small particle size gave the maximum reaction as measured by the yield of acetylene.

The products consisted of gas and soot, but there was an absence of tarry material, in sharp contrast to the products obtained by the more conventional carbonization (i.e., slow heating to 1000°C.). The main gaseous products were hydrogen, carbon monoxide, and acetylene. Acetylene formed over 95% of the hydrocarbons produced, the remainder comprising small quantities of ethylene, methane, and other saturated and unsaturated compounds of low molecular weight. Acetylene yields of 20% in an argon plasma and 40% in a 90% argon plus 10% hydrogen plasma were achieved, provided that the coal feed rate did not exceed 0.3 gram/min. Introducing nitrogen into the plasma produced hydrogen cyanide with a corresponding reduction in acetylene; a 20% conversion of carbon to hydrogen cyanide was achieved in a pure nitrogen plasma.

Publication Date: January 1, 1966 | doi: 10.1021/ba-1966-0055.ch041

Acknowledgments

The authors wish to thank L. A. King of the Electrical Research Assoc. for advice on the design of the plasma jet and I. F. Galbraith for its construction. We are also grateful to E. Pritchard for carrying out the gas chromatographic analysis, to R. Bent for the infrared analyses, to M. P. Mendoza for the microchemical analysis, and to R. Wheatley for preparing the sized coals.

This work is published by permission of the British Coal Utilisation Research Association. One of us (R.L.B.) gratefully thanks the National Science Foundation for making it possible to present this paper.

Literature Cited

(1) Badzioch, S., *B.C.U.R.A. Monthly Bulletin* **25,** 285 (1961).
(2) Baumann, P., *Angew. Chem.* **20,** 257 (1948).

(3) Bond, R. L., Galbraith, I. F., Ladner, W. R., McConnell, G. I. T., *Nature* **200**, 1313 (1963).
(4) British Standards Institution, B.S. **1016**, Part 3 (1957).
(5) Hawk, C. O., Schlesinger, M. D., Hiteshue, R. W., *U.S. Bur. Mines, Rept.* **R.I. 6264** (1963).
(6) I. G. Farbenind, A. G. British Patent **286,825** (1928).
(7) I. G. Farbenind, A. G. British Patent **389,165** (1933).
(8) King, L. A., private communication.
(9) Littlewood, K., McGrath, I. A., *Intern. Conf. Coal Sci., 5th, Cheltenham,* 1963.
(10) Lowry, H. H., Ed., "Chemistry of Coal Utilization," Suppl. Ed., John Wiley and Sons, New York, 1963.
(11) Rau, E., Eddinger, R. T., *Fuel* **43**, 246 (1964).
(12) Rau, E., Seglin, L., *Fuel* **43**, 147 (1964).
(13) Sharkey, A. G., Shultz, J. L., Friedel, R. A., *Nature* **202**, 988 (1964).
(14) Standard Oil Dev. Co., British Patent, **455,567** (1936).
(15) Van Krevelen, D. W., "Coal," p. 29, Elsevier, Amsterdam, 1961.

RECEIVED July 13, 1965.

42

Thermodynamic Aspects of the Reactions of Carbon and Coal at High Temperatures

D. M. L. GRIFFITHS and H. A. STANDING

Coal Research Establishment, National Coal Board, Cheltenham, England

Publication Date: January 1, 1966 | doi: 10.1021/ba-1966-0055.ch042

Published thermodynamic data on the reactions between carbon, hydrogen, nitrogen, and oxygen are surveyed over a wide range of temperatures with particular reference to the formation of acetylene, cyanogen, and hydrogen cyanide from carbon or coal. Consideration of the free energies of formation of hydrocarbons and their variations with temperature shows that acetylene could be formed as an intermediate, unstable product at temperatures of about 1800°K., the yield then being governed by kinetics. At temperatures above 3000°K., acetylene can exist in equilibrium with carbon and hydrogen, and the equilibrium yields have been calculated. Cyanogen can exist in equilibrium with carbon and nitrogen at high temperatures, and theoretical equilibrium yields have been calculated over a range of temperatures and pressures. If hydrogen is present, hydrogen cyanide is also formed at high temperatures.

The importance of chemical kinetics to coal carbonization is generally recognized and is featured in much of the recent fundamental research on coal carbonization (*4*). Nevertheless, thermodynamic considerations provide a useful guide to the type and yield of gaseous products which might be obtained at high temperatures. This paper reviews some of the thermodynamic work on the reactions between carbon, hydrogen, and nitrogen. The equilibrium yields of acetylene, hydrogen cyanide, and cyanogen are given over a wide range of temperature and pressure, the results for the first two compounds being taken from published work while those for cyanogen were derived by the authors.

In Coal Science; Given, P.;
Advances in Chemistry; American Chemical Society: Washington, DC, 1966.

At temperatures between 900° and 2000°K. most hydrocarbons have a positive free energy of formation which, with the exception of acetylene, increases with increasing temperature (Figure 1). If coal carbonization could attain thermodynamic equilibrium over this temperature range, the hydrocarbon by-products would be decomposed mainly to carbon and hydrogen while any oxygen in the coal would be evolved as carbon monoxide. In

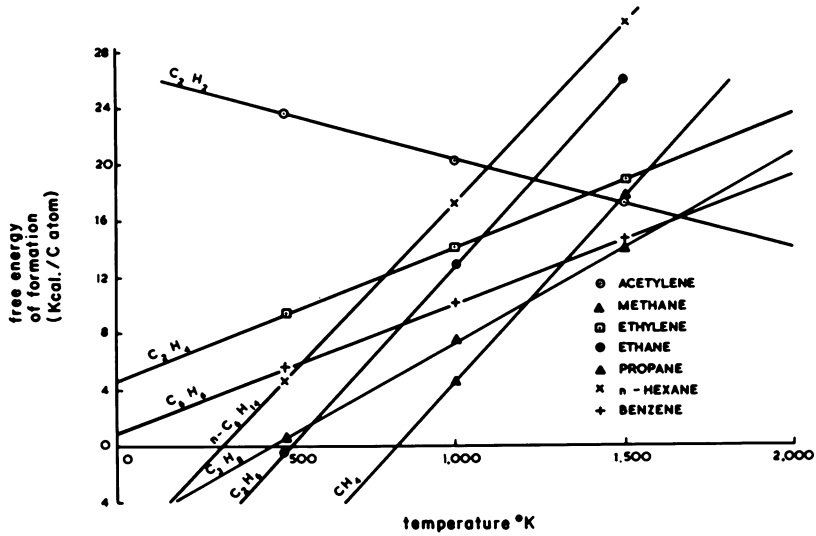

Figure 1. Free energy of formation of hydrocarbons at various temperatures

practice, thermodynamic equilibrium is not attained, and the composition of the hydrocarbon by-products is mainly determined by the temperature and the kinetics of the process. At temperatures above 1700°K. acetylene has a lower free energy of formation than the other hydrocarbons, but it is still thermodynamically unstable. Consequently, acetylene can be obtained by rapidly carbonizing coal at about 1800°K., but the yield is still mainly governed by chemical kinetics. The reaction time must be sufficiently long to permit the decomposition of other hydrocarbons to acetylene but sufficiently short to prevent any appreciable decomposition of the acetylene formed to carbon and hydrogen.

The Carbon-Hydrogen System

At temperatures of about 4000°K., the free energy of formation of acetylene from its elements approaches zero, and the equilibrium yield of acetylene is appreciable. The system is complicated, however, by other reactions and phase changes which occur at these high temperatures. Carbon sublimes at about 4000°K., various species of carbon C_1, C_2, and C_3 are formed, and dissociation of molecular hydrogen occurs.

Publication Date: January 1, 1966 | doi: 10.1021/ba-1966-0055.ch042

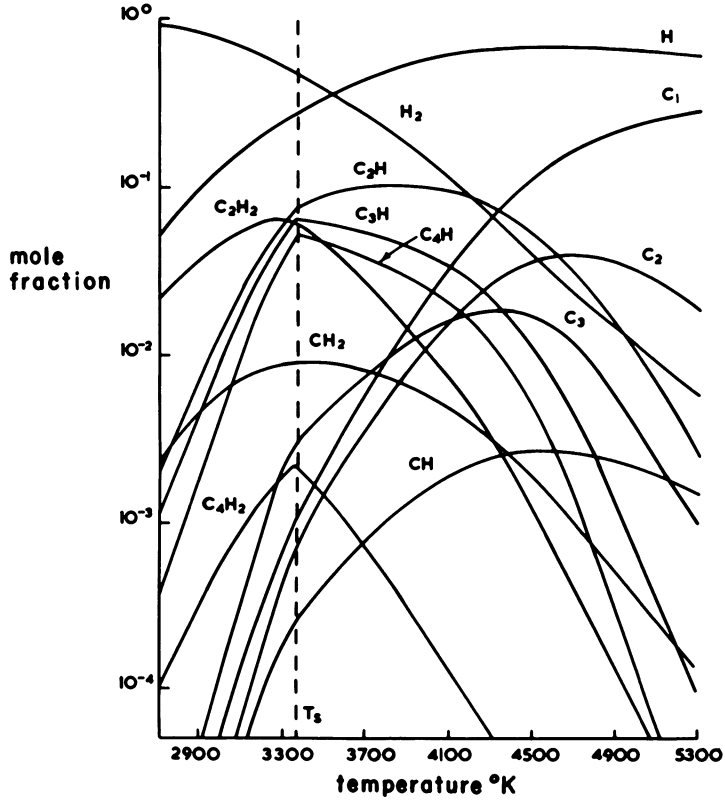

Figure 2. Equilibrium diagram for system C + H_2 at 1 atm. pressure

The equilibrium between carbon and hydrogen at high temperatures has been treated thermodynamically by several authors (*1*, *2*, *5*, *7*). The approach is to formulate the various reactions which could occur, to apply to each the appropriate mass action equation, and to solve the set of simultaneous equations so obtained. A distinction is made between heterogeneous and homogeneous systems since for the latter it is necessary to specify the ratio of carbon to hydrogen in the system.

Baddour and Blanchet (*1*) paid particular attention to the possible existence of C_2H, C_3H, C_4H, CH, and CH_2 in the equilibrium mixture. They assumed that at temperatures above 3000°K. the equilibrium mixture contained the following species: C_1, C_2, C_3, H, H_2, C_2H_2, C_2H, C_3H, C_4H, C_4H_2, CH, and CH_2, the last two becoming significant above 4000°K. Values of the free energy functions and the equilibrium constants for the 16 reactions were calculated by Blanchet by the method of Bauer and Duff (*2*). The calculated values necessarily depend upon the values assumed for the heat of formation and may require revision for certain species as new data become available.

On this basis Baddour and Blanchet derived the equilibrium diagram shown in Figure 2 for the carbon-hydrogen system at 1 atm., the ratio of

Publication Date: January 1, 1966 | doi: 10.1021/ba-1966-0055.ch042

carbon to hydrogen being one. The dotted line represents the sublimation temperature for this particular set of conditions. The mole fraction of acetylene in the equilibrium mixture passes through a maximum with temperature, the value being 0.07 at about 3300°K., that of C_2H is 0.1 at about 3800°K.

The concentration of acetylene in the quenched gas was calculated on the assumption that all the C_2H_2, H_2, and C_4H_2 remained unchanged on quenching whereas C_2H recombined with hydrogen to yield more C_2H_2. The other equilibrium species were assumed to go to solid carbon and hydrogen. On this basis Baddour and Blanchet showed that the theoretical maximum acetylene concentration in the quenched gas depended on the temperature and carbon-hydrogen ratio of the system; at 4300°K. and a ratio of 15, the theoretical maximum concentration was 50%. Experiments with a high intensity arc reactor gave a maximum acetylene concentration of 26% which was considerably higher than any value previously obtained but was still below the 40–50% theoretically possible.

The Carbon-Nitrogen System

The theoretical yields of cyanogen obtained by the reaction of carbon and nitrogen can also be derived from thermodynamic data. At high temperatures cyanogen is partly dissociated into cyanogen radicals, and the following simultaneous equilibria must be considered:

$$\begin{aligned}
C_1 &\rightarrow C(s) & K_1 &= 1/P_{C1} \\
2C_1 &\rightarrow C_2 & K_2 &= P_{C2}/P^2_{C1} \\
3C_1 &\rightarrow C_3 & K_3 &= P_{C3}/P^3_{C1} \\
2C(s) + N_2 &\rightarrow C_2N_2 & K_4 &= P_{C2N2}/P_{N2} \\
2N_1 &\rightarrow N_2 & K_5 &= P_{N2}/P^2_{N1} \\
C_1 + N_1 &\rightarrow CN & K_6 &= P_{CN}/P_{C1}P_{N1} \\
2C_1 + 2N_1 &\rightarrow C_2N_2 & K_7 &= P_{C2N2}/P^2_{C1}P^2_{N1}
\end{aligned}$$

The mass-action equations have been written in the same form as those given by Marynowski *et al.* (*6*) so that the equilibrium constants can be used directly. (Should more accurate data become available, the equilibrium yields calculated here will require revision.) The fourth equation, which applies to the heterogeneous equilibrium between carbon and nitrogen, is included for completeness but is unnecessary for the general solution. It can be shown that when the total pressure of the system is P, the partial pressure of cyanogen radicals is given by the equation:

$$\frac{1}{K^2_6}\left[\frac{K_5}{P^2_{C1}} + K_7\right]P^2_{CN} + \left[\frac{1}{K_6P_{C1}} + 1\right]P_{CN} + \left[P_{C1} + K_2P^2_{C1} + K_3P^3_{C1} - P\right] = 0$$

When the system is heterogeneous—i.e., the temperature and pressure are such that solid carbon exists in equilibrium with its vapor, the value of P_{C1} is uniquely determined by the temperature and can be calculated directly from the equilibrium constant K_1. Hence in a heterogeneous system, the partial pressure of cyanogen radicals and of cyanogen depend only on the temperature

Publication Date: January 1, 1966 | doi: 10.1021/ba-1966-0055.ch042

and pressure of the system. The value of P_{CN} at a given temperature and pressure can be readily calculated from the quadratic equation, and hence the corresponding partial pressures of the other components.

When the system is homogeneous, the value of P_{CN} is no longer uniquely determined by the temperature; it depends also on the atomic ratio C/N of carbon to nitrogen initially present in the system. Thus, for a homogeneous system the concentration of cyanogen radicals and cyanogen in the equilibrium mixture depends on three variables—temperature, pressure, and the C/N ratio. For a given temperature and pressure the equilibrium concentration of cyanogen radicals is a maximum when the C/N ratio is 1. The method used to calculate the partial pressures of the components in a homogeneous system with a C/N ratio of 1 was as follows. At a given temperature and pressure, the value of P_{CN} corresponding to an arbitrary value of P_{C_1} can be calculated, and hence the corresponding partial pressures of the other components and also the C/N ratio. By choosing a series of arbitrary values of P_{C_1}, the values of the equilibrium partial pressures corresponding to a C/N ratio of 1 can be determined by successive approximations.

The effect of temperature on the equilibrium composition of the carbon-nitrogen system at 1 atm. pressure is shown in Figure 3. At temperatures above 4000°K. the system is homogeneous, and the C/N ratio is fixed at 1. The partial pressure of cyanogen (expressed as a percentage of the total pressure)

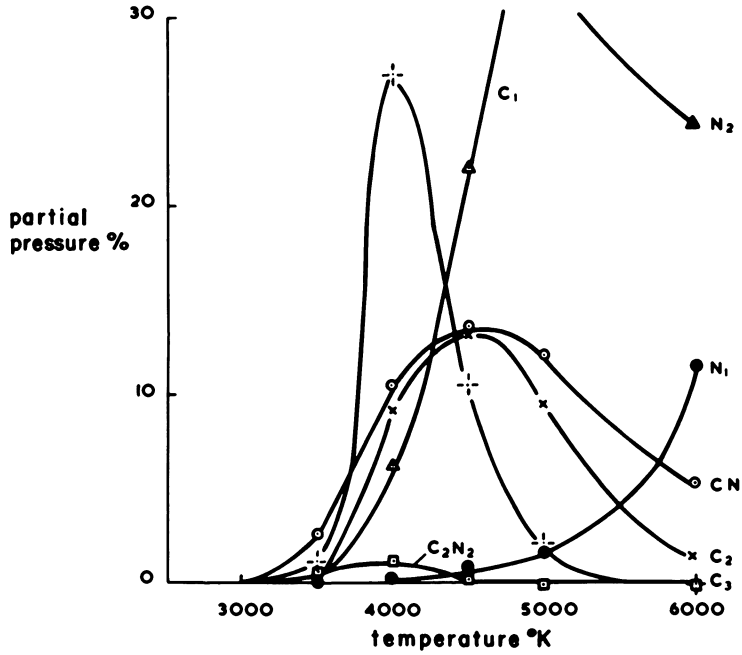

Figure 3. Effect of temperature on equilibrium composition of the carbon-nitrogen system at 1 atm. pressure

Publication Date: January 1, 1966 | doi: 10.1021/ba-1966-0055.ch042

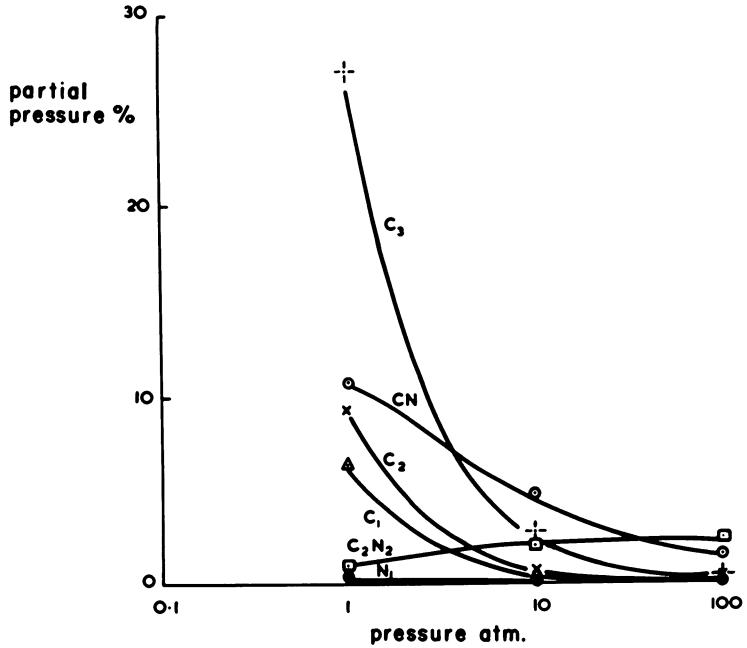

Figure 4. Effect of pressure on equilibrium composition of the carbon-nitrogen system at 4500°K.

passes through a maximum of 1% at 4000°K.; that of cyanogen radicals passes through a higher maximum of 13.6% at 4500°K. When the equilibrium mixture is quenched rapidly enough to prevent the decomposition of cyanogen to its elements, carbon will condense and the effective concentration of cyanogen will be increased. Moreover, the cyanogen radicals will combine to form cyanogen. On this basis the theoretical concentration of cyanogen in the quenched gas from the equilibrium mixture at 4500°K. would be 15% by volume.

The influence of pressure on the carbon-nitrogen equilibrium depends on whether the system is homogeneous or heterogeneous. When the system is heterogeneous, the vapor pressure of carbon is constant and the total pressure can only be varied by varying the partial pressure of nitrogen. In a homogeneous system, however, the partial pressures of carbon vapor and nitrogen vary simultaneously with the total pressure. In order to determine whether or not the system is homogeneous, it is necessary to specify not only the temperature and pressure, but also the ratio C/N of carbon to nitrogen initially present in the system. The present calculations on the effect of pressure on homogeneous systems were confined to a C/N ratio of 1. The equilibrium constants given by Marynowski *et al.* for the system C(s), C_1, C_2 and C_3 were used to calculate the total vapor pressure of carbon.

At 4000°K. the total vapor pressure of carbon is 0.43 atm. Consequently, the system is heterogeneous at 1 atm. pressure, and higher pressures can only be achieved by increasing the partial pressure of nitrogen. At pressures up

Publication Date: January 1, 1966 | doi: 10.1021/ba-1966-0055.ch042

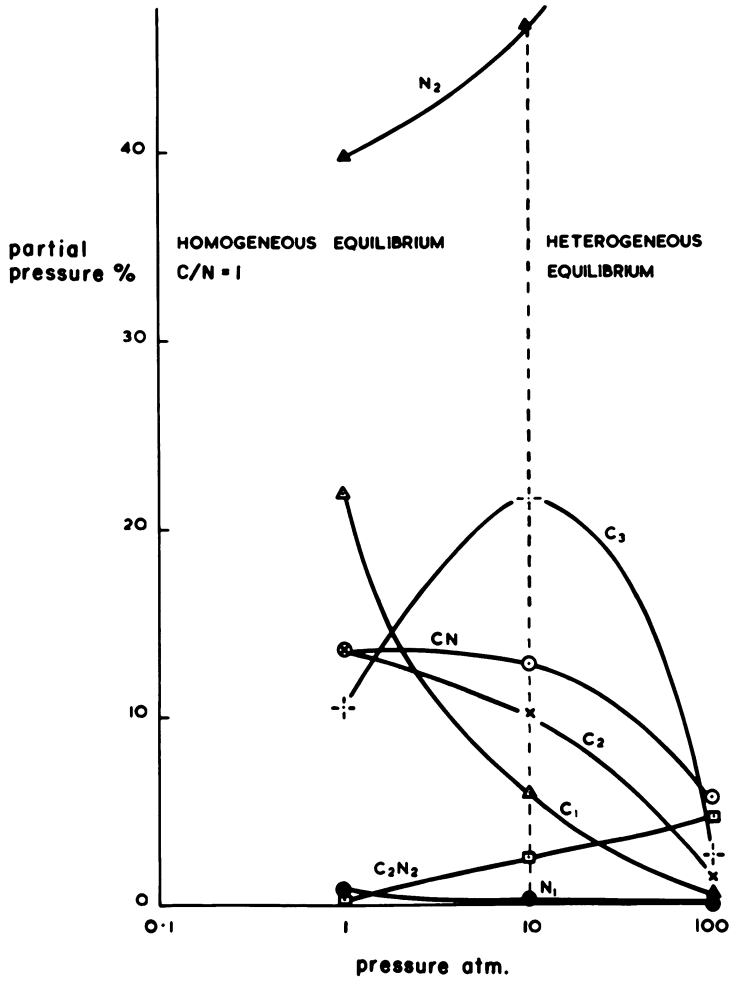

Figure 5. Effect of pressure on equilibrium composition of the carbon-nitrogen system at 4000°K.

to a few atmospheres, the ratio of the partial pressures of nitrogen to the total pressure increases with increasing pressure. Consequently pressure has an effect on the heterogeneous equilibrium

$$2C(s) + N_2 \rightleftharpoons C_2N_2$$

which at first sight appears to be independent of pressure. The other equilibrium—dissociation of cyanogen into cyanogen radicals—is obviously pressure dependent.

Figure 4 shows the effect of pressure (1–100 atm.) on the equilibrium composition of the carbon-nitrogen system at 4000°K. The partial pressure of each constituent is plotted as a percentage of the total pressure and therefore

Publication Date: January 1, 1966 | doi: 10.1021/ba-1966-0055.ch042

corresponds to the concentration by volume of that constituent in the equilibrium mixture. The cyanogen concentration increases with increasing pressure and at 100 atm. pressure approaches a limiting value of 2.4% by volume. This arises because at high pressures the ratio P_{N_2}/P tends to 1. By contrast, the concentration of cyanogen radicals decreases from 11% at 1 atm. to 1.5% at 100 atm. If the cyanogen radicals form cyanogen when the equilibrium mixture is rapidly quenched, then over the pressure range 1–100 atm. the concentration of cyanogen in the quenched gas will steadily decrease from 12 to 3% by volume.

Figure 5 shows the effect of pressure (1–100 atm.) on the carbon-nitrogen system at 4500°K., the partial pressures again being plotted as percentages of the total pressure. At this temperature the total vapor pressure of carbon is 4.2 atm., and it is possible to maintain a homogeneous system with a C/N ratio of 1 up to 10 atm. but not beyond this. Throughout the homogeneous region below 10 atm. the partial pressure of carbon increases with increasing pressure, but the formation of triatomic C_3 is favored at the expense of C_1. This affects the equilibrium between C_1, N_1 and CN. Thus between 1 and 10 atm. the concentration of cyanogen radicals in the equilibrium mixture decreases slightly while that of cyanogen increases. Assuming that the cyanogen radicals form cyanogen, the concentration of cyanogen in the quenched gas remains almost constant at 15% by volume as the equilibrium pressure is increased from 1 to 10 atm. In the heterogeneous region between 10 and 100 atm. the vapor pressure of carbon remains constant; the concentration of cyanogen radicals decreases appreciably while that of cyanogen continues to increase. Thus over the entire pressure range 1–100 atm. the concentration of

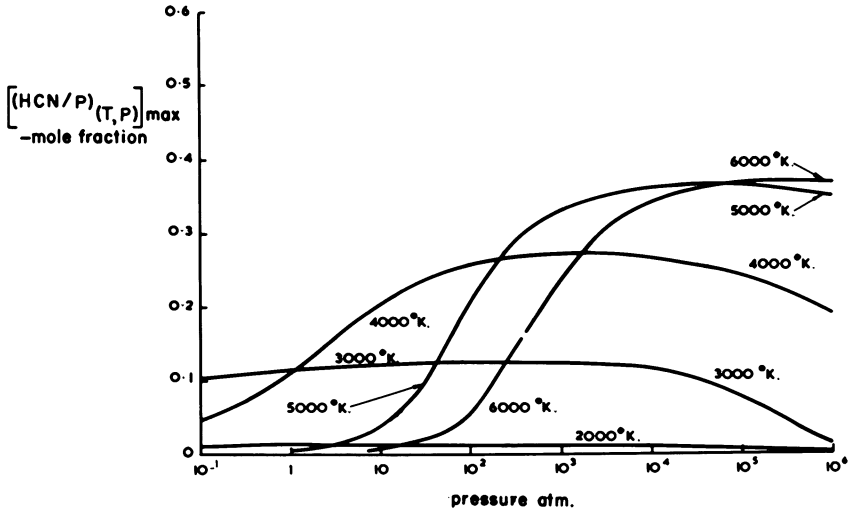

Figure 6. Maximum equilibrium HCN concentration as a function of pressure for five temperatures

Publication Date: January 1, 1966 | doi: 10.1021/ba-1966-0055.ch042

cyanogen in the quenched gas decreases from 15 to 8% by volume, but the decrease is confined to the region above 10 atm.

The Carbon-Hydrogen-Nitrogen System

When the ternary system carbon-hydrogen-nitrogen is subjected to high temperatures, many products are formed including hydrogen cyanide, acetylene, and cyanogen. The equilibrium yields of hydrogen cyanide have been calculated by Marynowski and co-workers (*6*). They showed that at any particular temperature and pressure the maximum yield of hydrogen cyanide was obtained when the system contained equal numbers of carbon, hydrogen, and nitrogen atoms.

Some results of their calculations are shown in Figure 6 which relates, at several definite temperatures, the maximum mole fraction of hydrogen cyanide in the equilibrium mixture to the pressure. At 2000°K. the concentration of hydrogen cyanide in the equilibrium mixture is small and does not vary much with pressure. At 4000°K. considerably higher concentrations of hydrogen cyanide are obtained, the concentration at first increasing with pressure and then passing through a maximum of about 28 mole % at 500 atm. Even higher concentrations can be obtained at 6000°K., but at this temperature, very high pressures—about 10^4 atm.—are necessary to counteract the dissociation reactions.

Publication Date: January 1, 1966 | doi: 10.1021/ba-1966-0055.ch042

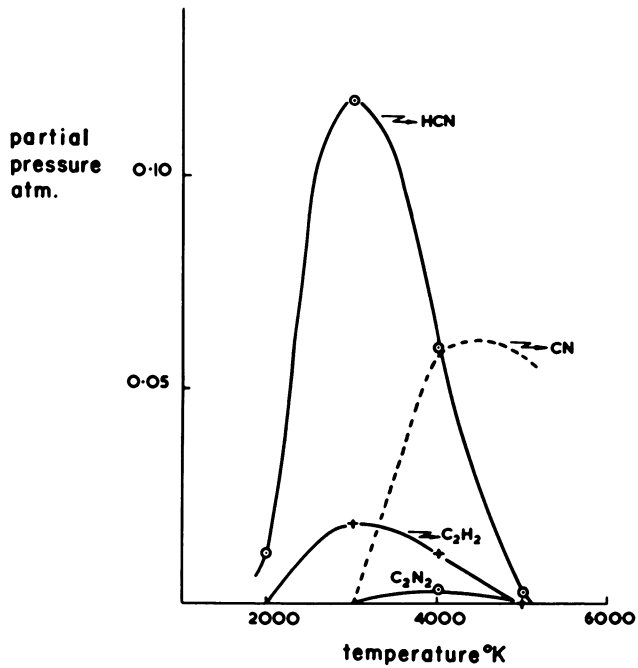

Figure 7. Equilibrium concentrations in the C-H-N system at 1 atm. pressure

Marynowski *et al.* confined themselves to the yields of hydrogen cyanide in the C-H-N system in which the numbers of carbon, hydrogen, and nitrogen atoms were equal. Smith and Robertson (*8*) have calculated the corresponding concentrations of other components. Typical results for the concentrations of hydrogen cyanide, acetylene, and cyanogen in the equilibrium mixture at atmospheric pressure are shown in Figure 7. The equilibrium concentrations of hydrogen cyanide, acetylene, and cyanogen pass through a maximum with increasing temperature. Over the whole temperature range, however, the equilibrium concentration of hydrogn cyanide exceeds that of cyanogen.

The equilibrium concentration of cyanogen radicals also passes through a maximum with increasing temperature, but the maximum occurs at a higher temperature than those of the other compounds. At 5000°K. and 1 atm pressure, the equilibrium concentration of cyanogen radicals exceeds that of hydrogen cyanide. The possibility therefore must be considered that the cyanogen radicals may form cyanogen when the equilibrium mixture is quenched. The equilibrium mixture, however, contains an excess of hydrogen atoms and, on quenching, these will probably combine with the cyanogen radicals to form hydrogen cyanide. Thus the general trend of the results for the C-H-N system is that at atmospheric pressure the concentration of hydrogen cyanide in the quenched gas will exceed that of cyanogen. This effect will be enhanced at higher pressures which favor the formation of hydrogen cyanide more than that of cyanogen radicals.

Publication Date: January 1, 1966 | doi: 10.1021/ba-1966-0055.ch042

High Temperature Carbonization of Coal

Lasers and plasma provide means for investigating the rapid carbonization of coal at high temperatures. Owing to the short residence time of coal particles in a plasma jet, it is unlikely that thermodynamic equilibrium or even thermal equilibrium will be attained. Moreover the gaseous products will be heavily diluted by the carrier gas. Nevertheless the thermodynamics presented here provide a useful guide to the type of products which may be expected at various temperatures and their relative yields.

The empirical formula of a typical low rank coal is $C_{100}H_{73}O_{10}N_1$. When the coal is rapidly carbonized at high temperatures, the volatile products probably will be evolved first, and this will raise the H/C ratio of the reactants above that of the coal. If the carbonization were carried out with an inert gas such as argon, the main gaseous product would be acetylene. Carbon monoxide would also be evolved from the oxygen in the coal along with traces of hydrogen cyanide. At atmospheric pressure, the optimum temperature range for acetylene formation would be between 3500° and 4500°K. Bond *et al.* (*3*) have reported yields of acetylene up to 25% by weight (on a carbon basis) from a low rank coal rapidly heated in an argon atmosphere by a plasma arc.

If the coal were carbonized at high temperatures in nitrogen, the main products would be hydrogen cyanide and acetylene. Very little cyanogen would be formed unless the nitrogen were greatly in excess of the hydrogen. At atmospheric pressure the optimum temperature for hydrogen cyanide formation would be about 3500°K.; higher yields should be obtained at higher

pressures. If cyanogen were required, it would be advisable to exclude hydrogen from the system by using coke or carbon instead of coal and heating it with nitrogen at about 4500°K.

Summary

Thermodynamics provide a useful guide to possible gaseous products from coal carbonization at high temperatures. This paper describes published and original work on the high temperature equilibria between carbon, hydrogen, and nitrogen.

Theoretical calculations by Baddour and Blanchet for the carbon-hydrogen equilibrium between 3500° and 4500°K. show that the quenched gas should contain high concentrations (40–50%) of acetylene. Theoretical calculations by the present authors for the carbon-nitrogen equilibrium at 4500°K. show that a cyanogen concentration of 15% should be obtained in the quenched gas. Marynowski *et al.* have shown that above 3000°K. the ternary system carbon-hydrogen-nitrogen should give appreciable yields of hydrogen cyanide. The implication of these results for coal carbonization has been discussed.

Acknowledgment

The work described in this paper was carried out as part of the research program of the Research and Development Department of the National Coal Board. The views expressed are those of the authors and not necessarily those of the Board.

Literature Cited

(1) Baddour, R. F., Blanchet, J. L., *Ind. Eng. Chem. Process Design Develop.* **3,** 258 (1964).
(2) Bauer, S. H., Duff, R. E., *Los Alamos Sci. Lab. Rept.* **LA-2556,** *Chem.,* **TID-4500.**
(3) Bond, R. L., Galbraith, I. F., Ladner, W. R., McConell, G. I. T., *Nature* **200,** 1313 (1963).
(4) Jones, W. Idris, *J. Inst. Fuel* **37,** 3 (1964).
(5) Kroepelin, H., Winter, E., "ASME Symposium on Thermal Properties," McGraw-Hill, New York, 1959.
(6) Marynowski, C. W., Phillips, T. C., Phillips, J. R., Hiester, N. K., *Ind. Eng. Chem. Fundamentals* **1,** 52 (1962).
(7) Plooster, M. N., Reed, T. B., *J. Chem. Phys.* **31,** 66 (1959).
(8) Smith, P. H., Robertson, V., private communication

RECEIVED October 5, 1964.

Discussion

Robert Friedel: In your calculations on the C-H-N system have you considered species related to hydrazine?

H. Alan Standing: Hydrazine was included in the general theoretical system of Marynowski and his co-workers. The theoretical concentration of hydrazine in the equilibrium mixture is small compared with that of HCN.

Gas Phase Chlorination of Coal

Construction and Evaluation of Apparatus and Reaction

S. C. SPALDING, JR. and J. O. BURCKLE

Chemstrand Co., Decatur, Ala.

W. L. TEISER

Esso Research & Engineering Co., Florham Park, N. J.

Publication Date: January 1, 1966 | doi: 10.1021/ba-1966-0055.ch043

To evaluate the chemical behavior of coal in a free radical environment when the coal solids themselves are in a condition of maximum free radical content, a fluidized bed gas phase reactor was set up; it is suitable for handling and heating the reactants to approximately 600°C. Evaluation runs indicate that the coal will undergo "chlorinolysis," and among the products will be carbon tetrachloride, phosgene, and possibly a chlorinated sulfur derivative together with a subliming solid as yet uncharacterized.

The extensive literature on the thermal degradation of variously ranked coals indicated that interesting products might be obtained if this reaction (depolymerization) were conducted in a chlorine environment. Because of its high reactivity, chlorine poses problems of containment, especially if it becomes wet or contaminated with hydrogen chloride or oxygen. Elevated temperatures exacerbate the containment problem as do heating and cooling of these gaseous mixtures.

Experimental

Self-bonded silicon carbide was used in that part of the apparatus where high temperatures were necessary together with high heat transfer rates. Borosilicate glass for tubing and condenser surfaces together with polypropylene plastic pipe were also used. In this way temperatures up to 600°C. could be tolerated by the reactor section, and heat transfer occurred easily by conduction through the reactor wall using Scotchlite beads as a fluidized bed material.

In Coal Science; Given, P.;
Advances in Chemistry; American Chemical Society: Washington, DC, 1966.

The design temperature of 600°C. was chosen by considering coal as a free radical source. Electron spin resonance studies of coals (*1*) indicate that a rather sharp maximum in nonspin-paired electron content occurs in coals when processed in this temperature zone—i.e., 500°–550°C. Chlorine moreover can be converted to atomic chlorine by several energy sources—corona discharge, silent electric discharge, *ca.* 4700 A. light, etc.

The coal was processed under these conditions using the experimental setup shown in Figures 1 and 2. In Figure 1 the process flow diagram is presented with indicator and/or controller points for both temperature and flow. The pressure indicator controller (PIC) was a cylinder regulator. A double diaphragm regulator was used on the nitrogen supply. The liquid chlorine maintained a constant cylinder pressure, and a double diaphragm valve was not necessary for constant flow to the system. Ammonia was also liquid in the

Publication Date: January 1, 1966 | doi: 10.1021/ba-1966-0055.ch043

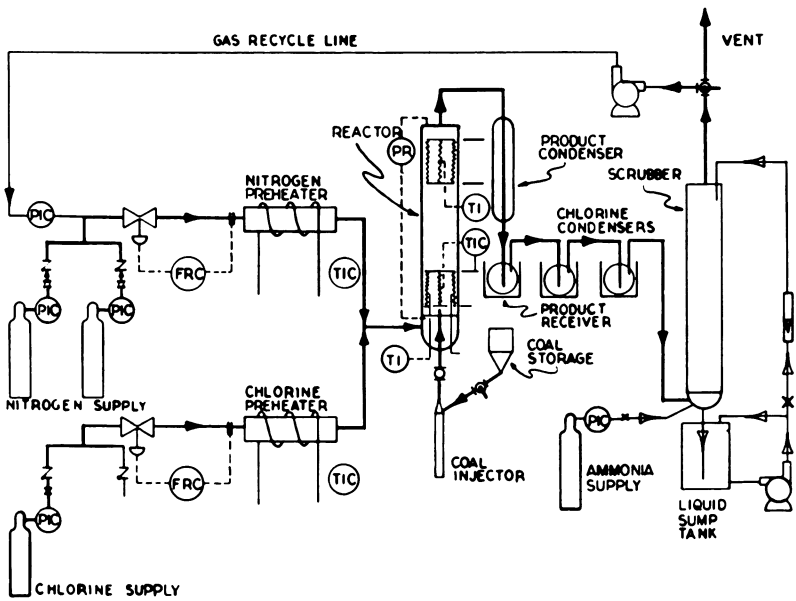

Figure 1. Process flow diagram

cylinder, and no difficulty was encountered in controlling these flows by simple, single diaphragm cylinder regulator valves. The pressure recorder (PR) was used to indicate the pressure differential across the fluidized bed and was a very effective monitor of the degree of fluidization. The flow recorder controller (FRC) represents closed loop flow control and recording of the gases used to fluidize the bed. The differential pressure across an orifice meter actuated pneumatic flow control-record system with reset and proportional band operation, which in turn actuated a pneumatic motor valve for delivering chlorine, nitrogen, or air to the system. Air and nitrogen were delivered

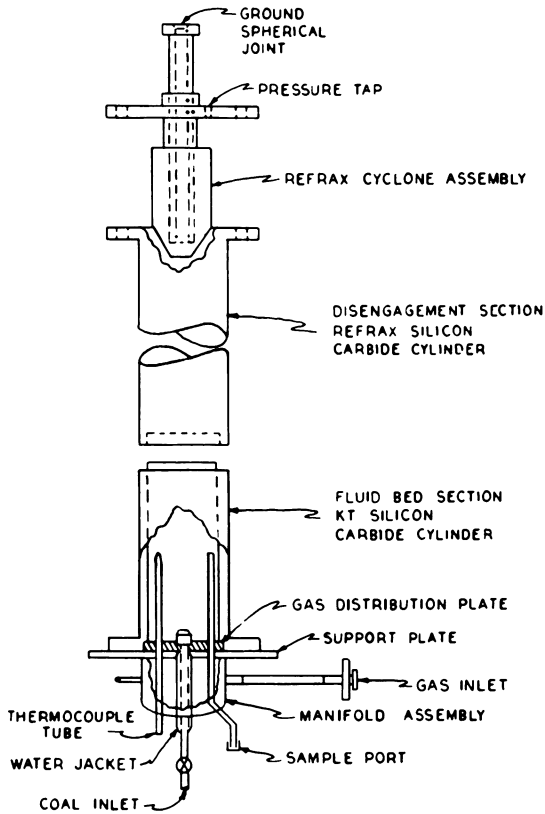

Figure 2. Reactor diagram

through the same piping, and only one FRC system was required. Chlorine was delivered separately by its own piping and FRC system.

The temperature control and/or indication was carried out more or less separately. Because the heating was electric, fairly close top temperature limits had to be observed. Monitoring and closed loop control were carried out at the critical surfaces-heating element faces or hot walls. Nickel may not be used in excess of 950°F. in chlorine duty; heater sheath temperatures carry 1200°F. and 1500°F. duty limits, and heating tapes may not exceed 800°F. Therefore, to achieve 500–525°C. for the gas temperature, the reactor was held at 650°C. using a temperature indicator-controller (TIC) system which was closed loop control in three stages. Initially the thermocouple signal unbalance was magnetically amplified for output to a small magnetic amplifier which generated a control signal for a saturable core reactor in series with the heating load. This control was characterized by limited reset and proportional band operation. This mode of temperature control was used for the two gas preheater furnaces. The reactor space temperature was obtained by a thermocouple inserted into a bulb which was about 8 inches above the reactor gas

Publication Date: January 1, 1966 | doi: 10.1021/ba-1966-0055.ch043

Table I. Operational Data

Run No.	Bed Temp., °C. Initial	Final	Corona Excitation	Coal in from	Charged Volume in ml. Beads	Coal	Coal to pass screen No.
6	394	403	No	Bottom	250	1500	200
8	250	250	Yes	Bottom	250	1500	200
9	27	54	Yes	Bottom	250	1500	200
11	25	78	Yes	Bottom	250	1500	200
13	475	390	Yes	Bottom	250	1500	200
14	525	470	Yes	Top	200	1500	200
15	520	500	Yes	Top	150	1500	50

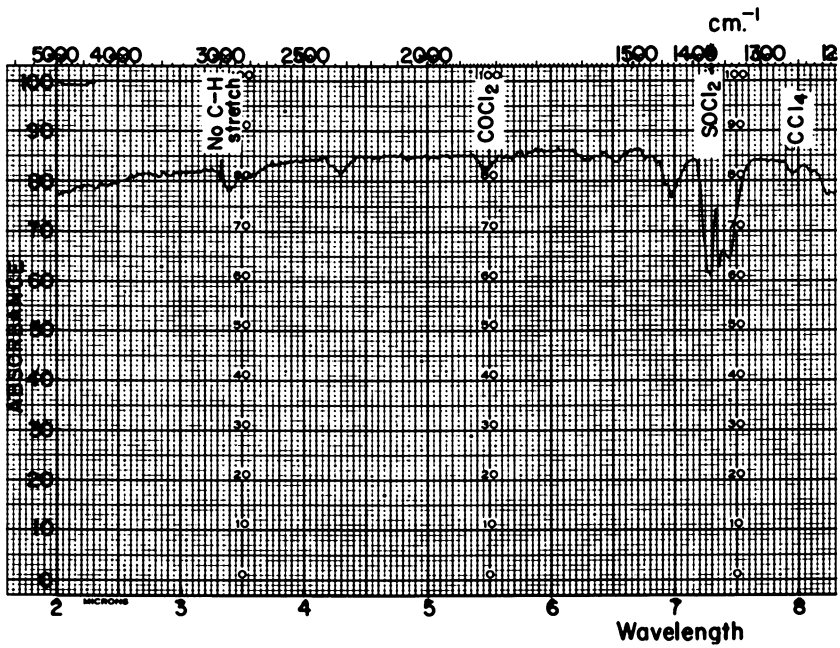

Figure 3. Infrared

distribution plate. This bulb was a two-piece assembly of silicon carbide inserted into the reaction space with a nickel coupling welded into the column support. There was no taper on these threads; hence, when the ceramic was screwed down tight, no compression was achieved, and gas leakage occurred with severe consequences to the thermocouple. The monitoring instrument was a 2200-ohm, 0–50 microammeter movement, standard 4-inch square face meter, which was calibrated using a standard thermocouple potentiometer. A ten point commutator was used for switching from point to point.

Figure 2 is a schematic diagram of the two-section reactor body and accessories. The fluid bed section was made of self-bonded silicon carbide, 16 inches high by 6¾ inches o.d. with a recessed flange. The recess accommodated a 120-mesh porosity silicon carbide gas distribution plate. The nickel manifold assembly was topped by a heavy support flange. This manifold sup-

Publication Date: January 1, 1966 | doi: 10.1021/ba-1966-0055.ch043

plied several services: pressure tap, gas inlet, cooled coal inlet, bed solids sample outlet, and thermocouple tube. The upper section, head, cyclone, etc. are well illustrated in Figure 1. The corona discharge electrode was inserted through the ceramic pipe with the label "ground spherical joint." A 1-inch glass tubing line with an outlet for the corona electrode coming straight out also connected this ceramic pipe to the product condenser as shown in Figure 1.

Chlorine excitation was obtained by a corona discharge on platinum wire points at 40 kv., 2 ma., and 4–5 Mc. from the tesla coil output of a vacuum system leak tester. According to Steacie (*3*) more than 40% atomic chlorine

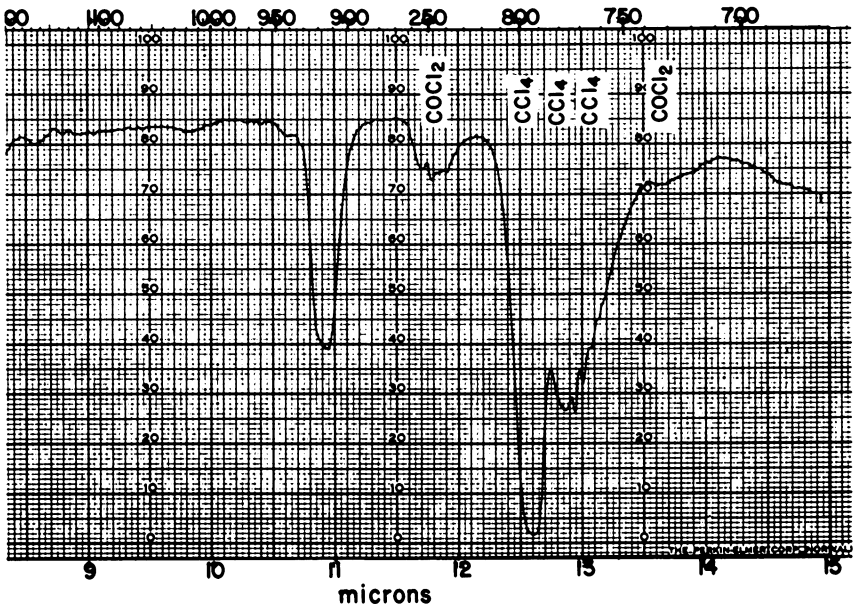

spectrum for residual gases, Run #15

can be formed using such techniques; however, without using such techniques, thermal dissociation is inconsequential at these temperatures.

Method. The reactor was brought on stream in the following manner: air was used to fluidize the bed while the heaters brought the bulb temperature in the bed space to between 500° and 535°C. This corresponds to thermal equilibrium with a heater sheath to reactor wall temperature of 650°C., the control point. Prepurified (99.8%) grade nitrogen was then used to displace the air from the system. The nitrogen, in turn, was displaced from the assembly by chlorine. The reactor bulb temperature site was monitored by spot temperatures taken by periodically inserting the thermocouple into the bulb. The reason for not leaving the thermocouple in the bulb throughout the reaction has been explained above, and mention here need only be made that the chlorine leakage consequent to the assembly method destroyed thermocouples if they were left in contact for any period of time. The complete displacement of nitrogen was indicated by condensation of chlorine in

Publication Date: January 1, 1966 | doi: 10.1021/ba-1966-0055.ch043

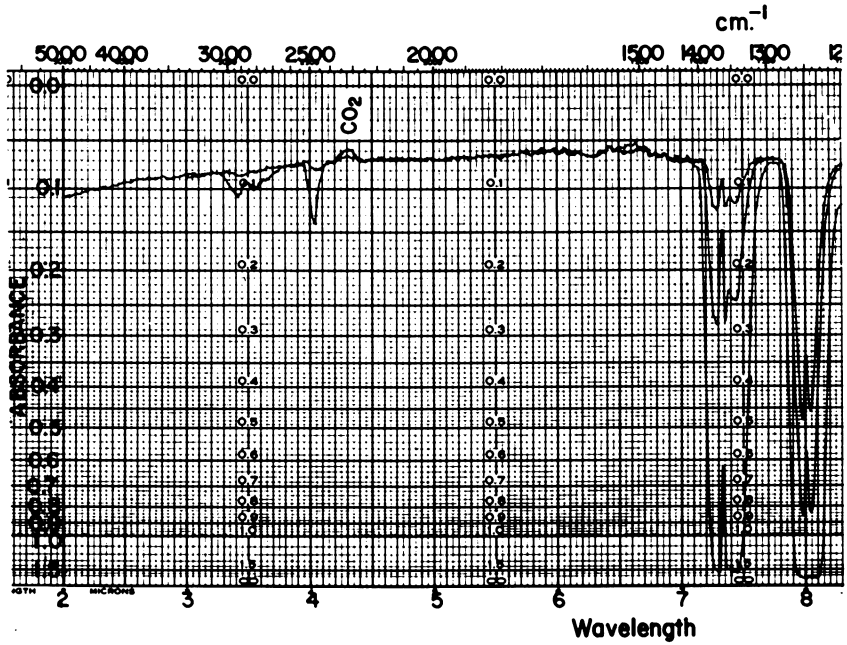

Figure 4. Infrared

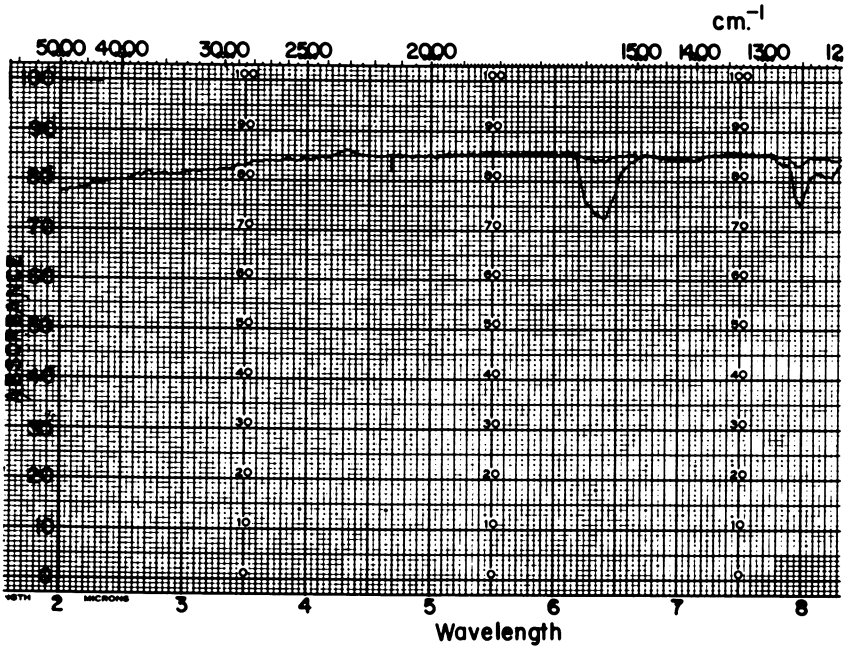

Figure 5. Infrared

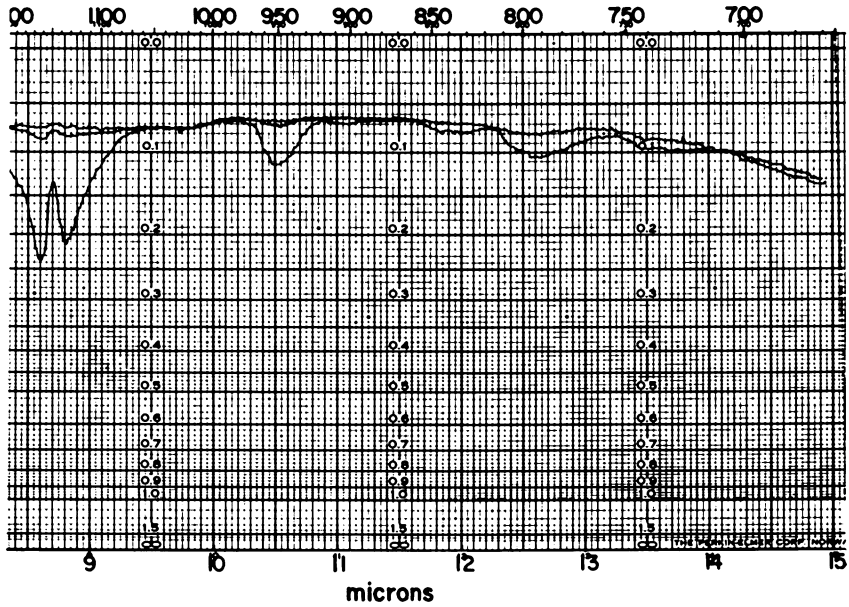

spectra for thionyl chloride

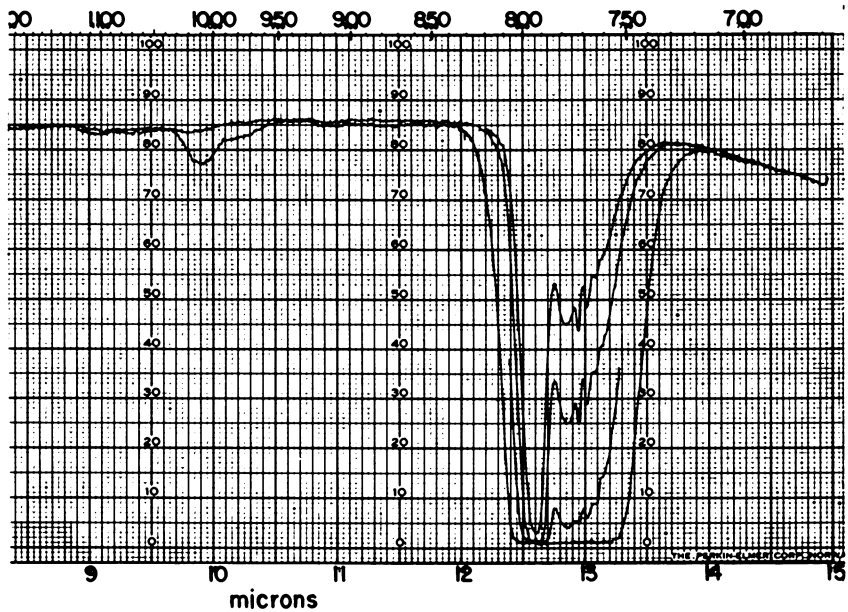

spectra for carbon tetrachloride

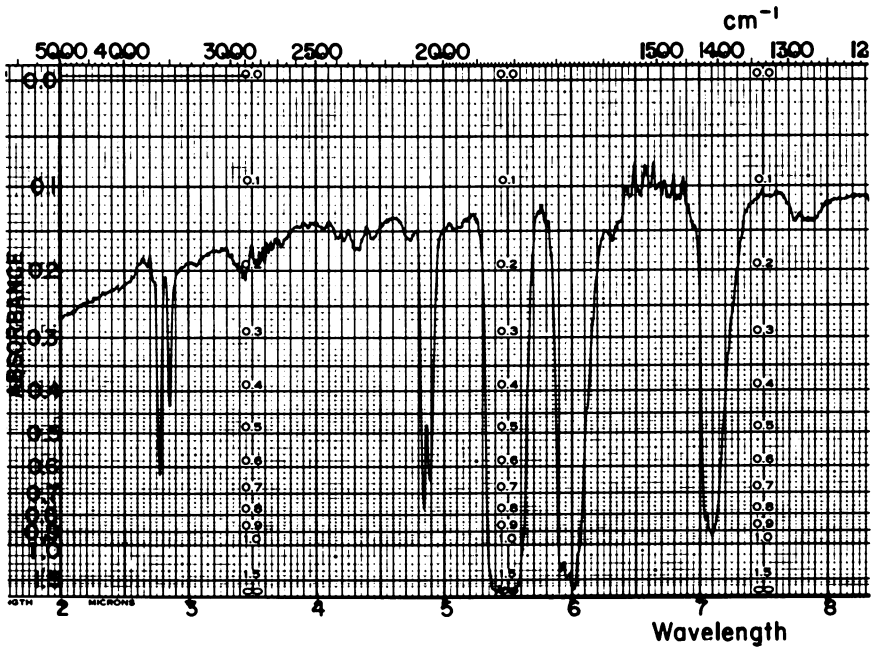

Figure 6. Infrared

the dry ice-methanol chilled condenser which led to the first tar chiller. When this time point was achieved, coal was slowly introduced by whichever feed device was used, chlorine of course was being passed through the apparatus continuously and was not recycled.

Results

In a given run for more than 3 hours as much as 2.5 liters of liquid chlorine accumulated in the last tar chiller. This large reservoir of chlorine introduced operational problems in the system and forced early termination of the runs.

The actual experiments reported here are exploratory and certainly qualitative in character. Table I shows some of the usual parameters for measuring and logging reactions. The unreported runs represented either failure of some part of the apparatus because of the extreme corrosiveness of the system studied or failure of the system to achieve design temperatures or runs using oxygen mixtures.

The significant runs, from the standpoint of characterized products, are No. 14 and No. 15. An infrared absorption spectrum (Figure 3) was obtained using the residual gases after chlorine was removed by distilling liquid chlorine. For comparison Figure 4 shows the spectra for thionyl chloride, Figure 5 for carbon tetrachloride at several concentrations, and Figure 6 for phosgene. Good evidence exists in Figure 3 for small amounts of phosgene, somewhat more carbon tetrachloride (*ca.* 0.25 atm.), together with a third compound

Publication Date: January 1, 1966 | doi: 10.1021/ba-1966-0055.ch043

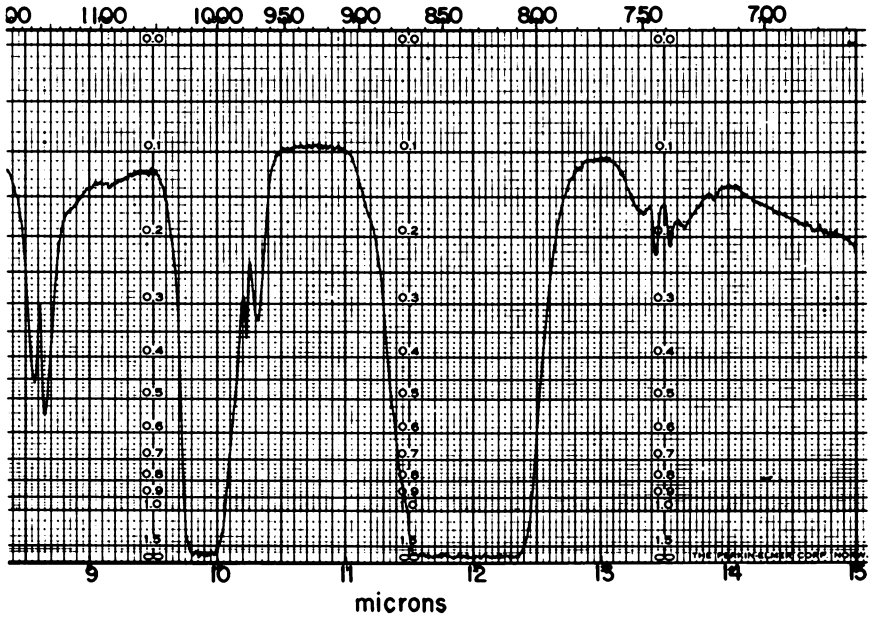

spectra for phosgene

closely related to thionyl chloride, as the triplet at 1360 cm.$^{-1}$ shows. Yet it otherwise is different. Also, neither carbon-hydrogen stretch frequencies nor carbonyl-oxygen frequencies were evident. The other product was a subliming white solid of cedary fragrance which was also difficult to dissolve. The remaining coal solids were readily burned out by air at a bed temperature of 500°C. The beads were left with a very pink residue which did not erode during the tumbling action of the bed but had to be dissolved in concentrated nitric acid then washed free of acidity by repeated washings with distilled water. The beads were washed free of acidity so that on reuse there would be no doubt concerning the presence of proton catalysis of the reaction rather than free radical reaction. The presence of phosgene in coal chlorination products when using ultraviolet light and lower temperatures has been observed by Pasha (*2*). Under these conditions phosgene was about three or more times more concentrated. However, in the products of these experiments no evidence was seen in the absorption spectra for either carbon tetrachloride or the sulfur compound.

Summary

Production as measured by lower molecular weight products is presently about 5% of the coal charged. So far, the evidence has favored only perchlorinated products. Provisions have been made to recycle the chlorine in order that longer runs would permit a closer approach to exhaustive chlorination of coal.

Publication Date: January 1, 1966 | doi: 10.1021/ba-1966-0055.ch043

Acknowledgment

The authors are deeply indebted to the extensive support provided by the National Science Foundation which made grants to obtain the apparatus and to support the research of Mr. Burckle.

Literature Cited

(1) Lowry, H. H., Ed., "Chemistry of Coal Utilization," Suppl. Ed., p. 78, John Wiley and Sons, New York, 1963.
(2) Pasha, M., Master's Thesis, University of Louisville, 1964.
(3) Steacie, E. W. R., "Atomic and Free Radical Reactions," p. 37, Reinhold Publishing Co., New York, 1946.

RECEIVED October 5, 1964. Contribution from the Chemical Engineering Department, Speed Scientific School, University of Louisville, Louisville, Ky.

Discussion

Bhupendra K. Mazumdar: I do not see how a significant amount of useful products could be obtainable by degradation in the presence of chlorine. We have found that treatment by chlorine before or during pyrolysis inhibits tar formation completely. Consequently, 93–94% of the carbon in the coal is fixed in the char. Thus, only a relatively small proportion of carbon could be devolatilized, leading to the formation of small amounts of "interesting products."

S. C. Spalding: Concerning the necessarily simple product spectrum from the chlorination, I would comment that the physical evidence on yields from the run at 500°C. would seem to preclude the possible formation of a structurally simple product. It seemed that about one-third of the coal appeared as an oil. Some white solid substance sublimed out of the reaction zone and precipitated in the cooler zones.

Pyrolysis of Polycyclic Compounds Containing Sulfur

P. X. MASCIANTONIO and J. W. WALTER

Applied Research Laboratory, U. S. Steel Corporation, Monroeville, Pa.

Publication Date: January 1, 1966 | doi: 10.1021/ba-1966-0055.ch044

The pyrolysis of polycyclic compounds has been of considerable interest in studying carbonization and the manufacture of carbon products. It is usually desirable to minimize the sulfur content of the carbonaceous residues resulting from pyrolysis of organic materials. To understand the disposition of sulfur during pyrolysis, a series of model polycyclic sulfur-containing compounds has been pyrolyzed at 625°C. A correlation between the sulfur distribution and the elemental composition of the model compounds has been observed. A mechanism of desulfurization that involves the probability of combining hydrogen and sulfur atoms during pyrolysis appears to fit the experimental data best. The study indicates that the volatile matter and oxygen content of the model compounds are also significant factors in desulfurization.

Most of the solid carbonaceous material available to industry is derived from the pyrolysis of petroleum residues, coal, and coal tar residues. Understanding the reactions occurring during pyrolysis would be beneficial in conducting materials research on the manufacture of carbonaceous products. The pyrolysis of aromatic hydrocarbons has been reported to involve condensation and polymerization reactions that produce complex carbonaceous materials (*1*). Interest in the mechanism of pyrolysis of aromatic compounds is evidenced in a recent study by Edstrom and Lewis (*2*) on the differential thermal analysis of 84 model aromatic hydrocarbons. The study demonstrated that carbon formation was related to the molecular size of the compound and to energetic factors that could be estimated from ionization potentials.

There has long been an interest in eliminating sulfur during pyrolysis of organic substances (*3*); however, little fundamental data pertinent to formation of carbonaceous residues are available on the pyrolysis of sulfur com-

In Coal Science; Given, P.;
Advances in Chemistry; American Chemical Society: Washington, DC, 1966.

pounds. The selection of materials suitable for conducting systematic studies presents a problem in such an investigation. Because petroleum residues, coal, and coal tar residues are very complex in chemical composition, it is difficult to study sulfur distribution during pyrolysis of such materials. Furthermore, the effects of mineral matter and other heteroatoms, such as oxygen and nitrogen, on pyrolysis and sulfur distribution are not well understood.

To study the effect of chemical composition on sulfur distribution during pyrolysis, it appeared desirable to study the pyrolysis of sulfur-containing model compounds of well-defined structure. The correlation of chemical composition and sulfur distribution during pyrolysis is the subject of this paper.

Experimental

Publication Date: January 1, 1966 | doi: 10.1021/ba-1966-0055.ch044

A series of 10 polycyclic compounds and blends with starch, Bakelite, and hydrogenated creosote were employed as model substances to examine the effect of carbon, hydrogen, and oxygen on sulfur distribution during pyrolysis at a temperature of about 625°C.

Materials. To satisfy the requirements for models for pyrolysis studies, it was necessary to select compounds that were of high purity and well-defined structure which would produce carbonaceous residues when subjected to high temperatures. Commercially available organic dyestuffs proved to be a ready source of model compounds containing various heterocyclic structures. It was necessary to purify these dyes by recrystallization and extraction to remove small quantities of organic impurities and residual inorganic contaminants. The identity, structure, and chemical composition of the model compounds can be seen in Table I and Figure 1.

Starch and Bakelite were obtained from stock supplies and were used as-received for pyrolysis studies of blends. Hydrogenated creosote was prepared in the laboratory by catalytically hydrotreating a 270°–355°C. creosote fraction to remove all heterocyclic impurities and to saturate completely the ring systems.

Apparatus. Pyrolysis experiments were conducted in a quartz tube heated by an induction furnace. A continuous flow of argon was used to sweep out gaseous pyrolysis products. The materials to be pyrolyzed were contained in alundum boats, which could be readily admitted and removed from the quartz pyrolysis tube.

Table I. Data on Pyrolysis

Compound	Composition, atom %			
	C	*H*	*O*	*S*
Ciba Pink B	57.2	28.6	7.14	7.14
Sulfur Black 2B	46.2	27.0	3.84	11.50
Hydron Blue G	56.3	22.0	7.80	7.80
Flavon GC	58.4	29.2	4.17	4.17
Alizarin Black B	49.2	32.1	13.20	1.89
Indanthrene Brown	60.0	30.0	5.00	5.00
Blue-Green FFB	66.7	25.9	3.71	3.71
Algol Orange RF	47.6	38.1	9.53	4.76
Ciba Orange R	62.6	25.0	8.34	4.17
Cibanone Yellow R	59.2	30.2	9.22	1.32

Procedure. Experiments were conducted in the following manner. A 3-gram sample of the material to be pyrolyzed was weighed into an alundum boat. The sample was then placed in the cold furnace within the quartz tube, and argon was passed slowly through the system. The tube was heated to 625°C. over 2 hours and then allowed to cool to room temperature with the flow of argon continuing throughout the cycle. The carbonaceous residue was then accurately weighed, and its elemental composition was determined. Volatile matter was calculated from the quantity of residue. Data were obtained from replicate experiments on model compounds and single experiments on the blended materials.

Results and Discussion

Experimental data were obtained on the carbonaceous residue (char), and sulfur distribution was calculated for the solid and gaseous products from the pyrolysis of model compounds. Sharp differences were observed in the quantity of char and the sulfur distribution for the different substances studied. The quantity of volatile matter varied from 21 to 43%. The sulfur retained by the char varied from 21 to 74% of the total present in the compound pyrolyzed (*see* Table I). The raw data show a possible relationship between the volatile matter and sulfur retention which indicates that as volatile matter decreases, sulfur retention generally increases (Table I). Neither structural features nor the molecular size of the various model compounds appear to have a significant relationship to sulfur distribution.

In an attempt to correlate sulfur distribution with elemental composition, the mechanism of sulfur elimination was assumed to involve two processes: (1) molecular fragmentation to form volatile sulfur-containing compounds, and (2) reactions between hydrogen and sulfur to form H_2S (*see* Figure 2). Therefore, the loss of sulfur by molecular fragmentation should be related to the volatile matter realized from the material pyrolyzed, and the formation of H_2S should be related to the hydrogen and sulfur contents of the substance pyrolyzed.

The sulfur ratio, defined as the ratio of weight percent sulfur in the char to the weight percent sulfur in the dye, provides an interesting parameter regarding sulfur volatilization. The three compounds with sulfur ratios between

of Model Compounds

Volatile Matter, wt %	*Sulfur Ratio*	*Sulfur Retained, wt %*	P_{H_2S} (10^4)	P_T (10^4)
43	0.38	21	3.15	1.35
42	0.40	23	5.86	2.46
31	0.43	30	4.38	1.36
29	0.56	40	2.50	0.73
35	0.64	42	0.84	0.22
34	0.74	49	3.00	1.02
21	0.70	56	1.71	0.36
37	0.91	58	3.75	1.39
39	0.97	59	1.09	0.43
25	0.98	74	0.56	0.14

Publication Date: January 1, 1966 | doi: 10.1021/ba-1966-0055.ch044

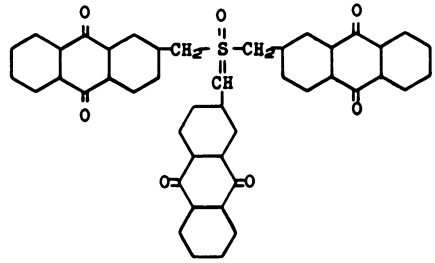

Cibanone Yellow R

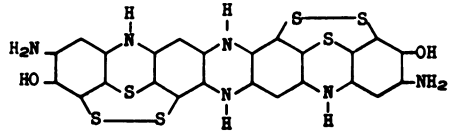

Sulfur Black 2B

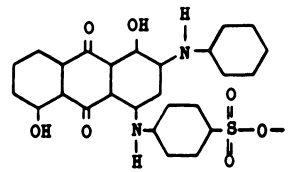

Alizarin Black B

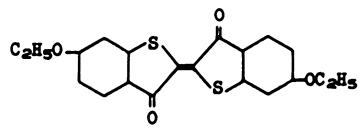

Algol Orange RF

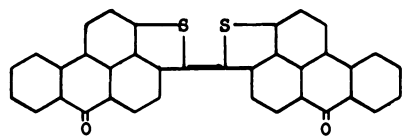

Blue-Green FFB

Figure 1. Structure

0.38 and 0.43 have a significant desulfurization reaction occurring during pyrolysis whereas compounds that exhibit values greater than 0.90 apparently lose sulfur principally by molecular fragmentation. To test this mechanism, the probability of H_2S formation was calculated for each of the model compounds using Equation 1.

$$P_{H_2S} = \frac{(H)}{(A)} \times \frac{(H-1)}{(A-1)} \times \frac{(S)}{(A-2)} \qquad (1)$$

Publication Date: January 1, 1966 | doi: 10.1021/ba-1966-0055.ch044

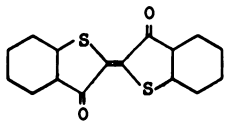

Ciba Pink B

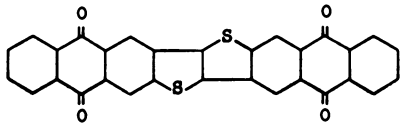

Ciba Orange R

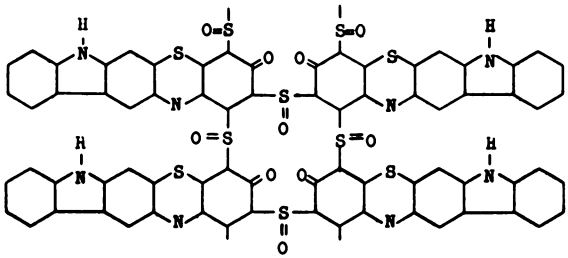

Hydron Blue G

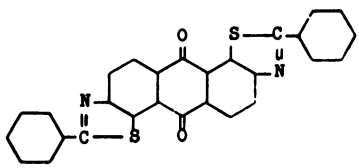

Flavon GC

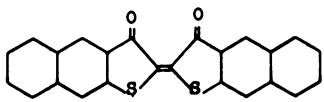

Indanthrene Brown

of model compounds

Here, P_{H_2S} = the probability of H_2S formation, H = total number of available hydrogen atoms, S = number of sulfur atoms, and A = total number of atoms. Because oxygen is a major component and since the quantity of hydrogen available for forming H_2S is affected by the amount of hydrogen that reacts with oxygen atoms to form H_2O, a correction was applied to the total hydrogen content of the pyrolyzed material to account for the effect of water formation. The expression $H = H_T - O_T$ was used for correction, where H_T and O_T are

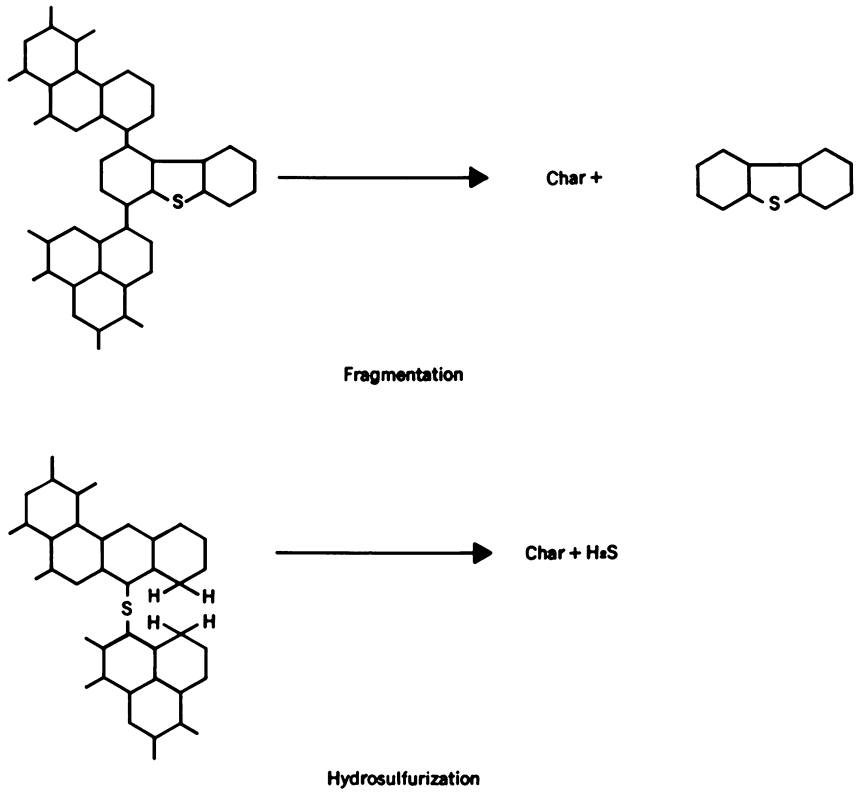

Figure 2. Process for sulfur elimination

the total hydrogen and oxygen, respectively. It was assumed that about one-half the oxygen would be involved in other reactions such as carbon monoxide formation. The values obtained for $P_{H,S}$ can be seen in Table I. Since sulfur distribution also involves fragmentation, the total sulfur elimination during pyrolysis should include a factor for volatile matter (V). The percentage weight loss during pyrolysis was taken as the value for V. An empirical expression representing a sulfur elimination factor (P_T) can then be expressed as

$$P_T = P_{H,S} \times V \quad (2)$$

Values of P_T calculated from Equation 2 also appear in Table I, and the relationship between P_T and experimental values of sulfur retained is presented graphically in Figure 3. The data indicate that sulfur retention by the char increases as the value of P_T decreases.

Because it was difficult to examine gradual changes in composition with the available model compounds, experiments were conducted using blends of starch, Bakelite, and hydrogenated creosote to obtain more data on the effect of oxygen and hydrogen atoms on sulfur distribution. Ciba Orange R was selected as the model compound for the blending experiments. The materials were blended by mixing together the solid components in a crucible.

Publication Date: January 1, 1966 | doi: 10.1021/ba-1966-0055.ch044

The composition of the various blends and the data resulting from the pyrolysis of the blends appear in Table II. Sulfur volatilization by fragmentation is not directly related to the volatile matter of the blend as was true with model compounds. For the same model compound (Ciba Orange R) in the various blends this factor is considered constant and has been neglected.

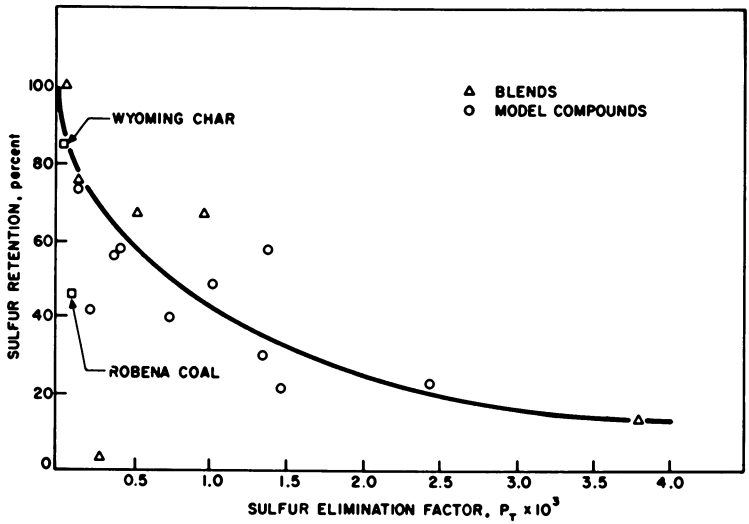

Figure 3. Sulfur elimination during pyrolysis

Table II. Data on Pyrolysis of Blends of Model Compounds

Blend	Composition, atom % C	H	O	S	Volatile Matter, wt %	Sulfur Retained, wt %	P_T (10^4)
1.0 Dye[a]	37.7	41.7	19.6	1.13	67	67	0.53
2.0 Starch 0.1 Dye	29.4	47.5	23.4	0.11	73	100	0.06
2.9 Starch 1.0 Dye	53.8	37.4	7.55	1.14	37	67	0.98
2.0 Bakelite 0.1 Dye	47.3	45.7	6.72	0.10	37	76	0.15
2.9 Bakelite 1.0 Dye	30.5	66.7	1.88	0.91	70	13	3.76
2.0 Naphthene 0.1 Dye	35.8	64.2	0.13	0.07	67	3	0.28
2.9 Naphthene Robena Coal[b]	53.4	42.6	3.64	0.28	29	46	0.12
3738–118–1 Wyoming Char	58.5	31.1	10.2	0.18	53	85	0.04
3940–64–2 Ciba Orange R	62.6	25.0	8.34	4.17	39	59	0.43

[a] Ciba Orange R
[b] Free of pyritic sulfur

Publication Date: January 1, 1966 | doi: 10.1021/ba-1966-0055.ch044

Values of P_T were therefore calculated from Equation 1 wherein $P_{H,S} = P_T$ for blended materials. The calculated values can be seen in Table II, and the graphical relationship between P_T and sulfur retained in the char can be seen in Figure 3. It is again apparent that sulfur retention increases as P_T decreases. The curve obtained from the data on the model compounds and blended materials can be used to predict the sulfur retention from the analytical data of the material pyrolyzed.

To test the usefulness of the curve depicted in Figure 3, samples of Robena coal and a char from Wyoming coal were examined. Pyrite was removed from the coal sample by extraction with molten caustic (*4*) before pyrolysis to eliminate interference from inorganic sulfur. The Wyoming char was prepared from Wyoming coal containing no detectable pyrite. Calculating P_T from analytical data on these materials (Table II) using Equation 2 gave a value of 0.12×10^{-3} for Robena coal and 0.04×10^{-3} for Wyoming char. The pyrolysis residues from these samples were analyzed, and sulfur retentions of 46% and 85%, respectively were observed. These values have been included in Figure 3 and appear to fit in a general way the data obtained from the model compounds.

Publication Date: January 1, 1966 | doi: 10.1021/ba-1966-0055.ch044

Summary

A series of model compounds has been examined to determine the sulfur distribution that occurs during pyrolysis at 625°C. The data indicate that there is a correlation between sulfur volatilization and the elemental composition of the material pyrolyzed. It is significant that volatile matter and oxygen content are important factors in addition to the concentration of hydrogen and sulfur. The molecular size and structure of model compounds appear to have little influence on sulfur retention. The equation correlating elemental composition and sulfur retention during pyrolysis appears to be applicable in a general way to experimental data from Robena coal and char from Wyoming coal.

Acknowledgment

The assistance of M. Katz and Genevieve Dudgeon in supplying analytical data for this investigation is gratefully acknowledged.

Literature Cited

(1) Conroy, J. S., Kinney, C. R., Murphy, D., Slysh, R. S., "Proceedings of the Third Conference on Carbon," Pergamon Press, London, 1959.
(2) Edstrom, T., Lewis, J. C., *Tech. Rept.* No. **WADD TR 61-72,** Wright-Patterson Air Force Base (1962).
(3) Given, P. H., Wyss, W. F., British Coal Utilization Research Association, Monthly Bulletin Vol. XXV, No. 5, May 1961.
(4) Masciantonio, P. X., "Abstracts of Papers," 148th Meeting, ACS, Aug.-Sept. 1964, p. 7L.

RECEIVED October 5, 1964.

Coalification of Woody Tissue as Deduced From a Petrographic Study of Brandon Lignite

WILLIAM SPACKMAN

The Pennsylvania State University, University Park, Pa.

ELSO S. BARGHOORN

Harvard University, Cambridge, Mass.

Publication Date: January 1, 1966 | doi: 10.1021/ba-1966-0055.ch045

The Lignogene suite of coal macerals is derived largely by vitrinization, fusinization, and micrinization of plant cell walls composed of cellulose or a cellulose-lignin complex. Early in coalification, unlignified cellulosic ray cell walls commonly transform with little evidence of developing a plastic phase. However, the lignified fiber-tracheid and fiber cell walls vitrinize to develop a semiplastic, sometimes almost fluid phase. The various fiber-tracheid and fiber wall layers respond differentially to vitrinization, and any single piece of wood appears to change heterogeneously. Sclerotic walls respond variously, yielding either high reflecting, dark-colord vitrinitic macerals, "normal" vitrinitic macerals, or low reflecting, cream-colored materials in lignitic coals. Source of at least three of the major maceral series was woody tissue of Brandon plants.

Coalification and carbonification are terms often used to describe collectively the processes involved in the formation and metamorphosis of coal substances. To be more definitive, such words as vitrinization, fusinization, or micrinization have been used. It is clear, however, that these terms describe sets or sequences of normal chemical reactions, in some instances accompanied by physical changes. Our ignorance of the details of coal substance formation and evolution has stimulated the use of these terms and the creation of others to indicate what we think we know concerning coalification. Vitrinization is

In Coal Science; Given, P.;
Advances in Chemistry; American Chemical Society: Washington, DC, 1966.

thought to involve a sequence of reactions different from fusinization, and both of these sets or sequences are probably different from the reaction sequence involved in forming macerals of the exinite series. Our present knowledge permits only general statements concerning the chemical changes occurring during maceral evolution and, in our opinion, this significantly deters advancing knowledge in many aspects of coal science.

What is the solution? First and foremost, the slow progress in this realm can be attributed to the coal petrographers. They undoubtedly have the initial role, for until the units comprising a heterogeneous mass are known, such units obviously cannot be sampled and studied. Fear of criticism has led the petrographer to adhere to simple concepts of coal seam constitution which regard all coals as consisting of less than a dozen common "macerals" and even fewer "lithotypes." Such reputed macerals and lithotypes often have been supplied to the chemist for study and were accepted as well-defined samples of high purity. Normally, the sample purity presented no problem, but the analytical data have often varied widely from sample to sample and when one investigator's study was compared with another. This has led to confusion and even disbelief in the value and importance of petrographic data. Of course, it is simply the result of including too many different entities in a single category.

It is useful for the petrologist to point to possible differences between coal substances as the first step in advancing basic coal science. His role, in this connection, is that of creating hypotheses which ascribe existence to certain coal substances and certain maceral-mineral aggregates so that the chemist and physicist may validate, refute, or amend the hypotheses to increase our knowledge of coal composition. The petrologist's job must be done first, simply because coal seams are rock masses, and the most expedient way to understand a rock mass thoroughly is to base one's study on that which can be perceived readily concerning entity distribution within the mass.

Because we are concerned with altered plant materials, the petrologist, as well as the chemist and physicist, should be aware of the hypotheses generated by paleobotanists concerning coal substance derivation and evolution. As in the case of the petrologist, the paleobotanist's contribution may often be restricted to creating hypotheses that will require validation, refution, or amending. This paper describes one type of contribution to coal petrology that can be made by the paleobotanist.

Materials Studied

The vitrinitic substances found in coal seams are commonly asserted to be derived from "wood" or "woody" tissue. The statement is usually made without any intention of being specific about what is meant by wood and, in fact, several non-wood tissues are often included intentionally in this broad generalization. It is generally agreed that various different substances are contained in these woody source materials and that several different biochemical, chemical, and physical processes may influence their alteration. In spite of this, our coal research has led many individuals to think of the vitrinites as forming a single maceral series. The coalified woods in the Brandon lignite

Publication Date: January 1, 1966 | doi: 10.1021/ba-1966-0055.ch045

provide us with an unusual opportunity to evaluate this concept and to examine some of the first products of the coalification of wood.

The Brandon lignite is a small deposit of Tertiary coal occurring in west central Vermont (*1*, *2*, *7*). It consists of a poorly stratified mass, composed of a mixture of coalified fragments of stems, roots, bark, seeds, fruits, flowers, and other plant parts in a matrix of organic and mineral debris. Prior reference has been made to the significance of this deposit with respect to coal petrology (*2*), and we would like to amplify the subject at this time with particular reference to the discrete fragments of coalified woody material. For the most part, we shall be concerned with the fragments of secondary xylem that are common in the deposits. These wood fragments are often identifiable as wood produced by plants belonging to the genera *Cyrilla*, *Persea*, and *Gordonia*. This being true, it is possible to associate paleobotanical and neobotanical facts, adding to one's knowledge of the original chemistry of the source materials. (The botanical identities of the coalified woods were determined by extensive comparative study using the Harvard Wood Collection. Identifications were confirmed by studying the other fossilized plant parts contained in the deposit.) Each wood is, of course, a complex tissue consisting of several cell types and several substances. The manner in which each has reacted to the coalifying conditions associated with the Brandon deposit may be valuable in understanding genetic interrelationships within the Lignogene maceral suite.

Publication Date: January 1, 1966 | doi: 10.1021/ba-1966-0055.ch045

Description of Observations

The lignitized materials will be discussed by comparing coalified products observed in each of the three wood types.

As in modern species (Figure 1), the secondary xylem found in the species of *Persea* represented in the Brandon deposit is composed of four basic cell types: (1) a matrix of fiber-tracheids, (2) vessels that commonly occur singly or in pairs, (3) ray parenchyma with "inflated" marginal ray cells, and (4) vascicentric xylem parenchyma. In the mature tree the first two cell types form the bulk of the wood. Both of these cell types are dead at maturity, hence devoid of protoplasm in the cell cavity. Their cellulosic cell walls are heavily impregnated with lignin, and the individual cell units are held together by an intercellular substance. The latter is initially composed of pectic compounds, and these are either heavily impregnated or replaced with lignin at maturity. Both primary and secondary walls are present, the latter being relatively thick. This cell wall material and the intercellular substances are about all these cell types offer to the coalifying processes. They form the bulk of the wood, and therefore these source materials are volumetrically important.

The cell walls of the vessels in *Persea* wood have reacted to the coalifying processes in a way that is different from the response of the fiber-tracheid walls, even though the two wall types may lie in juxtaposition. Microscopic study of thin sections, cut on a microtome, show that the vessel walls are yellow-tan in color, anisotropic, and morphologically intact though often deformed. In contrast, the fiber-tracheid walls have been converted to a yellow-brown to orange-brown, isotropic material that exhibits little of the original

anatomical structure (compare Figure 1 with Figures 2 and 3). This is interpreted to mean that much of the original cellulosic framework remains in the vessel element walls and that it has been destroyed in the walls of the fiber-tracheids. The anisotropy exhibited in Figure 4 also suggests this, and further confirmation has been obtained by extraction studies (2). The vessel cavities may contain a dark, reddish-brown, isotropic material (Figure 2), a yellow-brown, granular, isotropic material (Figure 3), a red-brown, granular, isotropic material, or the cavity may be devoid of any solid substance. A common feature of this wood is the presence of tyloses in the vessel. These are portions of adjacent parenchymatous cells that have grown into the vessel cavity through perforations in the side walls. In the wood studied they have become "sclerotic." Secondary wall layers have been deposited by the tylose cell, and these have become lignified. These tylose walls have responded to coalification in a distinctive manner, often yielding both a light yellow and a dark red product (*see* Figure 5). The primary wall (and probably the outermost secondary wall layer) commonly gives rise to the light-colored product, and the inner layers of the secondary wall frequently are converted into the dark-colored substance. In many instances there remains only a dark red product with no evidence of the original laminae that composed the wall. However, in all instances observed, the coalified secondary wall of the tyloses contrasted markedly with the light yellow or buff color of the vessel elements' secondary wall. This is shown in Figure 6. The tylose wall yields another product that deserves description—a granular material that ranges from a red-brown color to an optically dense state (*see* Figures 7 and 8).

Publication Date: January 1, 1966 | doi: 10.1021/ba-1966-0055.ch045

Figure 1. Transverse section of secondary xylem of Persea borbonia → *showing characteristic form of vessels, fiber-tracheids, vascicentric xylem parenchyma, and ray parenchyma in uncoalified wood.* 220×

Figure 2. Transverse section of coalified Persea *secondary xylem for comparison with Figure 1. At least three coaly products are shown: dark colored cell inclusions, vessel wall derivatives, and fiber-tracheid wall derivatives.* 304×

Figure 3. Transverse section of coalified Persea *wood showing: yellow-tan vessel wall material, orange-brown fiber-tracheid wall material, pale tan granular material in vessel lumen (just above center of picture), and dark colored tylose walls within vessel cavities.* 88×

Figure 4. Same as Figure 3 but with light partially polarized. Note anisotropy of vessel walls, suggesting retention of cellulosic framework. 88×

Figure 5. Transverse section of coalified Persea *wood showing a single vessel packed with tyloses. Note that the tylose walls are composed of a dark colored material that contrasts with the vessel wall residue.* 284×

Figure 6. Longitudinal section showing the yellow-tan, anisotropic material that typically forms the remnant vessel walls in the coalified Persea *wood. The contact between two vessel elements is shown with the dark red-brown tylose wall material in contact with the upper vessel element wall and extending across the perforation plate area into the lower element.* 784×

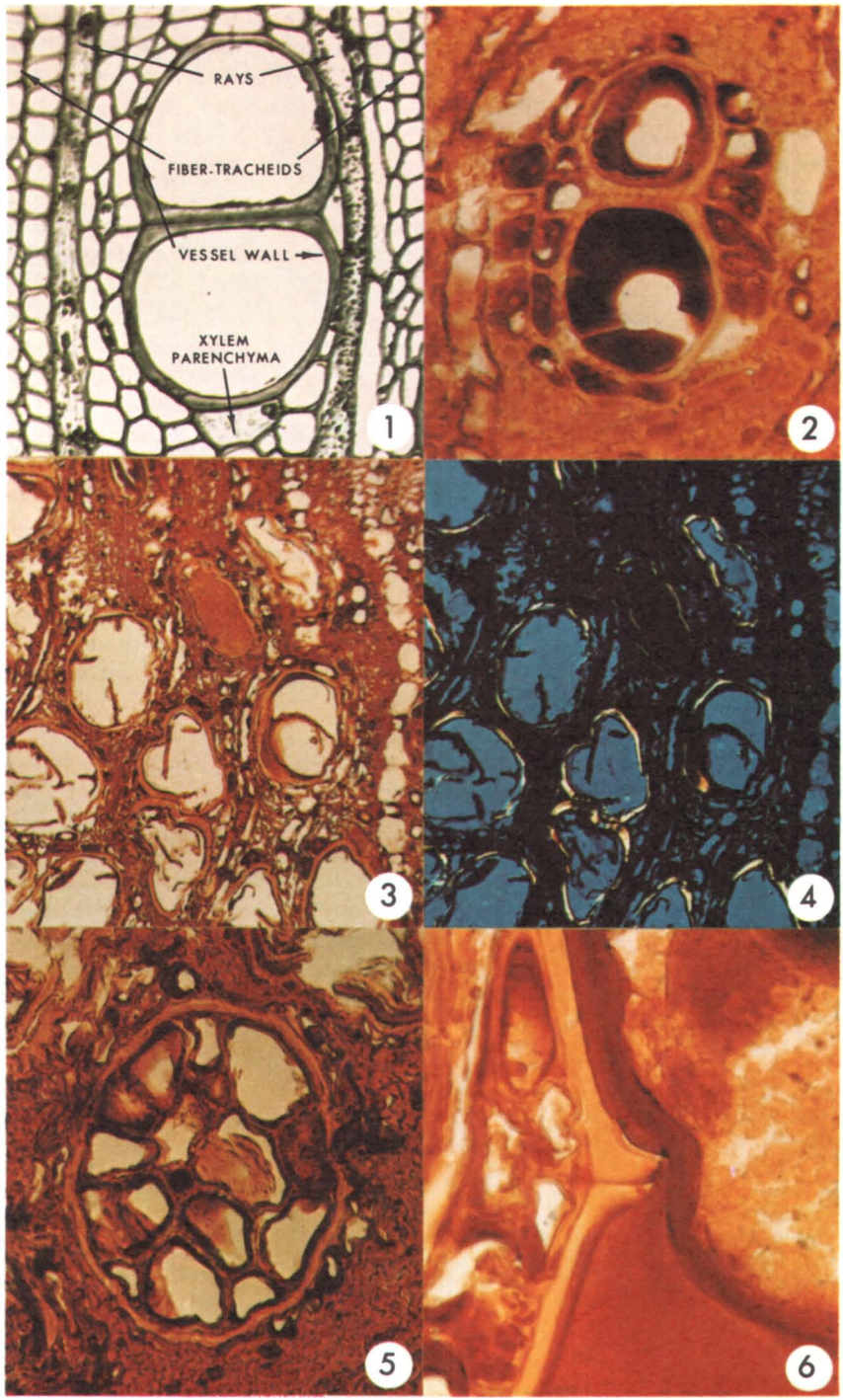

Publication Date: January 1, 1966 | doi: 10.1021/ba-1966-0055.ch045

In addition, the parenchymatous cells in the xylem appear to yield at least two lignitic materials. One is a dark red-brown material that may be derived from inclusions originally present in the cell. This material is common and may be observed in Figures 2, 3, 5, 6, 7, and 8. The other coalified product associated with this cell type is yellowish in color and derived from the wall of the cell (Figures 2 and 6). Ray parenchyma and longitudinal xylem parenchyma typically form only a primary wall, and usually the wall is devoid of lignin. It is of interest that this wall layer is preserved and that it is frequently possible to observe the simple pits that are characteristic of this cell type (Figure 2).

Contrasting with the response of the *Persea* wood, is that of the wood of *Cyrilla*. As previously mentioned, the vessel walls of *Persea* often have remained "morphologically intact." The comparable walls of *Cyrilla* exhibit responses ranging from in situ minor alteration to complete destruction or transformation to either a granular or a textureless residue. As Figure 9 shows, the vessel element walls frequently have become swollen as a result of coalification, and the innermost surface of the wall often exhibits a tuberculate or granular appearance. In some instances the swollen wall appears to have reduced the cell cavity to a fraction of its original size or to have eliminated the lumen completely. All transitions can be observed from an anatomically undistorted wall that has merely taken on some color as the result of coalification, through various degrees of swelling and granulation, to situations in which the original cell outline is faithfully preserved, but no recognizable wall or lumen remains. In the latter case, the area formerly occupied by the wall and lumen is now filled with either a vitreous, cream-colored material or a pale tan to brown granular substance (*see* Figure 9). It is difficult to envision the manner in which the large volume of material required to occupy the wall and lumen areas could be derived from the original wall substance. Longitudinal sections show no evidence that material flowed from one level in the vessel to a collecting site. It is possible that the vitreous and granular materials represent lignitized products of substances that occluded certain vessels in the living tree. Such vessel inclusions are not typical of *Cyrilla* wood, but they do occasionally occur. The frequency of this phenomenon in the lignitic wood casts doubt on this explanation, but the perfection of the cell outline argues for an emplacement of the material inside a walled chamber. If, during coalification, the vessel wall were in the process of swelling and approaching a plastic state and if the encasing matrix of fiber-tracheids were also in a plastic or semiplastic condition, it is difficult to conceive of a synchronous filling of the lumen without distortion of the cell outline. One possibility is that the thin primary wall of the vessel resisted any appreciable degradation until after the secondary wall was altered and the lumen eliminated, either by being filled with the by-products of secondary wall coalification or by infiltration of a foreign substance, derived, perhaps, from fiber-tracheid degradation.

Regardless of origin, four materials are found in the lignitic wood in the place of the vessels. These are: (1) buff colored, friable, isotropic material clearly derived from vessel walls, (2) yellow-brown, friable, isotropic material derived from vessel walls, (3) pale tan to brown, granular, isotropic secondary

Publication Date: January 1, 1966 | doi: 10.1021/ba-1966-0055.ch045

cell wall degradation material and lumen fillings, and (4) cream colored, vitreous, vessel lumen fillings.

The fiber-tracheids of *Cyrilla* yielded large quantities of an orange-brown, isotropic substance (Figures 9 and 10) with small quantities of a pale yellow anisotropic material that probably represents a remnant of the primary walls. "Wound tissue" is formed by *Cyrilla* under certain conditions. This consists of tangential layers of fibers that possess exceptionally thick walls and a very small lumina (Figure 10). The massive, multilaminate, secondary wall is composed of a pale yellow, anisotropic material, except that the outermost layer often is altered to an orange-brown substance that is indistinguishable from the material so commonly derived from fiber-tracheid walls (*see* left half of Figure 10). In Figure 10, a red-brown to optically dense material can be seen occupying the lumen of one of the centrally located fiber-tracheids. In the living tree the fiber-tracheids and parenchyma strands in the zone of "wound tissue" often contain dark colored inclusions. This granular material appears to have been derived from such a source. The ring of deep red-brown material in the cell adjacent to that containing the granular product probably is a cell wall derivative.

Although associated with *Persea* and *Cyrilla* wood in the same lignitic matrix, the wood of *Gordonia* was altered in a way quite different from that characteristic of the other woods. In almost all of the specimens examined, the vessel walls and cavities have been destroyed completely. This process of vessel wall destruction is so effective that previous investigators (*4*, *5*) mistakenly identified the wood as a conifer, calling it a *Pityoxylon*. Hence, in the case of the coalified *Gordonia* wood, virtually nothing remains that is identifiable as the derivative of vessel substances whereas in the case of both *Persea* and *Cyrilla* four or more coal substances were readily associated with vessel source materials. Another interesting feature of the response of *Gordonia* wood to coalification is the development of a homogeneous appearing, amber-brown substance from the walls, or at least in the position of the walls, of ray parenchyma cells (Figure 11). This was unexpected because of the presumed nonlignified nature of these walls. Although the amber-brown substance was usually formed, occasionally a cell in the ray yielded an almost colorless mass of material with a poorly defined wall remnant that also is almost colorless (*see* left half, Figure 11). These may represent cells that never reached maturity and whose walls were never impregnated with the source material, whatever it may be, of the amber-brown substance.

Figures 11 and 12 show that the coalified product derived from the fiber-tracheid walls, although lighter in color, is similar to that derived from such walls in the case of the other woods. Worthy of note, however, is the colorless material shown in both small and large strands in Figure 12. These appear to be remnants of portions of fiber-tracheid walls (the small strands) and ray parenchyma cell walls (the larger strand in the right half of the photograph). Material of this type studied thus far has proved to be isotropic.

Table I summarizes these observations by listing the coalified products derived from each cell type in the xylem. Only the more common materials are listed.

Publication Date: January 1, 1966 | doi: 10.1021/ba-1966-0055.ch045

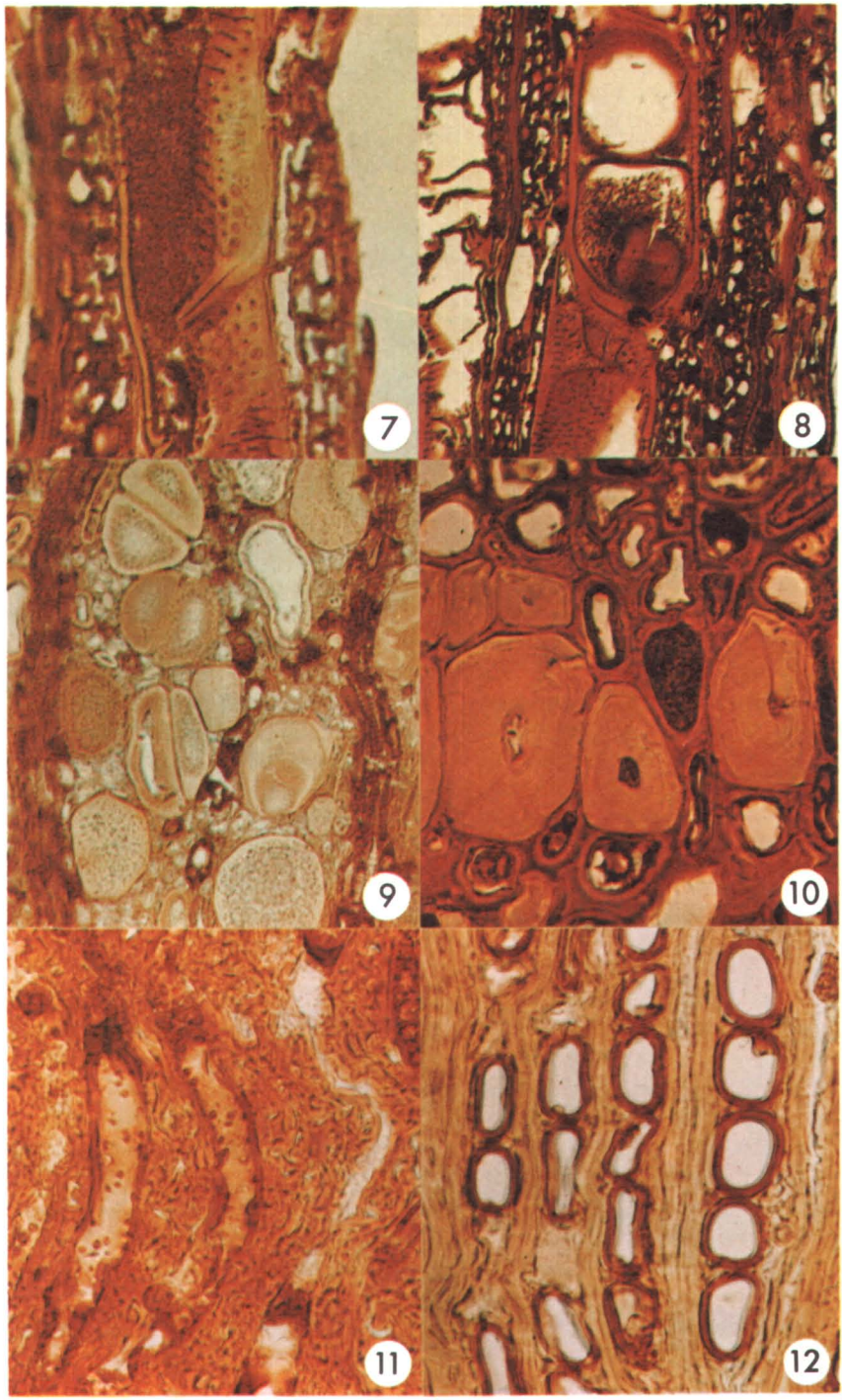

Publication Date: January 1, 1966 | doi: 10.1021/ba-1966-0055.ch045

In Coal Science; Given, P.;
Advances in Chemistry; American Chemical Society: Washington, DC, 1966.

Possible Relationships of Materials with Coal Macerals of Higher Rank

Although it is premature to assign the materials that have been described and illustrated to particular maceral classes, it may be useful to suggest possible affinities. At least four types of source materials are involved: vessel walls, fiber walls, parenchyma walls, and cell inclusions. This morphological classification of source materials is not a fully satisfactory basis for discussing coal substance development. More rational interpretations of maceral evolution could be made if the source materials could be differentiated on the basis of their chemical compositions. Lacking such knowledge, the four-fold differentiation of source materials suggested above does distinguish between the initial plant substances involved and, although the distinctions made are primarily botanical, there is a general implication concerning the chemical nature of the substances. For example, the vessel and fiber cell walls will typically contain large amounts of cellulose and lignin with pectins between the juxtaposed primary walls where the parenchyma walls are primarily cellulosic but are also surrounded with pectins, and the cell inclusions may be varied in composition but devoid of cellulose and lignin.

Publication Date: January 1, 1966 | doi: 10.1021/ba-1966-0055.ch045

← *Figure 7. Tangential section of coalified* Persea *wood showing the yellow-tan material derived from the vessel walls and a red-brown granular material derived from alteration of the tylose wall.* 113×

Figure 8. Tangential section of coalified Persea *wood cut thicker than that shown in Figure 7 to show effect of variable thickness on appearance. Note that the various coalified products are still readily differentiated.* 113×

Figure 9. Transverse section of coalified Cyrilla *wood showing various stages of vessel wall alteration. Note granular residue in vessel near bottom of photograph and vitreous material in small vessel near the center of the picture.* See *text for discussion.* 176×

Figure 10. Transverse section of coalified Cyrilla *wood through "wound tissue." Note differential response of the thick fiber wall layers to coalification. The outermost wall layers have produced an isotropic, orange-brown material whereas the bulk of the secondary wall has yielded a pale yellow, strongly anisotropic coal substance. A ring of dark red material has been produced from the inner secondary wall in the fiber-tracheid shown in the left center of the photograph and a semiopaque, granular product is seen in an adjacent tracheary element.* 323×

Figure 11. Tangential section of coalified Gordonia *wood showing amber-brown material produced from, or in the position of ray parenchyma walls. Note nearly colorless cell walls in the two rays on the left. Matrix of yellowish-brown material has been formed from alteration of fiber-tracheid walls.* 465×

Figure 12. Transverse section of coalified Gordonia *wood. The yellow-brown matrix material is derived from fiber-tracheid walls, the reddish material from ray parenchyma inclusions. Note colorless material in right half of photograph.* 607×

Table I. Summary of Common Maceral Materials in "Anthraxylon" from the Brandon Lignite

	Code Numeral[a]
Anisotropic Macerals	
1. Pale yellow material derived from normal or sclerotic fibers (Figures 9, 10)	[VI]
2. Yellow-tan material forming remnants of vessel walls (Figures 2, 3, 4, 5, 6)	[I]
Isotropic Macerals	
Hyaline material	
1. Colorless material occurring as cell wall remnants (Figures 11, 12)	[X]
2. Cream colored vessel lumen fillings (Figure 9)	[IV]
Granular material	
1. Pale tan to brown material: vessel derived (Figure 9)	[V]
2. Yellow-brown to red-brown material: tylose derived (Figures 3, 6, 7, 8)	[XII]
3. Red-brown to optically dense material: fiber-tracheid derived (Figure 10)	[IX]
Textureless material	
1. Buff colored, friable material forming remnants of vessel walls (Figure 9)	[II]
2. Yellow-brown, friable material forming remnants of vessel walls (Figure 9)	[III]
3. Orange-brown to brown material forming remnants of fiber-tracheid walls (Figures 3, 5, 10)	[VII]
4. Amber-brown material forming, or in position of, parenchyma wall remnants (Figure 11)	[XI]
5. Dark red or red-brown material occurring as cell inclusions (Figures 2, 5, 8, 9)	[XIII]
6. Dark red-brown material occurring as remnant cell walls (Figure 10)	[VIII]

[a] Numerals used to identify the different coalified products in Figure 13.

These four classes of source materials have given rise to at least 13 coalified products that appear to be optically distinguishable. These 13 products may represent as many as nine separate sequences in which plant substances are altered to coal substances and in which the coal substances are further metamorphosed from one maceral to another.

Figure 13 presents a diagrammatic representation of the relationships postulated for the wood-derived materials in the Brandon lignite. Each line represents the progressive alteration of some class of source substances by a particular sequence of processes. Each of the 13 coalified products described above is positioned on one of the lines by an identifying Roman numeral (*see* Table I). The height of the numeral on its particular evolutionary line represents a subjective assessment of the "degree of coalification." The presence of more than one Roman numeral on a line implies a genetic relationship between the materials designated by the numerals. In addition, the maceral groups to which the materials are related are identified at the upper end of each line. Hence, it is suggested that the vessel walls of *Persea* have been altered to an

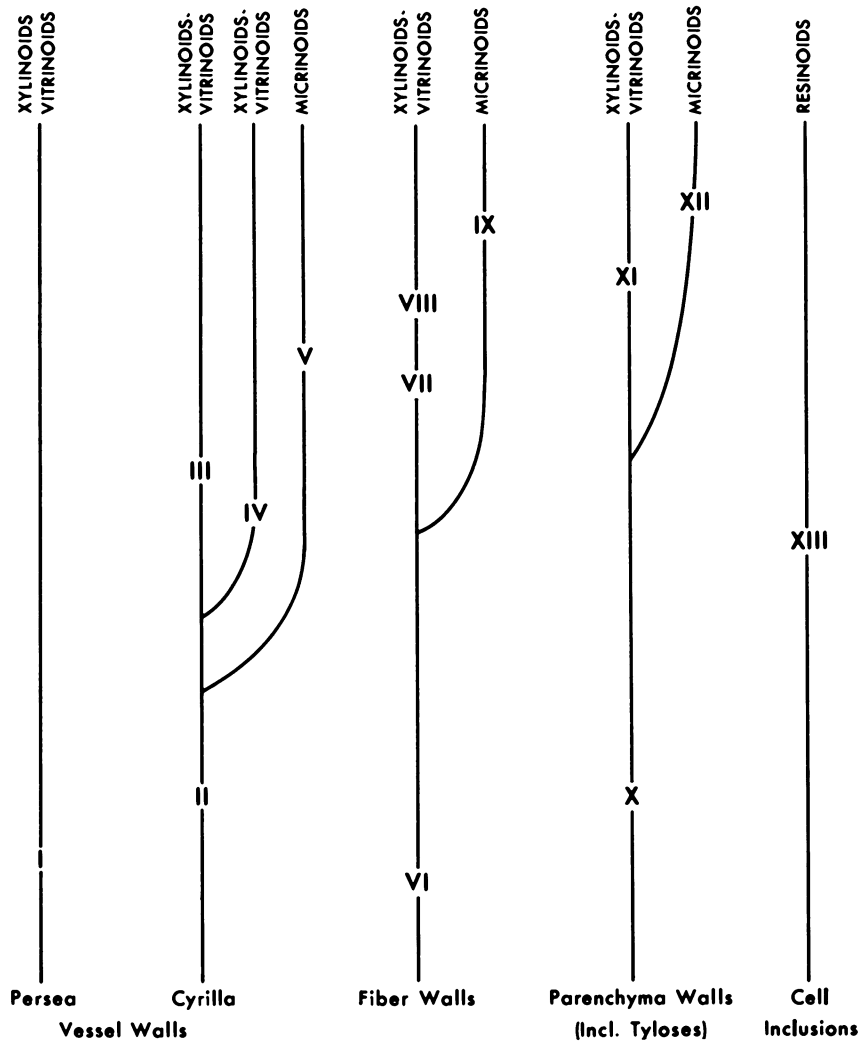

Figure 13. Postulated genetic relationships and suggested maceral affinities of wood-derived materials in the Brandon lignite. See Table I for key to Roman numerals.

anisotropic, yellow-tan material (I) that is probably related to the xylinoid-vitrinoid maceral groups. Similarly, the vessel walls of *Cyrilla* appear to have been altered to a buff-colored, isotropic material (II), and in some instances the alteration has proceeded further to a yellow-brown, isotropic material (III). In other cases, after arriving at the buff-colored stage, the vessel walls may have been altered in another direction to produce the collinitic material identified as IV. In still other instances the *Cyrilla* vessel walls appear to have been

granulated after reaching the buff-colored stage, giving rise to a material that may be related to the micrinite maceral series.

Extended discussion of these speculative relationships is unwarranted until more critical information is available. The "multilinear" aspect of coalification described previously (*3*, *6*) appears to be well illustrated by the Brandon woods. It seems evident that from a single plant tissue various dissimilar materials may result as products of coalification. Those described represent macerals related to the vitrinite, micrinite, and resinite maceral series. Because of the position of these materials in their respective series—i.e., only slightly metamorphosed and anatomically relatable to the woods of extant plants—their detailed study using appropriate chemical and physical methods should reveal useful information concerning the basic composition of coals of both higher and lower rank and simultaneously add to our knowledge of the coalification process.

Publication Date: January 1, 1966 | doi: 10.1021/ba-1966-0055.ch045

Literature Cited

(1) Barghoorn, E. S., Spackman, W., Jr., *Am. J. Sci.* **247,** 33 (1949).
(2) Barghoorn, E. S., Spackman, W., Jr., *Econ. Geol.* **45,** 344 (1950).
(3) Dutcher, R. R., Ph.D. Thesis, The Pennsylvania State University, 1960.
(4) Jeffrey, E. C., Chrysler, M. A., *Rept. Vermont State Geol.* **5,** 1 (1906).
(5) Knowlton, F. H., *Rept. Vermont State Geol.* **4,** 153 (1902).
(6) Spackman, W., Thompson, R. R., *Compt. Rend. Congr. Intern. Strat. Geol. Carboniferous,* **15,** 239 (1964).
(7) Traverse, A., *U.S. Bur. Mines Rept. Invest.* **5151,** 1 (1955).

RECEIVED March 18, 1966.

Discussion

Peter A. Hacquebard: The differentiation of various vitrinic compounds so beautifully shown in the Brandon lignite—e.g., between cell wall material and cell-content material, can also be observed in bituminous coals. I have been able to show this on polished sections by using an etching technique. How has Dr. Spackman shown this in thin sections, and what would be the effect of rank increase on the existence of these two types of vitrinite—i.e., types derived from cell walls and cell contents?

W. Spackman: The lignite sections shown were simply cut on a sliding microtome and no special techniques were required to display the effects of differential coalification of the wall layers. All sections are unstained. Bituminous coals prepared by normal thin sectioning procedures display the metamorphosed equivalents of the "collinitic" and "telenitic" substances found in lignites. Chemical etching will assist both the incident and transmitted light inspection of the materials. Increasing the "rank" of the individual materials merely moves them along on the "coalification line" they are following.

George R. Hill: What is the present geographic distribution of the plant genera found in the Brandon lignites?

Dr. Spackman: The Brandon flora includes 43 extant genera of which 37 are found in the vegetation of southeastern U. S. The remaining six genera are components of the modern floras of eastern Asia. *Gordonia, Persea, Magnolia, Cyrilla, Ilex, Planera, Nyssa, Vitis, Rhus, Quercus,* and *Symplocos* (to mention a few) are characteristic elements in the vegetation of the interfluvial swamp areas of southern Georgia and northern Florida. These genera are abundantly represented in the Brandon lignite, and it seems reasonable to conclude that the Brandon vegetation grew under similar environmental conditions.

Peter H. Given: As I understand it, cell walls that are distinct anatomically but similar in chemical composition may be differentiated in the lignite (a) by color in thin section, (b) by degree of mechanical or physical breakdown of the tissue. The authors consider that differences in color may represent different degrees or processes of coalification. There seems to be an alternative possibility—i.e., that flavonoid pigments from the cytoplasm of living cells elsewhere in the original plant, or other colored materials formed in decay, migrated into the xylem and were adsorbed to different extents on different types of cell walls; the adsorbed materials polymerized in situ to insoluble flavolans or otherwise remained fixed, conferring different depths of color on the cell walls. I am sure that the authors appreciate that in some cases differences in color may reflect adventitious circumstances and not real chemical differences. I merely suggest one possible set of adventitious circumstances.

The fact that different types of cell wall respond differently to the decay conditions is clear and extremely interesting. These differentiations no doubt arise partly from differences in the chemical nature of the substances in the walls and lumina. But could they not also arise in part from differences in physical structure—e.g., a porosity or surface accessibility to enzymes or other reaction-inducing substances?

Dr. Spackman: Several different, coalified, cell wall products have been described. In some instances the source walls were anatomically similar, and similar coalified products resulted. In other cases, the source walls were anatomically distinct and each type yielded a distinct coalified product. Moreover, the walls of each cell type seemed to respond consistently to coalification. When the walls of a particular cell type were compared with their analogs in coalified wood of a different plant genus, sometimes the products were similar, but instances were observed in which the coaly products were quite dissimilar. The latter was inferred to reflect an initial and heretofore, unrecognized difference in the nature of the source materials involved.

The authors agree with Dr. Given that initial physical structure and initial chemical composition both influence the course of coalification. The materials described should be studied further to clarify the significance of each and to evaluate the suggestion that the coalification processes have involved saturation of cell wall residues with foreign, flavonoid pigments.

Publication Date: January 1, 1966 | doi: 10.1021/ba-1966-0055.ch045

46

Coal Metamorphism and Igneous Intrusives in Colorado

RUSSELL R. DUTCHER, DONNA L. CAMPBELL, and CHARLES P. THORNTON

Department of Geology and Geophysics, The Pennsylvania State University, University Park, Pa.

Publication Date: January 1, 1966 | doi: 10.1021/ba-1966-0055.ch046

Two general areas in Colorado exhibit extensive alteration of coals by igneous intrusives. The first locality is near Somerset in the west central part of the state, and the second area is the Spanish Peaks region near Trinidad and Walsenburg. Drill core samples, outcrop samples, materials from active mines, and thin sections of the intrusive rocks were studied. The results show that mean maximum reflectance of the altered coal or natural coke increases as the distance from an intrusive body decreases. Carbon and ash values increase as the distance from intrusive decreases whereas volatile matter values decrease. Sulfur data are variable. Hydrogen values increase as the distance from an intrusive increases. Hydrogen and reflectance are considered the most sensitive and reliable indicators of degree of alteration.

Numerous areas in the U.S. contain examples of coal which has been altered by igneous bodies. These have been reported extensively in the literature. In 1906 Fenneman and Gale reported on the effect of intrusions in the Yampa coal field of Colorado (*4*). McFarlane in 1929 reported on both coals of the Yampa field and others from the U. S. (*12*). In 1939 Dapples worked extensively with altered coals from the Anthracite-Crested Butte area of Colorado (3). Clegg (2) has studied coals in southern Illinois which have been altered by intrusives. Johnson, working in the Spanish Peaks region of Colorado has reported extensive areas of alteration by intrusives (*9, 10*).

This paper reports the chemical and physical alteration of coals from two general areas in Colorado. An index map is included as Figure 1 to help in

In Coal Science; Given, P.;
Advances in Chemistry; American Chemical Society: Washington, DC, 1966.

understanding the general areas from which samples were studied. The first area is in the west central part of the state in the vicinity of Somerset. Two diamond drill core samples were available for study from this area. The coals in these two core samples have been altered by sills. Alteration in the second area, the Spanish Peaks region, has been caused by sills on the south side of the peaks and by dikes on the north side. Material altered by both dikes and sills has been studied from the Spanish Peaks area. Samples in this region were obtained from active mines on the north and from road-cut exposures and outcrops on the south. One exposure in the vicinity of Medina Plaza, Colo., is of great interest in that here a xenolith of natural coke occurs in a sill of "basaltic" composition. The xenolith is approximately 16 inches thick and 9½ feet long.

Experimental work is being conducted to determine the temperatures and pressures associated with the intrusions and alterations of the samples described in this paper.

Publication Date: January 1, 1966 | doi: 10.1021/ba-1966-0055.ch046

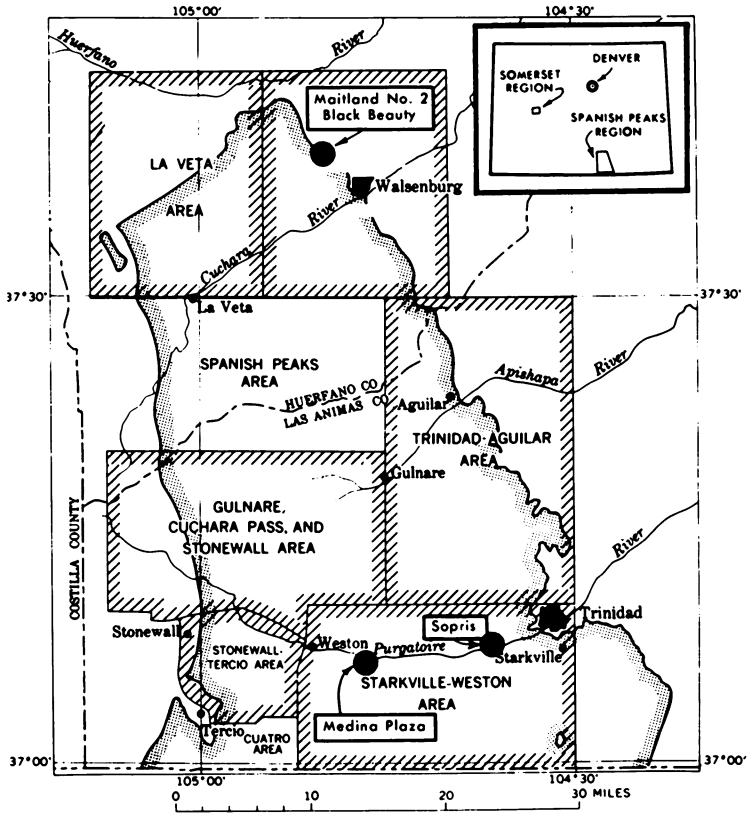

Figure 1. Index map. Insert in upper right corner shows location of two general regions in Colorado. Main map shows sample sites in the Spanish Peaks region. Modified from Johnson (9)

Somerset Area Samples

Two diamond drill cores, designated DDH-A and DDH-B were obtained from central Colorado. DDH-B is from the vicinity of Redstone, Gunnison County, and core DDH-A is from the vicinity of Somerset in Delta County. These samples were particularly interesting since there is a transition from unaltered high volatile bituminous coal to natural coke at the igneous contacts. Both cores are of Cretaceous age coal. All core samples are from depths in excess of 1500 feet below the surface.

These samples were studied by chemical and microscopic methods. Chemical data include moisture, ash, volatile matter, total carbon, and hydrogen. Microscopic data include reflectance measurements on samples from both cores and maceral analyses of core DDH-B.

Publication Date: January 1, 1966 | doi: 10.1021/ba-1966-0055.ch046

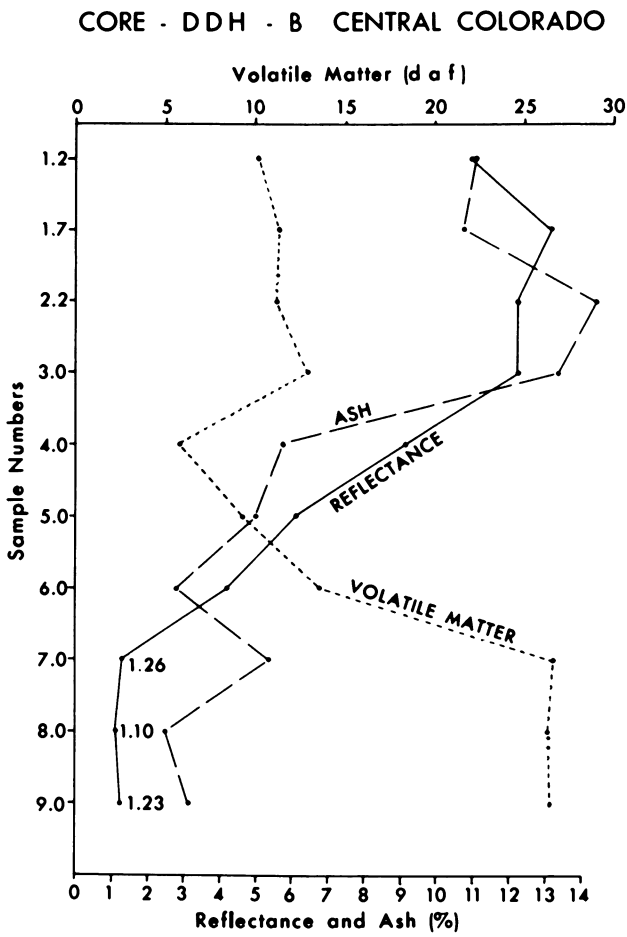

Figure 2. Volatile matter (daf), ash, and reflectance values in core DDH-B

Table I. Analyses of DDH-B

Sample	*Moisture*	*Total Carbon (daf)*	*Hydrogen (daf)*
DDH-B-1.2	0.72	92.3	0.80
DDH-B-1.7	0.08	94.3	0.94
DDH-B-2.2	0.94	92.1	0.78
DDH-B-3.0	0.60	90.4	1.07
DDH-B-4.0	1.10	94.5	1.76
DDH-B-5.0	0.90	91.9	3.16
DDH-B-6.0	1.28	89.6	3.60
DDH-B-7.0	1.08	87.5	5.18
DDH-B-8.0	1.34	87.2	4.96
DDH-B-9.0	1.28	87.9	5.30

Figure 2 shows the ash, volatile matter, and reflectance data of DDH-B plotted *vs.* the distance from the contact. There is a coke/sill contact at Sample 1.2 and between Samples 2.2 and 3.0 at position 2.6. The sill above Sample 1.2 is 15 inches thick, and that at position 2.6 is 3 inches in thickness. All these sample numbers are positions measured in feet along the core. As the distance from the sill contact increases, the volatile matter increases, and the ash decreases. Johnson, Gray, and Schapiro (*11*) reported similar results for cores from the same general area.

Moisture, carbon, and hydrogen analyses for DDH-B are listed in Table I. The most striking results are the hydrogen data. Hydrogen increases from 0.80% at the coke/sill contact to 5.30% at the 9-foot interval where essentially unaltered coal exists. Carbon data show relatively the same values throughout this range of samples. Hydrogen is possibly then an indicator of the degree of thermal alteration of a coal. However, reflectance values provide probably the most reliable indication of this alteration because they are less affected by the presence of mineral matter. This has also been suggested by Johnson, Gray, and Schapiro (*11*). Figure 2 shows the results of reflectance measurements made on polished pellets of the coal and coke samples using a Leitz Ortholux microscope and Photovolt photometer. Reflectance increases as the distance from the coke/sill contact decreases, with values from 1.23 to 13.2%.

Maceral analyses—i.e., coal constituent analyses—were made on polished pellets of the coal samples from 9, 7, and 6 feet from the sill contact. A Leitz Ortholux microscope at approximately 750× magnification was used. At a distance of less than 6 feet from the sill contact it was impossible to distinguish any specific macerals in the coal samples. At 6 feet it was possible to distinguish the macerals, and a ratio of reactives to inerts of 20:80% was found. At 9 feet there was an approximate ratio of 70:30% of reactives to inerts. The bulk of the increase is caused by carbonization of other macerals.

Figure 3 shows optically visible changes in the coal of DDH-B. Photograph a is of natural coke at a sill contact; vesicles are well developed. The coke appears completely opaque in transmitted light. Photograph b, a thin section of the coal 4 feet from the sill, appears slightly translucent red. Flow structure is visible around the two large vesicles of the large grain in the center of the photograph. At 6 feet from the sill the coal appears brown in transmitted light (photograph c). The essentially unaltered coal at 9 feet from the sill appears red in photograph d.

Publication Date: January 1, 1966 | doi: 10.1021/ba-1966-0055.ch046

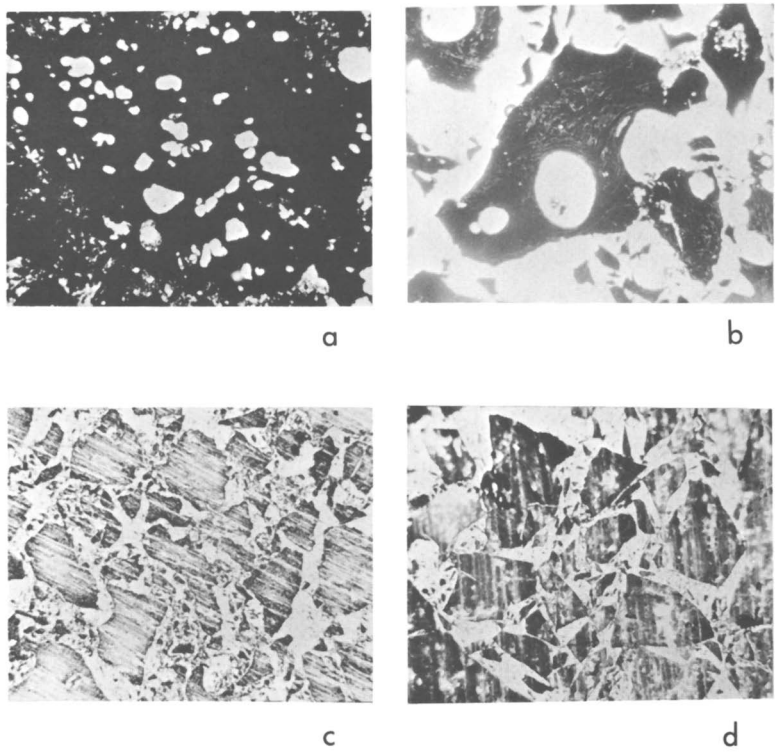

Figure 3. Photographs of thin sections of altered coal from core DDH-B showing the gradual increase in translucency away from the contact with sill. × 46

(a) Opaque natural coke at the contact of coal seam and sill.
(b) Highly altered coal at a distance of 4 feet from the sill; slightly deep red translucent; flow structure apparent around vesicles.
(c) Altered coal at a distance of 6 feet from the sill; very few areas remain opaque; color is light brown.
(d) Slightly altered coal at a distance of 9 feet from the sill; color is red and lighter than red areas of photograph b.

Drill core DDH-B shows the effect of a sill on a coal bed over a distance of 9 feet. McFarlane (*12*) noted that, except where the intrusion represents a flow channel or conduit, the coal is carbonized to "anthracite" only for distances ranging up to one-third the thickness of a sill, both above and below it. The sill in drill core DDH-B is just over 1 foot thick though the coal is coked for more than 4 feet from the contact, indicating that this sill must have been a flow channel or conduit. The greatest observable change in hydrogen, volatile matter, and reflectance occurs in samples 5.0 and 6.0 which are 4–5 feet from the sill, respectively.

All the carbonaceous material of core DDH-A is coked rather uniformly as can be seen by the reflectance measurements given in Figure 4. This figure

also shows a correlation of ash and volatile matter data. These data suggest some effect caused by mineralization, particularly by carbonates. Unfortunately the presence of carbonate minerals was not known when the analyses were requisitioned, and therefore they are not corrected for the loss of CO_2 in the ash and volatile matter tests or for the enclosing of this CO_2 in the carbon contents. The peaks in the volatile matter curve may be caused largely by the lack of these corrections. However, the values in Table II suggest that most of the analyses were not greatly affected by the presence of carbonate. Moreover, it is difficult to see how there could be any marked trend in carbon content

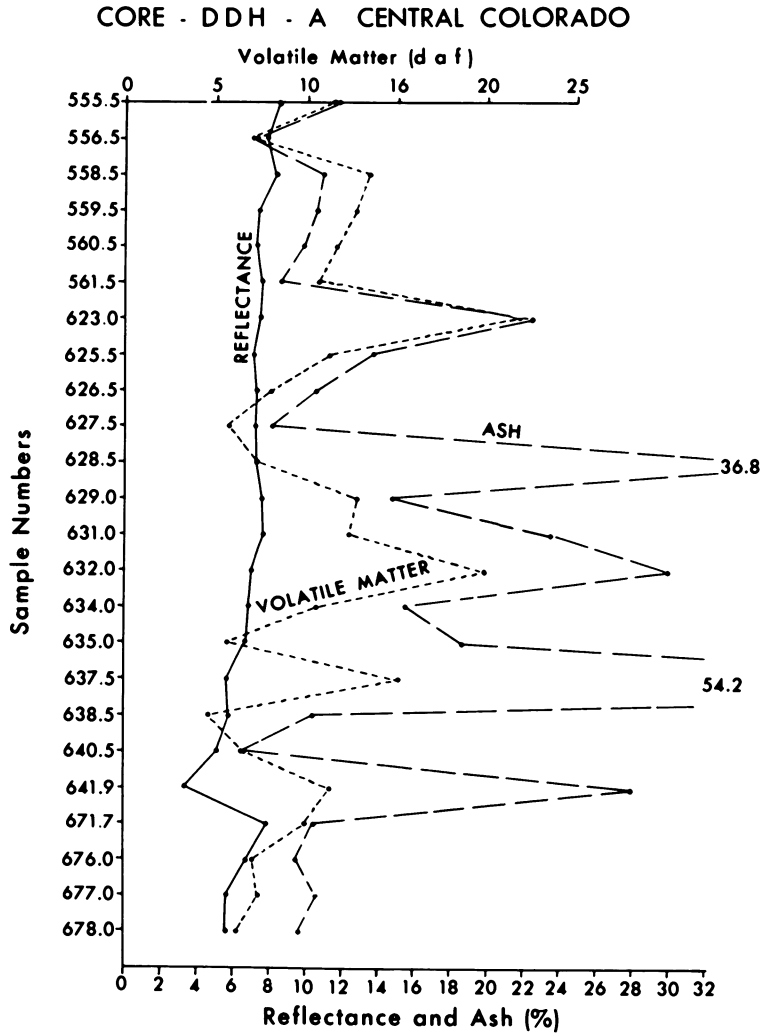

Figure 4. Volatile matter (daf), ash, and reflectance values in core DDH-A

with distance from the sill even if all values for percent carbon were fully corrected. This is in contrast to the result with the DDH-B core. A parallel contrast was found by Given and Binder in their study of the electron spin resonance properties of samples from the same two cores (5).

Table II. Analyses of DDH-A

Sample	*Moisture*	*Total Carbon (daf)*	*Hydrogen (daf)*
DDH-A-555.5	0.56	90.2	0.81
DDH-A-559.5	0.54	90.5	0.87
DDH-A-623.0	0.64	84.2	0.67
DDH-A-628.5	0.98	91.1	0.93
DDH-A-632.0	0.50	84.4	0.84
DDH-A-634.0	1.14	93.5	1.14
DDH-A-637.5	1.68	84.8	2.03
DDH-A-640.5	3.60	89.8	1.67
DDH-A-641.9	2.78	70.9	2.00
DDH-A-676.0	0.54	93.6	1.25

The hydrogen content is higher where the reflectance values noticeably decrease. This break in the uniform reflectance curve occurs where there is a greater concentration of coked carbonaceous material, without a large admixture of igneous material.

Drill core DDH-A offers an excellent opportunity for studying sill-coke relationships. Several of the contact relationships between coke and intrusive rock are shown in Figure 5. The intrusive is intermittently mixed through the coal. The igneous material is a strongly carbonatized and hydrated porphyritic mafic rock that rather intimately intrudes the coke. In the igneous rock, the approach of a contact is indicated by a noticeable darkening of the cryptocrystalline to microcrystalline, altered ground mass. Just at the contact, coke and igneous material often are separated by a thin zone of medium-grained, usually colorless carbonate mineral. Beyond the contact the coke is cut by numerous veinlets consisting mainly of colorless carbonate, but containing, in addition, occasional crystals of quartz and a complexly twinned mineral, probably a zeolite; similar veinlets cut the igneous rock, but apparently less commonly than the coke. In addition, the coke is cut by rare apophyses (0.5–1 mm. thick) of the igneous rock itself. Finally, at least near the intrusion, the vesicles in the coke are filled by mineral matter apparently derived from the sill: by carbonate, in part iron-stained; by quartz; and by igneous rock.

Spanish Peaks Region

Black Beauty and Maitland Samples. Approximately three miles northwest of Walsenburg, Colo., coal beds of the Vermejo formation are cut by a northeast-trending, nearly vertical dike which is approximately 25 feet thick. Fortunately, at this locality two coal mines have operated—one on either side of the dike. Both mines have been developed by "drifting in" from the outcrop of the seam. The Black Beauty mine on the south side of the dike has developed down dip more or less parallel to the strike of the dike. The main slope of the Maitland No. 2 mine on the north side has developed down dip and

Publication Date: January 1, 1966 | doi: 10.1021/ba-1966-0055.ch046

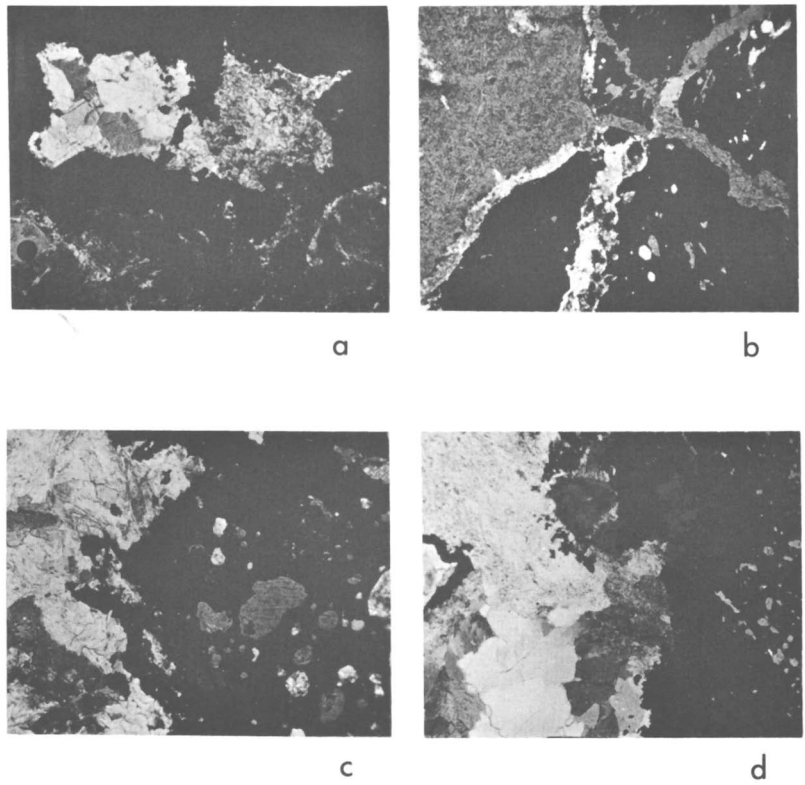

Figure 5. Photographs of thin sections from core DDH-A showing some of the features along contact zone of the sill and natural coke. × 46

(a) Carbonate minerals filling large, irregular cavities in coke. Carbonate in cavity on the right is iron-stained; that in cavity on the left is clear. Altered igneous rock of the sill forms the lower third of the photograph.

(b) Contact relations between altered igneous rock (mottled gray), coke (black), and carbonate minerals (white and uniform gray).

(c) Vesicles in coke (black) filled with carbonate minerals (white) and quartz (gray).

(d) Carbonate vein (left half) containing a single subhedral zeolite crystal (dark gray, top) cutting coke (right half).

is oriented nearly at right angles to the strike of the dike. The general relationships of these mines to the dike and the samples areas are shown in Figure 6.

Exposures in the Black Beauty mine, near the surface in the main slope, show "normal" unaltered coal of a high volatile C rank. That this has most probably been affected by the intrusion of the dike is evidenced by high concentrations of spheroidal coal or "coal apples." Johnson (*10*) has reported on spheroidal coal and concluded that development of these structures is related in this area to the igneous intrusions. Further into this mine the entire seam becomes altered to natural coke in rooms headed toward the dike. In these areas mining had to be terminated for this reason. Large areas are exposed,

Publication Date: January 1, 1966 | doi: 10.1021/ba-1966-0055.ch046

and the transition from coal to coke can be followed. The coke itself is a massive, dense, dark gray material. The original banding of the coal is readily visible; no evidence of flow or extensive vesiculation was noted. There is a high mineral matter content.

Within the Black Beauty mine the spheroidal coal has a reflectance value of 0.75%. Reflectance of the coke described above is 2.86%.

Representative samples taken from the face of the main slope (approximately 900 feet from the dike) of the Maitland No. 2 mine (samples M-1 and M-3) and a third sample back approximately 100 feet (M-2) show reflectance values of 0.65%, 0.61%, and 0.65%, respectively. Two additional samples taken approximately 1600 feet from the dike (M-4 and M-6) have reflectance values of 0.48% and 0.47%, respectively. None of the coal material exposed at any place in the mine is visibly altered by the intrusion. However, the reflectance values are quite sensitive and have recorded some effect from the heat of the dike rock.

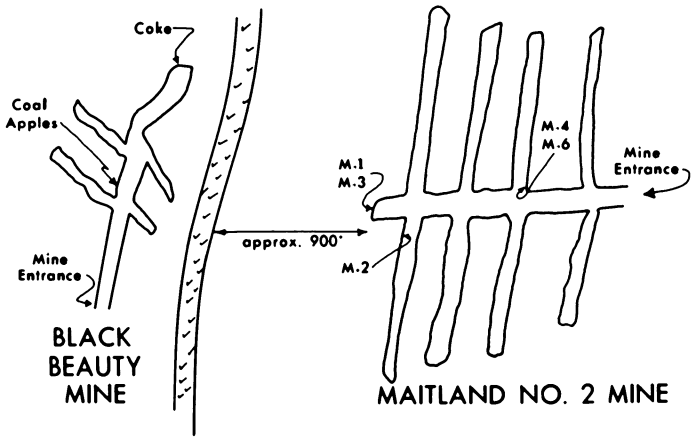

Figure 6. Generalized schematic to show relationships of sample areas in the Black Beauty and Maitland No. 2 mines to the dike (band with checks)

Normally, alteration at this distance (approximately 900 feet) is not expected with a dike of this size. The miner's "rule" is that one foot of coal will be "coked" on each side of a dike for each foot of thickness of the dike rock. The coal beyond these limits rarely appears to be altered at all. Clegg (2) reports a very narrow zone of visible alteration in his work.

Natural Coke at Sopris. At Sopris, Colo., approximately four and one-half miles west of Trinidad, on Colorado State Highway 12, there are some striking exposures of a "basaltic" sill which has completely altered a coal seam and in some areas almost entirely replaced it. The natural coking process has been so extensive in this area that attempts were made years ago to actually mine "coke." Figure 7 shows an exposure at Sopris where the sill material has invaded the coal seam in several layers. The lighter, more massive beds are the

Figure 7. Natural coke and "basaltic" sill at Sopris locality. Silver dollar, for scale, rests against band of well-"fingered" natural coke. A band of the sill is lighter material beneath

igneous rock. The darker, well "jointed" bands or layers are natural coke. The coke is well "fingered," and these fingers are oriented at right angles to the heating surface—the layers of the sill.

This orientation of coke blocks is shown well toward the top of the photograph where a mass of the igneous rock roughly semicircular in outline is shown. The coke fingers along the upper surface of this conduit-like mass exhibit a clear radial pattern. In the photograph the very light circle is a silver dollar included for scale. The natural coke itself is not at all unlike commercial coke in appearance although it obviously has a higher than desirable ash content.

Associated with the igneous material are masses of carbonate—almost exclusively calcite. These occur as veinlets within the rock and as linings of cavities in the sill material. Most of the calcite is massive, but some small crystals are present. Within one small cavity lined with carbonate, a small quartz crystal ("herkimer diamond") was encountered, which bridged from one side of the cavity to the other.

Figure 8 is a photograph taken approximately 400 yards west along the road from that area shown in Figure 7. Here the sill is present as a series of conduits roughly circular in outline and from 3½ to 4 feet in diameter. Some of these masses are bulged out at their base. These units, such as the one in the center of Figure 8, are wholly within the upper and lower boundaries of

Publication Date: January 1, 1966 | doi: 10.1021/ba-1966-0055.ch046

the "coal seam" and are spaced from 15 to 30 feet apart along a 150-foot exposure.

The seam at this locality was approximately 6 feet thick. The top and bottom of the seam are still readily located and these boundaries appear horizontal in the photograph. The apparent uparching of material over the conduit is caused primarily by the coking action. The fingering here is not well developed, but that which exists radiates outward from the upper areas of the igneous mass. Coal which has not reached the coke stage is present in the upper left hand portion of the photograph. Coal which megascopically does not appear to be altered also occurs in some of the intervals between conduits. The direction of movement of the molten igneous rock was most likely toward the viewer, in a southerly direction.

Publication Date: January 1, 1966 | doi: 10.1021/ba-1966-0055.ch046

Figure 8. Coal seam highly altered by "basaltic" sill at Sopris locality. Large conduit-like mass of sill rock in center with natural coke surrounding. Coke arches up and over the conduit-like mass. Seam is underlain by black shale and capped with a thin black shale and a massive light gray sandstone

The presence of the mass of igneous rock in conduits, not as a sheet, coupled with the localized nature of much of the coking suggest that this area may be at the outer limits of the sill and the magma was moving as a cooler, more viscous mass with a higher concentration of solids than in other nearby areas. The sill is not present at the same horizon across the valley on the south side of the Purgatoire River. It is possible, however, that it may have "jumped section" and for that reason is not present to the south.

In Coal Science; Given, P.;
Advances in Chemistry; American Chemical Society: Washington, DC, 1966.

Oriented vertically and passing through the center of the conduit is a dark zone shown in Figure 8. This is a fissure that extends from the top of the coke over the igneous rock downward through the "basalt" and at least 12 inches into the underlying black shale. The fissure is 1–1¼ inches wide at the top and ⅛–¼ of an inch wide at the base in the shale. All of this fissure is filled with a noncoked, nongraphitized coal material. The material must

Figure 9. Natural coke xenolith in sill, one-half mile east of Medina Plaza. Sill has replaced most of the coal seam in this area. The letters A and B in the photograph indicate the longest dimension of the xenolith. It is approximately 9½ feet between these stations

necessarily have been forced into this fissure after cooling and solidification of the conduit. There are other similar occurrences—dikes of apparently unaltered coal material, homogeneous and vitrain-like, cutting both the sill and underlying shale. One of these, at least 9 feet long, occurs at the xenolith locality east of Medina Plaza. One feasible explanation is that these are the result of condensed volatiles from coal being pyrolized in adjacent areas.

Medina Plaza Xenolith. About one-half mile east of Medina Plaza on Colorado Highway 12, a sill has replaced much of a coal seam in the Raton formation. This locality has been studied and illustrated by Johnson (9). Within a part of this sill there is a large mass of natural coke completely surrounded by igneous rock. This xenolith of natural coke is about 16 inches thick, 9½ feet long and occurs in the base of the 8-foot thick sill. Figure 9 is a photograph of the exposure. Samples of the xenolith were taken in 2-inch increments from the top to the bottom. The coke had a definite columnar structure and was well "fingered." The fingers occurred in 1½–2-inch lengths.

Publication Date: January 1, 1966 | doi: 10.1021/ba-1966-0055.ch046

These coke samples were studied by chemical, x-ray diffraction, and microscopic techniques. Chemical data include total carbon, volatile matter, ash, and sulfur determinations.

Figure 10 shows the percent total carbon and percent volatile matter plotted *vs.* the distance across the xenolith. The total carbon (daf), ranging from 85 to 93%, increases toward the center of the xenolith whereas the volatile matter, ranging from 6.5 to 16%, decreases. This may be explained by the movement of volatiles outward to the top and bottom of the xenolith.

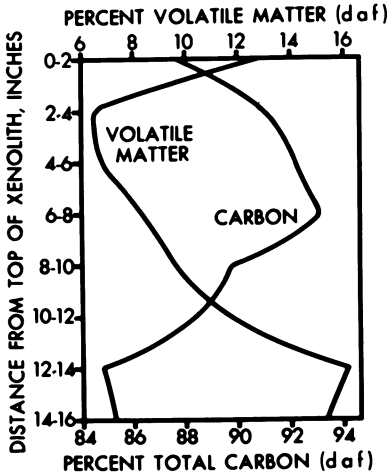

Figure 10. Carbon and volatile matter distribution across xenolith of natural coke

Heating progressing inward may have coked the outer edges prior to the center and the volatiles from the central portion were condensed or trapped by the outer coke structure. Thin sections show that translucent material is present in some vesicles and microfissures of the outer zones of coke. This also explains the increase in reflectance as being real in this case even though coupled with an increase in volatile matter. Figure 11 shows carbon and ash plotted *vs.* the distance across the xenolith. As expected, the ash decreases as the distance from the contacts increases. The ash content is extremely high, from 18.6 to 37.6%.

Sulfur data were variable, but the values were so small they were almost negligible. There was, however, a slight increase from the top to the bottom of the xenolith; the values ranged from 0.08 to 0.26%.

The mineral matter in the coke was extremely difficult to identify because it was finely disseminated throughout. X-ray diffraction techniques were used to gain some insight into the mineral content of the coke. In order to obtain x-ray diffraction patterns of the mineral matter, the interference of carbon had to be reduced to a minimum; this was accomplished by grinding the coke to —200 mesh, sink-floating it in a 2.30-specific gravity liquid, and centrifuging.

Publication Date: January 1, 1966 | doi: 10.1021/ba-1966-0055.ch046

This eliminated enough of the carbon to get readable patterns. The major minerals determined were quartz, calcite, kaolinite, and chlorite. The most obvious and abundant mineral, quartz, decreased in relative amounts toward the center of the xenolith, and this trend was apparent in all the other minerals. Diffraction patterns of the ash from the whole coke, in general, showed the same mineral decrease trend except, of course, no calcite at all was detectable. Calcination or emission of carbon dioxide from calcite occurs at 898°C. (7), significantly below the ashing temperature of 950°C.

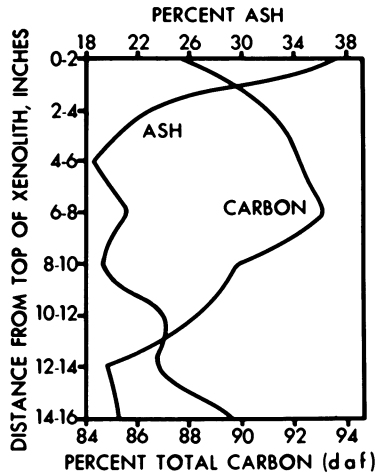

Figure 11. Carbon and ash distribution across xenolith of natural coke

In order to substantiate further the mineral matter content information received from the x-ray diffraction analyses, several coke pellets were scanned for sulfur, iron, calcium, silicon, aluminum and potassium in the electron microprobe. Electron probe results showed abundant silicon, suggesting quartz (SiO_2), considerable aluminum, suggesting kaolinite [$Al_2Si_2O_5(OH)_4$] and, relatively speaking, little iron, sulfur, calcium, or potassium.

Most of the mineral matter appeared to be of secondary origin. This was verified by the following. First, the mineral matter was more concentrated at the outer limits of the xenolith, increasing 20% from the center of the xenolith to the contacts with the greatest increase at the top contact. Secondly, kaolinite which was found to be present, is always a mineral of secondary origin being derived by the alteration of aluminum silicates (8). With a few minor exceptions all igneous rock-forming minerals are silicates, and since all of the minerals present are silicates (except calcite), this tends to establish further the idea of secondary mineralization. Finally, McFarlane (12) suggests that coal near a basalt contact is heated to well over 1200°C., and temperatures exceed 1000°C. 1 foot from the sill. It would seem that most minerals present in the coal at the time of the intrusion would not be preserved in their original state.

Publication Date: January 1, 1966 | doi: 10.1021/ba-1966-0055.ch046

Polished pellets and thin sections were made of each incremental fraction across the xenolith for reflected and transmitted light microscopic examination. Thin sections revealed little because of the opacity of the coke. However, the pellets, which were made by mounting the coke in plastic, were invaluable to the study.

Reflectance readings of the polished pellets were made on all fractions across the xenolith, utilizing a Leitz Ortholux microscope and a Photovolt photometer. Figure 12 shows the mean reflectance values of each fraction plotted *vs.* the distance across the xenolith. These values generally decrease toward the center of the xenolith as the distance from the sill increases. The mean reflectance values range from 5.7 to 8.1%.

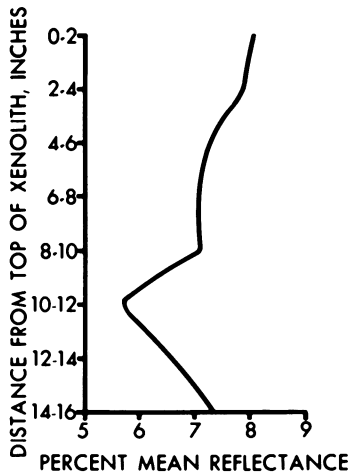

Figure 12. Variation in mean maximum reflectance across xenolith of natural coke

In addition to reflectance measurements, the pellets were studied microscopically employing a gypsum plate. This is one of the most effective ways of observing coke differences without relying on mechanical measurements. The appearance of the various constituents of the coke, whether flat, mottled or striated and the degree of anisotropy readily indicated the type of coal from which the coke is produced (*1*). Utilizing the gypsum plate, microscopically this natural coke appeared striated and anisotropic. Production coke from a low volatile coal has this same appearance.

The coal bed from which this natural coke was formed has not been traced to an unaltered area. However, data reported previously indicated that the coal seams of this general area are in the high volatile range. This discrepancy between the reported volatility and the character of the "coal" particles in the coke may be a result of a relatively rapid increase in the stage of metamorphism immediately prior to coking of the coal by the heat from the igneous intrusion.

In Coal Science; Given, P.;
Advances in Chemistry; American Chemical Society: Washington, DC, 1966.

Conclusions

A preliminary examination of coal materials associated with igneous intrusions from two general areas in Colorado has been completed. A study of the field relationships, petrographic examination, chemical analyses, and reflectance studies has been conducted. Results can be summarized as follows:

(1) Ash values are greatest at contacts and decrease with increasing distance from the contacts.

(2) Reflectance is highest at contacts and decreases as distance increases from the igneous intrusion.

(3) Hydrogen increases as the distance from the igneous intrusion increases.

(4) Reflectance and hydrogen content are the best parameters for correlating distance from an igneous contact within a coal bed.

(5) Volatile matter is a very poor parameter for correlations because of the possible interference of inorganic materials, especially carbonates, and because volatiles from adjacent areas can be trapped in coke structures.

(6) Use of reflectance most probably can detect alteration at greater distances than previous techniques allowed.

(7) Fissures or dikes of homogeneous vitrain-like coal cutting sills and underlying rock are probably caused by condensed volatiles.

(8) The conduits encountered at Sopris probably represent the outer limits of this particular sill where the magma was cooler and more viscous.

Publication Date: January 1, 1966 | doi: 10.1021/ba-1966-0055.ch046

Acknowledgments

The authors wish to acknowledge the support of the National Science Foundation (Grant No. NSF GP-137). Ross Johnson of the U.S. Geological Survey has been of great assistance in all phases of the work. His help is gratefully acknowledged. We also wish to thank the owners of the Red Ash Coal Co. who helped in collecting samples from the Maitland No. 2 mine.

Literature Cited

(1) Benedict, L. G., personal communication.
(2) Clegg, K. E., *Illinois State Geol. Surv., Rept. Invest.* **178** (1955).
(3) Dapples, E. C., *Econ. Geol.* **34**, 369 (1939).
(4) Fenneman, N. M., Gale, H. S., *U.S. Geol. Surv., Bull.* **297** (1906).
(5) Given, Peter H., Binder, C. R., *Proc. Conf. Organic Geochem., Paris, 1964* (in press).
(6) Hurlbut, C. S., Jr., "Dana's Manual of Mineralogy," 15th ed., John Wiley & Sons, New York, 1941.
(7) *Ibid.*, p. 382.
(8) *Ibid.*, p. 303.
(9) Johnson, Ross B., *U.S. Geol. Surv., Bull.* **1112-E**, 129 (1961).
(10) Johnson, Ross B., *U.S. Geol. Surv., Profess. Papers* **424-C**, C20 (1961).
(11) Johnson, Vard, Gray, R. J., Schapiro, N., "Abstracts of Papers," 145th Meeting, ACS, September 1963, p. 3K.
(12) McFarlane, George C., *Econ. Geol.* **24**, 1 (1929).

RECEIVED March 16, 1966.

47

The Determination and Use of Specific Surface Values For Coals

D. H. T. SPENCER and R. L. BOND

The British Coal Utilisation Research Association, Leatherhead, Surrey, England

Publication Date: January 1, 1966 | doi: 10.1021/ba-1966-0055.ch047

Several methods used during the last 30 years in attempts to measure the specific surfaces of coals include gas and vapor adsorption and heats of immersion. The specific surface value obtained for a given coal can vary according to both the type of method used and the particular variant of the method used—e.g., vapor adsorption at different temperatures. The consequent controversies that have been evoked by such contradictory results have led to considerable confusion. Growing evidence suggests that the concept of "specific surface," when applied to sorbents containing pores with diameters of a few tenths A. or less, has no physical meaning.

Much effort has been expended during the last 30 years on investigating the sorptive properties of coals (*12*, *13*). Many different sorbates, under various conditions of temperature and pressure, have been used; rare gases, nitrogen, oxygen, carbon dioxide, carbon monoxide, nitrous oxide, sulfur dioxide, hydrocarbons, alcohols, etc. have been sorbed from the gas or vapor phase, and a wide range of liquids of different molecular sizes and properties has been used in experiments on heats of immersion. Following directly from these measurements, specific surface values have often been deduced in attempts to elucidate coal structure and to explain the behavior of coals and their chars in various processes such as gasification or carbonization. Disaccord between the values obtained with the different methods or sorbates used has given rise to much controversy, which some workers believe has now been resolved.

Coal Structure

The main area of doubt was generally thought to be the uncertainty regarding the extent to which the molecules of a particular sorbate could pene-

In Coal Science; Given, P.;
Advances in Chemistry; American Chemical Society: Washington, DC, 1966.

trate the pore structure and regarding the role of specific interactions between the sorbate molecules and the coal. However, we believe there is a more important fundamental area of doubt—namely, the meaning that can be ascribed to computed values for the specific surfaces of coals. We have reached these views by considering the dual structural character of coals.

Coal is microporous, with certain partial molecular sieve properties. (A microporous solid herein refers to that which contains pores with diameters of a few tens of A. or less.) Micropores can be considered as entities capable of sorbing foreign molecules, and it is known that additivity of their sorption potential fields enhances the sorption owing to dispersion interactions. As the pores become progressively narrower, the vapor adsorption isotherm (Figure 1) in the initial region up to point B becomes progressively steeper (toward the

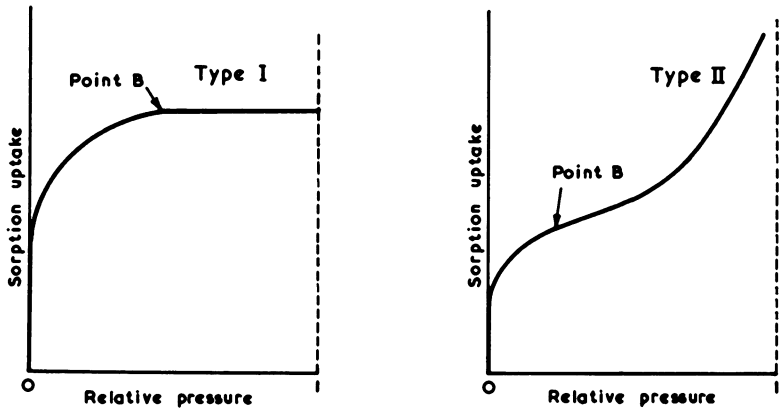

Figure 1. Type I and Type II BET sorption isotherms

sorption uptake ordinate). The differential heat of adsorption shows a corresponding rise. The magnitude of the effect, and the pore-diameter below which it becomes apparent are all different for different sorbates. Such enhancement, which may act across several molecular diameters of sorbed molecules by induction (*38*), can lead to the micropores' becoming completely filled by "condensed" sorbate in the region of apparent monolayer formation. Although such a drastically distorted isotherm (Type I) can still be represented mathematically by the Langmuir and BET equations, values derived for specific surface by using these equations (or from the point B value) lack meaning. References to the literature in which these problems are discussed are indicated in Table I.

Coals are "macromolecular,"—i.e., low rank coals, at least, appear to be able to absorb certain molecules such as methanol and hydrocarbons. In low and medium rank coals the ultimate units are linked by chemical and physical forces, and in high rank coals physical forces predominate. The presence of hydroaromatic structures in low rank coals must lead to rather distorted frameworks. Although it is not difficult to visualize that spaces exist in which foreign

Publication Date: January 1, 1966 | doi: 10.1021/ba-1966-0055.ch047

Table I. Some References to Literature on the Pore-Narrowing Effect and the Sorptive Behavior of Microporous Solids

Material Type	*Reference*[a]
Silicas[b]	*20, 22, 23, 24, 26, 28, 29, 30, 39,* and *see 3*
Dehydrated zeolites	*5, 6, 7, 11, 16, 31*
A phosphomolybdate	*18*
Carbons	*2, 4, 8, 14, 15, 19, 23, 25, 31, 32, 34, 36, 37, 38*

[a] The general comments of Gregg (*17*) are noteworthy.
[b] The studies of Kiselev and his co-workers particularly exemplify the pore-narrowing effect and the role of specific (*1, 21, 27*) sorbate/adsorbent interactions, such as hydrogen bonding, which are not affected by pore narrowing.

molecules may be accommodated and that the entrances, at least, to these spaces must be of molecular diameter, doubt must be expressed as to the meaning of the term specific surface when applied to such a structure. This argument, which has been mentioned briefly by Dryden (*13*), is in line with the recent views of Dubinin and his co-workers (*16*) on dehydrated zeolites and other microporous solids such as active carbons.

Micropore Filling by Methanol

We should like to give one example illustrating our contentions. Previous work (*34, 37*) has indicated that micropore filling by methanol at 273°K. occurred with a polymer carbon (treated with hydrogen) and the polymer carbon steam-activated to high burn-off; the activation caused a shift of the knee of the Type I isotherm to higher relative pressures. This is in accord with some widening of the pores that must have occurred, and it indicates that the pore-narrowing effect must have been more intense in the unactivated material. We obtained Type I methanol isotherms at 298°K. for a high rank coal (*9*), its 600°C. char (*9*), and the same char steam-activated to high burn-off, with a similar shift in the knee of the isotherm between char and activate. In contrast, although a 600°C. low rank coal char (*9*) and activates gave Type I isotherms up to at least a relative pressure of 0.95, that of the raw coal (*9*) was Type II, apparently owing to absorption.

Summary

Our current views, with some elaboration, are summarized below. We do not consider it meaningful with coals, or with microporous solids in general, to deduce specific surface values from sorption data, nor even to apply the concept of "specific surface" to these materials. We believe that "sorption uptake" (moles per unit weight or volume of a given adsorbent) under defined conditions is the correct parameter that should be used to describe the sorptive properties of such materials. Thus, whenever the sorption uptake by an active carbon, for a particular sorbate, is required in a practical application such as solvent recovery, purification, or gas sorption, what should be determined in the laboratory is the uptake under the conditions for which the value is to be used; it is not possible to predetermine unequivocally the value for one

Publication Date: January 1, 1966 | doi: 10.1021/ba-1966-0055.ch047

sorbate from the behavior of other sorbates—except inasmuch as it might be useful to find that in the absence of molecular sieve or absorption behavior, the maximum uptakes (expressed as volume of bulk liquid) of different vapors by a given microporous structure appear to be constant. In particular, "specific surface" values, determined under one set of conditions, should not be used to calculate sorption uptakes for different practical conditions.

Notwithstanding the above comments, we do not deny that adsorption/desorption isotherms can give revealing information on the pore structures of microporous solids and on the changes these undergo upon various treatments. Further, the heat of immersion "molecular probe" technique should still be regarded as a valuable tool for revealing partial molecular sieve behavior in a *given* carbon, but we feel it should not be used to estimate specific surface values, of coals for example or even of wide-pore carbonaceous materials since adequate reference materials are not available. Thus, for example, while we ourselves (*10*) have used heats of immersion values for a series of carbons to show the relative gross effect that progressively increasing burn-off has on the accessibility of the pore structures to penetrating molecules, we do not now consider it valid to translate the values into specific surface values.

Since with very fast gas-carbon reactions, where reaction occurs at the external surface and in large pores that effectively extend the external surface, the use of any computed specific surface value that includes a contribution owing to micropores or fine pores must be incorrect, we suggest that greater attention should be given to characterizing directly the structure of such large pores. Among the methods that might be considered for this application are x-ray stereo-microradiography with electron staining (*35*), mercury injection porosimetry, and the silver impregnation procedure (*33*) for obtaining replicas of the pores whose surface area could then be computed. In studies of slower reactions in which the role of fine pores and micropores may become important, the use of a specific surface value involving a contribution owing to the latter must also be inadequate, and here it is more realistic to include an investigation of the penetration behavior, at the same elevated temperature, of a nonreactive counterpart of the reacting gas.

Publication Date: January 1, 1966 | doi: 10.1021/ba-1966-0055.ch047

Acknowledgment

Acknowledgment is made to the British Coal Utilisation Research Association for permission to publish this communication.

Literature Cited

(1) Aristov, B. G., Kiselev, A. V., *Zh. Fiz. Khim.* **37,** 2520 (1963).
(2) Avgul', N. N. Kiselev, A. V. Kovalyova, N. V,. Khrapova, E. V., *Proc. Intern. Congr. Surface Activity, 2nd, London, 1957,* **2,** 218 (1957).
(3) Babkin, I. Yu., Kiselev, A. V., *Zh. Fiz. Khim.* **37,** 228 (1963).
(4) Barrer, R. M., *Proc. Roy. Soc. (London)* **A161,** 476 (1937).
(5) Barrer, R. M., *Proc. Symp. Colston Res. Soc.* **10,** 6, 53 (1958).
(6) Barrer, R. M., Bultitude, F. W., Sutherland, J. W., *Trans. Faraday Soc.* **53,** 1111 (1957).
(7) Barrer, R. M., Sutherland, J. W., *Proc. Roy. Soc. (London)* **A237,** 439 (1956).
(8) Beebe, R. A., Millard, B., Cynarski, J., *J. Am. Chem. Soc.* **75,** 839 (1953).

(9) Bond, R. L., Spencer, D H. T., "Industrial Carbon and Graphite," p. 231, Society of Chemical Industry, London, 1958.
(10) Bond, R. L., Spencer, D. H. T., *Proc. Conf. Carbon, 3rd, Buffalo, 1957*, 357 (1959).
(11) Breck, D. W., Eversole, W. G., Milton, R. M., Reed, T. B., Thomas, T. L., *J. Am. Chem. Soc.* **78**, 5963 (1956).
(12) Chiche, P., *J. Chim. Phys.* **60**, 792 (1963).
(13) Dryden, I. G. C., "Chemistry of Coal Utilization," Suppl. Vol., H. H. Lowry, ed., p. 232, Wiley & Sons, New York, 1963.
(14) Dubinin, M. M., *Chem. Rev.* **60**, 235 (1960).
(15) Dubinin, M. M., "Industrial Carbon and Graphite," p. 219, Society of Chemical Industry, London, 1958.
(16) Dubinin, M. M., Zhukovskaya, E. G., Murdmaa, K. O., *Zh. Fiz. Khim.* **37**, 426 (1963).
(17) Gregg, S. J., "Powders in Industry," pp. 79, 93, Society of Chemical Industry, London, 1961.
(18) Gregg, S. J., Stock, R., *Trans. Faraday Soc.* **53**, 1355 (1957).
(19) Kipling, J. J., Wilson, R. B., *Trans. Faraday Soc.* **56**, 562 (1960).
(20) Kiselev, A. V., Gas Chromatog., *Proc. Symp., 4th, Hamburg, 1962*, **XXXIV** (1962).
(21) Kiselev, A. V., *Rev. Gén. Caout.* **41**, 377 (1964).
(22) Kiselev, A. V., *Proc. Intern. Congr. Surface Activity, 2nd, London, 1957*, **2**, 179 (1957).
(23) *Ibid.*, p. 189.
(24) Kiselev, A. V., "Surface Chemical Compounds and Their Role in Adsorption Phenomena," Moscow University Press, 1957; transl. by U.S. At. Energy Comm., AEC-tr-3750, p. 93.
(25) Kiselev, A. V., *Proc. Symp. Colston Res. Soc.* **10**, 51 (1958).
(26) Kiselev, A. V., *Ibid.*, p. 195.
(27) Kiselev, A. V., *Quart. Rev. Chem. Soc. (London)* **15**, 99 (1961).
(28) Kiselev, A. V., *Uspekhi Khim.* **25**, 705 (1956).
(29) Kiselev, A. V., El'tekov, Yu. A., *Proc. Intern. Congr. Surface Activity, 2nd, London, 1957*, **2**, 228 (1957).
(30) Kiselev, A. V., Kulichenko, V. V., Isirikyan, A. A., *Ibid.*, p. 199.
(31) Lamond, T. G., Marsh, H., *Carbon* **1**, 281 (1964).
(32) Lamond, T. G., Marsh, H., *Carbon* **1**, 293 (1964).
(33) Lang, F. M., Magnier, P., private communication.
(34) Millard, B., Beebe, R. A., Cynarski, J., *J. Phys. Chem.* **58**, 468 (1954).
(35) Nelson, J. B., *Proc. Conf. Carbon, 5th, Univ. Park, Penna., 1961*, **1**, 438 (1962).
(36) Pierce, C., *J. Phys. Chem.* **63**, 1076 (1959).
(37) Pierce, C., Smith. R. N., *J. Phys. Chem.* **54**, 354 (1950).
(38) Pierce, C., Wiley, J. W., Smith, R. N., *J. Phys. Chem.* **53**, 669 (1949).
(39) Sing, K. S. W., Swallow, D., *J. Appl. Chem.* **10**, 171 (1960).

RECEIVED March 15, 1966.

Discussion

R. B. Anderson: We certainly agree with Mr. Bond that "surface area" in solids with pores of molecular size has little meaning; however, adsorption studies have provided much insight into the physical structure of coal. A word of caution is in order on the method of estimating "surface areas" using adsorption of gases at high temperatures. Near the boiling point of the adsorbate, physical adsorption may be regarded as enhanced condensation; this process is relatively nonspecific, and the success of the BET method probably results from this factor.

At high temperatures the surface is only sparsely occupied by adsorbate, and the number of molecules adsorbed probably varies significantly with the

number and kind of high energy sites on the surface. Adsorption will occur only on these sites of high energy. For this reason "surface areas" estimated from high temperature adsorption may be incorrect by factors possibly as large as 3 to 5.

It must be remembered, in interpreting adsorption isotherms on coal, that coal expands sizably when temperature is increased, and coal swells appreciably during adsorption. These factors are relatively unimportant for porous inorganic solids. On heating from —195°C. to room temperature the volume of coal expands about 10%, and at least more or less consistent with this, pore openings at —195°C. seem to be 4A. while at room temperature they are about 5A. Further, on adsorption of water or methanol the volume of coal increases 10–20%, and with some exceptional polar "adsorbates" coal eventually dissolves.

Publication Date: January 1, 1966 | doi: 10.1021/ba-1966-0055.ch047

Philip L. Walker, Jr.: I was interested in Mr. Bond's suggestion that we should no longer report the surface area of coals since the figure has little meaning. I would agree that there is some question as to what areas should be assigned to adsorbate molecules in the case of adsorption in the very fine pore structure of coals. However, Dr. Lamond has shown recently that surface areas reported for solids containing pores primarily less than 10A. in diameter, calculated from the BET equation or the PE equation, agree closely (5). Therefore, I do not think that we need be concerned that the areas we report are too high because of the confusion of capillary condensation and multilayer adsorption, which is a problem in activated carbons.

K. A. Kini: The paper by Bond and Spencer shows the skepticism with which they view the problem of the surface area of coal. More than two decades have passed since the question was first raised, and we are still debating it. I wonder whether this debate needs to continue in view of the work on CO_2 adsorption by coals by Kini (3), Walker and Geller (9), Anderson and co-workers (2), and the recent work using krypton and xenon under pressure by Kini (4). Surely, the data in these papers represent reasonably acceptable values of the total surface areas of coals. The meaning of "surface area" in pores of molecular dimensions is admittedly a difficult question, but I feel that the difficulties are exaggerated by the authors.

George R. Kapo: An interesting technique has been developed for determining the surface areas of carbon blacks by fatty acid soap adsorption from aqueous solutions (7). The technique used is relatively simple and is based on a break in the potentiometric titration curve of the carbon black with a standard soap solution. It was confirmed that the break in the curve corresponded to a monolayer of soap covering the available surface area. Generally the soap adsorption gave a much lower surface area than the BET area presumably owing to the 10' difference in diffusivities and to pore size restriction to the large soap molecules. This work was done on carbon blacks to provide a more meaningful criterion for ability of a black to act as a rubber reinforcement agent.

It is suggested that this technique be applied to coal and coke to provide a realistic estimate of the available surface area (compared with the BET area)

for liquid phase reaction involving large molecules. For example, semicokes and coke breeze (which have different BET areas) have been found to have the same capacity for absorbing large molecules such as thermobitumens (*6*).

Also, Naucke has reported a method for determining the surface area of cokes by phenol adsorption from solution (*8*).

R. L. Bond: We are grateful to the contributors for their comments. It is clear that various techniques for estimating apparent specific surfaces of coals provide reproducible values and that the sorption data provide useful comparative information. However, we still feel that the only reliable data are the "sorption uptakes" of a given sorbate by a given adsorbent, and these should not be converted into specific surface values, i.e., by using values for apparent monolayer capacities.

We hope to support our contentions more fully elsewhere, and the comments of the various contributors will be given full consideration, but we would like to note here with respect to Dr. Kini's remarks that BET specific surface values for low rank coal, using CO_2 at 195°K. (*3*) or xenon at 273°K. (*4*) as sorbate, can agree with the corresponding values obtained using methanol at 303°K. (*1*, *4*) which are spurious.

Literature Cited

(1) Anderson, R. B., Hall, W. K., Lecky, J. A., Stein, K. C., *J. Phys. Chem.* **60,** 1548 (1956).
(2) Anderson, R. B., Hofer, L. J. E., Bayer, J., *Fuel* **41,** 559 (1962).
(3) Kini, K. A., *Rept. Intern. Congr. Ind. Chem., 27th, Brussels* **2,** 110 (1954).
(4) Kini, K. A., *Fuel* **43,** 173 (1964).
(5) Lamond, T. G., Marsh, H., *Carbon* **1,** 281 (1964).
(6) Lowry, H. H., "Chemistry of Coal Utilization," Suppl. Vol., p. 182, John Wiley &
(7) Maron, S. H., Bobalek, E. G., Fok, S. M., *J. Colloid Sci.* **11,** 21 (1956).
(8) Naucke, W., *Brennstoff-Chem.* **44,** 302 (1963).
(9) Walker, P. L., Jr., Geller, I., *Nature* **178,** 1001 (1956).

Publication Date: January 1, 1966 | doi: 10.1021/ba-1966-0055.ch047

General Discussion

Peter H. Given: There are two general matters related to the theme of this session on which I should be interested to hear discussion.

In some coal combustion systems the ignition process occurs at relatively low temperatures. No doubt the character of this process depends on the particle size and mode of ignition (by radiation, flow of hot air, etc.) and hence on the radiation intensity or air temperature and flow rate. However, if one compares the ignition of a series of whole coals of different rank under the same physical conditions, the property of the coal that determines the change of ignition characteristics with rank is no doubt the nature and quantity or rate of release of volatile matter in the crucial temperature range (350°–450°C., approximately); this idea was implied in Dr. Essenhigh's paper in this session (Dr. Essenhigh's verbal presentation with J. B. Howard on "Coal Combustion Phenomena and the Two-Component Hypothesis of Coal Constitution"). If this idea is accepted, then the ignition characteristics of a coal may well depend on its petrographic composition. The volatile matter released by exinites is different in composition from that released by vitrinites, the yield of volatile matter is much greater (2–3 times with many bituminous coals), and the rate of release at 350°–450°C. is probably higher. On the other hand, the inert macerals yield little volatile matter at all, and virtually none at low temperatures. It may well happen therefore that two whole coals of apparently similar rank but different petrographic makeup could have different ignition characteristics. This seems to be a worthwhile topic for research.

We have heard several papers on the reactions of coal or coal volatiles under conditions of very high energy input (in plasmas, laser irradiation, etc.). Potentially useful yields of valuable chemical raw materials result. The work therefore appears to be a new variety of cook-book preparative chemistry in which new and highly active species are involved as intermediates, and it is not easy for the ordinary chemist to visualize what goes on and what these intermediates are. Would any of the authors care to comment?

Marie-Therese Mackowsky: I believe that during combustion in wet or dry boilers, especially in wet boilers in which one has a temperature in the fire chamber around 1700°C., the differences between macerals are not as important as transport phenomena.

I am involved with coal petrology and coal microscopy, but I feel that there are some problems which can't be solved by coal petrology.

R. H. Essenhigh: Dr. Given has accurately summarized and interpreted our views—namely, that ignition appears to be established in the first pulse of volatiles generated in the temperature range (300°–450°C.). Given that condition, coals of nominally similar rank (by total carbon or VM %) but having different ignition characteristics because of different "inflammabilities" are most likely to have these differing characteristics because of different petrographic makeup. We would agree with Dr. Given that this could be a most worthwhile and fruitful topic for research.

Publication Date: January 1, 1966 | doi: 10.1021/ba-1966-0055.ch047

Experimental results obtained very shortly after this Conference demonstrated a need to modify our views to some extent. We expected coals to break up at their normal decomposition temperature, even in flames under conditions of fast heating. In the plug flow reactor we have been operating, the rates of heating are 10⁴°C./sec., and the new results show that this is so fast that the particles can reach temperatures of 1000°C. before significant pyrolysis sets in; we would expect the previous comments to hold true only under conditions of *slow* heating, say not exceeding 10²°C./sec. However, we would still expect inflammability characteristics to depend on petrographic makeup.

In reply to Dr. Mackowsky's comments we would concede that other factors may well dominate in boilers at 1700°C.; we would submit that the influence of coal constitution may perhaps still be felt. In the first place the combustion of coal up to 1500° or 1600°C. at least is no longer regarded as being determined completely by transport processes. It is now clear that the role of boundary layer diffusion has been substantially overestimated. That being so, the nature of the reactant and its reactivity become important. The results referred to above indicate that there can be a significant residue of volatiles left in the solid coke (identified as the carbonization pole). The temperatures involved (1500°C.) are within 200° of those cited by Dr. Mackowsky, and the influence times (approaching one second) are also comparable. We must therefore accept the probability that the material burning out is a carbon-hydrogen complex—even in wet bottom boilers—and is therefore likely to have a higher reactivity than pure carbon. As far as the rank or petrographic constituents are concerned, these however, should not affect the situation if it is true that (a) all pyrolyzing coals pass through the carbonization pole, and (b) they stop pyrolyzing at the pole (even in boilers) provided that the coal is initially of lower equivalent rank than the carbonization pole. This, of course, says nothing of ignition. Broadly speaking, rank does affect ignition; otherwise there would be no difficulty in burning anthracites and no need for designing different boilers for anthracites.

The significant point, nevertheless, is the strong possibility of finding volatiles still in the residue, even in boiler combustion chambers operating at 1700°C.

Andrew G. Sharkey, Jr.: Positive, negative, and neutral species have been found by probe techniques in flames. Direct mass spectrometric techniques should lead to identification of many of the primary species obtained by heating coal to extreme temperatures.

Robert A. Friedel: To Dr. Sharkey's remarks on mass spectroscopy I would like to add a few pertinent comments on other types of spectroscopy which would be applicable to the study of species obtained from coal subjected to plasma, laser irradiation, and similar high energy processes.

High speed emission spectroscopy has been used to study free radicals and positive, negative, and multiple ions produced in explosions and flames. Many excited states would exist for many different species from coal subjected to high energy. Complex spectra would result. The combination of electronic-vibration-rotation transitions observable in emission spectroscopy

Publication Date: January 1, 1966 | doi: 10.1021/ba-1966-0055.ch047

would further complicate the spectra. However, the spectra may not be any more complex than coal itself.

High speed infrared spectroscopy is also available and has been used to study explosions and shock-tube experiments. Specific information on vibration and rotation states can be obtained by this method. Again the spectral information would be complex, but at least the electronic transitions are hereby eliminated.

Microwave spectroscopy is another possibility for studying high energy processes. The technique is most suitable for investigating rotational ground and excited states of small molecules. Practically all vibration transitions are eliminated by operating in this region of the spectrum. The technique closely allied to microwave spectroscopy—electron paramagnetic resonance—is certainly a feasible method for studying free radicals *in situ* in high energy processes. Studies of radiation processes *in situ* are being carried out. For example, the free radicals produced from organic vapors bombarded by electrons and gamma rays can be measured during the radiation process. It should be possible to use similar techniques for investigating organic substances subjected to high energy.

In addition to direct measurements on high energy processes it should also be possible to isolate species from a plasma—for example, by freezing them on cold surfaces or in matrices. Observations by various spectral methods, including absorption, scattering (Raman), and emission (luminescence), could then be used at leisure to study ions, radicals, and other species.

For studying metals in high energy processes, the flame emission technique should be applicable. A more sensitive technique for investigating metal ions is the atomic absorption method, in which the high energy flame or plasma absorbs the energy from a source emitting the spectrum of the metal being studied.

H. R. Linden: High temperature pyrolysis of coal with high energy sources seems to follow readily predictable paths similar to hydrocarbon pyrolysis. The effects of pressure, gas atmosphere, reaction time, and the "volatile matter" content of the coal bear the same relationship to yields of methane, ethane, ethylene, acetylene, and hydrogen as for simple hydrocarbons. Effective reaction temperature, although not directly measurable, could be estimated by means of a suitable chemical thermometer, such as the C_2H_2-C_2H_4-H_2 system which approaches equilibrium very rapidly. As Dr. Given also noted, equating the "volatile matter" to the reactive portion of the coal is an oversimplification but adequate for empirical purposes; the C H ratio of the coal would probably be more suitable.

Dr. Sharkey: Attempts were made to use C H ratio following laser irradiation as an indication of the reaction temperature, as Dr. Linden suggests. Collecting the irradiated coal was difficult, and special techniques are now being devised. Use of a spectrum-line reversal technique is another possibility.

R. L. Bond: In studying high temperature systems the problems associated with minerals in coal should also be investigated, and I would make a plea that as much work should be done on the minerals at high temperatures as on the carbon/hydrogen-containing particles.

Publication Date: January 1, 1966 | doi: 10.1021/ba-1966-0055.ch047

Publication Date: January 1, 1966 | doi: 10.1021/ba-1966-0055.ch047

INDEX

A

B

In Coal Science; Given, P.;
Advances in Chemistry; American Chemical Society: Washington, DC, 1966.

C

Publication Date: January 1, 1966 | doi: 10.1021/ba-1966-0055.ix001

D

E

Publication Date: January 1, 1966 | doi: 10.1021/ba-1966-0055.ix001

F

G

H

Publication Date: January 1, 1966 | doi: 10.1021/ba-1966-0055.ix001

I

J

K

L

M

Publication Date: January 1, 1966 | doi: 10.1021/ba-1966-0055.ix001

N

O

Publication Date: January 1, 1966 | doi: 10.1021/ba-1966-0055.ix001

P

Q

R

Publication Date: January 1, 1966 | doi: 10.1021/ba-1966-0055.ix001

S

T

Publication Date: January 1, 1966 | doi: 10.1021/ba-1966-0055.ix001

U

V

W

X

Y

Z

Publication Date: January 1, 1966 | doi: 10.1021/ba-1966-0055.ix001